

Dedication

To the love of my life, my beautiful wife Angela to whom I have been devoted for thirty six years

Michael R. Hamblin

To my parents and aunt, Seda, Debora, Esin, Berna, Begum and Ozan whose advise, encouragement and support have been genuine and precious

Pinar Avci

To my loving wife, Natalie, and to my son and my daughter, Jacob and Jasmine for their unwavering support and love

Tarl W. Prow

NANOSCIENCE IN DERMATOLOGY

Edited by

MICHAEL R. HAMBLIN

*Wellman Center for Photomedicine, Massachusetts General Hospital, Boston, MA, USA;
Department of Dermatology, Harvard Medical School, Cambridge, MA, USA*

PINAR AVCI

Department of Dermatology, Harvard Medical School, Cambridge, MA, USA

TARL W. PROW

*Dermatology Research Centre, University of Queensland, School of Medicine,
Translational Research Institute, Brisbane, Australia*



ELSEVIER

AMSTERDAM • BOSTON • HEIDELBERG • LONDON
NEW YORK • OXFORD • PARIS • SAN DIEGO
SAN FRANCISCO • SINGAPORE • SYDNEY • TOKYO

Academic Press is an imprint of Elsevier



Academic Press is an imprint of Elsevier
125 London Wall, London EC2Y 5AS, United Kingdom
525 B Street, Suite 1800, San Diego, CA 92101-4495, United States
50 Hampshire Street, 5th Floor, Cambridge, MA 02139, United States
The Boulevard, Langford Lane, Kidlington, Oxford OX5 1GB, United Kingdom

Copyright © 2016 Elsevier Inc. All rights reserved.

No part of this publication may be reproduced or transmitted in any form or by any means, electronic or mechanical, including photocopying, recording, or any information storage and retrieval system, without permission in writing from the publisher. Details on how to seek permission, further information about the Publisher's permissions policies and our arrangements with organizations such as the Copyright Clearance Center and the Copyright Licensing Agency, can be found at our website: www.elsevier.com/permissions.

This book and the individual contributions contained in it are protected under copyright by the Publisher (other than as may be noted herein).

Notices

Knowledge and best practice in this field are constantly changing. As new research and experience broaden our understanding, changes in research methods, professional practices, or medical treatment may become necessary.

Practitioners and researchers must always rely on their own experience and knowledge in evaluating and using any information, methods, compounds, or experiments described herein. In using such information or methods they should be mindful of their own safety and the safety of others, including parties for whom they have a professional responsibility.

To the fullest extent of the law, neither the Publisher nor the authors, contributors, or editors, assume any liability for any injury and/or damage to persons or property as a matter of products liability, negligence or otherwise, or from any use or operation of any methods, products, instructions, or ideas contained in the material herein.

Library of Congress Cataloging-in-Publication Data

A catalog record for this book is available from the Library of Congress

British Library Cataloguing-in-Publication Data

A catalogue record for this book is available from the British Library

ISBN: 978-0-12-802926-8

For information on all Academic Press publications
visit our website at <https://www.elsevier.com/>



Publisher: Mica Haley

Editorial Project Manager: Lisa Eppich

Production Project Manager: Lucía Pérez

Designer: Mark Rogers

Typeset by TNQ Books and Journals

Contributors

- Mona M.A. Abdel-Mottaleb** Ain Shams University, Cairo, Egypt; University of Franche Comte, Besancon, France; University of Bonn, Bonn, Germany
- Allesandro Afornali** Grupo Boticário, São José dos, Paraná, Brazil; The Pontifical Catholic University of Paraná (PUCPR), Curitiba, Paraná, Brazil
- Marcel Ameloot** Hasselt University, Diepenbeek, Belgium
- Firoz Anwar** King Abdul-Aziz University, Jeddah, Kingdom of Saudi Arabia
- F.A. Al-Abbasi** King Abdul-Aziz University, Jeddah, Kingdom of Saudi Arabia
- Anthony A. Attama** University of Nigeria, Nsukka, Enugu State, Nigeria
- Giuseppina Barrera** University of Turin, Turin, Italy
- Sarwar Beg** Panjab University, Chandigarh, India
- Heather A.E. Benson** Curtin University of Technology, Perth, WA, Australia
- Aaron J. Brady** Queen's University Belfast, Belfast, United Kingdom
- Jiezhong Chen** University of Newcastle, Callaghan, NSW, Australia; The University of Queensland, Brisbane, QLD, Australia
- Lucy L. Chen** University of Miami Miller School of Medicine, Miami, FL, United States
- Eric Stefano Ciamporcerro** University of Turin, Turin, Italy
- Martina Daga** University of Turin, Turin, Italy
- Sarah Deville** Hasselt University, Diepenbeek, Belgium; Flemish Institute for Technological Research, Mol, Belgium
- Chiara Dianzani** University of Turin, Turin, Italy
- Ryan F. Donnelly** Queen's University Belfast, Belfast, United Kingdom
- Labiba El-Khourdagui** Alexandria University, Alexandria, Egypt
- Nesma El-Sayed** Saarland University, Saarbruecken, Germany; Alexandria University, Alexandria, Egypt
- Socorro Espuelas** University of Navarra, Pamplona, Spain
- Anitha Ethirajan** Hasselt University, Diepenbeek, Belgium
- Conor L. Evans** Wellman Center for Photomedicine, Harvard Medical School, Charlestown, MA, United States; Harvard University Program in Biophysics, Boston, MA, United States
- Carlo Ferretti** University of Turin, Turin, Italy
- Matthew C. Foote** Princess Alexandra Hospital, Brisbane, QLD, Australia
- Adam Friedman** George Washington School of Medicine and Health Sciences, Washington, DC, United States
- Casimiro Luca Gigliotti** University of Eastern Piedmont, "Amedeo Avogadro", Novara, Italy
- Yolanda Gilaberte** Hospital San Jorge, Huesca, Spain
- Ee Teng Goh** University College London (UCL), London, United Kingdom
- Jeffrey E. Grice** The University of Queensland School of Medicine - Translational Research Institute, Woolloongabba, QLD, Australia
- Aswathi R. Hegde** Manipal University, Manipal, Karnataka, India
- Van L.T. Hoang** The University of Queensland, Brisbane, QLD, Australia
- G. Louis Hornyak** Asian Institute of Technology, Klong Luang, Pathum Thani, Thailand
- Sasan Jalili-Firoozinezhad** University of Lisbon, Lisbon, Portugal
- Ángeles Juarranz** Universidad Autónoma, Madrid, Spain
- Georgia Kirby** University College London (UCL), London, United Kingdom; University of Cambridge, Cambridge, United Kingdom
- Vikas Kumar** Sam Higginbottom Institute of Agriculture, Technology & Sciences (SHIATS), Allahabad, India
- Angelo Landriscina** Montefiore—Albert Einstein College of Medicine, Bronx, NY, United States
- Jun Li** Huazhong University of Science and Technology (HUST), Wuhan, PR China
- Zongxi Li** Wellman Center for Photomedicine, Harvard Medical School, Charlestown, MA, United States
- Xing-Jie Liang** Chinese Academy of Sciences (CAS), Beijing, China
- Lynlee L. Lin** The University of Queensland, Brisbane, QLD, Australia
- Márcio Lorencini** Grupo Boticário, São José dos, Paraná, Brazil
- Morteza Mahmoudi** Tehran University of Medical Sciences, Tehran, Iran; Stanford University School of Medicine, Stanford, CA, United States
- Giovanni Maina** University of Turin, Turin, Italy
- Jyothsna Manikkath** Manipal University, Manipal, Karnataka, India
- Srujan Kumar Marepally** Institute for Stem Cell Biology and Regenerative Medicine (inStem), GKVK-Campus, Bangalore, Karnataka, India

- Omid Mashinchian** Nestlé Institute of Health Sciences, Lausanne, Switzerland; École Polytechnique Fédérale de Lausanne (EPFL), Lausanne, Switzerland
- Yousuf Mohammed** The University of Queensland School of Medicine - Translational Research Institute, Woolloongabba, QLD, Australia
- Breanne Mordorski** Montefiore—Albert Einstein College of Medicine, Bronx, NY, United States
- Esther Moreno** University of Navarra, Pamplona, Spain
- Srinivas Mutalik** Manipal University, Manipal, Karnataka, India
- Mohammad Norouzi** Stem Cell Technology Research Center, Tehran, Iran
- Joshua D. Nosanchuk** Montefiore—Albert Einstein College of Medicine, Bronx, NY, United States
- Ebele B. Onuigbo** University of Nigeria, Nsukka, Enugu State, Nigeria
- Megan J. Osmond-McLeod** CSIRO, North Ryde, NSW, Australia
- Harendra S. Parekh** The University of Queensland, Brisbane, QLD, Australia
- Ievgenia Pastushenko** Université Libre de Bruxelles (ULB), Brussels, Belgium
- Rozhin Penjweini** University of Pennsylvania, Philadelphia, PA, United States; Hasselt University, Diepenbeek, Belgium
- Stefania Pizzimenti** University of Turin, Turin, Italy
- Lucia Prieto-Torres** Hospital Clínico Universitario Lozano Blesa, Zaragoza, Spain
- Tarl W. Prow** The University of Queensland, Brisbane, QLD, Australia
- Mahfoozur Rahman** Sam Higginbottom Institute of Agriculture, Technology & Sciences (SHIATS), Allahabad, India
- Jayakumar Rajadas** Stanford University, Stanford, CA, United States
- Fiorenza Rancan** Charité – Universitätsmedizin Berlin, Berlin, Germany
- Anil K. Rao** Metropolitan State University of Denver, Denver, CO, United States
- Joy N. Reginald-Opara** University of Nigeria, Nsukka, Enugu State, Nigeria
- Michael S. Roberts** The University of Queensland School of Medicine - Translational Research Institute, Woolloongabba, QLD, Australia; University of South Australia, Adelaide, SA, Australia
- Jamie Rosen** Montefiore—Albert Einstein College of Medicine, Bronx, NY, United States
- Federica Rossi** University of Turin, Turin, Italy
- Ricardas Rotomskis** Vilnius University, Vilnius, Lithuania
- Marc Schneider** Saarland University, Saarbruecken, Germany
- Juana Schwartz** University of Navarra, Pamplona, Spain
- Masoud Soleimani** Tarbiat Modares University, Tehran, Iran
- Aaron Tan** University College London (UCL), London, United Kingdom; Stanford University, Stanford, CA, United States
- Juan Tao** Huazhong University of Science and Technology (HUST), Wuhan, PR China
- Shima Tavakol** Iran University of Medical Sciences, Tehran, Iran; Tehran University of Medical Sciences, Tehran, Iran
- Emmanuel M. Uronnachi** Nnamdi Azikiwe University, Awka, Anambra State, Nigeria
- Praveen Kumar Vemula** Institute for Stem Cell Biology and Regenerative Medicine (inStem), GKVK-Campus, Bangalore, Karnataka, India; Ramalingaswami Re-Entry Fellow, Government of India
- Min Wang** Nanyang Technological University, Singapore
- Steven Q. Wang** Memorial Sloan-Kettering Cancer Center, New York, NY, United States
- Chenjie Xu** Nanyang Technological University, Singapore
- Miko Yamada** The University of Queensland, Brisbane, QLD, Australia
- Gian Paolo Zara** University of Turin, Turin, Italy
- Xu Dong Zhang** University of Newcastle, Callaghan, NSW, Australia
- Yi Zhang** Huazhong University of Science and Technology (HUST), Wuhan, PR China

Preface

It has been said that dermatology is one of the slowest medical disciplines to embrace new technologies. In fact, some have even said that dermatology is a medical discipline that lags behind the technology curve. After developing this book, we have come to the conclusion that perhaps it is more accurate to say that clinical dermatology may lag behind the technology curve at present, but dermatology research is cutting edge and is indeed expected to be pushing new technologies into the clinic in the coming years. One example of the advent of this advanced technology is the use of innovative imaging techniques and automated image processing (as described in the companion book to this volume, *Imaging and Dermatology*). Clinical dermatology is incredibly visual in nature. The amount of imaging data being gathered by innovative modalities these days is unprecedented and growing. The driving force behind this growth has been the emergence of empowered patients with high-resolution mobile phones, not to mention the explosion in skin-specific “Apps”. Patient empowerment is powerful, especially with the right mix of technology, accessibility, and the promise of improved healthcare. We are seeing similar growth in the field of nanotechnology with up-to-date researchers who have access to an impressive array of nanoparticle-based technologies that promise to change the dermatology drug delivery and imaging landscapes forever. One example of this is the nanoparticle-based imaging technology described in Chapter 6 that enables in vivo oxygen sensing. Imaging is one of the key technologies supporting nanoparticle research in dermatology. Chapters 9, 14, 16, 21, 22, and 24 all contain significant information about imaging nanoparticles on and in skin. We see that the combination of nanotechnology and advanced imaging is a powerful combination that supports a vast amount of research in this area.

A significant, but largely unappreciated, aspect of this wave of research is the establishment of toxicity testing through global networks. The single best example of this is the rollercoaster ride that our scientific and clinical community has witnessed over the last 5 to 10 years concerning zinc oxide nanoparticle research. Industry had generated organic sunscreens with ZnO as physical UV blockers and marketed them. They worked. Then the scientific community was gripped by uncertainty typified by conflicting reports concerning nanoparticle toxicity. We as a scientific and clinical research

community had to go back to our roots and develop new ways to assess nanoparticle exposure and toxicity risk. Chapter 16 takes the reader through this journey where we now have much more sophisticated and relevant ways to test topical nanoparticles. As a community, we now know how to move more assuredly forward in the areas of nanotechnology in dermatology.

We have seen dermatology move rapidly to the cutting edge of medical technology with a huge number of people using nanotechnology on their skin in the form of sunscreens and cosmetics. The controversy and even confusion that this realization generated have had a ripple effect that has been felt in other high-impact areas, like nanotechnology in food science and environmental science. So, perhaps dermatology can be viewed as being a bit more “avant-garde” than it is usually credited.

As we journey through the table of contents for this book, it becomes clear that “nanodermatology” is now at the cutting edge of medical science. Why is that? Perhaps it is for the same reason that companies were able to confidently deploy tons of nanomaterials into the consumer market without too many negative consequences. The skin is an incredible barrier to the penetration of almost everything, and moreover the skin is easily accessible. Almost every chapter in this book describes a novel nanotechnology being tested in human skin, or at the very least in animal models. The amount of volunteer and patient testing in the field of nanotechnology in dermatology is unprecedented. Undoubtedly, this aspect of dermatology is on the vanguard with few competitors. The majority of this work is in the field of topical drug delivery.

Nanotechnology has had a significant impact on drug delivery in general, and there are constantly renewed promises of revolutionary improvements in drug bioavailability, controlled release, and sophisticated drug targeting. Chapter 4 describes the use of microneedle technology to improve topical drug delivery. Microneedles have been used to dramatically improve the delivery of large payloads like nanoparticles. This combination of micro- and nanotechnology in skin is another example of cutting-edge research in dermatology. Drug delivery is another major theme in this book. Several chapters, including Chapters 5–7, 9, 10–13, 15–19, and 23, all discuss roles for nanoparticles as drug carriers or nanoparticles as active agents for use as preventatives or therapeutics.

Readers may be somewhat surprised to see Chapter 25 by Attama and colleagues included in this book, as the chapter deals with ophthalmology, and the book is actually concerned with dermatology. Nevertheless, the editors felt that the delivery of nanomaterials into the eye and into the skin had much in common. Both organs are accessible for topical application of nanodrugs, and

similar considerations of penetration and toxicology apply in both cases.

Michael R. Hamblin
Pinar Avci
Tarl W. Prow

Anatomy and Function of the Skin

Y. Gilaberte¹, L. Prieto-Torres², I. Pastushenko³, Á. Juarraz⁴

¹Hospital San Jorge, Huesca, Spain; ²Hospital Clínico Universitario Lozano Blesa, Zaragoza, Spain; ³Université Libre de Bruxelles (ULB), Brussels, Belgium; ⁴Universidad Autónoma, Madrid, Spain

OUTLINE

Introduction	1	Hypodermis	7
The Epidermis	2	Epidermal Appendages	8
<i>Structure of the Epidermis</i>	3	<i>Apocrine Glands and Eccrine Sweat Glands</i>	8
<i>Keratinocytes</i>	3	<i>Hair Follicle and Sebaceous Glands</i>	9
<i>Epithelial Stem Cells</i>	3	<i>Nails</i>	11
Basal Layer or Stratum Germinativum	3	Functions of the Skin	11
Squamous Cell Layer, Also Called the Prickle Cell Layer or Stratum Spinosum	4	<i>Regulation of Body Temperature</i>	11
The Granular Layer or Stratum Granulosum	4	<i>Preventing Loss of Essential Body Fluids, and</i>	
Cornified Layer or Stratum Corneum	5	<i>Protecting Against Penetration of Toxic</i>	
<i>Nonkeratinocyte Cells</i>	5	<i>Substances</i>	11
Melanocytes	5	<i>Immunological Function</i>	11
Langerhans Cells	5	<i>Sensory Organ for Touch, Heat, Cold, Sociosexual,</i>	
Merkel Cells	6	<i>and Emotional Sensations</i>	12
<i>The Dermal-Epidermal Junction: The Epidermal</i>		<i>Endocrine Function</i>	12
<i>Basement Membrane</i>	6	Conclusion	12
Dermis	6	Acknowledgments	12
<i>Dermal Blood and Lymphatic Vessels</i>	7	References	12
<i>Muscles</i>	7		
<i>Nerves</i>	7		
<i>Mast Cells</i>	7		

INTRODUCTION

The skin is the single largest human organ, with 2 m² of surface and 3.6 kg of weight in adults. It acts as a waterproof, insulating shield, protecting the body against environmental stresses. It also produces antimicrobial peptides that prevent infections, and hormones, neuropeptides, and cytokines that exert biological effects, not only locally on the skin but also systemically throughout the whole body.

The integumentary system develops from surface ectoderm and the underlying mesenchyme. It consists of the skin and the appendages, its derivative structures, which include hair follicles, nails, and sebaceous and sweat glands. The skin is composed of three layers: the epidermis, the dermis, and the hypodermis. It provides a life-sustaining interface between the body and the external environment, carrying out very important functions such as protection, preservation of water and electrolytes, regulation of temperature, and water and fat

storage, and it plays a major role in the endocrine and immunological systems.

THE EPIDERMIS

The epidermis is the most external layer of the skin and can range in total thickness from 0.5 mm (eyelid) to 1.5 mm (palms and soles). It is formed by a stratified squamous epithelial layer and is composed basically of keratinocytes and melanocytes that form a binary system [1]. The epidermis harbors a number of other cell populations such as Langerhans cells (LCs) and

Merkel cells, but keratinocytes are by far the most predominant cell type.

The epidermis is a perpetually regenerating tissue with cells continuously undergoing terminal differentiation and death. The total renewal time is approximately 2 months. The epidermis gives rise to other structures like nails, sweat glands, and pilosebaceous units. The epidermis penetrates down into the dermis through the rete ridges, while the dermis projects upward into the epidermis by the dermal papillae that occur between these rete ridges (Fig. 1.1). The epidermis is separated from the dermis by the basement membrane, which will be explained in this chapter.

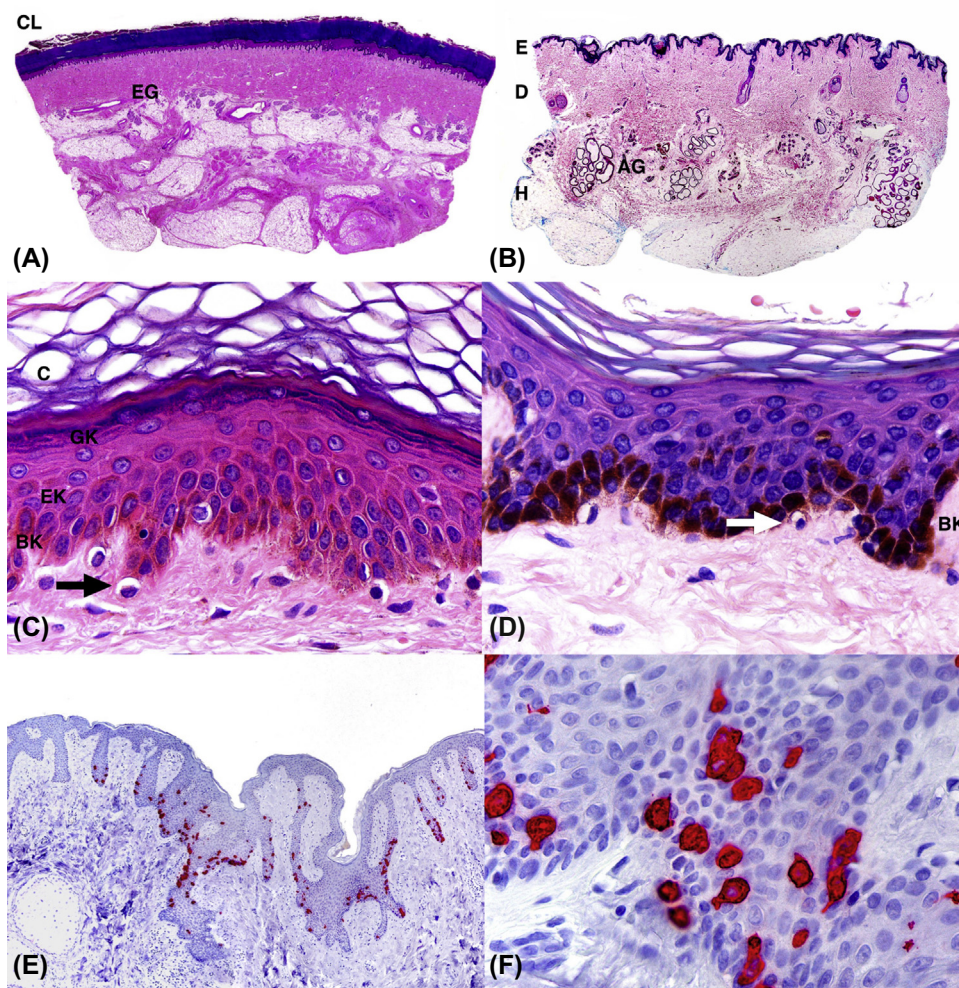


FIGURE 1.1 Normal epidermis. (A) Biopsy of the sole skin, where a thick stratum corneum and multiple eccrine glands are observed in the interphase between the dermis and the hypodermis. CL, Cornified layer; EG, Eccrine glands. (B) Scanning view of the skin of the axilla; unlike the sole in the axilla, the stratum corneum is thinner, there are multiple apocrine glands, and all the skin layers can be observed. E, Epidermis; D, Dermis; H, Hypodermis; AG, Apocrine glands. (C) Skin of a phototype II person; the arrow points the melanocytes located at the dermo-epidermal junction. BK, Basal keratinocytes; EK, Spinous cell layer keratinocytes; GK, Granular cell layer keratinocytes; C, Corneocytes. (D) Black skin with a higher degree of melanization, the presence of larger melanosomes, and a greater amount of them among basal cell keratinocytes (BKs). The arrow shows a melanocyte, with the clear halo around it. (E) Scanning view of the epidermis with scattered Merkel cells stained with immunohistochemical stain CAM 5.2. (F) Higher magnification showing the oval-shaped Merkel cells with cytoplasmic processes extending into and between keratinocytes. Courtesy of Prof. Luis Requena.

Structure of the Epidermis

The epidermis is usually divided into four layers, taking into account the morphology and location of the keratinocytes (Fig. 1.1). Resting directly on the basement membrane is the basal layer, which is formed in part by the rapidly proliferating cells. Some cells leave this layer to continue differentiation by ascending up to the next stratum, the stratum spinosum or prickly cell layer, but other cells die by apoptosis either as a consequence of an intrinsic program or as a consequence of an imbalance of signaling molecules [2]. The next outer layer, the granular cell layer (stratum granulosum), is the last stratum that contains living cells. In the final steps of differentiation, the keratinocytes suffer a transformation into flat, anucleated dead cells, the corneocytes that form the stratum corneum, the most superficial layer of the skin, which functions as the main element of the skin barrier.

Keratinocytes

Keratinocytes represent ectodermal derived cells, which make up 80% of the total cell populations in the epidermis. Keratinization is defined as cytoplasmic events that take place in keratinocytes that move through the different layers of the epidermis to finally differentiate into corneocytes. Keratinization has two different phases: one of them is related to synthesis of keratin, and the other is related to degradation of keratin [3]. When cells that are destined to differentiate reach the stratum spinosum, their cytoplasm becomes larger and several bundles of keratin intermediate filaments are formed inside them. The main function of these keratin filaments is to provide the stiffness to the cells that allows them to withstand the environmental stress that is inflicted upon them when they perform their role as an environmental barrier [4]. It is believed that each keratin intermediate filament is formed by approximately 20,000–30,000 individual polypeptides. There are more than 30 different types of tissue-specific keratins, of which about 20 are epithelial keratin proteins and 10 are hair keratins [5,6]. Epithelial keratins are classified depending on their molecular weight and their isoelectric point into two types; type I keratins, which are acidic and have lower molecular weight, and type II keratins, which are neutral or basic with a higher molecular weight. Besides this, keratins are further subdivided numerically. Type I keratins include molecules numbered from K10 to K20, and type II keratins are those from K1 to K9 [5,6]. Except for K15 [7], each type I keratin is expressed alongside a type II keratin as a molecular partner. Depending on the keratin type, its location within the epidermis varies. For example, in the basal layer the keratinocytes contain K5 and K14, while

in the suprabasal layers they contain K1 and K10. These keratin filaments converge at the plasma membrane, forming intercellular junctions called *desmosomes*. Mutations in the genes that encode keratin proteins have been implicated in the pathogenesis of numerous skin diseases, mainly in ichthyosis, some types of keratoderma, some types of hereditary bullous epidermolysis, and some pigmentation disorders [8].

Epithelial Stem Cells

The homeostasis of the epidermis relies heavily upon stem cells to replenish and repair wounds and continuously replace the many cells that die and are shed from the surface. Stem cells are characterized by their ability to self-renew and differentiate into the different cell lineages characteristic of their tissue of origin.

There are two types of proliferating cells in the basal layer of the epidermis: the epidermal stem cells and the epidermal progenitor cells. The stem cells are characterized by very slow division rates (4–6 times per year), have a long life span, and express high levels of integrin alpha 6. The progenitor cells in the basal layer express involucrin, divide much faster (once per week), and have a shorter lifespan [9].

The hair follicle stem cells are responsible for the growth of hair in the hair follicle and regeneration, and they reside in the lower part of the permanent portion of the hair follicle called the bulge. These cells express CD34, Lgr5, and keratin 15 as markers [10].

Recently, at least three more types of epithelial stem cells have been identified in the skin: stem cells homing to the sebaceous glands, the infundibulum, and the sweat glands. The sebaceous glands are maintained by unipotent stem cells expressing Lgr6 [11]. Stem cells from the infundibulum are multipotent and are characterized by the expression of Lrig1 as a marker [12]. Finally, four different types of progenitor cells have been identified in the epithelium of the sweat glands [13].

Basal Layer or Stratum Germinativum

The basal layer is formed by column-shaped keratinocytes that are attached to the basement membrane zone. They comprise a single layer of cells with dark-staining oval nuclei containing melanin pigment, which would have been transferred by melanocytes located right next to them [14]. Most authors admit the presence within the epidermal basal layer of a keratinocyte subpopulation that meets the functional definition of stem cells, but there is no consensus concerning their location, organization, and activity with regard to the whole epithelium [15]. To the best of our knowledge,

keratinocyte stem cells are considered to be the long-term guardians of integrity of the epidermis. Chadli et al. postulated that the basal layer contained both early progenitor cells, which were close to stem cells, and late progenitor cells, which can differentiate and undergo the keratinization process [16]. It takes about 26–42 days for the individual cells to migrate from the basal layer up to the granular layer, and then the transit through the cornified layer requires an additional 14 days.

Squamous Cell Layer, Also Called the Prickle Cell Layer or Stratum Spinosum

The squamous cell layer is formed by a variety of cells, which differ in shape, structure, and subcellular properties depending on their location. This layer is five to six cells thick [14]. The suprabasal cells are polyhedral with a rounded nucleus, while the upper spinous layer cells are larger and flatter, and have lamellar granules in their cytoplasm. These granules consist of a type of lysosomal vesicles containing glycoproteins, phospholipids, glycolipids, free sterols, acid hydrolases like lipases, proteases, phosphatases, and glycosidases. The granules are more active in the interphase between the stratum granulosum and corneum, but they appear for the first time in the upper spinous layer [17]. There are abundant desmosomes in the intercellular spaces between the spinous cells. Desmosomes are adhesive intercellular junctions that join adjacent cells closely together by linking desmosomal cadherins

with the keratin intermediate filaments, which form the cytoskeletal network. They link these proteins together through densely clustered cytoplasmic plaque proteins, including plakoglobin and plakophilin, and some other members of the plakin family like desmoplakin [18,19] (Fig. 1.2). These junctions are very important for the correct function of the skin and other organs; in fact, mutations in genes related with desmosomes cause cardiomyopathy and disorders of keratinization. Moreover, autoantibodies or bacterial toxins that selectively target desmosomal cadherins cause pemphigus or staphylococcal scalded-skin syndrome, respectively [20,21].

The Granular Layer or Stratum Granulosum

The granular layer is the most superficial layer of the epidermis that still has living cells. It is composed of flattened cells with abundant keratohyaline granules. These granules are basophilic and irregular in shape and size, and they result from the accumulation of newly synthesized proteins, the most relevant being profilaggrin (>400 kDa). This insoluble multiunit protein is dephosphorylated and degraded to produce monomeric filaggrin molecules in the stratum corneum and then further proteolyzed to release its component amino acids. Filaggrin is a histidine-rich protein that binds to keratins 1 and 10 and to other intermediate filament proteins within the keratinocyte cytoskeleton to form tight bundles, causing collapse of the granular cells that become flattened anuclear squames (thin flakes).

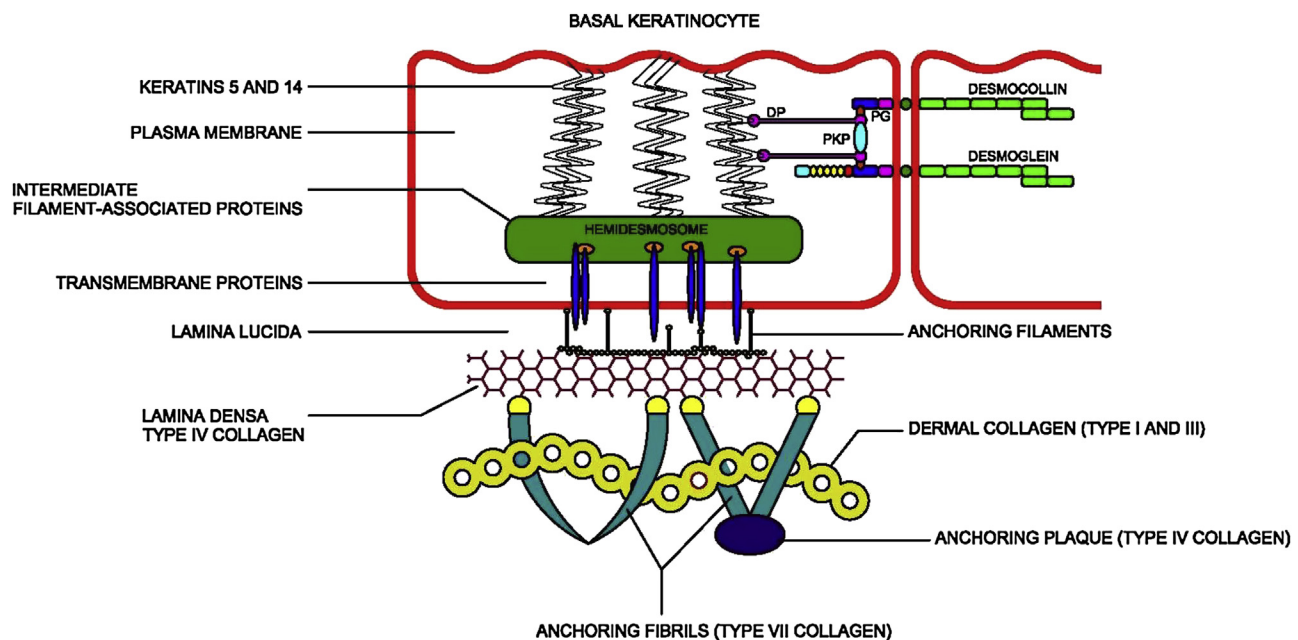


FIGURE 1.2 Basement membrane diagram representing its main components and the intercellular desmosome (not to scale). DP, Desmoplakin; PG, Plakoglobin; PKP, Plakophilin.

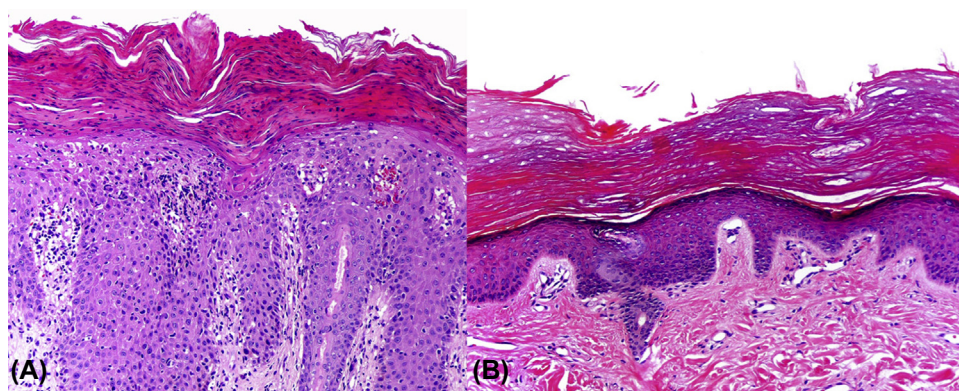


FIGURE 1.3 (A) Skin of a psoriasis patient without a granular layer and with intense parakeratosis in the stratum corneum. (B) Skin with granular layer and a compact orthokeratotic stratum corneum. *Courtesy of Dr Luis Requena.*

Filaggrin has a fundamental role in the development and maintenance of the skin barrier, and its alteration is implicated in numerous skin diseases such as atopic dermatitis or ichthiosis vulgaris [22,23]. Depending on the overlying horny cell layer, the stratum spinosum varies in thickness. In locations with a thin cornified layer like the trunk, it may only be one to three cells thick, whereas in locations like the palms and soles, which have a thicker cornified layer, it could be more than 10 times thicker. In some diseases like psoriasis, in which there is parakeratosis (the presence of cell nuclei within the cornified layer), there is an absence of granular cells (Fig. 1.3).

Cornified Layer or Stratum Corneum

The stratum corneum is formed by corneocytes that are dead cells linked together by corneodesmosomes. An insoluble barrier called the cornified envelope, which replaces the plasma membrane and is composed of proteins and lipids, covers the corneocytes. This cornified cell envelope is a critical structure for the skin barrier function formed by covalent cross-linking of component proteins such as involucrin, loricrin, and the small proline-rich protein. This coupling reaction requires transglutaminase, which is a calcium-dependent enzyme catalyzing the formation of an intermolecular isopeptide bond between proteins [24]. The physical and biochemical characteristics of corneocytes vary between the upper cells and the supragranular cells in order to facilitate desquamation. During desquamation, corneodesmosomes undergo proteolytic degradation.

The intercellular lipids, the corneocytes, some amino acids, other salts from sweat and sebaceous secretions, and degradation products from corneal proteins besides lipids all contribute to the overall barrier effect, preventing loss of water and keeping the skin pH at its optimum condition (5.5).

Nonkeratinocyte Cells

Melanocytes

Melanocytes are cells derived from the neural crest, which migrate through the developing embryo to specific locations in the fetal body, mostly to the skin and hair follicles [25]. In the epidermis, they are confined predominantly to the basal layer, where they come into contact with keratinocytes through cytoplasmic extensions (dendrites). Melanocytes contain melanosomes, tissue-specific “lysosome-related” organelles characteristic of pigment cells in which melanin molecules are synthesized and stored. During the biosynthesis of melanin, toxic intermediates are generated. There are two different forms of melanin in mammals: eumelanin, which is black or dark brown, and pheomelanin, which is yellow or red. The melanin is transferred from melanocytes to keratinocytes. Deeply pigmented skin may be due to an increased production of melanosomes, to a higher degree of melanization, to the presence of larger melanosomes, to a greater dispersion of melanosomes in the keratinocytes, or to slower degradation of melanosomes [26,27].

Langerhans Cells

LCs are antigen-presenting dendritic cells involved in several T-cell responses. They reside in the epidermis, constituting between 2% and 8% of the total epidermal cell population, and most of them are located in the squamous and granular layers. These dendritic cells are derived from the bone marrow and do not form intercellular unions with keratinocytes as do melanocytes. The Birbeck granules are a unique organelle found in LCs, and they can be seen with the electron microscope as having a shape resembling that of a tennis racquet. The phenotypic hallmark of LCs is their expression of the C-type lectin receptor called langerin or CD207 [28].

Merkel Cells

Merkel cells were discovered by Friedrich Sigmund Merkel in 1875 [29]. They are found in the basal layer of the epidermis. Merkel cells are oval-shaped, and their membrane interacts with nerve endings in the skin with synapse-like structures. On their opposite side, they have cytoplasmic processes that extend into and between the keratinocytes and to which they are linked by desmosomes. Merkel cells function as type 1 mechano-receptors and can sense light touches. They are part of the tactile-end organs in the skin, which include Merkel discs, Pacinian corpuscles, Meissner's corpuscles, and Ruffini endings [30].

The Dermal-Epidermal Junction: The Epidermal Basement Membrane

The epidermal basement membrane is a thin extracellular matrix separating the epidermis from the dermal connective tissue, located in the dermo-epidermal junction [31]. It has four major components: basal cell plasma membrane, the lamina lucida, the lamina densa, and the sublamina densa fibrillar zone that includes the anchoring fibrils [32] (Fig. 1.2).

The plasma membrane and hemidesmosome plaques of the basal keratinocytes are the outer part of the basement membrane [31]. Keratin intermediate filaments (K5 and K14) insert into hemidesmosomes. There act as anchoring filaments through the plasma membrane, lamina lucida, and lamina densa.

The lamina lucida, a 35–40 nm wide zone that appears transparent under an electron microscope, is the weakest link in the dermal-epidermal junction. It is traversed by anchoring filaments, including laminin 5, laminin 6, uncein, laminin 1, nidogen, and epiligrin [33,34].

The lamina densa is an electron-dense zone between 35 and 60 nm thick, whose main component is a specific collagen protein, type IV collagen, produced by both keratinocytes and fibrocytes [35]. Other components of the lamina densa are laminin 1, percelan, nidogen, and chondroitin sulfate proteoglycan.

The sublamina densa is a less well-defined zone that could be considered to be the top of the papillary dermis. It contains distinct structures, including the anchoring fibrils; the collagen fibers type I and III, looping from the dermis in close apposition to the lamina densa; the microfibrils, components of elastic fibers in the lower dermis; the micro-thread-like fibers; and the anchoring plaques, which contain type IV collagen and laminin-1. Anchoring fibrils are composed of collagen VII and laminin 332, and their major function is linking the epidermis with the dermis through the lamina densa and anchoring plaques of the dermis [36]. Understanding this structure is of great importance because genetic alterations of their components

and the presence of auto-antibodies produced against these proteins are responsible for most subepidermal bullous disorders.

DERMIS

Beneath the epidermis, a thick layer of fibrous and elastic tissue, called the dermis, provides structural and nutritional support. The dermis comprises two layers: the thin and superficial papillary dermis, and a thicker and deeper reticular dermis. The papillary dermis lies below the dermoepidermal junction and contains loosely arranged collagen fibers. The reticular dermis is formed by thicker bundles of collagen running parallel to the skin surface. The dermis contains stromal cells such as fibroblasts, fibrocytes, and structural cells of the blood and lymph vessels. In addition, many different populations of myeloid and lymphoid immune cells either reside in or traffic through the dermis.

Most of the constituents of the dermis are of mesodermal origin, except for the nerves, which, like melanocytes, derive from the neural crest [37]. Until week 6 of fetal development, the dermis is formed mainly by dendritic-shaped cells, which are precursors of fibroblasts. By week 12 the fibroblasts are producing collagen and elastic fibers, and by week 24 the vascular network and the hypodermis appear.

The dermis is composed of a mucopolysaccharide gel held together by collagen and elastic fibers. Collagen fibers make up 70% of the dermis, giving it strength and toughness, while elastin maintains normal elasticity and flexibility and proteoglycans provide viscosity and hydration. This extracellular matrix of the dermis is constantly being degraded by proteolytic enzymes called matrix metalloproteinases (MMPs) and replaced by new matrix components. MMPs are a group of zinc-dependent extracellular proteinases that remodel the extracellular matrix. There are three predominant groups: collagenases, gelatinases, and stromelysins. The collagenases (MMP-1, MMP-8, MMP-13, and MMP-18) cleave interstitial collagen, with MMP-1 as the predominant one. Gelatinases (MMP-2 and MMP-9) degrade basement membrane collagens and denatured structural collagens. The stromelysins (MMP-3, MMP-10, MMP-11, and MMP-19) degrade basement membrane collagens and proteoglycans, and matrix glycoproteins. Other MMP family members include membrane-type MMPs, matrilynsins, elastase (MMP-12), and others [38]. MMPs are regulated by tissue inhibitors of MMPs (TIMPs), especially TIMP-1 and TIMP-2 [39]. The balance between MMPs and TIMPs is important in the maintenance of the dermal matrix structure. MMPs are mainly produced by keratinocytes, fibroblasts, neutrophils, and mast cells. Transforming growth factor- β (TFG- β) is an important regulator of the

expression of MMPs, stimulating their expression in keratinocytes and inhibiting cell growth [38]. The production of MMPs is increased in several physiological and pathological processes, such as wound repair, skin aging, or tumoral invasion.

Dermal blood and lymphatic vessels, nerves, sweat and sebaceous glands, hair roots, mast cells, and small quantities of muscle are embedded within the fibrous tissue.

Dermal Blood and Lymphatic Vessels

Blood and lymphatic vessels fulfill important homeostatic functions such as providing nutrients for the skin and regulating the immunologic processes. In the dermis, the blood vascularization is organized into a deep plexus and a superficial horizontal plexus, with capillaries arising from the latter one [40,41]. The lymphatic vessels also form two plexuses in proximity to the vascular blood system. Branches from the superficial lymphatic vessel plexus extend into the dermal papillae and drain into the larger lymphatic vessels in the lower dermis [42]. While the blood microvasculature is located immediately below the epidermis, the lymphatic vessels reside more deeply within the dermis [43].

Muscles

The involuntary muscles of the skin comprise the arrector pili, the muscle fibers of veins and arteries, and the glomus bodies. The fibers of the arrector pili are located in the upper dermis and are fixed to the hair follicle below the sebaceous gland, pulling the hair follicle into a vertical position during contraction. Glomus bodies consist of an arteriovenous shunt surrounded by a capsule of smooth muscle cells, and they are found on the digits (toes and fingers), palms, and soles. Their function is to regulate body temperature by shunting blood away from the skin surface when exposed to cold temperature, thus preventing heat loss, and allowing maximum blood flow to the skin in warm weather to allow heat to dissipate.

Voluntary muscles can be found in the skin of the face, as these muscles are responsible for facial expressions, and in the skin of the neck as platysma (a broad sheet of muscle fibers extending from the collarbone to the angle of the jaw).

Nerves

The skin is an important sensory organ, being the principal interface with the environment. The network of sensory nerves allows the perception of touch, temperature, pain, and itch [44]. The autonomous nervous system is of great importance in maintaining cutaneous

homeostasis by controlling vasomotor functions, pilomotor activities, and glandular secretions.

Nerves in the skin contain both myelinated and unmyelinated fibers. In general, the myelinated (or type-A) fibers are motor neurons that interface with striated muscles and include a subgroup of sensory neurons, while unmyelinated (or type-C) fibers correspond to autonomic and sensory fibers. After losing the myelin sheaths, cutaneous nerves terminate as free nerve endings, either in association with receptors or as special nerve-end organs.

Meissner corpuscles mediate touch perception and are located in the dermal papillae. Vater–Pacinian corpuscles are located in the deeper dermis and are large nerve endings that create the perception of pressure. The unmyelinated nerve fibers are responsible for pain, temperature, and itch sensations.

The autonomic nervous system provides the motor innervation of the skin. Adrenergic fibers innervate the blood vessels, hair erector muscles, and apocrine glands, while cholinergic fibers innervate eccrine sweat glands. The secretion of sebaceous glands is not innervated by autonomic fibers but is regulated by the endocrine system.

Mast Cells

Mast cells are multifunctional immune cells that play an important role in both adaptive and innate immune responses. These cells attract other key players of the immune system by secreting cytokines and chemokines. Skin mast cells contain metachromatic granules, which release histamine, leukotrienes, prostanoids, proteases, and many cytokines and chemokines after activation by surface antigen binding or cytokine-dependent events. In addition to their role in allergic responses, mast cells have been implicated in other inflammatory responses, host defense, innate immunity, as well as cell growth and adhesion [45].

HYPODERMIS

Embryologically, at the end of the fifth month of gestation, fat cells begin to develop in the subcutaneous fetal tissue. The hypodermis serves as a reserve energy supply, protects the skin, and allows mobility by sliding over underlying structures. The hypodermis is primarily formed by adipocytes, which are organized into lobules defined by fibrous connective tissue (septa). Nerves, blood, and lymphatic vessels are located within the septa. The subcutaneous tissue stores energy through the following biological reactions: exotrophy, deposition, and endotrophy. Adiponectin is a specific mediator of subcutaneous adipocytes. In addition, subcutaneous tissue is considered to be an endocrine organ,

converting androstenedione into estrone by the aromatase enzyme. Moreover, the adipocytes produce leptin, a hormone that regulates body weight [46].

EPIDERMAL APPENDAGES

Besides the epidermis, there are some ectodermal-derived structures in the skin, called adnexa or epidermal appendages. They include pilosebaceous units, eccrine ducts, apocrine glands, and nails. Some authors claim that the skin appendages promote wound healing by encouraging re-epithelialization after injury through the migration of keratinocytes from the pilosebaceous units to the damaged epidermis [47].

Apocrine Glands and Eccrine Sweat Glands

Evolutionarily, apocrine glands were the first to appear. In humans, their presence has been limited to the periumbilical area, areola, axillae, mons pubis, labia, scrotum, foreskin, perianal region, free edge of

the eyelids (Moll's gland), and ear canal (ceruminous gland) [48]. Eccrine glands appeared later phylogenetically and are found throughout the surface of the body; the only variation between different locations are their density, ranging from 100 to 600/cm². This makes eccrine glands the most abundant skin adnexa. The absence of eccrine glands in normal skin is found in a condition called anhidrotic ectodermal dysplasia. The embryonic origins of the eccrine and apocrine glands are not the same. Whereas apocrine glands appear first during embryonic development (third month) and are derived from the same epithelial germ cells from which the hair follicles originate, the eccrine glands originate later (fourth month) from different epithelial germ cells.

Histologically, the excretory duct structure is roughly similar in both glands and consists of bilayered cubic cells that are surrounded by a basement membrane, and a lack of myoepithelial cells (Fig. 1.4D). The cells of the inner layer are larger than the cells of the outer layer. Excretory ducts differ in their outlet portion; while the apocrine duct opens into the infundibulum of the pilosebaceous unit, the eccrine duct penetrates through

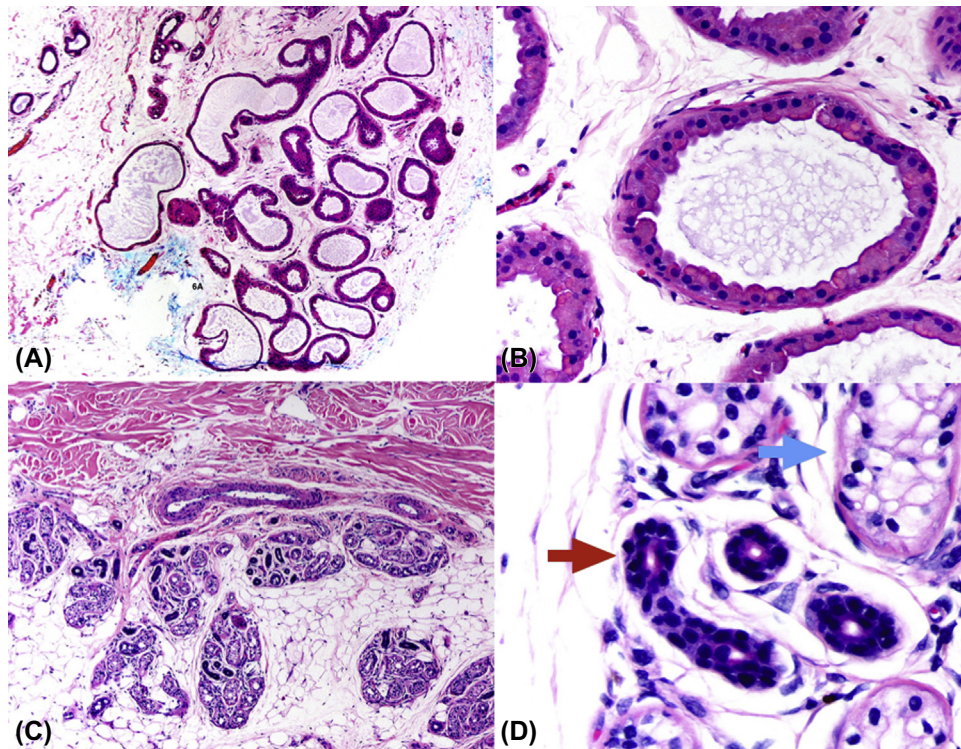


FIGURE 1.4 (A) Axillae skin with multiple apocrine glands with a large lumen. (B) The apocrine glands have one columnar secretory cell type with an oval basal nucleus arranged in more cylindric or cuboidal shapes surrounded by myoepithelial cells. (C) Eccrine glands and ducts located between the dermis and the subcutaneous tissue. (D) The blue arrow shows the secretory portion of the eccrine gland with the clear and dark cells, and the red arrow points ducts with bilayered cubic cells that are surrounded by basement membrane and lack of myoepithelial cells. Their cytoplasm delimits the lumen with a wide eosinophil density of tonofilaments (cuticle). *Courtesy of Prof. Luis Requena.*

the epidermis, and this epidermal portion of the eccrine duct is called the acrosyringium. The structure of the secretory portion differs in both glands. The eccrine secretory portion consists of three types of cells: glycogen-rich clear secretory cells, dark mucoidal cells, and myoepithelial cells with specialized contractile properties. The apocrine secretory portion only has one type of columnar secretory cell with an oval basal nucleus arranged in a more cylindrical or cuboidal shape surrounded by myoepithelial cells [48] (Fig. 1.4).

The type of material discharged is not the same in both glands; eccrine glands have a merocrine secretion process where the secretions of the cells are excreted via exocytosis into an epithelial-walled duct, and apocrine glands undergo apocrine secretion where a portion of the plasma membrane buds off the cell, containing the secretion [48]. Nearly isotonic primary sweat is produced as the secretion from eccrine glands, and then the reabsorption of NaCl, results in the secretion of hypotonic sweat to the surface of the skin. In apocrine glands, the luminal portion of secretory cells is pinched off and released into the secretory lumen; this mode of secretion is called decapitation secretion.

Sato and colleagues reported in 1987 a new gland type in humans, the apoecrine gland, which was found only in adult axillae and had a capacity to produce much higher sweat output than the eccrine gland, but no other authors have since reported this unusual structure, which is why its existence remains controversial [49,50].

Hair Follicle and Sebaceous Glands

Hair follicles are structures derived from the epidermis as a downward-projecting epithelial bud. Basal cells of the epidermis, which generate hair follicles, are guided by an accumulation of dermal mesenchymal cells from which the dermal papillae are formed [51]. Hair follicles are distributed throughout the whole body except on the palms and soles. They form units with the associated structures, the sebaceous glands and arrector pili muscle; and in those body locations where apocrine glands are found, such as the axillae, this apocrine gland is also connected to the pilosebaceous unit.

Two different types of hair shaft are produced by the hair follicle. The first type is terminal hair located in the scalp, which is usually heavily pigmented and thicker, and which projects into the deep dermis or the subcutis. The second type is vellous hair, which is lightly pigmented, shorter, and thinner, and which only extends into the upper reticular dermis. Both terminal and vellous hair have similar life cycles except that the length of the anagen phase is longer in terminal hair follicles [52].

The hair follicle may be divided into four anatomical regions (Fig. 1.5):

1. The infundibulum is a funnel-shaped structure filled with sebum, which extends from the skin surface to the sebaceous duct. Its cells show epidermal keratinization, and it serves as a reservoir for sebum.
2. The isthmus, which extends from the sebaceous duct to the exertion of the arrector pili muscle. This region is very important because it contains the bulge and the follicular trochanter [53]. The bulge region contains follicular stem cells, which stain with antibodies against CK19, CK15, and CD200.
3. The suprabulbar region between the isthmus and the hair bulb.
4. The hair bulb is the expanded lower end of the follicle and encloses the dermal papilla, dermal papilla cells, mucopolysaccharide-rich stroma, nerve fibers, and a single capillary loop. The follicular papilla instructs the hair follicle to grow; moreover, it is an important source of growth factors (keratinocyte growth factor, bone morphogenetic protein, insulin-like growth factor, and stem cell factor) that are critical for hair growth and melanogenesis [54] (Fig. 1.5E).

Hair color is determined by the size and the position of the melanosomes in the hair shaft. The shape of the hair shaft depends on the disposition of the hair follicles. The hair follicles in people who have straight hair are oval shaped and are oriented at an acute angle to the skin, whereas in people who have curly hair the hair follicle is elliptical and the orientation is perpendicular to the skin surface (Fig. 1.5C).

The terminal hair shaft is composed of three concentric layers: the innermost medulla, the intermediate cortex, and the outermost cuticle. The hair cortex has a covering formed by a single row of overlapping cells, called the shaft cuticle. The part of the hair that remains in the follicle has the inner (internal) root sheath outside the cuticle composed of three layers: an inner sheath cuticle, which is in contact with the shaft cuticle; a layer called Huxley's layer; and an outer Henle's layer, which is the first keratinized layer. In this part, the epithelium is continuous with the keratinized epidermis and is covered by an intact stratum corneum. External to the inner root sheath, the terminal hair follicle has the outer (external) root sheath that has clear cells because of a high glycogen content; it is formed by a single layer of cells except for the isthmus zone, where it is thicker and forms a small place of tricholemmal keratinization. Surrounding the hair follicle, there is a vitreous "glassy" layer, which stains with periodic acid Schiff stain. The fibrous root sheath is connected to the lower part of the dermal papilla [55] (Fig. 1.5B and D).

Hair formation is a cyclical process that can be divided into three phases: anagen, catagen, and telogen.

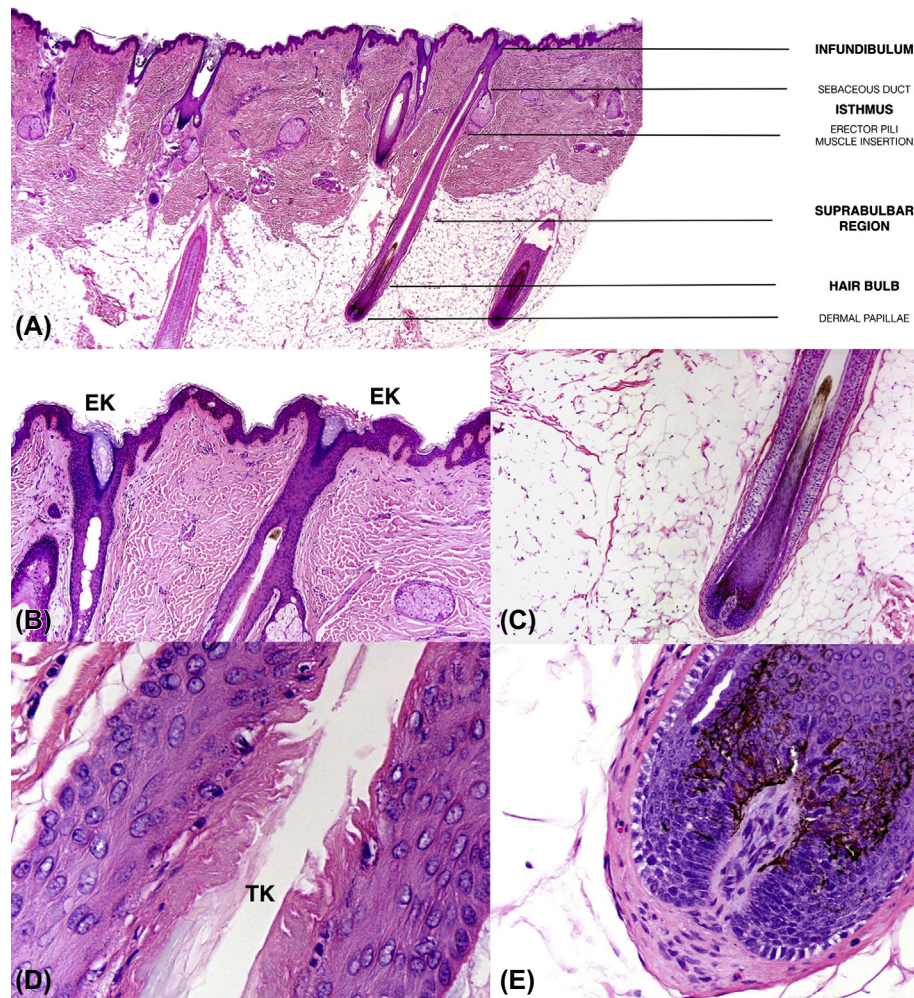


FIGURE 1.5 (A) Terminal hair follicles in a skin biopsy of the scalp. (B) Infundibulum showing an infundibular keratinization (EK) with granular cells and basophilic orthokeratotic keratin. (C) Hair bulb with the hair shaft. (D) Tricholemmal keratinization (TK) at the level of the isthmus without granular cells and with the formation of eosinophilic orthokeratotic keratin. (E) Higher magnification shows matricial cells of the hair bulb and melanin. *Courtesy of Prof. Luis Requena.*

The anagen phase is the phase of active hair production. Of the 100,000 hair follicles in the normal human scalp, approximately 85–90% are in the anagen phase, with a mean duration of 2–7 years [56]. There is a regional variation in the duration of this phase, being longer in the terminal hair of the scalp and shorter in hair in the axilla or pubic region (where it lasts only some months). Catagen is an involutionary phase in which a massive loss of cells by apoptosis occurs, with cessation of mitotic activity in the matrix and arrest of melanin production by melanocytes in the hair bulb. Histologically, scattered apoptotic cells in the outer root sheath can be observed [56]. Finally, the telogen phase lasts approximately 3–4 months, and there are 10–15% of scalp hair follicles in this stage. During this phase, there is no active hair production, and it is followed by a new anagen phase with a regrowth of the hair [56]. There are some hormonal factors controlling hair growth,

with androgens being one of the most important. On the other hand, the human hair follicle appears to represent a specialized compartment of the skin immune system, and it is considered as an immune-privileged site [49]. For that reason, different endocrine and immunological disorders can cause hair diseases or alopecia [56].

The sebaceous gland has a common origin with the hair follicle and the apocrine gland. It is found at the level of the infundibulum between the apocrine gland and the bulge. Sebaceous glands consist of lobes and a sebaceous duct. Each lobe consists of a group of sebocytes carrying out a holocrine secretion, which means that the secretion involves the disintegration of the entire gland. The sebaceous duct is the channel that connects one or more sebaceous lobules to the base of the follicular infundibulum (Fig. 1.5A).

In the facial area, many vellous hair follicles have a high number of sebaceous gland acini (compared to

other hair follicles) that occupy the main axis of the follicle sebaceous unit. These follicles are called sebaceous follicles [48].

Nails

The nail plate is a thin structure (0.25–0.6 mm for fingernails and up to 1.3 mm for toenails). It is hard, although slightly elastic; is translucent; has a convex shape; and comprises approximately 25 layers of dead, keratinized, flattened cells. It is the permanent product of the germinative epithelium of the nail matrix, which has a keratinization process that occurs without the formation of a granular layer. The proximal element forms the third of the nail nearest the cuticle, whereas the distal element provides the remaining two-thirds. The hard keratin of the nail lies perpendicular to the nail growth axis and parallel to the surface of the nail plate. The keratin fibers are held together by globular, cysteine-rich proteins, whose disulfide bonds bind them together. In normal conditions, the nail plate growth occurs from week 15 in the embryo until death. In a healthy person, the growth rate of a fingernail (3 mm/month) is faster than that of a toenail (1 mm/month) [57]. The nail provides protection and counter-pressure to the pulp that are essential to the tactile sensation of the fingers [58].

FUNCTIONS OF THE SKIN

The primary functions of the skin are to serve as a barrier to the entry of foreign pathogens, to protect against damaging sunlight and other harmful physical or chemical agents, and to prevent loss of water and extracellular fluid. Regulation of body temperature, sensory perception, absorption of some substances, immunological reactions, and synthesis of hormones are other relevant functions performed by the skin. All the functions are summarized in Table 1.1, and some of them are described in detail in this section.

TABLE 1.1 Functions of the Skin

- Regulation of body temperature
- Preventing loss of essential body fluids, and penetration of toxic substances
- Protection of the body from harmful effects of the sunlight and infections
- Excretion of toxic substances with sweat
- Mechanical support
- Sensory organ
- Immunological function
- Hormone synthesis
- Storing fat, water, and vitamin D

Regulation of Body Temperature

If the skin temperature drops below 37°C, a variety of responses are initiated in the skin to retain the heat within the body and to increase heat production. These include vasoconstriction, cessation of sweating, and erection of hairs to increase insulation. On the contrary, sweating begins at a skin temperature of 37°C, and also some additional mechanisms are activated to remove heat by processes such as radiation, conduction, convection, and perspiration [59].

Preventing Loss of Essential Body Fluids, and Protecting Against Penetration of Toxic Substances

The skin, especially the epidermis, acts as a two-way barrier to prevent the inward or outward passage of water and electrolytes. Regarding the passage of toxic substances or therapeutic drugs through the epidermis, there are three possible routes: the transcellular route (which is probably the major pathway for polar substances), the appendageal route (eg, hair follicles), and the intercellular route. Low-molecular-weight and lipophilic molecules can gain systemic entry by the transcellular route, by passive diffusion across the epithelial cells. In this sense, compounds with a molecular weight higher than 500 Da do not permeate through the stratum corneum, although the contribution of appendageal routes must be also taken into consideration [60].

Some factors that can influence the penetration of substances through the skin are:

1. Age: penetration is higher in newborns and children than in adults.
2. Skin condition: injured or abraded skin surfaces have increased penetration.
3. Hydration of the skin: hydrated skin is more permeable than dry skin.
4. Hyperemia: vasodilatation of the blood vessels increases the penetration.

Immunological Function

Human skin contains an extensive interacting network of immune cells that belong to both the innate and adaptive immune systems, which together act as a crucial barrier to infections. LCs present antigens that activate T cells and are called professional antigen-presenting cells. After capturing the antigen within the epidermis, LCs migrate through the epidermis and the dermis to finally reach the lymph nodes, in the same way as other classes of dendritic cells. Keratinocytes are also active components of the immunoregulatory network in the skin, and different types of myeloid

and lymphoid cells with specialized functional properties are also involved. The identification of skin-resident memory T-cell populations that have key roles in controlling cutaneous immune responses has revealed the existence of local tissue immunological memory and its importance in host defense [61]. Another important point is that cutaneous commensal bacteria control skin-resident T-cell function and protective immunity against cutaneous pathogens [62]. *Staphylococcus epidermidis* was shown to promote the growth of IL-17A and CD8+ T cells that reside in the epidermis, limiting pathogen invasion and improving the innate immune barrier.

Sensory Organ for Touch, Heat, Cold, Sociosexual, and Emotional Sensations

In order to protect our body from possible hazardous external contacts, the skin has developed an effective sensory and signaling system to react to changes in the external environment. Meissner corpuscles mediate the sense of touch and occur in greater quantity on the hands, especially in the fingertips. Vater–Pacini corpuscles are large nerve-end organs that detect pressure and are located in the deep dermis of weight-bearing surfaces and the perineal region. Sensing of pain, temperature, and itch are conducted by unmyelinated nerve fibers located around hair follicles and in the papillary dermis.

Endocrine Function

The skin possesses the capacity to produce various hormones and substances with hormone-like activity, such as sex steroids, melatonin, and vitamin D [63]. These hormones have biologic effects on the skin through paracrine, autocrine, intracrine, and endocrine mechanisms. Besides its capacity to produce hormones, the human skin is able to metabolize hormones by either activating or inactivating them. Characteristic examples are the metabolic pathways of the corticotrophin-releasing hormone–proopiomelanocortin axis, sex steroids, vitamin D, and retinoids [64].

The skin is the unique site of cholecalciferol synthesis. When ultraviolet B (UVB) radiation contained in sunlight (specifically at a wavelength of 300 ± 5 nm) hits the skin, the precursor molecule, 7-dehydrocholesterol (contained in the plasma membranes of keratinocytes), is converted to previtamin D₃. This is then converted to vitamin D₃ via a thermal, nonenzymatic process in the plasma membrane. With additional exposure to UVB, previtamin D₃ can be nonenzymatically converted to the inactive products, lumisterol and tachysterol, preventing vitamin D intoxication after prolonged sun

exposure. Vitamin D₃ is released and is bound by vitamin D–binding protein in the plasma, and it is transported first to the liver and then to the kidney for enzymatic hydroxylation [65].

CONCLUSION

The skin is a highly complex organ, including three multistructured layers and additional epidermal appendages. The skin serves not only to prevent the loss of fluids and electrolytes but also as an effective protective shield against trauma, solar radiation, toxic substances, and invading infections. The epidermis is able to continuously replace dying cells and maintain the tissue barrier that keeps harmful agents out and retains vital body fluids. In addition, the skin is a vast reserve of stem and progenitor cells to rejuvenate the body surface and repair wounds.

A good knowledge of the skin anatomy and physiology is essential to understand the pathogenesis of a variety of dermatological diseases, and to allow the search for optimal treatments to be soundly based. Nanoscience offers a new approach to preserve and restore the normal anatomy and functions of the skin using new molecular assemblies on the scale of individual cells, subcellular organelles, or even smaller components (large proteins). Nanotherapeutics facilitates the penetration of small molecules across skin, nails, and pilosebaceous units, which could be an advantage for providing targeted drug therapy to cutaneous or even to internal diseases. The available data suggest that healthy, intact skin represents a significant barrier to certain nanomaterials [66], but ways of overcoming this barrier are being discovered. In this scenario, the interaction of different nanoparticles with keratinocytes and keratin proteins, the mechanisms used by nanoparticles to cross the basal membrane, the effects they have on dermal structures, and their ability to gain entry to blood vessels by transdermal absorption are some of the questions to be solved for the successful future use of nanoscience in dermatology.

Acknowledgments

We wish to thank Prof. Luis Requena for providing us all the histological figures that appear in this chapter.

References

- [1] Javier B, Ackerman AB. Keratinocyte? Dermatopathol Pract Conceptual 2001;7(3):175–8.
- [2] Haake AR, Polakowska RR. Cell death by apoptosis in epidermal biology. J Invest Dermatol 1993;101(2):107–12.
- [3] Chu DH. Overview of biology, development, and structure of skin. In: Wolff K, Goldsmith LA, Katz SI, Gilchrist BA,

- Paller AS, Leffell DJ, editors. *Fitzpatrick's dermatology in general medicine*. 7th ed. New York: McGraw-Hill; 2008. p. 57–73.
- [4] McGowan KM, Coulombe PA. Keratin 17 expression in the hard epithelial context of the hair and nail, and its relevance for the pachyonychia congenita phenotype. *J Invest Dermatol* 2000; 114(6):1101–7.
 - [5] Smack DP, Korge BP, James WD. Keratin and keratinization. *J Am Acad Dermatol* 1994;30(1):85–102.
 - [6] Schweizer J, Bowden PE, Coulombe PA, et al. New consensus nomenclature for mammalian keratins. *J Cell Biol* 2006;174(2): 169–74.
 - [7] Waseem A, Dogan B, Tidman N, et al. Keratin 15 expression in stratified epithelia: downregulation in activated keratinocytes. *J Invest Dermatol* 1999;112(3):362–9.
 - [8] Irvine AD, McLean WHI. Human keratin diseases: the increasing spectrum of disease and subtly of the phenotype-genotype correlation. *Br J Dermatol* 1999;140(5):815–28.
 - [9] Blanpain C, Fuchs E. Plasticity of epithelial stem cells in tissue regeneration. *Science* 2014;344(6189):1242281.
 - [10] Pastushenko I, Prieto L, Gilaberte Y, Blanpain C. Skin stem cells: at the frontier between the laboratory and clinical practice. Part1. Epidermal Stem Cells. *Actas Dermosifiliográficas* 2015;106(9): 725–32.
 - [11] Horsley V, O'Carroll D, Tooze R, Ohinata Y, Saitou M, Obukhanych T, et al. Blimp 1 defines a progenitor population that governs cellular input to the sebaceous gland. *Cell* 2006; 126(3):597–609.
 - [12] Jensen KB, Collins CA, Nascimento E, Tan DW, Frye M, Itami S, et al. Lrig1 expression defines a distinct multipotent stem cell population in mammalian epidermis. *Cell Stem Cell* 2009;4(5):439.
 - [13] Lu CP, Polak L, Rocha AS, Pasolli HA, Chen SC, Sharma N, et al. Identification of stem cell population in sweat glands and ducts reveal roles in homeostasis and wound repair. *Cell* 2012;150(1): 136–50.
 - [14] Murphy GF. Histology of the skin. In: Elder D, Elenitsas R, Jaworsky C, Johnson Jr B, editors. *Lever's histopathology of the skin*. 8th ed. Philadelphia: Lippincott Williams & Wilkins; 1997. p. 5–45.
 - [15] Fortunel N, Martin M. Cellular organization of the human epidermal basal layer: clues sustaining a hierarchical model. *Int J Radiat Biol* 2012;88(10):677–81.
 - [16] Chadli L, Martin MT, Fortunel NO. Investigating human keratinocyte stem cell identity. *Eur J Dermatol* 2011;21(Suppl. 2):4–11.
 - [17] Haake AR, Hollbrook K. The structure and development of skin. In: Freedberg I, Eisen A, Wolff K, Austen K, Goldsmith L, Katz S, et al., editors. *Fitzpatrick's dermatology in general medicine*. 5th ed. New York: McGraw-Hill; 1999. p. 70–111.
 - [18] Thomason HA, Scothern A, McHarg S, Garrod DR. Desmosomes: adhesive strength and signalling in health and disease. *Biochem J* 2010;429(3):419–33.
 - [19] Delva E, Tucker DK, Kowalczyk AP. The desmosome. *Cold Spring Harbour Perspect Biol* 2009;1(2):a002543.
 - [20] Saito MT, Kholhorst D, Niessen CM, Kowalczyk AP. Classical and desmosomal cadherins at a glance. *J Cell Sci* 2012;125(Pt11): 2547–52.
 - [21] Kowalczyk AP, Green KJ. Structure, function and regulation of desmosomes. *Prog Mol Biol Trans Sci* 2013;116:95–118. <http://dx.doi.org/10.1016/B978-0-12-394311-8.00005-4>.
 - [22] Armengot-Carbo M, Hernández-Martín A, Torrelo A. The role of filaggrin in the skin barrier and disease development. *Actas Dermosifiliográficas* 2015;106(2):86–95.
 - [23] Brown SJ, McLean WHI. One remarkable molecule: filaggrin. *J Invest Dermatol* 2012;132(3 Pt 2):751–62.
 - [24] Hitomi K. Transglutaminases in skin epidermis. *Eur J Dermatol* 2005;15(5):313–9.
 - [25] Mort RL, Jackson IJ, Patton EE. The melanocyte lineage in development and disease. *Development* 2015;142(4):620–32.
 - [26] Flaxman BA, Sosis AC, Van Scott EG. Changes in melanosome distribution in Caucasoid skin following topical application of nitrogen mustard. *J Invest Dermatol* 1973;60(5):321–6.
 - [27] Olson RL, Nordquist J, Everett MA. The role of epidermal lysosomes in melanin physiology. *Br J Dermatol* 1970;83(1):189–99.
 - [28] Romani N, Clausen BE, Stoitzner P. Langerhans cells and more: langerin-expressing dendritic cell subsets in the skin. *Immunological Rev* 2010;234(1):120–41.
 - [29] Baumann KI, Halata Z, Moll I. The Merkel cell. Structure-development-function-cancerogenesis. New York: Springer-Verlag Berlin Heidelberg; 2003.
 - [30] Johnson KO. The roles and functions of cutaneous mechanoreceptors. *Curr Opin Neurobiol* 2001;11(4):455–61.
 - [31] Eady RAJ. The basement membrane. Interface between the epithelium and the dermis: structural features. *Arch Dermatol* 1988; 124(5):709–12.
 - [32] Woodley DT, Chen M. The basement membrane zone. In: Freinkel RK, Woodley DT, editors. *The biology of the skin*. New York, USA: Parthenon Publishing; 2001. p. 133–51.
 - [33] Fine J-D. Antigenic features and structural correlates of basement membranes. Relationship to epidermolysis bullosa. *Arch Dermatol* 1988;124(5):713–7.
 - [34] Fine J-D. International symposium on epidermolysis bullosa. *J Invest Dermatol* 1994;103(6):839–43.
 - [35] Sellheyer K. Which cells produce the basement membrane? *Dermatopathol Pract Conceptual* 2000;6:63–4.
 - [36] Stanley JR, Woodley DT, Katz SI, Martin GR. Structure and function of basement membrane. *J Invest Dermatol* 1982;79(Suppl. 1): 69s–72s.
 - [37] Smith LT, Holbrook KA. Embryogenesis of the dermis in human skin. *Pediatr Dermatol* 1986;3(4):271–80.
 - [38] Philips N, Auler S, Hugo R, Gonzalez S. Beneficial regulation of matrix metalloproteinases for skin health. *Enzyme Res* 2011;Mar 8;2011:427285. <http://dx.doi.org/10.4061/2011/427285>.
 - [39] Pérez-García LJ. Metaloproteinasas y piel. *Actas Dermosifiliográficas* 2004;95(7):413–23.
 - [40] Braverman IM. Ultrastructure and organization of the cutaneous microvasculature in normal and pathologic states. *J Invest Dermatol* 1989;93(2Suppl):2s–9s.
 - [41] Detmar M, Hiraoka S. Vascular biology. In: *Text book of dermatology*. 3rd ed. British: Elsevier; 2012. p. 1679–89.
 - [42] Huggenberger R, Detmar M. The cutaneous vascular system in chronic skin inflammation. *J Invest Dermatol Symp Proc* 2011; 15(1):24–32.
 - [43] Skobe M, Detmar M. Structure, function and molecular control of the skin lymphatic system. *J Invest Dermatol Symp Proc* 2000;5(1): 14–9.
 - [44] Weddell G. The anatomy of cutaneous sensibility. *Br Med Bull* 1945;3(7–8):167–72.
 - [45] Lippert U, Artuc M, Grutzkau A, Möller A, Kenderessy-Szabo A, Schadendorf D, et al. Human skin mast cells express H2 and H4, but not H3 receptors. *J Invest Dermatol* 2004;123(1):116–23.
 - [46] Kolarsick PAJ, Kolarsick MA, Goodwin C. Anatomy and physiology of the skin. *J Dermatol Nurses Assoc* 2011;3(4): 202–13.
 - [47] James WD, Berger TG, Elston DM. *Andrews' diseases of the skin: clinical dermatology*. 10th ed. Philadelphia: Elsevier Saunders; 2006.
 - [48] Simón P, Sánchez Yus E, Requena L. In: Requena L, editor. *Neoplasias anexas cutáneas*. 1st ed. Madrid: Spain; 2004. p. 1–10.
 - [49] Sato K, Leidal R, Sato F. Morphology and development of an apocrine gland in human axillae. *Am J Physiol* 1987;252(1Pt2): R166–80.

- [50] Sato K, Sato F. Sweat secretion by human axillary apoeccrine sweat gland in vitro. *Am J Physiol* 1987;252(1Pt2):R181–7.
- [51] Messenger AG. The control of hair growth: an overview. *J Invest Dermatol* 1993;101(1Suppl.):4S–9S.
- [52] Sperling LC. Hair anatomy for the clinician. *J Am Acad Dermatol* 1991;25(1Pt1):1–17.
- [53] Tiede S, Kloepper JE, Whiting DA, Paus R. The “follicular trochanter”: an epithelial compartment of the human hair follicle bulge region in need of further characterization. *Br J Dermatol* 2007;157(5):1013–6.
- [54] Buffoli B, Rinaldi F, Labanca M, Sorbellini E, Trink A, Guanzioli E, et al. The human hair: from anatomy to physiology. *Int J Dermatol* 2014;53(3):331–41.
- [55] Weedon D. *Weedon’s skin pathology: expert consult-online and print*. Elsevier Health Sciences; 2009.
- [56] Bernárdez C, Molina-Ruiz AM, Requena L. Histologic features of alopecias-part I: nonscarring alopecias. *Actas Dermosifiliográficas* April 2015;106(3):158–67.
- [57] Bologna JL, Jorizzo JL, Schaffer JV, Cerroni L, Heymann WR, Callen JP. *Dermatology*. 3rd ed. Elsevier health science; 2012.
- [58] Baran R. The nail in the elderly. *Clin Dermatol* 2011;29(1):54–60.
- [59] Guyton AC, Hall JE. *Textbook of medical physiology*. 10th ed. Philadelphia: W.B.Saunders; 2000. p. 822–33.
- [60] Wertz PW. Pertinent to skin penetration: skin biochemistry. *Skin Pharmacol Physiol* 2013;26(4–6):217–26.
- [61] Nakamizo S, Egawa G, Honda T, Nakajima S, Belkaid Y, Kabashima K. Commensal bacteria and cutaneous immunity. *Semin Immunopathol* 2015;37(1):73–80.
- [62] Pasparakis M, Haase I, Nestle FO. Mechanisms regulating skin immunity and inflammation. *Nat Rev Immunol* 2014;14(5):289–301.
- [63] Nejati R, Kovacic D, Slominski A. Neuro-immune-endocrine functions of the skin: an overview. *Expert Rev Dermatol* 2013;8(6):581–3.
- [64] Zouboulis CC. The skin as an endocrine organ. *Dermato-Endocrinology* 2009;1(5):250–2.
- [65] Kannan S, Lim HW. Photoprotection and vitamin D: a review. *Photodermatol Photoimmunology Photomed* 2014;30(2–3):137–45.
- [66] Basavaraj KH. Nanotechnology in medicine and relevance to dermatology: present concepts. *Indian J Dermatol* 2012;57(3):169–74.

Fundamentals of Nanoscience (and Nanotechnology)

G.L. Hornyak¹, A.K. Rao²

¹Asian Institute of Technology, Klong Luang, Pathum Thani, Thailand; ²Metropolitan State University of Denver, Denver, CO, United States

OUTLINE

Introduction	15	<i>Chemical Reactivity</i>	21
<i>Nanoscience and Nanotechnology</i>	15	<i>Penetration, Permeability, Solution, and Transport</i>	
<i>Nanomaterials and the Sizes of Things</i>	16	<i>Properties</i>	21
Different Kinds of Nanomaterials	17	<i>Advanced Surfaces</i>	23
<i>Zero-Dimensional and Larger Spherical</i>		<i>Optical and Magnetic Properties</i>	23
<i>Nanomaterials</i>	17	Synthesis of Nanomaterials	24
<i>One-Dimensional Nanomaterials</i>	17	<i>Self-Assembly and Self-Organization</i>	25
<i>Two-Dimensional Nanomaterials</i>	18	<i>Bottom-Up Synthesis of Nanocarriers</i>	25
Physical and Chemical Properties	18	Conclusion	27
<i>Collective and Specific Surface Area</i>	18	References	28
<i>Surface-to-Volume Ratio and Particle Shape</i>	19		
<i>Surface Energy and Particle Stability</i>	19		
<i>Intermolecular Interactions</i>	20		

INTRODUCTION

Nanoscience and Nanotechnology

One aspect of nanoscience refers to the study of Nature's nanomaterials and phenomena, or equivalently put, Nature's nanotechnology. Natural examples of enzymes, cell membranes, spider silk, nanoclays, and interference colors come to mind. Life processes, too, such as metabolism, homeostasis, and protein synthesis are all mediated at the nanoscale. On the other hand, from the perspective of human beings, nanotechnology is defined as the application of nanoscience for the purposes of industry and commerce. Nanotechnology *is* the application of nanoscience. The use of quantum dots (QDs)

for image enhancement, carbon nanotubes for making light-emitting diodes (LEDs), and Teflon nanoparticles to make textiles water repellant are all classified as nanotechnology (ie, practical applications of nanoscience). Nanoscience and nanotechnology are related through nanomaterials; therefore, no attempt is made in this text to strike a clear boundary between them.

Nanotechnology, according to accepted definitions, is the study and application of phenomena, substances and devices with at least one dimension between 1 and 100 nm. The definitions also take account of the remarkable properties associated with nanomaterials, since it is only when material dimensions drop below 100 nm that special physical and chemical properties start to emerge

(eg, properties that differ significantly from those in the bulk form), with the most remarkable change in properties occurring when particle sizes dip below 20 nm. The classic example is provided by sub-10 nm QDs that exhibit dramatic size-dependent fluorescence properties. Additionally, gold clusters 20 nm in diameter display a striking ruby red color in solution. Under these circumstances, gold is no longer the lustrous malleable inert metal that we have grown accustomed to throughout the ages. Furthermore, when made even smaller, say to a few nanometers, gold is no longer metallic and has transformed into an active catalyst—a property that is quite the opposite of its bulk counterpart. Nanotechnology has also made an impact on dermatology [1–5]. We begin the discussion with the size scale and the different kinds of nanomaterials.

Nanomaterials and the Sizes of Things

Nanomaterials are materials that have one or more of their dimensions, internal or external, that are nanoscale in size (1 nm, one-billionth of a meter, or 10^{-9} m). The human hair, a commonly applied reference, is in the range of 50–100 μm in diameter (1 μm , one-millionth of a meter, or 10^{-6} m). A carbon nanotube with 1 nm diameter, therefore, is 50,000–100,000 times thinner

than a human hair. A scale shown in Fig. 2.1 depicts the relative relationships of size within the context of dermatology.

Our bodies consist of a vast array of nanomaterials. Enzymes, membranes of cells and organelles, nucleic acids (DNA and RNA), and collagen nanofibrils in tendons are just a few examples of nanomaterials that naturally exist within us. Nature's in vivo nanotechnology is composed of macromolecular assemblages of proteins, carbohydrates, lipids, and nucleotides. Proceeding from the bottom up, amino acids (technically not nanomaterials) range in size from 0.42 nm (glycine) to 0.67 nm (tryptophan). Fatty acids with 10–30 carbons range in size from 1.4 to 4.2 nm in length. The average globular protein is circa 4 nm in diameter. Enzymes range in size from a few to several nanometers (eg, adenosine triphosphate (ATP) synthase: 12×20 nm). Glycogen containing 54,000 glucose residues is 25 nm in diameter. The average membrane thickness is about 5 nm. Lysosomes range from 200 to 500 nm in diameter or even larger. Microfibrils in tendons can be long but are only 3.5 nm in diameter. The helical diameter of DNA is 2.2 nm, which persists over a length of 50 nm. Therefore, any nanotechnology that we create, whether it be a targeted drug nanocarrier or an imaging QD or a contrast agent, has to interface with the complex

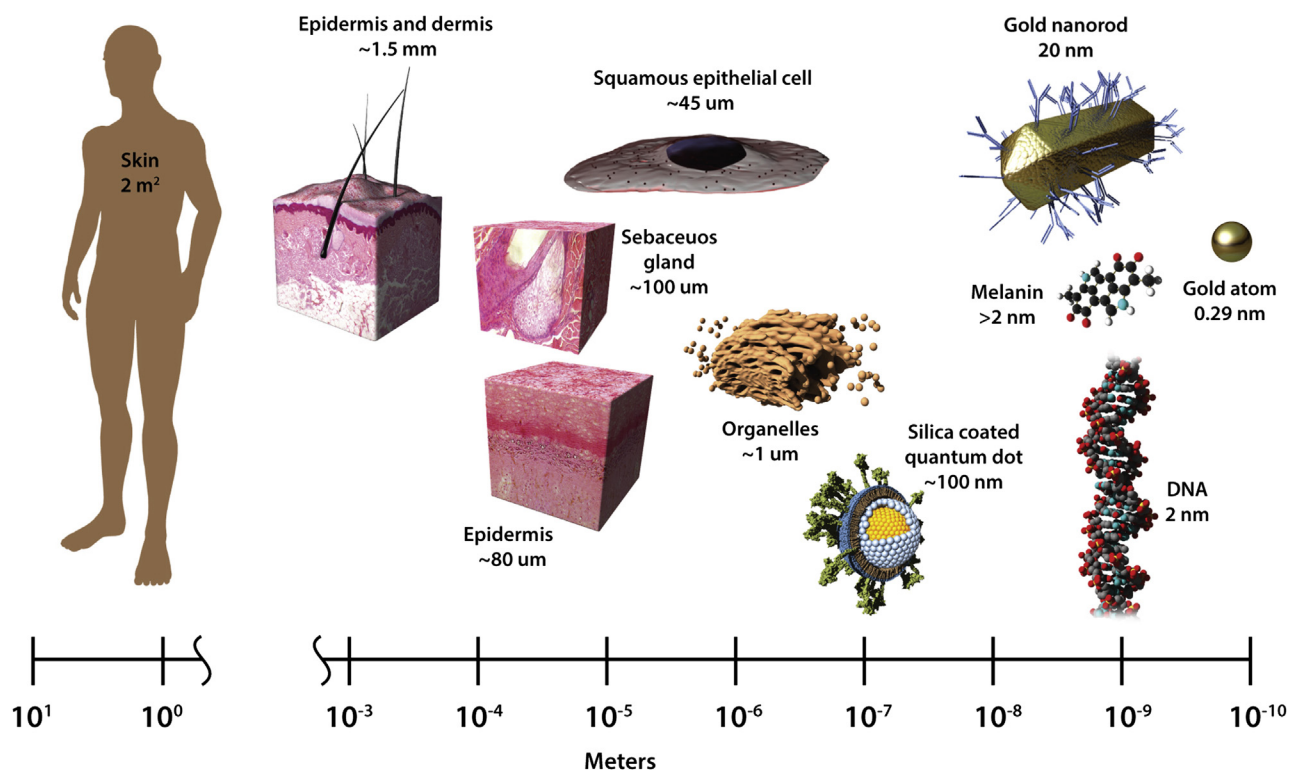


FIGURE 2.1 A log scale is used to provide perspective for the size of things from a dermatological point of view. Nanoscale structures range from less than 1 μm to 1 nm in size. However, according to strict definitions, the dimensions of nanoscale materials are confined between 1 and 100 nm. Nanomaterials exist at the interface between bulk materials and atoms and molecules. An interface between Nature and our technology is also defined at the nanoscale.

crowded environment of the submicron biological domain—one that is dominated by nanoscale materials (and intermolecular interactions).

DIFFERENT KINDS OF NANOMATERIALS

Nanomaterials are made from any major class of engineering material—metals, semiconductors, ceramics, organics, polymers, and even materials derived from living organisms that are considered to be “soft matter”. Nanocomposites containing nanomaterials incorporated into larger scale bulk materials can demonstrate superior mechanical, electrical, thermal, and optical properties. Within our synthetic domain, nanomaterials can be classified as zero-dimensional (0D), one-dimensional (1D), or two-dimensional (2D). A third category of nanomaterial was added recently, the three-dimensional (3D) nanomaterial [6]. With regard to dermatology, there is a preponderance of research reporting mostly 0D and larger spherical formulations of nanomaterials. Therefore, we focus our attention on spherical particles (and, to a lesser extent, nanowires) for this reason.

Zero-Dimensional and Larger Spherical Nanomaterials

Examples of 0D materials are QDs—spherical materials in which there is spatial (electron) confinement in the x , y , and z directions. In order to qualify as a QD, all three dimensions must be within the small end of the nanoscale. Physical properties of 0D materials are intermediate between those of the macroscopic form (continuous properties) and the molecular or even atomic forms (discrete properties). In other words, the physiochemical properties of 0D materials lie at the bulk–quantum scale boundary. Larger particles such as colloids are not considered to be QDs per se but still exhibit remarkable properties due to extrinsic size factors, rather than intrinsic size factors that are due to quantum effects [7]. QDs are usually made of metals, metal oxides, or semiconductor materials, although the fullerene C_{60} molecule is considered by some to be a QD.

It is the 0D formulation of these classes of materials that have made dramatic contributions to the fields of diagnostic imaging and therapeutics. The unrivaled example of a 0D material is the semiconductor QD. For example, taking advantage of their intense fluorescent properties, semiconductor QDs made of CdSe–ZnS core–shell coated with methoxy polyethylene glycol (mPEG) were used to measure QD biodistribution (migration and localization) in skin following subcutaneous injection [8]. From evidence acquired with confocal fluorescence microscopy, tracking of QD

migration was facilitated. Due to fluorescent tracking of such QDs, it was found that the basement membrane and connective tissue networks restricted the distribution of QDs with limited penetration into the epidermis, hair follicles, sebaceous glands, and sweat glands. In another study involving larger nanoparticles used in sunscreens, ZnO and TiO₂ nanoparticles were shown not penetrate beyond the stratum corneum layer of the skin following application [9a]. In this case, the particles were tracked with nuclear microscopy—a technique capable of in vivo assessment of elemental distribution and percutaneous absorption. Scanning transmission ion microscopy and particle-induced X-ray emission are examples of nuclear microscopy [9b].

Hyperthermic application for treatment of skin cancers is usually accomplished with spherical nanoparticles or shells, but nanorods and other shaped particles have also been utilized. In hyperthermic treatment, cancer cells are selectively annihilated by application of heat produced by nanoparticles exposed to an external energy field. Following exposure to near-infrared (near-IR) radiation, gold nanoshells, bare gold nanoparticles, and coated gold nanoparticles can all be effective agents for ablation therapy of skin tumors [10]. Superparamagnetic hematite (Fe_2O_3)-targeted nanospheres, due to their highly specified nanoscale dimensions, undergo unique modes of heating when exposed to an alternating external magnetic field [11].

One-Dimensional Nanomaterials

1D materials are called *quantum wires*. Materials designated as nanofibers, nanobelts, nanorods, and nanoribbons are considered to be 1D nanomaterials [12]. Electron confinement for 1D materials is along the x and y transverse dimensions. Along the longitudinal axis of the wire, there is no electron confinement and the material can display bulk behavior. Carbon nanotubes are made purely of carbon atoms in a hexagonal configuration like graphite, rolled into a tube similar to chicken wire, and serve as a reasonably good example of a 1D nanomaterial. Physical properties such as heat transfer and electrical conductivity along the x and y transverse coordinates demonstrate confined (discrete) behavior. In one study, single-walled carbon nanotubes conjugated with cyclic RGD peptides (arginine, glycine, and asparagine) have been used as contrast agents for photoacoustic imaging of tumors [13]. Carbon nanotubes have also shown potential as oxidizing agents and ingredients in artificial skin.

In another case of nanofibers in dermatology, naturally occurring chitin molecules have been used as ingredients in antiaging creams and are able to provide assistance in repair of damaged tissues. Chitin is a

polymeric form of glucosamine and N-acetyl glucosamine that ranges in size from 5–7 nm in diameter and circa 250 nm in length [14]. Chitin fibers are nonallergenic, have high specific surface area (400 m²/g), are recognizable by enzymes, and are stable in water. Its chemical structure is similar to hyaluronic acid. Chitin nanofibrils, depending on local chemical conditions, can form complexes with antioxidants (eg, lutein and melatonin) and immune modulators (ectoin, etc.) [15].

Finally, nanoscale wires of octadecylsiloxane (ODS) formed via template synthesis within the pore channels of anodic aluminum oxide (ca. 20–50 nm diameter with 50 μ m length) can serve as carriers for the drug paclitaxel [16a]. Paclitaxel is an effective anticancer drug but has low water solubility that hinders its effectiveness in vivo. Within the 35 nm diameter nanowires, the paclitaxel drug is distributed within the hydrophobic ODS core. The hydrophilic outer layer facilitates transport in aqueous media and in vitro is able to inhibit cancer cell proliferation within the first 24 h of application.

Two-Dimensional Nanomaterials

2D nanomaterials are considered to be quantum wells, or in generic terms, as thin films. In 2D materials, there is electron confinement only in one direction. Ultrafine chitin nanofibers (CNFs) can be made into membrane structures when incorporated into biopolymers [14]. Applications of CNF-biopolymers include serving as templates in tissue development and skin regeneration. Membranes, not necessarily of nanoscale thickness, have been applied successfully as transdermal drug delivery vehicles, an important mode of drug transport. CNF-reinforced chitosan films for use as wound medicaments showed enhanced healing capacity due to the synergistic reaction between chitosan salts and the CNF [16b].

PHYSICAL AND CHEMICAL PROPERTIES

It should be noted that equations show the dependence of numerous physical properties on, for example, the reciprocal radius— $1/r$ or higher orders thereof. Whether these properties are geometric, thermodynamic, physical, or biological, this inverse relationship seems to be ubiquitous. The principal consequence of this relationship is that any property as a function of size has the characteristic of changing rapidly once small enough dimensions are acquired. The physical properties of bulk materials remain constant over a wide range of size—all the way down to micron and even submicron dimensions. When materials achieve smaller

dimensions, physical properties can change rapidly and perhaps even radically. Quantum size effects take place when materials reach a few nanometers in size.

From statistical mechanics, the thermodynamic limit is defined by numbers of particles N divided by volume V in a relationship where, as $N \rightarrow \infty$, $V \rightarrow \infty$, $\frac{N}{V} = C$, where C is a constant. In other words, the ratio N/V represents an intensive density term that is invariant with size, because the volume increases in proportion to particle numbers. This is fundamental and validates the tenets of macroscopic thermodynamics. However, at the nanoscale, N is countable and V is variable due to the influence of environmental fluctuations and energetic adaptations. In other words, N/V might represent a nonintensive term that is variable with size. Nonintensity, nonextensivity, and the need (perhaps) for a 4th Law of Thermodynamics are the contributions that nanoscience has made to our fundamental understanding of the nature of things. We begin our discussion from the geometric perspective, starting with surface area.

Collective and Specific Surface Area

Collective surface area is an extensive property. Collective surface area is the sum of the surface areas of all particles within a system, usually composed of a single material. The generalized form is given as $A_C = \sum_{i=1}^n a_i$, where a_i is the area of a single particle. If a sphere of some material with 1 m³ volume is broken into 10^{27} individual smaller spheres each with 1 nm³ volume, then the collective surface area is equal to 4836 km²—a one-billion-fold increase of area over that of the singular parent sphere. At the nanoscale, pores and cavities in zeolites, charcoals, and anodic oxides; ZnO nanorods and TiO₂ nanoparticles in solar cells; metal catalysts in catalytic converters; and polymer filler materials in nanocomposites all exert their respective functions by contributing an enormous collective surface area or interfacial surface area (Fig. 2.2).

Another means of gauging surface area is specific surface area, specific for a selected material in terms of area per mass. The formula for specific surface area is as follows: $S_A = \frac{S_m}{\rho_m V_m} = \frac{m^2}{g}$, where m is some specific material; and V_m , ρ_m , and S_m are the volume, density, and surface area of that material, respectively. Why are collective and specific surface areas important to dermatology? The reasoning is straightforward. First, for equivalent materials with the same total mass, many smaller particles with higher specific surface area have a higher probability of interaction with targets than do fewer but larger particles. Second, with equivalent collective surface area, less material is required if a greater number of smaller particles are applied. Without considering the other benefits of using nanoparticles (eg, tuned

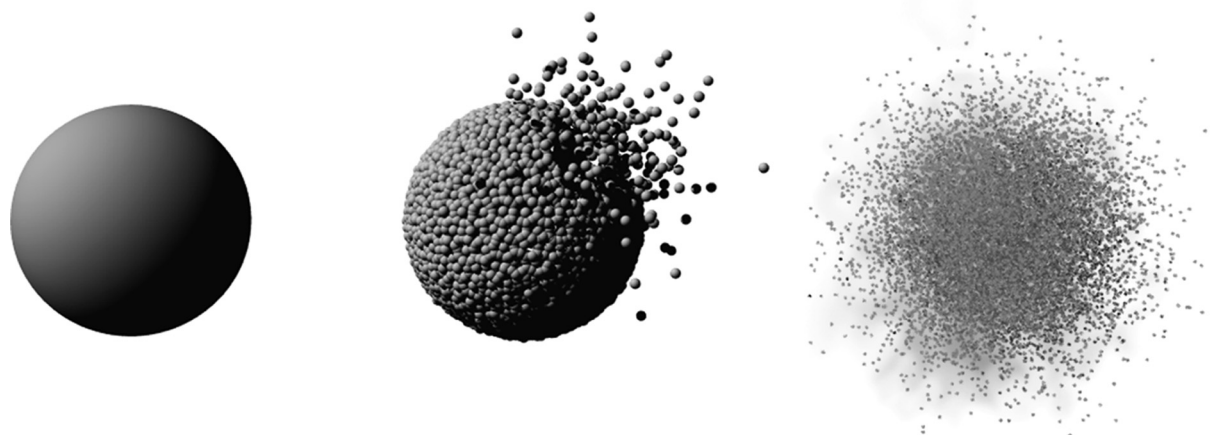


FIGURE 2.2 Collective surface becomes enormous with smaller particles. The sphere depicted on the left has a volume of 1 m^3 with surface area equal to 4.836 m^2 . The total volume and collective surface area of spheres depicted on the right are 1 m^3 and 4836 km^2 , respectively—a billion-fold increase.

solubility), this is advantageous in regard to drug delivery efficiency, reduced dosage, potential side effects, and long-term manufacturing costs.

Surface-to-Volume Ratio and Particle Shape

Surface-to-volume (S/V) ratio is defined in its most simplistic form as $\frac{S}{V} = \frac{\text{m}^2}{\text{m}^3} = \frac{1}{\text{m}}$. Therefore, S/V ratio increases exponentially as particle size decreases for any kind of volume. Spherical things have the lowest S/V ratio of any geometric shape with equivalent volume. The S/V ratios for some common geometric shapes at unit volume are as follows: tetrahedron 7.21, cube 6, octahedron 5.72, icosahedron 5.148, and sphere 4.836. It is easy to see the trend. The surface-to-volume ratio of a cube normalized to that of a sphere of the same volume is 1.24 times that of the sphere. Rod- and disc-shaped nanoparticles have increasingly higher surface-to-volume ratios. As mentioned in this chapter, most of the nanomaterials used in dermatology appear to be spherical particles. What, then, does this simple S/V ratio imply? If we consider the case of a high S/V ratio leading to particle instability (more about that in the “Surface Energy and Particle Stability” section), then reduction of the S/V ratio should increase the stability of the particle—because then particles become larger or more spherical. A high S/V ratio correlates directly with a high surface-atom-to-volume-atom ratio. This is an inherent component of the thermodynamic driving force for the persistence of spherical particles, especially nanoparticles, as the spherical forms yield the most stable configuration. On the other hand, for living cells, the S/V ratio is actually maximized in order to maintain homeostasis, energy exchange, and nutrient and waste balance.

Surface Energy and Particle Stability

Surface energy is the work per unit area required to create a new surface (J/m^2). For liquids, this phenomenon is known as the surface tension. If a material is cleaved along some crystal plane, energy is required to break bonds to create two new surfaces—described in the simple relation $w = \gamma A$, where w is energy in terms of work, γ is the surface energy, and A is area. The energy required to form a new surface is called *excess surface energy*—energy in excess of the volume or cohesion energy of a material that is required to break bonds. Consequently, atoms on the newly formed surface are missing nearest neighbors and therefore are in an undercoordinated state. For example, gold is a face-centered (*fcc*) cubic material. If cleaved along the $[111]$ crystal plane, three bonds per atom are broken. The excess surface energy per atom is given by $E_{\text{atom}[111]} = \frac{3\Delta H_{\text{sub}}}{ZN_A} = \frac{\Delta H_{\text{sub}}}{4N_A}$ where Z is the coordination number ($Z = 12$ for gold *fcc*), ΔH_{sub} is the enthalpy of sublimation and equals 368 kJ/mol ; and N_A is the Avogadro’s number 6.02×10^{23} [17]. For lattice planes that require more bonds to break during cleavage (eg, 4 for the $[100]$ *fcc* plane), then the excess surface energy is higher, $E_{\text{atom}[100]} = \frac{\Delta H_{\text{sub}}}{3N_A}$. The excess in surface energy condition is exacerbated as the materials approach and finally attain nanoscale dimensions with concomitant higher S/V ratio. Furthermore, for metallic and semiconductor clusters, the edge and corner atoms start to exert more influence on reactivity by imparting even greater unsaturation and, hence, greater instability.

Another form of instability for nanoscale materials is bond strain. C_{60} is a fullerene made of 60 carbon atoms in evenly distributed hexagonal and pentagonal structures. Its instability is due to bond angle strain, resulting in circa 44 kJ/mol per atom greater instability over

that of graphite, the most stable form of carbon. Along with its inherent dependency on shape, the chemical reactivity of C_{60} is directed by the 60 π -electrons that fill its molecular orbital [18]. These factors render C_{60} thermodynamically unstable (metastable or kinetically stable) and therefore reactive. As a result, numerous fullerenes have recently been shown to possess antioxidant properties by quenching the activity of radical oxygen species in the skin [19]. Fullerenes have also demonstrated antiinflammatory [20] and antimicrobial activity [21].

In order to preserve the unique properties of nanomaterials, the particles must not be allowed to agglomerate, aggregate, or coalesce. Surface energy mitigation is required for stabilization. Processes include surface sorption and chemisorption along with strong chemical binding of ligand species to the surface. Colloidal solutions can be stabilized via electrostatic repulsion. Other mechanisms are also available to stabilize the surface—crystal structure relaxation, restructuring, phase segregation, and surface enrichment. For example, achieving a spherical shape yields a favored state of a minimized S/V ratio and, hence, reduced surface energy. Last, excess surface energy is reduced if the particle size is increased by coalescence, aggregation, particle agglomeration, or Ostwald ripening. Incidentally, nanoscale biological materials show neither undersaturation nor bond strain and, within narrowly defined physiological environments, are quite stable.

In summary, a high S/V ratio results in a high surface-atom-to-volume-atom ratio, and this leads to higher reactivity—driven by excess surface energy for enhancement of physiochemical reactions. This state of affairs is exploited by the relative ease with which nanoparticle surfaces can be modified chemically. To the greatest extent, nanodermatology applications depend on the ability to functionalize nanoparticle surfaces.

Intermolecular Interactions

Along the electrostatic bonding continuum, there are two generalized kinds of electrostatic interactions that form chemical bonds. The first is designated as the *intramolecular* bond, and the second is the *intermolecular* bond. Intramolecular bonding is defined as strong bonding between atoms within a molecule formed mostly under kinetically controlled conditions. Ionic, metallic, and covalent bonds are examples of intramolecular kinds of bonding. Intermolecular bonds, on the other hand, are noncovalent bonds between molecules that are weaker and in many cases are formed under thermodynamically controlled conditions. Examples of intermolecular bonding include the ion–dipole interactions, hydrogen bonding, dative bonding, π -bonding, the hydrophobic effect, and the various

types of van der Waals forces (Keesom, Debye, and London). Intermolecular bonds, however, possess important distinctions—reactions associated with intermolecular bonding are reversible and can be highly specific, a factor of primary importance in targeted drug delivery by nanocarriers.

The dependence of electrostatic attraction energy is inversely proportional to the distance between two particles, once again proportional to $1/r$ or higher orders thereof. Table 2.1 shows this dependence of attraction energy on distance. Van der Waals forces are the weakest variety and are relevant only when molecules (or particles) get very close together. DLVO theory is applicable to nanoparticles and to larger colloidal materials, and describes the balance between van der Waals attractions and electrostatic repulsions in a liquid medium. In vivo, one would certainly expect a nanoparticle to interact with its environment by a multitude of intermolecular attractions—factors that certainly impact the in vivo transport of nanoparticles.

Intermolecular bonding is fundamental to supramolecular self-assembly and also to disassembly of these complexes in systems that allow for reversibility. Antibiofouling surfaces, avoidance of uptake in vivo by the reticuloendothelial system (RES) and other immune responses, biological absorption, minimal aggregation of nanoparticles, increased circulation lifetime, and decreased premature systemic clearance are all properties that are desirable in nanoparticles in medicine, and all these features depend on the many different

TABLE 2.1 Intermolecular Bonding: Dependence on Distance

Type of bond energy	Inverse dependence on r	Comments
Ion–ion	r	Sodium chloride cationic–anionic interaction
Ion–dipole	r^2	Valinomycin and potassium cation interaction can be considered to be a form of dative bonding
Dipole–dipole	r^3	Hydrogen bonding in water in which two electronegative atoms share a hydrogen atom
Keesom VDW	r^6	Bonding between molecules with permanent dipoles
Debye VDW	r^6	Dipole–induced dipole
London VDW	r^6	Induced dipole–induced dipole interactions or polarizability
DLVO theory	VDW attraction + electrostatic repulsion	Colloid solution stability

VDW, van der Waals interaction.

kinds of intermolecular bonding. The example of biofouling is provided to illustrate the importance of intermolecular bonding.

Proteins in particular have the ability to adhere to synthetic surfaces, whether hydrophilic (via hydrogen bonding) or hydrophobic (via conformational adjustment to expose inner nonpolar residues). If a nanoparticle or synthetic layer is coated with unwanted proteins (called the *protein corona*), then its efficacy is compromised. For example, nanoencapsulated luteolin (used in Chinese traditional medicine to treat cancer) was used successfully to treat squamous cell carcinoma of the head and neck area of laboratory mice [22]. The drug was encapsulated in a double layer consisting of a hydrophobic poly(lactic acid) (PLA) inner shell and a poly(ethylene glycol) monomethyl (or methoxy) ether (or mPEG) outer shell. PLA is insoluble in water and served to stabilize the nonpolar guest molecule luteolin by appropriate intermolecular bonding. The mPEG coating rendered the nanoparticle water-soluble. Apparently, such pegylated surfaces reduce biofouling by production of a hydration layer. The hydration layer provides a tightly bound layer of water between the external media and the surface. According to investigators, in the absence of a pegylated surface, protein adsorption is facilitated by entropy-driven elimination of water both from the surface and from the protein to initiate adhesion [23]. A more aggressive approach to restrict the binding of nonspecific proteins involved application of superhydrophilic zwitterionic (mixed-charge) molecules like carboxybetaines that provided an even stronger hydration layer [24–26]. Poly(carboxybetaine acrylamide) (polyCBAA) coatings on nanoparticles were shown to function well in complex media such as blood plasma [27].

Chemical Reactivity

The chemical reactivity of nanomaterials is size dependent, the best example provided by the reactivity of catalysts. Chemical reactivity in the case of nanomaterials, then, is expected to increase with diminishing size, due to the previously mentioned increase in the population of surface atoms compared to volume atoms. If the composition of a material is already characterized by a high chemical potential (whether electrical, chemical, or otherwise), the reactivity is expected to further increase when nanoscale dimensions are achieved.

The chemical reactivity of nanoscale titanium dioxide (TiO_2) is dependent on its crystalline form in addition to its size (eg, anatase, rutile, or brookite are different mineral forms of TiO_2). Titanium dioxide nanoparticles in an aqueous medium are capable of generating superoxide and hydroxyl radicals when exposed to ultraviolet (UV) and even to visible light [28]. It was shown that

the anatase form of TiO_2 was able to generate reactive oxygen species (ROS), while the rutile form did not [29]. Anatase with a positive charge on the particles adhered strongly to the skin and caused structural rearrangement of lipid bilayers in the stratum corneum when illuminated. Negatively charged rutile particles produced no such effects. It is thought that the structural rearrangement was due to oxidative reactions related to ROS generation [30]. As a result, scientists in Europe are encouraging that the safer rutile form of TiO_2 be used in cosmetics and sunscreens.

Bulk silver metal is relatively inert and does not react with hydrochloric acid. However, an unusually high reactivity of silver nanoparticles with hydrochloric acid has been demonstrated [31]. At smaller sizes, the standard electrode potentials shift to the negative compared to the bulk metal due to the altered electronic structure. This altered electronic state results in an increase in reactivity [31]. Coarse-grained silver particles of 74 μm diameter did not show any reactivity toward HCl. Therefore, the atomic structure and the size of metallic nanoparticles determined the extent of reactivity [32]. Gold clusters supported on a titanium dioxide film showed high catalytic activity for oxidation of carbon monoxide [33]. Deliquescence, efflorescence, and the saturation molality of sodium chloride and ammonium sulfate nanoscale crystals were shown to change significantly with diminishing particle size—especially below 20 nm diameter. Nanoparticles are indeed a different phase of materials.

Penetration, Permeability, Solution, and Transport Properties

Addition of nanoparticles to liquids (mostly water) alters the viscosity of the fluid in ways that cannot be explained by classical theories [34]. In particular, Einstein's formula for effective viscosity of a dilute suspension states that viscosity increases as particle concentration is increased by $\eta = \eta_0[1 + 2.5\phi]$, where η_0 is the viscosity of the base fluid and ϕ is the volume fraction of dispersed particles. This equation does not take into account the type of nanomaterial, the size of the material, or the fact that nanoparticles might agglomerate in solution, and at higher concentrations could transform into a non-Newtonian fluid with variable viscosity. Therefore, such equations based on classical thermodynamic approaches have a way of describing physical behavior without needing to address molecular (or even nanoscale) interactions. Once again, nanoparticles offer a challenge to traditional thermodynamics as their solubility can be described as a nonextensive property rather than as an extensive property [35]. Nanoparticle properties are susceptible to

environmental fluctuations and do not depend necessarily on initial conditions! From another perspective, the Stokes–Einstein equation relates the diffusion of a hard sphere in a viscous liquid: $D = \frac{k_B T}{6\pi\eta r}$ where k_B is the Boltzmann constant, T is temperature in Kelvin, η is the fluid viscosity, and r is the particle radius. Therefore, by this equation, diffusion of a material through a liquid is increasingly facilitative for smaller and smaller particles, and it depends only on the viscosity of the fluid and the size of the particle. At first glance, it seems as if this equation aptly describes the diffusion of particles down to the nanoscale and beyond. Yet again, from recent work, it was found that there is a lower particle size threshold limit, estimated to be a few nanometers, below which the Stokes–Einstein equation is no longer valid [36]. Nanoparticles used in dermatology applications are definitely not hard spheres. Rather, they have appendages and coatings that have the potential to interact in unpredictable ways once administered in vivo. Molecular dynamic (MD) simulations showed that van der Waals forces exerted an increasingly important role in particle diffusion behavior as the particle diameter approached molecular dimensions. For a 6 nm diameter core preparation of Au nanoparticles decorated with dodecanethiol, it was shown that there was strong interaction (and significant intermixing) between the ligands and the solvent via van der Waals forces [37].

The biodistribution of nanoparticles in vivo is impacted by the size of the nanoparticle and its surface modification. For example, polyethylene glycol (PEG) and derivatives can be used as coatings that enhance the hydrodynamic diameter to increase circulation lifetime of nanoparticles in the bloodstream. In addition, a larger particle serves to hinder recognition by the macrophage system (RES), thereby enhancing the opportunity to be recognized instead by the target cancer cells for proper binding. In the dermal layers, transport mechanisms for drugs include intercellular and transcellular mechanisms and penetration via follicular pathways [38]. Surface-modified nanoparticles that can be loaded with therapeutic chemicals can be designed to overcome the obstacles to penetration provided by the skin's inherent defenses. Nanoscale particles (nanocarriers), ranging in size from a few nanometers to submicron dimensions, can be modified to adjust to the chemical environment of the skin to increase permeability and lifetime [38].

Large silica nanoparticles (ca. 100 nm diameter) were found to penetrate into the skin, but were not able to actually permeate through the skin. Therefore, they were contained for the most part within the epidermal and upper dermal layers [39]. Nanoparticle transport, in addition to plasma and extracellular solubility conditions, is also impacted by endocytotic and exocytotic

mechanisms of cells. Endocytosis is the physical mechanism of nanoparticle uptake into cells whereby therapeutic payloads can be delivered. Exocytosis involves the removal of nanoparticles from cells for eventual expulsion from the human body. According to a recent summary report, there exist four kinds of endocytotic mechanisms: phagocytosis, pinocytosis, micropinocytosis, and the clathrin–caveolar-mediated form of endocytosis [40]. The authors concluded that smaller nanoparticles were more effective in entering and leaving cells, while spherical particles had an advantage over rod-shaped particles. Furthermore, nanoparticles with positive charges demonstrated higher rates of endocytosis than those with negative or neutral electrical charges.

Ingested silver nanoparticles undergo a variety of transport processes and chemical reactions. Colloidal silver nanoparticles within the dermal environment in combination with UV stimulation react to give a darkly colored silver chalcogenide that imparts a relatively irreversible bluish hue to the skin—a condition called argyria [41]. Upon entering the body, zero-valent silver is not transported intact in its original engineered particle form, but rather in ionic and modified particulate forms that undergo numerous reactions and transformations, including dissolution by stomach acids, binding to organic thiols and proteins, and reduction, complexation, and photochemical reactions to form silver–sulfide–selenide complexes [42a]. Recent research has shown that fine granules were concentrated in the region of the eccrine glands and pilosebaceous structures of patients that drank colloidal silver solutions for treatment of diabetes [42b]. Due to the ever-increasing use of antibacterial silver nanoparticles in commercial products, more research needs to be conducted in order to understand the in vivo transport and fate of silver nanoparticles.

The toxicity of zinc oxide nanoparticles is classified into two categories: first, the toxicity of the nanoparticle itself, and, second, the toxicity of the Zn^{2+} cation released from the nanoparticle under conditions when it dissolves. It is well known that the Zn^{2+} cation can be highly toxic to plants and bacteria. However, Zn^{2+} is taken regularly as a health supplement in the form of zinc gluconate or zinc acetate without any serious side effects. Perhaps more significant is the formation of ROS by zinc oxide nanoparticles—well-known photochemical sensitizers. ZnO nanoparticles (especially those produced from industrial sources) are today classified as toxic [43]. However, a study of ZnO nanoparticles applied onto rat skin showed that there was no increased mortality of experimental rats compared to controls. The study concluded that the dermal layers limited the transport of ZnO into the systemic circulation. Furthermore, ZnO was shown not to be a dermal

sensitizer or a skin irritant [44]. This study concluded that there was no observable impact of ZnO nanoparticles applied dermally up to the maximal level studied—1000 mg ZnO per kilogram body mass [45]. On the other hand, skin sensitization from exposure to nickel nanoparticle powder produced a positive result for allergic contact dermatitis using a T.R.U.E. patch test (Thin Layer Rapid Use Epicutaneous test) [46,47]. There is a need to know how these nickel nanoparticles are distributed within the layers of skin and what exactly are the mechanisms of sensitization.

Magnetic particle focusing in vivo is another approach to carry out drug targeting. What happens first is injection of magnetic nanoparticle cargo carriers into the bloodstream. External magnets are then applied to control their transport for eventual accumulation at the target site [48]. By using fundamental, well-established physical relationships derived from in vivo environments, a model was generated that predicted distribution and accumulation of these magnetic particles in dermatological tissues. This was accomplished by applying dimensionless classical parameters related to the magnetic force–drag force ratio and various convection–diffusion ratios in blood, membranes, and tissues. The model predicts the concentration of NPs in membranes (C_M) and tissue (C_T) as a function of time (eg, $\frac{\partial C_M}{\partial t}$ and $\frac{\partial C_T}{\partial t}$) [48]. Computer simulations will play an increasingly complementary role in unraveling the mechanisms behind in vivo nanoparticle transport, chemical reactivity, and physical behavior.

Advanced Surfaces

The water contact angle (WCA) maximum of hydrophobic surfaces is circa 120 degree, for example of a bulk, flat Teflon surface. WCA is the angle formed tangential to the water droplet at the air–liquid–solid interface. A WCA less than 90 degree is an indication of a wettable surface; a WCA greater than 90 degree indicates poor wettability. In order to exceed this 120 degree WCA limit, a surface that is “roughened” with hierarchical micro-nanostructures is required. Then WCA values of 160 degree or higher are possible (180 degree is the maximum value for WCA). The surfaces of nanoparticles can also be made to contribute to superhydrophobic, superhydrophilic, and/or oleophobic coatings. Superhydrophobic surfaces were first found in Nature. The lotus leaf surface is a combination of micron-scale roughness (nubs) decorated with nanoscale structures. The result is a self-cleaning surface with a WCA greater than 160 degree. Although WCA is not a practical measurement for a nanoparticle, it is relevant on substrate surfaces composed of nanoparticles.

A new line of socks was developed to keep feet dry and was produced by interweaving a superhydrophobic inner layer with a hydrophilic outer layer. Subsequently, it was proposed that patients with hyperhidrosis (increased sweating) and recurrent inflammation due to *tinea pedis* infections (like athlete’s foot) could benefit from this new fiber combination by keeping moisture away from the skin [49].

Optical and Magnetic Properties

For metals, especially for the noble metals, there exist “surface plasmons” with resonances in the visible range of the electromagnetic spectrum. A surface plasmon is the collective oscillation of free electrons at a metal–dielectric interface. Resonance occurs when the frequency of the incident radiation corresponds to the natural frequency of the oscillation. Gold, when very small, appears ruby red at circa 520 nm excitation; silver is yellow at circa 400 nm excitation. As gold nanoparticles become smaller, the resonance shifts to shorter wavelengths due to extrinsic (not quantum) size effects [7]. Particle shape and orientation with regard to the electric field of the incident light are also considered in selection of desired optical response. The condition of plasmon resonance for metal nanoparticles embedded within an oxide host is given by the following expression: $\epsilon'_m = -2\epsilon'_o$, where ϵ'_m is the real part of the wavelength-dependent complex dielectric function of the metal, 2 is the shape factor (or screening parameter) related to spheres, and ϵ'_o is the real part of the wavelength-dependent dielectric function (related to the refractive index) of the oxide host. The important thing to glean from this discussion is that tuning of optical properties of nanometallic particles is possible by manipulation of composition, size, shape, and orientation with respect to the propagation line of radiation. At longer wavelengths (eg, in the near-IR range), gold nanoparticles rapidly convert absorbed energy into heat [50]. This physical property is exploited by anti-cancer treatments that rely upon stimulated heating of gold nanoparticles.

Gold nanoshells are capable of strong absorption in the near-infrared (NIR) region of the electromagnetic spectrum [51]. Localized temperature increases (above 43°C) are responsible for the onset of protein denaturing, membrane blebbing, and disruption of other organelle structures within the cell. NIR radiation does not interact strongly with water or hemoglobin, and penetration depths of several centimeters can be achieved for soft tissue [52]. Losses are primarily due to scattering and absorption. The optical and photothermal properties of gold nanoparticles and gold nanorods can be tuned by controlling the particle aspect ratio, particle size, and surface chemistry and by conjugating

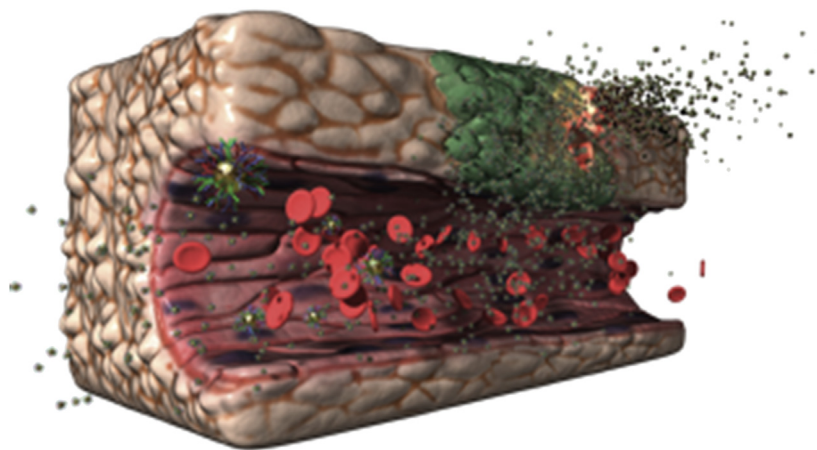


FIGURE 2.3 A generalized method for tumor ablation, using a generic crystalline plasmonic metal, is depicted. Functionalized metallic nanoparticles, nanoshells, or nanorods are injected into the blood supply and directed to the tumor site via targeting ligands (ie, epithelial growth factor receptor antibodies, or anti-EGFR). The tumor is then exposed to near-infrared radiation that stimulates the plasmonic metal to produce heat. Heating of the tumor cells causes their demise. Normal cells are spared because they do not adsorb the gold nanorods effectively. Gold nanoparticles, nanoshells, and nanorods have been used successfully as ablation agents to mitigate the growth of tumors [51,52].

various species to the surface. Photothermal therapy using gold nanorods has been successfully applied to treat squamous cell carcinoma, a form of skin cancer. Gold nanoparticles, in addition to causing heating when exposed to near-IR radiation, enhance X-rays delivered to tumor cells as a radiosensitizer [53] (Fig. 2.3).

Semiconductor QDs provide intense fluorescence emission due to alterations in the band gap of the native material as the particle size is decreased. The phenomenon is described by the fundamental Brus equation. The radius of a QD can be calculated from the position of energy emission in the spectrum.

$$\Delta E(r) = E_g + \frac{h^2}{8r^2} \left(\frac{1}{m_e^*} + \frac{1}{m_h^*} \right) - \frac{1.8e^2}{4\pi\epsilon_0\epsilon_r r}$$

where E_g is the band

gap energy of the semiconductor material in the bulk phase; h is the Planck's constant; r is the radius of the particle; m_e^* and m_h^* are the material-dependent effective masses of the electrons and holes, respectively, and e is the elementary electron charge; and ϵ_0 and ϵ_r are the permittivity of free space and the dielectric constant of the semiconductor material, respectively. The second term represents the additional energy gained as a result of quantum confinement with $1/r^2$ dependence. The important thing to glean from this discussion is to understand that the energy band gap depends on the particle radius. For emission in the violet region of the spectrum, QDs with smaller r and larger $\Delta E(r)$ are required. For emission in the red region of the spectrum, QDs with larger r and smaller $\Delta E(r)$ are required. Semiconductor QDs are used in imaging for the purpose of cancer detection.

The coercivity (intensity of external magnetic field required to remove magnetization of a material) of magnetic nanoparticles varies with the decreasing

size of the nanoparticles. It changes from multidomain to single domain and finally to superparamagnetic with the smallest sizes. Phase transition properties are also susceptible to diminishing size, and there are proposals that recommend use of particle size as a vital component of phase diagrams [54]. Exposing superparamagnetic nanoparticles to an alternating magnetic field (kHz to MHz) leads to heating above 43°C via the phenomenon of Néel relaxation loss. This physical property is, as expected, size dependent. Aside from destroying cancer cells in the targeted organ, such hyperthermia treatments can also lead to tumor-specific immune response that can be active at sites well away from the targeted organ.

SYNTHESIS OF NANOMATERIALS

Synthetic routes to form nanomaterials are varied in scope, but there exist some underlying patterns to all of them, especially with regard to preparation of nanoparticles. Once the ingredients and conditions have been determined in the design phase, we can let the self-assembly or mildly boosted self-assembly processes play out—in a layer-by-layer manner. As with any kind of controlled nanoparticle synthesis procedure, control over composition, size, size distribution, and particle shape is paramount. There are many kinds of bottom-up synthesis procedures that can be used to fabricate synthetic nanomaterials. They involve both intramolecular and intermolecular types of bond formation. Most types of bottom-up synthesis are usually accomplished in liquid media, although gas phase, solid-state, supercritical-fluid, and vacuum media can also be suitable. The second and/or third steps involve chemical modification of the surface with moieties that

serve to achieve transport objectives and/or to sequester or carry a payload.

Self-Assembly and Self-Organization

Self-assembly is defined as a process of synthesis in which only a minimal input of energy and direction is required. The innate beauty of nanomaterial synthesis carried out from the bottom up is that much of it can happen automatically—and at reasonable temperatures, ambient pressures, and relatively mild chemical conditions of pH and concentration of chemical components. Self-assembly is governed by thermodynamic control rather than kinetic control, although a hard line cannot be drawn between the two domains. For example, the synthesis of gold-55 nanoparticles requires a precursor solution (chloroauric acid [HAuCl₄]), a reducing agent (sodium borohydride [NaBH₄]), a ligand-binding agent (triphenyl phosphine [PPhe₃]), and mild conditions to help boost the reactions (temperature ca. 100°C). The result is gold-55 QDs—a monodisperse product that is ligand stable [55].

Self-assembled monolayers (SAMs) are one of the most powerful of all nanotechnology bottom-up fabrication methods [56]. Chemisorption of thiols onto gold surfaces, for example, produces SAMs with a vast array of functionalities. SAMs on gold substrates in electronics and gold nanoparticles in medical applications provide some notable examples. Other reactive ligand groups include carboxylic acids, silanes, and amines. Langmuir–Blodgett films employ long-chain aliphatic or fatty acids such as stearic acid to form monolayers on liquid surfaces (primarily water) that can act as gene or drug transport vehicles.

Supramolecular chemistry is chemistry beyond that of the individual molecule. It is chemistry characterized by formation of intermolecular bonds. It is the chemistry of the host–guest relationship. Supramolecules are combinations of molecules bonded by intermolecular forces that form a new “supramolecule” with different functions. Considerations at the design phase of synthesis involve solvent effects, choice of host–guest pairs, and thermodynamic and kinetic factors [57]. Layer-by-layer methods employ a variety of intermolecular and intramolecular bond formations to accomplish the objectives. The simplest of these involves ionic interactions in which oppositely charged species attract each other to form layers.

Bottom-Up Synthesis of Nanocarriers

Nanocarriers are vehicles that deliver diagnostic, therapeutic, or theranostic products. They come in three general varieties [58]. The first type sequesters products within its volume. In the case of liposomes, a polar cavity for water-soluble drugs and a nonpolar lipid bilayer

for water-insoluble drugs are both made available for drug encapsulation. Second, components can be tethered onto the surface of the nanocarriers. The surface can include a combination of targeting (homing) proteins or peptides; hydrophilic, hydrophobic, or amphiphilic groups to facilitate transport through complex media; and, of course, the therapeutic or diagnostic payload itself. Lastly, nanocarriers that are porous in nature are able to control the selective release of a therapeutic moiety. A generic representation is presented in Fig. 2.4.

A nanocarrier should possess some of the following properties. First, it should be nonimmunogenic, be resistant to microbial contamination, and avoid clearance by the RES. Second, it must be able to protect the therapeutic payload. Third, the nanocarrier should be nontoxic. Fourth, it should not be prematurely cleared from the body. And, fifth, the nanocarrier should have a suitable duration (transport lifetime) in vivo to reach its target effectively. Nanocarriers exist in several forms. Viruses can actually function as a nanocarrier. Polymeric nanocarriers offer great latitude for chemical modification and tuning of their properties. PLGA [poly(lactic-co-glycolic acid)] nanospheres are part of a family of biodegradable polymers together with nanoparticles of poly(amino esters), poly(anhydrides), poly(lactides), and chitosan that are degraded in vivo by hydrolysis [58]. Lipid-based nanocarriers such as liposomes are created from amphiphilic molecules, usually of the phospholipid family. The lipid nanocarrier can be solid or can contain a hydrophilic cavity. Dendrimers are highly branched supramolecular structures formed by strictly controlled rounds of synthesis. Dendrimers can encapsulate or be used to conjugate a drug cargo. If there is functionalization, the drug can be released by application of biodegradable chemical linking groups. There are many more varieties of nanocarriers.

As noted before, spherical particles have special significance. They are the most simple in terms of synthesis, and their physical properties are easiest to model due to highly symmetrical degeneracies in the electronic and physical states. We provide a few examples of synthetic processes of such ‘0D’ materials. Fig. 2.5 shows a representation of three kinds of nanoparticle systems. All are made from the bottom up in stepwise, layer-by-layer methods, although the shortcut of simultaneous assembly methods can be possible in some applications.

Silica nanoparticles are excellent vehicles for therapeutic delivery, enabling DNA transport into cells and targeted imaging of cancer cells, and they have made inroads into numerous cosmetic and dermatological applications [59]. Silica nanoparticles, like many other kinds of nanoparticles, are capable of facilitated skin penetration in transcutaneous vaccinations with sustained drug release. Their synthesis is straightforward

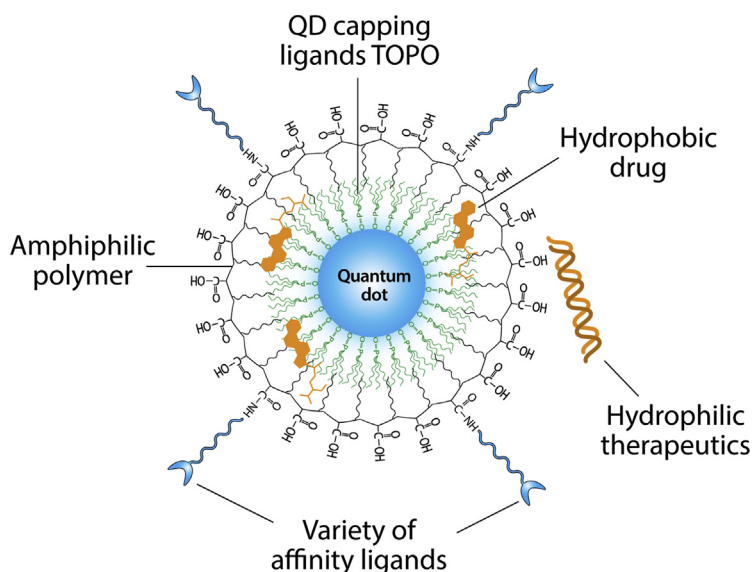


FIGURE 2.4 A generic nanocarrier is depicted. The carrier might actually be a theranostic agent as it contains a quantum dot that can be used for imaging. Hydrophobic drugs are sequestered within the hydrophobic inner layer interface between the TOPO (triethylphosphine oxide) and the amphiphilic polymer. Hydrophilic therapeutics are tethered to the surface via carboxylic acid group intermolecular interactions, most likely by hydrogen bonds. Homing ligands (affinity ligands) help to direct the ensemble to its proper destination.

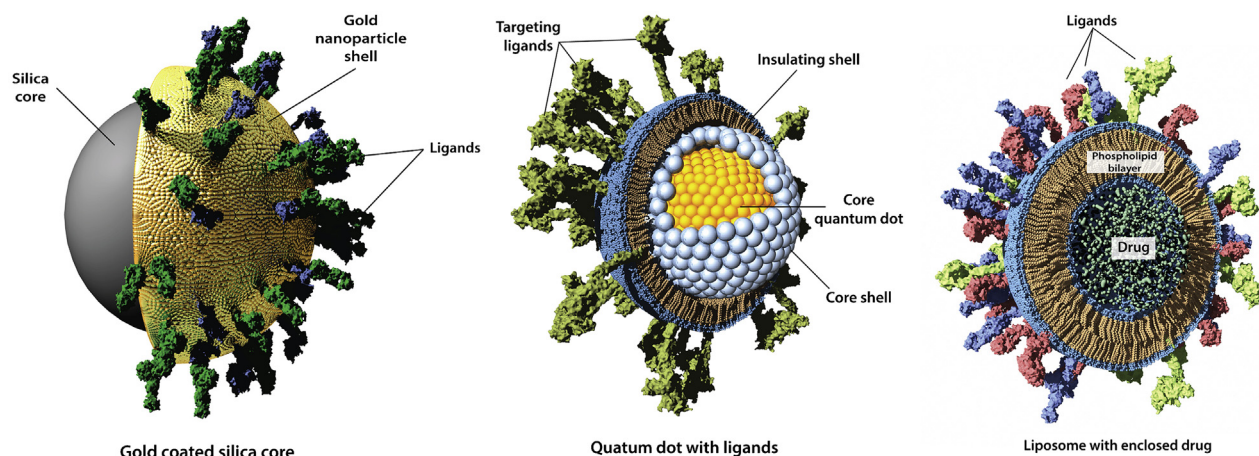


FIGURE 2.5 Various formulations of chemically and biochemically modified nanoparticles are depicted. Left: A gold nanoshell structure is formed on a silica particle. It is tagged with molecular recognition moieties that will target its delivery. Middle: Multilayer quantum dots are shown with a protective layer decorated with multifunctional ligands. Right: A therapeutic is encapsulated within a liposomal cavity. The liposome consists of a phospholipid bilayer that forms a polar cavity. Anti-immune system protective ligands and homing peptides are anchored to the surface. Lipid-soluble drugs are sequestered within the nonpolar interface between layers, while water-soluble drugs are situated in the polar cavity. There is a unifying simplicity to all of these schemes.

via the sol–gel process (eg, the Stöber process that was developed well before nanotechnology became popular) [60]. The alkylloxysilane tetraethylorthosilicate (TEOS or $[\text{Si}(\text{OC}_2\text{H}_5)_4]$) is an often used chemical precursor in the formation of silica nanoparticles by the sol–gel process. Hydrolysis of TEOS in the presence of catalytic acids like hydrochloric acid or catalytic bases like ammonia or sodium hydroxide yields silanol monomeric groups that undergo condensation to form the polymerized silica nanoparticles: $\text{Si}(\text{OR})_4 + 2\text{H}_2\text{O} \rightarrow \text{SiO}_2 + 4\text{ROH}$. Particle

growth occurs by addition of monomers or by controlled aggregation.

Gold nanoshell fabrication first involves the synthesis of a spherical dielectric core material (eg, silica) that serves as the structural core with a chemically modifiable surface (Fig. 2.5, left). The size of silica particles depends on the proportions of the reactants (ethanol, water, ammonia, ammonium hydroxide, and the TEOS) [61]. Particles in diameter from circa 50 nm to circa 440 nm are produced in this way. Silanes are an extremely versatile family of

chemicals that spontaneously self-assemble to form a wide variety of silicate structures. The next step involves surface functionalization with a silane derivative like 3-aminopropyltriethoxysilane (APTES) at 80°C with vigorous mixing. The important aspect of functionalization is to produce an amine-terminated group for subsequent binding of the gold species. Hydrogen tetrachloroaurate [$\text{HAuCl}_4 \cdot 3\text{H}_2\text{O}$] is added in the presence of sodium hydroxide to form gold hydroxide seed nanoparticles. The amine-functionalized silica nanoparticles are then added until a brownish color change is observed. Then, reduction of HAuCl_4 by sodium borohydride [NaBH_4] results in a continuous gold layer shell. The shell thickness is monitored by observation of the color of the solution ranging from reddish, purplish, and bluish to greenish. Addition of trisodium citrate dihydrate [$\text{Na}_3\text{C}_6\text{H}_5\text{O}_7 \cdot 2\text{H}_2\text{O}$] (a ligand that is also a reducing agent) serves to cap the gold nanoshell and help control the thickness of the layer. Therefore, core size and shell thickness are determined by the size of the silica nanoparticle, the amount of gold stock solution, and the timing of addition and concentration of a stabilization agent used for capping. The capping agent can be removed in a ligand exchange reaction to produce a new species with a specified surface activity.

The synthesis of semiconductor QDs is also straightforward—at least from the bottom-up perspective. Sizes ranging from a few nanometers to greater than 50 nm can be achieved. Core-shell semiconductor QDs, pictured in Fig. 2.5 (middle), can be fabricated by precipitation, sol-gel, or microemulsion, or via application of inverse micelles. CdSe-ZnS core-shell QDs of circa 5 nm diameter are synthesized using a mild temperature inverse-micelle microemulsion process [62]. Inverse micelles form spontaneously due to the hydrophobic effect (provided by one of the intermolecular components). Material requirements include water, *n*-heptane, dioctylsulfosuccinate sodium salt (the surfactant AOT), and the QD chemical ingredients, including zinc nitrate, cadmium nitrate, ammonium sulfide, sodium sulfite, and selenium powder. The selenium powder is converted into a water-soluble formulation (Na_2SeSO_3) in order to react with Cd^{2+} cations within the polar core of the inverse micelle to form the CdSe QDs: $\text{Cd}^{2+} + \text{SeSO}_3^{2-} + 2\text{OH}^- \rightarrow \text{CdSe}_{(s)} + \text{SO}_4^{2-} + \text{H}_2\text{O}$. A vortex mixer is used to enhance the efficiency of the reaction. Second, microemulsions of $(\text{NH}_4)_2\text{S}$ and $\text{Zn}(\text{NO}_3)_2$ are added to the CdSe mixture, also with strong vortex mixing, to form the core-shell structure [62]—all accomplished under relatively mild conditions.

Liposomes, discovered by a dermatologist in the 1960s, range in size from as small as 30 nm diameter to a diameter over microns, and have become one of the

premier biocompatible vehicles to deliver therapeutics, with their relatively simple synthesis that can be executed without the need for complicated apparatus [63–66]. Liposomes (Fig. 2.5, right) are formed primarily due to the hydrophobic effect in which amphiphilic phospholipids like lecithin self-organize in water into a bilayer with an aqueous core and a hydrophobic region within the lipidic domain of the membrane. Depending on chemical conditions, smaller unilamellar liposomes with a nonpolar core and multilamellar structures can also be formed. Electrostatic forces, hydrogen bonding, and van der Waals forces in addition to the hydrophobic effect all play a role in stabilizing the liposome. Polar drugs can be encapsulated within the hydrophilic cavity of the bilayered micelle, whereas nonpolar drugs interact within the hydrophobic lipid bilayer. Liposomes can undergo endocytosis by macrophages within the RES. The sequestered drug is released slowly, thereby reducing the accumulation of drugs while prolonging their action [66].

Recently, the encapsulation of a natural immune-regulatory compound called a salidroside (extracted from the flower “rose root” or *Rhodiola rosea*, found in cold regions of the Himalayas) has been accomplished with high-efficiency encapsulation into liposomes [66]. Salidroside is also known to play an important role in stabilizing liposome solutions by prevention of agglomeration and subsequent fusion [67]. The function of the salidroside liposomes as a vaccine adjuvant was tested using a porcine circovirus type 2 (PCV-2). The procedure was as follows. Phospholipid, cholesterol, and a nonionic surfactant were first dispersed in ethanol (via ethanol injection). Once stabilized, the mixture was then added to an aqueous ammonium sulfate solution. Following evaporation of the ethanol, the ammonium sulfate was removed by dialysis. The drug salidroside was added then to form the complex with encapsulation efficiency greater than 94%. The salidroside liposomes were mixed with inactivated PCV-2 as an antigen. Following experiments, it was shown that the salidroside liposome adjuvant was capable of enhancing PCV-2-specific IgG production and was able to maintain high levels for extended periods of time [67].

CONCLUSION

We have presented a very brief overview of nanotechnology from the perspective of physiochemical properties, phenomena, and synthesis. Examples scattered throughout have been chosen to link nanotechnology with dermatology via recent articles gleaned from the literature. Nanotechnology is all about size, and it is that special size domain that is responsible for imparting

the remarkable behavior that differs from the bulk form. If one understands the impact of size, the complex interactions of particles with intermolecular forces, and the subtleties involved within the crowded physiological ambiance of membranes, tissue, intracellular matrices, and plasma, then there is no limit to the synthetic possibilities yet to come. There also exists an impressive unifying simplicity in this technology.

We have not been able to adequately cover the extremely wide and diverse technology platform that is nanotechnology. Furthermore, the important field of nanotoxicology has not been addressed directly, but it most certainly presents great challenges facing future products derived from nanotechnology. Nanometrology and characterization techniques represent other challenges, along with the creation of regulatory standards that require rapid development to keep pace with the incredible avalanche of new research [68]. Nanodermatology has indeed arrived.

References

- [1] Nasir A. Nanotechnology and dermatology: part I – potential of nanotechnology. *Clin Dermatol* 2010;28(4):458–66.
- [2] DeLouise LA. Applications of nanotechnology in dermatology. *Journal Invest Dermatol* 2012;132:964–75.
- [3] Bangale MS, Mitkare SS, Gattani SG, Sakarkar DM. Recent nanotechnological aspects in cosmetics and dermatological preparations. *Int J Pharm Pharm Sci* 2012;4(2):88–98.
- [4] Walter P, Welcomme E, Hallégot P, Zaluzec NJ, Deeb C, Castaing J, Veyssière P, Bréniaux R, Lévêque J-L, Tsoucaris G. Early use of PbS nanotechnology for an ancient hair dyeing formula. *Nano Lett* 2006;6(10):2215–9.
- [5] Rodríguez G, Barbosa-Barros L, Rubio L, Cócera M, Fernández-Campos F, Calpena A, Fernández E, De La Maza A, López O. Bicelles: new lipid nanosystems for dermatological applications. *J Biomed Nanotechnol* 2015;11(2):282–90.
- [6] Pokropuvny VV, Skorokhod VV. *Mater Sci Eng C* 2007;27(5–8):990–3.
- [7] Kreibitz U, Vollmer M. Optical properties of metal clusters. Springer series in materials science, vol. 25. Berlin: Springer-Verlag; 1995.
- [8] Kulvietis V, Zurauskas E, Rotomskis R. Distribution of polyethylene glycol coated quantum dots in mice skin. *Exp Dermatol* 2013;22:141–59.
- [9] [a] Filipe P, Silva JN, Silva R, Cirne de Castro JL, Marques Gomes M, Alves LC, Santos R, Pinheiro T. Stratum corneum is an effective barrier to TiO₂ and ZnO nanoparticle percutaneous absorption. *Skin Pharmacol Physiol* 2009;22(5):266–75.
[b] Verissimo A, Alves LC, Filipe P, Silva JN, Silva R, Ynsa MD, Gontier E, Moretto P, Pallon J, Pinheiro T. Nuclear microscopy: a tool for imaging elemental distribution and percutaneous absorption in vivo. *Microsc Res Tech* April 2007;70(4):302–9.
- [10] Kennedy LC, Bickford LR, Lewinsky NA, Coughlin AJ, Hu Y, Day EM, West JL, Dresek RA. A new era for cancer treatment: gold-nanoparticle-mediated thermal therapies. *Small* 2011;7(2):169–83.
- [11] Kovziridze Z, Heinrich JH, Goerke R, Mamniashvili G, Chachkhani Z, Mitskevich N, Donadze G. Production of supraparamagnetic nanospheres for hyperthermic therapy of surface skin cancer diseases. *IOP Conf Ser Mater Sci Eng* 2011;18:192018.
- [12] Tiwari JN, Tiwari RN, Kim KS. Zero-dimensional, one-dimensional, two-dimensional, and three-dimensional nanostructured materials for advanced electrochemical energy devices. *Prog Mater Sci* 2012;57:724–803.
- [13] De La Zerda A, Zavaleta C, Keren S, Vaithilingham S, Bodapati S, Liu Z, Levi J, Smith BR, Ma T-E, Oralkan O, Cheng Z, Chen X, Dai H, Khuri-Yakub BT, Gambhir SS. Carbon nanotubes as photoacoustic molecular imaging agents in living mice. *Nat Nanotechnol* 2008;3:557–62.
- [14] Morganti P, Carezzi F, Del Clotto P, Morganti G, Nunziata ML, Gao XH, Duo-Chen H, Tishenko G, Yudin VE. Chitin nanofibrils: a natural multifunctional polymer. Physicochemical characteristics, effectiveness and safeness. In: Phonix DA, Ahmed W, editors. Chapter 1, Nanobiotechnology. UK: One Central Press; 2014. p. 1–31.
- [15] Morganti P. Chitin-nanofibrils in skin treatment. *J Appl Cosmetol* 2009;27:251–70.
- [16] [a] Mohamed HA, Al-Suwaidan A, Al-Kaysi O. Effect of surface modified paclitaxel nanowires on U937 cells in vitro: a novel drug delivery vehicle. *J Nanomater* 2012;328520:6.
[b] Muzzarelli RAA, Morganti P, Morganti G, Palombo P, Palombo M, Biagini G, Belmonte MM, Giantomassi F, Orlandi F, Muzzarelli C. Chitin nanofibrils/chitosan glycolate composites as wound medicaments. *Carbohydrate Polymers* 2007;70:274–84.
- [17] Howe JM. Interfaces in materials: atomic structure, thermodynamics and kinetics of solid–vapor, solid–liquid, and solid–solid interfaces. New York: John Wiley & Sons Inc.; 1997.
- [18] Hirsch A. Principles of fullerene reactivity, topics in current chemistry. *Fullerenes Rel Struct* 1999;199:1–65.
- [19] Lens M. Recent progress in application of fullerenes in cosmetics. *Recent Pat Biotechnol* 2011;5(2):67–73.
- [20] Ryan JJ, Bateman HR, Stover A, Gomez G, Norton SK, Zhao W, Schwartz LB, Lenk R, Kepley CL. Fullerene nanomaterials inhibit allergic response. *J Immunol* 2007;179(1):665–72.
- [21] Tegos GP, Demidova TN, Arcilla-Lopez D, Lee H, Wharton T, Gali H, Hamblin MR. Cationic fullerenes are effective and selective antimicrobial photosensitizers. *Chem Bio* 2005;12(10):1127–35.
- [22] Majumdar D, Jung K-H, Zhang H, Nannapaneni S, Wang X, Ruhul Amin ARM, Chen Z, Chen ZG, Shin DM. Luteolin nanoparticle in chemoprevention: in vitro and in vivo anticancer activity. *Cancer Prev Res* 2014;7(1):65–73.
- [23] Chen S, Yu F, Yu Q, He Y, Jiang S. Strong resistance of a thin crystalline layer of balanced charged groups to protein adsorption. *Langmuir* 2006;22(19):8186–96.
- [24] Yang W, Xue H, Carr LR, Wang J, Jiang SY. Zwitterionic poly(carboxybetaine) hydrogels for glucose biosensors in complex media. *Biosens Bioelectron* 2011;26:2454–9.
- [25] Chen S, Li L, Zhao C, Zheng J. Surface hydration: Principles and applications toward low-fouling/non-fouling biomaterials. *Polymer* 2010;51:5283–93.
- [26] Sin M-C, Chen S-H, Chang Y. Hemocompatibility of zwitterionic interfaces and membranes. *Polymer J* 2014;46:436–43.
- [27] Yang W, Zhang L, Wang S, White AD, Jiang S. Functionalizable and ultra stable nanoparticles coated with zwitterionic poly(carboxybetaine) in undiluted blood serum. *Biomater* 2009;30:5617–21.
- [28] Baruah S, Mahmood MA, Myint MTZ, Bora T, Dutta J. Enhanced visible light photocatalysis through fast crystallization of zinc oxide nanorods. *Beilstein J Nanotechnol* 2010;1:14–20.
- [29] Jin C, Tang Y, Yang FG, Li XL, Xu S, Fan XY, Huang YY, Yang YJ. Cellular toxicity of TiO₂ nanoparticles in anatase and rutile crystal phase. *Biol Trace Element Res* 2011;141(1–3):3–15.
- [30] Turci F, Peira E, Corazzari I, Fenoglio I, Trotta M, Fubini B. Crystalline phase modulates the potency of nanometric TiO₂ to adhere and perturb the stratum corneum of porcine skin under indoor light. *Chem Res Toxicol* 2013;26(10):1579–90.

- [31] Li L, Zhu Y-J. High chemical reactivity of silver nanoparticles toward hydrochloric acid. *J Colloid Interf Sci* 2006;303(2):415–8.
- [32] Viñes F, Gomes J, Illas F. Understanding the reactivity of metallic nanoparticles: beyond the extended surface model for catalysis. *Chem Soc Rev* 2014;43:4922–39.
- [33] Choudhary TV, Goodman DW. Oxidation catalysis by supported gold nano-clusters. *Top Catal* 2002;21(1–3):25–34.
- [34] Rudyak VY. Viscosity of nanofluids – why it is not described by the classical theories. *Adv Nanopart* 2013;2:266–79.
- [35] Letellier P, Mayaffre A, Turmine M. Solubility of nanoparticles: nonextensive thermodynamic approach. *J Phys-Condens Mat* 2007;19(43):436229.
- [36] Li Z. Critical particle size where the Stokes–Einstein relation breaks down. *Phys Rev E* 2009;80:061204.
- [37] Poddar NN, Amar JG. Adsorption and diffusion of colloidal Au nanoparticles at a liquid-vapor interface. *J Chem Phys* 2014;140(24):244702.
- [38] Gupta S, Bansal R, Gupta S, Jindal N, Jindal A. Nanocarriers and nanoparticles for skin care and dermatological treatments. *Indian Dermatol Online J* 2013;4(4):267–72.
- [39] Staronova K, Nielsen JB, Roursgaard M, Knudsen LE. Transport of SiO₂ nanoparticles through human skin. *Basic Clin Pharmacol Toxicol* 2012;111:142–4.
- [40] Oh N, Park J-H. Endocytosis and exocytosis of nanoparticles in mammalian cells. *Intl J Nanomed* 2014;9(1):51–63.
- [41] Gottesman SP, Goldberg GN. Immediate successful treatment of Argyria with a single pass of multiple Q-switched laser wavelengths. *JAMA Dermatol* 2013;149(5):623–4.
- [42] [a] Liu J, Wang Z, Liu FD, Kane AB, Hurt RH. Chemical transformations of nanosilver in biological environments. *ACS Nano* 2012;6(11):9887–99.
[b] Park S-W, Shin H-T, Lee K-T, Lee D-Y. Medical concern for colloidal silver supplementation: Argyria of the nail and face. *Ann Dermatol* February 2013;25(1):111–2.
- [43] Saptarshi SR, Feltis BN, Wright PFA, Lopata AL. Investigating the immunomodulatory nature of zinc oxide nanoparticles at sub-cytotoxic levels in vitro and after intranasal installation in vivo. *J Nanobiotechnol* 2015;13:6.
- [44] Jang YS, Lee EY, Park Y-H, Jeong SH, Lee SG, Kim Y-R, Kim M-K, Son SW. The potential for skin irritation, phototoxicity, and sensitization of ZnO nanoparticles. *Mol Cell Toxicol* 2012;8:171–7.
- [45] Ryu HJ, Seo MY, Jung SK, Maeng EH, Lee SY, Jang DH, Lee TJ, Jo KY, Kim YR, Cho KB, Kim MK, Lee BJ, Son SW. Zinc oxide nanoparticles: a 90-day repeated dose dermal toxicity study in rats. *Int J Nanomed* 2014;9(2):137–44.
- [46] Journeay WS, Goldman RH. Occupational handling of nickel nanoparticles: a case report. *Am J Ind Med* 2014;57(9):1073–6.
- [47] Geraci CL, Schulte P, Murashov V. Nickel nanoparticles: a case sensitization associated with occupational exposure. *NIOSH Science Blog: Safer Healthier Workers*. May 28, 2014. <http://blogs.cdc.gov/niosh-science-blog/2014/05/28/nickel-nano/>.
- [48] Nacev A, Beni C, Bruno O, Shapiro B. Magnetic nanoparticle transport within flowing blood and into surrounding tissue. *Nanomed-UK* 2010;5(9):1459–66.
- [49] Martinho E. New double layer socks keep feet dry. drymaxsocks.com/files/263913_final.pdf, American Academy of Dermatology, viewed 2015.
- [50] Huang X, El-Sayed MA. Plasmonic photo-thermal therapy (PPTT). *Alexandria J Med* 2011;47:1–9.
- [51] O’Neal DP, Hirsch LR, Halas NJ, Payne JD, West JL. Photo-thermal tumor ablation in mice using near infrared-absorbing nanoparticles. *Cancer Lett* 2004;209(2):171–6.
- [52] Dickerson EB, Dreaden EC, Huang X, El-Sayed IH, Chu H, Pushpanketh S, McDonald JF, El-Sayed MA. Gold nanorod assisted near-infrared plasmonic photothermal therapy (PPTT) of squamous cell carcinoma in mice. *Cancer Lett* 2008;269:57–66.
- [53] Hainfeld JF, Lin L, Slatkin DN, Dilmanian A, Vadas TM, Smilowitz HM. Gold nanoparticle hyperthermia reduces radiotherapy doses. *Nanomed* 2014;10(8):1607–9.
- [54] Cheng Y, Su H, Koop T, Mikhailov E, Pöschl U. Size dependence of phase transitions in aerosol nanoparticles. *Nature Commun* 2015;6:5923.
- [55] Schmid G, Corain B. Nanoparticulated gold: synthesis, structures, electronics and reactivities. *Euro J Inorg Chem* 2003;3081–98.
- [56] Love JC, Estroff LA, Kriebel JK, Nuzzo RG, Whitesides GM. Self-assembled monolayers of thiolates on metals as a form of nanotechnology. *Chem Rev* 2005;105:1103–69.
- [57] Hornyak GL, Dutta J, Tibbals HF, Rao AK. Introduction to Nanoscience. Boca Raton, USA: CRC Press; 2008.
- [58] Prasad PN. Introduction to nanomedicine and nanobioengineering. Hoboken, NJ: John Wiley & Sons, Inc; 2012.
- [59] Nafisi S, Schäfer-Korting M, Maibach HI. Perspectives on percutaneous penetration: silica nanoparticles. *Nanotoxicol* October 6, 2014:1–15.
- [60] Störber W, Fink A, Bohn E. Controlled growth of monodisperse silica spheres in the micron size range. *J Colloid Interf Sci* 1968;26(1):62–9.
- [61] Kah JCY, Phonthammachai N, Wan RCY, Song J, White T, Mhaisalkar S, Ahmad I, Sheppard C, Olivo M. Synthesis of gold nanoshells based on the deposition-precipitation process. *Gold Bull* 2008;41(1):23–36.
- [62] Matthew S, Bhardwaj BS, Saran AD, Radhakrishnan P, Nampoori VPN, Vallabhan CPG, Bellare JR. Effect of ZnS shell on optical properties of CdSe-ZnS core-shell quantum dots. *Opt Mater* 2015;39:46–51.
- [63] Zhang L, Zhang L. Lipid-polymer hybrid nanoparticles: synthesis, characterization and applications. *Nano LIFE* 2010;1 & 2:163–73.
- [64] Yogita P, Sameer J. Novel methods for liposome preparation. *Chem Phys Lipids* 2014;177:8–18.
- [65] Dua JS, Rana AC, Bhandari AK. Liposome: methods of preparation and applications. *Int J Pharm Studies Res* 2012;III(II):14–20.
- [66] Feng Y, Zhao X, Lv F, Zhang J, Deng B, Zhao Y, Hu Y, Wang D, Liu J, Yu L, Bo R, Liu Z. Optimization on preparation conditions of solidoside liposome and its immunological activity on PCV-2 in mice. *Evidence-Based Com Alt Med* 2015:178128.
- [67] Fan M, Xu S, Xia S, Zhan X. Effect of different preparation methods on physicochemical properties of solidoside liposomes. *J Agric Food Chem* 2007;55(8):3089–95.
- [68] Hornyak GL, Moore JJ, Tibbals HF, Dutta J. Fundamentals of nanotechnology. Boca Raton, USA: CRC Press; 2009.

An Overview of Nanomaterials in Dermatology

B. Mordorski¹, A. Landriscina¹, A. Friedman²

¹Montefiore—Albert Einstein College of Medicine, Bronx, NY, United States; ²George Washington School of Medicine and Health Sciences, Washington, DC, United States

OUTLINE

Introduction	31	<i>Nanoemulsions for Cosmetic Dermatology</i>	40
Therapeutic Roles of Nanomaterials	32	<i>Nanopigments for Cosmetic Dermatology</i>	40
<i>Nanoparticles</i>	33	Diagnostic Roles of Nanomaterials	41
Nanoparticles for Infectious Disease	33	<i>Quantum Dots for Diagnostic Dermatology</i>	41
Nanoparticles for Inflammatory Disease	35	<i>Nanoparticles for Diagnostic Dermatology</i>	41
Nanoparticles for Cutaneous Neoplasms	36	Safety Considerations	42
Nanoparticles for Photoprotection	37	Conclusions	42
<i>Nanoliposomes</i>	38	Glossary	42
Nanoliposomes for Cutaneous Neoplasms	38	List of Acronyms and Abbreviations	43
<i>Nanoemulsions</i>	38	References	43
Nanoemulsions for Acne and Actinic Keratoses	39		
Nanoemulsions for Infectious Disease	39		
<i>Nanoscaffold Wound Dressings</i>	39		
Cosmetic Roles of Nanomaterials	40		

INTRODUCTION

Nanomaterials are defined as materials that measure on the nanoscale (1–100 nm) or materials that contain nanoscale structures internally or on their surfaces [1]. They can be designed with a wide variety of chemical compositions, structures, and surface characteristics, and their magnetic, electronic, and optical features may also be varied. The small size of nanomaterials allows for the exploitation of unique properties of matter on this scale [2]. For example, their small size can increase their permeation through tissues—such as the skin, hair, and nails—in addition to facilitating selective accumulation within these tissues [3]. Furthermore, the outer coating of nanomaterials can be altered to target specific molecular structures and cell types. One way this can be achieved is by coating a nanomaterial with

a monoclonal antibody that has affinity for a certain type of cell receptor, thereby targeting the material to specific neoplastic, infected, or inflammatory cells [4,5]. Since nanomaterials may be only a few atoms wide, their surface area-to-volume ratio is extremely large. Therefore, a large percentage of atoms that make up a nanomaterial are localized to its surface, increasing their interaction with the surrounding environment. Surface atoms also have fewer neighboring atoms with which to bond, thereby conferring higher reactivity.

Another important feature of nanomaterials is their ability to encapsulate both established and emerging therapeutic agents that may not otherwise be bioavailable in vivo secondary to poor solubility, short half-life, or inability to maintain contact with their biological target. Thus, nanomaterials can increase the diversity of available therapeutics for a variety of

different diseases. Nanomaterials can serve as a depot of encapsulated agents by facilitating their release at a sustained rate over time and allowing continuous interface with their biological target. Release rate can also be conveniently controlled by altering nanomaterial composition and physical characteristics. Sustained release avoids the rapid saturation and washout of a bolus dose, thereby allowing the delivery of potent drugs while minimizing side effects, as it limits the maximum amount of drug that is in contact with the skin at one time. Given these properties, nanomaterials can enhance therapeutic efficiency due to greater specificity for disease targets, increased bioactivity of encapsulated agents, and decreased drug levels required in vivo to achieve therapeutic results.

Nanodermatology, the use of nanomaterials for dermatologic applications, is a growing field of interest. For example, nanoparticles and nanoscaffold wound dressings exhibit therapeutic roles for nanomaterials in the setting of infectious and inflammatory diseases and wound healing; nanoemulsions and nanopigments demonstrate cosmetic roles by reversing skin damage and evening skin tone; and quantum dots and specialized nanoparticles play important diagnostic roles, namely in the detection of neoplasms. This chapter will provide an overview of nanomaterials in therapeutic, cosmetic, and diagnostic dermatology.

THERAPEUTIC ROLES OF NANOMATERIALS

Topical therapeutics are the mainstay of dermatologic therapy, and the stratum corneum is the primary barrier for their delivery. The stratum corneum can be conceptualized as a brick wall, consisting of layers of anucleate polyhedral cells with thickened membrane envelopes (bricks) as well as intercellular lipids (mortar). Involucrin, a protein in the outer portion of the corneocyte envelope, is responsible for aligning the first layer of intercellular lipids, while the remaining lipids self-assemble in bilayers [6]. The lipid content of the stratum corneum has been considered the primary rate-limiting factor for diffusion [7], and studies have found 13-nm-sized pores between the hydrophilic lipid heads [8]. However, through hydration of the stratum corneum, topical vehicles may create larger aqueous channels between the lipids [9], and the compilation of several studies suggests that the size of the aqueous channels in the stratum corneum may vary, with diameters ranging from 0.4 to 36 nm [8]. While the small size of nanomaterials may enable diffusion through these pores, size alone does not confer penetration of the stratum corneum. For example, cutaneous penetration of 95.3 nm nanoparticles was enabled by the

addition of positively charged chitosan, demonstrating disruption of stratum corneum morphology on transmission electron microscopy (TEM) [10]. This confirms that surface chemical properties play a role in nanomaterial penetration as well (Fig. 3.1).

For nanomaterials that do not readily penetrate the stratum corneum, selective accumulation within the pilosebaceous unit may occur, a phenomenon that is well documented [11,12]. In fact, nanomaterials can be designed to specifically target this structure [13]. The pilosebaceous unit contains a single hair follicle and expels lipophilic sebum through pores ranging in size from 10 to 210 μm (10,000–210,000 nm), depending on location [14]. However, the role of the pilosebaceous unit may be limited in transcutaneous drug delivery. For one, its pores comprise only 0.1% of the skin surface, restricting its utility as a route to deeper cutaneous structures [13]. Second, nanomaterials themselves do not necessarily enter the skin from the pilosebaceous unit [11,15]. Rather, the structure can serve as a reservoir for nanomaterials, protecting them from the continuous desquamation of the stratum corneum. From this reservoir, drugs encapsulated by nanomaterials may enter the epidermis or dermis, though without nanoencapsulation within the skin their therapeutic effect may be muted [16]. Although topical penetration through the pilosebaceous unit is a limited pathway, it can be utilized by nanomaterials, especially when applying topical therapeutics to areas with an increased density of pores (Fig. 3.2).

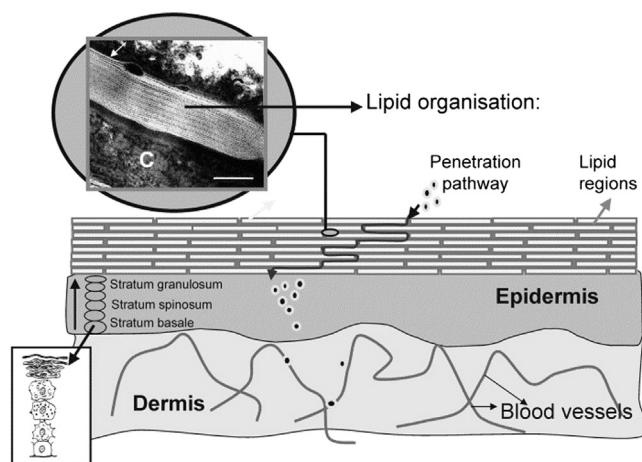


FIGURE 3.1 The stratum corneum is the primary barrier for delivery of topical drugs. The cross-sectional illustration depicts a brick-and-mortar arrangement of anucleate cells and intercellular lipids in the stratum corneum, the uppermost layer of the epidermis. A black arrow demonstrates the tortuous path of intercellular penetration through the stratum corneum. The micrograph inset reveals the lamellar configuration of intercellular lipids, arranged parallel to corneocyte surfaces. (C) is a corneocyte filled with keratin. Scale bar = 100 nm. Reproduced from Bouwstra JA, Honeywell-Nguyen PL, Gooris GS, Ponc M. Structure of the skin barrier and its modulation by vesicular formulations. *Prog Lipid Res* 2003;42:1–36, with permission from Elsevier.

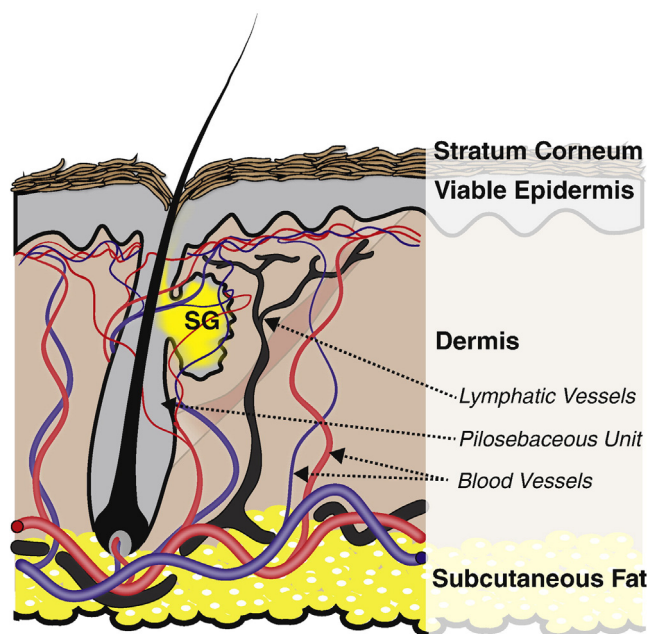


FIGURE 3.2 Selective accumulation of nanomaterials may occur in the pilosebaceous unit. The pilosebaceous unit is a dermal structure that includes a hair follicle, sebaceous gland (SG), and erector pili muscle. The role of the pilosebaceous unit may be limited in transcutaneous drug delivery as nanomaterials themselves do not necessarily enter the skin from the pilosebaceous unit. Rather, the pilosebaceous unit may serve as a reservoir for nanomaterials with potential for release of encapsulated substances. *Reproduced from Simonsson C, Stenfeldt AL, Karlberg AT, Ericson MB, Jonsson CAM. The pilosebaceous unit—a phthalate-induced pathway to skin sensitization. Toxicol Appl Pharmacol 2012;264(1):114–20, with permission from Elsevier.*

Through these routes described, the size, shape, and surface properties of nanomaterials may be exploited to overcome the stratum corneum barrier, the largest obstacle to the successful employment of topically applied nanotherapies. In order to deliver a diverse array of therapeutic substances, nanomaterials themselves come in a wide variety of structures. Nanoparticles, with all three dimensions measuring on the nanoscale, can be composed of a host of different materials and include special subtypes, such as nanoliposomes and nanoemulsions. Other nanomaterials may contain dimensions greater than 100 nm, such as nanofibers, which can be used to create nanoscaffold wound dressings. All of these materials have the potential to provide therapeutic benefits in the field of dermatology.

Nanoparticles

Nanoparticles can be engineered from a variety of materials, including metals (gold, silver), metal oxides (TiO_2 , ZnO), synthetic polymers (polylactic acid, polycaprolactone), natural polymers (chitosan, gelatin), and

lipids (triglycerides, waxes). Metal nanoparticles are recognized for their antimicrobial properties, while metal oxides are known for photoprotection [17]. Polymeric nanoparticles consist of a polymeric skeleton in which drugs are encapsulated and released through gaps or “pores.” Pore size, and thereby drug release rate, can be conveniently controlled by varying chemical reagents. For example, polyethylene glycol (PEG) 200 was incorporated into a polymeric nitric oxide–releasing nanoparticle to create small-sized pores and a slow NO release rate. Conversely, PEG 3000, a much larger molecule, produced a more rapid, burst-like release. Lipid-based nanoparticles include solid lipid nanoparticles (SLNs), nanostructured lipid carriers (NLCs), and lipid drug conjugates (LDCs). These particles create an ultrafine film and controlled occlusion, which are advantageous for topical drug delivery. NLCs improve upon the loading capacity of SLNs, and LDCs extend the advantages of lipid-based delivery to lipophobic drugs [18,19]. Given their diversity, nanoparticles can be employed against a wide variety of dermatologic diseases.

Nanoparticles for Infectious Disease

Antibiotic resistance is rising at an alarming rate, especially in the setting of skin and soft tissue infections. The rate of antibiotic innovation has unfortunately fallen behind the pace of microbial mutation rates, thereby leading biomedical researchers to search for new delivery platforms [20]. Nanoparticles may be favored in combating resistant pathogens for several reasons. For one, they have a large surface area and small size relative to most microbes, which often measure on the micron scale or the higher end of the nanoscale, thereby increasing the interaction of pathogens with antimicrobial substances [21]. As mentioned in this chapter, the surface characteristics of nanoparticles can be modified for specific cellular targeting; in this case, they can be designed to have a higher affinity for bacterial or fungal structures. Nanoparticles have also demonstrated the ability to circumvent antimicrobial resistance by encapsulating substances with multimechanistic antimicrobial activity, encapsulating more than one antimicrobial substance, and overcoming specific resistance mechanisms such as drug efflux and biofilm formation [22].

Nanoparticles for infectious disease largely fall into one of two categories: those that utilize materials with inherent antimicrobial activity that have not previously been therapeutically usable in their native form, and those that incorporate already-available antimicrobials to increase their therapeutic effect and mitigate resistance. Nitric oxide–releasing nanoparticles (NO-np) are an example of the former, as NO is an endogenous molecule that employs multiple mechanisms for

antimicrobial activity; however, it is not available in the clinical space due to its high reactivity and extremely short half-life. Its mechanisms include formation of cytotoxic reactive nitrogen oxide species (RNOS), inactivation of enzymes, DNA damage, and peroxidation of membrane lipids [23–25]. In vivo, NO is generated by macrophages, neutrophils, eosinophils, fibroblasts, epithelial cells, endothelial cells, and glial cells to engage in a wide variety of biological processes. Nanoparticles are well suited for the therapeutic delivery of NO, as particles themselves can be targeted to desired tissues where they offer a stable, sustained reservoir that provides continuous NO release over time.

NO-np, including those with nitrite (Fig. 3.3) [26–30] and diazeniumdiolate [31,32] NO donors, have demonstrated antimicrobial activity in vitro against *Staphylococcus aureus*, *Staphylococcus epidermidis*, *Streptococcus pyogenes*, *Enterococcus faecalis*, *Pseudomonas aeruginosa*, *Escherichia coli*, *Klebsiella pneumoniae*, *Acinetobacter baumannii*, and *Candida albicans*, inhibiting growth as well as biofilm formation in a dose-dependent fashion. These in vitro data have been mirrored by promising in vivo results. For example, NO-np have demonstrated antimicrobial activity against methicillin-resistant *S. aureus* (MRSA)-infected superficial skin infections [27], subcutaneous abscesses [28], and intramuscular abscesses [29]. NO-np have also been effective against *A. baumannii* wound infections [30] and *C. albicans* burn infections [33], in addition to accelerating wound closure.

Curcumin, a component of turmeric with antimicrobial, antiinflammatory, and antineoplastic activity, is another example of successful nanoencapsulation of a therapeutic molecule that was previously undeliverable

by topical formulation. Curcumin exhibits antibacterial activity through inhibition of cellular proteins FtsZ [34] and sortase A [35], as well as downregulation of quorum sensing and biofilm initiation [36], although its full breadth of antimicrobial mechanisms remains incompletely characterized. Curcumin's potential as an antimicrobial agent has been limited due to poor aqueous solubility, short half-life, and an unsightly color, limitations that have been overcome by nanoencapsulation in the form of curcumin nanoparticles (curc-np). Unlike free curcumin, curc-np are freely dispersible in water [37], exhibit sustained activity allowing 24 h dosing schedules in mice, and form colorless solutions [38]. Curc-np have demonstrated much greater in vitro activity against *S. aureus*, *Bacillus subtilis*, *E. coli*, *P. aeruginosa*, and *Aspergillus niger* [37], as well as against MRSA [38], in comparison to free curcumin. In vivo, curc-np have shown a significant reduction in bacterial burden compared to free curcumin when applied topically in MRSA-infected murine burn wounds, in addition to accelerating wound healing [38]. Together, these examples demonstrate that nanoparticle encapsulation enables the therapeutic use of previously unutilized molecules with intrinsic antimicrobial activity.

Another major approach for the employment of nanoparticles in the fight against skin and soft tissue infections includes the nanoencapsulation of readily-available antibiotics. Nanoparticle encapsulation can increase their antimicrobial activity through improved targeting, increased surface area-to-volume ratio, and potential for evasion of resistance mechanisms [22]. The benefits of nanoencapsulation have been demonstrated by ampicillin, which was incorporated into n-butylcyanoacrylate nanoparticles. In this form,

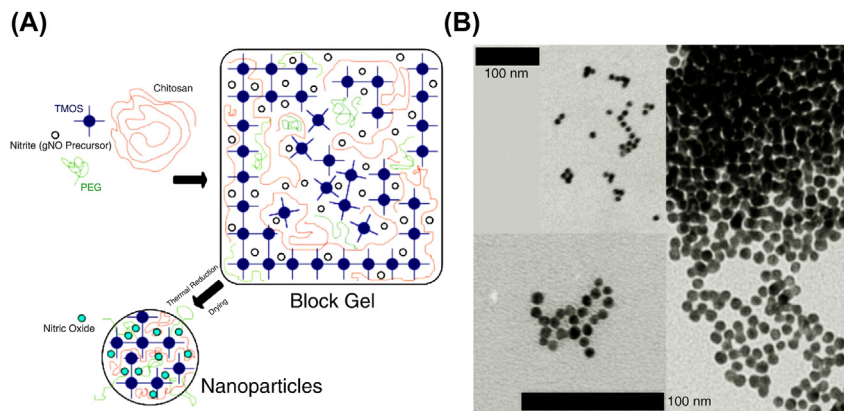


FIGURE 3.3 Nanoparticles can release encapsulated drugs through pores in their skeleton. (A) This schematic depicts a nitric oxide-releasing nanoparticle (NO-np). Tetramethyl orthosilicate (TMOS) is used to generate an O–Si–O lattice with interspersed chitosan polymer. Polyethylene glycol (PEG) controls pore size and thereby NO release rate from the lattice, while nitrite serves as a source of gaseous NO. These components exist in a sol–gel, which is then dried, and nitrite is converted to NO via thermal reduction. (B) This TEM image depicts NO-np with scale bar = 100 nm. Reproduced from Cabrales P, Han G, Roche C, Nacharaju P, Friedman AJ, Friedman JM. Sustained release nitric oxide from long-lived circulating nanoparticles. *Free Radical Biol Med* 2010;49:530–8, with permission from Elsevier.

ampicillin demonstrated potent antibacterial activity against highly virulent MRSA strains with mutated penicillin binding proteins and β -lactamase activity. The minimum inhibitory concentration (MIC) for *Enterococcus faecium* was also cut in half compared to treatment with ampicillin alone [39]. In addition to antibacterial agents, antifungal agents also can reap the benefits of nanoencapsulation. One such antifungal is Amphotericin B (AmB), a potent drug with severe side effects and potential for multiple organ damage that has thus far been restricted to parenteral delivery. AmB nanoparticles (AmB-np) have enabled topical delivery of this drug, which demonstrated potent in vitro activity against *Candida* spp. and inhibited biofilm formation. In vivo, topically applied AmB-np significantly reduced and even eliminated fungal burden in a *C. albicans* burn infection model in mice [40]. Thus, nanoparticles may offer a means to avoid systemic administration of a toxic drug, and also reduce potential for the generation of resistance during treatment of burn wound infections.

Nanoparticles for Inflammatory Disease

The pathogenesis of many of the most common dermatologic diseases, including atopic dermatitis, psoriasis, and even acne, are characterized by inappropriate and excessive inflammation [41,42]. Current treatments act to modulate inflammatory pathways and provide relief through a variety of therapeutic drugs, including corticosteroids, calcineurin inhibitors, methotrexate, retinoids, and biologics, all of which have been encapsulated by nanoparticles to demonstrate improved drug delivery [43–46].

Corticosteroids are a mainstay of treatment for atopic dermatitis and psoriasis, and they are used topically and orally to modulate inflammation. Three different corticosteroids—prednisolone, prednicarbate, and betamethasone—have been incorporated into SLNs. SLNs were found to significantly improve cutaneous penetration for all three drugs [47]. Additionally, specific targeting of the drugs to the epidermis was observed only with SLN encapsulation, particularly with prednisolone and prednicarbate. A study with fluocinolone, another corticosteroid, reported similar findings with specific epidermal targeting that only occurred when the drug was encapsulated by SLNs [48]. This is an important finding that may be useful in the treatment of diseases with known epidermal dysfunction. Epidermal targeting may also decrease the risk of atrophy, which is commonly seen with prolonged topical corticosteroid use, due to fibroblast inhibition and collagen cross-linking [49,50].

Tacrolimus, a calcineurin inhibitor with specific T-lymphocyte inhibition, has been encapsulated in liquid crystalline nanoparticles (LCNs) [51]. LCNs are

an additional variety of lipid-based nanocarrier made of monoolein, and they are known for permeation enhancement via ceramide extraction, thereby increasing lipid fluidity [52]. When encapsulated by LCNs, tacrolimus demonstrated increased cutaneous permeation and retention in mice. In addition, LCN-encapsulated tacrolimus outperformed tacrolimus alone in a murine psoriasis model by eliminating erythema and scale, as well as inducing a marked reduction in skin thickening and inflammatory cell infiltration on histology. These findings warrant further in vivo study for LCN encapsulation of dermatologic drugs, especially in the treatment of psoriasis [51].

Methotrexate is yet another important drug in the treatment of psoriasis, as well as other inflammatory and neoplastic diseases. Methotrexate can be delivered orally or parenterally, and its side effects are extensive, including liver toxicity, myelosuppression, and gastrointestinal (GI) distress [45]. Thus, topical administration is an attractive alternative with the potential for eliminating systemic side effects. In one recent study, methotrexate was delivered topically via NLC encapsulation in an in vitro porcine model [53]. By incorporating methotrexate into NLCs, the drug attained significantly increased cutaneous penetration, as well as enhanced concentration and permeation within the skin, compared to free methotrexate. Given their ability to increase cutaneous drug concentrations, these nanoparticles have the potential for targeted delivery of methotrexate with a lower risk of systemic side effects associated with its use. However, further studies are needed to determine whether improved in vitro penetration and permeation can translate into effective in vivo treatment. This investigation is important as topical methotrexate could increase patient compliance and satisfaction by providing a treatment option for psoriasis that is easier and more comfortable to use.

SLNs have also been loaded with adapalene, a third-generation retinoid for acne treatment that modulates cellular differentiation and keratinization as well as inflammatory processes. SLN encapsulation demonstrated sustained adapalene release over a 48 h period, and ex vivo experiments demonstrated significantly greater drug localization to the epidermis while decreasing and even eliminating systemic penetration, compared to adapalene alone [54].

In addition to enhancing the delivery of known therapeutics, nanotechnology has enabled the use of natural products in the treatment of acne. Chitosan is a polysaccharide derived from chitin, a component of crustacean exoskeletons, with antimicrobial and antiinflammatory properties that make it an ideal agent against *Propionibacterium acnes*, an important target for mitigating inflammation [55]. In one study, chitosan–alginate

nanoparticles displayed antiinflammatory properties by inhibiting IL6 and IL12 production in human monocytes and keratinocytes following *P. acnes* exposure, in addition to demonstrating direct activity against *P. acnes* via disruption of its cell wall [55]. Furthermore, these chitosan–alginate nanoparticles were loaded with benzoyl peroxide to exhibit superior activity against *P. acnes* with less eukaryotic toxicity compared to benzoyl peroxide alone. This demonstrates that nanoparticles can be engineered to wield a variety of biologic activities in one therapeutic structure, thereby conferring the ability to treat diseases through a multifaceted approach.

Nanoparticles for Cutaneous Neoplasms

According to the American Cancer Society (ACS), 80,100 new cases of skin cancer are projected to be diagnosed in 2015, excluding basal and squamous cell carcinomas. Including all skin cancers, more than 3 million cases are diagnosed annually [56]. Current treatments for skin cancers include surgery, immunotherapy, radiation, and cytotoxic chemotherapy. However, despite our available treatments, the ACS predicts 13,340 deaths from skin cancer in the United States in 2015, excluding basal and squamous cell carcinomas [56].

The treatment of skin cancer is complicated by cancer cells' rapid development of resistance to available treatments due to accelerated, unchecked cell replication. This can be demonstrated in melanoma patients who experience profound tumor regression with the revolutionary BRAF inhibitor therapy, only to exhibit disease progression within 6–8 months due to development of resistance [57]. A major mechanism of resistance includes overexpression of the multiple drug resistance (MDR)-conferring P-glycoprotein (otherwise known as MDR1), a nonspecific drug efflux pump [58]. Furthermore, cancer cells can activate antiapoptotic pathways, such as by overexpression of Bcl-2, a pro-survival antiapoptosis regulator [59].

Nanoparticles offer many advantages for cancer treatment by selectively targeting cancer cells, thereby minimizing treatment toxicity, as well as by overcoming resistance mechanisms for improved response to treatment. For example, nanoparticles can selectively accumulate in tumor tissue due to the overabundance of new vessels in the tumor that are hastily formed, irregular, and leaky. Nanoparticles less than 100 nm in diameter can pass through the relatively large gaps in these vessels, while normal vessels remain impermeable to most nanoparticles, with pores ranging 2–6 nm in size [60]. Poor lymphatic drainage systems, characteristic of tumor tissue, help retain nanoparticles in the tumor interstitium, further enhancing this effect. The inherent tumor-targeting capacity of nanomaterials

has been termed *enhanced permeability and retention* (EPR), and it has the potential to revolutionize treatments in the field of oncology [61]. In one study, FDA-approved abraxane, an albumin-bound paclitaxel-loaded nanoparticle, demonstrated increased antitumor activity compared to paclitaxel alone, while limiting taxane-associated toxicities such as myelosuppression, peripheral neuropathy, and GI distress [62]. Tumor cells can also be targeted by exploiting their tendency to overexpress folate receptors. For example, Pinhassi et al. studied folate-bearing arabinogalactan nanoparticles with methotrexate incorporated via an endosomally cleavable peptide, creating a target-activated release mechanism. These nanoparticles demonstrated 6.3-fold higher toxicity for folate receptor–rich tumor cells, compared to cells without increased folate receptor expression [63].

In addition to selective targeting, nanoparticles can be utilized to overcome cancer cells' resistance mechanisms. For example, chemotherapeutics can be co-delivered with chemosensitizers, agents that enhance tumor cells' sensitivity to the effects of chemotherapeutic drugs. This has been demonstrated by nanoencapsulation of paclitaxel with MDR1 small interfering RNAs (siRNAs). With siRNA-mediated downregulation of MDR1 efflux activity, paclitaxel treatment exhibited an enhanced cytotoxic effect against ovarian carcinoma cells. Furthermore, paclitaxel–siRNA nanoparticles delivered to paclitaxel-resistant cells produced a cytotoxic effect equivalent to the effect seen in cells that are paclitaxel sensitive [64]. In another study, nanoparticles delivered doxorubicin with Bcl-2 siRNAs to doxorubicin-resistant ovarian carcinoma cells, increasing doxorubicin cytotoxicity 132-fold [65].

As mentioned before, nanoparticles enable the delivery of drugs that were previously difficult or impossible to deliver for therapeutic benefit. One example is IL2, a cytokine glycoprotein that enhances tumor immunogenicity and tumor regression in metastatic melanoma. However, its use is limited by profound systemic side effects and a short half-life in vivo [66]. Recently, IL2 has been incorporated into polyethylenimine nanoparticles conjugated with folate, and peritumoral nanoparticle injection was shown to suppress tumor growth and prolong survival in mice with melanoma grafts [67]. This treatment increased tumor infiltration with CD8+, CD4+, and natural killer cells, while avoiding the severe multiorgan toxicity associated with high-dose IL2 treatments that are currently available.

In addition to enhancing chemotherapy and immunotherapy for cancer treatment, nanoparticles can be used to improve photodynamic therapy (PDT). PDT is a less invasive alternative to surgery that lacks the morbidity of radiation treatment. It relies on photosensitizers that

are preferentially taken up by tumor cells, in conjunction with a light beam aimed at the cancerous lesion. When the light strikes cells that have taken up a photosensitizing molecule, a chemical reaction occurs that induces cell injury and subsequent death. However, the selectivity of current photosensitizers is suboptimal and can put patients at risk for severe burns anywhere on the body that is exposed to light within 1–30 days of treatment, depending on the photosensitizer used [68]. For these reasons, it is not surprising that biomedical researchers are actively seeking improved photosensitizing agents.

One group has investigated HPPH (3-(1'-hexyloxyethyl)pyropheophorbide-a), a novel red-light-absorbing photosensitizer derived from chlorophyll-a [69]. It is effective for PDT with low skin phototoxicity, and when conjugated with cyanine dye it is also effective for near-infrared fluorescence imaging that can aid diagnosis and staging, as well as treatment. However, the dose of this conjugate required for therapy is eight- to 10-fold higher than that required for imaging due to undesired singlet oxygen quenching by cyanine dye. This problem can be overcome by encapsulating HPPH within polyacrylamide hydrogel nanoparticles in a 2:1 ratio with cyanine. When administered intravenously in BALB/c mice with subcutaneously grafted colon adenocarcinoma, the polyacrylamide 2:1 nanoconstructs demonstrated greater PDT treatment response compared to nonencapsulated HPPH–cyanine dye conjugates or HPPH alone. The nanoconstructs also served as an efficient tumor-imaging probe, demonstrating greater and more rapid tumor uptake compared to free cyanine. In addition to enhancing tumor uptake of photosensitizing agents via nanoencapsulation, which is aided by the EPR effect [69], uptake may be further augmented by conjugating nanoparticle carriers with specific tumor-targeting molecules, thereby offering even greater treatment efficacy and reduction of damage to nontarget tissues [70]. In another study, the photosensitizer 5,10,15,20-tetrakis(4-hydroxyphenyl)-21H,23H-porphine (tHPP) was loaded into iron oxide nanoparticles that were coated with chitosan and gold and conjugated with human epidermal growth factor receptor (hEGFR)-specific peptide for enhanced tumor-targeting effect. When used in PDT *in vitro*, these nanoparticles demonstrated peptide-specific uptake and subsequent cell death in ovarian adenocarcinoma cells. Additionally, the nanoparticles were administered to mice with subcutaneously grafted ovarian adenocarcinoma, where they exhibited preferential distribution in tumor cells and enhanced PDT response compared to tHPP alone or nanoencapsulated tHPP without hEGFR-specific peptide. The targeted nanoparticles decreased the required amount of tHPP by more than 56-fold, indicating the great potential for

nanotechnology to enhance the efficacy and specificity of PDT [70].

In addition to improving PDT for cancer treatment, nanoparticles may augment photothermal cancer therapy due to their unique physical properties. For example, nanoparticles formulated with a metallic shell overlying a glass surface exhibit plasmon excitation within the metallic shell when struck by a specific wavelength of light, thereby generating heat. These nanoparticles can also be conjugated with antibodies to enhance their tumor-targeting effect [17]. In one recent study, two squamous carcinoma cell lines and one benign epithelial cell line were incubated with anti-epidermal growth factor receptor (anti-EGFR) antibody-conjugated gold nanoparticles, which enabled selective laser destruction of malignant cells while using less than half of the light energy required to destroy benign cells. When no nanoparticles were present, no destruction was observed for all types of cells, even when using four times the laser energy required to kill malignant cells in the presence of nanoparticles [68]. These findings demonstrate the utility of nanoparticles as selective photothermal agents, which enable the improved use of laser therapy at lower powers and reduce the potential for damage to normal, healthy skin. Overall, nanoparticles can be engineered to include multiple biological properties and functions, enabling them to destroy cancer cells via a multifaceted approach. Nanoparticles offer enormous potential benefits by overcoming cancer cells' resistance mechanisms and offering improved cellular targeting, thereby limiting the negative side effects of cancer treatment.

Nanoparticles for Photoprotection

Another equally important way to fight skin cancer is prevention. Straightforward, cost-effective prevention can be achieved by protecting the skin from ultraviolet (UV) radiation. Excess UV radiation can lead to sunburn, photoaging, photoimmunosuppression, and photocarcinogenesis through the action of UVB (290–320 nm) and UVA (320–400 nm) [71]. While UVB radiation primarily produces sunburn and direct DNA damage (ie, thymidine dimers), UVA penetrates deeper into the skin and generates reactive oxygen species (ROS). ROS damage nucleic acids (especially guanine), lipids, and proteins. ROS also accelerate collagen breakdown and decrease collagen synthesis, thereby increasing the appearance of wrinkles [72].

The benefit of nanoparticle formulations in photoprotection is demonstrated by zinc oxide (ZnO) and titanium oxide (TiO₂). Both are highly effective UV filters that reflect and scatter UV radiation, and they have been used for decades in commercially available sunscreens. However, their use was previously limited as they also reflected light in the visible spectrum,

creating an undesirable white discoloration of the skin, in addition to leaving a grainy residue when applied. Commercially available sunscreens with ZnO and TiO₂ nanoparticles have overcome these challenges by increasing transparency of the formulation while optimizing photoprotection with particles that are 40–60 nm in size [73]. Because these nanoparticles do not disperse incident light, patients are more likely to adhere to sunscreen application, thereby increasing the opportunity for skin cancer prevention. Additionally, smaller particle sizes reflect and scatter UV radiation more efficiently, improving skin protection [71]. Finally, as with their non-nanoparticle formulations, ZnO and TiO₂ nanoparticles do not penetrate the stratum corneum [74]. Rather, they remain on the skin surface, as desired, to exert photoprotective effects.

Nanoliposomes

Liposomes are spherical phospholipid bilayers, analogous to those of cell membranes, and their amphiphilic nature enables encapsulation of both hydrophilic and hydrophobic substances. Other advantages include increased drug stability, as well as promotion of drug uptake by targeted tissues [75,76]. Despite these advantages, a major drawback of liposomes for drug delivery is their aggregation within the stratum corneum, resulting in limited topical penetration, and thereby ineffective delivery of the encapsulated drug [77]. This limitation has been overcome by nanoliposomes that, like nanoparticles, can be engineered to deliver a variety of therapeutic compounds and selectively affect molecular targets. For example, nanoliposomes can be designed to release their contents only at a desired pH or temperature, and they can be synthesized with surface ligands to influence phagocytosis by specific cell types [78]. The main therapeutic challenge with nanoliposomes is their readily deformable structure and intrinsic instability. They change shape and may even lyse when compressed or vigorously shaken, and can readily aggregate, precipitate, and fuse into non-nanosized structures, disrupting an evenly dispersed emulsion intended for topical therapy [78]. Despite these shortcomings, several recent studies have indicated their therapeutic potential.

Nanoliposomes for Cutaneous Neoplasms

Nanoliposomes have been employed for the delivery of siRNAs, a therapy that is difficult to administer due to rapid nuclease degradation in vivo. Nanoliposomes can overcome this limitation and harness siRNAs for gene knockdown therapy in melanoma by protecting and delivering V^{600E}B-raf and Akt3 siRNAs directly to cancer cells. B-raf and Akt3 signaling cascades regulate the cell

cycle, and deregulation of these cascades commonly occurs in the development of melanoma. For example, the B-raf gene contains the activating V600E mutation in approximately 60% of malignant melanomas, resulting in 10.7 times greater signaling activity compared to B-raf in normal cells [79]. The ability of siRNAs to target specific genes is therapeutically desirable, as agents that target both normal and mutant B-raf genes and agents that target all three Akt isoforms demonstrate greater side effects.

In one study, cationic nanoliposomes loaded with V^{600E}B-Raf and Akt3 siRNAs were applied to melanomas in in vitro human skin, and in vivo mouse skin models, using a low-frequency ultrasound to enhance penetration. Together, the dual siRNA therapies led to cooperative growth inhibition of melanoma cells [79]. Another study investigated folate-conjugated nanoliposomes loaded with doxorubicin against murine lung carcinoma [80]. Fluorescence microscopy confirmed internalization of liposomes by folate-overexpressing cancer cells, with doxorubicin release into the cytoplasm and doxorubicin detection in the nucleus of cancer cells shortly thereafter. In contrast to free doxorubicin, liposomal doxorubicin uptake was unaffected by P-glycoprotein efflux. Higher drug levels in whole cells and nuclei of both MDR and non-MDR cancer cells were also achieved with folate-targeted liposomes. These findings indicate the potential for increased specificity of cancer treatments, as well as the potential to evade common resistance mechanisms with nanoliposome formulations. However, it is important to bear in mind the aforementioned limitations of nanoliposomes, and remember that nanoliposomes were topically applied in these experiments under ideal conditions. Due to complications of lysis and aggregation within therapeutic nanoliposome emulsions, future research must ensure that topical formulations have adequate stability for practical use.

Nanoemulsions

Topical emulsions are made by dispersing either oil in water, or water in oil with a surfactant, and are widely used in dermatology. Since the active ingredient dissolves in the continuous phase, oil-in-water emulsions are best for delivering water-soluble drugs, and water-in-oil emulsions are better for lipid-soluble agents [81]. Following application, the aqueous phase evaporates, leaving active ingredients on the skin with an occlusive lipophilic film to aid in absorption. Nanoemulsions are made with emulsified droplets ranging on the nanoscale (<100 nm), and have been shown to increase stability and bioavailability of active ingredients, thereby lowering required doses. Additionally, emulsions that are typically opaque become transparent

when the dispersed droplets are less than 70 nm in diameter, improving cosmesis and patient satisfaction [82,83].

Nanoemulsions for Acne and Actinic Keratoses

Topical retinoids, a popular treatment for both acne and photoaging, are one example of improved drug delivery via nanoemulsion. Microencapsulated retinol (0.1%) with a triple nanoemulsion was more effective at combating structural and biochemical signs of skin aging than the leading commercial product (tretinoin 0.1%) or microencapsulated retinol alone [84]. Nanoemulsions can also be used in conjunction with PDT, as demonstrated by a nanoemulsion containing the common photosensitizer, 5-aminolaevulinic acid (ALA), used with PDT for ablation of actinic keratoses (AKs). A phase III clinical trial of AK treatment with ALA (10%) nanoemulsion and PDT demonstrated an excellent lesion clearance rate as high as 96% with optimal light sources, even though the nanoemulsion contained less ALA than non-nanoemulsions (20%), which are currently the first line of care [85]. Two additional trials have demonstrated ALA nanoemulsion with PDT to be more effective than methyl-5-aminolaevulinate (MAL) with PDT, another first-line treatment for AKs [86,87].

Nanoemulsions for Infectious Disease

As mentioned in this chapter, antibiotic resistance is on the rise, and the small size and multimechanistic potential of nanomaterials are ideal for combating a variety of pathogens. For example, a recent study investigated the use of NB-201, a simple antimicrobial nanoemulsion of vegetable oil, water, surfactants, and alcohol, against *P. aeruginosa*—infected murine burn wounds [88]. Topical NB-201 reduced bacterial burden by 1000-fold, outperforming mafenide acetate, the standard of care. NB-201 also attenuated neutrophil sequestration, reduced hair follicle cell apoptosis, and, unlike mafenide acetate, significantly diminished proinflammatory cytokines IL1 β and IL6. Thus, the nanoemulsion exhibited potent antimicrobial activity against a robust pathogen, and even demonstrated antiinflammatory effects, which are ideal to promote faster wound healing.

Another antimicrobial nanoemulsion, NB-002 was tested against four different dermatophytes responsible for skin, hair, and nail infections (*Trichophyton rubrum*, *Trichophyton mentagrophytes*, *Epidermophyton floccosum*, and *Microsporum* spp.), as well as 12 other genera of filamentous fungi [89]. Fungal infections are difficult to treat topically, especially when infecting the nails, and oral treatments such as terbinafine and azoles can have undesirable side effects such as liver toxicity, cardiac side effects, and drug–drug interactions. NB-002 is an oil-in-water emulsion of

cetylpyridinium chloride, a molecule found in mouthwashes and toothpastes, and its cationic quaternary ammonium structure is oriented at the oil–water interface for enhanced stability. When compared to ciclopirox, tolnaftate, naftifine, terbinafine, itraconazole, and griseofulvin, NB-002 was the only antifungal that was consistently fungicidal against all four dermatophytes. The other 12 filamentous fungi were almost all susceptible to ≤ 4 $\mu\text{g/mL}$ of NB-002, with MICs ranging from 0.06 to 8 $\mu\text{g/mL}$. NB-002 was even fungicidal against azole-susceptible and azole-resistant *C. albicans* yeast isolates. The broad coverage offered by NB-002, including fungicidal activity against resistant fungi, warrants further investigation into nanoemulsions for infectious disease.

Nanoscaffold Wound Dressings

In the United States alone, chronic wounds affect approximately 6.5 million patients, causing significant morbidity and mortality, especially in the setting of chronic disease. Acute wounds in the surgical and trauma settings are also a major healthcare concern, and postsurgical wound infections remain the most expensive complications following surgery [90].

Proper wound healing is essential for minimizing healthcare costs and preventing the development of chronic wounds. This requires an inflammatory phase of appropriate duration, free of complications such as infection, as well as an adequate proliferative phase during which a strong, functional extracellular matrix (ECM) is restored. To aid the wound-healing process, nanoscaffold wound dressings have been developed with antimicrobial properties, as well as an intricate nanostructure that imitates the topographical features of the ECM. By mimicking the structure of the lost ECM, nanoscaffold wound dressings promote epithelial migration for reepithelialization. These dressings also facilitate fibroblast homing for formation of endogenous ECM, providing a steady foundation on which to form healthy granulation tissue.

One recent study of nanoscaffold wound dressings investigated a bacterial cellulose nanofiber matrix impregnated with silver nanoparticles (Ag-np) for added antimicrobial activity. This dressing demonstrated activity against *E. coli*, *S. aureus*, and *P. aeruginosa*; facilitated attachment and growth of keratinocytes; and provided an ideal moist, absorbent barrier with high wet strength [91]. This dressing was made by synthesizing Ag-np directly onto the cellulose nanofibers, allowing sustained release of silver ions while preventing the release of free Ag-np. This is an effective approach as Ag-np microbicidal activity has been attributed to the release of free silver ions, with negligible activity attributed to the particles themselves, and stabilization of Ag-np within the

nanoscaffold dressing allows sustained release of silver ions into nearby tissue [92]. In another recent study, a PGLA—silk fibroin nanofiber dressing was investigated in diabetic rats, where it demonstrated an increased reduction in wound size compared to traditional dressings, in addition to increased fibroblast attachment and proliferation [93]. Another study investigated polyurethane nanofiber dressing which improved dermal organization and accelerated reepithelialization in guinea pigs, in addition to creating a moist, oxygenated environment while promoting exudate drainage [94]. Together, these findings demonstrate that nanomaterials can be harnessed to increase the efficacy of traditional wound dressings, thus presenting the opportunity to decrease the morbidity and mortality associated with wounds.

COSMETIC ROLES OF NANOMATERIALS

Thus far, our discussion of nanomaterials has largely been focused on drug delivery with an emphasis on promoting drug stabilization, bioavailability, and targeting. Nanomaterials are also attractive for the optimization of cosmetic formulations, offering benefits to enhance color, transparency, solubility, and chemical reactivity [95].

Nanoemulsions for Cosmetic Dermatology

As previously mentioned, nanoemulsions increase the stability and bioavailability of their active ingredients, while offering increased transparency and improved cosmesis of topical formulations. These properties have been applied to enhance a variety of cosmetics, including those containing antioxidants. Many cosmetic products contain antioxidants, such as vitamins C and E, which have the potential to protect the skin and decrease aging by neutralizing the effects of ROS and UV radiation. However, it has been demonstrated that some antioxidants do not maintain *in vivo* activity when applied in current topical formulations. In some cases, antioxidant content may be advantageous for marketing purposes while offering little, if any, consumer benefit. Therefore, it is important to ensure that antioxidants are effectively formulated for cosmetic products with adequate reactivity, concentration, stability, and topical penetration [96].

In one recent study, aqueous extracts of the antioxidants propolis (a botanical substance utilized by honeybees) and lycopene (a phytochemical found in red fruits and vegetables) were incorporated into a nanoemulsion that demonstrated sustained release of active ingredients over at least 8 h. The nanoemulsion outperformed control suspensions in the treatment of UV-burned

guinea pigs, significantly reducing the activity of collagenase and decreasing markers of inflammation by 75–100% [97]. In addition to products with UV protection, topical products offering increased moisture are in high demand, in both cosmetic applications and the treatment of skin disorders. As such, another recent study investigated rice bran oil, an antioxidant component of sunscreens and antiaging products. When delivered in a nanoemulsion, it increased moisture by 38% in normal skin patients and by 30% in patients with atopic dermatitis or psoriasis [98].

Stratum corneum lipids have also been included in nanoemulsions to fortify their barrier and decrease transepidermal water loss. For example, one study incorporated ceramide 3, cholesterol, and palmitic acid into an oil-in-water nanoemulsion with a net positive charge for increased epithelial membrane interaction. By enhancing the stratum corneum's barrier properties, this nanoemulsion demonstrated a significant increase in skin hydration and elasticity in healthy patients, without causing erythema [99].

Nanopigments for Cosmetic Dermatology

Nanopigments are nanosized aggregates of metals and metallic compounds that impart color, and their use has gained substantial interest in makeup formulation. Makeup includes a wide variety of cosmetic products that are utilized to smooth skin tone and conceal imperfections caused by comedones, papules, erythema, and areas of hypo- or hyperpigmentation. Additionally, makeup can be used to enhance aesthetic appearance with products such as eye shadow and lipstick. Thus, a variety of colors and tones are desired in the formulation of these cosmetic products.

By mixing cyan, magenta, yellow, and black, it is possible to create the full color spectrum, and nanopigments have demonstrated superiority over their micro-pigment counterparts in generating a wider array of hues [100]. With pigments on the nanoscale, both quantum and optical properties must be considered, including absorption, scattering, and emission, to predict the variety of cosmetic outcomes. In one approach to cosmetic nanopigments, Alfano et al. has suggested the employment of a two-color system. First, a color similar to the consumer's skin is created using a variety of pigments, including ZnO, TiO₂, and magnesium oxide nanoparticles. Then, a second color can be used to counteract undesirable colors. For example, silver and gold nanospheres can be optimized to reflect blue and green hues, which neutralize red tones reflected by areas of erythema [101]. In fact, every color of the spectrum can be achieved with metal nanoparticles due to surface plasmon activity, which enables

absorption of certain colors and emission or reflection of others. Silver nanospheres with 40 nm diameter appear blue, 25 nm gold nanospheres are red, and 100 nm gold nanospheres are yellow, demonstrating the variety of color achieved by modulating metal composition and size [101]. Ha et al. has also described gold, silver, and gold–silver alloy nanoparticles, which produce a variety of colors. They can be designed as nanospheres, nanorods, nanoshells, nanocubes, and nanoprisms for a wide variety of cosmetic applications [102].

DIAGNOSTIC ROLES OF NANOMATERIALS

Nanomaterials have the potential for significant impact in the diagnosis of cutaneous neoplasms, as thus far, noninvasive diagnosis has been limited to visual inspection. The use of dermatoscopes has increased diagnostic accuracy, and total body photography may be used in patients with multiple atypical nevi to establish a baseline, identify changes, and minimize unnecessary biopsies. However, when a lesion has raised significant clinical suspicion, a biopsy is almost always required. Current research has demonstrated the ability to image potentially malignant lesions noninvasively using nanomaterials, in conjunction with various imaging techniques [103].

Quantum Dots for Diagnostic Dermatology

Quantum dots are derived from semiconductor materials, including cadmium selenide, cadmium telluride, indium phosphide, and indium arsenide. They are useful as fluorescent markers following excitation by an external light source, and can be used to specifically target tumor biomarkers [17]. Their bright fluorescence signals are stable for hours at a time, allowing for continuous imaging of potentially malignant tissue [103]. Following injection into tumors, quantum dots have also been utilized to identify sentinel lymph nodes and enhance precision in mapping lymph nodes [104]. In addition to establishing early diagnosis of tumors, quantum dots may be utilized in Mohs surgery for visualization, as well as in PDT for both visualization and photosensitization, due to their ability to generate free radicals [17]. Limitations remain for the use of quantum dots in the diagnosis of cutaneous neoplasms, as heavy metal exposure is cytotoxic. This can be circumvented by coating quantum dots with PEG, which has been shown to decrease activation of inflammatory cytokines and prevent cytotoxicity. Despite this finding, quantum dots are the smallest nanomaterials (usually $\leq 10 \mu\text{m}$), and their extensive permeation of tissues raises fears

of systemic absorption. Thus, several toxicological studies will be required, focusing on both local and systemic effects, before quantum dots can potentially be used for the diagnosis of cutaneous neoplasms [105].

Nanoparticles for Diagnostic Dermatology

Nanoparticles are desirable for cancer diagnosis due to selective tumor targeting. This can be achieved by the EPR effect, as described in this chapter, as well as via nanoparticle surface modification. For example, gold nanoparticles (Au-np) have been conjugated with melanocyte-stimulating hormone (MSH), tripling their targeting efficiency for melanoma tumors in mice compared to PEG-conjugated Au-np. When combined with photoacoustic tomography (PAT), Au-np have shown promise for cancer detection [106]. PAT is a hybrid biomedical imaging technique based on the photoacoustic effect, whereby absorbed light energy can be transformed into acoustic energy [107]. When a pulsed light source strikes a photoabsorbent contrast agent, such as Au-np, the electromagnetic energy leads to thermal expansion that generates acoustic waves, detectable by high-frequency ultrasound. In fact, agents with a strong photoacoustic effect can be used to generate shock waves that kill cancerous cells. For example, folate-conjugated gold nanorods (Au-NRs) were used against human epithelial carcinoma tumors in mice. When subjected to laser irradiation, tumor volume was markedly decreased and tumor cells demonstrated a much lower growth rate [107] (Fig. 3.4).

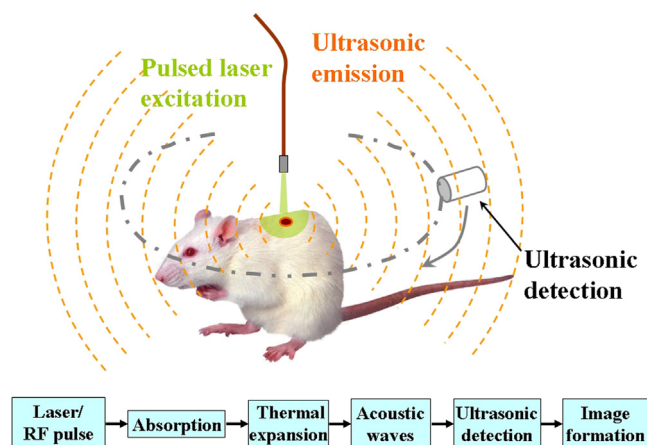


FIGURE 3.4 Nanoparticles can be used in photoacoustic tomography for cancer detection. When a pulsed light source strikes a photo-absorbent nanoparticle, the electromagnetic energy leads to thermal expansion that generates acoustic waves, detectable by high-frequency ultrasound. Reproduced from © 2007 User:Bme591wiki-project, Schematic illustration of photoacoustic imaging, Wikimedia Commons: http://en.wikipedia.org/wiki/Image:PASchematics_v2.png. License: <https://creativecommons.org/licenses/by-sa/3.0/legalcode>.

Another diagnostic modality includes radiolabeled silica nanoparticles, which have recently been approved for clinical trials in tumor targeting, differential tumor burden, nodal mapping, and determination of lymphatic drainage patterns [108]. These dye-encapsulating particles are surface functionalized with cyclic arginine–glycine–aspartic acid peptide ligands as well as radioiodine. The nanoparticles demonstrate high specificity for $\alpha v \beta 3$ integrin, a marker of neovascularization in melanoma that has enabled the detection of melanoma xenografts in mice. Furthermore, the nanoparticles enabled visualization of tumor burden, as well as lymph node mapping with drainage patterns in real time, demonstrating the potential for staging metastatic melanoma in the clinical setting [108].

SAFETY CONSIDERATIONS

Despite the plethora of potential benefits offered by nanomaterials, concerns remain regarding possible side effects, which will be discussed in detail later in this book. With the scientific literature that is currently available, it is difficult to address these concerns, as many studies provide conflicting evidence. A major problem includes the lack of standardized methods to assess local and systemic side effects of nanomaterials, and current in vitro methods may not be sufficient for evaluating in vivo effects. As such, the data regarding toxicology of nanomaterials is incomplete, and further development of methods for toxicological evaluation is warranted.

CONCLUSIONS

Nanomaterials exhibit a wide range of applications in therapeutic, cosmetic, and diagnostic dermatology, and overall they hold great promise to advance the field of medicine. As described, nanomaterials offer many useful properties due to their large surface area–to-volume ratio, unique surface reactivity, and ability to overcome stability and solubility barriers of active agents via nanoencapsulation and sustained-release activity. Furthermore, their capacity for specific molecular targeting and selective accumulation within tissues can enhance the specificity of current interventions. The studies presented have demonstrated that all of these properties can be exploited to provide better drug delivery, improved cosmetic outcomes, and increasingly effective imaging modalities to augment cancer detection. The full range of benefits offered by nanomaterials in dermatology will be further explored throughout this book. While the data are promising, the field of nanodermatology is lacking in human clinical trials, which are

necessary to ensure translatability of nanomaterials from the bench to the bedside. Further studies are needed to explore the clinical utility of nanomaterials in dermatology and also to elucidate their potential risks for toxicity.

Glossary

5-aminolaevulinic acid A photosensitizer used with a blue light source for photodynamic therapy in the treatment of actinic keratoses.

$\alpha v \beta 3$ integrin A biomarker of tumor-associated angiogenesis.

β -lactamase A bacterial enzyme that disrupts the 4-membered β -lactam ring of β -lactam antibiotics, including penicillins, cephalosporins, and carbapenems.

Abraxane An albumin-bound paclitaxel-loaded nanoparticle used in the treatment of a variety of cancers, including off-label use in melanoma.

Akt3 A serine–threonine kinase involved in cell proliferation, differentiation, and apoptosis; is encoded by AKT3, an oncogene.

Amphotericin B An antifungal drug that binds ergosterol in fungal membranes, causing leakage of cell components and cell death.

Azoles A class of antifungal drugs, including itraconazole, which inhibit ergosterol synthesis and thereby fungal membrane formation.

Bcl-2 An antiapoptotic signaling protein encoded by BCL2, an oncogene.

Benzoyl peroxide A topical drug that oxidizes bacterial proteins, thereby reducing the number of anaerobic skin bacteria; used in the treatment of acne vulgaris and acne rosacea.

Biofilm A resistance mechanism employed by microbes to avoid contact with antibiotics whereby cells adhere to each other on a surface, embedded within a matrix of extracellular polymeric substance.

B-raf A serine–threonine kinase involved in cell proliferation and differentiation, which is encoded by BRAF, an oncogene.

V600E B-raf B-raf protein with the V600E mutation, which leads to 10.7 times greater activity, thereby promoting oncogenesis.

Calcineurin inhibitors A class of immunosuppressant drugs, including tacrolimus, which block interleukin-2 (IL2) transcription and thereby T-cell activation.

Chemosensitizer An agent that enhances tumor cell sensitivity to the effects of chemotherapeutic drugs.

Chitosan A polysaccharide derived from the deacetylation of chitin, a component of crustacean exoskeletons, with favorable structural properties as well as antimicrobial activity against bacteria, fungi, and viruses.

Collagenase An enzyme that degrades the peptide bonds of collagen.

Corneocytes Terminally differentiated keratinocytes in the stratum corneum.

Corticosteroids A wide class of immunosuppressant drugs that bind the glucocorticoid receptor and inhibit mechanisms of both acquired and innate immunity; includes betamethasone, fluocinolone, prednicarbate, and prednisolone.

Curcumin Otherwise known as diferuloylmethane, a component of turmeric with antimicrobial, antiinflammatory, and antineoplastic activity.

Dermatophytes Three genera of fungi that infect the skin, hair, and nails: *Trichophyton*, *Epidermophyton*, and *Microsporum*.

Doxorubicin A chemotherapeutic drug that intercalates DNA and is used in the treatment of a variety of cancers.

Enhanced permeability and retention A phenomenon whereby enhanced permeability of tumor vasculature enables the accumulation of nanomaterials in tumors.

Granulation tissue Highly vascularized connective tissue composed of type III collagen, which is generated following a wound.

Inflammasome A multiprotein complex and agent of the innate immune system that promotes the release of inflammatory cytokines.

Keratinization The process by which viable cells of the epidermis become part of the stratum corneum.

Keratinocytes Keratin-producing cells of the epidermis.

Mafenide acetate A topical antimicrobial treatment for burn wounds.

Methotrexate An immunosuppressant and antineoplastic drug that inhibits folate metabolism; used in the treatment of a variety of cancers as well as psoriasis and rheumatoid arthritis.

Methyl-5-aminolaevulinate A photosensitizer used with a red light source for photodynamic therapy in the treatment of actinic keratoses.

Mohs surgery A surgical technique for locally invasive skin cancers that involves continuous histological examination of excised tissues and mapping of residual tumor, thereby allowing complete tumor excision with maximal preservation of surrounding tissue.

Multidrug resistance protein 1 See P-glycoprotein.

Nanodermatology The use of nanomaterials for dermatologic applications.

Nanomaterials Matter that has a particulate size on the nanoscale.

Nanoscale A size range from 1 to 100 nanometers.

NB-002 An oil-in-water nanoemulsion of cetylpyridinium chloride.

NB-201 A nanoemulsion of vegetable oil, water, surfactants, and alcohol.

Paclitaxel A chemotherapeutic drug that inhibits microtubule disassembly and is used in the treatment of a variety of cancers.

P-glycoprotein Otherwise known as multidrug resistance protein 1, a cell membrane protein that pumps foreign substances, including drugs, out of cells, thereby conferring resistance to chemotherapy.

Penicillin binding proteins A group of bacterial proteins and therapeutic targets of β -lactam antibiotics that, when mutated or overproduced, may contribute to β -lactam resistance.

Photoacoustic effect The generation of acoustic waves following light absorption.

Photoacoustic tomography A hybrid biomedical imaging technique based on the photoacoustic effect. It utilizes a contrast agent with optical absorption properties as well as a pulsed light source. Electromagnetic energy absorbed by the contrast agent leads to thermal expansion, which generates acoustic waves, detectable by high-frequency ultrasound.

Photodynamic therapy The use of light-sensitive molecules (photosensitizers) coupled with a light source to cause selective destruction of malignant or other diseased cells.

Photosensitizer A molecule preferentially taken up by tumor cells that, when struck by light of an appropriate wavelength, initiates a chemical reaction that leads to cellular death.

Pilosebaceous unit A dermal structure that includes a hair follicle, sebaceous gland, and erector pili muscle.

Plasmon A quantum of plasma oscillation.

Quorum sensing A coordinated signaling system within a local population of bacteria, which is used to modulate gene expression based on population density.

Retinoids A class of drugs derived from vitamin A, including topical drugs used in the treatment of acne vulgaris such as adapalene and tretinoin.

Stratum corneum The outermost layer of the epidermis that is composed of nonviable cells filled largely with keratin, interspersed with intercellular lipids.

Terbinafine An antifungal drug that inhibits sterol synthesis and thereby fungal membrane formation.

List of Acronyms and Abbreviations

A. baumannii *Acinetobacter baumannii*
ACS American Cancer Society
Ag-np Silver nanoparticles
AK Actinic keratosis
ALA 5-aminolaevulinic acid
AmB Amphotericin B
AmB-np Amphotericin B nanoparticles
Au-np Gold nanoparticles
AuNR Gold nanorods
C. albicans *Candida albicans*
Candida spp. *Candida* species
Curc-np Curcumin nanoparticles
ECM Extracellular matrix
E. coli *Escherichia coli*
EGFR Epidermal growth factor receptor
EPR Enhanced permeability and retention
GI Gastrointestinal
IL Interleukin
LCN Liquid crystalline nanoparticle
LDC Lipid drug conjugate
MAL Methyl-5-aminolaevulinate
MDR Multiple drug resistance
MDR1 Multidrug resistance protein 1
MIC Minimum inhibitory concentration
MRSA Methicillin-resistant *Staphylococcus aureus*
MSH Melanocyte stimulating hormone
NLC Nanostructured lipid carriers
NO Nitric oxide
NO-np Nitric oxide releasing nanoparticles
P. acnes *Propionibacterium acnes*
P. aeruginosa *Pseudomonas aeruginosa*
PAT Photoacoustic tomography
PDT Photodynamic therapy
PEG Polyethylene glycol
RNOS Reactive nitrogen oxide species
ROS Reactive oxygen species
S. aureus *Staphylococcus aureus*
siRNA Small interfering RNA
SLN Solid lipid nanoparticle
TEM Transmission electron microscopy
TiO₂ Titanium oxide
UV Ultraviolet
ZnO Zinc oxide

References

- [1] National nanotechnology initiative: frequently asked questions. <http://www.nano.gov/nanotech-101/nanotechnology-facts> [accessed on 20.08.15].
- [2] Kim BY, Rutka JT, Chan WC. Nanomedicine. *New Engl J Med* 2010;363(25):2434–43.
- [3] Alvarez-Román R, Naik A, Kalia Y, Guy RH, Fessi H. Skin penetration and distribution of polymeric nanoparticles. *J Control Release* 2004;99(1):53–62.
- [4] Zhou W, Wang Y, Jian J, Song S. Self-aggregated nanoparticles based on amphiphilic poly (lactic acid)-grafted-chitosan copolymer for ocular delivery of amphotericin B. *Int J Nanomedicine* 2013;8:3715.
- [5] Janát-Amsbury M, Ray A, Peterson C, Ghandehari H. Geometry and surface characteristics of gold nanoparticles influence their biodistribution and uptake by macrophages. *Eur J Pharm Biopharm* 2011;77(3):417–23.

- [6] Baroli B. Penetration of nanoparticles and nanomaterials in the skin: fiction or reality? *J Pharm Sci* 2010;99(1):21–50.
- [7] Elias PM, Menon GK. Structural and lipid biochemical correlates of the epidermal permeability barrier. *Adv lipid Res* 1991;24: 1–26.
- [8] Bouwstra JA, Ponc M. The skin barrier in healthy and diseased state. *Biochim Biophys Acta (BBA)-Biomembranes* 2006;1758(12): 2080–95.
- [9] Weiss SC. Conventional topical delivery systems. *Dermatol Ther* 2011;24(5):471–6.
- [10] Tan Q, Liu W, Guo C, Zhai G. Preparation and evaluation of quercetin-loaded lecithin-chitosan nanoparticles for topical delivery. *Int J Nanomed* 2011;6:1621.
- [11] Lademann J, Richter H, Teichmann A, Otberg N, Blume-Peytavi U, Luengo J, et al. Nanoparticles—an efficient carrier for drug delivery into the hair follicles. *Eur J Pharma Biopharm* 2007;66(2):159–64.
- [12] Fang C-L, Aljuffali IA, Li Y-C, Fang J-Y. Delivery and targeting of nanoparticles into hair follicles. *Ther Deliv* 2014;5(9):991–1006.
- [13] Patzelt A, Richter H, Knorr F, Schäfer U, Lehr C-M, Dähne L, et al. Selective follicular targeting by modification of the particle sizes. *J Control Release* 2011;150(1):45–8.
- [14] Kierszenbaum AL, Tres L. Histology and cell biology: an introduction to pathology. Elsevier Health Sciences; 2015.
- [15] Lademann J, Weigmann H-J, Rickmeyer C, Barthelmes H, Schaefer H, Mueller G, et al. Penetration of titanium dioxide microparticles in a sunscreen formulation into the horny layer and the follicular orifice. *Skin Pharmacol Physiol* 1999;12(5):247–56.
- [16] Rolland A, Wagner N, Chatelus A, Shroot B, Schaefer H. Site-specific drug delivery to pilosebaceous structures using polymeric microspheres. *Pharm Res* 1993;10(12):1738–44.
- [17] Boixeda P, Feltes F, Santiago J, Paoli J. Future prospects in dermatologic applications of lasers, nanotechnology, and other new technologies. *Actas Dermo-Sifiliográficas (English Edition)* 2015;106(3):168–79.
- [18] Müller R, Petersen R, Hommoss A, Pardeike J. Nanostructured lipid carriers (NLC) in cosmetic dermal products. *Adv Drug Deliv Rev* 2007;59(6):522–30.
- [19] Wilczewska AZ, Niemirowicz K, Markiewicz KH, Car H. Nanoparticles as drug delivery systems. *Pharmacol Rep* 2012;64(5): 1020–37.
- [20] Huh AJ, Kwon YJ. “Nanoantibiotics”: a new paradigm for treating infectious diseases using nanomaterials in the antibiotics resistant era. *J Control Release* 2011;156(2):128–45.
- [21] Landriscina A, Rosen J, Friedman AJ. Biodegradable chitosan nanoparticles in drug delivery for infectious disease. *Nanomedicine* 2015;10(10):1609–19.
- [22] Pelgrift RY, Friedman AJ. Nanotechnology as a therapeutic tool to combat microbial resistance. *Adv Drug Deliv Rev* 2013; 65(13):1803–15.
- [23] De Groote MA, Fang FC. NO inhibitions: antimicrobial properties of nitric oxide. *Clin Infect Dis* 1995;21(Suppl. 2):S162–5.
- [24] Liew F, Cox F. Nonspecific defence the role of nitric oxide. *Parasitol Today* 1991;7(3):17–21.
- [25] Bogdan C. Nitric oxide and the immune response. *Nat Immunol* 2001;2(10):907–16.
- [26] Friedman A, Blecher K, Sanchez D, Tuckman-Vernon C, Gialanella P, Friedman JM, et al. Susceptibility of gram-positive and-negative bacteria to novel nitric oxide-releasing nanoparticle technology. *Virulence* 2011;2(3):217–21.
- [27] Martinez LR, Han G, Chacko M, Mihi MR, Jacobson M, Gialanella P, et al. Antimicrobial and healing efficacy of sustained release nitric oxide nanoparticles against *Staphylococcus aureus* skin infection. *J Invest Dermatol* 2009;129(10):2463–9.
- [28] Han G, Martinez LR, Mihi MR, Friedman AJ, Friedman JM, Nosanchuk JD. Nitric oxide releasing nanoparticles are therapeutic for *Staphylococcus aureus* abscesses in a murine model of infection. *PLoS One* 2009;4(11):e7804.
- [29] Schairer DO, Martinez LR, Blecher K, Chouake JS, Nacharaju P, Gialanella P, et al. Nitric oxide nanoparticles: pre-clinical utility as a therapeutic for intramuscular abscesses. *Virulence* 2012; 3(1):62–7.
- [30] Mihi MR, Sandkovsky U, Han G, Friedman JM, Nosanchuk JD, Martinez LR. The use of nitric oxide releasing nanoparticles as a treatment against *Acinetobacter baumannii* in wound infections. *Virulence* 2010;1(2):62–7.
- [31] Hetrick EM, Shin JH, Paul HS, Schoenfisch MH. Anti-biofilm efficacy of nitric oxide-releasing silica nanoparticles. *Biomaterials* 2009;30(14):2782–9.
- [32] Hetrick EM, Shin JH, Stasko NA, Johnson CB, Wespe DA, Holmuhamedov E, et al. Bactericidal efficacy of nitric oxide-releasing silica nanoparticles. *ACS Nano* 2008;2(2):235–46.
- [33] Macherla C, Sanchez DA, Ahmadi MS, Vellozzi EM, Friedman AJ, Nosanchuk JD, et al. Nitric oxide releasing nanoparticles for treatment of *Candida albicans* burn infections. *Front Microbiol* 2012;3.
- [34] Rai D, Singh J, Roy N, Panda D. Curcumin inhibits FtsZ assembly: an attractive mechanism for its antibacterial activity. *Biochem J* 2008;410:147–55.
- [35] Park B-S, Kim J-G, Kim M-R, Lee S-E, Takeoka GR, Oh K-B, et al. *Curcuma longa* L. constituents inhibit sortase A and *Staphylococcus aureus* cell adhesion to fibronectin. *J Agric Food Chem* 2005;53(23):9005–9.
- [36] Rudrappa T, Bais HP. Curcumin, a known phenolic from *Curcuma longa*, attenuates the virulence of *Pseudomonas aeruginosa* PAO1 in whole plant and animal pathogenicity models. *J Agric Food Chem* 2008;56(6):1955–62.
- [37] Basniwal RK, Buttar HS, Jain V, Jain N. Curcumin nanoparticles: preparation, characterization, and antimicrobial study. *J Agric Food Chem* 2011;59(5):2056–61.
- [38] Krausz AE, Adler BL, Cabral V, Navati M, Doerner J, Charafeddine RA, et al. Curcumin-encapsulated nanoparticles as innovative antimicrobial and wound healing agent. *Nanomed Nanotechnol Biol Med* 2015;11(1):195–206.
- [39] Tonegawa J, Ohtuka K, Nakano M, Shirotake S. Reinforcement of antibiotic activity by nanoencapsulation of ampicillin against β -lactamase producing and non-producing strains of methicillin-resistant *Staphylococcus aureus*. *Pharm Pharmacol* 2015;190.
- [40] Sanchez DA, Schairer D, Tuckman-Vernon C, Chouake J, Kutner A, Makdisi J, et al. Amphotericin B releasing nanoparticle topical treatment of *Candida* spp. in the setting of a burn wound. *Nanomed Nanotechnol Biol Med* 2014;10(1):269–77.
- [41] Farrar MD, Ingham E. Acne: inflammation. *Clin Dermatol* 2004; 22(5):380–4.
- [42] Nomura I, Goleva E, Howell MD, Hamid QA, Ong PY, Hall CF, et al. Cytokine milieu of atopic dermatitis, as compared to psoriasis, skin prevents induction of innate immune response genes. *J Immunol* 2003;171(6):3262–9.
- [43] Nowicki R, Trzeciak M, Wilkowska A, Sokołowska-Wojdyło M, Ługowska-Umer H, Barańska-Rybak W, et al. Atopic dermatitis: current treatment guidelines. Statement of the experts of the dermatological section, Polish Society of Allergology, and the Allergology Section, Polish Society of Dermatology. *Adv Dermatol Allergology/Postępy Dermatol Alergol* 2015; 32(4):239.
- [44] Freeman AK, Linowski GJ, Brady C, Lind L, VanVeldhuisen P, Singer G, et al. Tacrolimus ointment for the treatment of psoriasis on the face and intertriginous areas. *J Am Acad Dermatol* 2003; 48(4):564–8.
- [45] Montaudé H, Sbidian E, Paul C, Maza A, Gallini A, Aractingi S, et al. Methotrexate in psoriasis: a systematic review of treatment

- modalities, incidence, risk factors and monitoring of liver toxicity. *J Eur Acad Dermatol Venereol* 2011;25(s2):12–8.
- [46] Kober M-M, Bowe WP, Shalita AR. Topical therapies for acne. Acneiform eruptions in dermatology. Springer; 2014. p. 19–25.
- [47] Schlupp P, Blaschke T, Kramer K, Hölte H-D, Mehnert W, Schäfer-Korting M. Drug release and skin penetration from solid lipid nanoparticles and a base cream: a systematic approach from a comparison of three glucocorticoids. *Skin Pharmacol Physiol* 2011;24(4):199–209.
- [48] Pradhan M, Singh D, Singh MR. Development characterization and skin permeating potential of lipid based novel delivery system for topical treatment of psoriasis. *Chem Phys Lipids* 2015; 186:9–16.
- [49] Fisher DA. Adverse effects of topical corticosteroid use. *West J Med* 1995;162(2):123.
- [50] Counts DF, Shull S, Cutroneo KR. Skin lysyl oxidase activity is not rate limiting for collagen crosslinking in the glucocorticoid-treated rat. *Connect Tissue Res* 1986;14(3):237–43.
- [51] Thapa RK, Yoo BK. Evaluation of the effect of tacrolimus-loaded liquid crystalline nanoparticles on psoriasis-like skin inflammation. *J Dermatol Treat* 2014;25(1):22–5.
- [52] Madheswaran T, Baskaran R, Thapa RK, Rhyu JY, Choi HY, Kim JO, et al. Design and in vitro evaluation of finasteride-loaded liquid crystalline nanoparticles for topical delivery. *AAPS PharmSciTech* 2013;14(1):45–52.
- [53] Pinto MF, Moura CC, Nunes C, Segundo MA, Lima SAC, Reis S. A new topical formulation for psoriasis: development of methotrexate-loaded nanostructured lipid carriers. *Int J Pharmaceutics* 2014;477(1):519–26.
- [54] Jain AK, Jain A, Garg NK, Agarwal A, Jain A, Jain SA, et al. Adapalene loaded solid lipid nanoparticles gel: an effective approach for acne treatment. *Colloids Surf B: Biointerfaces* 2014;121:222–9.
- [55] Friedman AJ, Phan J, Schairer DO, Champer J, Qin M, Pirouz A, et al. Antimicrobial and anti-inflammatory activity of chitosan–alginate nanoparticles: a targeted therapy for cutaneous pathogens. *J Invest Dermatol* 2013;133(5):1231–9.
- [56] Society AC. Cancer facts and figures 2015. American Cancer Society; 2015.
- [57] Sullivan RJ, Flaherty KT. Resistance to BRAF-targeted therapy in melanoma. *Eur J Cancer* 2013;49(6):1297–304.
- [58] Chen Y, Bathula SR, Li J, Huang L. Multifunctional nanoparticles delivering small interfering RNA and doxorubicin overcome drug resistance in cancer. *J Biol Chem* 2010;285(29):22639–50.
- [59] Shapira A, Livney YD, Broxterman HJ, Assaraf YG. Nanomedicine for targeted cancer therapy: towards the overcoming of drug resistance. *Drug Resist Updates* 2011;14(3):150–63.
- [60] Grossman JH, McNeil SE. Nanotechnology in cancer medicine. *Phys Today* 2012;65(8):38.
- [61] Chen J, Shao R, Zhang XD, Chen C. Applications of nanotechnology for melanoma treatment, diagnosis, and theranostics. *Int J Nanomed* 2013;8:2677.
- [62] Miele E, Spinelli GP, Miele E, Tomao F, Tomao S. Albumin-bound formulation of paclitaxel (Abraxane® ABI-007) in the treatment of breast cancer. *Int J Nanomed* 2009;4:99–105.
- [63] Pinhasi RI, Assaraf YG, Farber S, Stark M, Ickowicz D, Drori S, et al. Arabinogalactan – folic acid – drug conjugate for targeted delivery and target-activated release of anticancer drugs to folate receptor-overexpressing cells. *Biomacromolecules* 2009;11(1): 294–303.
- [64] Yadav S, van Vlerken LE, Little SR, Amiji MM. Evaluations of combination MDR-1 gene silencing and paclitaxel administration in biodegradable polymeric nanoparticle formulations to overcome multidrug resistance in cancer cells. *Cancer Chemother Pharmacol* 2009;63(4):711–22.
- [65] Chen AM, Zhang M, Wei D, Stueber D, Taratula O, Minko T, et al. Co-delivery of doxorubicin and Bcl-2 siRNA by mesoporous silica nanoparticles enhances the efficacy of chemotherapy in multidrug-resistant cancer cells. *Small* 2009;5(23):2673–7.
- [66] Dummer R, Rochlitz C, Velu T, Acres B, Limacher J-M, Bleuzen P, et al. Intraleisional adenovirus-mediated interleukin-2 gene transfer for advanced solid cancers and melanoma. *Mol Ther* 2008;16(5):985–94.
- [67] Yao H, Ng SS, Huo L-F, Chow BK, Shen Z, Yang M, et al. Effective melanoma immunotherapy with interleukin-2 delivered by a novel polymeric nanoparticle. *Mol Cancer Ther* 2011;10(6): 1082–92.
- [68] El-Sayed IH, Huang X, El-Sayed MA. Selective laser photothermal therapy of epithelial carcinoma using anti-EGFR antibody conjugated gold nanoparticles. *Cancer Lett* 2006;239(1): 129–35.
- [69] Gupta A, Wang S, Pera P, Rao K, Patel N, Ohulchanskyy TY, et al. Multifunctional nanoplatforms for fluorescence imaging and photodynamic therapy developed by post-loading photosensitizer and fluorophore to polyacrylamide nanoparticles. *Nanomed Nanotechnol Biol Med* 2012;8(6):941–50.
- [70] Narsireddy A, Vijayashree K, Irudayaraj J, Manorama SV, Rao NM. Targeted in vivo photodynamic therapy with epidermal growth factor receptor-specific peptide linked nanoparticles. *Int J Pharm* 2014;471(1):421–9.
- [71] Chen LL, Tooley I, Wang SQ. Nanotechnology in photoprotection. *Nanotechnology in dermatology*. Springer; 2013. p. 9–18.
- [72] Fisher GJ, Kang S, Varani J, Bata-Csorgo Z, Wan Y, Datta S, et al. Mechanisms of photoaging and chronological skin aging. *Arch Dermatol* 2002;138(11):1462–70.
- [73] Wiechers JW, Musee N. Engineered inorganic nanoparticles and cosmetics: facts, issues, knowledge gaps and challenges. *J Biomed Nanotechnol* 2010;6(5):408–31.
- [74] Filipe P, Silva JN, Silva R, Cirne de Castro JL, Marques Gomes M, Alves LC, et al. Stratum corneum is an effective barrier to TiO₂ and ZnO nanoparticle percutaneous absorption. *Skin Pharmacol Physiol* 2009;22(5):266–75.
- [75] Manosroi A, Wongtrakul P, Manosroi J, Sakai H, Sugawara F, Yuasa M, et al. Characterization of vesicles prepared with various non-ionic surfactants mixed with cholesterol. *Colloids Surf B Biointerfaces* 2003;30(1):129–38.
- [76] Gupta M, Goyal AK, Paliwal SR, Paliwal R, Mishra N, Vaidya B, et al. Development and characterization of effective topical liposomal system for localized treatment of cutaneous candidiasis. *J liposome Res* 2010;20(4):341–50.
- [77] Kirjavainen M, Urtti A, Jääskeläinen I, Marjukka Suhonen T, Paronen P, Valjakka-Koskela R, et al. Interaction of liposomes with human skin in vitro – The influence of lipid composition and structure. *Biochim Biophys Acta – Lipids Lipid Metab* 1996;1304(3):179–89.
- [78] Draelos Z. Enhancement of topical delivery with nanocarriers. In: Nasir A, Friedman A, Wang S, editors. *Nanotechnology in dermatology*. New York: Springer; 2013. p. 87–93.
- [79] Tran MA, Gowda R, Sharma A, Park E-J, Adair J, Kester M, et al. Targeting V600EB-Raf and Akt3 using nanoliposomal-small interfering RNA inhibits cutaneous melanocytic lesion development. *Cancer Res* 2008;68(18):7638–49.
- [80] Goren D, Horowitz AT, Tzemach D, Tarshish M, Zalipsky S, Gabizon A. Nuclear delivery of doxorubicin via folate-targeted liposomes with bypass of multidrug-resistance efflux pump. *Clin Cancer Res* 2000;6(5):1949–57.
- [81] Strober B, Washenik K, Shupack J. Principles of topical therapy. *Fitzpatrick's Dermatol Gen Med* 2004;2:2319–23.
- [82] Tadros T, Izquierdo P, Esquena J, Solans C. Formation and stability of nano-emulsions. *Adv Colloid Interf Sci* 2004;108:303–18.
- [83] Sonnevile-Aubrun O, Simonnet J-T, L'allouet F. Nanoemulsions: a new vehicle for skincare products. *Adv Colloid Interf Sci* 2004; 108:145–9.

- [84] Afornali A, Vecchi Rd, Stuart RM, Dieamant G, Oliveira LLd, Brohem CA, et al. Triple nanoemulsion potentiates the effects of topical treatments with microencapsulated retinol and modulates biological processes related to skin aging. *An Bras Dermatol* 2013;88(6):930–6.
- [85] Szeimies RM, Radny P, Sebastian M, Borrosch F, Dirschka T, Krähn-Senfleben G, et al. Photodynamic therapy with BF-200 ALA for the treatment of actinic keratosis: results of a prospective, randomized, double-blind, placebo-controlled phase III study. *Br J Dermatol* 2010;163(2):386–94.
- [86] Dirschka T, Radny P, Dominicus R, Mensing H, Brüning H, Jenne L, et al. Photodynamic therapy with BF-200 ALA for the treatment of actinic keratosis: results of a multicentre, randomized, observer-blind phase III study in comparison with a registered methyl-5-aminolaevulinate cream and placebo. *Br J Dermatol* 2012;166(1):137–46.
- [87] Neittaanmäki-Perttu N, Karppinen T, Grönroos M, Tani T, Snellman E. Daylight photodynamic therapy for actinic keratoses: a randomized double-blinded nonsponsored prospective study comparing 5-aminolaevulinic acid nanoemulsion (BF-200) with methyl-5-aminolaevulinate. *Br J Dermatol* 2014;171(5):1172–80.
- [88] Hemmila MR, Mattar A, Taddonio MA, Arbabi S, Hamouda T, Ward PA, et al. Topical nanoemulsion therapy reduces bacterial wound infection and inflammation after burn injury. *Surgery* 2010;148(3):499–509.
- [89] Pannu J, McCarthy A, Martin A, Hamouda T, Ciotti S, Fothergill A, et al. NB-002, a novel nanoemulsion with broad antifungal activity against dermatophytes, other filamentous fungi, and *Candida albicans*. *Antimicrob Agents Chemother* 2009;53(8):3273–9.
- [90] Sen CK, Gordillo GM, Roy S, Kirsner R, Lambert L, Hunt TK, et al. Human skin wounds: a major and snowballing threat to public health and the economy. *Wound Repair Regen* 2009;17(6):763–71.
- [91] Wu J, Zheng Y, Song W, Luan J, Wen X, Wu Z, et al. In situ synthesis of silver-nanoparticles/bacterial cellulose composites for slow-released antimicrobial wound dressing. *Carbohydr Polym* 2014;102:762–71.
- [92] Xiu Z-m, Zhang Q-b, Puppala HL, Colvin VL, Alvarez PJ. Negligible particle-specific antibacterial activity of silver nanoparticles. *Nano Lett* 2012;12(8):4271–5.
- [93] Shahverdi S, Hajimiri M, Esfandiari MA, Larijani B, Atyabi F, Rajabiani A, et al. Fabrication and structure analysis of poly (lactide-co-glycolic acid)/silk fibroin hybrid scaffold for wound dressing applications. *Int J Pharm* 2014;473(1):345–55.
- [94] Khil M-S, Cha D-I, Kim H-Y, Kim I-S, Bhattarai N. Electrospun nanofibrous polyurethane membrane as wound dressing. *J Biomed Mater Res Part B Appl Biomater* 2003;67B(2):675–9.
- [95] Raj S, Jose S, Sumod U, Sabitha M. Nanotechnology in cosmetics: opportunities and challenges. *J Pharm bioallied Sci* 2012;4(3):186.
- [96] Wang SQ, Osterwalder U, Jung K. Ex vivo evaluation of radical sun protection factor in popular sunscreens with antioxidants. *J Am Acad Dermatol* 2011;65(3):525–30.
- [97] Butnariu MV, Giuchici CV. The use of some nanoemulsions based on aqueous propolis and lycopene extract in the skin's protective mechanisms against UVA radiation. *J Nanobiotechnol* 2011;9(3):495.
- [98] Bernardi DS, Pereira TA, Maciel NR, Bortoloto J, Viera GS, Oliveira GC, et al. Formation and stability of oil-in-water nanoemulsions containing rice bran oil: in vitro and in vivo assessments. *J Nanobiotechnol* 2011;9(44):1–9.
- [99] Yilmaz E, Borchert H-H. Effect of lipid-containing, positively charged nanoemulsions on skin hydration, elasticity and erythema—an in vivo study. *Int J Pharm* 2006;307(2):232–8.
- [100] Nejad FM, Baghshahi S, Bakhtiari L. Advantages of nano pigments over micro pigments in obtaining larger spectra of colours in CMYK system. *Trans Indian Ceram Soc* 2011;70(2):93–9.
- [101] Alfano R, Ni X, Zevallos M. Changing skin-color perception using quantum and optical principles in cosmetic preparations. Google Patents. 2007.
- [102] Ha TH, Jeong JY, Jung BH, Kim JK, Lim YT. Cosmetic pigment composition containing gold or silver nano-particles. Google Patents. 2007.
- [103] Kim JK, Nasir A, Nelson KC. Nanotechnology and the diagnosis of cutaneous malignancies. *Nanotechnology in dermatology*. Springer; 2013. p. 127–32.
- [104] Ballou B, Ernst LA, Andreko S, Harper T, Fitzpatrick JA, Waggoner AS, et al. Sentinel lymph node imaging using quantum dots in mouse tumor models. *Bioconjug Chem* 2007;18(2):389–96.
- [105] Lowe AC, Hunter-Ellul LA, Wilkerson MG. Nanotoxicology. *Nanotechnology in dermatology*. Springer; 2013. p. 231–51.
- [106] Kim C, Cho EC, Chen J, Song KH, Au L, Favazza C, et al. In vivo molecular photoacoustic tomography of melanomas targeted by bioconjugated gold nanocages. *ACS nano* 2010;4(8):4559–64.
- [107] Zhong J, Wen L, Yang S, Xiang L, Chen Q, Xing D. Imaging-guided high-efficient photoacoustic tumor therapy with targeting gold nanorods. *Nanomed Nanotechnol Biol Med* 2015;11(6):1499–509.
- [108] Benezra M, Penate-Medina O, Zanzonico PB, Schaer D, Ow H, Burns A, et al. Multimodal silica nanoparticles are effective cancer-targeted probes in a model of human melanoma. *J Clin Invest* 2011;121(7):2768.

Clinical Impact and Patient Safety: The Potential of Microneedles in Changing the Form and Perception of Transdermal Drug Delivery

A.J. Brady, R.F. Donnelly

Queen's University Belfast, Belfast, United Kingdom

OUTLINE

Introduction	47	Regulatory Issues: New Dosage Form or Existing Delivery System?	52
Microneedle Materials: From Concept to Present	48	Microneedles as a Viable Commercial Technology	53
Potential Future Applications	50	Conclusion	54
Assuring Patient Confidence in Microneedles	50	Expectations for Microneedle Technology	55
Opinions on Microneedles by Patients and Healthcare Professionals	51	References	55
Ensuring Patient Safety: Risk of Infection and Immune Reaction	51		

INTRODUCTION

Despite the limited number of drugs deliverable across the skin, due to the formidable barrier properties of the stratum corneum, the value of the worldwide transdermal product market is predicted to increase from \$20 to \$32 billion by 2015 [1]. The major reasons cited for such expansion are greater patient acceptance leading to wider market penetration, lowered development costs, and introduction of novel technologies instigating market growth. Transdermal delivery of peptide- and protein-based drugs is an increasingly important area for development. There are over 100 biotechnology-derived medicines currently marketed, covering nine major therapeutic areas, now representing approximately 15% of all prescriptions written in the United Kingdom. A major challenge to successful

clinical use of these hydrophilic, high-molecular-weight molecules is drug delivery. Due to enzymatic breakdown and poor gastrointestinal absorption, they cannot be given orally and so must be injected. Microneedle (MN)-based transdermal delivery systems have the potential to effectively overcome this problem and may also eliminate transdermal dosing variability, which may be at least partially due to the heterogeneous nature of skin at different sites and on different patients, as they completely bypass the skin's barrier. MN arrays are micron-scale, minimally invasive devices that bypass the skin's stratum corneum barrier. To date, they have been produced from a range of materials, ranging from silicon and stainless steel to aqueous polymer blends (Fig. 4.1). Furthermore, since MNs do not penetrate the skin deeply enough to contact dermal nerves or blood vessels, application is

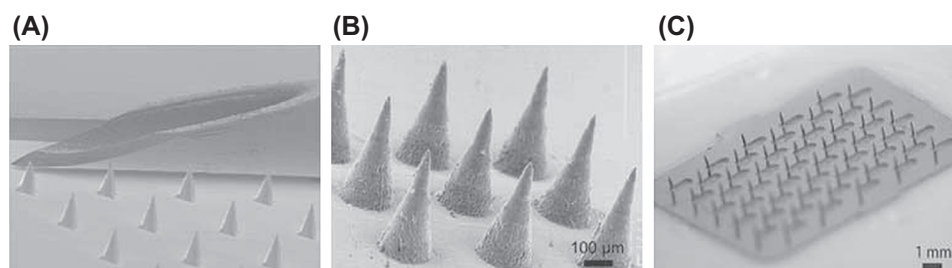


FIGURE 4.1 Examples of microneedles (MNs) used to facilitate drug delivery transdermally. (A) Scanning electron micrograph (SEM) that compares the bevel of a 26G needle to a silicon MN on an ImmuPatch device. (Reproduced with permission Carey JB, Pearson FE, Vrdoljak A, et al. *Microneedle array design determines the induction of protective memory CD8+ T cell responses induced by a recombinant live malaria vaccine in mice. PLoS One* 2011;6(7):e22442.) (B) SEM of polymeric MNs approximately 300 µm in height, prepared from aqueous blends containing 20% Gantrez AN-139. (C) Magnified image of an array of stainless-steel MNs that are 750 µm in height. (Reproduced with permission Norman JJ, Meltzer MI, Prausnitz MR, et al. *Microneedle patches: usability and acceptability for self-vaccination against influenza. Vaccine* 2014;32:1856–62.)

painless and minimally invasive. As efficient transdermal transport will no longer depend on drug physicochemical properties, MN systems could significantly increase the size of the transdermal market. Conventional MNs have already successfully delivered a wide range of biomolecules, both in vitro and in vivo [2]. Indeed, a recent report estimated the potential global market for MN-based drug delivery systems at just under \$400 million in 2012 [3]. Since MNs are frequently targeted not only to the \$20 billion transdermal drug delivery and \$25 billion global vaccine markets, but also to the \$120 billion global biologics market, significant further growth is anticipated.

MICRONEEDLE MATERIALS: FROM CONCEPT TO PRESENT

The first two MN-based products successfully marketed, Micronject and Soluvia, are based on silicon and metal MNs, respectively (Fig. 4.2). However, silicon is not biodegradable, and implanted silicon is prone to biofouling [4–6]. Therefore, silicon MNs left behind in skin due to brittle fracture of baseplates during insertion could cause skin problems. Moreover, the possible problems resulting from inappropriate disposal of silicon or metal MNs, which both remain intact post removal, have led to most researchers in this field focusing on MNs made from US Food and Drug Administration (FDA)-approved polymeric materials [7]. Initially, the hot polymer and carbohydrate melts used to make this second generation of MNs caused breakdown of biologics during processing [8]. Accordingly, the majority of recent research has focused on dissolving MNs prepared from aqueous polymer blends [9–12] (Fig. 4.1).

To overcome the limited dosing capacity for macromolecules loaded into dissolving MNs, we recently developed MNs made from hydrogel-forming polymers. These MNs contain no active drug themselves

[9,13]. Instead, they are hard in the dry state, but rapidly take up skin interstitial fluid upon insertion to form discrete hydrogel pathways between an attached patch-type drug reservoir and the dermal microcirculation. In this way, the dose of drug is not limited to what can be loaded into, or coated on the surface of, the MNs themselves. These MNs possess inherent antimicrobial properties and deposit no polymer in skin, yet are sufficiently soft after only 1 min of insertion to prevent reinjection, thus enhancing patient safety [9,13].

While the idea of MN-based delivery systems was first proposed in the 1970s, the first practical demonstration was not until the late 1990s [14,15]. Since then, the MN field has continued to develop due to enhancements in methods of manufacture and the use of ever-more sophisticated designs (Fig. 4.2). Researchers are gradually realizing the importance of material biocompatibility and the challenges of keeping the bioburden low. The introduction of biocompatible polymeric MN devices may herald a new era in the development of MN technology, overcoming a number of disadvantages of previous MN designs. It is obvious that MNs may have a major role to play in enhanced vaccine delivery strategies. By targeting the intradermal layer, which is replete with antigen-presenting cells, lower vaccine doses could potentially be used to achieve comparable levels of immune protection to conventional intramuscular and subcutaneous injections using needles and syringes [16–18]. Cold-chain storage may be obviated by formulation of vaccines in the solid state in MN-based products. Needlestick injuries and the need for reconstitution prior to administration will be eliminated, and, if MNs can be shown to be inserted into skin without specialist training, it could mean significant savings for healthcare providers. Clearly, those in the developing world stand to benefit greatly from MN-based vaccination.

The compounds delivered by MNs to date have typically been of high potency, meaning only a low dose is

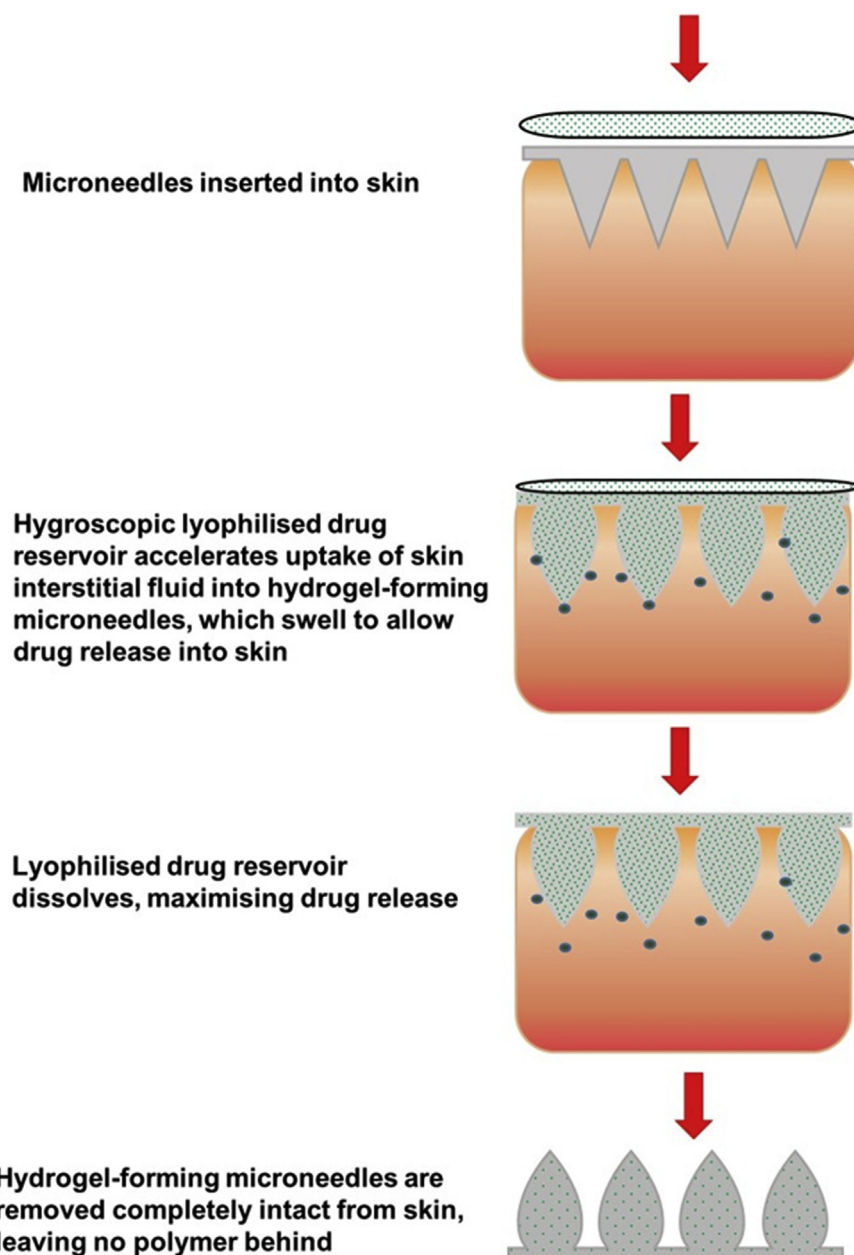


FIGURE 4.2 Schematic representation of the concept of combining hydrogel-forming microneedles prepared from super-swelling polymers and lyophilized wafer-type drug reservoirs for enhanced transdermal delivery of proteins and high-dose low-potency drug substances. *Reproduced with permission Donnelly RF, McCrudden MT, Zaid Alkilani A, et al. Hydrogel-forming microneedles prepared from “super swelling” polymers combined with lyophilized wafers for transdermal drug delivery. PLoS One 2014;9(10):e111547.*

required to achieve a therapeutic effect (eg, insulin) [9,16] or elicit the required immune response [17,18]. Clearly, the majority of marketed drug substances, including many antibodies, are not low-dose, high-potency molecules. Indeed, many drugs require doses of several hundred milligrams per day in order to achieve therapeutic plasma concentrations in humans. Until now, such high doses could not be delivered transdermally from a patch of reasonable size, even for

molecules whose physicochemical properties are ideal for passive diffusion across the skin's stratum corneum barrier. Therefore, transdermal delivery has traditionally been limited to fairly lipophilic, low-molecular-weight, high-potency drug substances. Since most drugs do not possess these properties, the transdermal delivery market has not expanded beyond around 20 drugs. Marketed MN-based patches are likely to increase this number of drugs in the coming years. However, this

increase will only be maximized if high-dose molecules can also be delivered in therapeutic doses using MNs. We have recently shown that suitably formulated dissolving MN platforms can deliver therapeutic doses of a low-potency, high-dose drug substance [19]. However, deposition of polymer in skin from a dissolving MN system may be undesirable if the system is to be used on an ongoing basis. The dissolving MN system employed in our study would deposit approximately 5–10 mg of polymer per square centimeter in skin [19]. If the patch size were 10 cm², then 50–100 mg of polymer would be deposited in the patient's skin every time the product is applied. While vaccines are used infrequently, most therapeutic agents need to be administered regularly. Accordingly, dissolving MN systems may be most appropriate for rapid delivery of low-dose vaccines, as we and others have described previously [17,20]. We have now modified our novel hydrogel-forming MN system to facilitate delivery of clinically relevant doses of a low-potency, high-dose drug substance and rapid delivery of a model protein by increasing swelling capabilities and using a hygroscopic lyophilized drug reservoir [21].

POTENTIAL FUTURE APPLICATIONS

The utility of MNs in bypassing formidable biological barriers, such as the skin's stratum corneum, opens up a range of additional applications, beyond transdermal and intradermal drug delivery. Drug delivery into the eye [22,23] and enhanced administration of active cosmeceutical ingredients [24,25] are currently under intense investigation in both academia and industry, while we have recently reviewed the increasing use of MNs for therapeutic drug-monitoring purposes [26–28]. If drug substances could be both monitored and delivered from the same, interconnected device, then the possibility of an MN-based closed-loop delivery system could become a reality. Thus, the potential uses for MN-based products are numerous, including vaccination; delivery of peptide, protein, and antibody therapeutics for at-home treatment of cancer, diabetes, and genetic diseases (eg, hemophilia); prolonged, convenient delivery of high-dose, low-molecular-weight drugs for treatment of numerous conditions (eg, hypertension, hypercholesterolemia, and Alzheimer's disease); treatment of diseases of the front (glaucoma) and back (age-related macular degeneration and diabetic retinopathy) of the eye; and cosmetic applications, such as delivery of skin fillers and active peptide ingredients.

As technological advances continue, MN arrays may well become one of the major pharmaceutical dosage forms and monitoring devices of the near future.

However, in order for new pharmaceutical products and medical devices based upon MN arrays to realize their undoubted potential and provide benefits for patients and industry, a number of factors will need to be taken into account. These include reliable patient application, user acceptability, safety, and cost-effective mass production.

ASSURING PATIENT CONFIDENCE IN MICRONEEDLES

If MN-based products are to be successfully developed and commercialized, then it will be important to know the dimensions of the micropores they create in patients' skin and how quickly normal skin barrier function recovers. Traditionally, colored dyes have been used to stain the pores created and transepidermal water loss (TEWL) measurements used to quantify disturbances in skin barrier function following MN removal [29–31]. Although these techniques confirm that the skin's stratum corneum barrier has been compromised, they provide no information with respect to the true depth of MN penetration.

Recently, optical coherence tomography (OCT), the optical analog of ultrasound imaging, has been used to investigate MN-mediated skin puncture [29–31]. Since it is capable of imaging the skin down to depths of 2.5 mm, OCT has been used to study insertion depth and micropore width. This work indicates that MNs do not usually penetrate fully into skin. For example, approximately 80% of the shaft length of 600 μ m MNs was shown to protrude beneath the stratum corneum in one study [31], with a micropore width of approximately 300 μ m. Importantly, the technique allows the influence of different MN design and application forces on insertion depth to be studied and, if used in conjunction with transparent polymeric MNs, can be used to follow MN dissolution/swelling in real time in vivo. Micropore closure kinetics can also be studied in real time. This has allowed researchers to show that, unless heavily occluded or treated with nonsteroidal anti-inflammatory drugs or lipid-lowering agents, MN-induced micropores close relatively quickly (completely by 24 h) [29–31]. However, extensive, controlled, clinical studies will inevitably be required to inform regulatory approvals. Indeed, we believe that OCT studies on MN insertion, in-skin behavior, and skin recovery will be essential components of any regulatory submissions for MN-based products. This is especially true because any long-term reductions in skin barrier function could lead to infection and any skin thickening occurring as a result of repeated MN insertion may reduce drug absorption when delivered using MNs to the same site.

Indeed, in order to gain acceptance from healthcare professionals, patients, and, importantly, regulatory authorities (eg, the FDA and the European Medicines Agency), it appears likely that some form of “dosing indicator” will need to be included within the overall MN “package.” Whilst a wide variety of applicator designs have been disclosed within the patient literature, only a few, relatively crude designs based upon high-impact and high-velocity insertion or rotary devices have been described [32]. Such device combinations are unlikely to enhance patient compliance and, currently, do not provide any feedback on successful skin insertion. Moreover, it is obvious that patients cannot “calibrate” their hands and will, therefore, apply MNs with different forces unless properly instructed. With this in mind, we have recently used OCT and TEWL measurements to illustrate that human volunteers can successfully insert our hydrogel-forming MNs into their own skin by hand to consistent depths to yield consistent transient disturbances of skin barrier function when counseled by a pharmacist and after having read a suitable patient information leaflet [33]. A similar study by the Prausnitz group also showed that consistent self-application is possible, once appropriate instructions are provided [34]. Moving toward commercialization, it is likely that patients will need a level of assurance that the MN device has actually been inserted properly into their skin. This would be especially true in cases of global pandemics or bioterrorism incidents, where self-administration of MN-based vaccines becomes a necessity. Accordingly, a suitable means of confirming that skin puncture has taken place may need to be included within the MN product itself.

OPINIONS ON MICRONEEDLES BY PATIENTS AND HEALTHCARE PROFESSIONALS

Whether MN-based products are ultimately a commercial success will depend upon not only their ability to perform as designed, but also their acceptability to patients and healthcare professionals. The study conducted by Birchall’s group [35] provided a range of opinions from healthcare professionals and members of the general public. The focus groups conducted showed clear patient benefits, including reduced pain and needlestick injuries, increased acceptability by people with needlephobia, and potential for self-administration. However, concerns were raised about effectiveness and how a patient would know the device had been used properly.

We also used focus groups to explore children’s views on MN use as an alternative approach to blood sampling in monitoring applications [36]. A total of 86 children

participated in 13 focus groups across seven schools in Northern Ireland. A widespread disapproval of conventional blood sampling using needles was evident, with pain, blood, and traditional needle visualization being particularly unpopular aspects. In general, MNs had greater visual acceptability and caused less fear. A patch-based design enabled minimal patient awareness of the monitoring procedure, with personalized designs (eg, cartoon themes) favored. Children’s concerns included possible allergy and potential inaccuracies with this novel approach. However, many had confidence in the judgment of healthcare professionals if the latter deemed this technique appropriate. They considered pediatric patient education critical for acceptance of this new approach and called for an alternative name, without any reference to “needles.” We concluded that a proactive response to these unique insights should enable MN array design to better meet the needs of this end-user group. Further work in this area is recommended to ascertain the perspectives of a purposive sample of children with chronic conditions who require regular monitoring. Indeed, such studies, when appropriately planned to capture the necessary demographics, will undoubtedly aid industry in taking necessary action to address concerns and develop informative labeling and patient counseling strategies to ensure safe and effective use of MN-based devices. Marketing strategies will, obviously, also be vitally important in achieving maximum market shares relative to existing and widely used conventional delivery and monitoring systems.

ENSURING PATIENT SAFETY: RISK OF INFECTION AND IMMUNE REACTION

Currently, little is known about any long-term effects that may occur due to repeatedly penetrating the skin with MNs. The skin is replete with antigen-presenting cells, so it is vital that delivery of biomolecules intradermally using MNs does not elicit immune responses to nonvaccine agents, such as insulin. It is likely that humanized versions of drug-like biomolecules will reduce this considerably, but nonimmunogenicity will probably have to be shown on a drug-by-drug basis. Moreover, it will be important that no local or systemic reactions to the materials used to fabricate MNs occur. It is statistically unlikely that MNs would ever be applied to exactly the same points on the skin’s surface due to the very small size of the devices, so it is probable that MN-based systems will have very favorable safety profiles, especially over conventional hypodermic needles. While mild skin erythema post MN removal may be concerning initially to some patients, skin barrier function will recover within a

matter of hours and any reddening of skin will be similarly transient, regardless of how long the MNs are in place [2,4].

Polymer deposition from dissolving MNs is of great interest currently. Poly(ethyleneglycol) and poly(vinylpyrrolidone) have a long history of safe intravenous use, and hyaluronic acid is now commonly used in cosmetic skin fillers. However, while most polymers used for MN production are typically approved pharmaceutical excipients, they have never before been used intradermally. Regulators may require information on the amounts of polymer left behind in skin after MN removal and information on clearance rates and routes. This may well be a nonissue for one-off vaccine administration, but it could be important if a dissolving MN was to be used regularly for insulin delivery, for example.

Two recent reports suggest that, when used inappropriately, MNs can indeed cause health problems, such as skin irritation and intradermal granulomas, as well as systemic hypersensitivity [37,38]. While exact details are scarce (including the MN types used and precise skin sites affected), in both cases it is likely that MNs were used in combination with cosmetic products that were not intended for application to MN-punctured skin. Such products contain multiple excipients and, importantly, are not sterile. Medical supervision of MN use was not present in either case. MN devices are not equivalent to conventional transdermal patches, in that they are not simply applied to the skin surface. Rather, MNs function principally by breaching the skin's protective stratum corneum barrier and often penetrate into the viable epidermis and dermis [2,4]. Such areas of the body are normally sterile. Accordingly, it is imperative that MNs, or products used with them, do not themselves contain microbial loads sufficient to cause skin or systemic infection. It is also important that bioburden be minimized to avoid immune stimulation, especially considering the rich immune cell population in the viable epidermis and dermis [39]. However, as we and others have shown [40,41], microbial penetration through MN-induced holes is minimal. Indeed, there have never been any reports of MN causing skin or systemic infections when MNs are used under medical supervision. This may be due to the action of the strong immune component of skin or the skin's nonimmune enzyme-based defense mechanisms. As the micropores created by MNs are aqueous in nature and very small in dimensions, there may not be a great tendency for microorganisms to traverse these openings. Accordingly, skin cleansing prior to MN insertion is unlikely to be necessary, but it should be investigated as part of product development studies. In an ideal situation, this would not be done. Accordingly, patients and healthcare professionals will not be

unnecessarily inconvenienced and may be more reassured about the safety of the delivery system, making the use of the product in the domiciliary setting appear more akin to application of a conventional transdermal patch than a self-administered injection. In our own experience as pharmacists, patients often do not follow instructions provided verbally by healthcare professionals or in written form in product inserts, especially if they consider them unnecessary or inconvenient. Accordingly, skin cleansing will be practically unenforceable outside the hospital or GP surgery.

At the end of the day, regulatory authorities will need to decide, based on the weight of available evidence. MNs may be classed as drug delivery systems, consumer products or medical devices, depending upon the intended use stated by their manufacturers. If MNs are considered to be more akin to an injection than a transdermal patch, then they may need to be produced or rendered sterile. Any contained microorganisms would have to be identified, and pyrogen content would need to be minimized. If sterile production is required, careful selection of the method to be used will be vital. Aseptic manufacture will be expensive and will present practical challenges if MNs are to be made on a very large scale, for example, with vaccine delivery products. Terminal sterilization using gamma irradiation, moist heat, or microwave heating may damage the MNs or biomolecule cargoes, while ethylene oxide may permeate polymeric MN materials, thus contaminating the delivery system.

REGULATORY ISSUES: NEW DOSAGE FORM OR EXISTING DELIVERY SYSTEM?

Manufacturing MNs aseptically or employing terminal sterilization procedures are likely to increase cost considerably. Scaling up MN production will require considerable thought. This is especially true given the plethora of small-scale production methods described in the literature. Very often a number of steps are required, especially for coated MNs. Silicon MNs require clean room conditions. Overall, it is likely that any manufacturer wishing to develop MN products will need to make a substantial initial capital investment, given that equivalent manufacturing technologies are not currently available. Similarly, a range of new quality control tests will now also become necessary. It is likely that the regulatory requirements set for the first MN products to be approved for human use will set the standards for follow-on products. Packaging will be important in protecting MNs from moisture and microbial ingress, and suitable advice will need to be provided to avoid damage during patient handling and insertion.

Overall, from a regulatory perspective, it seems likely that MNs will be classed as a new dosage form, rather than an adjunct technology to existing transdermal patch drug delivery systems. In summary, the key regulatory questions that may need to be addressed are as follows:

- **Ensuring MN sterility and/or microbial limits.** Under current FDA guidelines, microbial limits for all nonsterile dosage forms are based on Total Aerobic Microbial Count (TAMC) and Total Combined Yeasts and Molds Count (TYMC). Specifically for transdermal products, the TAMC and TYMC are limited at 10^2 and 10^1 cfu/mL following appropriate incubation, while the absence of *Staphylococcus aureus* and *Pseudomonas aeruginosa* is mandatory. Unlike transdermal patches, which simply adhere to the skin surface, MNs penetrate the stratum corneum. As one of the stratum corneum's main functions is to protect underlying tissue from infection, the microbiological content of MN products is an inevitable regulatory consideration. Whether MNs need to be sterile or designated with a "low" bioburden remains to be determined and will only be known once one or more products have been commercialized.
- **Is active MN content uniform? (Depending on system design.)** It is likely that this pharmacopeial requirement, which is internationally harmonized, will be applied to MN systems, as it is for transdermal patch dosage forms.
- **Robust manufacture and packaging.** The normal aspects of quality, including security of packaging (which may also require a demonstration of adequate protection from, eg, water ingress), will apply.
- **Benefits versus risk of MN reuse.** Many current MN systems, notably those made of silicon, can be removed intact from the skin and, therefore, could be reused by the patient or others. Thus, for reasons of safety, a self-disabling system ensuring single use only may be required.
- **Safe disposal or degradation?** MN materials that are not dissolvable or biodegradable may be a hazard, therefore this environmental aspect of their use may be an issue.
- **Will MN materials be retained in skin tissue, especially in the context of prolonged use?** Dissolvable, polymeric MNs will deposit in the skin the materials from which they were fabricated. This could lead to long- or short-term adverse skin effects, such as granuloma formation or local erythema, particularly where repeated use is a factor. This can be mitigated by varying the application site and may be less of an issue where the use is occasional, such as in vaccination.
- **Patient approval: ease and reliability of use.** As with all dosage forms, patients must be able to use the product properly, without significant inconvenience.
- **Reliable indication of MN dosing.** Since there is no obvious sensation on applying an MN dosage form, some indication of correct application and delivery (particularly for vaccination applications) may be required.
- **Immunological effect of MN application.** Repeated insult of the skin, an immunologically active site, by MNs may result in an immunological reaction, depending on the material involved. Some assurances as to immunological safety may be required by regulators.

MICRONEEDLES AS A VIABLE COMMERCIAL TECHNOLOGY

Over the past decade, there has been a substantial increase in MN technologies. Indeed, the number of academic publications on the subject has more than quadrupled since 2004. While biological agents have been the main focus, water-soluble drugs not currently suitable for passive transdermal delivery are also of great interest. A number of companies are investing heavily in development of MN-based delivery systems in particular. These include 3M, Corium, Zosano Pharma, Becton–Dickinson, Vaxxas, and Nanopass Technologies [42–47]. Fig. 4.3 shows some examples of MNs currently undergoing clinical studies and in early stages of commercial development.

Zosano has successfully conducted Phase I and II clinical trials using the Macroflux technology originally developed at Alza. In December 2014, Zosano granted Eli Lilly and Co. exclusive global commercialization rights to ZPPTH, its MN patch system for severe osteoporosis. There appears to be a good chance of success in the upcoming Phase III study delivering parathyroid hormone to postmenopausal women, based on the results of the earlier clinical studies and the positive feedback obtained in focus groups made up of the participants [42].

Nanopass Technologies have shown their Micronjet device to be useful in delivery of insulin, influenza vaccines, and local anesthetics in some clinical studies. However, it should be remembered that this device is more akin to four very short needles attached to the barrel of a conventional syringe, rather than a true microneedle array. Meanwhile, 3M's microstructured transdermal systems (MTS), based on either hollow or coated solid MNs, have been evaluated in a range of preclinical studies focused on delivery of proteins, peptides, and vaccines [44].

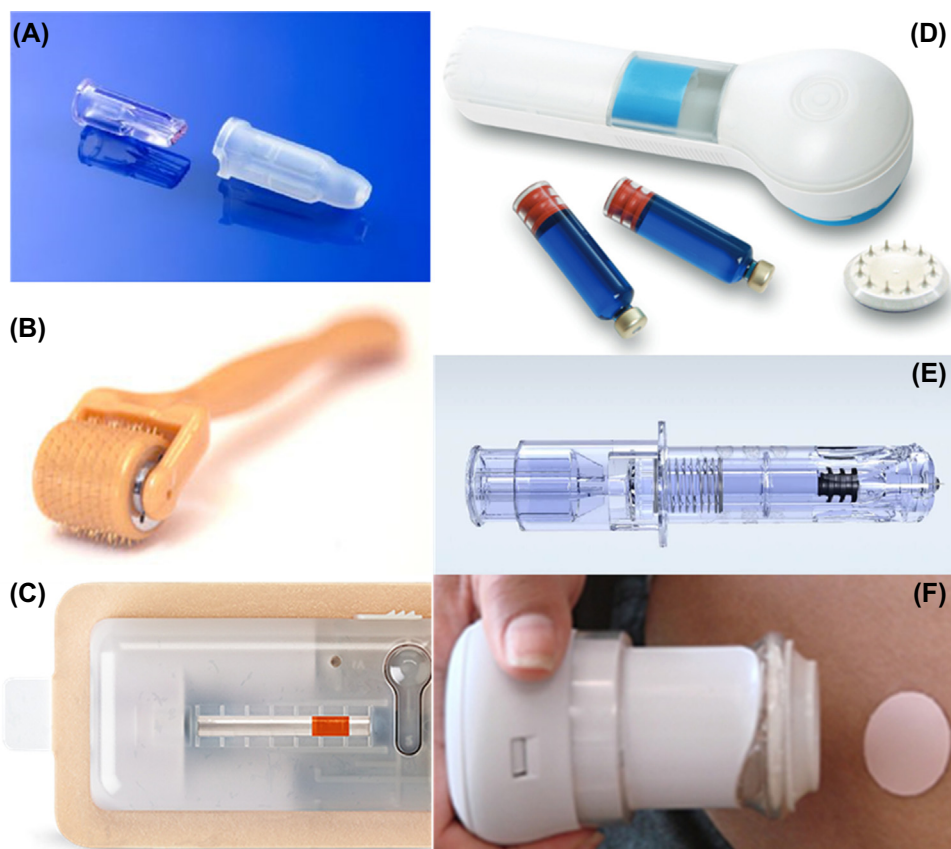


FIGURE 4.3 Microneedle devices: (A) MicronJet; (B) Dermaroller; (C) h-Patch; (D) 3M Microchannel Skin System; (E) Fluzone; and (F) Macroflux. Available at:

(A) <http://www.nanopass.com/content-e.asp?cid=19#>;

(B) <http://www.dermarollersystem.com/index.html>;

(C) https://www.valeritas.com/technologies/h_patch;

(D) http://solutions.3m.com/3MContentRetrievalAPI/BlobServlet?lmd=1410811883000&locale=en_WW&assetType=MMM_Image&assetId=1361805169080&blobAttribute=ThumbnailImage;

(E) <http://www.fluzone.com/fluzone-intradermal-vaccine.cfm>; and

(F) <http://www.zosanopharma.com/index.php/20091103117/Research/Research-General/Technology-Platform.html>.

Whilst the earlier-mentioned MN devices have been based upon solid or hollow MN systems, it is envisaged that devices based upon FDA-approved, biodegradable/dissolving polymeric MN formulations will, in the future, receive increased attention from pharma companies. This is due to the self-disabling nature of such systems. Once inserted into skin, these MNs will either dissolve or swell, thus making insertion into another patient post removal virtually impossible. This will, therefore, reduce transmission of infection by preventing needlestick injuries associated with conventional needles. Disposal issues will also be bypassed, since there is no “sharp” remaining. Ultimately, the impact on healthcare in the developing world in particular could be significant.

Corium has stated that they are exploring several applications of dissolving MNs with pharma partners [46]. Most notably, perhaps, Lohmann Therapie-Systeme AG

(LTS), the world’s largest transdermal patch manufacturer, have now indicated that they have entered the MN field and are inviting partners to collaborate on development of new MN products based on such technology [48]. Given the manufacturing capabilities, expertise, and customer base already possessed by LTS, it will be surprising if they do not claim a sizeable proportion of the developing MN market in the coming years.

CONCLUSION

The future appears to be very bright for new delivery and, potentially, monitoring systems based upon MN technologies. The ever-increasing amount of fundamental knowledge appears to be feeding industrial

development. MNs have many advantages over conventional needle-and-syringe-based delivery systems for biological agents, in particular in terms of reduced pain, reduced infection risk, and the ability to control administration. Skin barrier function disturbance is minimal, and recovery rapid. Once regulatory hurdles are overcome and manufacturing processes developed, optimized, and validated to current good manufacturing practice standards, the benefits for patients and, ultimately, industry will be considerable.

EXPECTATIONS FOR MICRONEEDLE TECHNOLOGY

Given the inherent safety features of MN systems, it is easy to foresee a time within the next 10 years when vaccination programs in the developing world are based around MNs. Because most MNs formulate biomolecules such as vaccine antigens in the dry state, the cold chain will be circumvented. Needlestick injuries also will be obviated. Such an intervention could massively improve the quality of life, life expectancy, and economic productivity of developing countries. Accordingly, the potential impacts of MN research and ultimate commercialization are vast. Once vaccine products are accepted by regulators, healthcare providers, and patients, other MN-based products for everyday patient and consumer use will become widely used to the benefit of the pharmaceutical, medical devices, and cosmetics industries and patients worldwide.

References

- [1] Pharmaceutical and Medical Packaging News (PMPN) Magazine. 2012. Available from: www.pmpnews.com/news/transdermal-delivery-market-predictedreach-315-billion-2015-pharmalive-special-report.
- [2] Donnelly RF, Thakur RRS, Morrow DIJ, et al. Microneedle-mediated transdermal and intradermal drug delivery. Oxford: Wiley-Blackwell; 2012.
- [3] Greystone Associates. Microneedles in medicine: technology, devices, markets and prospects. Amherst, NH: Greystone Associates; 2012.
- [4] Chow AY, Pardue MT, Chow VY, et al. Implantation of silicon chip microphotodiode arrays into the cat subretinal space. *IEEE Trans Neural Syst Rehabil Eng* 2001;9:86–95.
- [5] Voskerician G, Shive MS, Langer R, et al. Biocompatibility and biofouling of MEMS drug delivery devices. *Biomaterials* 2003;24:1959–67.
- [6] Schmidt S, Horch K, Normann R. Biocompatibility of silicon-based electrode arrays implanted in feline cortical tissue. *J Biomed Mater Res* 1993;27:1393–9.
- [7] Pierre MB, Rossetti FC. Microneedle-based drug delivery systems for transdermal route. *Curr Drug Targets* 2014;15:281–91.
- [8] Donnelly RF, Morrow DIJ, Thakur RRS, et al. Processing difficulties and instability of carbohydrate microneedle arrays. *Drug Dev Ind Pharm* 2009;35:1242–54.
- [9] Migalska K, Morrow DIJ, Donnelly RF, et al. Laser-engineered dissolving microneedle arrays for transdermal macromolecular drug delivery. *Pharm Res* 2011;28:1919–30.
- [10] Garland MJ, Caffarel-Salvador E, Donnelly RF, et al. Dissolving polymeric microneedle arrays for electrically assisted transdermal drug delivery. *J Control Release* 2012;159:52–9.
- [11] Demir YK, Akan Z, Kerimoglu O. Characterization of polymeric microneedle arrays for transdermal drug delivery. *PLoS One* 2013;8(10):e77289.
- [12] Park JH, Prausnitz MR. Analysis of mechanical failure of polymer microneedles by axial force. *J Korean Phys Soc* 2010;56:1223–7.
- [13] Donnelly RF, Thakur RRS, Garland MJ, et al. Hydrogel-forming microneedle arrays for enhanced transdermal drug delivery. *Adv Funct Mater* 2012;22:4879–90.
- [14] Gerstel MS, Place VA. Drug delivery device. US Patent No. 3964482; 1976.
- [15] Henry S, McAllister DV, Prausnitz MR, et al. Microfabricated microneedles: a novel approach to transdermal drug delivery. *J Pharm Sci* 1998;87:922–5.
- [16] McCrudden MTC, Thakur RRS, Donnelly RF, et al. Strategies for enhanced peptide and protein delivery. *Ther Deliv* 2013;4:593–614.
- [17] Zaric M, Donnelly RF, Kissenpfennig A, et al. Targeting of skin dendritic cells *via* microneedle arrays laden with antigen encapsulated PLGA nanoparticles induces efficient anti-tumour and antiviral immune responses. *ACS Nano* 2013;7:2042–55.
- [18] Koutsoukos DG, Compans RW, Skountzou I. Targeting the skin for microneedle delivery of influenza vaccine. *Adv Exp Med Biol* 2013;785:121–32.
- [19] McCrudden MTC, McCrudden C, Donnelly RF, et al. Design and physicochemical characterisation of novel dissolving polymeric microneedle arrays for transdermal delivery of high dose, low molecular weight drugs. *J Control Release* 2014;28(180):71–80.
- [20] Raphael AP, Crichton ML, Kendall MA, et al. Targeted, needle-free vaccinations in skin using multilayered, densely-packed dissolving microprojection arrays. *Small* 2010;16:1785–93.
- [21] Donnelly RF, McCrudden MT, Zaid Alkilani A, et al. Hydrogel-forming microneedles prepared from “super swelling” polymers combined with lyophilised wafers for transdermal drug delivery. *PLoS One* 2014;9(10):e111547.
- [22] Patel SR, Lin AS, Prausnitz MR, et al. Suprachoroidal drug delivery to the back of the eye using hollow microneedles. *Pharm Res* 2011;28:166–76.
- [23] Lee CY, You YS, Lee SH, et al. Tower microneedle minimizes vitreal reflux in intravitreal injection. *Biomed Microdevices* 2013;15:841–8.
- [24] Park KY, Kim HK, Kim SE, et al. Treatment of striae distensae using needling therapy: a pilot study. *Dermatol Surg* 2013;38:1823–8.
- [25] Seo KY, Kim DH, Lee SE, et al. Skin rejuvenation by microneedle fractional radiofrequency and a human stem cell conditioned medium in Asian skin: a randomized controlled investigator blinded split-face study. *J Cosmet Laser Ther* 2013;15:25–33.
- [26] Donnelly RF, Mooney K, Caffarel-Salvador E, et al. Microneedle-mediated minimally-invasive patient monitoring. *Ther Drug Monit* 2014;36:10–7.
- [27] Coffey JW, Corrie SR, Kendall MA. Early circulating biomarker detection using a wearable microprojection array skin patch. *Biomaterials* 2013;34:9572–83.
- [28] Yeow B, Coffey JW, Kendall MA, et al. Surface modification and characterization of polycarbonate microdevices for capture of circulating biomarkers, both in vitro and in vivo. *Anal Chem* 2013;85:10196–204.
- [29] Enfield J, O'Mahony C, Leahy M, et al. *In vivo* dynamic characterization of microneedle skin penetration using optical coherence tomography. *J Biomed Opt* 2010;15:046001.

- [30] Coulman S, Birchall JC, Alex A. *In vivo, in situ* imaging of micro-needle insertion into the skin of human volunteers using optical coherence tomography. *Pharm Res* 2011;28:66–81.
- [31] Donnelly RF, Garland MJ, Morrow DIJ, et al. Optical coherence tomography is a valuable tool in the study of the effects of microneedle geometry on skin penetration characteristics and in-skin dissolution. *J Control Release* 2011;147:333–41.
- [32] Thakur RRS, Dunne NJ, Donnelly RF, et al. Review of patents on microneedle applicators. *Recent Pat Drug Deliv Formul* 2011;5: 11–23.
- [33] Donnelly RF, Moffatt K, Zaid-Alkilani A, et al. Hydrogel-forming microneedle arrays can be effectively inserted in skin by self-application: a pilot study centred on pharmacist intervention and a patient information leaflet. *Pharm Res* 2014;31:1989–99.
- [34] Norman JJ, Meltzer MI, Prausnitz MR, et al. Microneedle patches: usability and acceptability for self-vaccination against influenza. *Vaccine* 2014;32:1856–62.
- [35] Birchall JC, Anstey A, John D, et al. Microneedles in clinical practice: an explanatory study into the views and opinions of healthcare professionals and the public. *Pharm Res* 2011;28: 95–106.
- [36] Mooney K, McElnay JC, Donnelly RF. Children's views on micro-needle use as an alternative to blood sampling for patient monitoring. *Int J Pharm Pract* 2014;22:335–44.
- [37] Daily Mail website, <http://www.dailymail.co.uk/femail/article-2026700/Microneedle-Therapy-System-potentially-lethal-Chinese-women-warned.html>; 2012.
- [38] Soltani-Arabshahi R, Wong JW, Duffy KL, et al. Facial allergic granulomatous reaction and systemic hypersensitivity associated with microneedle therapy for skin rejuvenation. *JAMA Dermatol* 2013;150:68–72.
- [39] Roby KD, Nardo AD. Innate immunity and the role of the antimicrobial peptide cathelicidin in inflammatory skin disease. *Drug Discov Today Dis Mech* 2013;10:3–4.
- [40] Donnelly RF, Thakur RRS, Tunney MM, et al. Microneedle arrays allow lower microbial penetration than hypodermic needles *in vitro*. *Pharm Res* 2009;26:2513–22.
- [41] Wei-Ze L, Mei-Rong H, Jian-Ping Z. Super-short solid silicon microneedles for transdermal drug delivery applications. *Int J Pharm* 2010;389:122–9.
- [42] Zosano Pharma website, www.zosanopharma.com/index.php?option=com_content&task=blogcategory&id=26&Itemid=169; 2015.
- [43] Nanopass website, www.nanopass.com; 2015.
- [44] 3M website, http://solutions.3m.com/wps/portal/3M/en_WW/DrugDeliverySystems/DDSD/technology-solutions/transdermal-technologies/microstructured-transdermal-systems/; 2015.
- [45] Beckton-Dickinson website, www.bdbiosciences.com/; 2015.
- [46] Corium website, www.coriumgroup.com/; 2015.
- [47] Vaxxas website, <http://www.vaxxas.com/>; 2015.
- [48] LTS website, www.ltslohmann.de/home.html; 2015.
- [49] Carey JB, Pearson FE, Vrdoljak A, et al. Microneedle array design determines the induction of protective memory CD8⁺ T cell responses induced by a recombinant live malaria vaccine in mice. *PLoS One* 2011;6(7):e22442.

Inorganic Nanoparticles for Transdermal Drug Delivery and Topical Application

M. Wang¹, S.K. Marepally², P.K. Vemula^{2,3}, C. Xu¹

¹Nanyang Technological University, Singapore; ²Institute for Stem Cell Biology and Regenerative Medicine (inStem), GKVK-Campus, Bangalore, Karnataka, India; ³Ramalingaswami Re-Entry Fellow, Government of India

OUTLINE

Introduction	57	<i>Iron Oxide Nanoparticles</i>	65
Design Criteria of Inorganic Nanoparticles	58	Inorganic Nanoparticles for Topical Application	66
<i>Skin Penetration Ability of Inorganic Nanoparticles</i>	58	<i>Silver Nanoparticles</i>	66
Surface Charge	58	<i>Titanium Dioxide and Zinc Oxide Nanoparticles</i>	68
Hydrophilicity	59	<i>Calcium Carbonate and Calcium Phosphate Nanoparticles</i>	68
Particle Size	60	<i>Quantum Dots</i>	68
Particle Shape	60	Conclusion	70
<i>Surface Engineering Strategies</i>	60	Acknowledgments	70
Inorganic Nanoparticles Used for Transdermal Drug Delivery	63	References	70
<i>Silica Nanoparticles</i>	63		
<i>Gold Nanoparticles</i>	64		
<i>Copper Sulfide Nanoparticles</i>	65		

INTRODUCTION

Transdermal drug delivery systems (TDDS) have generated extensive interest as a preferred alternative to oral drug delivery and hypodermic injections, ever since the first scopolamine transdermal patch for motion sickness was approved by the US Food and Drug Administration in 1979 [1]. Compared to oral or systemic dosage systems, TDDS can offer a controlled release of the drugs through the skin into the patients, which could reduce the first-pass metabolism effects, lessen systemic side effects, improve the dosage efficacy by enabling steadier blood drug profiles throughout the treatment, and enhance patient compliance [2]. However, extensive applications of TDDS are limited by the

excellent barrier function of the skin, in particular the stratum corneum, which is a stratified organ to prevent the invasion of external molecules [3]. Only a few drugs can passively penetrate through the skin to reach an effective concentration in the blood for treatment of diseases. Usually these drugs are expected to be highly potent, are lipophilic, and have a low molecular mass (<600 Da).

During the past two decades, enormous efforts have focused on improving the penetration of drugs through the intact skin by a wide range of physical and chemical techniques such as iontophoresis [4], sonophoresis [5], electroporation [6], microneedles [7], magnetophoresis [8], and electron beam irradiation [9]. Unfortunately, most of these methods may suffer from a risk of skin

irritation, which would decrease patient compliance. Recently, due to the unique physicochemical properties of nanoparticles, they have been introduced into a wide array of biomedical devices as the nanocarriers of drugs for imaging, diagnosis, and therapy of a wide array of medical conditions and diseases. In the case of TDDS, nanoparticles could significantly improve the penetration of macromolecular drugs across the stratum corneum, with the potential to reduce immunogenicity and improve the bioavailability [10]. The most common nanoparticles used for transdermal drug delivery are self-assembled liposomes [11,12], solid-lipid nanoparticles (SLNs) [13], polymeric micelles [14], and inorganic nanoparticles [15,16]. Compared with organic nanoparticles, inorganic nanoparticles such as gold, silica, and iron oxide nanoparticles offer higher chemical and mechanical stability, have easier surface functionalization, and possess a tunable particle size and varied morphology. Thus, developing novel transdermal nanodevices based on inorganic nanoparticles is one of the fastest growing fields in nanomedicine.

In this chapter, we focus on the selection and design criteria of inorganic nanoparticles for topical and transdermal drug delivery and summarize those that have been successfully used so far, including silica nanoparticles, gold nanoparticles (AuNPs), copper sulfide nanoparticles (CuSNPs), and iron oxide nanoparticles (Fe_3O_4 NPs). In addition, some inorganic nanoparticles, which themselves possess a very poor ability for skin penetration, can be placed on the surface of the skin for topical use, based on their unique properties like their antimicrobial function, light-scattering effect for photoprotection, and high affinity for metal ions. These nanoparticles include silver nanoparticles (AgNPs), titanium dioxide nanoparticles (TiO_2 NPs), zinc oxide nanoparticles (ZnONPs), and calcium carbonate nanoparticles (CaCO_3 NPs), which are also summarized in this chapter. At the end, we discuss the existing concerns and perspectives regarding inorganic nanoparticles-based TDDS and topical applications.

DESIGN CRITERIA OF INORGANIC NANOPARTICLES

The physical parameters of various nanoparticles such as the size, composition and morphology influence their ability to penetrate the skin. Previous findings that were conducted to study the rate of skin penetration of a wide range of inorganic nanoparticles for biomedical applications, suggested that the composition, surface chemistry, particle size and morphology were the critical parameters for optimizing the inorganic nanoparticle design to meet the safety requirement, while at the same time enhancing the skin penetration.

Skin Penetration Ability of Inorganic Nanoparticles

The efficiency of different TDDS has always been primarily determined by their ability to penetrate the skin. Effective skin penetration is the first criterion to be considered during the design and evaluation of nanoparticles for transdermal drug delivery. The physicochemical properties including the surface charge, hydrophilicity/hydrophobicity, size, and shape have been shown to influence the skin penetration of nanoparticles. Nanoparticles can penetrate the skin via three possible routes: (1) through the lipidic matrix (the intact horny layer or stratum corneum), (2) through sweat gland pores, and (3) through hair follicles with their associated sebaceous glands (Fig. 5.1) [17].

The stratum corneum, which is the uppermost layer of the skin and known to be acidic [18], lipophilic, and more compact than the intact skin, is the primary barrier against nanoparticle penetration. It is generally accepted that the inorganic nanoparticles with positive charge, high surface lipophilicity, and a small particle size (<10 nm) could passively penetrate the stratum corneum and reach the deeper layers of the skin [19].

Surface Charge

Inorganic nanoparticles can carry different charges (positive, negative, or neutral) on their surface. The integrity and stability of the nanoparticle solution critically depend on the surface charge. At the isoelectric point, where there is no surface charge, the nanoparticles can agglomerate due to the lack of any electrostatic repulsion among them to keep them apart. The surface charge of nanoparticles can also affect the interaction between the nanoparticles and the skin, thus affecting their penetration ability. In relation to the cell uptake of nanoparticles with an anionic surface charge, the acidic skin, which carries negative charges under neutral pH conditions, may also electrostatically repel the negatively charged nanoparticles, resulting in the aggregation of the nanoparticles, and further impacting their penetration. Yoo and colleagues reported that cationic liposomes exhibited a larger skin permeability than both anionic and neutral liposomes due to the "Donnan exclusion effect" of the skin [21]. Monteiro-Riviere and colleagues studied the influence of the surface charges borne by quantum dots (QDs) on their skin penetration. QDs were coated with polyethylene glycol (PEG) (neutral), PEG-amine (cationic), and PEG-carboxylic acid (anionic), respectively. The results showed that cationic charged QDs could penetrate deeper into the skin (dermal layers), compared to the neutral and anionic counterparts (which only reached the epidermal layer), within 8 h [22]. Baroli's group

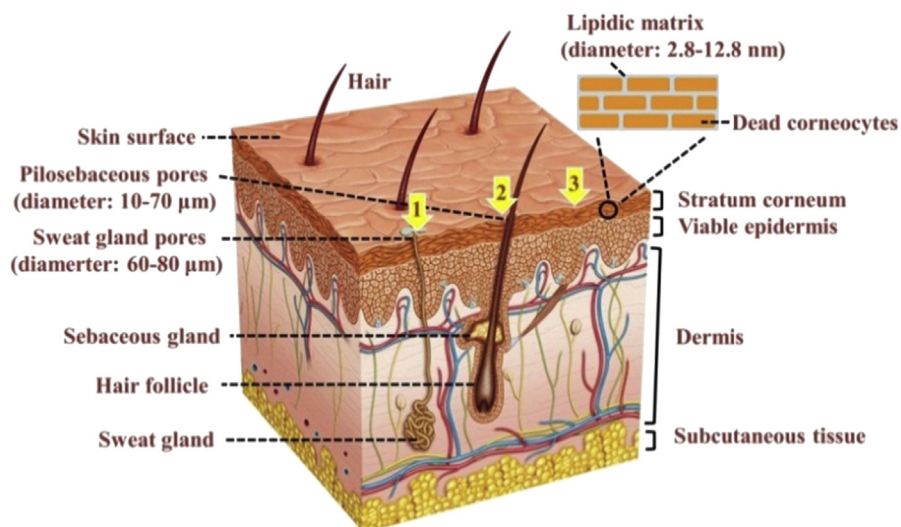


FIGURE 5.1 Structure of the skin and the potential penetration routes of nanoparticles (marked by yellow arrows): (1) through the lipidic matrix (the intact horny layer; pore diameters of the lipidic matrix between dead corneocytes: 2.8 ± 1.3 nm for aqueous pores and below 12.8 nm for the lipophilic region); (2) through sweat gland pores (diameter: 60–80 μm); and (3) through the hair follicles with the associated sebaceous glands (diameter: 10–70 μm) [20]. Modified from the skin figure that was downloaded from <http://www.brighterlooks.com/how-it-works/>.

reported that tetramethylammonium hydroxide (TMAOH)-stabilized maghemite nanoparticles with negative charges (the isoelectric point was pH 6.3 and 6.9 ± 0.9 nm) flocculated within the outermost layers of the stratum corneum, whereas a fraction of the positively charged nanoparticles succeeded in entering the skin and flocculated in the deeper layers of the skin [20]. Rancan and colleagues found that amorphous silica nanoparticles functionalized with positively charged groups exhibited an enhanced cellular uptake by different types of skin cells, in vitro [23]. Recently, Kanaras' group studied the influence of the surface charge of gold nanoparticles on the interactions between the skin and nanoparticles. They also pointed out that the penetration amount of positively charged nanoparticles coated with PEG-amine was larger (2–6 times) than that of the negatively charged ones (coated with PEG-carboxylic acid) (Fig. 5.2) [24]. In summary, the normally acidic skin may preferentially facilitate the penetration of cationic charged nanoparticles.

Hydrophilicity

A unique feature of skin is its varying values for hydrophilicity that change across the different layers. This changing hydrophilicity–hydrophobicity ratio limits the penetration of both hydrophilic and hydrophobic molecules into the deeper layers. Molecules with an amphiphilic nature (a balance between hydrophilicity and lipophilicity, possibly in different regions of the same molecule) can penetrate through the skin efficiently. Several findings have demonstrated that nanoparticles with an amphiphilic nature penetrate

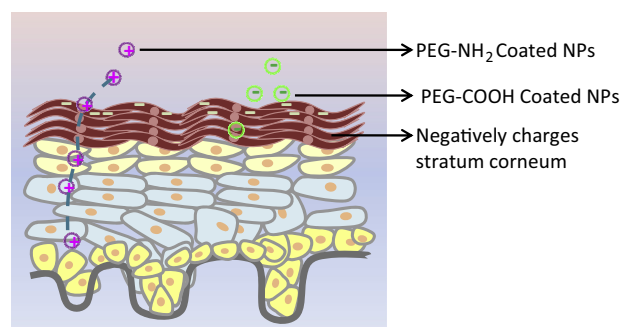


FIGURE 5.2 Schematic representation of charged nanoparticles' penetration into the skin.

deeper layers of skin than either hydrophilic or hydrophobic molecules. Recently, Iannuccelli and colleagues studied the in vivo skin penetration of bare (noncoated) hydrophilic silica nanoparticles (B-silica) and lipid-coated silica nanoparticles (LC-silica) across the human stratum corneum, and found that the hydrophobic lipid-coated silica particles exhibited greater skin penetration ability than the hydrophilic bare ones (Table 5.1) [25]. However, it was reported that hydrophilic PEG-coated QDs with a diameter of about 4.6 nm could also penetrate the dermis, while skin penetration with PEG-coated QDs with a diameter of 37 nm did not occur in intact mouse skin [22,26]. These results suggest that variations in the particle size may show a greater impact on skin penetration than the hydrophilicity. Particularly, in the case of inorganic nanoparticles, size plays a pivotal role in skin permeation compared with hydrophilicity.

TABLE 5.1 In Vivo Silica Permeation Amounts Following B-Silica or LC-Silica Application on the Volar or Dorsal Forearm Side

Sample	Nonpermeated (Tape 1)	Permeated (Tapes 2–12)
B-silica (volar side)	37.76 ± 2.22	46.62 ± 3.22
B-silica (dorsal side)	41.83 ± 3.28	52.97 ± 4.77
LC-silica (volar side)	14.02 ± 1.50	90.10 ± 5.46
LC-silica (dorsal side)	12.35 ± 0.96	87.88 ± 7.04

Reproduced by permission from Iannuccelli V, Bertelli D, Romagnoli M, Scalia S, Maretti E, Sacchetti F, et al. In vivo penetration of bare and lipid-coated silica nanoparticles across the human stratum corneum. *Colloid Surface B* 2014;122:653–61.

Particle Size

The size of the nanoparticles plays a critical role in modulating the skin penetration. Many efforts have been devoted to study the effect of particle size on the depth of skin penetration. However, the extent of correlation of skin permeation with the size of nanoparticles is still debated. It is widely accepted that rigid nanoparticles less than 10 nm are able to penetrate the skin through the lipidic matrix of the stratum corneum and through hair follicle orifices. Some may reach the deepest layers of the stratum corneum and even the viable epidermis [20]. Nanoparticles larger than 20 nm penetrate the skin through the hair follicles and then reach the deeper tissue layers (like the perifollicular dermis) of the skin. Sometimes, nanoparticles are trapped in hair follicles and slowly released by the ongoing sebum production. However, the orifices of hair follicles occupy only 0.1% of the total surface area of the intact human skin, and therefore the role of skin penetration through the hair follicles is often neglected and its importance is debated [27]. In addition, the principles of correlation of penetration with size are not absolute. Most investigators have pointed out that TiO₂ nanoparticles (applied eg, in sunscreen) remain in the very outermost layers of the stratum corneum and could not penetrate the deeper layers regardless of their size, shape, or surface properties [28]. Furthermore, it has been suggested that flexing of the skin and massages could enhance the skin penetration of inorganic nanoparticles [29,30].

Particle Shape

Earlier studies were directed toward understanding the effect of the shape and morphology of nanoparticles on their skin penetration ability. Monteiro-Riviere and colleagues compared the penetration ability of spherical-shaped core-shell QDs with the ones that had an ellipsoid shape. The spherical nanoparticles deeply penetrated the dermal layers, while the ellipsoid

nanoparticles just localized superficially in the epidermal layer within 8 h, which was ascribed to the difference in the shape, since both the nanoparticles possessed the same cationic surface charge and had similar hydrodynamic sizes [22]. Recently, Kanaras and colleagues observed that gold nanorods were found in the skin in higher amount than gold nanospheres, which suggests that shape of the nanoparticles (everything else being equal) does significantly influence their ability to penetrate the skin [24].

Surface Engineering Strategies

As discussed above, the physico-chemical parameters such as surface charge, hydrophilicity, and particle size are critical in engineering the surface of inorganic nanoparticles to achieve higher rates of skin penetration. In addition, the surface modification will have an impact over the drug-loading and drug release characteristics, and will also affect the stability of nanoparticles.

Currently, surface modification of nanoparticles is achieved either during or after the synthesis of the particles. To obtain a relatively stable suspension of nanoparticles, it is customary for them to be modified with various stabilizers during the synthesis processes. For example, gold nanoparticles are often prepared with a citrate coating to obtain a stable dispersion in aqueous solutions prepared via chemical reduction of gold salts. Upconversion nanoparticles have usually been obtained with surface hydrophobicity by coating with oleic acid via a solvo-thermal approach. Until now, there have been a variety of different strategies for the surface modification of inorganic nanoparticles, including physical adsorption, covalent bonding, layer-by-layer assembly, ligand exchange, and in situ polymerization (Fig. 5.3) [31,32].

Physical adsorption approaches are based on the hydrophobic–hydrophobic interactions that occur between the amphiphilic coating species and the nanoparticles. The hydrophilic upconversion nanoparticles were successfully prepared by coating the amphiphilic PEG or chitosan onto the surface of the hydrophobic nanoparticles via physical adsorption [33,34]. For example, Jon and colleagues prepared superparamagnetic iron oxide nanoparticles by coating with various antibiofouling amphiphilic polymers via hydrophobic–hydrophobic van der Waals interactions for an application involving cancer imaging in vivo [35].

Covalent bonding is the most common strategy for the surface modification of nanomaterials. In the case of noble metal nanoparticles, sulfhydryl-containing molecules (like thiols and thiolated DNAs) are often used via the formation of the metal–sulfur bonds, which allows the introduction of coatings with various reactive

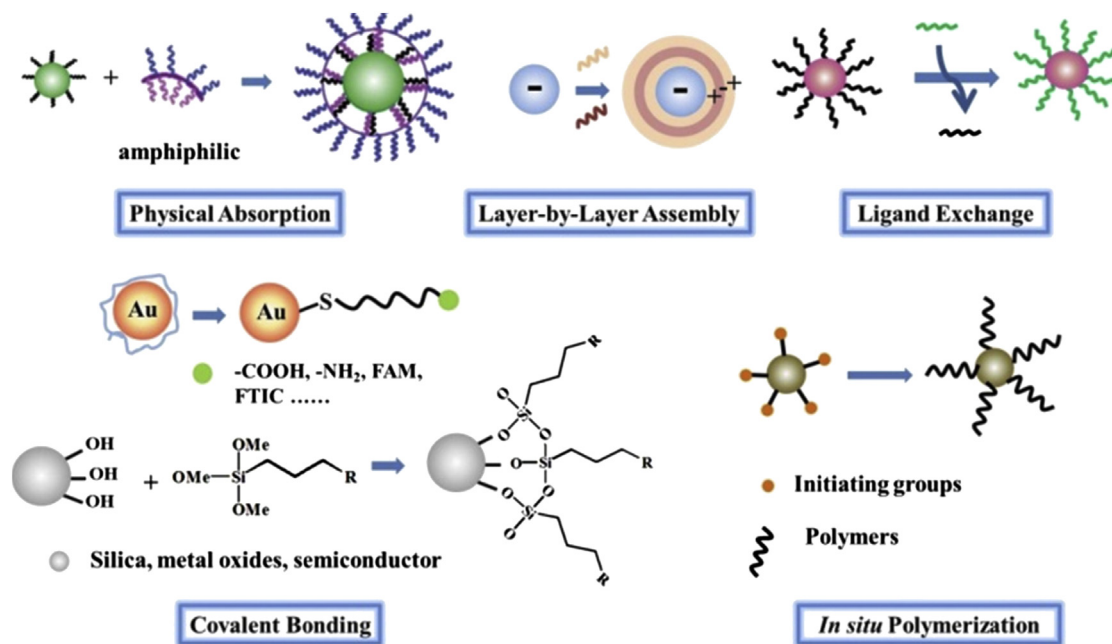


FIGURE 5.3 Common strategies of surface modification of inorganic nanoparticles.

groups (eg, $-\text{COOH}$, $-\text{NH}_2$, $-\text{OH}$) and with electrochemical fluorescent probes. Biomolecules (like aptamers, antibodies, oligonucleotides, and proteins) could also be subsequently attached via electrostatic interaction or by covalent reactions for various applications. The most common covalent reaction for modification is the amidation reaction between the carboxyl groups and amino groups in the presence of *N*-ethyl-*N*-(3-dimethyl-aminopropyl) carbodiimide hydrochloride (EDC) and *N*-hydroxysuccinimide (NHS). For example, Lucarini and colleagues prepared different thiol-modified gold nanoparticles through Au–S bonding, and used them as putative hosting systems for determining their affinities to different radical probes [36]. Mirkin and colleagues modified citrate-capped gold nanoparticles with thiolated small interfering RNA (siRNA) duplexes for suppressing expression of different genes in the skin using RNA interference [16]. Besides, surface silanization with silane reagents is another useful technique for the covalent surface modification of hydroxyl-containing nanomaterials such as silica, metal oxides, and semiconductors. Ying and colleagues reported the synthesis of functionalized nanoparticles by surface coating with commercially available silanes [37]. Li and colleagues synthesized the novel acetylated 3-aminopropyltrimethoxysilane (APTMS)-coated iron oxide nanoparticles for *in vitro* and *in vivo* magnetic resonance imaging. Furthermore, surface modification of nanoparticles based on other covalent reactions has also been reported. Lin and colleagues synthesized

boronic acid–functionalized molecularly imprinted silica nanoparticles via the free-radical polymerization process for glycoprotein recognition and enrichment (Fig. 5.4A) [38]. Binder functionalized luminescent CdSe nanoparticles with polar ligands via Cu(I)-mediated “click” chemistry for guiding a supramolecular recognition process (Fig. 5.4B) [39].

Layer-by-layer (LbL) assembly for modifying nanoparticles is based on the weak electrostatic attraction between positively and negatively charged species, which may allow a high drug loading onto nanoparticles. Venkatraman and colleagues encapsulated “secreted protein, acidic, and rich in cysteine” (SPARC)-siRNA in the multilayers of the commercially available hydroxyapatite (HA) nanoparticles modified through layer-by-layer self-assembly with poly(L-arginine) (ARG) and dextran sulfate (DXS) (denoted as HA/ARG/DXS/ARG/SPARC-siRNA/ARG). In turn, a higher coating efficiency of SPARC-siRNA (97%) was obtained with 0.4 pmole SPARC/ μg of LbL nanoparticles. SPARC-siRNA could be released into the cytoplasm by the layer structure delamination for efficient gene knockdown in fibroblasts [40]. Pishko and colleagues coated a solid dexamethasone (DXM) core with a poly-(diallyldimethylammonium chloride)–poly(styrene sulfonate) (PDAC–PSS) layer-by-layer nanoshell for thermo-responsive drug delivery. Based on the low water solubility of the drug DXM, the solid DXM nanoparticles with an average size of 200 ± 100 nm were prepared by a dual-solvent evaporation technique. Subsequently, the DXM-

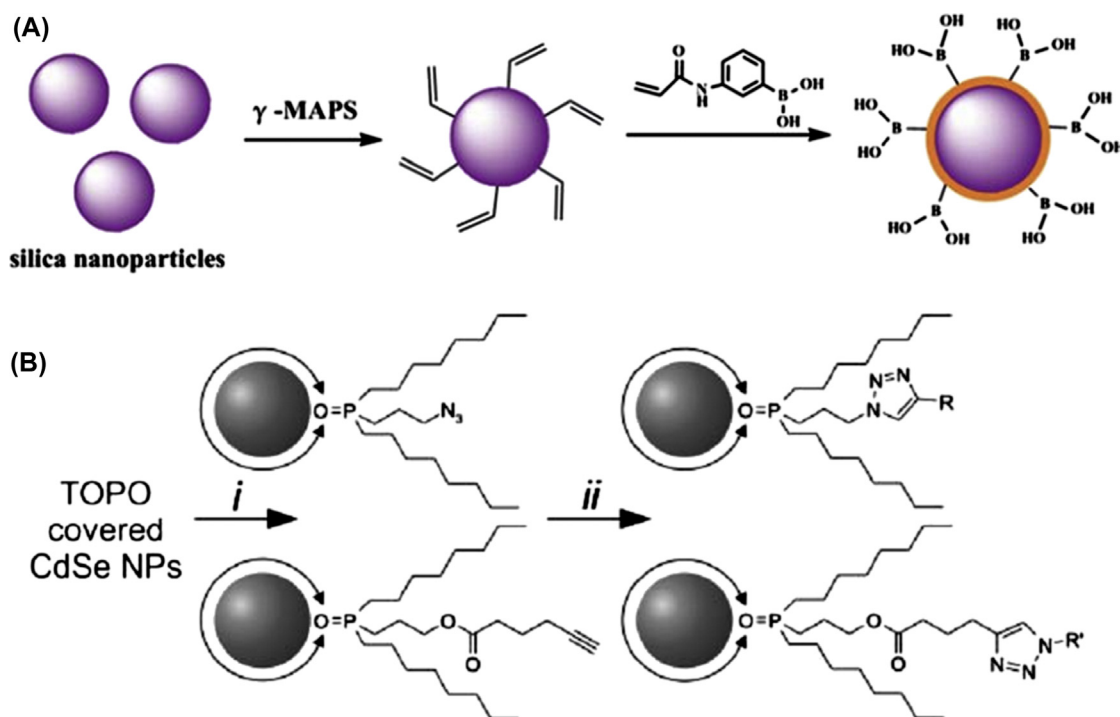


FIGURE 5.4 (A) Synthesis of boronic acid-functionalized silica nanoparticles. (Reproduced by permission from Lin Z, Sun L, Liu W, Xia Z, Yang H, Chen G. *Synthesis of boronic acid-functionally imprinted silica nanoparticles for glycoprotein recognition and enrichment*. *J Mater Chem B* 2014; 2(6):637–43.) (B) Modification of the CdSe nanoparticles using the “click” reaction. Starting from CdSe nanoparticles with a native trioctylphosphine oxide (TOPO) surface: (i) fixation of an azido-moiety or, alternatively, an acetylene moiety by ligand exchange; and subsequent (ii) thermal or Cu(I)-mediated “click” reaction. (Reproduced by permission from Binder WH, Sachsenhofer R, Straif CJ, Zirbs R, *Surface-modified nanoparticles via thermal and Cu (I)-mediated “click” chemistry: generation of luminescent CdSe nanoparticles with polar ligands guiding supramolecular recognition*. *J Mater Chem* 2007;17(20):2125–32.)

encapsulated LbL core-shell nanoparticles were obtained by assembling the alternating layers of the positively charged PDAC and negatively charged PSS onto the negatively charged DXM nanoparticles. DXM could be efficiently released at 60°C due to their increased water solubility or raised diffusion coefficient upon heating. In addition, the rate of drug release was inversely proportional to the number of PDAC-PSS layers [41].

Passivation of the surface by ligand exchange dictates the altered physiochemical properties of nanoparticles. The principle of ligand exchange is that the new ligands must show higher affinity to the nanoparticles than the original ones. Huang and colleagues reported a strategy to graft abundant carboxyl groups containing conjugated polymers onto the surface of Fe₃O₄ nanoparticles through ligand exchange with oleic acid. These grafted conjugated polymer-coated nanoparticles were then ionized with sodium carbonate for applications in cellular imaging and drug delivery [42]. Buriak and colleagues reported the preparation of the stable Zn₃P₂ colloidal nanoparticles using ligand exchange with three different types of anionic type ligands for surface chemistry studies [43].

In situ polymerization is defined as initiating the polymerization from initiating chemical groups attached on the surface of the nanoparticles to achieve controlled surface modification of nanoparticles. Among them, the radical polymerization method is one of the most powerful and widely used approaches for surface modification of metal oxide and silica nanoparticles. Messersmith and colleagues grafted polymethylmethacrylate (PMMA) polymer shells onto TiO₂ nanoparticles by in situ activation of a surface-initiated atom transfer radical polymerization (SI-ATRP) process [44]. Liu and colleagues reported the synthesis of hyperbranched polymer-coated ZnO hybrids by self-condensing SI-ATRP onto ZnO surfaces using *p*-chloromethyl styrene (CMS) as the monomer and 1,10-phenanthroline/Cu(I)Br as the catalyst [45]. Abdollahi and colleagues presented a novel approach for the surface modification of silica nanoparticles via the hydrophilic sulfonated monomers (styrene sulfonic acid sodium salt (SSA) and 2-acrylamido-2-methyl-1-propane sulfonic acid (AMPS)) initiating SI-ATRP onto the surface of brominated silica nanoparticles [46].

INORGANIC NANOPARTICLES USED FOR TRANSDERMAL DRUG DELIVERY

Due to their unique chemical, physical, mechanical, and optical properties, inorganic nanoparticles have been widely used in a wide range of fields such as catalysis, sensors, solar cells, and nanomedicine [47–50]. Recently, several inorganic nanoparticles have been successfully utilized for transdermal drug delivery based on the rational design of nanoparticles as discussed in this chapter.

Silica Nanoparticles

Colloidal silica is extensively used as a rheological additive in personal care products to control flowability. In the recent past, mesoporous silica nanoparticles have been explored as nanocarriers for delivering drugs and genes. Silica nanoparticles possess a wide range of particle size, controllable pore volumes, a high drug-loading capacity, and an abundant number of silanol groups for surface modification and functionalization, and they have been widely used in drug delivery [51]. Increasing efforts have been made to investigate their skin penetration ability and toxicity. Rancan and colleagues demonstrated that silica nanoparticles were taken up by skin cells in a size-dependent manner and the human skin could efficiently block the penetration of particles larger than 75 nm, even after mild disruption of the skin barrier using cyanoacrylate biopsy [23]. Findings from Iannuccelli's group have suggested that lipophilic silica nanoparticles could penetrate deeper layers of skin than the hydrophilic counterparts [25]. Son and colleagues found that the silica nanoparticles with smaller sizes (20 nm) had more toxicity than the larger ones (200 nm), and negatively charged silica particles had more toxicity than the ones with weakly negative charges [52]. Choy and colleagues encapsulated vitamin C into the interlayers of the layered zinc oxide by a co-precipitation reaction to obtain vitamin C-hydrated zinc oxide with a nanoporous silica shell by the hydrolysis of tetraethylorthosilicate (denoted as Vitabrid-C). The results showed that the absolute penetration amounts of vitamin C through the skin, *in vitro*, were 12.0, 10.4, and 7.9 $\mu\text{g}/\text{cm}^2$ for Vitabrid-C powder, Vitabrid-C-containing water in oil emulsion, and pure vitamin C-containing oil in water emulsion, respectively, which may be explained by the fact that the Vitabrid-C exhibited a large absorption of chemical species (like NaCl and fatty acids) that are present in sweat and skin secretions and the subsequent exchange reaction between the absorbed species and vitamin C may have enhanced the release of vitamin C. These

results suggested that the Vitabrid-C nanohybrids were helpful in the delivery of vitamin C into the skin [53]. Gasperlin's group demonstrated that the addition of colloidal silica into microemulsions (MEs) could enhance the delivery of both vitamin C and vitamin E into the excised skin samples. These results were explained by the dual influence of colloidal silica: (1) the addition of colloidal silica to MEs significantly increased the vitamin solubility in MEs (230-fold for hydrophobic vitamin E and 1.2-fold for hydrophilic vitamin C), and hence the skin bioavailability of both vitamins and (2) colloidal silica penetrated the upper layers of the stratum corneum and significantly increased the amount of both vitamins that permeated the epidermis [54].

Scalia and colleagues compared two different permeation enhancers, lipid nanoparticles (LNs; 527 nm) and colloidal silica nanoparticles (486 nm), for delivering quercetin into *in vivo* human skin. They discovered that the addition of LNs did not significantly change the accumulation of quercetin in the outermost layers, whereas the addition of colloidal silica increased the permeated amount of quercetin in the stratum corneum from 18.1% to 26.7% compared to the control emulsion. These results may be ascribed to the high amount of colloidal silica (58.9% of the applied particles) that penetrates the stratum corneum [55]. Yoshikawa and colleagues investigated the effects of amorphous silica particles with different sizes (30–1000 nm) on the atopic dermatitis (AD)-like skin lesions by a combined intradermal injection of silica particles and *Dermatophagoides pteronyssinus* (Dp; the mite antigen for inducing the AD-like skin lesions). They showed that the co-injection of smaller silica particles (<100 nm) and Dp significantly enhanced the ear thickening and caused more severe inflammatory cell infiltration, acanthosis, scabs, and scleroderma than Dp alone, suggesting severe AD-like histological changes, which may be ascribed to the fact that the silica nanoparticles enhanced interleukin-18 (IL18) and thymic stromal lymphopoietin (TSLP) production in the skin lesions and hence enhanced the systemic Th2 immune responses (Fig. 5.5) [56]. Al-Remawi and coworkers loaded the hydrophobic drug curcumin into hydrophilic and negatively charged mesoporous silica particles (363 ± 11.3 nm) and found that curcumin incorporated into silica nanoparticles penetrated through rabbit skin and was detected in the recipient chamber of Franz diffusion cells after 2.73 h, while the curcumin dispersed in an aqueous or an oleic acid medium without nanoparticles did not show any skin permeation. In addition, the curcumin-loaded nanoparticles exhibited a better antiinflammatory effect and higher analgesic activity compared to the controls [57].

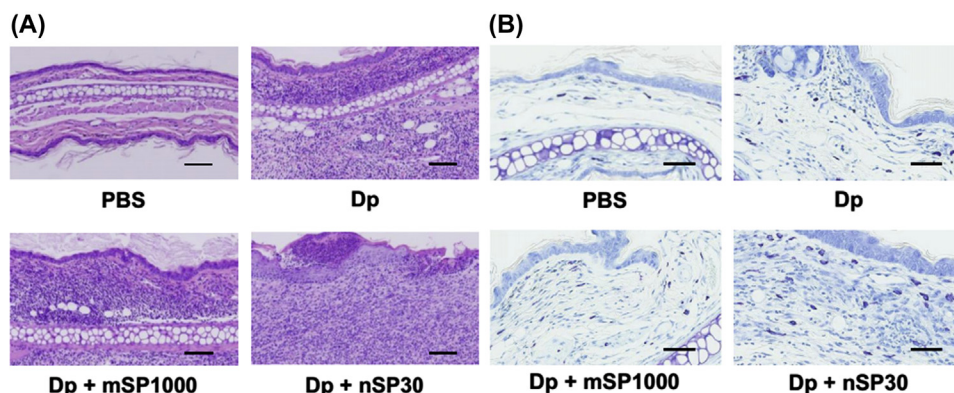


FIGURE 5.5 The ears were removed 24 h after the last intradermal injection. Sections were prepared, and the ears were stained with hematoxylin and eosin (H&E) to assess representative symptoms of AD (A), or with toluidine blue to assess mast cell infiltration (B). Scale bars: 100 μm (A) and 50 μm (B). Reproduced by permission from Hirai T, Yoshikawa T, Nabeshi H, Yoshida T, Tochigi S, Ichihashi K-i, et al. Amorphous silica nanoparticles size-dependently aggravate atopic dermatitis-like skin lesions following an intradermal injection. *Part Fiber Toxicol* 2012;9(3):8977–9.

Gold Nanoparticles

Metallic gold nanoparticles have garnered tremendous interest due to their chemical inertia, nontoxicity, ability to have tuned core sizes over a wide range of 1–150 nm, and unique localized surface plasmon resonance property [58]. During the past decade, gold nanoparticles have been emerging as lead candidates in the field of nanotechnology. Makino and colleagues investigated the skin penetration of citrate-coated gold nanoparticles (15, 102, and 198 nm diameter) through rat skin ex vivo. They demonstrated that the 15-nm-sized gold nanoparticles showed the maximum number density of 1.12×10^{18} in the rat skin at the end of 24 h, while a maximum density of 8.99×10^{15} with a lag time of 3 h and a maximum density of 2.98×10^{14} with a lag time of 6 h were observed for 102-nm-sized and 198-nm-sized gold nanoparticles, respectively. These results suggested that the smaller nanoparticles penetrated the skin in a higher amount and at a faster penetration rate [59]. Similarly, Filon's group and Kanaras's group also confirmed the enhanced in vitro skin penetration of gold nanoparticles.

Subsequently, preclinical studies were carried out with gold nanoparticles including gold nanorods and gold nanospheres. Niidome and colleagues developed a solid-in-oil (SO) dispersion system based on the surfactant/protein-coated gold nanorods and nanocomplexes for transdermal protein delivery and skin vaccination. The methoxy(polyethylene glycol)-thiol (mPEG)-coated gold nanorods (Rod) and ovalbumin (OVA)-based complexes Rod/OVA/SO penetrated the viable epidermis with a depth of 500 μm under the effect of irradiation with near-infrared (near-IR) light. However, the Rod/OVA/SO without near-IR light and OVA/SO with near-IR light only accumulated at

the outermost layer of the epidermis. In addition, with the irradiation of near-IR light, the Rod/OVA/SO exhibited 2.5 and 5 times higher antibody delivery than Rod/OVA/SO without near-IR light and OVA/SO with near-IR light, respectively. These results suggested that gold nanorods could significantly enhance the skin penetration of hydrophilic macromolecules such as proteins with the aid of near-IR irradiation, which may be due to the partial ablation of the stratum corneum by localized photothermal heating mediated by the nanorods [60]. Mirkin and colleagues coated citrate-capped gold nanoparticles with thiolated-EGFR (epidermal growth factor receptor) siRNA duplexes (SNA-NCs) via Au–S bonding for gene silencing (Fig. 5.6A). SNA-NCs penetrated through the stratum corneum and into the epidermis and dermis in both mouse skin and human skin within 3 h after topical application without inducing any cutaneous inflammation, ulceration, scaling, or color alteration. After 3 weeks of topical use, a 65% reduction in EGFR messenger RNA (mRNA) expression was observed (Fig. 5.6B), which subsequently suppressed downstream ERK phosphorylation, reduced the epidermal thickness, and inhibited cell proliferation in the epidermis of hairless mouse skin in vivo (Fig. 5.6C) [16]. Recently, Venuganti and colleagues coated polyethylene-imine (PEI)-modified gold nanoparticles with anionic polystyrene sulfonate (PSS) and cationic PEI via a layer-by-layer approach for electrostatically encapsulating the anticancer reagent imatinib mesylate (IM). Anodal iontophoresis (0.47 mA/cm², one of the physical enhancement methods for skin penetration) facilitated the topical delivery of IM-loaded layer-by-layer (LbL) gold nanoparticles and subsequently enhanced 6.2-fold IM skin permeation compared with

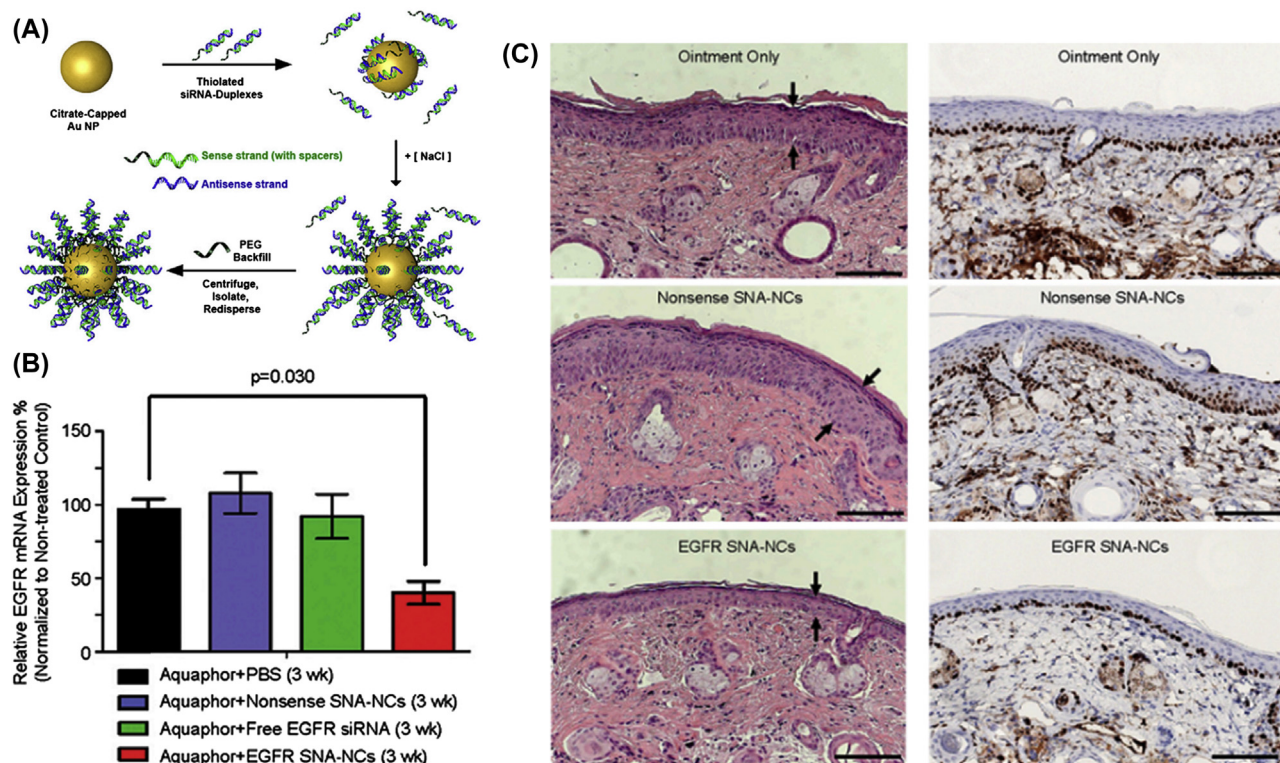


FIGURE 5.6 (A) Scheme of the synthesis of EGFR siRNA-based SNA-NCs. (B and C) Targeted gene knockdown by SNA-NCs correlates with biological effects in vivo. Scale bars: 100 μ m. Reproduced by permission from Zheng D, Giljohann DA, Chen DL, Massich MD, Wang X-Q, Iordanov H, et al. Topical delivery of siRNA-based spherical nucleic acid nanoparticle conjugates for gene regulation. *Proc Natl Acad Sci USA* 2012;109(30):11975–80.

passive application. In addition, IM-loaded LbL-Au nanoparticles delivered 7.8- and 4.9-fold greater IM, when compared with free IM, into the stratum corneum and viable skin, respectively, and exhibited a higher ability to inhibit the cancer cell growth [61].

Copper Sulfide Nanoparticles

Semiconductor CuS nanoparticles are a new class of photothermal nanoparticles that can absorb near-IR light. Lu et al. developed a photothermal ablation-enhanced transdermal drug delivery approach based on the intense photothermal coupling effects of hollow CuS nanoparticles (HCuSNPs). With the aid of irradiation by a nanosecond-pulsed near-IR laser, this approach needed only very short periods of irradiation but generated extremely high temperatures in local regions, which induced the depth-tunable thermal ablation of the stratum corneum via adjustment of the laser power. No histological damage of the skin could be observed without laser treatment or with HCuSNP gel, while significant histological changes were observed in the presence of HCuSNP gel and the laser treatment. The higher laser power resulted in thermal ablation penetrating the deeper layers (viable epidermis) (Fig. 5.7) [62]. This

approach offers a new platform for the transdermal delivery of macromolecular drugs.

Iron Oxide Nanoparticles

Iron oxide (Fe_3O_4) nanoparticles have been widely used for drug delivery due to their unique magnetic responsiveness, high drug loading, and good targeting efficiency [63]. However, there are only a few reports about the application of Fe_3O_4 nanoparticles in transdermal drug delivery. Recently, Lu and coworkers covalently attached a model anticancer agent, epirubicin (EPI), to the functionalized superparamagnetic Fe_3O_4 nanoparticles (EPI-SPION) through a pH-sensitive amide bond for the targeted transdermal chemotherapy of skin tumors. The results showed that the EPI-SPION exhibited good biocompatibility and could inhibit tumor proliferation in a dose-dependent manner. In addition, these hybrid nanocomposites could penetrate the skin barrier into the deep subcutaneous tissue via a transfollicular approach with the aid of an externally applied magnetic field, and EPI could be released from the pH-sensitive EPI-SPION in the acidic environment (pH: 4.5–6.8) for skin cancer therapy (Fig. 5.8) [64].

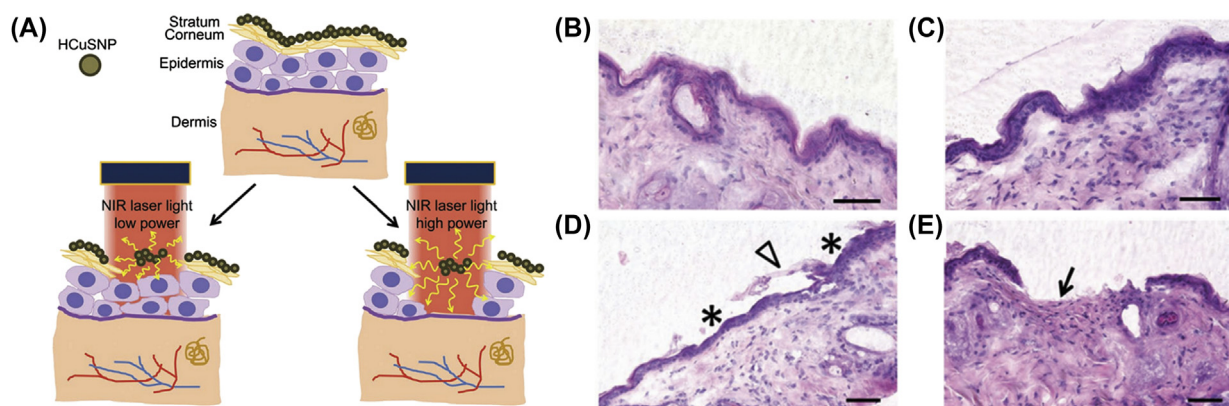


FIGURE 5.7 (A) Illustration of near-IR laser-triggered photothermal ablation of skin mediated by HCuSNPs. H&E staining of the skin sections from the anesthetized nude mice pretreated with (B) HCuSNP gel, (C) blank gel plus laser (2.6 W/cm^2), (D) HCuSNP gel plus laser (1.3 W/cm^2), and (E) HCuSNP gel plus laser (2.6 W/cm^2). Reproduced by permission from Ramadan S, Guo L, Li Y, Yan B, Lu W. Hollow copper sulfide nanoparticle-mediated transdermal drug delivery. *Small* 2012;8(20):3143–50.

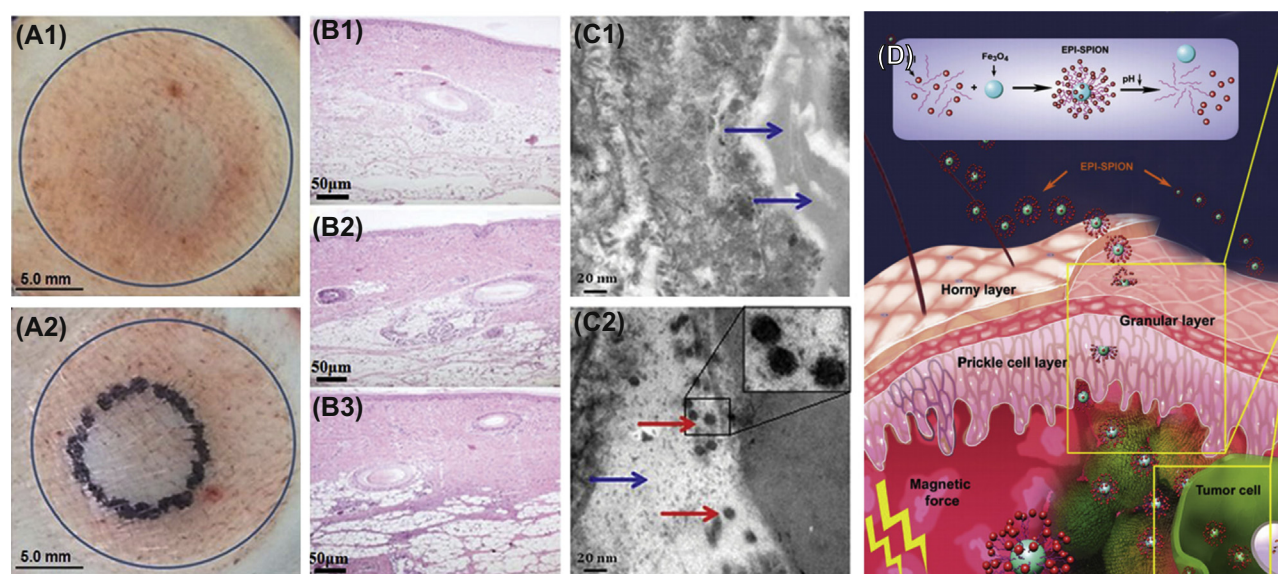


FIGURE 5.8 (A) Dermal localization of the EPI-SPION particles is shown in the absence (A1) and presence (A2) of an external permanent ferromagnet. (B) H&E-stained external section for control (B1) and EPI-SPION (B2, B3). (C) TEM images: blue arrows indicate the pilosebaceous unit, and red arrows indicate EPI-SPION particles. (D) Schematic mechanism of EPI-SPION for magnetic transdermal delivery to combat skin cancer. Reproduced by permission from Rao YF, Chen W, Liang XG, Huang YZ, Miao J, Liu L, et al. Epirubicin-loaded superparamagnetic Iron-Oxide nanoparticles for transdermal delivery: cancer therapy by circumventing the skin barrier. *Small* 2015;11(2):239–47.

INORGANIC NANOPARTICLES FOR TOPICAL APPLICATION

In some case, inorganic nanoparticles that have poor skin penetration ability are placed onto the surface of the skin for topical applications such as wound healing, suppressing local skin inflammation, and preventing allergens from entering the skin. In this section, we summarize the inorganic nanoparticles that have been successfully used in topical applications, including silver nanoparticles (AgNPs), titanium dioxide (TiO_2), zinc oxide (ZnO), and calcium carbonate (CaCO_3)–calcium phosphate (CaPO_4) nanoparticles.

Silver Nanoparticles

Silver nanoparticles have attracted increasing interest due to their chemical stability, catalytic activity, localized surface plasma resonance, and high conductivity [65]. In addition, previous reports showed that the reactive oxygen species (ROS) formed at the surface of the silver nanoparticles or by the released free silver ions under certain conditions may induce cell death of either mammalian cells or microbial cells, which endows the silver nanoparticles with unique antibacterial and antifungal effects [66]. Based on these effects, silver nanoparticles hold great potential in preventing wound

inflammation and hence promoting wound healing in the form of topical administration. For topical use, the skin penetration ability and safety of silver nanoparticles should be assessed.

The skin penetration ability of silver nanoparticles is much lower compared to that of other inorganic metal nanoparticles such as gold, since a larger percentage of free ions are precipitated as Ag–S in the outermost layers of the stratum corneum. Larese and colleagues evaluated the skin penetration of polyvinylpyrrolidone-coated silver nanoparticles (25 nm) through intact and damaged human skin using a series of *in vitro* assays. Their results showed that the penetration amount of silver nanoparticles was very low but still detectable (0.46 ng/cm^2) for intact skin, while an increased amount of penetration (2.32 ng/cm^2) was observed for damaged skin [67]. TEM micrographs showed that silver nanoparticles could passively penetrate the deepest layers of the stratum corneum [67]. George and colleagues analyzed the dermal and systemic absorption of silver nanoparticles through the healthy human skin *in vivo*. The results showed that the penetration of silver nanoparticles was restricted to the reticular dermis of intact human skin, and large aggregates of silver (up to 750 nm) could be observed below the epidermis without affecting the concentration of silver ions in the circulation [68]. In addition, Monteiro-Riviere evaluated the toxicity of three types of silver nanoparticles (unwashed, washed, and carbon-coated) toward skin *in vivo* and against keratinocytes *in vitro*. The results showed that

it was safe to use washed and carbon-coated silver nanoparticles for delivering topical drugs, while the toxicity of unwashed silver nanoparticles could be related to remaining contaminants such as formaldehyde [69].

Based on their good antimicrobial function and non-toxicity, silver nanoparticles have been used as an effective topical application for improving wound healing. Wong and coworkers studied the influence of silver nanoparticles in an animal model of wound healing by using silver sulfadiazine as a control. These results showed that wounds treated with silver nanoparticles better resembled the normal skin structure with a thin epidermis and nearly normal hair follicles within 25 days, while wounds treated with silver sulfadiazine showed a poorer cosmetic appearance with thickened epidermis and no evidence of hair growth, which demonstrated that silver nanoparticles exerted positive effects through their antimicrobial properties to reduce wound inflammation and thus promote wound healing (Fig. 5.9) [70]. Recently, Hazra and coworkers studied the influence of silver nanoparticles (40 nm) on postsurgical wound healing and also confirmed that silver nanoparticles exhibited a positive effect on wound healing. Importantly, silver nanoparticles exhibited superior antimicrobial properties, compared to conventional silver preparations, by interacting with the microbial membranes and, in consequence, lowering the drug concentration and limiting the toxicity of silver. However, the observation that silver nanoparticles induced local tissue edema raised serious concerns, which may limit

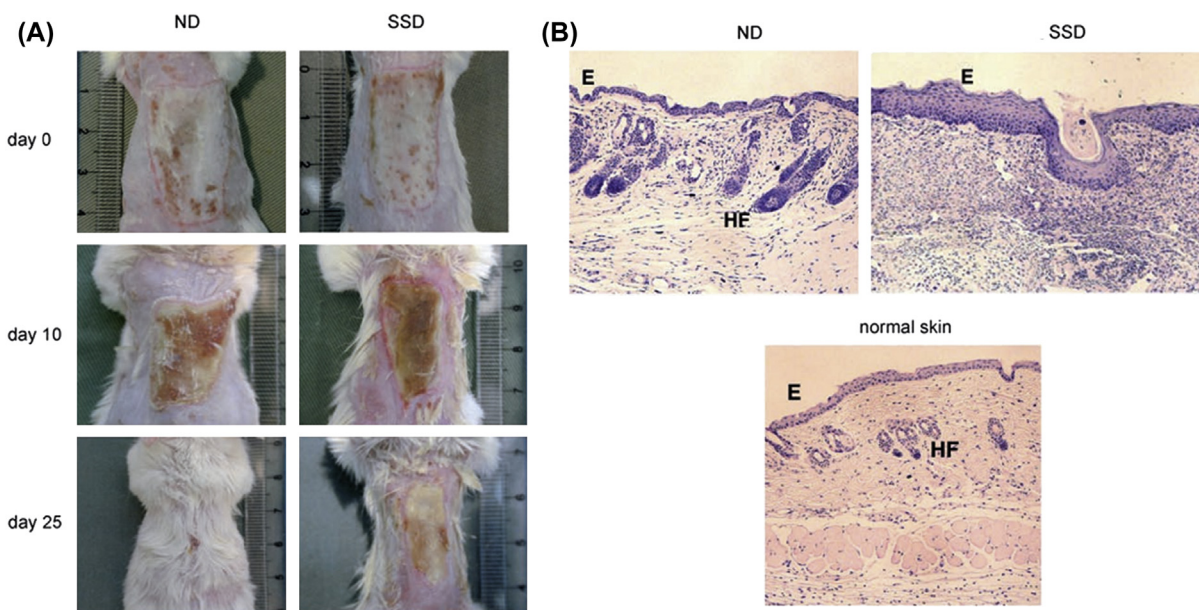


FIGURE 5.9 (A) Photographs of wounds from animals treated with silver nanoparticles (ND) and silver sulfadiazine (SSD) on days 0, 10, and 25 after burn injury. (B) H&E staining of histological sections of healed wounds from animals treated with ND, SSD, or no treatment (E = epidermis, HF = hair follicle). Reproduced by permission from Tian J, Wong KK, Ho CM, Lok CN, Yu WY, Che CM, et al. Topical delivery of silver nanoparticles promotes wound healing. *ChemMedChem* 2007;2(1):129–36.

the clinical applications of silver nanoparticles and urgently need to be addressed [71].

Titanium Dioxide and Zinc Oxide Nanoparticles

Metallic oxide nanoparticles such as titanium dioxide (TiO_2) and zinc oxide (ZnO) have been widely used as mineral-based sunscreen agents as they are able to absorb and scatter incident UV irradiation and thus protect the skin against harmful UV rays. Abundant results have shown that both the TiO_2 and ZnO nanoparticles could not penetrate the skin without use of chemical enhancers regardless of the particle size and the surface coating [28,72,73].

Ravenzwaay and coworkers investigated the in vitro absorption of microfine TiO_2 and ZnO particles in cosmetic formulations through porcine skin and pointed out that neither Ti–Zn ions nor microfine TiO_2 – ZnO particles were able to penetrate the stratum corneum of the skin [28]. Zvyagin and colleagues found that most of the ZnO nanoparticles in the formulation containing caprylic–capric triglycerides were retained on the stratum corneum surface, while a few of them drifted into the skin folds or the hair follicle roots but did not penetrate the deeper layers of the skin [72]. However, with the aid of chemical enhancers such as oleic acid, ethanol, and an oleic acid–ethanol mixture, ZnO nanoparticles penetrated the skin with a depth of 30, 25, and 20 μm from the skin surface, whereas only 10 μm of penetration depth was observed for ZnO nanoparticles without any permeation enhancers. This enhanced penetration was explained by the argument that the chemical enhancers increased the intercellular lipid fluidity, or else extracted lipids from the stratum corneum [73]. Recently, Keller and colleagues investigated the effect of photo-induced disaggregation of TiO_2 nanoparticles on the transdermal penetration. The results showed that after the light irradiation within a few minutes, the hydrodynamic diameter of TiO_2 aggregates was reduced from 280 to 230 nm. 200 mg/kg of TiO_2 in the skin was detected in the presence of natural sunlight compared to only 75 mg/kg under the control dark condition, which suggested the significant influence of the light on the skin penetration and raised a health concern for the topical use of TiO_2 nanoparticles in sunscreens [74].

Besides their applications in sunscreens, TiO_2 and ZnO nanoparticles have potential applications as topical treatments for other indications. Lim and colleagues studied the photo-stability of ketoprofen (KP) after the incorporation of TiO_2 nanoparticles into skin-adherent patches. KP is known as a widely used transdermal drug, and its instability may induce a photo-allergic reaction. The results showed that TiO_2 nanoparticles could prevent the photo-degradation of KP and

thus reduce the possible photo-allergic reaction [75]. Alenius' group investigated the penetration abilities of both nanosized ZnO nanoparticles (ca. 20 nm) and bulk-sized ones (ca. 100 nm) through injured skin and injured allergic skin in the mouse model of AD, and found that nanosized ZnO particles could suppress the local skin inflammation and could induce systemic production of IgE antibodies [76]. Vanoirbeek and colleagues studied the ability of TiO_2 nanoparticles to modulate the dermal sensitization process mediated by the potent dermal sensitizer, dinitrochlorobenzene (DNCB). They found that TiO_2 nanoparticles indeed increased the dermal sensitization potency of DNCB and could hold great potential in the field of immunomodulation [77,78].

Calcium Carbonate and Calcium Phosphate Nanoparticles

It is well-known that many people suffer from a particular metal-induced contact dermatitis, and functionalized nanoparticles hold great potential to reduce the penetration of metal ions through skin by enhancing the skin barrier properties and thus prevent these metal allergies. Previously, we evaluated the abilities of calcium carbonate (CaCO_3) and calcium phosphate (CaPO_4) nanoparticles to capture Ni^{2+} ions and minimize their penetration through the skin of pigs (in vitro) and mice (in vivo). The results showed that these nanoparticles could indeed capture the Ni^{2+} ions through a cation exchange process and showed a higher capture efficacy compared with the standard chelating agent, ethylenediaminetetraacetic acid (EDTA). In addition, the coated nanoparticles were retained on the surface of the skin and could be easily removed by washing with water without leaving any residue containing nickel or nanoparticles. Application of a combination of CaCO_3 and CaPO_4 nanoparticles could significantly reduce skin exposure to nickel ions, which suggested that these nanoparticles (smaller than 500 nm) hold great potential in the prevention of nickel allergy (Fig. 5.10) [15].

Quantum Dots

QDs are hybrid nanoparticles with a colloidal semiconductor core surrounded by various surface coatings. The QD surface can be coated with different chemical entities based on their specific applications. These surface coatings may affect both absorption and toxicity. QDs have potential biomedical applications as diagnostic and imaging agents due to their excellent optical activity [79,80]. However, their poor penetration properties and toxicity issues have restricted their applications [81,82]. Zhang and Monteiro-Riviere found negligible

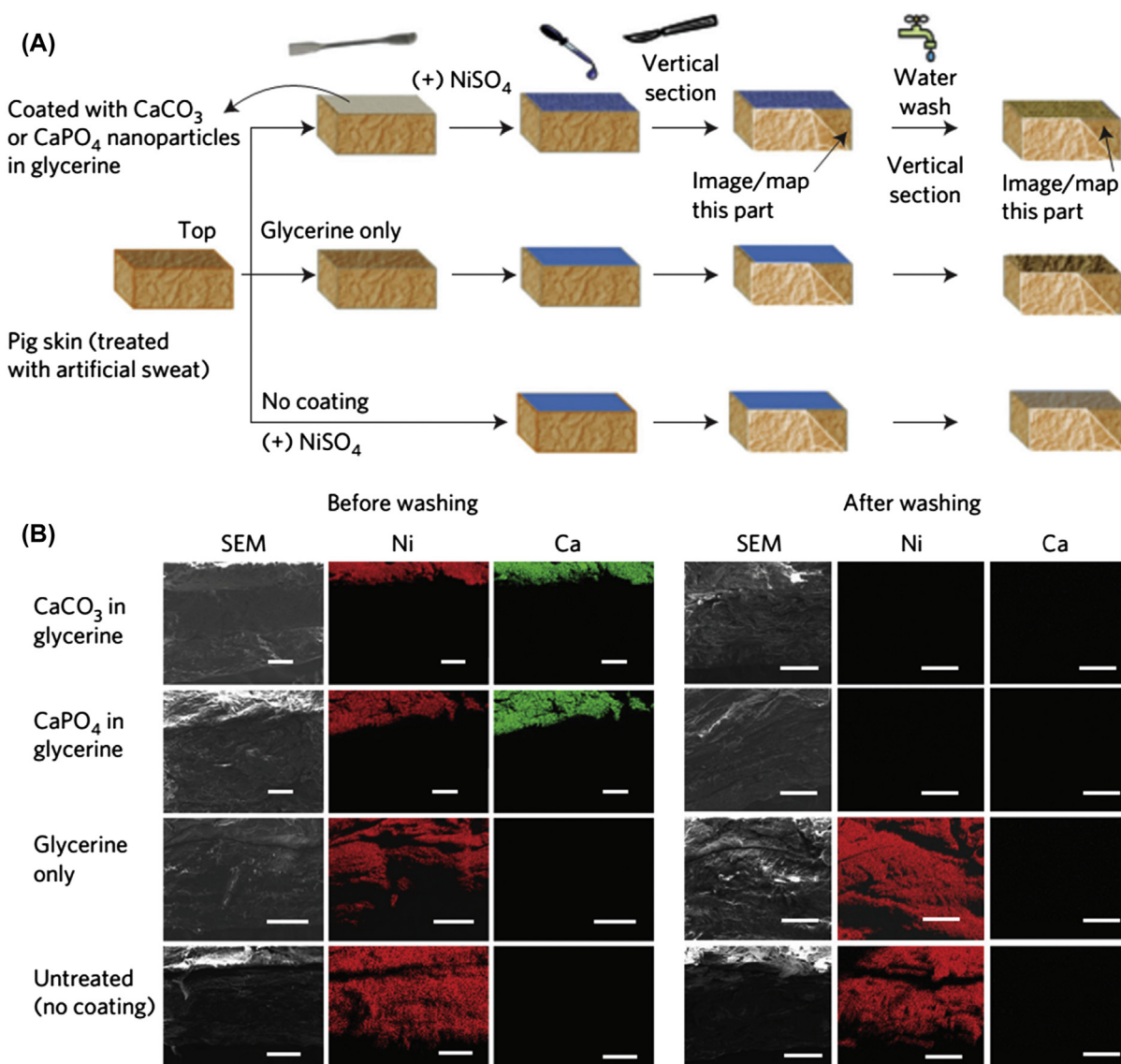


FIGURE 5.10 (A) Schematic of nickel permeation experiment with and without a nanoparticle coating on full-thickness pig skin. (B) Scanning electron microscopy (SEM) and elemental mapping images of vertically sectioned pigskin before (left) and after (right) rinsing with water. Scale bars: 200 μm . Reproduced by permission from Vemula PK, Anderson RR, Karp JM. Nanoparticles reduce nickel allergy by capturing metal ions. *Nat Nanotechnol* 2011;6(5):291–5.

penetration of QDs through the intact skin barrier, independent of species [81]. To understand the penetration properties of QDs, numerous studies have been performed with coatings with varying surface charge [79,80]. Gopee and Mortensen et al. compared the penetration of neutrally charged, PEG-coated, nail-shaped QDs (CdSe–CdS core–shell, 37 nm) with negatively charged, dihydrolipic acid-coated, sphere-shaped QDs (CdSe–ZnS core–shell, 15 nm) in dermabraded SKH hairless mice skin. Elemental analysis of the Cd ion concentration present in different organs convincingly demonstrated that neutral charged QDs (ca. 2% of the applied dose accumulated in the liver) have better

transdermal properties than negatively charged QDs (less than 0.001% of the applied dose in the lymph nodes) [26,80]. Understanding the fate and transport of topically applied QDs is critical for optimizing translational applications. Pedata et al. reported keratinocytes exposed to QDs with different surface coatings, including neutral, positive, and negative charges. Their findings demonstrated that neutral QDs are least as toxic as positively and negatively charged QDs. Among them all, the negatively charged QDs were found to be highly toxic at 20 nM concentrations [82]. These structure–activity findings will help in developing efficacious QDs for biomedical applications.

CONCLUSION

We have summarized the common inorganic nanoparticles that have been successfully used for topical and transdermal delivery. Inorganic nanoparticles may exhibit different nanotoxicity properties and varying skin penetration ability with different chemical components, shapes, sizes, and surface coatings (surface charges and hydrophilicity). The nanoparticles with a small size (<10 nm), high lipophilicity, and pronounced positive charges may be expected to passively penetrate the skin across the lipid matrix of the SC, while the larger nanoparticles penetrate the skin through the hair follicles and sweat glands. Some types of nanoparticles (TiO₂ and ZnO) hardly penetrate the skin at all and are just localized on the surface of the skin regardless of the size and surface coating. The smaller nanoparticles may exhibit higher nanotoxicity to the skin than the larger ones. Therefore, nanoparticles must be rationally and carefully selected and designed according to the practical purpose in each case.

Inorganic nanoparticles offer several advantages as nanocarriers for delivering drugs and genes into the skin, including protecting the therapeutic payload from enzymatic degradation, better delivery to the target site, and minimizing cellular toxicity during transport, without provoking adverse immune consequences. To date, numerous inorganic nanoparticles have been constructed for topical and transdermal applications such as gene regulation, wound healing, prevention of metal allergy, improved sunscreens, and immunomodulatory agents. However, the potential deleterious effects of these nanoparticles have yet to be completely evaluated. There is a growing concern regarding the toxicity of many heavy metals used in the preparation of nanoparticles. It is interesting and challenging to develop and design other inorganic nanoparticles that could be the ideal transdermal carriers in light of a comprehensive analysis of their nanotoxicity and skin permeability, which holds great potential for macromolecular drug delivery. In addition, direct quantitative evidence about the routes of skin penetration of nanoparticles still remains elusive. Above all, the future of the arena is emerging bright with the increased prevalence of skin problems in the world today.

Acknowledgments

XCJ is grateful for support from NTU-NU Institute of Nanomedicine. PKV thanks the Department of Biotechnology for a Ramalingaswami Re-Entry Fellowship and BIRAC for a Biotechnology Ignition Grant. SKM thanks the Department of Science and Technology for a Fast Track Fellowship.

References

- [1] Prausnitz MR, Langer R. Transdermal drug delivery. *Nat Biotechnol* 2008;26(11):1261–8.
- [2] Sharma A, Saini S, Rana A. Transdermal drug delivery system: a review. *Int J Res Pharm Biomed Sci* 2013;4(1):286–92.
- [3] Proksch E, Brandner JM, Jensen JM. The skin: an indispensable barrier. *Exp Dermatol* 2008;17(12):1063–72.
- [4] Cázares-Delgadillo J, Naik A, Ganem-Rondero A, Quintanar-Guerrero D, Kalia Y. Transdermal delivery of cytochrome C-A 12.4 kDa protein-across intact skin by constant-current iontophoresis. *Pharm Res* 2007;24(7):1360–8.
- [5] Alvarez-Román R, Merino G, Kalia YN, Naik A, Guy RH. Skin permeability enhancement by low frequency sonophoresis: lipid extraction and transport pathways. *J Pharm Sci* 2003;92(6):1138–46.
- [6] Lombry C, Dujardin N, Pr  at V. Transdermal delivery of macromolecules using skin electroporation. *Pharm Res* 2000;17(1):32–7.
- [7] Prausnitz MR. Microneedles for transdermal drug delivery. *Adv Drug Deliv Rev* 2004;56(5):581–7.
- [8] Murthy SN, Sammeta SM, Bowers C. Magnetophoresis for enhancing transdermal drug delivery: mechanistic studies and patch design. *J Control Release* 2010;148(2):197–203.
- [9] Kotiyan P, Vavia P, Bhardwaj Y, Sabarwal S, Majali A. Electron beam irradiation: a novel technology for the development of transdermal system of isosorbide dinitrate. *Int J Pharm* 2004;270(1):47–54.
- [10] Dianzani C, Zara GP, Maina G, Pettazzoni P, Pizzimenti S, Rossi F, et al. Drug delivery nanoparticles in skin cancers. *BioMed Res Int* 2014;2014:1–13.
- [11] Palac Z, Engesland A, Flaten GE, Škalko-Basnet N, Filipovic-Grcic J, Vanic Z. Liposomes for (trans) dermal drug delivery: the skin-PVPA as a novel in vitro stratum corneum model in formulation development. *J Liposome Res* 2014;24(4):313–22.
- [12] Kwon SS, Kim SY, Kong BJ, Kim KJ, Noh GY, Im NR, et al. Cell-penetrating peptide-conjugated liposomes as transdermal delivery system of polygonumaviculare L. extract. *Int J Pharm* 2015;483:26–37.
- [13] Han SB, Kwon SS, Jeong YM, Yu ER, Park SN. Physical characterization and in vitro skin permeation of solid lipid nanoparticles for transdermal delivery of quercetin. *Int J Cosmet Sci* 2014;36(6):588–97.
- [14] Lapteva M, Mondon K, M  ller M, Gurny R, Kalia YN. Polymeric micelle nanocarriers for the cutaneous delivery of tacrolimus: a targeted approach for the treatment of psoriasis. *Mol Pharm* 2014;11(9):2989–3001.
- [15] Vemula PK, Anderson RR, Karp JM. Nanoparticles reduce nickel allergy by capturing metal ions. *Nat Nanotechnol* 2011;6(5):291–5.
- [16] Zheng D, Giljohann DA, Chen DL, Massich MD, Wang X-Q, Iordanov H, et al. Topical delivery of siRNA-based spherical nucleic acid nanoparticle conjugates for gene regulation. *Proc Natl Acad Sci USA* 2012;109(30):11975–80.
- [17] Uchechi O, Ogbonna JD, Attama AA. Nanoparticles for dermal and transdermal drug delivery. In: Demir Sezer A, editor. *Appl. Nanotechnol. Drug Deliv*; 2014. Chapter 6.
- [18] Schmid-Wendtner M-H, Korting HC. The pH of the skin surface and its impact on the barrier function. *Skin Pharm Physiol* 2006;19(6):296–302.
- [19] Prow TW, Grice JE, Lin LL, Faye R, Butler M, Becker W, et al. Nanoparticles and microparticles for skin drug delivery. *Adv Drug Deliv Rev* 2011;63(6):470–91.
- [20] Baroli B, Ennas MG, Loffredo F, Isola M, Pinna R, L  pez-Quintela MA. Penetration of metallic nanoparticles in human full-thickness skin. *J Invest Dermatol* 2007;127(7):1701–12.
- [21] Shanmugam S, Song C-K, Nagayya-Sriraman S, Baskaran R, Yong C-S, Choi H-G, et al. Physicochemical characterization and

- skin permeation of liposome formulations containing clindamycin phosphate. *Arch Pharmacol Res* 2009;32(7):1067–75.
- [22] Ryman-Rasmussen JP, Riviere JE, Monteiro-Riviere NA. Penetration of intact skin by quantum dots with diverse physicochemical properties. *Toxicol Sci* 2006;91(1):159–65.
- [23] Rancan F, Gao Q, Graf C, Troppens S, Hadam S, Hackbarth S, et al. Skin penetration and cellular uptake of amorphous silica nanoparticles with variable size, surface functionalization, and colloidal stability. *ACS Nano* 2012;6(8):6829–42.
- [24] Fernandes R, Smyth NR, Muskens OL, Nitti S, Heuer-Jungemann A, Arden-Jones MR, et al. Interactions of skin with gold nanoparticles of different surface charge, shape, and functionality. *Small* 2015;11(6):713–21.
- [25] Iannuccelli V, Bertelli D, Romagnoli M, Scalia S, Maretti E, Sacchetti F, et al. In vivo penetration of bare and lipid-coated silica nanoparticles across the human stratum corneum. *Colloid Surface B* 2014;122:653–61.
- [26] Gopee NV, Roberts DW, Webb P, Cozart CR, Siitonen PH, Latendresse JR, et al. Quantitative determination of skin penetration of PEG-coated CdSe quantum dots in dermabrased but not intact SKH-1 hairless mouse skin. *Toxicol Sci* 2009;111(1):37–48.
- [27] Desai P, Patlolla RR, Singh M. Interaction of nanoparticles and cell-penetrating peptides with skin for transdermal drug delivery. *Mol Membr Biol* 2010;27(7):247–59.
- [28] Gamer A, Leibold E, Van Ravenzwaay B. The in vitro absorption of microfine zinc oxide and titanium dioxide through porcine skin. *Toxicol In Vitro* 2006;20(3):301–7.
- [29] Rouse JG, Yang J, Ryman-Rasmussen JP, Barron AR, Monteiro-Riviere NA. Effects of mechanical flexion on the penetration of fullerene amino acid-derivatized peptide nanoparticles through skin. *Nano Lett* 2007;7(1):155–60.
- [30] Wiechers JW, Musee N. Engineered inorganic nanoparticles and cosmetics: facts, issues, knowledge gaps and challenges. *J Biomed Nanotechnol* 2010;6(5):408–31.
- [31] Kango S, Kalia S, Celli A, Njuguna J, Habibi Y, Kumar R. Surface modification of inorganic nanoparticles for development of organic–inorganic nanocomposites—a review. *Prog Polym Sci* 2013;38(8):1232–61.
- [32] Sedlmeier A, Gorris HH. Surface modification and characterization of photon-upconverting nanoparticles for bioanalytical applications. *Chem Soc Rev* 2015;44:1526–60.
- [33] Li X, Wu Y, Liu Y, Zou X, Yao L, Li F, et al. Cyclometallated ruthenium complex-modified upconversion nanophosphors for selective detection of Hg 2+ ions in water. *Nanoscale* 2014;6(2):1020–8.
- [34] Cui S, Chen H, Zhu H, Tian J, Chi X, Qian Z, et al. Amphiphilic chitosan modified upconversion nanoparticles for in vivo photodynamic therapy induced by near-infrared light. *J Mater Chem* 2012;22(11):4861–73.
- [35] Park J, Yu MK, Jeong YY, Kim JW, Lee K, Phan VN, et al. Antibiofouling amphiphilic polymer-coated superparamagnetic iron oxide nanoparticles: synthesis, characterization, and use in cancer imaging in vivo. *J Mater Chem* 2009;19(35):6412–7.
- [36] Boccalon M, Bidoggia S, Romano F, Gualandi L, Franchi P, Lucarini M, et al. Gold nanoparticles as drug carriers: a contribution to the quest for basic principles for monolayer design. *J Mater Chem B* 2015;3(3):432–9.
- [37] Jana NR, Earhart C, Ying JY. Synthesis of water-soluble and functionalized nanoparticles by silica coating. *Chem Mater* 2007;19(21):5074–82.
- [38] Lin Z, Sun L, Liu W, Xia Z, Yang H, Chen G. Synthesis of boronic acid-functionalized molecularly imprinted silica nanoparticles for glycoprotein recognition and enrichment. *J Mater Chem B* 2014;2(6):637–43.
- [39] Binder WH, Sachsenhofer R, Straif CJ, Zirbs R. Surface-modified nanoparticles via thermal and Cu (I)-mediated “click” chemistry: generation of luminescent CdSe nanoparticles with polar ligands guiding supramolecular recognition. *J Mater Chem* 2007;17(20):2125–32.
- [40] Tan YF, Mundargi RC, Chen MHA, Lessig J, Neu B, Venkatraman SS, et al. Layer-by-layer nanoparticles as an efficient siRNA delivery vehicle for SPARC silencing. *Small* 2014;10(9):1790–8.
- [41] Zhou J, Pishko MV, Lutkenhaus JL. Thermoresponsive layer-by-layer assemblies for nanoparticle-based drug delivery. *Langmuir* 2014;30(20):5903–10.
- [42] Lu X, Jiang R, Yang M, Fan Q, Hu W, Zhang L, et al. Monodispersed grafted conjugated polyelectrolyte-stabilized magnetic nanoparticles as multifunctional platform for cellular imaging and drug delivery. *J Mater Chem B* 2014;2(4):376–86.
- [43] Mobarok MH, Buriak JM. Elucidating the surface chemistry of zinc phosphide nanoparticles through ligand exchange. *Chem Mater* 2014;26(15):4653–61.
- [44] Fan X, Lin L, Messersmith PB. Surface-initiated polymerization from TiO₂ nanoparticle surfaces through a biomimetic initiator: a new route toward polymer-matrix nanocomposites. *Compos Sci Technol* 2006;66(9):1198–204.
- [45] Liu P, Wang T. Surface-graft hyperbranched polymer via self-condensing atom transfer radical polymerization from zinc oxide nanoparticles. *Polym Eng Sci* 2007;47(9):1296–301.
- [46] Shahabadi R, Abdollahi M, Sharif A. Preparation, characterization and properties of polymer electrolyte nanocomposite membranes containing silica nanoparticles modified via surface-initiated atom transfer radical polymerization. *Int J Hydrogen Energy* 2015;40(9):3749–61.
- [47] Chen G, Zhao Y, Fu G, Duchesne PN, Gu L, Zheng Y, et al. Interfacial effects in Iron–Nickel Hydroxide–Platinum nanoparticles enhance catalytic oxidation. *Science* 2014;344(6183):495–9.
- [48] Radhakrishnan S, Krishnamoorthy K, Sekar C, Wilson J, Kim SJ. A highly sensitive electrochemical sensor for nitrite detection based on Fe₂O₃ nanoparticles decorated reduced graphene oxide nanosheets. *Appl Catal B* 2014;148:22–8.
- [49] Dar MI, Chandiran AK, Grätzel M, Nazeeruddin MK, Shivashankar SA. Controlled synthesis of TiO₂ nanoparticles and nanospheres using a microwave assisted approach for their application in dye-sensitized solar cells. *J Mater Chem A* 2014;2(6):1662–7.
- [50] Montalti M, Prodi L, Rampazzo E, Zaccheroni N. Dye-doped silica nanoparticles as luminescent organized systems for nanomedicine. *Chem Soc Rev* 2014;43(12):4243–68.
- [51] Nakamura T, Sugihara F, Matsushita H, Yoshioka Y, Mizukami S, Kikuchi K. Mesoporous silica nanoparticles for ¹⁹F magnetic resonance imaging, fluorescence imaging, and drug delivery. *Chem Sci* 2015;6:1986–90.
- [52] Park Y-H, Bae HC, Jang Y, Jeong SH, Lee HN, Ryu W-I, et al. Effect of the size and surface charge of silica nanoparticles on cutaneous toxicity. *Mol Cell Toxicol* 2013;9(1):67–74.
- [53] Yang J-H, Lee S-Y, Han Y-S, Park K-C, Choy J-H. Efficient transdermal penetration and improved stability of L-ascorbic acid encapsulated in an inorganic nanocapsule. *Bull Korean Chem Soc* 2003;24(4):499–503.
- [54] Rozman B, Gosenca M, Gasperlin M, Padois K, Falson F. Dual influence of colloidal silica on skin deposition of vitamins C and E simultaneously incorporated in topical microemulsions. *Drug Dev Ind Pharm* 2010;36(7):852–60.
- [55] Scalia S, Franceschinis E, Bertelli D, Iannuccelli V. Comparative evaluation of the effect of permeation enhancers, lipid nanoparticles and colloidal silica on in vivo human skin penetration of quercetin. *Skin Pharm Physiol* 2012;26(2):57–67.
- [56] Hirai T, Yoshikawa T, Nabeshi H, Yoshida T, Tochigi S, Ichihashi K-i, et al. Amorphous silica nanoparticles size-dependently aggravate atopic dermatitis-like skin lesions following an intradermal injection. *Part Fibre Toxicol* 2012;9(3):8977–9.

- [57] Hamam F, Al-Remawi M. Novel delivery system of curcumin through transdermal route using sub-micronized particles composed of mesoporous silica and oleic acid. *J Funct Foods* 2014;8:87–99.
- [58] Ghosh P, Han G, De M, Kim CK, Rotello VM. Gold nanoparticles in delivery applications. *Adv Drug Deliv Rev* 2008;60(11):1307–15.
- [59] Sonavane G, Tomoda K, Sano A, Ohshima H, Terada H, Makino K. In vitro permeation of gold nanoparticles through rat skin and rat intestine: effect of particle size. *Colloid Surface B* 2008;65(1):1–10.
- [60] Pissuwan D, Nose K, Kurihara R, Kaneko K, Tahara Y, Kamiya N, et al. A solid-in-oil dispersion of gold nanorods can enhance transdermal protein delivery and skin vaccination. *Small* 2011;7(2):215–20.
- [61] Labala S, Mandapalli PK, Kurumaddali A, Venuganti VVK. Layer-by-layer polymer coated gold nanoparticles for topical delivery of imatinib mesylate to treat melanoma. *Mol Pharm* 2015;12:878–88.
- [62] Ramadan S, Guo L, Li Y, Yan B, Lu W. Hollow copper sulfide nanoparticle-mediated transdermal drug delivery. *Small* 2012;8(20):3143–50.
- [63] Kievit FM, Wang FY, Fang C, Mok H, Wang K, Silber JR, et al. Doxorubicin loaded iron oxide nanoparticles overcome multi-drug resistance in cancer in vitro. *J Control Release* 2011;152(1):76–83.
- [64] Rao YF, Chen W, Liang XG, Huang YZ, Miao J, Liu L, et al. Epirubicin-loaded superparamagnetic Iron-Oxide nanoparticles for transdermal delivery: cancer therapy by circumventing the skin barrier. *Small* 2015;11(2):239–47.
- [65] Tran QH, Le A-T. Silver nanoparticles: synthesis, properties, toxicology, applications and perspectives. *Adv Nat Sci: Nanosci Nanotechnol* 2013;4(3):033001.
- [66] Levard C, Hotze EM, Lowry GV, Brown Jr GE. Environmental transformations of silver nanoparticles: impact on stability and toxicity. *Environ Sci Technol* 2012;46(13):6900–14.
- [67] Larese FF, D'Agostin F, Crosera M, Adami G, Renzi N, Bovenzi M, et al. Human skin penetration of silver nanoparticles through intact and damaged skin. *Toxicology* 2009;255(1):33–7.
- [68] George R, Merten S, Wang TT, Kennedy P, Maitz P. In vivo analysis of dermal and systemic absorption of silver nanoparticles through healthy human skin. *Australas J Dermatol* 2014;55(3):185–90.
- [69] Samberg ME, Oldenburg SJ, Monteiro-Riviere NA. Evaluation of silver nanoparticle toxicity in skin in vivo and keratinocytes in vitro. *Environ Health Perspect (Online)* 2010;118(3):407.
- [70] Tian J, Wong KK, Ho CM, Lok CN, Yu WY, Che CM, et al. Topical delivery of silver nanoparticles promotes wound healing. *Chem-MedChem* 2007;2(1):129–36.
- [71] Chowdhury S, De M, Guha R, Batabyal S, Samanta I, Hazra SK, et al. Influence of silver nanoparticles on post-surgical wound healing following topical application. *Eur J Nanomed* 2014;6(4):237–47.
- [72] Zvyagin AV, Zhao X, Gierden A, Sanchez W, Ross JA, Roberts MS. Imaging of zinc oxide nanoparticle penetration in human skin in vitro and in vivo. *J Biomed Opt* 2008;13(6):064031.
- [73] Kuo T-R, Wu C-L, Hsu C-T, Lo W, Chiang S-J, Lin S-J, et al. Chemical enhancer induced changes in the mechanisms of transdermal delivery of zinc oxide nanoparticles. *Biomaterials* 2009;30(16):3002–8.
- [74] Bennett SW, Zhou D, Mielke R, Keller AA. Photoinduced disaggregation of TiO₂ nanoparticles enables transdermal penetration. *PLoS ONE* 2012;7(11):e48719.
- [75] Choi Y-G, Lee JH, Bae I-H, Ah Y-C, Ki H-M, Bae J-H, et al. Titanium dioxide inclusion in backing reduce the photoallergenicity of ketoprofen transdermal patch. *Arch Toxicol* 2011;85(3):219–26.
- [76] Ilves M, Palomäki J, Vippola M, Lehto M, Savolainen K, Savinko T, et al. Topically applied ZnO nanoparticles suppress allergen induced skin inflammation but induce vigorous IgE production in the atopic dermatitis mouse model. *Part Fibre Toxicol* 2014;11(1):38.
- [77] Hussain S, Smulders S, De Vooght V, Ectors B, Boland S, Marano F, et al. Nano-titanium dioxide modulates the dermal sensitization potency of DNCB. *Part Fibre Toxicol* 2012;9(1):1–9.
- [78] Smulders S, Golanski L, Smolders E, Vanoirbeek J, Hoet P. Nano-TiO₂ modulates the dermal sensitization potency of dinitrochlorobenzene after topical exposure. *Br J Dermatol* 2015;172:392–9.
- [79] Mortensen LJ, Glazowski CE, Zavislan JM, DeLouise LA. Near-IR fluorescence and reflectance confocal microscopy for imaging of quantum dots in mammalian skin. *Biomed Opt Express* 2011;2(6):1610–25.
- [80] DeLouise LA. Applications of nanotechnology in dermatology. *J Invest Dermatol* 2012;132(3 Pt 2):964–75.
- [81] Zhang LW, Monteiro-Riviere NA. Assessment of quantum dot penetration into intact, tape-stripped, abraded and flexed rat skin. *Skin Pharm Physiol* 2008;21(3):166–80.
- [82] Pedata P, Boccellino M, La Porta R, Napolitano M, Minutolo P, Sgro LA, et al. Interaction between combustion-generated organic nanoparticles and biological systems: in vitro study of cell toxicity and apoptosis in human keratinocytes. *Nanotoxicology* 2012;6(4):338–52.

Biodegradable, Biocompatible, and Bioconjugate Materials as Delivery Agents in Dermatology

Safe Drug Delivery to Skin

F. Rancan*

Charité – Universitätsmedizin Berlin, Berlin, Germany

OUTLINE

Introduction	73	<i>Biocompatible Inorganic Nanocarriers</i>	80
Types of Nanocarriers	74	Nanocarrier Biodegradability and Biocompatibility in Skin	80
<i>Biological Nanocarriers</i>	74	Conclusions	83
<i>Bioconjugates</i>	76	Abbreviations	83
<i>Biodegradable Organic Nanocarriers</i>	77	References	84
Polypeptides	77		
Polysaccharides	78		
Synthetic Polymers	78		
<i>Biocompatible Organic Nanocarriers</i>	79		

INTRODUCTION

The increasing use of nanocarriers in medicine is mainly due to the peculiar properties of nanomaterials. First of all, as their name indicates, they can carry a therapeutic cargo and improve its pharmacokinetics. Nanocarriers protect drugs from rapid degradation or excretion, allowing for enhanced bioavailability with respect to free drug formulations. Surface functionalization confers further special characteristics such as long circulating and targeting properties. In addition, stimuli-responsive nanocarriers allow the release of

drugs in response to environment-specific conditions. In particular, genetically engineered biopharmaceuticals have brought new challenges with regard to their delivery, biodistribution, and potential side effects. Due to their instability, mechanism of action, and production costs, these drugs need to be administered by parenteral routes and get effectively transported to the target site. The rapidly developing nanotechnology field offers tailor-made solutions for these new classes of pharmaceuticals. Cancer immunotherapy is another rapidly developing field that is strongly supported by nanotechnology. Increasingly, nanoparticle-based antitumor

*Part of this work was included in the thesis submitted by Dr F. Rancan to the Charité—Universitätsmedizin Berlin for the degree of assistant professor in experimental dermatology.

vaccination strategies use the intradermal or subcutaneous administration route to create antigen depots and target antigens to skin immune system cells [1].

One of the most important aspects of nanocarrier-based drug delivery is biocompatibility. Considering the unique interactions between nanocarriers and biological materials [2], their compatibility with the host organism is of major importance to ensure the safety of nanotechnology-based therapies.

There are different types of classification for nanocarriers. When considering the constituting material, classification can be made into inorganic nanocarriers, which are made of inorganic materials (eg, metals or metal oxides), and organic nanocarriers, which are made of materials derived from living organisms and containing predominantly the elements carbon, hydrogen, as well as oxygen and nitrogen. Two types of organic nanocarriers can be distinguished: synthetic or biological ones. Synthetic nanocarriers are made of polymers, branched polymers, and dendrimers, which organize in supramolecular structures like micelles, nanocapsules, and spherical or elongated nanoparticles. Biological nanocarriers are complex particles derived from or resembling living organisms or parts thereof. They are made of lipids, proteins, and nucleic acids. Viruses, bacteria, proteins, virosomes, and virus-like particles belong to this category. Bioconjugates can also be considered as nanocarriers. These macromolecules are drugs covalently conjugated to biological molecules that serve as targeting units.

Depending on the toxicity of the constituting material, and the ways it is metabolized or excreted after administration, nanocarriers are classified as biodegradable and/or biocompatible. From the ecological point of view, the term *biodegradable* means environmentally friendly degradation of a material as a result of biological processes. In medicine, a material can be considered biodegradable when it decomposes to products that have low toxicity and can be metabolized and/or excreted. In contrast, a matter can be considered *biocompatible* when, even if not biodegradable, it exerts no local or systemic side effects. Biocompatible materials have been used in medicine for decades (eg, orthopedic implants and fillers). However, other than medical implants, penetrated nanocarriers cannot be removed. Thus, even if they have no acute toxicity, to be considered as safe, they have to be eliminated by biliary or renal excretion. In addition, even if nanocarriers are made of nontoxic material, impurities may cause toxicity (eg, reagents and solvents used in the synthesis or biological contaminants in the case of biopharmaceuticals). Therefore, each promising nanocarrier intended for human use needs to be subjected to comprehensive toxicology as well as pharmacokinetics studies. Different *in vitro* and *in vivo* tests have to be

applied, depending on the administration route, doses and duration of the designed therapy, target organ, and possible nonspecific toxicity. Carcinogenic risks have to be identified as well as possible metabolites or degradation products, which might exert toxic effects. In addition, the potential induction of an immune reaction has to be evaluated. Nanocarriers are often taken up by phagocytes and other immunoactive cells, with consequent release of cytokines and induction of inflammatory or allergic reactions. Thus, systemic and local increase of markers for irritation and inflammation as well as inflammatory cell infiltrates at the site of application should be monitored.

Because biodegradability and biocompatibility strictly depend on the constituting materials, in this chapter, we classify and describe the most relevant drug delivery systems according to their composition as well as their compatibility and degradability in the human body. In general, most biological nanocarriers are biodegradable. However, among organic nanocarriers, we can distinguish between biodegradable and nonbiodegradable ones. Biocompatible nanocarriers are nonbiodegradable delivery agents with no or minimal toxicity, depending on the intended application and administration route. In the following section, five types of nanocarriers are described: (1) biological biodegradable carriers, (2) bioconjugates, (3) organic biodegradable carriers, (4) organic biocompatible carriers, and (5) inorganic biocompatible carriers (Fig. 6.1). It has to be noted that this is a general classification and that several delivery agents are hybrid architectures consisting of both biodegradable and nonbiodegradable units, or both organic and inorganic units.

TYPES OF NANOCARRIERS

Biological Nanocarriers

Supramolecular architectures that derive or resemble structures from living organisms can be classified as biological nanocarriers. Virus-like particles (VLPs), virosomes, bacteria ghosts, lipoproteins, and protein-based nanocarriers are typical examples. Their disassembling or enzymatic degradation results in molecules that can be metabolized or excreted. Endogenous enzymes like protease, lipase, and nuclease can degrade biological nanocarriers with kinetics depending on the carrier composition and the site of accumulation (eg, extracellular space and lysosomes). Enzymatic activity can also be exploited to favor the release of drugs to specific target areas such as diseased tissue or cell populations with a particularly high enzymatic activity. Nanocarriers mimicking natural microorganisms, able to penetrate biological barriers and

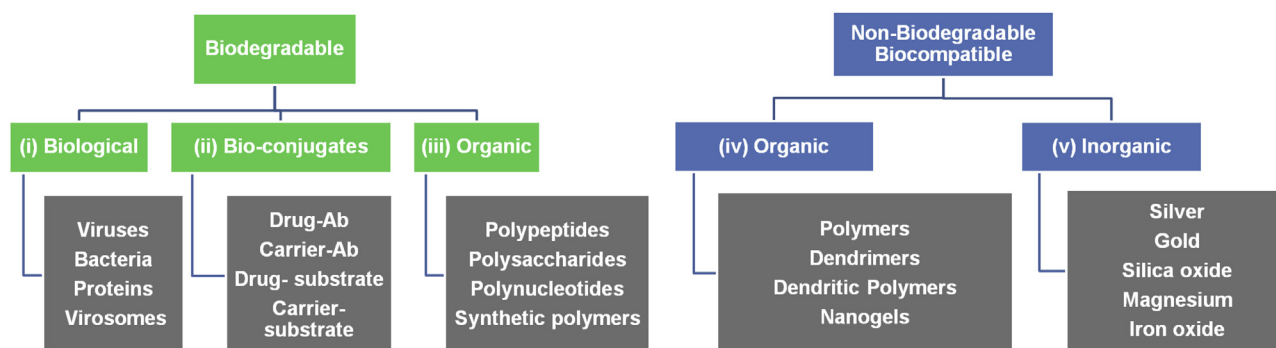


FIGURE 6.1 General classification of nanocarriers considering their composition, biodegradability, and biocompatibility. Not all types of nanocarriers fit in this classification, such as nanocarriers made of biodegradable subunits coupled to nonbiodegradable biocompatible moieties. Ab, Antibody.

enter cells, are promising drug delivery strategies. The main drawbacks of these nanocarriers are their virulent and immunogenic properties. For example, cell-penetrating peptides (CPPs), which are often conjugated to nanocarriers, can induce membrane leakage with consequent cytotoxicity [3]. Moreover, microorganisms like viruses have the natural ability to deliver their genetic material into host cells. Therefore, viral gene vectors are widely used to transfect cells in vitro and in vivo, and they were also tested in Phase I–III clinical trials [4]. However, to reduce concerns with regard to off-target effects (ie, transfection of unwanted cell populations), these vectors have to be genetically modified to enhance their specificity to target cells.

Besides inactivated viruses, there are many other types of biological nanocarriers. VLPs are genetically engineered nanocarriers made of virus proteins that can autoassemble to form empty virus capsids. They are nonvirulent and can transport antigens, fusion proteins, as well as drugs and nucleic acids [5]. They are extensively investigated as antigen carriers for vaccination strategies. VLPs carrying the L1 capsid protein of human papillomavirus subtypes 16 and 18 are actually on the market (Gardasil and Carvarix). VLPs are also investigated for transcutaneous vaccination strategies. A VLP-based influenza vaccine was administered by intradermal injection or microneedles, showing host responses including activation and migration of dendritic cells as well as their interaction with T cells [6].

Virosomes are liposome-like structures containing inserted glycoproteins of viral provenience. Glycoproteins like hemagglutinin and neuraminidase confer on them adjuvant properties as well as cell-targeting and endosome-escaping abilities, making them ideal nanocarriers for vaccination purposes and for cancer and gene therapy [7].

Invasomes are liposomes containing small amounts of penetration enhancers like ethanol and terpenes, which have been shown to improve drug delivery to skin. For example, invasomes containing different

penetration enhancers like ethanol cineole, citral, and D-limonene were useful for the delivery of temoporfin, a photosensitizer for photodynamic therapy, to both the epidermis and dermis [8].

Bacteria generally regarded as safe and with low virulence degree can be used to transport drugs, taking advantage of their cell-penetrating ability. Empty bacterial ghosts can be loaded with drugs or with nanoparticles carrying plasmid deoxyribonucleic acid (DNA) adsorbed on their surface. Recombinant bacteria can also be prepared with inserted plasmid vectors encoding for therapeutic proteins like interleukins and enzymes. For example, bacteria producing interleukin-10 (IL10) were used to treat inflammatory bowel disease [9].

Proteins are also used as carrier systems. They can be directly linked to drugs (bioconjugates) or be used as units to form nanoparticles for the transport of active molecules. Various synthetic methods were utilized (eg, cross-linking, heat, coacervation, nanoprecipitation, emulsification, and solvent evaporation) in order to prepare nanoparticles starting from natural proteins and encapsulate drugs. Because nanocarriers based on natural proteins have low homogeneity, recombinant proteins have been used with defined structures, defined cross-linking and drug-binding groups, as well as defined degradable sequences in order to improve stability as well as the loading and release capacity. One important drawback of nanocarriers based on human or animal proteins is that, as most nanocarriers are of hydrophilic nature, they release encapsulated drugs very quickly [10]. To control release kinetics, the degree of cross-linking can be enhanced, but a high degree of cross-linking might reduce nanoparticle biodegradation or give rise to toxicity once the cross-linker is released during biodegradation [10]. In general, low immunotoxicity was detected for most protein-based nanocarriers [11–13].

Human serum albumin, as a natural carrier system able to cross the endothelial barrier by receptor-mediated endocytosis, is extensively investigated as a

nonimmunogenic delivery system for biomacromolecules. Different albumin-based drugs are already on the market for the treatment of cancer (eg, paclitaxel loaded on albumin nanoparticles (Abraxane)) or diabetes, or as a diagnostic agent. Albumin-based particles were also used as delivery agents for transcutaneous antigen delivery in a study on melanoma cancer vaccination by means of micro-needles [14].

Other animal proteins used as nanocarriers are animal proteins like collagen, gelatin, fibrin, and milk proteins. Collagen is a widely abundant protein that forms bundles and is responsible for the mechanical stability of tissues. In a small study on five postmenopausal woman, hydrogels containing either estradiol loaded on collagen-based nanoparticles or the same amount of drug without nanoparticles were compared and demonstrated the superiority of the particle-based 17β -estradiol-hemihydrate formulation [15]. Gelatin is derived from collagen, and, thanks to its denaturated form, it has low immunogenicity. Cationized gelatin microspheres were used to deliver small interfering RNA (siRNA) to hair follicles in a mice model of alopecia areata [16]. Casein is the most abundant milk protein, and it is formed from both hydrophilic and hydrophobic sequences and tends to spontaneously assemble to form micelles. Elastin is a component of the extracellular matrix with the function to make tissues resilient and elastic.

Typical plant proteins used to prepare nanocarriers are zein (from corn kernels), gliadin (from wheat gluten), soy proteins, and lectins. These proteins hydrolyze slower in aqueous solution than most animal proteins do, thanks to hydrophobic amino acids or sulfide bonds. This results in slower degradation and release kinetics with prolonged and sustained drug release [10]. The presence of neutral and hydrophobic domains makes these nanocarriers more mucoadhesive and suitable for the release of lipophilic drugs. Plant-derived lectins have attracted attention because of their affinity to the glycosylated components of cell membranes, which can be exploited to enhance cellular uptake and the targeting of diseased cells overexpressing certain types of glycoproteins. Lectin-conjugated gliadin nanoparticles were used to target an antimicrobial drug to *Helicobacter pylori* [17], suggesting that similar nanoparticle formulations might be useful to treat skin and wound infections.

Other types of nanocarriers resembling natural biological structures are those made predominantly of lipids. Natural carriers belonging to this category are the low and high-density lipoproteins (LDLs and HDLs, respectively), vesicles that transport lipophilic substances in the blood. Lipid-based nanocarriers mimic these natural transporters. Liposomes, for example, are made of phospholipids organized in double layers and forming spheres with a hydrophobic compartment, a

hydrophilic surface, and a hollow core. They can be produced at the nanometer scale with all the advantages of nanoparticle formulations. Liposomes loaded with siRNA have been used in combination with low-frequency ultrasound to increase skin permeability and treat early or invasive cutaneous melanoma reducing systemic toxicity [18]. Solid lipid nanoparticles (SLNs) and nanostructured lipid carriers (NLCs) were developed to improve the performance of nanoemulsions, in that the liquid lipid phase is substituted with a solid one (SLN) or a blend of solid and liquid lipids (NLC) [19]. They are made by natural solid or liquid lipids forming matrix-filled nanoparticles where the core is made by solid or liquid lipids. Such lipid-based nanocarriers are disassembled, and their components (lipids and lipoproteins) are metabolized and excreted by endogenous pathways. They are ideal for the delivery of hydrophobic drugs and are widely used in dermatology because of their ability to form a film on skin surface, which reduces water loss and improves skin hydration (occlusive effect). They were also widely investigated because of their affinity to the hydrophobic extracellular matrix of the stratum corneum (SC) and their ability to destabilize its ordered structure, improving skin barrier permeability [20]. As an alternative to transdermal application, depots of drugs in the dermis or subcutaneous tissue allow for a prolonged and sustained delivery. Tristearin SLNs were used to deliver siRNA to skin. After intradermal injection in mouse footpads, prolonged siRNA release over a period of 10–13 days could be measured [21].

Bioconjugates

Bioconjugates are made of biological molecules, mostly serving as targeting or penetrating units, chemically bound to molecules possessing a functional property such as a drug or a diagnostic agent. A typical example is antibodies conjugated to drugs (ie, antibody–drug conjugates), which are used to enhance drug tissue targeting. Antibodies with specific therapeutic activities can also be conjugated to a drug to enhance efficacy [22]. Also, architectures in which the drug is loaded on a carrier unit (eg, nanoparticle), which is linked to a targeting biological unit (eg, antibody), can be considered as bioconjugates. Antibodies can also be conjugated to multiunit carrier systems, where a drug cargo is loaded on nanocarriers that are decorated with different surface molecules with stabilizing or imaging functions [23].

Another type of bioconjugate architecture is CPPs grafted on nanocarriers. These peptides resemble the penetrating units of viruses and increase the intracellular uptake of nanocarriers avoiding their

entrapment in endosomes. Fusion proteins between CPPs and catalase or superoxidismutase were investigated as antioxidative agents and were shown to penetrate the epidermis as well as the dermis after topical application [24]. CPPs were also used to enhance skin penetration of antigenic peptides for vaccination purposes [25]. CPP–elastin complexes were prepared to deliver elastin to fibroblasts [26]. Furthermore, CPPs were coupled to SLNs, resulting in enhanced skin penetration and delivery of a model antiinflammatory drug [27]. Filaggrin was administered topically as a strategy to restore skin barrier function in atopic dermatitis. The protein was delivered conjugated to CPPs in order to increase skin penetration and cellular uptake. After topical application of the conjugate to filaggrin-deficient mice, the recombinant protein was reprocessed with consequent restoration of the normal skin phenotype [28].

Proteins like transferrin, which are recognized by specific membrane receptors and internalized by cells, have been conjugated to drugs and used as targeting units. Similarly, because of their ability to bind to glycoproteins and to enhance endocytosis and transcytosis, lectins have been covalently bound to drugs and nanocarriers in order to enhance intestinal drug delivery as well as drug administration across blood–brain and mucosal barriers [29]. Fusion proteins between elastin and growth factors for the acceleration of wound healing were also self-assembled to form nanoparticles [30].

Folic acid is a vitamin of the B group that is important for DNA and cell replication. Many cancer cells overexpress folate receptors. For this reason, coupling drugs or carriers to folic acid enhance drug targeting to tumor cells and even their internalization [31].

Hyaluronic acid, a carbohydrate polymer found in the extracellular matrix, can also bind to cellular receptors. It has been covalently and physically conjugated to therapeutics such as siRNA and imaging agents, in order to exploit its targeting ability and enhance cellular uptake [32]. Targeting of B16-F10 murine melanoma cells was also achieved by functionalizing liposomes with anisamide, a ligand of the sigma one receptor that is overexpressed in several cancer cells [33]. Conjugates were also tested for the transdermal lymphatic delivery of doxorubicin in order to target tumor metastases in lymph nodes. After administration on Wistar rat dorsal skin, transferosomes loaded with the drug and conjugated with hyaluronic acid were found to penetrate the dermis and to accumulate in the lymph nodes much better than transferosomes without targeting units [34].

Biodegradable Organic Nanocarriers

Biodegradable organic materials are polymers that can be degraded by natural or enzymatic hydrolysis.

Biodegradable organic polymers can be divided into biologic and synthetic ones. Synthetic polymers are prepared by chemical reactions using monomers. Biological polymers (eg, polypeptides and polysaccharides) consist of repetitive simple amino acid or carbohydrate sequences. They can be obtained from natural sources or prepared by bioengineering. Thanks to their hydrophilic groups, biological polymers have high water-absorbing capacity and can form hydrogels and nanogels when chemically or physically cross-linked, and they are therefore ideal carriers for hydrophilic drugs. On the other hand, hydrophobic synthetic polymers, such as polylactic acid (PLA), organize to form particles with low water content, which are more adequate for the incorporation of hydrophobic molecules. A wide variety of block copolymers have been prepared by linking polymers with different degrees of hydrophilicity and hydrophobicity. Block copolymers can self-assemble to form micelles, nanospheres, nanocapsules, and polymersomes and encapsulate drugs [35]. Very often, block copolymers have been prepared by linking biodegradable polymers to the nonbiodegradable polymer (PEG) in order to take advantage of its water solubility and surface properties.

Polypeptides

Polypeptides are made of amino acids similar to proteins but are classified as polymers because they consist of one or a few repetitive peptides. Nanocarriers made of elastin-derived polymers are typical examples. Elastin-like polymers are genetically engineered by use of transfected cells that can produce protein variants with different hydrophobicity degrees. Modification of amino acids can also be employed to incorporate DNA-binding polylysine domains or targeting units [36]. Other genetically engineered polypeptides are derived from silk proteins or a combination of the two (a silk–elastin-like protein). Also, these polypeptides can be modified for conjugation to targeting units or cross-linked to form nanosized structures with different degradation and delivery properties [36]. Another example of biodegradable polypeptides is poly(γ -glutamic acid), which is produced by certain bacteria and can be degraded by γ -glutamyl transpeptidase.

A special class of polypeptides are depsipeptides, which are made of natural or synthetic amino acids connected by both amide and ester bonds. The presence of ester bonds accelerates the degradation of the polymers via hydrolysis. Some natural and synthetic short depsipeptides have biological activities (eg, antimicrobial or protease *inhibitory* effects), whereas poly-depsipeptides can be used as nanocarriers for drug delivery. Beside biodegradability, the advantage of synthetic poly-depsipeptides is that they can be tailored to build specific interactions with the drug to be transported by

choosing the appropriate amino acids. The type of binding will then determine the drug release kinetics [37]. Materials based on poly-depsipeptides have already been investigated as growth factor–loaded biodegradable scaffolds for tissue engineering [38], whereas their use as agents for dermal and transdermal drug delivery has not yet been fully explored.

Polysaccharides

Chitosan is a polysaccharide derived from shrimps and other crustacean shells. The basic monomers are D-glucosamine and its acetylated derivative. Because of its water solubility, permeability-enhancing property, and positive charge, chitosan was extensively investigated as a carrier for negatively charged molecules such as nucleotides. Nanoparticles made of chitosan were conjugated to γ -poly(glutamic acid) to enhance skin penetration and deliver DNA to skin [39]. Choi et al. delivered enzymes to human skin via chitosan-functionalized Pluronic-based nanocarriers and showed that the activity of the delivered enzyme still persisted after skin penetration [40].

Hyaluronic acid is a carbohydrate polymer that consists of N-acetyl-D-glucosamine and β -glucuronic acid and is distributed in the extracellular matrix with lubrication, stabilization, and protective functions. It is water soluble, is nonimmunogenic, and has been shown to have antioxidative immunomodulating properties. Hyaluronic acid–based nanocarriers have been investigated for intracellular drug delivery. In fact, this polymer binds to specific cellular receptors that are overexpressed in tumor cells and favor nanocarrier internalization [41]. Hyaluronic acid is also useful to enhance skin penetration. α -Tocopherol was incorporated as a model hydrophobic drug in hyaluronic acid–based nanoemulsions. These nanocarriers showed enhanced percutaneous delivery with respect to an ethanolic solution without any sign of irritation [42]. Particles based on trimethyl chitosan and hyaluronic acid were also developed for intradermal vaccination purposes [43].

Another carbohydrate used to prepare nanocarriers is starch. Nanoparticles based on starch, modified in order to make the polymer more hydrophobic and slow its hydrolysis, improved the sustained transdermal delivery of flufenamic acid, a nonsteroidal antiinflammatory drug [44]. Further polysaccharides used to prepare nanocarriers are alginate, pullulan, and dextran.

Cyclodextrins are oligomers of glucose organized to form rings that can be used to make hydrophobic moieties water soluble by forming inclusion complexes. They were widely investigated for drug delivery, and β -cyclodextrins are used as delivery agents for topical formulations of iodine and dermal delivery of dexamethasone in products marketed in Japan [45]. Different types

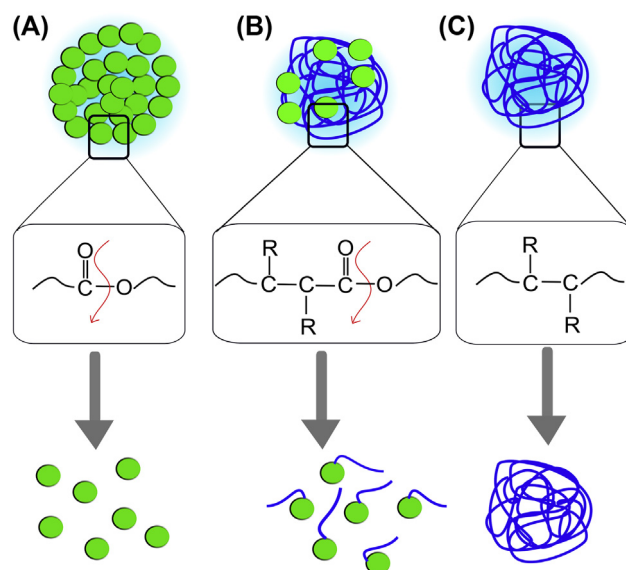


FIGURE 6.2 Schematic representation of three nanocarriers made of (A) a synthetic biodegradable polymer, in which all monomers are linked by hydrolyzable bonds; (B) a polymer made biodegradable by the introduction of hydrolyzable bonds; and (C) a non biodegradable polymer, in which all monomers are linked by non hydrolyzable bonds.

of polymers containing cyclodextrins have also been prepared and investigated as drug delivery agents. For example, linear cyclodextrin-containing poly-lactic-co-glycolic acid–polyethylene glycol (PLGA-PEG) particles have been used as carriers for transdermal delivery of flurbiprofen, showing improved drug retention in human excised skin and no irritation in rabbit skin [46].

Synthetic Polymers

In medicine, polymers are considered biodegradable when, once administered, they hydrolyze to products that are nontoxic and small enough to be excreted. Depending on the type of synthesis, polymers with different backbones can be synthesized. Radical polymerization leads to carbon–carbon bonds, which are not hydrolyzable and therefore nonbiodegradable, whereas condensation, ring-opening polymerization, or metal catalysts reactions result in hydrolyzable esters, amide, urethane, and carbonate bonds (Fig. 6.2). The introduction of hydrolyzable bonds in the backbone of a nonbiodegradable polymer results in partial degradation to small products that can be excreted.

The degradation rate is different depending on the type of chemical bond, with esters having the fastest reaction rates. Synthetic polymers have been largely used to prepare biodegradable material for implants, joints, and stents, and in their particulate form, they are also investigated as drug delivery systems. The most studied biodegradable synthetic polymers are PLGA, poly(D,L-lactic acid) (PLA), and poly(ϵ -caprolactone) (PCL).

Whereas the degradation kinetics of PLA polymer is slow and requires several months, poly(glycolic acid) (PGA) hydrolyzes more rapidly. PLGA, the copolymer of PLA and PGA, has therefore been prepared, adjusting the ratio of the two monomers in order to control the degradation rate depending on the desired degradation kinetics. In fact, besides the safety issue, the degradation process plays a central role with respect to the release of loaded drugs. Materials with selected degradation rates can be used to get fast or slow drug release, depending on the therapeutic application.

The degradation of particulate materials is a complex process, as shown by the nonlinear kinetics describing the release of encapsulated drugs, and can also interfere with the release of the drug [47]. To enhance the biodegradability of a delivery agent and control drug release, enzymes can be incorporated that actively and selectively digest the carrier matrix. Baier and coworkers immobilized the enzyme proteinase K into PLA particles in order to modulate the delivery of octenidine, a bactericidal drug [48]. Polymers can also be degraded by enzymes in the target organism. For example, PCL was used as the outer shell for nanogels loaded with vancomycin. Once the carrier were added to lipase-secreting *Staphylococcus aureus* cultures, the polymers were degraded, allowing the release of the drug [49]. The intracellular enzymatic activity can also be exploited. Polymersomes (polymer-based liposomes) were made sensitive to the lysosomal enzyme cathepsin B by introducing a peptide unit in between the two polymer blocks (methoxy PEG and PLA) and were used to enhance the intracellular delivery of fluorescently labeled dextran [50].

Biodegradable organic nanocarriers have been extensively investigated as delivery agents for dermal and transdermal applications. It has been shown that biodegradable PLA particles accumulate in the SC and in the hair follicles with different dye release kinetics and patterns, depending on the physicochemical properties of the loaded dyes [51,52]. For example, the hydrophobic fluorophore Nile red localized in both the epidermis and sebaceous glands with maximum dye concentrations after 8 and 16 h, respectively. More hydrophilic compounds localized mainly in the stratum and epidermis with maximum dye concentration at 4 h. The stability of surfactant-free PLA particles upon topical application on human excised skin was also tested at different time points, showing particle destabilization and loss of the particulate form after 16 h of incubation [53]. PLA particles loaded with the human immunodeficiency virus-1 (HIV-1) p24 antigen have been developed for particle-mediated transcutaneous vaccination and shown to enable the delivery of the p24 antigen to activated Langerhans cells after topical application on human skin explants [54]. PLA nanospheres with and without PEG

coating were used to deliver an antitumor drug, camptothecin, to mice that had been inoculated with B16-F10 melanoma cells and had metastatic spreads in the lungs [55]. In a comparison study, both PLGA and PLA were found to favor the retention of the synthetic hormone levothyroxine in the skin [56]. Finally, using a human skin culture model, the penetration and biological effects of PCL nanoparticle-mediated delivery of cyclosporin A were investigated showing that the particles induced no toxic effects and significantly reduced the release of anti-inflammatory mediators [57]. PCL-based nanoparticles were also shown to increase the antiinflammatory activity of nimesulide after topical application on animal models of chronic arthritis and granuloma formation [58].

Biocompatible Organic Nanocarriers

Synthetic nonbiodegradable linear or hyperbranched polymers as well as dendrimers have been used to prepare a wide variety of drug delivery agents. Polymers such as polystyrene, polyacrylates, PEG, and polyglycerol are not biodegradable but have been shown to be safe and biocompatible. PEG is one of the most used nonbiodegradable polymers in nanomedicine and has been approved by the US Food and Drug Administration (FDA) for many medical uses. This synthetic polymer has been conjugated to protein-based drugs in order to increase their molecular weight and retard their excretion. In addition, it is extensively used as a coating agent for different types of nanocarriers in order to enhance their colloidal stability and reduce opsonization and internalization by mononuclear phagocyte system cells [59]. PEG is also used as a hydrophilic unit in block co-polymers that self-assemble to form micelles, capsules, and polymersomes [35]. For example, micelles of the biocompatible methoxy-poly(ethylene glycol)-dihexyl substituted polylactide (MPEG-dihex-PLA) diblock copolymer were used to deliver tacrolimus after topical application, showing their superiority with respect to the commercial preparation (Protopic) [60]. Along with PEG, poly(N-vinylpyrrolidone) (PVP), poly(N-isopropylacrylamide) (PNIPA), and poly(acrylic acid) (PAA) are the polymers that are mostly used to build up block copolymer micelles [61]. Another polyether used for the preparation of nanocarriers is polyglycerol. Linear polyglycerol has been used as surface coating to reduce cellular uptake [62], whereas branched polyglycerol can be used to prepare hyperbranched and core-multishell nanocarriers [63] as well as nanogels [64]. Some of these architectures have already been tested for skin drug delivery after topical application with promising results [65,66]. Poly(N-(2-hydroxypropyl) methacrylamide) (PHPMA)

is another biocompatible polymer that, conjugated to anticancer drugs, has already reached clinical trials. Copolymers based on PHPMA are investigated as nanocarriers and surface coating of biomaterials [67].

In general, all these polymers have low toxicity and low immunogenicity. However, in order to make them biocompatible, it is also necessary to ensure their excretion and avoid organ retention. For this purpose, hydrolyzable bonds can be introduced in the nanocarriers' architecture by preparing copolymers, coupling block polymers by esterification, or using biodegradable cross-linkers [68] (Fig. 6.2). Dendrimers based on poly(amidoamine) (PAMAM) and carriers based on poly(ethylenimine) (PEI) and poly(propylenimine) (PPI) are very attractive as drug delivery agents because of their cell-penetrating properties and DNA complexation ability, but they are accompanied by toxic effects due to cationic charges that can impair cell membrane functions [69]. Nevertheless, nitric oxide (NO)-releasing PPI dendrimers were shown to have low toxicity toward fibroblasts, whereas they were effective against both Gram-negative and Gram-positive bacteria. Moreover, it was shown that size and surface functionalization effected the antibacterial activity [70]. Similarly, NO-releasing PAMAM dendrimers were tested against Gram-negative *Pseudomonas aeruginosa* biofilm-building strains, revealing dependency of antibacterial activity to size and surface hydrophobicity of the nanocarrier [71].

Biocompatible Inorganic Nanocarriers

Inorganic colloids such as metal and metal oxide nanoparticles, as well as certain fullerene derivatives, have acceptable low toxicity and can be degraded by erosion or excreted. They are therefore considered as biocompatible and have been investigated for drug delivery purposes. Inorganic particles are characterized by mechanical stability; a large variety of possible surface functionalization, including biological and synthetic polymers; and the possibility to prepare them in different forms (eg, spheres, prisms, wires, and rods). Drugs can be adsorbed on the particle surface or loaded in the matrix pores. The dimension of the pores can be adjusted in order to modulate drug release. In addition, functionalization of the particle surface with targeting and stimuli-responsive moieties allows for targeted and triggered drug delivery.

Mesoporous silica oxide particles are intensively investigated as delivery agents for different types of drugs [72]. They exert toxic effects only at high concentrations. Recently, the issue of organ deposition, which was a matter of concern because of possible long-term toxicity, has been resolved showing that theranostic mesoporous nanoparticles were eroded in vitro as well

as in vivo and cleared from cells within 3 weeks [73]. Amorphous silica oxide nanoparticles have also been investigated as delivery agents, especially for gene therapy [74]. Calcium phosphate has been used to prepare nanoparticles for transfection as well as bioimaging and therapeutic applications [75]. For example, calcium phosphate nanoparticles coated with polysaccharides and albumin were applied intradermally and on mice skin pretreated with tape stripping, resulting in an antibody titer higher than that of samples treated with albumin only [76].

The best known inorganic particles applied on skin are silver nanoparticles, which are incorporated as antimicrobials in wound dressing and function as delivery agents for silver ions [77]. It is still not clear if nanoparticle-associated toxic effects contribute to the antimicrobial activity of nanosilver [78]. Colloidal gold and iron oxide nanoparticles are considered as biocompatible materials and have been used for diagnostic and therapeutic purposes as well as adjuvants in vaccination strategies. Coating their surface with organic polymers allows to load them with drugs and thus to act as theranostic agents [79]. Recently, the delivery of siRNA in wounds of type 2 diabetic mice by means of spherical nucleic-acid gold–nanoparticle conjugates has been reported. The delivered siRNA induced the knockdown of ganglioside–monosialic acid three synthase, a mediator of impaired wound healing [80]. Very often, organic-inorganic hybrid nanocarriers have been developed and investigated. For example, a hydrogel–glass composite made of tetramethylorthosilicate, chitosan, and PEG was prepared, where nitrite was reduced by glucose during nanoparticle synthesis, resulting in a powder able to release NO once rehydrated. These nanoparticles were efficient against *S. aureus*–infected wounds and accelerated wound healing [81]. Core–shell silica nanoparticles loaded with the fluorescent probe cyanin-5 and coated with methoxy-terminated PEG chains were functionalized with targeting peptides conjugated to ^{124}I (a positron-emitting imaging agent). These sophisticated nanocarriers were successfully used to visualize an M21 melanoma in a xenograft mouse model. Importantly, these nanoparticles had a diameter of 7 nm to facilitate their renal excretion and avoid tissue accumulation [82].

NANOCARRIER BIODEGRADABILITY AND BIOCOMPATIBILITY IN SKIN

The biocompatibility of a material highly depends on the site of application. Thus, when developing nanocarriers for dermal and transdermal delivery, it is important to understand how nanocarriers interact with skin, including possible effects that the delivery method

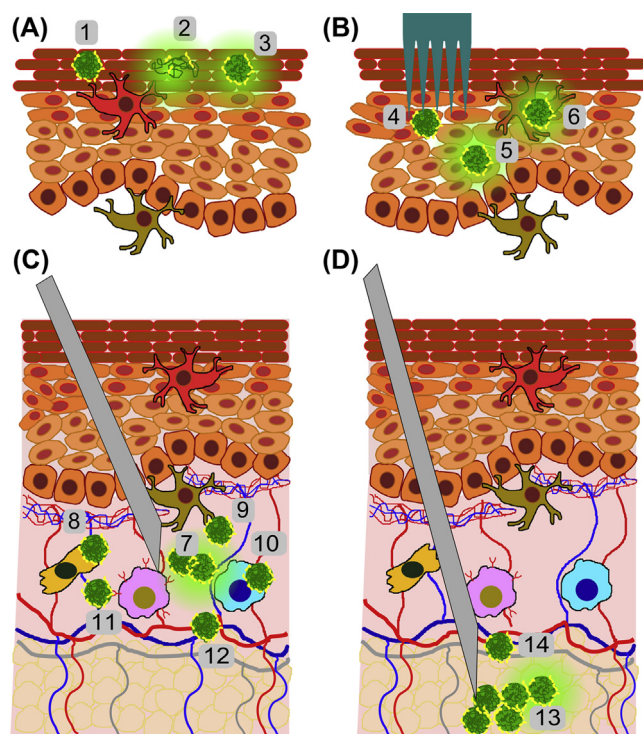


FIGURE 6.3 Schematic representation of nanocarriers' possible interactions with skin. Nanocarriers can be applied to different skin layers: (A) on the skin surface; (B) to the epidermis, for example by means of microneedles; (C) in the dermis; or (D) in the subcutaneous tissue by means of injection. Independent of the administration route, nanoparticles are likely to adsorb proteins on their surface (yellow). Typically applied nanocarriers can accumulate in the stratum corneum (1), destabilize and lose their particulate state (2), or undergo degradation (3). Nanocarriers that reach the epidermis can localize in the intercellular space or be taken up by keratinocytes. Nonbiodegradable nanocarriers (4) will be eliminated during the epidermal turnover. Biodegradable nanocarriers (5) can hydrolyze spontaneously or by extracellular or lysosomal enzymatic digestion. They can also be recognized by Langerhans cells (6) and be degraded or transported to the lymph nodes. Intradermally injected nanocarriers can accumulate and/or degrade in the intercellular space (7). They can interact or be taken up by cells like fibroblasts (8), dermal dendritic cells (9), macrophages (10), and mast cells (11), or translocate to the lymphatic and blood vessels reaching lymph nodes and the systemic compartment (12). Subcutaneous injection results in accumulation of nanocarriers in the fat tissue, where they can persist till their degradation (13) or translocate to the lymphatic and blood systems (14).

may have on skin physiology. Possible degradation and clearance processes as well as eventual reactions of skin immune system and toxicity toward skin cells have to be taken into consideration. Biocompatibility is not an absolute but rather a relative attribute, which depends on the specific properties of the nanomaterial, possible impurities, dose and duration of the treatment, and risk–benefit considerations [83]. Once nanocarriers are applied on skin, different interactions and reactions can take place, which will determine nanocarriers' distribution, biodegradation, drug release kinetics, as well as toxicity or biocompatibility (Fig. 6.3).

Different routes of nanocarrier administration to skin can be chosen, depending on the therapeutic application. Nanocarriers can be (1) applied on the skin surface, with or without skin penetration enhancement; (2) delivered in the epidermis, such as by means of microneedles; (3) injected in the dermis; or (4) injected subcutaneously. Typically applied nanocarriers may accumulate in the SC, degrade, or disassemble while interacting with the components of the SC. Extracellular proteins may adsorb on the surface of applied nanocarriers, including products of skin bacterial flora [84]. The protein corona will influence all further interactions with skin (eg, the cellular uptake by immune system cells may take place through pattern recognition receptors) [85]. In cases when nanocarriers can cross the skin barrier, such as due to penetration enhancement or because they are applied to an impaired skin barrier, they will interact with epidermal and dermal cells. Langerhans cells, dermal dendritic cells, and macrophages are skin resident immune system cells that recognize and react to penetrated foreign material. If methods such as detergents, tape stripping, or microneedles are used to disrupt the skin barrier, cytokines will be released [86]. These will attract immune system cells and induce their activation [87]. Next to phagocytic cells, other cell populations may interact with nanocarriers. Keratinocytes in the epidermis are also immune active cells and can release cytokines when they are damaged or exposed to dangerous exogenous materials [88]. On the other hand, nonbiodegradable nanocarriers, which accumulate in keratinocytes, will be possibly eliminated together with terminally differentiated corneocytes during epidermal cell turnover and the skin's natural exfoliation. Intradermally injected nanocarriers may interact with connective tissue fibers and fibroblasts, the most represented cell population in the dermis. Mast cells may also interact with nanoparticles reaching the dermis [89]. These cells react not only to physical stimuli but also to chemical and immunologic stimuli, releasing heparin and histamine, which in turn induce vasodilatation, granulocyte extravasation, and inflammation. Internalized by cells, nanocarriers can be processed in the endosomes and lysosomes. In these acidic organelles, depending on their nature and features, nanocarriers can be degraded or exocytosed, accumulate, or induce endosome disruption (endosomal escape) [2]. After internalization, endosomal escape, or exocytosis, nanocarriers might have a different protein corona acquiring new properties and toxicity [90,91]. Nanocarriers reaching the dermis can enter the blood system or be transported to the lymph nodes by dendritic cells or by lymphatic drainage [92]. Nanocarriers injected in the subcutaneous tissue are designed to set depots for sustained drug delivery that can last for hours, days, or months, depending on their degradation rate.

The released drugs are absorbed through the lymphatic and capillary network. Depending on their size and type of surface, nanocarriers can also translocate to the lymphatic and blood systems [93]. Once in the blood system, nanocarriers can be excreted by renal clearance, or redistribute to other organs and accumulate in the reticular connective tissue.

The degradation of a nanocarrier, once it has penetrated the skin, can take place by spontaneous hydrolysis or by means of skin enzymatic activity, and it depends on the type of constituting material, skin temperature, pH, and oxidative status. Skin is rich in enzymes, and biological nanocarriers can be degraded by proteases, lipases, hyaluronidase, and so on. In the SC, proteases like kallikreins are found that are involved in the SC exfoliation process [94] and may interact with topically applied nanocarriers. After internalization by endocytosis, nanocarriers encounter degrading enzymes like chatepsins. Granulocytes and mast cells contain several types of proteases in their granules [95]. In addition, specific enzymatic activity such as that of metalloproteinases is induced during skin damage and inflammatory conditions [96].

The main concern with regard to biological nanoparticles is related to their immunogenicity. Components of biological nanocarriers or carried molecules can be recognized as dangerous and activate the different arms of the immune system. Skin, as a biological barrier to the external environment, has a very efficient network of immune cells. Depending on the type of cells and the involved mediators, different reactions can be triggered that range from immune responses to allergic reactions toward nanocarrier constituents behaving as antigen or haptens [85]. Langerhans cells in the epidermis as well as macrophages and dermal dendritic cells are specialized in the uptake of particulate materials. Different uptake pathways exist involving different receptors on antigen presenting cells that might recognize molecules adsorbed or linked to the surface of nanocarriers [97]. Some of these pathways induce proinflammatory responses, whereas other pathways, such as the scavenger-receptor-mediated pathway, do not elicit inflammation. In addition, coating with hydrophilic negatively charged polymers such as PEG has been shown to reduce nanocarrier recognition and internalization by antigen presenting cells. Thus, depending on the nanocarrier surface decoration (eg, polysaccharides, antibody, or PEG) or on the type of adsorbed proteins (eg, complement), the immune system can be activated or avoided. Once internalized, biological nanoparticles or biological material loaded on nanocarriers can be processed and presented as antigen to T cells. Depending on the antigen concentration and on the presence of additional stimuli, such as cytokines and co-stimulatory molecules, tolerance or an immune response specific for the

nanocarrier or the associated antigens can take place [98]. These properties are convenient for vaccination purposes, whereas they lead to undesired reactions such as inflammation and tissue damage when drug delivery only is pursued. It also has to be considered that most nanocarriers investigated for dermatological therapies will be applied on diseased skin. In cases of atopic dermatitis, psoriasis, skin cancer, or infections, the skin immune system is often activated, and nanocarriers might amplify or suppress ongoing immune reactions. For example, it has been found that ZnO nanoparticles can induce the release of IgE when applied on a mouse model for atopic dermatitis [99]. Nanoparticles can also act as adjuvants, enhancing an immune response or allergic reactions. The mechanisms by which nanocarriers promote an immune response are not fully understood, but it seems that they act by forming a depot of antigen at the site of application and enhancing the uptake and presentation of antigens [100]. Such properties of nanoparticles may also cause exacerbation of allergic reactions. It has been shown that negatively charged silica nanoparticles could act as adjuvants in allergy processes, whereas positively charged silica nanoparticles were found to be safe and did not exacerbate induced allergic contact dermatitis in mice [101].

In cases of toxicity toward immune system cells or interference with the immunogenic processes, nanocarriers can also have immunosuppressive or antiinflammatory activity. For example, PAMAM-based dendrimers were shown to inhibit cytokine secretion, whereas polymerized lipid nanoparticles and butyrate-conjugated SLNs have been shown to inhibit leukocyte adhesion to activated endothelial cells, reducing cell infiltration in inflamed tissue [97]. Silver nanoparticles have been shown to exert antiinflammatory activity, for example in a model of contact dermatitis [102]. The mechanism of action is still not fully understood, but it seems to be related to increase of apoptosis and reduction of pro-inflammatory cytokines. The most frequently reported mechanism for nanoparticle cytotoxicity is the induction of oxidative stress. This may result in secretion of pro-inflammatory mediators, apoptosis, and also necrosis with consequent inflammation and skin irritation. Another important aspect of nanocarrier-induced toxicity is their potential carcinogenicity, which is directly correlated with direct or indirect DNA damage.

Independent of the constituting material, nanocarrier properties like size and surface polarity can influence their interaction with skin and determine their toxicity or biocompatibility. Size influences the penetration profile of nanoparticles in both healthy and diseased skin. If injected intradermally or subcutaneously, large particles form depots in the tissues, whereas smaller particles are more easily transported to the lymph nodes by the

lymphatic drainage [92], from which they can reach the systemic compartment. Particles smaller than 200 nm can be internalized by most types of skin cells, whereas particles larger than 200 nm are more suited for the targeting of phagocytosing cells [103]. As a consequence, size can also influence the immunomodulating properties of nanocarriers. Nanoparticle shape can influence skin penetration and cell internalization. It has been shown that phagocytic cells can internalize spherical particles more readily than elongated ones, especially when the aspect ratio increases [104]. Surface charge and functionalization may influence particle colloidal stability, penetration across skin barrier, and cellular uptake. Positively charged nanocarriers are internalized by cells better than negatively charged ones [103]. Whereas negatively charged dendrimers were found to permeate across the skin in the acceptor medium, dendrimers with positive surface charge were shown to accumulate in different skin layers depending on their size [105]. Surface functionalization can also determine biocompatibility. Quantum dots with neutral, cationic, or anionic coatings were found to have different cytotoxicity toward human keratinocytes, with carboxylic acid-coated particles being the most toxic ones [106]. Functional groups like PEG confer on nanocarriers colloidal stability upon topical application. For example, PEG was used to stabilize liposomes loaded with calcipotriol [107]. PEG also reduces the absorption of proteins on particle surfaces, and, thus, it serves to avoid internalization and clearance by skin phagocytosing cells.

Finally, softness of particles seems to be an important parameter for penetration in the SC. Elastic vesicles or particles are claimed to squeeze between the lamellar lipid layers. The first report was given by Cevc and Blume, who showed that intact transferosomes can cross the skin barrier [108].

CONCLUSIONS

Several skin diseases (eg, inflammatory skin conditions) can be treated only symptomatically. The therapies are often not satisfactory when considering that these diseases are not life-threatening, but can be managed only with drugs that display severe side effects and have to be applied during prolonged times or even for the patient's entire life. On this regard, genetically engineered biopharmaceuticals have high therapeutic potential. Nevertheless, they need to be delivered efficiently and specifically to the target cells. Thus, delivery systems represent essential tools for the development of these next-generation therapies. A number of reviews have been published on nanoparticulate carrier systems and their applications in dermatology [109–115]. Results from several dermatological and

pharmacological research fields show that nanocarriers have the potential to improve the outcome of many existing treatments and are important tools for the development of new treatment strategies. The number of nanoscaled delivery systems is continuously growing whereby properties like loading capacity, targeting ability, stealth, and stimuli responsiveness are being continuously improved. Nevertheless, in order to realize and even accelerate the clinical translation of these new therapeutic options, systematic investigations with respect to biodegradability and biocompatibility of these new delivery materials after their administration to skin are mandatory. Correlation between nanocarrier physicochemical properties and their biodegradability as well as biocompatibility would help to develop new, improved, and safe dermatological treatments [116]. Especially, a deeper understanding of the interactions between nanocarriers and the skin immune system as well as further new insights on the mechanisms of toxicity are necessary. For example, the effects of nanocarriers on Langerhans cells' ability to internalize and present antigens has not been investigated yet [112]. Similarly, the interaction of nanocarriers with mast cells and influence of their function are still open questions. Also, systematic studies on the potential carcinogenicity of the new delivery agents in healthy as well as diseased skin are necessary. Ideally, preclinical efficacy and toxicity studies should be conducted using models of the specific disease to be treated. It is also very important to consider that results can be very different depending on the *in vivo* and *in vitro* models that are used. In particular, animal skin and the associated immune system are anatomically and biologically different from those of humans [117].

In conclusion, along with the further improvement of nanocarriers' drug delivery efficiency, nanodermatology would strongly profit from a better understanding of the parameters influencing nanocarriers' biodegradability and biocompatibility, especially taking into consideration differences between healthy and diseased skin. A bright spectrum of potential interactions between skin and nanocarriers exists, which includes different biodegradation, clearance, or toxic processes. Systematic studies investigating how nanocarrier characteristics influence their mode of interaction with skin are urgently needed in order to fully exploit the potential of nanotechnology applied to dermatology.

Abbreviations

Ab	Antibody
CPP	Cell-penetrating peptide
DNA	Deoxyribonucleic acid
FDA	Food and Drug Administration
HDL	High-density lipoprotein
HIV-1	Human immunodeficiency virus one

IL Interleukin
 LDL Low-density lipoprotein
 MPEG Methoxy-poly(ethylene glycol)
 NLC Nanostructured lipid carrier
 NO Nitric oxide
 PAA Poly(acrylic acid)
 PAMAM Poly(amidoamine)
 PCL Poly(ϵ -caprolactone)
 PEG Polyethylene glycol
 PEI Poly(ethylenimine)
 PGA Poly(glycolic acid)
 PHPMA Poly(N-(2-hydroxypropyl)methacrylamide)
 PLA Poly(D,L-lactic acid)
 PLGA Poly(D,L-lactic-co-glycolic acid)
 PNIPA Poly(N-isopropylacrylamide)
 PPI Poly(propylenimine)
 PVP Poly(N-vinylpyrrolidone)
 siRNA Small interfering ribonucleic acid
 SC Stratum corneum
 SLN Solid lipid nanoparticle
 VLP Virus-like particle

References

- [1] Amoozgar Z, Goldberg MS. Targeting myeloid cells using nanoparticles to improve cancer immunotherapy. *Adv Drug Deliv Rev* 2014. <http://dx.doi.org/10.1016/j.addr.2014.09.007>.
- [2] Nel AE, Madler L, Velegol D, et al. Understanding biophysicochemical interactions at the nano–bio interface. *Nat Mater* 2009;8(7):543–57.
- [3] Saar K, Lindgren M, Hansen M, et al. Cell-penetrating peptides: a comparative membrane toxicity study. *Anal Biochem* 2005; 345(1):55–65.
- [4] Yoo J-W, Irvine DJ, Discher DE, Mitragotri S. Bio-inspired, bio-engineered and biomimetic drug delivery carriers. *Nat Rev Drug Discov* 2011;10(7):521–35.
- [5] Ma Y, Nolte RJ, Cornelissen JJ. Virus-based nanocarriers for drug delivery. *Adv Drug Deliv Rev* 2012;64(9):811–25.
- [6] Pearton M, Pirri D, Kang SM, Compans RW, Birchall JC. Host responses in human skin after conventional intradermal injection or microneedle administration of virus-like-particle influenza vaccine. *Adv Healthcare Mater* 2013;2(10):1401–10.
- [7] Kaneda Y. Virosome: a novel vector to enable multi-modal strategies for cancer therapy. *Adv Drug Deliv Rev* 2012;64(8):730–8.
- [8] Dragicevic-Curic N, Scheglmann D, Albrecht V, Fahr A. Development of different temoporfin-loaded invasomes—novel nanocarriers of temoporfin: characterization, stability and in vitro skin penetration studies. *Colloids Surf B* 2009;70(2):198–206.
- [9] Yuvaraj S, Peppelenbosch MP, Bos NA. Transgenic probiotics as drug delivery systems: the golden bullet? *Int J Nanomed* 2007; 4(1):1–3.
- [10] Elzoghby AO, Samy WM, Elgindy NA. Protein-based nanocarriers as promising drug and gene delivery systems. *J Controlled Release* 2012;161(1):38–49.
- [11] Elzoghby AO, El-Fotoh WSA, Elgindy NA. Casein-based formulations as promising controlled release drug delivery systems. *J Controlled Release* 2011;153(3):206–16.
- [12] Tang Q-S, Chen D-Z, Xue W-Q, et al. Preparation and bio-distribution of ^{188}Re -labeled folate conjugated human serum albumin magnetic cisplatin nanoparticles (^{188}Re -folate-CDDP/HSA MNPs) in vivo. *Int J Nanomed* 2011;6:3077.
- [13] Lai L, Guo H. Preparation of new 5-fluorouracil-loaded zein nanoparticles for liver targeting. *Int J Pharm* 2011;404(1):317–23.
- [14] Bhowmik T, D'Souza B, Shashidharamurthy R, Oettinger C, Selvaraj P, D'Souza MJ. A novel microparticulate vaccine for melanoma cancer using transdermal delivery. *J Microencapsulation* 2011;28(4):294–300.
- [15] Nicklas M, Schatton W, Heinemann S, Hanke T, Kreuter J. Preparation and characterization of marine sponge collagen nanoparticles and employment for the transdermal delivery of 17β -estradiol-hemihydrate. *Drug Dev Ind Pharm* 2009;35(9): 1035–42.
- [16] Nakamura M, Jo J-i, Tabata Y, Ishikawa O. Controlled delivery of T-box21 small interfering RNA ameliorates autoimmune alopecia (Alopecia Areata) in a C3H/HeJ mouse model. *Am J Pathol* 2008;172(3):650–8.
- [17] Umamaheshwari R, Jain N. Receptor mediated targeting of lectin conjugated gliadin nanoparticles in the treatment of *Helicobacter pylori*. *J Drug Target* 2003;11(7):415–24.
- [18] Tran MA, Gowda R, Sharma A, et al. Targeting V600EB-Raf and Akt3 using nanoliposomal-small interfering RNA inhibits cutaneous melanocytic lesion development. *Cancer Res* 2008;68(18): 7638–49.
- [19] Puglia C, Bonina F. Lipid nanoparticles as novel delivery systems for cosmetics and dermal pharmaceuticals. *Expert Opin Drug Deliv* 2012;9(4):429–41.
- [20] Prausnitz MR, Langer R. Transdermal drug delivery. *Nat Biotechnol* 2008;26(11):1261–8.
- [21] Lobovkina T, Jacobson GB, Gonzalez-Gonzalez E, et al. In vivo sustained release of siRNA from solid lipid nanoparticles. *ACS Nano* 2011;5(12):9977–83.
- [22] Sievers EL, Senter PD. Antibody-drug conjugates in cancer therapy. *Annu Rev Med* 2013;64:15–29.
- [23] Torchilin VP. Multifunctional nanocarriers. *Adv Drug Deliv Rev* 2012;64:302–15.
- [24] Jin LH, Bahn JH, Eum WS, et al. Transduction of human catalase mediated by an HIV-1 TAT protein basic domain and arginine-rich peptides into mammalian cells. *Free Radical Biol Med* 2001;31(11):1509–19.
- [25] Lopes LB, Furnish E, Komalavilas P, et al. Enhanced skin penetration of P20 phosphopeptide using protein transduction domains. *Eur J Pharm Biopharm* 2008;68(2):441–5.
- [26] Nasrollahi SA, Fouladdel S, Taghibiglou C, Azizi E, Farboud ES. A peptide carrier for the delivery of elastin into fibroblast cells. *Int J Dermatol* 2012;51(8):923–9.
- [27] Patlolla RR, Desai PR, Belay K, Singh MS. Translocation of cell penetrating peptide engrafted nanoparticles across skin layers. *Biomaterials* 2010;31(21):5598–607.
- [28] Stout TE, McFarland T, Mitchell JC, Appukuttan B, Stout JT. Recombinant filaggrin is internalized and processed to correct filaggrin deficiency. *J Invest Dermatol* 2014;134(2):423–9.
- [29] Bies C, Lehr C-M, Woodley JF. Lectin-mediated drug targeting: history and applications. *Adv Drug Deliv Rev* 2004;56(4):425–35.
- [30] Koria P, Yagi H, Kitagawa Y, et al. Self-assembling elastin-like peptides growth factor chimeric nanoparticles for the treatment of chronic wounds. *Proc Natl Acad Sci USA* 2011;108(3):1034–9.
- [31] Lu Y, Low PS. Folate-mediated delivery of macromolecular anticancer therapeutic agents. *Adv Drug Deliv Rev* 2012;64:342–52.
- [32] Saravanakumar G, Deepagan V, Jayakumar R, Park JH. Hyaluronic acid-based conjugates for tumor-targeted drug delivery and imaging. *J Biomed Nanotechnol* 2014;10(1):17–31.
- [33] Chen Y, Bathula SR, Yang Q, Huang L. Targeted nanoparticles deliver siRNA to melanoma. *J Invest Dermatol* 2010;130(12): 2790–8.
- [34] Kong M, Hou L, Wang J, et al. Enhanced transdermal lymphatic drug delivery of hyaluronic acid modified transfersomes for tumor metastasis therapy. *Chem Commun* 2015;51(8):1453–6.
- [35] Letchford K, Burt H. A review of the formation and classification of amphiphilic block copolymer nanoparticulate structures: micelles, nanospheres, nanocapsules and polymersomes. *Eur J Pharm Biopharm* 2007;65(3):259–69.

- [36] Shi P, Gustafson JA, MacKay JA. Genetically engineered nanocarriers for drug delivery. *Int J Nanomed* 2014;9:1617.
- [37] Feng Y, Lu J, Behl M, Lendlein A. Progress in decapeptide-based biomaterials. *Macromol Biosci* 2010;10(9):1008–21.
- [38] Ohya Y, Matori J, Ouchi T. Preparation of growth factor-loaded biodegradable matrices consisting of poly (decapeptide-co-lactide) and cell growth on the matrices. *React Funct Polym* 2014; 81:33–9.
- [39] Liu Z, Jiao Y, Wang Y, Zhou C, Zhang Z. Polysaccharides-based nanoparticles as drug delivery systems. *Adv Drug Deliv Rev* 2008;60(15):1650–62.
- [40] Choi WI, Lee JH, Kim J-Y, Kim J-C, Kim YH, Tae G. Efficient skin permeation of soluble proteins via flexible and functional nanocarrier. *J Controlled Release* 2012;157(2):272–8.
- [41] Choi KY, Saravanakumar G, Park JH, Park K. Hyaluronic acid-based nanocarriers for intracellular targeting: interfacial interactions with proteins in cancer. *Colloids Surf B* 2012;99: 82–94.
- [42] Kong M, Chen XG, Kweon DK, Park HJ. Investigations on skin permeation of hyaluronic acid based nanoemulsion as transdermal carrier. *Carbohydr Polym* 2011;86(2):837–43.
- [43] Verheul RJ, Slütter B, Bal SM, Bouwstra JA, Jiskoot W, Hennink WE. Covalently stabilized trimethyl chitosan-hyaluronic acid nanoparticles for nasal and intradermal vaccination. *J Controlled Release* 2011;156(1):46–52.
- [44] Santander-Ortega M, Stauner T, Loretz B, et al. Nanoparticles made from novel starch derivatives for transdermal drug delivery. *J Controlled Release* 2010;141(1):85–92.
- [45] Davis ME, Brewster ME. Cyclodextrin-based pharmaceuticals: past, present and future. *Nat Rev Drug Discov* 2004;3(12): 1023–35.
- [46] Vega E, Egea MA, Garduño-Ramírez ML, et al. Flurbiprofen PLGA-PEG nanospheres: role of hydroxy- β -cyclodextrin on ex vivo human skin permeation and in vivo topical anti-inflammatory efficacy. *Colloids Surf B: Biointerfaces* 2013;110: 339–46.
- [47] Azevedo HS, Reis RL. Understanding the enzymatic degradation of biodegradable polymers and strategies to control their degradation rate. In: *Biodegradable systems in tissue engineering and regenerative medicine*. Boca Raton, FL: CRC Press; 2005. p. 177–201.
- [48] Baier G, Cavallaro A, Friedemann K, et al. Enzymatic degradation of poly (L-lactide) nanoparticles followed by the release of octenidine and their bactericidal effects. *Nanomed: Nanotechnol, Biol Med* 2014;10(1):131–9.
- [49] Xiong M-H, Bao Y, Yang X-Z, Wang Y-C, Sun B, Wang J. Lipase-sensitive polymeric triple-layered nanogel for “on-demand” drug delivery. *J Am Chem Soc* 2012;134(9):4355–62.
- [50] Lee JS, Groothuis T, Cusan C, Mink D, Feijen J. Lysosomally cleavable peptide-containing polymersomes modified with anti-EGFR antibody for systemic cancer chemotherapy. *Biomaterials* 2011;32(34):9144–53.
- [51] Fernandes B, Silva R, Ribeiro A, et al. Improved Poly (D, L-lactide) nanoparticles-based formulation for hair follicle targeting. *Int J Cosmet Sci* 2015. <http://dx.doi.org/10.1111/ics.12197>.
- [52] Rancan F, Papakostas D, Hadam S, et al. Investigation of polylactic acid (PLA) nanoparticles as drug delivery systems for local dermatotherapy. *Pharm Res* 2009;26(8):2027–36.
- [53] Rancan F, Todorova A, Hadam S, et al. Stability of polylactic acid particles and release of fluorochromes upon topical application on human skin explants. *Eur J Pharm Biopharm* 2012;80(1): 76–84.
- [54] Rancan F, Amselgruber S, Hadam S, et al. Particle-based transcutaneous administration of HIV-1 p24 protein to human skin explants and targeting of epidermal antigen presenting cells. *J Controlled Release* 2014;176:115–22.
- [55] Loch-Neckel G, Nemen D, Puhl AC, et al. Stealth and non-stealth nanocapsules containing camptothecin: in-vitro and in-vivo activity on B16-F10 melanoma. *J Pharm Pharmacol* 2007;59(10): 1359–64.
- [56] Azarbayjani AF, Khu JV, Chan YW, Chan SY. Development and characterization of skin permeation retardants and enhancers: a comparative study of levothyroxine-loaded PNIPAM, PLA, PLGA and EC microparticles. *Biopharm Drug Dispos* 2011; 32(7):380–8.
- [57] Frusić-Zlotkin M, Soroka Y, Tivony R, et al. Penetration and biological effects of topically applied cyclosporin A nanoparticles in a human skin organ culture inflammatory model. *Exp Dermatol* 2012;21(12):938–43.
- [58] Lenz QF, Guterres SS, Pohlmann A, Alves MP. Semi-solid topical formulations containing nimesulide-loaded nanocapsules showed in-vivo anti-inflammatory activity in chronic arthritis and fibrovascular tissue models. *Inflamm Res* 2012; 61(4):305–10.
- [59] Otsuka H, Nagasaki Y, Kataoka K. PEGylated nanoparticles for biological and pharmaceutical applications. *Adv Drug Deliv Rev* 2012;64:246–55.
- [60] Lapteva M, Mondon K, Möller M, Gurny R, Kalia YN. Polymeric micelle nanocarriers for the cutaneous delivery of tacrolimus: a targeted approach for the treatment of psoriasis. *Mol Pharm* 2014;11(9):2989–3001.
- [61] Elsabahy M, Wooley KL. Design of polymeric nanoparticles for biomedical delivery applications. *Chem Soc Rev* 2012;41(7): 2545–61.
- [62] Weinhart M, Grunwald I, Wyszogrodzka M, Gaetjen L, Hartwig A, Haag R. Linear poly (methyl glycerol) and linear polyglycerol as potent protein and cell resistant alternatives to poly (ethylene glycol). *Chem Asian J* 2010;5:1992–2000.
- [63] Gupta S, Tyagi R, Parmar VS, Sharma SK, Haag R. Polyether based amphiphiles for delivery of active components. *Polymer* 2012;53(15):3053–78.
- [64] Cuggino JC, Strumia MC, Welker P, et al. Thermosensitive nanogels based on dendritic polyglycerol and N-isopropylacrylamide for biomedical applications. *Soft Matter* 2011;7(23):11259–66.
- [65] Kumar S, Alnasif N, Fleige E, et al. Impact of structural differences in hyperbranched polyglycerol–polyethylene glycol nanoparticles on dermal drug delivery and biocompatibility. *Eur J Pharm Biopharm* 2014;88(3):625–34.
- [66] Witting M, Molina M, Obst K, et al. Thermosensitive dendritic polyglycerol-based nanogels for cutaneous delivery of biomacromolecules. *Nanomed: Nanotechnol, Biol Med* 2015; 11(5):1179–87.
- [67] Kopeček J, Kopečková P. HPMA copolymers: origins, early developments, present, and future. *Adv Drug Deliv Rev* 2010; 62(2):122–49.
- [68] Hu M, Chen M, Li G, et al. Biodegradable hyperbranched polyglycerol with ester linkages for drug delivery. *Biomacromolecules* 2012;13(11):3552–61.
- [69] Leroueil PR, Berry SA, Duthie K, et al. Wide varieties of cationic nanoparticles induce defects in supported lipid bilayers. *Nano Lett* 2008;8(2):420–4.
- [70] Sun B, Slomberg DL, Chudasama SL, Lu Y, Schoenfish MH. Nitric oxide-releasing dendrimers as antibacterial agents. *Biomacromolecules* 2012;13(10):3343–54.
- [71] Lu Y, Slomberg DL, Shah A, Schoenfish MH. Nitric oxide-releasing amphiphilic poly (amidoamine)(PAMAM) dendrimers as antibacterial agents. *Biomacromolecules* 2013;14(10):3589–98.
- [72] Slowing II, Vivero-Escoto JL, Wu C-W, Lin VS-Y. Mesoporous silica nanoparticles as controlled release drug delivery and gene transfection carriers. *Adv Drug Deliv Rev* 2008;60(11):1278–88.
- [73] Kempen PJ, Greasley S, Parker KA, et al. Theranostic mesoporous silica nanoparticles biodegrade after pro-survival drug

- delivery and ultrasound/magnetic resonance imaging of stem cells. *Theranostics* 2015;5(6):631.
- [74] Wang L, Zhao W, Tan W. Bioconjugated silica nanoparticles: development and applications. *Nano Res* 2008;1(2):99–115.
- [75] Xie Y, Chen Y, Sun M, Ping Q. A mini review of biodegradable calcium phosphate nanoparticles for gene delivery. *Curr Pharm Biotechnol* 2013;14(10):918–25.
- [76] Sahdev P, Podaralla S, Kaushik RS, Perumal O. Calcium phosphate nanoparticles for transcutaneous vaccine delivery. *J Biomed Nanotechnol* 2013;9(1):132–41.
- [77] Aziz Z, Abu S, Chong N. A systematic review of silver-containing dressings and topical silver agents (used with dressings) for burn wounds. *Burns* 2012;38(3):307–18.
- [78] Chernousova S, Epple M. Silver as antibacterial agent: ion, nanoparticle, and metal. *Angew Chem Int Edition* 2013;52(6):1636–53.
- [79] Gautier J, Allard-Vannier E, Munnier E, Soucé M, Chourpa I. Recent advances in theranostic nanocarriers of doxorubicin based on iron oxide and gold nanoparticles. *J Controlled Release* 2013;169(1):48–61.
- [80] Randeria PS, Seeger MA, Wang X-Q, et al. siRNA-based spherical nucleic acids reverse impaired wound healing in diabetic mice by ganglioside GM3 synthase knockdown. *Proc Natl Acad Sci USA* 2015;201505951.
- [81] Martinez LR, Han G, Chacko M, et al. Antimicrobial and healing efficacy of sustained release nitric oxide nanoparticles against *Staphylococcus aureus* skin infection. *J Invest Dermatol* 2009;129(10):2463–9.
- [82] Benezra M, Penate-Medina O, Zanzonico PB, et al. Multimodal silica nanoparticles are effective cancer-targeted probes in a model of human melanoma. *J Clin Invest* 2011;121(7):2768–80.
- [83] Naahidi S, Jafari M, Edalat F, Raymond K, Khademhosseini A, Chen P. Biocompatibility of engineered nanoparticles for drug delivery. *J Controlled Release* 2013;166(2):182–94.
- [84] Wigginton NS, Titta A, Piccapietra F, et al. Binding of silver nanoparticles to bacterial proteins depends on surface modifications and inhibits enzymatic activity. *Environ Sci Technol* 2010;44(6):2163–8.
- [85] Fadeel B. Clear and present danger? Engineered nanoparticles and the immune system. *Swiss Med Wkly* 2012;142:w13609.
- [86] Glenn GM, Kenney RT, Ellingsworth LR, Frech SA, Hammond SA, Zoetewij JP. Transcutaneous immunization and immunostimulant strategies: capitalizing on the immunocompetence of the skin. *Expert Rev Vaccines* 2003;2(2):253–67.
- [87] Vogt A, Hadam S, Deckert I, et al. Hair follicle targeting, penetration enhancement and Langerhans cell activation make cyanoacrylate skin surface stripping a promising delivery technique for transcutaneous immunization with large molecules and particle-based vaccines. *Exp Dermatol* 2015;24(1):73–5.
- [88] Partidos C, Muller S. Decision-making at the surface of the intact or barrier disrupted skin: potential applications for vaccination or therapy. *Cell Mol Life Sci CMLS* 2005;62(13):1418–24.
- [89] Aldossari AA, Shannahan JH, Podila R, Brown JM. Influence of physicochemical properties of silver nanoparticles on mast cell activation and degranulation. *Toxicol Vitro* 2015;29(1):195–203.
- [90] Lundqvist M, Stigler J, Cedervall T, et al. The evolution of the protein corona around nanoparticles: a test study. *ACS Nano* 2011;5(9):7503–9.
- [91] Sakhtianchi R, Minchin RF, Lee K-B, Alkilany AM, Serpooshan V, Mahmoudi M. Exocytosis of nanoparticles from cells: role in cellular retention and toxicity. *Adv Colloid Interf Sci* 2013;201:18–29.
- [92] Mahe B, Vogt A, Liard C, et al. Nanoparticle-based targeting of vaccine compounds to skin antigen-presenting cells by hair follicles and their transport in mice. *J Invest Dermatol* 2009;129(5):1156–64.
- [93] McLennan DN, Porter CJ, Charman SA. Subcutaneous drug delivery and the role of the lymphatics. *Drug Discov Today Technol* 2005;2(1):89–96.
- [94] Rawlings AV, Voegeli R. Stratum corneum proteases and dry skin conditions. *Cell Tissue Res* 2013;351(2):217–35.
- [95] Hellman L, Thorpe M. Granule proteases of hematopoietic cells, a family of versatile inflammatory mediators—an update on their cleavage specificity, in vivo substrates, and evolution. *Biol Chem* 2014;395(1):15–49.
- [96] Wiedow O, Wiese F, Streit V, Kalm C, Christophers E. Lesional elastase activity in psoriasis, contact dermatitis, and atopic dermatitis. *J Invest Dermatol* 1992;99(3):306–9.
- [97] Dobrovolskaia MA, McNeil SE. Immunological properties of engineered nanomaterials. *Nat Nanotechnol* 2007;2(8):469–78.
- [98] Irvine DJ, Swartz MA, Szeto GL. Engineering synthetic vaccines using cues from natural immunity. *Nat Mater* 2013;12(11):978–90.
- [99] Landriscina A, Rosen J, Friedman AJ. Nanotechnology, inflammation and the skin barrier: innovative approaches for skin health and cosmesis. *Cosmetics* 2015;2(2):177–86.
- [100] Awate S, Babiuk LA, Mutwiri G. Mechanisms of action of adjuvants. *Front Immunol* 2013;4(114):1–10.
- [101] Ostrowski A, Nordmeyer D, Mundhenk L, et al. AHAPS-functionalized silica nanoparticles do not modulate allergic contact dermatitis in mice. *Nanoscale Res Lett* 2014;9(1):1–7.
- [102] Nadworny PL, Wang J, Tredget EE, Burrell RE. Anti-inflammatory activity of nanocrystalline silver in a porcine contact dermatitis model. *Nanomed: Nanotechnol, Biol Med* 2008;4(3):241–51.
- [103] Rancan F, Gao Q, Graf C, et al. Skin penetration and cellular uptake of amorphous silica nanoparticles with variable size, surface functionalization, and colloidal stability. *ACS Nano* 2012;6(8):6829–42.
- [104] Liu Y, Tan J, Thomas A, Ou-Yang D, Muzykantov VR. The shape of things to come: importance of design in nanotechnology for drug delivery. *Ther Deliv* 2012;3(2):181–94.
- [105] Yang Y, Sunoqrot S, Stowell C, et al. Effect of size, surface charge, and hydrophobicity of poly (amidoamine) dendrimers on their skin penetration. *Biomacromolecules* 2012;13(7):2154–62.
- [106] Ryman-Rasmussen JP, Riviere JE, Monteiro-Riviere NA. Surface coatings determine cytotoxicity and irritation potential of quantum dot nanoparticles in epidermal keratinocytes. *J Invest Dermatol* 2007;127(1):143–53.
- [107] Knudsen NØ, Rønholt S, Salte RD, et al. Calcipotriol delivery into the skin with PEGylated liposomes. *Eur J Pharm Biopharm* 2012;81(3):532–9.
- [108] Cevc G, Blume G. Lipid vesicles penetrate into intact skin owing to the transdermal osmotic gradients and hydration force. *Biochim Biophys Acta (BBA)-Biomembr* 1992;1104(1):226–32.
- [109] Papakostas D, Rancan F, Sterry W, Blume-Peytavi U, Vogt A. Nanoparticles in dermatology. *Arch Dermatol Res* 2011;303(8):533–50.
- [110] Prow TW, Grice JE, Lin LL, et al. Nanoparticles and microparticles for skin drug delivery. *Adv Drug Deliv Rev* 2011;63(6):470–91.
- [111] Gupta M, Agrawal U, Vyas SP. Nanocarrier-based topical drug delivery for the treatment of skin diseases. *Expert Opin Drug Deliv* 2012;9(7):783–804.
- [112] DeLouise LA. Applications of nanotechnology in dermatology. *J Invest Dermatol* 2012;132:964–75.
- [113] Badri W, Eddabra R, Fessi H, Elaissari A. Biodegradable polymer based nanoparticles: dermal and transdermal drug delivery. *J Colloid Sci Biotechnol* 2014;3(2):141–9.
- [114] Rancan F, Blume-Peytavi U, Vogt A. Utilization of biodegradable polymeric materials as delivery agents in dermatology. *Clin Cosmet Investig Dermatol* 2014;7:23–34.

- [115] Foldvari M, Rafiee A. Perspectives on using nanoscale delivery systems in dermatological treatment. *Curr Dermatol Rep* 2015: 1–7.
- [116] Rivera-Gil P, Jimenez De Aberasturi D, Wulf V, et al. The challenge to relate the physicochemical properties of colloidal nanoparticles to their cytotoxicity. *Acc Chem Res* 2012;46(3):743–9.
- [117] Schmook FP, Meingassner JG, Billich A. Comparison of human skin or epidermis models with human and animal skin in *in-vitro* percutaneous absorption. *Int J Pharm* 2001;215(1):51–6.

Peptide Dendrimers in Delivery of Bioactive Molecules to Skin

J. Manikkath¹, A.R. Hegde¹, H.S. Parekh², S. Mutalik¹

¹Manipal University, Manipal, Karnataka, India; ²The University of Queensland, Brisbane, QLD, Australia

OUTLINE

Introduction	89	Transdermal Drug Delivery Approaches	93
The Dendrimeric Structure	90	Peptide Dendrimers in Transdermal Drug Delivery	93
Types of Dendrimers	90	Development of a Validated RP-HPLC Method for Quantification of Peptide Dendrimers	93
Applications of Dendrimers in Drug Delivery	90	Sonophoresis-Mediated Permeation and Retention of Peptide Dendrimers Across Human Epidermis	94
What Makes Dendrimers Different in Comparison With Other Nanoparticles?	90	Iontophoresis-Mediated Permeation and Retention of Peptide Dendrimers Across the Human Epidermis	94
Dendrimer-Aided Solubility Enhancement of Drugs	91	Peptide Dendrimers as Drug Carriers	96
Peptide Dendrimers: An Alternative Class of Dendrimers	91	Effect of Drug–Peptide Dendrimeric Conjugates on Transdermal Permeation	96
Synthesis of Peptide Dendrimers	91	Conclusion	96
Advantages of Peptide Dendrimers	92	List of Acronyms and Abbreviations	96
Transdermal Drug Delivery	92	Glossary	97
Ideal Transdermal Candidates	92	References	97
Stratum Corneum: Impediment to Transdermal Drug Delivery	93		

INTRODUCTION

One of the additions to “new age” drug delivery is dendrimers. Created by Fritz Vogtle in 1978, dendrimers are artificial molecules of high molecular weight, with unique physicochemical and biological properties. They are onion-skin-like discrete nanostructures. Starting from a core, these nanoparticles grow sequentially, producing stepwise buildup in size [1]. Dendrimers

have been tailored to have myriad elemental compositions and can be derived from any element [2].

Dendrimers are considered to be “nature inspired” as they resemble the structure of a tree; thereby the name *dendrimer*, which is derived from *dendron*, the Greek equivalent for *tree* [3]. Although they are macromolecules, dendrimers are hyperbranched with globular architecture, which offers them nanoscopic shapes and surfaces. This allows them easy passage across biological

barriers. These features, along with low polydispersity, precisely controllable molecular weight, chemical composition, biodegradability, and biocompatibility, make them ideal vectors for drug delivery.

THE DENDRIMERIC STRUCTURE

There are three basic components in dendrimer structure:

1. A multifunctional core (other molecules can be trapped here),
2. Branched units extending from the core, and
3. External capping groups.

The size, shape, topology, flexibility, and surface functionality of a dendrimer can be controlled at the molecular level. The outcome of this is precise molecular weight and chemical composition. Narrow molecular weight distribution leads to reproducible pharmacokinetic behavior [4].

The highly branched units of a dendrimer are organized in layers called generations. Dendrimers are generally produced in iterative steps, with each iteration leading to a higher dendrimer generation, and doubling the number of end groups. Thus, the molecular weight of each new generation will be approximately double that of the previous generation. With every consecutive generation (G), the dendrimer mass is increased (approximately twice) and geometrically increases the peripheral functional groups (ie, $2G$). At the same time, the diameter is increased systematically by approximately 1 nm per generation.

In a series of generations (Generations 0–5), each dendrimer is a body of distinct composition, having precise molecular mass, molecular formulas, elemental constitution, number of surface groups, and sizes (in nanometers). In each generation, a distinct macromolecular structure having precise molecular mass and monodispersity may be obtained. The external functional groups of a dendrimer can be designed so as to reduce cytotoxicity, increase *trans*-epithelial transport, and promote interaction with coupling molecules.

TYPES OF DENDRIMERS

Although there are more than 100 different dendrimers and more than 1000 surface chemistries, they can be classified into two main categories: covalent type and supramolecular type. The most widely known classes of dendrimers [5] are:

1. Polyamidoamine (PAMAM) dendrimers
2. Tecto dendrimers

3. Chiral dendrimers
4. Peptide dendrimers
5. Poly(amidoamine-organosilicon) (PAMAMOS) dendrimers
6. Hybrid dendrimers
7. Multilingual dendrimers
8. PPI (Polypropylene imine) dendrimers
9. Amphiphilic dendrimers
10. Frechet-type dendrimers.

APPLICATIONS OF DENDRIMERS IN DRUG DELIVERY

General applications of dendrimers involve conjugating other chemical species to the dendrimer surface that can function as detecting agents (dye molecules), affinity ligands, targeting compounds, radioligands, imaging agents, or pharmaceutically active compounds.

In drug delivery, dendrimers can act as carriers for a range of molecules that can be enclosed in the internal regions of the dendrimer or can interact directly with the terminal head groups of the dendrimer [6]. Dendrimers can be used to modify drug properties and may include solubility enhancement, drug protection, controlled release, and targeted delivery.

In the delivery of drugs, dendrimers interact with drug molecules in different ways: (1) drug is entrapped noncovalently in the dendrimer's interior, (2) drug is bound to the dendrimer as a result of electrostatic interaction between drug molecules and surface groups of the dendrimer, or (3) multiple copies of drug are covalently conjugated to form a macromolecular prodrug system.

PAMAM dendrimers have been the most widely researched dendrimers to date possibly due to ease of availability; differing generations of PAMAM are commercially available with diverse molecular masses, number of end groups, and terminal group functionality.

WHAT MAKES DENDRIMERS DIFFERENT IN COMPARISON WITH OTHER NANOPARTICLES?

Apart from dendrimers, there are other nanoparticles like micelles and liposomes that aid drug delivery. But dendrimers present advantages that are not possessed by these agents.

Micelles and liposomes are carriers that have amphiphilic properties, but these are metastable. Whereas micelles rearrange into liposomes depending on the specific system, liposomes eventually rearrange to form planar bilayers.

It is extremely difficult to isolate and stabilize drug molecules of nanometer size. Additionally, in the bulk production of drugs, the particle size reduction that is practically achievable is limited. Dendrimers offer a different route to produce discrete nanostructures that are appropriate for the purpose of drug solubilization.

Dendrimer synthesis can be precisely controlled to form distinct molecules that are similar in size to proteins and still do not cause immunogenic reactions. This monodisperse control of size is at present impossible with conventional polymers.

Dendrimer–drug conjugates are typically <10 nm in size. These dimensions can cause more extensive infiltration into tumors and excretion through the renal route.

Dendrimers have distinct nanoscale configurations that are degradable (eg, bis-MPA dendrimers), biodegradable (eg, poly-L-lysine dendrimers degrade into the natural amino acid L-lysine and undergo endogenous metabolism), self-immolative, or suitable for desired routes of distribution and excretion.

Dendrimer–drug conjugates may generally be easily lyophilized to form water-soluble powders that have high drug solubility. This avoids the possible toxic side effects of solubilizing agents in the formulation.

DENDRIMER-AIDED SOLUBILITY ENHANCEMENT OF DRUGS

Dendrimers possess a hydrophobic interior capable of encapsulating hydrophobic drugs with a hydrophilic exterior for solubilization. Thus, drugs that are poorly soluble can be entrapped within the dendritic structure or can interact with terminal groups to improve their solubility. Dendrimers exert their solubilizing properties by ionic interactions, hydrogen bonding, and hydrophobic interactions.

PEPTIDE DENDRIMERS: AN ALTERNATIVE CLASS OF DENDRIMERS

Peptide dendrimers are radial or wedge-like molecules, of high molecular weight, that comprise basic amino acids (eg, arginine, histidine, or lysine) linked through peptide or amide bonds that are found both inside the branching core and on the outer surface [7]. Amino acid–based peptide dendrimers are increasingly gaining significance as promising scaffolds for the effective delivery of drug and genes. Peptide dendrimers are divided into three categories:

1. Grafted peptide dendrimers: These contain peptides only as surface functionalities.
2. Peptide dendrimers: These are composed entirely of amino acids.
3. Dendrimers: Dendrimers contain amino acids in the branching core and in the surface functional groups, but with nonpeptide branching units.

SYNTHESIS OF PEPTIDE DENDRIMERS

The synthesis of peptide dendrimers can be carried out using either a divergent approach or convergent approach. Solid-phase combinatorial methods, which are widely available, enable large libraries of peptide dendrimers to be produced and screened for desired properties.

Solid-phase peptide synthesis (SPPS) is one of the widely used methods to prepare synthetic peptides. The advantages of solid support synthesis are its speed, versatility, ease of automation, and low costs [8]. SPPS is based on sequential addition of α -amino and side-chain-protected amino acid residues to an insoluble polymeric support (resin). The acid-labile tert-butyl carbamates (Boc) group or base-labile 9-fluorenylmethyl carbamate (Fmoc) group is used for N- α -protection. After removal of this protecting group, the next protected amino acid is added using a coupling reagent. The resulting peptide is attached to resin, via a linker, through its C-terminus and may be cleaved to yield a peptide acid or amide depending on the linking agent used. This process is continued in succession till the desired dendrimer generation is obtained. The efficiency of each step in the amino acid coupling is verified by the ninhydrin test, and the next amino acid is coupled only after completing at least 99% coupling with the previous amino acid. Final cleavage of peptidyl resin and side-chain deprotection requires a strong acid such as HF (hydrofluoric acid) in Boc chemistry and TFA (trifluoroacetic acid) in Fmoc chemistry. Dichloromethane (DCM) and N,N-dimethylformamide (DMF) are the primary solvents used for resin deprotection, coupling, and washing. The SPPS process is briefly outlined here.

An example of an amino acid–based peptide dendrimer is shown in Fig. 7.1. Lysine is the most common amino acid branching unit from which peptide dendrimers are assembled. Lysine core dendrimers having tetrapeptide and octapeptide units on the surface have been used as antimicrobial agents. Lysine peptide dendrimers not only were reported to be more water soluble, less liable to proteolysis, and less toxic to human cells than their linear polymeric analogs, but also demonstrated comparable antimicrobial potency. Lysine core dendrimers having arginine surface residues have been devised as antiangiogenesis agents. Azobenzene residues on the surface added to a lysine core have brought about photo-responsive drug delivery systems.

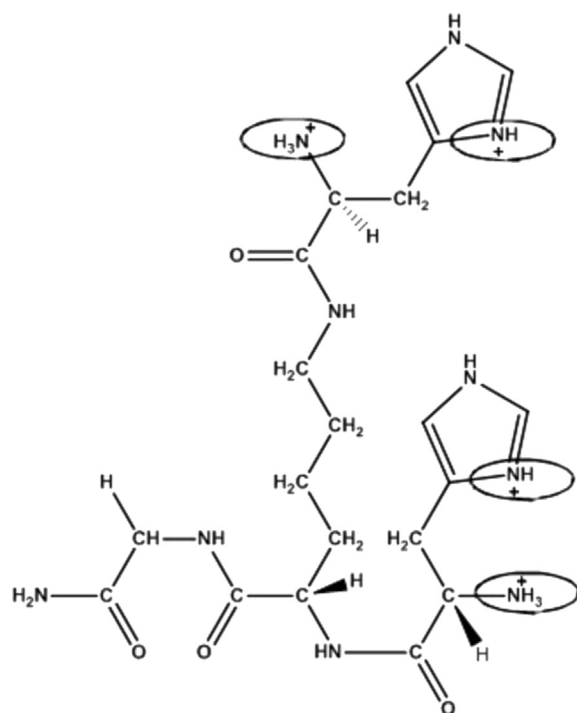


FIGURE 7.1 Structure of 4⁺ peptide dendrimer with histidine as terminal amino acid (sequence: Gly–Lys–(His)₂; [M + H]⁺ = 476.53). Produced with permission from Mutalik S, Nayak UY, Kalra R, et al. Sonophoresis-mediated permeation and retention of peptide dendrimers across human epidermis. *Skin Res Technol* 2011;1–7.

Peptide dendrimers can also be used as protein mimics, immunogens, and catalysts in reactions of ester hydrolysis.

ADVANTAGES OF PEPTIDE DENDRIMERS

The peptide dendrimers have advantages over the widely studied and reported PAMAM dendrimers, and some of the merits are given here:

- Lower or no toxicity (in contrast, PAMAM dendrimers break down endogenously, releasing toxic byproducts, such as acrylates).
- Endogenous peptidases break down peptide dendrimers into simple, natural amino acids.
- Synthesis of peptide dendrimers is cost-effective; synthesis and scale-up are relatively easy.
- Purification of peptide dendrimers is easily done by preparative reverse-phase high-performance liquid chromatography (RP-HPLC).

TRANSDERMAL DRUG DELIVERY

Transdermal drug delivery is the transport of drug molecules across the skin, and it has several advantages over

the traditional methods [9]. It eliminates gastric irritation, prevents hepatic first-pass metabolism, prevents gastric degradation of drug, provides sustained release of drug, is noninvasive, and improves patient compliance.

The skin of an average adult body covers a surface of approximately 2 m² and receives about one-third of the blood circulating through the body. The skin surface contains an average of 200–250 sweat ducts and 10–70 hair follicles in each square centimeter. Therefore, it provides a large surface area for drug absorption and is one of the most readily accessible organs of the human body. Transdermal drug delivery systems (TDDS) make use of the opportunity of this easy accessibility of the skin.

Compared to oral drug delivery, transdermal drug delivery has several advantages:

First-pass effect, which is an added limitation of oral drug delivery, can be evaded through the transdermal route.

Drugs that cause gastrointestinal (GI) irritation can be administered through the transdermal route as this route circumvents direct irritant effects on the GI tract. Drugs that undergo enzymatic degradation or acid degradation in the GI tract can be administered through the transdermal route.

Transdermal delivery also provides steady and consistent permeation of drug through the skin. This leads to more constant drug levels in plasma, which is usually the goal of therapy. Lack of peaks and troughs in plasma concentration can reduce the risk of side effects. Drugs that require relatively consistent plasma levels are generally good candidates for transdermal drug delivery.

An added advantage of TDDS is that, if toxicity develops from a transdermal system, this effect could be limited by removing the patch. TDDS can also provide sustained release of the drug for up to 7 days; therefore, TDDS require once-weekly application. Such a dosage regimen is simple and greatly improves patient compliance.

TDDS may be utilized as an alternative route of drug administration in patients who cannot tolerate oral dosage forms, are nauseated, or are unconscious.

Compared to intravenous, hypodermic, and other parenteral routes, TDDS has major advantages like elimination of pain, possibility of infection, and risk of disease transmission by needle reuse. Hence, with all these qualities, TDDS generally offer better patient compliance.

IDEAL TRANSDERMAL CANDIDATES [10]

Ideal properties as prerequisites for transdermal delivery of drugs include:

- Drugs with molecular mass that are only up to a few hundred Daltons.

- Drugs that have high octanol–water partition coefficients.
- Drugs that are required in low doses of milligrams per day.

But these ideal limits are not met by most of the drugs that have come through high-throughput screening processes. So, for these types of molecules that are required to be transported through the skin, some strategy for permeation enhancement is required to be used.

STRATUM CORNEUM: IMPEDIMENT TO TRANSDERMAL DRUG DELIVERY

Skin is an extraordinary miracle of evolution, which encapsulates an organism physically and acts as an interface between the organism and its surroundings. It is also continuously involved in the construction of an efficient homeostatic barrier. The enormous barrier properties of skin are because of the stratum corneum (SC), the outermost dead layer of the skin. The SC is about 15 μm thick and consists of densely packed disc-like keratinocytes. In between the water-filled (50% v/v) keratinocytes, multicellular lipid bilayers are present that function as “cement.” Typically, 10 lipid bilayers fill up the region between two keratinocytes. The highly ordered structure formed by multiple alterations of hydrophilic and lipophilic elements leads to the SC being practically impermeable.

TRANSDERMAL DRUG DELIVERY APPROACHES

Before going into detail about the application of peptide dendrimers in skin delivery of bioactive molecules, it is better to understand the different transdermal approaches to deliver drugs. If the barrier of the SC can be breached, introduction of drug molecules or biomolecules can be easily accomplished. In order to improve the transdermal permeation of drugs to clinically useful levels, permeation promoters can be added to the drug delivery systems. Various approaches have evolved to expand the number of drugs delivered through skin [11]. These include:

1. **Formulation manipulation**, like the use of supersaturated solution, microemulsion, liposomal systems, transfersome, and drug modification by derivatization (eg, esterification of betamethasone into its 17-valerate analog increases its potency 450 times);
2. **Chemical enhancement** using permeation enhancers such as surfactants, polyalcohols, amines, amides,

sulfoxides, esters, fatty acids terpenes, pyrrolidones, alkanes, and phospholipids; and

3. **Physical penetration** enhancement methods, like iontophoresis, sonophoresis, electroporation, magnetophoresis, and so on.

In recent years, dendrimers have been identified as permeation enhancers for skin delivery of drugs. The potential of dendrimers as drug vehicles or scaffolds is now being researched as one of the most active fields of biomedical and pharmaceutical sciences [12].

PEPTIDE DENDRIMERS IN TRANSDERMAL DRUG DELIVERY

Use of peptide dendrimers in transdermal drug delivery was pioneered and widely explored by Mutalik et al. [13–16]. The first step toward this was the development of a simple, robust, and validated analytical HPLC method for quantifying the dendrimers into and across the skin.

Development of a Validated RP-HPLC Method for Quantification of Peptide Dendrimers [14]

Though analytical methods for PAMAM dendrimers were well established, there were no reports on a suitable HPLC method for poly(amino acid) dendrimers. Peptide dendrimers with arginine and histidine as terminal amino acids and having varied positive charges (arginine group: 4⁺, 8⁺, and 16⁺; and histidine group: 4⁺, 8⁺, and 16⁺) were synthesized using SPPS and purified by semipreparative HPLC. Heptafluorobutyric acid (HFBA; 0.02% v/v) was used as an ion-pairing agent (which retains peptides on RP columns) to quantify the synthesized dendrimers. At all the tested concentrations of HFBA, dendrimers of the same charge (whether in the arginine or histidine class) showed almost similar column retention times. This indicated that the density of their positive charge is an important factor for the separation of these cationic poly(amino acids).

A preliminary study involving both passive diffusion and iontophoresis was conducted with human skin, to test whether this developed and validated RP-HPLC method could be used to quantify the cationic poly(amino acids) in transdermal permeation experiments. It was found that, compared to passive diffusion, the synthesized peptide dendrimers permeated to a much higher extent via iontophoresis. Peptide dendrimers have physicochemical properties (charged; high molecular weight, ~400–2300) that make them unsuitable for passive transdermal administration. It is widely accepted that molecules of size >500 Da are not fit for skin permeation by passive diffusion [17]. On the other

hand, iontophoresis, which is an electrically aided drug delivery technology, provides for a controlled, noninvasive route of delivery for charged molecules of even high molecular masses [18].

Sonophoresis-Mediated Permeation and Retention of Peptide Dendrimers Across Human Epidermis [13]

Once it was understood that iontophoresis successfully enhances the skin permeation of peptide dendrimers through skin, the next logical strategy was to determine the effect of sonophoresis, also a physical transdermal permeation enhancement technique like iontophoresis, on the skin permeation and deposition of peptide dendrimers.

Sonophoresis implies the application of ultrasound energy to drive molecules into and across skin [19,20]. Depending upon the frequency of ultrasound used, it can be classified into low-frequency ultrasound (20–100 kHz) and therapeutic-frequency ultrasound (1–3 MHz). But transdermal permeation enhancement induced by ultrasound of low frequency (<100 kHz) was found to be more remarkable than that caused by ultrasound of high frequency [21–23]. The experiments of Levy et al. [24] using sonophoresis showed that when the skin was exposed to 3–5 min of exposure to therapeutic ultrasound (1 MHz, 1.5 W/cm²), the permeation of physostigmine and mannitol through hairless rat skin was increased in vivo by 15-fold. Also, the lag time usually found in transdermal delivery was nearly completely abolished after exposure to therapeutic ultrasound. Several phenomena may occur in the skin upon exposure to ultrasound. They include thermal effects, acoustic streaming, and cavitation effects.

- **Thermal effects:** When a medium absorbs ultrasound, it leads to an increase in the temperature. Tissues such as bone, which have higher ultrasound absorption coefficients than tissues like muscle, experience severe thermal effects. The absorption coefficient of a medium is not constant; instead, it increases proportionally with the ultrasound frequency. This indicates that ultrasound-associated thermal effects are proportional to the frequency of the ultrasound. When a medium is exposed to ultrasound at a given frequency, the rise in temperature varies in proportion to the ultrasound intensity and the time of exposure. Thermal effects can be considerably decreased by pulsed application of ultrasound.
- **Acoustic streaming:** Formation of time-dependent large fluid velocities in a medium, due to the influence of ultrasound, is known as *acoustic streaming*. The primary causes of acoustic streaming

are the reflection and other distortions of wave propagation. Oscillation of cavitation bubbles may also contribute to acoustic streaming. The shear stresses developed by streaming velocities may affect the neighboring structures.

- **Cavitation effects:** This refers to the formation of gaseous cavities in a medium upon exposure to ultrasound. Cavitation is primarily caused by the pressure variations of the medium induced by ultrasound. This involves either transient cavitation (ie, the growth followed by collapse of a bubble rapidly) or stable cavitation (ie, the oscillatory slow movement of the bubble in an ultrasound field). The effects of cavitation on tissues are many. Specifically, cavitation bubbles collapse to release a shock wave that may then induce structural alterations in the surroundings. Tissues of biological origin contain numerous air pockets trapped inside the fibrous structures. These air pockets upon ultrasound exposure may act as nuclei for the process of cavitation. The possible mode of enhanced SC permeability through cavitation is shown in Fig. 7.2 [25]. Although cavitation disrupts SC lipid structure and skin permeability for many hours, deeper tissues are saved from damage [11].

Compared to passive diffusion, application of ultrasound substantially increased the permeation of peptide dendrimers [13]. The extent of permeation was found to depend on the molecular weight of dendrimers, and permeation decreased with an increase in molecular weight of the dendrimer. The most important reason for ultrasound-aided transdermal permeation and delivery of drugs has been found to be cavitation-induced lipid bilayer disordering [20]. Also, the retention of peptide dendrimers within the skin was assessed. A similar trend was observed in that dendrimers of high molecular weight showed the greatest retention within the skin.

This approach could pave the way for various applications of high-molecular-weight or low-molecular-weight dendrimers in clinical research. Ultrasound-mediated transdermal permeation of dendrimers has an important future role in the transport of drug and gene–dendrimer complexes through or into the skin, for the effective management of localized skin conditions, as well as immune-modulation and systemic effects while using skin delivery strategies that are noninvasive.

Iontophoresis-Mediated Permeation and Retention of Peptide Dendrimers Across the Human Epidermis [15]

Iontophoresis indicates the application of an electric current to increase the penetration of ionized or charged drugs into superficial tissues. The electrical principle of

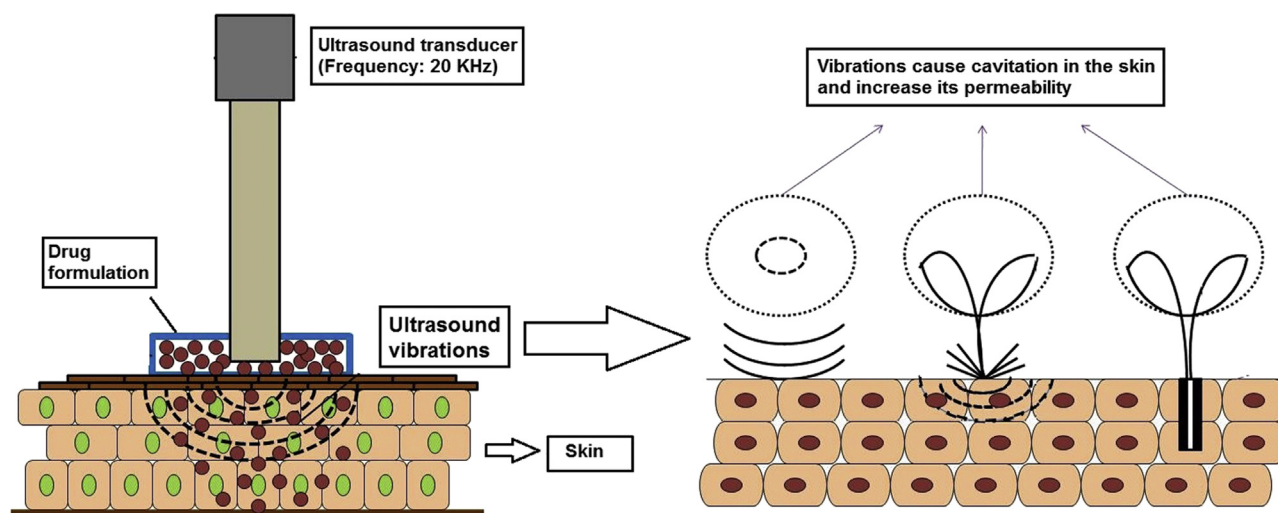


FIGURE 7.2 Possible mode through which inertial cavitation may enhance SC permeability.

“like charges repel each other and opposite charges attract” is the reason by which electrical energy aids in the movement of ions across the SC [26]. Generally, dendrimers are charged macromolecules at physiological pH, and hence the application of a harmless electric current ($\approx 0.5 \text{ mA/cm}^2$) via iontophoresis is a promising technique proposed to enhance the transdermal permeation of dendrimers or drug–dendrimer complexes across skin [18].

Iontophoresis employs an electrical current (usually $\approx 0.5 \text{ mA/cm}^2$) to promote the transfer of molecules through the skin. When an electrical potential develops across the membrane, it repels charged species into and through the skin. The efficiency of the process of iontophoresis depends upon the valency, polarity, and ionic mobility of the permeant and the composition of the formulation and the electric current applied [27].

In iontophoresis, the drug is applied under an electrode of the same charge. An electrode of charge opposite to the drug is placed on the body surface at a neutral site. An electric current below the level of the pain threshold of the patient ($\approx 0.5 \text{ mA/cm}^2$) is selected and allowed to flow for an appropriate duration of time. The electrical current increases the penetration of the drug into surface tissues significantly by repelling like charges and attracting opposite charges.

For iontophoretic treatment, there are certain prerequisites:

- The drug must be charged (or modified so as to become charged).
- The disease or site of drug requirement must be at or near a body surface [28].

However, iontophoresis can be applied to deliver the molecules into systemic circulation.

To elaborate the mechanism involved in iontophoretic skin permeation of peptide dendrimers through skin, a series of passive diffusion studies and iontophoresis studies were carried out. Akin to sonophoresis, the penetration of peptide dendrimers through skin depended on the molecular weight of dendrimers. Interestingly, molecular weight played a key determinant factor for permeation across skin, more so than the charge that the dendrimers possess. The isoelectric point of the skin is also likely to play a role in the enhanced iontophoretic transdermal permeation of peptide dendrimers. The isoelectric point of skin is four to five, and it is negatively charged at physiological pH. Cationic peptide dendrimers therefore have an intrinsic affinity for negatively charged skin, and hence higher skin permeation of peptide dendrimers may be a result of their nonspecific, charge-related binding to skin. In tune with the results obtained with sonophoresis, high-molecular-weight dendrimers demonstrated greatest skin retention upon application of iontophoresis.

Electromigration is the general mechanism behind the iontophoretic transdermal permeation enhancement of small charged molecules (ie, the cathode is used to deliver an anion, and the anode is used to deliver a cation). The electromigration-dominant mechanism may well be attributed to the positive charge of the dendrimers, which drives the dendrimers into the receptor compartment (cathode) under the influence of a current in the donor compartment (anode). Due to the permselectivity of skin to cations, the solvent and dendrimer within are expected to flow from the anode to cathode at physiological pH during iontophoresis. Hence, peptide dendrimers could be used in iontophoretic delivery of drugs and macromolecules.

Peptide Dendrimers as Drug Carriers [16]

Previous studies have reported that dendrimers can function as drug carriers either by encapsulating drugs within the dendritic structure or by attaching drugs to their terminal functional groups via electrostatic or covalent bonds (prodrug) [29].

Upon establishing the fate of peptide dendrimers following passive diffusion as well as assessing the effects of sonophoresis and iontophoresis on the skin delivery of peptide dendrimers, Mutalik et al. further elucidated the applicability of peptide dendrimers in enhancing the transdermal permeation of therapeutically relevant molecules. 5-fluorouracil (5-FU) was selected as a model drug based on previous reports available on the use of chemicals to enhance the skin permeation of 5-FU [30–32]. To study the mechanism underlying the peptide dendrimer-assisted permeation of 5-FU across human epidermis, a series of arginine-terminated peptide dendrimers of varying positive charge and molecular weights (4^+ , 8^+ , and 16^+ ; 515.8, 1084.4, and 2222.5 Da) were synthesized by Fmoc-SPPS, purified by preparative HPLC, and characterized by RP-HPLC and ESI⁺-MS for the molecular ion ($[M + H]^+$) peak. The skin permeation studies in the presence of dendrimers were conducted by either (1) simultaneously application of drug and dendrimer or (2) pretreating skin with dendrimers 2 h prior to application of drug solution [13].

For simultaneous application studies: Drug + Dendrimer in donor solution followed by adding a little quantity of 5-FU to make it a suspension. Entire mixture used for skin permeation studies.

For pretreatment studies: After hydration, skin treated with dendrimer for predetermined time (2 h). After complete removal of dendrimer solution, suspension of drug prepared, and in vitro skin permeation studies carried out.

From the results, they concluded that the peptide dendrimers considerably increased the permeation of 5-FU across human epidermis. This could be due to: (1) increased oil–water partition coefficient of drug by peptide dendrimers; (2) formation of drug–peptide dendrimer complex, which shows better skin permeation compared to plain drug; and (3) disruption of the well-organized structure of skin by peptide dendrimers via interacting with lipid and/or protein structures of skin. However, the presence of “free” peptide dendrimers (uncomplexed) is essential for superior skin deposition and permeation of drugs.

Encouraged by the results obtained from the previous studies, an attempt was made to study the skin permeation and deposition of ketoprofen, a model drug, using peptide dendrimers (unpublished results). The effects of sonophoresis and iontophoresis on the skin delivery of ketoprofen were also assessed.

Effect of Drug–Peptide Dendrimeric Conjugates on Transdermal Permeation

The linkage of a dendrimer to a drug covalently forms a stable system, which does not depend on dynamic equilibrium or those thermodynamic factors that are applicable in matrix systems like drug encapsulation by micelles or dendrimers [33]. Drug release from a prodrug results from chemical or enzymatic cleavage of a hydrolytically labile bond. Since peptide dendrimers break down into harmless amino acids, this strategy was used to design a ketoprofen–peptide dendrimer conjugate and to study the transdermal permeation of dendrimeric conjugate of ketoprofen in the presence of ultrasound and electric current across mice skin.

Different dendrimeric prodrugs of ketoprofen with arginine and lysine as amino acids and with varying positive charges were successfully synthesized by Fmoc SPPS. The rate of skin permeation of ketoprofen was considerably less from dendrimeric conjugates when compared with that from plain ketoprofen, which might be due to higher molecular weight of dendrimeric prodrugs (≈ 1000) as compared to ketoprofen (MW = 254). Sonophoresis substantially increased the skin permeation of both ketoprofen and its dendrimeric conjugates when compared to simple passive diffusion. The results of iontophoresis also demonstrated that the peptide dendrimeric conjugates of ketoprofen could be successfully applied to enhance the transdermal permeation of the drug.

CONCLUSION

Peptide dendrimers have an important role to play in the transdermal permeation. They themselves have the ability to penetrate the skin. In addition, they enhance the permeation of the drugs. They have been found more effective in conjunction with iontophoresis or sonophoresis in delivering the drugs across or into the skin. The role of peptide dendrimers in skin delivery of bioactive molecules is yet to be explored in detail.

List of Acronyms and Abbreviations

Bis-MPA	Bis(methylol)propionic acid
Boc	tert-Butyl carbamates
DSC	Differential scanning calorimetry
Fmoc	9-Fluorenylmethyl carbamate
FTIR	Fourier transform infrared
G	Generation
GI	Gastrointestinal
KHz	Kilo-Hertz
MHz	Mega-Hertz
MS	Mass spectrometry
MW	Molecular weight
nm	Nanometer

Pa Pascal
PAMAM Poly(amidoamine)
PAMAMOS Poly(amidoamine-organosilicon)
PLL Poly-L-lysine
RP-HPLC Reverse phase-high performance liquid chromatography
SPPS Solid phase peptide synthesis
Da Dalton

Glossary

Dendrimer A dendrimer is an artificially manufactured or synthesized molecule built up from branched units called monomers.

Iontophoresis Introduction of an ionized substance (as a drug) through intact skin by the application of a direct electric current.

Passive diffusion Movement of biochemicals and other atomic or molecular substances across cell membranes. Unlike active transport, it does not require an input of chemical energy, being driven by the growth of entropy of the system.

Peptide dendrimers Radially branched macromolecules that contain a peptidyl core and/or peripheral peptide chains.

Solid phase peptide synthesis Solid-phase peptide synthesis (SPPS) can be defined as a process in which a peptide anchored by its C-terminus to an insoluble polymer is assembled by the successive addition of the protected amino acids constituting its sequence.

Sonophoresis Movement of the drugs through skin into the subcutaneous tissues under the influence of ultrasound.

Transdermal drug delivery system Transdermal therapeutic systems are defined as self-contained, discrete dosage forms, which when applied to the intact skin deliver the drug at a controlled rate to the systemic circulation.

References

- [1] Tomalia DA, Baker H, Deqald J, et al. A new class of polymers: starburst-dendritic macromolecules. *Polym J* 1985;17:117–32.
- [2] Kannan RM, Nance E, Kannan S, et al. Emerging concepts in dendrimer-based nanomedicine: from design principles to clinical applications (review). *J Intern Med* 2014;276:579–617.
- [3] Nanjwade BK, Bechra HM, Derkar GK, et al. Dendrimers: emerging polymers for drug-delivery systems. *Eur J Pharm Sci* 2009;38(3):185–96.
- [4] Jain K, Kesharwani P, Gupta U, et al. Dendrimer toxicity: let's meet the challenge. *Int J Pharm* 2010;394(1–2):122–42.
- [5] Malik A, Chaudhary S, Garg G, et al. Dendrimers: a tool for drug delivery. *Adv Biol Res* 2012;6(4):p165–169.
- [6] Svenson S. Dendrimers as versatile platform in drug delivery applications. *Eur J Pharm Bio-pharm* 2009;71(3):445–62.
- [7] Neiderhafner P, Sebestik J, Jezek J. Peptide dendrimers (review). *J Pept Sci* 2005;11:757–88.
- [8] Parekh HS, Marano RJ, Rakoczy EP, et al. Synthesis of a library of polycationic lipid core dendrimers and their evaluation in the delivery of an oligonucleotide with hVEGF inhibition. *Bioorg Med Chem* 2006;14:4775–80.
- [9] Kumar KP, Radhika PR, Sivakumar T. Ethosomes-A priority in transdermal drug delivery. *Int J Adv Pharm Sci* 2010;1(2):111–211.
- [10] Keleb E, Sharma RK, Mosa EK, et al. Transdermal drug delivery system-design and evaluation. *Int J Adv Pharm Sci* 2010;1:201–11.
- [11] Prausnitz MR, Langer R. Transdermal drug delivery. *Nat Biotechnol* 2008;26(11):1261–8.
- [12] Cheng Y, Xu T. Dendrimers as drug carriers: applications in different routes of drug administration. *J Pharm Sci* 2008;97(1):123–43.
- [13] Mutalik S, Nayak UY, Kalra R, et al. Sonophoresis-mediated permeation and retention of peptide dendrimers across human epidermis. *Skin Res Technol* 2011;1–7.
- [14] Mutalik S, Hewavitharana AK, Shaw PN, et al. Development and validation of a reversed-phase high-performance liquid chromatographic method for quantification of peptide dendrimers in human skin permeation experiments. *J Chromatogr B Analyt Technol Biomed Life Sci* 2009;877:3556–62.
- [15] Mutalik S, Parekh HS, Anissimov YG, et al. Iontophoresis-mediated transdermal permeation of peptide dendrimers across human epidermis. *Skin Pharmacol Physiol* 2013;26:127–38.
- [16] Mutalik S, Shetty PK, Kumar A, et al. Enhancement in deposition and permeation of 5-fluorouracil through human epidermis assisted by peptide dendrimers. *Drug Deliv* 2014;21(1):44–54.
- [17] Schuetz YB, Naik A, Guy RH, et al. Emerging strategies for the transdermal delivery of peptide and protein drugs. *Expert Opin Drug Deliv* 2005;2(3):533–48.
- [18] Kalia YN, Naik A, Guy RH, et al. Iontophoretic drug delivery. *Adv Drug Deliv Rev* 2004;56(5):619–58.
- [19] Mutoh M, Ueda H, Nakamura Y, et al. Characterization of transdermal solute transport induced by low-frequency ultrasound in the hairless rat skin. *J Controlled Release* 2003;92(1–2):137–46.
- [20] Polat BE, Hart D, Langer R, et al. Ultrasound-mediated transdermal drug delivery: mechanisms, scope, and emerging trends. *J Controlled Release* 2011;152(3):330–48.
- [21] Tezel A, Sens A, Mitragotri S, et al. Frequency dependency of sonophoresis. *Pharm Res* 2001;18(12):1694–700.
- [22] Boucaud A, Garrigue MA, Machel L, et al. Effect of sonication parameters on transdermal delivery of insulin to hairless rats. *J Controlled Release* 2002;81(1–2):113–9.
- [23] Mitragotri S, Kost J. Low-frequency sonophoresis: a review. *Adv Drug Deliv Rev* 2004;5:589–601.
- [24] Levy D, Kost J, Meshulam Y, et al. Effect of ultrasound on transdermal drug delivery to rats and guinea pigs. *J Clin Invest* 1989; 83:2074–8.
- [25] Joshi A, Raje J. Sonicated transdermal drug transport. *J Controlled Release* 2002;83(1):13–22.
- [26] Rai R, Srinivas CR. Iontophoresis in dermatology. *Indian J Dermatol Venerol Leprol* 2005;71(4):236–41.
- [27] Naik A, Kalia YN, Guy RH. Transdermal drug delivery: overcoming the skin's barrier function. *Pharm Sci Technol Today* 2000;3(9):318–26.
- [28] Akimoto M, Maeda K, Nishimura T, et al. Photodynamic therapy in the dermatological field and enhanced cutaneous absorption of photosensitizer. *Piers Online* 2010;6(8):754–8.
- [29] Jansen JF, de Brabander van den Berg EM, Meijer EW. Encapsulation of guest molecules into a dendritic box. *Science* 1994;266: 1226–9.
- [30] Raja MH, Ping Q, Gao Z. Penetration enhancing effect of tetrahydrogeraniol on the percutaneous absorption of 5-fluorouracil from gels in excised rat skin. *J Controlled Release* 1998;55:297–302.
- [31] Elka T, Lizette A. Effect of propylene glycol, azone and n-decylmethyl sulphoxide on skin permeation kinetics of 5-fluorouracil. *Int J Pharm* 1985;27:89–98.
- [32] Marjukka TT, Servet B, Nadir B, et al. Enhanced delivery of 5-fluorouracil through shed snake skin by two new transdermal penetration enhancers. *Int J Pharm* 1993;92:89–95.
- [33] Aulenta F, Hayes W, Rannard S. Dendrimers: a new class of nanoscopic containers and delivery devices. *Eur Polym J* 2003;39: 1741–71.

Insights Into Interactions of Gold Nanoparticles With the Skin and Potential Dermatological Applications

N. El-Sayed^{1,2}, L. El-Khourdagui², M. Schneider¹

¹Saarland University, Saarbruecken, Germany; ²Alexandria University, Alexandria, Egypt

OUTLINE

Introduction	99	Chemical Penetration Enhancers	107
Dermatological Applications of Gold Nanoparticles	100	Ultrasound	107
Skin Cancer Treatment and Imaging	101	Thermal Ablation	107
Topical and Transdermal Drug Delivery	101	Iontophoresis	108
Other Applications	102	Dermaportation	108
		Dermabrasion	108
Interactions of Gold Nanoparticles With the Skin Barrier	102	Potential Mechanisms of Skin Penetration of Gold Nanoparticles	108
Factors Affecting Skin Penetration of Gold Nanoparticles	102	Future Perspectives and Recommendations	110
Physicochemical Properties of Gold Nanoparticles and Formulation Adjuvants	102	Conclusion	110
Skin Origin and Condition	104	List of Acronyms and Abbreviations	110
Experimental Variables and Experimental Configuration	105	Acknowledgments	111
Evaluation Methods (Quantification of Gold Nanoparticles Interactions and Imaging and Tracking of Their Penetration)	106	Endnote	111
Skin Penetration Enhancers of Colloidal Gold	107	References	111

INTRODUCTION

Nanotechnology is an exciting research area that is expected to pave the way for the design and discovery of nanomedicines as a new class of drugs. Among nanomaterials with great potential in nanomedicine, gold nanoparticles (AuNPs) have recently gained widespread interest due to their unique physicochemical

properties [1]. The skin is an attractive route of administration for noninvasive entry of nanoparticulates, for either local dermal applications [2] or systemic transdermal purposes [3]. In skin-based biomedical applications, AuNPs have been investigated for theranostics and the delivery of drugs and vaccines. For instance, AuNPs were explored for diagnosis of skin cancers [4] and cancer treatment with photothermal therapy

[5,6]. Furthermore, AuNPs have been applied for the delivery of small actives [7] and biomacromolecules [8–12]. In this respect, they have been utilized for percutaneous immunization [10] and for gene-suppressing therapy when conjugated with small interfering RNAs (siRNAs) [12]. Similarly, transdermal delivery of other macromolecules such as insulin has been improved by AuNPs along with near-infrared (near-IR) radiation [8].

Despite easy topical application, dermatological uses of AuNPs are challenged by the formidable barrier function of the skin, being the first line of defense against xenobiotics [13]. This is obvious from the dense structure of the stratum corneum (SC) representing the main physical barrier [14]. For efficient development of skin nanotherapeutics, the SC is to be overcome to reach the deeper skin layers. Therefore, strategies have been adopted to enhance the diffusion of AuNPs through the SC, such as the use of physical [11] and chemical [15] penetration enhancers. Furthermore, it is essential to understand the possible diffusion mechanisms of AuNPs through the skin. This will allow one

to assess the impact of different variables and penetration enhancers for the development of optimized nanomedicines.

In this chapter, we shed light on the potentials of AuNPs for dermatological applications along with the key element in their effectiveness, which is the ability to penetrate through the SC. In this regard, the variables that potentially affect the penetration process are discussed. The different experimental designs (configurations and variables) and evaluation methods are highlighted. Furthermore, the penetration enhancement and the potential mechanisms of AuNP penetration are summarized. Finally, we discuss the current state of the art and recommendations for the future.

DERMATOLOGICAL APPLICATIONS OF GOLD NANOPARTICLES

A representative illustration of AuNPs' potential dermatological applications is shown in Fig. 8.1.

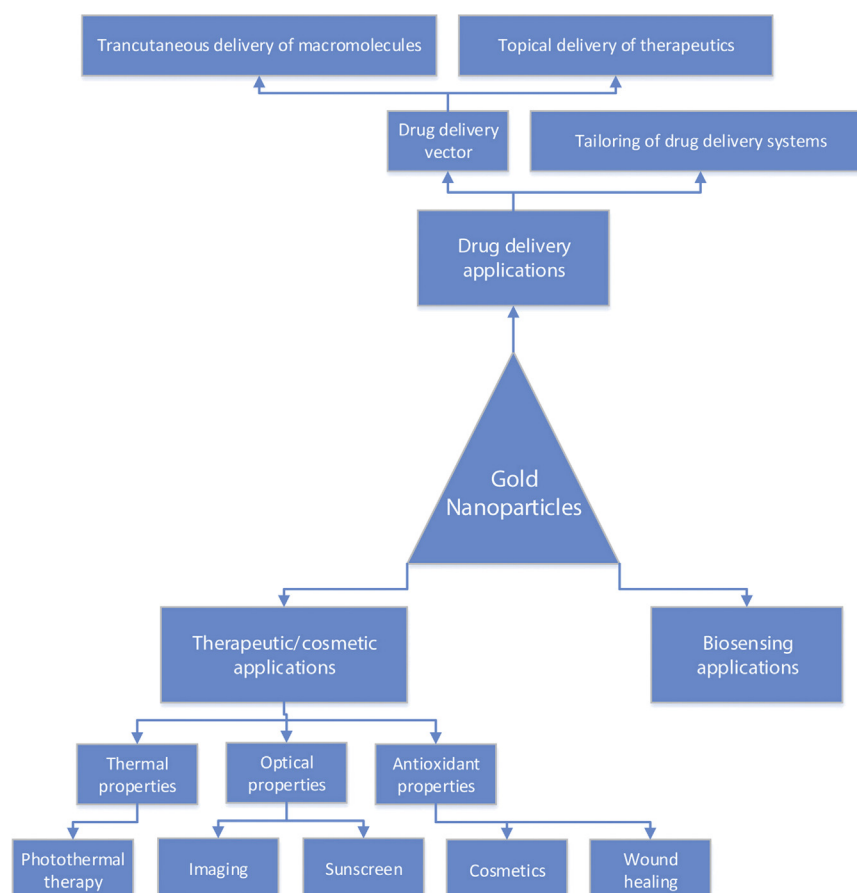


FIGURE 8.1 Diagram illustrating the dermatological applications of gold nanoparticles. Gold nanoparticles in various researches were applied topically or systemically for treatment of dermal conditions, transcutaneous delivery of therapeutics, or treatment and diagnosis of skin cancer.

Skin Cancer Treatment and Imaging

Skin cancers are an uprising challenging clinical problem worldwide, representing the most common malignancy induced by environmental effectors, especially extensive exposure to ultraviolet radiation [16]. Surgical excision remains the standard treatment modality for skin cancers [16,17]. However, developing new treatment strategies could offer great benefits regarding reduced morbidity and mortality [16]. Several researches have explored the use of AuNPs in fighting cancer cells. Systemically applied nanosized objects may accumulate in cancer cells due to the enhanced permeability and retention effect [18]. Alternatively, AuNPs can be decorated with targeting ligands, for instance antibodies that can bind selectively to certain antigens overexpressed on the cancer cells [6,19–21].

For local hyperthermia with near-IR radiation, gold nanorods functionalized with epidermal growth factor receptor antibody (anti-EGFR) were developed to target EGFR that is overexpressed in squamous carcinoma cells. The conjugate showed efficient *in vitro* cellular uptake by human squamous carcinoma cells A431. Furthermore, in the presence of near-IR, the conjugate was able to induce apoptotic cell death [6].

Moreover, AuNPs have been explored as a vector for the delivery of anticancer therapeutics. Zn(II)-phthalocyanine disulfide–AuNP conjugates were developed for anticancer and showed two- to threefold higher biodistribution of phthalocyanine compared to free phthalocyanine in amelanotic melanoma subcutaneously transplanted in a mouse model [22]. As an example of another anticancer therapy, an epigallocatechin-3-gallate–AuNP conjugate showed higher anticancer activity compared to the free molecules against melanoma cells *in vitro* and *in vivo* in a mouse model when applied intratumorally [23].

Another important application of AuNPs is the optical detection of skin cancers for diagnostic purposes and tracing of malignant cells for complete tumor excision in surgeries [24]. The usage of surface plasmon resonance allows for enhanced light absorption and scattering cross-sections [25]. This permits various imaging techniques to distinguish discrete AuNP-labeled cancerous cells from the unlabeled healthy cells [26]. Squamous cell carcinoma was imaged *ex vivo* using anti-EGFR-conjugated gold nanorods and near-IR radiation with narrow-band imaging [24]. Furthermore, photoacoustic imaging of AuNP-labeled melanoma cells was exploited [4] by relying on the heat formed when AuNPs absorb light, creating acoustic waves [26]. Another application of AuNPs is for skin cancer diagnosis via immunosensing of melanoma adhesion molecule antigen (CD146) providing higher sensitivity for detection [27].

Overall, the potential applications of AuNPs in skin cancer treatment and imaging are various. Studies for *in vivo* delivery of AuNPs to skin cancer were conducted via intravenous or intratumoral administration. In contrast, topical application of nanotherapeutics seems like an attractive easy route to reach these skin-localized cancers. This raises the question about the possibility of combining the beneficial medicinal effects of AuNPs with the ease of dermal application.

Topical and Transdermal Drug Delivery

AuNPs were adopted in various laboratories for different drug delivery strategies, due to the ease of preparation, surface modification, and control of particle size and shape, in addition to their stability and their special properties that enable imaging and tracking in biological tissues. Among the attempts for tailoring and controlling drug delivery to skin, pH-responsive liposomes were developed and stabilized by AuNPs as a platform to deliver antibacterial agents to infected skin regions [28]. Liposomes smaller than 100 nm exhibit poor stability and tend to fuse to decrease surface tension [29]. This tremendously reduces skin penetration ability and effective drug delivery [30]. Electrostatic binding of carboxyl-modified AuNPs (4 nm) to the surface of cationic sub-100-nm liposomes was shown to stabilize them and prevent early fusion at neutral pH. When the system is applied to the skin, AuNPs detach from the surface of liposomes due to the drop of pH, especially in infectious lesions, with free liposomes regaining their ability to fuse with biological membranes. Therefore, AuNPs in environments where there is an alteration of the pH may offer the advantage of activating drug delivery systems selectively in infectious skin lesions [28].

Another area of interest is the transdermal delivery of therapeutics, especially biomacromolecules—for instance, peptides and proteins for transcutaneous vaccination. Skin layers contain antigen presenting cells, such as Langerhans cells in the epidermis, that initiate an immune response against exogenous antigens invading the skin. Transcutaneous vaccination will be an attractive needle-free immunization strategy [31]. However, the delivery of the hydrophilic peptides and proteins through the SC to deeper skin layers is challenging. Huang et al. speculated, during experiments on naked mice, that 5 nm AuNP can alter the integrity of the SC due to interactions with intercellular lipids forming transient openings. AuNPs were found to concentrate in the SC and epidermis, with limited distribution in the dermis and follicles. The co-administration of AuNPs with two protein drug models (horseradish peroxidase and β -galactosidase) revealed similar

penetration results. This penetration enhancement was also shown to be a temporal effect, which was demonstrated via use of a small fluorescent dye (rhodamine B). Diffusion of the dye into deeper skin layers was allowed only by co-application with AuNPs; in contrast, this was not observed for the dye applied after AuNP removal. Finally, the efficiency of AuNPs to induce transcutaneous immunization in mice when co-administered with ovalbumin was tested. The results showed a robust, persistent immune response observed from the significantly increased level of anti-ovalbumin–immunoglobulin G (IgG) over the immunization course [10].

Other Applications

Because of their antioxidant and antiinflammatory properties, AuNPs may exhibit cosmeceutical effects [32–34] and promote wound healing [35–37]. AuNPs have the potential to inhibit glycation of skin collagen, and hence they would enhance skin elasticity and act against skin aging [38]. They also have been combined with skin nutrients for cosmetic purposes; for instance, a facial mask composed of nanofibers loaded with AuNPs, ascorbic acid, retinoic acid, and collagen has been developed [32]. Furthermore, AuNPs were considered to replace conventional sunscreen nanomaterials such as titanium dioxide and zinc oxide owing to their light absorption and light-scattering properties [34]. Apart from cosmetic applications, the wound-healing-enhancing effect of AuNPs has also attracted the attention of some laboratories. Topically applied AuNPs together with other antioxidants (epigallocatechin gallate and α -lipoic acid) were found to accelerate cutaneous wound healing in mouse models [35,36]. Moreover, combining AuNPs with microelectrical current stimulation was reported to enhance the healing of burn wounds [37].

Finally, the various potential applications of AuNPs in therapeutics and drug delivery indicate the large expectations put onto these systems. However, translation of laboratory data to topical clinical applications appears to be still remote, as a result of the firmness of the skin as a barrier that is difficult to be penetrated passively. There are less promising reports with respect to particles' penetration into intact skin [39–41]. Accordingly, a deeper understanding of the penetration behavior of nanoparticulates is necessary for a better design of nanotherapeutics and specific selection of the efficient enhancement methods.

INTERACTIONS OF GOLD NANOPARTICLES WITH THE SKIN BARRIER

The SC has a bricks-and-mortar wall-like structure [14], where rigid corneocytes, which are dead cells filled

with keratin, are connected by intercellular lipids organized in lamellar phases with liquid, hexagonal, or orthorhombic lateral packing. The orthorhombic pattern, with a very dense lipid organization, is the most prominent in human skin [42]. Consequently, SC is the main barrier against the translocation of molecules and nanoparticles and the limiting factor for the effectiveness of nanotherapeutics.

Recently, the ability of AuNPs to penetrate the skin received pronounced attention in different laboratories [40,43–47]. Penetration studies of AuNPs were conducted with the aim of drug delivery [8–11], as studies to explore the potential pathways of skin penetration of nanoparticles [15,45,47], or to evaluate their potential toxicity [40,48]. AuNPs are considered as a very good model for such studies, due to their optical properties facilitating imaging in tissues and complex media [26]. However, the results of different studies were controversial; some showed the penetration ability of AuNPs [43,47], while another concluded the opposite [40]. Taking into consideration that this field of research was established recently, this variability in results could be attributed to the lack of standardization of experimental configurations in different laboratories and the complexity of the multifactorial skin penetration process [49]. The physicochemical properties of AuNPs, formulation adjuvants (eg, solvents and surfactants), origin and condition of the skin sample, and experimental variables along with experimental configuration need to be adjusted to potentially control the results of skin penetration studies. A potential design for AuNPs skin penetration and permeation experiments and possible evaluation methods is illustrated in Fig. 8.2.

Factors Affecting Skin Penetration of Gold Nanoparticles

Physicochemical Properties of Gold Nanoparticles and Formulation Adjuvants

Based on literature, the physicochemical properties of AuNPs play an important role in controlling their interaction with skin and consequently their skin penetration and permeation abilities. Interaction of AuNPs with skin is a complex process involving a combination of different variables, mainly particle size [40,43,45], morphology [47], physical or aggregation state [45], surface charge [46,47], and polarity [45] of the nanoparticles. Experimental results are always related to the parameters tested in the experiment and the experimental configuration (ie, the results are individualized for each experiment). Nevertheless, overall generalized trends relating the physicochemical properties of nanoparticles to their behavior within the skin could be derived from the results of different experiments. These established relationships could be the first step toward a better design of optimized AuNPs for dermal and transdermal biomedical applications.

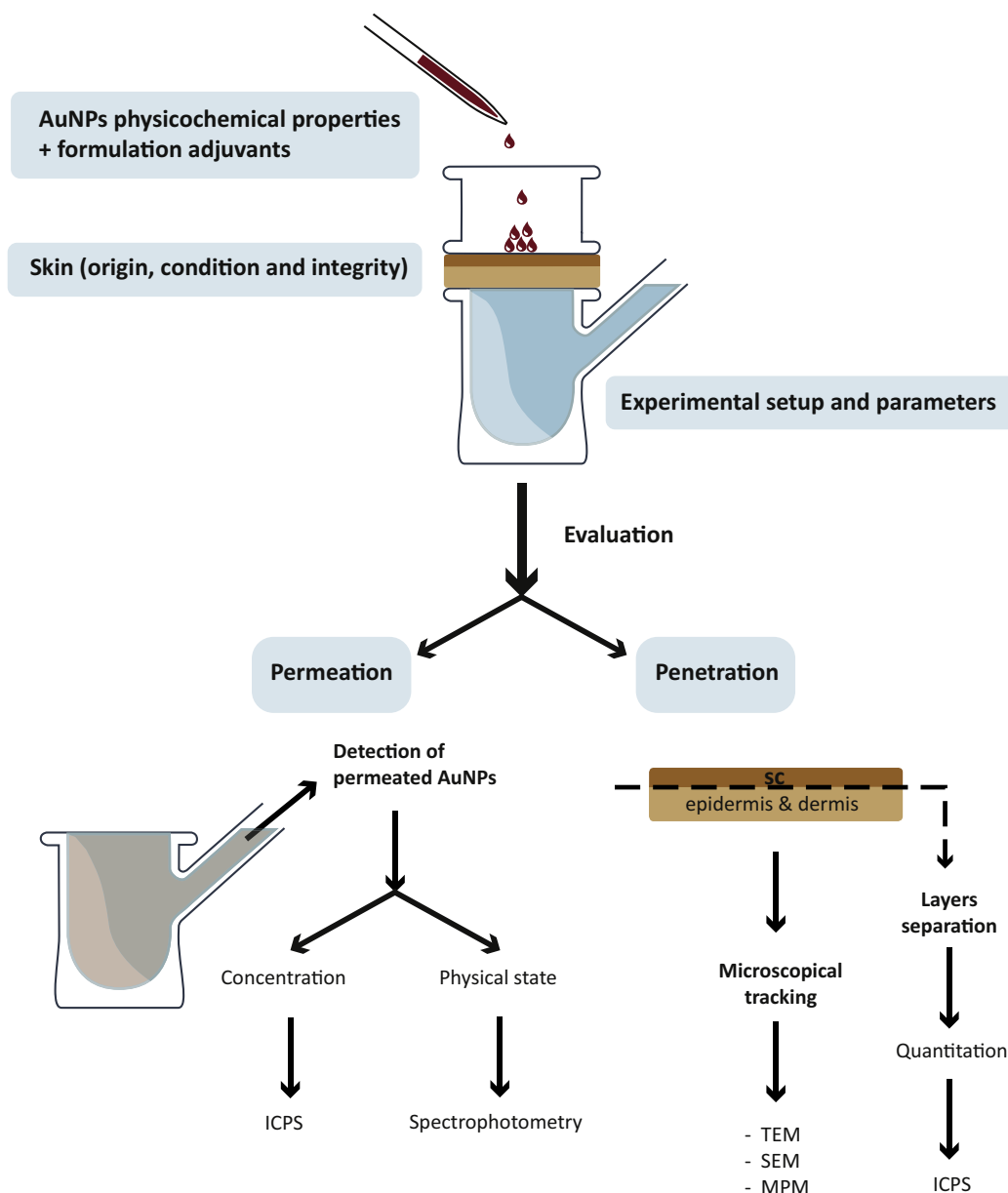


FIGURE 8.2 Illustration of the potential experimental design and evaluation of AuNPs penetration and permeation through skin. ICPS, inductively coupled plasma spectroscopy; MPM, multiphoton microscopy; SEM, scanning electron microscopy; TEM, transmission electron microscopy.

To figure out how particle size can affect the interaction with skin, different studies have adopted AuNPs of different sizes. For instance, Sonavane et al. explored the penetration of 15, 102, and 198 nm sized AuNPs through rat skin. Results showed a size-dependent permeation of the tested nanoparticles. Permeability coefficient and diffusion coefficient decreased by increasing the particle size. Additionally, increasing particle size led to increased lag time, which was 3 and 6 h for 102 and 198 nm AuNPs, respectively. Moreover, transmission electron microscopy (TEM) revealed the ability of the smaller particles to reach deeper in the skin than the larger particles [43]. The study is indicative of size-dependent penetration of nanoparticles through the skin. However, rat skin as a skin model might allow

more skin penetration of nanoparticles in comparison to human skin because of the former's different composition and less compact structure. On the other hand, reports on the penetration of AuNPs into human skin were controversial. While lack of significant penetration of citrate-stabilized AuNPs of 10, 30 and 60 nm size beyond the SC barrier of freshly excised human skin was reported by Liu et al. [40], 12.6 nm citrate-stabilized AuNPs were shown by Filon et al. to penetrate the epidermis and dermis of thawed human skin [44]. This controversy may arise from differences in the integrity of the human skin samples used in the two studies.

For examining the effects of different physicochemical characteristics on AuNP penetration, Labouta et al. designed a study where four AuNP types of

different size and surface polarity (6 nm dodecanethiol-coated AuNPs in toluene, 6 nm lecithin-coated AuNPs in water, 15 nm citrate-coated AuNPs in water, and 15 nm cetrimide-coated AuNPs in toluene) have been examined for their penetration into human skin. The study revealed that the smaller 6 nm AuNPs penetrate deeper skin layers in higher numbers than the larger 15 nm counterparts of the corresponding surface polarity, as semiquantitatively analyzed by multiphoton microscopy (MPM). Moreover, hydrophobic surface-modified AuNPs showed higher penetration to deeper skin layers than their hydrophilic counterparts of the same or even smaller size. In this regard, the authors postulated that AuNPs penetration behaves like molecular penetration [45] but with a lower diffusion rate due to their particulate nature, as expected [14]. Another important parameter to be considered upon studying skin penetration of nanoparticles is their physical state while interacting with skin. Aggregation can prevent skin penetration of small nanoparticles. For AuNPs, aggregation can be easily detected by monitoring the change in the plasmon resonance bands of the particles after skin exposure [45]. Besides, other good tools are present to observe aggregation of AuNPs within the skin layers, for instance dermoscopy and reflectance confocal microscopy (RCM) [48]. In this context, the inability of 15-nm citrate surface-modified AuNPs dispersed in water to penetrate the SC was attributed to their tendency to aggregate when coming in contact with the skin. Their aggregation probably arose from the exchange of citrate ions with skin proteins [45].

As the geometry of particles can affect their interactions with biological barriers [50,51], it may also have an effect on skin penetration. Fernandes et al. found that gold nanorods penetrate the skin at a higher percentage than nanospheres [47]. This is surprising, as the geometry of nanorods necessitates a specific orientation of the particles to penetrate through the densely packed SC. Moreover, they found that positively charged nanoparticles penetrate into human skin in higher numbers than their negatively charged counterparts, and attributed this to the favorable interaction of the positive moieties with the negatively charged skin. However, another study by Lee et al. revealed the opposite: skin penetration is in favor of negatively charged AuNPs, possibly as a result of reduced particle–tissue interaction [46]. This controversy in results regarding the influence of nanoparticles' charge on skin penetration prevents clear conclusions based on these data. However, these arguments emphasize the necessity to optimize the surface charge of nanoparticles for efficient skin penetration. On one hand, highly negatively

charged particles could be hindered from entering skin due to the repulsive forces within skin tissue; and, on the other hand, too high positive charge could hinder the particles' diffusion within the skin due to attractive forces to the tissue. Alternatively, functionalization of AuNPs can be used as a penetration enhancement tool. For example, functionalization of AuNPs with the cell-penetrating peptides TAT and R₇ induced more pronounced skin penetration compared to their polyethylene glycol–functionalized counterpart [47].

In order to apply AuNPs to the skin surface or enhance their penetration ability, vehicles or formulation adjuvants can be employed. Their influence on penetration should be the core of more studies. Another aspect to be considered when studying the effect of vehicles, especially organic solvent, is their potential toxicological hazards when humans are exposed to nanoparticles combined with solvents in research or industry [48]. In this context, demonstrating the influence of toluene revealed a toxic effect on living tissue and hampering of the skin metabolism that was determined to be a disruption of cellular membranes and reduction of NADPH [48]. However, a minor enhancement of nanoparticle penetration was detected after skin preincubation with toluene [45]. The penetration improvement was attributed to the effect of toluene on weakening the lamellar lipid structure in the SC. However, its effect on the SC barrier function is weak, as ceramides, which are the main component of the SC lipids, were not extracted by toluene [52]. Thus, it is highly recommended to extend the research to more types of organic solvents. Moving to formulation adjuvants, AuNPs may be applied in another form rather than colloidal gold, for instance in the form of an oil-based formulation as introduced by the Niidome group where the oil phase and surfactant used in the formulation would contribute to facilitate AuNPs skin penetration, which was further enhanced by near-IR [8,9].

Skin Origin and Condition

In addition to physicochemical properties of AuNPs and formulation factors, skin model origin and integrity are important contributors regarding the extent and speed of nanoparticle skin penetration. Among skin models, human skin is considered as the gold standard for penetration studies [40,49,53,54]. However, the ethical and availability limitations of human skin for research encouraged researchers to identify alternatives. In this regard, mammalian skins were utilized. Despite their general structural similarity to human skin, interspecies variability in barrier integrity does play a role [47,54]. In literature, AuNPs skin penetration studies were conducted on porcine skin [7,53], which is a closely

related model to human skin, as well as on mouse [8,9,11,46,47] and rat [43] skin. But penetration results obtained from rodents' skin must be processed with caution not to misinterpret the data. AuNPs were found to penetrate in a higher amount and rate in mouse than human skin, as mouse skin is thinner and less compact [47]. Another significant difference between human and animal skin is the density of hair follicles, which could affect the deposition and penetration of nanoparticles.¹ Consequently, it is important to select an animal skin model with the lowest density of hair follicles, for instance by using hairless animal skin [46] or skin from newly born animals where hair follicles are still under development [47]. Importantly, in the latter condition, the decreased barrier function is a drawback to be considered.

Apart from the origin of the skin model, both skin viability and integrity have key roles in penetration studies. For instance, 12.6 nm AuNPs showed penetration in thawed human skin [44], whereas 10 nm AuNPs failed to penetrate freshly excised human skin [40]. On the other hand, for keeping the results reliable, the barrier integrity of the skin should be assured by, for instance, electrical resistivity [53], histological examination [47], or transepidermal water loss (TEWL) measurement [40,48]. Some studies have investigated the effect of skin integrity variation on AuNPs penetration, by weakening or removing the SC barrier. Abrasion of human skin was found to enhance the penetration of AuNPs, but interestingly no significant increase was observed concerning permeation [44]. In another study, skin-nonpenetrating 15-nm citrate-stabilized AuNPs in aqueous dispersion were applied to human skin samples of different barrier function integrity as follows: surface lipids were extracted with toluene, the total SC lipids were extracted with a methanol–chloroform mixture, and SC was completely removed by tape stripping [45]. It was found that removal of the SC lipids allowed for the penetration of AuNPs beyond the SC barrier, whereas the highest penetration was observed upon complete removal of the SC. This supports the idea that the process is governed by the whole complex structure of the SC, and intercellular lipids are not solely responsible to limit particle penetration. In another report, induction of mechanical damage to skin by pricking allowed the penetration of the previously nonpenetrating 247×22 nm gold nanorods into the dermis [55].

Extending the research scope to find more alternative penetration models to human skin has recently received interest [46,56–58]. In this context, reconstructed skin equivalents have been developed by culturing keratinocytes and fibroblasts. These were tested for AuNPs

penetration and compared to human skin data obtained at the same laboratory. Because of the lower compactness of the in vitro developed skin model, higher and faster penetration of AuNPs was observed when compared to human skin as expected. Although the model might be useful for faster screening of the potential penetration of nanoparticles, further experiments are required to establish a relationship to human skin data [56].

Finally, it is important to select the skin model that gives relevant data and answers the questions posed. In in vitro permeation studies on full-thickness skin, the dermis could act as a reservoir that interacts with macromolecules or nanoparticles, hindering their permeation [53]. In this context, Seto et al. have developed a pig skin model for testing the permeation of AuNPs for transdermal drug delivery purposes with the aid of combined mechanical and chemical penetration enhancers (ultrasound/sodium lauryl sulfate (SLS)). The model was a split-thickness skin (700 μm thick) that was prepared by removing much of the dermis. When it was compared to the full-thickness skin in an in vitro permeation study, it allowed for a larger amount of AuNPs to diffuse to the receiver solution, due to the reduced thickness of the dermal layer [53].

Experimental Variables and Experimental Configuration

Both AuNP concentration and incubation time with skin can affect the efficiency of the penetration process. Testing different concentrations and different time intervals of exposure, if possible, is necessary for a better understanding of the nanoparticles' penetration process. For instance, Filon et al. found that the permeation of 12.6 nm AuNPs through human skin is dose and time dependent, for doses of 15 and 45 $\mu\text{g}/\text{cm}^2$ and time intervals up to 24 h [44]. These findings were also supported for smaller particles; 6 nm dodecanethiol-coated AuNPs in toluene penetrated deeper in skin at a concentration of 437 compared to 90 $\mu\text{g}/\text{mL}$ [45]. Moreover, the higher concentration required a shorter exposure time of 2 h versus 6 h for the lower concentration to penetrate beyond the SC. Furthermore, increasing the exposure time from 0.5 to 24 h gradually increased the penetration into the SC and deeper skin layers for both of the tested concentrations [45].

In any event, a well-designed experimental setup is very important for reliable results. Regarding experimental setup, a Franz diffusion cell is a commonly used device for penetration and permeation studies [15,43–45,48,53,59–62]. However, it exposes the skin to excessive pressure and shear stress that may affect the

delicate skin alternatives [47,56]. Sometimes, another experimental configuration consisting of transwell plates is used, especially for less compact skin models such as mice skin [47] or skin equivalents [56]. Another important parameter is to preserve the condition and the integrity of the skin throughout the whole experimental time [47]. Typically, most *in vitro* permeation and penetration studies on human skin were terminated at 24 h [15,44,45,47,48,59,63–66], as this would be the maximum duration for which the skin maintains its structure. This time would vary for other skin models; for instance, the maximum time for newly born mouse skin to keep integrity was 6 h, as detected by histological examination [47].

Evaluation Methods (Quantification of Gold Nanoparticles Interactions and Imaging and Tracking of Their Penetration)

In AuNP skin permeation and penetration studies, gold could be detected in the receiver solution and the skin layers, respectively, by inductively coupled plasma spectroscopy (ICPS) [43,46,47,53]. In this technique, the mass content of elemental gold in nanoparticles is detected quantitatively [43,47,67]. Nevertheless, the permeated or the penetrated amount of gold may not represent the number of the diffused particles, considering the particles' size distribution [43]. For bio-distribution studies, different skin layers can be separated; for instance, SC by tape stripping, and the epidermis and dermis by heat separation, and then analyzed individually for the penetrated gold [44]. Another technique that would be used for detection of elemental gold is energy-dispersive X-ray spectroscopy (EDS) [43,55]. However, these techniques give no idea about the spatial distribution of the particles within the skin [47].

For imaging and spatial tracking of AuNPs within the skin, there are different microscopical techniques that rely on the specific properties of AuNPs; light scattering, absorption, and luminescence. For instance, TEM [43,44,47], scanning electron microscopy (SEM) [55], and scanning transmission X-ray microscopy (STXM) [55] have been utilized to detect AuNPs within different skin layers. However, these techniques are qualitative and just give an idea about nanoparticles' locations. Aspects to be taken into consideration for selecting the appropriate imaging techniques are the resolution and the ease of sample processing along with its influence on the tissue. In general, each imaging technique has pros and cons. For instance, TEM gives high resolution, but skin preparation is complicated and samples should be ultrathin [44,68] (90 nm thick [47]). A combination of more than one imaging technique would help to give

complementary results for a better understanding of the penetration process.

Another imaging technique that allows for scanning thicker skin samples noninvasively is MPM [47,69]. Herein, AuNPs are excited with two or more photons simultaneously with a wavelength in the infrared region. In response, AuNPs emit photoluminescence that is clearly distinguishable from that of its surrounding [69–71]. Imaging of AuNPs offers an advantage over other fluorophores of avoiding photobleaching [72]. However, their signal strength may be less than that of fluorescent dyes or quantum dots [26]. MPM can also be used in combination with fluorescence lifetime imaging (FLIM) for imaging of AuNPs and living tissue [40,48].

Although MPM is a promising optical tool for tracking AuNPs in the skin [56,69], it still suffers limitations with depth in biological tissues [73]. Accordingly, the complex dense structure of the skin causes absorption and scattering of the incident light and in turn attenuation of the AuNPs' signals with depth [69]. Moreover, the compactness of the tissue and presence of wrinkles govern the maximum detection depth. For instance, AuNPs were detected at variable depths from the skin surface (14–23 μm , 20–50 μm , and 20–100 μm in human skin and fixed and nonfixed reconstructed skin, respectively), due to the different degrees of tissue compactness. Furthermore, the presence of wrinkles would affect the accuracy of depth detection of AuNPs penetration, which sometimes is critical to detect whether particles penetrate deep enough in the SC or pass to the viable epidermis [69]. For imaging, another important parameter is the resolution to individually distinguish single particles. This can be detected by measurement of point spread function (PSF) [69]. However, there are still limitations with this method as PSF is diffraction limited and, consequently cannot distinguish the aggregation of very small particles below the detection limit. Hence, for the detection of separate individual particles, measuring the intensity of the emitted light from the spot image can be considered [74]. The suitability of this method for nanoparticles imaging in skin might be questionable. In general, to avoid imaging problems regarding penetration into tissues, examination of skin longitudinal sections, though invasive, is an option. Nevertheless, skin sectioning is prone to the introduction of artifacts, and a possible depth change of nanoparticles could happen. In this context, a useful protocol might be cutting the skin longitudinally when it is perpendicular to the cutting blade to avoid the vertical translocation of the nanoparticles between the different skin layers [47,75].

Using more than one technique for evaluation of nanoparticles' skin penetration is essential to get

confirmative results, especially with the very low concentrations of AuNPs penetrating skin. Furthermore, development of methods that would combine spatial and quantitative detection of AuNPs in the skin would be very beneficial for easier and more time-managed evaluation. In this regard, Labouta et al. have introduced a semiquantitative method for the detection of the weighed number of AuNPs penetrating different skin layers [75,76]. The method relies on the conjugated simultaneous transmission and multiphoton imaging of longitudinal sections of skin. MPM images were superimposed to transmission light images for detecting the SC-viable epidermis junction. Images were then analyzed for the pixel frequency of the luminescent particles in the respective skin layers. Furthermore, the total pixel frequency was summed from all skin sections, and the weighed number of particles was calculated based on the resolution-limited spot size of a single particle to obtain a measure for the particles number [76].

Skin Penetration Enhancers of Colloidal Gold

A number of skin penetration enhancement techniques have been adopted for the aim of deeper skin translocation of AuNPs, which could be a potential approach for transdermal delivery of molecules.

Chemical Penetration Enhancers

Different classes of chemical compounds are used currently for enhancing skin penetration of active substances with different contributing mechanisms [77–79]. A study investigating the effect of different chemical enhancers on AuNP penetration into skin was carried out [15]. The AuNPs used were hydrophilic and were proven earlier not to penetrate the skin [45], to exclude any interfering factor and investigate the bare effect of the studied enhancers. The enhancers tested were either (1) affecting the corneocytes' protein and hence the intracellular pathway (urea, SLS, polysorbate 80, and dimethyl sulfoxide (DMSO) up to 50%) or (2) inducing lipid disruption addressing the intercellular pathway (DMSO 80% and 100%). The influence of the different enhancers on the physical stability of the studied nanoparticles was also taken into consideration. It was found that the different chemical enhancers studied affect the aggregation state of AuNPs to varying extents. Both urea and SLS at 5% concentration resulted in high AuNP aggregation, and hence no AuNPs were observed to penetrate beyond the SC due to the strongly reduced concentration of single nanoparticles [15]. Moving to polysorbate 80, a limited amount of AuNPs reached the deep skin layers with a lesser extent of AuNPs aggregation observed. DMSO showed an increasing penetration pattern of AuNPs to deeper skin layers by

increasing DMSO concentration up to 80% [15]. The mechanism of penetration enhancement of DMSO is concentration dependent, where less than 60% affects protein conformation; however, when exceeding 60%, DMSO has an additional effect on the lipid structure [15,77,80]. It was found that the effect of increasing DMSO from 50% to 80% has a more pronounced effect on AuNPs' penetration in SC and deeper skin layers than raising the concentration from 20% to 50%. This suggests that the main barrier for AuNPs penetration is the intercellular pathway [15]. Finally, the selection of the ideal chemical enhancer depends on how much it would affect the physical properties of the applied AuNPs and the mechanism by which the enhancer operates.

Ultrasound

Low-frequency ultrasound waves are a known skin penetration enhancement technique that induces disruption of the SC lipids mainly by acoustic cavitation (ie, gaseous bubbles that induce pore formation) [81]. The use of ultrasound as a mechanical penetration enhancement approach was previously accompanied with chemical enhancers [82–84] for a postulated synergistic effect. A study conducted by Seto et al. demonstrated the effect of the simultaneous application of ultrasound and SLS on AuNP penetration through porcine skin models [53]. However, the main aim of the study was to establish a good skin model for studying the effect of the already established combination of penetration enhancers (ultrasound and SLS) for the aim of transdermal drug delivery, as discussed in Section "Skin Origin and Condition".

Thermal Ablation

For transdermal delivery of hydrophilic macromolecules, thermal ablation of SC seems like a promising technique. A research team led by Niidome has developed a surfactant–ovalbumin–gold nanorod complex (170.6 nm in size) formulated as solid-in-oil dispersion [9]. As hypothesized, gold nanorods along with the surfactant and the hydrophobicity of the oil phase could enhance the protein passage through the SC. However, skin penetration studies through shaved mice skin *in vitro* revealed low penetration ability of the complex to deep skin layers with high concentration in the SC. For further penetration enhancement, the system was combined with near-IR irradiation (6 W/cm², 20 min) that resulted in localized heating of gold nanorods and hence a thermal ablation of the SC and enhancement of ovalbumin penetration to a detected skin depth of 500 μ m. Furthermore, *in vivo* transcutaneous immunization in mice showed 2.4 times higher immune response (antibodies production) for the near-IR-irradiated complex compared to the complex without

near-IR radiation [9]. Similarly, an insulin-containing complex/near-IR radiation combination was tested in diabetic mice. After 10 h of keeping the patch containing the therapeutic complex on the dorsal skin of the mice, blood glucose level decreased to 15% for the complex/near-IR radiation compared to 60% for the nonirradiated complex [8]. For effective thermal ablation of the SC without side effects to the deeper skin layers, a study was conducted to compare between the effect of continuous-wave (CW) near-IR laser and pulsed near-IR laser of 920 nm wavelength on skin penetration of protein with the aid of gold nanorods. First, gold nanorods were applied to skin, followed by ovalbumin solution and then near-IR application. The results showed that both CW–near-IR and pulsed near-IR lasers enhanced ovalbumin skin penetration. Studying the effect of both lasers on skin revealed that CW–near-IR laser application in the presence of gold nanorods increased the skin temperature along with necrotic cell death and obvious histological changes, whereas no changes have been observed when pulsed near-IR light was applied. The contrast between the effect of both lasers is attributed to the temporal heating when using the pulsed laser affecting only the vicinity of the particles, compared to the tissue heating effect induced by the CW-laser, which causes protein denaturation and tissue damage as the heat is accumulating and cannot be dissipated fast enough [11]. Overall, gold nanorods and pulsed near-IR lasers are an interesting option to improve the delivery of peptides and proteins.

Iontophoresis

Iontophoresis is a physical technique that uses microelectric current to enhance the transport of charged moieties through the skin by electronic repulsion between similar charges (electromigration) and enforcing solvent to enter the SC (electro-osmosis) [77,85]. In this context, the use of anodal iontophoresis was envisaged to enhance the skin penetration of positively charged layer-by-layer polyelectrolyte-coated AuNPs loaded with imatinib mesylate (an anticancer agent in phase II clinical studies) for the treatment of melanoma. The *in vitro* study revealed that iontophoresis could significantly enhance skin permeation of imatinib mesylate–AuNPs compared to passive application, accompanied with a significant enhancement of the retained amounts in both SC and viable skin [7]. Enhancement of skin penetration and permeation achieved by iontophoresis was attributed to the increased pore size of the SC's hydrophilic channels in the presence of the electric current, along with the small particle size of AuNPs and their high positive charge density, which enhances their interactions with the negatively charged skin [7].

Dermaportation

The use of pulsed electromagnetic field could affect the SC integrity and enhance the translocation of molecules and particles through the skin, what is known as dermaportation [86,87]. A preliminary study was conducted on pulsed electromagnetic field–assisted skin penetration of AuNPs. Dermaportation was found to enhance the penetration of 10 nm AuNPs in SC and epidermis. The application of pulsed electromagnetic field enhanced AuNPs penetration by 200 times as observed by MPM–FLIM [87].

Dermabrasion

Dermabrasion is a well-known technique that is used for cosmetic purposes, where the surface layer of the skin is abraded. In addition, this technique can be used for absorption enhancement of drugs or nanoparticles through skin. In this regard, a study was conducted investigating the penetration and permeation of 12.6 nm AuNPs through intact and abraded skin. The results showed that permeation in both cases was not statistically different, though skin penetration was more pronounced in the case of abraded skin [44].

POTENTIAL MECHANISMS OF SKIN PENETRATION OF GOLD NANOPARTICLES

Studies on AuNP skin penetration were for the purpose of either biomedical applications, such as transdermal drug delivery, or mechanistic studies. As SC penetration is the crucial step for dermal applications of AuNPs, understanding the penetration mechanism would pave the way for the development of optimized nanomedicines. Nanoparticle penetration throughout the SC is potentially achievable through three pathways: the intercellular, intracellular, and transfollicular pathways [2,14]. Mechanistic studies were exploring the effect of different variables of known penetration enhancement mechanisms on the penetration behavior of AuNPs, and hence a better insight of the potential contributing mechanisms could be attained. When Labouta et al. examined different chemical penetration enhancers acting by different mechanisms on the penetration of the nonpenetrating citrate-stabilized AuNPs, they found that the enhancers acting on lipid disruption enhanced the penetration of the tested nanoparticles [15]. This would be in favor of the speculation that the intercellular pathway is the main pathway for nanoparticle penetration through the SC. Moreover, Huang et al. attributed the permeation of 5 nm polyvinylpyrrolidone-coated AuNPs through mouse skin to their interaction with the intercellular lipids

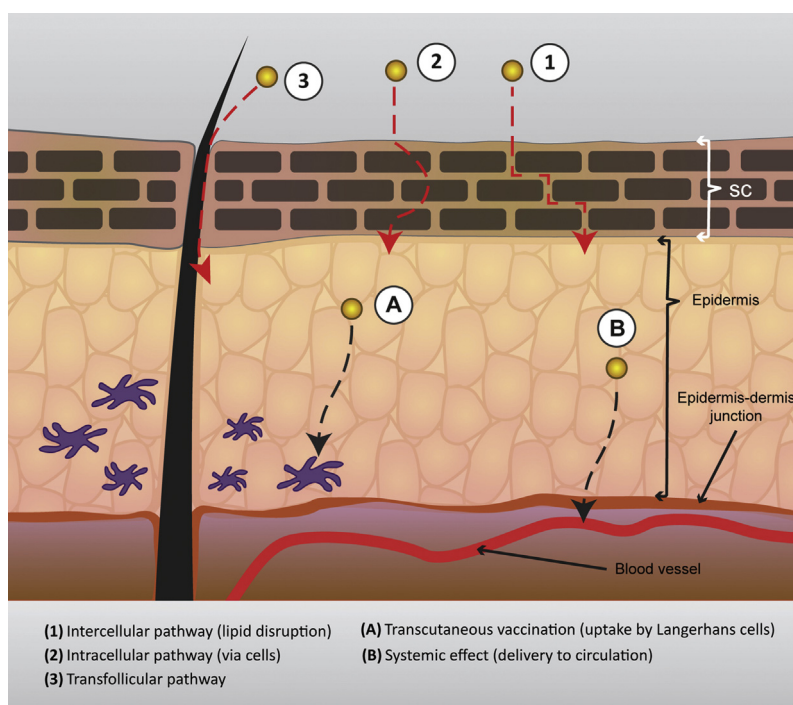


FIGURE 8.3 Illustration for the potential penetration pathways of AuNPs through the SC and their final targets in the viable deeper skin layers.

and the formation of transient reversible pores in the SC [10]. This idea can be also verified by reports on the ability of AuNPs to disrupt lipid bilayers [88,89]. When micrographs presented for AuNPs [43,46–48,75] or other particles [57,66,90,91] are analyzed, a spot-like penetration is observed. This is also an indication of the non-abundant penetration pathway that could be related to pores or induced pores [10]. Conversely, the intercellular pathway seems not to be the only contributor to the diffusion of AuNPs through the SC. The removal of the SC lipids enhanced the diffusion of AuNPs to deeper skin layers; nevertheless, a more pronounced influence on AuNP translocation was observed after the complete removal of the SC. This gives an impression that the penetration of AuNPs is controlled by the whole complex structure of the SC [45].

However, the intracellular pathway through the rigid corneocytes, which are actually dead cells filled with keratin and surrounded by an impermeable cornified envelope [14,42], is an unlikely pathway for nanoparticle diffusion. Functionalization of AuNPs with cell-penetrating peptides improved their penetration behavior, allowing to observe the nanoparticles inside the skin cellular compartments [47]. Generally, cell-penetrating peptides have the ability to enter cellular compartments by different mechanisms. Regarding skin, the situation would be different due to the nonviable nature of SC. The exact contributing mechanism for skin penetration enhancement is still unknown [92,93].

Alternatively, penetration through the transfollicular pathway is a particle size-controlled process, where hair movement is claimed to pump the particles into the hair follicle [94]. A report indicated a size range of 400–700 nm for deep diffusion (compared to smaller or larger particles) through porcine hair follicles, which are similar to human hair follicles in size ratio [95]. In contrast, another report showed that 40 nm particles can diffuse deep through the hair follicles of human skin rather than larger particles (eg, 750 nm and 1.5 μ m) [96]. In this regard, the contribution of this pathway to the penetration of AuNPs is debatable. Regardless, skin appendages are of limited area compared to the total human skin surface area [93], so their contribution to particles penetration will be limited.

For efficient development of skin nanotherapeutics, it is a prerequisite to overcome the SC to allow translocation to deeper skin layers. Passing through the SC and diffusing within the viable epidermis would finally allow nanoparticles aimed for drug delivery to reach their targets. They deliver their cargos to the Langerhans cells in the epidermis for the aim of transcutaneous immunization, or to the circulation through the capillaries located just below the epidermis. The detailed potential pathways of AuNPs through the SC and epidermis for the aim of transdermal drug delivery are shown in Fig. 8.3. However, passive diffusion through the skin layers forming different biological barriers is difficult. Even with successful penetrating systems, the

delivery of an optimized and reproducible dose is challenging. Generally, for nanoparticle skin penetration, it is not a necessity that the particles reach the deeper skin layer intact [93,97]. For instance, liposomes may decrease the barrier integrity of SC by fusion of phospholipids with the lipids of the SC, and hence facilitate the release and diffusion of the drug cargo to deeper skin layers [2,3,93]. For AuNPs, the situation is different since they are rigid, nondeformable inorganic particles of much smaller size than polymeric and lipid nanoparticles and consequently might react differently with the skin barrier. This would leave us with open questions regarding the penetration of AuNPs: is this related to their extremely small size (several nanometers), their presumed ability to alter the lipid bilayer structure, or other contributing mechanisms? To which extent can AuNPs penetrate intact human skin without any helping factors, and to what extent are the experimental setups relevant to a real situation of skin exposure to nanoparticles? Understanding the behavior of AuNPs within the skin could help to select the most suitable penetration enhancement approaches for the ultimate goal of effective topically applied nanotherapeutics.

FUTURE PERSPECTIVES AND RECOMMENDATIONS

As discussed in this chapter, nanoparticles' interaction with the skin barrier is controlled by multiple factors. The variability between different laboratories in terms of tested skin's origins, conditions or experimental configurations, and parameters could lead to contradictory results. For this reason, experimental results should be always accompanied with a full detailed description of the contributing factors. Moreover, the main goal of such experiments is to ensure and/or improve the health of humans whether by preventing hazards or developing drug delivery systems. Consequently, results of experiments, at which skin alternatives or skins of animals are used, would ideally be extrapolated to human data derived in the same laboratory. This in turn will help with the standardization of results and with judging the alternative experimental conditions and their appropriateness for the penetration studies. Furthermore, this will help to build up a database in each laboratory and hence lead to easier comparison between the results of experiments carried out in different laboratories under different conditions. Some parameters should be taken into account, for instance the maximum possible retention time of topical formulations on skin. Another important aspect that should be controlled during experiments is skin hydration. Excessive skin hydration, as in Franz diffusion cells, can hamper the integrity of the SC, and consequently

misleading higher penetration results might be obtained [44]. In setups allowing for less hydrated skin (eg, the Saarbrücken penetration model), no penetration (quantum dots: 3.5 nm) was observed [41].

Another important issue is the evaluation techniques for nanoparticles skin penetration. Imaging techniques comprise the main confirmative method for AuNP translocation in different skin layers. However, there are limitations in the currently used imaging techniques, either in depth monitoring or resolution issues, due to the complex structure of the skin. Consequently, validated skin alternatives for penetration should be developed, for instance skin equivalents from cultured skin cells. Nevertheless, results must still be processed with caution, especially when extrapolated to human data. Another strategy might be investigating the interaction of AuNPs with skin components individually, for instance examining the *in vitro* cellular uptake or the diffusion of the particles within SC lipids. Although the interaction with the complex skin tissue would rather differ, this strategy will help to exclude many distracting factors that arise from the skin complexity and will give a close view on how AuNPs interact with the skin components.

CONCLUSION

Gold nanoparticles are well known for their diverse biomedical applications in cancer treatment and drug delivery. Studies are conducted on AuNPs with the final aim of treatment of various diseases, even though their dermatological applications are challenging. Ideally, skin seems not to allow for substantial passive penetration of particles even if they are very small (<10 nm). The current chapter illustrated the recent integration of AuNPs with dermatology for treatment of local skin disorders, transcutaneous immunization, or transdermal drug delivery with the aid of penetration enhancers. Cracking the skin barrier transiently is the key step for the effectiveness of AuNP-based dermatological applications. Studying and manipulating the different factors that could enhance skin penetration will allow researchers to reveal the underlying mechanism not known today. Overall, because this is a recent field of research, many questions are not answered yet and more research efforts are still needed to get better insights into AuNPs' interactions with skin.

List of Acronyms and Abbreviations

Anti-EGFR Epidermal growth factor receptor antibody
AuNPs Gold nanoparticles
CW-NIR Continuous wave near-infrared
DMSO Dimethyl sulfoxide

EDS Energy-dispersive X-ray spectroscopy
FLIM Fluorescence lifetime imaging
ICPS Inductively coupled plasma spectroscopy
MPM Multiphoton microscopy
near-IR Near-infrared
PSF Point spread function
SC Stratum corneum
SEM Scanning electron microscopy
siRNA Small interfering ribonucleic acid
SLS Sodium lauryl sulfate
STXM Scanning transmission X-ray microscopy
TEM Transmission electron microscopy
TEWL Transepidermal water loss

Acknowledgments

We would like to thank the Ministry of Higher Education, Cultural Affairs and Missions Sector, Egypt, for financially supporting the current work.

Endnote

1. The area of the skin covered by hair follicles is typically only ~1%. Specific targeting of the follicles might allow for relatively higher penetration.

References

- [1] Giljohann DA, Seferos DS, Daniel WL, Massich MD, Patel PC, Mirkin CA. Gold nanoparticles for biology and medicine. *Angew Chem Int Ed Engl* 2010;49(19):3280–94.
- [2] Prow TW, Grice JE, Lin LL, Faye R, Butler M, Becker W, et al. Nanoparticles and microparticles for skin drug delivery. *Adv Drug Deliv Rev* 2011;63(6):470–91.
- [3] Cevc G, Vierl U. Nanotechnology and the transdermal route: a state of the art review and critical appraisal. *J Control Release* 2010;141(3):277–99.
- [4] McCormack DR, Bhattacharyya K, Kannan R, Katti K, Viator JA. Enhanced photoacoustic detection of melanoma cells using gold nanoparticles. *Lasers Surg Med* 2011;43(4):333–8.
- [5] Salas-García I, Fanjul-Vélez F, Ortega-Quijano N, Lavín-Castanedo A, Mingo-Ortega P, López-Escobar M, et al., editors. Effect of gold nanoparticles in the local heating of skin tumors induced by phototherapy. *Medical Laser Applications and Laser-Tissue Interactions V*. Munich: Optical Society of America; 2011.
- [6] R CS, Kumar J, R V, V M, Abraham A. Laser immunotherapy with gold nanorods causes selective killing of tumour cells. *Pharmacol Res* 2012;65(2):261–9.
- [7] Labala S, Mandapalli PK, Kurumaddali A, Venuganti VV. Layer-by-layer polymer coated gold nanoparticles for topical delivery of imatinib mesylate to treat melanoma. *Mol Pharm* 2015;12(3):878–88.
- [8] Nose K, Pissuwan D, Goto M, Katayama Y, Niidome T. Gold nanorods in an oil-base formulation for transdermal treatment of type 1 diabetes in mice. *Nanoscale* 2012;4(12):3776–80.
- [9] Pissuwan D, Nose K, Kurihara R, Kaneko K, Tahara Y, Kamiya N, et al. A solid-in-oil dispersion of gold nanorods can enhance transdermal protein delivery and skin vaccination. *Small* 2011;7(2):215–20.
- [10] Huang Y, Yu F, Park YS, Wang J, Shin MC, Chung HS, et al. Co-administration of protein drugs with gold nanoparticles to enable percutaneous delivery. *Biomaterials* 2010;31(34):9086–91.
- [11] Tang H, Kobayashi H, Niidome Y, Mori T, Katayama Y, Niidome T. CW/pulsed NIR irradiation of gold nanorods: effect on transdermal protein delivery mediated by photothermal ablation. *J Control Release* 2013;171(2):178–83.
- [12] Zheng D, Giljohann DA, Chen DL, Massich MD, Wang X-Q, Iordanov H, et al. Topical delivery of siRNA-based spherical nucleic acid nanoparticle conjugates for gene regulation. *Proc Natl Acad Sci USA* 2012;109(30):11975–80.
- [13] Roberts MS, Walters KA. Human skin morphology and dermal absorption. In: *Dermal absorption and toxicity assessment*. 2nd ed. 2007. p. 1–15.
- [14] Schneider M, Stracke F, Hansen S, Schaefer UF. Nanoparticles and their interactions with the dermal barrier. *Dermatoendocrinol* 2009;1(4):197–206.
- [15] Labouta HI, El-Khordagui LK, Schneider M. Could chemical enhancement of gold nanoparticle penetration be extrapolated from established approaches for drug permeation? *Skin Pharmacol Physiol* 2012;25(4):208–18.
- [16] Simoes MC, Sousa JJ, Pais AA. Skin cancer and new treatment perspectives: a review. *Cancer Lett* 2015;357(1):8–42.
- [17] Dianzani C, Zara GP, Maina G, Pettazzoni P, Pizzimenti S, Rossi F, et al. Drug delivery nanoparticles in skin cancers. *Biomed Res Int* 2014;2014:13.
- [18] Bertrand N, Wu J, Xu X, Kamaly N, Farokhzad OC. Cancer nanotechnology: the impact of passive and active targeting in the era of modern cancer biology. *Adv Drug Deliv Rev* 2014;66(0):2–25.
- [19] Qu X, Yao C, Wang J, Li Z, Zhang Z. Anti-CD30-targeted gold nanoparticles for photothermal therapy of L-428 Hodgkin's cell. *Int J Nanomedicine* 2012;7:6095–103.
- [20] Zhang Z, Jia J, Lai Y, Ma Y, Weng J, Sun L. Conjugating folic acid to gold nanoparticles through glutathione for targeting and detecting cancer cells. *Bioorg Med Chem* 2010;18(15):5528–34.
- [21] El-Sayed IH, Huang X, El-Sayed MA. Selective laser photothermal therapy of epithelial carcinoma using anti-EGFR antibody conjugated gold nanoparticles. *Cancer Lett* 2006;239(1):129–35.
- [22] Camerin M, Magaraggia M, Soncin M, Jori G, Moreno M, Chambrier I, et al. The in vivo efficacy of phthalocyanine-nanoparticle conjugates for the photodynamic therapy of amelanotic melanoma. *Eur J Cancer* 2010;46(10):1910–8.
- [23] Chen CC, Hsieh DS, Huang KJ, Chan YL, Hong PD, Yeh MK, et al. Improving anticancer efficacy of (-)-epigallocatechin-3-gallate gold nanoparticles in murine B16F10 melanoma cells. *Drug Des Devel Ther* 2014;8:459–74.
- [24] Puvanakrishnan P, Diagaradjane P, Kazmi SM, Dunn AK, Krishnan S, Tunnell JW. Narrow band imaging of squamous cell carcinoma tumors using topically delivered anti-EGFR antibody conjugated gold nanorods. *Lasers Surg Med* 2012;44(4):310–7.
- [25] Huang X, Jain PK, El-Sayed IH, El-Sayed MA. Gold nanoparticles: interesting optical properties and recent applications in cancer diagnostics and therapy. *Nanomedicine (Lond)* 2007;2(5):681–93.
- [26] Cai W, Gao T, Hong H, Sun J. Applications of gold nanoparticles in cancer nanotechnology. *Nanotechnol Sci Appl* 2008;2008(1):17–32.
- [27] Ren X, Yan T, Zhang Y, Wu D, Ma H, Li H, et al. Nanosheet Au/Co₃O₄-based ultrasensitive nonenzymatic immunosensor for melanoma adhesion molecule antigen. *Biosens Bioelectron* 2014;58:345–50.
- [28] Pornpattananangkul D, Olson S, Aryal S, Sartor M, Huang CM, Vecchio K, et al. Stimuli-responsive liposome fusion mediated by gold nanoparticles. *ACS Nano* 2010;4(4):1935–42.
- [29] Gao W, Hu C-MJ, Fang RH, Zhang L. Liposome-like nanostructures for drug delivery. *J Mater Chem B* 2013;1(48):6569–85.
- [30] Sinico C, Fadda AM. Vesicular carriers for dermal drug delivery. *Expert Opin Drug Deliv* 2009;6(8):813–25.

- [31] Karande P, Mitragotri S. Transcutaneous immunization: an overview of advantages, disease targets, vaccines, and delivery technologies. *Annu Rev Chem Biomol Eng* 2010;1(1):175–201.
- [32] Fathi-Azarbayjani A, Qun L, Chan YW, Chan SY. Novel vitamin and gold-loaded nanofiber facial mask for topical delivery. *AAPS PharmSciTech* 2010;11(3):1164–70.
- [33] Padamwar MN, Patole MS, Pokharkar VB. Chitosan-reduced gold nanoparticles: a novel carrier for the preparation of spray-dried liposomes for topical delivery. *J Liposome Res* 2011;21(4):324–32.
- [34] Borase HP, Patil CD, Salunkhe RB, Suryawanshi RK, Salunke BK, Patil SV. Phytolates synthesized gold nanoparticles as novel agent to enhance sun protection factor of commercial sunscreens. *Int J Cosmet Sci* 2014;36(6):571–8.
- [35] Leu JG, Chen SA, Chen HM, Wu WM, Hung CF, Yao YD, et al. The effects of gold nanoparticles in wound healing with antioxidant epigallocatechin gallate and alpha-lipoic acid. *Nanomedicine* 2012;8(5):767–75.
- [36] Chen SA, Chen HM, Yao YD, Hung CF, Tu CS, Liang YJ. Topical treatment with anti-oxidants and Au nanoparticles promote healing of diabetic wound through receptor for advance glycation end-products. *Eur J Pharm Sci* 2012;47(5):875–83.
- [37] Silveira PC, Venancio M, Souza PS, Victor EG, de Souza Notoya F, Paganini CS, et al. Iontophoresis with gold nanoparticles improves mitochondrial activity and oxidative stress markers of burn wounds. *Mater Sci Eng C Mater Biol Appl* 2014;44:380–5.
- [38] Kim JH, Hong CO, Koo YC, Choi HD, Lee KW. Anti-glycation effect of gold nanoparticles on collagen. *Biol Pharm Bull* 2012;35(2):260–4.
- [39] Campbell CSJ, Contreras-Rojas LR, Delgado-Charro MB, Guy RH. Objective assessment of nanoparticle disposition in mammalian skin after topical exposure. *J Control Release* 2012;162(1):201–7.
- [40] Liu DC, Raphael AP, Sundh D, Grice JE, Peter Soyer H, Roberts MS, et al. The human stratum corneum prevents small gold nanoparticle penetration and their potential toxic metabolic consequences. *J Nanomater* 2012;2012:8.
- [41] Gratieri T, Schaefer UF, Jing L, Gao M, Kostka KH, Lopez RFV, et al. Penetration of quantum dot particles through human skin. *J Biomed Nanotechnol* 2010;6(5):586–95.
- [42] Bouwstra JA, Gooris GS. The lipid organisation in human stratum corneum and model systems. *Open Dermatol J* 2010;4:10–3.
- [43] Sonavane G, Tomoda K, Sano A, Ohshima H, Terada H, Makino K. In vitro permeation of gold nanoparticles through rat skin and rat intestine: effect of particle size. *Colloids Surf B Biointerfaces* 2008;65(1):1–10.
- [44] Filon FL, Crosera M, Adami G, Bovenzi M, Rossi F, Maina G. Human skin penetration of gold nanoparticles through intact and damaged skin. *Nanotoxicol* 2011;5(4):493–501.
- [45] Labouta HI, El-Khordagui LK, Kraus T, Schneider M. Mechanism and determinants of nanoparticle penetration through human skin. *Nanoscale* 2011;3(12):4989–99.
- [46] Lee O, Jeong SH, Shin WU, Lee G, Oh C, Son SW. Influence of surface charge of gold nanorods on skin penetration. *Skin Res Technol* 2013;19(1):e390–6.
- [47] Fernandes R, Smyth NR, Muskens OL, Nitti S, Heuer-Jungemann A, Arden-Jones MR, et al. Interactions of skin with gold nanoparticles of different surface charge, shape, and functionality. *Small* 2015;11(6):713–21.
- [48] Labouta HI, Liu DC, Lin LL, Butler MK, Grice JE, Raphael AP, et al. Gold nanoparticle penetration and reduced metabolism in human skin by toluene. *Pharm Res* 2011;28(11):2931–44.
- [49] Labouta HI, Schneider M. Interaction of inorganic nanoparticles with the skin barrier: current status and critical review. *Nanomedicine* 2013;9(1):39–54.
- [50] Arnida, Janát-Amsbury MM, Ray A, Peterson CM, Ghandehari H. Geometry and surface characteristics of gold nanoparticles influence their biodistribution and uptake by macrophages. *Eur J Pharm Biopharm* 2011;77(3):417–23.
- [51] Daum N, Tscheka C, Neumeyer A, Schneider M. Novel approaches for drug delivery systems in nanomedicine: effects of particle design and shape. *Wiley Interdiscip Rev Nanomed Nanobiotechnol* 2012;4(1):52–65.
- [52] Reiter LV, Torres SMF, Wertz PW. Characterization and quantification of ceramides in the nonlesional skin of canine patients with atopic dermatitis compared with controls. *Vet Dermatol* 2009;20(4):260–6.
- [53] Seto JE, Polat BE, Lopez RF, Blankschtein D, Langer R. Effects of ultrasound and sodium lauryl sulfate on the transdermal delivery of hydrophilic permeants: comparative in vitro studies with full-thickness and split-thickness pig and human skin. *J Control Release* 2010;145(1):26–32.
- [54] Barbero AM, Frasch HF. Pig and guinea pig skin as surrogates for human in vitro penetration studies: a quantitative review. *Toxicol In Vitro* 2009;23(1):1–13.
- [55] Graf C, Nordmeyer D, Ahlberg S, Raabe J, Vogt A, Lademann J, et al., editors. Penetration of spherical and rod-like gold nanoparticles into intact and barrier-disrupted human skin. *Colloidal nanoparticles for biomedical applications X*; 2015.
- [56] Labouta HI, Thude S, Schneider M. Setup for investigating gold nanoparticle penetration through reconstructed skin and comparison to published human skin data. *J Biomed Opt* 2013;18(6):061218.
- [57] Jeong SH, Kim JH, Yi SM, Lee JP, Kim JH, Sohn KH, et al. Assessment of penetration of quantum dots through in vitro and in vivo human skin using the human skin equivalent model and the tape stripping method. *Biochem Biophys Res Commun* 2010;394(3):612–5.
- [58] Asbill C, Kim N, El-Kattan A, Creek K, Wertz P, Michniak B. Evaluation of a human bio-engineered skin equivalent for drug permeation studies. *Pharm Res* 2000;17(9):1092–7.
- [59] Marepally S, Boakye CHA, Shah PP, Etukala JR, Vemuri A, Singh M. Design, synthesis of novel lipids as chemical permeation enhancers and development of nanoparticle system for transdermal drug delivery. *PLoS One* 2013;8(12):e82581.
- [60] Bianco C, Adami G, Crosera M, Larese F, Casarin S, Castagnoli C, et al. Silver percutaneous absorption after exposure to silver nanoparticles: a comparison study of three human skin graft samples used for clinical applications. *Burns* 2014;40(7):1390–6.
- [61] Han SB, Kwon SS, Jeong YM, Yu ER, Park SN. Physical characterization and in vitro skin permeation of solid lipid nanoparticles for transdermal delivery of quercetin. *Int J Cosmet Sci* 2014;36(6):588–97.
- [62] Bikkad ML, Nathani AH, Mandlik SK, Shrotriya SN, Ranpise NS. Halobetasol propionate-loaded solid lipid nanoparticles (SLN) for skin targeting by topical delivery. *J Liposome Res* 2014;24(2):113–23.
- [63] Trauer S, Patzelt A, Otberg N, Knorr F, Rozycki C, Balizs G, et al. Permeation of topically applied caffeine through human skin – a comparison of in vivo and in vitro data. *Br J Clin Pharmacol* 2009;68(2):181–6.
- [64] Staronová K, Nielsen JB, Roursgaard M, Knudsen LE. Transport of SiO₂ nanoparticles through human skin. *Basic Clin Pharmacol Toxicol* 2012;111(2):142–4.
- [65] Brain KR, Walters KA, Green DM, Brain S, Loretz LJ, Sharma RK, et al. Percutaneous penetration of diethanolamine through human skin in vitro: application from cosmetic vehicles. *Food Chem Toxicol* 2005;43(5):681–90.
- [66] Baroli B, Ennas MG, Loffredo F, Isola M, Pinna R, Lopez-Quintela MA. Penetration of metallic nanoparticles in human full-thickness skin. *J Invest Dermatol* 2007;127(7):1701–12.
- [67] Fabricius A-L, Duester L, Meermann B, Ternes T. ICP-MS-based characterization of inorganic nanoparticles—sample preparation

- and off-line fractionation strategies. *Anal Bioanal Chem* 2014; 406(2):467–79.
- [68] Cheville NF, Stasko J. Techniques in electron microscopy of animal tissue. *Vet Pathol* 2014;51(1):28–41.
- [69] Labouta HI, Hampel M, Thude S, Reutlinger K, Kostka KH, Schneider M. Depth profiling of gold nanoparticles and characterization of point spread functions in reconstructed and human skin using multiphoton microscopy. *J Biophotonics* 2012;5(1):85–96.
- [70] Dowling MB, Li L, Park J, Kumi G, Nan A, Ghandehari H, et al. Multiphoton-absorption-induced-luminescence (MAIL) imaging of tumor-targeted gold nanoparticles. *Bioconjug Chem* 2010; 21(11):1968–77.
- [71] Farrer RA, Butterfield FL, Chen VW, Fourkas JT. Highly efficient multiphoton-absorption-induced luminescence from gold nanoparticles. *Nano Lett* 2005;5(6):1139–42.
- [72] He H, Xie C, Ren J. Nonbleaching fluorescence of gold nanoparticles and its applications in cancer cell imaging. *Anal Chem* 2008;80(15):5951–7.
- [73] Muriello PA, Dunn KW. Improving signal levels in intravital multiphoton microscopy using an objective correction collar. *Opt Commun* 2008;281(7):1806–12.
- [74] Li K, Schneider M. Quantitative evaluation and visualization of size effect on cellular uptake of gold nanoparticles by multiphoton imaging-UV/Vis spectroscopic analysis. *J Biomed Opt* 2014; 19(10):101505.
- [75] Labouta HI, Kraus T, El-Khordagui LK, Schneider M. Combined multiphoton imaging-pixel analysis for semiquantitation of skin penetration of gold nanoparticles. *Int J Pharm* 2011;413(1–2): 279–82.
- [76] Labouta HI, Schaefer UF, Schneider M. Laser scanning microscopy approach for semiquantitation of in vitro dermal particle penetration. *Methods Mol Biol* 2013;961:151–64.
- [77] Trommer H, Neubert RH. Overcoming the stratum corneum: the modulation of skin penetration. *Skin Pharmacol Physiol* 2006; 19(2):106–21.
- [78] Thong HY, Zhai H, Maibach HI. Percutaneous penetration enhancers: an overview. *Skin Pharmacol Physiol* 2007;20(6): 272–82.
- [79] Escobar-Chávez JJ, Rodríguez-Cruz IM, Domínguez-Delgado CL. Chemical and physical enhancers for transdermal drug delivery. In: Gallelli L, editor. *Pharmacology*; 2012.
- [80] Anigbogu ANC, Williams AC, Barry BW, Edwards HGM. Fourier transform Raman spectroscopy of interactions between the penetration enhancer dimethyl sulfoxide and human stratum corneum. *Int J Pharm* 1995;125(2):265–82.
- [81] Polat BE, Hart D, Langer R, Blankschtein D. Ultrasound-mediated transdermal drug delivery: mechanisms, scope, and emerging trends. *J Control Release* 2011;152(3):330–48.
- [82] Ueda H, Isshiki R, Ogihara M, Sugibayashi K, Morimoto Y. Combined effect of ultrasound and chemical enhancers on the skin permeation of aminopyrine. *Int J Pharm* 1996;143(1): 37–45.
- [83] Shetty PK, Suthar NA, Menon J, Deshpande PB, Avadhani K, Kulkarni RV, et al. Transdermal delivery of lercanidipine hydrochloride: effect of chemical enhancers and ultrasound. *Curr Drug Deliv* 2013;10(4):427–34.
- [84] Mitragotri S, Ray D, Farrell J, Tang H, Yu B, Kost J, et al. Synergistic effect of low-frequency ultrasound and sodium lauryl sulfate on transdermal transport. *J Pharm Sci* 2000;89(7):892–900.
- [85] Marro D, Kalia YN, Delgado-Charro MB, Guy RH. Contributions of electromigration and electroosmosis to iontophoretic drug delivery. *Pharm Res* 2001;18(12):1701–8.
- [86] Namjoshi S, Chen Y, Edwards J, Benson HAE. Enhanced transdermal delivery of a dipeptide by dermaporation. *Pept Sci* 2008;90(5):655–62.
- [87] Krishnan G, Edwards J, Chen Y, Benson HA. Enhanced skin permeation of naltrexone by pulsed electromagnetic fields in human skin in vitro. *J Pharm Sci* 2010;99(6):2724–31.
- [88] Lin J-Q, Zheng Y-G, Zhang H-W, Chen Z. A simulation study on nanoscale holes generated by gold nanoparticles on negative lipid bilayers. *Langmuir* 2011;27(13):8323–32.
- [89] Hou W-C, Moghadam BY, Corredor C, Westerhoff P, Posner JD. Distribution of functionalized gold nanoparticles between water and lipid bilayers as model cell membranes. *Environ Sci Technol* 2012;46(3):1869–76.
- [90] Larese FF, D'Agostin F, Crosera M, Adami G, Renzi N, Bovenzi M, et al. Human skin penetration of silver nanoparticles through intact and damaged skin. *Toxicology* 2009;255(1–2):33–7.
- [91] Ryman-Rasmussen JP, Riviere JE, Monteiro-Riviere NA. Penetration of intact skin by quantum dots with diverse physicochemical properties. *Toxicol Sci* 2006;91(1):159–65.
- [92] Nasrollahi SA, Taghibiglou C, Azizi E, Farboud ES. Cell-penetrating peptides as a novel transdermal drug delivery system. *Chem Biol Drug Des* 2012;80(5):639–46.
- [93] Desai P, Patlolla RR, Singh M. Interaction of nanoparticles and cell-penetrating peptides with skin for transdermal drug delivery. *Mol Membr Biol* 2010;27(7):247–59.
- [94] Lademann J, Knorr F, Richter H, Jung S, Meinke MC, Rühl E, et al. Hair follicles as a target structure for nanoparticles. *J Innov Opt Health Sci* 2015;8(4):1530004.
- [95] Patzelt A, Richter H, Knorr F, Schäfer U, Lehr C-M, Dähne L, et al. Selective follicular targeting by modification of the particle sizes. *J Control Release* 2011;150(1):45–8.
- [96] Vogt A, Combadiere B, Hadam S, Stieler KM, Lademann J, Schaefer H, et al. 40 nm, but not 750 or 1500 nm, nanoparticles enter epidermal CD1a+ cells after transcutaneous application on human skin. *J Invest Dermatol* 2006;126(6):1316–22.
- [97] Watkinson A, Bunge A, Hadgraft J, Lane M. Nanoparticles do not penetrate human skin—a theoretical perspective. *Pharm Res* 2013; 30(8):1943–6.

Formulation Effects on Topical Nanoparticle Penetration

H.A.E. Benson¹, Y. Mohammed², J.E. Grice², M.S. Roberts^{2,3}

¹Curtin University of Technology, Perth, WA, Australia; ²The University of Queensland School of Medicine - Translational Research Institute, Woolloongabba, QLD, Australia; ³University of South Australia, Adelaide, SA, Australia

OUTLINE

Nanoparticles and the Skin	115	Combination of Nanoparticles With Penetration Enhancers	124
Nanoformulations for the Skin	115	Nanoparticles for Targeted Delivery to the Hair Follicles and Sebaceous Glands	124
Flexible Nanoparticles and Nanovesicles	116	Conclusion	124
Metal Oxide Nanoparticles	120	References	124
Solid Lipid Nanoparticles	121		
Nanostructured Lipid Carriers	122		
Polymer-Based Nanoparticles	123		

NANOPARTICLES AND THE SKIN

Nanotechnology is a hot topic in science and is increasingly utilized in a wide variety of agricultural, industrial, and health applications. Consequently, nanoparticles (NPs) may come into contact with the skin by deliberate topical application, such as via a sunscreen product, or by accident through contact with nanotechnology-based industrial or agricultural products. As the primary protective organ of the body, the skin is well designed to prevent the penetration of materials deposited on its surface. Therefore, whereas significant advances in biomaterial engineering have and continue to facilitate nanotechnological applications for health diagnostics and therapeutics by other routes of administration, the skin has provided a much tougher challenge. Our understanding of the skin barrier, and the way in which materials interact with and penetrate

it, has developed rapidly over the past 40 years. Advanced analytical and visualization techniques [1] now provide information at the nanoscale and molecular levels; thus, scientists can evaluate the influence of formulation parameters on skin interaction and permeation. This chapter reviews the current knowledge of NP skin penetration and the formulation parameters that influence their penetration.

NANOFORMULATIONS FOR THE SKIN

Many colloidal systems are utilized for topical application to the skin (Fig. 9.1). These include liposomes, and vesicles composed of various materials that can confer elasticity and flexibility on the liposomal structure. Whereas conventional liposomes do not penetrate the stratum corneum barrier, flexible vesicles have been

shown to enhance skin permeation [2]. There remains considerable controversy about whether these flexible vesicles carry their payload intact into the skin or act due to their components' effects on occlusion, hydration, and enhanced solubility within the stratum corneum. Nanoemulsions composed of oils, aqueous vehicles, and emulsifiers that can be processed to generate a stable system of nanosized globules are increasingly popular in cosmetic formulations. For example, the NanoGel platform developed by Tri-K Industries (now Kemira Specialty) provides a simple production process for elegant nanoemulsion products that reduce transepidermal water loss (TEWL) and are well suited to a range of indications, such as sunscreens, antiaging products, and moisturizers. These emulsion and vesicle-based formulations are liquid, but there are a number of examples of solid and semisolid particle-based nanoformulations that are applied to the skin. Metal oxides such as zinc oxide and titanium dioxide are widely used in sunscreens. Solid lipid nanoparticles (SLNs) and nanostructured lipid carriers (NLCs) have received increasing attention for delivery of a range of compounds to the skin and hair follicles [3]. NPs composed of a range of polymers are

increasingly used in drug targeting following parenteral injection but have received limited attention for skin delivery. In a recent investigation of three nanocarrier systems based on nanoemulsion, SLNs, and NLCs with similar physicochemical properties, Schwarz et al. [4] suggested that all nanocarriers provided similar enhanced skin deposition. This chapter focuses on the formulation of NP-based delivery systems and their application to the skin. Table 9.1 provides a summary of representative studies on the influence of NPs on skin permeation.

FLEXIBLE NANOPARTICLES AND NANOVESICLES

Flexible NPs or vesicles were first described by Gregor Cevc (Idea, Munich) who termed them transfersomes [5]. Like conventional liposomes, they are composed of phospholipids, but also contain surfactant that acts as an "edge activator" to destabilize the lipid bilayers and increase deformability of the vesicle [6,7]. The formulation may also contain some ethanol. Cevc claimed that the flexibility conferred on the liposomes by the surfactant molecules allow transfersomes to "squeeze" through channels in the stratum corneum lipid lamellar regions. Other scientists contest this theory, believing that these vesicles do not carry their payload intact but, rather, it is the influence of the formulation components (the combination of surfactants, ethanol, and lipids) that interact with the stratum corneum to enhance skin permeation. Cevc originally utilized phosphatidylcholine in combination with the surfactant sodium cholate [8] for his transfersomes, but many other compositions of flexible nanovesicles have also been developed and evaluated. In general, phosphatidylcholine (soya, egg, or hydrogenated) is used as the lipid. Surfactants used include sodium cholate and deoxycholate, surfactant L-595 (sucrose laurate ester), PEG-8-L (octaoxyethylene laurate ester) [9,10], dipotassium glycyrrhizinate [11,12], Spans, and Tweens [13–15]. The cationic lipid 1,2-diethyl-3-triethylammonium-propane (DOTAP), in combination with Tween 20 nonionic surfactant, has been used to form positively charged flexible vesicles that are attracted to the negatively charged skin, thereby enhancing skin retention [15,16]. Geusens et al. [17,18] described the development of 57.7 nm flexible nanovesicles, termed *secosomes* (surfactant, ethanol, and cholesterol nanosomes), composed of DOTAP, cholesterol, sodium cholate, and 30% ethanol. They showed good loading capacity for small interfering RNA (siRNA), stability of the siRNA for at least 4 weeks, and transport through intact human skin in vitro. There is considerable opportunity to manipulate the composition of

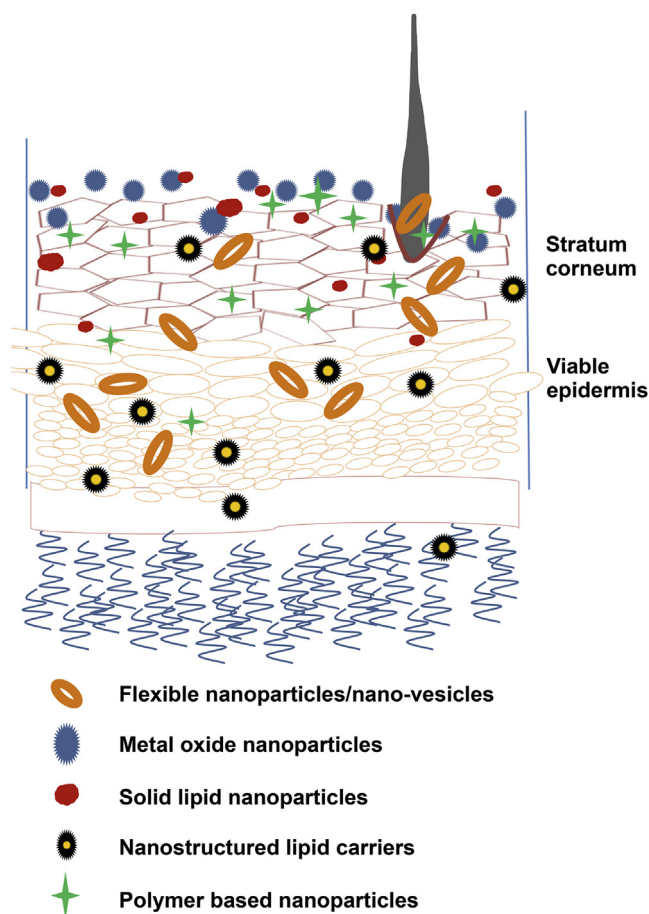


FIGURE 9.1 Penetration of various types of NPs into and across the skin. Figure drawn based on literature reports.

TABLE 9.1 Representative Studies of Nanoparticle Application to Skin

Nanoformulation type	Active/model compound	Formulation details	Experimental details	Key findings	References
Flexible nanoparticles, nanovesicles	Diclofenac	Transfersome; PC:sodium cholate (75:25) and 10% ethanol	Applied unoccluded to excised human epidermis	Diclofenac flux from transfersome: $4.8 \pm 3.2 \mu\text{g}/\text{cm}^2 \text{ h}$ (vesicle) compared to $2.3 \pm 2.2 \mu\text{g}/\text{cm}^2 \text{ h}$ from conventional liposome	[82]
	Estradiol	PC:sodium cholate (86:14) PC:Span 80 (86.7:13.3) PC:Tween (84.5:15.5) PC (conventional) (Includes 7% ethanol)	Applied unoccluded to excised human epidermis	Estradiol flux (max) increased by 18-, 16-, and 15-fold and skin deposition by 8-, 7-, and 8-fold compared with control	[13]
	siRNA	DOTAP, cholesterol, sodium cholate, and 30% ethanol (57.7 nm)	Applied unoccluded to excised human skin for 1 h followed by visualization with confocal microscopy and MPM	MPM–FLIM visualization within keratinocytes	[17,18]
	Diclofenac	PC containing a water-miscible penetration enhancer Transcutol; 10%, 20%, and 30% v/v	Applied unoccluded to excised newborn pig skin for 8 h. Tape strips, epidermis, dermis, and receptor solution analyzed.	Amount accumulated in skin ($\mu\text{g}/\text{cm}^2$) and (flux values $\mu\text{g}/\text{cm}^2 \text{ h}$) for Transcutol vesicles: 0%: $81, 1.2 \pm 0.6$ 10%: $128, 3.0 \pm 0.9$ 20%: $216, 7.7 \pm 0.9$ 30%: $215, 7.1 \pm 0.8$	[22]
Metal oxide nanoparticles	ZnO	Coated ($63 \pm 44 \text{ nm}$) and uncoated ($94 \pm 55 \text{ nm}$) ($\pm\text{SD}$) NP	In vivo application to human volunteers; MPM–FLIM real time	NPs remained in superficial SC layers and furrows	[30]
	ZnO and TiO_2	Microfine particles	In vitro pig skin; tape strips and receptor analysis	All particles removed in 5 tape strips	[27]
	ZnO	Zinclear spherical NP	In vitro human epidermis	Less than 0.03% of the applied zinc content penetrated the epidermis	[28]
	ZnO and TiO_2	20 nm TiO_2 and ZnO NPs in commercial products	In vivo application to human volunteers; biopsy	NP deposition limited to superficial SC even after 48 h with occlusion. No detectable deposition in viable epidermis	[40]
	ZnO		In vitro and in vivo human skin; analysis by MPM, SEM, and EXD	ZnO NPs detected in SC, skin folds, and hair follicles only	[25]

Continued

TABLE 9.1 Representative Studies of Nanoparticle Application to Skin—cont'd

Nanoformulation type	Active/model compound	Formulation details	Experimental details	Key findings	References
Solid lipid nanoparticles	Vitamin A (retinol)	Compritol (glyceryl behenate) SLNs in hydrogel; compared to nanoemulsion and o/w cream	In vitro application to pig skin; vitamin A extracted from skin after 6 and 24 h analyzed by HPLC	Vitamin A predominantly in outer 100 μm of skin: significantly greater amount from SLNs and nanoemulsion at 6 and 24 h, respectively	[44]
	Aconitine	Compritol (glyceryl behenate) SLNs in hydrogel; compared to nanoemulsion	In vitro application to excised rat skin	Aconitine skin deposition was higher and flux was lower from SLNs than from nanoemulsion ($p < .05$)	[46]
	Betamethasone 17-valerate	Monostearin SLNs (135.7 ± 15.1 nm) and beeswax SLNs (125.7 ± 11.8 nm) compared to commercial lotion	In vitro application to human epidermis from a single donor	Drug flux ($\mu\text{g}/\text{cm}^2$ h): Lotion: 0.64 ± 0.14 Monostearin: 0.16 ± 0.01 Beeswax: 0.40 ± 0.04 Deposition in the epidermis was: monostearin SLNs > lotion > beeswax SLNs	[52]
	Tocopheryl acetate	Labrafac (medium-chain acid triglycerides: 16.5%, w/w), Lipoid S-75 (soybean lecithin: 1.75%, w/w), and Solutol (mixture of free polyethylene glycol 660 and polyethylene glycol 660 hydroxystearate: 16.25%, w/w) mixture as SLNs (50.8 ± 0.5 nm)	In vitro application to pig skin for 24 h: analysis by skin stripping	Approximately 10% of the applied dose was recovered from the epidermis and dermis; viscosity of the formulation did not affect skin deposition	[53]
	pEGFP-C1 plasmid DNA	DOTAP, DOPE, Tween 20, and tricaprln (1:1:1:1.67, w/w) cationic SLNs (80.6 ± 7.9 nm)	In vivo application to Balb/c mouse skin for 24 h: expression of GFP mRNA was examined in the skin tissue and blood	Dose-dependent mRNA expression was detected in the skin and blood	[54]
	Retinyl palmitate	Gelucire 50/13 (glyceryl palmitostearate) and Precirol ATO5 (PEG-32 glyceryl stearate) SLNs with dicetyl phosphate for anionic surface charge	In vitro application to Sprague–Dawley rat skin for 12 h: analysis in skin and receptor; in vivo to hairless mice with wrinkle score assessment over 38 days	Retinyl palmitate predominately in upper 200 μg of skin; negative SLNs 4.8 \times neutral SLNs; dose-dependent wrinkle reduction: high-dose negative SLNs comparable to those of commercial product	[55]

Nanostructured lipid carriers	Coenzyme Q10	Cetyl palmitate, Labrafac Lipophile WL1349 (medium-chain triglycerides), and Tego Care 450 (polyglyceryl-3 methylglucose distearate) NLCs (151.7 nm)	In vitro application to Sprague–Dawley rat skin for 24 h: analysis of Q10 in receptor fluid and skin by HPLC; comparison with emulsion	Amount of Q10 accumulated in skin from NLCs was 10× emulsion; NLC compositions with range of viscosity did not alter skin accumulation. Skin “rinsed” with water prior to extraction of Q10: it is unclear how effectively this would remove a lipophilic formulation from the skin surface	[60]
	Flurbiprofen	Phosphatidylcholine, stearic acid, and coconut oil NLCs (214 ± 18 nm)	In vitro application to rat skin for 24 h followed by HPLC (skin shaved and wiped with alcohol prior to application); in vivo to Wistar rats with blood samples and carrageenan paw pain model over 24 h; comparison with commercial gel	In vitro data show 100% applied dose from commercial gel penetrated rat skin within 6 h compared to 80% penetration from NLCs in 24 h; in vivo reported Tmax 8 and 6 h, Cmax 34.18 ± 1.28 and 38.42 ± 1.37 µg/mL for commercial gel and NLCs, respectively; despite this, edema reduction was reported to be greater for NLCs up to 4 h, then similar up to 8 h	[62]
	Psoralens	Glyceryl palmitostearate and squalene, Poloxamer 188 (Pf), glyceryl stearate (g), Tween 80 (Tw), and phosphatidylcholine	In vitro application to nude mouse skin for 24 h, followed by HPLC (receptor solution 30% ethanol); comparison with suspension, SLN, and emulsion	Flux (nmol/cm ² /h) of 8-methoxypsoralen: Suspension: 60.48 ± 15.69 SLN: 67.17 ± 8.89 NLC-Pf: 96.71 ± 6.22 NLC-Tw: 107.51 ± 8.57 Emulsion: 38.31 ± 5.31	[66]
	Fluorescent dye, Spantide II, and ketoprofen	Range of formulations using phosphatidylcholine, caprylic/capric triglyceride, 1,2-dioleoylsn-glycero-3-((N-(5-amino-1-carboxypentyl) imidodiacetic acid) succinyl nickel salt), glyceryl behenate, glycerol distearate, monosterol, poloxamer, and Span 80 NLCs (140 ± 20 nm) with surface modified with cell-penetrating peptides (CPPs)	In vivo application of fluorescent dye to hairless rats with confocal Raman imaging; in vitro application to hairless rat skin for 24 h; receptor fluid and skin analyzed by HPLC	NLC–CPPs increased penetration of dye into the epidermis compared to NLCs in vivo and penetration of drugs in vitro. Number of arginines in CPPs affected penetration.	[70]
	Olanzapine and simvastatin	Tripalmitin, caprylic/capric triglyceride, propylene glycol dicaprylocaprate, oleic acid, and Tween 80 NLCs, with penetration enhancers terpenes and ethanol	In vitro application to newborn pig skin for 48 h with HPLC analysis of receptor fluid	Combination of NLCs with enhancers gave enhancement ratios for flux up to 60 compared to NLCs alone	[73]

nanovesicles to control the size, charge, and flexibility. An interesting formulation approach is the incorporation of chemicals known to be skin penetration enhancers, such as oleic acid and limonene, as the edge activators [19]. Manconi et al. [20–22] used soy lecithin or phosphatidylcholine as the vesicle base and varied the amounts of the penetration enhancers 2-(2-ethoxyethoxy)ethanol (Transcutol), capryl-caproyl macrogol 8-glyceride (Labrasol), propylene glycol, and cineole. These *penetration enhancer vesicles* (PEVs) showed increased delivery of tretinoin [23] and minoxidil [24] to the skin, with minimal transdermal delivery.

METAL OXIDE NANOPARTICLES

Zinc oxide nanoparticles (ZnO NPs) and titanium dioxide nanoparticles (TiO₂ NPs) act as effective physical ultraviolet A and B (UVA and UVB) filters [25] and are widely used in sunscreens to protect consumers from the deleterious effects of UV radiation [26]. The aim of these formulations is that they remain at or near the skin surface as there is no rationale for their permeation into the skin. Most published studies have examined the penetration of NPs into skin using in vitro animal models and excised tissue [27,28]. Recently, a number of studies have examined the penetration of topically applied ZnO NPs into in vivo human skin under “in-use” conditions using in vivo imaging [25,29,30]. Gulson et al. [31,32] applied ZnO highly enriched with ⁶⁸Zn to human volunteers and found small amounts of ⁶⁸Zn in blood and urine. This suggests that penetration occurred under the application conditions but provides no information as to whether the particles penetrated the skin or dissolved to release the ⁶⁸Zn that then penetrated and was detected. There is considerable debate surrounding the safe topical use of NPs in cosmetics and sunscreens due to concerns regarding their potential to overcome the stratum corneum barrier and diffuse into the viable epidermis to cause cellular toxicity. Toxic effects have been reported when ZnO NPs are incubated with viable cells in vitro, resulting in a loss of mitochondrial function, elevated reactive oxygen species production, and the induction of apoptosis and genotoxicity [33–35]. However, despite these observations in vitro, no toxicity has been reported following topical application of ZnO NP sunscreen products on in vivo human skin [30,36]. This would suggest that the stratum corneum provides an effective barrier to skin penetration of these NPs. The current literature regarding skin penetration and toxicity of sunscreen NPs has been reviewed in the chapter by Osmond-McLeod. Our focus is on the formulation effects that can influence the skin penetration and distribution of sunscreen NPs. Important formulation factors

are the NP size, the NP coating, and the vehicle in which the NPs are presented to the skin surface.

The small size and high specific surface area of NPs increase their reactivity and propensity to release free radicals when exposed to light [37,38]. A formulation strategy that has been used to reduce this reactivity is to coat the NPs with a silicone-based material. Examples of coated ZnO NPs used in sunscreen products are Z-Cote HP1 and Z-Cote Max (BASF), ZnO MDM (Symrise GmbH), and Zano 10 Plus (Umicore) [39]. Uncoated ZnO NPs are amphiphilic and preferentially incorporated into the water phase of an emulsion. In contrast, the silicone coating confers hydrophobicity to the NPs that are then predominately incorporated into the oil phase of an emulsion sunscreen product. This can also have the advantage of better retention of the NPs on the skin during sweating and general activity. Our group recently investigated the effect of the coating on ZnO NPs on their skin permeation in human volunteers [30]. Multiphoton tomography with fluorescence lifetime imaging microscopy (MPT–FLIM) permitted simultaneous assessment of the distribution of ZnO NPs and potential changes in NAD(P)H fluorescence characteristics within the viable epidermis. ZnO NPs (10%; mean diameter 63 and 94 nm coated and uncoated NPs, respectively) were incorporated into three formulations: a gel, oil-in-water (o/w) emulsion, and water-in-oil (w/o) emulsion. All formulations contained glycerol as a hydrating agent, the emulsions contained lanolin and caprylic acid–capric triglyceride, and the w/o emulsion also contained petrolatum and liquid paraffin. Thus, the degree of hydration and occlusion from the emulsions would be expected to be w/o > o/w > gel, although TEWL data showed little change in skin hydration from any formulation after 4 h of topical application. After 6 h of topical application, the ZnO NPs remained predominantly in the superficial layers of the stratum corneum and skin furrows, with no metabolic changes detected from ZnO NP permeation to the viable epidermis.

Filipe et al. [40] also reported only superficial skin localization of ZnO and TiO₂ NPs even after 48 h when applied topically in a range of formulations. The consensus based on in vitro [28,41] and in vivo [25,30,40] studies is that metal oxide NPs do not permeate beyond the superficial layers of the stratum corneum, regardless of their formulation. Indeed, Monteiro-Riviere et al. applied ZnO NP– and TiO₂ NP–containing sunscreen formulations to weanling pig skin that had been exposed to UVB to induce moderate sunburn [42]. Four sunscreen formulations were applied: 10% coated TiO₂ NPs in o/w lotion, TiO₂ NPs in w/o lotion, 5% coated ZnO NPs in o/w lotion, and 5% uncoated ZnO NPs in o/w lotion. The mean particle size was 200 and 140 nm for TiO₂ and ZnO NPs, respectively.

They reported slightly higher penetration in the sunburned skin overall, but even in this damaged skin the coated and uncoated ZnO NPs were localized to the upper one to two stratum corneum layers. TiO₂ NPs penetrated 13 layers of the stratum corneum in sunburn-damaged skin compared to seven layers in normal skin. The formulation was reported to affect skin penetration in damaged skin, with greater TiO₂ NP penetration from the w/o lotion. In all cases, there was no evidence of transdermal penetration despite the use of skin from weanling piglets, which is known to be more permeable than human skin.

SOLID LIPID NANOPARTICLES

SLNs (Nanopearls) are composed of lipids that are solid at room temperature with a surface covering of surfactant to stabilize them as a nanodisperser [3]. They are prepared by high-pressure homogenization and offer good solubility for hydrophobic actives such as vitamin A, vitamin E [43], and coenzyme Q10. This can facilitate the loading of these poorly water-soluble compounds within a gel or cream product. Traditionally, these hydrophobic compounds would be formulated in an ointment with poor aesthetic qualities and consumer acceptability; thus, SLN encapsulation offers the opportunity to formulate them in cosmetically elegant products. They also provide a significant advantage in protecting labile compounds to generate stable formulations. Retinol, a compound utilized in cosmetic and dermatological products, is prone to decomposition in the presence of light and oxygen. SLN formulation stabilizes the retinol, but the choice of lipid and surfactant influences the degree of stabilization [44,45]. SLNs also offer the potential for controlled delivery of actives to the skin. This was demonstrated by Zhang et al. [46], who showed a more sustained release of aconitine from SLNs compared with a microemulsion of similar sized vesicles (70–90 nm). Aconitine deposition in the stratum corneum was approximately 3.2-fold higher but flux across the skin lower for the SLN formulation. Using an NP tracking analysis, the authors determined that neither the SLNs nor microemulsion vesicles penetrated the rat skin to the receptor compartment intact.

When applied topically, SLN formulations form a film on the skin surface that combines with the skin lipid film to reduce water loss, increase skin hydration, and help to protect the barrier function of the stratum corneum. SLNs are reported to adhere effectively to the stratum corneum surface [47,48], thereby optimizing presentation of the applied compound to the skin, a property that could be particularly useful in sunscreen products where wash-off due to sweating and bathing can lead to unforeseen sunburn.

Thus, there are likely to be multiple mechanisms by which SLNs enhance skin permeation, including the prolonged contact with the skin surface and the occlusive nature of the SLN formulation hydrating the skin [49]. In addition, the interaction between formulation lipids with lipids in the stratum corneum bilayers will promote permeation of actives that are soluble in the SLN lipids. Küchler et al. [50] used scanning electron microscopy to show the loss of SLN platelet structure 2 h after administration on the surface of pig skin. They suggested that this occurred due to the interaction of the glycerol dibehenate SLN lipids with stratum corneum lipids in the stratum corneum of the pig skin. This mechanism was confirmed by differential scanning calorimetry (DSC) and Fourier transform infrared spectroscopy (FT-IR), which showed shifts of phase transition temperature and stretching bands due to the interaction between cetyl palmitate SLN lipids and stratum corneum lipids [51].

Given the mechanism of action of SLNs, it is clear that the formulation will influence their performance. First, the solubility of actives, and thus the loading capacity in the SLNs, will influence the amount of active deposited on the skin surface. It was this that drove the development of NLCs (discussed in the “[Nanostructured Lipid Carriers](#)” section), as the liquid lipid component of NLCs substantially increases their solubilization ability. Formulation in SLNs can also provide a controlled release from the NPs to localize delivery to the skin and prolong the duration of action. Zhang et al. [52] observed that prolonged and localized delivery of betamethasone 17-valerate could be achieved with monostearin SLNs. The permeation of the steroid through the skin was highly dependent on the lipid content of the SLNs, with other lipids such as beeswax showing no effect on in vitro human skin permeation.

NPs also alter the viscosity of a gel by facilitating association and cross-linking of the macromolecular chains in the gel matrix. Moddaresi et al. [53] assessed the interactions of tocopheryl acetate-loaded SLNs (<100 nm) with its hyaluronic acid (HA) gel vehicle and the effect on permeation in porcine skin. Gel viscosity was measured by cone and plate rheometer, and NP tracking analysis was used to monitor SLN mobility within the gels. They demonstrated a strong gel–SLN interaction that increased the viscoelasticity of the gel. Increasing the HA content increased the gel viscoelasticity and decreased SLN mobility within the gel. However, there was no significant difference in tocopheryl acetate permeation in the skin. The authors concluded that drug release from the SLN was the rate-limiting step in the permeation of a hydrophobic compound through the skin and not the SLN–vehicle–skin interactions.

Altering the lipid content of the SLNs can be used to manipulate their formulation properties, particularly their solubilization of encapsulated actives and particle size. In addition, surface modification can alter their interactions with vehicles and the skin, and enhance stability of these colloidal dispersions. The cationic phospholipids 1,2-dioleoyl-3-trimethylammonium-propane (DOTAP) and dioleoylphosphatidylethanolamine (DOPE) offer the opportunity of charge interaction to the negatively charged skin surface. Jin and Kim [54] formulated highly positively charged (51 mV) NPs (<100 nm) using DOTAP, DOPE, Tween 20 as surfactant, and tricaprins as a solid lipid core, encapsulating plasmid DNA. They showed enhanced *in vitro* permeation into mouse skin and expression levels of mRNA *in vivo* in mice after topical application.

In contrast, Jeon et al. [55] incorporated dicetyl phosphate to generate a negative charge on the surface of their SLNs with the aim of increasing the skin distribution of the retinyl palmitate payload. They reported increased penetration of retinyl palmitate into rat skin *in vitro* and reduced wrinkle formation in response to UV light in a mouse model, when compared to controls (including a commercial cosmetic product).

NANOSTRUCTURED LIPID CARRIERS

NLCs are mixtures of solid and fluid lipids, with the fluid lipid phase reported to be embedded into the solid lipid matrix [3] or localized at the surface of solid platelets and the surfactant layer [56]. They are generally prepared by a hot-melt homogenization technique. The spatial structure of the lipids allows greater drug loading and better stability compared to SLNs [57]. For example, Xia et al. [58] reported 70% loading capacity of sunscreen in NLCs compared to 10–15% in SLNs, thus offering the opportunity to develop skincare products with higher sun protection factors (SPFs). Yue et al. [59] reported increased fluorescence in rat skin following the topical administration of 60-nm-sized NLCs containing Nile Red to shaved areas of anesthetized rats when compared to an emulsion formulation. Chen et al. [60] incorporated coenzyme Q10 in NLCs composed of varied amounts of lipid and emulsifier. The optimized Q10-NLC formulation (particle size 151.7 ± 2.31) showed 10.11 times accumulation in rat epidermis *in vitro* compared to Q10 emulsion. In addition, the formulation provided a significant improvement in stability as the amount of Q10 in Q10-NLC decreased only 5.59% compared to decreases of 24.61% and 49.74% in, respectively, the Q10 emulsion and Q10-ethanol solution. The combination of NLCs and hydrogel vehicle also showed improved stability and skin delivery of coenzyme Q10 [61]. Kawadkar et al. [62]

reported increased stability, *in vitro* dermal delivery to rat skin (1.7-fold), and antiinflammatory effect in a carrageenan-induced rat paw edema model for flurbiprofen–NLC compared to a commercial gel. It should also be noted that much of the skin penetration evaluation of NLCs has been undertaken in rat skin, which is considerably more permeable than human skin. In addition, the skin treatment should also be considered. For example, Kawadkar et al. [62] shaved and washed the rat skin with isopropyl alcohol, which is likely to permeabilize the skin. Indeed, they reported 100% penetration of flurbiprofen from commercial gel through their treated rat skin in 6 h. There is no note of how they ensured skin integrity.

The mechanism of skin permeation enhancement reported for NLCs is similar to that of SLNs, namely occlusion and lipid mixing between the formulation and skin. The increased solubilization of the liquid lipid component allows for greater loading of the active in the NLCs and thus greater skin deposition. This improved skin deposition has been demonstrated for a number of compounds, including coenzyme Q10 [60,63], tacrolimus [64,65], and psoralen [66].

A number of different lipids and surfactants have been utilized in NLC formulations with different sizes and zeta potentials, but it is not possible to directly compare the formulation effects on skin permeation across studies due to the varied experimental models used. Increasing the liquid lipid content was shown to alter the zeta potential but not the particle size of NLCs in one study [67]. Increasing the content of medium-chain triglycerides led to increased skin deposition of Nile Red, which the authors suggested was due to improved occlusion.

Like SLNs, surface modification has been used for enhancing the delivery and targeting of NLCs to the skin. Of particular interest is the coupling of NLCs with cell-penetrating peptides, which is well established for targeting NPs following other routes of administration. Patlolla et al. [68] reported greater epidermal deposition of a fluorescent probe and the lipophilic drug celecoxib applied in transactivating transcriptional activator TAT-NLCs, compared to control NLCs, which were found mainly in the hair follicles following topical administration to *in vitro* rat skin. In a subsequent study, they increased celecoxib and changes in related inflammatory markers in skin monitored by microdialysis for the TAT-NLCs compared with control NLCs [69]. Shah et al. [70] investigated the effect of polyarginine chain length and number of arginines that provide optimized surface modification of NLCs (140 nm) for skin delivery of a payload of Spantide II and ketoprofen. Based on confocal imaging of rat skin and reduced inflammation in a mouse model, they concluded that surface modification of

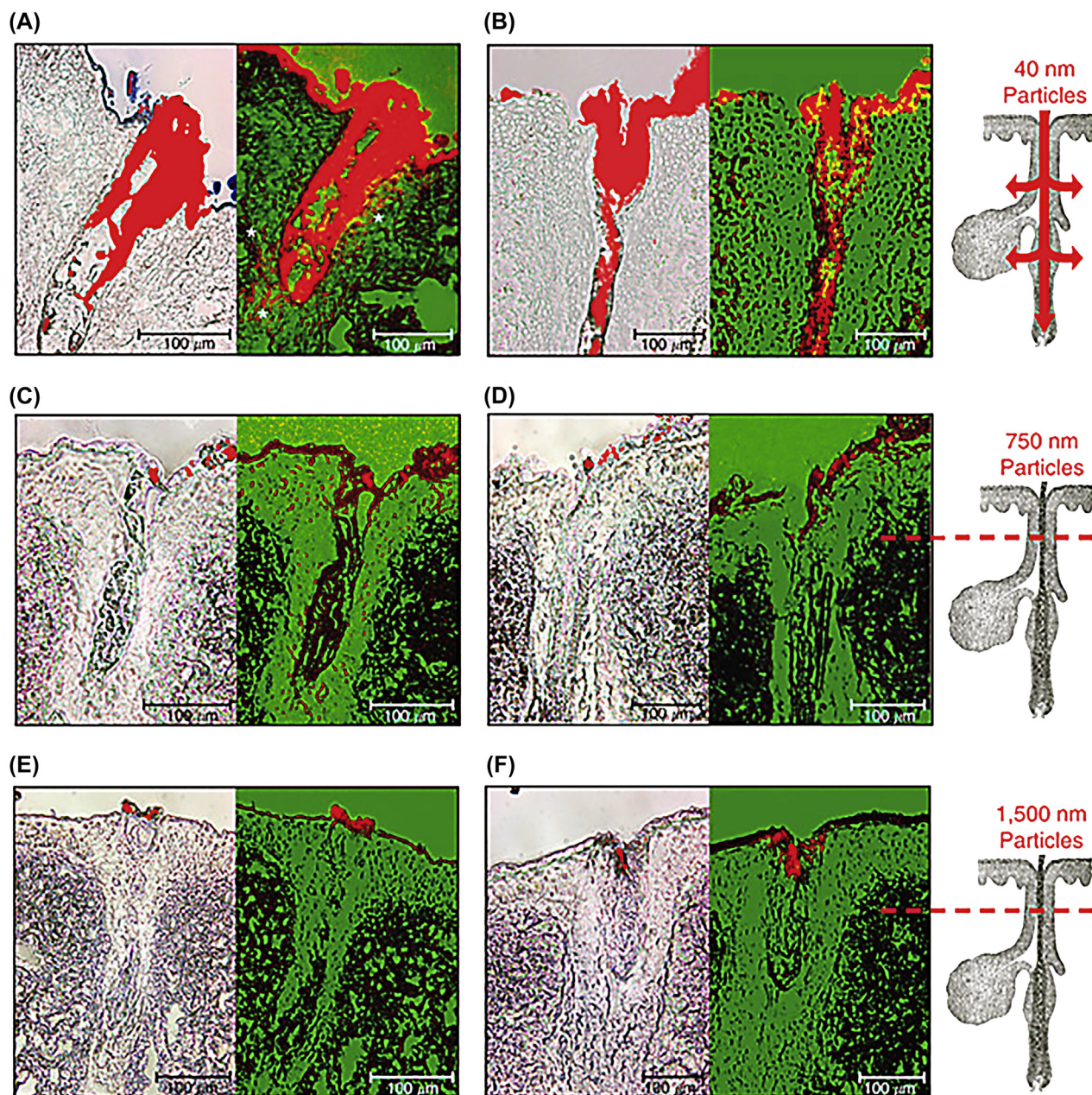


FIGURE 9.2 Penetration of variably sized NPs via the hair follicle. Laser scan microscopy was performed on skin samples treated with variably size particles. It was found that 40 nm particles (A and B) penetrated deep into hair follicles. In contrast, 750 nm particles (C and D) and 1500 nm particles (E and F) aggregated in the infundibulum. Reprinted from Vogt A, Combadiere B, Hadam S, Stieler KM, Lademann J, Schaefer H, et al. 40 nm, but not 750 or 1,500 nm, nanoparticles enter epidermal CD1a+ cells after transcutaneous application on human skin. *J Invest Dermatol* 2006;126: 1316–22, published by Nature Publishing Group, 2006.

the NLCs with a cell-penetrating peptide containing 11 arginines had significant permeation-enhancing ability compared to other polyarginines and TAT peptides.

POLYMER-BASED NANOPARTICLES

Polymer-based NPs are widely used in drug targeting via parenteral administration but have received limited

attention for application by topical administration to the skin. Shah [71] investigated the skin permeation of polymeric NPs composed of poly(lactic-co-glycolic acid) (PLGA) and chitosan, a common composition used for other routes of administration. Permeation of Spantide II and ketoprofen loaded in the NPs was assessed in dermatomed human skin in vitro, and response to ketoprofen monitored in a mouse model of allergic contact dermatitis. The NPs showed little enhanced delivery

compared to control. However, when the surface was modified by incorporation of oleic acid, skin permeation was deeper and skin retention increased significantly.

COMBINATION OF NANOPARTICLES WITH PENETRATION ENHANCERS

As the above study shows, there has been interest in the combination of NPs with penetration enhancers, both chemical and physical. Nonionic surfactants can be incorporated into liposomes and can act as penetration enhancers. As previously described, Manconi et al. showed that the skin deposition of both minoxidil [72] and tretinoin [23] was significantly enhanced by PEVs compared to application as conventional liposomes or penetration enhancer solutions. In both cases, permeation into and deposition within the skin was enhanced rather than transdermal delivery.

Vitorino et al. [73] investigated the combination of NLCs containing simvastatin and olanzapine with terpene penetration enhancers (menthol, limonene, and cineole) and ethanol in the applied vehicle. They found that all terpenes enhanced the permeation across pig skin of the drugs when combined with NLCs. The optimal combination of limonene + ethanol + NLCs provided an enhancement ratio of 60 and 64 for simvastatin and olanzapine, respectively, when compared with NLCs alone. Although beyond the scope of this chapter, the combination of NPs that offer enhanced stability to their drug payload but limited skin penetration, with a physical enhancer such as microneedles to generate transient pores in the epidermis, is a logical combination for many applications [74,75] but may not always add to the skin permeation of optimized formulations [76].

NANOPARTICLES FOR TARGETED DELIVERY TO THE HAIR FOLLICLES AND SEBACEOUS GLANDS

It is generally accepted that NPs with a size greater than 10 nm do not penetrate intact human skin to any great extent [77]. However, hair follicles and sebaceous glands offer routes of less resistance than the intact stratum corneum and thus are potential sites for NP deposition. This can offer a significant advantage for targeting conditions associated with the skin appendages, such as alopecia and acne [78–80].

Particle size is an important parameter in targeting hair follicles, with NPs of around 640 nm shown to provide optimal and deeper penetration when applied in combination with massage. Patzelt and Lademann [78]

provide an excellent review of the topic, summarizing the properties of particulate carriers that influence follicular deposition and the experimental models suitable for specifically monitoring transfollicular penetration. Particle size is the primary determinant for optimizing follicular deposition (Fig. 9.2), whereas other formulation parameters such as miscibility with sebum can be used to control drug release from the particulate carriers within the appendage.

CONCLUSION

Nanodelivery systems have been available for application to the skin for many years. Although there has been controversy regarding the safety of nanotechnology, there is little evidence to suggest there is a risk to health from topical application. Continued formulation development has generated a range of NP types and a variety of vehicles in which they are presented to the skin surface. Important NP formulation parameters include particle size, composition, and the presence of coatings. In addition, the way in which the vehicle components, particularly oils, surfactants, and alcohols, interact with the NPs and stratum corneum can influence the skin distribution and performance of the NPs. This is a complex area, but recent research is beginning to enhance our understanding of the ways in which formulation influences the interaction of NPs with the skin.

References

- [1] Lin LL, Nufer KL, Tomihara S, Prow TW. Non-invasive nanoparticle imaging technologies for cosmetic and skin care products. *Cosmetics* 2015;2:196–210.
- [2] Benson HA. Elastic liposomes for topical and transdermal drug delivery. *Curr Drug Deliv* 2009;6:217–26.
- [3] Muller RH, Radtke M, Wissing SA. Solid lipid nanoparticles (SLN) and nanostructured lipid carriers (NLC) in cosmetic and dermatological preparations. *Adv Drug Deliv Rev* 2002;54(Suppl. 1):S131–55.
- [4] Schwarz JC, Weixelbaum A, Pagitsch E, Low M, Resch GP, Valenta C. Nanocarriers for dermal drug delivery: influence of preparation method, carrier type and rheological properties. *Int J Pharm* 2012;437:83–8.
- [5] Cevc G, Blume G. Lipid vesicles penetrate into intact skin owing to the transdermal osmotic gradients and hydration force. *Biochim Biophys Acta* 1992;1104:226–32.
- [6] Bouwstra JA, De Graaff A, Groenink W, Honeywell L. Elastic vesicles: interaction with human skin and drug transport. *Cell Mol Biol Lett* 2002;7:222–3.
- [7] Honeywell-Nguyen PL, Gooris GS, Bouwstra JA. Quantitative assessment of the transport of elastic and rigid vesicle components and a model drug from these vesicle formulations into human skin in vivo. *J Invest Dermatol* 2004;123:902–10.
- [8] Cevc G. Transfersomes, liposomes and other lipid suspensions on the skin: permeation enhancement, vesicle penetration, and transdermal drug delivery. *Crit Rev Ther Drug Carrier Syst* 1996;13: 257–388.

- [9] van den Bergh BA, Bouwstra JA, Junginger HE, Wertz PW. Elasticity of vesicles affects hairless mouse skin structure and permeability. *J Control Rel* 1999;62:367–79.
- [10] van den Bergh BA, Vroom J, Gerritsen H, Junginger HE, Bouwstra JA. Interactions of elastic and rigid vesicles with human skin in vitro: electron microscopy and two-photon excitation microscopy. *Biochim Biophys Acta* 1999;1461:155–73.
- [11] Trotta M, Peira E, Debernardi F, Gallarate M. Elastic liposomes for skin delivery of dipotassium glycyrrhizinate. *Int J Pharm* 2002;241:319–27.
- [12] Trotta M, Peira E, Carloti ME, Gallarate M. Deformable liposomes for dermal administration of methotrexate. *Int J Pharm* 2004;270:119–25.
- [13] El Maghraby GM, Williams AC, Barry BW. Oestradiol skin delivery from ultradeformable liposomes: refinement of surfactant concentration. *Int J Pharm* 2000;196:63–74.
- [14] El Maghraby GM, Williams AC, Barry BW. Skin delivery of oestradiol from lipid vesicles: importance of liposome structure. *Int J Pharm* 2000;204:159–69.
- [15] Song YK, Kim CK. Topical delivery of low-molecular-weight heparin with surface-charged flexible liposomes. *Biomaterials* 2006;27:271–80.
- [16] Kirjavainen M, Urtti A, Jaaskelainen I, Suhonen TM, Paronen P, Valjakka-Koskela R, et al. Interaction of liposomes with human skin in vitro—the influence of lipid composition and structure. *Biochim Biophys Acta* 1996;1304:179–89.
- [17] Geusens B, Lambert J, De Smedt SC, Buyens K, Sanders NN, Van Gele M. Ultradeformable cationic liposomes for delivery of small interfering RNA (siRNA) into human primary melanocytes. *J Control Rel* 2009;133:214–20.
- [18] Geusens B, Van Gele M, Braat S, De Smedt SC, Stuart MC, Prow TW, et al. Flexible nanosomes (SECosomes) enable efficient siRNA delivery in cultured primary skin cells and in the viable epidermis of ex vivo human skin. *Adv Funct Mat* 2010;20:4077–90.
- [19] El Maghraby GM, Williams AC, Barry BW. Interactions of surfactants (edge activators) and skin penetration enhancers with liposomes. *Int J Pharm* 2004;276:143–61.
- [20] Mura S, Manconi M, Sinico C, Valenti D, Fadda AM. Penetration enhancer-containing vesicles (PEVs) as carriers for cutaneous delivery of minoxidil. *Int J Pharm* 2009;380:72–9.
- [21] Manconi M, Sinico C, Caddeo C, Vila AO, Valenti D, Fadda AM. Penetration enhancer containing vesicles as carriers for dermal delivery of tretinoin. *Int J Pharm* 2011;412:37–46.
- [22] Manconi M, Caddeo C, Sinico C, Valenti D, Mostallino MC, Lampis S, et al. Penetration enhancer-containing vesicles: composition dependence of structural features and skin penetration ability. *Eur J Pharm Biopharm* 2012;82:352–9.
- [23] Manconi M, Sinico C, Valenti D, Lai F, Fadda AM. Niosomes as carriers for tretinoin: III. A study into the in vitro cutaneous delivery of vesicle-incorporated tretinoin. *Int J Pharm* 2006;311:11–9.
- [24] Mura S, Manconi M, Fadda AM, Sala MC, Perricci J, Pini E, et al. Penetration enhancer-containing vesicles (PEVs) as carriers for cutaneous delivery of minoxidil: in vitro evaluation of drug permeation by infrared spectroscopy. *Pharm Dev Technol* 2013;18:1339–45.
- [25] Zvyagin AV, Zhao X, Gierden A, Sanchez W, Ross JA, Roberts MS. Imaging of zinc oxide nanoparticle penetration in human skin in vitro and in vivo. *J Biomed Opt* 2008;13:064031.
- [26] Maverakis E, Miyamura Y, Bowen MP, Correa G, Ono Y, Goodarzi H. Light, including ultraviolet. *J Autoimmun* 2010;34:J247–57.
- [27] Gamer AO, Leibold E, van Ravenzwaay B. The in vitro absorption of microfine zinc oxide and titanium dioxide through porcine skin. *Toxicol Vitro* 2006;20:301–7.
- [28] Cross SE, Innes B, Roberts MS, Tsuzuki T, Robertson TA, McCormick P. Human skin penetration of sunscreen nanoparticles: in-vitro assessment of a novel micronized zinc oxide formulation. *Skin Pharmacol Physiol* 2007;20:148–54.
- [29] Lin LL, Grice JE, Butler MK, Zvyagin AV, Becker W, Robertson TA, et al. Time-correlated single photon counting for simultaneous monitoring of zinc oxide nanoparticles and NAD(P)H in intact and barrier-disrupted volunteer skin. *Pharm Res* 2011;28:2920–30.
- [30] Leite-Silva VR, Le Lamer M, Sanchez WY, Liu DC, Sanchez WH, Morrow I, et al. The effect of formulation on the penetration of coated and uncoated zinc oxide nanoparticles into the viable epidermis of human skin in vivo. *Eur J Pharm Biopharm* 2013;84:297–308.
- [31] Gulson B, McCall M, Korsch M, Gomez L, Casey P, Oytam Y, et al. Small amounts of zinc from zinc oxide particles in sunscreens applied outdoors are absorbed through human skin. *Toxicol Sci* 2010;118:140–9.
- [32] Gulson B, Wong H, Korsch M, Gomez L, Casey P, McCall M, et al. Comparison of dermal absorption of zinc from different sunscreen formulations and differing UV exposure based on stable isotope tracing. *Sci Total Environ* 2012;420:313–8.
- [33] Chiang HM, Xia Q, Zou X, Wang C, Wang S, Miller BJ, et al. Nano-scale ZnO induces cytotoxicity and DNA damage in human cell lines and rat primary neuronal cells. *J Nanosci Nanotech* 2012;12:2126–35.
- [34] Kocbek P, Teskac K, Kreft ME, Kristl J. Toxicological aspects of long-term treatment of keratinocytes with ZnO and TiO₂ nanoparticles. *Small* 2010;6:1908–17.
- [35] Sharma V, Singh SK, Anderson D, Tobin DJ, Dhawan A. Zinc oxide nanoparticle induced genotoxicity in primary human epidermal keratinocytes. *J Nanosci Nanotechnol* 2011;11:3782–8.
- [36] Raphael AP, Sundh D, Grice JE, Roberts MS, Soyer HP, Prow TW. Zinc oxide nanoparticle removal from wounded human skin. *Nanomed* 2013;8:1751–61.
- [37] Oberdorster G, Maynard A, Donaldson K, Castranova V, Fitzpatrick J, Ausman K, et al. Principles for characterizing the potential human health effects from exposure to nanomaterials: elements of a screening strategy. Part I. *Fibre Toxicol* 2005;2:8.
- [38] Popov AP, Lademann J, Priezzhev AV, Myllylä R. Effect of size of TiO₂ nanoparticles embedded into stratum corneum on ultraviolet-A and ultraviolet-B sun-blocking properties of the skin. *J Biomed Opt* 2005;10:064037.
- [39] European Commission Scientific Committee on Consumer Safety (SCCS). Opinion on Zinc Oxide (nano form). 2012, 1489/12.
- [40] Filipe P, Silva JN, Silva R, Cirne de Castro JL, Marques Gomes M, Alves LC, et al. Stratum corneum is an effective barrier to TiO₂ and ZnO nanoparticle percutaneous absorption. *Skin Pharmacol Physiol* 2009;22:266–75.
- [41] Baroli B, Ennas MG, Loffredo F, Isola M, Pinna R, Lopez-Quintela MA. Penetration of metallic nanoparticles in human full-thickness skin. *J Invest Dermatol* 2007;127:1701–12.
- [42] Monteiro-Riviere NA, Wiensch K, Landsiedel R, Schulte S, Inman AO, Riviere JE. Safety evaluation of sunscreen formulations containing titanium dioxide and zinc oxide nanoparticles in UVB sunburned skin: an in vitro and in vivo study. *Toxicol Sci* 2011;123:264–80.
- [43] Dingler A, Blum RP, Niehus H, Muller RH, Gohla S. Solid lipid nanoparticles (SLN/Lipopearls)—a pharmaceutical and cosmetic carrier for the application of vitamin E in dermal products. *J Microencapsulation* 1999;16:751–67.
- [44] Jennings V, Gysler A, Schafer-Korting M, Gohla SH. Vitamin A loaded solid lipid nanoparticles for topical use: occlusive properties and drug targeting to the upper skin. *Eur J Pharm Biopharm* 2000;49:211–8.

- [45] Jennings V, Schafer-Korting M, Gohla S. Vitamin A-loaded solid lipid nanoparticles for topical use: drug release properties. *J Control Rel* 2000;66:115–26.
- [46] Zhang YT, Wu ZH, Zhang K, Zhao JH, Ye BN, Feng NP. An in vitro and in vivo comparison of solid and liquid-oil cores in transdermal aconitine nanocarriers. *J Pharm Sci* 2014;103:3602–10.
- [47] Kuntsche J, Bunjes H, Fahr A, Pappinen S, Ronkko S, Suhonen M, et al. Interaction of lipid nanoparticles with human epidermis and an organotypic cell culture model. *Int J Pharm* 2008;354:180–95.
- [48] Chen H, Chang X, Du D, Liu W, Liu J, Weng T, et al. Podophyllotoxin-loaded solid lipid nanoparticles for epidermal targeting. *J Control Rel* 2006;110:296–306.
- [49] Wissing SA, Muller RH. The influence of solid lipid nanoparticles on skin hydration and viscoelasticity—in vivo study. *Eur J Pharm Biopharm* 2003;56:67–72.
- [50] Kuchler S, Radowski MR, Blaschke T, Dathe M, Plendl J, Haag R, et al. Nanoparticles for skin penetration enhancement—a comparison of a dendritic core-multishell-nanotransporter and solid lipid nanoparticles. *Eur J Pharm Biopharm* 2009;71:243–50.
- [51] Khurana S, Bedi PM, Jain NK. Preparation and evaluation of solid lipid nanoparticles based nanogel for dermal delivery of meloxicam. *Chem Phys Lipids* 2013;175–176:65–72.
- [52] Zhang J, Smith E. Percutaneous permeation of betamethasone 17-valerate incorporated in lipid nanoparticles. *J Pharm Sci* 2011;100:896–903.
- [53] Moddarelli M, Brown MB, Zhao Y, Tamburic S, Jones SA. The role of vehicle-nanoparticle interactions in topical drug delivery. *Int J Pharm* 2010;400:176–82.
- [54] Jin SE, Kim CK. Charge-mediated topical delivery of plasmid DNA with cationic lipid nanoparticles to the skin. *Colloids Surf B Biointerfaces* 2014;116:582–90.
- [55] Jeon HS, Seo JE, Kim MS, Kang MH, Oh DH, Jeon SO, et al. A retinyl palmitate-loaded solid lipid nanoparticle system: effect of surface modification with dicetyl phosphate on skin permeation in vitro and anti-wrinkle effect in vivo. *Int J Pharm* 2013;452:311–20.
- [56] Jores K, Haberland A, Wartewig S, Mader K, Mehnert W. Solid lipid nanoparticles (SLN) and oil-loaded SLN studied by spectrofluorometry and Raman spectroscopy. *Pharm Res* 2005;22:1887–97.
- [57] Uner M. Preparation, characterization and physico-chemical properties of solid lipid nanoparticles (SLN) and nanostructured lipid carriers (NLC): their benefits as colloidal drug carrier systems. *Pharmazie* 2006;61:375–86.
- [58] Xia Q, Saupe A, Muller RH, Souto EB. Nanostructured lipid carriers as novel carrier for sunscreen formulations. *Int J Cosmet Sci* 2007;29:473–82.
- [59] Yue Y, Zhou H, Liu G, Li Y, Yan Z, Duan M. The advantages of a novel CoQ10 delivery system in skin photo-protection. *Int J Pharm* 2010;392:57–63.
- [60] Chen S, Liu W, Wan J, Cheng X, Gu C, Zhou H, et al. Preparation of coenzyme Q10 nanostructured lipid carriers for epidermal targeting with high-pressure microfluidics technique. *Drug Dev Ind Pharm* 2013;39:20–8.
- [61] Junyaprasert VB, Teeranachaideekul V, Souto EB, Boonme P, Muller RH. Q10-loaded NLC versus nanoemulsions: stability, rheology and in vitro skin permeation. *Int J Pharm* 2009;377:207–14.
- [62] Kawadkar J, Pathak A, Kishore R, Chauhan MK. Formulation, characterization and in vitro-in vivo evaluation of flurbiprofen-loaded nanostructured lipid carriers for transdermal delivery. *Drug Dev Ind Pharm* 2013;39:569–78.
- [63] Lohan SB, Bauersachs S, Ahlberg S, Baisaeng N, Keck CM, Muller RH, et al. Ultra-small lipid nanoparticles promote the penetration of coenzyme Q10 in skin cells and counteract oxidative stress. *Eur J Pharm Biopharm* 2015;89:201–7.
- [64] Pople PV, Singh KK. Development and evaluation of colloidal modified nanolipid carrier: application to topical delivery of tacrolimus. *Eur J Pharm Biopharm* 2011;79:82–94.
- [65] Pople PV, Singh KK. Development and evaluation of colloidal modified nanolipid carrier: application to topical delivery of tacrolimus, part II—in vivo assessment, drug targeting, efficacy, and safety in treatment for atopic dermatitis. *Eur J Pharm Biopharm* 2013;84:72–83.
- [66] Fang JY, Fang CL, Liu CH, Su YH. Lipid nanoparticles as vehicles for topical psoralen delivery: solid lipid nanoparticles (SLN) versus nanostructured lipid carriers (NLC). *Eur J Pharm Biopharm* 2008;70:633–40.
- [67] Teeranachaideekul V, Boonme P, Souto EB, Muller RH, Junyaprasert VB. Influence of oil content on physicochemical properties and skin distribution of Nile red-loaded NLC. *J Control Rel* 2008;128:134–41.
- [68] Patlolla RR, Desai PR, Belay K, Singh MS. Translocation of cell penetrating peptide engrafted nanoparticles across skin layers. *Biomaterials* 2010;31:5598–607.
- [69] Desai PR, Shah PP, Patlolla RR, Singh M. Dermal microdialysis technique to evaluate the trafficking of surface-modified lipid nanoparticles upon topical application. *Pharm Res* 2012;29:2587–600.
- [70] Shah PP, Desai PR, Channer D, Singh M. Enhanced skin permeation using polyarginine modified nanostructured lipid carriers. *J Control Rel* 2012;161:735–45.
- [71] Shah PP, Desai PR, Singh M. Effect of oleic acid modified polymeric bilayered nanoparticles on percutaneous delivery of spantide II and ketoprofen. *J Control Rel* 2012;158:336–45.
- [72] Mura S, Manconi M, Valenti D, Sinico C, Vila AO, Fadda AM. Transcutol containing vesicles for topical delivery of minoxidil. *J Drug Target* 2011;19:189–96.
- [73] Vitorino C, Almeida J, Goncalves LM, Almeida AJ, Sousa JJ, Pais AA. Co-encapsulating nanostructured lipid carriers for transdermal application: from experimental design to the molecular detail. *J Control Rel* 2013;167:301–14.
- [74] Gomaa YA, Garland MJ, McInnes FJ, Donnelly RF, El-Khordagui LK, Wilson CG. Microneedle/nanoencapsulation-mediated transdermal delivery: mechanistic insights. *Eur J Pharm Biopharm* 2014;86:145–55.
- [75] Donnelly RF, Morrow DI, Fay F, Scott CJ, Abdelghany S, Singh RR, et al. Microneedle-mediated intradermal nanoparticle delivery: potential for enhanced local administration of hydrophobic preformed photosensitisers. *Photodiagnosis Photodyn Ther* 2010;7:222–31.
- [76] Vitorino C, Almeida A, Sousa J, Lamarche I, Gobin P, Marchand S, et al. Passive and active strategies for transdermal delivery using co-encapsulating nanostructured lipid carriers: in vitro vs. in vivo studies. *Eur J Pharm Biopharm* 2014;86:133–44.
- [77] Baroli B. Penetration of nanoparticles and nanomaterials in the skin: fiction or reality? *J Pharm Sci* 2010;99:21–50.
- [78] Patzelt A, Lademann J. Drug delivery to hair follicles. *Expert Opin Drug Deliv* 2013;10:787–97.
- [79] Lademann J, Richter H, Meinke MC, Lange-Asschenfeldt B, Antoniou C, Mak WC, et al. Drug delivery with topically applied nanoparticles: science fiction or reality. *Skin Pharmacol Physiol* 2013;26:227–33.
- [80] Lademann J, Richter H, Schanzer S, Knorr F, Meinke M, Sterry W, et al. Penetration and storage of particles in human skin: perspectives and safety aspects. *Eur J Pharm Biopharm* 2011;77:465–8.
- [81] Vogt A, Combadiere B, Hadam S, Stieler KM, Lademann J, Schaefer H, et al. 40 nm, but not 750 or 1,500 nm, nanoparticles enter epidermal CD1a+ cells after transcutaneous application on human skin. *J Invest Dermatol* 2006;126:1316–22.
- [82] Boinpally RR, Zhou SL, Poondru S, Devraj G, Jasti BR. Lecithin vesicles for topical delivery of diclofenac. *Eur J Pharm Biopharm* 2003;56:389–92.

Nitric Oxide—Releasing Nanoparticles as an Antimicrobial Therapeutic

J. Rosen, A. Landriscina, J.D. Nosanchuk

Montefiore—Albert Einstein College of Medicine, Bronx, NY, United States

OUTLINE

Introduction	127	Nitric Oxide Releasing Nanoparticles as an Antifungal Agent	131
Nitric Oxide: Physical Characteristics and Physiological Role	128	Future Directions	132
Nitric Oxide Releasing Nanoparticles: Characteristics	128	Conclusion	133
Nitric Oxide Releasing Nanoparticles as an Antibacterial Agent	129	References	133

INTRODUCTION

The development of antimicrobial agents represents a definitive turning point in medicine. The development of antibiotics in the early 20th century and the subsequent growth of the antimicrobial armamentarium allowed for the treatment of previously incurable ailments and a sharp decline in morbidity and mortality. However, the pace of development of new antimicrobial drugs continues to lag behind microbial mutation rates, with multidrug resistant organisms reaching critical levels in both nosocomial and community settings. The current landscape of infectious disease calls for a new approach to antimicrobial therapy.

A promising solution to this challenge is nanotechnology, an approach that exploits the unique properties of substances at the nanoscale (1–100 nm). Nanotherapies tailored for antimicrobial treatment have shown promise in the treatment of several species of bacteria and fungi [1,2]. While a host of

nanoencapsulated drugs have shown promise as antimicrobials (traditional antibiotics, plant extracts), there has been considerable interest in harnessing the antimicrobial efficacy of endogenous substances [3,4]. By encapsulating endogenous molecules with inherent antimicrobial activity and low levels of resistance, we can mimic and augment the body's own immune mechanisms to provide both a fortified response to infection and minimal resistance potential.

One such molecule of interest is nitric oxide (NO). NO is a short-lived, diatomic, lipophilic gas with key functions in vascular modulation, cell cycle regulation, inflammation and immunity [1]. Its wide-ranging functionality has encouraged many attempts to harness this molecule for a variety of uses, though its utilization has been limited due to the lack of effective delivery vehicles [1,2]. This challenge has been overcome by the development of nanoparticle platforms that deliver sustained quantities of NO over time [20]. This chapter outlines the role of NO in combating infection and

recent advances in NO-releasing nanoparticle platforms (NO-np) as antimicrobial therapy.

NITRIC OXIDE: PHYSICAL CHARACTERISTICS AND PHYSIOLOGICAL ROLE

NO is an amphiphilic natural gas composed of a nitrogen and an oxygen atom linked by a double covalent bond. With its relatively small Stokes radius, NO is readily able to cross most cell membranes [5]. NO is synthesized from arginine in varying concentrations by three NO Synthase (NOS) enzymes: neuronal NOS, endothelial NOS, and inducible NOS (iNOS). Neuronal and endothelial NOS produce low fluxes ($<1\ \mu\text{M}$) of NO over short time periods [6,7]. At these low concentrations, NO interacts with soluble guanylyl cyclase (sGC) resulting in increases in cyclic guanosine monophosphate levels and protein kinase G activation. There are numerous downstream effects of these interactions including vasodilation, temperature modulation, and neurotransmission [8–10]. In contrast, iNOS produces high concentrations of NO ($>1\ \mu\text{M}$) in response to various stimuli (cytokines, bacterial polysaccharides, endotoxins, neuropeptides), resulting in nitrosation, nitration, and oxidation. Furthermore, iNOS is less susceptible to feedback inhibition than its counterparts, allowing for sustained synthesis of NO for defense against microbes. NO can also be produced independently from NOS via the conversion of nitrite ion to NO by nitrite reductase and nitrite anhydrase [11,12].

NO's antimicrobial action can be attributed to several mechanisms. The first is the formation of reactive nitrogen oxide intermediates (RNOS) such as peroxyxynitrite (OONO^-), nitrogen dioxide (NO_2), and dinitrogen trioxide (N_2O_3). These RNOS are formed by several mechanisms, most commonly through oxidation of NO by reactive oxygen species [5]. RNOS have several effects on microbial cells, including DNA deamination and double strand breaks, enzyme inactivation, and interference of signal transduction [13–16].

All of these characteristics make NO ideally suited as an antimicrobial therapy. However, several factors have made the delivery of NO challenging. As a gas, NO is very difficult to handle, requiring complete exclusion from oxygen to prevent oxidation to the cytotoxic NO_2 , though this gaseous form is still used for the treatment of persistent pulmonary hypertension in certain clinical settings [17]. Furthermore, NO has a short half-life, easily diffuses down its concentration gradient from the site of production, and is readily scavenged in most physiologic conditions. Hence, the sustained delivery of appropriate concentrations to tissue is highly problematic.

NITRIC OXIDE RELEASING NANOPARTICLES: CHARACTERISTICS

The development of an NO-releasing nanoparticle platform provides a solution for the challenges mentioned earlier. The delivery of NO using nanomaterials can be achieved either by the use of NO-donating substances such as s-nitrosothiols or NONOates or by the delivery of substances that can then be converted into NO. The majority of these platforms have relied on the sol–gel technique for synthesis of nanoparticles [18]. This technique uses metal or inorganic compounds, water, and an alcoholic solvent as its raw materials. Such solutions are then hydrolyzed with an acidic or basic catalyst to form Si-OH groups. Upon condensation, Si-O-Si is formed. These bonds result in a lattice, which forms the skeleton of the nanoparticles. This substance takes the form of a gel. The final product, nanoscaled particles, is formed after removal of the solvent via drying. A variety of substances such as antibiotics, chemotherapeutics, and endogenously produced molecules can be added to the solvent for encapsulation. Furthermore, the addition of reagents such as polyethylene glycol (PEG) and chitosan allows for control over release via alterations in pore size as well as enhances its microbial efficacy and targeting.

Shin et al. described a sol–gel-based platform for complexing N-diazeniumdiolate (an NO-donating molecule) within silica nanoparticles (Fig. 10.1A). The NO-releasing silica nanoparticles have been characterized and exhibit a variety of nanoscale sizes (ranging from 20 to 500 nm in diameter), release characteristics (maximum release ranging from 10 to 5500 ppb/mg) and half-lives (0.1–12 h) [19]. In contrast, another platform, developed by our group, relies on the encapsulation of nitrite that is thermally reduced to NO by electrons from included sugars, resulting in a slow and sustained release of nitric oxide (Fig. 10.1B) [20]. These NO-np are appropriately nanoscaled (10 nm in an anhydrous environment, 130 nm upon aggregation), and release NO in a sustained fashion over 24 h when dispersed in an aqueous solution (Fig. 10.2) [20]. These NO-np showed minimal toxicity to fibroblasts in culture and upon IV administration in a hamster model [21]. Several metal-based NO-np have also been described [22–24]. These platforms release large quantities of NO and have additional benefits such as added heat stability and photodelivery of NO. While the antimicrobial efficacy of other metal-containing nanoplateforms has been shown, there is no data relating to metal-containing NO-np for antimicrobial therapy [25]. Additionally, the use of metal-based NO-np is limited due to lack of toxicity data and considerable cost of metals such as gold and platinum.

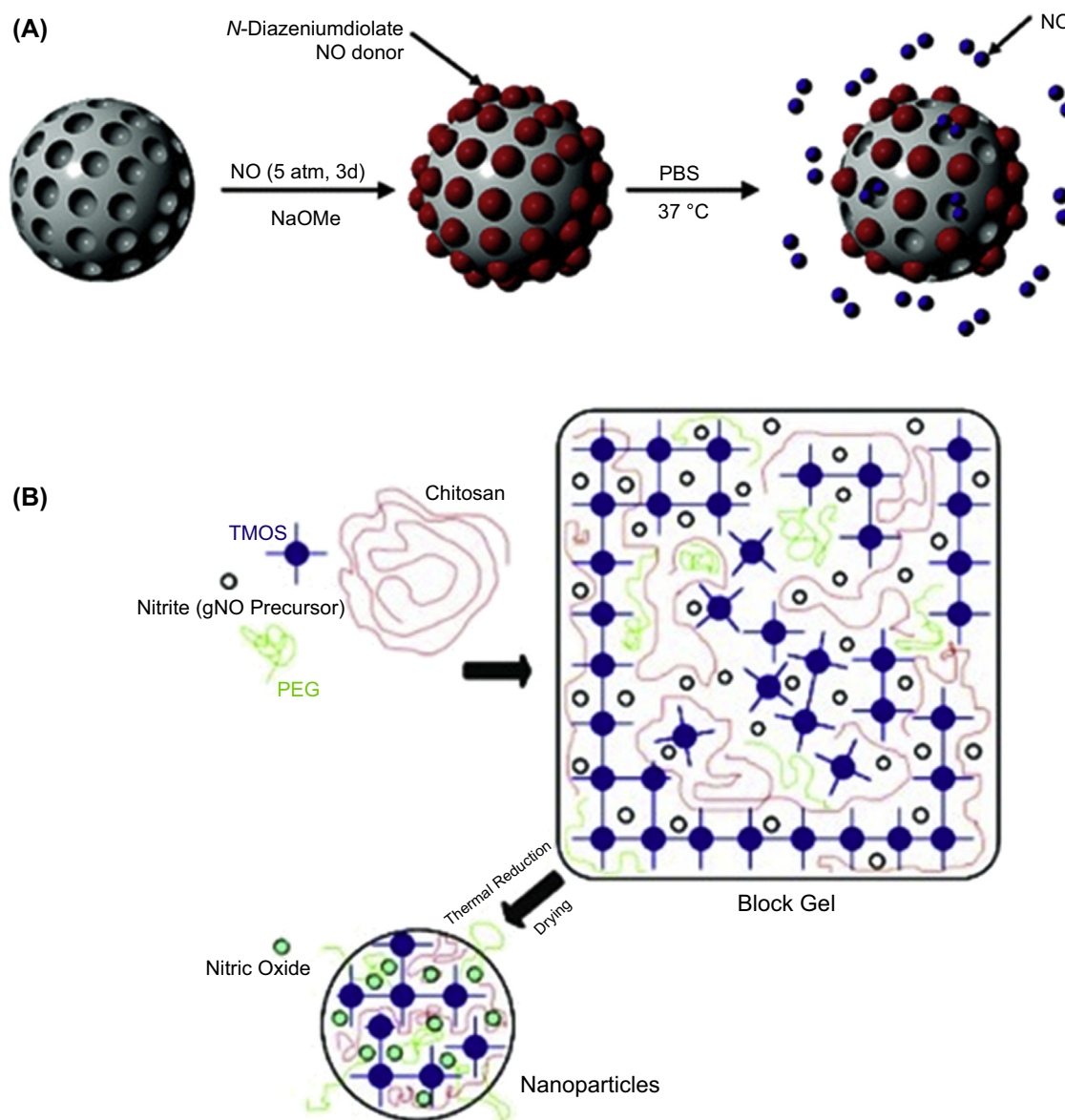


FIGURE 10.1 Nitric oxide releasing sol-gel nanoplateforms. (A) Synthesis of N-diazeniumdiolate-modified silica nanoparticles. (Reprinted from Shin JH, Metzger SK, Schoenfisch MH. Synthesis of nitric oxide-releasing silica nanoparticles. *J Am Chem Soc* 2007;129(15):4612–9, with permission from ACS Publishing.) (B) Schematic of nitrite-containing nitrogen dioxide-releasing nanoparticle platform synthesis. Abbreviations as follows: TMOS (tetramethoxysilane) and PEG (polyethylene glycol). (Reprinted from Schairer DO, Chouake JS, Nosanchuk JD, Friedman AJ. The potential of nitric oxide releasing therapies as antimicrobial agents. *Virulence* 2012;3(3):271–9, under the Creative Commons Attribution Noncommercial License.)

These nanoparticulate platforms have a variety of unique properties that make them an attractive candidate for antimicrobial therapy. The majority are inexpensive, easy to produce, and nontoxic [21]. Their customizability allows for the creation of drugs tailored to specific disease processes. They also allow for sustained release of the drug over time, with the potential to avoid complicated dosing schedules. Furthermore, they allow for the use of unstable molecules like NO. The potential for NO-np as an antimicrobial has been demonstrated through multiple studies, which are outlined later in this chapter.

NITRIC OXIDE RELEASING NANOPARTICLES AS AN ANTIBACTERIAL AGENT

NO-np have shown efficacy in the treatment of a variety of microbes. To date, NO-np have shown significant antimicrobial activity against both gram-positive and gram-negative bacteria, including strains resistant to traditional antibiotics. Nanomaterials incorporating NO-donating molecules have been shown effective against *Staphylococcus aureus*, *Staphylococcus epidermidis*, *Pseudomonas aeruginosa*, and *Escherichia coli*, inhibiting

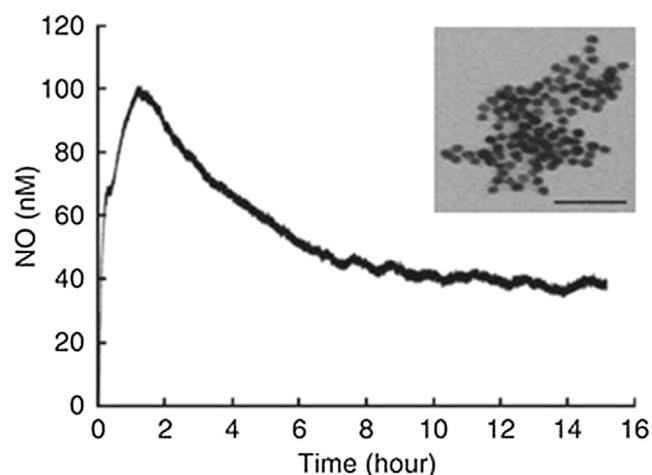


FIGURE 10.2 Characterization of nitrite-containing nitrogen dioxide-releasing nanoparticle platform (NO-np). Amperometric analysis revealed sustained release of NO from NO-np over time. Inset transmission electron microscopy shows 10 nm diameter of NO-np. Scale bar = 100 nm. Reprinted from Martinez LR, Han G, Chacko M, Mihi MR, Jacobson M, Gialanella P, et al. Antimicrobial and healing efficacy of sustained release nitric oxide nanoparticles against *Staphylococcus aureus* skin infection. *J Invest Dermatol* 2009;129(10):2463–9, with permission from Nature Publishing Group.

both growth and biofilm formation in vitro [26,27]. NO-np utilizing encapsulated nitrite have been shown effective against a variety of gram-positive (*S. aureus*, *Streptococcus pyogenes*, and *Enterococcus faecalis*) and gram-negative bacteria (*E. coli*, *P. aeruginosa*, *Klebsiella pneumoniae*, and *Acinetobacter baumannii*) in a dose-dependent manner [1,28–31]. A combined approach of forming NO donors using NO-np and glutathione

(GSH), which forms s-nitrosoglutathione (GSNO) in the presence of NO, resulted in even greater efficacy against several bacterial species [32]. This approach was found to provide sustained GSNO over 24 h, and was more effective than GSH, GSNO, or NO-np alone. A similar result was seen using s-nitrosocaptopril nanoparticles (SNO-CAP-np) in the presence of GSH [33]. SNO-CAP-np + GSH demonstrated sustained GSNO production as well as increased antimicrobial activity against *E. coli* and methicillin-resistant *S. aureus* (MRSA) in a dose-dependent fashion.

The strong in vitro data led to in vivo studies assessing the application of NO-releasing nanoplateforms in the setting of bacterial infections. Han et al. investigated the susceptibility of MRSA to NO-np both in vitro and in vivo [28]. NO-np significantly reduced bacterial growth compared to both untreated control and control (empty) nanoparticles (control-np). In a murine subcutaneous abscess model, intradermal and topical administration of NO-np resulted in a decreased microbial burden and abscess area (Fig. 10.3) as well as preservation of skin architecture (minimized collagen degradation) as visualized by histological analysis. Furthermore, NO-np treatment altered the cytokine milieu of the abscess, resulting in a more favorable molecular profile to fight infection. Treatment with NO-np was also shown to have antiangiogenic effects in abscesses, a mechanism that may prevent systemic dissemination of infection. Martinez et al. expanded on these results by demonstrating NO-np's efficacy against MRSA in vitro (Fig. 10.4) and in the setting of a superficial skin infection, again with a significant decrease in bacterial burden,

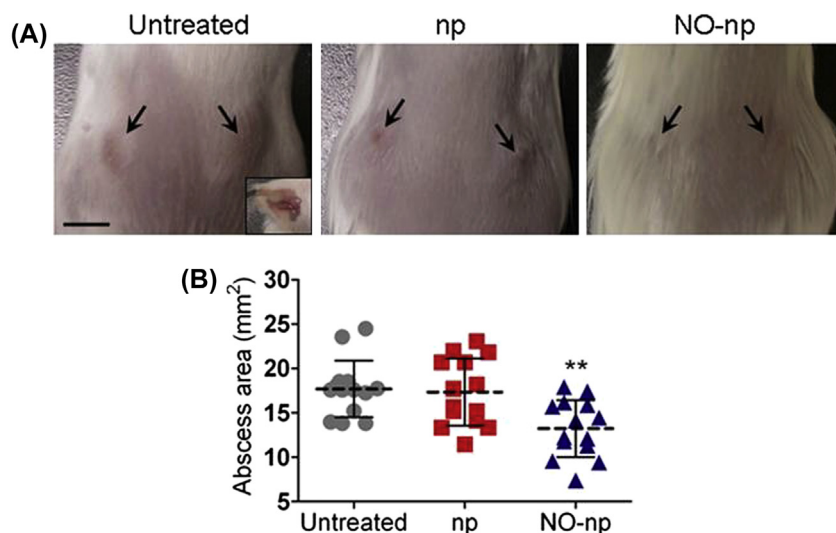


FIGURE 10.3 Subcutaneous abscess area decreased after treatment with nitrogen dioxide-releasing nanoparticle platform (NO-np). (A) MRSA abscesses in mice following 4 days of nontreatment, control-np treatment, and NO-np treatment. (B) Area analysis of subcutaneous abscesses. Abscesses infected with MRSA were untreated, treated with control-np, or NO-np. Each point represents a single abscess. The dashed line represents the average abscess area. Error bars denote SD. $**p < .001$. Reprinted from Han G, Martinez LR, Mihi MR, Friedman AJ, Friedman JM, Nosanchuk JD. Nitric oxide releasing nanoparticles are therapeutic for *Staphylococcus aureus* abscesses in a murine model of infection. *PLoS One* 2009;4(11):e7804, under the Creative Commons Attribution License.

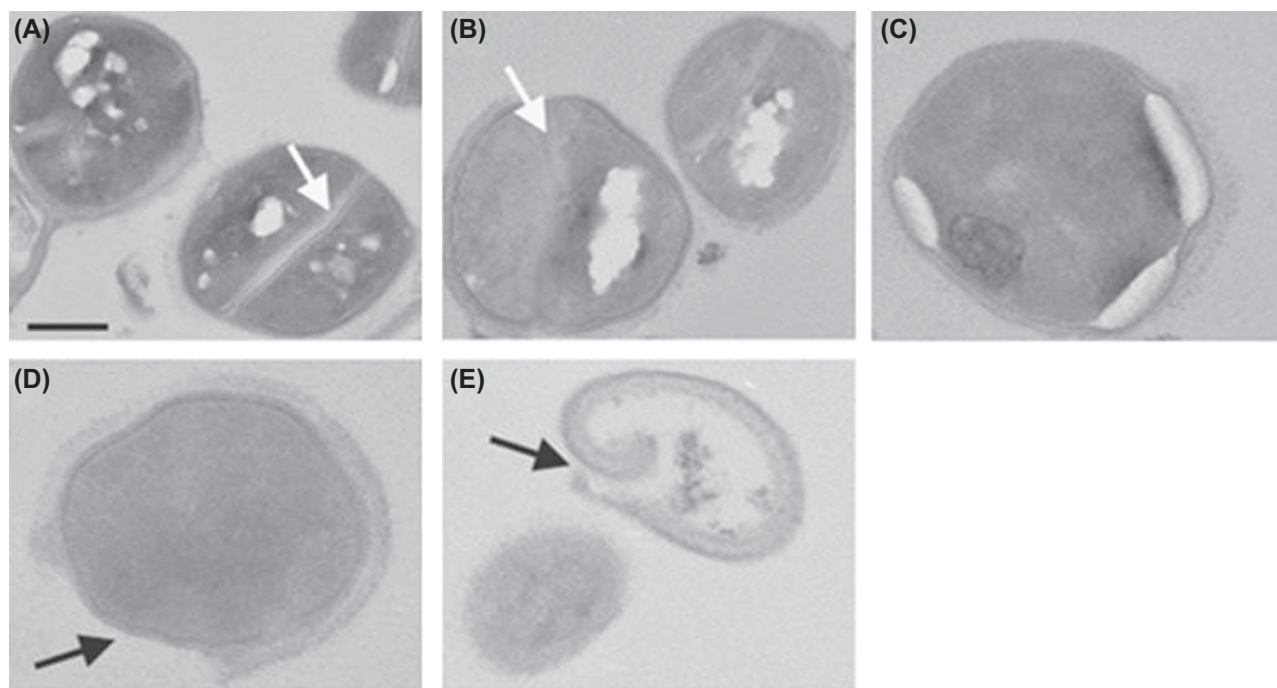


FIGURE 10.4 Nitrogen dioxide–releasing nanoparticle platforms (NO-np) have antimicrobial efficacy against *Staphylococcus aureus*. Transmission electron microscopy of *S. aureus* in the absence of NO-np (A) and presence of NO-np over 1 (B), 4 (C), 7 (D), and 24 h (E) with increasing loss of cell architecture, cell lysis, and edema. White arrow denotes cross wall damage after treatment. Black arrow denotes cell wall damage after treatment. Scale bar = 2 μ M. Reprinted from Martinez LR, Han G, Chacko M, Mihu MR, Jacobson M, Gialanella P, et al. Antimicrobial and healing efficacy of sustained release nitric oxide nanoparticles against *Staphylococcus aureus* skin infection. *J Invest Dermatol* 2009;129(10):2463–9, with permission from Nature Publishing Group.

prevention of collagen degradation as well as enhanced wound healing were observed [29]. Prolonged wound healing renders individuals susceptible to microbial infections due to a weakened barrier function and altered inflammatory status. Therefore, enhanced wound healing in the setting of NO-np treatment represents a unique way to defend against infection. This is achieved by increasing fibroblast migration and enhancing collagen deposition as well as increasing vascularization via the recruitment of TGF- β and alteration of leukocyte migration [34]. Schairer et al. compared NO-np's efficacy to that of vancomycin, a gold standard treatment for MRSA, in the setting of a murine intramuscular abscess [30]. In this model, subcutaneous vancomycin decreased bacterial burden by 94% while intralesional and topical NO-np reduced bacterial burden by 98% and 99%, respectively. NO-np also limited muscular damage due to infection in this model. NO-np have also been found effective in vivo against multidrug resistant gram-negatives including *A. baumannii* [31]. Given these results, it can be postulated that NO-np represents a comparable-to-superior treatment for resistant organisms, with the added benefit of multiple modes of administration.

NITRIC OXIDE RELEASING NANOPARTICLES AS AN ANTIFUNGAL AGENT

NO-np has also been investigated for use as an antifungal agent. Hetrick et al. described NO-np's efficacy against *Candida albicans* biofilm formation in vitro [27]. Macherla et al. also showed NO-np's activity against *C. albicans* with in vitro and in vivo methods (Fig. 10.5) [2]. NO-np inhibited fungal growth in vitro as determined by Bioscreen C analysis. Furthermore, time-lapse microscopy showed a reduction in the rate of cell division, bud formation, and filamentation. The study also evaluated the efficacy of NO-np in *C. albicans* burn infections, finding decreased fungal burden and accelerated wound closure in NO-np treated mice. These results were mirrored by histology, which showed a lack of fungal hyphal structures within the dermis, augmented collagen and fibrin deposition, and attenuated inflammation in NO-np treated burns. The data suggest that these antifungal effects are due not only to known antifungal activity of NO (interference with adhesion, tissue penetration, and dissemination) but also to some interaction between fungi and nanoparticle structures. The findings specifically indicate that

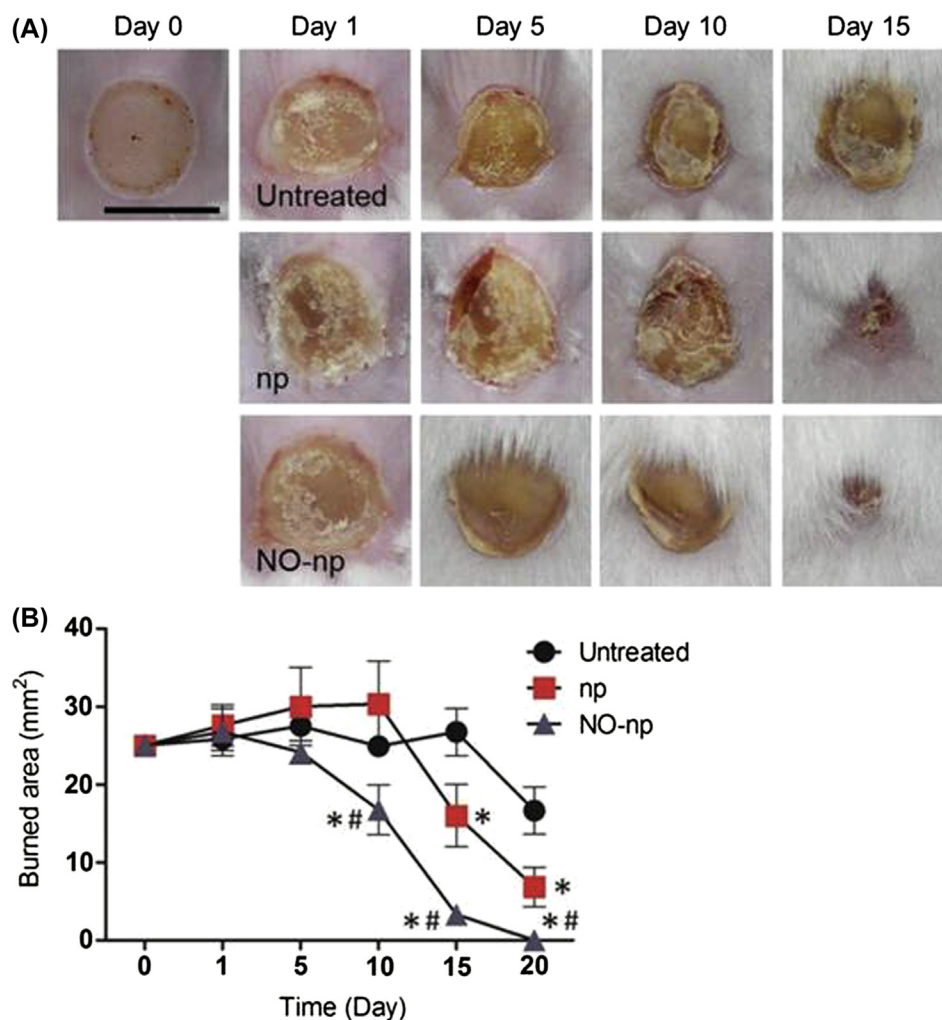


FIGURE 10.5 Nitrogen dioxide–releasing nanoparticle platform (NO-np) is effective in treating *Candida albicans* infected burn wounds in vivo. (A) Burns untreated and treated with control-np and NO-np throughout the study. Scale bar = 5 mm. (B) Burn area closure relative to day 0. Error bars denote SD. * $p < .001$ comparing control-np versus untreated. # $p < .001$ comparing control-np versus NO-np. Reprinted from Macherla C, Sanchez DA, Ahmadi MS, Vellozzi EM, Friedman AJ, Nosanchuk JD, et al. Nitric oxide releasing nanoparticles for treatment of *Candida albicans* burn infections. *Front Microbiol* 2012;3:193, under the Creative Commons Attribution Noncommercial License.

nanoparticles may interfere with cell–cell interactions and quorum sensing.

To date, unpublished data have revealed NO-np's activity against the dermatophyte *Trichophyton mentagrophytes* (unpublished findings). Investigations in the area of NO-np's antifungal activity are limited compared to studies of its antibacterial efficacy. This dearth of data underscores the need for further studies.

FUTURE DIRECTIONS

Though the aforementioned data are promising, many questions are still unanswered. Future research may provide more information about the efficacy and safety of NO-np as an antimicrobial therapy. Specific areas of study should be directed at assessing activity

against additional pathogens, especially fungi, viruses, and parasites, as there is a paucity of this data. Additionally, while NO-np have exhibited a low potential for toxicity thus far, further studies are needed to fully elucidate their safety before translation to and during clinical trials. Interestingly, a double blind, randomized clinical trial found that a topical nanofiber NO-releasing patch was effective in treating cutaneous leishmaniasis in a small percentage of patients (37.1%) at the 3-month follow-up as compared to meglumine antimoniate (94.8%) with a significant decrease in the number of adverse effects [35]. Notably, clinical evaluation of an NO-releasing nanocompound treatment for acne vulgaris and human papilloma virus (HPV) is underway. Preliminary results from a phase 2a clinical trial demonstrate a significant reduction in inflammatory lesion count in subjects with acne vulgaris after

12 weeks of therapy, with 80% less sebum on the skin surface compared to those treated with a vehicle control [36]. Furthermore, in a preclinical HPV rabbit model, there was a statistically significant cessation of papilloma growth after treatment with the same drug [37]. Further studies are needed to ascertain data about bioavailability and localization of nanoparticles during in vivo use, especially when delivered by different routes of administration. Moreover, little is known about the long-term use of NO-np, and the potential side effect profile that may be associated with prolonged use, for applications such as suppression of acne or treatment of onychomycosis. While serious adverse events are not expected based on current studies, extended toxicological analysis is needed before widespread use can occur.

The nanoparticulate platforms mentioned earlier are versatile and readily modifiable. Therefore, the nanoparticle vehicle can be tailored for use against specific pathogens, by different routes of administration, or for use in specific tissues. Many of the studies described earlier have only presented in vitro data or pertain to localized infections. In fact, various concentrations of NO-np injected into hamsters for systemic use induced no adverse events [21]. Furthermore, unpublished data demonstrated that NO-np used systemically was able to significantly attenuate inflammatory cytokine secretion in septic mice (unpublished data). These data taken together show promise for the possible use of NO-np in systemic infections and sepsis, further reinforcing their broad applicability in the setting of infection.

CONCLUSION

NO-releasing nanomaterials represent a promising therapeutic strategy for the treatment of infectious disease. These nanoparticulate platforms harness the antimicrobial potential of NO using innovative delivery vehicles. Their efficacy against bacteria and fungi have been shown through a variety of in vitro and in vivo studies. Further studies are needed to elucidate their full therapeutic potential as well as safety profile to progress from bench to bedside.

References

- [1] Friedman A, Blecher K, Sanchez D, Tuckman-Vernon C, Gialanella P, Friedman JM, et al. Susceptibility of Gram-positive and -negative bacteria to novel nitric oxide-releasing nanoparticle technology. *Virulence* 2011;2(3):217–21.
- [2] Macherla C, Sanchez DA, Ahmadi MS, Vellozzi EM, Friedman AJ, Nosanchuk JD, et al. Nitric oxide releasing nanoparticles for treatment of *Candida albicans* burn infections. *Front Microbiol* 2012;3:193.
- [3] Krausz AE, Adler BL, Cabral V, Navati M, Doerner J, Charafeddine R, et al. Curcumin-encapsulated nanoparticles as innovative antimicrobial and wound healing agent. *Nanomedicine* 2014;11(1):195–206.
- [4] Sanchez DA, Schairer D, Tuckman-Vernon C, Chouake J, Kutner A, Makdisi J, et al. Amphotericin B releasing nanoparticle topical treatment of *Candida spp.* in the setting of a burn wound. *Nanomedicine* 2014;10(1):269–77.
- [5] Fang FC. Perspectives series: host/pathogen interactions. Mechanisms of nitric oxide-related antimicrobial activity. *J Clin Invest* 1997;99(12):2818–25.
- [6] Thomas DD, Ridnour LA, Isenberg JS, Flores-Santana W, Switzer CH, Donzelli S, et al. The chemical biology of nitric oxide: implications in cellular signaling. *Free Radic Biol Med* 2008;45(1):18–31.
- [7] Wink DA, Mitchell JB. Chemical biology of nitric oxide: insights into regulatory, cytotoxic, and cytoprotective mechanisms of nitric oxide. *Free Radic Biol Med* 1998;25(4–5):434–56.
- [8] Schmidt HH, Lohmann SM, Walter U. The nitric oxide and cGMP signal transduction system: regulation and mechanism of action. *Biochim Biophys Acta* 1993;1178(2):153–75.
- [9] Kaster MP, Rosa AO, Santos AR, Rodrigues ALS. Involvement of nitric oxide – cGMP pathway in the antidepressant-like effects of adenosine in the forced swimming test. *Int J Neuropsychopharmacol* 2005;8(4):601–6.
- [10] Steiner AA, Antunes-Rodrigues J, McCann SM, Branco LG. Antipyretic role of the NO-cGMP pathway in the anteroventral preoptic region of the rat brain. *Am J Physiol Regul Integr Comp Physiol* 2002;282(2):R584–93.
- [11] Shiva S, Gladwin MT. Shining a light on tissue NO stores: near infrared release of NO from nitrite and nitrosylated hemes. *J Mol Cell Cardiol* 2009;46(1):1–3.
- [12] Gladwin MT, Grubina R, Doyle MP. The new chemical biology of nitrite reactions with hemoglobin: R-state catalysis, oxidative denitrosylation, and nitrite reductase/anhydrase. *Acc Chem Res* 2009;42(1):157–67.
- [13] Wink DA, Kasprzak KS, Maragos CM, Elespuru RK, Misra M, Dunams TM, et al. DNA deaminating ability and genotoxicity of nitric oxide and its progenitors. *Science* 1991;254(5034):1001–3.
- [14] Juedes MJ, Wogan GN. Peroxynitrite-induced mutation spectra of pSP189 following replication in bacteria and in human cells. *Mutat Res* 1996;349(1):51–61.
- [15] Ischiropoulos H, al-Mehdi AB. Peroxynitrite-mediated oxidative protein modifications. *FEBS Lett* 1995;364(3):279–82.
- [16] Murad F. Regulation of cytosolic guanylyl cyclase by nitric oxide: the NO-cyclic GMP signal transduction system. *Adv Pharmacol* 1994;26:19–33.
- [17] Friedman A, Friedman J. New biomaterials for the sustained release of nitric oxide: past, present and future. *Expert Opin Drug Deliv* 2009;6(10):1113–22. <http://dx.doi.org/10.1517/17425240903196743>.
- [18] Gupta R, Kumar A. Bioactive materials for biomedical applications using sol-gel technology. *Biomed Mater* 2008;3(3):034005.
- [19] Shin JH, Metzger SK, Schoenfisch MH. Synthesis of nitric oxide-releasing silica nanoparticles. *J Am Chem Soc* 2007;129(15):4612–9.
- [20] Friedman AJ, Han G, Navati MS, Chacko M, Gunther L, Alfieri A, et al. Sustained release nitric oxide releasing nanoparticles: characterization of a novel delivery platform based on nitrite containing hydrogel/glass composites. *Nitric Oxide* 2008;19(1):12–20.
- [21] Cabrales P, Han G, Roche C, Nacharaju P, Friedman AJ, Friedman JM. Sustained release nitric oxide from long-lived circulating nanoparticles. *Free Radic Biol Med* 2010;49(4):530–8.

- [22] Rothrock AR, Donkers RL, Schoenfisch MH. Synthesis of nitric oxide-releasing gold nanoparticles. *J Am Chem Soc* 2005; 127(26):9362–3.
- [23] Caruso EB, Petralia S, Conoci S, Giuffrida S, Sortino S. Photodelivery of nitric oxide from water-soluble platinum nanoparticles. *J Am Chem Soc* 2007;129(3):480–1.
- [24] Polizzi MA, Stasko NA, Schoenfisch MH. Water-soluble nitric oxide-releasing gold nanoparticles. *Langmuir* 2007;23(9): 4938–43.
- [25] Hajipour MJ, Fromm KM, Akbar Ashkarran A, Jimenez de Aberasturi D, de Larramendi IR, Rojo T, et al. Antibacterial properties of nanoparticles. *Trends Biotechnol* 2012;30(10):499–511.
- [26] Hetrick EM, Shin JH, Stasko NA, Johnson CB, Wespe DA, Holmuhamedov E, et al. Bactericidal efficacy of nitric oxide-releasing silica nanoparticles. *ACS Nano* 2008;2(2):235–46.
- [27] Hetrick EM, Shin JH, Paul HS, Schoenfisch MH. Anti-biofilm efficacy of nitric oxide-releasing silica nanoparticles. *Biomaterials* 2009;30(14):2782–9.
- [28] Han G, Martinez LR, Mihu MR, Friedman AJ, Friedman JM, Nosanchuk JD. Nitric oxide releasing nanoparticles are therapeutic for *Staphylococcus aureus* abscesses in a murine model of infection. *PLoS One* 2009;4(11):e7804.
- [29] Martinez LR, Han G, Chacko M, Mihu MR, Jacobson M, Gialanella P, et al. Antimicrobial and healing efficacy of sustained release nitric oxide nanoparticles against *Staphylococcus aureus* skin infection. *J Invest Dermatol* 2009;129(10):2463–9.
- [30] Schairer DO, Chouake JS, Nosanchuk JD, Friedman AJ. The potential of nitric oxide releasing therapies as antimicrobial agents. *Virulence* 2012;3(3):271–9.
- [31] Mihu MR, Sandkovsky U, Han G, Friedman JM, Nosanchuk JD, Martinez LR. The use of nitric oxide releasing nanoparticles as a treatment against *Acinetobacter baumannii* in wound infections. *Virulence* 2010;1(2):62–7.
- [32] Friedman AJ, Blecher K, Schairer D, Tuckman-Vernon C, Nacharaju P, Sanchez D, et al. Improved antimicrobial efficacy with nitric oxide releasing nanoparticle generated S-nitrosoglutathione. *Nitric Oxide* 2011;25(4):381–6.
- [33] Mordorski B, Pelgrift R, Adler B, Krausz A, da Costa Neto AB, Liang H, et al. S-nitrosocaptopril nanoparticles as nitric oxide-liberating and transnitrosylating anti-infective technology. *Nanomedicine* 2015;11(2):283–91. <http://dx.doi.org/10.1016/j.nano.2014.09.017>.
- [34] Han G, Nguyen LN, Macherla C, Chi Y, Friedman JM, Nosanchuk JD, et al. Nitric oxide – releasing nanoparticles accelerate wound healing by promoting fibroblast migration and collagen deposition. *Am J Pathol* 2012;180(4):1465–73.
- [35] Lopez-Jaramillo P, Rincon MY, Garcia RG, Silva SY, Smith E, Kampeerappun P, et al. A controlled, randomized-blinded clinical trial to assess the efficacy of a nitric oxide releasing patch in the treatment of cutaneous leishmaniasis by *Leishmania (V.) panamensis*. *Am J Trop Med Hyg* 2010;83(1):97–101.
- [36] Rico JQJ, Hollenbach S, Enloe C, Stasko N. Phase 2 study of efficacy and safety of SB204 in the treatment of acne vulgaris. Durham (NC): Novan Therapeutics; 2015. Available from: http://www.novantherapeutics.com/files/9113/9949/9564/Novan_Therapeutics_SB204_Nitric_Oxide_Treatment_for_Acne_Vulgaris.pdf.
- [37] Coggan KBK, Johnston B, Martin M, Zhang Y, Doxey R, Hollenbach S, et al. Antiviral efficacy of nitric oxide – releasing drug candidates in vivo utilizing the cottontail rabbit papilloma-virus model. Durham (NC): Novan Therapeutics; 2015. Available from: http://www.novantherapeutics.com/files/4214/1026/8096/ICAAC2014_28Aug14.pdf.

Nanoparticles in the Topical Treatment of Cutaneous Leishmaniasis: Gaps, Facts, and Perspectives

S. Espuelas, J. Schwartz, E. Moreno

University of Navarra, Pamplona, Spain

OUTLINE

A Brief Introduction to Cutaneous Leishmaniasis: Current Status of the Disease and the Therapy	135	<i>Reports of Nanoparticles for Topical Therapy of Cutaneous Leishmaniasis: Facts</i>	146
Skin Features in Cutaneous Leishmaniasis Lesions: A Chronic Inflammation	137	Liposomal Conventional Drugs	146
Turning Around Paromomycin Efficacy: Optimizing the Therapy	139	Nitric Oxide Delivery Systems	147
<i>Pharmacokinetic Considerations: Penetration or Permeation?</i>	139	Failure of Silver Nanoparticles (AgNPs) in <i>Leishmania major</i> —Infected BALB/c Mice	147
<i>Immunological Considerations: Activation or Suppression?</i>	140	Liposomes in Photodynamic Therapy: Only In Vitro Studies	148
Nanoparticles in the Topical Therapy of Cutaneous Leishmaniasis	143	Perspectives in Nanoparticles for Cutaneous Leishmaniasis Topical Therapy	148
<i>Nanoparticles and Their Interaction With Pathological Skin Lesions: Translation to Cutaneous Leishmaniasis Lesions</i>	143	Glossary	149
		List of Abbreviations	150
		References	150

A BRIEF INTRODUCTION TO CUTANEOUS LEISHMANIASIS: CURRENT STATUS OF THE DISEASE AND THE THERAPY

The term “leishmaniasis” includes a range of diseases caused by different species of protozoa of the genus *Leishmania* that are transmitted by phlebotomine (blood-sucking) sandflies. *Leishmania* parasites are injected into the vertebrate host as a promastigote (the elongated form with an external flagellum), which is

uptaken by different phagocytic cells. Within the cells of the mononuclear phagocyte system (their natural habitat), promastigotes differentiate into amastigotes (the round form without an external flagellum) and proliferate, thus establishing the infection [1].

Leishmaniasis encompasses visceral and tegumentary forms [2]. Visceral leishmaniasis (VL), which is fatal if untreated, is the most severe form in which parasites migrate to vital organs. Tegumentary leishmaniasis is one of the major tropical dermatoses of immense public health significance. It is endemic in 88

countries and it is estimated that 350 million people worldwide are at risk of infection, with an estimated prevalence of 12 million cases and an annual incidence of 1.5 million cases per year. Most of the cases (90%) are reported in Africa (mainly Morocco, Ethiopia, and Tunisia), the Middle East (Afghanistan, Pakistan, Iran, Iraq, Syria, and Saudi Arabia), and Latin America (Brazil, Bolivia, Colombia, Ecuador, Peru, and Venezuela) [2,3]. It is also increasing in travelers returning from endemic areas [4]. Despite the fact that cutaneous leishmaniasis (CL) is a growing social and health problem worldwide, it receives less attention than VL because it is not directly fatal [2].

CL [3] is divided into three major clinical phenotypes: localized cutaneous leishmaniasis (LCL), diffuse cutaneous leishmaniasis (DCL), and mucocutaneous leishmaniasis (MCL) whose manifestations range from small cutaneous nodules to gross mucosal tissue destruction. A fourth form of CL, happens as a sequel of VL, known as post-kala-azar dermal leishmaniasis (PKDL). This clinical diversity is a consequence of the numerous *Leishmania* species responsible for the disease pathogenesis as well as the degree of immune response and the genetic susceptibility of the host to infection. In general terms, species that are prevalent in the Old World (OWCL; Africa, Asia, and Southern Europe) produce limited clinical manifestations compared to New World species (NWCL; Latin America).

Current treatment of CL can be topical, systemic, or none in the self-curing form ("wait and see") [5]. In any case, treatment is recommended to expedite healing, reduce the risk of scarring, prevent parasite dissemination, and reduce the chance of relapse [6,7]. In general, parenteral treatment is required for severe CL and established MCL. It mainly consists of antimonial derivatives, which are the first line treatment and that are given daily for 21 days. However, systemic antimonials are associated with considerable toxicity and need close monitoring. In addition, there are reports of emerging leishmanial resistance. Amphotericin B (AmB), pentamidine, or paromomycin (PM) can be used as first line agents because they have been found to be as effective as the antimonials, but their use is also limited by toxicity and route of administration.

The choice for local therapy is usually determined by the following factors: (1) low risk of developing MCL; (2) few in number (<4) and small in size (<4 cm) lesions; (3) lesions not localized on joints or on esthetically compromised areas like nose, eyelashes, or lips; and (4) no signs of lymphangitic dissemination or immunosuppression [6]. In OWCL caused by species such as *Leishmania major*, *Leishmania tropica*, and *Leishmania aethiopica*, topical treatments are

the chosen option because lesions may heal spontaneously without dissemination. Furthermore, in NWCL due to *Leishmania mexicana*, *Leishmania panamensis*, or *Leishmania amazonensis*, the possibility of developing MCL is rare and topical treatments are a reasonable preference [8].

Local therapies tested in clinical practice include local chemotherapy [9] that can be either topical or intralesional or physical therapies that include intralesional antimonials, topical PM with 12% methylbenzethonium chloride (PM-MBCL), cryotherapy, or thermotherapy. More recently, photodynamic therapy (PDT) with 5-aminolevulinic acid (5-ALA) or immunotherapy with imiquimod (IMQ) in a cream have also been evaluated. However, there are several difficulties in determining which of these local therapies were really effective, mainly because of the heterogeneity in the clinical features of CL lesions. Moreover, clinical trials usually failed to define common clinical end-points or follow-up periods, and they rarely included placebo controls, which are important given the potential of CL to resolve spontaneously, making it difficult to assess their relative merits [10,11].

In general, most studies have found the highest clinical efficacy and lowest recurrence rates with intralesional antimonials [12,13]. Thermotherapy was more effective than or as effective as parenteral antimonials for the treatment of *L. major* and NWCL infections, respectively. Furthermore, PDT was superior to topical PM-MBCL in *L. major* infections.

As far as topical PM-MBCL is concerned, a meta-analysis of 14 randomized controlled trials published in 2009 confirmed that the efficacy of topical PM was similar to intralesional antimonials in treating OWCL, and was inferior against NWCL, although the ointment produced skin irritation [14]. Other formulations were further designed to be effective but also nonirritative, for example, WR279396, prepared with a hydrophilic vehicle containing 15% PM and 0.5% gentamicin. A recent clinical trial confirmed this was effective and well-tolerated in ulcerative CL infections produced by *L. major* [15] and *L. panamensis* [16]. There are not sufficient clinical trials to support the use of topical immunotherapy with 5% IMQ although the treatment led to higher cure rates than placebo and a cure rate of 90% when given in combination with systemic antimonials at the beginning of the therapy. Besides, clinical trials using topical AmB did not provide sufficient evidence for its use in OWCL or NWCL [12,13].

The World Health Organization (WHO) and other organizations such as the Drugs for Neglected Diseases initiative (DNDi) encourage the topical treatment of CL and advise using parenteral treatment only if the topical therapy fails or cannot be performed. This is

due to the fact that topical therapies can facilitate treatment access, decrease the risk-benefit ratio, improve patient compliance, and reduce costs [2].

Thus, topical therapy of CL needs new, better, and safer treatment options. Concerning new topical products, it is expected not only that they are able to accelerate the clearance of the parasites, but also lead to more rapid and stable healing processes that do not lead to scars and disfigurement. In addition, new treatments should prevent the occurrence of mucosal lesions [7]. By achieving these benefits, local therapy could extend its range of application, currently restricted to LCL, to more severe forms of tegumentary leishmaniasis possibly in combination with parenteral drugs.

This book chapter describes the histological and immunological skin alterations that characterize CL lesions and makes an effort to understand the success or failure of previously reported therapies on the basis of both pharmacokinetic and immunological considerations.

The role of nanotechnology in improving the current topical therapy is discussed taking into consideration its benefits (as sustained release systems and skin permeation enhancers), its risks (as inductors of proinflammatory cytokines and oxidation), and limitations (ability to penetrate deeply into the skin).

SKIN FEATURES IN CUTANEOUS LEISHMANIASIS LESIONS: A CHRONIC INFLAMMATION

As we have previously discussed, there are four main types of CL: LCL, DCL, MCL, and PKDL [2]. These clinical manifestations and their severity degree are determined by factors related to the parasite (species) and the host (immune status and genetic susceptibility) [3,7]. LCL is caused by *L. major*, *L. tropica* and *L. aethiopica* in the regions of North and East Africa, Central Asia, and the Middle East. *L. mexicana* and *L. amazonensis* cause LCL in parts of Central and South America, the United States, and Mexico [3]. CL lesions vary in size, appearance (papule, plaque, nodule, or ulcer), time of lesion development, progression, and resolution time after disease onset. LCL lesions start with the development of erythema that develops after a variable period at the site where an infected sandfly has bitten the host. It eventually evolves into an asymptomatic, small, pink, or red papule. The papule slowly evolves to a firm, inflamed, smooth nodule with an “iceberg” configuration. It ulcerates over a period of weeks to months, when the parasite spreads to lymph nodes and triggers an immunological response. Indeed, papules, nodules, and ulcers appear progressively in the period after

infection as the extent of the inflammatory response to the parasite progresses. The nodule enlarges progressively and eventually ulcerates over a period of 2 weeks to 6 months, becoming crusted in the center. The contour of the lesion from the margin toward the central ulcer or crust slopes upwards smoothly. Thus, the shallow ulcer with its raised indurated border has the characteristic appearance of a volcanic crater. Peripheral extension usually stops after 2 months. Gradually, the nodule loses its turgid feel and becomes firmer, indicating the replacement of the macrophage granulomas by fibrosis in the process of spontaneous healing. Ulcerated nodules persist for another 3–6 months. Five to twelve months after the initial appearance, the noduloulcerative lesions begin to regress from the center and, with time, will resolve completely, leaving a sharply demarcated and irregular scar which is often hyperpigmented and disfiguring [17].

Under certain conditions, *L. aethiopica*, *L. Mexicana*, and *L. amazonensis* also cause a diffuse form of the disease which is characterized by the development of non-ulcerative lesions away from the initial site of infection (DCL). These lesions do not have a tendency to self-cure. On the other hand, the migration of parasites to oropharyngeal mucosal sites leads to disfiguring mucosal lesions (in MCL) which is typically caused by *Leishmania braziliensis* in South America, parts of Central America, and Mexico [3]. MCL, like DCL, does not heal spontaneously and can be fatal. In addition, lesions are usually seen months or years after the first CL symptom [2].

A sandfly is a very small insect, and it seems that the labrum of *Phlebotomus* spp. is just long enough to obtain a blood meal in the subpapillary plexus of the human skin. Thus, the depth of occurrence of the leishmanial granuloma (ie, papule or nodule) does not depend on the sandfly, but is most likely governed by the specific features of the lymphatic and blood microvasculature in the particular anatomic sites of exposure. The peculiar properties of lymphatic drainage lead to the formation of an area of limited parasitic replication in the papillary dermis (leading to the formation of a papule/plaque) or in the reticular dermis (a nodule) [17]. Further morphological alterations are a consequence of the intensity of the immune response. Accordingly, the higher the tissue damage, the higher the inflammatory response [18]. Currently, it is well accepted that tissue necrosis observed in CL lesions is provoked by the immune response and not directly by the parasite. Ulcerative lesions are associated with relatively low infectious loads and nonulcerative CL or DCL with impaired parasite clearance. However, the role of the immune cells and factors responsible for the pathology as well as if it is possible to reduce the

skin pathology without affecting the parasite control need to be further investigated.

Microscopic and histological examinations show significant alterations in the skin structure in CL lesions (Fig. 11.1). The center of the ulcer is composed by the dermis layer, either directly exposed to the surface or protected by a fibrin crust. A profound necrosis characterizes this region. The induration that contours the ulcer (or the nonulcerative lesions as papules, plaques, or nodules) presents a thickened epidermis due to acanthosis and spongiosis [19]. The dermis beneath harbors the infiltrate of immune cells (macrophages, plasma cells, and T lymphocytes) and parasites forming granulomas [20,21]. In any case, the stratum corneum (SC) has been removed. The neutrophils are detected in the necrotic and perinecrotic areas [22].

The importance of T cells bias in the resolution of *Leishmania* spp. infections is well known [23–26]. The paradigm of Th1-protection versus Th2-susceptible was determined in works using animal models. Thus, while in BALB/c mice infected with *L. major* a Th2 immune response prevails and allows parasite

multiplication, C57BL/6 mice are able to control infection with a strong Th1 immune response. However, in other *Leishmania* species and in humans, the Th1/Th2 paradigm does not quite explain the natural outcome of the disease, while a misbalance among the different Th subsets may be involved. In ulcerative lesions, there is an exacerbated Th1 immune response that coexists with an elevated presence of T-regulatory cells expressing IL-10 and TGF- β that could explain the progression of the disease in spite of the high production of IFN- γ and TNF- α , detected both in blood and tissue. However, lymphocytes from DLC patients (characterized by nodular lesions) show anergy and do not produce IFN- γ upon in vitro stimulation with *Leishmania* antigens. Thus, a Th1 bias may be desired for parasite killing although it is also mainly responsible for skin ulceration in CL. Accordingly, the size of CL lesions and the healing time are well-correlated with IFN- γ and TNF- α levels in patients with CL [27]. CD8+ T cells and their cytolytic activity seem to be also implicated in the pathology of the disease. These cells express granzyme B and perforin and the expression of these

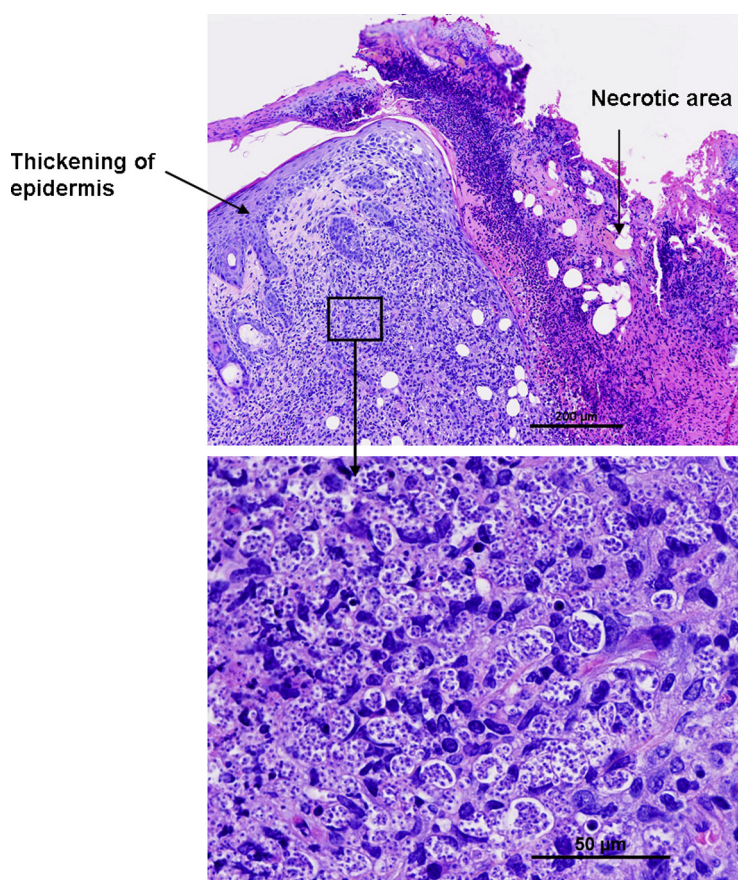


FIGURE 11.1 H&E stained skin sections obtained from the tail vein of an *Leishmania major* infected BALB/c mouse. In the cutaneous leishmaniasis lesion, two clear areas can be distinguished: the necrotic tissue and the inflamed area with epidermal hyperplasia and impressive infiltration of infected macrophages and free parasites (magnified) in dermis.

proteases is positively correlated with necrosis intensity and lesion size [28].

Leishmania parasites have developed several mechanisms for immune evasion [29]. Firstly, upon infection of the host, parasites induce the recruitment of neutrophils and delay their death by apoptosis [29]. This delay may be beneficial for the arrival of more macrophages. The uptake of apoptotic neutrophils by macrophages induces their differentiation toward an “M2-like” macrophage phenotype characterized by depressed killing functions such as the oxidative burst and nitric oxide (NO) production [30]. This phenotype also exhibits low IL2p70 and high IL-10, TGF- β production, cytokines that promote Th17, and T regulatory immune response, rendering the area of infection an immune-privileged site for parasite survival and replication. However, the production of TNF- α remains high. TNF- α and Th17 cells can induce the recruitment of new waves of neutrophils that amplify and loop the immune circuit. This inflammatory scenario upregulates Fas and TNF-related apoptosis-inducible ligand (TRAIL) in keratinocytes [31,32], induces their hyperproliferation and the production of more TNF- α and other inflammatory cytokines such as IL-6, IL-1, and IL-8. Then, they act as instigators of inflammation [33] and attract more neutrophils, macrophages, FasL-expression T cells, and TRAIL-expressing inflammatory cells that lead to keratinocyte apoptosis and ulceration. The persistence of neutrophils contributes to the chronicity of the inflammatory reaction as these cells harbor the most destructive potency for host cells and their apoptosis is required for macrophages to switch from M1 to M2 phenotypes in a normal process of wound repair [34]. On the other hand, M1-macrophages are initially required in the process of wound repair to clear infection and dying cells as well as to stimulate the proliferation of keratinocytes and fibroblasts. However, their accumulation and persistence have been detected in pathological healing conditions [35]. The proinflammatory cytokines produced by these macrophages stimulate the production of several matrix metalloproteinases (MMPs), such as MMP-2 [36] and MMP-9 [37], while inhibiting the synthesis of tissue inhibitors of matrix metalloproteinases (TIMPs). Their elevated and prolonged expression lead to excessive extracellular matrix (ECM) degradation and impaired wound healing [38], as occurs in CL lesions.

Overall, the description of CL lesions and their immunopathology allow us to estimate the complexity of designing an effective topical therapy against CL aiming at both parasite elimination and scarless wound healing. The immunological modulation required for the eradication of the parasite (a clear Th1–M1 polarization) contrasts with the Th2 immune polarization required for avoiding residual scarring. Scarless fetal wounds are

characterized by absence of an inflammatory phase [39] and their prolongation—observed, for instance, in venous leg ulcers—has been related to excessive scar formation [40].

Another major drawback is the deep location of the parasites (Fig. 11.1). The infected macrophages remain either in the papillary or reticular dermis below thickened and hypertrophic epidermis. Even in ulcerative lesions without epidermis, parasites do not appear directly exposed to the surface, or immediately under the fibrotic scab, but rather are hidden under the elevated borders of the induration area. In skin delivery, the accumulation of a drug in the dermis is only possible if the drug (through its interaction with skin components or leached plasma proteins) has a low rate of dermal clearance, or else the physiopathological skin conditions decrease the blood flow or lymphatic efflux because the dermis, compared to the epidermis, is highly perfused.

TURNING AROUND PAROMOMYCIN EFFICACY: OPTIMIZING THE THERAPY

Pharmacokinetic Considerations: Penetration or Permeation?

The aminoglycoside PM was originally formulated in an ointment with the surfactant MBCL and in the hydrophilic vehicle WR279396 [15,16,41]. PM is currently the only effective topical chemotherapy in use against ulcerative OWCL lesions [14].

Many studies in topical therapy have been devoted to theoretically predict the dermatopharmacokinetics of drugs and their therapeutic potential after local application. The selection of optimal candidate drugs should take into consideration their physicochemical properties, their intrinsic activity, and their dermal clearance (Cl). A higher ratio between input (flux, J) and output (Cl) allows the accumulation of the drug in the skin [42]. Drugs retained at concentrations higher than those required for activity could be candidates for topical therapy. Thus, the higher the drug potency, the lower the concentration required to penetrate into the skin for efficacy. J o flux depends of the parameter K_p , the concentration of the drug in the formulation, the area and time of application. According to the empirical Potts–Guy equation [43], K_p increases with the lipophilicity of the permeant and decreases with its molecular weight (MW). In intact skin, MW < 500 Da, log P ~ 1–3, low melting point, solubility parameter 9–10, and few functional groups capable of hydrogen binding are considered to be the ideal physicochemical properties for a topical drug candidate [44]. Finally, a high drug concentration in the formulation in parallel

with a tendency to escape from the vehicle into the skin or the thermodynamic activity [45,46] will dictate the kinetic diffusion process through the skin or J .

The shortcomings of these guidelines for selecting candidates for CL topical therapy could perhaps explain the unexpected efficacy of PM, in comparison with other tested drugs such as AmB or miltefosine (MIL) [47]. PM is a drug with a high MW (800), freely soluble in water ($\log P \sim -8.3$), with more than 11 functional groups capable of hydrogen binding and positively charged at physiological pH. It shows a low penetration rate into and through the intact skin because the SC prevents the penetration of highly hydrophilic drugs. Moreover, its antileishmanial activity (expressed in terms of half maximal effective concentration, EC_{50}) is rather low compared to many other antileishmanial agents. Thus, high PM accumulation (higher than EC_{50}) is necessary for efficacy.

A mismatch currently found in the research for CL topical therapy is the selection of drugs and formulations with high J [47]. Candidates for CL treatment should penetrate into the skin instead of permeate through it. The dermal location of the infected macrophages is probably responsible for the confusion in this issue, because drugs that reach the dermis are assumed to reach the systemic circulation later in time, taking into consideration the high blood and lymphatic irrigation of this skin layer.

Next, the dermal Cl parameter of drugs has been ignored. The computational models for Cl estimation [48] and/or its experimental determination by the microdialysis technique are tedious and not easy to address [49]. Some of these theoretical approaches calculate the Cl on the basis of the fact that diffusion is the only mode of transport, and they ignore the blood and lymphatic transport and the possible interactions of the drugs with skin compounds or plasma proteins [50]. Once the convective transport is involved, a crossover at approximately 16 kDa has been established. Further, the interactions with plasma or skin compounds greatly changes this cutoff [50].

The fate of the drugs in healthy or intact skin is a huge gap in knowledge that involves all these estimations. The skin barrier properties are currently oversimplified to just include the SC layer, because it is certain that SC is the main barrier responsible for the protection exerted by the skin against the environment. Moreover, the SC is more lipophilic than both the epidermis and the dermis, which resemble more an aqueous hydrogel. In skin lesions, the SC and even the epidermis (in ulcers) have been removed. Although the papules or nodules show a thickened epidermis, the SC removal and epidermal alterations tend to increase the permeability of drugs and most significantly for hydrophilic compounds that have low penetration rates into the intact

skin [51–54]. On the other hand, the blood and lymphatic clearance are profoundly altered in CL lesions characterized by a more or less intense influx of inflammatory cells and leakage of plasma proteins from the blood. This inflammatory status has a strong effect on the lymphatic/blood clearance of drugs that bind to proteins and can drastically modify the Cl theoretical estimation [55].

Thus, we can suppose that the removal of the SC makes skin CL lesions more permeable to PM than expected. In fact, it was determined that PM permeation increases between 2 and 52 times when different formulations of the drug were evaluated with intact or stripped hairless skin (skin without SC) of mice, respectively [56]. On the other hand, the cationic charge of PM at physiological pH could delay its rapid removal from the skin, and enable its accumulation in time enough to exert its activity. In fact, the drug was detected in the epidermis and dermis of patients that received WR279,396 containing 15% of PM and 0.5% of gentamicin after 10 days of daily application [57]. The pharmacokinetics of PM systemic absorption, five times more on day 20 than on day 1, also indicated the progressive accumulation of the drug in the skin and its saturation after daily application [58].

Other common drugs that have been tested for topical therapy of CL include AmB [59], buparvaquone [60], sitamaquine [61], MIL [62], fluconazole [63], allopurinol [59], or pentamidine [59]. In spite of their general higher intrinsic antileishmanial activity and lower hydrophilicity they were not significantly more effective in clinical practice [47]. The critical influence of formulation in topical delivery was ignored. For example, El-On et al. used the same cream (prepared by adding water to Ceto-macrogol Ointment BP) for the more than 20 drugs tested [59]. The vehicle and its interaction with the drug and the skin will dictate the thermodynamic activity of the drug and its tendency to move from the formulation into the skin.

Immunological Considerations: Activation or Suppression?

Another aspect that has been disregarded in leishmaniasis treatment is the local immunomodulatory effect of the drugs, as well as their effects on other cells apart from the parasites and macrophages. After topical application, the drugs first encounter the keratinocytes present in the papules, nodules, and indurations around the ulcers. From the center of the ulcer (necrotic and fibrotic dermal tissue), the drug should diffuse toward the edges to reach the granulomas composed of infected macrophages and T cells. Thus, any stimulating or toxic effects on the keratinocytes (strong instigators of

inflammation) will affect the overall therapeutic effect of the drug. Despite this fact, little data about the effects on keratinocytes has been reported so far for the current antileishmanial drugs. In the lesions of *L. tropica*–infected patients that received intralesional meglumine antimoniate, the decrease in parasite load was concomitant with upregulation of T cells and a decrease in the number of macrophages and neutrophils [64].

The type of cell death induced by the different drugs (necrosis, apoptosis, and many others [65]) could also affect their immunomodulatory effect. Apoptosis is a general way of causing cell death avoiding excessive inflammation. Neutrophil apoptosis shifts the inflammatory response toward the resolution phase during the process of wound healing [34]. The ability of the parasite to induce apoptosis in several immune cells has been described as a mechanism of immune evasion [29].

The immunostimulatory effect of antileishmanial agents [66,67] is currently considered as positive, and this has already been well-described for many of them, such as AmB, antimonials, and MIL, both in vitro and in vivo after systemic administration. Immunomodulation, as a treatment option, could counteract the mechanisms of immune evasion and immunosuppression caused by *Leishmania* parasites, such as abrogation of the oxidative burst, suppression of MHC II mediated antigen presentation, and inhibition of Th1 immune response [68]. Antimonials increase phagocytosis, production of proinflammatory cytokines (IL-6, IL-1 β , and TNF- α) and production of oxidants (reactive oxygen species [ROS] and NO) in *Leishmania* infected phagocytes, human monocytes, and neutrophils. MIL stimulates T cells and macrophages, increases secretion of proinflammatory cytokines, including IFN- γ , and enhances the production of oxidants. An increase in IFN- γ has been observed in vivo after MIL therapy. The antileishmanial effect of AmB was also partially due to a proinflammatory activity.

Thus, although a Th1-bias, and a proinflammatory effect or suppression of antiinflammatory cytokines such as IL-10, could be helpful in the eradication of parasites [23], antileishmanial drugs with antiinflammatory effects, when locally applied, could be more suitable for the healing of the lesions without scarring [35]. It is important to keep in mind that tissue injury is produced by an exacerbated immune response [40] and scarless fetal wound healing occurs without inflammation [39]. In that sense, aminoglycosides had ROS scavenging activities [67] and reduced oxidation. They also reduced the neutrophil chemotaxis through inhibition of protein kinase C (PKC) and phospholipase A2 (PLA2). In contrast, peritoneal macrophages from PM-treated BALB/c mice showed an enhanced T cell–stimulating ability and generation of ROS, NO, and TNF- α . In

Leishmania donovani in vitro infected macrophages, PM killed the parasites by inducing release of TNF- α and NO in a TLR4-dependent manner. The immunosuppression should be locally and temporally restricted and combined with a direct antileishmanial effect to achieve the elimination of the parasite [23]. Otherwise, systemic immunosuppression would predispose people to *Leishmania* infections or reactivation of healing infections, as previously reported [69,70].

On the other hand, previous works have not supported the use of immunomodulators as a monotherapy for CL. The combination of immunomodulators with chemotherapy was always required. IMQ, originally approved for the topical treatment of external anogenital warts, has been evaluated with success in combination with pentavalent antimonials for the treatment of NWCL (*L. braziliensis*), and is awaiting further studies to obtain robust clinical evidence of the synergistic combination [71]. The benefit of IMQ was less clear in OWCL infections (*L. tropica*) although the compound was active in vitro and in vivo against *L. major* infected mice [72,73]. Differences in the permeability of skin to IMQ (higher in ulcers of patients infected with *L. braziliensis* than in nodular lesions of *L. tropica*), as well immunopathological differences in the response between both species could explain the variations in the efficacy [74]. In that sense, data about the local immunomodulatory effect of IMQ in CL lesions are scarce. Topical administration of IMQ in patients with OWCL produced by *L. tropica* had a similar effect, although less intense than that previously described with intralesional antimonials. Therefore, IMQ monotherapy is less effective than intralesional chemotherapy alone or in combination with IMQ [64].

More studies with IMQ and other Toll-like receptor (TLR) agonists should be undertaken. TLR9 and TLR3 agonists have successfully been tested as adjuvants in leishmania vaccines [75]. Furthermore, TLRs are not only expressed on macrophages and DC, but also by keratinocytes and fibroblasts, and could benefit the healing of the lesions without need of deep skin penetration [76,77]. Furthermore, wound healing studies utilizing TLR3 [78] or TLR9 [79] deficient mice resulted in significantly delayed wound healing compared to wild-type controls. In addition, topical application of poly(I:C) or CpG oligonucleotides (CpG ODN) to human and mouse wounds resulted in significantly improved healing times and increased macrophage infiltration. Constraints to the therapeutic effect of poly(I:C) and CpG ODN will be the need of intracellular penetration because TLR9 and TLR3, in contrast to other TLR, are endosomal receptors, whose function is to detect intracellular infections.

Another possible therapeutic option is the combination of antileishmanial drugs with compounds that specifically inhibit inflammatory cells or factors implicated

in tissue injury that do not themselves have significant effect in parasite clearance [18]. Currently, the negative effect of $\text{TNF-}\alpha$, the protease granzyme B, and several metalloproteinases such as MMP-2 and MMP-9 are clearly established. Apoptosis of keratinocytes and FasL expression is also a hallmark of ulcerative lesions. Monoclonal antibodies, antisense oligonucleotides, or siRNA specifically designed to block these factors involved in the pathogenesis of tissue damage could significantly improve the healing process and reduce the scar formation.

Oral pentoxifylline, a $\text{TNF-}\alpha$ inhibitor, has also been successfully used as an adjuvant to intramuscular meglumine antimoniate (IMMA) in the treatment of OWCL and NWCL [80]. Although intact skin constitutes a barrier to topical delivery of antibodies, some alterations to the skin barrier as a result of diseases have been reported to allow their penetration [81]. Repeated administrations of the $\text{TNF-}\alpha$ specific antibody Infliximab (a chimeric IgG) as a solution onto the skin covered with an adhesive sheet, or as a gel formulation under a hydrofiber dressing, were able to cure leg ulcers [82], and there was a report of a rapid improvement in pyoderma gangrenosum, a reaction causing local skin ulceration [83]. Thus, application of Infliximab could be tested in CL lesions (Fig. 11.2).

PDT is a therapeutic modality whereby diseased cells and tissues are destroyed by a combination of special drugs, called photosensitizers (PS), and light of the correct wavelength to be absorbed by the PS, in the presence of oxygen. The excited PS transfers energy to molecular oxygen and produces ROS such as singlet oxygen and hydroxyl radicals, killing the cells and tissues where the PS is localized prior to photoactivation. According to the Cochrane database [12,13], a weekly session of PDT with 5-ALA or its derivative methyl-ALA (MAL) for 4 weeks against *L. major*/*L. tropica* infections showed higher cure rates and similar cosmetic results compared to topical daily treatment with PM for 28 days. A recent study has corroborated the efficacy of another inexpensive PDT regimen based on methylene blue (MB) as a PS and a noncoherent light source to treat CL caused by *L. amazonensis* [84].

As 5-ALA has no direct phototoxic effect on the parasites themselves, its efficacy seems to be indirectly mediated by the PDT effect on the immune cells, although there are some disagreements about whether 5-ALA PDT produced macrophage cytotoxicity or Th1-immunostimulating effects. The good cosmetic results observed in patients [85,86] contrasts with the tissue destruction, depopulation of macrophages, and increased levels of MCP-1 and IL-6 previously reported

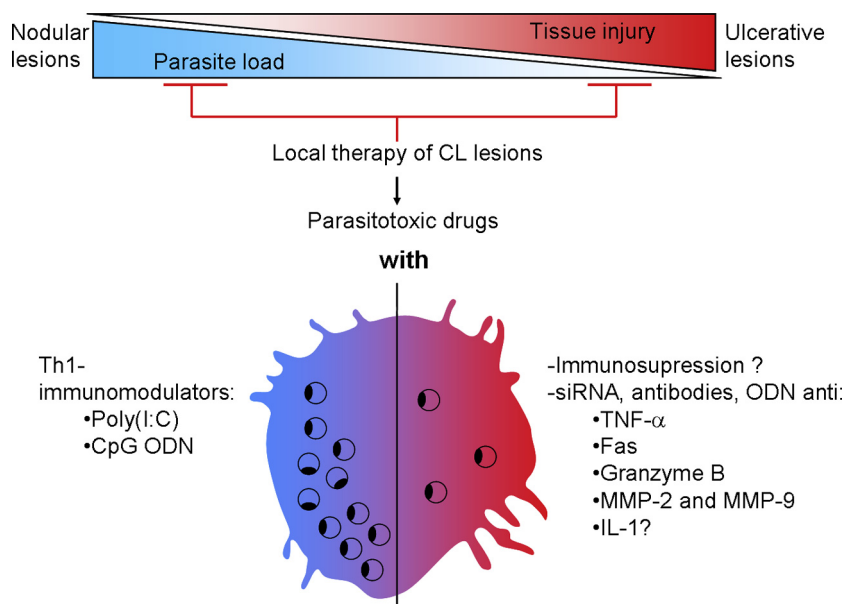


FIGURE 11.2 Types of cutaneous leishmaniasis (CL) lesions and options for their treatment. CL lesions range from papules, nodules to ulcers. Nodular lesions show high parasite load and low skin-tissue necrosis. On the contrary, parasites are scanty and tissue destruction is prominent in ulcerative lesions. In accordance with these two extreme situations, the local therapy of CL could range from Th1-immunostimulation addressed to eliminate the parasite in nodular lesions to immunosuppression in ulcers where the overinflammation produced tissue destruction. Immunotherapy should be able to modulate the delicate balance between protection and overinflammation as well as the immune response to *Leishmania* so that the antileishmanial effects are maximized but tissue destruction minimized. Then, instead of inespecific immunosuppression, the specific inhibition of factors directly implicated in the tissue destruction, such as $\text{TNF-}\alpha$, matrix metalloproteinase, and FasL, would be a safer therapeutic option. Combining immunomodulatory agents with a parasitotoxic drug (a drug with direct and nonmacrophage-mediated effect) is mandatory for all types of lesions. *Poly(I:C)*, Polyinosinic:polycytidylic acid; *CpG ODN*, Oligonucleotides with CpG motifs; *MMPs*, Metalloproteinases.

in the skin of *L. major* infected BALB/c mice that received 5-ALA PDT [87,88]. This mismatch in results is probably due to dose-dependent and light wavelength-dependent effects of PDT in the immune system [89]. Low levels of irradiance reduced inflammation and stimulated tissue repair (reduction of IL-6 and increased expression of IL-10) whereas high light intensity induced high IL-6, low IL-10 production, and cytotoxic effects. 5-ALA PDT and phototherapy of psoriasis induced Fas–FasL mediated apoptosis in keratinocytes and T cells, inhibition of proinflammatory cytokines, reduction of the inflammatory cell infiltrate in the dermis, and normalization of keratinocyte proliferation [90]. Low light and low PS doses accelerated the healing of chronic wounds by upregulating the expression of growth factors and antiinflammatory cytokines (TGF- β , IL-10, vascular endothelial growth factor [VEGF], and other growth factors).

Strategies designed to improve the current PDT protocols against CL involve the synthesis of novel PS with better parasitocidal effect in vitro, as well as improved photoactivable properties.

New generation of PS, such as chlorins or phthalocyanine derivatives are more effective in the generation of singlet oxygen after light exposure, compared to traditional phenothiazinium derivatives and are activated at longer wavelengths. The ideal PS should be photoactivated mainly in the red and far-red spectral regions. PS that absorb light at longer wavelengths may be photoactivated in deeper tissue layers and promote a more effective photoactivation in these regions [91]. This is especially important in CL because parasites reside deeply in the dermis. Several PS with confirmed in vitro activity against *Leishmania* spp. promastigotes and amastigotes have been previously reported [92,93]. However, phototoxicity was still higher for the macrophages than for the parasites. Moreover, the new generation PS have higher MWs. Either they are highly hydrophobic molecules, tending to form inactive aggregated complexes, or they are highly hydrophilic molecules. Anyway, the new generations of PS are likely to have more problems to move across the skin and to interact with biological membranes. The most challenging issue in the development of PS for PDT against CL would be to ensure the intracellular localization of the PS and its selective parasite destruction [94].

Finally, one of the biggest handicaps in the research of novel topical therapies, is the fact that the animal models of CL and MCL do not accurately mimic the human disease [18]. Injecting a low dose of infective promastigotes intradermally leads to a natural course of disease that mimics the human pathological changes during CL. However, this model does not reflect the correlation between parasitic load and tissue destruction

evident in the human disease, where ulcerative CL is predominantly associated with relatively low infectious loads, and nonulcerative CL is associated with impaired parasite clearance. In contrast, the susceptible BALB/c murine CL model is associated with widespread tissue destruction and uncontrolled parasite replication. The self-healing C57BL/6 *L. major* model is typically associated with low parasitic loads and mild to moderate immunopathology.

NANOPARTICLES IN THE TOPICAL THERAPY OF CUTANEOUS LEISHMANIASIS

Current topical therapy application is limited by its variation in its clinical efficacy, as well as by the fact that it has no effect on the process of reepithelialization and healing of the lesions with reduced scarring. We discuss now if nanotechnology-based products could overcome the drawbacks of the current therapy.

Nanoparticles and Their Interaction With Pathological Skin Lesions: Translation to Cutaneous Leishmaniasis Lesions

The application of nanotechnology for the design of novel drug delivery systems has provided topical drug delivery with new opportunities. Many types of nanoparticles (NPs), mostly lipid-based in nature, have been evaluated as drug carriers aiming at an improvement either in local (dermal delivery) [95] or systemic effect (transdermal delivery) [96]. As a function of their physicochemical properties, composition, and interaction with the drug and the skin, NPs can enhance the solubility of poorly soluble drugs [97], promote drug penetration into the SC [98], or permeate through the skin and/or serve as rate-limiting membrane barriers that control the drug release rate [99]. This may result in an increased amount of drug accumulated in the different skin layers and a sustained drug release that reduce the absorption into the blood and systemic side effects [95].

The mechanisms by which NPs act as drug permeation enhancers, drug transporters, or agents that localize drugs in the skin have not yet been clearly established. There is no consensus about the penetration/permeation pathways for nanomaterials and their ability to penetrate into the skin [100]. These difficulties are due to the different types of NPs tested, the different experimental skin materials, as well as variations in the conditions and techniques used for the determination.

In general, NPs can be divided into two large groups: (1) biodegradable and (2) nonbiodegradable. The

different types of vehicles intended for drug delivery are: lipid-based, such as liposomes, solid lipid NP (SLNPs), nanostructured lipid carriers (NLCs), or polymeric NPs, such as poly lactic-co-glycolic acid (PLGA) NPs or niosomes. They all belong to the first group [45,96]. In this category, we can also include highly deformable vesicles such as transfersomes and highly elastic vesicles like ethosomes or invasomes. Among the nonbiodegradable NPs, we can distinguish noble metallic NPs (silver (Ag) and gold), magnetic NPs, semiconductor metal oxide TiO_2 , ZnO , SiO_2 (silica NPs) currently incorporated in cosmetic sunscreen products, quantum dots (QDs) under investigation for diagnostics, or fullerenes, which are NPs discovered to be present in atmospheric aerosols [101].

Their mechanism and skin penetration depth of NPs as well as their biological effects (toxicity, immune interactions) depend on their composition and their physicochemical properties such as size, aggregation, surface charge, hydrophobicity, solubility of the particles in the skin, solubilizing properties of particles toward skin lipids, and whether the particles change on passing from the product to the skin (film forming ability and deformability [99]). The particular status of the skin is also a decisive factor. The interaction of these carriers has usually been investigated only in healthy skin, and this is surprising because many topical products are designed to be applied for the treatment of localized skin disorders (psoriasis, eczema, skin cancer, fungal infections, wounds, scars, or CL in our case). Even cosmetic products are often applied in non-healthy skin. Skin structure and permeability are significantly altered under pathological conditions as in CL lesions, which was explained at the beginning of this chapter.

In healthy skin, the general trend is that inorganic [101] and biodegradable polymeric NPs [102] tend to accumulate in the hair follicle openings and on the SC surface. Some studies reported the localization of NPs in the deepest layers of the SC, the viable epidermis and in the lowest section of the hair follicles. Sporadically, penetration into the dermis has been reported for very small NPs [103,104]. These NPs are supposed to use the transepidermal intercellular lipidic route. On the other hand, particles can persist in the hair follicles 10 times longer than in the SC [105].

The mechanism of skin interaction with soft matter nanocarriers is also highly affected by their composition [106]. Rigid liposomes such as those containing cholesterol or saturated lipids, tend to act as depot formulations and produce sustained local delivery of drugs. Several studies have excluded the possibility that intact liposomes may permeate through the skin layers. It is more likely that a disintegration of the liposome at the skin surface occurs, and that their individual

components integrate into the skin lipids [107]. This may lead to an overall increase in the skin permeability to topically applied drugs that overcome the SC and diffuse to deeper skin layers at a rate that depends on drug-partitioning properties.

SLNPs and NLCs have also demonstrated their ability to enhance epidermal drug accumulation, but their mechanism seems to be different [108]. Due to their solid nature, water evaporation that occurs after application of the preparation to the skin produces the formation of an occlusive film that has a hydrating effect and enhanced drug permeation. Also, their lipid transition at skin temperature could expel the drug from the matrix facing the skin forming a supersaturated solution that increased the drug penetration to a great extent.

In a step forward, highly flexible and highly deformable vesicles were designed aiming to enhance the penetration depth of conventional liposomes, and thus increase delivery of the loaded drugs [109]. Transfersomes are characterized by a high degree of elasticity/deformability that allows them to penetrate biological pores much smaller than their own size. The driving force for movement from the skin surface should be the transdermal osmotic skin gradient, that exclusively occurs under nonocclusive conditions, independently of the diffusion gradient for the drug concentration [109]. Compared to conventional liposomes that accumulate in the upper layers of the SC, transfersomes accumulate in the viable epidermis. The loaded drugs are then released and can diffuse into systemic circulation. The permeation enhancer properties of ethosomes occur by a different mechanism. Ethosomes contain phospholipids, and alcohol in relative high concentrations and water. Theoretically, the ethanol initially disturbs the lipid organization of the SC. Ethosomes, which are much more flexible than conventional liposomes, squeeze through the compromised horny layer. Compared to classical vesicles, ethosomes enable drugs to reach deeper skin layers and/or the systemic circulation. Ethosomes showed much more stability than transfersomes [110].

Studies of NP interactions with pathological skin conditions have started to be addressed [106], although they have been focused on inorganic NPs that are incorporated in cosmetics [111,112]. Skin barrier impairment tends to increase the cutaneous uptake of NPs in the same way as it does for drugs, and gives better access to the viable epidermis. This trend also applied in hyperkeratosis disorders; although the SC is thicker, the barrier function is weakened due to loose connection between the corneocytes. In artificially damaged skin (ie, delipidized by treatment with organic solvents or tape-stripped), psoriatic, or atopic dermatitis skin lesions, NPs were never detected in significant amounts in the dermis.

Possible health concerns associated with the penetration of NPs into skin is also a hot topic [113]. Most NPs (and especially inorganic NP) have been shown to induce oxidative stress [114], had a proinflammatory effect, and showed cytotoxicity in fibroblasts and keratinocytes [115]. In vivo studies with normal skin indicate that NPs did not cause phototoxicity, acute cutaneous irritation, or skin sensitization, probably due to the protection provided by the SC layer. However, neither in vitro studies nor acute administration of high doses of NP correlated with the more realistic scenario of chronic exposure to lower amounts of NPs. In these conditions, 50-nm silver (Ag) NPs did not induce a cytotoxic response but activated sustained stress and signaling responses [116]. Compared to inorganic and nonbiodegradable NPs, the toxic and inflammatory effects of biodegradable and soft matter nanocarriers should be lower. However, they are not inert carriers.

The activation of NALP-3 inflammasome is a common feature of NPs because of particulate dimensions [117,118]. Besides, many cationic lipids have been described to activate NF- κ B signaling pathways [119].

From this quick overview of current status of NPs for topical administration to the skin, we can estimate their possible benefits and risks upon application in CL therapy. The major drawback should be their inability to selectively target the dermal infected macrophages. Even applied onto ulcerative lesions they should diffuse through the necrotic and fibrotic dermal tissue to reach the infected cells accumulated in the borders of the ulcers. NPs could have difficulties to move through the dermis in this state (Fig. 11.3). Another concern is their toxic or proinflammatory effects in keratinocytes and fibroblasts through induction of oxidative stress and NALP-3 signaling pathways. Although they could have a positive effect for the

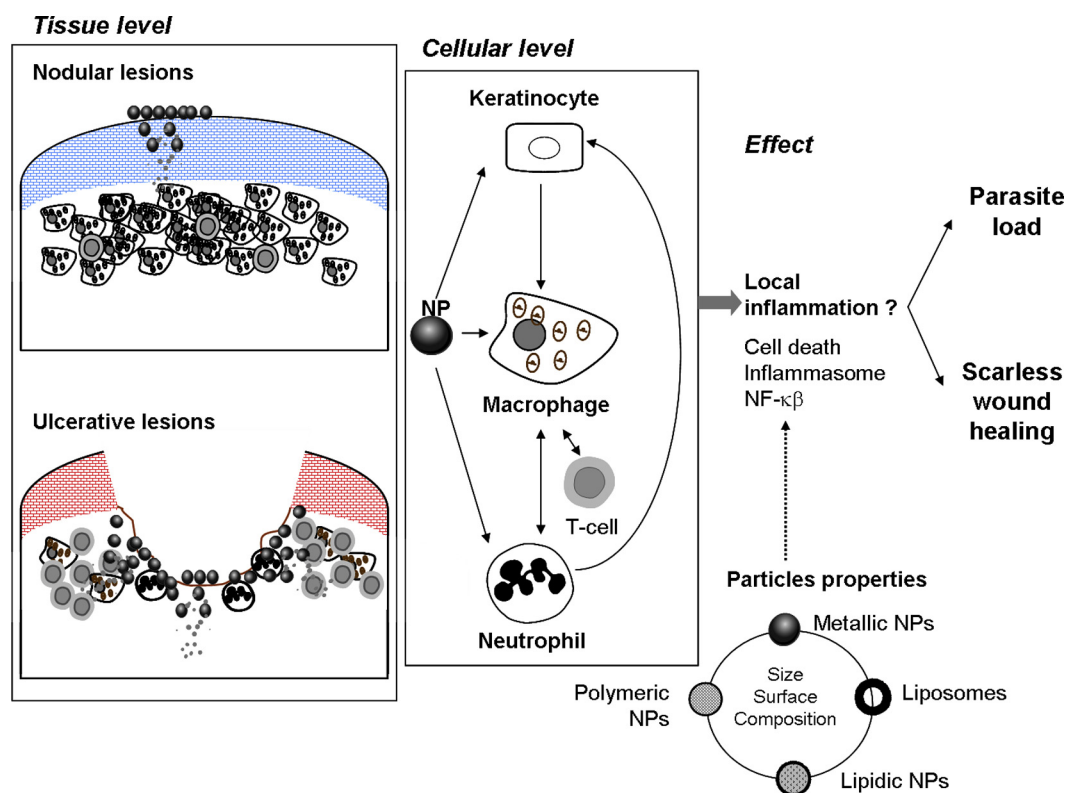


FIGURE 11.3 Interaction of nanoparticles (NPs) with cutaneous leishmaniasis lesions and effect on their resolution. Nodular lesions show high parasite load, poor lymphocytes infiltrate, and low skin tissue necrosis. On the contrary, in the ulcerative lesions the parasite load is low, whereas the infiltrate of lymphocytes and tissue injury are strong. Infected macrophages and lymphocytes are located in the indurated border of the ulcers whereas the neutrophils accumulate in the necrotic area. In nodular lesions, NPs first encounter with hypertrophic epidermis and keratinocytes whereas in the ulcers (center), NPs face to fibrotic and necrotic dermal tissue with infiltration of neutrophils. In nodular lesions, according to their physicochemical properties, NPs remain in the surface, penetrate into the epidermis (small, deformable NPs), and/or fuse with the epidermis. The drug is then released and will diffuse to the dermis where it will encounter the infected macrophage and it will be removed by blood and lymphatic clearance. The time of dermal retention is critical for the activity. In ulcerative lesions, NPs have a higher chance to directly contact infected macrophages. Either through their direct effect in macrophages or indirectly mediated by their effect in keratinocytes and neutrophils and according to their physicochemical properties, NPs can induce stress and proinflammatory signaling that can promote parasite elimination, wound healing, or exacerbate the tissue necrosis. NPs should be engineered to maximize the parasite elimination and minimize the tissue injury.

elimination of the parasite, they may not benefit the healing of the lesions without scarring. The solubilization, sustained release, and permeation enhancer properties of NPs can improve and prolong the accumulation of the drug in the dermis. As no NPs that can penetrate through the dermis have been designed so far, the drugs will get into the dermis in their free form. Thus, compounds with high dermal clearance are not good candidates for topical therapy of CL even if they are administrated in topical NPs, because the carriers cannot prevent their rapid removal.

Reports of Nanoparticles for Topical Therapy of Cutaneous Leishmaniasis: Facts

Liposomal Conventional Drugs

Studies performed with NPs in the particular context of CL are scarce, and mostly concerned with drugs currently in use for the treatment of the disease by the parenteral route: PM, AmB, or antimonials (Table 11.1). It means that two of the three critical factors conditioning the topical efficacy, namely flux into the skin (*J*) and dermal clearance (*Cl*), are not really taken into consideration before their evaluation. Thus, these drugs could be said to have “entered blind” into topical NP delivery.

The clearest example is PM and its formulation into NPs. Because of the physicochemical properties of the drug (high MW, hydrophilic, and cationic character), it was supposed that PM would show low penetration and permeation through the skin. Then, it was loaded

into different liposomal formulations [120–122]. Ex vivo permeation studies across mouse skin however indicated that the enhancement in PM topical efficacy correlated with higher skin drug retention, because the permeation of PM when applied in a cream was superior [122,123]. In fact, a nontoxic systemic absorption of PM has been reported in humans after 20 days of daily treatment with a cream containing 15% of PM and 0.5% of gentamicin in the base WR279396 [58].

Although liposomal PM was successfully tested in *L. major* infected BALB/c mice (ulcerative lesions), we have not found any information about the results in clinical trials that were apparently completed in 2012.

The wrong idea, that PM suffered difficulties to penetrate deeply into the skin and target the infected macrophages in the dermis, was also used to justify the use of transfersomes (highly deformable vesicles) [123]. However, if in fact PM needs better retention instead of better penetration, the use of rigid liposomes could be more beneficial. On the other hand, the water gradient of skin hydration, the driving force for movement of transfersomes, probably does not exist in CL lesions.

For delivery of AmB by liposomes, three different AmB lipidic formulations (AmBisome, Amphocil, Albacet) were successfully commercialized for the parenteral treatment of VL and then moved toward topical CL therapy. In *L. major* infected mice, their administration in 2–25% ethanolic solution was necessary to observe a reduction in the lesion size. Subsequently, the ethanolic Amphocil solution was used to treat CL lesions caused by *L. major* in patients from

TABLE 11.1 Preclinical or Clinical Studies Addressed With Nanocarriers

Agent	Nanoparticle formulation	Composition size	Preclinical/clinical studies
PM	Liposomes	PC:Chol ~500 nm	Animals: Absence of parasite burden in the spleen and complete wound healing 8 weeks after infection in BALB/c mice infected with <i>Leishmania major</i> treated twice a day for 4 weeks with 5–7.5 mg PM/mice. No comparison with ointment [120,122].
	Transfersomes	PC:Chol: DOC ~200 nm	Animals: More effective than the cream in <i>L. major</i> –infected BALB/c mice after treatment twice a day for 4 weeks with absence of parasites in spleen and reduction of lesion size [123].
AmB	Ethanolic solution of lipidic carriers	Amphocil: CS:AmB ~100 nm nanodisks Abelcet: DMPC:DMPG: AmB 2–5 µm ribbon-like	Animals: Efficacy of Amphocil and Abelcet in <i>L. major</i> –infected BALB/c mice following 21-day administration [158] compared with Fungizone. Humans: No evidences of efficacy in OWCL [13]. Humans: One trial with 17 patients in Israel treated with Amphocil dispersed in 5% ethanol. Lesions healed faster than placebo [124,125].
Silver	Nanosilver	~100 nm in solution	Animals: No differences with control group in <i>L. major</i> –infected BALB/c mice [140].
SbV	Liposomes	PC:Chol PC:CHOL:OA ~100 nm	Animals: Decrease of spleen parasite burden and smaller lesion size after twice a day treatment of <i>L. major</i> –infected BALB/c mice for 4 weeks. No differences were observed between both formulations. The antimonial derivative was meglumine antimoniate [159].

AmB, amphotericin B; Chol, cholesterol; CS, cholesterol sulfate; DMPC, dimethyl phosphatidyl choline; DMPG, dimethylphosphatidyl glycerol; DOC, sodium deoxycholate; OA, oleic acid; OWCL, old world CL; PC, phosphatidylcholine; PM, paromomycin; SbV, pentavalent antimonial compounds.

Israel. The Amphocil treated lesions healed faster compared with the placebo lesions [124,125]. An in-house liposomal AmB formulation showed similar efficacy compared to intralesional antimonials in a clinical trial launched with 110 patients in Iran [126]. Ex vivo penetration studies conducted with skin from pig ears confirmed the higher retention of AmB in the skin after application of Amphocil compared with Fungizone (a micellar solution of AmB with sodium deoxycholate) [127]. However, no differences between aqueous and ethanolic Amphocil were reported. AmB is one of the most active antileishmanial drugs. Its destabilizing effect on the cell membranes could account for this drug's skin penetration ability. Furthermore, a strong interaction and affinity with lipid compounds in the liposomes can decrease AmB's thermodynamical activity and affect the tendency to move from the formulation to the skin. It is still worth investigating AmB for CL topical therapy.

Nitric Oxide Delivery Systems

The use of NO as a therapeutic agent is particularly appealing for the topical treatment of CL because of two of its important therapeutic properties. Among the microbicidal mechanisms exhibited by phagocytic cells, NO production by activated macrophages has been shown to be one of the most important for eliminating *Leishmania* parasites. IFN- γ produced by Th1 cells induces the expression of the NO synthase enzyme (iNOS) by macrophages. This enzyme catalyzes NO production, which kills the parasite [128,129]. However, *Leishmania* reduced NO production in macrophages by increasing the expression of arginase [130]. Thus, the exogenous supply of NO using several different NO donors has been evaluated with more or less success in mice [131] and in humans [132]. The limitations of these molecules (NO donors) such as their limited concentration and too rapid release can be improved with the use of nanotechnology-based NO release systems [133]. In topical application, NO is a small molecule that can easily permeate into and through the skin [134]. Thus, the sustained release over time that can be provided by NPs [135] is the major advantage over other NO donors or NO-generating creams [136] that produce burst release of large or low amounts of NO with a rapid return to baseline. A wide range of organic and inorganic (silica) NPs have been developed as carriers of NO donors [133,137], and one of them, more specifically a patch, has been tested for the topical treatment of CL. In patients infected with *L. panamensis*, the cure rates after 3 months were 94.8% for the group that received parenteral Glucantime compared with 37.1% in the group topically treated with the patch [138].

On the other hand, NO has also emerged as an important molecule in the process of wound healing and not only for its antimicrobial activity [139]. Because of the program for changes in M1–M2 polarization during the process of infection resolution and wound healing, NO levels increased rapidly after skin damage and gradually decreased as the healing process progressed. NO participates in several events involved in the wound-healing process, including angiogenesis, chemoattraction of cytokines, monocytes, and neutrophils, control of collagen deposition, and fibroblast migration. Thus, it has been reported that a decrease in NO production resulted in impairment of wound healing and conversely, the supplementation of NO levels using L-arginine or NO donors increased wound closure. In vitro and in vivo studies have demonstrated that NO-NPs enhanced the wound-healing process [139].

NO-based therapy raises some concerns when it is exploited in topical CL therapy. The concentrations of NO in the affected area should change during the course of the treatment. A high NO concentration will be initially needed to eliminate the parasite. However, prolonged high NO levels may needlessly prolong the inflammatory phase of wound healing, leading to scarring. Thus, NP should be designed to tightly control the amount of NO released over time.

Failure of Silver Nanoparticles (AgNPs) in *Leishmania major*–Infected BALB/c Mice

Within the context of inorganic metallic NPs, the efficacy of AgNPs has been investigated in *L. major*–infected BALB/c mice without success, probably due to the limited capacity of these NP to penetrate into the skin and reach the infected macrophages [140]. In fact, it has been previously reported that the penetration profile of metallic NPs through the skin is greatly affected by the particle size and skin state. At most, small AgNPs (around 10 nm) could be detected in the deepest layers of the SC and the uppermost strata of the viable epidermis of abraded human skin samples [141]. In human samples of burned skin treated with an AgNP-containing dressing, AgNPs were found in the upper part of the dermis of unhealed and healed lesions [142]. Because of the localization of infected macrophages in CL, we can assume that only silver ions released from AgNPs from the skin surface could diffuse through the skin deep enough to eliminate the parasites. Their antileishmanial effect should be produced by Ag⁺ ions released from AgNPs that accumulate in the skin surface. Thus, in the context of CL, the main advantage of AgNPs is their lower toxicity compared to other forms of Ag administration [143]. Other factors limiting the benefits of metallic NPs for the topical treatment of CL will be their low selectivity

index with regard to parasites versus macrophages [144]. In general, mechanisms of activity mediated by generation of ROS are usually unspecific and tightly associated with inflammatory and cytotoxic constrains. The persistent sustained oxidative stress produced by AgNPs in vitro in HaCaT cells contrasts [116] with the antiinflammatory effect recorded by other authors during burn wound healing [142]. Topical administration of AgNPs reduced the neutrophil infiltration and local MMP levels. AgNP also decreased the expression of IL-6 and TGF- β 1, whereas levels of IL-10, VEGF, and IFN- γ were higher, which explains why wound healing was enhanced [145].

Liposomes in Photodynamic Therapy: Only In Vitro Studies

NPs have been extensively investigated to improve the performance of PDT [146,147] in skin cancer treatment. One of the advantages of delivering PS by means of NPs is, as previously described for chemotherapeutic drugs, the enhancement of their penetration through the skin. In fact, improved 5-ALA penetration and higher skin production and accumulation of protoporphyrin IX has been demonstrated with several types of ALA-containing NPs [148]. Additionally, NPs can avoid the tendency toward aggregation and subsequent inactivation of the novel second-generation PS. Ultradeformable liposomes (UDL) enhanced the amount and depth of penetration of a hydrophobic PS, zinc phthalocyanine (ZnPC), in ex vivo studies performed with abdominal human skin. In vitro studies with *L. braziliensis* infected macrophages indicated an enhancement of PS activity from 20% after light irradiation for the PS alone until 80% antiamastigote activity at the same light dose applied with these ZnPC NPs [149]. The same system (UDL) encapsulating chloroaluminum phthalocyanine (a hydrophilic cationic phthalocyanine) also enhanced 10-times the photoactivity of the free PS against intracellular amastigotes of *L. chagasi* and *L. panamensis* [150]. However, the effect was indirectly mediated by macrophage toxicity and loss of membrane integrity. In vivo studies evaluating the performance of NP in PDT against CL have not been addressed yet.

The encapsulation of PS has been described as a strategy to favor their mitochondrial and lysosomal accumulation and shifts the tumoral cell death mechanism of PS from necrosis to apoptosis [151]. The necrosis would be produced by PS ROS generation outside the target cells and further cytoplasmic membrane alteration. The process of apoptosis is a general way of causing cell death avoiding excessive inflammation. Thus, NP delivery of PS to cause PDT-induced macrophage apoptosis could

mitigate the tissue damage caused by PS administered in conventional formulations.

PERSPECTIVES IN NANOPARTICLES FOR CUTANEOUS LEISHMANIASIS TOPICAL THERAPY

CL lesions are produced by the infection with the parasite *Leishmania* and the induced immune response which tries to eliminate the parasite eventually produces tissue destruction. Certainly, the parasite infection is ultimately responsible for the immunological deregulation. However, as the ulcerative lesions are characterized by a low parasite load, and nonulcerative lesions have a high number of infected macrophages, the clinical cure of CL should be designed to clear the parasite load and also to modulate the immune response or at least to avoid skin destruction, ulceration, scarring, and disfiguration. It poses a challenge because the immune response required to eliminate the parasite (IFN- γ , NO, TNF- α) is the opposite of the response that favors lesion healing without scarring (IL-10, TGF- β). The best way to avoid residual scarring is suppressing the inflammatory response or to shorten its duration. Because general immunosuppressive environments have risks, the combination of antileishmanial drugs with specific inhibitors of cytokines and factors directly responsible for the ulceration would be safer. There are still many gaps in our knowledge of how to achieve this goal. Currently, the negative effect of TNF- α , the protease granzyme B, and several metalloproteinases such as MMP-2 and MMP-9 are clearly established. Apoptosis of keratinocytes and FasL expression is also a hallmark of ulcerative lesions. Monoclonal antibodies, antisense oligonucleotides, or siRNA specifically designed to block these factors involved in the pathogenesis of tissue damage could significantly improve the healing process and reduce the scar formation.

The key issue is the access of these compounds to their targets. In nonulcerative CL lesions, the first interaction of a topically applied drug and the vehicle takes place with the keratinocytes that form the hypertrophic and thicker epidermis. Beneath the epidermis, the dermis houses an intense infiltrate of infected macrophages and T cells. In ulcerative lesions, infected macrophages are scanty and restricted to the prominent indurated edges. In the center of the ulcers, NPs first encounter neutrophils and could also have the chance to encounter the target, the infected macrophages, although the fibrotic and necrotic status of the dermis does not facilitate their diffusion. The border of the

ulcers has also a thicker epidermis with apoptotic keratinocytes.

There is still no evidence that NPs are able to reach the dermis and selectively target the antileishmanial drugs to the parasite located inside the infected dermal macrophages. However, NPs can protect labile biotechnological products (DNA, RNA, proteins, and peptides) from degradation, and sustain their release over time from the skin surface or deeper epidermal layers, where flexible or deformable vesicles can access. Thus, NPs open the opportunity to enhance the therapeutic efficacy of these labile molecules, ie, anti-TNF- α antibodies.

In view of the free access of NPs to keratinocytes in CL lesions (the SC has been removed), the effect of NPs in these cells should be analyzed in detail, not only to avoid toxicity but also for profiting the indirect effects that alteration of the keratinocytes may have in the immune system, healing of the lesion, and evolution of the infection. Inorganic NPs tend to induce the production of ROS and the production of proinflammatory cytokines (IL-6, IL-8, IL-1) by keratinocytes. However, their composition and their physicochemical properties can tightly modulate their inflammatory effects. For example the proinflammatory effects of AgNPs (ROS and TNF- α production) was downregulated by their coating with tannic acid [152]. Cationic lysine-based surfactants in SLNP induced the production of IL-1 α by keratinocytes, which was inhibited with the incorporation of cholesterol [153]. Lipids participate in skin homeostasis because of their effect on skin permeability. Moreover, some lipids act as specific lipid mediators (ie, eicosanoids or sphingolipids, lipoxins, resolvins, maresins) involved in skin inflammation and immunity [154,155]. Cationic lipids or polymers (ie, chitosan) have been shown to activate NF- κ B and/or NALP3-inflammasome system and induce IL-1 production, implicated in inflammatory skin diseases.

NPs can also enhance the endosomal delivery of poly(I:C) and CpG ODN and improve their skin penetration in the same degree. We have previously demonstrated their beneficial effect in processes of wound healing and Th1-bias. However, we are not sure how their loading into NP will influence their effect in keratinocytes as cells with limited capacity of endocytosis.

Neutrophils can also be considered as a therapeutic target in view of their localization near to the surface in ulcerative lesions (Fig. 11.3), their high phagocytic capacity, and the harmful effect of their persistence in chronic skin lesions. A recent work reported the inhibition of neutrophil chemotaxis by albumin NP delivery as a strategy to prevent vascular inflammation [156]. We have recently conducted a study in which

β -lapachone was loaded in lecithin-chitosan NP that were topically applied in *L. major* infected BALB/c mice. This treatment decreased the number of the neutrophils in the skin lesion and lessened the tissue damage although the parasite load was not actually reduced [157].

Glossary

Cutaneous leishmaniasis The most common form of leishmaniasis.

Usually cutaneous leishmaniasis (CL) refers to localized cutaneous leishmaniasis (LCL) rather than to much less common forms, such as diffuse cutaneous leishmaniasis (DCL) and disseminated CL. Different *Leishmania* species cause Old World and New World (American) CL. In the Old World, etiological agents include *L. tropica*, *L. major*, and *L. aethiopica*, as well as *L. infantum* and *L. donovani*. The main species in the New World belong either to the *L. mexicana* species complex (*L. mexicana*, *L. amazonensis*, and *L. venezuelensis*) or to the subgenus *Viannia* (*L. (V.) braziliensis* species complex.) In general, CL causes skin lesions, which can persist for months or sometimes years. Skin lesions usually develop within several weeks or months after the exposure to the parasites but occasionally first appear years later. Lesions typically evolve from papules to nodular plaques to ulcerative lesions with a raised border and central depression and which can be covered by scab or crust. However, some lesions persist as nodules.

Ethosomes Highly fluid vesicles prepared from phospholipids, a high proportion of the permeation enhancer ethanol and water. The presence of ethanol enhances the ability of these vesicles to penetrate into the skin compared to liposomes.

Inflammasome A molecular complex of several proteins, including members of the NOD-like receptor family (such as NALP3) that upon assembly cleaves pro-interleukin-1 β (pro-IL-1 β) and pro-IL-18, thereby producing active cytokines. Nanoparticles, depending on their physicochemical properties, can activate NALP3.

Leishmaniasis Diseases caused by protozoan parasites from more than 20 *Leishmania* species that are transmitted to humans by the bites of infected female phlebotomine sandflies. There are three main forms of the disease: CL, mucocutaneous leishmaniasis, and VL, or kala-azar. According to the WHO, leishmaniasis is a category 1 disease, which means that it is emergent and uncontrolled.

Liposomes Vesicular particles consisting of one or more lipid bilayers enclosing an aqueous phase. They can be classified as large multilamellar liposomes (MLV), small unilamellar vesicles (SUV), and large unilamellar vesicles (LUV) depending on their size and the number of lipid bilayers. Water soluble compounds can be included within the aqueous compartment and lipophilic and amphiphilic compounds can be associated with the lipid bilayer.

Metalloproteinases A family of zinc endopeptidases which are expressed by a number of cell types during different phases of healing (including inflammatory cells, fibroblasts, endothelial cells, and keratinocytes). They are capable of degrading the components of the ECM and facilitate many of the pathways leading to the regeneration of injured tissues, including the clearance of damaged protein and destruction of the provisional matrix, facilitation of cellular migration to the wound area, and granulation tissue formation. MMPs do not only act in the direct remodeling of ECM components, but also degrade growth factors and their receptors as well as angiogenic factors and ultimately influence cellular behavior. The control of their expression is a critical part of normal wound healing. Elevated and prolonged expression can lead to excessive ECM degradation associated with impaired wound healing.

Nanoparticles Microscopic particles whose size is measured in nanometers. In general, NPs can be divided into two large groups: biodegradable and nonbiodegradable NPs. Biodegradable NPs can be lipidic, such as liposomes, solid lipid nanoparticles, or NLCs, or they can be polymeric. Among the nonbiodegradable nanoparticles we can distinguish metallic NPs (silver and gold), magnetic NPs, semiconductive metal oxide TiO_2 , ZnO , SiO_2 (silica NPs)—currently incorporated in cosmetic sunscreen products—quantum dots (QDs)—under investigation for diagnostics—or fullerenes, which are accidental NPs presented in atmospheric aerosols.

Nanostructured lipid carriers Nanoparticles composed of a lipid core consisting of a mixture or solid and liquid lipids stabilized with surfactants. They stand between solid lipid nanoparticles and nanoemulsions. The lipids that are used to prepare them are triglycerides, fatty acids, and waxes. They minimize some problems associated with solid lipid nanoparticles such as low payloads for some drugs and drug expulsion on storage.

Nodule A nodule is a raised solid lesion that measures more than 1 cm.

Papule A small circumscribed, superficial, solid elevation of the skin with a diameter of less than 1 cm (0.5 cm according to some authorities).

Polymeric nanoparticles Nanoparticles that are constituted of biodegradable or nonbiodegradable polymers, such as polysaccharides (ie, chitosan) or polyesters (ie, poly(ϵ -caprolactone) or PLGA copolymers.

Skin wound healing The restoration of structure and function of injured skin. The process of skin wound healing proceeds in four phases: (1) hemostasis; (2) inflammation; (3) granulation tissue formation and myofibroblast-driven wound contraction and; (4) matrix deposition and remodeling. This sequence is orchestrated via the movement of neutrophils, macrophages and fibroblasts, and secretion of signaling molecules, such as IL-1, TNF- α , metalloproteinases, nitric oxide, ROS, TGF- β , IL-10, and growth factors.

Solid lipid nanoparticles Nanoparticles composed of a solid lipid core and that is stabilized with surfactants. Lipid matrices can be composed of fats and waxes or other solids at room temperature. Common disadvantages are inherent poor drug loading due to the crystalline structure of the solid lipid and poor stability on storage.

Toll-like receptor Cell surface molecules on phagocytes and other cell types (such as keratinocytes) that are involved in the recognition of microbial structures such as endotoxin and the generation of signals that lead to the activation of innate immune responses

Transfersomes Ultradeformable vesicular particles, consisting of at least one inner aqueous compartment surrounded by a lipid bilayer able to penetrate pores much smaller than their own size. They are made of phospholipids but the addition of surfactants facilitates their deformability.

Ulcer A local defect or excavation of the surface of an organ or tissue which is produced by sloughing of necrotic inflammatory tissue.

DNDi Drugs for Neglected Diseases initiative

EC₅₀ Half maximal effective concentration

ECM Extracellular matrix

FasL Fas ligand

IFN- γ Interferon gamma

IgG Immunoglobulin G

IL Interleukin

IMMA Intramuscular meglumine antimoniate

IMQ Imiquimod

iNOS Inducible nitric oxide synthase

J Flux

K_p Permeability coefficient

LCL Localized Cutaneous Leishmaniasis

M1, M2 Macrophage type 1 or 2

MAL Methyl-ALA

MB Methylene blue

MBCL Methyl benzethonium chloride

MCL Mucocutaneous leishmaniasis

MHCII Major histocompatibility complex II

MIL Miltefosine

MMP Matrix metalloprotease

MW Molecular weight

NALP-3 NACHT, LRR, and PYD domains-containing protein 3 (NALP3) or cryopyrin

NF- κ B Nuclear factor kappa-light-chain-enhancer of activated B cells

NLCs Nanostructured lipid carriers

NO Nitric oxide

NPs Nanoparticles

NWCL New world cutaneous leishmaniasis

ODN Oligodeoxynucleotides

OWCL Old world cutaneous leishmaniasis

PDT Photodynamic therapy

PKC Protein kinase C

PKDL Post-kala-azar dermal leishmaniasis

PLA2 Phospholipase A2

PLGA Poly lactic-co-glycolic acid

PM Paromomycin

Poly(I:C) Polyinosinic-polycytidylic acid

PS Photosensitizers

QDs Quantum dots

ROS Reactive oxygen species

SC Stratum corneum

siRNA Small interfering RNA

SLNPs Solid lipid nanoparticles

TGF- β Tumor growth factor- β

Th T-helper cell (1, 2, 17)

TIMPS Tissue inhibitors of matrix metalloproteinases

TLR Toll-like receptor

TNF- α Tumor necrosis factor alpha

TRAIL TNF-related apoptosis-inducing ligand

UDL Ultradeformable liposomes

VEGF Vascular endothelial growth factor

VL Visceral leishmaniasis

WHO World Health Organization

List of Abbreviations

5-ALA 5-Aminolevulinic acid

Ag Silver

AgNPs Silver nanoparticles

AmB Amphotericin B

CD8 Cluster of Differentiation 8

Cl Clearance

CL Cutaneous leishmaniasis

CpG ODN Oligonucleotides containing CpG motifs (cytosine-guanine)

DCL Diffuse cutaneous leishmaniasis

References

- [1] Kaye P, Scott P. Leishmaniasis: complexity at the host-pathogen interface. *Nat Rev Microbiol* August 2011;9(8):604–15.
- [2] WHO. Control of the leishmaniasis: report of a meeting of the WHO Expert Committee on the control of leishmaniasis, Geneva, 22–26 March 2010. WHO technical report series 949. 2010. pp. 1–185.

- [3] Reithinger R, Dujardin JC, Louzir H, Pirmez C, Alexander B, Brooker S. Cutaneous leishmaniasis. *Lancet Infect Dis* September 2007;7(9):581–96.
- [4] Blum J, Buffet P, Visser L, Harms G, Bailey MS, Caumes E, et al. LeishMan recommendations for treatment of cutaneous and mucosal leishmaniasis in travelers, 2014. *J Trav Med* March–April, 2014;21(2):116–29.
- [5] Monge-Maillo B, Lopez-Velez R. Therapeutic options for old world cutaneous leishmaniasis and new world cutaneous and mucocutaneous leishmaniasis. *Drugs* November 2013;73(17):1889–920.
- [6] Sundar S, Chakravarty J. Leishmaniasis: an update of current pharmacotherapy. *Expert Opin Pharmacother* January 2013;14(1):53–63.
- [7] David CV, Craft N. Cutaneous and mucocutaneous leishmaniasis. *Dermatol Ther* November–December, 2009;22(6):491–502.
- [8] Hodiamont CJ, Kager PA, Bart A, de Vries HJC, van Thiel PPAM, Leenstra T, et al. Species-directed therapy for leishmaniasis in returning travellers: a comprehensive guide. *Plos Negl Trop Dis* May 2014;8(5).
- [9] Ameen M. Cutaneous leishmaniasis: advances in disease pathogenesis, diagnostics and therapeutics. *Clin Exp Dermatol* October 2010;35(7):699–705.
- [10] Gonzalez U, Pinart M, Reveiz L, Rengifo-Pardo M, Tweed J, Macaya A, et al. Designing and reporting clinical trials on treatments for cutaneous leishmaniasis. *Clin Infect Dis* August 15, 2010;51(4):409–19.
- [11] Oliaro P, Vaillant M, Arana B, Groggl M, Modabber F, Magill A, et al. Methodology of clinical trials aimed at assessing interventions for cutaneous leishmaniasis. *PLoS Negl Trop Dis* 2013;7(3):e2130.
- [12] Gonzalez U, Pinart M, Rengifo-Pardo M, Macaya A, Alvar J, Tweed JA. Interventions for American cutaneous and mucocutaneous leishmaniasis. *Cochrane Database Syst Rev* 2009;(2):CD004834.
- [13] Gonzalez U, Pinart M, Reveiz L, Alvar J. Interventions for old world cutaneous leishmaniasis. *Cochrane Database Syst Rev* 2008;(4):CD005067.
- [14] Kim DH, Chung HJ, Bleys J, Ghohestani RF. Is paromomycin an effective and safe treatment against cutaneous leishmaniasis? A meta-analysis of 14 randomized controlled trials. *PLoS Negl Trop Dis* 2009;3(2):e381.
- [15] Ben Salah A, Ben Messaoud N, Guedri E, Zaatour A, Ben Alaya N, Bettaieb J, et al. Topical paromomycin with or without gentamicin for cutaneous leishmaniasis. *N Engl J Med* February 7, 2013;368(6):524–32.
- [16] Sosa N, Capitan Z, Nieto J, Nieto M, Calzada J, Paz H, et al. Randomized, double-blinded, phase 2 trial of WR 279,396 (paromomycin and gentamicin) for cutaneous leishmaniasis in Panama. *Am J Trop Med Hyg* September 2013;89(3):557–63.
- [17] Akilov OE, Khachemoune A, Hasan T. Clinical manifestations and classification of Old World cutaneous leishmaniasis. *Int J Dermatol* February 2007;46(2):132–42.
- [18] Nylen S, Eidsmo L. Tissue damage and immunity in cutaneous leishmaniasis. *Parasite Immunol* December 2012;34(12):551–61.
- [19] Dantas ML, de Oliveira JM, Carvalho L, Passos ST, Queiroz A, Guimaraes LH, et al. Comparative analysis of the tissue inflammatory response in human cutaneous and disseminated leishmaniasis. *Mem Inst Oswaldo Cruz* April 2014;109(2):202–9.
- [20] Cangussu SD, Souza CC, Campos CF, Vieira LQ, Afonso LC, Arantes RM. Histopathology of *Leishmania major* infection: revisiting *L. major* histopathology in the ear dermis infection model. *Mem Inst Oswaldo Cruz* September 2009;104(6):918–22.
- [21] Araujo AP, Giorgio S. Immunohistochemical evidence of stress and inflammatory markers in mouse models of cutaneous leishmaniasis. *Arch Dermatol Res* April 21, 2015;307.
- [22] Boaventura VS, Santos CS, Cardoso CR, de Andrade J, Dos Santos WL, Clarencio J, et al. Human mucosal leishmaniasis: neutrophils infiltrate areas of tissue damage that express high levels of Th17-related cytokines. *Eur J Immunol* October 2010;40(10):2830–6.
- [23] Hartley MA, Kohl K, Ronet C, Fasel N. The therapeutic potential of immune cross-talk in leishmaniasis. *Clin Microbiol Infect* February 2013;19(2):119–30.
- [24] da Silva Santos C, Brodskyn CI. The role of CD4 and CD8 T Cells in human cutaneous leishmaniasis. *Front Public Health* 2014;2:165.
- [25] Kedzierski L, Evans KJ. Immune responses during cutaneous and visceral leishmaniasis. *Parasitology* July 30, 2014;1–19.
- [26] Carvalho LP, Passos S, Schrieffer A, Carvalho EM. Protective and pathologic immune responses in human tegumentary leishmaniasis. *Front Immunol* 2012;3:301.
- [27] Oliveira F, Bafica A, Rosato AB, Favali CB, Costa JM, Cafe V, et al. Lesion size correlates with *Leishmania* antigen-stimulated TNF-levels in human cutaneous leishmaniasis. *Am J Trop Med Hyg* July 2011;85(1):70–3.
- [28] Novais FO, Carvalho LP, Graff JW, Beiting DP, Ruthel G, Roos DS, et al. Cytotoxic T cells mediate pathology and metastasis in cutaneous leishmaniasis. *PLoS Pathog* 2013;9(7):e1003504.
- [29] Cecilio P, Perez-Cabezas B, Santarem N, Maciel J, Rodrigues V, Cordeiro da Silva A. Deception and manipulation: the arms of *Leishmania*, a successful parasite. *Front Immunol* 2014;5:480.
- [30] Murray PJ, Wynn TA. Protective and pathogenic functions of macrophage subsets. *Nat Rev Immunol* November 2011;11(11):723–37.
- [31] Tasew G, Nylen S, Lieke T, Lemu B, Meless H, Ruffin N, et al. Systemic FasL and TRAIL neutralisation reduce leishmaniasis induced skin ulceration. *PLoS Negl Trop Dis* 2010;4(10):e844.
- [32] Rethi B, Eidsmo L. FasL and TRAIL signaling in the skin during cutaneous leishmaniasis – implications for tissue immunopathology and infectious control. *Front Immunol* 2012;3:163.
- [33] Pasparakis M, Haase I, Nestle FO. Mechanisms regulating skin immunity and inflammation. *Nat Rev Immunol* May 2014;14(5):289–301.
- [34] Wilgus TA, Roy S, McDaniel JC. Neutrophils and wound repair: positive actions and negative reactions. *Adv Wound Care (New Rochelle)* September 2013;2(7):379–88.
- [35] Novak ML, Koh TJ. Phenotypic transitions of macrophages orchestrate tissue repair. *Am J Pathol* November 2013;183(5):1352–63.
- [36] Maretti-Mira AC, de Oliveira-Neto MP, Da-Cruz AM, de Oliveira MP, Craft N, Pirmez C. Therapeutic failure in American cutaneous leishmaniasis is associated with gelatinase activity and cytokine expression. *Clin Exp Immunol* February 2011;163(2):207–14.
- [37] Campos TM, Passos ST, Novais FO, Beiting DP, Costa RS, Queiroz A, et al. Matrix metalloproteinase 9 production by monocytes is enhanced by TNF and participates in the pathology of human cutaneous leishmaniasis. *PLoS Negl Trop Dis* November 2014;8(11):e3282.
- [38] McCarty SM, Percival SL. Proteases and delayed wound healing. *Adv Wound Care (New Rochelle)* October 2013;2(8):438–47.
- [39] Yates CC, Hebda P, Wells A. Skin wound healing and scarring: fetal wounds and regenerative restitution. *Birth Defects Res C Embryo Today* December 2012;96(4):325–33.
- [40] Shaw TJ, Kishi K, Mori R. Wound-associated skin fibrosis: mechanisms and treatments based on modulating the inflammatory

- response. *Endocr Metab Immune Disord Drug Targets* December 2010;10(4):320–30.
- [41] Ben Salah A, Buffet PA, Morizot G, Ben Massoud N, Zaatour A, Ben Alaya N, et al. WR279,396, a third generation aminoglycoside ointment for the treatment of *Leishmania major* cutaneous leishmaniasis: a phase 2, randomized, double blind, placebo controlled study. *PLoS Negl Trop Dis* 2009;3(5):e432.
 - [42] Davis A. Getting the dose right in dermatological therapy. In: Walters HR, Roberts MS, editors. *Dermatologic, cosmeceutic, and cosmetic development: therapeutic and novel approaches*. New York: Informa Healthcare USA, Inc; 2008. p. 197–213.
 - [43] Potts RO, Guy RH. Predicting skin permeability. *Pharm Res* May 1992;9(5):663–9.
 - [44] Forster M, Bolzinger MA, Fessi H, Briancon S. Topical delivery of cosmetics and drugs. *Molecular aspects of percutaneous absorption and delivery*. *Eur J Dermatol* 2009 ;19(4):309–23.
 - [45] Akomeah FK. Topical dermatological drug delivery: quo vadis? *Curr Drug Deliv* October 2010;7(4):283–96.
 - [46] Lane ME, Hadgraft J, Oliveira G, Vieira R, Mohammed D, Hirata K. Rational formulation design. *Int J Cosmet Sci* December 2012;34(6):496–501.
 - [47] Moreno E, Schwartz J, Fernandez C, Sanmartin C, Nguewa P, Irache JM, et al. Nanoparticles as multifunctional devices for the topical treatment of cutaneous leishmaniasis. *Expert Opin Drug Deliv* April 2014;11(4):579–97.
 - [48] Anissimov YG, Jepps OG, Dancik Y, Roberts MS. Mathematical and pharmacokinetic modelling of epidermal and dermal transport processes. *Adv Drug Deliv Rev* February 2013;65(2):169–90.
 - [49] Herkenne C, Alberti I, Naik A, Kalia YN, Mathy FX, Preat V, et al. In vivo methods for the assessment of topical drug bioavailability. *Pharm Res* January 2008;25(1):87–103.
 - [50] Ibrahim R, Nitsche JM, Kasting GB. Dermal clearance model for epidermal bioavailability calculations. *J Pharm Sci* June 2012; 101(6):2094–108.
 - [51] Chiang A, Tudela E, Maibach HI. Percutaneous absorption in diseased skin: an overview. *J Appl Toxicol* August 2012;32(8): 537–63.
 - [52] Gattu S, Maibach HI. Enhanced absorption through damaged skin: an overview of the in vitro human model. *Skin Pharmacol Physiol* 2010;23(4):171–6.
 - [53] Gattu S, Maibach HI. Modest but increased penetration through damaged skin: an overview of the in vivo human model. *Skin Pharmacol Physiol* 2011;24(1):2–9.
 - [54] Nielsen JB, Nielsen F, Sorensen JA. Defense against dermal exposures is only skin deep: significantly increased penetration through slightly damaged skin. *Arch Dermatol Res* November 2007;299(9):423–31.
 - [55] Oshima S, Suzuki C, Yajima R, Egawa Y, Hosoya O, Juni K, et al. The use of an artificial skin model to study transdermal absorption of drugs in inflamed skin. *Biol Pharm Bull* 2012;35(2):203–9.
 - [56] Castro GA, Nascimento DS, Fernandes AP, Nunan EA, Ferreira LAM. In vitro skin permeation of paromomycin from topical formulations across normal and stripped hairless mouse skin. *Stp Pharma Sci* May–June, 2003;13(3):203–8.
 - [57] Ben Salah A, Zaatour A, Ben Messaoud N, Kidar A, Smith PL, Kopydlowski KM, et al. Parasite load decrease during application of a safe and easily applied antileishmanial aminoglycoside cream. *PLoS Negl Trop Dis* May 2014;8(5):e2749.
 - [58] Ravis WR, Llanos-Cuentas A, Sosa N, Kreishman-Deitrick M, Kopydlowski KM, Nielsen C, et al. Pharmacokinetics and absorption of paromomycin and gentamicin from topical creams used to treat cutaneous leishmaniasis. *Antimicrob Agents Chemother* October 2013;57(10):4809–15.
 - [59] El-On J, Jacobs GP, Witzum E, Greenblatt CL. Development of topical treatment for cutaneous leishmaniasis caused by *Leishmania major* in experimental animals. *Antimicrob Agents Chemother* November 1984;26(5):745–51.
 - [60] Garnier T, Mantyla A, Jarvinen T, Lawrence MJ, Brown MB, Croft SL. Topical buparvaquone formulations for the treatment of cutaneous leishmaniasis. *J Pharm Pharmacol* January 2007; 59(1):41–9.
 - [61] Garnier T, Brown MB, Lawrence MJ, Croft SL. In-vitro and in-vivo studies on a topical formulation of sitamaquine dihydrochloride for cutaneous leishmaniasis. *J Pharm Pharmacol* August 2006;58(8):1043–54.
 - [62] Dorlo TP, Balasegaram M, Beijnen JH, de Vries PJ. Miltefosine: a review of its pharmacology and therapeutic efficacy in the treatment of leishmaniasis. *J Antimicrob Chemother* November 2012; 67(11):2576–97.
 - [63] Mussi SV, Fernandes AP, Ferreira LA. Comparative study of the efficacy of formulations containing fluconazole or paromomycin for topical treatment of infections by *Leishmania (Leishmania) major* and *Leishmania (Leishmania) amazonensis*. *Parasitol Res* May 2007;100(6):1221–6.
 - [64] Shamsi Meymandi S, Javadi A, Dabiri S, Shamsi Meymandi M, Nadji M. Comparative histological and immunohistochemical changes of dry type cutaneous leishmaniasis after administration of meglumine antimoniate, imiquimod or combination therapy. *Arch Iran Med* July 2011;14(4):238–43.
 - [65] Poon IK, Lucas CD, Rossi AG, Ravichandran KS. Apoptotic cell clearance: basic biology and therapeutic potential. *Nat Rev Immunol* March 2014;14(3):166–80.
 - [66] Saha P, Mukhopadhyay D, Chatterjee M. Immunomodulation by chemotherapeutic agents against Leishmaniasis. *Int Immunopharmacol* November 2011;11(11):1668–79.
 - [67] Labro MT. Immunomodulatory effects of antimicrobial agents. Part II: antiparasitic and antifungal agents. *Expert Rev Anti Infect Ther* March 2012;10(3):341–57.
 - [68] Dalton JE, Kaye PM. Immunomodulators: use in combined therapy against leishmaniasis. *Expert Rev Anti Infect Ther* July 2010; 8(7):739–42.
 - [69] van Griensven J, Carrillo E, Lopez-Velez R, Lynen L, Moreno J. Leishmaniasis in immunosuppressed individuals. *Clin Microbiol Infect* April 2014;20(4):286–99.
 - [70] Neumayr AL, Morizot G, Visser LG, Lockwood DN, Beck BR, Schneider S, et al. Clinical aspects and management of cutaneous leishmaniasis in rheumatoid patients treated with TNF-alpha antagonists. *Trav Med Infect Dis* November–December, 2013; 11(6):412–20.
 - [71] Arevalo I, Ward B, Miller R, Meng TC, Najjar E, Alvarez E, et al. Successful treatment of drug-resistant cutaneous leishmaniasis in humans by use of imiquimod, an immunomodulator. *Clin Infect Dis* December 1, 2001;33(11):1847–51.
 - [72] El-On J, Bazarsky E, Sneider R. *Leishmania major*: in vitro and in vivo anti-leishmanial activity of paromomycin ointment (Leshcutan) combined with the immunomodulator Imiquimod. *Exp Parasitol* June 2007;116(2):156–62.
 - [73] Khalili G, Dobakhti F, Mahmoudzadeh-Niknam H, Khaze V, Partovi F. Immunotherapy with Imiquimod increases the efficacy of Glucantime therapy of *Leishmania major* infection. *Iran J Immunol* March 2011;8(1):45–51.
 - [74] Carneiro G, Aguiar MG, Fernandes AP, Ferreira LA. Drug delivery systems for the topical treatment of cutaneous leishmaniasis. *Expert Opin Drug Deliv* September 2012;9(9):1083–97.
 - [75] Singh RK, Srivastava A, Singh N. Toll-like receptor signaling: a perspective to develop vaccine against leishmaniasis. *Microbiol Res* September 6, 2012;167(8):445–51.
 - [76] Portou MJ, Baker D, Abraham D, Tsui J. The innate immune system, toll-like receptors and dermal wound healing: a review. *Vascul Pharmacol* August 2015;71:31–6.

- [77] Dasu MR, Isseroff RR. Toll-like receptors in wound healing: location, accessibility, and timing. *J Invest Dermatol* August 2012; 132(8):1955–8.
- [78] Lin Q, Wang L, Lin Y, Liu X, Ren X, Wen S, et al. Toll-like receptor 3 ligand polyinosinic:polycytidylic acid promotes wound healing in human and murine skin. *J Invest Dermatol* August 2012; 132(8):2085–92.
- [79] Sato T, Yamamoto M, Shimosato T, Klinman DM. Accelerated wound healing mediated by activation of Toll-like receptor 9. *Wound Repair Regen* November–December, 2010;18(6):586–93.
- [80] Machado PR, Lessa H, Lessa M, Guimaraes LH, Bang H, Ho JL, et al. Oral pentoxifylline combined with pentavalent antimony: a randomized trial for mucosal leishmaniasis. *Clin Infect Dis* March 15, 2007;44(6):788–93.
- [81] Jones RG, Martino A. Targeted localized use of therapeutic antibodies: a review of non-systemic, topical and oral applications. *Crit Rev Biotechnol* January 20, 2015:1–15.
- [82] Streit M, Belezny Z, Braathen LR. Topical application of the tumour necrosis factor- α antibody infliximab improves healing of chronic wounds. *Int Wound J* September 2006;3(3):171–9.
- [83] Teich N, Klugmann T. Rapid improvement of refractory pyoderma gangrenosum with infliximab gel in a patient with ulcerative colitis. *J Crohns Colitis* January 2014;8(1):85–6.
- [84] Song D, Lindoso JA, Oyafuso LK, Kanashiro EH, Cardoso JL, Uchoa AF, et al. Photodynamic therapy using methylene blue to treat cutaneous leishmaniasis. *Photomed Laser Surg* October 2011;29(10):711–5.
- [85] Baptista MS, Wainwright M. Photodynamic antimicrobial chemotherapy (PACT) for the treatment of malaria, leishmaniasis and trypanosomiasis. *Braz J Med Biol Res* January 2011; 44(1):1–10.
- [86] van der Snoek EM, Robinson DJ, van Hellemont JJ, Neumann HA. A review of photodynamic therapy in cutaneous leishmaniasis. *J Eur Acad Dermatol Venereol* August 2008;22(8): 918–22.
- [87] Akilov OE, Kosaka S, O'Riordan K, Hasan T. Parasitocidal effect of delta-aminolevulinic acid-based photodynamic therapy for cutaneous leishmaniasis is indirect and mediated through the killing of the host cells. *Exp Dermatol* August 2007;16(8):651–60.
- [88] Kosaka S, Akilov OE, O'Riordan K, Hasan T. A mechanistic study of delta-aminolevulinic acid-based photodynamic therapy for cutaneous leishmaniasis. *J Invest Dermatol* June 2007;127(6): 1546–9.
- [89] Reinhard A, Sandborn WJ, Melhem H, Bolotine L, Chamaillard M, Peyrin-Biroulet L. Photodynamic therapy as a new treatment modality for inflammatory and infectious conditions. *Expert Rev Clin Immunol* May 2015;11(5):637–57.
- [90] Racz E, Prens EP. Phototherapy and photochemotherapy for psoriasis. *Dermatol Clin* January 2015;33(1):79–89.
- [91] Sharma SK, Dai T, Kharkwal GB, Huang YY, Huang L, De Arce VJ, et al. Drug discovery of antimicrobial photosensitizers using animal models. *Curr Pharm Des* 2011;17(13):1303–19.
- [92] Akilov OE, Kosaka S, O'Riordan K, Song X, Sherwood M, Flotte TJ, et al. The role of photosensitizer molecular charge and structure on the efficacy of photodynamic therapy against *Leishmania* parasites. *Chem Biol* August 2006;13(8):839–47.
- [93] Akilov OE, Kosaka S, O'Riordan K, Hasan T. Photodynamic therapy for cutaneous leishmaniasis: the effectiveness of topical phenothiaziniums in parasite eradication and Th1 immune response stimulation. *Photochem Photobiol Sci* October 2007;6(10): 1067–75.
- [94] Dutta S, Ongarora BG, Li H, Vicente Mda G, Kolli BK, Chang KP. Intracellular targeting specificity of novel phthalocyanines assessed in a host-parasite model for developing potential photodynamic medicine. *PLoS One* 2011;6(6):e20786.
- [95] Gupta M, Agrawal U, Vyas SP. Nanocarrier-based topical drug delivery for the treatment of skin diseases. *Expert Opin Drug Deliv* July 2012;9(7):783–804.
- [96] Schroeter A, Engelbrecht T, Neubert RH, Goebel AS. New nano-sized technologies for dermal and transdermal drug delivery. A review. *J Biomed Nanotechnol* October 2010;6(5):511–28.
- [97] Kaur IP, Kakkar S. Topical delivery of antifungal agents. *Expert Opin Drug Deliv* November 2010;7(11):1303–27.
- [98] Pierre MB, Dos Santos Miranda Costa I. Liposomal systems as drug delivery vehicles for dermal and transdermal applications. *Arch Dermatol Res* November 2011;303(9):607–21.
- [99] Zhang Z, Tsai PC, Ramezanli T, Michniak-Kohn BB. Polymeric nanoparticles-based topical delivery systems for the treatment of dermatological diseases. *Wiley Interdiscip Rev Nanomed Nanobiotechnol* 2013 May–June;5(3):205–18.
- [100] Baroli B. Penetration of nanoparticles and nanomaterials in the skin: fiction or reality? *J Pharm Sci* January 2010;99(1):21–50.
- [101] Labouta HI, Schneider M. Interaction of inorganic nanoparticles with the skin barrier: current status and critical review. *Nanomedicine* January 2013;9(1):39–54.
- [102] Rancan F, Blume-Peytavi U, Vogt A. Utilization of biodegradable polymeric materials as delivery agents in dermatology. *Clin Cosmet Investig Dermatol* 2014;7:23–34.
- [103] Choksi AN, Poonawalla T, Wilkerson MG. Nanoparticles: a closer look at their dermal effects. *J Drugs Dermatol* May 2010; 9(5):475–81.
- [104] Landsiedel R, Fabian E, Ma-Hock L, van Ravenzwaay B, Wohlleben W, Wiench K, et al. Toxicity/biokinetics of nanomaterials. *Arch Toxicol* July 2012;86(7):1021–60.
- [105] Knorr F, Lademann J, Patzelt A, Sterry W, Blume-Peytavi U, Vogt A. Follicular transport route—research progress and future perspectives. *Eur J Pharm Biopharm* February 2009;71(2): 173–80.
- [106] Abdel-Mottaleb MM, Try C, Pellequer Y, Lamprecht A. Nanomedicine strategies for targeting skin inflammation. *Nanomedicine (Lond)* August 2014;9(11):1727–43.
- [107] Sinico C, Fadda AM. Vesicular carriers for dermal drug delivery. *Expert Opin Drug Deliv* August 2009;6(8):813–25.
- [108] Puglia C, Bonina F. Lipid nanoparticles as novel delivery systems for cosmetics and dermal pharmaceuticals. *Expert Opin Drug Deliv* April 2012;9(4):429–41.
- [109] Romero EL, Morilla MJ. Highly deformable and highly fluid vesicles as potential drug delivery systems: theoretical and practical considerations. *Int J Nanomedicine* 2013;8:3171–86.
- [110] Mbah CC, Builders PF, Attama AA. Nanovesicular carriers as alternative drug delivery systems: ethosomes in focus. *Expert Opin Drug Deliv* January 2014;11(1):45–59.
- [111] Alnasif N, Zoschke C, Fleige E, Brodwolf R, Boreham A, Ruhl E, et al. Penetration of normal, damaged and diseased skin—an in vitro study on dendritic core-multishell nanotransporters. *J Control Release* July 10, 2014;185:45–50.
- [112] Ostrowski A, Nordmeyer D, Boreham A, Brodwolf R, Mundhenk L, Fluhr JW, et al. Skin barrier disruptions in tape stripped and allergic dermatitis models have no effect on dermal penetration and systemic distribution of AHAPS-functionalized silica nanoparticles. *Nanomedicine* October 2014;10(7):1571–81.
- [113] Smijs TG, Bouwstra JA. Focus on skin as a possible port of entry for solid nanoparticles and the toxicological impact. *J Biomed Nanotechnol* October 2010;6(5):469–84.
- [114] Vogt A, Rancan F, Ahlberg S, Nazemi B, Choe CS, Darvin ME, et al. Interaction of dermatologically relevant nanoparticles with skin cells and skin. *Beilstein J Nanotechnol* 2014;5:2363–73.
- [115] Lowe A, Hunter-Ellul L, Wilkerson M. Nanotoxicology. In: Nasir A, editor. *Nanotechnology in dermatology*. New York: Springer Science; 2013. p. 231–51.

- [116] Comfort KK, Braydich-Stolle LK, Maurer EI, Hussain SM. Less is more: long-term in vitro exposure to low levels of silver nanoparticles provides new insights for nanomaterial evaluation. *ACS Nano* April 22, 2014;8(4):3260–71.
- [117] Dunne A. Inflammasome activation: from inflammatory disease to infection. *Biochem Soc Trans* April 2011;39(2):669–73.
- [118] Neumann S, Burkert K, Kemp R, Rades T, Rod Dunbar P, Hook S. Activation of the NLRP3 inflammasome is not a feature of all particulate vaccine adjuvants. *Immunol Cell Biol* July 2014;92(6):535–42.
- [119] Lonez C, Vandenbranden M, Ruysschaert JM. Cationic lipids activate intracellular signaling pathways. *Adv Drug Deliv Rev* December 2012;64(15):1749–58.
- [120] Carneiro G, Santos DC, Oliveira MC, Fernandes AP, Ferreira LS, Ramaldes GA, et al. Topical delivery and in vivo antileishmanial activity of paromomycin-loaded liposomes for treatment of cutaneous leishmaniasis. *J Liposome Res* March 2010;20(1):16–23.
- [121] Ferreira LS, Ramaldes GA, Nunan EA, Ferreira LA. In vitro skin permeation and retention of paromomycin from liposomes for topical treatment of the cutaneous leishmaniasis. *Drug Dev Ind Pharm* March 2004;30(3):289–96.
- [122] Jaafari MR, Bavarsad N, Bazzaz BS, Samiei A, Soroush D, Ghorbani S, et al. Effect of topical liposomes containing paromomycin sulfate in the course of *Leishmania major* infection in susceptible BALB/c mice. *Antimicrob Agents Chemother* June 2009;53(6):2259–65.
- [123] Bavarsad N, Fazly Bazzaz BS, Khamesipour A, Jaafari MR. Colloidal, in vitro and in vivo anti-leishmanial properties of transfersomes containing paromomycin sulfate in susceptible BALB/c mice. *Acta Trop* October 2012;124(1):33–41.
- [124] Vardy D, Barenholz Y, Cohen R, Zvulunov A, Biton A, Klaus S, et al. Topical amphotericin B for cutaneous leishmaniasis. *Arch Dermatol* July 1999;135(7):856–7.
- [125] Vardy D, Barenholz Y, Naftoliev N, Klaus S, Gilead L, Frankenburg S. Efficacious topical treatment for human cutaneous leishmaniasis with ethanolic lipid amphotericin B. *Trans R Soc Trop Med Hyg* March–April, 2001;95(2):184–6.
- [126] Zvulunov A, Cagnano E, Frankenburg S, Barenholz Y, Vardy D. Topical treatment of persistent cutaneous leishmaniasis with ethanolic lipid amphotericin B. *Pediatr Infect Dis J* June 2003;22(6):567–9.
- [127] Santos CM, de Oliveira RB, Arantes VT, Caldeira LR, de Oliveira MC, Tabosa Egito ES, et al. Amphotericin B-Loaded nanocarriers for topical treatment of cutaneous leishmaniasis: development, characterization, and in vitro skin permeation studies. *J Biomed Nanotechnol* April 2012;8(2):322–9.
- [128] Horta ME, Mendes BP, Roma EH, Noronha FS, Macedo JP, Oliveira LS, et al. Reactive oxygen species and nitric oxide in cutaneous leishmaniasis. *J Parasitol Res* 2012;2012:203818.
- [129] Olekhnovitch R, Ryffel B, Muller AJ, Bousso P. Collective nitric oxide production provides tissue-wide immunity during *Leishmania* infection. *J Clin Invest* April 2014;124(4):1711–22.
- [130] Olivier M, Gregory DJ, Forget G. Subversion mechanisms by which *Leishmania* parasites can escape the host immune response: a signaling point of view. *Clin Microbiol Rev* April 2005;18(2):293–305.
- [131] Costa IS, de Souza GF, de Oliveira MG, Abrahamsohn ID. S-nitrosoglutathione (GSNO) is cytotoxic to intracellular amastigotes and promotes healing of topically treated *Leishmania major* or *Leishmania braziliensis* skin lesions. *J Antimicrob Chemother* June 19, 2013;68.
- [132] Davidson RN, Yardley V, Croft SL, Konecny P, Benjamin N. A topical nitric oxide-generating therapy for cutaneous leishmaniasis. *Trans R Soc Trop Med Hyg* 2000 ;94(3):319–22.
- [133] Riccio DA, Schoenfisch MH. Nitric oxide release: part I. Macromolecular scaffolds. *Chem Soc Rev* May 21, 2012;41(10):3731–41.
- [134] Lancaster Jr JR. Simulation of the diffusion and reaction of endogenously produced nitric oxide. *Proc Natl Acad Sci USA* August 16, 1994;91(17):8137–41.
- [135] Oplander C, Muller T, Baschin M, Bozkurt A, Grieb G, Windolf J, et al. Characterization of novel nitrite-based nitric oxide generating delivery systems for topical dermal application. *Nitric Oxide* January 15, 2013;28:24–32.
- [136] Weller RB. Nitric oxide-containing nanoparticles as an antimicrobial agent and enhancer of wound healing. *J Invest Dermatol* October 2009;129(10):2335–7.
- [137] Quinn JF, Whittaker MR, Davis TP. Delivering nitric oxide with nanoparticles. *J Control Release* May 10, 2015;205:190–205.
- [138] Lopez-Jaramillo P, Rincon MY, Garcia RG, Silva SY, Smith E, Kampeerapappun P, et al. A controlled, randomized-blinded clinical trial to assess the efficacy of a nitric oxide releasing patch in the treatment of cutaneous leishmaniasis by *Leishmania* (V.) *panamensis*. *Am J Trop Med Hyg* July 2010;83(1):97–101.
- [139] Han G, Nguyen LN, Macherla C, Chi Y, Friedman JM, Nosanchuk JD, et al. Nitric oxide-releasing nanoparticles accelerate wound healing by promoting fibroblast migration and collagen deposition. *Am J Pathol* April 2012;180(4):1465–73.
- [140] Nilforoushzadeh MA, Shirani-Bidabadi LA, Zolfaghari-Baghbaderani A, Jafari R, Heidari-Beni M, Siadat AH, et al. Topical effectiveness of different concentrations of nanosilver solution on *Leishmania major* lesions in Balb/c mice. *J Vector Borne Dis* December 2012;49(4):249–53.
- [141] Larese FF, D'Agostin F, Crosera M, Adami G, Renzi N, Bovenzi M, et al. Human skin penetration of silver nanoparticles through intact and damaged skin. *Toxicology* January 8, 2009; 255(1–2):33–7.
- [142] Rigo C, Ferroni L, Tocco I, Roman M, Munivrana I, Gardin C, et al. Active silver nanoparticles for wound healing. *Int J Mol Sci* 2013;14(3):4817–40.
- [143] Brandt O, Mildner M, Egger AE, Groessl M, Rix U, Posch M, et al. Nanoscale silver possesses broad-spectrum antimicrobial activities and exhibits fewer toxicological side effects than silver sulfadiazine. *Nanomedicine* May 2012;8(4):478–88.
- [144] Jebali A, Kazemi B. Nano-based antileishmanial agents: a toxicological study on nanoparticles for future treatment of cutaneous leishmaniasis. *Toxicol In Vitro* September 2013;27(6):1896–904.
- [145] Gunasekaran T, Nigusse T, Dhanaraju MD. Silver nanoparticles as real topical bullets for wound healing. *J Am Coll Clin Wound Spec* December 2011;3(4):82–96.
- [146] Dragicevic-Curic N, Fahr A. Liposomes in topical photodynamic therapy. *Expert Opin Drug Deliv* August 2012;9(8):1015–32.
- [147] Chatterjee DK, Fong LS, Zhang Y. Nanoparticles in photodynamic therapy: an emerging paradigm. *Adv Drug Deliv Rev* December 14, 2008;60(15):1627–37.
- [148] Fang YP, Wu PC, Tsai YH, Huang YB. Physicochemical and safety evaluation of 5-aminolevulinic acid in novel liposomes as carrier for skin delivery. *J Liposome Res* 2008;18(1):31–45.
- [149] Montanari J, Maidana C, Esteva MI, Salomon C, Morilla MJ, Romero EL. Sunlight triggered photodynamic ultradeformable liposomes against *Leishmania braziliensis* are also leishmanicidal in the dark. *J Control Release* November 1, 2010;147(3):368–76.
- [150] Hernandez IP, Montanari J, Valdivieso W, Morilla MJ, Romero EL, Escobar P. In vitro phototoxicity of ultradeformable liposomes containing chloroaluminum phthalocyanine against New World *Leishmania* species. *J Photochem Photobiol B* December 5, 2012;117:157–63.
- [151] Deda DK, Pavani C, Carita E, Baptista MS, Toma HE, Araki K. Control of cytolocalization and mechanism of cell death by encapsulation of a photosensitizer. *J Biomed Nanotechnol* August 2013;9(8):1307–17.
- [152] Orłowski P, Krzyżowska M, Zdanowski R, Winnicka A, Nowakowska J, Stankiewicz W, et al. Assessment of in vitro

- cellular responses of monocytes and keratinocytes to tannic acid modified silver nanoparticles. *Toxicol In Vitro* September 2013; 27(6):1798–808.
- [153] Rubert Nogueira D, Carmen Moran M, Mitjans M, Martinez V, Perez L, Pilar Vinardell M. New cationic nanovesicular systems containing lysine-based surfactants for topical administration: toxicity assessment using representative skin cell lines. *Eur J Pharm Biopharm* January 2013;83(1):33–43.
- [154] Kendall AC, Nicolaou A. Bioactive lipid mediators in skin inflammation and immunity. *Prog Lipid Res* January 2013; 52(1):141–64.
- [155] Headland SE, Norling LV. The resolution of inflammation: principles and challenges. *Semin Immunol* April 21, 2015;27.
- [156] Wang Z, Li J, Cho J, Malik AB. Prevention of vascular inflammation by nanoparticle targeting of adherent neutrophils. *Nat Nanotechnol* March 2014;9(3):204–10.
- [157] Moreno E, Schwartz J, Larrea E, Conde I, Font M, Sanmartin C, et al. Assessment of beta-lapachone loaded in lecithin-chitosan nanoparticles for the topical treatment of cutaneous leishmaniasis in *L. major* infected BALB/c mice. *Nanomedicine* November 2015;11(8):2003–12.
- [158] Frankenburg S, Glick D, Klaus S, Barenholz Y. Efficacious topical treatment for murine cutaneous leishmaniasis with ethanolic formulations of amphotericin B. *Antimicrob Agents Chemother* December 1998;42(12):3092–6.
- [159] Kalat SA, Khamesipour A, Bavarsad N, Fallah M, Khashayarmanesh Z, Feizi E, et al. Use of topical liposomes containing meglumine antimoniate (Glucantime) for the treatment of *L. major* lesion in BALB/c mice. *Exp Parasitol* August 2014;143:5–10.

Nanotechnology-Based Nano-Bullets in Antipsoriatic Drug Delivery: State of the Art

M. Rahman¹, S. Beg², F. Anwar³, F.A. Al-Abbasi³, V. Kumar¹

¹Sam Higginbottom Institute of Agriculture, Technology & Sciences (SHIATS), Allahabad, India; ²Panjab University, Chandigarh, India; ³King Abdul-Aziz University, Jeddah, Kingdom of Saudi Arabia

OUTLINE

Introduction	157	Emulsion-Based Nanocarriers	164
Pathophysiology and Pharmacotherapy for Psoriasis	157	Polymeric Nanocarriers	164
Nanomedicines for Antipsoriatic Drug Therapy	160	Conclusion	165
Lipid Based Vesicular Nanocarriers	160	References	165
Nanoparticulate Carriers	163		

INTRODUCTION

Psoriasis is a T cell-mediated autoimmune-based skin disorder characterized by skin inflammation, keratinocyte proliferation, and differentiation. It is also an important risk factor for cardiovascular disease. Globally, psoriasis affects 2–4% of the world's population. It may appear in various forms such as plaque psoriasis, guttate psoriasis, pustular psoriasis, and erythrodermic psoriasis [1]. Spontaneous remission and relapse are not uncommon. Although etiology is still unclear, environmental factors and several other factors such as streptococcal infection, cutaneous trauma, drugs, alcohol, cigarette smoking, and exposure to ultraviolet (UV) radiation may aggravate psoriasis [2]. Several drugs are available for treatment of psoriasis but their prolonged use causes severe toxicity and it could provide only limited benefits. There is no complete cure of management of psoriasis. The challenges in the treatment of psoriasis thus call for the effective and safe delivery systems [1,2]. An extensive study has demonstrated that nanomedicine as a drug vehicle can be effective in the treatment of psoriasis [1,2].

Nanomedicines have unique advantages over conventional drug carriers. They have high drug loading capacity, specific targeted action, cause reduced side effects, and enhance patient compliance, which makes the nanoparticle an attractive drug delivery system [3]. However, challenges still exist regarding their wide acceptance, due to high cost of production, stability, reproducibility, safety, and regulatory obstacles [3]. The present chapter gives an overview on various targeted nanomedicines for effective treatment of psoriasis. Pathophysiology involved in psoriasis, available therapies, and their challenges are also covered.

PATHOPHYSIOLOGY AND PHARMACOTHERAPY FOR PSORIASIS

T lymphocyte activation is a principle pathway involved in pathogenesis of psoriasis. Epidermis and dermis are populated with antigen-presenting cells which can pick up the antigen and present it on their cellular surface in the context of major histocompatibility complex (MHC) molecules. Antigen is ultimately

transported to lymph nodes and binding with T lymphocyte receptors produces T cell activation and further formation of synapses such as cluster differentiation 2 (CD2) and lymphocyte functional antigen (LFA-3), etc. Thus, an activated T cell rapidly enters into systemic circulation and further migrates to various skin layers, which ultimately produces various cytokines and chemokines (Fig. 12.1). This process is responsible for hyperkeratosis and neovascularization in psoriasis [1,2]. Dendritic cells (DCs) and macrophages are associated with CD4 and CD8-T cells, which are profound in psoriatic lesions. They are responsible for cytokines production such as IL-12, IL-23, and TNF- α and β . These cytokines regulate the production of T helper (Th1) and Th17/Th22 cells, which further leads to production of IL-4, IL-13, IL-5 IL-17A, and IL-23R [2,4]. Among all, IL-17A and IL-23R were reported

as leading biomarkers for keratinocyte hyperproliferation in psoriasis [5,6]. Moreover, there are several predisposing factors in the pathogenesis of psoriasis which include eicosanoid metabolism, lymphokine secretion, and free radical generation [4,7]. Current pharmacotherapy for psoriasis includes vitamin D analogs, corticosteroids, dithranol, coal tar, retinoids, tacrolimus, babchi oil, and 8-methoxypsoralen with UVA radiation (PUVA), which are delivered either topically or through the systemic route [1,2]. These are enlisted in Table 12.1. Topical therapies gained wider popularity in psoriasis treatment, but they suffer from limited absorption of drugs through skin, limiting their therapeutic effectiveness [3]. Systemic administration of drug such as methotrexate, cyclosporine, hydroxycarbamide, fumaric acid esters, etc. But these have numerous limitations such as immunosuppression,

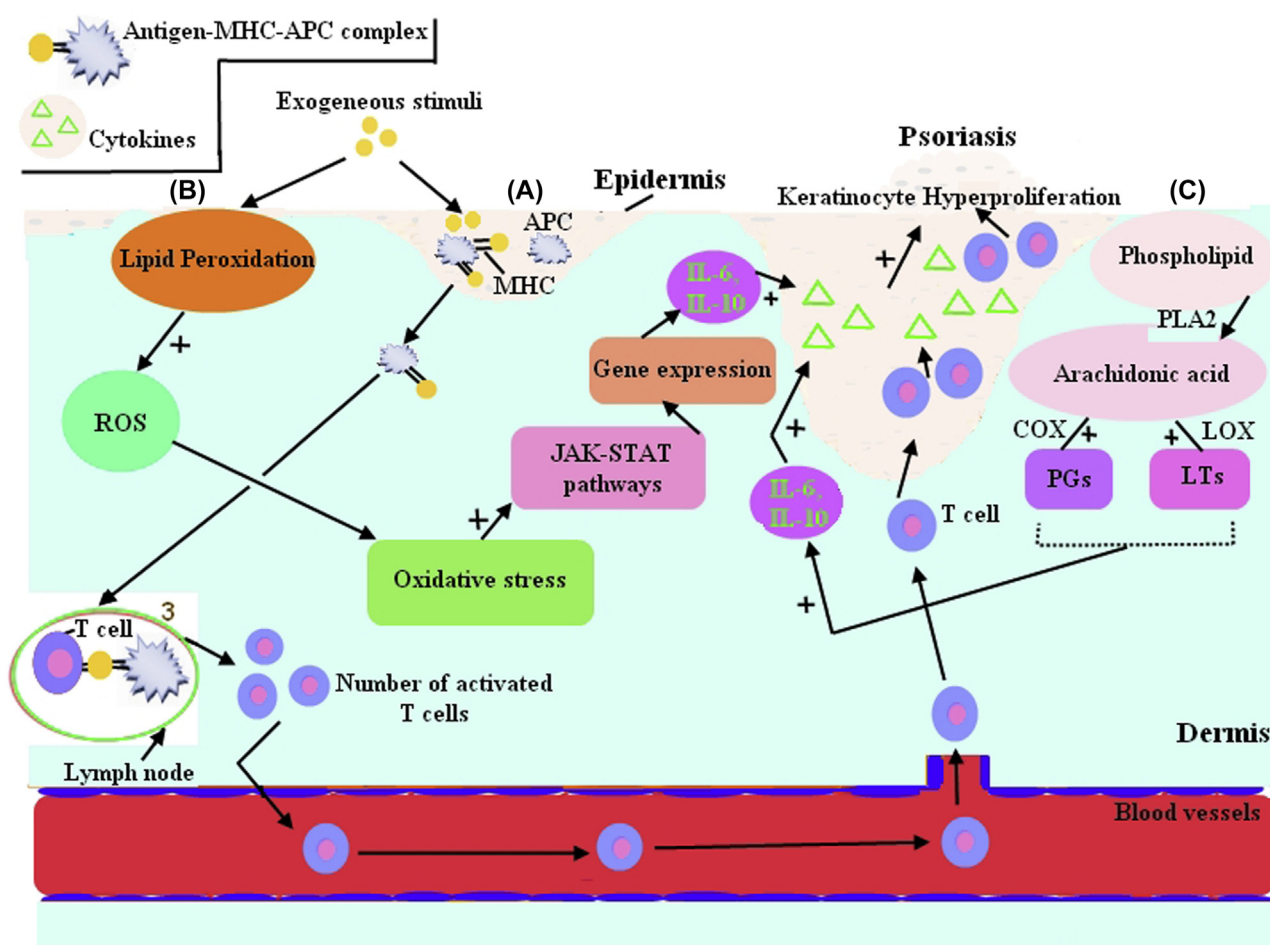


FIGURE 12.1 Various eminent pathways in the pathogenesis of psoriasis: (A) Exogenous stimuli produce reactive oxygen species (ROS), their accumulation leads to oxidative stress, which stimulates the JAK-STAT pathway and regulates gene expression and keratinocyte hyperproliferation in psoriasis. (B) Binding of antigen to major histocompatibility complex (MHC) of antigen-presenting cells to form a complex, which migrates to the lymph nodes and produces a number of activated T cells; T cells through the blood vessels reach the epidermis and release cytokines, which stimulate keratinocyte hyperproliferation. (C) Cell membranes are composed of phospholipids; an enzymatic action produces arachidonic acid (AA), which acts as a substrate for prostaglandins (PGs) and leukotriens (LTs), that are responsible for IL secretion and keratinocyte hyperproliferation in psoriasis.

TABLE 12.1 Current Psoriasis Pharmacotherapy With Conventional Formulation

Antipsoriatic drugs	Route of administration	Advantages	Limitations	References
Corticosteroids	Topical	<ul style="list-style-type: none">Convenient and effective	<ul style="list-style-type: none">Possible risk of remission of psoriasis and cutaneous atrophyCalcipotriol causes irritant reactionTacalcitol causes risk of hypercalcemiaNeed constant treatment	[1]
Vitamin D analogs (calcipotriol, tacalcitol)				
Emollients		<ul style="list-style-type: none">Easy in application and effective	<ul style="list-style-type: none">Need constant treatmentLimited in efficacy	[2]
Dithranol (anthralin)		<ul style="list-style-type: none">Safe and effective	<ul style="list-style-type: none">Causes skin irritation and skin staining	[2]
Tar (crude coal tar, tar extracts)		<ul style="list-style-type: none">Effective and safe	<ul style="list-style-type: none">Has unpleasant smell, long contact time required, and possible risk of carcinogenicity	[1,2]
Retinoids (tazarotene)		<ul style="list-style-type: none">Effective and safe	<ul style="list-style-type: none">Causes irritation and teratogenic	[1,2]
Tacrolimus		<ul style="list-style-type: none">Highly effective in face psoriasis	<ul style="list-style-type: none">Restricted with combination of phototherapy and causes burning sensation	[1,2]
Phototherapy				
UV light	Topical	<ul style="list-style-type: none">Effective	<ul style="list-style-type: none">Causes squamous cell carcinoma	
UVB (290–320 nm); produces broad bands of wavelength		<ul style="list-style-type: none">Effective	<ul style="list-style-type: none">Leads to carcinogenicity	[2,3]
UVA (320–400 nm)		<ul style="list-style-type: none">More effective when applied with a photosensitizing agent such as psoralen	<ul style="list-style-type: none">Produces skin irritation and carcinogenic	[2,3]
				[2,3]
Cyclosporine	Systemic (Oral and Parentera)	<ul style="list-style-type: none">Effective and relatively safe	<ul style="list-style-type: none">Immune suppression, nephrotoxicity, and hypertension	
Fumaric acid esters		<ul style="list-style-type: none">Safe and effective	<ul style="list-style-type: none">Causes flushing, diarrhea, and lymphopenia	[1–3]
Hydroxyurea		<ul style="list-style-type: none">Effective and compatible in renal or hepatic impairment psoriatic patient	<ul style="list-style-type: none">Produces bone marrow suppression	[1–3]
Methotrexate		<ul style="list-style-type: none">Effective	<ul style="list-style-type: none">Drawbacks such as bone marrow suppression, nausea, and hepatic fibrosis	[2,3]
Biological agents				
Adalimumab	Systemic (IV and SC)	<ul style="list-style-type: none">More effective	<ul style="list-style-type: none">Has a high cost, causes immunosuppression, and can be administered only with injection	[1,2]
Etanercept		<ul style="list-style-type: none">More effective	<ul style="list-style-type: none">Has a high cost, causes immunosuppression, and can be administered only with injection	[1,2]
Infliximab		<ul style="list-style-type: none">Quick action and more effective	<ul style="list-style-type: none">Has a high cost, causes immunosuppression, and can be administered only with injection	[1]
Ustekinumab		<ul style="list-style-type: none">Highly effective	<ul style="list-style-type: none">Has a high cost, causes immunosuppression, and can be administered only with injection	[1]

UVA, Ultraviolet A; UVB, Ultraviolet B.

suboptimal therapeutic effects, poor patient compliance, and significant toxicity [3]. Other than these therapies, biological agents have been employed in psoriasis treatment. Biological agents are proteins which are obtained from microorganisms and exhibit fewer side effects. However, they are not common in clinical practice due to their immunosuppressive effects, high cost, and availability in only injection form which leads to poor patient compliance [1,2].

NANOMEDICINES FOR ANTIPSORIATIC DRUG THERAPY

Nanomedicines, or nanocolloidal carriers, are growing as versatile nanocarriers, owing to their unique features and spectacular importance in antipsoriatic drug delivery. They are mainly classified as lipid based and polymeric nanocarriers [2,3,8,9]. Lipid-based nano-vehicles include vesicular carriers, particulate carriers, and emulsion-based carriers, while polymeric carriers subclassify as particulate and capsular carriers [10].

Lipid Based Vesicular Nanocarriers

Lipid based vesicular nanocarriers are mainly composed of physiological lipids; they may further be classified as liposomes, ethosomes, niosomes, and transfersomes. Liposome is a vesicular nanocarrier, which may compose of phospholipids and cholesterol. Its size varies from nanometer to several 100 micrometers, depending on whether it is a unilamellar or multilamellar vesicle [11]. They can encapsulate hydrophilic and hydrophobic drugs in the central core and in bilayer, respectively. Moreover, they exhibit higher encapsulation efficiency, enhanced biocompatibility, and controlled drug release [11]. Dithranol is an old drug used in treatment of psoriasis which acts through IL receptors of keratinocyte cells. However, it does not penetrate well through the skin, cause irritation and staining of the skin [2]. Katare et al. have developed dithranol-loaded liposomes and applied against plaque psoriasis at a reduced dose of 0.5%. As a result, the group found greater efficacy as compared to 1.15% dithranol ointment [12]. Reactive oxygen species (ROS) are oxygen-centered radicals; their overproduction and reduced elimination results in oxidative stress. This may alter the function of keratinocytes in psoriasis by acting on various signaling pathways such as MAPK, NF- κ B, and Janus kinase signal transducers [1]. Antioxidants have been beneficial in treatment of psoriasis [1]. Resveratrol is an antioxidant, used in management of psoriasis [13]. In one study, resveratrol was loaded in transfersomes with 70% encapsulation efficiency and demonstrated higher skin permeation across porcine skin

while inhibiting the production of ROS and lipid peroxidation in H₂O₂ stimulated human keratinocyte cells [14]. An ex vivo study compared niosomes and liposomes containing resveratrol in terms percutaneous absorption, and concluded that niosomes showed better behavior than liposomes [15]. Cyclosporine A (CsA) is an immunosuppressant drug and widely used in management of psoriasis by blocking the activity of T cells via binding of cytosolic immunophilin. Their application is hindered due the systemic toxicity and restricted permeation [2,4,16]. To overcome these limitations, researchers have developed CsA-loaded lecithin vesicular carriers and delivered them through a transdermal route. Higher skin permeation was observed, which may be attributed to the flexibility of vesicles [17]. In another study iontophoresis was applied on lecithin vesicular carrier with monoolein which acts as a permeation enhancer; they received appreciable drug transport across the human cadaver skin [18]. Similarly, Verma et al. reported enhanced CsA skin permeation with ethosomes [19]. Another group of researchers developed multicompartamental liposomes and a micro-emulsified system and found enhanced skin permeation of CsA through psoriatic skin [20]. M-tetrahydroxyphenylchlorin (mTHPC) loaded cationic flexible liposomes were also investigated for their use in photodynamic therapy of psoriasis; higher stability, and greater skin permeation as compared to conventional liposomes, neutral, and anionic liposomes were reported. These properties of mTHPC may be attributed to the presence of cations on the vesicles [21,22]. Tamoxifen is an antiestrogen prodrug and reported to be beneficial in psoriasis. It is metabolized by the liver to its active metabolite 4-hydroxytamoxifen which has a higher affinity to estrogen receptor than tamoxifen itself. Applications of tamoxifen are limited due to inappropriate solubility, limited absorption, and systemic side effects [23]. To overcome these obstacles, Katare et al. developed multilamellar topical liposomes for tamoxifen delivery. Higher skin permeation and drug retention were observed [24].

Methotrexate (MTX; 4 amino-N10 methyl pterolglutamic acid) is a potent immune-modulating drug, widely used for severe and recalcitrant psoriasis. It inhibits the conversion of dihydrofolate to tetrahydrofolate, in turn results in inhibition of DNA and RNA synthesis [1,2]. Although MTX's exact mechanism of action on psoriasis is not well understood, studies demonstrate that MTX exerts its antiinflammatory effects via promoting intracellular accumulation of 5-aminoimidazole-4-carboxamide ribonucleotide which in turn increases adenosine release [1–4]. In an attempt to avoid systemic side effects of MTX, liposomal MTX hydrogel was tested on six psoriasis patients in conjunction with an 80-J diode laser, and the results

showed that during 8 months follow-up, 60% of the patients had no recurrence [25].

Emulsomes, a different type of vesicular nanocarrier, are proven to be highly efficacious in treatment of topical diseases including psoriasis by reducing the problems such as incompatibility with skin. As previously discussed, dithranol, although a highly effective drug for psoriasis, has limitations and unwanted effects for patients. To overcome these limitations, dithranol was encapsulated into emulsomes, which was reported to enhance antipsoriatic activity in an *in vivo* model. In addition to enhanced skin permeation and retention, unlike dithranol administered alone, dithranol-loaded emulsomes were quite nonirritant [26].

Trotta et al. have prepared elastic liposomes by utilizing phosphatidylcholine and dipotassium glycyrrhizinate for the topical delivery of MTX. They have found three to four times higher skin permeation as compared to conventional liposomes [27].

Ethosomes are ethanol-based lipid vesicular nanocarriers. Presence of high amount of ethanol in vesicles may help in easy penetration of drugs into the stratum corneum [3]. Due to this unique feature, they are suitable agents for the treatment of skin disease [3]. Photodynamic therapy with 5-aminolevulinic acid (5-ALA) was found to be beneficial for psoriasis; however 5-ALA has poor penetration ability into the skin [28]. To overcome this problem, researchers tested the use of ethosomes for delivery of ALA and achieved enhanced skin permeation of the drug in psoriasis lesions [29]. Temoporfin (mTHPC) is a potent second generation

synthetic photosensitizer with low penetration ability, but when loaded into ethosomes they showed higher skin penetration through abdominal skin as compared to liposomes [30]. In a separate study tacrolimus loaded into ethosomes exhibited higher entrapment efficiency with higher skin permeation as compared to liposomes [31]. MTX has also been loaded into ethosomes and when tested on human cadaver skin, they showed higher transdermal flux with decreased lag time [32].

Niosomes are nonionic surfactant-based lipid vesicular nanocarriers; they have the ability to encapsulate both hydrophobic and hydrophilic drugs [33]. As compared to liposomes and ethosomes, they have better resistance against oxidation. Niosomes have been widely investigated for psoriasis treatment as they can minimize side effects of the current drugs and improve patient compliance [33]. Katare et al. have prepared dithranol-encapsulated niosomes cream, and reported enhanced flux up to $7.78 \mu\text{g}/\text{cm}^2/\text{h}$ on mouse abdominal skin whereas conventional cream showed only $4.10 \mu\text{g}/\text{cm}^2/\text{h}$ [12]. In a double blind controlled clinical study, niosomal MTX in chitosan gel was compared to a conventional MTX gel for efficacy, tolerability, and patient compliance. After 3 months, both psoriasis area and severity index were significantly reduced and niosome MTX in chitosan gel was found to be better in all three aspects investigated [34]. Various nano-bullets investigated as delivery vehicles for the treatment of psoriasis are illustrated and summarized in Fig. 12.2 and Table 12.2, respectively. Gidwani reported that dithranol in combination with and without salicylic

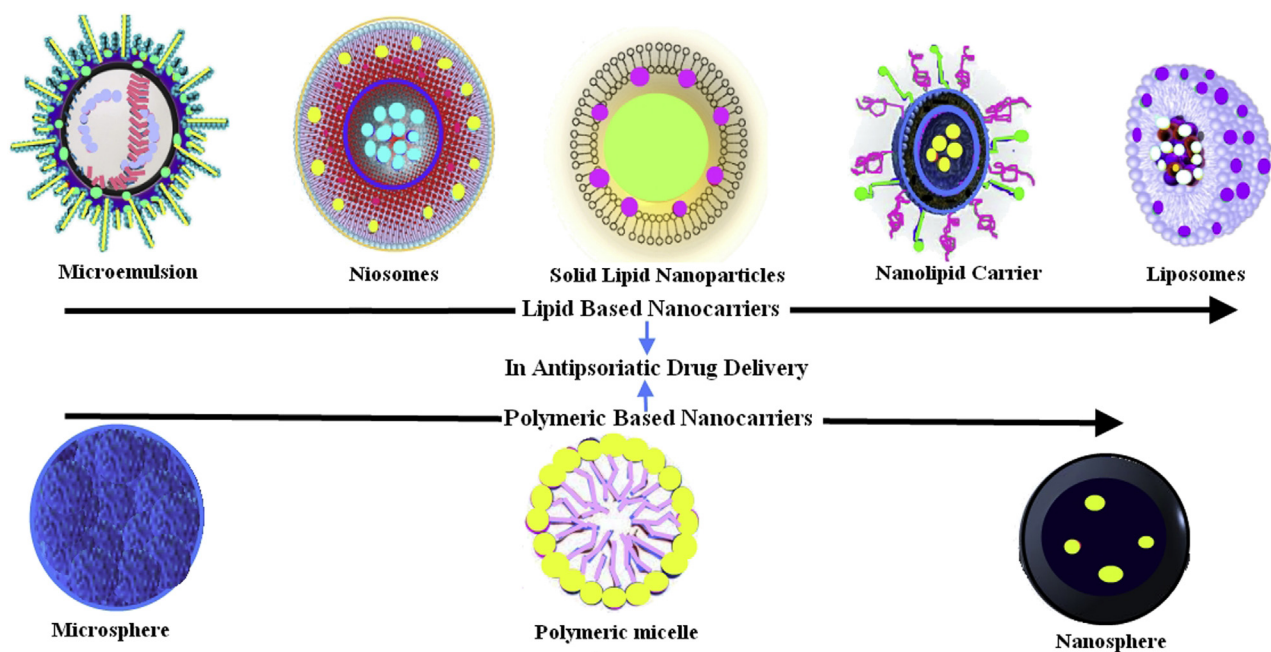


FIGURE 12.2 Nano-bullets in antipsoriatic drug delivery.

TABLE 12.2 Nanocarriers in Antipsoriatic Drug Delivery

Antipsoriatic drug molecules	Nano-bullets	Outcomes	References
Clobetasol propionate	Microspheres	Showed prolonged drug release as compared to conventional cream	[64]
Betamethasone dipropionate (BD) with salicylic acid	Microemulsion gel	Three times higher inhibition of inflammation compared to a marketed formulation	[57]
Betamethasone 17-valerate (BMV)	Solid lipid nanoparticles (SLN)	Increased permeation and presence of monostearin-enabled specific targeting to epidermal cells in psoriasis lesions	[42]
BD	Hydrogel thickened nanoemulsion	Better stability and permeation and presence of omega-3 fatty acids as oil phase synergized the antiinflammatory action over placebo	[60]
Dithranol	Liposomes	0.5% dithranol-loaded lipogel was applied to 20 psoriasis patients; they received better permeation and enhanced efficacy with lower staining	[12]
Dithranol	Niosomes	Better skin permeation in laca mice over conventional cream	[12]
Cyclosporin A (CsA)	Iontophoresis based lecithin vesicular carriers	Provided better site specific targeted action in psoriasis as compared to microemulsion	[18]
CsA	Multicompartmental liposomes and microemulsified systems	High entrapment efficiency (EE) and better compliance was achieved	[20]
Tacrolimus	Microemulsion	Provides higher drug permeation, while in ointment form shows lesser penetration	[3]
Tacrolimus	Modified nanolipid carrier (MNLC)	They provide better skin penetration, avoid biodisposition to other organs and produce less irritation in guinea pig as compared to commercial ointment	[50]
Methotrexate (MTX)	Elastic liposomes	Three to four times higher skin permeation of dipotassium glycyrrhizinate for MTX delivery across in porcine skin as compared to conventional liposomes	[27]
MTX	Niosomal systems in chitosan gel (0.25%)	Three times reduction in PASI better efficacy compared to a marketed formulation	[34]
MTX	SLNs	Tested on 24 psoriasis patients. Improved therapeutic index in terms of average percent improvement in healing of lesions and reduction in degree of erythema	[43]
MTX	Ethosomes	Higher skin flux in human cadaver skin as compared to liposomes	[32]
MTX	O/W microemulsion gel	Higher percentage of skin retention of MTX over microemulsion	[3]
Babchi oil (<i>Psoralea corylifolia</i>)	Microemulsion gel	Higher skin permeation and enhanced accumulation of psoralen without systemic side effects	[62]
Tretinoin (TTN)	Liposomes, niosomes, SLNs, and nanocapsules	Enhanced efficacy, less skin irritation, and more sustained release	[49,50]
TRE	SLNs	Higher EE and enhanced permeation	[49]
Acitretin	Nanostructured lipid carriers (NLCs)	Higher EE and 81.38% acitretin skin deposition, whereas skin deposition was 47.28% for acitretin conventional gel	[48]
Resveratrol	Liposomes	Higher stability and loading efficiency	[15]
Resveratrol	Transferosomes	Higher skin permeation in porcine skin and enhanced therapeutic efficacy in psoriasis	[14]

BD, Betamethasone dipropionate; SLN, solid lipid nanoparticles; KG, dipotassium glycyrrhizinate; MTX, methotrexate; CsA, cyclosporine A; NLCs, nanostructured lipid carriers; APIH, average percent improvement in healing; PASI, psoriasis area and severity index; ROS, reactive oxygen species; MOP, methoxy psoralen; EE, entrapment efficiency; Act, acitretin; PEG, polyethylene glycol; TTN, tretinoin; MNLC, modified nanolipid carrier; BMV, Betamethasone 17-valerate.

acid were loaded into mixed vesicular systems and tested on 12 psoriatic patients. Patients were followed up for 4 weeks, and authors reported enhanced efficacy, absence of irritation and staining problems [35]. Transfersomes are known to be elastic liposomes with better penetration ability than conventional liposomes. Curcumin has been suggested to have antiinflammatory effects in psoriasis via inhibition of IL-1 β /IL-6 and indirectly downregulating IL-17A/IL-22 which both have an impact on impacting the IL-23/IL-17A axis [36]. However curcumin has limited transdermal delivery efficacy, poor stability, and can stain skin as well as clothes during treatment [36]. In an attempt to enhance its delivery by taking the advantage of transfersomes, curcumin-loaded lecithin gel has been developed and compared to a marketed curcumin gel. The proposed system was found to be more stable, demonstrated higher entrapment efficiency, improved permeability of curcumin over time, and can be used as a self-penetration enhancer [36]. Tar is obtained from coal at temperatures between 900 and 1200 °C. It exerts its effects against psoriasis by suppression of DNA synthesis in keratinocytes. Conventional loaded preparation has many drawbacks such as skin irritation and cloth staining, and it is difficult to remove by washing [2]. To avoid these problems, tar has been loaded into lipid-based lecithinized self-assembled nanocarriers which provided targeted action and covered large surface area of skin with minimum skin irritation and staining [37].

Nanoparticulate Carriers

Solid lipid nanoparticles (SLNs) are lipid-based nanoparticulate carriers with a size range from 50 to 1000 nm [38]. They are composed of phospholipids dispersed in the aqueous solution of surfactant. It has meticulous properties such as enhanced biocompatibility, availability of high surface area, high drug loading, and extended drug release [39]. Another type is nanostructured lipid carriers (NLCs), which are composed of solid lipid and liquid lipids. It provides higher stability, enhanced biocompatibility, and higher skin permeation across the skin [40–41].

Betamethasone 17 valerate was loaded into SLNs with the help of monostearin; for localized skin delivery, the results revealed higher therapeutic effects with minimum adverse events [42]. To minimize systemic side effects of MTX, it was loaded into SLN gel which was applied on 24 psoriasis patients for up to 6 weeks, and resulted in improved healing of lesions and significant reduction in average score of erythema and scaling [43]. Tacrolimus (FK506) is a macrolide immunosuppressant. It is obtained from fermentation broth of *Streptomyces tsukubaensis* and has been widely used in treatment of psoriasis, exerting its effects via acting on

FKBP-immunophilin (cytoplasmic receptor) and inhibition of the T lymphocyte activation [44]. FK506 has been loaded into SLNs (FK506-SLNs) and converted into a gel. Higher entrapment efficiency with greater skin permeation and retention was observed as compared to ointment [45]. Triptolide (TP) is a diterpenoid triepoxide obtained from *Tripterygium wilfordii*. It is effective against psoriasis due to its strong inhibitory action on DCs, T cells, and T helper's cells [46]. However, it has poor water solubility and has several side effects such as diarrhea, skin rashes, and pigmentation [46]. To alleviate its disadvantages, it has been loaded into SLN to enable controlled release [47]. Better skin penetration as well as enhanced antiinflammatory activity was achieved, but the authors suggested further studies on toxicity of different formulations of triptolide.

Acitretin is a second-generation retinoid; it controls cell differentiation, keratinocyte hyperproliferation and reduce cellular inflammation in psoriasis by acting on the retinoic acid receptor (PAR α , β , and γ) and retinoid X receptor (RXR α , β , and γ). Conventional formulation for acitretin delivery has several drawbacks including limited solubility, bioavailability, instability, and higher systemic toxicity [2,4]. To minimize these problems, acitretin loaded into NLC gel, which enabled 80% drug release whereas acitretin suspension provided only 46.2% drug release [48]. Furthermore, improvement in therapeutic index as well as a reduction in psoriatic index was observed [48].

Tretinoin (TTN) is natural retinoid, similar in action to isotretinoin. There are several reports regarding its use in treatment of psoriasis. However, it also has several drawbacks such as instability, limited permeation, and improper bioavailability [2]. Recently, it has been loaded into SLNs to achieve higher encapsulation efficiency, better skin permeation, and lesser skin irritation as compared to methanolic TTN solution [49]. In another study when loaded into NLCs, they received better photostability compared to liposomes, ethosomes, and niosomes [50]. Tacrolimus have limited penetration ability; to overcome this problem, modified nanolipid nanocarrier was utilized, which improved entrapment efficiency, skin penetration, and stability [51]. Vitamin D and its analogs such as calcitriol, calcipotriol, maxacalcitol, and tacalcitol inhibit IL-8 production, which results in decreased keratinocyte proliferation and differentiation. They have numerous disadvantages, such as getting rapidly metabolized [52]. Lin et al. developed lipophilic calcipotriol and hydrophilic MTX-loaded NLCs to provide dual therapy with enhanced skin permeation and reduced skin irritation. Dual drug-loaded NLCs demonstrated reduced skin permeation of calcipotriol but in case of MTX amount permeating the skin was around three times greater than the control [53]. Capsaicin is a tetra-terpenoid obtained

from red pepper. It is effective against psoriasis by causing downregulation of the translation of HIF-1 α mRNA and TRPV1 receptors, which are upregulated in keratinocytes of psoriasis [54]. It leads to inhibition of abnormal keratinocyte hyperproliferation in psoriasis lesions. Conventional formulations have limited skin permeation; to overcome this problem it was loaded into SLNs and NLCs, which both showed higher capsaicin skin permeation [55].

Emulsion-Based Nanocarriers

Emulsion-based nanocarriers are produced by mixing a water-immiscible oil phase into an aqueous phase with a high-stress, mechanical extrusion process. They are subclassified as microemulsion and nanoemulsion. Microemulsion is an isotropic dispersion of lipids, surfactants, and cosurfactants. They have been widely investigated in topical drug delivery, due to their high surface area and permeation [56]. Corticosteroids, owing to their immunosuppressive, antiinflammatory, and antiproliferative properties, are widely used in the treatment of psoriasis, but their use is restricted due to the cutaneous and systemic side effects [2,7]. To improve their safety profile, researchers have developed nanocarriers for their delivery in psoriasis treatment. Baboota et al. developed betamethasone dipropionate and salicylic acid-loaded microemulsion gel, and when applied topically, 72.1% reduction in inflammatory response was observed as compared to the marketed gel with 43.9% reduction only. This could be attributed to enhanced drug penetration via skin [57]. Omega-3 fatty acids were reported to exhibit beneficial effects in treatment of psoriasis by indirect inhibition of 5-lipoxygenase of mononuclear cells, thus limiting the synthesis of pro-inflammatory leukotriene's [58]. Rahman et al. prepared omega-3 fatty acid-loaded microemulsion gel by using linseed oil and showed higher skin permeation for better management of psoriasis [59]. In a different study investigators developed nanoemulsion gel containing fish oil as the oil phase for topical delivery of betamethasone dipropionate, and showed 87.64% inhibition in inflammation associated with psoriasis [60].

As mentioned earlier, curcumin has limited bioavailability and transdermal delivery is challenging, although there is ongoing research aiming to overcome these obstacles [36]. Liu and Chang studied the solubility of curcumin in various oils, surfactants, and cosurfactants to find the optimal components that can be used for an ideal transdermal delivery vehicle for curcumin. Among several microemulsion systems, composed of eucalyptol, polysorbate 80, ethanol, and water, the eucalyptol microemulsion system was found to be the most promising [61]. Betamethasone dipropionate-loaded nanoemulsion-based hydrogels have been developed

with eucalyptus oil and babchi oil and tested in vivo as a potential vehicle for topical delivery in treatment of psoriasis. In addition to acting as a vehicle for nano emulsion, babchi oil itself exerts antipsoriatic activity owing to having psoralen as its chief constituent [62]. The optimized formulation demonstrated chemical stability, high viscosity, enhanced permeation, and sustained the drug release for the desired period of time. Inhibition of edema was observed at 77.83% while the marketed gel used as a comparison showed only 40.97% inhibition. In addition to improved antiinflammatory activity, presence of eucalyptus oil's antiseptic properties prevented microbial infection in the treated area [62].

Polymeric Nanocarriers

Microspheres are examples of polymeric nanocarriers having a size range of 1 to 1000 μm . They provide sustained drug delivery with reduced dosing frequency and enhanced patient compliance [63]. Furthermore, they have the ability to increase the drug targeting specificity. Microsphere-based topical formulations have gained wider importance in the treatment of psoriasis due to their ability for controlled drug delivery and enhanced therapeutic effectiveness for prolonged periods of time [63]. Clobetasol is a potent corticosteroid used in treatment of psoriasis. It was loaded into polylactic-co-glycolic acid microspheres and prolonged duration of action as well as reduced dose-related side effects were achieved as compared to marketed products [64]. Another study reported use of TTN-loaded microspheres, which provided controlled drug release as compared to the cream form [65]. TTN has been loaded into nanocapsules which were prepared by interfacial deposition of preformed polymer (poly-epsilon-caprolactone) using two different oily phases: capric/caprylic triglycerides and sunflower seed oil, and with both oily phases used, greater TTN photostability was reported [66]. Curcumin has been loaded into poly (butyl) cyanoacrylate nanoparticles and higher skin permeation of curcumin was shown together with controlled release [67].

The New Jersey Center for Biomaterials has developed a new tyrosine derived triblock copolymer called TyroSpheres as a topical delivery system, to enhance paclitaxel (a mitotic inhibitor that promotes assembly and stabilization of microtubules and thus inhibits cell division) solubility, enable sustained dose-controlled release and selective accumulation which in turn would eliminate side effects associated with systemic exposure [68]. TyroSpheres were mainly composed of copolymers with hydrophobic blocks of oligomer of desaminotyrosyl tyrosine esters, diacids, and hydrophilic blocks of polyethylene glycol. Drug-loaded TyroSpheres showed

numerous advantages such as reproducible particle sizes, enhancement of drug stability, and higher encapsulation ability with higher skin permeation [68]. Together with the possibility to incorporate TyroSpheres into a gel-like formulation, which would allow enhanced skin contact as well as ease of application, paclitaxel-TyroSpheres seems to be a promising modality for treatment of psoriasis [68].

CONCLUSION

Many antipsoriatic drugs have been developed and are being used in psoriasis pharmacotherapy. None of them have been sufficient for effective treatment of psoriasis; they have numerous drawbacks which hindered their efficacy. Nanomedicines such as liposomes, ethosomes, niosomes, lipid based nanoparticles, and microspheres have been successfully loaded with antipsoriatic drugs and shown to improve their therapeutic potential. They provide better therapeutic efficacy, lesser toxicity, dose reduction, and drug specific targeting. However, clinical studies are still scarce. Establishing their safety and efficacy is urgent and crucial as nanopharmaceuticals demonstrate significant potential for treatment of psoriasis.

References

- [1] Rahman M, Zaki Ahmad M, Kazmi I, Akhter S, Beg S, Gupta G, et al. Insight into the biomarkers as the novel antipsoriatic drug discovery tool: a contemporary viewpoint. *Curr Drug Discov Technol* 2012;9:48–62.
- [2] Rahman M, Alam K, Ahmad MZ, Gupta G, Afzal M, Akhter S, et al. Classical to current approach for treatment of psoriasis: a review. *Endocr Metab Immune Disord Drug Targets* 2012;12:287–302.
- [3] Rahman M, Akhter S, Ahmad J, Ahmad MZ, Beg S, Ahmad FJ. Nanomedicine-based drug targeting for psoriasis: potentials and emerging trends in nanoscale pharmacotherapy. *Expert Opin Drug Deliv* 2015;12:635–52.
- [4] Lynde CW, Poulin Y, Vender R, Bourcier M, Khalil S. Interleukin 17A: toward a new understanding of psoriasis pathogenesis. *J Am Acad Dermatol* 2014;71(1):141–50.
- [5] Mudigonda P, Mudigonda T, Feneran AN, Alamdari HS, Sandoval L, Feldman SR. Interleukin-23 and interleukin-17: importance in pathogenesis and therapy of psoriasis. *Dermatol Online J* 2012;18(10):1.
- [6] Yang J, Sundrud MS, Skepner J, Yamagata T. Targeting Th17 cells in autoimmune diseases. *Trends Pharmacol Sci* 2014;35(10):493–500.
- [7] Lowes MA, Suárez-Fariñas M, Krueger JG. Immunology of psoriasis. *Annu Rev Immunol* 2014;32:227–55.
- [8] Rawat M, Singh D, Saraf S. Nanocarriers: promising vehicle for bioactive drugs. *Biol Pharm Bull* 2006;29:1790–8.
- [9] Rahman M, Beg S, Ahmad MZ, Kazmi I, Ahmed A, Rahman Z, et al. Omega-3 fatty acids as pharmacotherapeutics in psoriasis: current status and scope of nanomedicine in its effective delivery. *Curr Drug Targets* 2013;14:708–22.
- [10] Lapteva M, Mondon K, Möller M, Gurny R, Kalia YN. Polymeric micelle nanocarriers for the cutaneous delivery of tacrolimus: a targeted approach for the treatment of psoriasis. *Mol Pharm* 2014;11(9):2989–3001.
- [11] Manconi M, Sinico C, Caddeo C, Vila AO, Valenti D, Fadda AM. Penetration enhancer containing vesicles as carriers for dermal delivery of tretinoin. *Int J Pharm* 2011;412:37–46.
- [12] Agarwal R, Katare OP, Vyas SP. Preparation and in vitro evaluation of liposomal/niosomal delivery systems for antipsoriatic drug dithranol. *Int J Pharm* 2001;228:43–52.
- [13] Bishtaba K, Wagnerb KH, Bulmer AC. Curcumin, resveratrol and flavonoids as anti-inflammatory, cyto- and DNA-protective dietary compounds. *Toxicology* 2010;278:88–100.
- [14] Scognamiglio I, De Stefano D, Campani V, Mayol L, Carnuccio R, Fabbrocini G, et al. Nanocarriers for topical administration of resveratrol: a comparative study. *Int J Pharm* 2013;440:179–87.
- [15] Pando D, Caddeo C, Manconi M, Fadda AM, Pazos C. Nanodesign of olein vesicles for the topical delivery of the antioxidant resveratrol. *J Pharm Pharmacol* 2013;65:1158–67.
- [16] Guo J, Ping Q, Sun G, Jiao C. Lecithin vesicular carriers for transdermal delivery of cyclosporine A. *Int J Pharm* 2000;194:201–17.
- [17] Guo JX, Ping QN, Wu T. Transdermal delivery mechanisms of lecithin nanoparticles with cyclosporin A through mice skin. *Yao Xue Xue Bao* 2000;35:782–5.
- [18] Boinpally RR, Zhou SL, Devraj G, Anne PK, Poondru S, Jasti BR. Iontophoresis of lecithin vesicles of cyclosporine A. *Int J Pharm* 2004;274:185–90.
- [19] Verma DD, Fahr A. Synergistic penetration enhancement effect of ethanol and phospholipids on the topical delivery of cyclosporin A. *J Control Release* 2004;97:55–66.
- [20] Katare OP, Kumar R, Bhoop BS, Dogra S. A multicompartamental liposomal system for topical drug delivery. *The Patent Off J* 2009:6210.
- [21] Dragicevic-Curic N, Gräfe S, Gitter B, Winter S, Fahr A. Surface charged temoporfin-loaded flexible vesicles: in vitro skin penetration studies and stability. *Int J Pharm* 2010;384:100–8.
- [22] Dragicevic-Curic N, Winter S, Krajisnik D, Stupar M, Milic J, Graefe S, et al. Stability evaluation of temoporfin-loaded liposomal gels for topical application. *J Liposome Res* 2010;20:38–48.
- [23] Boyd AS, King Jr LE. Tamoxifen-induced remission of psoriasis. *J Am Acad Dermatol* 1999;41:887–9.
- [24] Bhatia A, Kumar R, Katare OP. Tamoxifen in topical liposomes: development, characterization and in-vitro evaluation. *J Pharm Pharm Sci* 2004;7:252–9.
- [25] Ali MF, Salah M, Rafea M. Liposomal methotrexate hydrogel for treatment of localized psoriasis: preparation, characterization and laser targeting. *Med Sci Monit* 2008;12:166–74.
- [26] Raza K, Katare OP, Setia A, Bhatia A, Singh B. Improved therapeutic performance of dithranol against psoriasis employing systematically optimized nanoemulsomes. *J Microencapsul* 2013;3:225–36.
- [27] Trotta M, Peira E, Debernardi FM, Gallarate M. Elastic liposomes for skin delivery of dipotassium glycyrrhizinate. *Int J Pharm* 2002;241:319–27.
- [28] Ibbotson SH. Topical 5-aminolaevulinic acid photodynamic therapy for the treatment of skin conditions other than non-melanoma skin cancer. *Br J Dermatol* 2002;146:178–88.
- [29] Fang YP, Huang YB, Wu PC, Tsai YH. Topical delivery of 5-aminolevulinic acid-encapsulated ethosomes in a hyperproliferative skin animal model using the CLSM technique to evaluate the penetration behavior. *Eur J Pharm Biopharm* 2009;73:391–8.
- [30] Dragicevic-Curic N, Scheglmann D, Albrecht V, Fahr A. Development of liposomes containing ethanol for skin delivery of temoporfin: characterization and in vitro penetration studies. *Colloids Surf B Biointerfaces* 2009;74:114–22.
- [31] Li G, Fan C, Li X, Fan Y, Wang X, Li M, et al. Preparation and in vitro evaluation of tacrolimus-loaded ethosomes. *Scientific World J* 2012;2012:874053.

- [32] Dubey V, Mishra D, Dutta T, Nahar M, Saraf DK, Jain NK. Dermal and transdermal delivery of an antipsoriatic agent via ethanolic liposomes. *J Control Release* 2007;123:148–54.
- [33] Madhav NVS, Saini A. Niosomes: a novel drug delivery system. *IJRPC* 2011;1:498–511.
- [34] Lakshmi PK, Devi GS, Bhaskaran S, Sacchidanand S. Niosomal methotrexate gel in the treatment of localized psoriasis: phase I and phase II studies. *Indian J Dermatol Venereol Leprol* 2007;73:157–61.
- [35] Gidwani SK, Singnurkar PS. Composition for delivery of dithranol. India: Eur Patent Off 2003:1–14.
- [36] Patel R, Singh SK, Singh S, Sheth NR, Gendle R. Development and characterization of curcumin loaded transfersome for transdermal delivery. *J Pharm Sci Res* 2009;1:71–80.
- [37] Bhatia A, Raza K, Singh B, Katare OP. Phospholipid-based formulation with improved attributes of coal tar. *J Cosmet Dermatol* 2009;8:282–8.
- [38] Puglia C, Bonina F. Lipid nanoparticles as novel delivery systems for cosmetics and dermal pharmaceuticals. *Expert Opin Drug Deliv* 2012;9(4):429–41.
- [39] Rawat M, Singh D, Saraf S, Saraf S. Lipid carriers: a versatile delivery vehicle for proteins and peptides. *Yakugaku Zasshi* 2008;128:269–80.
- [40] Abdullah R, How CW, Abbasalipourkabir R. Characterization and stability of nanostructured lipid carriers as drug delivery system. *Afr J Biotechnol* 2011;10:1684–9.
- [41] Xia Q, Saupe A, Muller RH, Souto EB. Nanostructured lipid carriers as novel carrier for sunscreen formulations. *Int J Cosmet Sci* 2007;29:473–82.
- [42] Sonawane R, Harde H, Katariya M, Agrawal S, Jain S. Solid lipid nanoparticles-loaded topical gel containing combination drugs: an approach to offset psoriasis. *Expert Opin Drug Deliv* 2014;11:1833–47.
- [43] Misra AK, Padhi BK, Chougule M. Methotrexate-loaded solid lipid nanoparticles for topical treatment of psoriasis: formulation & clinical implications. *Drug Del Tech* 2004;4:8.
- [44] Remitz A, Reitamo S, Erkkö P, Granlund H, Lauerma AI. Tacrolimus ointment improves psoriasis in a microplaque assay. *Br J Dermatol* 1999;141:103–7.
- [45] Wang R, Li L, Wang B, Zhang T, Sun L. FK506-loaded solid lipid nanoparticles: preparation, characterization and in vitro transdermal drug delivery. *Afr J Pharm Pharmacol* 2012;6:904–13.
- [46] Zhou ZL, Yang YX, Ding J, Li YC, Miao ZH. Triptolide: structural modifications, structure–activity relationships, bioactivities, clinical development and mechanisms. *Nat Prod Rep* 2012;29:457–75.
- [47] Mei Z, Chen H, Weng T, Yang Y, Yang X. Solid lipid nanoparticle and microemulsion for topical delivery of triptolide. *Eur J Pharm Biopharm* 2003;56:189–96.
- [48] Agrawal Y, Petkar KC, Sawant KK. Development, evaluation and clinical studies of Acitretin loaded nanostructured lipid carriers for topical treatment of psoriasis. *Int J Pharm* 2010;401:93–102.
- [49] Nasrollahi SA, Abbasian AR, Farboud ES. In vitro comparison of simple tretinoin-cream and cream loaded with tretinoin-SLN. *J Pharm Technol Drug Res* 2013;2:13.
- [50] Raza K, Singh B, Lohan S, Sharma G, Negi P, Yachha Y. Nano lipoidal carriers of tretinoin with enhanced percutaneous absorption, photostability, biocompatibility and antipsoriatic activity. *Int J Pharm* 2013;456:65–72.
- [51] Pople PV, Singh KK. Development and evaluation of colloidal modified nanolipid carrier: application to topical delivery of tacrolimus. *Eur J Pharm Biopharm* 2011;79:82–94.
- [52] Prufer K, Jirikowski GF. Liposomal incorporation changes the effect of 1,25-dihydroxyvitamin D3 on the phospholipase C signal transduction pathway and the eicosanoid cascade on keratinocytes in vitro. *Biochem Pharmacol* 1996;51:247–52.
- [53] Lin YK, Huang ZR, Zhuo RZ, Fang JY. Combination of calcipotriol and methotrexate in nanostructured lipid carriers for topical delivery. *Int J Nanomedicine* 2010;5:117–28.
- [54] Bernstein JE, Parish LC, Rapaport M. Effects of topically applied capsaicin on moderate and severe psoriasis vulgaris. *J Am Acad Dermatol* 1986;15:504–7.
- [55] Agrawal U, Gupta M, Vyas SP. Capsaicin delivery into the skin with lipidic nanoparticles for the treatment of psoriasis. *Artif Cells Nanomed Biotechnol* 2013:16.
- [56] Gupta S, Moulik SP. Biocompatible microemulsions and their prospective uses in drug delivery. *J Pharm Sci* 2008;97:22–43.
- [57] Baboota S, Alam MS, Sharma S, Sahni JK, Kumar A, Ali J. Nanocarrier-based hydrogel of betamethasone dipropionate and salicylic acid for treatment of psoriasis. *Int J Pharm Investig* 2011;3:139–47.
- [58] Balbás GM, Regaña MS, Millet PU. Study on the use of omega-3 fatty acids as a therapeutic supplement in treatment of psoriasis. *Clin Cosmet Investig Dermatol* 2011;4:73–7.
- [59] Baboota S, Rahman M, Kumar A, Sharma S, Sahni J, Ali J. Submicron size formulation of linseed oil containing Omega-3 fatty acids for topical delivery. *J Disp Sci Technol* 2012;33:1259–66.
- [60] Sharma S, Kumar A, JK S BS, Ali J. Nanoemulsion based hydrogels containing omega -3 fatty acids as a surrogate of betamethasone dipropionate for topical delivery. *Adv Sci Lett* 2012;6:221–31.
- [61] Liu CH, Chang FY. Development and characterization of eucalyptol microemulsions for topic delivery of curcumin. *Chem Pharm Bull (Tokyo)* 2011;59:172–8.
- [62] Ali J, Akhtar N, Sultana Y, Baboota S, Ahuja A. Antipsoriatic microemulsion gel formulations for topical drug delivery of babchi oil (*Psoralea corylifolia*). *Methods Find Exp Clin Pharmacol* 2008;30:277–85.
- [63] Alagusundaram M, Chetty MS, Umashankari K, Badarinath AV, Lavanya C, Ramkanth S. Microspheres as a novel drug delivery system- a review. *Int J Chem Tech Res* 2009;1:526–34.
- [64] Badilli U, Sen T, Tarımcı N. Microparticulate based topical delivery system of clobetasol propionate. *AAPS Pharm Sci Tech* 2011;12:949–57.
- [65] Dinarvand R, Rahmani E, Farbod E. Gelatin microspheres for the controlled release of all-trans-retinoic acid topical formulation and drug delivery evaluation. *Iranian J Pharm Res* 2003;2:47–50.
- [66] Ourique AF, Pohlmann AR, Guterres SS, Beck RC. Tretinoin-loaded nanocapsules: preparation, physicochemical characterization, and photostability study. *Int J Pharm* 2008;20(352):1–4.
- [67] Mulik R, Mahadik K, Paradkar A. Development of curcuminoids loaded poly (butyl) cyanoacrylate nanoparticles: physicochemical characterization and stability study. *Eur J Pharm Sci* 2009;37:395–404.
- [68] Kilfoyle BE, Sheihet L, Zhang Z, Laohoo M, Kohn J, Michniak-Kohn BB. Development of paclitaxel-TyroSpheres for topical skin treatment. *J Control Release* 2012;163:18–24.

Nanoparticles for Treatment of Atopic Dermatitis

M.M.A. Abdel-Mottaleb^{1,2,3}

¹Ain Shams University, Cairo, Egypt; ²University of Franche Comte, Besancon, France;

³University of Bonn, Bonn, Germany

OUTLINE

Atopic Dermatitis	167	<i>Use of Nanoparticles for the Treatment of Atopic Dermatitis</i>	170
Pathophysiology	167	<i>Potential Risks and Challenges in Use of Nanoparticles</i>	173
Clinical Features	168	References	173
Epidemiology	168		
Treatment	169		

ATOPIC DERMATITIS

Atopic dermatitis (AD) is a common relapsing chronic inflammation of the skin. The term atopic indicates the inherited tendency of sufferers from this disease to produce immunoglobulin E (IgE) antibodies in response to environmental or food allergens such as pollen, house dust, mites, and some ingested proteins [1]. Due to the potential of this disease to cause relapsing episodes of intense pruritis in AD [2], it could be a major cause of psychosocial problems to the patients and their families. Moreover, in severe cases AD may progress to allergic rhinitis and asthma in a process called “atopic march” [3].

PATHOPHYSIOLOGY

The pathophysiology of AD involves a complex interaction between environmental and genetic factors [4]. It is considered the classic example of dermatitis in which the endogenous component is of great importance.

Due to its immunologic background, AD patients have also tended to develop asthma, hay fever, and type I allergic reactions to different allergens such as latex or hair from dogs or cats. The genetic basis for the AD has been linked to several genes with strong evidence implicating a loss of function of the gene for the keratinocyte protein filaggrin, that also explains the disruption of skin barrier function seen in AD [5,6].

AD is considered one of the most common, chronically relapsing inflammatory eczematous skin conditions with immunological abnormalities associated with abnormalities in the epithelial skin barrier and defective tight junctions [7]. Immunological abnormalities include elevated serum levels of IgE with the involvement of different cell types, which makes the understanding of and distinguishing the causative and promoting factors very challenging [8]. It was found that the acute lesions of AD are Th2-mediated with increased infiltration of T-cell lymphocytes, while the chronic lesions are Th1-regulated with increased presence of dendritic cells and monocytes. Decreased stratum corneum (SC) lipids (especially ceramide 1) has

been observed in both lesional and nonlesional skin, which is considered of major importance for the insufficiency of the SC function in AD patients [9].

CLINICAL FEATURES

AD is often characterized by papules, bouts of itching and lichenification (or leathery induration), and skin thickening with hyperkeratosis. It is commonly found in asthma and hay fever patients reflecting some common immunologic problems among these diseases. Dissemination over the entire body, and formation of pustules (pustulation) due to the occurrence of secondary infections, are common complications of AD [10]. AD is characterized by a high tendency toward skin drying especially in the winter. This drying is expressed as chapping of the dorsal sides of the hand and the lips, and generalized skin dryness that might lead to irritant contact dermatitis [11]. The danger of AD lies in the impairment of barrier function of the skin that protects the body from environmental contaminants, microbial infections, and toxins as well as body hydration control. With the state of chronic inflammation, the proliferation of epidermal progenitor cells leads to epidermal hyperplasia and tissue remodeling and subsequent spongiosis. Spongiosis is the separation of keratinocytes in the epidermis, which disrupts the architecture of the normal skin structure [8]. Concurrent bacterial, viral, or fungal infections are commonly seen in AD patients. Atopic dermatitis is the one of the most common inflammatory skin conditions that can affect the patients' quality of life, especially considering that most of the AD patients are children. Caring for AD child patients is sometimes similar to caring for type I diabetic children. Scratching and rubbing of the skin are common, leading to sleep disturbance and significant distress.

EPIDEMIOLOGY

The prevalence of AD has increased significantly over the past 30 years. It is estimated that 10–20% of children and 1–3% of adults in developed countries are affected by this disorder. Those developing AD in their childhood mostly have a severe form of the disease, while the adult-onset type is mainly manifested by hand eczema [12].

Other studies claim that AD affects about one fifth of all individuals, but the distribution varies greatly throughout the world [13]. Around 50% of AD patients develop symptoms within the first year of their life, and probably as many as 95% experience disease onset below the age of 5 years [1]. In around 75% of the children suffering from AD, a spontaneous remission is

observed before adolescence, while the remaining 25% continue to have eczema into adulthood.

The frequency of AD was found to be highly correlated to genetic predisposition, where a higher incidence of disease had been reported in family members of affected people. For example, the incidence was found to be 75% in monozygotic twins and 30% in dizygotic twins showing that genetic factors are of prime importance [14]. A strong correlation was found between many specific genes and the development of AD, especially genes concerned with encoding epidermal structural proteins or key elements of the immune system. Mutations in the filaggrin gene positioned on chromosome 1, which increases the transepidermal water loss (TEWL), and the passive transfer of protein allergens have particularly been implicated.

The risk of developing AD has been correlated with several factors such as climate, diet, duration of breastfeeding and delayed weaning, skin barrier disruption, and sensitization [15]. It was found that the symptoms of AD correlated positively with latitude and negatively with outdoor temperature. Ultraviolet (UV) exposure seems to play a role in the aggravation of AD symptoms due to its immunosuppressive effects. UV exposure is known to facilitate the isomerization of the skin barrier product, trans-urocanic acid into the immunosuppressive cis-urocanic acid isoform [16]. Other environmental factors including humidity and seasonal changes in pollen counts are likely to be involved, with the higher prevalence in cities compared with the countryside apparently due to higher environmental pollution and subsequent higher allergen exposure [17].

The effect of diet on the increase of AD risk has revealed that the frequent consumption of fresh fruits has a protective effect against AD, while the continuous use of fast food can lead to increased prevalence of AD [18]. The intake of large quantities of vegetables, nuts, and fish also led to lower occurrence of AD [19]. This could be attributed to the antiinflammatory effect of n-3 polyunsaturated fatty acids (n-3 PUFAs) and the low content of proinflammatory n-6 PUFAs [20]. Another consistent finding was that the rate of AD was increased in association with a high maternal intake of n-6 PUFA during pregnancy, and also with the increased consumption of margarine rather than butter in children [20,21]. Effects of other variables like duration of breastfeeding, age of weaning, exposure to pollutant and tobacco smoke, obesity and physical exercise seem to be related to the incidence of AD, but no strong evidence for these associations has been found which necessitates further investigation [15].

Some environmental factors have been found to be strongly correlated with the prevalence of AD. Although no solid indication was found on the correlation between living on a farm and the protection from AD

risk, the consumption of unpasteurized farm milk during the first 2 years of life was found to be a protective factor against AD [22]. The protective effects may be linked to microbial contamination or other protein constituents of the milk that are destroyed once boiled. In addition, direct and regular contact with farm animals either prenatally, postnatally for pregnant mothers, or during early childhood seem to reduce the risk of AD suggesting that priming of the immune system is of particular importance [23]. The immunity priming effects were claimed to be correlated with exposure to endotoxins found on the associated gram-negative bacteria which are known to be good inducers of IL-10 and INF-gamma [15]. Moreover, the intake of antibiotics was found to be strongly correlated to an increased risk of AD. It was found that the probability of developing AD in the offspring was increased by 41% in those who received at least one course of antibiotics in early life [24]. The effect is probably related to the changes in the normal microbiota caused by antibiotics with subsequent changes in the development of the immune system and altered response to different allergens.

TREATMENT

Symptomatic treatment of AD depends mainly on emollients, topical steroids, and oral antihistamines for relieving the itchiness and dryness of the skin [7]. Refractory cases require more powerful treatment modalities. The different treatments offered for AD are mostly used in combination because they address different aspects of AD pathogenesis.

The nonpharmacologic treatments used for the management of AD include several interventions, of which the use of moisturizers is the most important one. Xerosis is known to be one of the most common clinical features of AD, resulting from the epidermal barrier dysfunction necessitating the use of moisturizers. Topical moisturizers with emollient components, occlusive oils, and humectants are used to increase skin hydration and soften the skin. This will help to lessen the symptoms of AD such as pruritus, erythema, fissuring, and lichenification. In addition, they might help to reduce the dose of antiinflammatory drugs required for disease control. Bathing is also recommended to remove scales, crust, irritants, and allergens from the skin surface, and when followed by application of moisturizers, a good hydration state can be ensured for the skin. In addition, therapy with wet wraps is sometimes recommended to decrease water loss, prevent scratching, and increase the efficiency of the topically applied medications via the increased occlusion, but care should be taken to avoid the enhanced systemic absorption of drugs with subsequent systemic risks [25].

The first line pharmacologic treatment of AD is the use of topical corticosteroids that are applied during the active inflammatory phase and also to prevent relapses. They function by binding to nuclear receptors, thus inducing suppression of different inflammatory cytokines, inhibition of T-cells and other inflammatory cells, and modulating the production of arachidonic acid, as well as the function of vascular and connective tissue [11]. The basic corticosteroid molecule was originally hydrocortisone, from which various new molecules were developed through chemical modifications of its four-ring structure. The topical corticosteroids can be classified on a four-point scale of potency: mild, moderate, potent, and very potent. Unfortunately the long-term use of corticosteroids is always accompanied by several side effects including skin atrophy, telangiectasia, focal hypertrichosis, acneiform, or rosacea-like eruptions and skin purpura with accompanying secondary infections. Therefore, intermittent usage schedules are recommended for avoidance of such side effects. The use of moderate- or high-potency corticosteroids for short courses for the control of significant acute flares is sometimes necessary, but for the long-term management of the disease, the least potent corticosteroid that is active in that patient should be used [25]. In addition, the use of appropriate strength corticosteroids for different body areas may help to reduce the undesirable effects. For example, the face should only be treated with mild steroids while the intertriginous areas can be treated with mild- to moderate-strength steroids [11].

Calcineurin antagonists (mainly tacrolimus and pimecrolimus) are now evolving as primary therapeutic agents for the treatment of AD, especially in nonimmunocompromised patients who have failed to respond to other treatments, or when the use of corticosteroids is not advisable. Tacrolimus and pimecrolimus topical ointments and creams have proved clinically efficient in the short- and long-term treatment of dermatitis including AD [26–28]. Additionally, tacrolimus ointment has demonstrated an effective reduction of the number of flare-ups, and can improve the quality of life in AD patients [29,30]. These compounds are principally T-cell suppressing agents used orally for systemic immunosuppression as required for organ transplantation. However, topical use has proved efficient against AD as well as other inflammatory conditions, as the inhibition of the calcineurin T-cell activation can block the secretion of proinflammatory cytokines and mediators involved in the AD process. Adverse effects include skin burning, warmth, redness and local allergic reactions, and a risk of secondary infections due to the reduced immunity. Systemic absorption also can lead to breathing difficulties, face swelling, and the associated systemic immunosuppressive effects with an increased risk of infections and

malignancy. The use of tacrolimus and pimecrolimus ointments is also accompanied by variable absorption rates and therapeutic efficiencies. Therefore, the use of nanotechnology for targeting the inflamed skin areas would avoid risks to the healthy skin as well as to the systemic circulation [31].

Atopic individuals are predisposed to skin infection since the physical barrier is already disrupted along with the impaired production of antimicrobial peptides. Therefore, topical antibiotics, antiseptics, or antibacterial soaps might be proposed as additional measures to enhance the treatment of AD. However, the addition of antibiotics was not found to improve the global outcome or disease severity thus they are not recommended in the treatment of AD, especially considering that their excessive use might increase the risk of antimicrobial drug resistance. Similarly, the use of topical antihistamines has been tried for the treatment of AD but did not demonstrate high utility, and therefore their use is not recommended because of the risk of systemic toxicity, particularly in children.

Use of Nanoparticles for the Treatment of Atopic Dermatitis

For the past few years, nanotechnology has gained an increasing role as innovative drug delivery systems. Nanostructures used for drug delivery are able to enhance the solubility and bioavailability of various drugs, increase their targeting potential, sustain their activity, and reduce the associated side effects. Different types of nanocarriers are used as drug carriers especially in the field of nanodermatology.

Nanoemulsions are considered a very attractive vehicle for the topical treatment of different skin diseases due to their fast and easy penetration through skin lipids, and their nongreasy pleasant feeling. The choice of lipids to be used in nanoemulsions should be biocompatible and biodegradable, and characterized by extra soothing effects that would be advantageous especially in case of inflammatory skin conditions like dermatitis [7]. The use of nanoemulsions for the treatment of AD has been recently explored. Prednicarbate has been formulated in a positively charged nanoemulsion using phytosphingosine (PS) as an essential element required for the production of ceramides to help healing and restoring of the normal skin barrier function. PS is also known to have significant anti-inflammatory effects and antimicrobial properties against *Propionibacterium acnes* and *Staphylococcus aureus*, making it a good choice for the treatment of dermatitis and acne. In addition, the positive charge of the nanoemulsion droplets helps to enhance the skin penetration by interaction with the negatively charged SC [32]. Nanoemulsions have been also investigated for the

topical delivery of DNazymes for the treatment of AD. DNazymes are considered to be of therapeutic potential against AD since they can interfere with Th2 cell differentiation and inflammatory reactions. Unfortunately, they are easily degraded by the enzymes of the normal skin microflora and have very poor skin penetration due to their high molecular weight (MW). Therefore, their inclusion into nanoemulsions was proposed to enhance their skin penetration, epidermal uptake, and stability [33].

On another side, the use of lipid nanoparticle preparations like solid lipid nanoparticles (SLNs) or nanostructured lipid carriers (NLCs) has been also explored for the treatment of AD. These structures consist of lipid nanoemulsions in which the liquid oil has been replaced by a solid lipid or a mixture of solid and liquid lipids for the SLNs and NLCs respectively. For their solid and oily content, they are known to have excellent occlusive properties, which help to enhance skin hydration and penetration. The encapsulation of prednicarbate into SLNs helped to enhance its stability and tolerability, in addition to providing increased epidermal localization, which was not even affected by dilution of the SLNs with a cream base [34]. Similarly, all-trans retinoic acid has shown marked increase in its photostability upon its formulation in SLNs. This encapsulation could also significantly reduce its irritant effect as seen from the remarkably reduced erythematic episodes when it was applied to rabbit skin compared to the marketed all-trans retinoic acid cream [35].

The encapsulation of tacrolimus into lipid nanoparticles led to significant accumulation of the drug into the SC compared to other conventional formulations, which makes it a good strategy to continuously supply the drug to deeper skin layers. It was found that the accumulation was 30.8 and 28.6 times higher than conventional formulations in the epidermis and dermis respectively, which are considered the main areas of interest for the treatment of AD since they contain most of the inflammatory and dendritic cells. In addition, bio-distribution data using radiolabeled formulations of tacrolimus showed significant localization of the radioactivity in the skin with no accumulation in any other body organs revealing a high targeting potential with enhanced bioavailability and reduced systemic side effects [36].

Another class of nanoparticulate carriers includes the vesicular systems like liposomes, transferosomes, ethosomes, and niosomes. Liposomes are composed of phospholipid bilayers enclosing an aqueous core and dispersed in aqueous medium. They vary in diameter from 20 to 100 nm for the unilamellar liposomes and up to 500 nm for the multilamellar ones [37]. Although liposomes are considered highly biocompatible and as excellent carriers for skin applications because they are

mostly composed from natural phospholipids, their use is often limited by different instability problems such as aggregation, variability in particle size, hydrolysis, and drug leakage [7]. An example of the optimization of a liposomal formulation for the treatment of AD was the encapsulation of PS in 1,2-dipalmitoyl-sn-glycero-3-phosphocholine (DPPC), a phospholipid that is known for its similarity with skin lipids and its ability to form liposomes with higher encapsulation rates for the topical delivery of PS. The incorporation of PS into DPPC liposomes led to significant enhancement of its skin retention with minimal transdermal or systemic availability, thus reducing the dose required as well as the dosing frequency [38]. Ethosomes are considered another type of vesicular carrier that have ethanol as an important constituent that helps the penetration of various drugs through the SC. Ethanol is a good organic solvent that can help the solubilization of various drugs to achieve higher drug loading compared to liposomes. In addition, the ability of ethanol to extract SC lipids helps the diffusion of drugs through the altered skin membrane. Tacrolimus-loaded ethosomes proved efficient in the treatment of AD in mice compared to the commercially available ointment or empty liposomes. The higher therapeutic efficacy was found to be related to the higher concentrations of drug achieved in the epidermal and dermal layers [39]. However, it is worth noting that the use of ethanol (especially in such high concentrations) might not be favorable for application in some AD patients because of the irritation risk. On the other hand, the use of transferosomes and niosomes has also been explored for various dermal applications, yet these vehicles are not yet considered to be advantageous in case of the treatment of skin diseases like AD. This is due to their ability to enhance the transdermal permeation of various drugs rather than increasing their skin localization. Niosomes are nonionic surfactant vesicles formed from the self-assembly of nonionic amphiphiles in aqueous media. These surfactants can disturb the intact structure of the SC and enhance the permeation (and hence the systemic availability) of various drugs. A clinical trial of the management of methyl nicotinate-induced erythema in human volunteer skin using ammonium glycyrrhizinate niosomes and ammonium glycyrrhizinate solution proved the superior efficacy of the niosomes, but also showed higher skin penetration with risks of associated systemic side effects. Transferosomes, also called “ultradeformable liposomes,” consist of phospholipid bilayers but with the inclusion of an edge activator which facilitates the deformability of these vesicles [40]. They have been proposed for the topical application of glucocorticoids (GCs) including hydrocortisone, dexamethasone, and triamcinolone acetonide [41–43]. Several theories have been presented for the permeation-enhancing

capabilities of transferosomes. They were claimed to be able to penetrate the skin as intact vesicles due to their unique ability to squeeze through the SC channels. Another theory suggests the enhancement of transdermal permeation via the creation of an osmotic gradient across the skin by applying the transferosomes under nonocclusive conditions [44]. However, other researchers have found that transferosomes never penetrated beyond the SC, and that the transdermal penetration of drugs was enhanced after the disintegration of the vesicles and depended mostly on the physicochemical properties of the drug [45,46]. When used for the localized delivery of GCs, transferosomes are supposed to penetrate the SC and form a sub-SC depot layer which can continuously release the drug over long duration periods of time providing a high localized drug concentration in the diseased skin. However, such localized effects were only attainable with low doses of the drug, while higher doses appeared to achieve higher systemic availability with subsequent risks, especially with hydrophilic drugs that tend to escape from the sub-SC depot to the washout of hydrophilic drugs by the systemic circulation [47].

The use of polymeric nanoparticles (PNP) has been proposed as an efficient method for the localization of topical drugs in the skin, and reducing the systemic absorption of drugs used for the topical treatment of skin diseases [48]. PNP also offer advantages of enhancing the stability and bioavailability of different lipophilic and hydrophilic drugs, as well as providing a more controlled release. Being small in size and mostly prepared from biodegradable polymers, they are biologically compatible with a high tendency to accumulate in hair follicles, and they can achieve a high concentration of drugs in the epidermis; they appear to have good potential to be an interesting carrier for the treatment of AD. Selective preferential accumulation of ethyl cellulose nanoparticles in the size range of 50–100 nm was detected in the hair follicles and sebaceous glands of inflamed skin in a dithranol-induced dermatitis model in mice compared to healthy normal skin [49]. Larger particles of 500–1000 nm behaved similarly in both dermatitis and healthy skin, and this indicated the significant effect of particle size on the enhanced localization potential in the inflamed skin. The results of therapeutic efficiency testing using betamethasone-loaded PNP revealed that the selective accumulation of the 100 nm particles led to enhanced efficacy of anti-inflammatory drugs. These attractive characteristics combined with the observed selective accumulation of small-sized PNP in inflamed skin have encouraged researchers to utilize them for the enhancement of AD treatment. Evidence of enhanced capillary permeability (by a similar mechanism to the enhanced permeation and retention effect seen in tumors) has been seen in

models of AD. Thus, passive targeting using nanoencapsulation techniques might be a beneficial strategy in the therapy of AD. Coencapsulation of hydrocortisone as a topical corticosteroid with the powerful oxygen free radical scavenger, hydroxytyrosol, has been performed to treat AD and to reduce the autooxidation and the free radical cell-damaging effects seen at the site of inflammation. The coencapsulated drugs showed higher epidermal and dermal accumulation with lower flux across the full thickness mouse skin, compared with the drugs in co-solution and with a commercial hydrocortisone product. In addition, higher therapeutic efficiency was also achieved [50].

Poly (ϵ -caprolactone) (PCL) nanoparticles containing hydrocortisone acetate were prepared by a solvent displacement method to provide a prolonged drug release for the local treatment of AD thus reducing the systemic side effects of corticosteroids [51]. However, the slowly biodegradable particles might show persistence and accumulation at the application site and possibly cause inflammation, so this necessitates performing a thorough investigation of the nanoparticles' potential for toxicity.

The use of double-stranded small interfering RNA (siRNA) has been introduced as a therapeutic modality to interfere with genes that promote or cause disease. This is due to their ability to induce specific gene silencing, leading to modification of the behavior of the immune system with subsequent reduction of disease symptoms [52]. However, these macromolecular nucleic acid moieties are considered very challenging to deliver if used topically for the management of dermatitis due to several factors. Their large MW significantly limits their skin permeation and their subsequent uptake by the deep targeted epidermal and dermal cells. In addition, they suffer from stability problems, with possible degradation by skin nuclease enzymes. Cationic polymers or cationic lipid molecules could offer a potential strategy to form complexes with siRNA thus protecting these nucleic acids from degradation, and enhancing their skin delivery through their interaction with the negatively charged skin phospholipids. Liquid crystalline nanodispersions of monoolein were combined with the cationic polymer, polyethylenimine (PEI), or the cationic lipid oleylamine (OAM) for siRNA delivery, for the knockdown of glyceraldehyde 3-phosphate dehydrogenase (GAPDH) protein that is responsible for skin irritation [52]. This polymeric nanodispersion proved to be efficient in delivering the macromolecules to the deep epidermis with preservation of their biological activity that was observed up to 48 h after application. On the other hand, the application of only a solution of siRNA did not show any gene silencing effects. The nanodispersions could also be deposited on the skin surface and could provide a

sustained release of the siRNA, which can be seen as the reason for the delayed biological activity.

Successful skin delivery of both siRNA and capsaicin, by using cyclic lipid polymeric nanostructures for the inhibition of neuropeptides involved in chronic skin inflammatory conditions, has been also investigated. The proposed carrier was composed of DSPE-PEG2000 surrounding a self-penetrating lipid synthesized with pyrrolidinium cyclic polar head groups enclosing a negatively charged poly lactic-co-glycolic acid-containing capsaicin layer. Enhanced drug delivery to the deeper skin layers was achieved by the interaction of the cationic lipid layer with the negatively charged residues of proteins and lipids of the SC, and the deposition into the hair follicles and skin furrows provided a sustained effect over longer duration of time [53].

UV-irradiated skin has been claimed to develop a kind of dermatitis which involves reactive oxygen species, which can be improved by the application of platinum. A nanoparticulate platinum preparation stabilized with polyacrylic acid was found to be more potent than macroparticulate platinum in HaCAT cells and in UV-irradiated mice [54]. AD could be exacerbated by nickel-induced contact allergy; therefore topical agents to reduce the penetration of nickel into skin have sometimes been proposed to avoid disease exacerbation. Nanoparticles in the size range of 500 nm containing calcium carbonate were able to capture nickel ions by cation exchange, and remained on the surface of the skin, allowing them to be removed by simple washing with water. Approximately 11-fold fewer nanoparticles by mass were required to achieve the same efficacy as the alternative chelating agent ethylenediamine tetra acetic acid [55].

Since one of the most important functions of the skin is to prevent dehydration and protect from the penetration of exogenous chemicals and infectious agents, the compromised skin barrier typical of AD might significantly affect the permeability of the skin thus changing the MW cutoff value of penetrants. The involved skin of AD patients was found to have elevated TEWL compared to the noninvolved skin which in turn had a higher TEWL compared to the skin of healthy individuals [56,57]. The penetration of a mixture of lipid-soluble and water-soluble dyes through the skin of clinically normal atopic patients and skin of healthy subjects was investigated using photoacoustic spectrometry. Dyes were found to penetrate faster through the clinically normal skin of atopic patients, compared with skin of healthy subjects. In addition, penetration of hydrophilic dyes were positively correlated with the serum IgE levels and with the disease severity [56]. Other studies compared the penetration of hydrocortisone after topical application to both AD skin and healthy skin and the penetration ranged from 4% to 19% and 0.3% to 3% of

the applied dose in case of atopic patients and healthy subjects respectively [58,59].

The recognition of the disrupted skin barrier properties in AD might suggest that macromolecules like peptides, proteins, or oligonucleotides would have significantly higher bioavailability after topical application to diseased skin compared to healthy skin. This suggests the potential for targeted drug delivery of these high MW molecules for the treatment of dermatitis, with the ability to minimize the undesirable local side effects on the surrounding healthy skin, and absorption into the systemic circulation. As the course of treatment progresses, the inflamed skin would heal gradually and restore the original barrier properties leading to a gradual reduction in the penetration of such large molecules, which will subsequently reduce any associated systemic risks.

Potential Risks and Challenges in Use of Nanoparticles

Developments in the field of nanotechnology, including the application of nanomaterials in a wide variety of different fields including cosmetics, food, and medicine, have made possible exposure to nanomaterials in everyday life unavoidable to some extent. Amorphous silica nanoparticles are widely used nanomaterials that were found to aggravate the symptoms of AD in a size-dependent manner (particles tested were in the size range from 30 to 1000 nm). AD was induced in NC/Nga mice by the intradermal injection of mite antigen *Dermatophagoides pteronyssinus*, and the combined injection of amorphous silica nanoparticles aggravated the AD symptoms mainly due to excessive induction of total IgE and a stronger systemic Th2-response associated with high levels of IL-18 and thymic stromal lymphopoietin (TSLP) in the skin lesions [60]. However, positively charged silica nanoparticles were found to have no effect on the course of oxazolone-induced allergic contact dermatitis during exposure for five consecutive days [61].

TiO₂ and ZnO are insoluble metal oxides that are commonly used in the cosmetic industry due to their opacifying, antimicrobial, and UV-protective properties. However, their efficient use has been hindered due to their poor dispersion properties and their comedogenic potential, encouraging the development of next-generation nanosized metal oxide particles for avoiding such problems. Therefore, sunscreens containing such nanoparticles are considered one of the products to which many people are deliberately exposed. A comparative study of the accumulation of nanosized ZnO particles to bulk-sized particles revealed a significant accumulation of the nanomaterial in the viable epidermal and dermal layers of AD-like skin lesions in

mice induced by ovalbumin and staphylococcal enterotoxin B after tape stripping. On the other hand, the bulk-sized ZnO was only detectable on the upper surface of the SC of the skin without any deeper penetration. In addition, significant superiority of the nanosized material was also observed in their ability to suppress the infiltration of inflammatory cells in the sensitized skin. However, elevated IgE levels have also been observed which means that the exposure of AD skin to nanosized ZnO might have a significant accumulation with some beneficial effects causing relief of inflammatory symptoms, but also with the risk of possible aggravation of IgE antibody secretion, leading it to be considered a “double edged sword” [4].

It was found that the disruption of the superficial skin barrier by tape in an allergic contact dermatitis model could neither lead to enhanced penetration of AHAPS–SiO₂ nanoparticles, nor their penetration below the SC with systemic uptake after topical application. Only after subcutaneous injection were the SiO₂ nanoparticles taken up by the macrophages in the skin and then delivered to the lymph nodes during a 5-day period. This indicated that these nanoparticles could be used for targeting the skin surface in intact or inflamed skin, but for deeper penetration purposes such as vaccination another route of delivery would be preferred [62].

In the light of the findings from earlier in this chapter, it is clear that nanotechnology can sometimes carry risk but also can be considered absolutely safe in some other cases. This disparity in findings necessitates a thorough investigation of each system, concentrating on the disease indication, the intended skin type it is to be used for, and under the specific in-use conditions that apply, to ensure the maximum safety and efficacy of the nanocarrier for each anticipated use.

References

- [1] Thomsen SF. Atopic dermatitis: natural history, diagnosis and treatment. ISRN Allergy 2014;2014. Article ID: 354250, 7 pages.
- [2] Bieber T. Atopic dermatitis. Ann Dermatol 2010;22:125–37.
- [3] Zheng T, Yu J, Oh MH, Zhu Z. The atopic march: progression from atopic dermatitis to allergic rhinitis and asthma. Allergy Asthma Immunol Res 2011;3:67–73.
- [4] Ilves M, Palomaki J, Vippola M, Lehto M, Savolainen K, Savinko T, et al. Topically applied ZnO nanoparticles suppress allergen induced skin inflammation but induce vigorous IgE production in the atopic dermatitis mouse model. Part Fibre Toxicol 2014;11:38–50.
- [5] Novak N, Bieber T, Allam J-P. Recent highlights in the pathophysiology of atopic eczema. Int Arch Allergy Immunol 2005;136(2): 191–7.
- [6] Palmer C, Irvine A, Terron-Kwiatkowski A, Zhao Y, Liao H, Lee S, et al. Common loss-of-function variants of the epidermal barrier protein filaggrin are a major predisposing factor for atopic dermatitis. Nat Genet 2006;38:441–6.
- [7] Abdel-Mottaleb MMA, Try C, Pellequer Y, Lamprecht A. Nanomedicine strategies for targeting skin inflammation. Nanomedicine 2014;9:1727–43.

- [8] Li C, Lasse S, Lee P, Nakasaki M, Chen S, Yamasaki K, et al. Development of atopic dermatitis-like skin disease from the chronic loss of epidermal caspase-8. *PNAS* 2010;107:22249–54.
- [9] Imokawa G, Abe A, Jin K, Higaki Y, Kawashima M, Hidano A. Decreased level of ceramides in stratum corneum of atopic dermatitis: an etiologic factor in atopic dry skin? *J Inv Dermatol* 1991;96: 523–7.
- [10] Bucks D. Permeability through diseased and damaged skin. In: Walters K, Roberts M, editors. *Dermatologic, cosmeceutic and cosmetic development, therapeutic and novel approaches*. New York: Informa Healthcare USA, Inc.; 2007. p. 157–67 [chapter 9].
- [11] Anderson C. Treatment of dermatitis. In: Walters K, Roberts M, editors. *Dermatologic, cosmeceutic and cosmetic development, therapeutic and novel approaches*. New York: Informa Healthcare USA, Inc.; 2007. p. 21–43 [chapter 3].
- [12] Watson W, Kapur S. Atopic dermatitis. *Allergy Asthma Clin Immunol* 2011;7(Suppl. 1):S4.
- [13] Asher MI, Montefort S, Björkstén B, Lai CK, Strachan DP, Weiland SK, et al. Worldwide time trends in the prevalence of symptoms of asthma, allergic rhinoconjunctivitis, and eczema in childhood: ISAAC Phases One and Three repeat multicountry cross-sectional surveys. *The Lancet* 2006;368(9537):733–43.
- [14] Thomsen SF, Ulrik CS, Kyvik KO, Hjelmborg Jv, Skadhauge LR, Steffensen I, et al. Importance of genetic factors in the etiology of atopic dermatitis: a twin study. *Allergy Asthma Proc* 2007; 28(5):535–9.
- [15] Flohr C, Mann J. New insights into the epidemiology of childhood atopic dermatitis. *Allergy* 2014;69:3–16.
- [16] Mijalovic H, Fallon PG, Irvine AD, Foster TJ. Effect of filaggrin breakdown products on growth of and protein expression by *Staphylococcus aureus*. *J Allergy Clin Immunol* 2010;126:1184–90.
- [17] Schram ME, Tedja AM, Spijker R, Bos JD, Williams HC, Spuls PI. Is there a rural/urban gradient in the prevalence of eczema? A systematic review. *Br J Dermatol* 2010;162:964–73.
- [18] Ellwood P, Asher MI, Garcia-Marcos L, Williams H, Keil U, Robertson C, et al. Do fast food cause asthma, rhinoconjunctivitis and eczema? Global findings from the International Study of Asthma and Allergies in Childhood (ISAAC) phase three. *Thorax* 2013;68:351–60.
- [19] Ellwood P, Asher MI, Björkstén B, Burr M, Pearce N, Robertson CF. Diet and asthma, allergic rhinoconjunctivitis and atopic eczema symptom prevalence: an ecological analysis of the International Study of Asthma and Allergies in Childhood (ISAAC) data. ISAAC Phase One Study Group. *Eur Respir J* 2001;17:436–43.
- [20] Sausenthaler S, Kompauer I, Borte M, Herbarth O, Schaaf B, Berg A, et al. Margarine and butter consumption, eczema and allergic sensitization in children. The LISA birth cohort study. *Pediatr Allergy Immunol* 2006;17:85–93.
- [21] Miyake Y, Sasaki S, Tanaka K, Ohfuji S, Hirota Y. Maternal fat consumption during pregnancy and risk of wheeze and eczema in Japanese infants aged 16–24 months: the Osaka Maternal and Child Health Study. *Thorax* 2009;64:815–21.
- [22] Loss G, Apprich S, Waser M, Kneifel W, Genuneit J, Buchele G, et al. The protective effect of farm milk consumption on childhood asthma and atopy: the GABRIELA study. *J Allergy Clin Immunol* 2011;128:766–73.
- [23] Roduit C, Wohlgensinger J, Frei R, Bitter S, Bieli C, Loeliger S, et al. Prenatal animal contact and gene expression of innate immunity receptors at birth are associated with atopic dermatitis. *J Allergy Clin Immunol* 2011;127:179–85.
- [24] Tsakok T, McKeever TM, Yeo L, Flohr C. Does early life exposure to antibiotics increase the risk of eczema? A systematic review. *Br J Dermatol* 2013;169:983–91.
- [25] Eichenfield L, Tom W, Berger T, Krol A, Paller A, Schwarzenberger K, et al. Guidelines of care for the management of atopic dermatitis. *J Am Acad Dermatol* 2014;71:116–32.
- [26] Ruzicka T, Bieber T, Schöpf E, Rubins A, Dobozy A, Bos J, et al. A short-term trial of tacrolimus ointment for atopic dermatitis. *N Engl J Med* 1997;337:816–21.
- [27] Reitamo S, Wollenberg A, Schöpf E, Perrot J, Marks R, Ruzicka T, et al. Safety and efficacy of 1 year of tacrolimus ointment monotherapy in adults with atopic dermatitis. *Arch Dermatol* 2000; 136:999–1006.
- [28] Meurer M, Fölster-Holst R, Wozel G, Weidinger G, Junger M, Brautigam M, et al. Pimecrolimus cream in the long-term management of atopic dermatitis in adults: a six-month study. *Dermatology* 2002;205:271–7.
- [29] Wollenberg A, Reitamo S, Girolomoni G, Lahfa M, Ruzicka T, Healy E, et al. Proactive treatment of atopic dermatitis in adults with 0.1% tacrolimus ointment. *Allergy* 2008;63:742–50.
- [30] Thaci D, Reitamo S, Gonzalez Ensenat MA, Moss C, Boccaletti V, Cainelli T, et al. Proactive disease management with 0.03% tacrolimus ointment for children with atopic dermatitis: results of a randomized, multicentre, comparative study. *Br J Dermatol* 2008;159:1348–56.
- [31] Pople PV, Singh KK. Targeting tacrolimus to deeper layers of skin with improved safety for treatment of atopic dermatitis-Part II: in vivo assessment of dermatopharmacokinetics, biodistribution and efficacy. *Int J Pharm* 2012;434(1):70–9.
- [32] Baspinar Y, Borchert HH. Penetration and release studies of positively and negatively charged nanoemulsions - is there a benefit of the positive charge? *Int J Pharm* 2012;430(1–2):247–52.
- [33] Schmidts T, Marquardt K, Schlupp P, Dobler D, Heinz F, Mäder U, et al. Development of drug delivery systems for the dermal application of therapeutic DNAs. *Int J Pharm* 2012;431(1):61–9.
- [34] Santos Maia C, Mehnert W, Schaller M, Korting HC, Gysler A, Haberland A, et al. Drug targeting by solid lipid nanoparticles for dermal use. *J Drug Target* 2002;10:489–95.
- [35] Shah KA, Date AA, Joshi MD, Patravale VB. Solid lipid nanoparticles (SLN) of tretinoin: potential in topical delivery. *Int J Pharm* 2007;345(1):163–71.
- [36] Pople PV, Singh KK. Targeting tacrolimus to deeper layers of skin with improved safety for treatment of atopic dermatitis. *Int J Pharm* 2010;398(1):165–78.
- [37] Korting HC, Schäfer-Korting M. Carriers in the topical treatment of skin disease. *Handb Exp Pharmacol* 2010;197:435–68.
- [38] Hasanovic A, Hoeller S, Valenta C. Analysis of skin penetration of phytosphingosine by fluorescence detection and influence of the thermotropic behaviour of DPPC liposomes. *Int J Pharm* 2010; 383(1):14–7.
- [39] Li G, Fan Y, Fan C, Li X, Wang X, Li M, et al. Tacrolimus-loaded ethosomes: physicochemical characterization and in vivo evaluation. *Eur J Pharm Biopharm* 2012;82(1):49–57.
- [40] Cevc G, Blume G, Schatzlein A. Transdermal drug carriers: basic properties, optimization and transfer efficiency in the case of epicutaneously applied peptides. *J Cont Rel* 1995;36:3–16.
- [41] Cevc G, Blume G, Schatzlein A. Transfersomes-mediated transepidermal delivery improves the regio-specificity and biological activity of corticosteroids in vivo. *J Cont Rel* 1997;45:211–26.
- [42] Cevc G, Blume G. Biological activity and characteristics of triamcinolone-acetonide formulated with the self-regulating drug carriers. *Transfersomes Biochim Biophys Acta* 2003;1614: 156–64.
- [43] Cevc G, Blume G. Hydrocortisone and dexamethasone in very deformable drug carriers have increased biological potency, prolonged effect, and reduced therapeutic dosage. *Biochim Biophys Acta* 2004;1663:61–73.

- [44] Cevc G, Schatzlein A, Richardsen H. Ultradeformable lipid vesicles can penetrate the skin and other semi-permeable barriers unfragmented. Evidence from double label CLSM experiments and direct size measurements. *Biochim Biophys Acta* 2002;1564:21–30.
- [45] Honeywell-Nguyen PL, Gooris GS, Bouwstra JA. Quantitative assessment of the transport of elastic and rigid vesicle components and a model drug from these vesicle formulations into human skin in vivo. *J Invest Dermatol* 2004;123:902–10.
- [46] Sinico C, Fadda AM. Vesicular carriers for dermal drug delivery. *Expert Opin Drug Deliv* 2009;6(8):813–25.
- [47] Romero E, Morilla M. Highly deformable and highly fluid vesicles as potential drug delivery systems: theoretical and practical considerations. *Int J Nanomed* 2013;8:1–16.
- [48] Abdel-Mottaleb MMA, Neumann D, Lamprecht A. Lipid nanoparticles for dermal application: a comparative study of lipid based versus polymer based nanocarriers. *Eur J Pharm Biopharm* 2011;79:36–42.
- [49] Abdel-Mottaleb MMA, Moulari B, Beduneau A, Pellequer Y, Lamprecht A. Nanoparticles enhance therapeutic outcome in inflamed skin therapy. *Eur J Pharm Biopharm* 2012;82:151–7.
- [50] Hussain Z, Katas H, Mohd Amin MC, Kumolosasi E, Buang F, Sahudin S. Self-assembled polymeric nanoparticles for percutaneous co-delivery of hydrocortisone/hydroxytyrosol: an ex vivo and in vivo study using an NC/Nga mouse model. *Int J Pharm* 2013;444(1):109–19.
- [51] Rosado C, Silva C, Reis CP. Hydrocortisone-loaded poly(ϵ -caprolactone) nanoparticles for atopic dermatitis treatment. *Pharm Dev Technol* 2013;18(3):710–8.
- [52] Vicentini FT, Depieri LV, Polizello AC, Del Ciampo JO, Spadaro AC, Fantini MC, et al. Liquid crystalline phase nanodispersions enable skin delivery of siRNA. *Eur J Pharm Biopharm* 2013;83(1):16–24.
- [53] Desai PR, Marepally S, Patel AR, Voshavar C, Chaudhuri A, Singh M. Topical delivery of anti-TNF α siRNA and capsaicin via novel lipid-polymer hybrid nanoparticles efficiently inhibits skin inflammation in vivo. *J Cont Rel* 2013;170(1):51–63.
- [54] Yoshihisa Y, Honda A, Zhao QL, Makino T, Abe R, Matsui K, et al. Protective effects of platinum nanoparticles against UV-light-induced epidermal inflammation. *Exp Dermatol* 2010;19(11):1000–6.
- [55] Vemula P, Anderson R, Karp J. Nanoparticles reduce nickel allergy by capturing metal ions. *Nat Nanotechnol* 2011;6(5).
- [56] Hata M, Tokura Y, Takigawa M, Sato M, Shioya Y, Fujikura Y, et al. Assessment of epidermal barrier function by photoacoustic spectrometry in relation to its importance in the pathogenesis of atopic dermatitis. *Lab Invest* 2002;82:1451–61.
- [57] Werner Y, Lindberg M. Transepidermal water loss in dry and clinically normal skin in patients with atopic dermatitis. *Acta Derm Venereol* 1985;65:102–5.
- [58] Aalto-Korte K, Turpeinen M. Quantifying systemic absorption of topical hydrocortisone in erythroderma. *Br J Dermatol* 1995;133:403–8.
- [59] Aalto-Korte K, Turpeinen M. Transepidermal water loss and absorption of hydrocortisone in widespread dermatitis. *Br J Dermatol* 1993;128:633–5.
- [60] Hirai T, Yoshikawa T, Nabeshi H, Yoshida T, Tochigi S, Ichihashi K, et al. Amorphous silica nanoparticles size-dependently aggravate atopic dermatitis-like skin lesions following an intradermal injection. *Part Fibre Toxicol* 2012;9:3.
- [61] Ostrowski A, Nordmeyer D, Boreham A, Brodwolf R, Mundhenk L, Fluhr J, et al. Skin barrier disruptions in tape stripped and allergic dermatitis models have no effect on dermal penetration and systemic distribution of AHAPS-functionalized silica nanoparticles. *Nanomedicine* 2014;10:1571–81.
- [62] Ostrowski A, Nordmeyer D, Mundhenk L, Fluhr J, Lademann J, Graf C, et al. AHAPS-functionalized silica nanoparticles do not modulate allergic contact dermatitis in mice. *Nanoscale Res Lett* 2014;9:524–30.

Challenges and Opportunities of Nanoparticle-Based Theranostics in Skin Cancer

S. Pizzimenti¹, C. Dianzani¹, G.P. Zara¹, C. Ferretti¹, F. Rossi¹, C.L. Gigliotti², M. Daga¹, E.S. Ciamporzero¹, G. Maina¹, G. Barrera¹

¹University of Turin, Turin, Italy; ²University of Eastern Piedmont, “Amedeo Avogadro”, Novara, Italy

OUTLINE

Introduction	177	Glossary	185
Nanoparticles in Cancer Theranostics	178	List of Acronyms and Abbreviations	185
Nanoparticles for Transdermal Drug Delivery	179	References	185
Skin Cancers	181		
Conclusions	185		

INTRODUCTION

Nanoparticles (NPs) offer remarkable potential for future biomedical technology with simultaneous applications for diagnosis and therapy of disease sites. They are an effective method of molecular imaging because of their intense and stable output, strong target binding via multiple ligands, multimodal signaling capacity, and controlled biodistribution [1]. NPs, with dimensions from one to hundreds of nanometers, are increasingly popular in imaging since they can interact with light, sound, and electromagnetic fields. Moreover, their use as drug carriers for therapeutic applications has long been studied, in particular in the context of cancer therapy. Indeed, when infused into the bloodstream they can accumulate in tumors owing to the enhanced permeability and retention effect (EPR) since the vasculature of immature tumors has pores smaller than 200 nm, permitting extravasation of NPs from blood into tumor

tissue [2]. The infusion of anticancer drugs carried by NPs results in an increased payload of drugs to the tumor, as compared with conventional infusion [3].

NPs are particularly intriguing when used for combination applications that are both therapeutic and diagnostic. The term theranostics describes technology with concurrent and complementary diagnostic and therapeutic capabilities [4]. Theranostics is particularly useful when used in the cancer treatment because of the tumor heterogeneity and adaptive resistance which require the ability to address these two intrinsic properties of this complex disease.

Skin cancer is the most common form of malignancy principally in the white population; in the United States and many other countries, more than 3.5 million cases are diagnosed each year and its incidence is progressively and worryingly increasing [5]. While surgery is the primary treatment used for local and nonmetastatic skin cancers, anticancer drugs are the choice currently

used in metastatic disease. The use of NPs for the treatment and diagnosis of metastatic skin cancers has increased along with efforts to identify new systems that can be used for theranostics.

NANOPARTICLES IN CANCER THERANOSTICS

The nature and physical chemistry of the nanomaterial clearly influence the *in vitro* and *in vivo* behavior of the theranostic particles [6]. Thus, a successful theranostic effect relies on the structure and formulation of the multifunctional nanoplateforms. Thereafter, significant characteristics of the nanomaterial that facilitate an optimum theranostic activity (with minimized toxicity) are the geometry (very small size, ≤ 100 nm and spherical shape), null or almost negligible surface electrical charge, hydrophilic character, biocompatibility, and controlled biodegradability. A proper nanostructure could even be of great help in the delivery and follow-up of drug molecules and contrast agents through the blood-brain barrier (BBB) [6,7]. To this concrete aim, the nanoplateform should be designed with a very small size, a slightly positive electrical charge, and, if possible, surface functionalized with adequate ligands that could facilitate NP endocytosis by ligand–receptor interactions [7,8]. With respect to the chemical composition, the nanoparticulate material can be based on inorganic material or organic matrix.

NPs are prepared with organic polymers (organic NPs) and/or inorganic elements (inorganic NPs). Polymer-based NPs, lipid-based NPs (liposomes, nanoe-mulsion, and solid-lipid NP), self-assembling nanostructures such as polymeric micelles, and dendrimers-based nanostructures are examples of organic NPs.

Therapeutic NPs with a highly defined lipid scaffold are mainly the liposomes. They are phospholipid vesicles (dimension of 50–100 nm and even larger) that have a bilayered membrane structure, similar to that of biological membranes, together with an internal aqueous phase. Liposomes are classified according to size and number of layers into multi-, oligo-, or unilamellar. The aqueous core can be used for encapsulation of water-soluble drugs, whereas the lipid bilayers may retain hydrophobic or amphiphilic compounds. To escape from reticuloendothelial system (RES) uptake after IV injection, PEGylated liposomes, “stealth liposomes,” were developed for reducing clearance and prolonging circulation half-life [9].

Liposomes show excellent circulation, penetration, and diffusion properties. The possibility to link the liposomes surface with ligands and/or polymers increases significantly the drug delivery specificity [10]. Currently, several liposomal formulations in the clinical practice

contain several drugs for the treating of ovarian cancer, AIDS-related Kaposi’s sarcoma, multiple myeloma, lymphoma, etc. [11]. New opportunities were proposed by Madaswamy Muthu and Si-Shen Feng [12] that developed a theranostic liposome, with the possibility of loading wide variety of diagnostic NP along with anticancer drug in combination with vitamin E TPGS coating.

A progressive type of lipid-based NP emerging in the therapeutic fields is the solid-lipid NPs (SLNs). SLNs present a high physical stability, they can protect the drugs against degradation, and they allow an easy control of the drug release. The preparation of SLNs does not require the use of organic solvents. They are biodegradable, biocompatible, and have low toxicity. In addition, the production and sterilization on a large scale are rather easy [13]. SLNs containing docetaxel improve the efficacy of this chemotherapeutic agent in colorectal (C-26) and malignant melanoma (A-375) cell lines in “*in vitro*” and “*in vivo*” experiments [14]. Cholesteryl butyrate SLNs have been shown to inhibit human umbilical vein endothelial cells’ adhesiveness to cancer cell lines derived from human colon-rectum, breast, prostate cancers, and melanoma [15].

Various multistimuli-responsive polymeric matrix system loaded with magnetic NPs have been developed to control the behavior of nanosystems. In particular, it is possible to trigger drug release in complex luminescent/magnetic nanosystems under magnetic guidance and near-infrared irradiation *in vivo* [16].

Other kinds of nanosystems include polymeric micelles; they are formed by two or more polymer chains with different hydrophobicity. These copolymers spontaneously assemble into a core-shell micellar structure [17]. The typical size of micelles for pharmaceutical applications ranges from 10 to 80 nm. Micelles, being smaller than liposomes, have a short circulation time, but they show a superior uptake by tumors, because of the EPR effect. Poorly soluble drugs, with high loading capacity (5–25 wt%) can be carried in the hydrophobic core, while the hydrophilic shell allows a steric protection for the micelle and thereby reduces their systemic toxicity. Functional groups suitable for ligands, such as antibodies, peptides, nucleic acid aptamers, carbohydrates, and small molecules, further increase their specificity and efficacy [18–20]. Polymeric micelles are usually more stable in blood than liposomes and other surfactant micelles. Due to their considerably large size, these polymeric micelle systems can also be used to co-deliver two or more drugs for combinational therapeutic modalities, such as radiation agents and drugs [9,21]. Polymeric micelles have been used for the treatment of B16F10 melanoma-bearing mice [22]. Paramagnetic metals, such as gadolinium (Gd) or manganese (Mn), normally used in

contrast agents, can also easily be incorporated into micelles for imaging applications.

Dendrimers are a unique class of repeatedly branched polymeric macromolecules with a nearly perfect 3D geometric pattern. They have been extensively studied in the area of therapeutics and diagnostics for cancer as well as for photodynamic therapy [23], boron neutron capture therapy [24], and hyperthermia therapies using gold NPs [25]. Their surface can be engineered with a variety of functionalities, enhancing their biocompatibility and biodegradability for widespread biomedical applications [26].

The inorganic NPs represent a different class of NPs that are usually much smaller, 5–40 nm, and they do not have the flexibility observed in liposomes and polymeric NPs. Inorganic theranostic nanotools are commonly based on quantum dots (semiconductor nanocrystals composed of cadmium selenide which exhibit significant fluorescence imaging properties) [27], metals (eg, silver, gold, dielectric silica cores coated by an ultrathin gold layer) [28], and superparamagnetic iron oxide NPs (SPION) [29]. By themselves, they have been classically used as signal emitters/contrast agents in MRI [30], optical coherence tomography [31], confocal imaging [32], photoacoustic tomography [33], and/or near-infrared tomography [34]. For instance, iron oxide NPs have been used for imaging tumors [35]. Additionally, iron oxide NPs can be guided to target sites such as a tumor using external magnetic field and they can be also heated to provide hyperthermia for cancer therapy [36].

Gold NPs (AuNP) are another kind of inorganic metal particle used in targeting tumors. Other examples include Ag, Ni, Pt, and TiO₂ NPs. AuNPs (1–150 nm) can be prepared with different geometries, such as nanospheres, nanoshells, nanorods, or nanocages. The advantages of AuNPs are their ease of preparation in a range of sizes, good biocompatibility, ease of functionality, and ability to conjugate with other biomolecules without altering their biological properties [37]. AuNPs with diameters ≤ 50 nm have been shown to cross the BBB [37]. They can be used to sensitize cells and tissue for treatment regimens [38], and to monitor and guide surgical procedures [1]. Different types of drugs, including proteins and DNA as well as smaller drug molecules, have been linked to the surface chemistry of AuNP, inducing a therapeutic effect in several types of tumors, including melanoma. They are also excellent labels for biosensors, because they can be detected by numerous techniques, such as optical absorption, fluorescence, and electric conductivity [39]. The use of the confocal reflectance microscope with antibody-conjugated AuNP has made the development of highly sensitive cancer imaging possible [40]. Furthermore, they are not toxic and biocompatible.

In fact, they do not elicit any allergic or immune responses [41].

Finally, organic–inorganic nanohybrids, that is, based on an inorganic core embedded into an organic matrix (such as, SPION/biodegradable polymer (core/shell) nanostructures) are of greater interest due to their multimodality imaging possibilities, capability for multidrug delivery, and additional treatment options (ie, hyperthermia, photodynamic therapy, photothermal therapy) [8,42,43]. In the ideal case, more than one signal emitter, photosensitizer agent, and drug molecule (or gene) could be incorporated into the organic matrix, while the inorganic core could also play a key role as contrast agent and/or as a significant functionalization structure for active targeting to nonhealthy sites; for example, SPION have been demonstrated to be efficient contrast agents for MRI, drug nanocarriers, and hyperthermic particles [44]. A prototype of carbon-coated SPION for sentinel lymph nodes mapping in melanoma and breast cancer patients has been developed [45].

NANOPARTICLES FOR TRANSDERMAL DRUG DELIVERY

The skin is the largest organ of the body, covering approximately 16% of body mass. Skin is composed of two primary layers, epidermis and dermis, which, in turn, are composed of cells of different origin: epithelial, mesenchymal, glandular, and neurovascular. Epidermis is the peripheral layer of skin that contacts with the environment, acting as a physiochemical barrier against environmental stressors such as pathogens, chemicals, and ultraviolet light [46]. The dermis, originated from the mesoderm, underlies the epidermis and anchors cutaneous structures such as hair follicles, nerves, sebaceous glands, and sweat glands. The most abundant cells of the epidermis are keratinocytes. Epidermal keratinocytes are a result of cell division by keratinocyte stem cells in the stratum basale (basal layer), and constitute the principal barrier of the epidermal coating [47].

The skin as a route of administration of drugs shows relevant benefits compared to oral or intravenous administration, the potential advantages of topical drug delivery including ease of application, dose termination, large surface area, patient compliance, less enzymatic and pH based drug degradation, and direct access to skin. The current global transdermal market is valued at \$30 billion, which is held by only a handful of molecules [48]. Such a figure is not surprising when we consider that the skin acts as a protective barrier, and that the rate of molecular transport through the stratum corneum (SC) is constrained and slow: it follows that transdermal drug delivery (TDD) as well as dermal

drug delivery (DDD) is suitable only for very potent drugs with adequate molecule's skin permeability profile (small molecular weight of <500 kDa, $\log P$ value of 5, melting point of 200°C , and appropriate lipophilicity) [49].

NPs possess inimitable properties of promoting drug absorption, allowing sustained drug release for prolonged time periods and protecting the encapsulated substance from chemical degradation; hence, they have the potential in effectively delivering drugs across the skin. Two main pathways are recognized as transdermal penetration mechanism: the transappendageal pathway and the transepidermal pathway (Fig. 14.1).

The first is also known as the "shunt route" because of the presence of natural openings in the skin (eg, sweat glands, hair follicles and areas of low cell-lipid packing such as wrinkles), which facilitate the permeation of drugs through the skin. These conduits are hydrophilic and have natural openings of at least a few microns [50,51]. However, this route of administration is limited by the fact that they constitute only 0.1% of the total skin surface area. The second pathway is subcategorized into two micropathways: the intercellular route, which is a continuous but tortuous way through the intercellular lipid domains surrounding the cells, and secondly, the transcellular pathway, where drug molecules partition into and diffuse across both corneocytes and intercellular lipid lamellae. The process of diffusing across both hydrophilic and hydrophobic domains is highly unfavorable for most drugs and for this reason, despite the relatively small surface area available, the intercellular pathway is the preferred route of administration. Hydrophilic molecules can permeate across aqueous pathways created by imperfections in the SC lipid bilayers. These can be due to missing lipids, steric constraints placed by the corneocytes,

and lipid bilayers or the packing defects associated with the different kinds of lipids that associate together in the lamellae. These defects can have a length scale of a few nanometers and it has been seen that the average porosity is of about $2 \times 10^{-5} \text{ cm}^2$. Depending on the physical–chemical characteristics of the permeating compound it will, however, permeate through the barrier according to a combination of all three pathways [52].

The types of nanocarriers that are used today have significantly increased in the last decades. These systems are designed around the two characteristics that are sought in the modern pharmacy: temporal delivery and spatial location. It is hard to say what is the ideal nanocarrier, because every day, new advantages and disadvantages of each are discovered. We can mention as general advantages improvements in drug solubility, permeability, half-life, bioavailability, and stability, among other properties, and the main disadvantages are low load capacity in many cases and lack of stability of the system per se [53].

An important point highlighted by Panariti et al. [54] is that physicochemical properties of nanocarrier systems determine the interaction with biological systems and nanocarrier cell internalization. The main physicochemical properties that affect cellular uptake are size, shape, rigidity, and charge in the surface of NPs.

Nanoparticulated systems can be administered into organisms by almost all routes including transdermal. The most used and investigated nanocarriers for topical/TDD as a function of the material used to prepare them include liposomes, transfersomes, ethosomes, niosomes, lipidic NPs, polymeric NPs, and nanoemulsions [55]. These nanovehicles mainly increase or decrease the flux, adapt the drug depot location and size, and even selectively permeabilize the SC. The mechanisms of interaction of nanoaggregates with skin structures and their microenvironment, that is, furrows, hair follicles, eccrine ducts, and so on, are absolutely significant for the enhancement of cutaneous drug delivery. The topically used nanomedicines offer promising opportunities in dermal delivery, and recent advances and modifications appear to have generated increased therapeutic potential. Amelioration and variation in their composition and structure result in vesicles with required tailored properties. The enhancement in skin permeation can be also obtained by mean active penetration techniques as electrical methods (iontophoresis, electroporation) mechanical methods (microneedles, abrasion, suction, stretching), and other techniques (magnetophoresis, photomechanical waves, electron beam irradiation, sonophoresis) [56].

Hence, nanosystems possess a promising, adjustable platform for the biocompatible, safe, and effective

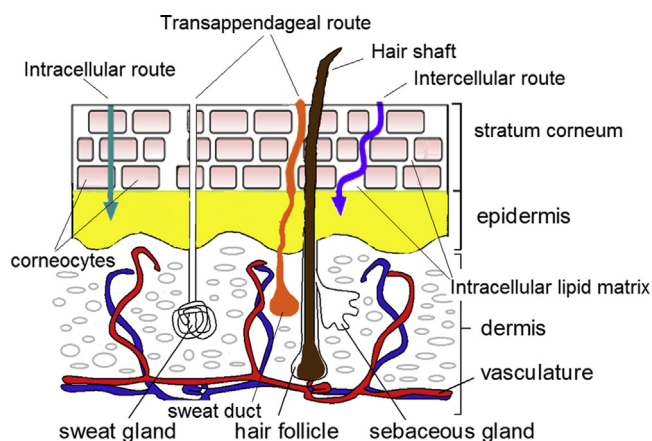


FIGURE 14.1 Schematic representation of the transdermal penetration mechanisms: transappendageal route and transepidermal route.

topical delivery of therapeutics, since they did not induce any short-term cytotoxicity or morphological changes in the SC [57].

Nanocarriers including liposomes, polymer, and lipid-based spherical NPs show a particle size >100 nm, while metal-based NPs can be prepared with particle size <100 nm. Several studies have demonstrated that some special NPs may possibly penetrate hair follicles [58] and the SC, reaching the viable epidermis [59]. Among these, AuNP has shown potential in varied biomedical applications such as nanocarrier systems and imaging agents. The initial interest in the topical application of AuNP was directed to study nanotoxicology [60]. Later, few studies reported AuNP as nanocarriers to deliver siRNA and protein products inside skin [61]. One of the bottlenecks in developing AuNP for drug delivery is to load the cargo in AuNP, but this approach involves complex chemistry, and often the resulting drug-conjugated AuNP is unstable in ionic medium. To overcome these limitations, Labala et al. [62] recently developed layer-by-layer polyelectrolyte coated AuNP (LbL-AuNP) as carrier for ionophoretic transport into skin of imatinib mesylate, an anticancer agent to treat melanoma in a phase II clinical study. The results of this study indicate that LbL-AuNP can be used for the topical delivery of a small anticancer drug, where iontophoresis application significantly enhances the skin penetration of imatinib. The application of SPION for drug delivery has been investigated in recent decades because of the intense magnetic responsiveness, strong drug-loading capacity, good biocompatibility, and high efficiency of targeted delivery of SPION [29]. A model anticancer agent, epirubicin (EPI), is attached to functionalized SPION. The covalent modification of the SPION results in EPI-SPION, a potential drug delivery vector that uses magnetism for the targeted transdermal chemotherapy of skin tumors. The spherical EPI-SPION composite exhibits excellent magnetic responsiveness with a saturation magnetization intensity of 77.8 emu/g. They feature specific pH-sensitive drug release, targeting the acidic microenvironment typical in common tumor tissues or endosomes/lysosomes. Cellular uptake studies using human keratinocyte HaCaT cells and melanoma WM266 cells demonstrate that SPION have good biocompatibility. After conjugation with EPI, the NPs can inhibit WM266 cell proliferation; its inhibitory effect on tumor proliferation is determined to be dose-dependent. In vitro transdermal studies demonstrate that the EPI-SPION composites can penetrate deep inside the skin driven by an external magnetic field circumventing the SC via follicular pathways, suggesting the potential of a SPION-based vector for feasible transdermal therapy of skin cancer [29].

SKIN CANCERS

The three main types of skin cancer are melanoma, basal cell carcinoma (BCC), and squamous cell carcinoma (SCC). SCC is a common disease with a prevalence of more than 700,000 cases each year in the United States [63].

The two major forms of skin cancer, BCC and SCC, both derived from epidermal keratinocytes, are less deadly than melanoma mainly due to their tendency to remain confined to their primary site of disease. Excision is the gold standard treatment for localized SCC and BCC. This can be obtained through curettage and desiccation, surgical excision, radiation therapy, cryosurgery, Mohs micrographic surgery, and micrographic surgery [64]. However, these treatments can result in significant disfigurement, leading to physical and emotional adverse consequences for the patients [65]. Moreover, although the majority of SCC and BCC remains locally invasive, 1–5% of primary SCC may diffuse to regional lymph nodes and distant sites, such as lungs, liver, brain, and other areas of the skin [66]. On the other hand, although very rare, BCC can metastasize to distant sites of the body, which is considered a terminal condition [66]. Therefore, for these types of skin cancers some drugs have been approved for the use in patients who refuse surgical treatment [67] or for situations in which postoperative healing is impaired, such as lesions that involve the lower limb in elderly patients or those with venous stasis disease [68]. Several formulations of NPs have been performed to improve the delivery of drugs used to treat skin lesions. In the case of SCC, magnetic nanocomposite spheres carrying 5-fluorouracil (5-Fu) were prepared [69] to improve the penetration of drug. Other methodological approaches to destroy SCC cells involved the use of gold nanorods, functionalized with epidermal growth factor receptor antibody-conjugated with gold nanorods which have been successfully used in an “in vitro” model of human SCC. Results obtained with laser photothermal therapy demonstrated that immunolabeled gold nanorods can selectively destroy the cancer cells and induce apoptosis through the reactive oxygen species (ROS) mediated mitochondrial pathway under low power laser exposure [70]. Photodynamic therapy (PDT) is a nonsurgical treatment that induces a cytotoxic effect by application of a photosensitizer (PS) followed by irradiation with wavelengths specific for its absorbance spectrum, in the presence of oxygen. Upon the photoirradiation of PS at specific wavelength(s), photodynamic reactions can generate cytotoxic ROS that oxidize subcellular organelles and biomolecules, ultimately leading to the destruction of diseased cells and tissues [71]. High efficacy is demonstrated for PDT using standardized protocols in nonhyperkeratotic actinic keratoses, Bowen’s

disease (SCC *in situ*), and superficial BCC [71]. Two PS agents, aminolevulinic acid (ALA) and methyl aminolevulinate (MAL) are currently available for use with PDT. However, due to the hydrophilic nature of ALA, ALA-PDT has been hindered by the rate of ALA uptake into neoplastic cells and its limited penetration into tissue. A first attempt has already been performed by using liposomes to better deliver ALA to the deep layers of epidermis [72]. ALA has also been carried by succinate-modified chitosan, and physically complexed with folic acid–modified chitosan [73] to improve drug penetration and release in the cellular lysosomes, and by polylactic-co-glycolic acid (PLGA) [74]. A new engineered polymer-based nanoplateform showing the convergence of two-photon fluorescence imaging and bimodal phototherapeutic activity in a single nanostructure has been suggested to be useful in the treatment of skin cancer. This structure has been achieved through the use of three different components: a β -cyclodextrin-based polymer acting as a suitable carrier, a zinc phthalocyanine emitting red fluorescence simultaneously as being a singlet oxygen ($(^1O_2)$) photosensitizer, and a tailored nitroaniline derivative, functioning as a nitric oxide (NO) photodonor. The self-assembly of these components results in photoactivable NPs, coencapsulating a multifunctional cargo, which can be delivered to carcinoma cells. The potential of dual therapeutic photodynamic action and two-photon fluorescence imaging capability in a single nanostructure make this system a candidate for theranostics [75]. In the latest years, general attention has been placed on studying the molecular composition of human skin. Indeed, it has been suggested that lipids, structural proteins, inflammatory mediators, nucleic acids, and small molecules in the skin can serve as disease biomarkers [76]. Moreover, the difference of molecular composition between the healthy and pathological skin may offer a cue to targeting NPs toward the disease site. In this context, magnetic/metallic NPs (MNPs) may be valuable for aspects of cell targeting [59]. Biomedical applications *in vivo* of MNPs may be separated in therapeutic (hyperthermia and drug-targeting) and diagnostic applications (magnetic resonance imaging) [77]. The transfer of magnetic energy to the particles in the form of heat can be used *in vivo* to increase the temperature of tumor tissues to destroy the cancer cells by hyperthermia. This method permits a restricted heating to the tumor area. In addition, drug-loaded MNPs, in combination with an external magnetic field and/or magnetizable implant, allow the delivery of particles to the desired area, fixing them at the local site while the drug is released. This leads to concentrating the anticancer drugs and retaining them locally for longer periods.

As well as the molecular composition in malignant keratinocytes that may offer important insight for targeting of drug-loaded NPs for SCC and BCC, the treatment of the more deadly skin cancer, melanoma, takes advantage of the molecular alterations present in melanoma cells with respect to normal melanocytes.

Melanoma is the major cause of skin cancer–related mortality, resulting in about 55,000 deaths worldwide in 2012 [5], with remarkable differences in stage-specific survival [78]. Localized disease is often curable through chirurgic excision, but advanced disease requires anticancer treatments [79]. Various biomarkers including BRAF V600E mutation of cutaneous melanoma [80] and KIT gene of mucosal melanoma [81] may help in the diagnosis of melanoma and in the choice of therapy. Moreover, these molecular alterations can give options for the detection of metastatic sites far from the primary lesion. Several melanomas show hyperactivation of the MAPK signaling pathway caused by activating mutation of BRAF ($\sim 50\%$ mutation frequency) and NRAS ($\sim 30\%$) or loss of function mutations of PTEN ($\sim 50\%$) [80]. Moreover, melanoma is one of the most immunogenic tumors in which immune evasion and immune suppression play an important role [82]. On the basis of these characteristics, small, targeted molecules, such as selective mutant BRAF V600E inhibitors vemurafenib and dabrafenib, an MEK inhibitor trametinib [83,84], and immune checkpoint inhibitor such as ipilimumab, an anticytotoxic T lymphocyte-associated antigen-4 (anti-CTLA-4) monoclonal antibody [85] have been developed and newly approved by the US Food and Drug Administration for the treatment of metastatic melanoma. Given the dependence of melanoma from hyperactivation of the MAPK signaling pathway, of particular interest appears the work reported by Basu and colleagues [86] which generated and tested NPs loaded with the MEK1 inhibitor PD98059 and proved its ability in enhancing the antitumor activity to cisplatin. Such study opened a new scenario on the possibility to combine highly effective targeted therapies in the field of melanoma such as combinations of BRAF inhibitors, MEK inhibitors, and PI3K inhibitors with the optimal delivery of the drugs also in difficult-to-reach sites such as brain metastasis.

Another potentially powerful application of NPs involves the use of RNA interference-based approaches. The possibility of tumor-selective delivery of small RNA or DNA molecules makes this application the most flexible and potentially powerful anticancer approach given that, in theory, every transcribed gene can be targeted. Recently, much attention has been directed to molecular beacons (MBs) as potential theranostic agents [87]. MBs

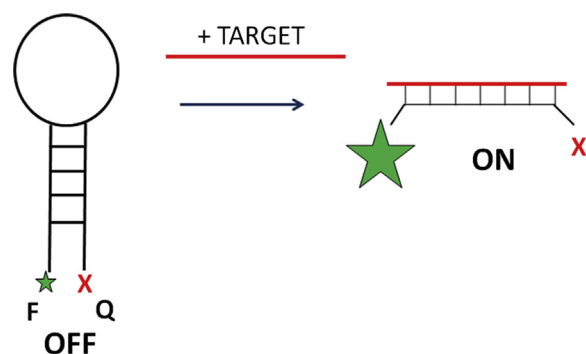


FIGURE 14.2 Molecular beacon: In the absence of the complementary mRNA the fluorescence of the fluorophore (F) is quenched by the closely located quencher (Q). The hybridization with target nucleic acid opens the hairpin and causes an optical oligonucleotide switch used for intracellular sensing.

are stem-loop-folded oligodeoxyribonucleotides with fluorophore and quencher dyes conjugated to the opposite ends of the hairpin. In the absence of the complementary nucleic acid target (mRNA), the fluorescence of the fluorophore is quenched by the closely located quencher [88]. Otherwise, the hybridization with target nucleic acid opens the hairpin, generates a probe-analyte duplex that physically separates the fluorophore from quencher, allowing a fluorescence signal to be emitted upon excitation (Fig. 14.2) [89,90].

MBs have been used to transfect into A375 and 501 melanoma cells. They generated high-signal intensity from the cytoplasm in surviving positive cells. Moreover, MB time dependently decreased surviving expression, induced apoptosis, and enhanced the pro-apoptotic effect of standard chemotherapeutic drugs tested at clinically relevant concentrations. The MB conjugating the ability of imaging with the pharmacological action may represent an innovative approach for cancer diagnosis and treatment [91]. As well as it regards NPs used for

theranostics in melanoma, one report demonstrated that a novel phospholipid-based microbubble formulation containing doxorubicin and perfluoropropane gas enhanced the inhibitory effects on the proliferation of B16BL6 melanoma murine cells in vitro and in vivo when combined with ultrasound (US) irradiation [92]. Additionally, US echo imaging showed high contrast enhancement of the DLMBs in the tumor vasculature.

An aptamer-conjugated theranostic magnetic hybrid graphene oxide–based assay for tumor cell detection from blood samples with combined therapy capability has been used in G361 human malignant melanoma cancer cells [93]. The authors demonstrated that indocyanine green-bound AGE-aptamer-attached hybrid graphene oxide provided selective imaging of G361 human malignant melanoma cancer cells and was capable of combined synergistic photothermal and photodynamic treatment of melanoma. Another NP model for imaging guided drug delivery application in melanoma cells has been provided by loading amphiphilic Gd(III) complex in PLGA-NPs [94]. The addition of gold nanoshells (including nanocages, nanorod-in-shell and NP-in-shell) to the nanomaterial-mediated photothermal effects, has been provided theranostic effects in the B16F0 melanoma tumor growth in mice. Indeed, these formulations not only were able to absorb near infrared light, but can also emit fluorescence, sensitize formation of singlet oxygen, and exert nanomaterial-mediated photodynamic therapeutic effects allowing the complete destruction of solid tumors [95]. Although different types of NPs have been proven to affect melanoma cell growth in vitro and in vivo, only a few types of nanovehicles have been approved for clinical trials. Several clinical trials comprise the use of drug-loaded nanovehicles together with conventional drugs. The therapeutic and diagnostic nanovehicles currently under clinical trial for melanoma are reported in Table 14.1.

TABLE 14.1 Nanovehicles in Therapy and Diagnosis of Skin Cancer

Drugs in nanovehicles as single therapeutic agents for skin cancers			
Nanomedicines	Condition	Trial ID	Phase, stage
Paclitaxel albumin-stabilized nanoparticles (alias nab-paclitaxel or Abraxane)	Pediatric patients with recurrent/refractory solid tumors, including melanoma	NCT01962103	Phase 1/2, recruiting
Nab-paclitaxel	Cutaneous squamous cell carcinoma	NCT02076243	Phase 2, not yet recruiting
PEGylated interferon-alpha-2a	Malignant melanoma stage IIA–IIIB	NCT00204529	Phase 3, ongoing, not recruiting
PEGylated interferon-alpha-2b	Melanoma stage I–III	NCT00871533	Phase 0, recruiting

Continued

TABLE 14.1 Nanovehicles in Therapy and Diagnosis of Skin Cancer—cont'd

Drugs in nanovehicles as single therapeutic agents for skin cancers			
Nanomedicines	Condition	Trial ID	Phase, stage
Docetaxel nanoparticles for injectable suspension (BIND-014)	Several advanced or metastatic cancer, including melanoma	NCT01300533	Phase 1, ongoing, not recruiting
Liposomes containing bifunctional short hairpin RNAs (shRNA) against human stathmin 1 (STMN1) (pbi-shRNA STMN1 LP)	Several metastatic tumors, including melanoma	NCT01505153	Phase 1, ongoing, not recruiting
Drugs in nanovehicles for combined therapy			
Combined Treatments	Condition	Trial ID	Phase, stage
Nab-paclitaxel in combination with bevacizumab	Patients with stage IV melanoma that cannot be removed by surgery	NCT02158520	Phase 2, recruiting
Nab-paclitaxel in combination with bevacizumab	BRAFwt metastatic melanoma	NCT01879306	Phase 2, recruiting
Nab-paclitaxel in combination with bevacizumab	Patients with stage IV melanoma that cannot be removed by surgery	NCT02020707	Phase 1, recruiting
Nab-paclitaxel in combination with ipilimumab	Metastatic melanoma	NCT01827111	Phase 2, recruiting
Nab-paclitaxel in combination with temozolomide and bevacizumab	Patients with metastatic melanoma with brain metastases	NCT02065466	Phase 1/2, recruiting
Nab-paclitaxel in combination with rituxan	Stage III and IV of melanoma	NCT02142335	Phase 2, recruiting
Nab-paclitaxel in combination with trametinib	Advanced unresectable or metastatic melanoma	NCT02300935	Phase 1, recruiting
Nab-paclitaxel in combination with PLX7486 (Fms/Trk tyrosine kinase inhibitor) and gemcitabine	Patients with advanced solid tumors, including melanoma	NCT01804530	Phase 1
Liposomal cytarabine (DepoCyt) in combination with lomustine and brain radiotherapy	Leptomeningeal metastasis from malignant melanoma	NCT01563614	Phase 1, ongoing, recruiting
Molecules in nanovehicles for diagnosis in skin cancers			
Nanoformulations	Purposes	Trial ID	Phase, stage
Magnetic nanoparticles	Using magnetic tracers, instead of radioactive tracers, to find the sentinel lymph nodes in patients with melanoma skin cancer	ISRCTN15768185	Phase 3, recruiting
Silica-based nanoparticles labeled with the fluorophore cyanine 5.5 (Cy5.5), and surrounded by polyethylene glycol (PEG) chains attached to cyclo-[Arg-Gly-Asp-Tyr] (cRGDY) peptides (fluorescent cRGDY PEG-Cy5.5 C dots)	For image-guided intraoperative sentinel lymph node mapping in head and neck melanoma, and other cancers	NCT02106598	Phase 0, recruiting

CONCLUSIONS

Skin cancers are common diseases whose treatment involves not only surgical excision but also transdermal and systemic chemotherapy. Among skin cancers, advanced melanoma represents the deadliest form, characterized by a high drug resistance. New drugs against skin cancer and melanoma cells, targeting specific molecular alteration or immunological characteristics, have proven to be vastly superior to conventional chemotherapy but their higher toxicity and the onset of resistance are the major limitations for their use. It is therefore clinically relevant to develop therapeutic strategies that can enhance drug effectiveness, overcome resistance, and reduce side effects. In this context, nanomedicine has offered several cues in improving drug transdermal and systemic delivery and release, and in reducing effective therapeutic doses. Nanotechnology in recent years has made significant progress in this field including highly effective targeted therapies and/or diagnostic markers.

The main opportunity offered by nanotheranostics is the possibility of combining the simultaneous noninvasive diagnoses and treatment of diseases with the possibility of monitoring in real time drug release and distribution, thus predicting and validating the effectiveness of the therapy. In the future, nanotheranostics could be used to perform a personalized medicine which will tailor optimized treatment to each patient, taking into account the individual variability.

However, nanotheranostics is still a young subject and little is known about the long-term exposure to nanomaterials. Thus, together with important opportunities, theranostics need to overcome several challenges that are not insignificant:

1. Definition of pharmacokinetic and pharmacodynamics profiles of the platform adopted. Although several reports demonstrated that some nanomaterials employed to make NPs are biologically inert, the loading of agents and ligands may change the toxicity of these particles. Moreover, although passive targeting based on the EPR effect increases the accumulation and retention of NPs in the tumor site, physical aspects such as size, shape, and charge can affect their pharmacokinetic and pharmacodynamic profiles.
2. Toxicity. The EPR effect does not mean that NPs go only to the tumors: most of the injected NPs end up in normal organs such as the liver, kidney, and spleen [96]. This means every NP should be tested for organ toxicity.
3. Effectiveness of targeting. The complexity of the EPR effect due to individual variability and tumor heterogeneity will have great influence on the efficacy of both passive and active targeting.

4. The lack of universal standards for evaluating the potent cytotoxicity of NPs and surfactants. This is an ineluctable problem that should be considered before NP commercialization.

In conclusion, for a successful transition of theranostic NPs to clinical practice, biodistribution, pharmacokinetics, metabolism, long-term toxicity, and degradation should be considered. Nonetheless, even though more research is necessary, nanotechnology may play an important role in the future of individualized medicine.

Glossary

Gold nanoshells Gold nanoshells are nanoparticles consisting of a silica core coated with a thin gold shell; they exhibit a strong optical resonance that depends sensitively on their core radius and shell thickness.

Molecular beacons Molecular beacons are hybridization probes for detection of nucleic acids in homogeneous solutions.

Nanoparticles Nanoparticles are carriers devices or systems sized in 1–100 nm range.

Nanotechnology Nanotechnology is the engineering of functional systems at nanoscale, thus being attractive for disciplines ranging from materials science to biomedicine. One of the most active research areas of the nanotechnology is nanomedicine, which applies nanotechnology to highly specific medical interventions for prevention, diagnosis, and treatment of diseases, including cancer disease.

Photosensitizer Photosensitizer is a light-sensitive molecule or atomic species that initiates a photochemical reaction.

Theranostics Theranostics is a combination of diagnostic and therapy and describes technology with concurrent and complementary diagnostic and therapeutic capabilities.

List of Acronyms and Abbreviations

ALA Aminolevulinic acid
AuNP Gold nanoparticle
BCC Basal cell carcinoma
DDD Dermal drug delivery
EPI–SPION Epirubicin attached to functionalized SPION
EPR Enhanced permeability and retention
Gd Gadolinium
LbL-AuNP Layer-by-layer polyelectrolyte coated AuNP
MAL Methyl aminolevulinic
MB Molecular beacon
Mn Manganese
MNPs Magnetic/metallic nanoparticles
PDT Photodynamic therapy
PLGA-NPs Polylactic-co-glycolic acid nanoparticles
PS Photosensitizer
RES Reticuloendothelial system
SCC Squamous cell carcinoma
SPION Superparamagnetic iron oxide nanoparticles
TDD Transdermal drug delivery
US Ultrasound

References

- [1] Jokerst JV, Gambhir SS. Molecular imaging with theranostic nanoparticles. *Acc Chem Res* 2011;44:1050–60.
- [2] Hobbs SK, Monsky WL, Yuan F, Roberts WG, Griffith L, Torchilin VP, et al. Regulation of transport pathways in tumor

- vessels: role of tumor type and microenvironment. *Proc Natl Acad Sci USA* 1998;95:4607–12.
- [3] Betty YS, Rutka JT, Chan WCV. *Nanomed N Eng J Med* 2010;363:2434–43.
 - [4] Sumer B, Gao J. Theranostic nanomedicine for cancer. *Nanomedicine* 2008;3:137–40.
 - [5] WHO. World cancer report 2014. World Health Organization; 2014. p. 14 [chapter 5].
 - [6] Arias JL. Micro- and nano-particulate drug delivery systems for cancer treatment. In: Spencer P, Holt W, editors. *Anticancer drugs: design, delivery and pharmacology*. New York: Nova Science Publishers Inc.; 2009. p. 1–85.
 - [7] Couvreur P, Vauthie C. Nanotechnology: intelligent design to treat complex disease. *Pharm Res* 2006;23:1417–50.
 - [8] Treat LH, McDannold N, Vykhodtseva N, Zhang Y, Tam K, Hynynen K. Targeted delivery of doxorubicin to the rat brain at therapeutic levels using MRI-guided focused ultrasound. *Int J Cancer* 2007;121:901–7.
 - [9] Zhang L, Zhang N. How nanotechnology can enhance docetaxel therapy. *Int J Nanomed* 2013;8:2927–41.
 - [10] Torchilin VP. Recent advances with liposomes as pharmaceutical carriers. *Nat Rev Drug Discov* 2005;4:145–60.
 - [11] Slingerland M, Guchelaar HJ, Gelderblom H. Liposomal drug formulations in cancer therapy: 15 years along the road. *Drug Discov Today* 2012;17:160–6.
 - [12] Muthu MS, Feng SS. Theranostic liposomes for cancer diagnosis and treatment: current development and pre-clinical success. *Expert Opin Drug Deliv* 2013;10:151–5.
 - [13] Yano J, Hirabayashi K, Nakagawa SI, Yamaguchi T, Nogawa M, Kashimori I, et al. Antitumor activity of small interfering RNA/cationic liposome complex in mouse models of cancer. *Clin Cancer Res* 2004;10:7721–6.
 - [14] Mosallaei N, Jaafari MR, Hanafi-Bojd MY, Golmohammadzadeh S, Malaekhe-Nikouei B. Docetaxel-loaded solid lipid nanoparticles: preparation, characterization, in vitro, and in vivo evaluations. *J Pharm Sci* 2013;102:1994–2004.
 - [15] Minelli R, Serpe L, Pettazoni P, Minero V, Barrera G, Gigliotti CL, et al. Cholesteryl butyrate solid lipid nanoparticles inhibit the adhesion and migration of colon cancer cells. *Br J Pharmacol* 2012;166(2):587–601.
 - [16] Baldi G, Ravagli C, Mazzantini F, Loudos G, Adán J, Masa M, et al. In vivo anticancer evaluation of the hyperthermic efficacy of anti-human epidermal growth factor receptor-targeted PEG-based nanocarrier containing magnetic nanoparticles. *Int J Nanomed* 2014;24:3037–56.
 - [17] Torchilin VP. Micellar nanocarriers: pharmaceutical perspectives. *Pharm Res* 2007;24:1–16.
 - [18] Fonseca MJ, Jagtenberg JC, Haisma HJ, Storm G. Liposome-mediated targeting of enzymes to cancer cells for site-specific activation of prodrugs: comparison with the corresponding antibody-enzyme conjugate. *Pharm Res* 2003;20:423–8.
 - [19] Schnyder A, Krähenbühl S, Drewe J, Huwylar J. Targeting of daunomycin using biotinylated immunoliposomes: pharmacokinetics, tissue distribution and in vitro pharmacological effects. *J Drug Target* 2005;13:325–35.
 - [20] Farokhzad OC, Cheng J, Teply BA, Sherifi I, Jon S, Kantoff PW, et al. Targeted nanoparticle-aptamer bioconjugates for cancer chemotherapy in vivo. *Proc Natl Acad Sci USA* 2006;103:6315–20.
 - [21] Zhang L, Gu FX, Chan JM, Wang AZ, Langer RS, Farokhzad OC. Nanoparticles in medicine: therapeutic applications and developments. *Clin Pharmacol Ther* 2008;83:761–9.
 - [22] Coimbra M, Rijcken CJ, Stigter M, Hennink WE, Storm G, Schiffelers RM. Antitumor efficacy of dexamethasone-loaded core-crosslinked polymeric micelles. *J Control Rel* 2012;163:361–7.
 - [23] Wolinsky JB, Grinstaff MW. Therapeutic and diagnostic applications of dendrimers for cancer treatment. *Adv Drug Deliv Rev* 2008;60:1037–55.
 - [24] Barth RF, Coderre JA, Vicente MGH, Blue TE. Boron neutron capture therapy of cancer: current status and future prospects. *Clin Cancer Res* 2005;11:3987–4002.
 - [25] Shi XG, Wang S, Meshinchi S, Van Antwerp ME, Bi X, Lee I, et al. Dendrimer-entrapped gold nanoparticles as a platform for cancer-cell targeting and imaging. *Small* 2007;3:1245–52.
 - [26] Kievit FM, Zhang M. Surface engineering of iron oxide nanoparticles for targeted cancer therapy. *Acc Chem Res* 2011;44:853–62.
 - [27] Ho YP, Leong KW. Quantum dot-based theranostics. *Nanoscale* 2010;2:60–8.
 - [28] Mody VV, Siwale R, Singh A, Mody HR. Introduction to metallic nanoparticles. *J Pharm Bioallied Sci* 2010;2:282–9.
 - [29] Liong M, Lu J, Kovochich M, Xia T, Ruehm SG, Nel A, et al. Multifunctional inorganic nanoparticles for imaging, targeting, and drug delivery. *ACS Nano* 2008;2:889–96.
 - [30] Rosenholm JM, Sahlgren C, Lindén M. Towards multifunctional, targeted drug delivery systems using mesoporous silica nanoparticles—opportunities & challenges. *Nanoscale* 2010;2:1870–83.
 - [31] Jung Y, Reif R, Zeng Y, Wang RK. Three-dimensional high resolution imaging of gold nanorods uptake in sentinel lymph nodes. *Nano Lett* 2011;11:2938–43.
 - [32] Tang SC, Fu YY, Lo WF, Hua TE, Tuan HY. Vascular labeling of luminescent gold nanorods enables 3-D microscopy of mouse intestinal capillaries. *ACS Nano* 2010;4:6278–84.
 - [33] Kim C, Cho EC, Chen J, Song KH, Au L, Favazza C, et al. In vivo molecular photoacoustic tomography of melanomas targeted by bioconjugated gold nanocages. *ACS Nano* 2010;4:4559–64.
 - [34] Pan D, Pramanik M, Senpan A, Wickline SA, Wang LV, Lanza GM. A facile synthesis of novel self-assembled gold nanorods designed for near-infrared imaging. *J Nanosci Nanotechnol* 2010;10:8118–23.
 - [35] Peng XH, Qian X, Mao H, Wang AY, Chen ZG, Nie S, et al. Targeted magnetic iron oxide nanoparticles for tumor imaging and therapy. *Int J Nanomed* 2008;3:311–21.
 - [36] Yu MK, Jeong YY, Park J, Park S, Kim JW, Min JJ, et al. Drug-loaded superparamagnetic iron oxide nanoparticles for combined cancer imaging and therapy in vivo. *Angew Chem Int Ed Engl* 2008;47:5362–5.
 - [37] Sonavane G, Tomoda K, Makino K. Biodistribution of colloidal gold nanoparticles after intravenous administration: effect of particle size. *Colloids Surf B Biointerfaces* 2008;66:274–80.
 - [38] Nazir S, Hussain T, Ayub A, Rashid U, MacRobert AJ. Nanomaterials in combating cancer: therapeutic applications and developments. *Nanomedicine* 2013;10:19–34.
 - [39] Huang X, Jain PK, El-Sayed IH, El-Sayed MA. Gold nanoparticles: interesting optical properties and recent applications in cancer diagnostics and therapy. *Nanomedicine* 2007;2:681–93.
 - [40] Kimling J, Maier M, Okenve B, Kotaidis V, Ballot H, Plech A. Turkevich method for gold nanoparticle synthesis revisited. *J Phys Chem* 2006;110:15700–7.
 - [41] Pan Y, Neuss S, Leifert A, Fischler M, Wen F, Simon U, et al. Size-dependent cytotoxicity of gold nanoparticles. *Small* 2007;3:1941–9.
 - [42] Liu G, Swierczewska M, Lee S, Chen X. Functional nanoparticles for molecular imaging guided gene delivery. *Nano Today* 2010;5:524–39.
 - [43] Hartman KB, Wilson LJ, Rosenblum MG. Detecting and treating cancer with nanotechnology. *Mol Diagn Ther* 2008;12:1–14.
 - [44] Gupta AK, Gupta M. Synthesis and surface engineering of iron oxide nanoparticles for biomedical applications. *Biomaterials* 2005;26:3995–4021.

- [45] Wang YX, Wang DW, Zhu XM, Zhao F, Leung KC. Carbon coated superparamagnetic iron oxide nanoparticles sentinel lymph nodes mapping. *Quant Imaging Med Surg* 2012;2:53–6.
- [46] Simões MCF, Sousa JJS, Pais AACC. Skin cancer and new treatment perspectives: a review. *Cancer Lett* 2015;357:8–42.
- [47] Proksch E, Brandner JM, Jensen JM. The skin: an indispensable barrier. *Exp Dermatol* 2008;17:1063–72.
- [48] Wiedersberg S, Guy RH. Transdermal drug delivery: 30+ years of war and still fighting! *J Control Rel* 2014;190:150–6.
- [49] Guy RH. Transdermal drug delivery. In: Schafer-Korting M, editor. *Drug delivery. Handbook of Experimental Pharmacology*, vol. 197. Springer; 2010. p. 399–410.
- [50] Mitragotri S. Modeling skin permeability to hydrophilic and hydrophobic solutes based on four permeation pathways. *J Control Rel* 2003;86:69–92.
- [51] Patzelt A, Lademann J. Drug delivery to hair follicles. *Exper Opin Drug Deliv* 2013;10:787–97.
- [52] Pegoraro C, MacNeil S, Battaglia G. Transdermal drug delivery: from micro to nano. *Nanoscale* 2012;4:1881–9.
- [53] Escobar-Chávez JJ, Marimuthu T, Choonara E, Kumar YP, du Toit C, Pillay V. Nanocarriers for transdermal drug delivery. *Res Rep Trans Drug Del* 2012;1:3–17.
- [54] Panariti A, Miserocchi G, Rivolta I. The effect of nanoparticle uptake on cellular behavior: disrupting or enabling functions? *Nanotechnol Sci Appl* 2012;5:87–100.
- [55] Gupta M, Agrawal U, Vyas S. Nanocarrier-based topical drug delivery for the treatment of skin diseases. *Expert Opin. Drug Deliv* 2012;9:783–804.
- [56] Alexander A, Dwivedi S, Giri TK, Saraf S, Tripathi DK. Approach for breaking the barriers of drug permeation through transdermal drug delivery. *J Control Rel* 2012;164:26–40.
- [57] Mieszawska AJ, Dwivedi S, Giri TK, Saraf S, Tripathi DK. Multifunctional gold nanoparticles for diagnosis and therapy of disease. *Mol Pharmaceutics* 2013;10:831–47.
- [58] Lademann S, Richter H, Schanzer S, Knorr F, Meinke M, Sterry W, et al. Penetration and storage of particles in human skin: perspectives and safety aspects. *Eur J Pharm Biopharm* 2011;77:465–8.
- [59] Baroli BM, Ennas MG, Loffredo F, Isola M, Pinna R, López-Quintela MA. Penetration of metallic nanoparticles in human full-thickness skin. *J Invest Dermatol* 2007;127:1701–12.
- [60] Filon FL, Crosera M, Adami G, Bovenzi M, Rossi F, Maina G. Human skin penetration of gold nanoparticles through intact and damaged skin. *Nanotoxicology* 2011;5:493–501.
- [61] Zheng D, Giljohann DA, Chen DL, Massich MD, Wang XQ, Iordanov H, et al. Topical delivery of siRNA-based spherical nucleic acid nanoparticle conjugates for gene regulation. *Proc Natl Acad Sci USA* 2012;109:11975–80.
- [62] Labala S, Mandapalli PK, Kurumaddali A, Venuganti VVK. Layer-by-layer polymeric coated gold nanoparticles of imatinib mesylate to treat melanoma. *Mol Pharmaceutics* 2015;12:878–88.
- [63] Geller AC, Annas GD. Epidemiology of melanoma and nonmelanoma skin cancer. *Semin Oncol Nurs* 2003;19:2–11.
- [64] Joseph MG, Zulueta WP, Kennedy PJ. Squamous cell carcinoma of the skin of the trunk and limbs: the incidence of metastases and their outcome. *Aust N Z J Surg* 1992;62:697–701.
- [65] Arunachalam D, Thirumoorthy A, Devi S. Quality of life in cancer patients with disfigurement due to cancer and its treatments. *Indian J Palliat Care* 2011;17:184–90.
- [66] Wadhera A, Fazio M, Bricca G, Stanton O. Metastatic basal cell carcinoma: a case report and literature review. How accurate is our incidence data? *Dermatol Online J* 2006;12. article 7.
- [67] Mandekou-Lefaki I, Delli F, Koussidou-Eremondi T, Mourellou-Tsatsou O, Dionyssopoulos A. Imiquimod 5% cream: a new treatment for Bowen's disease. *Int J Tissue React* 2005;27:31–8.
- [68] Goette DK. Topical chemotherapy with 5-fluorouracil. *J Am Acad Dermatol* 1981;4:633–49.
- [69] Misak H, Zacharias N, Song Z, Hwang S, Man KP, Asmatulu R, et al. Skin cancer treatment by albumin/5-Fu loaded magnetic nanocomposite spheres in a mouse model. *J Biotech* 2013;164: 130–6.
- [70] Huang Z, Xu H, Meyers AD, Musani AI, Wang L, Tagg R, et al. Photodynamic therapy for treatment of solid tumors—potential and technical challenges. *Technol Cancer Res Treat* 2008;7:309–20.
- [71] Morton CA, McKenna KE, Rhodes LE. Guidelines for topical photodynamic therapy: update. *Br J Dermatol* 2008;159:1245–66.
- [72] Casas A, Batlle A. Aminolevulinic acid derivatives and liposome delivery as strategies for improving 5-aminolevulinic acid-mediated photodynamic therapy. *Curr Med Chem* 2006;13: 1157–68.
- [73] Yang SJ, Lin CF, Kuo ML, Tan CT. Photodynamic detection of oral cancers with high-performance chitosan-based nanoparticles. *Biomacromolecules* 2013;14:3183–91.
- [74] Shi L, Wang X, Zhao F, Luan H, Tu Q, Huang Z, et al. In vitro evaluation of 5-aminolevulinic acid (ALA) loaded PLGA nanoparticles. *Int J Nanomed* 2013;8:2669–76.
- [75] Kandath N, Kirejev V, Monti S, Gref R, Ericson MB, Sortino S. Two-photon fluorescence imaging and bimodal phototherapy of epidermal cancer cells with biocompatible self-assembled polymer nanoparticles. *Biomacromolecules* 2014;15:1768–76.
- [76] Ogura M, Paliwal S, Mitragotri S. Sampling of disease biomarkers from skin for theranostic applications. *Drug Deliv Transl Res* 2012; 2:87–94.
- [77] Akbarzadeh A, Samiei M, Davaran S. Magnetic nanoparticles: preparation, physical properties, and applications in biomedicine. *Nanoscale Res Lett* 2012;7:144.
- [78] Balch CM, Soong SJ, Atkins MB, Buzaid AC, Cascinelli N, Coit DG, et al. An evidence-based staging system for cutaneous melanoma. *CA Cancer J Clin* 2004;54:131–49.
- [79] Ramsay D, Weary PE. Primary care in dermatology: whose role should it be? *J Am Acad Dermatol* 1996;35:1009–11.
- [80] Flaherty KT, Hodi FS, Fisher DE. From genes to drugs: targeted strategies for melanoma. *Nat Rev Cancer* 2012;12:349–61.
- [81] Quintas-Cardama A, Lazar AJ, Woodman SE, Kim K, Ross M, Hwu P. Complete response of stage IV anal mucosal melanoma expressing KIT Val560Asp to the multikinase inhibitor sorafenib. *Nat Clin Pract Oncol* 2008;5:737–40.
- [82] Jacobs JF, Nierkens S, Figdor CG, de Vries IJM, Adema GJ. Regulatory T cells in melanoma: the final hurdle towards effective immunotherapy? *Lancet Oncol* 2012;13:e32–42.
- [83] Chapman PB, Hauschild A, Robert C, Haanen JB, Ascierto P, Larkin J, et al. Improved survival with vemurafenib in melanoma with BRAF V600E mutation. *N Engl J Med* 2011;364:2507–14.
- [84] Falchook GS, Lewis KD, Infante JR, Gordon MS, Vogelzang NJ, DeMarini DJ, et al. Activity of the oral MEK inhibitor trametinib in patients with advanced melanoma: a phase 1 dose-escalation trial. *Lancet Oncol* 2012;13:782–9.
- [85] Hodi FS, O'Day SJ, McDermott DF, Weber RW, Sosman JA, Haanen JB, et al. Improved survival with ipilimumab in patients with metastatic melanoma. *N Engl J Med* 2010;363:711–23.
- [86] Basu R, Harfouche R, Soni S, Chimote G, Mashelkar AR, Sengupta S, et al. *Proc Natl Acad Sci USA* 2009;106:7957–61.
- [87] Wang Q, Chen L, Long Y, Tian H, Wu J. Molecular beacons of xeno-nucleic acid for detecting nucleic acid. *Theranostics* 2013;3: 395–408.
- [88] Kolpashchikov DM. An elegant biosensor molecular beacon probe: challenges and recent solutions. *Scientifica* 2012;2012: 1–17. ID 928783.
- [89] Santangelo P, Nitin N, Bao G. Nanostructured probes for RNA detection in living cells. *Ann Biomed Eng* 2006;34:39–50.
- [90] Giannetti A, Tombelli S, Baldini F. Oligonucleotide optical switches for intracellular sensing. *Anal Bioanal Chem* 2013;405: 6181–96.

- [91] Carpi S, Fogli S, Giannetti A, Adinolfi B, Tombelli S, Da Pozzo E, et al. Theranostic properties of a survivin-directed molecular beacon in human melanoma cells. *PLoS One* 2014;11:9.
- [92] Abdalkader R, Kawakami S, Unga J, Suzuki R, Maruyama K, Yamashita F, et al. Evaluation of the potential of doxorubicin loaded microbubbles as a theranostic modality using a murine tumor model. *Acta Biomater* 2015;19:112–8.
- [93] Viraka Nellore BP, Pramanik A, Chavva SR, Sinha SS, Robinson C, Fan Z, et al. Aptamer-conjugated theranostic hybrid graphene oxide with highly selective biosensing and combined therapy capability. *Faraday Discuss* 2014;175:257–71.
- [94] Mariano RN, Alberti D, Cutrin JC, Geninatti Crich S, Aime S. Design of PLGA based nanoparticles for imaging guided applications. *Mol Pharm* 2014;11:4100–6.
- [95] Vankayala R, Lin CC, Kalluru P, Chiang CS, Hwang KC. Gold nanoshells-mediated bimodal photodynamic and photothermal cancer treatment using ultra-low doses of near infra-red light. *Biomaterials* 2014;35:5527–38.
- [96] Bae YH, Park K. Targeted drug delivery to tumors: myths, reality, and possibility. *J Control Rel* 2011;153:198–205.

Nanodelivery of Anticancer Agents in Melanoma: Encouraging, But a Long Way to Go

J. Chen^{1,2}, X.D. Zhang¹

¹University of Newcastle, Callaghan, NSW, Australia; ²The University of Queensland, Brisbane, QLD, Australia

OUTLINE

Introduction	189	Nanotechnology in Targeting Mitochondrial Apoptotic Pathway	195
Potential Benefits of Nanodelivery in Melanoma Therapy	190	Nanotechnology in Melanoma Immunotherapy	195
Examples of Nanoparticle Drug Delivery Systems Relevant to Melanoma	191	Immunostimulation	196
Nanotechnology in the Chemotherapy of Melanoma	192	Immune Checkpoint	196
Nanotechnology in Targeted Therapy Against Melanoma	192	CD47	196
MAPK Pathway	193	PD-L1	197
PI3K/Akt Pathway	194	CTLA4	197
Nanotechnology in Other Signaling Pathways in Melanoma	194	Nanotechnology in Combination Therapy of Melanoma	197
Combination of siRNAs Against BRAF and Akt Carried in a Nanoparticle	195	Conclusions	198
		References	198

INTRODUCTION

Melanoma is an aggressive malignancy, which is difficult to treat, and this has led to a very low survival rate [1,2]. Although it represents only a small proportion of skin cancer cases, melanoma accounts for the vast majority of skin cancer deaths [3]. Early-stage melanoma, which has not spread to other organs, can be treated by surgical removal, with a cure rate of 97–99.8% [4]. However, metastasized irremovable melanoma needs to be treated by therapies including chemotherapy, radiotherapy, targeted therapy, and immunotherapy [5,6]. Unfortunately, the outcomes of all these approaches are not satisfactory. Patients with

metastasized melanomas only have a 6–10 month median survival time and less than 20% for a 5-year survival rate [7–9]. Patients' responses to chemotherapy are very poor. There is a 5–10% response rate for most commonly used Food and Drug Administration (FDA) chemotherapeutic drugs including dacarbazine (DTIC) [10]. Targeted therapy against mutated BRAF can greatly increase the response rate to more than 80% [11,12]. However, almost all patients develop acquired drug resistance and relapse after 6 months of treatment. The activation of the MAPK pathway and/or other signaling pathways, such as PI3K/Akt and NF-κB, has been considered to be the major reason. Thus, combination therapy with both BRAF and MEK inhibition has

been applied in melanoma therapy. Combination therapy improves the response rate, increases progression-free survival time, and reduces some severe side effects and has been used in phase III clinical trials [13,14]. A clinical trial showed that MEK inhibitor, trametinib, improved the effectiveness of BRAF inhibitor, dabrafenib, increasing progression survival time from 5.8 to 9.4 months and treatment response rate from 54% to 76%, while reducing cutaneous squamous cell carcinoma incidence from 19% to 7% [14]. These treatment outcomes are still far from satisfactory. Immunotherapy against immune checkpoint proteins has been promising, but only limited patients show a response [15,16]. Therefore, further research into melanoma therapy is required.

The application of nanotechnology in melanoma treatment brings new hope for curing the disease by increasing treatment efficacy and reducing side effects. Nanotechnology involves materials in nanoscale from 1 to 100 nm and has been extensively studied for improving the diagnosis and treatment of disease [17,18], forming a new research area referred to as nanomedicine. In cancer, the delivery of anticancer agents has been highly regarded and several nanodelivered drugs have been used clinically. Many nanoparticles (NPs) have been studied for the treatment of melanoma including liposomes, dendrimers, polymersomes, carbon-based NPs, inorganic NPs, and protein-based NPs [17,19–21]. Each has its own characteristic for certain therapeutic agents. In this chapter, we introduce the recent progress in the application of nanotechnology for the treatment of melanoma with emphasis on the delivery of anticancer agents for targeted therapy and immunotherapy.

POTENTIAL BENEFITS OF NANODELIVERY IN MELANOMA THERAPY

A key problem in the current treatment of melanoma is the off-target side effects that prevent the dosage of anticancer agents necessary to eliminate melanoma cells from being administered. Nanodelivery can concentrate the anticancer agents at the tumor site and increase the penetration of the drugs into cancer cells. The accumulation of drugs at the tumor site is achieved by enhanced permeability and retention (EPR) at the tumor site or targeted delivery [22]. Nanoparticles can be made to approximately 100 nm, allowing them to pass through the leakiness of tumor vasculature but not normal vessels [22]. The vasculature of a tumor is poorly organized and thus has larger gaps between endothelial cells. In addition, the lymphatic drainage in a tumor is blocked, resulting in the retention of the NPs at the tumor site.

Therefore, off-target side effects can be reduced and dosages used can be increased.

EPR, however, does not reduce off-target side effects on the immune system because the NPs are engulfed by immune cells. Therefore, specific targeted delivery has been developed. The targeted delivery is realized by attachment of specific antibodies, peptides, nuclear acid-based ligands, or small molecules that bind to proteins specifically and are highly expressed on cancer cells. Therefore, targeting delivery can greatly increase the interactions of NPs with targeted cancer cells. BIND-014 is a good sample for targeting delivery, and is based on highly expressed prostate specific membrane antigen (PSMA) in many cancers [23,24]. The 100 nm polymeric NP contains docetaxel and the PSMA-specific ligand, accurins. Clinical trials of BIND-014 have shown promising outcomes, with a proportion of patients having complete or partial responses [24,25]. Some highly expressed proteins have been selected as targets for melanoma in targeting nanodelivery such as transferrin receptors, folic acid receptor, and CD44 receptor, MCR-1 receptor, fibroblast growth factor receptor, laminin receptor, somatostatin receptor (SSTR), and sigma receptor [26,27]. Hyaluronic acid has been used to guide NPs to melanoma, which binds to CD44 overexpressed on melanoma cells. Inclusion of the CD44 antibody in NPs increased drug delivery to melanoma cells [28], greatly improving the concentration of NPs in tumor cells. The use of folic acid has a similar effect as its receptor is also increased in melanoma. However, all of these proteins are also expressed in normal cells. Therefore, off-target side effects are still a problem although they may be reduced.

Nanoparticles can protect drugs from biochemical degradation in the human body, thereby increasing circulating time [29]. Nanoparticles provide a shield for carried drugs, enabling them to avoid contact with enzymes in the blood. For example, liposomes can contain hydrophilic drugs in their core aqueous phase, protecting the drugs by their bilayer of lipids. Nanodelivery has also been shown to protect siRNAs, enabling siRNA-mediated gene silencing *in vivo*.

Nanodelivery can facilitate combination therapy as it can carry multiple drugs simultaneously. Combination therapy is highly regarded as it can combine different anticancer modes to increase treatment efficacy. Co-delivery allows all agents contained in an NP to have similar pharmacokinetics and thus facilitate their coordinated effects. For example, layered double hydroxide NPs have been used to deliver siRNA against signaling molecule and chemotherapeutic drug 5-FU, showing a synergistic anticancer effect [30] (Fig. 15.1).

As an NP can carry many different agents together, it has been studied to include a diagnostic agent in a therapeutic NP so that the treatment effect can be

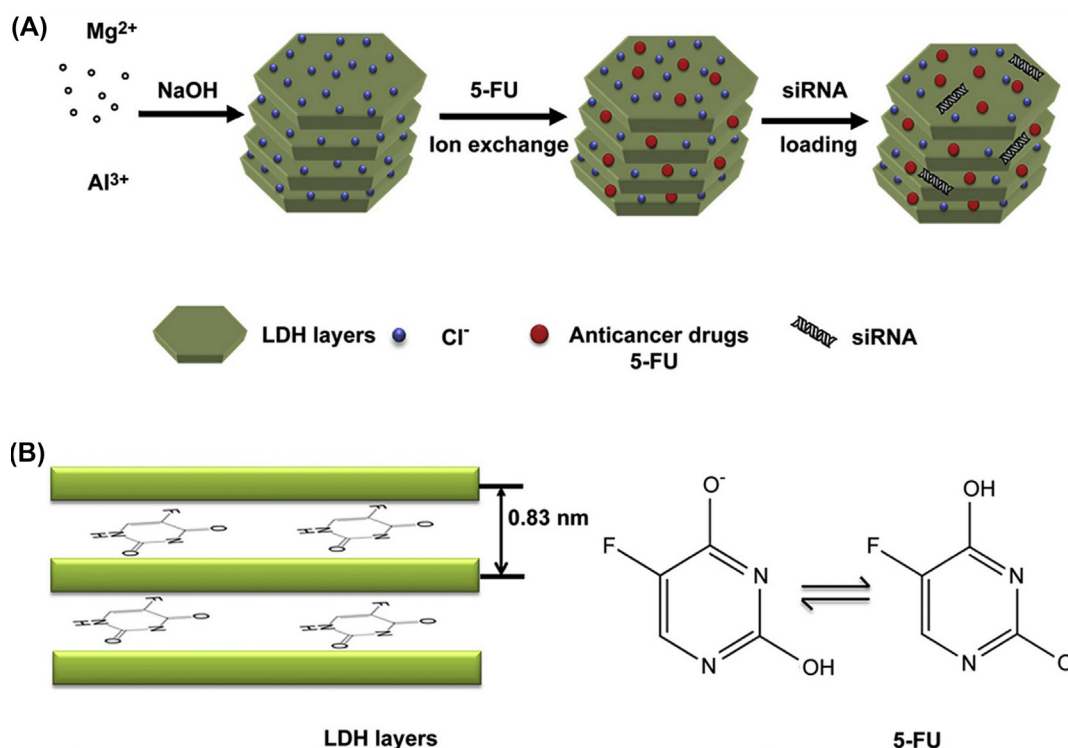


FIGURE 15.1 A nanoparticle containing both 5-FU and siRNA. Nanoparticle layer double hydroxide nanoparticles can carry both siRNA and the chemotherapeutic agent 5-FU. SiRNA is used to target the death receptor pathway while 5-FU is a chemotherapeutic agent. (Panel A) a nanoparticle containing both siRNA and 5-FU; (Panel B) a nanoparticle containing 5-FU. The scheme is adopted from Li L, Gu W, Chen J, Chen W, Xu ZP. Co-delivery of siRNAs and anti-cancer drugs using layered double hydroxide nanoparticles. *Biomaterials* 2014;35(10):3331–9 Scheme 1 with permission from Elsevier.

monitored in a real-time fashion [31,32]. Liposomes and polymersomes are the most commonly used NPs for this purpose to include imaging agents for magnetic resonance imaging, radionuclide imaging, and fluorescence imaging. The theranostic approach has also been studied in melanoma [33,34]. A fluorescent, dye DiR, has been included in a lipid-based nanomicelle which delivers doxorubicin (DOX) [35]. This has facilitated the detection of distribution of NPs in the blood and tumor cells. For example, fluorescent reagent rhodamine has also been included in an NP and tested in melanoma [36]. A biodegradable polymer NP containing paclitaxel, quantum dots, and magnetic NP was shown to have both imaging function and cytotoxic effect [37].

EXAMPLES OF NANOPARTICLE DRUG DELIVERY SYSTEMS RELEVANT TO MELANOMA

Several nanodelivered drugs have been used clinically. Extensive descriptions of common medical NPs are well presented in several reviews [18,27,38,39]. Lipid-based NPs consist of two layers of phospholipid

membranes and thus can carry both hydrophobic and hydrophilic drugs. They are the most common NPs used for drug delivery as they are biocompatible and easy to produce. As they have very low toxicity and are compatible with the human body, these NPs have been studied most extensively for anticancer drug delivery. Various lipid-based NPs have been developed including liposomes, solid lipid NPs, niosomes, and nanoemulsions. A marketed NP made from lipids, Doxil, that delivers DOX has also been used for a clinical trial in melanoma [40].

Polymers are another type of NP commonly used for cancer treatment. There are many types of polymers including polymeric NP, polymeric micelle, dendrimer, polymersome, polyplex, polymer-lipid hybrid, and polymer-drug/protein conjugates [41]. Polymers can be formed as dendrimers such as poly(aminoamine), poly(propyleneimine) and poly-L-lysine dendrimers. They are particularly suitable for siRNA carriers as they have low toxicity and form a complex with siRNA with high loading capacity. They are stable and thus protect siRNA from serum degradation. BIND-014, a polymer containing DOX has been in clinical trials [42,43]. Chitosan, a natural polymer, has been used to deliver siRNAs showing promising results.

Human albumin is known to have low toxicity due to its biocompatibility [36]. The first FDA-approved nanodelivery drug nab-paclitaxel is a human albumin NP containing paclitaxel, which is now used clinically for the treatment of breast cancer. Nab-paclitaxel is made by mixing paclitaxel and human albumin under pressure to form 130 nm NPs. Paclitaxel is a mitosis inhibitor through blocking microtubule dynamics in cell division. It is a hydrophobic drug and is therefore difficult to dissolve in water; human albumin increases its solubility. In animal experiments, nanodelivery increased paclitaxel transportation to the tumor site and decreased side effects. Clinical trials of nab-paclitaxel in breast cancer increased response rate and overall survival time. Nab-paclitaxel has also been tested in melanoma in a few clinical trials.

NANOTECHNOLOGY IN THE CHEMOTHERAPY OF MELANOMA

Chemotherapy is still a first-line therapy for cancer including melanoma. Chemotherapeutic agents kill both malignant and normal cells that are dividing [44]. Therefore, they are very toxic, limiting the dosage that can be safely administered. The low therapeutic index of chemotherapy is a major problem. The common chemotherapeutic agents used in melanoma are DTIC, vinblastine, and temozolomide. The response rates to DTIC, vinblastine, and temozolomide are only 7%, 9.5%, and 28%, respectively [10]. The application of nanodelivery to these chemotherapeutic agents has increased treatment efficacy and reduced side effects, enabling more chemotherapeutic agents to be applied to melanoma treatment.

Nab-paclitaxel, a human albumin-based NP, is the most successful nanodelivered anticancer agent [36]. The outcomes of the trials in breast cancer are encouraging due to greatly improved pharmacokinetics and pharmacodynamics [45]. Thus it was also used for clinical trials for other cancers including metastatic melanoma. Several phase II clinical trials in melanoma showed that nab-paclitaxel increased treatment responses to more than 20% compared to less than 10% for free paclitaxel [46,47]. These trials showed that nab-paclitaxel was more tolerated and more effective against melanoma than free paclitaxel [46,48]. However, side effects like neutropenia, thrombocytopenia, neurosensory problems, fatigue, nausea, and vomiting are still common [47]. Thus, studies for further improvement are warranted.

Encouraged by nab-paclitaxel, NPs have been used to deliver other chemotherapeutic agents including DOX and etoposide for melanoma treatment. DOX delivered by gold NPs or dendrimers showed increased

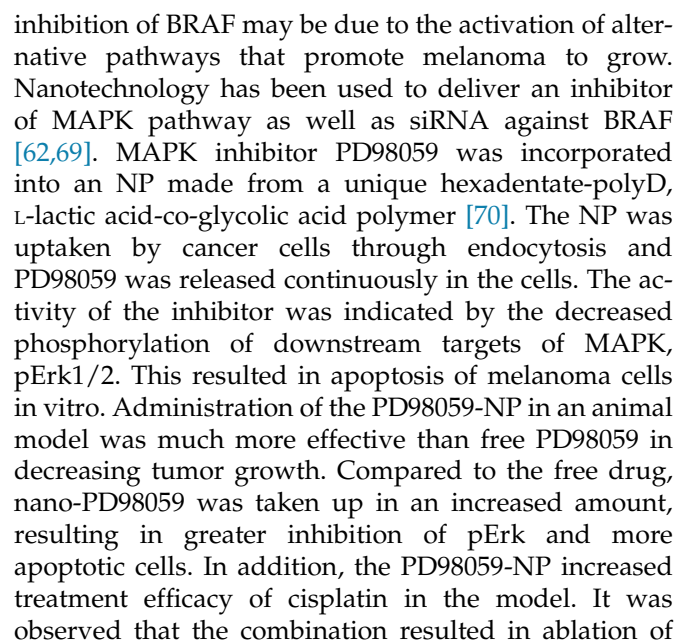
effectiveness in comparison with free DOX in melanoma cell lines [49,50]. The addition of an antibody against CD44 to a liposome NP-delivered DOX achieved specific targeting malignant cells [28]. In a xenograft mouse model inoculated with melanoma cells, B16F10, DOX-carrying NPs decreased xenograft melanoma by 60% while nontargeted, DOX-NPs were ineffective. DOX was encapsulated into liposomes by the creation of an ammonium sulfate gradient [51]. Due to decreased side effects, the maximum tolerated dose of DOX-NP increased five-fold. These preclinical studies may lead to clinical trials for nanodelivered DOX in melanoma.

NPs have also been developed to deliver etoposide and cisplatin for melanoma treatment. An NP with cholesterol-rich nanoemulsion (LDE) has been used to deliver etoposide and tested in a mouse model of melanoma [52]. The concentration of etoposide at the tumor site was fourfold higher than free etoposide. Thus, it decreased tumor growth markedly compared with free etoposide. A lipid NP was used to deliver iodinated cisplatin to increase its water solubility [53]. It was tested in two xenograft melanoma models in mice. The NP delivery greatly increased the efficacy of cisplatin in inhibiting tumor growth. Targeted delivery may be necessary to further improve the treatment efficacy for these NPs in melanoma.

NANOTECHNOLOGY IN TARGETED THERAPY AGAINST MELANOMA

Intracellular signaling pathways play a key role in carcinogenesis and cancer progression, metastasis, and drug resistance. These pathways are aberrantly activated in cancer cells either by genetic alterations or growth factors/cytokines in the blood and the tumor microenvironment (Fig. 15.2) [54]. For example, increased blood levels of TNF- α , IL-6, insulin, estrogen, and leptin can activate multiple signalling pathways including MAPK, PI3K, and STAT3 to increase cancer incidence and lead to poorer prognosis [55–58].

Viral infections can also cause the activation of multiple signaling pathways to promote cancer. Many viruses have oncogenes that express oncoproteins to alter host cellular signaling pathways [59,60]. Genetic defects are well known to cause cancer via alterations of signaling pathways such as BRAF mutation [61]. Signaling pathways have been associated with the prognosis of melanoma and inhibition of these signaling pathways has been studied for the treatment of melanoma [56,62]. Among them, MAPK and PI3K/Akt are the most common pathways activated. In the MAPK pathway, mutation frequencies of BRAF, NRAS, KRAS, and HRAS are 50–70%, 15–30%, 2%, and 1%, respectively [63–65].



tumors in some mice. This indicates that combination therapy with nanodelivered signaling molecule inhibitors and free chemotherapeutic agents has an additive effect. NPs containing both MAPK inhibitor and cisplatin may increase treatment effect, but this has not been studied.

SiRNA against BRAF was loaded in a liposome NP, which was able to reduce tumor size in a xenograft melanoma model [71]. Although siRNA against BRAF is effective in reducing melanoma cell growth, it is not practical in vivo as siRNA can be degraded quickly in blood and is therefore unable to reach the tumor site. Liposomes were shown to protect siRNA from serum degradation and nano-siRNA was successfully introduced into the melanoma cells. The effect of this nano-siRNA was verified by decreased expression of mutated BRAF in grafted melanoma cells, decreased cell proliferation, and reduced tumor size.

Taken together, nanodelivery is valuable in increasing treatment efficacy for BRAF inhibition by siRNA and MEK inhibition by a small molecule inhibitor [70,71]. Moreover, combination use of the nano-MEK inhibitor and free cisplatin resulted in the ablation of tumors in some animals with xenograft melanomas [70]. This encourages further effort into the application of nanotechnology in melanoma. The following work may increase BRAF mutated melanoma treatment: nanodelivery of BRAF small molecule inhibitors; co-delivery of BRAF inhibitors and MEK inhibitors; and co-delivery of BRAF inhibitors, MEK inhibitors, and chemotherapeutic agents. It is expected that the co-delivery of BRAF and MEK inhibitors will be more effective than the present regimen using combination therapy of BRAF and MEK inhibitors only. A combination of free BRAF and MEK inhibition together has been shown to be much more effective than a single inhibitor.

PI3K/Akt Pathway

The PI3K/Akt pathway is also commonly activated and is responsible for the drug resistance to BRAF inhibitors [72]. In addition, a large proportion of patients have no BRAF mutations as BRAF mutations only account for 50% of melanoma patients [73]. In these patients, PI3K/Akt may act with other signaling pathways to play key roles in melanoma pathogenesis and resistance to treatment [66]. Nanotechnology has been used in the delivery of inhibitors of Akt and its downstream targets such as myc and NF- κ B. Myc is a mitogenic gene which promotes cancer progression. NF- κ B is a transcriptional factor, which increases cancer cell survival.

Myc is downstream of WNT RTK and TCR and is transcriptionally upregulated. It promotes carcinogenesis, metabolism, and metastasis. Inhibition of the pathway has been proposed for cancer therapy [74,75]. An NP has been designed to carry siRNA against

oncogene c-Myc to target melanoma cells B16F10 and has demonstrated effectiveness against melanoma [76].

A polymeric NP PLGA was used to deliver the PDK/Akt inhibitor, PH-427 [77]. It was shown that nanodelivering of PH-427 greatly reduced tumor size compared to free PH-427 in a mouse model of pancreatic cancer. A polymer micelle was used to pack rapamycin together with paclitaxel, showing significantly superior effects in reducing tumor size in a xenograft breast cancer model compared to rapamycin or paclitaxel alone [78].

Biodegradable PEI has been used to deliver shRNA against the p65 unit of NF- κ B, showing effectiveness in a breast cancer model [79]. The NP showed constant release of shRNA, leading to apoptosis and decreased proliferation. In a xenograft model injected with MDA-MB-435, the nanodelivered shRNA almost abolished the tumor. These NP-deliveries of inhibitor or siRNA against PI3K/Akt key signaling molecules have not yet been tested in melanoma.

Nanotechnology in Other Signaling Pathways in Melanoma

Vascular endothelial growth factor (VEGF) is a major regulator of angiogenesis. In order for cancer cells to proliferate quickly, they need a sufficient supply of blood. Therefore, inhibition of VEGF can be used in the treatment of cancer. A humanized VEGF-A antibody bevacizumab has been used clinically. Nanotechnology has been used to further improve the treatment efficacy of anti-VEGF therapy. A chitosan NP has been used to deliver VEGF siRNA and was demonstrated to improve therapeutic efficacy [80]. The NPs were successfully transferred to B16-F10 and siRNA was shown to last for a longer time, indicating that the siRNA was nano-protected from RNase degradation. This leads to a 40% silencing efficacy. Nanotechnology has also been used for improving the effect of bevacizumab but it has not yet been tested in melanoma [81,82].

STAT3 is a transcriptional factor which plays a key role in cancer development and progression. STAT3 is activated by IGF-1, EGFR, PDGFR, and Src [83–86]. Activation of STAT3 results in increased cell proliferation, survival, and mobility. STAT3 has been considered as a key mediator in melanoma, promoting brain metastasis [87]. Inhibition of phosphorylated STAT3 has been shown to increase efficacy of TNF- α for melanoma [88]. A functional graphene oxide to deliver a plasmid-based STAT3 siRNA showed significantly reduced xenograft tumor growth [89]. Graphene oxide is a two-dimensional carbon nanomaterial with a large surface for siRNA to attach. The optimal ratio of GO-PEI-PEG to si-STAT3 is 4:1 and transfection efficacy of GO-si-STAT3 is 60%. In a B16 xenografted model, at day 30, the average tumor weight was 4.2 ± 1.0 g while in the GO-si-STAT3 group, it was 0.1 ± 0.1 g. Western blotting and qPCR showed that STAT3 mRNA and protein were

greatly reduced in the GO-si-STAT3 group. In vitro cell culture, introduction of GO-si-STAT3 induced apoptosis and decreased proliferation indicated by TUNEL assay and decreased expression of proliferation-associated antigen (PCNA), with decreased downstream target proteins of STAT3 including c-myc and bcl-2.

Combination of siRNAs Against BRAF and Akt Carried in a Nanoparticle

As activation of two pathways in cancer may have a synergistic effect, simultaneous inhibition of key molecules in two different signaling pathways has been tested. Simultaneous inhibition of both MAPK and PI3K/Akt pathways has been shown to have a synergistic effect in the treatment of melanoma [90]. Nanotechnology has been used to develop such a system to carry siRNAs to silence two signaling molecules simultaneously. Both siRNAs specifically targeting mutated BRAF and Akt3 were loaded into a liposome NP (average size 50 nm), which was applied to the skin topically after ultrasound treatment at a frequency of 20 kHz. An in vitro test showed that siRNAs were protected from serum degradation. In animal models, the NP was used topically after the ultrasound treatment. The effect of the NP containing two siRNAs is superior compared to that containing a single siRNA [91].

Overall, NP-delivered siRNAs or inhibitors against key molecules increased the effectiveness. However, the tumor is only reduced not eradicated. As siRNAs are unable to eliminate signaling molecules, it is not surprising they are unable to kill all cancer cells. The currently invented new technique CRISPR/Cas9 can manipulate genes and thus knock out a gene completely [92]. Its application in cancer treatment may result in better outcomes than with siRNAs [93]. The side effects are also a problem for this new technology, thus limiting its application in the clinic. Nanotechnology may also help deliver CRISPR/Cas9 to reduce side effects.

In addition, it may be necessary to combine siRNAs with chemotherapeutic agents or immune stimulating agents so that the cancer cells weakened by inhibition of signaling pathways can be eradicated. Furthermore, liposome NPs are also taken up by normal cells. An approach is needed to improve the specificity of the NP to cancer cells so that side effects are eliminated and thus, the dosage could be increased to eradicate cancer cells.

NANOTECHNOLOGY IN TARGETING MITOCHONDRIAL APOPTOTIC PATHWAY

Mitochondrion is a key organelle regulating cell apoptosis through the Bcl-2 family. The pathway is

regulated by many factors. Both PI3K/Akt and MAPK are regulators of the mitochondrial apoptotic pathway. The Bcl-2 family includes both proapoptotic proteins and antiapoptotic proteins. The former includes bak, bax, Bid, Bim, Bad, NOXA, and PUMA and the later Bcl-2, Bcl-xL, Bcl-w, Mcl-1, and A1 [94]. Activation of PI3K/Akt and MAPK can increase the expression of antiapoptotic proteins and decrease the expression of proapoptotic proteins, thus increasing melanoma cell survival [95]. Inhibition of antiapoptotic proteins has been used to cause melanoma cell apoptosis [96]. ABT-737, which can inhibit Bcl-2, Bcl-xL, and Bcl-w, but not Mcl-1, is not a very effective drug in melanoma treatment, as Mcl-1 is highly expressed in melanoma. However, further inhibition of Mcl-1 by fenretinide can cause massive melanoma cell apoptosis via activation of NOXA, indicating that manipulation of the mitochondrial apoptotic pathway could be an approach for melanoma treatment [97].

Nanotechnology has been studied to increase the therapeutic effect of Bcl-2 inhibition. SiRNA against Bcl-2 was packed into an arginine-grafted biodegradable polymer NP (ABP) for the treatment of melanoma [98]. In a mouse model with xenografted B16 melanoma cells systemic administration of ABP-bcl-2 siRNA led to the accumulation of the NP at the tumor site. It reduced both mRNA and protein levels of Bcl-2 as well as tumor size. It is possible that the combination delivery with Mcl-1 may further increase its effectiveness. A dendrimer NP has been used to deliver a cocktail containing siRNAs against Bcl-2, Bcl-xL, and Mcl-1 in Hela and HL-60 cells, showing much better effectiveness than a single siRNA [99]. This approach may be tested in melanoma cells that have highly expressed Mcl-1.

Recently, a sophisticated method has been developed to deliver NPs into mitochondria to improve specificity and reduce side effects. Rhodamine has been used for a carbon NP carrying cisplatin to target mitochondria specifically [100]. It was found that the rhodamine-coated NP colocalized with mitochondria at 80% compared to 20% for that without rhodamine. The efficacy of the NP to cause cancer cell death was seven- to eightfold of that without rhodamine.

NANOTECHNOLOGY IN MELANOMA IMMUNOTHERAPY

Immune responses are important in cancer development and treatment. Deficiency in the immune system is associated with increased cancer incidence and drug resistance. Immunotherapy has been developed for cancer treatment either through stimulation of the immune system or suppression of immune checkpoint proteins. The major issues in cancer immune therapy are the low rate of responses and side effects such as autoimmune diseases. Nanotechnology has been used to

improve approaches in immunotherapy to increase treatment efficacy and reduce side effects.

Immunostimulation

Immunotherapy is used to improve the immune responses in patients with melanoma by increasing the clearance of cancer cells by cytotoxic T-cells or macrophages. In melanoma, several cytokines have been shown to have initial effects but the effects are limited by side effects [101]. The commonly used immune stimulators in melanoma are IL-2, IFN- α , ipilimumab and thymosin alpha-1 [102–105]. IL-2 has been reported to increase remission time but high-doses of IL-2 can cause severe side effects including death [101,104].

NPs have been used to deliver immunotherapeutic agents to reduce side effects [106,107]. Plasmids expressing IL-2 have been packed inside a polymeric NP (poly-ethylenimine [PEI]) which is linked to β -cyclodextrin, conjugated with folate [108]. In a mouse model with xenograft melanoma, peritumoral injection of the NP inhibited tumor growth and prolonged the survival of the melanoma-bearing mice [108]. An engineered IL-2Fc with anti-CD137 was packed into a PEGylated liposome and injected into the tumor in a xenograft melanoma mouse model [109]. It increased the number of CD8 T-cells and decreased the number of regulatory T-cells, leading to the eradication of a majority of the tumors. The NP approach has also been used for the delivery of other cytokines [110].

IFN- α has been packed in a nanoporous miniature device made from a biodegradable polymer, poly(ϵ -caprolactone) (PCL). It was shown to constantly release IFN- α after subcutaneous implantation into a xenograft melanoma mouse model and also reduced tumor size [111]. The released cytokine was able to phosphorylate STAT1, which is a mediator of IFN- α -induced immune responses. Furthermore, the ligands of immune cells have also been loaded into NPs to stimulate an immune response. For example, CD40L expressing plasmids have been packed into a polymeric NP formed from PEI, which greatly increased cytotoxicity of CD8 T-cells and ablated tumors in a xenograft mouse melanoma model [112].

Immune Checkpoint

Several immune checkpoint proteins including CD47, CD-1, and CTLA4 have been identified to play key roles in cancer immune escape (Fig. 15.3). Inhibition of these proteins using antibodies has been investigated. Clinical trials revealed long-lasting effectiveness but the response rate was not high enough even with combination therapy. Nanodelivery of antibodies and siRNAs against these proteins has been tested to improve the efficacy of these inhibitors [113,114].

CD47

Macrophages have been identified as major players in the pathogenesis of cancer. Macrophages can either

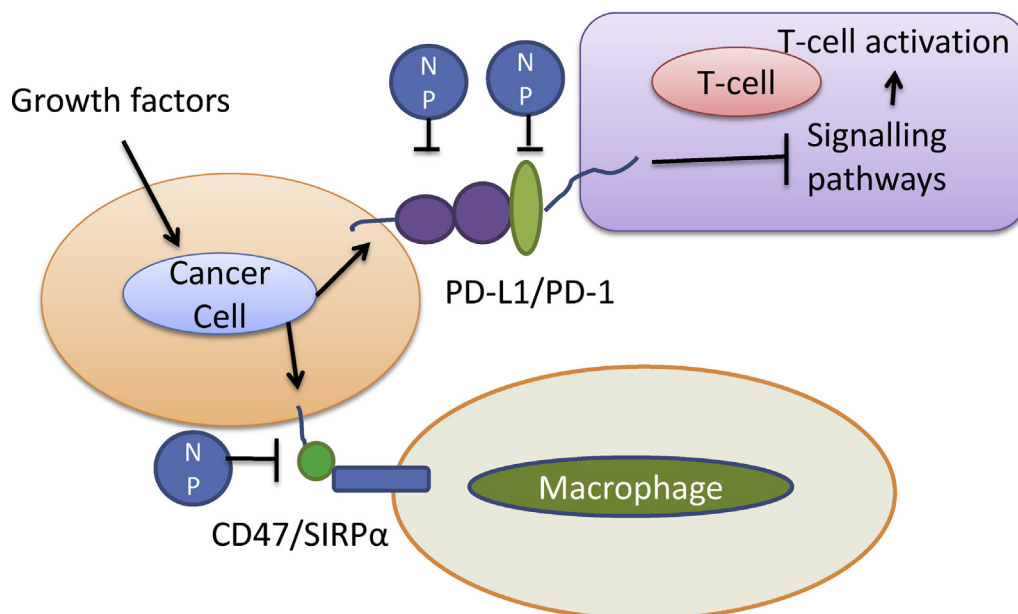


FIGURE 15.3 Nanotechnology in T-cell and macrophage activation. T-cell function is regulated by both stimulation systems such as TCR and inhibitory checkpoints such as PD-L1/PD-1. Cancer cells have an increased expression of PD-L1 to inhibit T-cells and CD47 to inhibit macrophages. Nanoparticles have been used to deliver anti-PD-1, anti-PD-L1, and anti-CD47 to activate immune cells.

promote cancer or prevent cancer development depending on the signals they receive. Macrophages promote phagocytosis, antigen presentation, and cytokine production to facilitate cancer cell elimination. However, cancer cells can express CD200 and CD47 to bind to the receptors on macrophages to inhibit their anticancer activities. CD47 binds to signal regulatory protein- α (SRP α) on macrophages to cause a signaling cascade, inhibiting phagocytosis [115,116]. Overexpression of CD47 has been shown to increase cancer aggressiveness while deficiency leads to decreased tumor size [117]. Inhibition of CD47/SIRP- α has been tested both in vivo and in vitro for the treatment of cancer. The approaches include the development of an antibody against CD47, a recombinant SIRP- α to bind to CD47 and antibody against SIRP- α [115]. As CD47 also exists on many normal cells, blockage of CD47 may also affect normal cell function, leading to side effects.

CD47 is increased in melanoma. Intravenous delivered siRNA against CD47 has been shown to decrease tumor growth and metastasis [113]. CD47 deficiency has been shown to increase melanoma cell resistance to radiotherapy [118]. A nanodelivery system to carry the CD47 antibody has been developed, showing increased efficacy [113]. Liposome-protamine-hyaluronic acid (LPH) was used to carry siRNAs against CD47 and tested them both in vitro and in vivo. In vitro LPH-siRNA against CD47 decreased expression of CD47 to 3.6%, resulting in increased colony formation. Knockdown of CD47 increased phagocytosis to 14%. C57Bl/6 mice inoculated with 2×10^5 B16F10 melanoma cells were intravenously injected with LPH (CD47) NPs every other day for a maximum of six times. The average tumor volume was reduced by 93%, this was not observed in mice with clodronate-depleted macrophages, indicating the effect was macrophage-dependent. The delivery specificity was demonstrated by unchanged CD47 expression on infiltrated leukocytes in tumors. Therefore, the immune system was minimally affected and autoimmune responses can be avoided.

PD-L1

One of the reasons for melanoma to escape immune attack is through increased expression of PD-L1, which binds to PD-1 to cause T-cell dysfunction and death [119,120]. Currently, antibodies against PD-L1/PD-1 have been developed and used for clinical trials. Two of them, nivolumab (anti-PD-1, Bristol-Myers Squibb) and pembrolizumab (anti-PD-1, Merck), have been approved by the FDA. The response rate to anti-PD-L1/anti-PD-1 treatment in melanoma achieved 17–28% [121,122]. However, the response rates to anti-PD-L1/anti-PD-1 are still too low. Additionally, anti-

PD-1 has been associated with autoimmune disease side effects [123]. Nanotechnology is being applied to help solve these problems.

An NP has been developed to deliver siRNA against PD-L1 to inhibit PD-L1/PD-1-caused T-cell death [114]. PEI was used to carry siRNA against PD-L1 while FA was used to obtain specific delivery to cancer cells. The addition of PEG was also used to avoid siRNA degradation in serum. The results showed that NP-carried siRNA against PD-L1 increased T-cell killing dramatically. Particularly, the addition of FA increased the uptake of NPs by cancer cells and reduced their uptake by monocytes, leading to decreased autoimmune side effects.

CTLA4

The anti-CTLA4 antibody has been shown to increase T-cell CTL activity. However, systemic inflammation is a severe side effect [124]. There are no reports at present about nanotechnology application for CTLA4. Specific site delivery of the anti-CTLA4 antibody or siRNA may greatly reduce the side effect of systemic inflammation. The application of nanotechnology in CTLA4 may be of particular importance as anti-CTLA4 produces higher immune stimulation. Use of nanotechnology may reduce the side effects by concentrating anti-CTLA4 antibody or siRNA at the tumor site.

NANOTECHNOLOGY IN COMBINATION THERAPY OF MELANOMA

As melanoma is highly heterogeneous, a single anti-cancer agent is usually ineffective, and combination therapy has been highly regarded. Resistance to mutated BRAF inhibitors can be caused by activation of either MEK/ERK or other signaling pathways such as the PI3K/Akt pathway [125,126]. In addition, melanomas with wild-type BRAF are dominated by various other pathways. One study showed that immunotherapy combined with both the BRAF inhibitor and the MEK inhibitor produced the strongest responses among all treatment regimens [127]. A single nanodelivered drug is not sufficient to lead to curable melanoma. Combination therapy has thus been explored to further increase the treatment efficacy of nanodelivered drugs.

Co-delivery of chemotherapeutic agents and signaling molecules in an NP has been achieved. Cisplatin and rapamycin are not compatible in PLGA. However, cisplatin was coated on dioleoylphosphatidic acid and then it was packed into PLGA together with rapamycin [128]. The NP containing both cisplatin and rapamycin is much more effective both in vitro cell culture systems and in vivo mouse melanoma models.

This effect was attributed to the effect of rapamycin on stroma cells where rapamycin inhibits intracellular signaling pathway (mTOR), leading to increased sensitivity of melanoma cells to cisplatin. This is consistent with the finding that inhibition of PI3K/mTOR by BEZ235 sensitized NP-packed 5-FU in cancer cells [129]. Targeted therapy against VEGF has been shown to increase the effect of nab-paclitaxel [47].

Co-delivery of siRNAs to inhibit multiple signaling molecules has been tested. An NP co-delivering siRNAs for bcl-2, VEGF, and myc showed increased effectiveness in animal melanoma models [98]. Gene expression for all three proteins was markedly decreased. The NP caused a 35–50% reduction of tumor weight in comparison to control.

Nanodelivered siRNA against TGF- β has been used to increase the effectiveness of vaccination in melanoma mouse models [130]. A polymeric NP has been used to carry three different melanoma antigens to retard tumor growth while a single antigen failed [71]. Co-delivery may also be applied to anti-PD-1 therapy. Nivolumab (anti-PD-1) has been tested together with ipilimumab (anti-CTLA-4) in melanoma, increasing the 2-year survival rate for all patients to 79% [131]. A clinical trial showed that objective responses can achieve up to 61% in BRAF wild-type tumors [132]. It is possible to use an NP to pack both siRNAs together to further increase treatment efficacy.

CONCLUSIONS

Although the discoveries of mutated BRAF inhibitors and anti-PD-L1/PD-1 therapy shed light on melanoma treatment, the overall outcomes are still not satisfactory. The application of nanotechnology in melanoma treatment may bring an effective approach as it can concentrate anticancer agents into the site of the tumor to increase efficacy and reduce side effects. So far, NP delivery has been studied to deliver various agents for chemotherapy, targeted therapy, immunotherapy, and so on. Results obtained from in vitro cell culture tests and in vivo animal experiments are promising. In addition, nanotheranotics allow us to monitor the distribution of nanodelivered drugs and therapeutic effects in a real-time fashion.

A new direction is the nanodelivery of combination therapy, which may greatly improve treatment efficacy. Although some studies have been carried out, extensive investigation is still needed to produce a practical approach for melanoma treatment. There are many types of combination treatments available for selection in melanoma therapy. At present it is difficult to judge which approach is most suitable in terms of efficacy and side effects.

References

- [1] Siegel R, DeSantis C, Virgo K, Stein K, Mariotto A, Smith T, et al. Cancer treatment and survivorship statistics, 2012. *CA Cancer J Clin* 2012;62(4):220–41.
- [2] Siegel R, Naishadham D, Jemal A. Cancer statistics, 2012. *CA Cancer J Clin* 2012;62(1):10–29.
- [3] Jerant AF, Johnson JT, Sheridan CD, Caffrey TJ. Early detection and treatment of skin cancer. *Am Fam Physician* 2000;62(2):357–68. 75–6, 81–2.
- [4] Zitelli JA, Mohs FE, Larson P, Snow S. Mohs micrographic surgery for melanoma. *Dermatol Clin* 1989;7(4):833–43.
- [5] Boyle GM. Therapy for metastatic melanoma: an overview and update. *Expert Rev Anticancer Ther* 2011;11(5):725–37.
- [6] Katipamula R, Markovic SN. Emerging therapies for melanoma. *Expert Rev Anticancer Ther* 2008;8(4):553–60.
- [7] Falkson CI, Ibrahim J, Kirkwood JM, Coates AS, Atkins MB, Blum RH. Phase III trial of dacarbazine versus dacarbazine with interferon alpha-2b versus dacarbazine with tamoxifen versus dacarbazine with interferon alpha-2b and tamoxifen in patients with metastatic malignant melanoma: an Eastern Cooperative Oncology Group Study. *J Clin Oncol* 1998;16(5):1743–51.
- [8] Atkins MB, Hsu J, Lee S, Cohen GI, Flaherty LE, Sosman JA, et al. Phase III trial comparing concurrent biochemotherapy with cisplatin, vinblastine, dacarbazine, interleukin-2, and interferon alfa-2b with cisplatin, vinblastine, and dacarbazine alone in patients with metastatic malignant melanoma (E3695): a trial coordinated by the Eastern Cooperative Oncology Group. *J Clin Oncol* 2008;26(35):5748–54.
- [9] Sharma A, Sharma AK, Madhunapantula SV, Desai D, Huh SJ, Mosca P, et al. Targeting Akt3 signaling in malignant melanoma using isoselenocyanates. *Clin Cancer Res* 2009;15(5):1674–85.
- [10] Khan KH, Goody RB, Hameed H, Jalil A, Coyle VM, McAleer JJ. Metastatic melanoma: a regional review and future directions. *Tumori* 2012;98(5):575–80.
- [11] Brose MS, Volpe P, Feldman M, Kumar M, Rishi I, Guerrero R, et al. BRAF and RAS mutations in human lung cancer and melanoma. *Cancer Res* 2002;62(23):6997–7000.
- [12] Davies H, Bignell GR, Cox C, Stephens P, Edkins S, Clegg S, et al. Mutations of the BRAF gene in human cancer. *Nature* 2002;417(6892):949–54.
- [13] Dossett LA, Kudchadkar RR, Zager JS. BRAF and MEK inhibition in melanoma. *Expert Opin Drug Saf* 2015;14(4):559–70.
- [14] Flaherty KT, Infante JR, Daud A, Gonzalez R, Kefford RF, Sosman J, et al. Combined BRAF and MEK inhibition in melanoma with BRAF V600 mutations. *N Engl J Med* 2012;367(18):1694–703.
- [15] Buchbinder EI, McDermott DF. Cytotoxic T-lymphocyte antigen-4 blockade in melanoma. *Clin Ther* 2015;37(4):755–63.
- [16] Mahoney KM, Freeman GJ, McDermott DF. The next immune-checkpoint inhibitors: PD-1/PD-L1 blockade in melanoma. *Clin Ther* 2015;37(4):764–82.
- [17] Bei D, Meng J, Youan BB. Engineering nanomedicines for improved melanoma therapy: progress and promises. *Nanomedicine (Lond)* 2010;5(9):1385–99.
- [18] Davis ME, Shin DM. Nanoparticle therapeutics: an emerging treatment modality for cancer. *Nat Rev Drug Discovery* 2008;7(9):771–82.
- [19] Sharifi S, Behzadi S, Laurent S, Forrest ML, Stroeve P, Mahmoudi M. Toxicity of nanomaterials. *Chem Soc Rev* 2012;41(6):2323–43.
- [20] Liao J, Wang C, Wang Y, Luo F, Qian Z. Recent advances in formation, properties, and applications of polymersomes. *Curr Pharm Des* 2012;18(23):3432–41.
- [21] Chen J, Shao R, Zhang XD, Chen C. Applications of nanotechnology for melanoma treatment, diagnosis, and theranostics. *Int J Nanomedicine* 2013;8:2677.

- [22] Prabhakar U, Blakey DC, Maeda H, Jain RK, Sevcik-Muraca EM, Zamboni W, et al. Challenges and key considerations of the enhanced permeability and retention effect (EPR) for nanomedicine drug delivery in oncology. *Cancer Res* 2013;73(8):2412–7.
- [23] Bourzac K. Nanotechnology: carrying drugs. *Nature* 2012;491(7425):S58–60.
- [24] Biosciences B. A phase 2 study to determine the safety and efficacy of BIND-014 (Docetaxel nanoparticles for injectable Suspension) as Secondline therapy to patients with non-small cell Lung Cancer. In: ClinicalTrials.gov [Internet]. Bethesda (MD): National Library of Medicine (US); 2013.
- [25] Hrkach J, Von Hoff D, Ali MM, Andrianova E, Auer J, Campbell T, et al. Preclinical development and clinical translation of a PSMA-targeted docetaxel nanoparticle with a differentiated pharmacological profile. *Sci Transl Med* 2012;4(128):128ra39.
- [26] Li J, Wang Y, Liang R, An X, Wang K, Shen G, et al. Recent advances in targeted nanoparticles drug delivery to melanoma. *Nanomedicine* 2014;11(3):769–94.
- [27] Peer D, Karp JM, Hong S, Farokhzad OC, Margalit R, Langer R. Nanocarriers as an emerging platform for cancer therapy. *Nat Nanotechnol* 2007;2(12):751–60.
- [28] Ndinguri MW, Zheleznyak A, Lauer JL, Anderson CJ, Fields GB. Application of collagen-model triple-helical peptide-amphiphiles for CD44-targeted drug delivery systems. *J Drug Deliv* 2012;2012:592602.
- [29] Moghimi SM, Hunter AC. Capture of stealth nanoparticles by the body's defences. *Crit Rev Ther Drug Carrier Syst* 2001;18(6):527–50.
- [30] Li L, Gu W, Chen J, Chen W, Xu ZP. Co-delivery of siRNAs and anti-cancer drugs using layered double hydroxide nanoparticles. *Biomaterials* 2014;35(10):3331–9.
- [31] Wang LS, Chuang MC, Ho JA. Nanotheranostics—a review of recent publications. *Int J Nanomedicine* 2012;7:4679–95.
- [32] Luk BT, Fang RH, Zhang L. Lipid- and polymer-based nanostructures for cancer theranostics. *Theranostics* 2012;2(12):1117–26.
- [33] Fraix A, Kandoth N, Manet I, Cardile V, Graziano AC, Gref R, et al. An engineered nanoplatform for bimodal anticancer phototherapy with dual-color fluorescence detection of sensitizers. *Chem Commun (Camb)* 2013;49.
- [34] Rolfe BE, Blakey I, Squires O, Peng H, Boase NR, Alexander C, et al. Multimodal polymer nanoparticles with combined ¹⁹F magnetic resonance and optical detection for tunable, targeted, multimodal imaging in vivo. *J Am Chem Soc* 2014;136(6):2413–9.
- [35] Ma M, Hao Y, Liu N, Yin Z, Wang L, Liang X, et al. A novel lipid-based nanomicelle of docetaxel: evaluation of antitumor activity and biodistribution. *Int J Nanomedicine* 2012;7:3389–98.
- [36] Vannucci L, Falvo E, Fornara M, Di Micco P, Benada O, Krizan J, et al. Selective targeting of melanoma by PEG-masked protein-based multifunctional nanoparticles. *Int J Nanomedicine* 2012;7:1489–509.
- [37] Liang R, Wang J, Wu X, Dong L, Deng R, Wang K, et al. Multifunctional biodegradable polymer nanoparticles with uniform sizes: generation and in vitro anti-melanoma activity. *Nanotechnology* 2013;24(45):455302.
- [38] Cho K, Wang X, Nie S, Shin DM. Therapeutic nanoparticles for drug delivery in cancer. *Clin Cancer Res* 2008;14(5):1310–6.
- [39] Misra R, Acharya S, Sahoo SK. Cancer nanotechnology: application of nanotechnology in cancer therapy. *Drug Discov Today* 2010;15(19):842–50.
- [40] Tsimberidou AM, Moulder S, Fu S, Wen S, Naing A, Bedikian AY, et al. Phase I clinical trial of hepatic arterial infusion of cisplatin in combination with intravenous liposomal doxorubicin in patients with advanced cancer and dominant liver involvement. *Cancer Chemother Pharmacol* 2010;66(6):1087–93.
- [41] Prabhu RH, Patravale VB, Joshi MD. Polymeric nanoparticles for targeted treatment in oncology: current insights. *Int J Nanomedicine* 2015;10:1001.
- [42] Zuckerman JE, Gritli I, Tolcher A, Heidel JD, Lim D, Morgan R, et al. Correlating animal and human phase Ia/Ib clinical data with CALAA-01, a targeted, polymer-based nanoparticle containing siRNA. *Proc Natl Acad Sci USA* 2014;111(31):11449–54.
- [43] Sanna V, Pala N, Sechi M. Targeted therapy using nanotechnology: focus on cancer. *Int J Nanomedicine* 2014;9:467.
- [44] Vanneman M, Dranoff G. Combining immunotherapy and targeted therapies in cancer treatment. *Nat Rev Cancer* 2012;12(4):237–51.
- [45] Viúdez A, Ramírez N, Hernández-García I, Carvalho F, Vera R, Hidalgo M. Nab-paclitaxel: a flattering facelift. *Crit Rev Oncol Hematol* 2014;92(3):166–80.
- [46] Hersh EM, O'Day SJ, Ribas A, Samlowski WE, Gordon MS, Shechter DE, et al. A phase 2 clinical trial of nab-paclitaxel in previously treated and chemotherapy-naïve patients with metastatic melanoma. *Cancer* 2010;116(1):155–63.
- [47] Kottschade LA, Suman VJ, Amatruda 3rd T, McWilliams RR, Mattar BI, Nikcevich DA, et al. A phase II trial of nab-paclitaxel (ABI-007) and carboplatin in patients with unresectable stage IV melanoma: a North Central Cancer Treatment Group Study, N057E(1). *Cancer* 2011;117(8):1704–10.
- [48] Montana M, Ducros C, Verhaeghe P, Terme T, Vanelle P, Rathelot P. Albumin-bound paclitaxel: the benefit of this new formulation in the treatment of various cancers. *J Chemother* 2011;23(2):59–66.
- [49] Zhang X, Chibli H, Kong D, Nadeau J. Comparative cytotoxicity of gold-doxorubicin and InP-doxorubicin conjugates. *Nanotechnology* 2012;23(27):275103.
- [50] Al-Jamal KT, Al-Jamal WT, Wang JT-W, Rubio N, Buddle J, Gathercole D, et al. Cationic poly-L-lysine dendrimer complexes doxorubicin and delays tumor growth in vitro and in vivo. *ACS Nano* 2013;7(3):1905–17.
- [51] Amselem S, Gabizon A, Barenholz Y. Optimization and upscaling of doxorubicin-containing liposomes for clinical use. *J Pharm Sci* 1990;79(12):1045–52.
- [52] Lo Prete AC, Maria DA, Rodrigues DG, Valduga CJ, Ibanez OC, Maranhao RC. Evaluation in melanoma-bearing mice of an etoposide derivative associated to a cholesterol-rich nanoemulsion. *J Pharm Pharmacol* 2006;58(6):801–8.
- [53] Guo S, Wang Y, Miao L, Xu Z, Lin C-HM, Huang L. Turning a water and oil insoluble cisplatin derivative into a nanoparticle formulation for cancer therapy. *Biomaterials* 2014;35(26):7647–53.
- [54] Chen J, Huang XF, Qiao L, Katsifis A. Insulin caused drug resistance to oxaliplatin in colon cancer cell HT29. *J Gastrointest Oncol* 2011;2:27–33.
- [55] Chen J. Multiple signal pathways in obesity-associated cancer. *Obes Rev* 2011;12(12):1063–70.
- [56] Chen J. Targeted therapy of obesity-associated colon cancer. *Transl Gastrointest Cancer* 2012;1(1):44–57.
- [57] Chen J, Wang MB. The roles of miRNA-143 in colon cancer and therapeutic implications. *Transl Gastrointest Cancer* 2012;1(2):169–74.
- [58] Chen J. Prevention of obesity-associated colon cancer by (-)-epigallocatechin-3 gallate and curcumin. *Transl Gastrointest Cancer* 2012;1(3):243–9.
- [59] Chen J. Signaling pathways in HPV-associated cancers and therapeutic implications. *Rev Med Virol* 2015;25(S1):24–53.
- [60] Doorbar J, Egawa N, Griffin H, Kranjec C, Murakami I. Human papillomavirus molecular biology and disease association. *Rev Med Virol* 2015;25(S1):2–23.
- [61] Holderfield M, Deuker MM, McCormick F, McMahon M. Targeting RAF kinases for cancer therapy: BRAF-mutated melanoma and beyond. *Nat Rev Cancer* 2014;14(7):455–67.

- [62] Inamdar GS, Madhunapantula SV, Robertson GP. Targeting the MAPK pathway in melanoma: why some approaches succeed and other fail. *Biochem Pharmacol* 2010;80(5):624–37.
- [63] Dhomen N, Da Rocha Dias S, Hayward R, Ogilvie L, Hedley D, Delmas V, et al. Inducible expression of (V600E) Braf using tyrosinase-driven Cre recombinase results in embryonic lethality. *Pigment Cell Melanoma Res* 2010;23(1):112–20.
- [64] Dhomen N, Reis-Filho JS, da Rocha Dias S, Hayward R, Savage K, Delmas V, et al. Oncogenic Braf induces melanocyte senescence and melanoma in mice. *Cancer Cell* 2009;15(4):294–303.
- [65] Maldonado JL, Fridlyand J, Patel H, Jain AN, Busam K, Kageshita T, et al. Determinants of BRAF mutations in primary melanomas. *J Natl Cancer Inst* 2003;95(24):1878–90.
- [66] Stahl JM, Sharma A, Cheung M, Zimmerman M, Cheng JQ, Bosenberg MW, et al. Deregulated Akt3 activity promotes development of malignant melanoma. *Cancer Res* 2004;64(19):7002–10.
- [67] Cheung M, Sharma A, Madhunapantula SV, Robertson GP. Akt3 and mutant V600E B-Raf cooperate to promote early melanoma development. *Cancer Res* 2008;68(9):3429–39.
- [68] Chen J, McMillan N, Gu W. Intra-tumor injection of lentiviral-vector delivered shRNA targeting human papillomavirus E6 and E7 oncogenes reduces tumor growth in a xenograft cervical cancer model in mice. *J Solid Tumors* 2012;2(4):4–10.
- [69] Basu S, Harfouche R, Soni S, Chimote G, Mashelkar RA, Sengupta S. Nanoparticle-mediated targeting of MAPK signaling predisposes tumor to chemotherapy. *Proc Natl Acad Sci USA* 2009;106(19):7957–61.
- [70] Basu S, Harfouche R, Soni S, Chimote G, Mashelkar RA, Sengupta S. Nanoparticle-mediated targeting of MAPK signaling predisposes tumor to chemotherapy. *Proc Natl Acad Sci USA* 2009;106(19):7957–61.
- [71] Tan S, Sasada T, Bershteyn A, Yang K, Ioji T, Zhang Z. Combinational delivery of lipid-enveloped polymeric nanoparticles carrying different peptides for anti-tumor immunotherapy. *Nanomedicine* 2014;9(5):635–47.
- [72] Perna D, Karreth FA, Rust AG, Perez-Mancera PA, Rashid M, Iorio F, et al. BRAF inhibitor resistance mediated by the AKT pathway in an oncogenic BRAF mouse melanoma model. *Proc Natl Acad Sci USA* 2015;112(6):E536–45.
- [73] Chapman PB, Hauschild A, Robert C, Haanen JB, Ascierto P, Larkin J, et al. Improved survival with vemurafenib in melanoma with BRAF V600E mutation. *N Engl J Med* 2011;364(26):2507–16.
- [74] Dang CV. MYC on the path to cancer. *Cell* 2012;149(1):22–35.
- [75] Dang CV, Kim J-W, Gao P, Yustein J. The interplay between MYC and HIF in cancer. *Nat Rev Cancer* 2008;8(1):51–6.
- [76] Chen Y, Bathula SR, Yang Q, Huang L. Targeted nanoparticles deliver siRNA to melanoma. *J Invest Dermatol* 2010;130(12):2790–8.
- [77] Lucero-Acuña A, Jeffery JJ, Abril ER, Nagle RB, Guzman R, Pagel MD, et al. Nanoparticle delivery of an AKT/PDK1 inhibitor improves the therapeutic effect in pancreatic cancer. *Int J Nanomedicine* 2014;9:5653.
- [78] Blanco E, Sangai T, Wu S, Hsiao A, Ruiz-Esparza GU, Gonzalez-Delgado CA, et al. Colocalized delivery of rapamycin and paclitaxel to tumors enhances synergistic targeting of the PI3K/Akt/mTOR pathway. *Mol Ther* 2014;22(7):1310–9.
- [79] Xiao J, Duan X, Yin Q, Miao Z, Yu H, Chen C, et al. The inhibition of metastasis and growth of breast cancer by blocking the NF- κ B signaling pathway using bioreducible PEI-based/p65 shRNA complex nanoparticles. *Biomaterials* 2013;34(21):5381–90.
- [80] Yang Y, Liu X, Zhang D, Yu W, Lv G, Xie H, et al. Chitosan/VEGF-siRNA nanoparticle for gene silencing. *J Control Release* 2011;152(Suppl. 1):e160–1.
- [81] Varshochian R, Riazi-Esfahani M, Jeddi-Tehrani M, Mahmoudi AR, Aghazadeh S, Mahbod M, et al. Albuminated PLGA nanoparticles containing bevacizumab intended for ocular neovascularization treatment. *J Biomed Mater Res Part A* 2015;103(10):3148–56.
- [82] Varshochian R, Jeddi-Tehrani M, Mahmoudi AR, Khoshayand MR, Atyabi F, Sabzevari A, et al. The protective effect of albumin on bevacizumab activity and stability in PLGA nanoparticles intended for retinal and choroidal neovascularization treatments. *Eur J Pharm Sci* 2013;50(3):341–52.
- [83] Quesnelle KM, Boehm AL, Grandis JR. STAT-mediated EGFR signaling in cancer. *J Cell Biochem* 2007;102(2):311–9.
- [84] Cordero JB, Ridgway RA, Valeri N, Nixon C, Frame MC, Muller WJ, et al. c-Src drives intestinal regeneration and transformation. *EMBO J* 2014;33(13):1474–91.
- [85] Tyryshkin A, Bhattacharya A, Eissa NT. Src kinase is a novel therapeutic target in lymphangioleiomyomatosis. *Cancer Res* 2014;74(7):1996–2005.
- [86] Blažević T, Schwaiberger AV, Schreiner CE, Schachner D, Schaible AM, Grojer CS, et al. 12/15-Lipoxygenase contributes to platelet-derived growth factor-induced activation of signal transducer and activator of transcription 3. *J Biol Chem* 2013;288(49):35592–603.
- [87] Xie TX, Huang FJ, Aldape KD, Kang SH, Liu M, Gershenwald JE, et al. Activation of stat3 in human melanoma promotes brain metastasis. *Cancer Res* 2006;66(6):3188–96.
- [88] Kong LY, Gelbard A, Wei J, Reina-Ortiz C, Wang Y, Yang EC, et al. Inhibition of p-STAT3 enhances IFN- α efficacy against metastatic melanoma in a murine model. *Clin Cancer Res* 2010;16(9):2550–61.
- [89] Yin D, Li Y, Lin H, Guo B, Du Y, Li X, et al. Functional graphene oxide as a plasmid-based Stat3 siRNA carrier inhibits mouse malignant melanoma growth in vivo. *Nanotechnology* 2013;24(10):105102.
- [90] Meier F, Busch S, Lasithiotakis K, Kulms D, Garbe C, Maczey E, et al. Combined targeting of MAPK and AKT signalling pathways is a promising strategy for melanoma treatment. *Br J Dermatol* 2007;156(6):1204–13.
- [91] Tran MA, Gowda R, Sharma A, Park EJ, Adair J, Kester M, et al. Targeting V600EB-Raf and Akt3 using nanoliposomal-small interfering RNA inhibits cutaneous melanocytic lesion development. *Cancer Res* 2008;68(18):7638–49.
- [92] Maddalo D, Manchado E, Concepcion CP, Bonetti C, Vidigal JA, Han Y-C, et al. In vivo engineering of oncogenic chromosomal rearrangements with the CRISPR/Cas9 system. *Nature* 2014;516(7531):423–7.
- [93] Zhen S, Hua L, Takahashi Y, Narita S, Liu Y-H, Li Y. In vitro and in vivo growth suppression of human papillomavirus 16-positive cervical cancer cells by CRISPR/Cas9. *Biochem Biophys Res Commun* 2014;450(4):1422–6.
- [94] Hocker TL, Singh MK, Tsao H. Melanoma genetics and therapeutic approaches in the 21st century: moving from the bedside to the bedside. *J Invest Dermatol* 2008;128(11):2575–95.
- [95] Hersey P, Zhang XD. Treatment combinations targeting apoptosis to improve immunotherapy of melanoma. *Cancer Immunol Immunother* 2009;58(11):1749–59.
- [96] Reuland SN, Goldstein NB, Partyka KA, Smith S, Luo Y, Fujita M, et al. ABT-737 synergizes with Bortezomib to kill melanoma cells. *Biol Open* 2012;1(2):92–100.
- [97] Mukherjee N, Reuland SN, Lu Y, Luo Y, Lambert K, Fujita M, et al. Combining a BCL2 inhibitor with the retinoid derivative fenretinide targets melanoma cells including melanoma initiating cells. *J Invest Dermatol* 2014;135(3):842–50.
- [98] Beloor J, Choi CS, Nam HY, Park M, Kim SH, Jackson A, et al. Arginine-engrafted biodegradable polymer for the systemic delivery of therapeutic siRNA. *Biomaterials* 2012;33(5):1640–50.

- [99] Dzmitruk V, Szulc A, Shcharbin D, Janaszewska A, Shcharbina N, Lazniewska J, et al. Anticancer siRNA cocktails as a novel tool to treat cancer cells. Part (B). Efficiency of pharmacological action. *Int J Pharm* 2015;485(1):288–94.
- [100] Yoong SL, Wong BS, Zhou QL, Chin CF, Li J, Venkatesan T, et al. Enhanced cytotoxicity to cancer cells by mitochondria-targeting MWCNTs containing platinum (IV) prodrug of cisplatin. *Biomaterials* 2014;35(2):748–59.
- [101] Poust JC, Woolery JE, Green MR. Management of toxicities associated with high-dose interleukin-2 and biochemotherapy. *Anticancer Drugs* 2013;24(1):1–13.
- [102] Keilholz U, Eggermont AM. The role of interleukin-2 in the management of stage IV melanoma: the EORTC melanoma cooperative group program. *Cancer J Sci Am* 2000;6(Suppl. 1):S99–103.
- [103] Jha G, Miller JS, Curtsinger JM, Zhang Y, Mescher ME, Dudek AZ. Randomized phase II study of IL-2 with or without an allogeneic large multivalent immunogen vaccine for the treatment of stage IV melanoma. *Am J Clin Oncol* 2012;37(3):261–5.
- [104] Schadendorf D, Vaubel J, Livingstone E, Zimmer L. Advances and perspectives in immunotherapy of melanoma. *Ann Oncol* 2012;23(Suppl. 10):x104–8.
- [105] Mackiewicz-Wysocka M, Zolnierok J, Wysocki PJ. New therapeutic options in systemic treatment of advanced cutaneous melanoma. *Expert Opin Investig Drugs* 2013;22(2):181–90.
- [106] Zhang Z, Tongchusak S, Mizukami Y, Kang YJ, Ioji T, Touma M, et al. Induction of anti-tumor cytotoxic T cell responses through PLGA-nanoparticle mediated antigen delivery. *Biomaterials* 2011;32(14):3666–78.
- [107] Perche F, Benvegna T, Berchel M, Lebegue L, Pichon C, Jaffres PA, et al. Enhancement of dendritic cells transfection in vivo and of vaccination against B16F10 melanoma with mannosylated histidylated lipopolyplexes loaded with tumor antigen messenger RNA. *Nanomedicine* 2011;7(4):445–53.
- [108] Yao H, Ng SS, Huo LF, Chow BK, Shen Z, Yang M, et al. Effective melanoma immunotherapy with interleukin-2 delivered by a novel polymeric nanoparticle. *Mol Cancer Ther* 2011;10(6):1082–92.
- [109] Kwong B, Gai SA, Elkhader J, Wittrup KD, Irvine DJ. Localized immunotherapy via liposome-anchored Anti-CD137+ IL-2 prevents lethal toxicity and elicits local and systemic antitumor immunity. *Cancer Res* 2013;73(5):1547–58.
- [110] Ragelle H, Riva R, Vandermeulen G, Naeye B, Pourcelle V, Le Duff CS, et al. Chitosan nanoparticles for siRNA delivery: optimizing formulation to increase stability and efficiency. *J Control Release* 2014;176:54–63.
- [111] He H, Grignol V, Karpa V, Yen C, LaPerle K, Zhang X, et al. Use of a nanoporous biodegradable miniature device to regulate cytokine release for cancer treatment. *J Control Release* 2011;151(3):239–45.
- [112] Stone GW, Barzee S, Snarsky V, Santucci C, Tran B, Langer R, et al. Nanoparticle-delivered multimeric soluble CD40L DNA combined with toll-like receptor agonists as a treatment for melanoma. *PLoS One* 2009;4(10):e7334.
- [113] Wang Y, Xu Z, Guo S, Zhang L, Sharma A, Robertson GP, et al. Intravenous delivery of siRNA targeting CD47 effectively inhibits melanoma tumor growth and lung metastasis. *Mol Ther* 2013;21(10):1919–29.
- [114] Teo PY, Yang C, Whilding LM, Parente-Pereira AC, Maher J, George AJ, et al. Ovarian cancer immunotherapy using PD-L1 siRNA targeted delivery from folic acid-functionalized polyethylenimine: strategies to enhance T cell killing. *Adv Healthc Mater* 2015;4(8):1180–9 [Epub ahead of print].
- [115] Chao MP, Weissman IL, Majeti R. The CD47–SIRP α pathway in cancer immune evasion and potential therapeutic implications. *Curr Opin Immunol* 2012;24(2):225–32.
- [116] Chao MP, Majeti R, Weissman IL. Programmed cell removal: a new obstacle in the road to developing cancer. *Nat Rev Cancer* 2012;12(1):58–67.
- [117] Jaiswal S, Jamieson CH, Pang WW, Park CY, Chao MP, Majeti R, et al. CD47 is upregulated on circulating hematopoietic stem cells and leukemia cells to avoid phagocytosis. *Cell* 2009;138(2):271–85.
- [118] Soto-Pantoja DR, Terabe M, Ghosh A, Ridnour LA, DeGraff WG, Wink DA, et al. CD47 in the tumor microenvironment limits cooperation between antitumor T-cell immunity and radiotherapy. *Cancer Res* 2014;74(23):6771–83.
- [119] Pardoll DM. The blockade of immune checkpoints in cancer immunotherapy. *Nat Rev Cancer* 2012;12(4):252–64.
- [120] Chen J, Zhang XD, Proud C. Dissecting the signaling pathways that mediate cancer in PTEN and LKB1 double-knockout mice. *Sci Signal* 2015;8(392):pe1.
- [121] Brahmer JR, Tykodi SS, Chow LQ, Hwu W-J, Topalian SL, Hwu P, et al. Safety and activity of anti–PD-L1 antibody in patients with advanced cancer. *N Engl J Med* 2012;366(26):2455–65.
- [122] Topalian SL, Hodi FS, Brahmer JR, Gettinger SN, Smith DC, McDermott DE, et al. Safety, activity, and immune correlates of anti–PD-1 antibody in cancer. *N Engl J Med* 2012;366(26):2443–54.
- [123] Hamid O, Robert C, Daud A, Hodi FS, Hwu W-J, Kefford R, et al. Safety and tumor responses with lambrolizumab (anti–PD-1) in melanoma. *N Engl J Med* 2013;369(2):134–44.
- [124] Voskens CJ, Goldinger SM, Loquai C, Robert C, Kaehler KC, Berking C, et al. The price of tumor control: an analysis of rare side effects of anti-CTLA-4 therapy in metastatic melanoma from the ipilimumab network. *PLoS One* 2013;8(1):e53745.
- [125] Greger JG, Eastman SD, Zhang V, Bleam MR, Hughes AM, Smitheman KN, et al. Combinations of BRAF, MEK, and PI3K/mTOR inhibitors overcome acquired resistance to the BRAF inhibitor GSK2118436 dabrafenib, mediated by NRAS or MEK mutations. *Mol Cancer Ther* 2012;11(4):909–20.
- [126] Jiang CC, Lai F, Thorne RF, Yang F, Liu H, Hersey P, et al. MEK-independent survival of B-RAFV600E melanoma cells selected for resistance to apoptosis induced by the RAF inhibitor PLX4720. *Clin Cancer Res* 2011;17(4):721–30.
- [127] Hu-Lieskovan S, Mok S, Moreno BH, Tsoi J, Robert L, Goedert L, et al. Improved antitumor activity of immunotherapy with BRAF and MEK inhibitors in BRAFV600E melanoma. *Sci Transl Med* 2015;7(279):279ra41.
- [128] Guo S, Lin CM, Xu Z, Miao L, Wang Y, Huang L. Co-delivery of cisplatin and rapamycin for enhanced anticancer therapy through synergistic effects and microenvironment modulation. *ACS Nano* 2014;8(5):4996–5009.
- [129] Chen J, Shao R, Li L, Xu ZP, Gu W. Effective inhibition of colon cancer cell growth with MgAl-layered double hydroxide (LDH) loaded 5-FU and PI3K/mTOR dual inhibitor BEZ-235 through apoptotic pathways. *Int J Nanomedicine* 2014;9:3403.
- [130] Xu Z, Wang Y, Zhang L, Huang L. Nanoparticle-delivered transforming growth factor- β siRNA enhances vaccination against advanced melanoma by modifying tumor microenvironment. *ACS Nano* 2014;8(4):3636–45.
- [131] Wolchok JD, Kluger H, Callahan MK, Postow MA, Rizvi NA, Lesokhin AM, et al. Nivolumab plus ipilimumab in advanced melanoma. *N Engl J Med* 2013;369(2):122–33.
- [132] Postow MA, Chesney J, Pavlick AC, Robert C, Grossmann K, McDermott D, et al. Nivolumab and ipilimumab versus ipilimumab in untreated melanoma. *N Engl J Med* 2015;372.

Targeted Nanoparticles for Drug Delivery to Melanoma: From Bench to Bedside

J. Li, Y. Zhang, J. Tao

Huazhong University of Science and Technology (HUST), Wuhan, PR China

OUTLINE

Introduction	203	Targeting Melanoma-Associated Antigen-Presenting Cells and Melanoma-Draining Lymph Nodes	208
<i>Melanoma: Mutational Landscape and Immunobiological Properties</i>	203	<i>Stimuli-Responsive Drug Delivery and Triggered Release</i>	209
<i>Limitations of Conventional Treatments for Melanoma</i>	204	pH Responsive	209
<i>Nanotechnology-Based Targeted Drug Delivery: A New Promising Strategy for Melanoma Treatment</i>	205	Temperature Responsive	209
Targeted Nanoparticles Drug Delivery for Melanoma Therapy	205	Light Responsive	209
<i>Passive Targeting to Extend the Blood Circulation Time and Increase the Accumulation of Therapeutic Nanoparticles at the Melanoma Site</i>	205	Ultrasound Responsive	210
<i>Active Targeting to Increase Uptake and Internalization of Therapeutic Nanoparticles</i>	206	<i>Multifunctionality: Nanotheranostics and Combination Therapy</i>	210
Targeting the Receptors on the Surface of Melanoma Cells	206	Theranostic Nanoparticles in Melanoma Imaging and Therapy	210
Targeting the Integrins on the Surface of Endothelial Cells Associated With Melanoma Neovasculation	208	Nanoparticles in Melanoma Combination Therapy	210
		Nanomedicine in Melanoma Clinical Trials	211
		Conclusion and Perspectives	212
		List of Acronyms and Abbreviations	213
		References	213

INTRODUCTION

Melanoma: Mutational Landscape and Immunobiological Properties

Melanoma arises from the malignant transformation of melanocytes, the melanin-producing cell type, which differentiates from the neural crest and migrates through the developing embryo to the skin, hair follicles,

eyes, and meninges. Melanoma is among the most aggressive and therapy-resistant human cancers. The incidence and mortality rates for malignant melanoma have been increasing steadily since the 1960s, with an estimated 76,100 new cases and 9710 deaths in the United States in 2014 [1]. Early genome studies identified some of the melanoma risk loci such as cyclin-dependent kinase inhibitor 2A (CDKN2A) and some melanin-related genes (eg, melanocortin 1 receptor

(MC1R), tyrosinase (TYR), etc.) [2,3]. High rate of somatic mutations, caused by increased exposure to natural ultraviolet radiation (UVR) with enrichment of cytosine (C) to thymine (T), or guanine (G) to adenine (A) mutations, promotes the malignant transformation of melanocyte to melanoma [4], especially in patients with the red hair/fair skin phenotype. With fast development and wide applications of next-generation sequencing technology, up to 70% of melanoma genetic mutations have been identified to be involved in the mitogen-activated protein kinase (MAPK) pathway (RTK-RAS-RAF-MEK-ERK), with mutation in BRAF (~50%) and NRAS (~30%) being the most prevalent [5]. Besides the hyperactivated MAPK signaling, the activation of phosphatidylinositol 3-kinase (PI3K/AKT) signaling pathway also plays an important role in melanoma development.

Major advances in immunology and an in-depth understanding of immune responses in tumorigenesis led to a shift in the prevailing dogma, so that now melanoma is considered not only a genetic disease, but also an immunological disorder. Melanoma can avoid immune recognition and elimination by disrupting antigen presentation mechanism, eg, downregulation of major histocompatibility complex class I molecules and disabling of the antigen processing machinery. Additionally, upregulation of programmed death

ligand-1 (PD-L1) expression on the surface of melanoma cells leads to the suppression of the effector function of tumor infiltrating lymphocytes (TILs) through the PD-1/PD-L1 interaction [6]. Widespread attention has been given to the role of immunosuppressive cells in melanomagenesis such as myeloid-derived suppressor cells (MDSCs) and regulatory T cells (Tregs), and the molecules and enzymes released by these cells, including reactive oxygen species (ROS), arginase-1 (ARG1), indoleamine 2,3-dioxygenase (IDO), etc., which are also important components of the suppressive tumor microenvironment [7] (Fig. 16.1).

Limitations of Conventional Treatments for Melanoma

Melanoma is highly curable if detected at a very early stage. Surgical resection is associated with a 5-year survival rate of 95% and 80% in patients with stage I and stage II lesions, respectively [8]. However, once the tumor has disseminated to distant sites and visceral organs (stage IV), melanoma is almost always incurable, with a median survival of 8–9 months and a 3-year overall survival (OS) rate less than 15% [9].

Before 2011, treatment was limited to dacarbazine (DTIC, 1975), interferon α -2b (IFN- α -2b, 1995), and interleukin 2 (IL-2, 1998), which were the only three

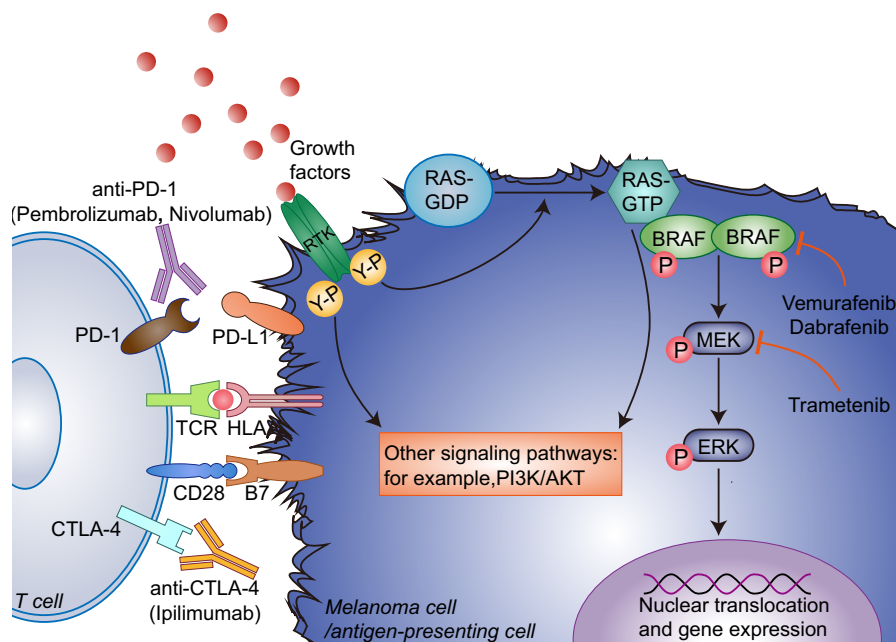


FIGURE 16.1 Schematic illustration of the genetic mutations and immunobiological changes in the development of melanoma. The majority of melanoma genetic mutations have been identified to be involved in the mitogen-activated protein kinase (MAPK) signaling pathway (RTK-RAS-RAF-MEK-ERK). Besides the hyperactivated MAPK pathway, other signaling pathway (eg, phosphatidylinositol 3-kinase [PI3K/Akt]) also plays an important role in melanoma development. Moreover, immune suppression and immune escape also participate in melanomagenesis. For example, tumor infiltrating T lymphocytes (TILs) are important effector cells which are capable of recognizing and killing tumor cells. Melanoma cells can upregulate the expression of programmed death ligand-1 (PD-L1), which specifically binds to the PD-1 receptors expressed on the surface of TILs and further inhibits the effector function of TILs through the PD-1/PD-L1 interaction.

therapeutic agents approved by the US Food and Drug Administration (FDA) for metastatic nonresectable melanoma [10–12]. The overall objective response rates with DTIC, high-dose IL-2, and recombinant IFN- α -2b are about 20%, 16%, and 15%, respectively [10–12]. Although the response rates are encouraging to some extent, the significant toxicity and lack of improvement in the OS limit their widespread use in melanoma treatment.

Breakthroughs in the treatment of metastatic melanoma are based on the progress in understanding the oncogenic mutations and immunobiological properties of this cancer. Selective small molecular inhibitors targeting the key genetic mutations on the MAPK signaling pathway, including BRAF inhibitors vemurafenib (2011) and dabrafenib (2013), along with trametinib (2013), an MEK inhibitor, have demonstrated high initial response rate and significant improvement on the progression-free survival (PFS) and OS. However, the results are unfortunately overshadowed by a short median length of response and a high relapse rate [13–15]. Immune check point inhibitors, ipilimumab (2011), an anticytotoxic T lymphocyte-associated antigen 4 (CTLA-4) monoclonal antibody (mAb), as well as pembrolizumab (2014) and nivolumab (2014), mAbs antagonizing the activity of PD-1, have also shown clear OS benefit in patients with advanced melanoma [16–18]. Although the responses are more durable, only a minority of patients achieve clear, objective responses in contrast with targeted therapy, in which a majority of patients obtain an objective response [16–18]. Moreover, immune-related adverse events with blockade of both CTLA-4 and PD-1 limit their clinical application [16–18].

Nanotechnology-Based Targeted Drug Delivery: A New Promising Strategy for Melanoma Treatment

One of the main reasons leading to the low efficacy and therapy resistance of the conventional drugs mentioned earlier is the lack of selective delivery of therapeutic agents to tumor tissues. Furthermore, high systemic exposure to these drugs inevitably results in serious dose-limiting toxicities. Therefore, targeted delivery is of utmost importance to overcome current limitations in melanoma therapy.

Rapid growth in nanotechnology and the application of nanoparticles (NPs) in medicine hold great promise to improve drug delivery, thereby increasing efficacy while decreasing the side effects of anticancer drugs. NPs are uniformly dispersed particles with nanoscaled size and favorable physicochemical characteristics, capable of carrying therapeutic entities with a high surface-to-

volume ratio. Compared with the administration of conventional free drugs, NPs offer numerous clinical advantages in cancer therapy. First, poor water solubility limits the bioavailability and reduces the efficacy of traditional anticancer drugs. By encapsulating these poorly soluble drugs in hydrophilic NPs, increased cell uptake and intracellular delivery can be achieved. Second, NPs can provide protection of therapeutic agents (eg, small interfering RNA [siRNA] and proteins) from biodegradation and thus influence their pharmacokinetic profiles. Third, stimuli-responsive NPs can be designed to release their payload to the required target sites upon internal or external triggers such as pH, temperature, light, and ultrasound. Fourth, surface modification of NPs (eg, PEGylation) can increase the circulation time, protects NPs from clearance from the blood by the mononuclear phagocytic system (MPS) and improve the accumulation of drugs in the tumor tissues. Moreover, conjugation with specific ligands can enhance the uptake of the therapeutic NPs by tumor cells and avoid adverse effects through both specific and enhanced interactions between the targeted tumor cells and the NPs. Finally, by incorporation of different therapeutic drugs (NP combination therapy), or therapeutic and diagnostic agents (NP theranostics) into a single NP, these approaches may help to overcome multidrug resistance (MDR) and offer the possibility of detecting and treating tumors simultaneously.

In this chapter, we focus on the preclinical research of targeted NP drug delivery for melanoma treatment, including passive targeting; active targeting; stimuli-responsive delivery and triggered release; melanoma-associated nanotheranostics and combination therapy; and the studies of nanomedicine in melanoma clinical trials. While the targeted NP drug delivery for melanoma treatment requires in-depth study on its own, the intentions of this chapter remain to provide only an overview of the relevant challenges and strategies.

TARGETED NANOPARTICLES DRUG DELIVERY FOR MELANOMA THERAPY

Passive Targeting to Extend the Blood Circulation Time and Increase the Accumulation of Therapeutic Nanoparticles at the Melanoma Site

The pathophysiological characteristics of tumors, eg, the increased vascular permeability as well as poor lymphatic drainage, enable NPs to accumulate at the tumor site through the enhanced permeability and retention (EPR) effect [19], which forms the basis of passive targeting and has been widely exploited for cancer therapy. The long circulation time of NPs is of

the great importance for optimal passive targeting to ensure sufficient drug delivery to targeted tumors. Surface modification with hydrophilic and flexible polymers, such as PEG, is the usual approach to obtain long-circulating NPs.

The first generation of NPs mainly aimed to improve the solubility/stability and reduce the toxicity, elongate the circulation time, and protect the anticancer drugs from degradation. Doxil (PEGylated liposomal doxorubicin) and Abraxane (based on the NP albumin-bound [nab] platform, nab-paclitaxel), approved by the FDA for the treatment of malignant tumors [20,21], including ovarian cancer, breast cancer, Kaposi's sarcoma, and pancreatic cancer, are two representative examples of first-generation nanomedicines based on passive targeting.

No chemotherapeutic drugs other than DTIC have been approved by the FDA for melanoma treatment since 1975. Although some drugs (eg, docetaxel [DTX], paclitaxel [PTX], and doxorubicin [DOX]) are capable of killing melanoma cells in vitro with high efficiency, poor solubility/chemical stability and severe toxicity to normal tissues have hampered their clinical use. Polymer bioconjugates, micelles, and liposomes are among the most commonly used nanocarriers for the delivery of these chemotherapeutic agents to melanoma to surmount the obstacles of low delivery efficiency and toxic adverse effects to normal tissues. For example, chitosan-DTX conjugates and polymeric micelles loaded with PTX or DOX could inhibit tumor growth and prolong the survival in a mouse model of melanoma more effectively but with less cytotoxicity than free drugs [22–24]. Liposomes for chemotherapeutic drug delivery have also shown enhanced ant melanoma efficacy and improved survival compared with free drugs, but with less side effects [25].

Gene therapy with siRNA has emerged as a strategy with great potential to revolutionize the treatment of cancers including melanoma. However, its clinical applications have been limited by rapid degradation by RNAases in the plasma, rapid clearance from the blood circulation, and low transfection efficiency due to poor cellular uptake of the nucleic acids. A variety of synthetic and natural NPs have been developed for siRNA delivery, with significantly improved efficacy and safety profiles. For example, VEGF-siRNA was successfully delivered to melanoma cells by using chitosan (CTS) NPs [26]. These CTS/siRNA NPs displayed improved transfection efficiency and enhanced gene silencing efficacy in B16–F10 melanoma cells without apparent cytotoxicity [26].

Although passive targeting based on the EPR effect enables NPs to accumulate and then release their therapeutic payloads within tumors, the EPR effect provides relatively modest specificity offering only 20–30%

increases in delivery and most NPs end up in or near normal tissues and organs such as the liver, kidney, and spleen [27]. Most importantly, the EPR effect cannot increase the uptake of NPs by tumor cells or the intracellular drug concentration. Therefore, the development of next-generation NPs with multifunctionalities is certainly warranted. Second-generation NPs are based on an alternative delivery system with an active targeting vector or smart nanocarriers with stimuli-responsive properties. Thus, second-generation NPs hold the promise of improved targeting, controlled release, and increased efficacy.

Active Targeting to Increase Uptake and Internalization of Therapeutic Nanoparticles

Active targeting mediated by specific ligand-receptor interactions is capable of complementing the defect of passive targeting since it not only enhances the affinity between NPs and tumor cells, but also facilitates the uptake of NPs by tumor cells via receptor-mediated endocytosis.

A wide variety of targeting moieties, including small molecules such as folic acid (FA) and carbohydrates, or macromolecules such as peptides, proteins, and antibodies, have been exploited for such purposes. For example, the second-generation NP, BIND-014, a DTX loaded PEG-PLGA (poly lactic-co-glycolic acid) polymeric NP targeting the prostate specific membrane antigen (PSMA), is currently being evaluated in clinical trials (phase 1/2) with clear responses in patients with nonsmall-cell lung cancer and prostate cancer [28]. An increasing number of preclinical experiments on actively targeted NPs for melanoma treatment have been carried out with many interesting and impressive data as well as a myriad of publications. Representative studies of the application of NPs in active targeting of melanoma are listed in Table 16.1 and will be discussed in more details in the following part.

Targeting the Receptors on the Surface of Melanoma Cells

Different receptors overexpressed on the surface of melanoma cells have been widely explored to improve the cellular uptake of NPs and to minimize offsite toxicity. Transferrin receptors (TfR) and FA receptors (FR) are two representative examples of receptors known for active melanoma targeting. The first siRNA clinical trial was performed in 2008 to treat patients with solid tumors by using a transferrin (TF)-conjugated NP preparation (denoted as CALAA-01 in the clinical version) targeting the TfR overexpressed on solid tumors, including melanoma [29]. Other examples include the use of TfR-targeted dendrimers and FA-conjugated NPs for the delivery of p73 and IL-2

TABLE 16.1 Active Targeting Melanoma and Melanoma-Associated Antigen-Presenting Cells (APCs) Through Ligand-Receptor-Mediated Interactions

Ligand	Receptor	Drug	Nanocarrier	References
TARGETING THE RECEPTORS ON THE SURFACE OF MELANOMA CELLS				
Transferrin (Tf)	Transferrin receptor (TfR)	RRM2 siRNA	Tf-bearing PEGylated cyclodextrin-based polymer (CALAA-01)	[29]
Tf	TfR	P73 plasmid DNA	Tf-bearing polypropylenimine dendrimer	[30]
Folic acid (FA)	Folic acid receptor (FR)	IL-2 plasmid DNA	Polyethylenimine linked by beta-cyclodextrin and conjugated with folate	[31]
Truncated human basic fibroblast growth factor (tbFGF)	Fibroblast growth factor receptor (FGFR)	Doxorubicin and paclitaxel	tbFGF conjugated liposomes	[32]
tbFGF	FGFR	Paclitaxel	tbFGF-PEG modified liposomes	[33]
Octreotide (Oct)	Somatostatin receptor (SSTR)	Doxorubicin	Oct-PEG-PE	[34]
Tyr-Ile-Gly-Ser-Arg peptide (YIGSR)	Laminin receptor	5-Fluorouracil	YIGSR-PEG nanospheres	[35]
YIGSR	Laminin receptor	Etoposide	YIGSR peptide conjugated micelles	[36]
Anisamide (AA)	Sigma receptor	c-Myc siRNA	AA modified NPs	[37]
AA	Sigma receptor	MDM2, c-myc, and VEGF-siRNA	Lipid/calcium/phosphate NP grafted with PEG and AA	[38]
MC1SP-peptide	Melanocortin 1 receptor (MC1R)	HSVtk	PEI-PEG-based polyplexes containing MC1SP-peptide	[39]
TARGETING THE INTEGRINS ON THE SURFACE OF MELANOMA VASCULATURES				
Cyclic Arg-Gly-Asp-d-Tyr-Lys peptide (cRGDyK)	Integrin $\alpha v \beta 3$	Doxorubicin and combretastatin A4	RFPs modified with PEG-PLA	[41]
Cyclic Arg-Gly-Asp-d-Phe-Lys peptide (cRGDFK)	Integrin $\alpha v \beta 3$	Paclitaxel and combretastatin A4	cRGDFK peptide conjugated with PLGA modified solid NPs	[42]
N-acetyl-Pro-His-Ser-Cys-Asp-amide peptide (Ac-PHSCN-NH(2))	Integrin $\alpha 5 \beta 1$	Doxorubicin	PHSCNK conjugated with stealth liposomes	[43]
C16Y peptide	Integrin $\alpha v \beta 3$ and $\alpha 5 \beta 1$		C16Y peptide modified liposomes	[44]
TARGETING DENDRITIC CELLS				
DC-SIGN-binding glycans	DC-specific intercellular adhesion molecule-3-grabbing nonintegrin (DC-SIGN)	Melanoma antigen recognized by T-cells 1 (MART-1)	DC-SIGN-binding glycans modified liposomes	[45]
CD11c and DEC-205 single chain antibody fragments	CD11c and DEC-205	OVA or OVA peptide antigen	CD11c and DEC-205 single chain antibody fragments conjugated stealth liposomes	[46]
Mannose	Mannose receptor	MART-1 mRNA	Mannosylated and histidylated lipopolyplexes	[47]

Oct-PEG-PE, Oct conjugated PEGylated phosphatidyl-ethanolamine; PEI-PEG-based polyplexes containing MC1SP-peptide, Polyetherimide-based PEGylated polyplexes containing MC1SP-peptide; RFPs modified with PEG-PLA, RFPs modified with PEGylated polylactic acid; cRGDFK peptide conjugated with PLGA modified solid NPs, cRGDFK peptide conjugated with poly(lactic-co-glycolic acid) modified solid NPs.

plasmid DNA to melanoma. Both of them inhibited tumor growth and extended survival in melanoma-bearing mice more efficiently and without apparent toxicity compared to the nontargeted control group [30,31]. Even though antitumor effects have been achieved to a certain extent by modifying nanocarriers with Tf and FA, the wide distribution of the TfR and FR on normal tissues and cells will pose the danger of off-target binding and side effects.

Besides TfR and FR, other receptors such as fibroblast growth factor receptor (FGFR), laminin receptor, somatostatin receptor (SSTR), sigma receptor, MC1R, etc., have also been utilized for specific melanoma targeting with high affinity and have shown promising results. For example, FGFR-targeted liposomes loaded with PTX or DOX showed higher accumulation in tumor tissues and internalization by melanoma cells with less toxicity to normal tissues compared with nontargeted liposomes or free PTX or DOX [32,33]. Liposomes conjugated with SSTR targeting moieties also showed a remarkable drug accumulation in melanoma with enhanced cytotoxicity to melanoma cells [34]. Laminin receptor-targeted nanospheres and polymeric micelles carrying 5-fluorouracil (5-FU) or etoposide demonstrated significant efficacy in the prevention of tumor growth and lung metastasis in melanoma mice model compared to free drugs and nontargeted NPs [35,36]. Sigma receptor-targeted NPs loaded with siRNA, as well as MC1R targeted polyplexes for melanoma gene therapy also showed significantly enhanced antimelanoma effect compared to nontargeted control [37–39].

Targeting the Integrins on the Surface of Endothelial Cells Associated With Melanoma Neovasculature

Integrins are heterodimeric transmembrane glycoprotein receptors essential for tumor cell adhesion, migration, and invasion. They are composed of an α subunit and a β subunit, which together modulate the interactions of tumor endothelial cells with proteins of the extracellular matrix [40].

Integrin family members $\alpha v \beta 3$, $\alpha v \beta 5$, and $\alpha 5 \beta 1$ are usually highly expressed on endothelial cells associated with melanoma neovasculature. Peptides such as Arg-Gly-Asp (RGD), cyclic Arg-Gly-Asp-d-Tyr-Lys (cRGDyK), and cyclic Arg-Gly-Asp-d-Phe-Lys (cRGDfK) show high affinity to these integrins and can be used for NP surface modification for actively targeting melanoma vasculatures [41–43]. Many studies have indicated that chemotherapeutic agent-loaded NPs conjugated with these peptides exhibited enhanced intracellular uptake and significant tumor growth inhibition compared with nontargeted control NP in melanoma-bearing mice [41–43]. Moreover, compared to mono-targeting,

dual-targeting seems to be an even more effective method for anticancer drug delivery. For example, C16Y, a synthetic peptide with 12 amino acids, can bind to integrins $\alpha v \beta 3$ and $\alpha 5 \beta 1$ on both tumor vasculature associated endothelial cells and tumor cells in melanoma-bearing mice [44]. More efficient melanoma growth inhibition using C16Y-modified liposomes was observed than that found with nontargeted control [44].

Targeting Melanoma-Associated Antigen-Presenting Cells and Melanoma-Draining Lymph Nodes

The great success obtained from the clinical trials of melanoma vaccines such as gp100 and Allovectin-7 suggests a new strategy in melanoma treatment. Dendritic cells (DCs) have long been known to be the most potent antigen-presenting cells (APCs). Owing to their remarkable ability to initiate an immune response with ultimate T-cell activation, a variety of NP vaccinations targeting DCs have been used in tumor immunotherapy. But the relatively low efficiency of antigen delivery to skin-derived conventional DCs, and DCs residing in the melanoma-draining lymph nodes (LNs), owing to the nonspecific uptake and endocytosis of NPs by MPS (eg, macrophages), is great challenge in melanoma vaccination. By modulating NPs with receptors/biomarkers specific to DC, including DC-specific intercellular adhesion molecule-3-grabbing nonintegrin (DC-SIGN), CD11c, and DEC-205, the improved delivery efficiency, the increased uptake and internalization of the melanoma antigens, as well as the enhanced antigen presentation capability to T lymphocytes can be achieved. For example, melanoma antigen recognized by T-cells 1 (MART-1) loaded liposome targeting DC-SIGN exhibited more efficient antigen presentation to T cells than nontargeted control [45]. CD11c and DEC-205-targeted liposomes loaded with B16-OVA also induced dramatic B16-OVA-specific cytotoxic T lymphocytes (CTLs) responses, significantly inhibited tumor growth, and extended melanoma-free survival [46]. MART-1 mRNA-loaded mannoseylated and histidylated lipopolyplexes could efficiently bind the mannose receptors on splenic DCs, deliver melanoma antigen mRNA to splenic DCs in B16-F10 melanoma-bearing mice, and induce significant antimelanoma immune responses and tumor growth inhibition [47].

Although the DC-targeted NP vaccination demonstrated its advantages over conventional vaccination methods, nonspecific phagocytosis and macropinocytosis of antigen-loaded NPs by macrophages in the tissue environment occur and greatly influence the efficiency of DC targeting. Thus, targeting melanoma-draining LNs has emerged as a promising strategy for more efficient antigen presentation to LN-resident DCs. For example, CpG-B or CpG-C oligonucleotides conjugated

to NPs showed better dual-targeting of adjuvant and antigen to the LNs, and induced the maturation of DCs more efficiently compared with the control group, which led to an active antitumor immune response and efficient tumor growth inhibition in a melanoma mouse model [48]. Synthesized CpG-DNA/peptide amphivaccine, as well as the combination of CpG-NP and PTX-NP could also accumulate in the melanoma-draining LNs and significantly suppress melanoma growth while greatly reducing systemic toxicity [49,50].

Stimuli-Responsive Drug Delivery and Triggered Release

Stimuli-responsiveness is currently one of the most impressive and promising approaches to targeted cancer therapy. Stimuli-responsive drug delivery, or “smart” delivery, is a popular form of active targeting with the capability of delivering the cargo at the desired site and at the required time. Pathophysiologic properties characteristic of tumors such as a more acidic extracellular microenvironment and a higher sensitivity to hyperthermia can act as “intrinsic stimuli.” Similarly, some stimuli can be induced at the tumor site, such as by applying alternating magnetic fields, near-infrared (NIR) light, or ultrasound to bring about local delivery of cargo, and are termed “extrinsic stimuli.” Upon exposure to extrinsic and/or intrinsic stimuli, stimuli-sensitive NPs undergo physical and chemical changes that act as triggers for the “on-demand” release of the associated cargo.

pH Responsive

The extracellular microenvironment of tumors is slightly acidic (pH ~6.5–7.2) compared to healthy tissues (pH ~7.4) due to the active metabolism and abnormal glycolysis of tumor cells, which has been utilized to achieve a controlled delivery and triggered drug release. The conformational and/or solubility changes of polymeric NPs with ionizable groups in response to pH variation, and the cleavage of acid-sensitive bonds anchored on the backbone of polymeric NPs, are two main strategies for pH-triggered drug release.

The delivery efficiency and therapeutic effect of a variety of pH-sensitive systems have been investigated in animal models of melanoma. For example, acid-sensitive micelles loaded with chemotherapeutic agents (eg, gemcitabine or DOX) were susceptible to pH-sensitive hydrolysis under tumor microenvironments and demonstrated higher cytotoxicity and better antitumor activity in a melanoma mouse model compared to acid-insensitive micelles and free drug [51,52]. NPs that are pH sensitive are also effective for nucleic acid delivery. For example, the increased

osmotic pressure formed by cationic NPs could lead to the swelling and rupture of the lysosomes. The so-called “proton sponge effect” enabled DNA-loaded NPs to escape from the endosomal compartment and significantly improved the transfection efficiency in melanoma-bearing mice [53].

Temperature Responsive

Ideally, thermo-responsive NPs remain stable at body temperature (~37°C), and rapidly release the drug within tumor tissues upon a local hyperthermia (~40–42°C) to prevent their payloads from undergoing rapid clearance from the circulation, and washout from the tumor. When exposed to alternating magnetic fields or heating with shortwave radio-frequency fields, the heat produced from the applied electromagnetic energy can kill melanoma cells either directly or through the heat-triggered drug release from thermal-responsive polymers. For example, when applying an external magnetic field, thermosensitive ferromagnetic particles (FMP) showed an increased antitumor effect compared to the control without FMP [54].

Light Responsive

Light-responsive drug delivery is also an attractive strategy owing to the noninvasiveness and the possibility of remote and precise spatiotemporal control. Light-responsive polymers can be designed by combining optically active substances (eg, functional dyes, metals, and photosensitive materials) with nanocarriers. These NPs are capable of changing the light energy into heat (photothermal), and photosensitive NP can release their loaded drugs when irradiated by ultraviolet (UV), visible light, or NIR light. For example, hollow gold nanospheres modified with an α -melanocyte-stimulating hormone (α -MSH) analog could specifically target melanoma cells and induce significant photothermal ablation of melanoma after NIR irradiation [55]. Photodynamic therapy (PDT) is now considered as one of the most promising strategies for the treatment of skin cancers owing to it being less invasive than surgery and with no long-term side effects. Photosensitizer (eg, aminolevulinic acid derivatives) conjugated NPs allowed enhanced permeation of photosensitizers through the skin and improved the PDT efficacy for superficial melanoma and other skin cancers after visible light irradiation [56]. For large and deep-seated tumors these visible light photosensitizers are less effective while NIR light can afford greater penetration depths than that of visible light. Upconversion fluorescent NPs are able to convert NIR light into visible wavelengths, and have shown significant tumor growth inhibition [57], providing a new and noninvasive approach for the treatment of large and deep-seated cancers.

Ultrasound Responsive

Ultrasound represents an appealing and effective method for “on-demand” drug release, owing to less harmful side effects to surrounding normal tissues, and absence of ionizing radiation. Furthermore, the depth of penetration is easy to be regulated by modulating the ultrasound frequency, energy, and exposure time. The acoustic energy absorbed by the fluid or tissues can produce a thermal effect, which can trigger the release of drugs. Also, the cavitation phenomena caused by the oscillation of ultrasound-induced bubbles can generate small transient holes in the cell membrane and facilitate the delivery of therapeutic agents into the cytosol. For example, under ultrasound, perfluoropropane gas-entrapping liposomes (bubble liposomes) and Man-PEG (2000) bubble lipoplexes can be used to deliver melanoma antigens directly into the cytosol of DCs more efficiently, with enhanced melanoma growth inhibition and prevention of metastasis [58,59].

Although a much better spatial and temporal control over the release of drugs can be achieved compared to the conventional delivery systems, stimuli-responsive systems are not completely devoid of off-target effects. For example, a lower pH may also be present in vivo in some normal organs and tissues as well as at inflammatory sites. As a result, the extent of the stimuli sensitivity of the developed NPs needs to be carefully considered. Furthermore, the quest for increasingly complex stimuli-responsive NPs often ignores their safety profiles (eg, the utilization of biomaterials with excellent multifunctionality but poor biocompatibility/bioavailability for NP modification), which will hinder the development of a safer NP delivery system.

Multifunctionality: Nanotheranostics and Combination Therapy

Theranostic Nanoparticles in Melanoma Imaging and Therapy

NPs hold great promise in the application of molecular imaging because of their intense and stable output and multimodal signaling capacity. The term “theranostic” indicates technology with simultaneous and complementary diagnostic and therapeutic capabilities [60]. By virtue of combining imaging modalities and therapeutic agents into a single biocompatible and biodegradable particle, theranostic NPs would enable both early diagnosis and therapy, the prediction of the therapeutic efficacy as well as the tracking of the tumors. Since the prognosis of melanoma is better if detected at a very early stage, it is of great importance that the enhanced signal-to-noise ratio and increased imaging resolution achieved by the application of theranostic

imaging NPs enables the discovery of very small lesions which are undetectable with traditional methods.

For example, magnetic NPs (MNPs) combined with chemotherapeutic drugs such as PTX, DOX, or curcumin can produce an increased dark contrast signal in magnetic resonance imaging (MRI) in tumor tissues and inhibited tumor growth with reduced side effects in melanoma-bearing mice [61–62]. Liposomes coencapsulated with cisplatin and quantum dots (QDs) also demonstrated concurrent capabilities of tumor imaging and tumor growth suppression in a melanoma mouse model [63]. Interestingly, coadministration of dual-color fluorescence imaging agents and chromo-fluorogenic components into a single NP can achieve dual-color imaging and enhanced melanoma killing effect [64].

Nanoparticles in Melanoma Combination Therapy

The combination of two or more therapeutic drugs to achieve a synergistic therapeutic efficacy better than that achieved with each of them individually has been a mainstay of cancer treatment for several decades. The combined cancer treatment regimens can act through different mechanisms to achieve a synergistic therapeutic effect and reduce the possibility of drug resistance.

The advantage of NPs combination therapy over conventional combination therapy lies in its capability to increase the delivery to the tumor site to reduce nonspecific and dose-limiting toxicities to healthy tissues, while bypassing many drug resistance mechanisms to overcome MDR. Examples include PTX and CA4 (an antiangiogenesis agent) coencapsulated into NPs that showed dramatic tumor growth inhibition and tumor vasculature disruption in melanoma-bearing mice [42]; the combination of imatinib-loaded sterically stabilized liposomes (SSL-IMA) and SSL-DOX significantly inhibited melanoma growth at a low dose in which neither SSL-DOX nor SSL-IMA showed obvious antitumor efficacy [65].

Accumulating evidence has revealed that some chemotherapy-based cancer treatments may activate the antitumor immune responses through different molecular and cellular mechanisms. The chemo-immunotherapy combination may thus be synergistic and enhance the clinical response while reducing the toxicity. For example, incorporation of the immunostimulant lipopolysaccharide and PTX in the same NP showed significantly higher antitumor activity and a higher percentage of activated TILs in a melanoma mouse model as compared to PTX-treated control [66]. PTX and an adenovirus vector encoding for IL-12 (Ad5-mIL-12) coencapsulated into anionic liposomes (AL) demonstrated a significantly enhanced antitumor effect in melanoma-bearing mice compared with mice treated with either AL/Ad5-mIL-12 or AL/PTX alone [67].

Although promising, the development of combination payload-containing NPs comes with its own challenges. A thorough physicochemical characterization of the combination of payloads by determining the optimal loading capacity of the NPs in the context of the synergistic ratio is the first aspect that needs to be considered. In addition, the combined therapeutic components should have no pharmacokinetic interactions and should be well tolerated in the ratios and concentrations used. Furthermore, the wrong sequence of drug release could reduce the synergistic effect of coencapsulated therapeutic drugs. Despite so many difficulties, the advances in understanding drug synergism and the development of nanotechnology may enable the development of robust combination NPs with an improved therapeutic efficacy and a reduced potential for unwanted and unknown toxicity concerns.

NANOMEDICINE IN MELANOMA CLINICAL TRIALS

A wide range of nanomedicines based on proteins, polymer bioconjugates, micelles, liposomes, and many other types of nanomaterials have been investigated in

the patients with metastatic melanoma, including Abraxane, Taxoprexin (docosahexaenoic acid-paclitaxel, DHA-paclitaxel), Marqibo (vincristine sulfate liposomes injection, VSLI), Caelyx (PEGylated liposomal doxorubicin), ADI-PEG-20 (PEGylated arginine deiminase), Allovectin-7 (HLA-B7/beta-2 microglobulin plasmid DNA/lipid complex), PEG-Intron (peginterferon- α -2b), etc. However, most clinical trials have focused on marketed products, such as Abraxane or PEG-Intron, either investigating new indications or testing therapies in combination with other anticancer agents. Representative studies involving nanomedicine in melanoma clinical trials are listed in Table 16.2 and will be discussed in more details in the following part.

The therapeutic efficacy and safety of Abraxane (also known as ABI-007), first approved by the FDA in 2005 for the treatment of metastatic breast cancer, have also been investigated in patients with metastatic melanoma. In a phase II trial, ABI-007 as a monotherapy achieved a clear objective response rate, along with an increased median PFS and OS in a chemotherapy-naïve group of patients with metastatic melanoma [68]. In addition, the effect of ABI-007 in combination with other therapeutic agents was also investigated. For example, the weekly combination of ABI-007 and carboplatin

TABLE 16.2 Nanomedicines in Melanoma Clinical Trials

NCT No	Phase	Number Enrolled	Nanomedicine	Outcome	References
NCT00093119	II	74	Nab-paclitaxel (Abraxane, ABI-007)	Chemotherapy-naïve group versus previously treated group: Response rate (21.6% vs 2.7%), median progression-free survival (PFS) (4.5 m vs 3.5 m), median survival (9.6 m vs 12.1 m), free of disease progression at 6 months (34% vs 27%); 22% discontinued therapy because of toxicities in previously untreated group	[69]
NCT00404235	II	76	Nab-paclitaxel	Chemotherapy-naïve group versus previously treated group: Response rate (25.6% vs 8.8%), median PFS (4.5 m vs 4.1 m), overall survival (OS) (11.1 m vs 10.9 m)	[70]
NCT00462423	II	50	Nab-paclitaxel	Combination therapy with Abraxane and bevacizumab: Objective response rate was 36%; PFS and OS were 7.63 m and 16.8 m, respectively; the rate of serious adverse events (SAEs) was 26%	[71]
NCT00864253	III	529	Nab-paclitaxel	ABI-007 versus dacarbazine: Median PFS (4.8 m vs 2.5 m), OS (12.8 m vs 10.7 m), SAEs (24.12% vs 20.93%)	[72]
NCT00044356	II	133	Allovectin-7	Objective response rate was 11.8%, median duration of response and median time-to-progression were 13.8 m and 1.6 m, respectively	[75]
NCT00395070	III	390	Allovectin-7	Allovectin-7 versus dacarbazine/temozolomide: Response rate (4.6% vs 12.3%), OS (18.8 m vs 24.1 m); but duration of response was marginally longer of Allovectin-7 than that of dacarbazine/temozolomide	[76]

appeared to be moderately well tolerated, with promising clinical activity as therapy in chemotherapy-naïve patients with stage IV melanoma and with modest anti-tumor activity in those previously treated patients [69]. Moreover, the combination of Abraxane and bevacizumab also seemed to be well tolerated and effective in melanoma patients with remarkable improvement on the response rate, median PFS, and OS [70]. A phase III comparison study of the efficacy and safety of ABI-007 and DTIC in patients with metastatic melanoma indicated that patients who received ABI-007 had much longer PFS than those who received DTIC despite there being no significant difference in participant survival between these two groups [71]. Although Abraxane has been proven to be beneficial, not all chemotherapeutic nanomedicines are effective for patients with malignant melanoma. Two phase II studies showed that PEGylated liposomal DOX as a monotherapy in patients with disseminated melanoma could not produce any positive response in the evaluable patients and enrollment was stopped due to lack of activity [72,73].

Besides chemotherapeutic nanomedicine, the efficacy and safety of NP vaccination as a melanoma treatment has also been evaluated. A phase II trial indicated that high-dose Allovectin-7 was effective and well tolerated for some stage III/IV metastatic melanoma patients [74]. A phase III pivotal trial to compare the safety and efficacy of Allovectin-7 versus DTIC/temozolomide in patients with recurrent stage III/IV metastatic melanoma showed that although the OS of the Allovectin-7 group was shorter than that of DTIC/temozolomide, the low toxicity, easy administration, and likely systemic immune responses of Allovectin-7 make it an attractive option in combination with other lines of therapy [75].

Although some progress has been made in the use of nanomedicine for melanoma treatment, many clinical results have not been so satisfactory as we expected. The discrepancy between the large amount of preclinical research devoted to NPs in melanoma therapy, and its limited translation to patients may lead to uncertainties arising about the future of nanomedicine. However, on the historical timescale of pharmaceutical research, the field of nanotechnology and its application in medicine is still in its infancy, and we have good reasons to believe that given more time, obstacles to the commercialization of nanomedicines will be cleared away.

CONCLUSION AND PERSPECTIVES

Although NPs have demonstrated a promising translational potential in preclinical cancer therapy, relatively few anticancer nanomedicines (eg, Doxil, DaunoXome, Mepact, DepoCyt, Abraxane, and Myocet) have come

onto the market over the past two decades. Here comes the question: why, with so many encouraging data, the road to its clinical translation is still so long and full of difficulties?

The potential answers to this question may be, firstly, that there is evidence that many promising preclinical data cannot be directly and easily translated into humans. For example, the EPR effect is much more heterogeneous in human melanoma patients than is seen in the most frequently used subcutaneous melanoma animal xenograft models because of higher heterogeneity in tumor vascular permeability and blood flow. In the meantime, the lack of standardization of preclinical studies often makes it difficult to compare these results among different experimental groups. In addition, whether active targeted NPs are more efficient for drug delivery than nontargeted NPs has long been debated because the ligand or antibody itself cannot produce propulsive forces to drive the NPs to reach the targeted tumors, despite their higher probability of binding to and being internalized by the tumor cells. Finally, the general batch-to-batch inconsistency and the complexity of the process of NP design and synthesis have also hampered their industrial production on a commercial scale.

On the other hand, the phenotypical plasticity of melanoma tumors resulting from the interplay of genetic mutations, epigenetic changes, and environmental factors poses great challenges for designing and preparing a “one size fits all” NP which is applicable to all different subsets of melanoma. Furthermore, the heterogeneity of melanoma may also influence the quantity, density, and clustering of the receptors that are overexpressed on melanoma cells. This heterogeneous landscape of receptor expression among different individuals or at different stages of melanoma may explain why an “off-target” effect can still happen despite the use of high-affinity ligands binding to these receptors. The off-target related drawbacks such as low drug delivery efficiency, toxicity to normal cells and tissues, and reduced sensitivity of early-stage imaging of metastatic melanoma also need to be taken into careful consideration.

In conclusion, when emphasizing the advantages of drug delivery by targeted NPs in melanoma treatment, the significance of an in-depth understanding of the EPR effect—the basis and key element of the targeted drug delivery system—cannot be ignored. Meanwhile, deep insight into the interplay of genetic mutations and immunobiological changes involved in melanoma-genesis is equally important. How to take full advantage of the EPR effect and further augment it [76], and how to combine nanotechnology with recently highlighted clinical progress in melanoma are the most urgent problems that need to be solved. Effective solutions to these problems will yield full translational potential of targeted NPs in melanoma treatment.

List of Acronyms and Abbreviations

5-FU 5-Fluorouracil
AL Anionic liposome
Anx Anginex
APC Antigen-presenting cell
ARG1 Arginase-1
CDKN2A Cyclin-dependent kinase inhibitor 2A
cRGDfK Cyclic Arg-Gly-Asp-d-Phe-Lys
cRGDyK Cyclic Arg-Gly-Asp-d-Tyr-Lys
CTL Cytotoxic T lymphocyte
CTLA-4 Cytotoxic T lymphocyte-associated antigen 4
CTS Chitosan
DC Dendritic cell
DC-SIGN DC-specific intercellular adhesion molecule-3-grabbing nonintegrin
DOX Doxorubicin
DTIC Dacarbazine
DTX Docetaxel
EPR Enhanced permeability and retention
FDA Food and Drug Administration
FGFR Fibroblast growth factor receptor
FMP Ferromagnetic particles
FR Folic acid receptor
IDO Indoleamine 2,3-dioxygenase
IFN- α -2b Interferon α -2b
IL-2 Interleukin 2
LN Lymph node
mAb Monoclonal antibody
MAPK Mitogen-activated protein kinase
MART-1 Melanoma antigen recognized by T-cells 1
MC1R Melanocortin 1 receptor
MDR Multidrug resistance
MDSC Myeloid-derived suppressor cell
MNP Magnetic nanoparticle
MPS Mononuclear phagocytic system
MRI Magnetic resonance imaging
NIR Near-infrared
NP Nanoparticle
OS Overall survival
PD-L1 Programmed death ligand-1
PDT Photodynamic therapy
PFS Progress-free survival
PI3K Phosphatidylinositol 3-kinase
PTX Paclitaxel
QD Quantum dot
RGD Arg-Gly-Asp
ROS Reactive oxygen species
siRNA Small interfering RNA
SSTR Somatostatin receptor
Tf Transferrin
TfR Transferrin receptor
TIL Tumor infiltrated lymphocyte
TYR Tyrosinase
UV Ultraviolet
UVR Ultraviolet radiation

References

- [1] <http://www.cancer.gov/cancertopics/pdq/treatment/melanoma/patient>.
- [2] Hussussian CJ, Struewing JP, Goldstein AM, Higgins PA, Ally DS, Sheahan MD, et al. Germline p16 mutations in familial melanoma. *Nat Genet* September 1994;8(1):15–21.
- [3] Bishop DT, Demenais F, Iles MM, Harland M, Taylor JC, Corda E, et al. Genome-wide association study identifies three loci associated with melanoma risk. *Nat Genet* August 2009;41(8):920–5.
- [4] Hodi E, Watson IR, Kryukov GV, Arold ST, Imielinski M, Theurillat JP, et al. A landscape of driver mutations in melanoma. *Cell* July 20, 2012;150(2):251–63.
- [5] Flaherty KT, Hodi FS, Fisher DE. From genes to drugs: targeted strategies for melanoma. *Nat Rev Cancer* May 2012;12(5):349–61.
- [6] Blank C, Brown I, Peterson AC, Spiotto M, Iwai Y, Honjo T, et al. PD-L1/B7H-1 inhibits the effector phase of tumor rejection by T cell receptor (TCR) transgenic CD8+ T cells. *Cancer Res* February 1, 2004;64(3):1140–5.
- [7] Mellman I, Coukos G, Dranoff G. Cancer immunotherapy comes of age. *Nature* December 22, 2011;480(7378):480–9.
- [8] Garbe C, Eigentler TK, Keilholz U, Hauschild A, Kirkwood JM. Systematic review of medical treatment in melanoma: current status and future prospects. *Oncologist* 2011;16(1):5–24.
- [9] Balch CM, Gershenwald JE, Soong SJ, Thompson JF, Atkins MB, Byrd DR, et al. Final version of 2009 AJCC melanoma staging and classification. *J Clin Oncol* December 20, 2009;27(36):6199–206.
- [10] Atkins MB, Lotze MT, Dutcher JP, Fisher RI, Weiss G, Margolin K, et al. High-dose recombinant interleukin 2 therapy for patients with metastatic melanoma: analysis of 270 patients treated between 1985 and 1993. *J Clin Oncol* July 1999;17(7):2105–16.
- [11] Hill 2nd GJ, Kremenz ET, Hill HZ. Dimethyl triazeno imidazole carboxamide and combination therapy for melanoma. IV. Late results after complete response to chemotherapy (Central Oncology Group protocols 7130, 7131, and 7131A). *Cancer* March 15, 1984;53(6):1299–305.
- [12] Phan GQ, Attia P, Steinberg SM, White DE, Rosenberg SA. Factors associated with response to high-dose interleukin-2 in patients with metastatic melanoma. *J Clin Oncol* August 1, 2001;19(15):3477–82.
- [13] Chapman PB, Hauschild A, Robert C, Haanen JB, Ascierto P, Larkin J, et al. Improved survival with vemurafenib in melanoma with BRAF V600E mutation. *N Engl J Med* June 30, 2011;364(26):2507–16.
- [14] Hauschild A, Grob JJ, Demidov LV, Jouary T, Gutzmer R, Millward M, et al. Dabrafenib in BRAF-mutated metastatic melanoma: a multicentre, open-label, phase 3 randomised controlled trial. *Lancet* July 28, 2012;380(9839):358–65.
- [15] Falchook GS, Lewis KD, Infante JR, Gordon MS, Vogelzang NJ, DeMarini DJ, et al. Activity of the oral MEK inhibitor trametinib in patients with advanced melanoma: a phase 1 dose-escalation trial. *Lancet Oncol* August 2012;13(8):782–9.
- [16] Hodi FS, O'Day SJ, McDermott DF, Weber RW, Sosman JA, Haanen JB, et al. Improved survival with ipilimumab in patients with metastatic melanoma. *N Engl J Med* August 19, 2010;363(8):711–23.
- [17] Robert C, Ribas A, Wolchok JD, Hodi FS, Hamid O, Kefford R, et al. Antiprogrammed-death-receptor-1 treatment with pembrolizumab in ipilimumab-refractory advanced melanoma: a randomised dose-comparison cohort of a phase 1 trial. *Lancet* September 20, 2014;384(9948):1109–17.
- [18] Topalian SL, Sznol M, McDermott DF, Kluger HM, Carvajal RD, Sharfman WH, et al. Survival, durable tumor remission, and long-term safety in patients with advanced melanoma receiving nivolumab. *J Clin Oncol* April 1, 2014;32(10):1020–30.
- [19] Matsumura Y, Maeda H. A new concept for macromolecular therapeutics in cancer chemotherapy: mechanism of tumorotropic accumulation of proteins and the antitumor agent smancs. *Cancer Res* December 1986;46(12 Pt 1):6387–92.
- [20] Ranson MR, Carmichael J, O'Byrne K, Stewart S, Smith D, Howell A. Treatment of advanced breast cancer with sterically stabilized liposomal doxorubicin: results of a multicenter phase II trial. *J Clin Oncol* October 1997;15(10):3185–91.

- [21] Ibrahim NK, Samuels B, Page R, Doval D, Patel KM, Rao SC, et al. Multicenter phase II trial of ABL-007, an albumin-bound paclitaxel, in women with metastatic breast cancer. *J Clin Oncol* September 1, 2005;23(25):6019–26.
- [22] Liu F, Feng L, Zhang L, Zhang X, Zhang N. Synthesis, characterization and antitumor evaluation of CMCS-DTX conjugates as novel delivery platform for docetaxel. *Int J Pharm* July 15, 2013; 451(1–2):41–9.
- [23] Zhang W, Shi Y, Chen Y, Hao J, Sha X, Fang X. The potential of pluronic polymeric micelles encapsulated with paclitaxel for the treatment of melanoma using subcutaneous and pulmonary metastatic mice models. *Biomaterials* September 2011;32(25):5934–44.
- [24] Zheng L, Gou M, Zhou S, Yi T, Zhong Q, Li Z, et al. Antitumor activity of monomethoxy poly(ethylene glycol)-poly (epsilon-caprolactone) micelle-encapsulated doxorubicin against mouse melanoma. *Oncology Reports* June 2011;25(6):1557–64.
- [25] Huang FY, Mei WL, Li YN, Tan GH, Dai HF, Guo JL, et al. The antitumor activities induced by pegylated liposomal cytochalasin D in murine models. *Eur J Cancer* September 2012;48(14):2260–9.
- [26] Yang Y, Liu X, Zhang D, Yu W, Lv G, Xie H, et al. Chitosan/VEGF-siRNA nanoparticle for gene silencing. *J Control Release* November 30, 2011;152(Suppl. 1):e160–1.
- [27] Bae YH, Park K. Targeted drug delivery to tumors: myths, reality and possibility. *J Control Release* August 10, 2011;153(3):198–205.
- [28] Hrkach J, Von Hoff D, Mukkaram Ali M, Andrianova E, Auer J, Campbell T, et al. Preclinical development and clinical translation of a PSMA-targeted docetaxel nanoparticle with a differentiated pharmacological profile. *Sci Transl Med* April 4, 2012;4(128): 128–39.
- [29] Davis ME, Zuckerman JE, Choi CH, Seligson D, Tolcher A, Alabi CA, et al. Evidence of RNAi in humans from systemically administered siRNA via targeted nanoparticles. *Nature* April 15, 2010;464(7291):1067–70.
- [30] Lemarie F, Croft DR, Tate RJ, Ryan KM, Dufes C. Tumor regression following intravenous administration of a tumor-targeted p73 gene delivery system. *Biomaterials* March 2012;33(9):2701–9.
- [31] Yao H, Ng SS, Huo LF, Chow BK, Shen Z, Yang M, et al. Effective melanoma immunotherapy with interleukin-2 delivered by a novel polymeric nanoparticle. *Mol Cancer Ther* June 2011;10(6): 1082–92.
- [32] Cai L, Wang X, Wang W, Qiu N, Wen J, Duan X, et al. Peptide ligand and PEG-mediated long-circulating liposome targeted to FGFR overexpressing tumor in vivo. *Int J Nanomedicine* 2012;7: 4499–510.
- [33] Chen X, Wang X, Wang Y, Yang L, Hu J, Xiao W, et al. Improved tumor-targeting drug delivery and therapeutic efficacy by cationic liposome modified with truncated bFGF peptide. *J Control Release* July 1, 2010;145(1):17–25.
- [34] Sun M, Wang Y, Shen J, Xiao Y, Su Z, Ping Q. Octreotide-modification enhances the delivery and targeting of doxorubicin-loaded liposomes to somatostatin receptors expressing tumor in vitro and in vivo. *Nanotechnology* November 26, 2010;21(47):475101.
- [35] Dubey PK, Singodia D, Vyas SP. Polymeric nanospheres modified with YIGSR peptide for tumor targeting. *Drug Deliv* 2010 September–October;17(7):541–51.
- [36] Ukawala M, Chaudhari K, Rajyaguru T, Manjappa AS, Murthy RS, Gude R. Laminin receptor-targeted etoposide loaded polymeric micelles: a novel approach for the effective treatment of tumor metastasis. *J Drug Target* January 2012;20(1):55–66.
- [37] Chen Y, Bathula SR, Yang Q, Huang L. Targeted nanoparticles deliver siRNA to melanoma. *J Invest Dermatol* December 2010; 130(12):2790–8.
- [38] Yang Y, Li J, Liu F, Huang L. Systemic delivery of siRNA via LCP nanoparticle efficiently inhibits lung metastasis. *Mol Ther* March 2012;20(3):609–15.
- [39] Durymanov MO, Beletkaia EA, Ulasov AV, Khramtsov YV, Trusov GA, Rodichenko NS, et al. Subcellular trafficking and transfection efficacy of polyethylenimine-polyethylene glycol polyplex nanoparticles with a ligand to melanocortin receptor-1. *J Control Release* October 28, 2012;163(2):211–9.
- [40] Kuphal S, Bauer R, Bosserhoff AK. Integrin signaling in malignant melanoma. *Cancer Metastasis Rev* June 2005;24(2):195–222.
- [41] Wang Y, Yang T, Wang X, Dai W, Wang J, Zhang X, et al. Materializing sequential killing of tumor vasculature and tumor cells via targeted polymeric micelle system. *J Control Release* February 10, 2011;149(3):299–306.
- [42] Wang Z, Chui WK, Ho PC. Nanoparticulate delivery system targeted to tumor neovasculature for combined anti-cancer and antiangiogenesis therapy. *Pharm Res* March 2011; 28(3):585–96.
- [43] Dai W, Yang T, Wang Y, Wang X, Wang J, Zhang X, et al. Peptide PHSCNK as an integrin alpha5beta1 antagonist targets stealth liposomes to integrin-overexpressing melanoma. *Nanomed* October 2012;8(7):1152–61.
- [44] Hamano N, Negishi Y, Fujisawa A, Manandhar M, Sato H, Katagiri F, et al. Modification of the C16Y peptide on nanoparticles is an effective approach to target endothelial and cancer cells via the integrin receptor. *Int J Pharm* May 30, 2012; 428(1–2):114–7.
- [45] Unger WW, van Beelen AJ, Bruijns SC, Joshi M, Fehres CM, van Bloois L, et al. Glycan-modified liposomes boost CD4+ and CD8+ T-cell responses by targeting DC-SIGN on dendritic cells. *J Control Release* May 30, 2012;160(1):88–95.
- [46] van Broekhoven CL, Parish CR, Demangel C, Britton WJ, Altin JG. Targeting dendritic cells with antigen-containing liposomes: a highly effective procedure for induction of antitumor immunity and for tumor immunotherapy. *Cancer Res* June 15, 2004;64(12): 4357–65.
- [47] Perche F, Benvegna T, Berchel M, Lebegue L, Pichon C, Jaffres PA, et al. Enhancement of dendritic cells transfection in vivo and of vaccination against B16F10 melanoma with mannoseylated histidylated lipopolyplexes loaded with tumor antigen messenger RNA. *Nanomed* August 2011;7(4):445–53.
- [48] Jeanbart L, Ballester M, de Titta A, Corthesy P, Romero P, Hubbell JA, et al. Enhancing efficacy of anticancer vaccines by targeted delivery to tumor-draining lymph nodes. *Cancer Immunol Res* May 2014;2(5):436–47.
- [49] Liu H, Moynihan KD, Zheng Y, Szeto GL, Li AV, Huang B, et al. Structure-based programming of lymph-node targeting in molecular vaccines. *Nature* March 27, 2014;507(7493):519–22.
- [50] Thomas SN, Vokali E, Lund AW, Hubbell JA, Swartz MA. Targeting the tumor-draining lymph node with adjuvanted nanoparticles reshapes the antitumor immune response. *Biomaterials* January 2014;35(2):814–24.
- [51] Zhu S, Lansakara PD, Li X, Cui Z. Lysosomal delivery of a lipophilic gemcitabine prodrug using novel acid-sensitive micelles improved its antitumor activity. *Bioconjug Chem* May 16, 2012; 23(5):966–80.
- [52] Talelli M, Iman M, Varkouhi AK, Rijcken CJ, Schiffrers RM, Etrych T, et al. Core-crosslinked polymeric micelles with controlled release of covalently entrapped doxorubicin. *Biomaterials* October 2010;31(30):7797–804.
- [53] Gu J, Wang X, Jiang X, Chen Y, Chen L, Fang X, et al. Self-assembled carboxymethyl poly (L-histidine) coated poly (beta-amino ester)/DNA complexes for gene transfection. *Biomaterials* January 2012;33(2):644–58.
- [54] Ito A, Saito H, Mitobe K, Minamiya Y, Takahashi N, Maruyama K, et al. Inhibition of heat shock protein 90 sensitizes melanoma cells to thermosensitive ferromagnetic particle-mediated hyperthermia with low Curie temperature. *Cancer Sci* March 2009;100(3): 558–64.

- [55] Lu W, Xiong C, Zhang G, Huang Q, Zhang R, Zhang JZ, et al. Targeted photothermal ablation of murine melanomas with melanocyte-stimulating hormone analog-conjugated hollow gold nanospheres. *Clin Cancer Res* February 1, 2009;15(3):876–86.
- [56] Ferreira DM, Saga YY, Aluicio-Sarduy E, Tedesco AC. Chitosan nanoparticles for melanoma cancer treatment by photodynamic therapy and electrochemotherapy using aminolevulinic acid derivatives. *Curr Med Chem* 2013;20(14):1904–11.
- [57] Idris NM, Gnanasammandhan MK, Zhang J, Ho PC, Mahendran R, Zhang Y. In vivo photodynamic therapy using upconversion nanoparticles as remote-controlled nanotransducers. *Nat Med* October 2012;18(10):1580–5.
- [58] Oda Y, Suzuki R, Otake S, Nishiie N, Hirata K, Koshima R, et al. Prophylactic immunization with bubble liposomes and ultrasound-treated dendritic cells provided a four-fold decrease in the frequency of melanoma lung metastasis. *J Control Release* June 10, 2012;160(2):362–6.
- [59] Un K, Kawakami S, Suzuki R, Maruyama K, Yamashita F, Hashida M. Suppression of melanoma growth and metastasis by DNA vaccination using an ultrasound-responsive and mannose-modified gene carrier. *Mol Pharm* April 4, 2011;8(2):543–54.
- [60] Sumer B, Gao J. Theranostic nanomedicine for cancer. *Nanomedicine (Lond)* April 2008;3(2):137–40.
- [61] Wang J, Liang R, Jiang H, Zhu J, Tu Y, Tao J. A simple route to prepare multifunctional PLA nanoparticles against melanoma. *J Control Release* November 28, 2013;172(1):E43–.
- [62] Wadajkar AS, Bhavsar Z, Ko CY, Koppolu B, Cui W, Tang L, et al. Multifunctional particles for melanoma-targeted drug delivery. *Acta Biomater* August 2012;8(8):2996–3004.
- [63] Zhang L, Wen C, Al-Suwayeh SA, Yen T, Fang J. Cisplatin and quantum dots encapsulated in liposomes as multifunctional nanocarriers for theranostic use in brain and skin. *J Nanoparticle Res* July 2012;14(7).
- [64] Fraix A, Kandoth N, Manet I, Cardile V, Graziano AC, Gref R, et al. An engineered nanoplatform for bimodal anticancer phototherapy with dual-color fluorescence detection of sensitizers. *Chem Commun (Camb)* May 18, 2013;49(40):4459–61.
- [65] Fan Y, Du W, He B, Fu F, Yuan L, Wu H, et al. The reduction of tumor interstitial fluid pressure by liposomal imatinib and its effect on combination therapy with liposomal doxorubicin. *Biomaterials* March 2013;34(9):2277–88.
- [66] Roy A, Chandra S, Mamilapally S, Upadhyay P, Bhaskar S. Anticancer and immunostimulatory activity by conjugate of paclitaxel and nontoxic derivative of LPS for combined chem-immunotherapy. *Pharm Res* August 2012;29(8):2294–309.
- [67] Cao L, Zeng Q, Xu C, Shi S, Zhang Z, Sun X. Enhanced antitumor response mediated by the codelivery of paclitaxel and adenoviral vector expressing IL-12. *Mol Pharm* May 6, 2013;10(5):1804–14.
- [68] Hersh EM, O'Day SJ, Ribas A, Samlowski WE, Gordon MS, Shechter DE, et al. A phase 2 clinical trial of nab-paclitaxel in previously treated and chemotherapy-naïve patients with metastatic melanoma. *Cancer* January 1, 2010;116(1):155–63.
- [69] Kottschade LA, Suman VJ, Amatruda 3rd T, McWilliams RR, Mattar BI, Nikcevich DA, et al. A phase II trial of nab-paclitaxel (ABI-007) and carboplatin in patients with unresectable stage IV melanoma: a North Central Cancer Treatment Group Study, N057E(1). *Cancer* April 15, 2011;117(8):1704–10.
- [70] Spitler LE, Boasberg P, O'Day S, Hamid O, Cruickshank S, Mesko S, et al. Phase II study of nab-paclitaxel and bevacizumab as first-line therapy for patients with unresectable stage III and IV melanoma. *Am J Clin Oncol* February 2015;38(1):61–7.
- [71] <https://clinicaltrials.gov/ct2/show/NCT00864253?term=NCT00864253&rank=1>.
- [72] Fink W, Zimpfer-Rechner C, Thoenke A, Figl R, Kaatz M, Ugurel S, et al. Clinical phase II study of pegylated liposomal doxorubicin as second-line treatment in disseminated melanoma. *Onkologie* December 2004;27(6):540–4.
- [73] Smylie MG, Wong R, Mihalicioiu C, Lee C, Pouliot JF. A phase II, open label, monotherapy study of liposomal doxorubicin in patients with metastatic malignant melanoma. *Invest New Drugs* April 2007;25(2):155–9.
- [74] Bedikian AY, Richards J, Kharkevitch D, Atkins MB, Whitman E, Gonzalez R. A phase 2 study of high-dose Allovectin-7 in patients with advanced metastatic melanoma. *Melanoma Res* June 2010;20(3):218–26.
- [75] Agarwala SS. Intralesional therapy for advanced melanoma: promise and limitation. *Curr Opin Oncol* March 2015;27(2):151–6.
- [76] Nakamura H, Jun F, Maeda H. Development of next-generation macromolecular drugs based on the EPR effect: challenges and pitfalls. *Expert Opin Drug Deliv* January 2015;12(1):53–64.

The Potential for Metal Nanoparticle-Enhanced Radiotherapy in Dermatology

V.L.T. Hoang¹, M.C. Foote², T.W. Prow¹

¹The University of Queensland, Brisbane, QLD, Australia; ²Princess Alexandra Hospital, Brisbane, QLD, Australia

OUTLINE

Introduction	217	Application of Metal Nanoparticles in Brachyradiation for Nonmelanoma Skin Cancers	223
Enhanced Radiosensitization With Metal Nanoparticles	218	Conclusion and Perspectives	225
<i>Gold Nanoparticle Production and Physicochemical Properties</i>	218	List of Acronyms and Abbreviations	225
<i>Mechanism of Metal Radiosensitization</i>	219	References	226
<i>In Vivo Studies</i>	219		
<i>Other Metal-Based Radiosensitizers</i>	220		
Targeted Delivery of Metal Nanoparticles to Tumor Tissues	221		

INTRODUCTION

The most significant impact of nanotechnology in dermatology has been in the area of ultraviolet (UV) protection, but to date nanotechnology has not had a dramatic impact on therapy. Nanoparticle-based sunscreens have been used globally to prevent skin cancer since the 1990s [1]. Skin cancer incidence is higher than all other cancers, and the rate of skin cancer is increasing worldwide despite the use of sunscreens. Nonmelanoma skin cancers, predominately squamous cell carcinoma and basal cell carcinoma, are extremely common [2]. Despite significant efforts to decrease the incidence of skin cancer through preventative strategies, the overall incidence is still expected to rise. Early diagnosis of skin cancer is important to provide effective local treatment, potentially avoiding disfiguring surgery, and in some cases improving survival. Although the majority of skin cancers are removed surgically, local treatment options include a variety of

physical (cryotherapy/curettage), chemical (topical 5-fluorouracil), and radiation therapy options. Current topical treatment methods are essentially agents that induce necrosis in the tumor; these have poor compliance, are painful, and have high recurrence rates because they do not target the core pathogenic mechanisms.

Radiation therapy in the treatment of cancer utilizes ionizing radiation with the goal of destroying all the diseased cells while sparing normal tissue. Two main radiation therapy modalities have emerged. External radiation therapy is where the radiation comes from a source outside the body (such as a beam of X-rays), and internal radiation therapy (also known as brachytherapy), where the radiation comes from implants or liquids placed inside the body or on the body surface. Irrespective of the modality, the common mechanism of action is to damage the DNA of the cancer cells either directly, or by creating charged particles (free radicals) within the cells that can in turn damage DNA. The ultimate goal of

radiation therapy is to destroy the cancer cells with minimal damage to the normal cells, thus improving the therapeutic ratio.

Radiation therapy has a long history in the local management of nonmelanoma skin cancers. This approach has often been preferred in the definitive (up front, curative) setting where the cosmetic and functional outcome is better compared to surgery, or if the extent of the disease is such that surgery is not feasible. This may be the case in some regions of the face, for example, on the nose, lip, or ear, or in patients with widespread lesions on most parts of the body. Radiation therapy is also an option in elderly patients with advanced lesions whereby complex surgery under general anesthesia is high risk [3].

Local control rates after radiation therapy for basal cell carcinoma are 90–95% [4,5]. The local control rate for an equivalent size squamous cell carcinoma is lowered by approximately 10% [4] and the control rate for both squamous cell carcinoma and basal cell carcinoma that have recurred after previous surgery is approximately 80% [4]. A range of radiation therapy dose schedules have been used that are more commonly based on institutional preference rather than best evidence and research, but taking into consideration a number of factors that are patient-specific (age, performance status, preference) and tumor-specific (site, depth, and histology). Despite this there is significant scope to investigate means to improve the therapeutic ratio in the treatment of nonmelanoma skin cancers treated with radiation therapy. Radiation therapy has its disadvantages including the possibility of radiation injury to the surrounding normal tissue. Moreover, the tumor cells can develop resistance to the radiation. Many efforts have been developed to enhance the susceptibility of tumor tissues to injury by exposure to radiation, in other words, to produce radiation sensitizers.

Nanoparticles have a number of characteristics that are ideally suited to oncological applications, and there has been significant interest in nanoparticle-enhanced radiation therapy [6]. Sensitizing cancer cells to the effects of radiation therapy (radiosensitization) is one way to improve the therapeutic ratio. The concept of high-Z radiation dose enhancement began in the 1980s with the ultimate aim of effecting lethal damage to the tumor target with sparing of adjacent normal tissue [7]. A range of high-Z inorganic nanoparticles have been used *in vitro* and *in vivo*; however, to this date, none are being used clinically [6]. Gold, for example, is a high-Z material ($Z = 79$) and an excellent absorber of X-rays with a well-known safety profile because it is inert (elemental gold). The low toxicity of gold and the correspondingly low radiation dose needed to examine enhancement lend itself to clinical investigation in nanoparticle-enhanced radiation therapy.

One of the major barriers for high-Z inorganic nanoparticles is the lack of clearance pathways which makes intravenous administration for radiosensitization impractical. Intratumoral injection has been investigated and suggested as the main route of administration; however, it presently has limited utility in clinical radiation oncology to date [6]. Cutaneous nanoparticle administration overcomes these barriers and nanoparticle-enhanced radiation therapy in the management of nonmelanoma skin cancers has potential to cross the regulatory hurdle into clinical use as an effective therapeutic option.

ENHANCED RADIOSENSITIZATION WITH METAL NANOPARTICLES

Gold Nanoparticle Production and Physicochemical Properties

The concept of using high-Z materials for dose enhancement in cancer radiotherapy was introduced over 20 years ago by Matsudaira et al. [8], who measured the radio-enhancing effect of iodine in cultured cells. Gold nanoparticles (GNPs) have emerged as promising agents for cancer therapy, and are being investigated as photothermal agents and radiosensitizers because of their good biocompatibility, easy chemical modification, and high X-ray absorption coefficients [7–9]. GNPs can be easily produced in uniform sizes and shapes, including nanospheres, nanorods, shells, and cages [10]. A variety of methods to prepare GNPs have been introduced including microemulsion, reverse micelles, seeding growth, sonochemistry, photochemistry, and radiolysis [11]. The Turkevich method is the most commonly used preparation for GNPs via the aqueous reduction of gold salt by sodium citrate at reflux temperatures [12]. The colloidal gold will form because the citrate ions act as both a reducing agent and a capping agent. Generally, particles synthesized by citrate reduction are modestly monodisperse spherical GNPs around 10–20 nm in diameter. They have a negative surface charge as a consequence of a weakly bound citrate coating. The Brust–Schiffrin method, or called two-phase synthesis method, uses NaBH_4 as a reducing agent and a mercapto-containing binding agent [13]. It involves the reaction of a chlorauric acid solution with tetraoctylammonium bromide solution in toluene and sodium borohydride as an anticoagulant and a reducing agent, respectively. In both methods, the particle size can be controlled by the initial reagent concentrations [12]. The size and shape of the nanocore can be measured by several techniques such as atomic force microscopy, transmission electron microscopy, small-angle X-ray scattering, and X-ray diffraction [14].

Mechanism of Metal Radiosensitization

Ionizing radiation generates reactive oxygen species (ROS), such as HO^\bullet , $\text{O}_2^{\bullet-}$, and H_2O_2 , through the radiolysis of H_2O molecules. These radiation-induced ROS have a strong destructive effect on the DNA because of their unpaired electron [15]. Electron beam radiation is often used to treat skin cancers because it only penetrates as far as the skin, and spares deeper organs and body tissues. This therapy is used as the main treatment in cases where a tumor is very large, is on an area of the skin that makes surgery difficult like the face, or in patients with poor general health. It damages the basal cell layer of the skin and layers above. The basal cells lose their integrity once the radiation dose reached 20–25 Gy, and the maximum depletion of basal cells occurred when the patient had received a dose of 50 Gy [16]. People react differently to radiotherapy depending on their general skin condition, general health, nutritional status, age, and comorbid diseases [17,18]. A number of outside factors appear to influence the success of radiation therapy including dose, energy, and fractionation regime. The increasing dose of radiotherapy, however, affects the severity of skin reactions experienced. Radiotherapy can significantly damage the surrounding healthy tissue if the energy waves are not properly directed to the targeted tissue. 85–87% of patients receiving this treatment can suffer from acute skin side reactions which can range from mild erythema to confluent moist desquamation and occasionally, ulceration [19].

Metal particles can scatter and/or absorb the high-energy gamma/X-ray radiation, which leads to more localized and consolidated damage to target cells. They provide new opportunities for developing targeted radiation therapy modalities to further increase radiation therapeutic efficacy. This new brachytherapy involves first targeting the tumor cells with GNPs and then irradiating the GNPs using low-energy γ -/X-ray sources to boost radiation therapeutic efficacy. Geng et al. [20] reported that GNPs enhanced the production of intracellular ROS when irradiated with 90 kVp or 6 MV X-rays in SKOV-3 human ovarian cancer cells. In addition, there are several reports showing that GNPs can induce cell apoptosis and regulate cell cycle in combination with radiation. Irradiation combined with GNPs in DU-145 prostate cancer cells accelerated the G1/S phase of the cell cycle and arrested cells in the G2/M phase [21]. These changes were accompanied by the downregulation of p53 and cyclinA expression, and the upregulation of cyclinB1 and cyclinE [21]. Similar result observed in A375 melanoma cells [22]. The efficacy of the radiation therapy can be increased and its adverse effects decreased if somehow the surrounding

healthy tissue can either be protected from this damage or made less radiation sensitive.

In Vivo Studies

The idea of using GNPs for treating skin diseases has been further supported by numerous in vivo studies which showed that GNPs delivered to tumor tissue can selectively enhance radiation therapy efficacy leading to differentially increased tumor cell killing. Herold et al. [23] injected 1.5–3.0 μm diameter GNPs directly into a mouse tumor model followed by irradiation carried out in a chamber with 8 Gy of 200 kVp X-rays. The average dose increased using the microparticles by 42–43%, which suggested that smaller GNPs could provide better targeting of tumors, while also enhancing radiotherapy. In another pioneering study, Hainfeld et al. [24] performed an in vivo experiment using GNPs on a mouse mammary carcinoma model, in which the tumor-bearing mice received a single injection of small (1.9 nm) GNPs in combination with 26 or 30 Gy using 250 kVp X-rays. Mice received 1.35–2.7 g GNPs per kilogram body weight injected via the tail vein. Both tumor volume and survival were monitored, with 100% survival time exceeding 1 year compared with only 20% survival for X-rays alone (Fig. 17.1). They also found that GNPs still had a significant radiosensitization effect on resistant tumor cells in their second study [25]. In these studies, the mass of gold in various tissues, including the tumor, was quantified by atomic absorption spectrometry. With this approach, the amount of particles measured at the tumor 5 minutes after injection was $4.9 \pm 0.6\%$ whereas the majority of the dose was in the kidney. The optimal ratio tumor-to-tissue ratio was 3.5 while this ratio was only $1.4 \pm 0.1\%$ for tumor-to-muscle.

In 2005, Cho et al. [26] reported a phantom-based estimation of the dose enhancement due to the use of GNPs. They evaluated the dose enhancement effect of GNPs with radiation from 140 kV X-rays, 4 and 6 MV photon beams, or ^{192}Ir γ rays. The most effective result that achieved a dose enhancement factor of 5.6 was the 140 kVp X-rays on a superficial target loaded with 30 mg GNPs per gram tumor, while the photon beam approach did not result in any appreciable improvements in dose enhancement (approximately 1–7%). For the ^{192}Ir γ rays, the dose enhancement ratio was 5–31% depending on the radial distance and the GNP concentration. The study showed that the dose enhancement was reasonably well correlated to the amount of gold present. Although this level of gold loading may not be within realistic ranges, it does illustrate that enhancement gains are possible. Results suggested a clinically relevant dose enhancement with ^{192}Ir rays

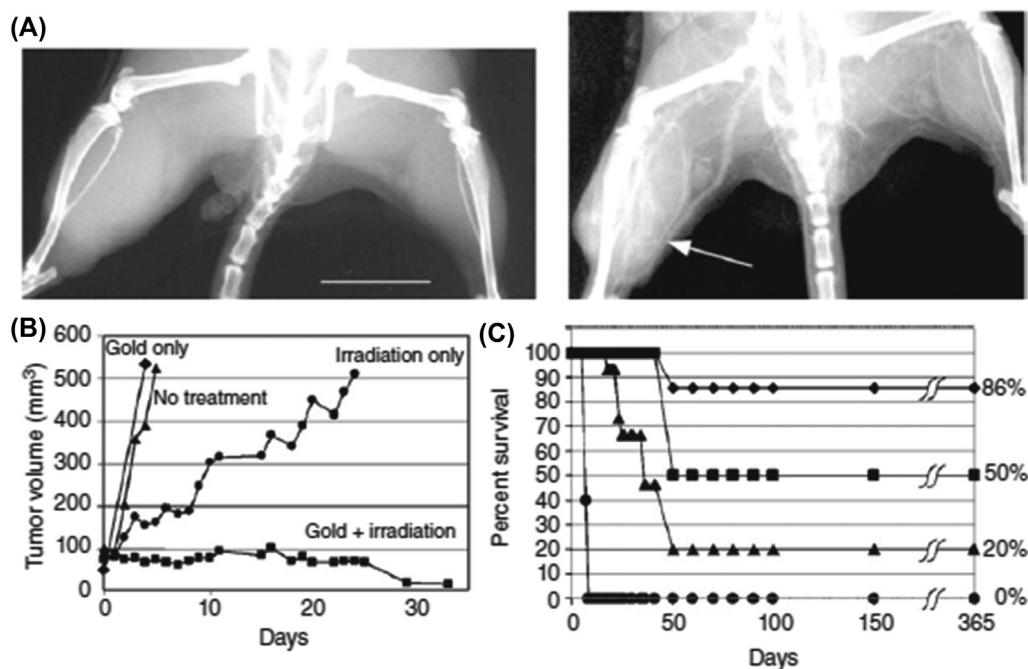


FIGURE 17.1 Gold nanoparticle (GNP) enhanced radiotherapy in a mouse model. There was a clear difference in X-ray imaging of the animals before (left panel) and 2 min after (right panel) injecting GNPs (Panel A). After irradiation, the tumor volume shrank dramatically in the GNP and radiotherapy group compared with the other controls (Panel B). This was also the case with percent survival shown in Panel (C).

was found with 30 mg gold per gram of tumor. However, the gold loading that gave a clinically relevant dose enhancement for X-rays and γ rays varied depending on the energy of the photon.

In another study by Cho et al. [27], the potential for enhanced radiotherapy with much lower doses of radiation was investigated through Monte Carlo–based calculations. Monte Carlo (MC) calculations facilitate the accurate estimation of the dose enhancement effect caused by GNPs, which takes into account the detailed energy deposition at the nanoscale [28]. Brachytherapy sources of ^{125}I , ^{169}Yb , or 50 kVp X-rays were used to calculate the macroscopic dose enhancement factor, which is a ratio of the average dose in the tumor region, with and without the presence of GNPs during tumor irradiation. Results showed respective MDEFs of 116%, 92%, and 108% for ^{125}I , 50 kVp, and ^{169}Yb , respectively, when a tumor was loaded with 18 mg Au/g. The corresponding macroscopic dose enhancement factor decreased to 68%, 57%, and 44% at 7 mg Au/g. These data suggest the favorable dose enhancement ratios were between 7 and 18 mg GNPs per gram tumor. The study also revealed that even at low-energy radiation brachytherapy, GNPs could also serve as radiation sensitizers. These are the first studies of using GNPs in the context of radiotherapy enhancement and proposing possible dose goals and sources for the elusive “clinically relevant dose.”

Other Metal-Based Radiosensitizers

Besides gold, other high-Z materials such as the metals silver and platinum have also received great interest in the potential to enhance radiotherapy. Silver nanoparticles are widely used in topical products such as wound dressings due to their antimicrobial activity [29]. A study by Larese et al. [30] showed that silver nanoparticles coated with polyvinylpyrrolidone were able to permeate into the stratum corneum (SC), and into the outermost surface of the *epidermis* of both intact and damaged skin in the Franz diffusion system. Several in vitro studies proved that 20 nm silver nanoparticles significantly enhanced radiation sensitivity of human U251 and SHG-44 glioma cells [31], MGC803 gastric cells [32], U231 breast cancer cells [33], and A549 lung cancer cells [34]. In an in vivo study by Liu et al. [35], C6 glioma-bearing rats were treated with a single dose of 10 Gy using 6 MV X-rays radiation alone or in combination with intratumoral administration of silver nanoparticles. The silver nanoparticles and radiation combination significantly increased the mean survival times to 100.5 days compared to 24.5 days with irradiated controls and 16.4 days with untreated controls. Several studies have reported biological effects of silver nanoparticles which have been attributed to causing oxidative stress, and influencing membrane fluidity [36,37]. These factors need to be taken into account to

address the mechanisms of silver nanoparticles radiosensitization.

There are few studies regarding *in vivo* skin absorption of platinum. Recently, Mauro et al. [38] demonstrated that platinum nanoparticles can permeate the skin in an *in vivo* system. The results showed significantly higher concentrations of platinum in damaged skin compared to intact skin, which is consistent with other damaged skin permeation studies [30,39]. Platinum has a similar atomic number to gold, therefore it has also been employed in radiotherapy. The combination of platinum nanoparticles with irradiation by fast ions (effectively used in hadron therapy) strongly enhanced lethal damage in DNA, with an efficiency factor close to two for double strand breaks [40]. The enhancing effect was due to auto-amplified electronic cascades inside the nanoparticles, which reinforced the energy deposition in the close vicinity of the metal. Gadolinium (Gd), a naturally occurring metalloid with semiconductor properties was suggested as another radiation sensitizer. Gd(III) texaphyrin was found to be an efficient radiation sensitizer *in vitro* in HT-29 cells [41] and also in a murine mammary carcinoma model. A new therapeutic strategy called gadolinium neutron capture therapy utilizes the “Gadolinium neutron capture reaction” to produce long-range gamma rays, internal conversion electrons, X-rays, and Auger electrons with a large total kinetic energy. Tokimitsu et al. [42] evaluated the effectiveness of this therapy in *in vivo* using chitosan nanoparticles as a novel gadolinium delivery vehicle. Mice with subcutaneous B16F10 melanoma were injected twice with this formulation intratumorally and then irradiated 8 h after the second administration. Mice treated with the Gd-nanoparticles showed much better therapeutic response as compared to those that were dosed with just the gadolinium solution despite the radioresistance of melanoma. Recently, bismuth nanoparticles have drawn great attention for application in radiosensitizing. At 350 mg/g, bismuth nanoparticles showed 1.25 and 1.29 times higher dose enhancements than gold and platinum nanoparticles for a given nanoparticle size [43].

TARGETED DELIVERY OF METAL NANOPARTICLES TO TUMOR TISSUES

The potential use of metal nanoparticles in the context of radiotherapy enhancement has been supported by many publications mentioned earlier in this chapter. Another focus in this field is on targeting the nanoparticles to the tumor to elevate the tumor nanoparticle dose. Metal nanoparticles can be delivered to tumor

tissue in a variety of ways. Direct routes of intratumoral injection and intraperitoneal administration have been mostly used [23,25]. Nanoparticles passively accumulate at tumor sites even in the absence of functionalization. Circulating nanoparticles preferentially accumulate at tumor sites due to the characteristically defective architecture of the vessels that supply oxygen and nutrients to these tissues [44]. This is known as the enhanced permeability and retention effect [45]. However, this delivery method is limited due to the heterogeneity of tumor vasculature, especially at the center of poorly vascularized areas of tumor. Moreover, delivery of an adequate nanoparticle concentration to the target site is hindered by rapid renal clearance and nonspecific phagocytosis of nanoparticles by the reticuloendothelial system [46].

Nanoparticle delivery to the skin is being increasingly used to facilitate local therapies. Skin disease usually affects relatively large areas of tissue, and in some cases such as psoriasis and skin cancer, the skin barrier thickens as a result of hyperkeratinization [52]. The main barrier of skin is the SC, which can be considered to be a lipid-rich compartment whereas the underlying tissue is a more aqueous environment [47]. Generally, nanoparticles need to pass through the SC and then need to gain access to the intercellular space to move through the various layers of the skin.

Nanoparticles can also penetrate into deeper skin layers via the appendageal route such as via hair follicles and sweat glands (Fig. 17.2). There is a rich capillary blood supply available in the subcutaneous layer to transport the solutes out of hair follicles [48]. It is important to note, however, hair follicles only occupy 0.1% of the skin surface, and moreover this route can be blocked by sebum “plugs” [49]. The capacity of nanoparticles to overcome the SC and reach the viable skin is dependent on the skin model studied, barrier integrity, nanoparticle (size, shape, surface properties, and charge), and nanoparticle degradation kinetics [50]. The uptake of GNPs across the skin barrier has attracted appreciable interest to exploit the potential benefits in skin cancer treatment.

The absorption and penetration of GNPs into the skin is dependent upon their size, shape and surface chemistry [51–53]. An *in vitro* study by Sonavane et al. [51] showed a size dependent permeation through rat skin. The permeation of GNPs through the skin was highest for 15 nm compared to 102 and 198 nm nanoparticles. They also found that GNPs with a small size could penetrate to deeper areas of the skin compared to larger-sized GNPs which were mostly located in the epidermal region. Another study by Huang et al. [52] reported that 5 nm GNPs could permeate rapidly through the *epidermis* in mouse skin. There is evidence of some

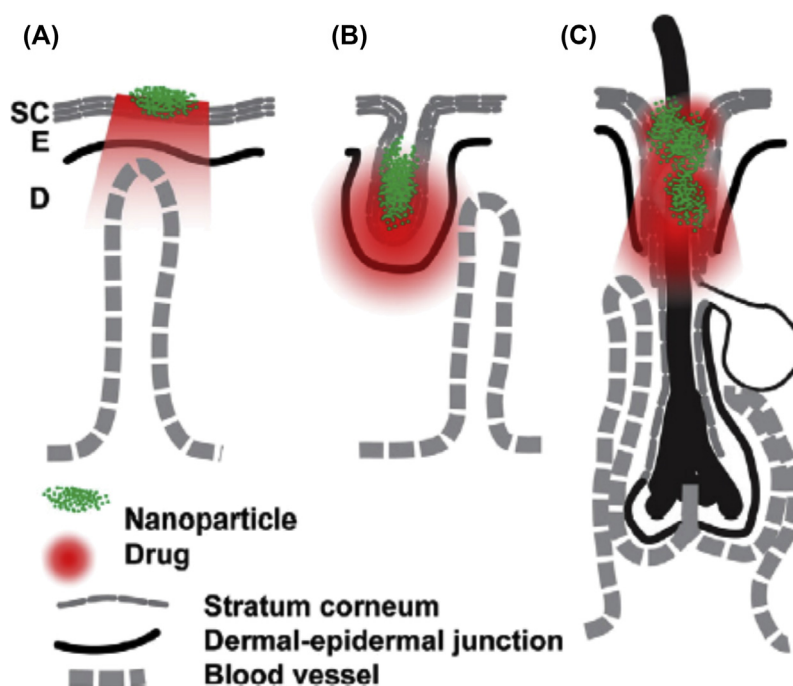


FIGURE 17.2 Sites in skin for nanoparticle delivery. Topical nanoparticle drug delivery takes place in three major sites: stratum corneum (SC) surface (panel A), furrows (dermatoglyphs; panel B), and openings of hair follicles (infundibulum; panel C). The nanoparticles are shown in green and the drug in red. Other sites for delivery are the viable *epidermis* (E) and dermis (D).

nanoparticle penetration into the SC of human skin, but not into the viable *epidermis* for very small particles up to 20 nm composed of gold, silver, and quantum dots [54]. There is one study based on Franz diffusion cells to evaluate permeation of GNPs (15, 102, and 198 nm) through rat skin [51]. The GNP suspension was placed on the donor side and collected at different time points for 24 h. The smallest particles were found to aggregate in deeper skin layers whereas the two larger types of particles only reached the viable *epidermis* and dermis. Generally, the potential of using GNPs delivery into the *epidermis* and dermis without barrier modification has met with little success. It is well known that compounds with a molecular mass > 500 Da cannot cross the skin barrier. Either mechanical or chemical stimuli should be considered to improve the penetration of nanoparticles through the skin barrier by for successful therapeutic applications.

Surface coating using polymeric materials has led to better regulation of the pharmacokinetic and targeting properties of GNPs, allowing greater accumulation in tumor tissue [55]. Labouta et al. [56] coated 6 nm gold nanoparticles with thiol compounds and investigated its *in vivo* skin penetration using multiphoton imaging-pixel analysis. Result showed that thiol-coated GNPs penetrated into the SC and later migrated to deeper layers of the skin. In another study later, Labouta et al. [53] investigated the penetration of GNPs at different surface modifications, sizes, vehicles, and

concentrations through the human skin. Nonpolar (dodecanethiol-coated gold of size 6 nm; cetrimide-coated gold of size 15 nm) and negatively charged (lecithin-coated gold of size 6 nm; citrate-coated gold of size 15 nm) GNPs were used for skin penetration. All types of gold could be detected at the SC except citrate-coated GNPs. The 15-nm cetrimide-coated GNPs could penetrate to deeper skin layers, which was probably due to their hydrophobic properties. Results also suggested the importance of the dispersion solvent and charge of GNPs in skin penetration of GNPs (Fig. 17.3).

Hainfeld et al. [57] suggested more specific tumor targeting by surface conjugation of antibodies that recognized markers overexpressed in tumors to improve cellular uptake of bare GNPs. For example, GNPs were coated with polyethylene glycol and covalently coupled to anti-Her2 antibodies [58], or with a plasma-polymerized allylamine to allow bioconjugation of tumor-targeting anti-EGFR monoclonal antibodies [59]. Both studies showed a preferential uptake in cognate tumors of the antibody-tagged GNPs. However, there are no associated irradiation studies with this method.

Other approaches such as sonophoresis [60], magnetophoresis [61], and microneedles [39] have also been used to enhance the efficacy of transdermal nanoparticle delivery. Etame et al. [62] used magnetic resonance image-guided focused ultrasound (MRI-GFU) to improve monitoring and delivery of 50 nm GNPs

Overlaid Multiphoton/Transmission

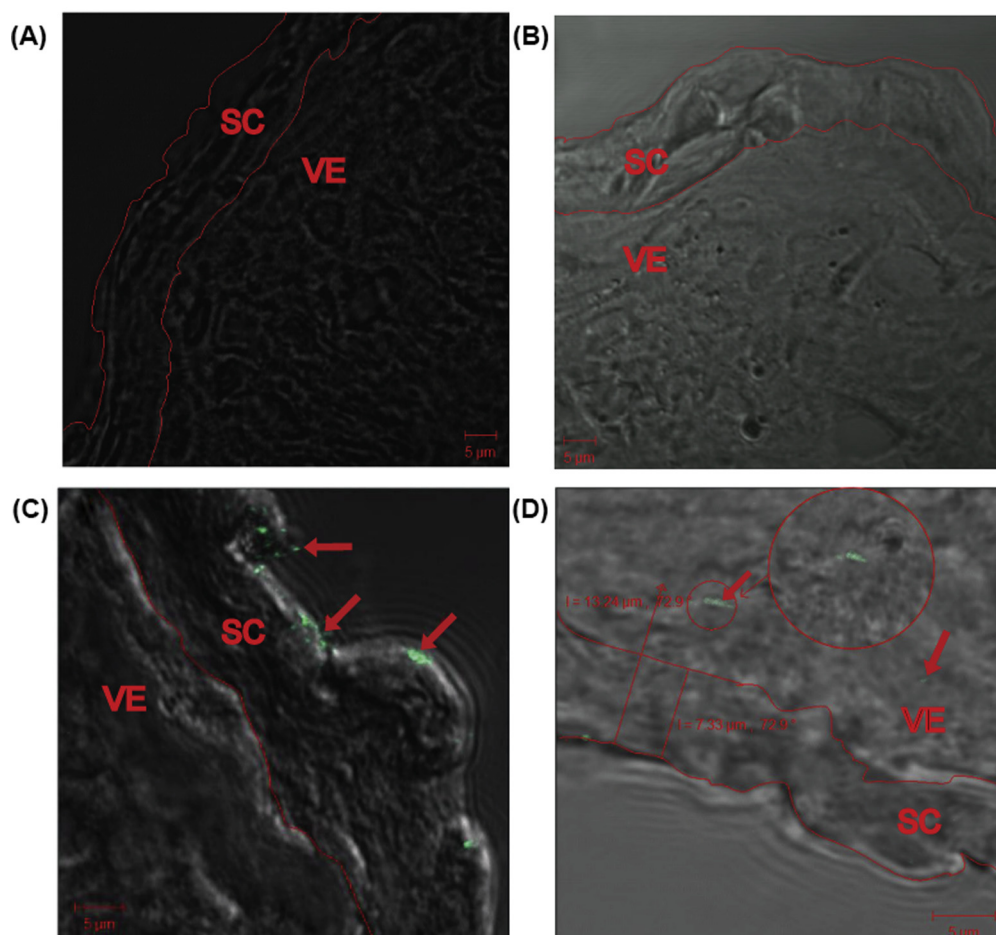


FIGURE 17.3 Multiphoton tomography of thawed skin treated for 24 h (A–D) 10 μm -thick cryosectioned skin from aqueous, toluene, gold nanoparticle (GNP) in aqueous solution (GNP-Aq), and GNP in toluene (GNP-TOL) groups. The images are overlays of light transmission and gold luminescence images. The stratum corneum and viable epidermis are labeled SC and VE; the SC is outlined in red. The red arrows indicate GNP in the GNP in aqueous solution image and the circle indicates GNP in the GNP in toluene image that is 13 μm deep.

vehicles to the rat central nervous system after saphenous vein injection. The results showed that GNPs were detected within the brain parenchyma of the MRI-GFU treated right hemisphere while leaving the untreated left part. MRI-GFU could transiently disrupt the blood–brain barrier, which allows focal delivery of nanoparticles. In another study, low-frequency ultrasound combined with the surfactant sodium lauryl sulfate (SLS: 1% w/v) was used to enhance the delivery of GNPs (5 nm) across split-thickness pig skin [63].

Magnetophoresis is a relatively new field of skin penetration enhancement. Benson's group utilized pulsed electromagnetic fields (PEMF) generated by the “dermaportation” technology to enhance the transport of 10 nm diameter GNPs across the skin [61]. GNP-treated human skin exposed to the PEMF had 200 times more GNP positive pixels than the skin exposed to GNPs without PEMF. This suggests that the PEMF facilitates penetration of the GNPs through the SC and that the channels through

which the nanoparticles move must be larger than the 10 nm diameter of these rigid particles.

APPLICATION OF METAL NANOPARTICLES IN BRACHYRADIATION FOR NONMELANOMA SKIN CANCERS

As mentioned earlier in this chapter, skin constitutes an excellent barrier and presents difficulties for the transdermal delivery of therapeutic agents [48,64]. Many physical and chemical approaches have been developed to enhance particle penetration into skin. To address these challenges, we have developed novel high-aspect ratio “elongated” EMPs to deliver particles to targeted skin areas [65]. The cylindrical-shaped solid silica EMPs have an aspect ratio of 33 ± 22 , a diameter of $9.3 \pm 0.9 \mu\text{m}$, and 50% of the EMPs have a length

between 120.1 and 483.2 μm [65]. Their unique size and morphology facilitates a relatively passive administration process. The microparticles can be easily applied and targeted to areas of interest without the use of complex devices or high forces. The EMPs are mixed with the drug and massaged into the skin, not restricted by application site or a large area [66]. This process gently pushes the EMPs into the viable *epidermis*. The EMPs penetrate the skin, resulting in increased permeability and drug penetration [66]. Penetration of the EMPs occurs predominantly within the *epidermis*, minimizing disruption of the dermis. Experiments in healthy volunteers have shown that the EMPs penetrate through the *epidermis* to the dermal–epidermal junction followed by natural removal from the skin through transepidermal elimination [65]. It can therefore significantly improve topical nanoparticle and microsphere delivery in an *in vivo* human model. A previous study showed a relatively continuous and uniform delivery of

therapeutically relevant compounds [65]. Confocal microscopy images can provide a visualization of the location of the particles into the skin and their aggregation around the EMPs.

We have extended these concepts by using microparticles for physically-targeted delivery of GNPs to skin. In our preliminary study, EMP nanoparticle delivery enhancement was evaluated in different formulations using GNPs and applied to the freshly excised healthy human skin using our previously published technique. These treated explants were then exposed to 6 Gy. The explants were embedded and snap frozen within 2 h of radiotherapy. Multiphoton microscopy was used to track the GNPs as previously described [67]. Histopathology sections were evaluated with haematoxylin and eosin (H&E) staining for epidermal disruption. Results showed that a cross-linked polymer approach to fabricate EMP was successfully applied to a number of payloads including 20 nm GNPs. EMPs appeared

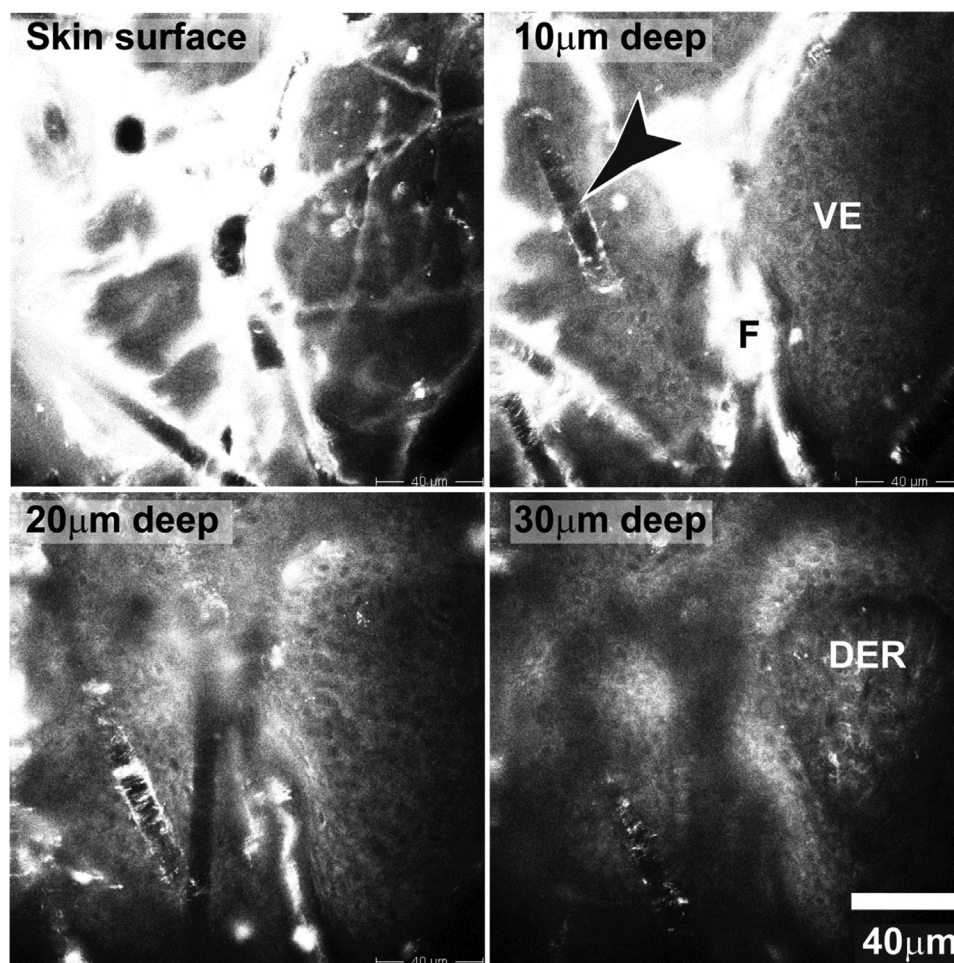


FIGURE 17.4 Viable human skin was treated with gold nanoparticles (GNPs) with elongated microparticles (EMPs). Multiphoton microscopy was used to simultaneously visualize skin autofluorescence, ie, NAD(P)H and collagen, and GNPs. The GNPs can be seen as a bright signal from the furrows (F) and as particulates on the EMPs (arrow head). The viable *epidermis* (VE) and dermis (DER) are characterized by perinuclear NAD(P)H signal and fibrous collagen bundles, respectively. EMPs appear to deliver gold nanoparticles deep into the VE.

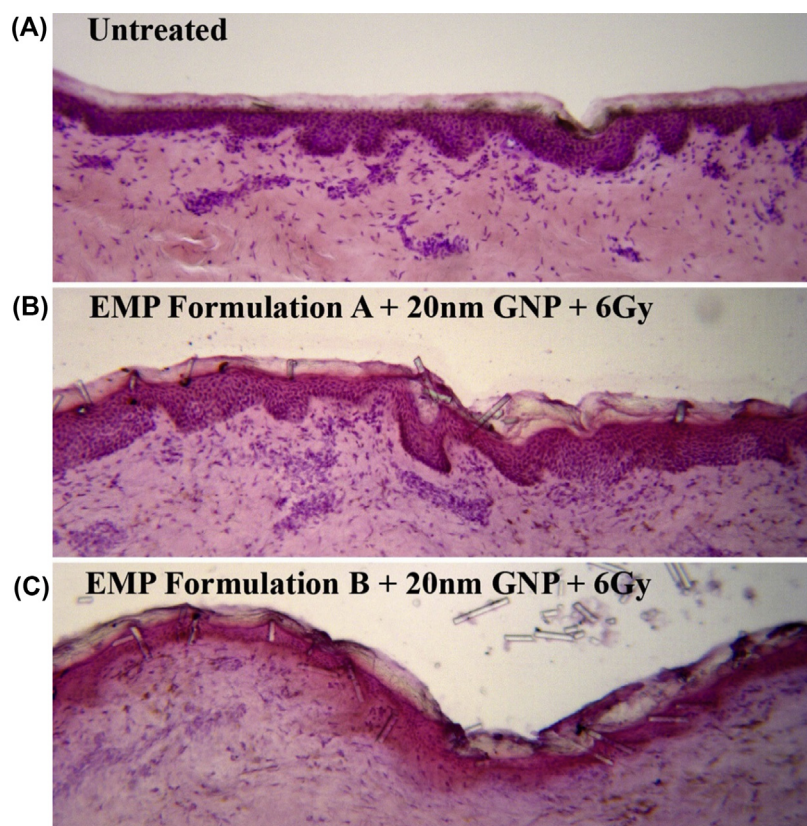


FIGURE 17.5 EMP enhanced radiotherapy in human skin. Panel (A) shows an untreated H&E stained skin section. Panel (B) shows skin treated with EMPs (arrow) Formulation A with a low dose of gold nanoparticles exposed to 6 Gy. Panel (C) shows a similarly treated piece of skin but with a higher dose of gold nanoparticles. There is a marked therapeutic improvement from Panel (B) to (C) in terms of disruption to the viable epidermis.

to improve the delivery of GNPs deep into the viable epidermis (Fig. 17.4) and resulted in a relatively uniform and continuous delivery profile within the treatment area when compared to identical delivery without EMPs (data not shown). The EMPs-delivered formulation B showed significant epidermal disruption (Fig. 17.5). These data support the further exploration of EMP-GNPs delivery for skin brachytherapy. Further investigations are required in the future to better control and release GNPs to the designated skin areas and to understand the relationship between nanoparticle dose and the energy required. The low toxicity of gold and the correspondingly low irradiation dose required encourage further testing in volunteers.

CONCLUSION AND PERSPECTIVES

Skin cancer rates are increasing worldwide, and the incidence of nonmelanoma skin cancer has steadily increased over the years despite preventative measures. Reducing the incidence and burden of skin cancer is one of the biggest health challenges. There is a need for new minimally invasive methods to treat nonmelanoma

skin cancers. This chapter focuses on the feasibility of GNP-enhanced radiotherapy. It is clear from these relatively early reports that there is indeed the potential for enhancement of radiotherapy mediated by GNP. We have discussed the underlying technology that is currently being exploited to enhance metal nanoparticle delivery. Nanoparticle penetration into and through the skin is not feasible using topical application alone. Many physical and chemical approaches have been developed to enhance particle penetration into skin. New techniques to noninvasively deliver GNPs in human skin were presented. Given the demonstrated high levels of radiosensitization by GNP at low energies, the conclusions from our pilot study support the hypothesis that it is clinically feasible to use EMP-formulated GNPs in treating skin diseases in combination with low dose brachytherapy.

List of Acronyms and Abbreviations

EMP Elongated silica microparticles
 GNP Gold nanoparticles
 MC Monte Carlo
 MRI GFU-Magnetic resonance image-guided focused ultrasound
 PEMF Pulsed electromagnetic fields
 SC Stratum corneum

References

- [1] Chen LL, Tooley IR, Wang SQ. Nanotechnology in photoprotection. In: Nasir A, Friedman A, Wang S, editors. *Nanotechnology in dermatology*. New York: Springer-Verlag; 2013. p. 9–18.
- [2] Sinclair R. Nonmelanoma skin cancer in Australia. *Br J Dermatol* 2013;168(1):1–2.
- [3] Morrison WH, Garden AS, Ang KK. Radiation therapy for nonmelanoma skin carcinomas. *Clin Plast Surg* 1997;24(4):719–29.
- [4] Locke J, et al. Radiotherapy for epithelial skin cancer. *Int J Radiat Oncol Biol Phys* 2001;51(3):748–55.
- [5] Schulte KW, et al. Soft x-ray therapy for cutaneous basal cell and squamous cell carcinomas. *J Am Acad Dermatol* 2005;53(6):993–1001.
- [6] Wang AZ, Tepper JE. Nanotechnology in radiation oncology. *J Clin Oncol* 2014;32(26):2879–85.
- [7] Yamada M, Foote M, Prow TW. Therapeutic gold, silver, and platinum nanoparticles. *Wiley Interdiscip Rev Nanomed Nanobiotechnol* 2015;7(3):428–45.
- [8] Matsudaira H, Ueno AM, Furuno I. Iodine contrast medium sensitizes cultured mammalian cells to x rays but not to gamma rays. *Radiat Res* 1980;144–8.
- [9] Jeremic B, Aguerri AR, Filipovic N. Radiosensitization by gold nanoparticles. *Clin Transl Oncol* 2013;15(8):593–601.
- [10] Cai W, et al. Applications of gold nanoparticles in cancer nanotechnology. *Nanotechnol Sci Appl* 2008;1:17–32.
- [11] Daniel MC, Astruc D. Gold nanoparticles: assembly, supramolecular chemistry, quantum-size-related properties, and applications toward biology, catalysis, and nanotechnology. *Chem Rev* 2004;104(1):293–346.
- [12] Turkevich J, Stevenson PC, Hillier J. A study of the nucleation and growth processes in the synthesis of colloidal gold. *Discuss Faraday Soc* 1951;11:55.
- [13] Brust M, et al. Synthesis of thiol-derivatized gold nanoparticles in a two-phase liquid-liquid system. *J Chem Soc Chem Commun* 1994:801–2.
- [14] Zhou J, et al. Functionalized gold nanoparticles: synthesis, structure and colloid stability. *J Colloid Interface Sci* 2009;331(2):251–62.
- [15] Chompoosor A, et al. The role of surface functionality on acute cytotoxicity, ROS generation and DNA damage by cationic gold nanoparticles. *Small* 2010;6(20):2246–9.
- [16] Archambeau JO, Pezner R, Wasserman T. Pathophysiology of irradiated skin and breast. *Int J Radiat Oncol Biol Phys* 1995;31(5):1171–85.
- [17] Sifton E. Early and late radiation-induced skin alterations. Part I: mechanisms of skin changes. *Oncol Nurs Forum* 1992;19(5):801–7.
- [18] Blackmar A. Radiation-induced skin alterations. *Medsurg Nurs* 1997;6(3):172–5.
- [19] Salvo N, et al. Prophylaxis and management of acute radiation-induced skin reactions: a systematic review of the literature. *Curr Oncol* 2010;17(4):94–112.
- [20] Geng F, et al. Thio-glucose bound gold nanoparticles enhance radio-cytotoxic targeting of ovarian cancer. *Nanotechnology* 2011;22(28):285101.
- [21] Roa W, et al. Gold nanoparticle sensitize radiotherapy of prostate cancer cells by regulation of the cell cycle. *Nanotechnology* 2009;20(37):375101.
- [22] Xu W, et al. RGD-conjugated gold nanorods induce radiosensitization in melanoma cancer cells by downregulating alpha(v) beta(3) expression. *Int J Nanomedicine* 2012;7:915–24.
- [23] Herold DM, et al. Gold microspheres: a selective technique for producing biologically effective dose enhancement. *Int J Radiat Biol* 2000;76(10):1357–64.
- [24] Hainfeld JF, Slatkin DN, Smilowitz HM. The use of gold nanoparticles to enhance radiotherapy in mice. *Phys Med Biol* 2004;49: N309–15.
- [25] Hainfeld JF, et al. Gold nanoparticles enhance the radiation therapy of a murine squamous cell carcinoma. *Phys Med Biol* 2010;55(11):3045–59.
- [26] Cho SH. Estimation of tumour dose enhancement due to gold nanoparticles during typical radiation treatments: a preliminary Monte Carlo study. *Phys Med Biol* 2005;50:N163–73.
- [27] Cho SH, Jones BL, Krishnan S. The dosimetric feasibility of gold nanoparticle-aided radiation therapy (GNRT) via brachytherapy using low-energy gamma-/x-ray sources. *Phys Med Biol* 2009;54(16):4889–905.
- [28] Spezi E, Lewis DG, Smith CW. Monte Carlo simulation and dosimetric verification of radiotherapy beam modifiers. *Phys Med Biol* 2001;46(11):3007–29.
- [29] Mijndonckx K, et al. Antimicrobial silver: uses, toxicity and potential for resistance. *Biomaterials* 2013;26(4):609–21.
- [30] Laresse FF, et al. Human skin penetration of silver nanoparticles through intact and damaged skin. *Toxicology* 2009;255(1–2):33–7.
- [31] Xu R, et al. Ag nanoparticles sensitize IR-induced killing of cancer cells. *Cell Res* 2009;19(8):1031–4.
- [32] Huang P, et al. Protein-directed one-pot synthesis of Ag microspheres with good biocompatibility and enhancement of radiation effects on gastric cancer cells. *Nanoscale* 2011;3(9):3623–6.
- [33] Lu R, et al. Egg white-mediated green synthesis of silver nanoparticles with excellent biocompatibility and enhanced radiation effects on cancer cells. *Int J Nanomed* 2012;7:2101–7.
- [34] Ma J, et al. Nanoparticle surface and nanocore properties determine the effect on radiosensitivity of cancer cells upon ionizing radiation treatment. *J Nanosci Nanotechnol* 2013;13(2):1472–5.
- [35] Liu P, et al. Silver nanoparticles: a novel radiation sensitizer for glioma? *Nanoscale* 2013;5(23):11829–36.
- [36] Franco-Molina MA, et al. Antitumor activity of colloidal silver on MCF-7 human breast cancer cells. *J Exp Clin Cancer Res* 2010;29:148.
- [37] Asharani PV, Hande MP, Valiyaveetil S. Anti-proliferative activity of silver nanoparticles. *BMC Cell Biol* 2009;10:65.
- [38] Mauro M, et al. Permeation of platinum and rhodium nanoparticles through intact and damaged human skin. *J Nanoparticle Res* 2015;17(6).
- [39] Zhang W, et al. Penetration and distribution of PLGA nanoparticles in the human skin treated with microneedles. *Int J Pharm* 2010;402(1–2):205–12.
- [40] Porcel E, et al. Platinum nanoparticles: a promising material for future cancer therapy? *Nanotechnology* 2010;21(8):85103.
- [41] Young SW, et al. Gadolinium(III) texaphyrin: a tumor selective radiation sensitizer that is detectable by MRI. *Proc Natl Acad Sci USA* 1996;93:6610–5.
- [42] Tokumitsu H, et al. Gadolinium neutron-capture therapy using novel gadopentetic acid-chitosan complex nanoparticles: in vivo growth suppression of experimental melanoma solid tumor. *Cancer Lett* 2000;150:177–82.
- [43] Hossain M, Su M. Nanoparticle location and material dependent dose enhancement in X-ray radiation therapy. *J Phys Chem C Nanomater Interfaces* 2012;116(43):23047–52.
- [44] Yuan F, et al. Vascular permeability in a human tumor xenograft: molecular size dependence and cutoff size. *Cancer Res* 1995;55(17):3752–6.
- [45] Fang J, Sawa T, Maeda H. Factors and mechanism of “EPR” effect and the enhanced antitumor effects of macromolecular drugs including SMANCS. *Adv Exp Med Biol* 2003;519:29–49.
- [46] Maki S, Konno T, Maeda H. Image enhancement in computerized tomography for sensitive diagnosis of liver cancer and semiquantitation of tumor selective drug targeting with oily contrast medium. *Cancer* 1985;56(4):751–7.

- [47] Schneider M, et al. Nanoparticles and their interactions with the dermal barrier. *Dermatoendocrinol* 2009;1:197–206.
- [48] Prow TW, et al. Nanoparticles and microparticles for skin drug delivery. *Adv Drug Deliv Rev* 2011;63(6):470–91.
- [49] Lademann J, et al. Nanoparticles – an efficient carrier for drug delivery into the hair follicles. *Euro J Pharma Biopharma* 2007;66(2):159–64.
- [50] Liu DC, et al. The human stratum corneum prevents small gold nanoparticle penetration and their potential toxic metabolic consequences. *J Nanomater* 2012;2012.
- [51] Sonavane G, et al. In vitro permeation of gold nanoparticles through rat skin and rat intestine: effect of particle size. *Colloids Surfaces B-Biointerfaces* 2008;65(1):1–10.
- [52] Huang YZ, et al. Co-administration of protein drugs with gold nanoparticles to enable percutaneous delivery. *Biomaterials* 2010;31(34):9086–91.
- [53] Labouta HI, et al. Mechanism and determinants of nanoparticle penetration through human skin. *Nanoscale* 2011;3(12):4989–99.
- [54] Baroli B, et al. Penetration of metallic nanoparticles in human full-thickness skin. *J Invest Dermatol* 2007;127(7):1701–12.
- [55] Dorsey JF, et al. Gold nanoparticles in radiation research: potential applications for imaging and radiosensitization. *Transl Cancer Res* 2013;2(4):280–91.
- [56] Labouta HI, et al. Combined multiphoton imaging-pixel analysis for semiquantitation of skin penetration of gold nanoparticles. *Int J Pharm* 2011;413(1-2):279–82.
- [57] Hainfeld JF, et al. Radioactive gold cluster immunoconjugates: potential agents for cancer therapy. *Int J Rad Appl Instrum B* 1990;17(3):287–94.
- [58] Hainfeld JF, et al. Micro-CT enables microlocalisation and quantification of Her2-targeted gold nanoparticles within tumour regions. *Br J Radiol* 2011;84(1002):526–33.
- [59] Marega R, et al. Antibodyfunctionalized polymer-coated gold nanoparticles targeting cancer cells: an in vitro and in vivo study. *J Mater Chem* 2012;22:21305–12.
- [60] Polat BE, Blankschtein D, Langer R. Low-frequency sonophoresis: application to the transdermal delivery of macromolecules and hydrophilic drugs. *Expert Opin Drug Deliv* 2010;7(12):1415–32.
- [61] Krishnan G, et al. Enhanced skin permeation of naltrexone by pulsed electromagnetic fields in human skin in vitro. *J Pharm Sci* 2010;99(6):2724–31.
- [62] Etame AB, et al. Enhanced delivery of gold nanoparticles with therapeutic potential into the brain using MRI-guided focused ultrasound. *Nanomedicine* 2012;8(7):1133–42.
- [63] Seto JE, et al. Effects of ultrasound and sodium lauryl sulfate on the transdermal delivery of hydrophilic permeants: comparative in vitro studies with full-thickness and split-thickness pig and human skin. *J Control Release* 2010;145(1):26–32.
- [64] Andrews SN, Jeong E, Prausnitz MR. Transdermal delivery of molecules is limited by full epidermis, not just stratum corneum. *Pharm Res* 2012;30:1099–109.
- [65] Raphael AP, et al. High aspect ratio elongated microparticles for enhanced topical drug delivery in human volunteers. *Adv Health Mater* 2014;3(6):860–6.
- [66] Raphael AP, et al. Enhanced delivery of nano- and submicron particles using elongated microparticles. *Curr Drug Deliv* 2015;12(1):78–85.
- [67] Labouta HI, et al. Gold nanoparticle penetration and reduced metabolism in human skin by toluene. *Pharm Res* 2011;28(11):2931–44.

Nanotechnology in Photoprotection

L.L. Chen¹, S.Q. Wang²

¹University of Miami Miller School of Medicine, Miami, FL, United States; ²Memorial Sloan-Kettering Cancer Center, New York, NY, United States

OUTLINE

Introduction	229	The Regulatory State of Nanoparticles in Sunscreens	234
Inorganic Filters: Nano TiO ₂ and ZnO	229	Conclusion	235
Organic Filters and Nanotechnology	231	References	235
Safety Concerns for Nano TiO ₂ and ZnO	232		

INTRODUCTION

Overexposure to ultraviolet (UV) radiation from the sun is a major risk factor for sun damage and sequelae such as sunburn, photoaging, and skin cancer. Topical sunscreen products have been developed to protect the public and prevent these damages caused by UV exposure. The UV spectrum (290–400 nm) can be further divided into UVB (290–320 nm), representing only 5% of the UV reaching the earth surface, and UVA (320–400 nm), approximately 95%. UVA radiation can generate a severe oxidative stress and lead to photocarcinogenesis, immunosuppression, and photoaging. UV filters are broadly divided into organic and inorganic filters. Titanium dioxide (TiO₂) and Zinc Oxide (ZnO) are the only inorganic filters approved for sunscreen use. Compared to organic UV filters, such as avobenzone and oxybenzone, inorganic filters have significantly lower risk for developing photoallergic and allergic reaction, and therefore more amenable to individuals with sensitive skin. TiO₂ and ZnO have been widely recommended as safe and effective UV filters in sunscreen. Despite these benefits, older formulations with inorganic filters had a poor cosmetic appearance secondary to poor dispersive qualities, leaving a white or opaque film on the skin and a grainy after-feel. Therefore, these

sunscreens had inconsistent and insufficient application of product, hindering wide acceptance by the public.

The texture and aesthetic problem associated with sunscreens with TiO₂ and ZnO have largely been solved by the introduction of nanotechnology, which involves the design, production, and application of materials in the size range of 1–100 nm. However, there is rising concern due to safety implications of these nanomaterials. In this chapter, application of nanotechnology to both inorganic and organic UV filters use in nanotechnology will be reviewed as well as the controversy over the toxicity and penetration of nanoparticles in topical administration.

INORGANIC FILTERS: NANO TiO₂ AND ZnO

Nanoparticulate TiO₂ and ZnO are increasingly being incorporated into photoprotection products, due to less skin whitening and improved UV reflectance and absorption. By 1990, these two nanosized UV filters were introduced on a large scale after garnering approval by various consortiums and organizations, including the US Food and Drug Administration (FDA) [1]. Over a 12-year period, the percentage of sunscreen products

containing ZnO increased from 3% to 16% [2]. The boon of these ingredients was due to its more pleasing aesthetic effects. Given that the average size of these minerals are less than 100 nm, this smaller particle size minimizes visible light scattering and results in a topical formulation that appears “transparent.” In reality, oxide nanoparticles appear transparent at or below concentration thresholds, thereby have less “whitening effect” and appear to easily blend into the skin. For example, visible light is maximally scattered at ZnO particle size of 0.8 μm (thereby appearing white). Visible scattering decreases below this size, so below 200 nm (0.2 μm), ZnO is virtually transparent. The reduction in particle size also is an advantage for UVB protection, since smaller size scatters and reflects UVB more efficiency. For cosmetic and effectiveness reasons, nanometal oxides appear to be an ideal choice in sunscreen products.

During the manufacturing process, nanosized TiO_2 and ZnO can exist in three different states: primary nanoparticles (5–20 nm), aggregates (30–150 nm), and agglomerates (1–100 μm) [3]. Primary nanoparticles have strong crystal attractions which form clustered, tightly bound aggregates (Fig. 18.1). Aggregates are the smallest particles which can be found in sunscreen formulations, because the forces required to break apart aggregates are far greater than those forces encountered during production or during application onto the skin. Visualization of nanoparticle-containing sunscreen emulsions by transmission electron microscopy (TEM) has allowed particles to be more precisely measured (Fig. 18.2A and B). In formulation, TiO_2 and ZnO are always present as aggregates, though it is common to specify “particle size” as the size of single crystals. The optimum particle size is calculated to be around 50 nm to maintain cosmetic elegance. On the market, TiO_2 particles range from ultra-fine size of 30 nm to microsize aggregates. In contrast, ZnO particles are larger grade, typically 60–200 nm [4,5]. Larger-sized agglomerates

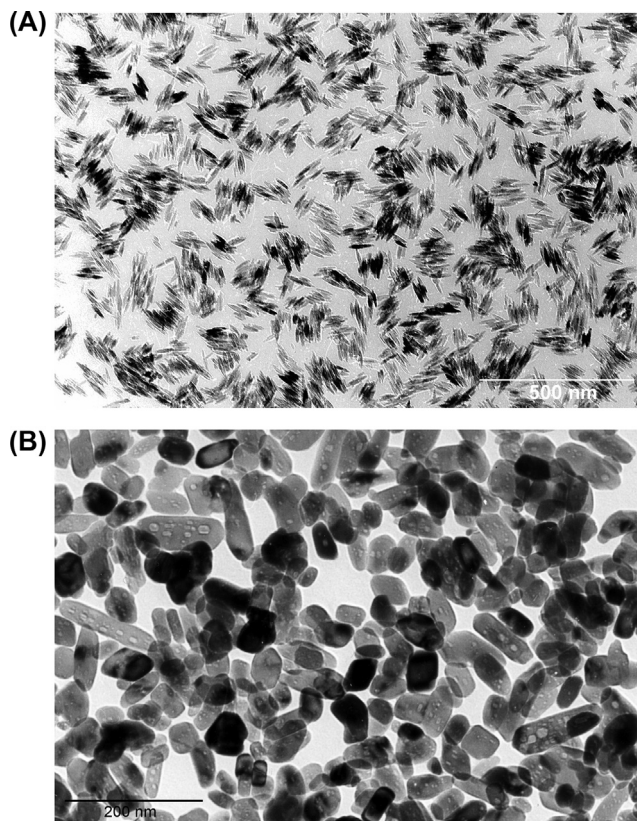


FIGURE 18.2 (A) 15 nm TiO_2 and (B) 35 nm TiO_2 primary particles and aggregates measured by TEM. Reprinted with permission from Chen et al.

are more loosely bound and can be a result of the drying and heat treatment processing during manufacturing. These larger sizes are ineffective at UV attenuation. Special coating materials (commonly silica or dimethicone) are applied to the surface of mineral particles to resist agglomeration and improve dispersion in the final sunscreen formulation [1]. This technique also diminishes the photoreactivity of both kinds of minerals. Special

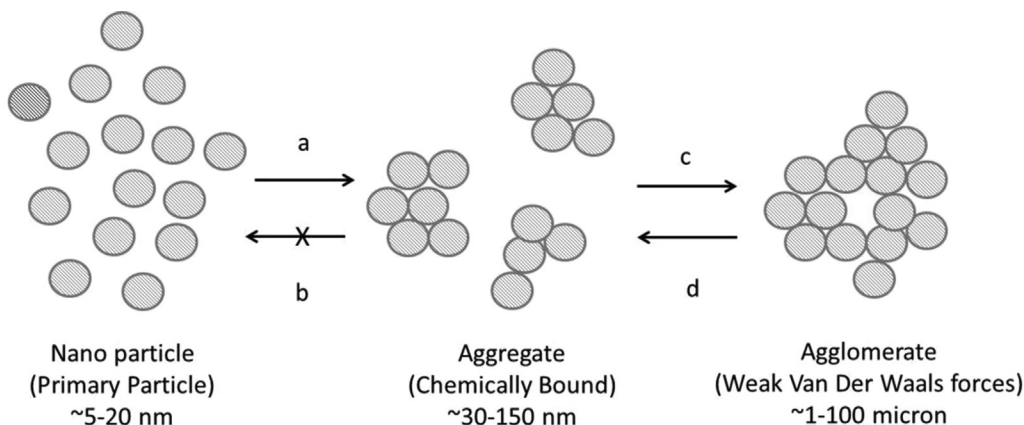


FIGURE 18.1 Formation of aggregates and agglomerates from nanoparticle building blocks. Reprinted with permission from Chen et al. [38].

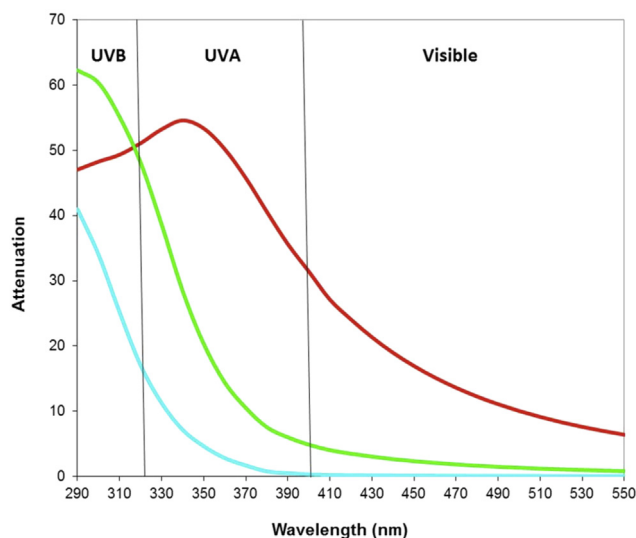


FIGURE 18.3 UV attenuation versus wavelength for spherical TiO_2 of varying particle size. Blue line, 20 nm; green line, 50 nm; and red line, 100 nm. Reprinted with permission from Chen et al.

modifications with a carbon coating can minimize the formation of reactive oxygen species and prevent adherence of nanoparticles to cells [6].

Sunscreen formulators must find an optimum particle size to achieve the desired UV attenuation profile, while delivering a pleasing aesthetic effect. UV attenuation is the sum of UV reflecting and absorbing properties and dependent on wavelength of light, particle size, and refractive index [1]. With a smaller size, nanoparticles attenuate shorter wavelengths of UV radiation, and thus they offer high UVB and less UVA coverage. Generally, TiO_2 is less effective than ZnO in the UVA I range (>340 nm). Therefore, the sunscreen with a smaller particle size will be a more transparent product but have poorer UVA protection (Fig. 18.3). It would make sense that the optimal sunscreen would be one containing a mixture of nanoparticle aggregate sizes: for TiO_2 ranging between 50 and 120 nm and for ZnO between 60 and 100 nm particles.

ORGANIC FILTERS AND NANOTECHNOLOGY

Some of the organic filters have the reputation to be photounstable, have higher allergenicity, and provoke skin sensitization. With recent nanotechnology advances, there have been great strides in reducing these adverse effects. With respect to sunscreen filters, photostability is defined as degradation of these filters following solar-stimulated UV radiation [7]. Organic UV filters absorb photo energy and transition into its excited energy state. The absorbed energy is dissipated

innocuously via heat, light, or more destructive processes such as isomerization, fragmentation, free radical production, or can react with other molecules. The functional degradation of these filters make them less effective in blocking UV radiation. Furthermore, it can lead to photoirritation, allergy, acute sunburn, or chronic actinic damages [7]. Therefore, photostability has a significant impact on the efficacy of a sunscreen, including achieving a desired SPF and broad-spectrum protection. SPF is a measure of the efficacy of a sunscreen to offer photoprotection, defined as the time factor that skin will be protected from sunburn when the sunscreen is used. For example, a sunscreen with SPF 30 allows for 30 times longer time with sun exposure compared to without the sunscreen before becoming sunburnt.

Avobenzone and oxybenzone, two common UVA filters, are known to exhibit photounstability (breaking down following exposure to UV radiation) and to have photoallergic contact potential from its degradation photoproducts [8]. However, when repeatedly tested in human skin, the risk of a true photoallergy has been low and the frequency of allergic reactions has remained constant despite increasing use of this filter in sunscreen products [9]. The photo instability can be ameliorated or worsened when these above UV filters are combined with other UV filters. For example, photostability of avobenzone can be achieved when it is combined with octocrylene. However, the combination of octinoxate and avobenzone should not be used in any formulation, because it leads to an accelerated state of photodegradation.

New innovations utilizing nanotechnology, such as nanoencapsulation, have been deployed to solve these issues of photounstability and penetration. For example, octyl methoxycinnamate (OMC) exists in both photostable *cis*- form to an unstable trans isomer. UV radiation converts OMC from the *cis*- to *trans*-form, and renders the OMC molecule photounstable. However, by encapsulating OMC with nanosized (D,L lactide) polymer, there is a significant reduction in photoisomerization from a photostable *cis*- form to an unstable trans isomer, which leads to a significant improvement in photostability and SPF protection [10]. Other authors used similar biocompatible nanopolymers and UV filters to show similar significant effects on photostability [11,12]. Theoretically, nanoencapsulation can reduce the contact between the sunscreen and skin surface by entrapping the product above the stratum corneum (SC) to prevent penetration into the skin and thereby limit photoallergic contact reactions. In addition, nanoencapsulated UV filters significantly decrease transdermal transport of UV filters, compared to formulation with nonencapsulated filter [13]. Indeed, after 24 hour of application of oil-containing polyamide-encapsulated ethylhexyl methoxycinnamate (EHMC) and avobenzone on pig ear

epidermal membranes, there was minimal epidermal penetration. Photostability of encapsulated sunscreens was improved by more than 50% as well.

In addition to polymers, inorganic matrices have been proposed as a strategy to increase sunscreen stability and prevent absorption into the skin. Porous materials such as hydrotalcites, zeolites, and mesoporous silicate (MCM-41) are suitable carriers of organic molecules due to their organized pore structure, narrow pore-size distribution, and high surface area [14,15]. By entrapping pores with an organic UV filter, a broader photoprotection range and enhanced photostability can be achieved. All these effects are attributable to the inclusion of filter within the matrix pores. These pores also offer an obstacle to sunscreen release, with low amounts of the UV filter (for example, oxybenzone) released based on *in vitro* assays [16]. Similar in notion to polymer encapsulation, porous entrapment offers a suitable vehicle for UV filters and attenuates sunscreen release, thus reducing direct contact or systemic absorption of potentially photounstable ingredients on the skin.

Aside from employing nanotechnology to encapsulate existing UV filters, there are now novel organic UV filters in the nanosized range. In April 2015, Tris-biphenyl triazine (Tinosorb A2B) became the first nanosized organic UV filter approved for use by the European Parliament and the Council. It is the first filter to be added on the list of the European Union (EU) Cosmetics Regulation (Annex VI) since the regulation came into effect in July 2013. Tinosorb A2B is a broad-spectrum filter that attenuates in the UVA II (320–340 nm) and UVB ranges (290–320 nm). It is also touted as photostable since its photoprotective abilities do not vary after two hours of solar-simulated irradiation [17]. Unlike other organic filters, it is considered skin safe up to 10% proportion in cosmetic formulations, with no significant potential to produce a photoallergy. In preclinical absorption testing, negligible to low concentrations of the particle were found beneath the skin [18]. Pending approval by the Australian Therapeutic Goods Administration, this filter will soon be incorporated into that nation's photoprotection repertoire [3,19].

SAFETY CONCERNS FOR NANO TiO₂ AND ZnO

These nanosized TiO₂ and ZnO have been welcomed as innovative technology, in the past decade, however there has been concern regarding their safety profile. One of the central issues was related to the phototoxicity of these nanosized filters. It has been demonstrated that, when exposed to UVR, these nanosized TiO₂ and ZnO can generate free radicals which induce the formation

of reactive oxygen species (ROS) and peroxides in the local environment with resulting cellular and DNA damage. This oxidative stress can impact the cellular and genetic integrity of a living cell, possibly driving toward apoptosis. For example, in the presence of TiO₂ particles after exposure to UV radiation, plasmid DNA had accelerated damage due to formation of hydroxyl radicals (OH) [3,20]. Other genetic targets included oxidative biomarkers such as 8-oxoguanosine [21], double-stranded DNA breaks, and structural chromosomal aberrations [22]. To determine whether phototoxicity was due to the metals oxides alone or a UV-mediated process, Dufor et al. examined the clastogenic (genotoxic) potential of ZnO in the presence of UV irradiation [23]. Chinese hamster ovarian cells were challenged to three conditions: (1) in the dark; (2) preirradiation followed by ZnO treatment; and (3) simultaneous irradiation with ZnO treatment. True photoclastogenic agents would have significantly higher potential under the simultaneous irradiated conditions. Interestingly, the results were identical in preirradiated and simultaneously irradiated groups with respect to severity of chromosomal aberrations. Therefore, the timing of UV exposure and ZnO treatment had no effect on the degree of severity. The authors concluded that UV radiation mediated an enhanced susceptibility of cells to ZnO but ZnO itself was not photoclastogenic. To minimize the production of free radicals, special coating materials (commonly silica or dimethicone) are applied to the surface of these nanosized particles to minimize the formation of ROS and prevent adherence of nanoparticles to cells [23]. The addition of antioxidants and free radical scavengers in sunscreen has the potential to further reduce the harmful effects of ROS products [1].

Another concern that has been raised in the safety debate is whether there is significant penetration of these nanoparticles into human skin. What are the risks of cosmetic formulations containing tiny molecules and their implications for systemic toxicity and exposure? The SC, the outermost layer of the epidermis, is approximately 15–20 μm thick in humans. Smaller-sized minerals have the possibility of penetration past the skin barrier of the SC and into the deeper viable portion of the epidermis and dermis. Key penetration studies, largely *ex vivo* and a few *in vivo* have been performed for both TiO₂ and ZnO that have concluded nanoparticles do not penetrate human or other animal skin [18,24]. By utilizing various imaging modalities such as electron and light microscopy, X-ray fluorescence, particle-induced X-ray emission, and electron emission spectrophotometry, all studies concluded that nanosized TiO₂ remained on the outermost layer of the skin. Similar penetration studies were performed with ZnO and these results were matching. A summary of these important findings are listed in Tables 18.1–18.3.

TABLE 18.1 TiO₂ Skin Penetration Studies

Study	Material	Particle size	Skin model/design	Results
Tan et al. [40]	TiO ₂ (no coating specified)	Not specified	Human skin, in vitro	No significant penetration into skin
Lademann et al. [31]	TiO ₂ (Al ₂ O ₃ , stearic acid coated)	150–170 nm	Human skin biopsy	Penetration into upper layers of stratum corneum (SC); ~1% of particles in follicular ostium
European Union SCCNFP opinion [24]	TiO ₂ (anatase and rutile forms, various coatings)	14–200 µm	Pig skin, in vitro; Human skin, tape stripping, or biopsy	No penetration beyond the SC
Pflucker et al. [41]	TiO ₂ (SiO ₂ , Al ₂ O ₃ , Al ₂ O ₃ + SiO ₂ coated)	10–100 nm	Human skin biopsy	Penetration into upper layers of the SC
Schulz et al. [42]	TiO ₂ (SiO ₂ ± Al ₂ O ₃ coated)	10–100 nm	Human skin biopsy	Penetration into the upper layers of the SC
Gottbrath and Muller-Goymann [43]	TiO ₂ -containing sunscreen (no coating specified)	Not specified	Human skin, tape stripping	Particles into upper layers of SC
Menzel et al. [44]	TiO ₂ (various forms, no coating specified)	45–150 nm	Pig skin, in vitro	Particles in SC; minimal penetration into stratum granulosum
Popov et al. [4]	TiO ₂ (rutile form)	100 nm	Human skin, tape stripping	No penetration beyond the SC
Mavon et al. [50]	TiO ₂ (SiO ₂ coated)	20 nm	Human skin, tape stripping, and in vitro	Penetration in upper layers of SC

Reprinted with permission from Newman MD, Stotland M, Ellis JI. The safety of nanosized particles in titanium dioxide- and zinc oxide-based sunscreens. *J Am Acad Dermatol* 2009; 61(4):685–92.

TABLE 18.2 ZnO Skin Penetration Studies

Pirot et al. [45]	ZnO (no coating specified)	Not specified	Human skin, in vitro	0.36% penetration in 72 h
European Union SCCNFP opinion [25]	ZnO	Not specified	Pig skin, in vitro Human nonpsoriatic and psoriatic skin	No increase in plasma zinc levels; in vitro, penetration <1% of dose; most ZnO recovered from stratum corneum (SC)
Cross et al. [5]	ZnO (siliconate coated)	15–30 nm	Human skin, in vitro	<3% of applied Zn recovered in SC; penetration into upper layers of the SC
Zvyagin [30]	ZnO (uncoated)	26–30 nm	Human skin, in vivo and in vitro	No penetration beyond SC, accumulation in skin folds and hair follicles

Reprinted with permission from Newman MD, Stotland M, Ellis JI. The safety of nanosized particles in titanium dioxide- and zinc oxide-based sunscreens. *J Am Acad Dermatol* 2009; 61(4):685–92.

There are several explanations as to why some studies still interpret that nanoparticles can penetrate past the skin. Most penetration studies under in vitro or in vivo conditions were performed using animal skin, such as rabbit, rodent and pig skin that are more permeable than human skin [25]. Additionally, there can be greater permeability if skin occlusion methods (which produce corneocyte swelling) were used. Finally, physical destruction of the skin prior to use such as tape stripping can artificially yield positive interpretation of epidermal

penetration if particles are seen in the skin furrows or deep hair follicles. In consideration of these findings, all studies to date suggest that TiO₂ and ZnO remain on the surface of skin and there remain negligible concentrations below the SC.

Why are nanoparticles poorly capable of penetration through the skin? From principles of transdermal drug delivery, we know that a drug that is skin penetrable can be no larger than 500 Da (2.5 nm) [26,27]. Topical steroids and antifungal medications all fall below this

TABLE 18.3 Combination TiO₂ and ZnO Skin Penetration Studies

Lansdown and Taylor [46]	TiO ₂ , ZnO (no coating specified)	<2–20 μ m	Rabbit skin, in vivo	Penetration into stratum corneum (SC) and outer hair follicle
Dussert et al. [47]	TiO ₂ , ZnO (no coating specified)	TiO ₂ : 50–100 nm ZnO: 20–200 nm	Human skin, in vitro	Penetration into upper layers of SC
Gamer et al. [48]	TiO ₂ (SiO ₂ , dimethicone coated) ZnO (uncoated)	TiO ₂ : 30–60 nm ZnO: <160 nm	Pig skin, in vitro	Penetration into upper layers of SC; 0.8–1.4% of applied dose recovered
Filipe et al. [49]	TiO ₂ (SiO ₂ \pm Al ₂ O ₃ -coated) ZnO	TiO ₂ : 20 nm ZnO: 20–60 nm	Human skin (intact, compromised and psoriatic), tape stripping	No penetration beyond SC
Durand et al. [51]	TiO ₂ (hydrophobically coated) ZnO coated)	TiO ₂ : 30–150 nm ZnO: 100–200 nm	Human skin, in vitro	Presence in SC and hair follicles

Reprinted with permission from Newman MD, Stotland M, Ellis JI. The safety of nanosized particles in titanium dioxide- and zinc oxide-based sunscreens. *J Am Acad Dermatol* 2009; 61(4):685–92.

molecular size and yield penetration beneath the SC. Nanoparticles tend to combine as aggregates and agglomerates in final sunscreen formulation as described earlier, so their final size often exceeds the permissible size for transcutaneous delivery. Besides size, various physical and chemical characteristics of the particles such as polarity, concentration, melting temperature, and solubility need to be considered. The host environment also has an important role in the ease of penetration. Hair follicles have long been studied as a pathway for nanomaterials to enter. This “follicular sink” was first described by Lademann et al. as a collectible reservoir for nanoparticles [28–30]. By tape stripping and evaluation of strips by spectroscopic measurements, nanoparticles were found in the follicular openings and superficial portion of the follicles at concentrations two times less than the upper part of the SC. However, after further work, it appeared that the hair growth cycle had a crucial role in the location of nanoparticles. Active hair growth and sebum production phases are needed to be present to find follicular nanoparticles. As such, growing hair shafts push these materials to the surface of the skin [31]. By a similar concept, the SC is constantly shedding and preventing deeper penetration of nanoparticles into viable skin tissue [32].

Theoretically there could be increased skin penetration of nanosized particles when exposed to a compromised or disrupted skin barrier. Compared to intact skin, sunburnt skin is shown to receive a higher percutaneous absorption of topical steroid lotion [32]. Skin conditions with a disrupted SC, such as eczema, or physical conditions like skin tape stripping can increase the penetration of topically applied substances [33]. One interesting study used four TiO₂ and ZnO sunscreen formulations on pig skin and treated the SC with UVB irradiation

[34]. Penetration of nanoparticles was enhanced in the irradiated skin (deeper in the layers of the SC), though there was no evidence of systemic absorption. Furthermore, the toxicity of aerosolized nanoparticles (spray sunscreens) and potential for systemic absorption is still to be determined. Though a significant amount of data has been utilized to deem nanoparticles safe for topical use in normal skin, their safety should be assessed under conditions of abnormal skin barrier and behavior.

THE REGULATORY STATE OF NANOPARTICLES IN SUNSCREENS

Given the increasing interest in new formulations of UV filters, regulatory strategies have been adopted by governing countries pertaining to nanomaterials, generally with favorable opinions. The EU initiated the “Cosmetics Regulation #1223/2009” in 2009 to impose more responsibility on the overall regulatory framework for cosmetics [35]. Beginning in 2013, this mandate required the labeling of cosmetic products that contain nanomaterials, safety assessment of these ingredients with particular attention to the nanosized components, and a 6-month notification period prior to beginning marketing of any new cosmetics. Any cosmetic or sunscreen with an ingredient smaller than 100 nm should be clearly labeled as “nano” in brackets and individually tested for safety. Also, cosmetic ingredients should be listed in regulatory documents known as Annexes as permitted, restricted, or banned to be up to date. In cases with safety concerns, the Scientific Committee on Consumer Safety may publish opinions about particular nanomaterial ingredients or cosmetic products.

Compared to the EU, the US FDA has no particular mandates regarding nanoparticle-containing topical products [36]. In contrast to the European counterpart, sunscreens are considered over-the-counter drug products and are under regulations from the FDA, rather than a cosmetics committee. The FDA included micronized TiO₂ and ZnO in the 1999 OTC Monograph for Sunscreen Products. A need has been recognized with the inception of the Nanotechnology Task Force in 2007, which recommended that the FDA provide guidance to manufacturers to consider good manufacturing practices for nanoscale-containing products, labeling and safety issues, and quality assurance. In fact, the budget for nanotechnology related work doubled over the time period between 2009 and 2012. However, to date the FDA has not issued any guidelines in providing clearer directives regarding its policy to regulate nanomaterials.

CONCLUSION

Nanotechnologies have been widely employed to enhance aesthetic and functional capability of sunscreens. There is no doubt that industry will continue to employ nanotechnology in future sunscreen products. The advantages of nanosized filters are well known, such as having more effective UV coverage and a cosmetically elegant formulation. Especially with burgeoning technologies generating more photostable organic filters, the appeal for nanoparticles continues to increase. However, concerns regarding toxicity and penetration about these nanosized ingredients will remain despite a wealth of evidence demonstrating no penetration beyond the top layers of the skin. There remains a need to test these sunscreens under real-life applications conditions; for example, following UV exposure, under compromised skin conditions or when used in a spray vehicle. Another recognized concern is at the level of the various government agencies that can authorize approval of these ingredients, in consideration of quality and safety issues. Formulators should be cognizant of all of these aspects when developing nanoparticle-containing sunscreen so that future generations can continue to safely use these UV filters without restriction or hesitation.

References

- [1] Mitchnick MA, Fairhurst D, Pinnell SR. Microfine zinc oxide (Z-cote) as a photostable UVA/UVB sunblock agent. *J Am Acad Dermatol* 1999;40(1):85–90.
- [2] Wang SQ, Tanner PR, Lim HW, Nash JF. The evolution of sunscreen products in the United States—a 12-year cross sectional study. *Photochem Photobiol Sci* 2013;12(1):197–202.
- [3] Bateman D. Super sunscreen soon to hit shelves, helping to lower Far North skin cancer rate. Australia. 2015. Available from: <http://www.cairnspost.com.au/lifestyle/super-sunscreen-soon-to-hit-shelves-helping-to-lower-far-north-skin-cancer-rate/story-fnpqql4s-1227330860489>.
- [4] Popov AP, Lademann J, Priezzhev AV, Myllyla R. Effect of size of TiO₂ nanoparticles embedded into stratum corneum on ultraviolet-A and ultraviolet-B sun-blocking properties of the skin. *J Biomed Opt* 2005;10(6):064037.
- [5] Cross SE, Innes B, Roberts MS, Tsuzuki T, Robertson TA, McCormick P. Human skin penetration of sunscreen nanoparticles: in-vitro assessment of a novel micronized zinc oxide formulation. *Skin Pharmacol Physiol* 2007;20(3):148–54.
- [6] Livraghi S, Corazzari I, Paganini MC, Ceccone G, Giamello E, Fubini B, et al. Decreasing the oxidative potential of TiO₂ nanoparticles through modification of the surface with carbon: a new strategy for the production of safe UV filters. *Chem Commun* 2010;46(44):8478–80.
- [7] Nash JF, Tanner PR. Relevance of UV filter/sunscreen product photostability to human safety. *Photodermatol Photoimmunol Photomed* 2014;30(2–3):88–95.
- [8] Dondi D, Albini A, Serpone N. Interactions between different solar UVB/UVA filters contained in commercial suncreams and consequent loss of UV protection. *Photochem Photobiol Sci* 2006;5(9):835–43.
- [9] Gaspar LR, Tharmann J, Maia Campos PM, Liebsch M. Skin phototoxicity of cosmetic formulations containing photounstable and photostable UV-filters and vitamin A palmitate. *Toxicol In Vitro* 2013;27(1):418–25.
- [10] Vettor M, Perugini P, Scalia S, Conti B, Genta I, Modena T, et al. Poly(D,L-lactide) nanoencapsulation to reduce photoinactivation of a sunscreen agent. *Int J Cosmet Sci* 2008;30(3):219–27.
- [11] Jimenez MM, Pelletier J, Bobin MF, Martini MC, Fessi H. Polye-epsilon-caprolactone nanocapsules containing octyl methoxycinnamate: preparation and characterization. *Pharm Dev Technol* 2004;9(3):329–39.
- [12] Perugini P, Simeoni S, Scalia S, Genta I, Modena T, Conti B, et al. Effect of nanoparticle encapsulation on the photostability of the sunscreen agent, 2-ethylhexyl-p-methoxycinnamate. *Int J Pharm* 2002;246(1–2):37–45.
- [13] Alvarez-Roman R, Naik A, Kalia YN, Guy RH, Fessi H. Enhancement of topical delivery from biodegradable nanoparticles. *Pharm Res* 2004;21(10):1818–25.
- [14] Deleted in review.
- [15] Ambrogi V, Latterini L, Marmottini F, Pagano C, Ricci M. Mesoporous silicate MCM-41 as a particulate carrier for octyl methoxycinnamate: sunscreen release and photostability. *J Pharm Sci* 2013;102(5):1468–75.
- [16] Perioli L, Ambrogi V, Bertini B, Ricci M, Nocchetti M, Latterini L, et al. Anionic clays for sunscreen agent safe use: photoprotection, photostability and prevention of their skin penetration. *Eur J Pharm Biopharm* 2006;62(2):185–93.
- [17] Ambrogi V, Latterini L, Marmottini F, Tiralti MC, Ricci M. Oxygen-benzene entrapped in mesoporous silicate MCM-41. *J Pharm Innov* 2013;8(4):212–7.
- [18] Chen L, Hu JY, Wang SQ. The role of antioxidants in photoprotection: a critical review. *J Am Acad Dermatol* 2012;67(5):1013–24.
- [19] Opinion on 1,3,5-triazine, 2,4,6-tris[1,1'-biphenyl]-4-yl-. European Commission Scientific Committee on Consumer Safety; 2011.
- [20] Dunford R, Salinaro A, Cai L, Serpone N, Horikoshi S, Hidaka H, et al. Chemical oxidation and DNA damage catalysed by inorganic sunscreen ingredients. *FEBS Lett* 1997;418(1–2):87–90.
- [21] Uchino T, Tokunaga H, Ando M, Utsumi H. Quantitative determination of OH radical generation and its cytotoxicity induced by TiO₂–UVA treatment. *Toxicol Vitro* 2002;16(5):629–35.
- [22] Wamer WG, Yin JJ, Wei RR. Oxidative damage to nucleic acids photosensitized by titanium dioxide. *Free Radic Biol Med* 1997;23(6):851–8.

- [23] Dufour EK, Kumaravel T, Nohynek GJ, Kirkland D, Toutain H. Clastogenicity, photo-clastogenicity or pseudo-photo-clastogenicity: genotoxic effects of zinc oxide in the dark, in pre-irradiated or simultaneously irradiated Chinese hamster ovary cells. *Mutat Res* 2006;607(2):215–24.
- [24] European Union's Scientific Committee on Cosmetic Products and Non-Food Products Brussels, Belgium; 2000. Available from: http://ec.europa.eu/health/archive/ph_risk/committees/sccp/documents/out135_en.pdf.
- [25] European Union's Scientific Committee on Cosmetic Products and Non-Food Products. Brussels, Belgium; 2003. Available from: http://ec.europa.eu/health/archive/ph_risk/committees/sccp/documents/out222_en.pdf.
- [26] Magnusson BM, Walters KA, Roberts MS. Veterinary drug delivery: potential for skin penetration enhancement. *Adv Drug Deliv Rev* 2001;50(3):205–27.
- [27] Subedi RK, Oh SY, Chun MK, Choi HK. Recent advances in transdermal drug delivery. *Arch Pharm Res* 2010;33(3):339–51.
- [28] Bos JD, Meinardi MM. The 500 Dalton rule for the skin penetration of chemical compounds and drugs. *Exp Dermatol* 2000;9(3):165–9.
- [29] Lademann J, Otberg N, Richter H, Weigmann HJ, Lindemann U, Schaefer H, et al. Investigation of follicular penetration of topically applied substances. *Skin Pharmacol Appl Skin Physiol* 2001;14(Suppl. 1):17–22.
- [30] Zvyagin AV, Zhao X, Gierden A, Sanchez W, Ross JA, Roberts MS. Imaging of zinc oxide nanoparticle penetration in human skin in vitro and in vivo. *J Biomed Opt* 2008;13(6):064031.
- [31] Lademann J, Weigmann H, Rickmeyer C, Barthelmes H, Schaefer H, Mueller G, et al. Penetration of titanium dioxide microparticles in a sunscreen formulation into the horny layer and the follicular orifice. *Skin Pharmacol Appl Skin Physiol* 1999;12(5):247–56.
- [32] Lademann J, Knorr F, Richter H, Blume-Peytavi U, Vogt A, Antoniou C, et al. Hair follicles—an efficient storage and penetration pathway for topically applied substances. Summary of recent results obtained at the Center of Experimental and Applied Cutaneous Physiology, Charité – Universitätsmedizin Berlin, Germany. *Skin Pharmacol Physiol* 2008;21(3):150–5.
- [33] Gunther C, Kecskes A, Staks T, Tauber U. Percutaneous absorption of methylprednisolone aceponate following topical application of Advantan lotion on intact, inflamed and stripped skin of male volunteers. *Skin Pharmacol Appl Skin Physiol* 1998;11(1):35–42.
- [34] Korting HC, Zienicke H, Schafer-Korting M, Braun-Falco O. Liposome encapsulation improves efficacy of betamethasone dipropionate in atopic eczema but not in psoriasis vulgaris. *Eur J Clin Pharmacol* 1990;39(4):349–51.
- [35] Monteiro-Riviere NA, Wiench K, Landsiedel R, Schulte S, Inman AO, Riviere JE. Safety evaluation of sunscreen formulations containing titanium dioxide and zinc oxide nanoparticles in UVB sunburned skin: an in vitro and in vivo study. *Toxicol Sci* 2011;123(1):264–80.
- [36] Henkler F, Tralau T, Tentschert J, Kneuer C, Haase A, Platzek T, et al. Risk assessment of nanomaterials in cosmetics: a European union perspective. *Arch Toxicol* 2012;86(11):1641–6.
- [37] Deleted in review.
- [38] Chen LL, Ian T, Wang SQ. Nanotechnology in photoprotection. In: Nasir A, Adam F, Wang S, editors. *Nanotechnology in dermatology*, 1. New York: Springer; 2013. p. 9–18.
- [39] Newman MD, Stotland M, Ellis JI. The safety of nanosized particles in titanium dioxide- and zinc oxide-based sunscreens. *J Am Acad Dermatol* 2009;61(4):685–92.
- [40] Tan MH, Commens CA, Burnett L, Snitch PJ. A pilot study on the percutaneous absorption of microfine titanium dioxide from sunscreens. *Australas J Dermatol* 1996;37(4):185–7.
- [41] Pflücker F, Wendel V, Hohenberg H, Gärtner E, Will T, Pfeiffer S, et al. The human stratum corneum layer: an effective barrier against dermal uptake of different forms of topically applied micronised titanium dioxide. *Skin Pharmacol Appl Skin Physiol* 2001;14(Suppl. 1):92–7.
- [42] Schulz J, Hohenberg H, Pflücker F, Gärtner E, Will T, Pfeiffer S, et al. Distribution of sunscreens on skin. *Adv Drug Deliv Rev* 2002;54(Suppl.):S157–63.
- [43] Gottbrath SM-GC. Penetration and visualization of titanium dioxide microparticles in human stratum corneum: effect of different formulations on the penetration of titanium dioxide. *SOFW J* 2003;129(3):11–7.
- [44] Menzel F, Reinert T, Vogt J, Butz T. Investigations of percutaneous uptake of ultrafine TiO₂ particles at the high energy ion nanoprobe LIPSION. *Nucl Instr Methods Phys Res Section B* 2004;219–220(1–4):82–6.
- [45] Pirot F, Millet J, Kalia YN, Humbert P. In vitro study of percutaneous absorption, cutaneous bioavailability and bioequivalence of zinc and copper from five topical formulations. *Skin Pharmacol* 1996;9(4):259–69.
- [46] Lansdown ABG, Taylor A. Zinc and titanium oxides: promising UV-absorbers but what influence do they have on the intact skin? *Int J Cosmet Sci* 1997;19(4):167–72.
- [47] Dussert AS, Gooris E, Hemmerle J. Characterization of the mineral content of a physical sunscreen emulsion and its distribution onto human stratum corneum. *Int J Cosmet Sci* 1997;19(3):119–29.
- [48] Gamer AO, Leibold E, van Ravenzwaay B. The in vitro absorption of microfine zinc oxide and titanium dioxide through porcine skin. *Toxicol In Vitro* 2006;20(3):301–7.
- [49] Filipe P, Silva JN, Silva R, Cirne de Castro JL, Marques Gomes M, Alves LC, et al. Stratum corneum is an effective barrier to TiO₂ and ZnO nanoparticle percutaneous absorption. *Skin Pharmacol Physiol* 2009;22(5):266–75.
- [50] Mavon A, Miquel C, Lejeune O, Payre B, Moretto P. In vitro percutaneous absorption and in vivo stratum corneum distribution of an organic and a mineral sunscreen. *Skin Pharmacol Physiol* 2007;20:10–20.
- [51] Durand L, Habran N, Henschel V, Amighi K. In vitro evaluation of the cutaneous penetration of sprayable sunscreen emulsions with high concentrations of UV filters. *Int J Cosmet Sci* 2009;31:279–92.

Nanoemulsions to Prevent Photoaging

A. Aforali^{1,2}, M. Lorencini¹

¹Grupo Boticário, São José dos, Paraná, Brazil; ²The Pontifical Catholic University of Paraná (PUCPR), Curitiba, Paraná, Brazil

OUTLINE

Introduction	237	Nanoemulsions Applied for Prevention and Treatment of Photoaging	242
Skin Permeability	238	Conclusion	243
Skin Aging	239	Glossary	243
Antiaging Cosmetics	240	List of Acronyms and Abbreviations	244
Nanoemulsions	240	References	244
Other Nanocarriers: Liposomes, Nisosomes, and Dendrimers	242		

INTRODUCTION

Human skin is the outermost tissue of the body and is the largest organ in terms of both weight and surface area. Skin occupies approximately 16,000 cm² on adults and represents approximately 8% of an adult's body weight. Skin has a very complex structure in which cells, fibers, and other components form a multilayer architecture permeated by large networks of veins, capillaries, and nerves. Furthermore, skin appendages such as hair follicles can be observed in some regions, whose presence or absence determines the classification of skin as hairy or glabrous, respectively [1]. Skin has a wide variety of functions resulting from chemical and physical reactions that take place inside its structure, and from interactions that skin undergoes with external environments. The primary function of skin is to act as a remarkable and selective barrier [2,3] against foreign and potentially toxic compounds and organisms. Skin contributes to the regulation of body temperature, the maintenance of fluid balance, the prevention of

excessive water loss, and protection against pathogens, chemicals, and dangerous sunlight effects [4–6].

The skin structure is composed of two primary layers: the epidermis and the dermis. Subcutaneous tissue or adipose tissue is located adjacent to skin, and this tissue is occasionally described in the literature as a third skin layer. The epidermis is the outermost skin layer, consisting of a multilamellar structure that is formed by keratinocytes (~85% of total cells), melanocytes, Langerhans cells, and Merkel cells. As a very dynamic tissue, the epidermis undergoes continuous renewal via a constant process of peeling [7]. Keratinocytes proliferate in the innermost portion of the epidermis and undergo differentiation as they are pushed to the epidermal surface by the emergence of new cells in an ongoing process that requires approximately 4 weeks from start to finish [8]. Keratinocytes differentiation includes changes in the molecular and structural levels of the cells and in their function, resulting in a stratified epidermis composed of the basal layer, stratum spinosum, stratum granulosum, and stratum corneum (SC) [8,9].

The dermis is the inner portion of the skin, whose structure is rich in extracellular matrix (ECM) components, such as collagen and elastin, blood vessels, lymph vessels, and nerve endings. The dermis is responsible for physical and nutritional support of skin, representing approximately 90% of the thickness of the skin. The structure of the dermis varies according to the region of the body: the papillary dermis is more superficial, thin, and composed of loose connective tissue with more sparse fibers; the reticular dermis is deeper, thick, and composed of dense and irregular connective tissue with a more compact fibrillar structure. Fibroblasts represent the major cell type located in the dermis. These cells are responsible for the synthesis of several ECM components, including proteins and other elements of amorphous ground substance, such as interstitial fluid, complex glycosaminoglycans (GAGs), and proteoglycans. In addition, the dermis also contains immune defense cells, including dendritic cells, macrophages, and neutrophils [10].

Based on the knowledge of the original skin structure and considering the effects of aging on skin, this chapter reviews relevant aspects that may be considered for preventive or corrective therapeutic approaches. Specifically, this chapter focuses on functional aspects of skin permeability, photoaging-related cutaneous damages, and the application of nanotechnology in the search for more effective dermatological and/or cosmetic solutions.

SKIN PERMEABILITY

Human skin has evolved a barrier function that exhibits low permeability to foreign substances, protecting the body from environmental threats such as toxins, harmful chemicals, and microorganisms. The SC provides the most significant barrier to diffusion of molecules, and even against some nanometric inorganic particles [11,12]. In fact, *in vivo* studies have demonstrated that approximately 70% of different products applied to the skin do not cross the SC [13]. However, nanoparticles smaller than 40 nm in diameter exhibit good skin permeation [14,15]. Skin permeability also varies according to different types of nanoparticles: spherical particles appear to have a better ability to penetrate skin compared with ellipsoidal particles. A study comparing the two forms revealed that spherical particles were located deep in the epidermis and the dermis, whereas ellipsoidal particles were mainly located in the layers of the SC and the epidermis [15].

Penetration of an active ingredient into the skin includes diffusion through the intact epidermis and/or migration through skin appendages, such as hair follicles and sweat glands, which occupy 0.1% of the total human skin area and represent shunt routes for the passage of molecules [16]. The three primary mechanisms (Fig. 19.1) of crossing the intact skin

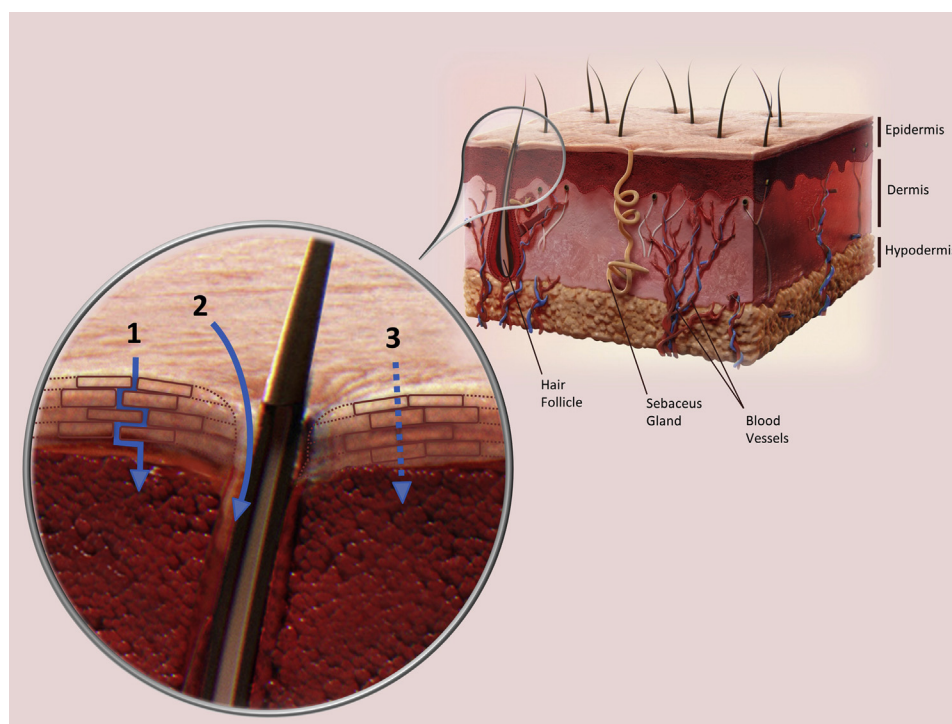


FIGURE 19.1 Skin barrier and the three possible penetration routes for topically applied substances: (1) intercellular; (2) follicular; and (3) transcellular.

barrier include: (1) intercellular; (2) transcellular; and (3) follicular routes. The intercellular lipid route refers to the passage of substances between corneocytes through interlamellar regions of the SC. In this case, fluid lipids are crucially important for the transepidermal diffusion of lipidic and amphiphilic molecules, whereas hydrophilic molecules diffuse predominantly “laterally” along surfaces of water-filled spaces or through free spaces between lamella and corneocyte outer membranes [17–19]. Transcellular routes involve molecules moving across corneocytes with their keratin-enriched intracellular macromolecular matrix and intervening lipids [20]. Although this route is considered a shorter path compared with intercellular routes, transcellular diffusion involves higher resistance to the passage of substances and therefore is not a feasible route for drug transportation [21]. Despite its relevance, follicular routes are often neglected because hair follicles represent only a small proportion of the total skin, but studies have reconsidered the efficiency of follicular routes [22–26]. Due to the morphological architecture of hair follicles, follicular penetration is a complex process that may have great potential for the absorption of substances below the skin surface.

Various factors influence percutaneous absorption of a topically applied product, such as skin age and anatomical site, skin temperature, peripheral circulation, the state of the skin, contact time, the degree of hydration, physicochemical properties of the product, and structural characteristics of the skin. Absorption is also influenced by external stimulation, such as iontophoresis, sonophoresis, electrical, and thermal stimuli or by suitable skin penetration enhancing agents [18]. The development of models to predict skin permeability is a fertile area that is highly relevant to the fields of transdermal drug delivery, the assessment of dermal exposure to industrial and environmental hazards, and understanding of different biotransport processes. New models have several parameters and are significantly more complex than simple permeability—molecular weight—partition coefficient relationships. Some approaches, including a combination of molecular orbital calculations with neural networks and random-walk models have been successfully employed to mathematically model skin permeability. Moreover, some models have also been proposed to explain the size dependence of skin permeation based on fundamental diffusion mechanisms [27]. With the advent of confocal Raman microscopy and other spectroscopic techniques, it is possible to model and interpret experimental concentration profiles of both the drug and the excipient *in vivo*, and to thereby analyze routes of drug penetration through the skin [27].

SKIN AGING

Skin aging is a complex biological process that is influenced by a combination of intrinsic factors (cellular metabolism, hormone, and metabolic processes) and extrinsic factors (chronic light exposure, pollution, ionizing radiation, chemicals, and toxins). These factors act synergistically, leading to cumulative structural and physiological alterations in the skin, and constant exposure to environmental aggressors accelerates or intensifies the process. Throughout one’s lifetime, especially after the mid-twenties, intrinsic structural changes in the skin occur as a natural consequence of aging and are generally genetically determined [28]. Major signs of intrinsic skin aging include diminished or defective synthesis of collagen and elastin in the dermis, resulting in thin, atrophic, finely wrinkled, and dry-aged cutaneous tissue. In aged skin, collapsed fibroblasts produce low levels of collagen and high levels of collagen-degrading enzymes. This imbalance promotes a self-perpetuating deleterious cycle of aging [28].

Extrinsic skin aging, also called photoaging, is most commonly caused by chronic exposure to ultraviolet (UV) radiation and is clinically characterized by deep coarse wrinkles, roughened skin, mottled pigmentation, and a marked loss of elastic recoil [29,30]. Histologically, photoaging causes epidermal thickening and significant remodeling of dermal ECM, affecting the molecular composition, architecture, and function of fibrillar collagens, elastic fibers, and GAGs [31]. In the first stage of aging, the thinnest fibers that occur in the more superficial dermis undergo fragmentation and lysis. In contrast, these thin fibers tend to thicken progressively in the deep dermis, which appears to be a compensatory mechanism to recover the resistance of the skin that becomes weaker at the surface. This process is thought to begin in parallel for the different distinct types of fibers but progresses faster in elastic fibers [32]. In addition, fragmentation of the fibers, a reduction in total collagen, and decreased cell-collagen fiber interactions also characterize aged skin [33,34]. Moreover, in solar-exposed areas, it is common to observe a build-up of dystrophic elastotic material and the accumulation of disorganized GAGs, most notably chondroitin sulfate and hyaluronic acid [35], within the deeper dermis. Additionally, the accumulation of reactive oxygen species (ROS) and aging-related oxidative stress contribute to the development of a senile skin phenotype characterized by chronic inflammatory activity and the development of melanoses, telangiectasia, poikiloderma, actinic keratoses, and malignant tumors [36,37].

A number of mechanisms have been proposed to explain dermal photoaging, and the most widely documented involves matrix metalloproteinase (MMP)

driven degradation. UV radiation increases the synthesis and activity of MMPs without affecting the production of tissue inhibitors of MMPs (TIMPs) [38]. UV-induced ROS play a role in dermal remodeling, and can potentially act as signaling intermediates that lead to the activation of MMP-1, -3, and -9 [39]. UV radiation may preferentially degrade proteins rich in UV-absorbing amino acids or other chromophores, driving some of the early photoaging events, such as the specific loss of the microfibril components fibrillin-1 and fibulin-5 from the papillary dermis [40–42]. UV radiation is also absorbed by DNA in the nuclei of cutaneous cells, producing various types of damage, including DNA strand breaks, sister chromatid exchange, DNA-protein crosslinks, sugar damage, a basic site, and base modifications. Cell death, chromosome changes, mutation, and morphological transformations are observed after cellular exposure to UV radiation [43].

ANTIAGING COSMETICS

Skin appearance is a primary indicator of chronological age. As the world population ages, skin aging considerations become increasingly important to individuals, contributing to confidence in their social lives. Leathery or wrinkly skin is associated with an older look, whereas smooth and supple skin suggests a younger appearance [44]. In this sense, antiaging skin-care cosmetics represent an alternative for quality-of-life improvements and improvements in appearance leading to better social inclusion [45].

Classical cosmetics include products that are intended to be rubbed, poured, sprinkled, sprayed, introduced, or otherwise applied to the human body or to any part thereof, for cleansing, beautifying, promoting attractiveness, or altering the appearance [46]. However, currently, skin treatment products are

intended not only to enhance a person's youthful appearance, but also to go toward meeting new standards of personal hygiene and health. Specifically, antiaging cosmetics remove aging signs from human skin, helping to reduce the appearance of wrinkles and increase cutaneous moisturization [45,47].

Emulsions, such as creams and lotions, are the most common type of formulation system used in cosmetics. An emulsion can be defined as a mixture of two or more immiscible phases with a third component (an emulsifier) to stabilize the dispersed droplets. Various types of emulsions are available: oil-in-water (O/W), water-in-oil (W/O), water-in-water (W/W) and oil-in-oil (O/O) [48]. Although emulsions typically enable the convenient delivery of antiaging active compounds to the skin, nanotechnology is a promising alternative to increase the efficacy of specific ingredients [47,49]. In particular, the moderate use of emulsifier concentrations in nanoemulsions is attracting attention in fields, such as cosmetics and pharmaceuticals [50].

NANOEMULSIONS

A nanoemulsion (Fig. 19.2) is a transparent or translucent system that generally includes particles that range in diameter from 20 to 500 nm [51]. Nanoemulsions are also called mini-emulsions, fine-disperse emulsions, submicron emulsions, or unstable microemulsions [50]. Due to the small droplet size, the Brownian motion of nanoemulsions is sufficiently high to overcome the physical destabilization caused by gravitational separation, flocculation, and/or coalescence [52–55]. Due to their long-term physical stability, nanoemulsions have been occasionally described as “approaching thermodynamic stability” [56,57]. When the maximum droplet size of an emulsion is less than 80 nm, it exhibits particular properties compared with conventional emulsions,

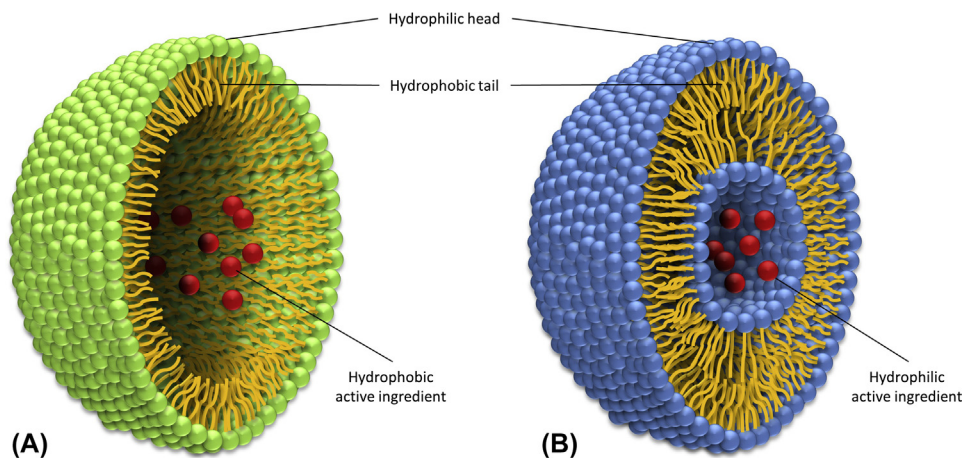


FIGURE 19.2 Nanocarriers system: (A) nanoemulsion (O/W); and (B) liposome.

such as optical transparency, high colloidal stability, and a large interfacial area-to-volume ratio [56]. Nanoemulsions are stable under temperature changes and/or dilutions; therefore, they are considered better nanocarriers compared with other emulsion systems [58,59]. Moreover, additional advantages of nanoemulsion include increased interest in research, and applications in personal care, health care, and cosmetics [60], such as rapid penetration of active ingredients through skin due to their large surface area; high aesthetic value due to their transparent appearance and lack of thickeners; the requirement of a very low emulsifier concentration; and uniform deposition on substrates due to their wetting, spreading, and penetration properties.

Two mechanisms are available to carry ingredients in nanoemulsions to the site of action (Figs. 19.3 and 19.4): (1) passive targeting and (2) active targeting. Passive or natural targeting corresponds to the normal distribution of a nanoemulsion according to the pattern of the molecules present at the surface of the particles, mostly composed of phospholipids or phospholipids and sterols [61–63]. In active targeting, molecular surfaces are altered via the insertion of charged lipids or the attachment of specific ligands, including proteins, peptides, polysaccharides, glycolipids, glycoproteins, and monoclonal antibodies, such that the normal distribution pattern of the nanoemulsion is modified and directed to specific target sites in a process called functionalization. This process not only enhances the therapeutic effect of the loaded active ingredient but also minimizes the side effects associated with its large and unspecific distribution [50]. Surface coating with polyethylene glycol (PEG) also contributes to active targeting strategies, prolonging the half-life of developed formulations.

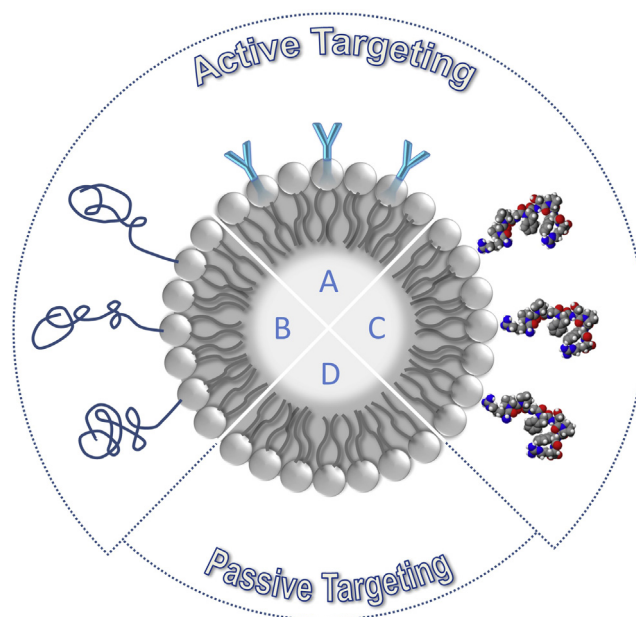


FIGURE 19.4 Different types of nanoemulsion's surface targeting: (A) antibodies; (B) propylene glycol; and (C) peptides. (D) illustrates the naked nanoemulsion's surface.

Several methods can be used to functionalize nanoparticles, thus providing different benefits.

Nanoemulsions were recently confirmed as good vehicles for the controlled delivery of cosmetics and for the optimized dispersion of active ingredients in particular skin layers or cells. Moreover, nanoemulsions are also recognized for their own intrinsic bioactive effects, such as reinforcement of barrier functions and the reduction of transepidermal water loss (TEWL). The incorporation of potentially irritating surfactants

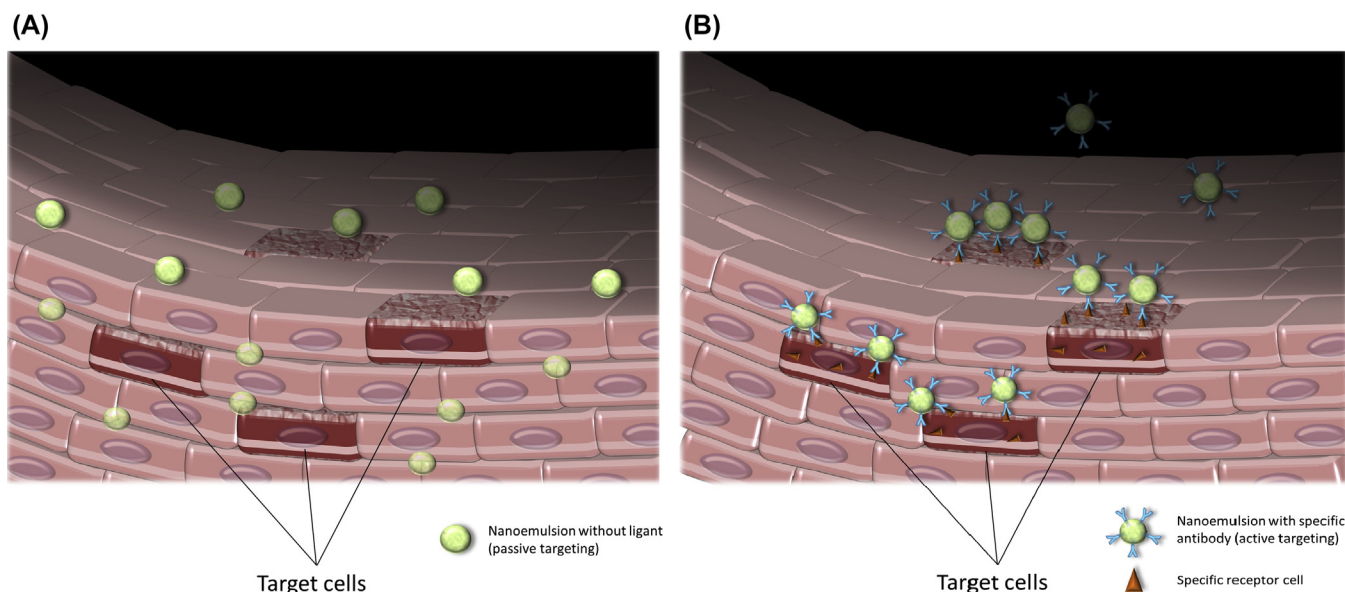


FIGURE 19.3 Nanoemulsion mechanisms of action: (A) passive targeting; and (B) active targeting.

can be avoided using high-energy equipment during the manufacturing process. PEG-free nanoemulsions for cosmetics have also been developed, and the formulations exhibited good stability.

OTHER NANOCARRIERS: LIPOSOMES, NIOSOMES, AND DENDRIMERS

Liposomes are vesicular structures with an aqueous core surrounded by a hydrophobic lipid bilayer created by the extrusion of phospholipids (Fig. 19.2). Liposomes are widely known cosmetic delivery systems and can vary in size from 15 nm up to several μm . Depending on the vesicles size and the number of bilayers, liposomes can be classified as small unilamellar vesicles and large unilamellar vesicles (containing a single bilayer) or multilamellar (multilayered) vesicles. The first liposomal cosmetic product, an antiaging cream, was launched onto the market in 1986. Since then, several other cosmetic companies have utilized liposomal technology, including those that produce hair products, after-shave, lipstick, sunscreen, and makeup [64]. Phosphatidylcholine is a common ingredient of liposomes that is widely used in skin care products and shampoos due to its softening and conditioning properties. Liposomes also facilitate the continuous supply of agents to cells and provide a reservoir for ingredients allowing sustained and controlled release, making liposomes an ideal candidate for the controlled delivery of vitamins and other molecules. Skin care preparations with empty or moisture-loaded liposomes reduce TEWL, supply lipids, and water to the SC and consequently combat dry skin [64].

Niosomes are vesicles composed of nonionic surfactants that have been mainly studied for their advantages compared with liposomes, including increased chemical stability and reduced manufacturing costs. In addition, niosomes do not require any special conditions for preparation and storage and are not associated with purity problems [64]. Regarding skin care applications, niosomes increase the stability of entrapped active compounds, improve the bioavailability of poorly absorbed ingredients, and enhance skin penetration. The first cosmetic product containing niosomes was manufactured in 1987. Other cosmetic applications based on niosomes are characterized by increased photostability for tretinoin and optimized delivery of ascorbylpalmitate and estradiol to the skin [64].

Dendrimers, which is a word derived from the Greek word “dendron” meaning tree, are monodisperse and repetitively branched molecules that conjugate with numerous functional groups. After the creation of a core, a series of stepwise cycles of syntheses (known as generations), are carried out by the consecutive addition

of monomers. This approach allows for an iterative synthesis, providing the ability to control both molecular weight and architecture such that the classification of dendrimers is based on specifying the number of generations. In addition, the use of branched monomers provides the opportunity for tailored “handles” for attachment of site-specific molecular recognition ligands and for encapsulation. Dendrimers can have a high surface-charge density due to the presence of ionizable groups that can bind active compounds via electrostatic forces. Furthermore, dendrimers can be positively or negatively charged, thus allowing them to complex with different types of active ingredients [64].

NANOEMULSIONS APPLIED FOR PREVENTION AND TREATMENT OF PHOTOAGING

Significant alterations in the skin caused by photoaging involve changes in tissue hydrophobicity, in mechanical properties, and in general appearance. Ribeiro and colleagues [65] demonstrated that O/W nanoemulsions containing 1% of *Opuntia ficus-indica* (L.) Mill hydroglycolic extract increased water content in the SC for 5 h and led to a significant difference compared with the vehicle formulation alone, indicating that the nanoemulsion was stable and efficient for cosmetic applications. Extract compositions rich in carbohydrates, such as galacturonic acid, glucose, rhamnose, and arabinose, associated with a nanoemulsion suggested a humectant and nonocclusion mechanism for skin hydration [65]. When loaded with C_{60} fullerene, a compound that acts as a strong free radical scavenger with better performance than natural antioxidants, nanoemulsions provided protection and regenerative effects against ROS-induced collagen breakdown in human skin [66–69]. Moreover, fullerene nanoemulsions exhibited other striking results: a high physicochemical stability against creaming and thermal stress after a storage period of 90 days; no cytotoxicity against 3T3 cells up to a concentration of 1000 mg/mL; a significant increase in skin hydration and TEWL reduction after 28 days of treatment; no dermal irritation; and a potential to increase dermal collagen content in an in vivo study [69].

Few articles have compared the drug delivery abilities and penetration enhancement attributes of various lipid-based colloidal carriers [70–72]. Retinoids, including vitamin A, retinyl palmitate, and other derivatives, are promising for dermatological disorders, such as photoaging, severe acne, and skin inflammation [73–75]. However, high lipophilicity or instability to oxidation, heat, light, moisture, and metals limits the use of retinoids in several formulations [76–79]. In this context, interest in lipid nanocarriers has increased

substantially due to their enhanced efficiency, reduction of irritant effects, immunogenic responses, and the intrinsic instability of retinoids [80]. Several lipid nanocarriers have been extensively studied for retinoid delivery with promising results [78]. The use of vitamin A in the form of fatty acid esters instead of as free retinol increases nanocarrier stability against oxidation [81]. Retinyl palmitate oil is the most stable form of vitamin A and plays an important role in cellular differentiation, epidermal thickening, and carcinogenesis prevention [82–85]. Clares and colleagues [86] compared the efficiency of solid lipid nanoparticles, liposomes, and a nanoemulsion for transportation of retinyl palmitate. Although all the nanocarriers were biocompatible, the nanoemulsions were associated with the highest retinyl palmitate permeation, reaching deeper skin layers [86]. Afornali and colleagues [49] also investigated the influence of retinoids on biological processes related to skin aging, and compared the effect of different retinoids and different delivery systems on cutaneous gene expression. When retinoids were associated with nanoemulsions, the results revealed an increased tretinoin-induced antiinflammatory response in *ex vivo* skin compared with other retinoids. Additionally, treatment using nanoemulsions associated with retinol microcapsules induced biological processes related to protection against oxidative stress reactions, ECM lipid metabolism, and cell proliferation compared with a leading commercial product (tretinoin or microencapsulated retinol, used separately). Nanoemulsion-retinoids have emerged as a new possibility for the treatment and prevention of skin aging.

Solar filters are another category of ingredients that can be effectively applied with nanoemulsions to prevent skin photoaging. They are designed for topical applications to protect skin against UV radiation. However, many are toxic substances that should be retained in the skin and prevented from reaching the bloodstream. The lipophilic nature of many UV filter molecules may cause bioaccumulation in humans and animals, with reported adverse side-reactions, including allergic and irritant contact dermatitis, phototoxic and photoallergic reactions, contact urticaria, and isolated cases of severe anaphylactic reactions [87]. The application of organic UV filters, such as benzophenone-3, diethylamino hydroxybenzoyl hexylbenzoate, octocrylene, and octylmethoxycinnamate, in nanoemulsions containing pomegranate extract and chitosan exhibited stability for at least 6 months, showed photostability when irradiated in a solar simulator and had effective photoprotective and antioxidant activities. Additionally, chitosan promoted the retention of nanoemulsion formulations in the epidermis, thus increasing their formulation safety [88]. Another important consideration is that sunscreen nanoemulsions may enhance

UV radiation protection without increasing the amount of organic UV filters. Nikolić and colleagues [89] optimized sunscreen formulations based on lipid nanoparticles and reported improved sun protection factor (SPF) values while maintaining constant active concentrations. For the mixture of three different UV filters used in this experiment, bis-ethylhexyloxyphenol methoxyphenyl triazine, ethylhexyl triazone, and ethylhexyl methoxycinnamate carnauba wax, nanostructured lipid carriers exhibited the best results, increasing SPF values by greater than 45% for the same concentrations of organic UV filters compared with beeswax and a reference emulsion [89].

CONCLUSION

There are currently two primary uses for nanotechnology in cosmetics: the development of nanoparticles, such as can be used for UV filters, and the improvement of the delivery of active treatments to the skin. Different formulation technologies may serve as supplementary tools to offer highly effective products for hydration, the reduction of signs of aging, and skin protection against injury from daily exposure to external factors [47]. Nanoemulsions constitute one of the most promising systems for improving the solubility and functionality of active ingredients applied to cosmetic formulations. In addition to increasing skin permeation, nanoemulsions can improve the delivery of agents to the desired target sites (also referred to as smart carrier systems) and increase the efficacy of active ingredients. Better sensorial and positive economic aspects of nanoemulsions must also be taken into consideration when compared with traditional emulsions.

Although not a recent scientific topic, the promising applications of nanoemulsions have been suggested in several research publications. Further studies are needed, including evaluation of a wide range of active compounds that can be carried, and the elucidation of the complete benefits of nanoemulsions for skin aging treatments. Therapeutic approaches based on targeted functionalization can also minimize side effects through the specific directed delivery of ingredients and consequent toxicity reduction. The application of nanotechnology to the development of cosmetics can significantly improve safety and efficacy of products, which aligns with market requirements and longer life expectancies of the worldwide aging population.

Glossary

3T3 cell Murine fibroblast cell line.

Amphiphilic A term describing a chemical compound possessing both hydrophilic and lipophilic properties.

Brownian motion Random motion of particles suspended in a fluid resulting from their collision with the quick atoms or molecules in the gas or liquid.

Chromophores A molecule that absorbs certain wavelengths of visible light and transmits or reflects others.

Coalescence Process in which two phase domains of the same composition come together and form a larger phase domain.

Corneocytes Terminally differentiated keratinocytes.

Emulsifier A surface-active agent promoting the formation and stabilization of an emulsion.

Extracellular matrix A collection of extracellular molecules secreted by cells that provide structural and biochemical support to the surrounding cells.

Iontophoresis Physical process in which ions flow diffusively in a medium driven by an applied electric field.

Sonophoresis The application of ultrasound to assist the adsorption of topical medicine through the skin.

List of Acronyms and Abbreviations

ECM Extracellular matrix
GAG Glycosaminoglycans
MMP Matrix metalloproteinase
Nm Nanometers
O/O Oil-in-oil
O/W Oil-in-water
PEG Propylene glycol
ROS Reactive oxygen species
SPF Sun protection factor
TEWL Transepidermal water loss
TIMPs Tissue inhibitors of MMPs
UV Ultraviolet
W/O Water-in-oil
W/W Water-in-water
µm Micrometers

References

- [1] Marks JG, Miller J. Lookingbill and Marks' principles of dermatology. 4th ed. Elsevier Inc.; 2006.
- [2] Mithal BM, Saha RN. A handbook of cosmetics. 1st ed. New Delhi: Vallabh Prakashan; 2006. p. 12–7.
- [3] Costin GE, Hearing VJ. Human skin pigmentation: melanocytes modulate skin color in response to stress. *FASEB J* 2007;21:976–94.
- [4] Hussein MR. Ultraviolet radiation and skin cancer: molecular mechanisms. *J Cutan Pathol* 2005;32:191–205.
- [5] Svobodova A, et al. Ultraviolet light induced alteration to the skin. *Biomed Pap Med Fac Univ Palacky Olomouc Czech Repub* 2006; 150:25–38.
- [6] Palma MD, et al. Update on photoprotection. *Dermatol Ther* 2007; 20:360–76.
- [7] Milstone LM. Epidermal desquamation. *J Dermatol Sci* 2004;36(3): 131–40.
- [8] Fuchs E, et al. Getting under the skin of epidermal morphogenesis. *Nat Rev Genet* 2002;3(3):199–209.
- [9] Simpson CL, et al. Deconstructing the skin: cytoarchitectural determinants of epidermal morphogenesis. *Nat Rev Mol Cell Biol* 2011;12(9):565–80.
- [10] Farage MA, et al. Psychological and social implications of aging skin: normal aging and the effects of cutaneous disease. In: Farage MA, Miller KW, Maibach HI, editors. *Textbook of aging skin*. Heidelberg: Springer; 2010.
- [11] Johnson ME, et al. Evaluation of solute permeation through the stratum corneum: lateral bilayer diffusion as the primary transport mechanism. *J Pharm Sci* 1997;86(10):1162–72.
- [12] Alvarez-Román R, et al. Skin penetration and distribution of polymeric nanoparticles. *J Control Release* 2004;99(1):53–62.
- [13] Baroli B. Penetration of nanoparticles and nanomaterials in the skin: fiction or reality? *J Pharm Sci* 2009;99:21–50.
- [14] Ryman-Rasmussen JP, et al. Penetration of intact skin by quantum dots with diverse physicochemical properties. *Toxicol Sci* 2006; 91(1):159–65.
- [15] Sonavane G, et al. In vitro permeation of gold nanoparticles through rat skin and rat intestine: effect of particle size. *Colloids Surf B Biointerfaces* 2008;65(1):1–10.
- [16] Illel B. Formulation for transfollicular drug administration: some recent advances. *Crit Rev Ther Drug Carrier Syst* 1997;14(3): 207–19.
- [17] Cevc G. Drug delivery across the skin. *Expert Opin Investig Drugs* 1997;6(12):1887–937.
- [18] Xiang TX, Anderson BD. Influence of chain ordering on the selectivity of dipalmitoylphosphatidylcholine bilayer membranes for permeant size and shape. *Biophys J* 1998;75(6):2658–71.
- [19] Geinoz S, et al. Quantitative structure-permeation relationships (QSPeRs) to predict skin permeation: a critical evaluation. *Pharm Res* 2004;21(1):83–92.
- [20] Potts RO, Guy RH. Predicting skin permeability. *Pharm Res* 1992; 9(5):663–9.
- [21] Mitragotri S. Modeling skin permeability to hydrophilic and hydrophobic solutes based on four permeation pathways. *J Control Release* 2003;86(1):69–92.
- [22] Meidan V, et al. Low intensity ultrasound as a probe to elucidate the relative follicular contribution to total transdermal absorption. *Pharm Res* 1998;15(1):85–92.
- [23] Ogiso T, et al. Transfollicular drug delivery: penetration of drugs through human scalp skin and comparison of penetration between scalp and abdominal skins in vitro. *J Drug Target* 2002; 10(5):369–78.
- [24] Dokka S, et al. Dermal delivery of topically applied oligonucleotides via follicular transport in mouse skin. *J Invest Dermatol* 2005;124(5):971–5.
- [25] Grams YY, et al. On-line diffusion profile of a lipophilic model dye in different depths of a hair follicle in human scalp skin. *J Invest Dermatol* 2005;125(4):775–82.
- [26] Teichmann A, et al. Semiquantitative determination of the penetration of a fluorescent hydrogel formulation into the hair follicle with and without follicular closure by microparticles by means of differential stripping. *Skin Pharmacol Physiol* 2006;19(2): 101–5.
- [27] Mitragotri S, et al. Mathematical models of skin permeability: an overview. *Int J Pharm* 2011;418(1):115–29.
- [28] Joshi B, et al. Antiaging cosmetics. *J Drug Del Ther* 2013;3(3): 158–62.
- [29] Smith JG, et al. Alterations in human dermal connective tissue with age and chronic sun damage. *J Invest Dermatol* 1962;39: 347–50.
- [30] Warren R, et al. Age, sunlight, and facial skin: a histologic and quantitative study. *J Am Acad Dermatol* 1991;25:751–60.
- [31] El-Domyati M, et al. Intrinsic aging vs. photoaging: a comparative histopathological, immunohistochemical, and ultra-structural study of skin. *Exp Dermatol* 2002;11:398–405.
- [32] Bonta M, et al. The process of ageing reflected by histological changes in the skin. *Rom J Morphol Embryol* 2013;54(3): 797–804.
- [33] Oikarinen A, et al. A biochemical and immunohistochemical study of collagen in sun-exposed and protected skin. *Photodermatol* 1989;6:24–31.
- [34] Varani J, et al. Decreased collagen production in chronologically aged skin: roles of age-dependent alteration in fibroblast function and defective mechanical stimulation. *Am J Pathol* 2006;168(6): 1861–8.

- [35] Bernstein EF, et al. Chronic sun exposure alters both the content and distribution of dermal glycosaminoglycans. *Br J Dermatol* 1996;135:255–62.
- [36] Dröge W. Aging-related changes in the thiol/disulfide redox state: implications for the use of thiol antioxidants. *Exp Gerontol* 2002;37(12):1333–45.
- [37] Caruso C, et al. Aging, longevity, inflammation, and cancer. *Ann N Y Acad Sci* 2004;1028:1–13.
- [38] Fisher GJ, et al. Molecular basis of sun-induced premature skin ageing and retinoid antagonism. *Nature* 1996;379:335–9.
- [39] Wlaschek M, et al. Solar UV irradiation and dermal photoaging. *J Photochem Photobiol B* 2001;63:41–51.
- [40] Kadoya K, et al. Fibulin-5 deposition in human skin: decrease with ageing and ultraviolet B exposure and increase in solar elastosis. *Br J Dermatol* 2005;153:607–12.
- [41] Watson R, et al. Damage to skin extra-cellular matrix induced by UV exposure. *Antioxid Redox Signal* 2014;21(7):1063–77.
- [42] Bradlec EJ, et al. Over-the-counter anti-ageing topical agents and their ability to protect and repair photoaged skin. *Maturitas* 2015;80:265–72.
- [43] Poljsak B, Dahmane R. Free radicals and extrinsic skin aging. *Dermatol Res Pract* 2012;2012:4.
- [44] Draelos ZD. What is anti-aging? *J Cosmet Dermatol* 2007;6:73–4.
- [45] Sharma B, Sharma A. Future prospect of nanotechnology in development of antiageing formulations. *Int J Pharm Pharm Sci* 2012;4(3):57–66.
- [46] Harry RG. In: Wilkinson JB, Clark R, Green E, McLaughlin TP, editors. *Modern cosmeticology*, vol. 1 (revision). London: Leonard Hill Ltd.; 1962.
- [47] Lorencini M, et al. New perspectives in the control of the skin aging process. In: Barel AO, Paye M, Maibach HI, editors. *Handbook of cosmetic science and technology*. 4th ed. Boca Raton: CRC Press; 2014. p. 245–50.
- [48] Tadros TF, Vincent B. *Encyclopedia of emulsion technology*. New York: Marcel Dekker; 1983.
- [49] Afornali A, et al. Triple nanoemulsion potentiates the effects of topical treatments with microencapsulated retinol and modulates biological processes related to skin aging. *An Bras Dermatol* 2013;88(6):930–6.
- [50] Liu W, et al. Formation and stability of paraffin oil-in-water nano-emulsions prepared by the emulsion inversion point method. *J Colloid Interf Sci* 2006;303:557–63.
- [51] Sole I, et al. Optimization of nano-emulsion preparation by low-energy methods in an ionic surfactant system. *Langmuir* 2006;22:8326–32.
- [52] Elaasser MS, et al. The miniemulsification process – different form of spontaneous emulsification. *Colloids Surf* 1988;29:103–18.
- [53] Benita S, Levy MY. Submicron emulsions as colloidal drug carriers for intravenous administration: comprehensive physicochemical characterization. *J Pharm Sci* 1993;82:1069–79.
- [54] Forgiarini A, et al. Formation of nano-emulsions by low-energy emulsification methods at constant temperature. *Langmuir* 2001;17:2076–83.
- [55] Morales D, et al. A study of the relation between bicontinuous microemulsions and oil/water nano-emulsion formation. *Langmuir* 2003;19:7196–200.
- [56] Tadros T, et al. Formation and stability of nano-emulsions. *Adv Colloid Interface Sci* 2004;99:303–18.
- [57] Bouchemal K, et al. Nano-emulsion formulation using spontaneous emulsification: solvent, oil and surfactant optimisation. *Int J Pharm* 2004;280:241–51.
- [58] Pouton CW. Formulation of self-emulsifying drug delivery systems. *Adv Drug Deliv Rev* 1997;25:47–58.
- [59] Anton N, Vandamme TF. Nano-emulsions and micro-emulsions: clarifications of the critical differences. *Pharm Res* 2011;28:978–85.
- [60] Guy R. *Transdermal drug delivery*. 2a ed. New York (USA): Marcel Dekker; 2003.
- [61] Santos N, Castanho M. Liposomes: has the magic bullet hit the target? *Quim Nova* 2002;25:1181–5.
- [62] Essa EA, et al. Human skin sandwich for assessing shunt route penetration during passive and iontophoretic drug and liposome delivery. *J Pharm Pharmacol* 2002;54(11):1481–90.
- [63] Bauer KH, et al. *Lehrbuch der pharmazeutischen technologie*. Stuttgart (Germany): Wissenschaftliche Verlagsgesellschaft mbH; 2012. 9 Auflage.
- [64] Patravale VB, Mandawgade SD. Novel cosmetic delivery systems: an application update. *Int J Cosmet Sci* 2008;30(1):19–33.
- [65] Ribeiro RCA, et al. Production and characterization of cosmetic nanoemulsions containing *Opuntia ficus-indica* (L.) mill extract as moisturizing agent. *Molecules* 2015;20:2492–509.
- [66] Wang IC, et al. C₆₀ and water-soluble fullerene derivatives as antioxidants against radical-initiated lipid peroxidation. *J Med Chem* 1999;42:4614–20.
- [67] Cataldo F. Solubility of fullerenes in fatty acids esters: a new way to deliver in vivo fullerenes. Theoretical calculations and experimental results. In: Cataldo F, Ros T, editors. *Medicinal chemistry and pharmacological potential of fullerenes and carbon nanotubes*. (Netherlands): Springer; 2008. p. 317–35.
- [68] Cataldo F. Interaction of C₆₀ fullerene with lipids. *Chem Phys Lipids* 2010;163:524–9.
- [69] Ngan CL, et al. Skin intervention of fullerene-integrated nanoemulsion in structural and collagen regeneration against skin aging. *Eur J Pharm Sci* 2015;70:22–8.
- [70] Doktorovova S, et al. Nanotoxicology applied to solid lipid nanoparticles and nanostructured lipid carriers – a systematic review of in vitro data. *Eur J Pharm Biopharm* 2014;87:1–18.
- [71] Raza K, et al. Nanolipoidal carriers of tretinoin with enhanced percutaneous absorption, photo-stability, biocompatibility and anti-psoriatic activity. *Int J Pharm* 2013;456:65–72.
- [72] Souza JG, et al. Topical delivery of ocular therapeutics: carrier systems and physical methods. *J Pharm Pharmacol* 2014;66:507–30.
- [73] Kim MS, et al. The effects of a novel synthetic retinoid, seletinoid G, on the expression of extracellular matrix proteins in aged human skin in vivo. *Clin Chim Acta* 2005;362:161–9.
- [74] Yamaguchi Y, et al. Successful treatment of photo-damaged skin of nano-scale atRA particles using a novel transdermal delivery. *J Control Release* 2005;104:29–40.
- [75] Suggs A, et al. Effect of botanicals on inflammation and skin aging: analyzing the evidence. *Inflamm Allergy Drug Targets* 2014;13:168–76.
- [76] Martins S, et al. Lipid-based colloidal carriers for peptide and protein delivery – liposomes versus lipid nanoparticles. *Int J Nanomedicine* 2007;2(4):595–607.
- [77] Eskandar NG, et al. Chemical stability and phase distribution of all-trans-retinol in nanoparticle-coated emulsions. *Int J Pharm* 2009;376:186–94.
- [78] Jeon HS, et al. A retinyl palmitate-loaded solid lipid nanoparticle system: effect of surface modification with dicetyl phosphate on skin permeation in vitro and anti-wrinkle effect in vivo. *Int J Pharm* 2013;452:311–20.
- [79] Abbasi A, et al. Stability of vitamin D₃ encapsulated in nanoparticles of whey protein isolate. *Food Chem* 2014;143:379–83.
- [80] Müller RH, et al. Solid lipid nanoparticles (SLN) and nanostructured lipid carriers (NLC) in cosmetic and dermatological preparations. *Adv Drug Deliv Rev* 2002;54:131–55.
- [81] Halbaut L, et al. Oxidative stability of semisolid excipient mixtures with corn oil and its implication in the degradation of vitamin A. *Int J Pharm* 1997;147:31–40.
- [82] Kurlandsky SB, et al. Auto-regulation of retinoic acid biosynthesis through regulation of retinol esterification in human keratinocytes. *J Biol Chem* 1996;271:15346–52.

- [83] Hansen LA, et al. Retinoids in chemoprevention and differentiation therapy. *Carcinogenesis* 2000;21:1271–9.
- [84] Shapiro SS, et al. Vitamin A and its derivatives in experimental photocarcinogenesis: preventive effects and relevance to humans. *J Drugs Dermatol* 2013;12:458–63.
- [85] Wang SQ, et al. Safety of retinyl palmitate in sunscreens: a critical analysis. *J Am Acad Dermatol* 2010;63:903–6.
- [86] Clares B, et al. Nanoemulsions (NEs), liposomes (LPs) and solid lipid nanoparticles (SLNs) for retinyl palmitate: effect on skin permeation. *Int J Pharm* 2014;473(1–2):591–8.
- [87] Lautenschlager S, et al. Photoprotection. *Lancet* 2007;370:528–37.
- [88] Cerqueira-Coutinho C, et al. Development of a photoprotective and antioxidant nanoemulsion containing chitosan as an agent for improving skin retention. *Eng Life Sci* 2015;1:1–12.
- [89] Nikolić S, et al. Skin photoprotection improvement: synergistic interaction between lipid nanoparticles and organic UV filters. *Int J Pharm* 2011;414(1–2):276–84.

Decoupling Hazard From Risk in Using Sunscreens Containing Metal Oxide Nanoparticles

M.J. Osmond-McLeod

CSIRO, North Ryde, NSW, Australia

OUTLINE

Introduction	247	Skin Barrier Disruption May Facilitate Low Levels of Nanoparticle Penetration	250
Decoupling In Vitro Nanotoxicity From Risk to Human Health	248	The Impact of Particle Characteristics on Nanoparticle Entry Through Skin Is Equivocal	252
Ex Vivo Studies Investigating the Passage of Nanoparticles Through Healthy Intact Skin Show Little to No Particle Penetration	248	Remaining Knowledge Gaps	252
In Vivo Studies Investigating the Passage of Nanoparticles Through Skin Highlight Variables That May Influence Nanoparticle Penetration	249	Conclusions	253
Particle/Ion Penetration Is More Likely to Occur With Longer Exposure Durations, Albeit Still at Very Low Levels	249	List of Acronyms and Abbreviations	254
		Glossary	254
		References	254

INTRODUCTION

Novel quantum-mechanical and physicochemical properties that can arise in materials at the nanoscale have been key to their increasing use in a range of new technologies, collectively referred to as nanotechnologies. The application of nanotechnologies to areas such as next-generation materials, pharmaceuticals, and the computing sector has met with relatively little consumer resistance. In contrast, nanotechnology-linked advances in products such as cosmetics and foods have focused attention on the question of whether new properties in materials engineered at the scale of

biological molecules might lead to unanticipated outcomes for human health and the environment.

Over recent decades, the intentional incorporation of metal oxide particles engineered at the nano-scale into sunscreen formulations has allowed consumers the option to choose highly effective, lightweight, and transparent topical barriers to prevent the damaging biological effects associated with prolonged sun exposure. Despite these benefits, however, an early conflation of in vitro toxicity, for example, the extrapolation [1,2] of damage under in vitro conditions to cells [3] unlikely to meet sunscreen nanoparticles under normal conditions of use, with a generalized risk to human health from

using sunscreens containing metal oxide nanoparticles resulted in consumer confusion about relative risk and safety [4] and, in some cases [5], active avoidance of these sunscreens.

Fortunately, collaborative research efforts over the past decade have resulted in an increasingly robust evidence-based framework supporting the safety of nanoparticles in sunscreens. A consensus is being reached that metal oxide nanoparticles in topically applied sunscreens are effective in protecting human skin from ultraviolet radiation (UVR), and are safe to use [6–10]. The aim behind this chapter is to summarize the evidence underlying this consensus, but to also highlight where continuing research efforts in this space might be effectively directed to close remaining knowledge gaps. Although cerium dioxide has shown recent promise as a UVR protective agent [11–13], the metal oxide nanoparticles used in sunscreens are most commonly titanium dioxide (TiO_2) or zinc oxide (ZnO), and therefore they will be the focus of this chapter.

DECOUPLING IN VITRO NANOTOXICITY FROM RISK TO HUMAN HEALTH

Particles of TiO_2 and ZnO have a long history of safe use in consumer products, typified by the “white zinc on the nose” sunscreens. However, when nano-sized particles of TiO_2 and ZnO were shown to be transparent and lightweight on the skin without compromising UVR-blocking efficacy, they began to be intentionally incorporated into sunscreen formulations. The question then arose as to whether the regulation of TiO_2 and ZnO nanoparticles in sunscreens should be assessed under the existing profiles for non-nano TiO_2 and ZnO , or considered as new chemicals, particularly in light of studies suggesting that nano-sized TiO_2 and ZnO were cytotoxic and/or genotoxic in vitro [14–16].

With respect to sunscreen, however, the critical point is less about the intrinsic toxicity of TiO_2 and ZnO nanoparticles and more about whether they can pass through the stratum corneum following topical application to reach the viable dermis, at which point the cell toxicity would become more relevant. Even then, it is also important to consider the toxicity of particles as they are commonly used in sunscreens. For example, ZnO and TiO_2 particles are typically coated (eg, with methicone, silica, or aluminum hydroxide) [17] to improve their dispersability in sunscreen formulations and/or reduce photocatalytic activity. These coatings have the additional benefit of decreasing intrinsic particle toxicity. For example, comprehensive in vitro work from our laboratory using human multipotent olfactory

[18] and primary hepatic stellate [19] cells showed that coating ZnO nanoparticles with silicon derivatives substantially mitigated the cellular stress responses induced by treatment with uncoated ZnO nanoparticles, as measured by multiple cell-signaling pathways, cellular functions, and whole-genome transcriptomics. Fundamentally, the immediate extrapolation from in vitro cell toxicity using uncoated nanoparticles to toxicity in humans under conditions of normal sunscreen use, without consideration of in what form or even whether the particles will reach viable cells in the first place, is arguably misguided. Nevertheless, in vitro studies are important for our understanding of the mechanisms of response to nanoparticles.

Research over the past decade has thus aimed to dissociate intrinsic hazard (ie, in vitro cell toxicity using uncoated nanoparticles) from actual risk to human health by using a variety of techniques and exposure protocols to assess the percutaneous absorption of, and responses to, TiO_2 and ZnO nanoparticles following topical application to skin. These studies have typically employed either ex vivo techniques, such as excised skin samples mounted on diffusion cells, or in vivo protocols involving the topical application of sunscreens to live small animals and/or humans. A subset of these is described in this chapter.

EX VIVO STUDIES INVESTIGATING THE PASSAGE OF NANOPARTICLES THROUGH HEALTHY INTACT SKIN SHOW LITTLE TO NO PARTICLE PENETRATION

The majority of metal oxide nanoparticle studies assessing percutaneous absorption have been performed using excised rodent [20], pig [21–23], or human [24–30] skin. Typically, TiO_2 or ZnO nanoparticles are dispersed in an application vehicle such as aqueous- or oil-based [21,24] sun cream formulations [25,26,28] or artificial physiological fluids [29], although in some instances a penetration-enhancing medium has been chosen [20]. Once dispersed, the particles are applied to the stratum corneum side of skin samples (most often mounted on static or flow-through diffusion cells; eg, Fig. 20.1) for short periods of time, typically up to 24 h. Very few studies using this type of protocol have reported nanoparticle penetration through to the viable dermal skin layers. Studies that did detect some degree of particle penetration were generally associated with some form of compromised skin, such as the movement of 35 nm coated TiO_2 nanoparticles into empty hair follicles (but not beyond) shortly after hair removal from minipig skin [21], or the use of penetration enhancers with 10 nm ZnO nanoparticles applied to nude mouse

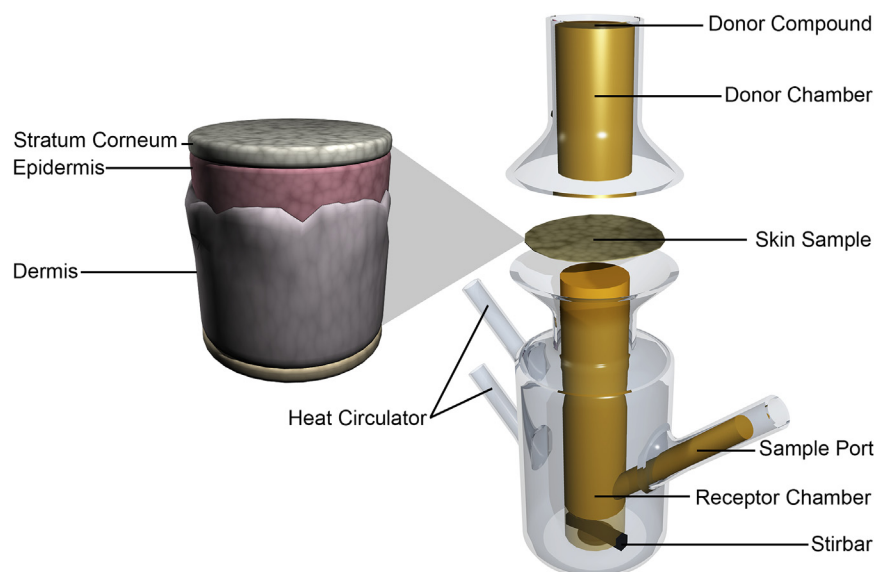


FIGURE 20.1 Franz diffusion cells comprise a donor and receptor chamber that is separated by a small piece of excised full- or partial-thickness skin. The receptor chamber generally contains representative physiological fluid in contact with the dermis side of the skin sample. For sunscreen experiments, the sunscreen is applied to the stratum corneum side of the skin sample and incubated for a defined period of time, during which samples from the receptor fluid can be taken, after which the receptor fluid and various skin layers are assessed for the presence of nanoparticles.

skin [20], which itself is inherently more penetrable than pig or human skin [31,32]. It can therefore be concluded that the overwhelming majority of ex vivo skin studies have shown little to no nanoparticle penetration through the stratum corneum to deeper skin layers in healthy excised skin. The potential for enhanced penetration through a defective skin barrier, however, is discussed in more detail in this chapter.

IN VIVO STUDIES INVESTIGATING THE PASSAGE OF NANOPARTICLES THROUGH SKIN HIGHLIGHT VARIABLES THAT MAY INFLUENCE NANOPARTICLE PENETRATION

Ex vivo skin samples lack functional vasculature and natural flexion; therefore, a reliance on diffusion cell studies might underestimate the risk of nanoparticle penetration in humans [33,34]. Furthermore, rapid skin deterioration after removal from the animal precludes long exposure protocols, again limiting the relevance to normal sunscreen use. Ex vivo results should therefore be considered alongside those obtained from in vivo experiments. Models for in vivo skin nanoparticle penetration studies are most often rodent [23,35–38], pig [30,39,40], or human [27,30,41–48]. Consistent with ex vivo results, the weight of in vivo data suggests that solid nanoparticles undergo little to no movement through the stratum corneum and therefore are not likely to reach the deeper skin layers.

Where nanoparticles have been detected deeper than the upper layers of the stratum corneum, they were generally associated with skin furrows and/or hair follicles [35,37,43] rather than true penetration, or were subject to some uncertainty around the interpretation of positive results [36,41,42], potentially confounded [23,38,40], or ascribed to experimental error [39]. Nevertheless, some factors have emerged more likely than others to influence the penetrability of nanoparticles, most particularly the duration of the treatment protocol, and the source, health, and integrity of the skin.

Particle/Ion Penetration Is More Likely to Occur With Longer Exposure Durations, Albeit Still at Very Low Levels

Although greatly hindered by the use of different models, different variables, and different particles, it can arguably be concluded that very low levels of nanoparticle penetration is more likely to be observed in experimental protocols where longer exposure durations are used, although the converse is not necessarily true. In 1996, Tan et al. reported elevated concentrations of Ti in the epidermis and dermis of human volunteers who had applied TiO₂ sunscreen twice daily for 2–6 weeks, although they did note no correlation between amount of Ti detected and length of exposure [41]. This result was ultimately not statistically significant due to an outlier control showing concentrations of Ti comparable to those of the experimental

volunteers, source unknown, but it was nevertheless an early indication that exposure duration may be an important consideration. Despite this, however, the majority of ex vivo and in vivo studies following Tan et al. that reported no percutaneous absorption lasted no longer than 48 h. Conversely, when some degree of penetration was observed, it was likely to be in a study involving longer protocols [23,36,42].

In particular, the Gulson et al. (2010) study, which showed very limited absorption of Zn into blood and urine from topically applied ZnO sunscreen, highlighted two important points. This experiment involved twice-daily applications of sunscreen enriched to >99% with a naturally occurring stable and traceable form of Zn (^{68}ZnO) (nano-size or larger) to the backs of human volunteers over the course of 5 days at a beach in Australia [42]. Based on very sensitive measurements made using multicollector inductively coupled plasma mass spectrometry (MC-ICP-MS), the authors reported that very small amounts of the tracer could be found in the blood and urine of human volunteers, with the highest absorption occurring in females receiving applications of the nano-form of the ZnO particles relative to the larger particles. Although the destructive nature of MC-ICP-MS precluded definitive identification of the tracer as particulate ^{68}ZnO or ^{68}Zn dissolved from the ^{68}ZnO , this study highlighted two key considerations. First, despite the highly sensitive techniques employed, ^{68}Zn was not detected until after the fourth sunscreen application on the afternoon of the second day, raising the possibility that many of the studies involving durations shorter than 48 h and/or less sensitive detection techniques that reported no penetration may have been limited by missing the window and/or sensitivity of detection, rather than no penetration per se. Second, although applications in the Gulson study lasted only 5 days, ^{68}Zn did not peak in blood samples until approximately day 14 [49], suggesting that hair follicles and/or skin furrows may act as a reservoir for sunscreen-derived particles, consistent with earlier studies [50].

To investigate the biodistribution of absorbed ^{68}Zn , our laboratory then applied the same nano and micro ^{68}ZnO sunscreens as used by Gulson et al., along with the sunscreen base formulation containing no ZnO, onto the backs of immune-competent hairless pregnant and not-pregnant mice six times over 4 days [36]. Bearing in mind the accepted limitations of the relatively permeable hairless mouse model as it relates to human skin (Fig. 20.2), the results of our work suggested that although ^{68}Zn was systemically absorbed from topically applied ^{68}ZnO in greater quantities from nano compared to the micro sunscreen, and also underwent transplacental transfer, it appeared to largely exchange with endogenous Zn rather than accumulate (ie, total organ

Zn concentrations remained the same). This result was indicative of solubilized ^{68}Zn rather than particulate ^{68}ZnO , and no particle-mediated adverse biological responses were observed. In fact, the only adverse response we found was a mild inflammatory reaction to the sunscreen formulation itself, which was mitigated by the presence of the ZnO, consistent with zinc's known wound-healing properties [51]. Interestingly, a recent study also showed that nanosized ZnO suppressed local skin inflammation in an atopic dermatitis mouse model [52].

Our conclusion that the ^{68}Zn detected in the blood and internal organs of hairless mice [36] was likely to be solubilized ^{68}Zn that exchanged with endogenous Zn rather than particulate ^{68}ZnO is arguably supported by more recent work in another laboratory [38] showing that daily treatment of (clipped) haired rats with up to 1000 mg/kg body weight topically applied ZnO nanoparticles over 90 days did not result in increases in internal ZnO as measured by ICP atomic emission spectroscopy. This work, however, did not utilize a traceable form of Zn and could therefore not distinguish whether exogenously sourced Zn had exchanged with endogenous Zn. No adverse biological effects were observed in mice apart from temporary and dose-dependent dermal inflammation at site of application. This is again consistent with our own published findings in the short term [36] as well as to-be-published results from our laboratory that show that weekly treatment of immune-competent hairless mice over 8 months with sunscreens containing nanoparticles of TiO_2 or $\text{ZnO} \pm \text{UVR}$ was not associated with nanoparticle-mediated adverse biological outcomes (Osmond-McLeod et al. unpublished work).

In contrast, Adachi et al. (2013) reported that hairless rats treated daily with topical applications of TiO_2 nanoparticles for up to 8 weeks did not show elevated levels of Ti in internal organs aside from the lungs, which was attributed to particle inhalation rather than dermal penetration [35]. Similarly, multiple applications of TiO_2 nanoparticles over a 4-week period were not associated with dermal absorption in minipigs [39]. Therefore, a message arising from these studies taken together may be that even when longer durations and multiple applications are incorporated, a contributing factor may be the solubility of the particle.

Skin Barrier Disruption May Facilitate Low Levels of Nanoparticle Penetration

The health and integrity of the skin to which the sunscreen is being applied have also been raised as important factors in how effectively it acts as a barrier to topically applied nanoparticles [16]. Sunscreen is often

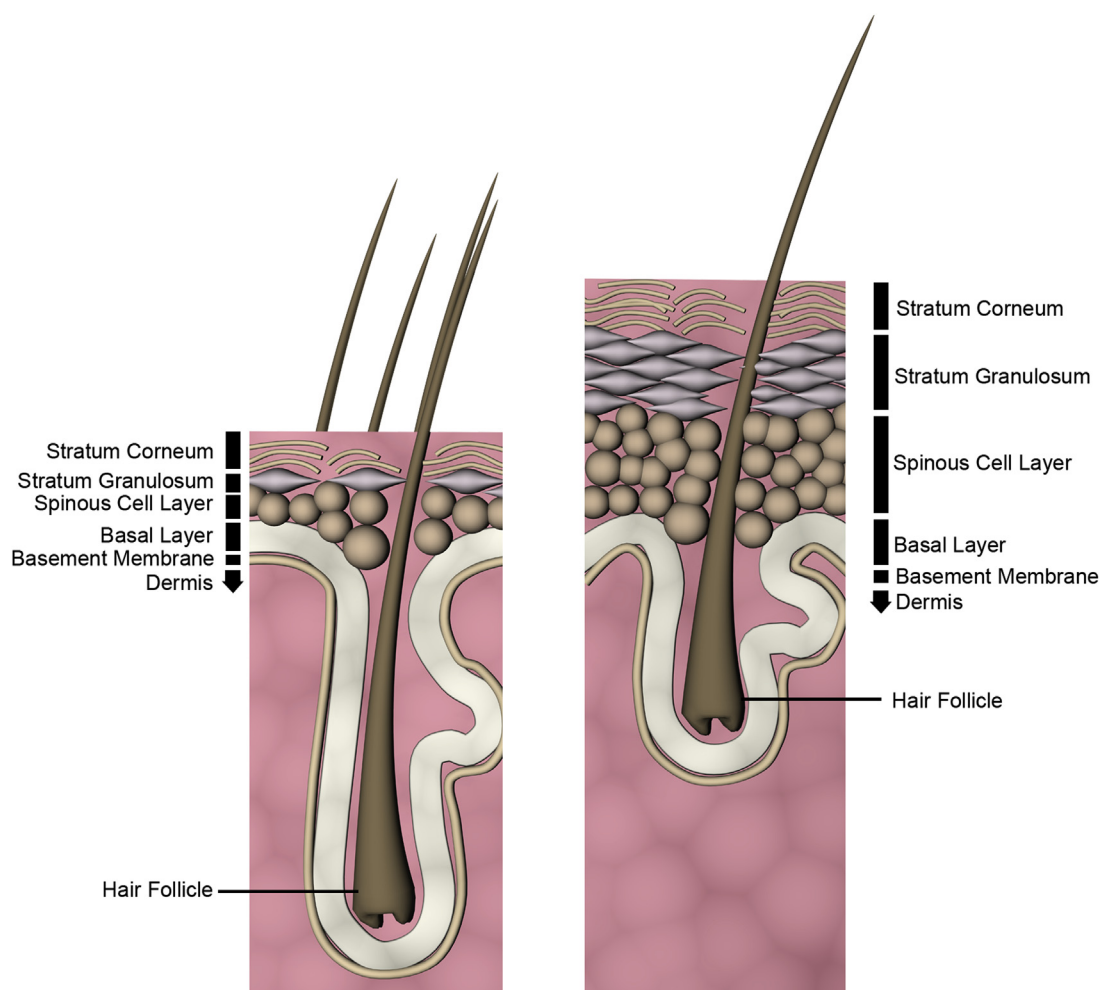


FIGURE 20.2 Mouse skin is generally considered to be more permeable to topically applied substances than human skin, largely because it has fewer epidermal cell layers. Mouse skin is also much more densely packed with hair follicles than human skin.

applied to skin that has already been burnt, has been shaved, or has been abraded and/or dehydrated by, for example, sand or wind at the beach, where sunscreen is often applied. These factors therefore warrant consideration when assessing the likelihood of nanoparticle penetration through the skin under conditions of normal sunscreen use. Currently, it appears that topical application to UV-damaged or otherwise barrier-disrupted skin can slightly facilitate the penetration of at least some nanoparticles.

UVB has been shown to temporarily disrupt the skin barrier [53–55]. A number of studies using a variety of nanomaterials have therefore addressed the question of whether sunburning the skin can facilitate the penetration of solid nanoparticles, including quantum dots [56,57] or nanoparticles of ZnO and/or TiO₂ [58,59]. Applying negatively-charged quantum dots dispersed in a glycerol vehicle to the backs of immune-competent hairless mice, either closely following their exposure to acute doses of UVB [57] or at the peak of

barrier disruption 3.5–4.5 days post irradiation [56], Mortensen and colleagues reported that UVB did indeed enhance their skin penetration and systemic uptake, typically via an intercellular lipid lamellae pathway (ie, around the skin cells rather than through them). Even in sun-damaged skin, however, the overall number of quantum dots penetrating through the stratum corneum remained low. An interesting point raised in this study was that low, but statistically significant, uptake of the quantum dots through undamaged skin was also observed. The authors ascribed this to movement through low-frequency defects in the stratum corneum (lacunar pathways [60]), which they postulated would not be detected by normal tissue histology using transmission electron microscopy (TEM) unless many sections are analyzed [56].

Surprisingly, given the relevance of UVR to sunscreen use, few studies have directly assessed the effect of sunburn on the penetration of TiO₂ or ZnO nanoparticles in vivo. One ex vivo diffusion cell experiment

using sunburned and damaged pig skin showed little enhanced TiO₂ nanoparticle penetration after 24 h [59], although, as discussed here, the shorter time frame employed is a limiting factor. In a slightly longer *in vivo* study using moderately sunburned white Yorkshire pigs, slightly enhanced penetration of TiO₂ nanoparticles and, to a lesser extent, ZnO nanoparticles into the dermis and epidermis was observed after 48 h, but internal organs were not assessed for systemic uptake [58]. The Gulson et al. experiment also incorporated sun exposure at the beach, and low concentrations of the traceable Zn were detected in blood and urine of human volunteers [42].

Disrupting the skin barrier by abrasion or wounding may facilitate particle entry more than UV damage. One recent study utilizing *in vivo* and *ex vivo* human skin models [8] compared ZnO nanoparticle removal from intact or damaged skin. *In vivo* skin samples were damaged by comprehensive tape stripping, whereas *ex vivo* skin samples were punctured using microneedles. The ZnO nanoparticles were topically applied and removed by washing with soapy water 2 h post application, and multiphoton tomography was used to compare the ZnO signal before and after washing. The authors reported that ZnO nanoparticles were less effectively removed in the presence of puncture wounds compared to the tape-stripped skin, raising the prospect that wounds might act as a reservoir for nanoparticles from sunscreens if applied to broken skin.

The Impact of Particle Characteristics on Nanoparticle Entry Through Skin Is Equivocal

In vitro, the surface properties of a nanoparticle (ie, surface charge and hydrophobicity) can influence its ability to disrupt the bilipid cell membrane, enter cells, and induce genotoxic and cytotoxic cellular responses, immune reactions, pharmacokinetics, bio-distribution, and protein denaturation in a complex and surface-interaction-dependent manner [61]. However, a lack of systematic and comparable data makes it very difficult to conclusively determine which, if any, particle characteristics influence solid nanoparticle movement through the skin, although it is possible that a positive surface charge may slightly facilitate entry [10]. Leite-Silva et al. [62] reported that the presence of a hydrophobic coating on ZnO nanoparticles dispersed in a water-in-oil vehicle slightly facilitated their movement through the stratum corneum to viable epidermal layers adjacent to skin furrows in human volunteers. However, the authors noted that the coated sample contained more particles with diameters smaller than 30 nm compared to the uncoated sample, which had an average diameter of 80 nm, giving rise to the

possibility that the effect was size—rather than surface characteristic—driven. Dispersion in the oil phase of an application vehicle also facilitated the penetration of 40 nm TiO₂ nanoparticles through human skin, whereas TiO₂ nanoparticles dispersed in the aqueous phase remained on the surface of the skin [63]. It is likely, however, that the surface properties of nanoparticles are less critical than particle size with respect to dermal penetration [64,65].

REMAINING KNOWLEDGE GAPS

Recently, the European Union (EU) Commission's Working Group on Cosmetics comprehensively assessed the safety dossiers for nanosized ZnO [66] and TiO₂ [9] in dermally applied cosmetic products and concluded that their inclusion up to 25% as UV filters was safe for human use. In 2009 [67] and again in 2013 [6], Australia's Therapeutic Goods Administration (TGA) deemed TiO₂ and ZnO nanoparticles as safe for human use in sunscreens. An exhaustive and cross-cutting review published in 2013 into the dermal absorption of nanomaterials (including ZnO and TiO₂ in sunscreens), commissioned under the Danish Environmental Protection Agency's "Better control of nano" Initiative 2012–15, concluded that whilst dermal penetration of nanoparticles was possible under some conditions, this was likely only to a very small degree [10]. Numerous reviews written by different groups and authors in scientific journals have reached similar conclusions. It is clear that a scientific consensus is being reached as our understanding of the factors involved and the influence of protocol limitations has matured. Nevertheless, despite general agreement that these nanoparticles are safe for human use in sunscreens, there is also acknowledgment of the difficulties in drawing definitive conclusions with respect to the impact of physicochemical and vehicle properties due to the lack of systematic and harmonized testing protocols [10], as well as uncertainties regarding long-term biological impacts, and the extent to which existing testing strategies are optimal [9]. The remainder of this chapter will review some remaining areas where coordinated research efforts could fully mature our understanding.

One critical point that remains to be addressed is whether the accumulation and retention of nanoparticles from sunscreens with photocatalytic activity [68–70] in hair follicles lead to adverse biological impacts. It is interesting to note that whereas research in the area of sunscreen safety has generally been aimed at demonstrating a lack of nanoparticle dermal penetration, the hair follicle is considered to be a potential route of entry of interest for therapeutic applications

[71–74]. In the epidermis, the majority of viable skin cells are in the process of differentiation whilst moving upward from the basal cell layer until they reach the stratified surface as terminally differentiated, keratin-packed corneocytes. Damage to fully differentiated cells at the skin's surface may have only transient effects as they are routinely shed. In fact, a basal skin cell takes only 4 weeks to reach terminal differentiation and be sloughed from the skin's surface [75]. Epidermal hair follicle stem cells, on the other hand, reside long term in the hair follicle bulge region and therefore may have a more significant impact if they are damaged as they are the source from which hair follicle cells are replenished during normal homeostasis as well as during wound repair [76,77]. Significant cell damage has the potential to diminish the capacity of these cells to replenish the hair follicle cell population, and targeted mutations could result in conversion to cancer cells.

Topically applied nanoparticles can reside in hair follicles and skin furrows for up to 10 days before being removed by natural means such as sebum flow [73]. Some sunscreens containing nanoparticles of ZnO and/or TiO₂ have been shown to generate free radicals on steel roofs in Australia [69] as well as on skin [70]. Consequently, the impact of free radical generation arising from UVR exposure of metal oxide nanoparticles deposited in the hair follicle on the viability and function of local epithelial hair follicle stem cells is a subtle but important consideration in the assessment of long-term sunscreen safety. Similarly, the buildup and localized dissolution of ZnO nanoparticles from sunscreen, which is enhanced by UVB radiation [78], in close proximity to stem cells warrants consideration given the toxicity of ZnO nanoparticles *in vitro* [16], which appears to be primarily mediated by released Zn²⁺ [79].

Another area where there is a relative lack of information is the impact of age, gender, and racial differences on the penetration of and reaction to topically applied TiO₂ and ZnO nanoparticles in sunscreen. For example, the higher follicular density in white skin compared to Asian or African-American skin [17] may influence the biological response to nanoparticle accumulation in hair follicles if this does indeed act as a source of free radical generation. Similarly, although gender is known to influence a number of skin properties [80], including the response to UVR [81] and possibly permeability [42], a potential gender bias in the penetration of nanoparticles from sunscreens remains to be addressed in a systematic manner.

A recent review [17] highlighted the paucity of research addressing the effect of skin disorders on the penetrability of ZnO and TiO₂ nanoparticles. Lin et al. observed no penetration into the viable skin layers in humans with psoriatic or atopic dermatitis lesions after

2 h of treatment with silicon-coated ZnO nanoparticles dispersed in caprylic–capric triglycerides [82], although the short treatment period was an acknowledged limitation of this work. Another group utilized an atopic dermatitis mouse model to investigate the impact of injured allergic skin on the penetration profile of ZnO nanoparticles compared to larger ZnO particles, reporting that the nanosized particles could penetrate deeper into the dermal layers of allergic skin compared to larger particles [52]. Furthermore, two other studies showed that polystyrene or silica nanoparticles co-injected intradermally with an allergen into the ears of mice with atopic dermatitis-like skin lesions exacerbated the inflammatory reaction. Importantly, both groups also reported that the nanoparticles themselves were capable of inducing an inflammatory response in these models [83,84]. With a growing proportion of the population suffering from allergic and contact sensitization disorders [17], using relevant models to assess the biological reaction to topically applied nanoparticles will be a priority over the coming years.

Last, the potential for unanticipated long-term biological impacts should be investigated, through both standard experimental protocols as well as human epidemiology studies, if possible at this stage. In particular, the latter would allow the general statement “ZnO and TiO₂ nanoparticles have been used for years in sunscreens with no adverse effects” to be supported by an evidence-based epidemiological framework.

CONCLUSIONS

Nanotoxicology has moved in recent years from extrapolating from intrinsic particle hazards to a more nuanced assessment of actual risk to human and environmental health under conditions of normal use. With respect to the use of metal oxide nanoparticles in sunscreen, this approach is now allowing a scientific consensus to be reached where reports of the relative toxicities of ZnO and TiO₂ nanoparticles compared to larger particles in unrealistic *in vitro* cell culture systems are considered within a context of numerous skin penetration studies indicating that solid nanoparticles are not likely to see those cells in healthy humans under conditions of normal use. However, remaining knowledge gaps—such as whether free radical generation and/or localized high concentrations of dissolved Zn²⁺ in the vicinity of hair follicle stem cells can induce aberrant cell behavior; the impact of factors such as race, gender, and skin disorders; and, of course, the potential for unanticipated biological outcomes with long-term use—should be addressed to fully mature our understanding and allow safety-by-design approaches to be utilized where appropriate.

List of Acronyms and Abbreviations

EU European Union

H Hour

MC-ICP-MS Multicollector inductively coupled plasma mass spectrometry

Nm Nanometer

TEM Transmission electron microscopy

TGA Therapeutic Goods Administration

TiO₂ Titanium dioxide

UV Ultraviolet

UVB Ultraviolet B

UVR Ultraviolet radiation

Zn Zinc

ZnO Zinc oxide

Glossary

Cytotoxic Toxic to cells.

Ex vivo Latin for “out of the living.” Experiments are conducted on tissue taken from an organism, where attempts are made to maintain the tissue at close to a physiological state.

Genotoxic Damaging to a cell’s genetic information.

Hazard Something that has the potential to harm.

In vitro Latin for “in glass.” Experiments are conducted using biological molecules or organisms outside their biological environment.

In vivo Latin for “in the living.” Experiments are conducted on whole, living organisms.

Risk The chance/probability that a hazard will actually cause harm.

UVB Ultraviolet radiation with wavelengths between 280 and 315 nm. The shorter, more damaging UVB wavelengths are largely absorbed by the ozone layer and do not reach the earth’s surface.

⁶⁸Zn A nonradioactive, naturally occurring stable isotope of ZnO.

References

- [1] FOE. Nanotechnology & sunscreens: a consumer guide for avoiding nano-sunscreens. 2007. http://www.foe.org/system/storage/877/23/9/634/Nanotechnology_and_sunscreens.pdf.
- [2] Ball P. Nanoparticles in sun creams can stress brain cells. *Nature* June 16, 2006.
- [3] Long T, Saleh N, Tilton R, Lowry G, Veronesi B. Titanium dioxide (P25) produces reactive oxygen species in immortalized brain microglia (BV2): implications for nanoparticle neurotoxicity. *Environ Sci Technol* 2006;40(14):4346–52.
- [4] DIISR. Australian community attitudes held about nanotechnology – trends 2005–2011. 2011.
- [5] AEU. Schools advised to use nano-free sunscreen; 2011, 2014.
- [6] TGA. Literature review on the safety of titanium dioxide and zinc oxide nanoparticles in sunscreens. 2013. <https://www.tga.gov.au/literature-review-safety-titanium-dioxide-and-zinc-oxide-nanoparticles-sunscreens>.
- [7] SCCS. Scientific committee on consumer safety, opinion on ZnO (nanoform) COLIPA S76. 2012. http://ec.europa.eu/health/scientific_committees/consumer_safety/docs/sccs_o_103.pdf.
- [8] Raphael A, Sundh D, Grice J, Roberts M, Soyer H, Prow T. Zinc oxide nanoparticle removal from wounded human skin. *Nanomedicine* 2013;8(11):1751–61.
- [9] SCCS, Chaudhry Q. Opinion of the Scientific Committee on Consumer safety (SCCS) – Revision of the opinion on the safety of the use of titanium dioxide, nano form, in cosmetic products. *Regul Toxicol Pharmacol* 2015;73:669–70.
- [10] Poland C, Read S, Varet J, Carse G, Christensen F, Hankin S. Dermal absorption of nanomaterials: part of the “Better control of nano” initiative 2012–2015. 2013. <http://www2.mst.dk/Udgiv/publications/2013/09/978-87-93026-50-6.pdf>.
- [11] Truffault L, Winton B, Choquenot B, et al. Cerium oxide based particles as possible alternative to ZnO in sunscreens: effect of the synthesis method on the photoprotection results. *Mater Lett* 2012;68:357–60.
- [12] Yabe S, Sato T. Cerium oxide for sunscreen cosmetics. *J Solid State Chem* 2003;171:7–11.
- [13] Herrling T, Seifert M, Jung K. Cerium dioxide: future UV-filter in sunscreen? *SOFW J* 2013;139:10–4.
- [14] Rampaul A, Parkin I, Cramer L. Damaging and protective properties of inorganic components of sunscreens applied to cultured human skin cells. *J Photochem Photobiol A* 2007;191:138–48.
- [15] Serpone N, Salinaro A, Emeline A. Deleterious effects of sunscreen titanium dioxide nanoparticles on DNA. Efforts to limit DNA damage by particle surface modification. In: Murphy C, editor. *SPIE*; 2001.
- [16] Osmond M, McCall M. Zinc oxide nanoparticles in modern sunscreens: an analysis of potential exposure and hazard. *Nanotoxicology* 2010;4(1):15–41.
- [17] Jatana S, DeLouise L. Understanding engineered nanomaterial skin interactions and the modulatory effects of ultraviolet radiation skin exposure. *WIREs Nanomed Nanobiotechnol* 2013; 6:61–79.
- [18] Osmond-McLeod M, Osmond R, Oytam Y, et al. Surface coatings of ZnO nanoparticles mitigate differentially a host of transcriptional, protein and signalling responses in primary human olfactory cells. *Part Fibre Toxicol* 2013;10:54.
- [19] Osmond-McLeod M, Oytam Y, Osmond R, Sobhanmanesh F, McCall M. Surface coatings protect against the in vitro toxicity of zinc oxide nanoparticles in human hepatic stellate cells. *Nanomed Nanotechnol* 2014;5:5.
- [20] Kuo T, Wu C, Hsu C, et al. Chemical enhancer induced changes in the mechanisms of transdermal delivery of zinc oxide nanoparticles. *Biomaterials* 2009;30:3002–8.
- [21] Senzui M, Tamura T, Miura K, Ikarashi Y, Watanabe Y, Fuji M. Study on penetration of titanium dioxide (TiO₂) nanoparticles into intact and damaged skin in vitro. *J Toxicol Sci* 2010;35:107–13.
- [22] Gamer A, Leibold E, Ravenzwaay B. The in vitro absorption of microfine zinc oxide and titanium dioxide through porcine skin. *Toxicol Vitro* 2006;20:301–7.
- [23] Wu J, Liu W, Xue C, et al. Toxicity and penetration of TiO₂ nanoparticles in hairless mice and porcine skin after subchronic dermal exposure. *Toxicol Lett* 2009;191(1):1–8.
- [24] Cross S, Innes B, Roberts M, Tsuzuki T, Robertson T, McCormick P. Human skin penetration of sunscreen nanoparticles: in vitro assessment of a novel micronized zinc oxide formulation. *Skin Pharmacol Physiol* 2007;20:148–54.
- [25] Mavon A, Miquel C, Lejeune O, Payre B, Moretto P. In vitro percutaneous absorption and in vivo stratum corneum distribution of an organic and a mineral sunscreen. *Skin Pharmacol Physiol* 2007;20:10–20.
- [26] Durand L, Habran N, Henschel V, Amighi K. In vitro evaluation of the cutaneous penetration of sprayable sunscreen emulsions with high concentrations of UV filters. *Int J Cosmet Sci* 2009;31: 279–92.
- [27] Roberts M, Roberts M, Robertson T, et al. In vitro and in vivo imaging of xenobiotic transport in human skin and in the rat liver. *J Biophotonics* 2008;1:478–93.
- [28] Dussert A, Gooris E, Hemmerle J. Characterization of the mineral content of a physical sunscreen emulsion and its distribution onto human stratum corneum. *Int J Cosmet Sci* 1997;19:119–29.

- [29] Crosera M, Prodi A, Mauro M, et al. Titanium dioxide nanoparticle penetration into the skin and effects on HaCat cells. *Int J Environ Res Public Health* 2015;12(8):9282–97.
- [30] Gontier E, Ynsa M-D, Biro T, et al. Is there penetration of titania nanoparticles in sunscreens through skin? a comparative electron and ion microscopy study. *Nanotoxicology* 2008;2:218–31.
- [31] Scott R, Walker M, Dugard P. a comparison of the *in vitro* permeability properties of human and some laboratory animal skins. *Int J Cosmet Sci* 1986;8:189–94.
- [32] Bond J, Barry B. Limitations of hairless mouse skin as a model for *in vitro* permeation studies through human skin: hydration damage. *The Soc Invest Dermatol* 1988;90(4):486–9.
- [33] Gulson B, McCall M, Bowman D, Pinheiro T. A review of critical factors for assessing the dermal absorption of metal oxide nanoparticles from sunscreens applied to humans, and a research strategy to address current deficiencies. *Arch Toxicol* 2015 [epub ahead of print].
- [34] Ryman-Rasmussen J, Riviere J, Monteiro-Riviere N. Penetration of intact skin by quantum dots with diverse physicochemical properties. *Tox Sci* 2006;91(1):159–65.
- [35] Adachi K, Yamada N, Yoshida Y, Yamamoto O. Subchronic exposure of titanium dioxide nanoparticles to hairless rat skin. *Exp Dermatol* 2013;22:278–83.
- [36] Osmond-McLeod M, Oytam Y, Kirby J, Gomez-Fernandez L, Baxter B, McCall M. Dermal absorption and short-term biological impact in hairless mice from sunscreens containing zinc oxide nano- or larger particles. *Nanotoxicology* 2013. <http://dx.doi.org/10.3109/17435390.2013.855832>.
- [37] Adachi K, Yamada N, Yoshida Y, Yamamoto K, Yamamoto O. In vivo effect of industrial titanium dioxide nanoparticles experimentally exposed to hairless rat skin. *Nanotoxicology* 2010;4(3):296–306.
- [38] Ryu H, Seo M, Jung S, et al. Zinc oxide nanoparticles: a 90-day repeated-dose dermal toxicity study in rats. *Int J Nanomed* 2014;15(9):137–44.
- [39] Sadrieh N, Wokovich A, Gopee N, et al. Lack of significant dermal penetration of titanium dioxide from sunscreen formulations containing nano- and submicron-size TiO₂ particles. *Toxicol Sci* 2010;115:156–66.
- [40] Menzel F, Reinert T, Vogt J, Butz T. Investigations of percutaneous uptake of ultrafine TiO₂ particles at the high energy ion nanoprobe LIPSION. *Nucl Instrum Meth Phys Res B* 2004;219–220:82–6.
- [41] Tan M, Commens C, Burnett L, Snitch P. A pilot study on the percutaneous absorption of microfine titanium dioxide from sunscreens. *Australas J Dermatol* 1996;37:185–7.
- [42] Gulson B, McCall M, Korsch M, et al. Small amounts of zinc from zinc oxide particles in sunscreens applied outdoors are absorbed through human skin. *Tox Sci* 2010;118(1):140–9.
- [43] Darvin M, König K, Kellner-Hoefer M, et al. Safety assessment by multiphoton fluorescence/second harmonic generation/hyper-Rayleigh scattering tomography of ZnO nanoparticles used in cosmetic products. *Skin Pharmacol Physiol* 2012;25:219–26.
- [44] Filipe P, Silva J, Silva R, et al. Stratum corneum is an effective barrier to TiO₂ and ZnO nanoparticle percutaneous absorption. *Skin Pharmacol Physiol* 2009;22:266–75.
- [45] Zvyagin A, Zhao X, Gierden A, Sanchez W, Ross J, Roberts M. Imaging of zinc oxide nanoparticle penetration in human skin in vitro and in vivo. *J Biomed Opt* 2008;13(6):064031.
- [46] Pflucker F, Wendel V, Hohenberg H, et al. The human stratum corneum layer: an effective barrier against dermal uptake of different forms of topically applied micronised titanium dioxide. *Skin Pharmacol Appl Skin Physiol* 2001;14(Suppl. 1):92–7.
- [47] Schulz J, Hohenberg H, Pflucker F, et al. Distribution of sunscreens on skin. *Adv Drug Deliv Rev* 2002;54(Suppl. 1):S157–63.
- [48] Pinheiro T, Pallon J, Alves L, et al. The influence of corneocyte structure on the interpretation of permeation profiles of nanoparticles across the skin. *Nucl Instrum Meth Phys Res B* 2007;260:119–23.
- [49] Larner F, Gulson B, McCall M, Oytam Y, Rehkamper M. An inter-laboratory comparison of high precision stable isotope ratio measurements for nanoparticle tracing in biological samples. *J Anal At Spectrom* 2013. <http://dx.doi.org/10.1039/c3ja50322d>.
- [50] Lademann J, Otberg N, Richter H, et al. Investigation of follicular penetration of topically applied substances. *Skin Pharmacol Appl Skin Physiol* 2001;12:247–56.
- [51] Lansdown A, Mirastschijski U, Stubbs N, Scanlon E, Agren M. Zinc in wound healing: theoretical, experimental, and clinical aspects. *Wound Repair Regen* 2007;15(1):2–16.
- [52] Ilves M, Palomaki J, Vippola M, et al. Topically applied ZnO nanoparticles suppress allergen induced skin inflammation but induce vigorous IgE production in the atopic dermatitis mouse model. *Part Fibre Toxicol* 2014;11:38.
- [53] Gellis C. Modification of *in vitro* skin penetration under solar irradiation: evaluation on flow-through diffusion cells. *Photochem Photobiol* 2002;75(6):598–604.
- [54] Jiang S, Chu A, Lu Z, Pan M, Che D, Zhou X. Ultraviolet B-induced alterations of the skin barrier and epidermal calcium gradient. *Exp Dermatol* 2007;16:985–92.
- [55] Haratake A, Uchinda Y, Schmutz M, et al. UVB-induced alterations in permeability barrier function: roles for epidermal hyperproliferation and thymocyte-mediated response. *J Invest Dermatol* 1997;108:769–75.
- [56] Mortensen L, Jatana S, Gelein R, et al. Quantification of quantum dot murine skin penetration with UVR barrier impairment. *Nanotox* 2013;7(8):1386–98.
- [57] Mortensen L, Oberdorster G, Pentland A, DeLouise L. In vivo skin penetration of quantum dot nanoparticles in the murine model: the effect of UVR. *NanoLetters* 2008;8:2779–87.
- [58] Monteiro-Riviere N, Wiench K, Landsiedel R, Schulte S, Inman A, Riviere J. Safety evaluation of sunscreen formulations containing titanium dioxide and zinc oxide nanoparticles in UVB sunburned skin: an *in vitro* and *in vivo* study. *Toxicol Sci* 2011;123(1):264–80.
- [59] Miquel-Jeanjean C, Crepel F, Raufast V, et al. Penetration study of formulated nanosized titanium dioxide in models of damaged and sun-irradiated skins. *Photochem Photobiol* 2012;88:1513–21.
- [60] Paliwal S, Menon G, Mitragotri S. Low-frequency sonophoresis: ultrastructural basis for stratum corneum permeability assessed using quantum dots. *J Invest Dermatol* 2006;126(5):1095–101.
- [61] Kim S, Saha K, Kim C, Rotello V. The role of surface functionality in determining nanoparticle cytotoxicity. *Acc Chem Res* 2013;46(3):681–91.
- [62] Leite-Silva V, Lamer ML, Sanchez W, et al. The effect of formulation on the penetration of coated and uncoated zinc oxide nanoparticles into the viable epidermis of human skin *in vivo*. *Eur J Pharmaceutics Biopharmaceutics* 2013;84:297–308.
- [63] Bennat C, Muller-Goymann C. Skin penetration and stabilization of formulations containing microfine titanium dioxide as physical UV filter. *Int J Cosmet Sci* 2000;22:271–83.
- [64] Rancan F, Gao Q, Graf C, et al. Skin penetration and cellular uptake of amorphous silica nanoparticles with variable size, surface functionalization, and colloidal stability. *ACS Nano* 2012;6(8):6829–42.
- [65] Vogt A, Combadiere B, Hadam S, et al. 40 nm, but not 750 or 1500 nm, nanoparticles enter epidermal CD1a+ cells after transcutaneous application on human skin. *J Invest Dermatol* 2006;126:1316–22.

- [66] SCCS. Addendum to the opinion SCCS/1489/12 on zinc oxide (nano form) COLIPA S76. 2014. http://ec.europa.eu/health/scientific_committees/consumer_safety/docs/sccs_o_137.pdf.
- [67] TGA. A review of the scientific literature on the safety of nanoparticulate titanium dioxide or zinc oxide in sunscreens. 2009.
- [68] Brezova V, Gabcova S, Dvoranova D, Stasko A. Reactive oxygen species produced upon photoexcitation of sunscreens containing titanium dioxide (an EPR study). *J Photochem Photobiol B* 2005; 79:121–34.
- [69] Barker P, Branch A. The interaction of modern sunscreen formulations with surface coatings. *Prog Org Coat* 2008;62(3): 313–20.
- [70] Millington K, Osmond M, McCall M. Detecting free radicals in sunscreens exposed to UVA radiation using chemiluminescence. *J Photochem Photobiol B* 2014;133:27–38.
- [71] Ossadnik M, Richter H, Teichmann A, et al. Investigation of differences in follicular penetration of particle- and nonparticle-containing emulsions by laser scanning microscopy. *Laser Phys* 2006;16(5):747–50.
- [72] Toll R, Jacobi U, Richter H, Lademann J, Schaefer H, Blume-Peytavi U. Penetration profile of microspheres in follicular targeting of terminal hair follicles. *The Soc Invest Dermatol* 2004;123: 168–76.
- [73] Lademann J, Richter H, Teichmann A, et al. Nanoparticles – an efficient carrier for drug delivery into the hair follicles. *Eur J Pharm Biopharm* 2007;66(2):159–64.
- [74] Blume-Peytavi U, Vogt A. Human hair follicle: reservoir function and selective targeting. *Br J Dermatol* 2011;165(Suppl. 2):13–7.
- [75] Fuchs E. Skin stem cells: rising to the surface. *JBC* 2008;180(2): 273–84.
- [76] Plikus M, Gay D, Treffeisen E, Wang A, Supapannachart R, Cotsarelis G. Epithelial stem cells and implications for wound repair. *Semin Cell Dev Biol* 2012;23(9):946–53.
- [77] Yang C, Cotsarelis G. Review of hair follicle dermal cells. *J Dermatol Sci* 2010;57(1):2–11.
- [78] Martorano L, Stork C, Li Y. UV irradiation-induced zinc dissociation from commercial zinc oxide sunscreen and its action in human epidermal keratinocytes. *J Cosmet Dermatol* 2010;9: 276–86.
- [79] Xia T, Kovochich M, Liong M, et al. Comparison of the mechanism of toxicity of zinc oxide and cerium oxide nanoparticles based on dissolution and oxidative stress properties. *ACS Nano* 2008;2(12): 2592.
- [80] Dao H, Kazin R. Gender differences in skin: a review of the literature. *Gend Med* 2007;4(4):308–28.
- [81] Reeve V, Allanson M, Domanski D, Painter N. Gender differences in UV-induced inflammation and immunosuppression in mice reveal male unresponsiveness to UVA radiation. *Photochem Photobiol Sci* 2012;11:173–9.
- [82] Lin L, Grice J, Butler M, et al. Time-correlated single photon counting for simultaneous monitoring of zinc oxide nanoparticles and NAD(P)H in intact and barrier-disrupted volunteer skin. *Pharm Res* 2011;11:2920–30.
- [83] Yanagisawa R, Takano H, Inoue K, Koike E, Sadakane K, Ichinose T. Size effects of polystyrene nanoparticles on atopic dermatitis-like skin lesions in NC/NGA mice. *Int J Immunopathol Pharmacol* 2010;23(1):131–41.
- [84] Hirai T, Yoshikawa T, Nabeshi H, et al. Amorphous silica nanoparticles size-dependently aggravate atopic dermatitis-like skin lesions following an intradermal injection. *Part Fibre Toxicol* 2012;9:3.

Nanoparticle Oxygen Sensing in Skin

Z. Li¹, C.L. Evans^{1,2}

¹Wellman Center for Photomedicine, Harvard Medical School, Charlestown, MA, United States; ²Harvard University Program in Biophysics, Boston, MA, United States

OUTLINE

Introduction	257	Oxygen Sensing Based on Magnetic Resonance	267
<i>The Need for Sensing Oxygen in Skin</i>	257	Techniques	267
<i>Existing Techniques for Tissue Oxygen Sensing</i>	258	<i>Introduction to Magnetic Resonance Techniques</i>	267
<i>Nanomaterials in Oxygen Sensing</i>	259	<i>Particle Oxygen Sensors for Magnetic Resonance</i>	268
Oxygen Sensing Based on Phosphorescence		<i>Techniques</i>	268
Quenching	259	<i>Skin Oxygen Sensing Based on Magnetic Resonance</i>	269
<i>Introduction to Phosphorescence Quenching</i>	259	<i>Techniques</i>	269
<i>Phosphorescent Probes</i>	260	Conclusions and Future Directions	270
<i>Sensor Matrix</i>	262	References	271
<i>Nanomaterial Oxygen Sensors</i>	263		
<i>Skin Oxygen Sensing Based on Phosphorescence</i>			
<i>Quenching</i>	265		

INTRODUCTION

The Need for Sensing Oxygen in Skin

Molecular oxygen is crucial for life, playing a key role in cellular respiration and energy generation. Cells, and by extension tissues, require a constant supply of oxygen to survive. Though tissues can temporarily withstand low levels of oxygenation, a condition known as hypoxia, normal skin homeostasis and growth are based on the continuous consumption of molecular oxygen. When skin oxygen supply or consumption is abnormal, a range of pathologies can arise with consequences ranging from compromised healing to the need for limb amputation [1].

In the clinic, a common condition caused by low oxygenation is the pressure, or decubitus, ulcer—also known as a bedsore [2,3]. These chronic wounds form when skin is compressed for a long period of time, such as during transport on a stiff surface or through continuous bed rest. Constant pressure on soft tissue

acts to reduce or obstruct blood flow, choking off the supply of oxygen and causing the skin and underlying tissue to undergo necrosis [4]. Fortunately, pressure ulcers are highly treatable in their early stage, provided that the reduced oxygen levels can be detected [5]. Diabetic ulcers are caused by a similar reduction in tissue oxygenation. Compounded by diabetic neuropathy, decreased oxygen supply to skin causes cellular death and the formation of open, chronic ulcers that routinely become infected. At their most extreme, diabetic ulcers can result in amputation and even death. Diabetic ulcers account for more than \$10 billion in health-related costs per year [6]. As a result, the ability to determine regions of reduced oxygen in skin prior to the formation of an ulcer could save patients considerable time, eliminate unnecessary procedures, prevent unnecessary limb amputations, and save the healthcare industry billions of dollars per year in the United States alone.

General wound healing, in which compromised skin undergoes re-epithelialization, is an active metabolic process, requiring the consumption of oxygen

to fuel the growth and cellular migration necessary for wound closure [7]. Poor tissue oxygenation, whether caused by the severity of the wound or a chronic condition such as diabetes, can considerably slow or even halt wound healing [3,8]. Prolonged healing times, unfortunately, may result in the bacterial colonization and infection of chronic wounds, leading to a cycle of skin injury, inflammation, and surgical debridement. These needs have prompted the rise of procedures that deliver oxygen to wounds either directly or indirectly. Hyperbaric oxygen therapy is one example where oxygen is supplied extracorporeally [9]. Alternatively, in negative-pressure wound therapy, a vacuum is placed over a wound site to draw fluids and oxygen into wounds to encourage healing [10]. However, in both cases, oxygen is supplied as a response to symptoms without knowledge of the underlying tissue oxygen content.

The current standard of care in wound healing, from open wounds to decubitus ulcers, is based on subjective measures made by a caregiver. These measures, ranging from sight to touch to smell, largely lack quantitative or objective character [11]. Despite the best efforts of physicians, patients still experience painful wounds and ulcers, and may need to undergo drastic, life-altering procedures like amputations due to poor wound healing [8]. Skin transplants and grafts, which are often required for pressure and diabetic ulcers, have similar oxygenation needs [12]. While large grafts, such as perforator flaps, receive oxygen supply via surgical anastomosis to local blood vessels, free flaps, as well as full-thickness/partial-thickness skin grafts, are fed via diffusion from underlying tissue. When oxygen supply is poor or compromised, in cases such as anastomotic failure, transplanted tissue can become necrotic, requiring surgical removal and retransplantation of new tissue.

Other than chronic wounds and skin grafts, the ability to monitor tissue oxygenation noninvasively would also benefit patients with cancer and peripheral vascular diseases. Avascular tumors or those with vascular malformations typically develop hypoxic cores that are linked to a number of chemotherapy resistance mechanisms. The ability to identify hypoxic regions in tissue could potentially serve as a diagnostic tool in various cancers. Conditions such as Raynaud's phenomenon or compartment syndromes could be better monitored and controlled with the help of a tissue oxygen sensor. In addition, a noninvasive transdermal oxygen sensor would also facilitate the treatment of burns, since access to oxygen profiles across burn wounds will allow surgeons to accurately determine burn depth during the debridement procedures. The ability to quantitatively measure skin oxygenation to gain an objective measure of tissue

health has immense potential to aid physicians and, by extension, patients in need [13,14].

Existing Techniques for Tissue Oxygen Sensing

There exist a number of physical tools and techniques aimed at the measurement of skin blood supply and oxygenation. The gold standard among these is the Clark electrode, a polarographic, electrochemical probe that measures local oxygen concentration via the reduction of molecular oxygen. The electrical current generated by the probe is linear with respect to the concentration of oxygen, giving a direct readout of oxygen tension [15]. Despite the utility of the Clark electrode, it has significant limitations in both research and clinical measurements of skin oxygenation. The electrodes, while precise, measure oxygen at just one point in the skin. Recording oxygenation across tissue or a wound requires either multiple electrodes or the introduction of the probe at multiple sites. The electrochemical probe is typically fashioned from a thin, fragile glass tip. Even though Clark electrodes can be encased within a sturdier needle, polarographic electrodes must still be inserted into the skin to measure oxygen tension, which can cause unwanted perturbation to sensitive, delicate wounds. Recently, more flexible, less fragile, fiber-based optrodes with a form factor similar to that of Clark electrodes have become popular [16]. Although these measurement tools, which make use of phosphorescence (explained in [Section "Introduction to Phosphorescence Quenching"](#)), remain both invasive and limited to point measurements, they will likely supersede polarographic electrodes due to their increased reliability and ease of use.

Transcutaneous oxygen tension ($TcPO_2$) devices based on polarographic technology are available and in active clinical use [9,14]. $TcPO_2$ devices are attached to the skin, usually via an adhesive, and include a heating element that elevates the local tissue temperature to approximately 45°C to increase gas diffusion rates. This heating alters the tissue from its normal physiological state. Furthermore, $TcPO_2$ sensors require full calibration at the bedside prior to use. Like Clark electrodes, $TcPO_2$ sensors measure tissue oxygenation at only a single point, necessitating multiple sensors for oxygen mapping.

Whereas electrode technology largely requires the insertion of a probe into tissue, optical technologies can avoid direct skin contact and thus offer advantages in the study of sensitive skin conditions such as wounds. One direct approach is to determine if tissue is receiving blood flow by measuring or mapping perfusion directly. These techniques look at blood flow within vessels either via the use of fluorescent dyes or by measuring

the rate of flow. Tools such as the SPY angiography system make use of intravenous injection of the fluorescent dye indocyanine green, which can be excited by near-infrared light and visualized with a sensitive camera system [17]. Operating in the dark, such an imaging system can determine if blood is flowing to a particular region of tissue, with measurement penetration depth up to 2 cm. Doppler imaging systems, in contrast, take advantage of the time-variant nature of the reflected ultrasonic signal caused by blood flow to determine the extent of local blood supply up to 2 mm deep [18]. Though useful, these methods measure blood flow, not actual tissue oxygenation.

Near-infrared oxygen sensing can provide a measure of both blood supply and tissue-related oxygen values [19]. These tools make use of the endogenous contrast provided by the binding of oxygen to heme – oxygen saturation (StO₂) – by probing the absorption of oxy- and deoxyhemoglobin. The most well-known of these techniques is the pulse oximeter, which measures tissue absorption at two wavelengths to determine the percentage of heme bound to oxygen in pulsating arterial blood [20]. Other near-infrared (NIR) StO₂ technologies include NIRS (near-infrared spectroscopy) [21], diffuse optical tomography and spectroscopy [22], photoacoustic tomography [23], and optical coherence tomography [24]. It is important to emphasize that these techniques measure blood oxygen saturation (StO₂) rather than oxygen tension (pO₂), which is a separate metric that is not always representative of local oxygen concentration. StO₂ measurements can detect only the level of heme binding to oxygen in blood, and as such do not directly report the oxygen concentration within tissue itself. Moreover, these tools only work where there is active blood supply; if tissue is poorly perfused or injured, the information gained through NIR StO₂ measurements can be limited.

While other methods offer considerable insight into tissue properties, no current clinical method provides direct, noninvasive measurement of tissue oxygen concentration by mapping oxygen over whole regions of tissue. Much effort, therefore, has been spent focusing on the development of new tools and methods that can deliver real-time, accurate measurements of skin pO₂.

Nanomaterials in Oxygen Sensing

Materials engineered to be micro- to nanometers in diameter feature a number of unique chemical and biological properties that make them advantageous over bulk materials [25]. For instance, sensors in the form of nanoparticles not only have a very high surface area-to-mass ratio, providing a large contact area between a sensor and its analytes, but also see ready uptake by

cells via endocytosis. Due to these unique properties, nanoparticles have been widely used to build oxygen-sensing materials, with the goals of improving the sensing capabilities, the biocompatibility, and the bio-distribution of the oxygen probes.

For example, the dynamic range of an oxygen sensor can be fine-tuned by embedding the probe molecule in particles that provide different levels of permeability toward oxygen gas [19,26]. In addition, the particle matrix can immobilize probe molecules, preventing excessive aggregation while also serving as a physical barrier between the probe molecules and the biological milieu [19,27]. These effects help reduce the potential toxicity of sensing probes and prevent unwanted interference or degradation by ions, enzymes, or proteins in the body. The surface properties of the particles can also be modified to maximize their accumulation in target tissues. Targeting is usually accomplished by tuning the charge and hydrophobicity of the particle surface or by covalently attaching targeting ligands [28].

OXYGEN SENSING BASED ON PHOSPHORESCENCE QUENCHING

Introduction to Phosphorescence Quenching

The largest group of oxygen-sensing molecules developed thus far is based on an optical principle called oxygen-dependent phosphorescence quenching [19,26,27,29,30]. Phosphorescence is a type of photoluminescence where the energy absorbed by a molecule is not re-emitted immediately, but rather over a longer time following the initial excitation. Therefore, the phosphorescence glow usually has a longer lifetime (from microseconds to minutes) compared to fluorescence emission (several nanoseconds).

The sensing mechanism relies on the energy transfer that occurs when oxygen physically collides with a phosphor, during which molecular oxygen receives energy from the phosphor's triplet excited state and allows the phosphor to decay to its ground state nonradiatively, thus quenching the phosphor's emission. Therefore, as the concentration of oxygen increases, both the intensity and the lifetime of the phosphorescence decrease. The oxygen-dependent quenching effect on the probe's phosphorescence intensity and lifetime is described by the Stern–Volmer equation:

$$\frac{I_0}{I} = \frac{\tau_0}{\tau} = 1 + K_q \tau_0 pO_2 \quad (21.1)$$

where I_0 and τ_0 are the phosphorescence intensity and lifetime in the absence of oxygen, respectively; I and τ are, respectively, the phosphorescence intensity and lifetime at a given oxygen concentration, pO₂; and k_q is a

constant related to the rate of bimolecular quenching between oxygen and the phosphor. The different types of phosphorescent oxygen sensors will be further described in Section “Phosphorescent probes”.

Probes that rely on oxygen-dependent phosphorescence quenching can be applied in a number of ways. The feasibility of utilizing so-called naked probe molecules is usually limited by their poor solubility in the medium of interest, interference by other species in the sample, ease of probe degradation, and poor dynamic range due to the high rate of molecular oxygen collision with the probe (ie, even the smallest quantities of molecular oxygen quench the probe's phosphorescence entirely) [26]. Many strategies have been developed to immobilize and stabilize the probe molecules so that oxygen sensors can be constructed into a desired form factor (eg, fiber-optics and planar sensor films) [19,27]. These methods include chemically modifying the probe's periphery, immobilizing the molecules onto the surface or inside the framework of solid particles, and embedding the molecules in a thin polymeric film. These approaches will be further discussed in Section “Sensor Matrix”.

Oxygen sensing based on phosphorescence quenching has been realized in a variety of systems such as spectrometers, fiber-optic sensors, cameras, and microscopes, providing quantitative measurements on different spatial and temporal scales in biological samples. Detailed discussions of phosphorescence-quenching measurement techniques can be found in a number of recent reviews [19,27,30]. Both intensity- and lifetime-based approaches have been utilized. Intensity-based approaches correlate the phosphorescence intensity measured by a photodetector with oxygen concentration. They are simple and can be easily adapted to existing systems such as CCD (charge-coupled device) and CMOS (complementary metal-oxide semiconductor) cameras [31]. An oxygen-independent dye co-localized with the sensing phosphor can provide a ratiometric measurement to correct for inhomogeneous illumination and probe distribution across a sample's two-dimensional surface [32]. In contrast, lifetime-based approaches have the advantage of being independent of excitation intensity, detector sensitivity, and probe concentration. However, their implementation requires more advanced optical systems, including pulsed light sources and time-gated cameras (used in time-domain lifetime measurements) [33] or modulated light sources and phase detection (used in frequency-domain measurements) [34].

Phosphorescent Probes

Transition metal complexes undergoing metal-ligand charge transfer can enter a long-lived excited triplet state

upon excitation. Many of these complexes have high phosphorescence quantum yield, and their phosphorescence emission is sensitive to quenching by molecular oxygen.

Early studies have shown that ruthenium(II), osmium(II), and iridium(III) complexes are strongly quenched by oxygen [30]. Osmium complexes present excellent photostability and can be made into effective oxygen-sensing probes [35]; however, they are highly toxic, and therefore not suitable for biomedical applications. Ruthenium complexes possess excited state lifetimes on the order of microseconds and represent the most common transition metal complexes used for oxygen sensors [19,27,30]. For example, the most commonly used complex, Ru(bpy)₃, has strong absorption in the blue region, emits in the red slightly above 600 nm, and has been incorporated into nanoparticles, thin films, and fiber-optics for sensing oxygen in biological systems. Iridium(II) complexes lack low-lying, nonemitting excited states that could lead to the nonradiative depopulation of the excited triplet state. As a result, they demonstrate stronger phosphorescence [quantum yield (QY): 0.2–1.0] compared to ruthenium(II) complexes (QY < 0.2). Many recent studies have focused on developing iridium-complexed oxygen sensors [36].

Over the past decade, these early sensors have been largely replaced by another, even larger group of transition metal complexes: the metalloporphyrins [19,26,27,30]. Compared to the Ru and Ir complexes, metalloporphyrins are equally quenchable by oxygen. In addition, they have higher structural versatility, enabling the design and synthesis of oxygen probes with highly tunable physical and chemical properties. Cu, Ni, Pt, Pd, and Zn metalloporphyrins have been explored as oxygen sensors; among these compounds, Pt(II) and Pd(II) porphyrins show the highest phosphorescence quantum yield and provide the quenching constants most suitable for oxygen measurements in the physiological pO₂ range [26]. Generally, Pt porphyrins possess a phosphorescence quantum yield (QY: 0.1–0.25) two to three times greater than that of Pd porphyrins (QY: 0.05–0.1). Advantageously, however, Pd porphyrins have a longer emission lifetime compared to their Pt counterparts (10^{−4} s vs. 10^{−5} s). The stronger spin–orbit coupling in the heavier metal complex (Pt) facilitates intersystem crossing into the triplet excited state as well as rapid phosphorescence decay back to the ground state [30]. Fig. 21.1 illustrates some of the transition metal complexes that have been commonly used as oxygen probes.

Since unmodified porphyrins have low water solubility, a number of strategies have been explored to modify the periphery of these metalloporphyrins to create probes compatible with a wide range of environments. These include chemically modifying the peripheral

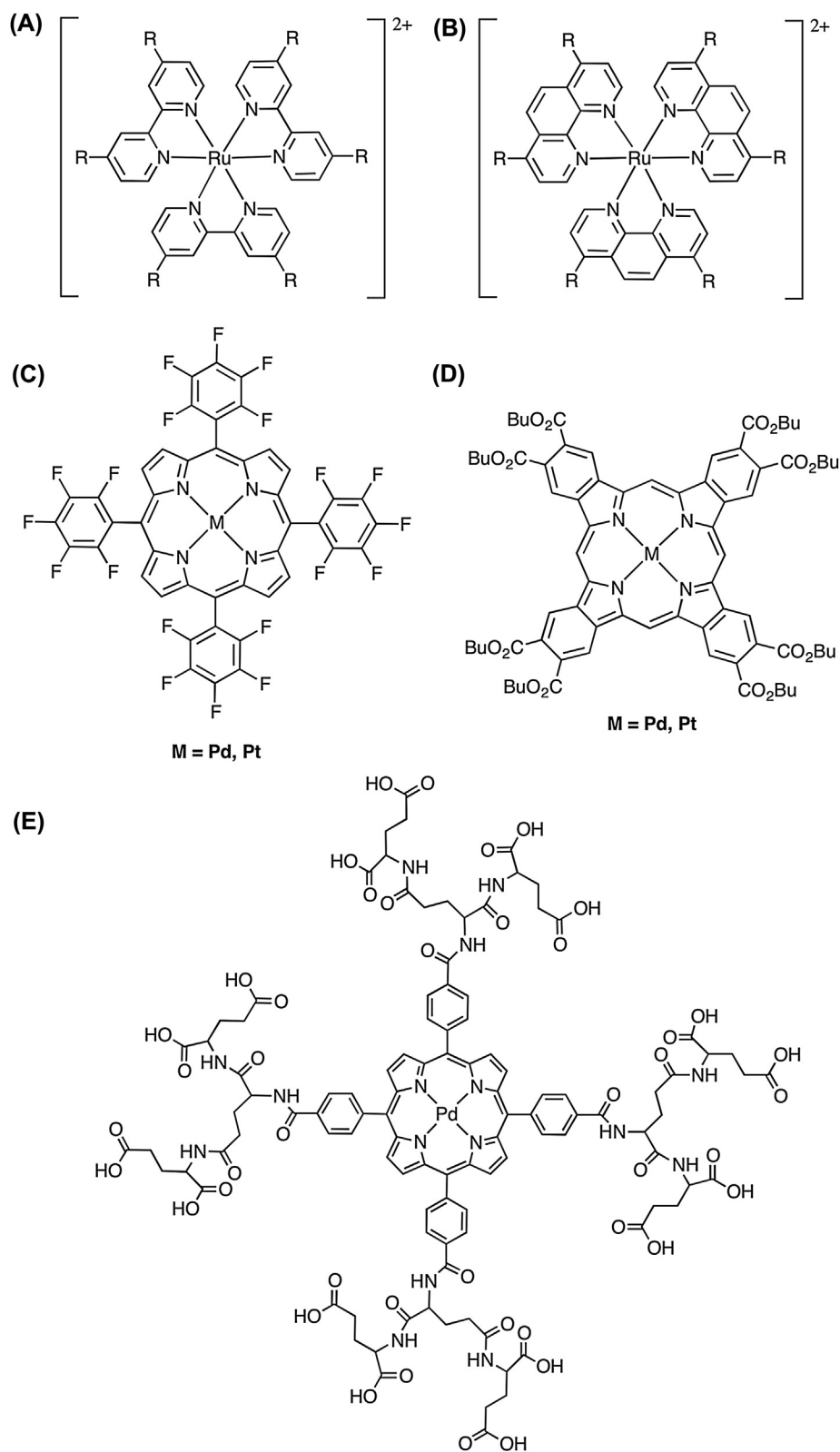


FIGURE 21.1 Chemical structures of commonly used oxygen-sensing phosphors. (A) Tris(bipyridine) ruthenium(II), also called $[\text{Ru}(\text{bpy})_3]^{2+}$; (B) tris(1,10-phenanthroline) ruthenium(II) ($[\text{Ru}(\text{phen})_3]^{2+}$); (C) platinum(II)- or palladium(II)-5,10,15,20-tetrakis-(2,3,4,5,6-pentafluorophenyl)-porphyrin (PtTFPP or PdTFPP, respectively); (D) platinum(II) or palladium(II) tetrabenzoporphyrin octabutylester (PtTBP(CO_2Bu)₈ or PdTBP(CO_2Bu)₈, respectively); and (E) Pd-meso-tetra-(4-carboxyphenyl)porphyrin-glutamate-dendrimer (Oxyphor R2).

groups of the metalloporphyrin, attaching dendritic structures to the central porphyrin, forming protein–porphyrin complexes, or embedding the porphyrin in micro- or nanoscale constructs. These modifications protect the probes from chemical degradation and interfering species (eg, metal ions and protein binding). More importantly, they serve to improve the sensitivity and dynamic range of the probe by fine-tuning the oxygen diffusion rate from the sample media to the metalloporphyrin cores, thereby producing the ideal quenching constant k_q required for the specific application.

Given these considerations, ideal oxygen-sensing phosphors should meet the following design criteria:

1. High phosphorescence intensity.
Determined by both the molar extinction coefficient and the phosphorescence quantum yield. Brighter sensors provide higher sensitivity and signal-to-noise ratio and are more likely to overcome background tissue autofluorescence. Some of the brightest sensors developed thus far are orange-emitting Ir(II) coumarin complexes and red/NIR-emitting Pt(II) porphyrins (both have molar extinction coefficients over $80,000 \text{ M}^{-1}\text{cm}^{-1}$ and phosphorescence quantum yields above 0.5).
2. Long excited state lifetime.
Lifetime affects both sensitivity and dynamic range. A longer lifetime makes collisional quenching by molecular oxygen more likely, giving rise to the highest possible measurement resolution. Long lifetime also makes it easier to separate the phosphorescence signal from any reflection or fluorescent background. Pd(II) porphyrins with long lifetimes (10^{-4} s) are more suitable for low oxygen concentration sensing, while Pt(II) porphyrins with lifetimes on the level of 10^{-5} s are most suitable for sensing with greater, more physiologically relevant ranges of oxygen concentration.
3. Appropriate quenching constant k_q .
The quenching constant k_q of the compound should be large enough to give high sensitivity, but not so high that the intensity/lifetime drops to zero at even the lowest oxygen concentrations.
4. Appropriate excitation and emission wavelength.
Excitation wavelength should ideally be compatible with common light sources (eg, LED, lasers in confocal microscopes, and camera flash). Longer, NIR excitation is preferred for deep tissue penetration. Excitation in the ultraviolet range should be avoided because of the background fluorescence in this range originating from many biological substances, sensor supports, optical components, and so on.
5. Good chemical stability.
For longer shelf life.
6. High photostability.
For good sensor reversibility in long-term application. Electron-withdrawing groups (halogens) enhance photostability.
7. High selectivity to oxygen, low cross-sensitivity to other parameters.
The probe should not be affected by other variables such as temperature, pH, metal ions, humidity, bacteria, and so on. For example, Ru(II) and Ir(II) complexes are more prone to thermal quenching than metalloporphyrins (the latter experience only a 0.05–0.2% change in decay time per 1K).
8. High solubility.
Probe molecules should be compatible with their media. Structural modification may be necessary to obtain the desired surface properties.
9. Biocompatible and nontoxic.
Compounds should be suitable for biological and medical applications. Some factors to be considered include the chemical toxicity caused by metal ions, the phototoxicity caused by singlet oxygen generation, and the liver–kidney toxicity of metabolic products. Embedding the probes within a polymeric matrix (nanoparticle or film) can reduce their toxicity. Enhancing the probe brightness also allows for a smaller amount to be used, thereby decreasing the active-to-lethal dose ratio.

Sensor Matrix

A number of phosphorescent probes can be directly solubilized for oxygen sensing in liquid-based environments (eg, blood) [37]. However, in order to be used for oxygen imaging in skin, the majority of phosphorescent probes need to be immobilized within a solid substrate so that the sensor's desired form factor (eg, sensor film and fiber) can be achieved, leaching of probe molecules into the skin is prevented, and the permeability of oxygen and other interfering species can be adjusted to enhance the sensitivity, selectivity, and stability of the probe molecule.

Micro- and nanoparticles synthesized from inorganic and organic polymers are excellent substrates for oxygen probes since they contain a large surface area for oxygen exchange, protect the probe molecules from chemical degradation, and offer a wide range of permeability to oxygen and other species. In fact, the first phosphorescent oxygen sensors were constructed with probe molecules absorbed onto the surface of silica particles [38]. Since this first demonstration in 1931, numerous other materials have been explored as substrates for phosphorescent oxygen probes, including polystyrene (PS), polydimethylsiloxane (PDMS), polyacrylonitrile (PAN), and ethylcellulose. These materials were chosen

for their unique solubility and permeability to oxygen, impermeability to interfering species such as water and metal ions, and excellent mechanical and adhesive properties [19,27].

Oxygen probe molecules can be incorporated into particles in three major ways:

1. Immobilized on the particle surface.
Surface adsorption of charged probe molecules can be readily achieved via electrostatic interactions with negatively charged (eg, silica, alumina, and carboxyl-terminated polymer beads) or positively charged particles (eg, amine-terminated silica or polystyrene beads). Probe molecules with reactive peripheral groups can also be covalently linked to the particle surface for stronger attachment.
2. Embedded throughout the particle framework.
Incorporating probes throughout the particle framework allows for the molecules to be more tightly enmeshed and therefore less likely to leach into the sample. Furthermore, the particle matrix protects the probe and offers different degrees of shielding toward oxygen. As a result, the quenching efficiency of the sensor can be tuned to a wide dynamic range.
3. Located at the center of a nanoconstruct.
Recently, a class of oxygen-sensing nanoconstructs has been developed in which dendritic branches are grown from a central probe molecule (Fig. 21.2) [26]. The resulting oxygen-sensing dendrimers have distinct sizes and structures [39]. Unlike particle-embedded probe molecules that experience a heterogeneous microenvironment, the probe molecules in a dendrimer nanoconstruct receive consistent shielding and therefore demonstrate highly uniform oxygen quenching.

In order to engineer oxygen sensors suitable for applications in skin, probe molecules or probe-containing particles can be further embedded in a polymer host and made into planar sensor films or fiber-optics. Fig. 21.3 illustrates the four most common approaches of embedding oxygen-sensing probes in a solid polymer host. The general considerations while selecting solid substrates for oxygen probes are summarized here. Specific examples of microparticle- and nanoparticle-based oxygen sensors will be provided in the next section.

1. Compatible with the probe molecule.
Charge, hydrophobicity, reactivity, and optical interactions between the probe and the substrate should be considered.
2. Provide optimal oxygen permeability.
Oxygen permeability of the substrate should be adjusted to maximize the probe's sensing dynamic range.

3. Appropriate solubility and surface properties.
To ensure sufficient solubility of the particle in its polymer host or biological media.
4. Transparent and optically inert.
The substrate needs to be optically transparent or at least minimally translucent for phosphorescence sensing.
5. Nontoxic and biocompatible.
The host matrix should not cause adverse effects to human or animal subjects. Leaching cannot be permitted.
6. Chemically stable.
Sensors should have optimal stability and degradability for their proposed uses.
7. Provide optimal mechanical properties.
Flexibility, strength, elasticity, and other mechanical properties should be adjusted according to the desired form factors, such as fiber-optics or sensor film conformable with skin.

Nanomaterial Oxygen Sensors

Ru(II) polypyridyl complexes with relatively high brightness and long lifetimes were some of the earliest phosphorescent probes to be incorporated into nanometer-sized oxygen sensors. For example, liposomes and microemulsions have been used to stabilize and deliver Ru(phen)₃ and Ru(bpy)₃ [40,41]. Ru(dpp)₃ (dpp: 4,7-diphenyl-1,10-phenanthroline), with its relatively long phosphorescence lifetime (6.4 μs) and high quantum yield (0.3), is also one of the most common Ru complexes to be incorporated into sensors [42–45]. PDMS microparticles containing a Ru complex have been used to map oxygenation throughout 3D cell scaffolds in vitro [46]. Silica and ormosil (organically modified silica gel) nanoparticles have also been developed, and new materials and formulations are still being explored [27,43,47,48].

Ru complexes have the advantage of being easy to synthesize, but they are limited by short phosphorescence lifetimes, moderate brightness, and severe temperature dependence. Since the early 2000s, they have been largely replaced by the brighter metalloporphyrin-based oxygen probes, which provide a wide range of structural variations that are suitable for a plethora of applications. Platinum octaethylporphyrin (PtOEP) was a popular probe due to its strong room temperature phosphorescence and long lifetime. It has been immobilized in nanoparticles created from organic (eg, PDMS and PS) [44,49] and inorganic (eg, silica and ormosil) materials [50,51]. However, PtOEP suffers from rather low photostability and has since largely been replaced by platinum tetrakis(pentafluorophenyl)porphyrin (PtTFPP), which contains

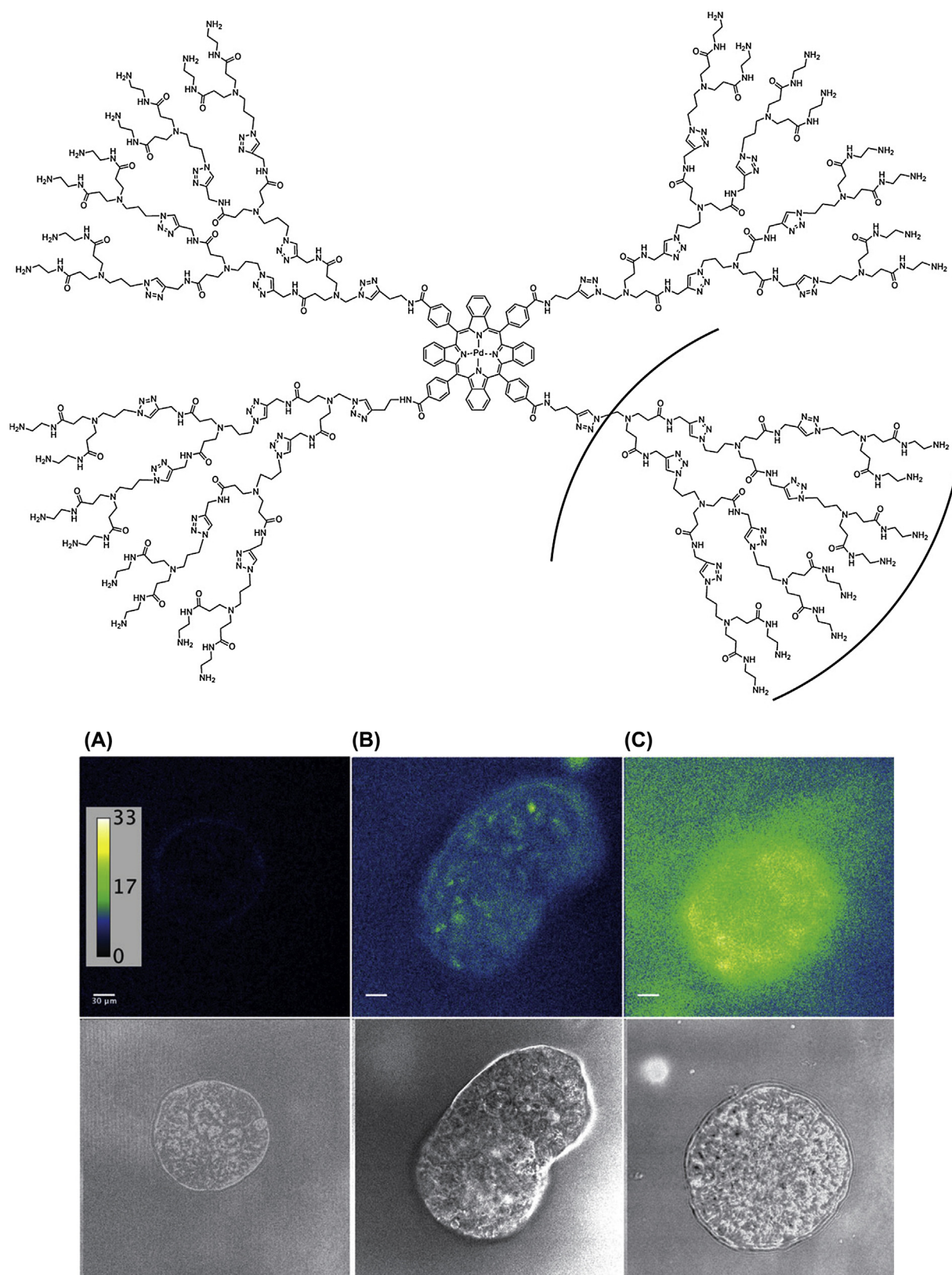


FIGURE 21.2 (Top) Chemical structure of the G3 CAOS sensor, a Pt(II) metalloporphyrin encapsulated within a third-generation glutamic acid dendrimer. (Bottom) Panels showing phosphorescence confocal microscopy images of 3D ovarian cancer spheroids (bottom/gray panels: transmission channel) corresponding to no treatment control (A), and to spheroids treated for 4 h with 2 μM G3 CAOS, imaged under air (B) or after a N₂ purge (C). The color scale bar shown in the top left image represents the number of photons collected. Adapted with permission from Nichols AJ, Roussakis E, Klein OJ, Evans CL. Click-assembled, oxygen-sensing nanoconjugates for depth-resolved, near-infrared imaging in a 3D cancer model. *Angew Chem Int Ed Engl* 2014;53(14):3671–4.

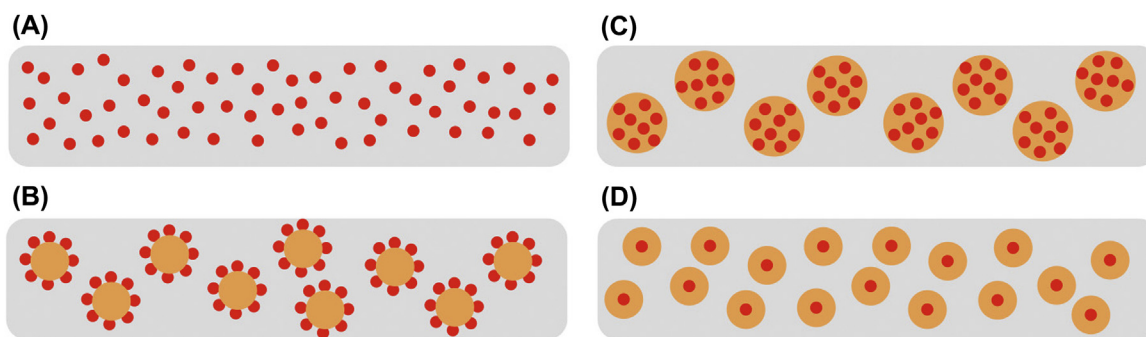


FIGURE 21.3 Scheme of four common approaches to immobilize oxygen probes in a solid substrate. (A) Oxygen probes (red dots) are directly embedded in the host matrix (gray); (B) oxygen probes are absorbed or covalently attached to micronanoparticles (orange) and then embedded in the matrix; (C) oxygen probes are immobilized throughout micro/nanoparticles and then embedded in the matrix; (D) oxygen probes are at the center of dendritic nanoconstructs and then embedded in the matrix.

electron-withdrawing perfluorophenyl substituents that reduce the tendency of the porphyrin ring to be oxidized by singlet oxygen. PtTFPP has also been embedded within nanoparticles composed of polystyrene [32,52,53], poly(styrene-block-vinylpyridine) [54,55], Eudragit RL-100 [56], and poly(N-isopropylacrylamide) [52], and applied to oxygen sensing in cell cultures [40]. Inorganic particles such as mesoporous silica offer unique properties in which metalloporphyrins can be covalently attached to the inside of the particle's nanochannels (Fig. 21.4) [48]. Other types of nanoparticles such as luminescent quantum dots have also been combined with oxygen probe molecules to create fluorescence resonance energy transfer (FRET)-based sensors or simply to serve as an oxygen-independent reference. [57].

One prominent class of nanoparticle oxygen probes is the PEBBLE (probe-encapsulated by biologically localized embedding) developed by Kopelman et al. Oxygen probe molecules (eg, Ru(dpp)₃, PtOEP, and Oxyphor G2) were noncovalently incorporated into nanoparticles (eg,

poly(acrylic acid), poly(decyl methacrylate), silica, and ormosil) [51,58,59]. The design of PEBBLE focuses on optimizing the biocompatibility and biodistribution of the sensor, by using nontoxic sensor matrix and/or surface-targeting moieties for selective delivery to specific cells or subcellular organelles (Fig. 21.5).

Skin Oxygen Sensing Based on Phosphorescence Quenching

A number of strategies have been used to create phosphorescent probes suitable for sensing oxygen in the skin. Early experiments involved coating the tip of glass fiber-optic sensor optrodes with a silicone film containing oxygen-sensing Ru(II) complexes [33,60]. When the tip is in contact with the target tissue, the oxygen concentration equilibrates between the tissue and the sensor. Excitation light can be delivered to the sensor molecules through the optical fiber, and the emitted light from the sensing layer can be collected by the fiber and later correlated to oxygen partial

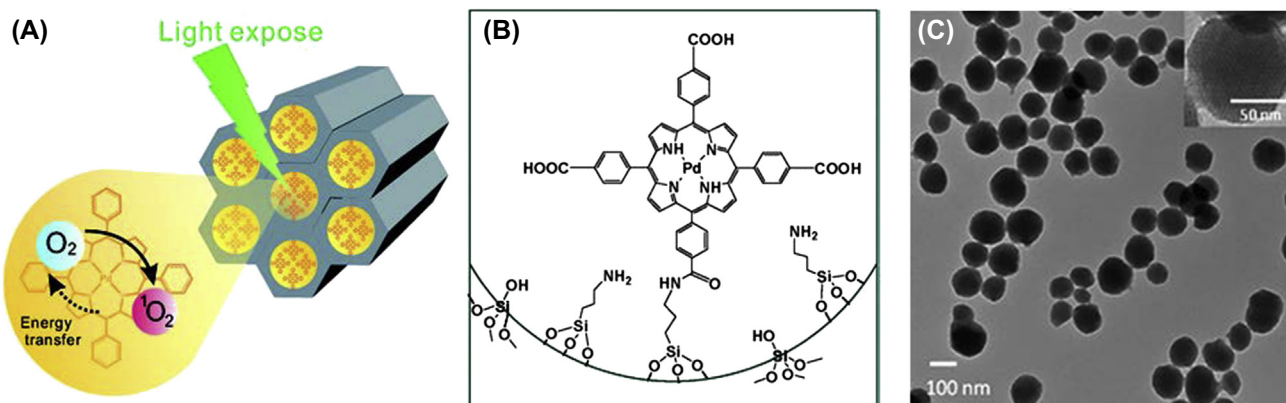


FIGURE 21.4 (A) A photodynamic model of mesoporous silica nanoparticles (MSNs); (B) the covalent modification of Pd tetraphenylporphyrin (PdTPP) onto the nanochannel surface of MSNs; (C) a TEM image of MSN-PdTPP. Adapted with permission from Cheng S-H, Lee C-H, Yang C-S, Tseng F-G, Mou C-Y, Lo L-W. Mesoporous silica nanoparticles functionalized with an oxygen-sensing probe for cell photodynamic therapy: potential cancer theranostics. *J Mater Chem* 2009;19:1252–7.

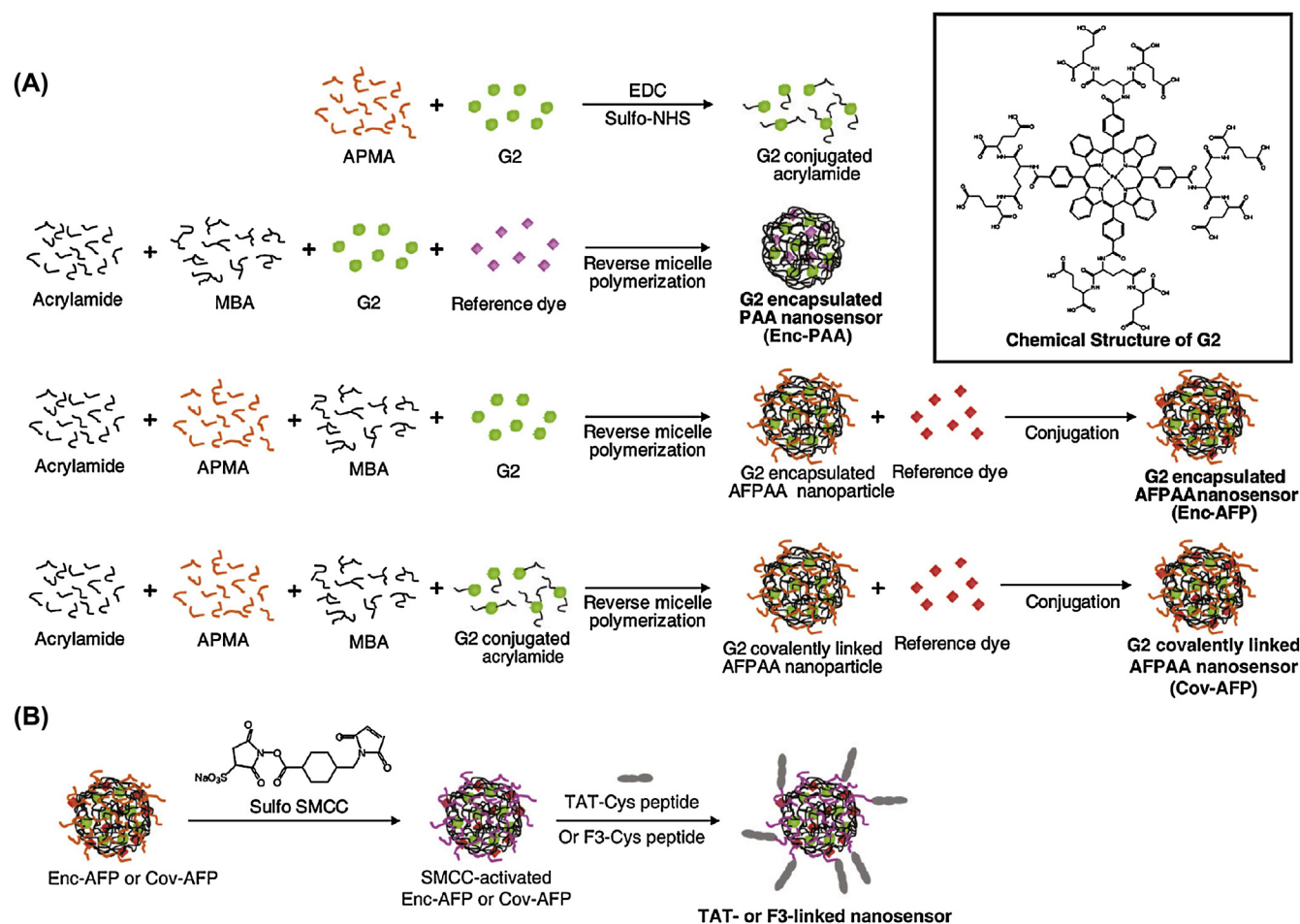


FIGURE 21.5 Synthesis of targeted ratiometric Oxyphor G2-loaded oxygen nanosensor. (A) Preparation of three kinds of G2-loaded poly(acrylic acid) (PAA) nanosensors; (B) conjugation of TAT or F3 peptide to the G2-loaded amine-functionalized PAA (AFPAA) nanosensor. The targeted G2-loaded ratiometric oxygen sensors were prepared with optimized oxygen sensitivity and brightness. Reprinted with permission from Lee YE, Ulbrich EE, Kim G, Hah H, Strollo C, Fan W, et al. Near infrared luminescent oxygen nanosensors with nanoparticle matrix tailored sensitivity. *Anal Chem* 2010;82(20):8446–55.

pressure. The technique is straightforward, and commercial oxygen-sensing micro-optrodes have been produced. However, such fiber-based sensors have the drawback of causing tissue perturbation and only provide point measurements.

Creating phosphorescent, oxygen-sensing films has been a major focus of research. A planar-sensing film is advantageous over a point measurement approach in that it provides oxygen-“mapping” capabilities over an entire area of interest and is especially suitable for skin oxygen sensing. Silicone is an excellent matrix for making oxygen-sensing films due to its outstanding oxygen permeability, and it has been widely used to immobilize hydrophobic probe molecules, such as Ru complexes [34,35,45,60,61]. Polystyrene is also a popular hydrophobic matrix and has been used to immobilize PtOEP to create subcutaneous or transcutaneous oxygen-imaging systems [55,62].

If hydrophilicity is a required characteristic of the matrix, ethylcellulose or nitrocellulose can be components of oxygen-sensing films, providing excellent biocompatibility and mechanical properties [34]. For example, a rapid-drying, paint-on bandage formulation of the oxygen sensor Oxyphor R2 in nitrocellulose was recently created. The resulting oxygen-sensing bandage conforms to the skin surface and has provided two-dimensional, transdermal oxygen maps in a number of animal models [63]. Other hydrophilic materials, such as polyurethane hydrogels, have demonstrated good oxygen permeability [64,65]. For example, Wolfbeis et al. applied a polyurethane hydrogel film containing three types of nanoparticles (ie, oxygen sensing, pH sensing, and reference) to the skin of human subjects and obtained maps of tissue pO_2 and pH across healthy skin, grafts, and acute wounds (Fig. 21.6) [65].

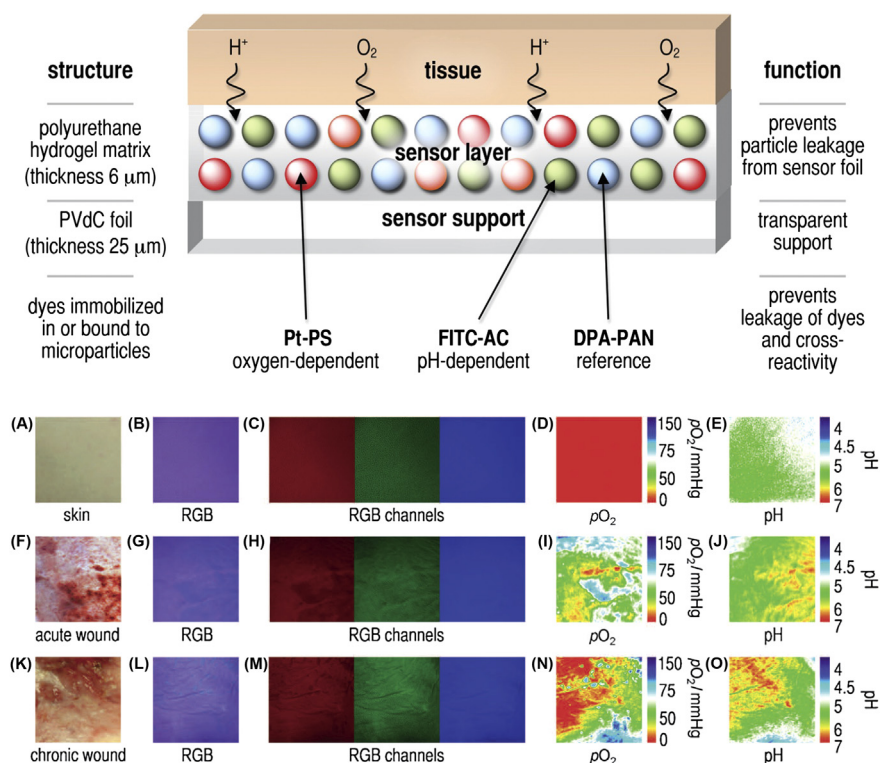


FIGURE 21.6 (Top) Sensor foil scheme. (Bottom) In vivo application of the dual sensor on the plain skin surface of a volar forearm (A–E), a skin graft donor site (postoperative, day 5) as a model for acute wound healing (F–J), and a chronic wound (K–O). (A,F,K) Pictures of skin and wound surfaces; (B, G, L) RGB pictures of skin and wound with an overlaying sensor. (C,H,M) The picture is split into the three respective color channels. (D,I,N) The R/B ratios show the distribution of oxygen; (E,J,O) the G/B ratios show the pH distribution on the surface of skin and wound. Adapted with permission from Meier RJ, Schreml S, Wang XD, Landthaler M, Babilas P, Wolfbeis OS. Simultaneous photographing of oxygen and pH in vivo using sensor films. *Angew Chem Int Ed Engl* 2011;50(46):10893–6.

Thanks to the continuing advances in designing brighter probes, the optical sensing of oxygen in skin can be carried out with growing sensitivity and less complex instrumentation. However, advanced micro- and nanoparticle formulations are needed to provide better biocompatibility and oxygen permeability for the probe molecule. Novel materials for constructing sensor matrices are also necessary to meet the chemical, optical, and mechanical challenges posed by the unique structure and topology of the skin. For instance, the intrinsic skin roughness and curvature may lead to uneven sensor attachment, and may cause only certain parts of the tissue to lie within the focal plane. An airtight seal needs to be formed between the sensor and the skin, so that an accurate reading from the tissue side can be obtained without being affected by oxygen in room air. In addition, effective mechanisms are needed to minimize the interference of strong autofluorescence from skin cells. In parallel to probe development, advances in optical detection and imaging devices have provided a wide range of portable and inexpensive systems that allow for the easy readout and quantification of sensor emission. Optical sensors for skin oxygen measurement can be fashioned into wearable and connected

devices, which provide continuous monitoring of tissue oxygenation during ischemic injuries, wound healing, and treatment response.

OXYGEN SENSING BASED ON MAGNETIC RESONANCE TECHNIQUES

Introduction to Magnetic Resonance Techniques

Despite the high sensitivity and resolution of oxygen sensing by phosphorescence quenching, optical techniques are inherently limited by the penetration depth of the excitation and emission light (typically, several hundred microns in tissue), and are thus suitable only for measuring oxygen on the surface of a subject. Magnetic resonance–based techniques have attracted tremendous attention due to their noninvasive nature and whole-body scanning capabilities, and have therefore experienced rapid advancement over the past 50 years. This section introduces oxygen-sensing techniques that utilize the spin resonance of atomic nuclei or electrons within magnetic fields, the advances in the

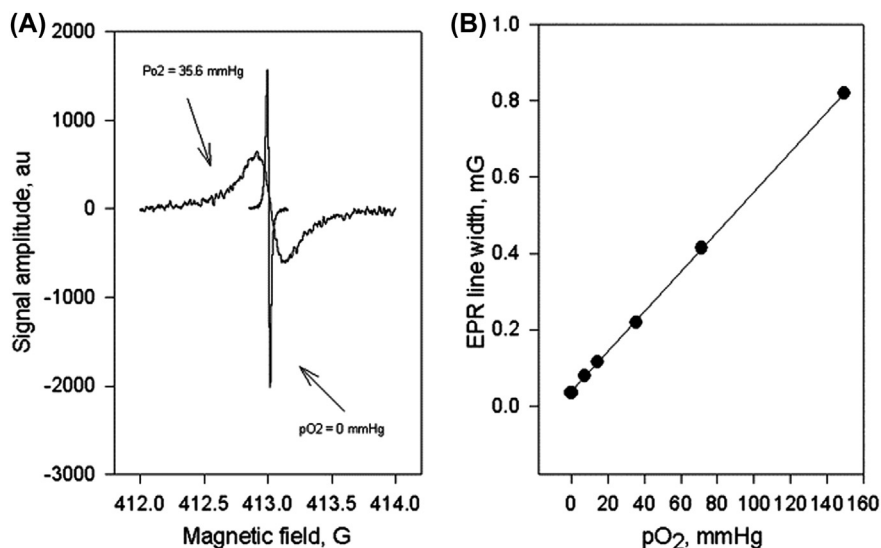


FIGURE 21.7 Oxygen calibration curve of LiPc. (A) EPR spectra showing the line shape in 0 and 35.6 mm Hg pO_2 . Note that the higher the pO_2 , the broader the line. (B) Calibration curve of LiPc against known gases. The linewidth is not sensitive to whether the material is in water, saline, or air. Calibrations are thus routinely done in air. Reprinted with permission from Dunn JF, Swartz HM. *In vivo electron paramagnetic resonance oximetry with particulate materials*. *Methods* 2003;30(2):159–66.

design of these types of probes and particles, and their applications in skin oxygen sensing.

The energy difference between two spin states of an atomic nucleus or electron is linearly proportional to the magnetic field in which the nucleus is located. As a result, nuclei and electrons in a magnetic field absorb and re-emit electromagnetic radiation at frequencies unique to their chemical environment. Resonance techniques take advantage of the noninvasive nature of the magnetic field by using radiofrequency or microwave radiation to detect specific chemical species in a biological system. Detailed descriptions of oxygen sensing based on these resonance techniques can be found in a number of recent reviews [19,66].

Nuclear magnetic resonance (NMR) techniques based on 1H and ^{19}F NMR can detect changes in the relaxation rate of either an endogenous or an exogenous contrast agent following an interaction with molecular oxygen. Commonly used exogenous contrast agents include perfluorocarbons (PFCs) for ^{19}F NMR [67] and hexamethyl-disiloxane (HMDSO) for 1H NMR [68]. In a typical *in vivo* experiment, a contrast agent is administered intravenously in an emulsion or nanocarrier several hours to a few days before the measurement [66]. NMR instruments constructed for *in vivo* studies utilize frequencies in the range of 10–400 MHz and associated magnetic fields between 0.4 and 10 T.

Techniques based on electron magnetic resonance mainly involve electron paramagnetic resonance (EPR). EPR utilizes paramagnetic contrast agents, including stable radicals such as nitroxides and particulate materials such as India ink, carbon black, and lithium

phthalocyanine (LiPc) [69,70]. The EPR spectra of these paramagnetic species are easily affected by the spin of nearby unpaired electrons in molecular oxygen, which exists as a triplet in its ground state. The orbital overlap of these unpaired electrons leads to energy exchange that shortens their relaxation times, resulting in broadening of their spectral features. The measured linewidth can be correlated with the pO_2 of the surrounding material (Fig. 21.7) [71]. Relevant design criteria of oximetric particulate materials include their spin density, the linewidth in the absence of oxygen, the change in linewidth per unit oxygen, and the range over which they respond to changes in oxygen.

Since the magnetic moment of the electron is much greater than that of the nucleus, an electron resonance instrument utilizes higher radiofrequencies and lower magnetic fields compared to an NMR instrument. As the magnetic field strength increases, the frequency increases proportionally along with the sensitivity of the technique. However, higher radiofrequencies suffer from reduced tissue penetration depth. Therefore, *in vivo* EPR systems tend to operate at the lower frequencies and field strengths. The frequencies commonly used for *in vivo* EPR are usually in the range of 300–1200 MHz, and magnets in the range of 0.01–0.04 T.

Particle Oxygen Sensors for Magnetic Resonance Techniques

Oxygen-sensing NMR contrast agents are usually introduced into systemic circulation or directly injected

into the tissue being measured. In order for the contrast agents to accumulate at a specific tissue location, contrast agents have been incorporated into nanoparticles and emulsions to create biocompatible, targeted delivery formulations. For example, Mason et al. have used a PFC emulsion, Oxypherol-ET, to measure subcutaneous tumor pO_2 in mice based on ^{19}F NMR. Measurements were performed after complete vascular clearance of the perfluorocarbon, enabling ^{19}F signal to be observed specifically from materials sequestered in tissue, thus avoiding flow artifacts [72]. Similarly, siloxane-based nanoprobe have been developed for 1H MRI oximetry. HMDSO nanoemulsions have been created that allow for measurement of intramuscular pO_2 [68]. Solid microparticles of PDMS have been formulated, containing dodecamethylpentasiloxane as contrast agent, which can be injected and retained within the muscle for up to one month, providing long-term monitoring of intramuscular pO_2 [73].

There are two classes of paramagnetic materials that are most commonly used as contrast agents for EPR oximetry: soluble free radicals such as nitroxides, triaryl methyl radicals, and insoluble particulate materials such as lithium phthalocyanine, coals, chars, inks, and carbon blacks [70,74,75]. A variety of delivery systems have been developed to optimize the biocompatibility and biodistribution and to maximize the sensitivity and stability of these agents. For example, nitroxides are unstable in biological media and are quickly converted into diamagnetic hydroxylamines. Nitroxides incorporated into unilamellar liposomes, however, have demonstrated higher stability in oxygen measurements in vivo [76]. Nitroxides have also been encapsulated in the organic phase of proteinaceous microspheres, which provide higher sensitivity compared to the liposome formulations due to higher solubility of oxygen in organic solvents [77].

Compared to soluble free radicals, insoluble micro- and nanoparticle paramagnetic materials have a much higher spin density that provides, in some cases, up to 1000 times greater sensitivity to oxygen [71]. Another great advantage of particulate contrast agents is their excellent stability. Biocompatible implants containing oxygen-sensitive EPR contrast agents have been developed that can be injected into tissue for long-term monitoring of oxygenation at a given site over several months [78]. Coating oxygen-sensitive particles with biocompatible materials can prevent aggregation, enable systemic injection of these agents, and help improve tissue tolerance by minimizing undesired immunological responses. For example, Gallez et al. suspended inks consisting of fusinite or carbohydrate char in an aqueous solution containing arabic gum to create 300 nm nanoparticles; this reduced the nanoparticles' toxicity while preserving the oxygen sensitivity

of the material [79]. The same group found that coating charcoals with cellulose nitrate could extend the responsiveness to oxygen of these charcoals from less than a week to over 2 months [80].

Skin Oxygen Sensing Based on Magnetics Resonance Techniques

The application of MR-based oximetry in skin is challenging because the signal interference at the tissue–air interface is more prominent in a strong magnetic field. EPR-based techniques are less affected by this artifact. In fact, EPR is more readily adapted to skin applications, since it is not limited by the weak penetration (less than 1 cm) of the higher frequency radiation. Measurements of oxygenation in the skin can be carried out using either low-frequency (1200 MHz) or higher frequency (2.5 or 9.0 GHz) systems [81]. The first EPR instrument for clinical use was constructed at Dartmouth Medical School (Fig. 21.8) [71]. Since the majority of EPR contrast agents have not been approved for use in humans, early EPR studies were performed on human subjects with preexisting tattoos, utilizing the carbon black in the tattoo ink as a contrast agent.

EPR oximetry measurements in skin can provide clinically important information on dermatological oncology, peripheral vascular diseases, and wound healing [81]. With implantable contrast agents, EPR oximetry can be used for long-term monitoring of tissue oxygenation during the development of disease or in response to therapy, and it is necessary for optimal treatment of cancer and peripheral vascular disease [82]. For example, measurements of subcutaneous pO_2 have been performed in the feet of human subjects to study peripheral vascular disease and perfusion in diabetic patients. Measurements in tumors during courses of radiation and chemotherapy have allowed for tumor pO_2 to be followed, so oxygen-dependent therapies can be optimized (Fig. 21.9) [75]. Ongoing studies in wound models may allow physicians to monitor wound oxygenation using EPR to signal the need for intervention should wound healing become suboptimal.

The clinical translation of resonance-based oxygen-sensing techniques relies on advancements in human-compatible scanners, which provide the magnetic field and radiation frequency required for ^{19}F MRI and EPR imaging. The spatial resolution of current resonance imaging system is limited by the magnetic field strength used by the scanner, and it needs to be improved in order to obtain resolution of features on the submillimeter scale. Furthermore, the safety of MR and EPR contrast agents must be demonstrated. Much effort is required to develop biocompatible formulations that allow for the safe use in humans.

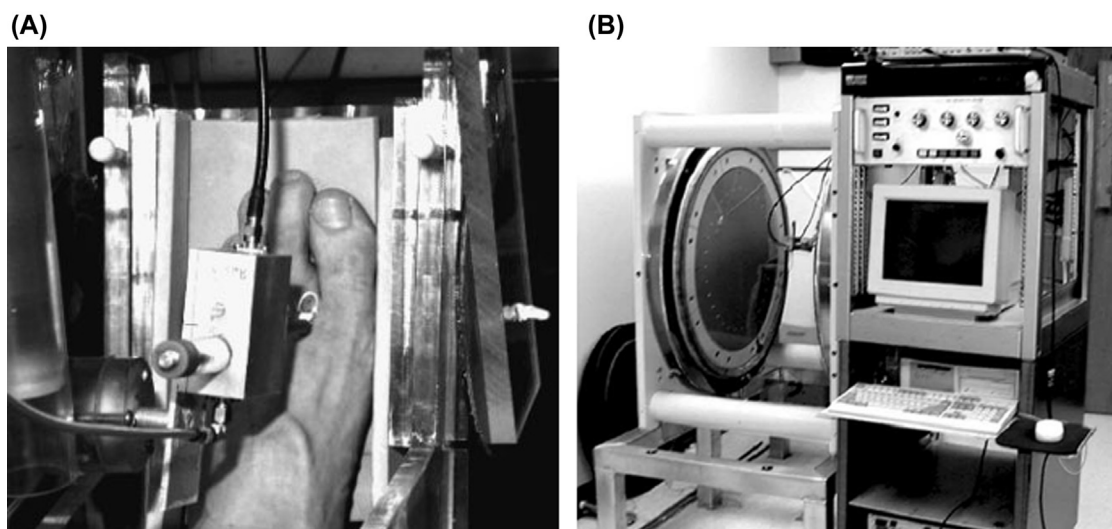


FIGURE 21.8 In vivo EPR oximetry systems. (A) A platform to position and stabilize the foot for measurements of pO_2 in the foot was designed and constructed based on the feedback from volunteers. The platform, resonator assembly, and deposit of India ink are visible in this photograph, which shows the position within the clinical magnet. (B) A 1.2 GHz frequency EPR system, installed in 2002 with a Sumitomo Special Metals Company magnet in the Dartmouth–Hitchcock Medical Center as the first dedicated clinically used human EPR system. The EPR magnet has a 105 cm diameter and a 50 cm gap. Adapted with permission from Swartz HM, Khan N, Buckley J, Comi R, Gould L, Grinberg O, et al. Clinical applications of EPR: overview and perspectives. *NMR Biomed* 2004;17(5):335–51; Dunn JF, Swartz HM. In vivo electron paramagnetic resonance oximetry with particulate materials. *Methods* 2003;30(2):159–66.

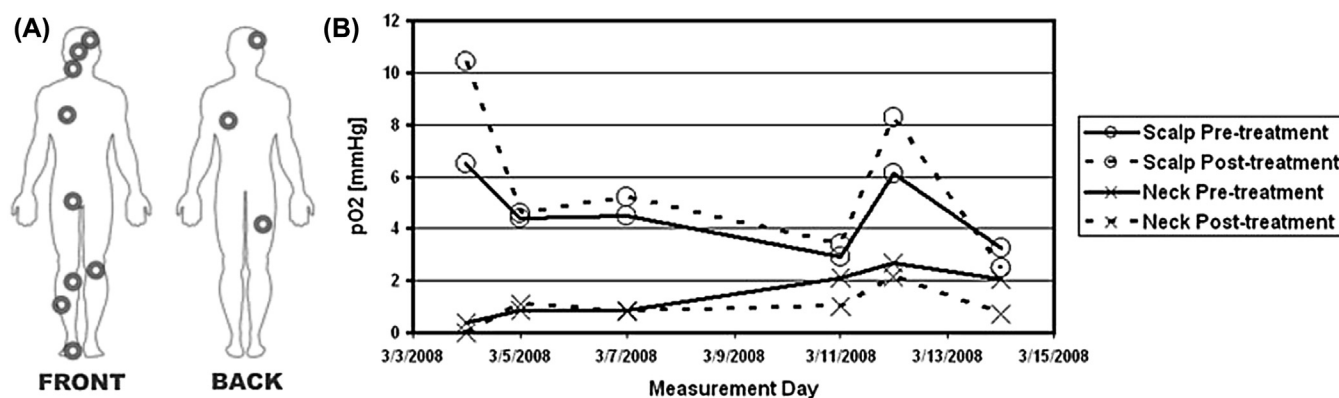


FIGURE 21.9 (A) Tumor pO_2 has been measured for 10 volunteers with different tumor locations from head to toe. (B) Tumor pO_2 was monitored in melanoma metastases at two sites, in the scalp and neck, during the course of radiation treatment. Spectra were recorded immediately before and after each fraction while the patient inspired room air. These results indicate hypoxic environments that vary on a day-to-day basis, but show little acute response in pO_2 due to radiation. Reprinted with permission from Williams BB, Khan N, Zaki B, Hartford A, Ernstoff MS, Swartz HM. Clinical electron paramagnetic resonance (EPR) oximetry using India ink. *Adv Exp Med Biol* 2010;662:149–56.

CONCLUSIONS AND FUTURE DIRECTIONS

Chemical, material, and nanoparticle systems for oxygen sensing have been engineered to span the myriad environments of the body, from blood to muscle and skin. Toolkits, ranging from optical sensors to EPR, offer nanomaterial platforms that have largely passed proof-of-concept research and development and are ready for use in the research space. There is

great promise in the utility of skin oxygen sensing in preclinical settings, especially as applied to chronic wounds such as diabetic ulcers. Platforms seeking to detect the early stages of ulcer formation are sorely needed and can be explored in animal models. Similarly, experiments focused on establishing the key parameters for optimal wound healing are imperative. For example, the optimal debridement, and thus available pO_2 , needed for skin grafting is not yet known. Research exploring this field will have a large impact

in the planning and execution of clinical protocols to benefit patients.

Much of the promise of these methods, however, can only be realized upon translation to the clinic. This highly interdisciplinary field is currently ripe for development. Research focused on the applications of these technologies to the skin is still a nascent field that will require close collaborations among dermatologists, plastic surgeons, chemists, and biomedical engineers across academia and industry. The creation and implementation of clinic-ready tools are expected to have profound effects on the routine management of skin diseases, wounds, and grafts.

References

- [1] Hopf HW, Rollins MD. Wounds: an overview of the role of oxygen. *Antioxid Redox Signal* 2007;9(8):1183–92.
- [2] [a] Ruangsetakit C, Chinsakchai K, Mahawongkajit P, Wongwanit C, Mutirangura P. Transcutaneous oxygen tension: a useful predictor of ulcer healing in critical limb ischaemia. *J Wound Care* 2010;19(5):202–6.
- [b] Bader DL, Gant CA. Changes in transcutaneous oxygen tension as a result of prolonged pressures at the sacrum. *Clin Phys Physiol Meas* 1988;9(1):33–40.
- [3] Baldwin KM. Transcutaneous oximetry and skin surface temperature as objective measures of pressure ulcer risk. *Adv Skin Wound Care* 2001;14(1):26–31.
- [4] Cox J. Predictors of pressure ulcers in adult critical care patients. *Am J Crit Care* 2011;20(5):364–75.
- [5] Faglia E, Ezio F, Clerici G, Giacomo C, Caminiti M, Maurizio C, et al. Evaluation of feasibility of ankle pressure and foot oximetry values for the detection of critical limb ischemia in diabetic patients. *Vasc Endovascular Surg* 2010;44(3):184–9.
- [6] Rice JB, Desai U, Cummings AK, Birnbaum HG, Skornicki M, Parsons NB. Burden of diabetic foot ulcers for medicare and private insurers. *Diabetes Care* 2014;37(3):651–8.
- [7] Schreml S, Szeimies RM, Prantl L, Karrer S, Landthaler M, Babilas P. Oxygen in acute and chronic wound healing. *Br J Dermatol* 2010;163(2):257–68.
- [8] Claeys LG, Horsch S. Transcutaneous oxygen pressure as predictive parameter for ulcer healing in endstage vascular patients treated with spinal cord stimulation. *Int Angiol* 1996;15(4):344–9.
- [9] Fife CE, Buyukcakir C, Otto GH, Sheffield PJ, Warriner RA, Love TL, et al. The predictive value of transcutaneous oxygen tension measurement in diabetic lower extremity ulcers treated with hyperbaric oxygen therapy: a retrospective analysis of 1144 patients. *Wound Repair Regen* 2002;10(4):198–207.
- [10] Hinck D, Franke A, Gatzka F. Use of vacuum-assisted closure negative pressure wound therapy in combat-related injuries—literature review. *Mil Med* 2010;175(3):173–81.
- [11] Boateng JS, Matthews KH, Stevens HN, Eccleston GM. Wound healing dressings and drug delivery systems: a review. *J Pharm Sci* 2008;97(8):2892–923.
- [12] Phillips JC. Understanding hyperbaric oxygen therapy and its use in the treatment of compromised skin grafts and flaps. *Plast Surg Nurs* 2005;25(2):72–80. quiz 81–2.
- [13] Sen CK. Wound healing essentials: let there be oxygen. *Wound Repair Regen* 2009;17(1):1–18.
- [14] Yip WL. Evaluation of the clinimetrics of transcutaneous oxygen measurement and its application in wound care. *Int Wound J* 2014;12(6):625–9.
- [15] [a] Clark LC, Wolf R, Granger D, Taylor Z. Continuous recording of blood oxygen tensions by polarography. *J Appl Physiol* 1953;6(3):189–93.
- [b] Takahashi GH, Fatt I, Goldstick TK. Oxygen consumption rate of tissue measured by a micropolarographic method. *J Gen Physiol* 1966;50(2):317–35.
- [16] Wang XD, Wolfbeis OS. Fiber-optic chemical sensors and biosensors (2008–2012). *Anal Chem* 2013;85(2):487–508.
- [17] Alander JT, Kaartinen I, Laakso A, Pätälä T, Spillmann T, Tuchin VV, et al. A review of indocyanine green fluorescent imaging in surgery. *Int J Biomed Imaging* 2012;2012:940585.
- [18] Benedik PS. Monitoring tissue blood flow and oxygenation: a brief review of emerging techniques. *Crit Care Nurs Clin North Am* 2014;26(3):345–56.
- [19] Roussakis E, Li Z, Nichols AJ, Evans CL. Oxygen-sensing methods in biomedicine from the macroscale to the microscale. *Angew Chem Int Ed Engl* 2015.
- [20] Goodell TT. An in vitro quantification of pressures exerted by earlobe pulse oximeter probes following reports of device-related pressure ulcers in ICU patients. *Ostomy Wound Management* 2012;58(11):30–4.
- [21] Scheeren TW, Schober P, Schwarte LA. Monitoring tissue oxygenation by near infrared spectroscopy (NIRS): background and current applications. *J Clin Monit Comput* 2012;26(4):279–87.
- [22] Busch DR, Choe R, Durduran T, Friedman DH, Baker WB, Maidment AD, et al. Blood flow reduction in breast tissue due to mammographic compression. *Acad Radiol* 2014;21(2):151–61.
- [23] Wang LV, Hu S. Photoacoustic tomography: in vivo imaging from organelles to organs. *Science* 2012;335(6075):1458–62.
- [24] Yi J, Wei Q, Liu W, Backman V, Zhang HF. Visible-light optical coherence tomography for retinal oximetry. *Opt Lett* 2013;38(11):1796–8.
- [25] Nel A, Madler L, Velegol D, Xia T, Hoek E, Somasundaran P, et al. Understanding biophysicochemical interactions at the nano-bio interface. *Nat Mater* 2009;8(7):543–57.
- [26] Vinogradov SA, Wilson DF. Porphyrin-dendrimers as biological oxygen sensors. *Designing dendrimers*. Wiley; 2012.
- [27] Wang XD, Wolfbeis OS. Optical methods for sensing and imaging oxygen: materials, spectroscopies and applications. *Chem Soc Rev* 2014;43(10):3666–761.
- [28] Dmitriev RI, Zhdanov AV, Ponomarev GV, Yashunski DV, Papkovsky DB. Intracellular oxygen-sensitive phosphorescent probes based on cell-penetrating peptides. *Anal Biochem* 2010;398(1):24–33.
- [29] Papkovsky DB, Dmitriev RI. Biological detection by optical oxygen sensing. *Chem Soc Rev* 2013;42(22):8700–32.
- [30] Quaranta M, Borisov SM, Klimant I. Indicators for optical oxygen sensors. *Bioanal Rev* 2012;4(2–4):115–57.
- [31] Rumsey WL, Vanderkooi JM, Wilson DF. Imaging of phosphorescence: a novel method for measuring oxygen distribution in perfused tissue. *Science* 1988;241(4873):1649–51.
- [32] Wang XD, Gorris HH, Stolwijk JA, Meier RJ, Groegel DBM, Wegener J, et al. Self-referenced RGB colour imaging of intracellular oxygen. *Chem Sci* 2011;2011:901–6.
- [33] Stucker M, Schulze L, Pott G, Hartmann P, Lubbers DW, Rochling A, et al. FLIM of luminescent oxygen sensors: clinical applications and results. *Sens Actuators B* 1998;51:171–5.
- [34] Hartmann P, Ziegler W, Holst G, Lubbers DW. Oxygen flux fluorescence lifetime imaging. *Sens Actuators B* 1997;38–39:110–5.
- [35] Bambot SB, Rao G, Romauld M, Carter GM, Sipior J, Terpetchnig E, et al. Sensing oxygen through skin using a red diode laser and fluorescence lifetimes. *Biosens Bioelectron* 1995;10(6–7):643–52.
- [36] Borisov SM, Klimant I. Luminescent nanobeads for optical sensing and imaging of dissolved oxygen. *Microchim Acta* 2009;164:7–15.

- [37] [a] Shonat RD, Richmond KN, Johnson PC. Phosphorescence quenching and the microcirculation: an automated, multipoint oxygen tension measuring instrument. *Rev Sci Instr* 1995;66: 5075–84.
[b] Sakadžić S, Roussakis E, Yaseen MA, Mandeville ET, Srinivasan VJ, Arai K, Ruvinskaya S, Wu W, Devor A, Lo EH, Vinogradov SA, Boas DA. Cerebral blood oxygenation measurement based on oxygen-dependent quenching of phosphorescence. *J Vis Exp* 2011;(51).
[c] Sakadžić S, Roussakis E, Yaseen MA, Mandeville ET, Srinivasan VJ, Arai K, Ruvinskaya S, Devor A, Lo EH, Vinogradov SA, Boas DA. Two-photon high-resolution measurement of partial pressure of oxygen in cerebral vasculature and tissue. *Nat Methods* 2010;7(9):755–9.
- [38] Kautsky H, Hirsch A. *Ber Dtsch Chem Ges B* 1931;64:2677–86.
- [39] Nichols AJ, Roussakis E, Klein OJ, Evans CL. Click-assembled, oxygen-sensing nanoconjugates for depth-resolved, near-infrared imaging in a 3D cancer model. *Angew Chem Int Ed Engl* 2014;53(14):3671–4.
- [40] Cheng Z, Aspinwall CA. Nanometre-sized molecular oxygen sensors prepared from polymer stabilized phospholipid vesicles. *Analyst* 2006;131(2):236–43.
- [41] [a] McNamara KP, Rosenzweig Z. Dye-encapsulating liposomes as fluorescence-based oxygen nanosensors. *Anal Chem* 1998;70: 4853–9.
[b] Velasco-García N, Valencia-González MJ, Díaz-García ME. Fluorescent organofilms for oxygen sensing in organic solvents using a fiber optic system. *Analyst* 1997;122(11):1405–9.
- [42] Coogan MP, Court JB, Gray VL, Hayes AJ, Lloyd SH, Millet CO, et al. Probing intracellular oxygen by quenched phosphorescence lifetimes of nanoparticles containing polyacrylamide-embedded $[\text{Ru}(\text{dpp}(\text{SO}_3\text{Na})_2)_3]\text{Cl}_2$. *Photochem Photobiol Sci* 2010;9(1):103–9.
- [43] Chojnacki P, Mistlberger G, Klimant I. Separable magnetic sensors for the optical determination of oxygen. *Angew Chem Int Ed Engl* 2007;46(46):8850–3.
- [44] Xu H, Aylott JW, Kopelman R, Miller TJ, Philbert MA. A real-time ratiometric method for the determination of molecular oxygen inside living cells using sol-gel-based spherical optical nanosensors with applications to rat C6 glioma. *Anal Chem* 2001;73(17): 4124–33.
- [45] He H, Fraatz RJ, Leiner MJP, Rehn MM, Tusa JK. Selection of silicone polymer matrix for optical gas sensing. *Sens Actuators B* 1995;29:246–50.
- [46] Acosta MA, Ymele-Leki P, Kostov YV, Leach JB. Fluorescent microparticles for sensing cell microenvironment oxygen levels within 3D scaffolds. *Biomaterials* 2009;30(17):3068–74.
- [47] [a] Zhang P, Guo J, Wang Y, Pang W. Incorporation of luminescent tris(bipyridine)ruthenium(II) complex in mesoporous silica spheres and their spectroscopic and oxygen-sensing properties. *Mater Lett* 2002;53:400–5.
[b] Tang Y, Tehan EC, Tao Z, Bright FV. Sol-gel-derived sensor materials that yield linear calibration plots, high sensitivity, and long-term stability. *Anal Chem* 2003;75(10):2407–13.
[c] Roche PJR, Cheung MC-K, Yao L, Kirk AG, Vamsy P, Chodavarapu, Enhancement of luminescent quenching-based oxygen sensing by gold nanoparticles: comparison between lumiphore:matrix:nanoparticle thin films on glass and gold coated substrates. *J Nanophotonics* 2010;4:043521.
- [48] Cheng S-H, Lee C-H, Yang C-S, Tseng F-G, Mou C-Y, Lo L-W. Mesoporous silica nanoparticles functionalized with an oxygen-sensing probe for cell photodynamic therapy: potential cancer theranostics. *J Mater Chem* 2009;19:1252–7.
- [49] [a] Cao Y, Lee Koo YE, Kopelman R. Poly(decyl methacrylate)-based fluorescent PEBBLE swarm nanosensors for measuring dissolved oxygen in biosamples. *Analyst* 2004;129(8):745–50.
[b] Wu C, Bull B, Christensen K, McNeill J. Ratiometric single-nanoparticle oxygen sensors for biological imaging. *Angew Chem Int Ed Engl* 2009;48(15):2741–5.
[c] Wang X-D, Zhou T-Y, Song X-H, Jiang Y, Yang CJ, Chen X. Chameleon clothes for quantitative oxygen imaging. *J Mater Chem* 2011;21:17651–3.
- [50] [a] Chu CS, Lo YL, Sung TW. Enhanced oxygen sensing properties of Pt(II) complex and dye entrapped core-shell silica nanoparticles embedded in sol-gel matrix. *Talanta* 2010;82(3): 1044–51.
[b] Wang X-H, Peng H-S, Ding H, You F-T, Huang S-H, Teng F, Dong B, Song H-W. Biocompatible fluorescent core-shell nanoparticles for ratiometric oxygen sensing. *J Mater Chem* 2012;22: 16066–71.
- [51] Koo YE, Cao Y, Kopelman R, Koo SM, Brasuel M, Philbert MA. Real-time measurements of dissolved oxygen inside live cells by organically modified silicate fluorescent nanosensors. *Anal Chem* 2004;76(9):2498–505.
- [52] Liu H, Yang H, Hao X, Xu H, Lv Y, Xiao D, et al. Development of polymeric nanoprobe with improved lifetime dynamic range and stability for intracellular oxygen sensing. *Small* 2013;9(15): 2639–48.
- [53] Cywinski PJ, Moro AJ, Stanca SE, Biskup C, Mohr GJ. Ratiometric porphyrin-based layers and nanoparticles for measuring oxygen in biosamples. *Sens Actuators B* 2009;135:472–7.
- [54] Borisov SM, Mayr T, Klimant I. Poly(styrene-block-vinylpyrrolidone) beads as a versatile material for simple fabrication of optical nanosensors. *Anal Chem* 2008;80(3):573–82.
- [55] Borisov SM, Nuss G, Klimant I. Red light-excitable oxygen sensing materials based on platinum(II) and palladium(II) benzoporphyrins. *Anal Chem* 2008;80(24):9435–42.
- [56] Fercher A, Borisov SM, Zhdanov AV, Klimant I, Papkovsky DB. Intracellular O_2 sensing probe based on cell-penetrating phosphorescent nanoparticles. *ACS Nano* 2011;5(7):5499–508.
- [57] [a] Collier BB, Singh S, McShane M. Microparticle ratiometric oxygen sensors utilizing near-infrared emitting quantum dots. *Analyst* 2011;136(5):962–7.
[b] Lemon CM, Karnas E, Bawendi MG, Nocera DG. Two-photon oxygen sensing with quantum dot-porphyrin conjugates. *Inorg Chem* 2013;52(18):10394–406.
- [58] Clark HA, Hoyer M, Philbert MA, Kopelman R. Optical nanosensors for chemical analysis inside single living cells. 1. Fabrication, characterization, and methods for intracellular delivery of PEBBLE sensors. *Anal Chem* 1999;71(21):4831–6.
- [59] Lee YE, Ulbrich EE, Kim G, Hah H, Strollo C, Fan W, et al. Near infrared luminescent oxygen nanosensors with nanoparticle matrix tailored sensitivity. *Anal Chem* 2010;82(20):8446–55.
- [60] [a] Shaw AD, Li Z, Thomas Z, Stevens CW. Assessment of tissue oxygen tension: comparison of dynamic fluorescence quenching and polarographic electrode technique. *Crit Care* 2002;6(1):76–80.
[b] Holst GA, Köster T, Voges E, Lubbers DW. FLOX an oxygen-flux-measuring system using a phase-modulation method to evaluate the oxygen-dependent fluorescence lifetime. *Sens Actuators B* 1995;29:231–9.
- [61] Klimant L, Wolfbeis OS. Oxygen-sensitive luminescent materials based on silicone-soluble ruthenium Diimine complexes. *Anal Chem* 1995;67:3160–6.
- [62] [a] Babilas P, Liebsch G, Schacht V, Klimant I, Wolfbeis OS, Szeimies RM, et al. In vivo phosphorescence imaging of pO_2 using planar oxygen sensors. *Microcirculation* 2005;12(6):477–87.
[b] Babilas P, Lamby P, Prantl L, Schreml S, Jung EM, Liebsch G, Wolfbeis OS, Landthaler M, Szeimies RM, Abels C. Transcutaneous pO_2 imaging during tourniquet-induced forearm ischemia using planar optical oxygen sensors. *Skin Res Technol* 2008;14(3): 304–11.

- [63] Li Z, Roussakis E, Koolen PG, Ibrahim AM, Kim K, Rose LF, et al. Non-invasive transdermal two-dimensional mapping of cutaneous oxygenation with a rapid-drying liquid bandage. *Biomed Opt Express* 2014;5(11):3748–64.
- [64] [a] Hofmann J, Meier RJ, Mahnke A, Schatz V, Brackmann F, Trollmann R, Bogdan C, Liebsch G, Wang X-D, Wolfbeis OS, Jantsch J. Ratiometric luminescence 2D in vivo imaging and monitoring of mouse skin oxygenation. *Methods Appl Fluoresc* 2013;1: 045002.
[b] Schreml S, Meier RJ, Wolfbeis OS, Maisch T, Szeimies RM, Landthaler M, Regensburger J, Santarelli F, Klimant I, Babilas P. 2D luminescence imaging of physiological wound oxygenation. *Exp Dermatol* 2011;20(7):550–4.
- [65] Meier RJ, Schreml S, Wang XD, Landthaler M, Babilas P, Wolfbeis OS. Simultaneous photographing of oxygen and pH in vivo using sensor films. *Angew Chem Int Ed Engl* 2011; 50(46):10893–6.
- [66] Yu JX, Hallac RR, Chiguru S, Mason RP. New frontiers and developing applications in 19F NMR. *Prog Nucl Magn Reson Spectrosc* 2013;70:25–49.
- [67] Liu S, Shah SJ, Wilmes LJ, Feiner J, Kodibagkar VD, Wendland MF, et al. Quantitative tissue oxygen measurement in multiple organs using 19F MRI in a rat model. *Magn Reson Med* 2011;66(6): 1722–30.
- [68] Gulaka PK, Rastogi U, McKay MA, Wang X, Mason RP, Kodibagkar VD. Hexamethyldisiloxane-based nanoprobe for (1) H MRI oximetry. *NMR Biomed* 2011;24(10):1226–34.
- [69] [a] Smirnov AI, Norby SW, Walczak T, Liu KJ, Swartz HM. Physical and instrumental considerations in the use of lithium phthalocyanine for measurements of the concentration of the oxygen. *J Magn Reson B* 1994;103(2):95–102.
[b] Swartz HM, Hou H, Khan N, Jarvis LA, Chen EY, Williams BB, Kuppusamy P. Advances in probes and methods for clinical EPR oximetry. *Adv Exp Med Biol* 2014;812:73–9.
- [70] Swartz HM, Liu KJ, Goda F, Walczak T. India ink: a potential clinically applicable EPR oximetry probe. *Magn Reson Med* 1994; 31(2):229–32.
- [71] Dunn JF, Swartz HM. In vivo electron paramagnetic resonance oximetry with particulate materials. *Methods* 2003; 30(2):159–66.
- [72] Mason RP, Nunnally RL, Antich PP. Tissue oxygenation: a novel determination using 19F surface coil NMR spectroscopy of sequestered perfluorocarbon emulsion. *Magn Reson Med* 1991; 18(1):71–9.
- [73] Liu VH, Vassiliou CC, Imaad SM, Cima MJ. Solid MRI contrast agents for long-term, quantitative in vivo oxygen sensing. *Proc Natl Acad Sci USA* 2014;111(18):6588–93.
- [74] Clarkson RB, Odintsov BM, Ceroke PJ, Ardenkjaer-Larsen JH, Fruianu M, Belford RL. Electron paramagnetic resonance and dynamic nuclear polarization of char suspensions: surface science and oximetry. *Phys Med Biol* 1998;43(7):1907–20.
- [75] Williams BB, Khan N, Zaki B, Hartford A, Ernstoff MS, Swartz HM. Clinical electron paramagnetic resonance (EPR) oximetry using India ink. *Adv Exp Med Biol* 2010;662:149–56.
- [76] Glockner JF, Chan HC, Swartz HM. In vivo oximetry using a nitroxide-liposome system. *Magn Reson Med* 1991;20(1): 123–33.
- [77] Liu KJ, Grinstaff MW, Jiang J, Suslick KS, Swartz HM, Wang W. In vivo measurement of oxygen concentration using sonochemically synthesized microspheres. *Biophys J* 1994;67(2):896–901.
- [78] Gallez B, Debuyst R, Liu KJ, Demeure R, Dejeht F, Swartz HM. Development of biocompatible implants of fusinite for in vivo EPR oximetry. *MAGMA* 1996;4(1):71–5.
- [79] Gallez B, Debuyst R, Dejeht F, Liu KJ, Walczak T, Goda F, et al. Small particles of fusinite and carbohydrate chars coated with aqueous soluble polymers: preparation and applications for in vivo EPR oximetry. *Magn Reson Med* 1998;40(1):152–9.
- [80] Gallez B, Jordan BF, Baudet C. Microencapsulation of paramagnetic particles by pyrroxylin to preserve their responsiveness to oxygen when used as sensors for in vivo EPR oximetry. *Magn Reson Med* 1999;42(1):193–6.
- [81] Swartz HM, Khan N, Buckley J, Comi R, Gould L, Grinberg O, et al. Clinical applications of EPR: overview and perspectives. *NMR Biomed* 2004;17(5):335–51.
- [82] Krzic M, Sentjurc M, Kristl J. Improved skin oxygenation after benzyl nicotinate application in different carriers as measured by EPR oximetry in vivo. *J Control Release* 2001; 70(1–2):203–11.

Investigating the Intracellular Dynamics of Hypericin-Loaded Nanoparticles and Polyvinylpyrrolidone-Hypericin by Image Correlation Spectroscopy

R. Penjweini^{1,2}, S. Deville^{2,3}, A. Ethirajan², M. Ameloot²

¹University of Pennsylvania, Philadelphia, PA, United States; ²Hasselt University, Diepenbeek, Belgium; ³Flemish Institute for Technological Research, Mol, Belgium

OUTLINE

Introduction	275	<i>Corrections for Immobile Species, the Flow Induced by Cell Movement, and Stage Drift</i>	281
Overview	275	Image Collection for Different Variants of ICS	281
Dermatological Application of Hypericin	276	Intracellular Dynamics of PLLA-Hyp Nanoparticles and PVP-Hyp	281
Dermatological Application of PLLA Nanoparticles	276	Conclusion	283
Distribution of the Nanoparticles and Hypericin in the Living Cells	277	List of Acronyms and Abbreviations	284
Characterization of PLLA-Hyp Nanoparticles	277	Acknowledgments	284
Incubation of the Cells With PLLA-Hyp Nanoparticles and PVP-Hyp Photosensitizer	277	References	284
Labeling of the Different Cell Organelles	278		
Image Correlation Spectroscopy	278		
Spatiotemporal Image Correlation Spectroscopy	278		
Temporal Image Correlation Spectroscopy	279		
Spatiotemporal Image Cross-Correlation Spectroscopy	279		

INTRODUCTION

Overview

Photodynamic therapy (PDT) is known as a minimally invasive technique for the treatment of oncologic diseases that avoids many of the side effects typical for ionizing radiation and chemotherapy [1–6]. PDT is based on the

use of photochemical reactions resulting from cytotoxic reactive oxygen species induced by a sensitizer after excitation by light (photosensitizer). PDT can take advantage of the high capacity of nanosystems to carry hydrophobic photosensitizing agents and increase cancer-selective drug delivery [7–14]. Some polymeric nanocarriers such as poly L-lactic acid (PLLA), polycaprolactone, and

poly-alkyl-cyanoacrylates have been approved by the US Food and Drug Administration (FDA) for clinical use due to their unique properties such as biocompatibility suitable for drug delivery applications [15,16]. NPs can travel through complex biological environments full of steric and adhesive obstacles [3,17]. They release their cargo by degradation in an acidic environment as well as by the action of enzymes such as esterases. Cellular components such as cytoplasm, endosomes, lysosomes, endoplasmic reticulum, Golgi apparatus, mitochondria, and nuclei maintain their own characteristic pH values ranging from 4.5 in the lysosome to about 8.0 in the mitochondria [18]. Therefore, the inherent pH conditions in addition to the presence of enzymes influence the intracellular degradation of the NPs [3,15,16].

The therapeutic efficacy and intracellular behavior of NPs depend primarily on how they interface to biomolecules and their surroundings [20–22]. Understanding NPs' biointeractions requires knowledge about the dynamic behavior of nanomaterials during their cellular uptake, the intracellular traffic, the mutual reactions with cell organelles, the fate of nanomaterials, and the respective cellular end points [20,21,23,24]. As intracellular location and interactions of NPs correlate with their characteristics, every nanomaterial has to be tested individually [15,16,18,20].

PLLA-based NPs are proposed for delivery of different photosensitizers in PDT of skin cancer [13,14]. Although in vivo PDT studies have shown that photosensitizer delivery using PLLA nanocarriers is more effective than using free photosensitizers in treating mouse bearing skin cancer, more attention has to be devoted specifically to understanding PLLA intracellular dynamics and localization. In this chapter, we use temporal and spatio-temporal image correlation spectroscopy to measure the directed and diffusive motions of hypericin-loaded PLLA (PLLA-Hyp) NPs and different cell organelles in the crowded intracellular environment. Using spatiotemporal image cross-correlation spectroscopy, we investigate the intracellular motions of NPs in association with individual early endosomes, late endosomes, lysosomes, and mitochondria. As the physicochemical nature of the hypericin is crucial for cellular studies, in addition for comparison, hypericin is introduced to the cells without nanocarriers by employing a water-soluble formulation of hypericin [25,26]. To make hypericin water-soluble, a formulation of hypericin with polyvinylpyrrolidone (PVP-Hyp; PVP: Mw. 4.0000; Sigma-Aldrich, St. Louis, MO, USA), in a ratio of 1:100, is prepared using the procedure described by Kubin et al. [25]. Human primary dendritic cells (DCs) and human cervical epithelial HeLa cells are used in this study. DCs are found in tissue that has contact with the outside environment such as the skin. DCs are leukocytes that, although infrequently represented in their tissues of origin (lymphoid and solid

organs and epithelia), are critically important in immunophysiology [27]. The importance of DCs can be attributed to their unique ability to function as antigen-presenting cells that can initiate responses in T cells, and to dictate the net outcome of this interaction as it relates to the character of the immune responses that ensue. Immunomodulatory properties of sulfonate- and phosphonate-functionalized polystyrene NPs have been suggested as a useful strategy for strengthening the efficacy of NP-based approaches in immunotherapy [12]. HeLa cells originate from the cervical cancer tumor. As HeLa cells are adherent and flat, they are the most widely used human cell line in biological and biomedical research.

Dermatological Application of Hypericin

Hypericin is known as an effective photosensitizer with several attributes that make it particularly attractive for investigating its clinical use in skin disorders, with potential advantages over phototherapy with psoralen plus ultraviolet A (UVA). Hypericin can be activated by white light, for example at wavelengths produced by the sodium lamp (590 nm), which significantly reduces the side effects associated with UV irradiation [28]. Hypericin-mediated PDT has been shown to be an effective treatment modality, through topical administration, for treatment of nonmelanoma skin cancers. Hypericin localization in the endoplasmic reticulum of cancer cells, shown by fluorescent microscopy [29,30], further supports a disruption in cellular processing and induction of cancer cell death. Furthermore, it is reported that hypericin accumulates in mitochondria that can cause a caspase-dependent apoptotic mode of cell death [31,32]. However, hypericin is known to induce skin phototoxicity not only after systemic administration but also after topical application, especially when applied as its precursor acetate ester [28,33]. Therefore, NPs can be used to shield hypericin till the target cells are reached.

Dermatological Application of PLLA Nanoparticles

Most organic photosensitizers are hydrophobic. On one hand, the hydrophobic characteristic allows the photosensitizer to penetrate the cell membrane and locate in photosensitive cellular compartments such as the membrane of organelles. On the other hand, conventional PDT drug delivery requires high systemic drug levels to provide therapeutic benefit. The poor water solubility of the photosensitizer makes it incompatible for systemic administration. Previously, polymer particles were studied for their disposition on and within the

skin following their topical application and were investigated for their potential utility for the local delivery of an associated “active” substance [11]. Nanocarriers, such as PLLA NPs, are promising drug delivery platforms to increase the delivery of the hydrophobic photosensitizers. Moreover, using nanocarriers reduces drug doses and minimizes the toxic side effects. Some studies have shown that using PLLA NPs for carrying the photosensitizers can exhibit cancer-selective targeting (in both a pretargeting and a direct approach), enhanced reduction of cancer cell viability, together with no significant reduction in viability of normal cells [3,9,13,15,34,35]. PLLA NPs enhance protoporphyrin IX (PpIX), assisted 5-aminolevulinic acid (ALA) PDT efficiency, and induce antitumor immune responses in squamous cell carcinoma (a common skin cancer) tumor-bearing mice [13,14,18].

DISTRIBUTION OF THE NANOPARTICLES AND HYPERICIN IN THE LIVING CELLS

Characterization of PLLA-Hyp Nanoparticles

PLLA-Hyp NPs are prepared using the mini-emulsion technique with the emulsion–solvent evaporation

method; a more detailed description can be found elsewhere [36,37]. The NPs are characterized using dynamic light scattering (DLS), transmission electron microscopy (TEM), and optical spectroscopy. The size distribution of the NPs is characterized by DLS using a Brookhaven Instrument. The morphology of the NPs (see Fig. 22.1A) is characterized by using a TECNAI Spirit TEM (FEI, Hillsboro, OR, USA) operating at an accelerating voltage of 120 kV. The sample is prepared by air drying the diluted sample in water on a carbon-coated copper grid.

The absorption spectrum of PLLA-Hyp NPs measured using a UV-visible–near-infrared (UV-vis–NIR) spectrophotometer has been shown in Fig. 22.1A. Fig. 22.1B shows the emission spectrum of the NPs obtained with a FluoroLog-3 spectrofluorometer. PLLA ($M_w = 101,700$ g/mol from Sigma-Aldrich, Bornem, Belgium) NPs have a mean effective diameter of 205 nm, containing about 0.7% (with respect to the polymer amount) encapsulated hydrophobic hypericin (Sigma-Aldrich, St. Louis).

Incubation of the Cells With PLLA-Hyp Nanoparticles and PVP-Hyp Photosensitizer

HeLa cells were cultured in Dulbecco’s modified Eagle’s medium (Gibco, Paisley, UK) with 10% fetal

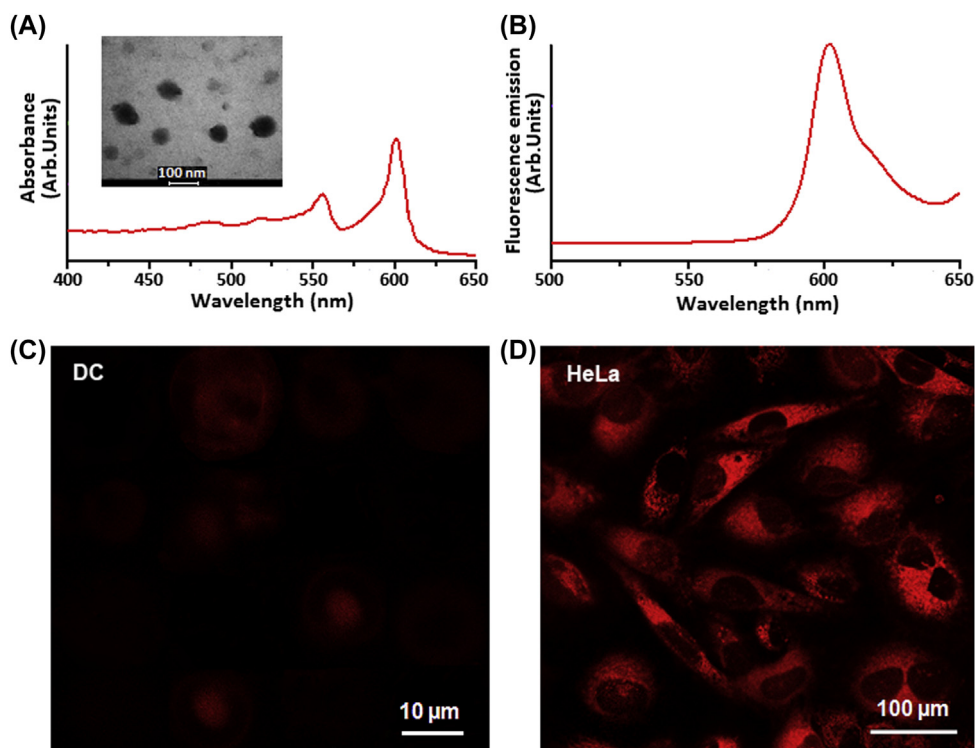


FIGURE 22.1 (A) UV–Vis absorbance; (B) fluorescence emission spectra of PLLA-Hyp NPs. The insert in (A) shows a TEM image of PLLA-Hyp NPs (scale bar: 100 nm). Fluorescence microscopy images of (C) DC and (D) HeLa cells incubated with PLLA-Hyp NPs. *This figure has been adapted from the supplementary material of reference Penjweini R, Deville S, D’Olieslaeger L, Berden M, Ameloot M, Ethirajan A. Intracellular localization and dynamics of hypericin loaded PLLA nanocarriers by image correlation spectroscopy. J Control Release 2015;218:82–93.*

bovine serum (FBS; Biochrom AG, Berlin, Germany) and 1% penicillin–streptomycin (P/S; Gibco). DCs were derived from CD34+ progenitor cells from human umbilical cord blood, which were induced to proliferate and differentiate toward immature DCs [38,39]. Human cord blood samples were collected from umbilical blood vessels of placentas of full-term infants, born at Heilig Hart hospital at Mol and St. Dimpna hospital at Geel, both in Belgium. Informed consent was given by the mothers, and the study was approved by the ethical commission of both hospitals. Then, DCs were cultured in Iscove's modified Dulbecco's medium with 10% FBS, 2% P/S, and 1% bovine serum albumin (Sigma-Aldrich, Belgium). One day before the experiments, the cells were plated in μ -Slide eight-well Petri dishes (Ibidi GmbH, Martinsried, Germany) with a density of 5×10^4 cells/chamber at 37°C and 5% CO₂ in a standard incubator. DCs were plated in μ -Slide eight-well Petri dishes coated overnight with 0.01% poly-L-lysine (Sigma-Aldrich).

Freshly prepared PLLA-Hyp NPs and PVP-Hyp photosensitizer were diluted in separate culture mediums at the final concentrations of 130 μ g/mL and 10 μ M, respectively. Then, two groups of each cell type (HeLa and DCs) were prepared, one for incubation with PLLA-Hyp NPs and another for PVP-Hyp photosensitizer. Each group was incubated for 1 h with the NP solution or 20 min with PVP-Hyp solution in the incubator at 37°C and 5% CO₂. The staining was stopped by washing several times with phosphate buffered saline (PBS). Finally, the cells were maintained in the culture medium with 10% FBS and were imaged with a commercial Zeiss LSM 510 META confocal laser scanning microscope. Figs. 22.1C and D show the NPs' fluorescence signals in DCs and HeLa cells.

Labeling of the Different Cell Organelles

Different types of cell organelles are labeled by staining with organelle-specific dyes (from Molecular Probes, Invitrogen, Paisley, UK; and Sigma-Aldrich, St. Louis): early and late endosomes with 25 particles per cell of CellLight Early Endosomes-GFP and CellLight Late Endosomes-GFP, both for 24 h; lysosomes with 5 μ M LysoTracker green DND-22 for 1 h; and mitochondria with 200 nM MitoTracker Green FM for 20 min.

IMAGE CORRELATION SPECTROSCOPY

Image correlation spectroscopy (ICS) is a fluorescence-based microscopic technique most appropriate for the study of biomolecular interactions, measurement of molecular diffusion, and directed transport (flow) on time scales ranging from

microseconds to milliseconds [40–42]. ICS allows utilizing the spatial information of small particles at a high density within a significant, homogeneous area of the specimen [31,43–47]. ICS implementations are subdivided according to whether fluorescence fluctuation information in space and/or time is analyzed within the image series [41,43,44]. Temporal ICS (TICS) involves the correlation analysis of the fluorescence fluctuations in time recorded in the pixels of an image time series. In spatiotemporal image correlation spectroscopy (STICS), the spatial information embedded in the two-dimensional spatial correlations is combined with the time-dependent transport measured by the temporal correlation. STICS determines flow directions of the fluorescently tagged macromolecules, enabling the mapping of the velocity vectors. To assess the dynamics of the associated motions of two populations, STICS is used via cross-correlation analyses (STICCS) of the two fluorescence detection channels [41–44,46].

For the analyses, image subsections of 64×64 pixels are selected from different regions of the cells. For all pairs of (sub) images separated by lag time τ , the average spatiotemporal autocorrelation function $r(\xi, \eta, \tau)$ is defined by [42,46,48]:

$$r(\xi, \eta, \tau) = \left\langle \frac{\langle \delta i(x, y, t) \delta i(x + \xi, y + \eta, t + \tau) \rangle_{XY}}{\langle i(x, y, t) \rangle_{XY} \langle i(x + \xi, y + \eta, t + \tau) \rangle_{XY}} \right\rangle_T \quad (22.1)$$

where x and y are spatial coordinates of the considered pixel and t is the time of the considered image in the time series; ξ and η are the spatial lag variables in x and y , respectively; $i(x, y, t)$ represents the intensity with (x, y) and time with t ; and $\delta i(x, y, t) = i(x, y, t) - \langle i(x, y, t) \rangle_{XY}$ defines the fluctuations of fluorescence intensity in an image series. The angle brackets denote averaging of the stack of images in space (XY) or time (T).

The spatial information of the autocorrelation $r(\xi, \eta, 0)$ is fit by nonlinear least squares with a two-dimensional Gaussian function [40]:

$$r(\xi, \eta, 0) = r(0, 0, 0) \exp \left\{ -\frac{\xi^2 + \eta^2}{\omega_0^2} \right\} + r_\infty \quad (22.2)$$

The zero-lags amplitude $r(0, 0, 0)$, the longtime offset r_∞ , and the e^{-2} radius of the point spread function of the optical setup ω_0 are the fit parameters; the latter can also be fixed to a value resulting from the experimentally determined point spread function.

Spatiotemporal Image Correlation Spectroscopy

In STICS, the full spatiotemporal information in the autocorrelation expressed in Eq. (22.1) is used. By locating the maximum of the $r(\xi, \eta, \tau)$ in spatial lag space

and fitting this with a translationally and radially adjustable two-dimensional Gaussian function, the space–time evolution of the correlation function is captured [41]:

$$r(\Delta\xi, \Delta\eta, \tau) = r(0, 0, \tau) \exp \left\{ -\frac{(\xi - \Delta\xi)^2 + (\eta - \Delta\eta)^2}{\omega_0(\tau)^2} \right\} + r_\infty \quad (22.3)$$

The time-dependent amplitude $r(0, 0, \tau)$, the position of the peak in lag space $(\Delta\xi, \Delta\eta)$, and the offset parameter r_∞ are obtained by fitting the experimental data.

The spatial autocorrelation function from each image will appear as a two-dimensional Gaussian peak, as shown in Fig. 22.2A [42,46,49]. In the case of stationary particles, the peak centered at $(\xi = 0, \eta = 0)$ stays unchanged for all values of τ . If some particles move between frames, depending on the kind of motion (diffusion and/or flow), the peak is going to change. In the case of diffusion, the peak decreases in amplitude and spreads in a radially symmetric fashion as a function of τ . However, the peak will stay centered at $(\xi = 0, \eta = 0)$. If the particles are only undergoing directed flow with the velocities v_x and v_y in, respectively, x and y directions, the correlation peak maintains its original shape as a function of time, but its center will be shifted to lag positions $\xi = -v_x\tau$ and $\eta = -v_y\tau$ (see Fig. 22.2B). If the macromolecules are undergoing a flow-biased diffusion, the autocorrelation function not only moves but also broadens because of the diffusion (see Fig. 22.2A). Only when the moving particles stay within the bounds of the analyzed region will the STICS analysis be valid.

Temporal Image Correlation Spectroscopy

For the same subregions of the images, the diffusion coefficient of the particles was calculated by using TICS [41,43,44]. Each pixel location yields an autocorrelation function, which all are averaged to obtain a single temporal autocorrelation function $r(0, 0, \tau)$ (see Fig. 22.2C):

$$r(0, 0, \tau) = \left\langle \frac{\langle \delta i(x, y, t) \delta i(x, y, t + \tau) \rangle_{XY}}{\langle i(x, y, t) \rangle_{XY} \langle i(x, y, t + \tau) \rangle_{XY}} \right\rangle_T \quad (22.4)$$

Based on the magnitude of the flow measured by STICS, $r(0, 0, \tau)$ is then fit to one of the three analytical decay models [46]:

1. Two-dimensional diffusion

$$r(0, 0, \tau) = r(0, 0, 0) \left(1 + \frac{\tau}{\tau_D} \right)^{-1} + r_\infty \quad (22.5)$$

2. Two-dimensional diffusion and flow for a single population

$$r(0, 0, \tau) = r(0, 0, 0) \left(1 + \frac{\tau}{\tau_D} \right)^{-1} \times \exp \left\{ -\left(\frac{|v_f| \tau}{\langle \omega_0 \rangle} \right)^2 \left(1 + \frac{\tau}{\tau_D} \right)^{-1} \right\} + r_\infty \quad (22.6)$$

3. Two-dimensional diffusion and flow for two populations ($i = 1, 2$)

$$r(0, 0, \tau) = r(0, 0, 0)_1 \left(1 + \frac{\tau}{\tau_{D1}} \right)^{-1} + r(0, 0, 0)_2 \times \exp \left\{ -\left(\frac{|v_{f2}| \tau}{\langle \omega_0 \rangle} \right)^2 \right\} + r_\infty \quad (22.7)$$

where, v_f and τ_D refer to the flow velocity and characteristic diffusion time, respectively. $\langle \omega_0 \rangle$ represents the average of ω_0 . The diffusion coefficient (D) is obtained from the best fit characteristic diffusion time, τ_D , combined with $\langle \omega_0 \rangle$:

$$D = \frac{\langle \omega_0 \rangle^2}{4\tau_D} \quad (22.8)$$

The fitting scheme weights the correlation from each pair of images equally. Thus, it gives a higher weight to the lower lags as compared to the higher lags, which contain fewer images [43,44].

Spatiotemporal Image Cross-Correlation Spectroscopy

Studying the intracellular destination of the NPs and photosensitizers as well as their co-transport with the target cell organelles requires STICS in a cross-correlation scheme (STICCS) [42,46,50]. STICCS needs the image time series in space and time from two fluorescence detection channels, a from fluorescent labeled NPs or fluorescent photosensitizers and b from the fluorescent labeled cell organelle. A modified version of $r(\xi, \eta, \tau)$ presented in Eq. (22.1) is used for the cross-correlation function [42,46,50]:

$$r_{ab}(\xi, \eta, \tau) = \left\langle \frac{\langle \delta i_a(x, y, t) \delta i_b(x + \xi, y + \eta, t + \tau) \rangle_{XY}}{\langle i_a(x, y, t) \rangle_{XY} \langle i_b(x + \xi, y + \eta, t + \tau) \rangle_{XY}} \right\rangle_T \quad (22.9)$$

The space–time evolution of the cross-correlation function is then captured by locating the maximum of $r_{ab}(\xi, \eta, \tau)$ and fitting this with a free Gaussian function as presented in Eq. (22.3).

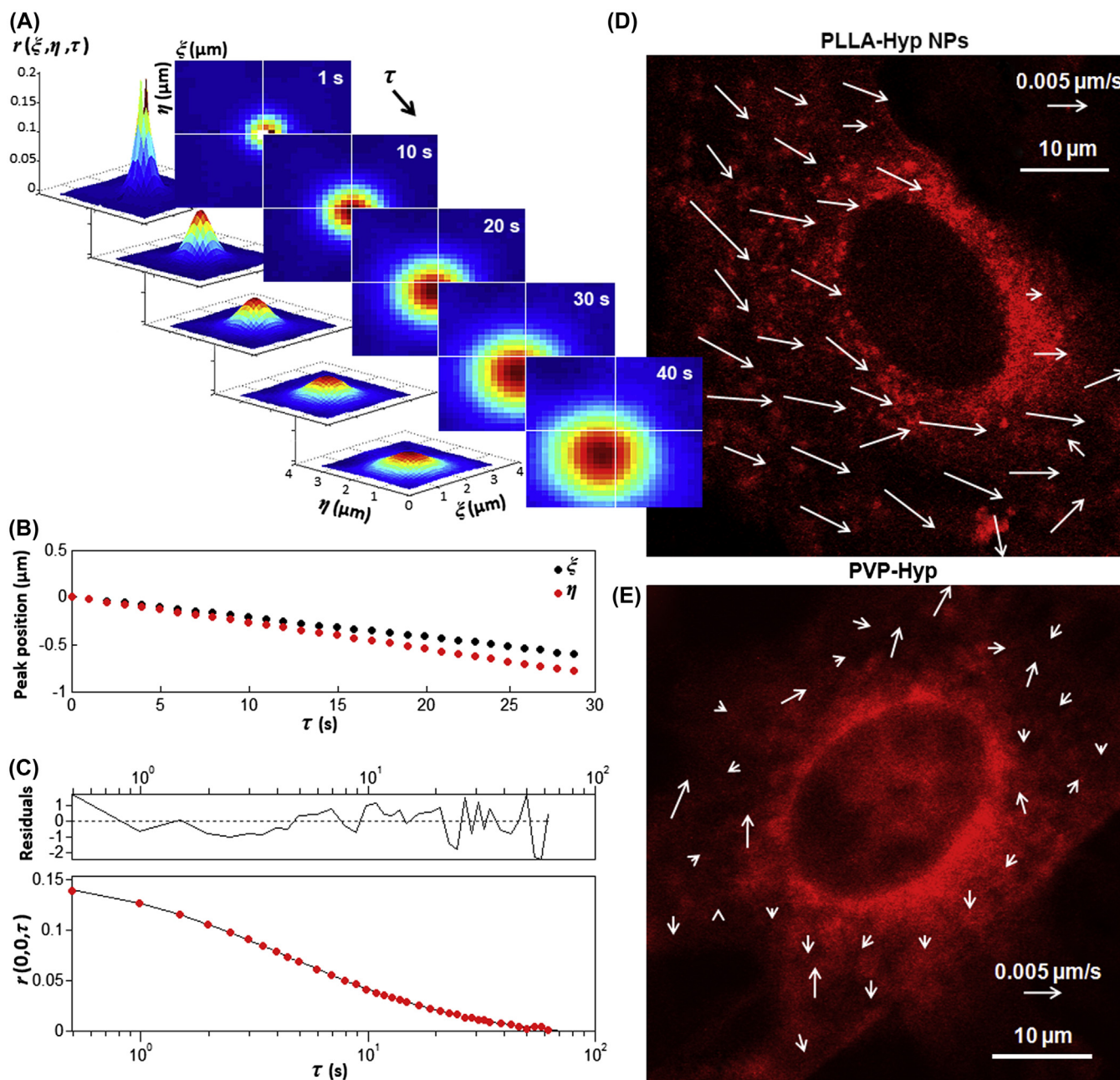


FIGURE 22.2 (A) Representation of a typical spatiotemporal autocorrelation function $r(\xi, \eta, \tau)$ and its contour plot. (B) Plots of the position of the $r(\xi, \eta, \tau)$ peak as a function of time-lag τ . (C) TICS fit to the temporal autocorrelation peak $r(0,0,\tau)$ gives an estimate of the particles diffusion coefficient. The flow mapping of (D) PLLA-Hyp NPs [6] and (E) PVP-Hyp (free hypericin) in living HeLa cells. STICS analyses applied to 30–33 different regions inside the cells give the average flow velocity of $V_{\text{STICS}} = (9.1 \pm 0.5) \times 10^{-3} \mu\text{m/s}$ for PLLA-Hyp NPs and $V_{\text{STICS}} = (2.4 \pm 0.2) \times 10^{-3} \mu\text{m/s}$ for PVP-Hyp photosensitizer. TICS fits to $r(0,0,\tau)$ of the same regions of the cells give an average diffusion coefficient of $D_{\text{TICS}} = (2.3 \pm 0.4) \times 10^{-3} \mu\text{m}^2/\text{s}$ for the NPs and $D_{\text{TICS}} = (7.0 \pm 1.7) \times 10^{-3} \mu\text{m}^2/\text{s}$ for PVP-Hyp.

If for zero time lag the cross-correlation between the two detection channels is nonzero, it means that the two species (NPs or photosensitizer and organelle-specific dye) are associated. In the case of stationary particles, then the cross-correlation stays unchanged for all values of τ and centers at $(\xi = 0, \eta = 0)$. Changes over time in the number of interacting and/or correlating molecules

will be reflected in the cross-correlation function as described for STICS.

The custom written MATLAB (R2013a, 64-bit; MATLAB, Boston, MA, USA) routines, which have been published previously by Wiseman Research Group, McGill University, are used in all the calculations and analyses [41,43,44,46].

Corrections for Immobile Species, the Flow Induced by Cell Movement, and Stage Drift

In cells, the mobile population is a small fraction of the total content. The correlations of the immobile or slowly diffusing populations issue a challenge to extract the velocity direction by following the Gaussian correlation peak [43,44,46,51]. Therefore, the immobile population contribution (which effectively remains centered at zero spatial lags) to the correlation function is removed from the regions of interest by Fourier filtering before the ICS analyses; more detailed descriptions can be found elsewhere [43,44,46,51].

IMAGE COLLECTION FOR DIFFERENT VARIANTS OF ICS

For different variants of ICS, various image series are obtained by using a confocal laser scanning microscope. We performed the image collection with a Zeiss LSM 510 META confocal laser scanning microscope on an inverted epifluorescence Axiovert 200M motorized frame equipped with an LD C-Apochromat $40\times/1.1$ W Corr UV-vis-IR water immersion objective. During the live cell imaging, a chamber with 37°C temperature and 5% CO_2 (Temp-control 37-2 digital; PeCon, Erbach, Germany) is fitted to the microscope, to provide an environment that is nonperturbing and suitable for the metabolism and growth of the cells.

The microscope is coupled to a 30 mW air-cooled argon ion laser emitting at 488 nm under the control of an acousto-optic modulator ($\sim 3\text{ }\mu\text{W}$ maximum radiant power at the sample position) for imaging of the PLLA-Hyp NPs, PVP-Hyp photosensitizer, MitoTracker, LysoTracker, Late Endosomes-GFP, and Early Endosomes-GFP. The laser light is directed to the sample using a dichroic mirror and beam splitters NFT 545 and HFT UV/488/543/633. Three bandpass filters BP 650-710 IR, BP 565-615 IR, and BP 500-550 IR are also used for detection and separation of different emitted fluorescence signals; the filter selection must avoid bleed-through artifacts. In all cases, point detection is achieved using one or two analog photomultiplier tubes (proprietary Zeiss information). The images (512×512 pixels) of each series are collected with no time delays between the sequential frames. The individual frames are acquired with the pixel size of $0.1\text{--}0.2\text{ }\mu\text{m}$ and pixel dwell times of 1.6 or $2.5\text{ }\mu\text{s}$. Fluorescence photobleaching and cytotoxicity (due to the reactive oxygen generation) of the photosensitizer limit the maximum continuous observation of the healthy

cells to 250 and 100 frames for cells incubated with PLLA-Hyp NPs and PVP-Hyp photosensitizer, respectively.

INTRACELLULAR DYNAMICS OF PLLA-HYP NANOPARTICLES AND PVP-HYP

Different concentrations of the freshly prepared PLLA-Hyp NPs and incubation times have been explored to minimize the intracellular degradation of the NPs before the start of the ICS measurements, and at the same time to strike a balance between a decent signal-to-noise ratio in the fluorescence intensity and a sufficient cellular uptake of the NPs. Among different protocols, incubation of the cells with $130\text{ }\mu\text{g/mL}$ NPs in complete culture medium for 1 h has been chosen as the optimum conditions for time-lapse fluorescence confocal microscopy [52–55]. Although the same amounts of the NPs and incubation procedure have been used for the distribution of the NPs in DCs and HeLa cells, a much lower fluorescence signal has been detected in DCs as compared to the HeLa cells (see Fig. 22.2C and D). For the given experimental condition, due to the low amounts of the NPs' uptake and the weak fluorescence signal, ICS could not be applied on DCs to measure the NPs' motion.

STICS has been applied on the different regions of the living HeLa cells to obtain the magnitude and direction of the velocity of the flowing PLLA-Hyp NPs and PVP-Hyp particles. Fitting for the displacement of the autocorrelation peak $r(\xi, \eta, \tau)$ in HeLa cells yields flow vectors of the NPs with magnitudes and directions presented in Fig. 22.2D. The flow mapping of PVP-Hyp photosensitizer has been shown in Fig. 22.2E. The obtained motions demonstrate a slower flow and a higher diffusion of PVP-Hyp compared to those observed for the NPs: $(9.1 \pm 0.5) \times 10^{-3}\text{ }\mu\text{m/s}$, $(2.3 \pm 0.4) \times 10^{-3}\text{ }\mu\text{m}^2/\text{s}$ for PLLA-Hyp NPs and $(2.4 \pm 0.2) \times 10^{-3}\text{ }\mu\text{m/s}$, $(7.0 \pm 1.7) \times 10^{-3}\text{ }\mu\text{m}^2/\text{s}$ for PVP-Hyp photosensitizer.

Friedman and Wilcoxon tests were also used to evaluate whether the flow velocity and diffusion in each of the two groups of samples, PLLA-Hyp NPs and PVP-Hyp, are significantly different from each other. Analyses were carried out using the SPSS 14.0 software (SPSS, Chicago, IL, USA), and statistical significance was defined at the $p < 0.05$ level (95% confidence level). Both flow and diffusion are statistically significantly different ($p < 0.001$). The higher diffusion for the PVP-Hyp photosensitizer can be expected due to the smaller size of the PVP-Hyp particles (about 5 nm) compared to the PLLA-Hyp NPs (205 nm).

Interaction between the organelles and NPs as well as their co-transport is necessary for the correct delivery of their cargo such as the photosensitizer. It is reported that the directed movements of the NPs can be related to the microtubules in the cytoskeleton and the dynamics of the cell organelles [56–60]. To quantify the dynamics of the mitochondria, lysosomes, and early and late endosomes, and to study the role of these organelles in the transport and motion of PLLA-Hyp NPs and PVP-Hyp photosensitizer, STICS and STICCS were used. For each type of organelle, various image subsections were selected from different regions of the cells, and the spatiotemporal autocorrelation function, $r(\xi, \eta, \tau)$, was calculated. Fitting for the displacement of the peak yields flow vectors of the organelles with magnitudes and directions presented in Table 22.1 and Fig. 22.3. For STICCS, two image time-series were collected via two fluorescence detection channels from PLLA-Hyp NPs or PVP-Hyp and Early Endosomes-GFP, Late Endosomes-GFP, LysoTracker, or MitoTracker. The result of the STICCS calculation was the appearance of the Gaussian cross-correlation peaks, $r(\xi, \eta, \tau)$, in some of the selected regions, which reveals an association of NPs and PVP-Hyp with the early endosomes, late endosomes, lysosomes, and mitochondria in those regions. The cross-correlation peaks broaden and appear to be mobile as a function of time, which represents a flow-biased diffusion of the NPs with the aforementioned organelles [31,54,55]. Fitting for the displacement of the cross-correlation peak yields flow velocity of the co-localized PLLA-Hyp NP or PVP-Hyp (Fig. 22.3, red signals) and organelle-specific dye (Fig. 22.3, green signals) populations, with average values presented in Table 22.1.

In most regions of the cells, the velocities of the co-transport populations are about 2–13 times bigger than those estimated for the entire population of the organelles and PLLA-Hyp NPs or PVP-Hyp photosensitizer in cytosol. STICCS implicitly selects the subpopulations of the PLLA-Hyp NPs, PVP-Hyp, and organelles that undergo a correlated motion. These subpopulations are smaller as compared to the corresponding populations as considered in STICS. Although there is a reduced averaging effect in STICCS, the considered autocorrelation functions still exhibited a good signal-to-noise ratio. Therefore, the results seem to suggest that the interaction of the PLLA-Hyp NPs and PVP-Hyp photosensitizer with the organelles affects their mutual directed motion, implying active transport [31,54,55]. These results also indicate that a higher fraction of the PLLA-Hyp NPs and PVP-Hyp are outside the organelles. Moreover, early endosomes, late endosomes, lysosomes, and mitochondria co-localized with NPs and photosensitizer (leading to associated motion) are a small fraction of the whole organelle populations (including associated and nonassociated motions). This subpopulation is characterized with a higher velocity as compared to the velocity obtained for the whole population.

For each individual cell, STICS analysis performed on the whole cell itself yields $|v_x| = (2.0 \pm 0.8) \times 10^{-3} \mu\text{m/s}$ and $|v_y| = (2.0 \pm 0.6) \times 10^{-3} \mu\text{m/s}$. These values are reported as mean \pm standard error of the mean (SEM), and they take the motions of the cell and the stage into account. All the measured flow velocities are corrected for the motions of the cell and stage.

TABLE 22.1 Flow Velocities of Organelles, PLLA-Hyp NPs, and PVP-Hyp Photosensitizer in HeLa Cells, Including the Velocity of Organelles' Co-transport With NPs or PVP-Hyp

Organelles	Cells incubated with NPs			Cells incubated with PVP-Hyp		
	$V_{\text{STICCS}}^{\text{a}} \times 10^{-3}$	$V_{\text{STICS}}^{\text{b}} \times 10^{-3}$		$V_{\text{STICCS}}^{\text{c}} \times 10^{-3}$	$V_{\text{STICS}}^{\text{d}} \times 10^{-3}$	
	($\mu\text{m/s}$)	($\mu\text{m/s}$)		($\mu\text{m/s}$)	($\mu\text{m/s}$)	
	Co-transport population	Organelle population	NPs	Co-transport population	Organelle population	PVP-Hyp
Early endosomes	$29 \pm 11^{\text{e}}$	4.2 ± 0.4	9.1 ± 0.5	21.7 ± 2.2	4.4 ± 0.2	2.4 ± 0.2
Late endosomes	25.3 ± 5.3	3.9 ± 0.3		29.2 ± 2.2	4.7 ± 0.4	
Lysosomes	38.7 ± 9.8	3.3 ± 0.2		26.2 ± 3.4	5.3 ± 0.7	
Mitochondria	17.2 ± 1.3	4.6 ± 0.4		16.6 ± 1.4	5.0 ± 1.0	

^aAverage velocity of the organelles' co-transport with PLLA-Hyp NPs; measured by STICCS.

^bFlow velocity of the NPs or entire population of the organelles treated; with PLLA-Hyp NPs and measured by STICS.

^cAverage velocity of the organelles' co-transport with PVP-Hyp photosensitizer; measured by STICCS.

^dAverage velocity of the PVP-Hyp or entire population of the organelles; treated with the photosensitizer and measured by STICS.

^eAll velocity values are reported as mean \pm SEM for 11–40 regions inside the cells.

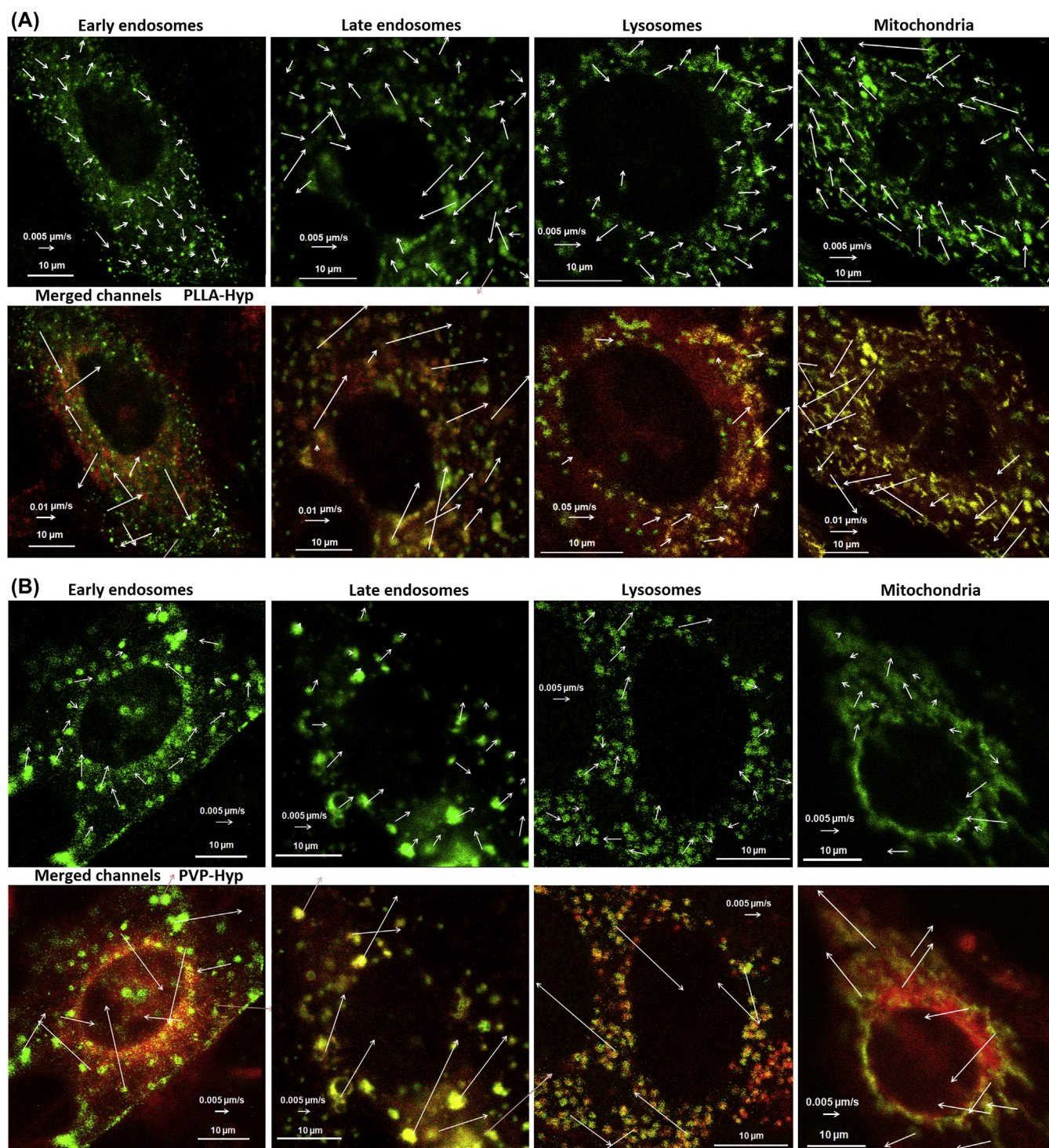


FIGURE 22.3 Directed movement characteristics of the early endosomes, late endosomes, lysosomes, and mitochondria of HeLa cells treated with (A) PLLA-Hyp NPs and (B) PVP-Hyp. For the STICCS analyses (merged images), the cells were stained with organelle-specific dyes. The spatial scale bars are 10 μm in all images.

CONCLUSION

In this chapter, the uptake and dynamics of the PLLA NPs carrying hypericin, a potent photosensitizer in PDT,

in DCs and HeLa cells have been studied. DCs are antigen-presenting cells (also known as accessory cells) of the mammalian immune system. Immune cell populations in the skin are predominantly composed of

DCs [27]. As HeLa cells are adherent and flat, they are suitable for image correlation spectroscopy and imaging. A substantially higher accumulation of the NPs was observed in HeLa cells. This finding is in agreement with the other studies that show PLLA-Hyp NPs exhibit cancer-selective targeting, enhanced reduction of cancer cell viability, together with no significant reduction in viability of the normal cells in comparison with hypericin alone [3,9,15,34]. Although, in our previous study [31], we detected a lower uptake of PVP-Hyp by DCs in comparison with HeLa cells, more detailed studies are required to evaluate whether using PLLA-Hyp NPs improves the cancer targeting or not. The intracellular dynamics of PLLA-Hyp NPs and PVP-Hyp photosensitizer was studied shortly after the end of the incubation period to avoid substantial NP degradation and photosensitizer-induced cytotoxicity. The quantification of the dynamics was based on TICS, STICS, and STICCS. The intracellular motion of the PLLA-Hyp NPs and PVP-Hyp photosensitizer and of early endosomes, late endosomes, lysosomes, and mitochondria were studied to provide insight into NP and PVP-Hyp behavior and cell interaction. TICS and STICS showed a higher diffusion and a lower flow for the PVP-Hyp photosensitizer as compared to the PLLA-Hyp NPs. The higher diffusion coefficient can be expected due to the smaller size of the PVP-Hyp particles (about 5 nm) as compared to the NPs (205 nm). We also obtained quantitative values for the directed motion of the cell organelles in the presence of PLLA-Hyp NPs and PVP-Hyp photosensitizer. In addition, we observed that there exists a difference between the dynamics of the co-transport and the organelle-only population, indicating that the presence of PLLA-Hyp NPs or PVP-Hyp influences the organelle dynamics [31,54,55]. STICCS targets the subpopulations of the PLLA-Hyp NPs or PVP-Hyp photosensitizer and organelles that undergo a correlated transport. These subpopulations are smaller as compared to the corresponding populations as considered in STICS. Based on the smaller flow velocity obtained by STICS for the PLLA-Hyp NPs and PVP-Hyp population as compared to the co-transported population, we might conclude that PLLA-Hyp and PVP-Hyp accumulate in a small fraction of the whole organelle population. Organelles associated with the PLLA-Hyp NPs or PVP-Hyp photosensitizer exhibit higher flow velocity as compared to those moving without them. These observations can be studied further to shed light on the intricacies involved in the cellular uptake of the nanocarriers as well as the fate of the cargo and the carrier at the subcellular level.

List of Acronyms and Abbreviations

ALA Assisted 5-aminolevulinic acid
DC Human primary dendritic cells

DLS Dynamic light scattering
FBS Fetal bovine serum
FDA Food and Drug Administration
ICS Image correlation spectroscopy
NP Nanoparticle
PBS Phosphate buffered saline
PDT Photodynamic therapy
PLLA Poly L-lactic acid
PLLA-Hyp Poly L-lactic acid-hypericin
PpIX Protoporphyrin IX
PVP-Hyp Polyvinylpyrrolidone-hypericin
SEM Standard error of the mean
STICCS Spatiotemporal image cross-correlation spectroscopy
STICS Spatiotemporal image correlation spectroscopy
TEM Transmission electron microscopy
TICS Temporal image correlation spectroscopy

Acknowledgments

The work was supported by Research Foundation Flanders (FWO-Vlaanderen), BELSPO (for supporting IAP P7/05 network), funding from INTERREG-IV A (BioMiMedics), and BOF (Hasselt University). A. Ethirajan is an FWO postdoctoral fellow. The authors acknowledge Rik Paesen and Nick Smisdom for the useful discussions concerning ICS technique. We also would like to thank Inge Nelissen and Jef Hooyberghs at the Flemish Institute for Technological Research, Environmental Risk for the preparation of DCs.

References

- [1] Penjweini R, Liu B, Kim MM, Zhu TC. Explicit dosimetry for 2-(1-hexyloxyethyl)-2-devinylpyropheophorbide-a-mediated photodynamic therapy: macroscopic singlet oxygen modeling. *J Biomed Opt* 2015;20(12):128003.
- [2] Lima AM, Pizzol CD, Monteiro FB, Creczynski-Pasa TB, Andrade GP, Ribeiro AO, et al. Hypericin encapsulated in solid lipid nanoparticles: phototoxicity and photodynamic efficiency. *J Photochem Photobiol B* 2013;125:146–54.
- [3] Zeisser-Laboube M, Lange N, Gurny R, Delie F. Hypericin-loaded nanoparticles for the photodynamic treatment of ovarian cancer. *Int J Pharm* 2006;326:174–81.
- [4] Jichlinski P, Jacqmin D. Photodynamic diagnosis in non-muscle-invasive bladder cancer. *Eur Urol* 2008;7:529–35.
- [5] Jocham D, Stepp H, Waidelich R. Photodynamic diagnosis in urology: state-of-the-art. *Eur Urol* 2008;53:1138–50.
- [6] Wang KK, Finlay JC, Busch TM, Hahn SM, Zhu TC. Explicit dosimetry for photodynamic therapy: macroscopic singlet oxygen modeling. *J Biophotonics* 2010;3:304–18.
- [7] Guduru R, Liang P, Runowicz C, Nair M, Atluri V, Khizroev S. Magneto-electric nanoparticles to enable field-controlled high-specificity drug delivery to eradicate ovarian cancer cells. *Sci Rep* 2013;3:2953.
- [8] Petros RA, DeSimone JM. Strategies in the design of nanoparticles for therapeutic applications. *Nat Rev Drug Discov* 2010;9:615–27.
- [9] Xie J, Lee S, Chen X. Nanoparticle-based theranostic agents. *Adv Drug Deliv Rev* 2010;62:1064–79.
- [10] Sutradhar KB, Amin ML. Nanotechnology in cancer drug delivery and selective targeting. *ISRN Nanotechnol* 2014;2014:12.
- [11] Wu X, Landfester K, Musyanovych A, Guy RH. Disposition of charged nanoparticles after their topical application to the skin. *Skin Pharmacol Physiol* 2010;23:117–23.
- [12] Frick SU, Bacher N, Baier G, Mailänder V, Landfester K, Steinbrink K. Functionalized polystyrene nanoparticles trigger

- human dendritic cell maturation resulting in enhanced CD4+ T cell activation. *Macromol Biosci* 2012;12:1637–47.
- [13] Wang X, Shi L, Tu Q, Wang H, Zhang H, Wang P, et al. Treating cutaneous squamous cell carcinoma using 5-aminolevulinic acid poly(lactic-co-glycolic acid) nanoparticle-mediated photodynamic therapy in a mouse model. *Int J Nanomedicine* 2015;10:347–55.
 - [14] da Silva CL, Del Ciampo JO, Rossetti FC, Bentley MV, Pierre MB. PLGA nanoparticles as delivery systems for protoporphyrin IX in topical PDT: cutaneous penetration of photosensitizer observed by fluorescence microscopy. *J Nanosci Nanotechnol* 2013;13: 6533–40.
 - [15] Kumari A, Yadav SK, Yadav SC. Biodegradable polymeric nanoparticles based drug delivery systems. *Colloids Surf B* 2010;75:1–18.
 - [16] Guo S, Huang L. Nanoparticles containing insoluble drug for cancer therapy. *Biotechnol Adv* 2013;32.
 - [17] Makadia HK, Siegel SJ. Poly(lactic-co-glycolic acid) (PLGA) as biodegradable controlled drug delivery carrier. *Polymers* 2011;3: 1377–97.
 - [18] Panariti A, Miserocchi G, Rivolta I. The effect of nanoparticle uptake on cellular behavior: disrupting or enabling functions? *Nanotechnol Sci Appl* 2012;5:87–100.
 - [19] Deleted in review.
 - [20] Hemmerich PH, von Mikecz AH. Defining the subcellular interface of nanoparticles by live-cell imaging. *PLoS One* 2013;8: e62018.
 - [21] Huang F, Dempsey C, Chona D, Suh J. Quantitative nanoparticle tracking: applications to nanomedicine. *Nanomedicine* 2011;6: 693–700.
 - [22] Huang Z, Xu H, Meyers AD, Musani AI, Wang L, Tagg R, et al. Photodynamic therapy for treatment of solid tumors—potential and technical challenges. *Technol Cancer Res Treat* 2008;7: 309–20.
 - [23] Lai SK, Hida K, Chen C, Hanes J. Characterization of the intracellular dynamics of a non-degradative pathway accessed by polymer nanoparticles. *J Control Release* 2008;125:107–11.
 - [24] Kulkarni RP, Wu DD, Davis ME, Fraser SE. Quantitating intracellular transport of polyplexes by spatio-temporal image correlation spectroscopy. *PNAS* 2005;102:7523–8.
 - [25] Kubin A, Kubin A, Loew HG, Loew HG, Burner U, Jessner G, et al. How to make hypericin water-soluble. *Die Pharmazie* 2008;63: 263–9.
 - [26] Penjweini R, Loew HG, Breit P, Kratky KW. Optimizing the anti-tumor selectivity of PVP-hypericin re A549 cancer cells and HLF normal cells through pulsed blue light. *Photodiagnosis Photodyn Ther* 2013;10:591–9.
 - [27] Malissen B, Tamoutounour S, Henri S. The origins and functions of dendritic cells and macrophages in the skin. *Nat Rev Immunol* 2014;14:417–28.
 - [28] Fox FE, Niu Z, Tobia A, Rook AH. Photoactivated hypericin is an anti-proliferative agent that induces a high rate of apoptotic death of normal, transformed, and malignant T lymphocytes: implications for the treatment of cutaneous lymphoproliferative and inflammatory disorders. *J Invest Dermatol* 1998;111: 327–32.
 - [29] Ritz R, Roser F, Radomski N, Strauss WS, Tatagiba M, Gharabaghi A. Subcellular colocalization of hypericin with respect to endoplasmic reticulum and Golgi apparatus in glioblastoma cells. *Anticancer Res* 2008;28:2033–8.
 - [30] Delaey EM, Obermueller R, Zupko I, De Vos D, Falk H, de Witte PA. In vitro study of the photocytotoxicity of some hypericin analogs on different cell lines. *Photochem Photobiol* 2001;74:164–71.
 - [31] Penjweini R, Smisdom N, Deville S, Ameloot M. Transport and accumulation of PVP-hypericin in cancer and normal cells characterized by image correlation spectroscopy techniques. *Biochim Biophys Acta* 2014;1843:855–65.
 - [32] Ali SM, Olivo M. Bio-distribution and subcellular localization of hypericin and its role in PDT induced apoptosis in cancer cells. *Int J Oncol* 2002;21:531–40.
 - [33] Boiy A, Roelandts R, van den Oord J, de Witte PA. Photosensitizing activity of hypericin and hypericin acetate after topical application on normal mouse skin. *Br J Dermatol* 2008;158: 360–9.
 - [34] Nobs L, Buchegger F, Gurny R, Allemann E. Biodegradable nanoparticles for direct or two-step tumor immunotargeting. *Bioconjug Chem* 2006;17:139–45.
 - [35] Shirali AC, Look M, Du W, Kassis E, Stout-Delgado HW, Fahmy TM, et al. Nanoparticle delivery of mycophenolic acid upregulates PD-L1 on dendritic cells to prolong murine allograft survival. *Am J Transplant* 2011;11:2582–92.
 - [36] Musyanovych A, Schmitz-Wienke J, Mailänder V, Walther P, Landfester K. Preparation of biodegradable polymer nanoparticles by miniemulsion technique and their cell interactions. *Macromol Biosci* 2008;8:127–39.
 - [37] Baier G, Baki A, Tomcin S, Mailänder V, Alexandrino E, Wurm F, et al. Stabilization of nanoparticles synthesized by miniemulsion polymerization using “green” amino-acid based surfactants. *Macromol Symp* 2014;337:9–17.
 - [38] Schoeters E, Verheyen GR, Nelissen I, Van Rompay AR, Hooyberghs J, Van Den Heuvel RL, et al. Microarray analyses in dendritic cells reveal potential biomarkers for chemical-induced skin sensitization. *Mol Immunol* 2007;44:3222–33.
 - [39] Lardon F, Snoeck HW, Berneman ZN, Van Tendeloo VF, Nijs G, Lenjou M, et al. Generation of dendritic cells from bone marrow progenitors using GM-CSF, TNF-alpha, and additional cytokines: antagonistic effects of IL-4 and IFN-gamma and selective involvement of TNF-alpha receptor-1. *Immunology* 1997;91:553–9.
 - [40] Petersen NO, Hoddellius PL, Wiseman PW, Seger O, Magnusson KE. Quantitation of membrane receptor distributions by image correlation spectroscopy: concept and application. *Biophys J* 1993;65:1135–46.
 - [41] Wiseman PW. Image correlation spectroscopy: mapping correlations in space, time, and reciprocal space. *Methods Enzymol* 2013;518:245–67.
 - [42] Toplak T, Pandzic E, Chen L, Vicente-Manzanares M, Horwitz AR, Wiseman PW. STICCS reveals matrix-dependent adhesion slipping and gripping in migrating cells. *Biophys J* 2012;103:1672–82.
 - [43] Kolin DL, Costantino S, Wiseman PW. Sampling effects, noise, and photobleaching in temporal image correlation spectroscopy. *Biophys J* 2006;90:628–39.
 - [44] Kolin DL, Wiseman PW. Advances in image correlation spectroscopy: measuring number densities, aggregation states, and dynamics of fluorescently labeled macromolecules in cells. *Cell Biochem Biophys* 2007;49:141–64.
 - [45] Geissbuehler M, Bonacina L, Shcheslavskiy V, Bocchio NL, Geissbuehler S, Leutenegger M, et al. Nonlinear correlation spectroscopy (NLCS). *Nano Lett* 2012;12:1668–72.
 - [46] Hebert B, Costantino S, Wiseman PW. Spatiotemporal image correlation spectroscopy (STICS) theory, verification, and application to protein velocity mapping in living CHO cells. *Biophys J* 2005; 88:3601–14.
 - [47] Ries J, Schille P. Fluorescence correlation spectroscopy. *Bioessays* 2012;34:361–8.
 - [48] Rossow M, Mantulin WW, Gratton E. Spatiotemporal image correlation spectroscopy measurements of flow demonstrated in microfluidic channels. *J Biomed Opt* 2009;14:024014.
 - [49] Wiseman PW, Brown CM, Webb DJ, Hebert B, Johnson NL, Squier JA, et al. Spatial mapping of integrin interactions and dynamics during cell migration by image correlation microscopy. *J Cell Sci* 2004;117:5521–34.

- [50] Staedler D, Magouroux T, Hadji R, Joulaud C, Extermann J, Schwung S, et al. Harmonic nanocrystals for biolabeling: a survey of optical properties and biocompatibility. *ACS Nano* 2012;6:2542–9.
- [51] Comeau JW, Kolin DL, Wiseman PW. Accurate measurements of protein interactions in cells via improved spatial image cross-correlation spectroscopy. *Mol Biosyst* 2008;4:672–85.
- [52] Ethirajan A, Musyanovych A, Chuvilin A, Landfester K. Biodegradable polymeric nanoparticles as templates for biomimetic mineralization of calcium phosphate. *Macromol Chem Phys* 2011;212:915–25.
- [53] Rivolta I, Panariti A, Lettiero B, Sesana S, Gasco P, Gasco MR, et al. Cellular uptake of coumarin-6 as a model drug loaded in solid lipid nanoparticles. *J Physiol Pharmacol* 2011;62:45–53.
- [54] Deville S, Penjweini R, Smisdom N, Notelaers K, Nelissen I, Hooyberghs J, et al. Intracellular dynamics and fate of polystyrene nanoparticles in A549 lung epithelial cells monitored by image (cross-) correlation spectroscopy and single particle tracking. *Biochim Biophys Acta* 2015;1853:2411–9.
- [55] Penjweini R, Deville S, D'Olieslaeger L, Berden M, Ameloot M, Ethirajan A. Intracellular localization and dynamics of hypericin loaded PLLA nanocarriers by image correlation spectroscopy. *J Control Release* 2015;218:82–93.
- [56] Garrison AK, Shanmugam M, Leung HC, Xia C, Wang Z, Ma L. Visualization and analysis of microtubule dynamics using dual color-coded display of plus-end labels. *PLoS One* 2012;7:e50421.
- [57] Jordan MA, Thrower D, Wilson L. Effects of vinblastine, podophyllotoxin and nocodazole on mitotic spindles. Implications for the role of microtubule dynamics in mitosis. *J Cell Sci* 1992;102(Pt 3):401–16.
- [58] Quintero OA, DiVito MM, Adikes RC, Kortan MB, Case LB, Lier AJ, et al. Human Myo19 is a novel myosin that associates with mitochondria. *Curr Biol* 2009;19:2008–13.
- [59] Manneville JB, Etienne-Manneville S, Skehel P, Carter T, Ogden D, Ferenczi M. Interaction of the actin cytoskeleton with microtubules regulates secretory organelle movement near the plasma membrane in human endothelial cells. *J Cell Sci* 2003;116:3927–38.
- [60] Otten M, Nandi A, Arcizet D, Gorelashvili M, Lindner B, Heinrich D. Local motion analysis reveals impact of the dynamic cytoskeleton on intracellular subdiffusion. *Biophys J* 2012;102:758–67.

Accelerated Wound Healing Using Nanoparticles

E.T. Goh¹, G. Kirby^{1,2}, R. Jayakumar³, X.-J. Liang⁴, A. Tan^{1,3}

¹University College London (UCL), London, United Kingdom; ²University of Cambridge, Cambridge, United Kingdom;

³Stanford University, Stanford, CA, United States; ⁴Chinese Academy of Sciences (CAS), Beijing, China

OUTLINE

Wound Healing	287	Stimulating Proliferation	295
<i>Inflammation</i>	288	Delivery and Elution of Biological Factors	295
<i>Proliferation</i>	289	Gene Therapy	297
<i>Maturation</i>	289	Maturation	297
Nanoparticles	290	Nitric Oxide	298
Nanoparticle Applications in Wound Healing	290	Toxicity of Nanoparticles	301
<i>Hemostasis</i>	290	What Next?	303
<i>Platelets</i>	290	List of Acronyms and Abbreviations	303
<i>Thrombin</i>	291	References	304
<i>Nanobridging</i>	292		
Antimicrobial Applications	292		
<i>Delivery of Antimicrobial Agents</i>	292		
<i>Inherent Antimicrobial Properties of Metal Nanoparticles</i>	293		
Stemming Inflammation	295		

WOUND HEALING

The skin is the largest organ of the human body, and it covers the entire external body surface. Besides forming a crucial barrier against microbial invasion, it is also important for many other functions, such as sensory detection, fluid homeostasis, and general protection against external insults. Having said that, a wound can be defined as an insult to the skin due to physical, chemical, or thermal damage. Wounds can also be caused by underlying physiological abnormalities or medical conditions that can ultimately compromise

the normal structure and function of the skin [2]. Fig. 23.1 gives a brief summary of how wounds can be classified [3].

Acute wounds can be healed within a reasonable period of time and are usually caused by specific, temporary insults such as mechanical trauma. Chronic wounds, on the other hand, are usually due to underlying pathologies and can take more than 12 weeks to heal, with a high chance of reoccurrence.

In the event the skin is damaged, there is a system in place to restore function and structural integrity. This is known as wound repair. The three basic stages of wound

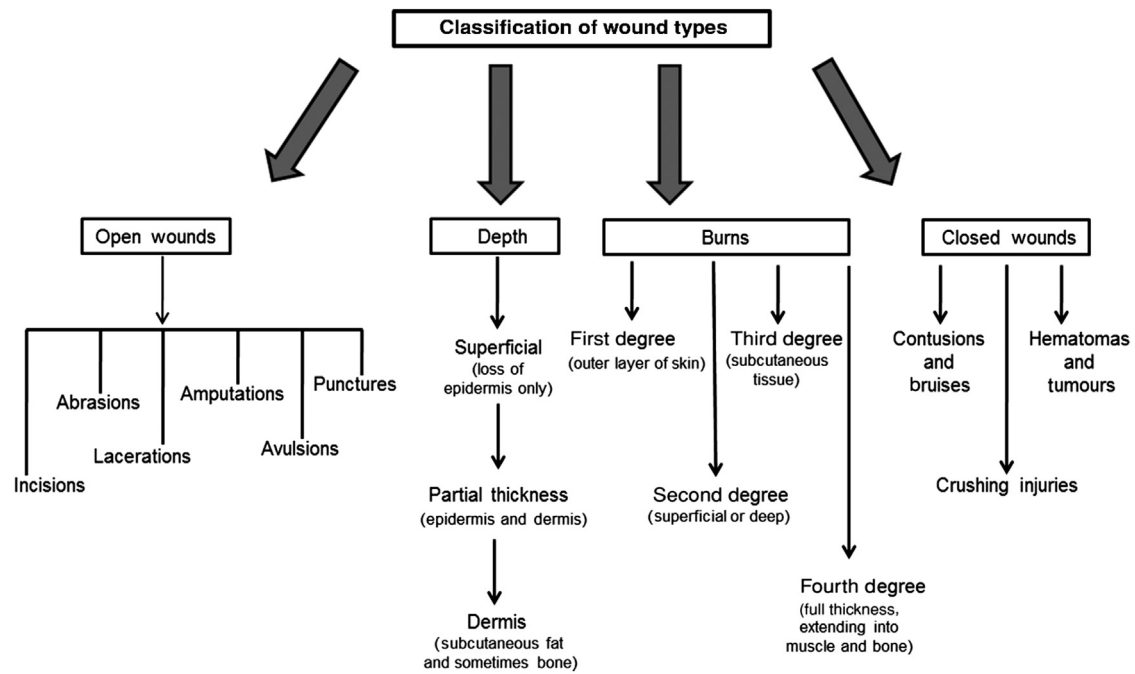


FIGURE 23.1 Classification of wound types. Reproduced with permission from Mayet N, Choonara YE, Kumar P, et al. A comprehensive review of advanced biopolymeric wound healing systems. J Pharm Sci 2014;103(8):2211–30.

repair are inflammation, proliferation, and maturation. The three stages may occur simultaneously, with individual processes within each stage overlapping as well [4]. Table 23.1 gives a brief overview of the stages involved in wound repair.

Inflammation

As an immediate reaction to an injury, hemostasis and inflammation take place. The purpose of this stage is to minimize damage, stop any bleeding, seal the injury site, and eliminate or contain any foreign bodies or microorganisms. At the wound site, there is increased vascular

permeability, secretion of cytokines and growth factors, as well as migration and activation of inflammatory cells.

When the damaged endothelium of blood vessels is exposed after injury, vasoconstriction occurs and the clotting cascade is activated. Platelet aggregation occurs at the same time, forming a platelet plug to stop the bleeding. Activated platelets not only trigger the coagulation system and the complement cascade, but also degranulate to release cytokines, growth factors, and vasoactive substances. A fibrin network is eventually formed, stopping further hemorrhage by trapping blood cells. Cytokines and other biomolecules such as platelet-derived growth factor, transforming growth factor β (TGF- β), fibroblast growth factor (FGF), vascular endothelial growth factor (VEGF), serotonin, bradykinin, prostaglandin, and histamine are released that result in increased vascular permeability and recruit inflammatory cells to the wound site (Fig. 23.2) [1]. These include neutrophils and mononuclear leukocytes, which mature into macrophages and, later on, lymphocytes [5]. The neutrophils then proceed to eliminate foreign debris and bacteria in the wound. They are then extruded or phagocytosed by macrophages. Macrophages also express important cytokines such as transforming growth factor α (TGF- α), TGF- β , insulin-like growth factor I, and others. The cytokines expressed by the inflammatory cells and damaged tissue are extremely important for new tissue formation in wounds.

TABLE 23.1 Stages of Wound Repair

Stage	Process
Inflammation (reactive)	Hemostasis
	Chemotaxis
	Epithelial migration
Proliferation (regenerative)	Proliferation
Maturation (remodeling)	Maturation
	Contraction
	Scar tissue formation
	Remodeling of scar

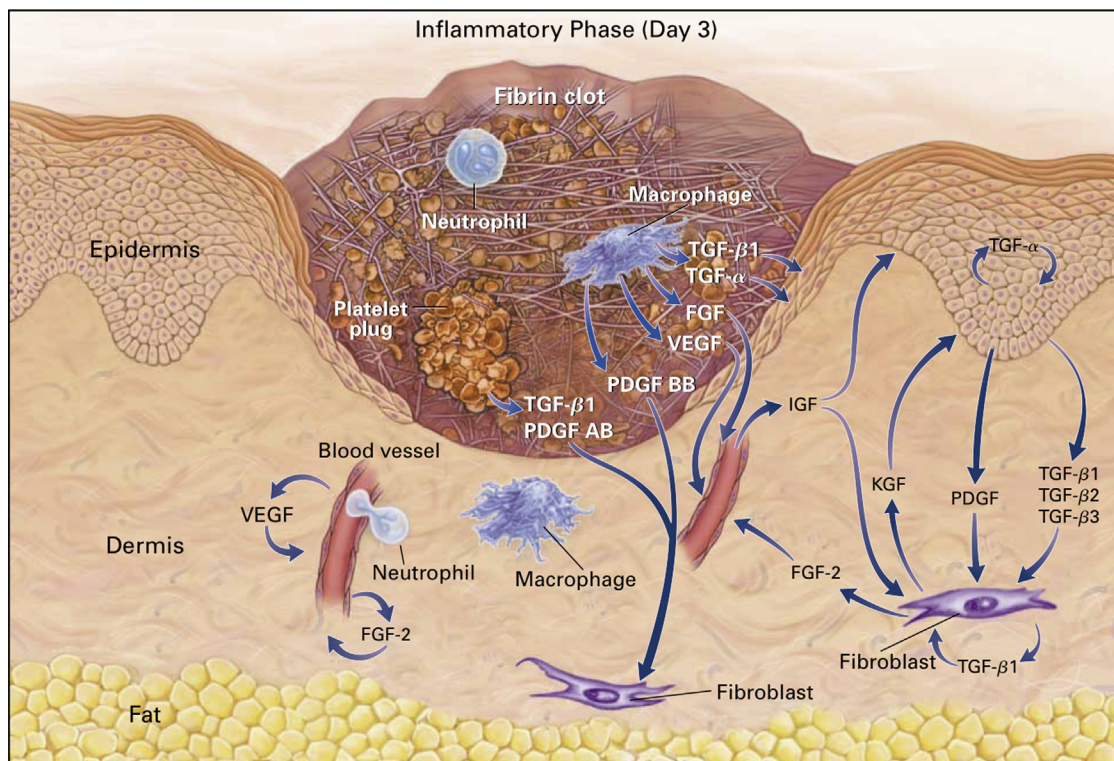


FIGURE 23.2 Cutaneous wound three days after injury. TGF, transforming growth factor; PDGF, plate-derived growth factor; VEGF, vascular endothelial growth factor; FGF, fibroblast growth factor; KGF, keratinocyte growth factor. Reproduced with permission from Singer AJ, Clark RAF. *Cutaneous wound healing. New Engl J Med* 1999;341(10):738–46.

Proliferation

The re-epithelialization of wounds happens within hours of injury and occurs alongside other processes. Epidermal cells and dermal cells at the wound margins undergo phenotypic alteration, which allows epidermal cells to migrate into the wound area. Later on, epidermal cells at the wound margins start to proliferate as well. This migration and proliferation of epidermal cells may be stimulated by the absence of neighbor cells as well as the release of growth factors. The basement membrane is reestablished in an orderly, zipper-like fashion from the wound margins, and the epidermal cells revert to their normal phenotype once their positions are fixed.

Granulation tissue then starts to form in the wound space. This occurs as macrophages, fibroblasts, and blood vessels enter the wound space. Growth factors secreted by the macrophages help to stimulate and sustain fibroplasia and angiogenesis. Fibroblasts lay down new extracellular matrix (ECM) to form the provisional ECM, which is then replaced by collagenous matrix. The new ECM supports cell ingrowth. Angiogenesis, in contrast, is necessary for the delivery of oxygen and nutrients to sustain the heightened metabolism at the wound site. Biomolecules that promote angiogenesis

include TGF- β , VEGF, angiogenin, FGFs, and many more. The collagenous matrix fills the wound space as re-epithelialization occurs and new blood vessels are formed [3].

Maturation

The granulation tissue matures, and there is continued accumulation of collagen. The vascularity of the wound and the number of inflammatory cells start to reduce. Microscopically, the scar becomes paler, a process known as blanching. By the end of one month, a complete scar can be seen with collagen at its maximum. If the wound area is large, wound contraction occurs to bring the edges of the wound closer together. Fibroblasts switch to a myofibroblast phenotype usually during the second week of wound repair. Contraction of the wound then occurs via the concerted effort of myofibroblasts, stimulatory cytokines, the attachments of fibroblasts to the collagen matrix, and cross-links between collagen bundles.

Remodeling of the wound then occurs to improve the tensile strength of the newly synthesized tissue. The degradation of preexisting collagen by proteolytic enzymes known as matrix metalloproteinases (MMPs) occurs, and new, fibrillar collagen accumulates. The

collagen bundles are larger, and more inter- and intramolecular cross-links are formed. The bundles are also aligned along lines of stress. This process occurs slowly over months, but the final product is still not as strong as unwounded tissue.

NANOPARTICLES

A nanoparticle is a minute fragment of matter that is less than 100 nm in diameter. Despite its miniscule size, a nanoparticle behaves as a whole unit with regard to its properties and transport. Nanoparticle research is one of the most widely researched fields currently due to its extensive applicability in numerous industries.

Nanoparticles are unique in the sense that they form the link between bulk material and materials at the atomic or molecular scale. Bulk materials usually retain their properties regardless of size. However, when the materials are reduced to the nanoscale, their physical and chemical properties change depending on size. For materials larger than 1 μm , the percentage of atoms on the surface area of the material is insignificant compared to the number of atoms making up the bulk of the material. In nanoparticles, the surface area is much more significant compared to the bulk of the particle, and this largely accounts for their different physical properties. This high surface area-to-volume ratio is extremely valuable in the sense that chemical reactions occur at a rate proportional to the available surface area of reactants. Nanoparticles are thus capable of producing more efficient reactions.

Physical and chemical properties of nanoparticles that may differ from the bulk forms of the same materials include color, melting temperature, chemical reactivity, electrical conductivity, magnetism, mechanical strength, or crystal structure. For instance, gold nanoparticles melt at approximately 300°C, while gold slabs melt at 1064°C.

Nanoparticles can be made up of a wide variety of materials. It would be beyond the scope of this topic to summarize all the different types and functions of nanoparticles, but broadly speaking, one can classify nanoparticles into several categories (Table 23.2).

TABLE 23.2 Different Categories of Nanoparticles

Different categories of nanoparticles
<ul style="list-style-type: none"> • Fullerenes and carbon nanotubes (CNTs) • Metals • Ceramics • Quantum dots • Polymers • Dendrimers • Liquid crystal-based nanoparticles

TABLE 23.3 Different Sources of Materials for Polymeric Nanoparticles

Natural sources	Synthetic sources
<ul style="list-style-type: none"> • Gelatin • Chitosan • Alginate • Nano-crystalline cellulose 	<ul style="list-style-type: none"> • Poly(lactic-co-glycolic)acid • Poly-n-(cyanoacrylate) • Polycaprolactone

Polymeric nanoparticles are synthesized from polymers that, in biomedical applications, are preferably biodegradable. The biodegradable polymers can come from either synthetic or natural sources. Table 23.3 lists some materials commonly used to synthesize polymeric nanoparticles.

Next-generation nanoparticles incorporate qualities of different materials. An example would be lipid-polymer hybrid nanoparticles (LPNs) [6]. LPNs are core-shell nanoparticles with polymer cores and lipid shells. They exhibit the physical stability of polymeric nanoparticles and the biocompatibility of liposomes. In essence, current development for biomedical applications is targeted toward creating nanoparticles that are stable, biocompatible, nontoxic, and easily synthesized.

NANOPARTICLE APPLICATIONS IN WOUND HEALING

As mentioned in this chapter, wound healing is a multistage process. Applications of nanoparticle technology to improve wound healing therefore aim to enhance these processes, supporting the body's ability to heal itself. By utilizing the unique properties of nanoparticles, we can aim to develop therapies that have greater efficacy, efficiency, and specificity, while reducing off-target side effects at the same time.

Hemostasis

Hemostasis takes top priority in wound healing. Any bleeding has to be arrested as soon as possible before healing can take place. A dynamic process, effective hemostasis requires the combined action of vascular, platelet, and plasma factors. Therapy options to improve hemostasis therefore aim to supplement these factors, including platelet and thrombin action.

Platelets

Anselmo et al. have recently reported the development of platelet-inspired nanoparticles for treating vascular injuries [7]. This is in conjunction with the recent paradigm of bio-inspired nanoparticle design

for better performance *in vivo* [8]. The platelet-inspired nanoparticles were said to simulate the key characteristics of platelets. First of all, the nanoparticles were synthesized using the layer-by-layer method, with attention being given to the natural biophysical attributes of platelets. The nanoparticles exhibit a discoidal morphology with enhanced mechanical flexibility. In addition, to match the biochemical properties of platelets, the nanoparticles were functionalized with wound adhesive and activated platelet aggregatory peptides. These consist of collagen-binding peptides (which bind to exposed collagen at wound sites), von Willebrand Factor (vWF)-binding peptides (which bind to vWF at wound sites), and linear fibrinogen-mimetic peptides (which bind specifically to integrin GPIIb–IIIa on activated natural platelets). The peptide ligands were conjugated to branched dendrimers and covalently bonded to the surface of the nanoparticles.

The platelet-like nanoparticles (PLNs) were subsequently able to aggregate under high shear conditions, and the authors suggested that this might be due to their physical morphology encouraging accumulation at the vessel wall under flow. Following injection of PLNs, improved hemostatic plug formation was observed, as activating circulating platelets and PLNs were able to bind to the injured endothelium and to each other.

This results in faster hemostasis, speeding up the wound-healing process. Using *in vivo* standard tail transection models, functionalized PLNs have been demonstrated to reduce bleeding times by up to 65%.

Thrombin

Thrombin is an endogenous protein involved in the coagulation cascade, where it has a key role in the formation of fibrin clots by converting fibrinogen to fibrin. Besides that, other functions of thrombin have been documented as well, including platelet activation, inflammatory cell chemotaxis, stimulation of endothelial changes, as well as the production of autocooids and cytokines (Fig. 23.3) [9]. As such, thrombin has been used for hemostasis and wound management for decades [10]. However, the half-life of thrombin in human plasma is less than 15 s, due to stringent regulation by protease inhibitors and blood vessel wall components [11]. Steps must therefore be taken to stabilize thrombin to ensure longer lasting effects at the wound site.

Ziv-Polat et al. managed to stabilize thrombin by binding it to maghemite ($\gamma\text{-Fe}_2\text{O}_3$) nanoparticles [12]. This was done by adsorption to a bovine serum albumin (BSA) coating on the nanoparticles. The study showed that this process resulted in thrombin being stabilized

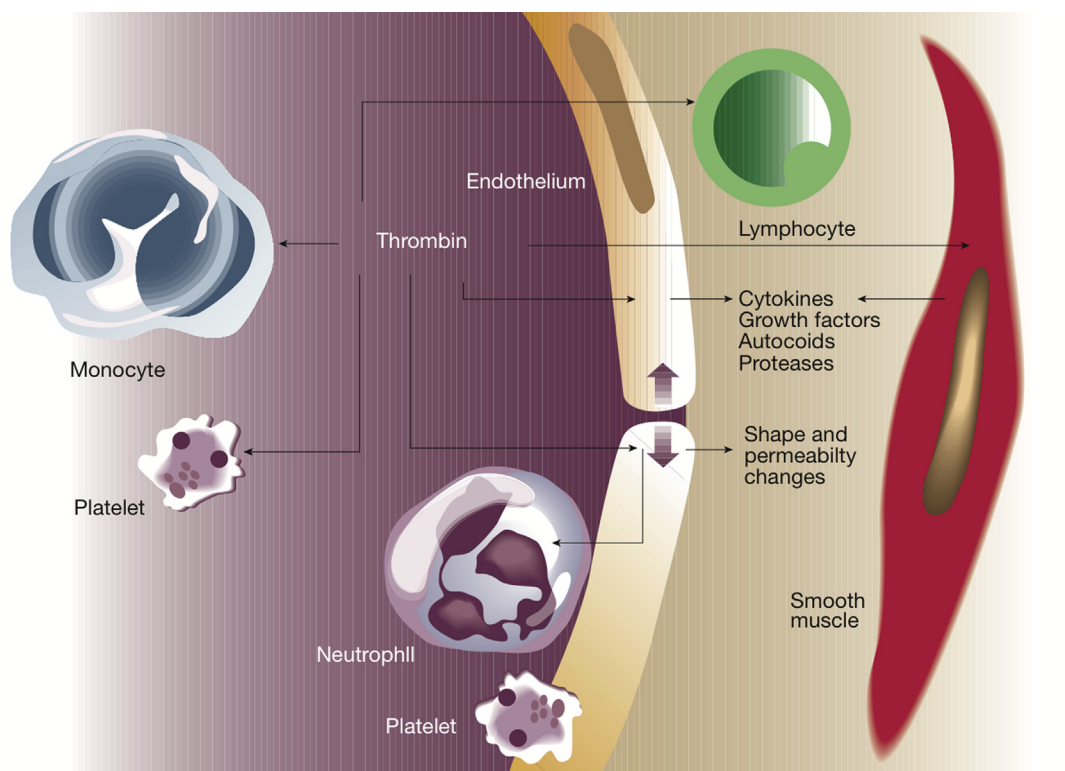


FIGURE 23.3 Thrombin has a role in the chemotaxis of immune cells, platelet activation, endothelial modification, and the synthesis of various endogenous molecules. Reproduced with permission from Jung SM, Yoon GH, Lee HC, Shin HS. Chitosan nanoparticle/PCL nanofiber composite for wound dressing and drug delivery. *J Biomater Sci Polym Ed* 2015;26(4):252–63.

against antithrombin III. In addition, the storage stability as well as clotting activity of thrombin were improved. In a further study, the same group managed to show that thrombin-conjugated $\gamma\text{-Fe}_2\text{O}_3$ nanoparticles promoted faster healing of incisional skin wounds as compared to free thrombin and untreated controls [13].

Nanobridging

A novel approach to wound closure and stopping bleeding involves the concept of nanobridging. By using nanoparticles instead of polymer adhesives, a different approach to hydrogel adhesion has been introduced. Nanoparticles are spread on gel surfaces and act as connectors to bring the gel pieces together. Meddahi-Pellé et al. investigated the applications of this new concept and found that for cutaneous wounds, nanobridging with a silica nanoparticle solution provided easy wound closure with favorable aesthetic quality [14]. Minimal training was needed for the procedure compared to other procedures such as suturing, and future research can be focused on utilizing nanoparticles that have beneficial effects for wound healing in the hydrogel solutions, such as antimicrobial metal nanoparticles.

ANTIMICROBIAL APPLICATIONS

Infection is a significant problem when it comes to wound healing, as it not only delays the repair process but also can exacerbate the severity of the wound. In the past, wound infection contributed significantly to mortality and morbidity before infection control measures were put in place [15]. Despite advancements in antimicrobial therapy since then, infection control today is not without its challenges. The emergence of multidrug-resistant pathogens has resulted in a race to develop antimicrobial therapies faster than the pathogens can evolve. The use of nanoparticles can potentially help to tackle these challenges through the targeted delivery of drugs and other antimicrobial substances or the intrinsic antimicrobial activity of the nanoparticles themselves.

Delivery of Antimicrobial Agents

Ironically enough, the evolution of stronger pathogens is spurred on by the selection pressure exerted on microbial populations from the inadequate use of antimicrobials. For example, the excessive and inappropriate use of penicillin has resulted in the emergence of penicillin-resistant strains of *Staphylococcus aureus* that produce penicillinase (an enzyme that breaks down the beta-lactam ring in penicillin).

This is a problem as *S. aureus* is one of the most common pathogens to infect wounds, resulting in severe complications such as sepsis and toxic shock syndrome [15].

Thus, there is extensive interest in the delivery of antimicrobial agents such as antibiotic drugs via nanoparticles. Due to their unique structures and modifiability, nanoparticles can be considered as novel delivery platforms for such endogenous substances, allowing for their controlled release over extended periods of time [16]. Besides that, specific structures or ligands can be conjugated to the surface of nanoparticles, allowing for both interaction with the biological environment as well as specific targeting to the intended site [17]. This will result in more targeted delivery with less dosage required to achieve the desired effect, thus reducing the risk of developing antibiotic resistance. This section will address some of the more recent developments in this area.

Vancomycin is a glycopeptide-class antibiotic and can be used against strains of bacteria that are resistant to beta-lactams. Several groups have suggested the delivery of vancomycin using nanoparticles to improve the efficiency and efficacy of drug administration. For instance, Chakraborty et al. loaded folic acid-tagged chitosan nanoparticles with vancomycin and utilized them as “Trojan horses” to deliver the vancomycin into bacteria [18]. The study results showed that the transport of vancomycin across epithelial surfaces and its drug action were improved by the nanoparticles, and that there is a strong bactericidal effect against vancomycin-resistant *S. aureus*.

N-methylthiolated β -lactams are a new form of antibiotics that has been proven to be effective against methicillin-resistant *S. aureus* (MRSA), as their mode of action is different from that of other beta-lactams. However, their use is limited by their low water solubility. To address this, Turos et al. incorporated the drug monomer into the polymeric matrix of a polyacrylate nanoparticle emulsion [19]. In vitro studies showed that the nanoparticles were nontoxic and were stabilized for 24 h in the blood serum.

More recently, another group has demonstrated the use of chitosan nanoparticles as a drug-unloading system attached to polycaprolactone (PCL) nanofiber mesh, incorporating both as a wound dressing [20]. They showed that the nanoparticles were able to infiltrate the wound site and could potentially provide continuous drug delivery without observable side effects. Another group also demonstrated the potential of Laponite, a clay mineral, as antibiotic-eluting (mafenide) nanoparticles to be used in wound dressings [21]. Laponite also releases Mg^{2+} ions, which can reduce the toxicity of mafenide. Studies such as the one by Alphonsa et al. [22] have also been undertaken to

evaluate the viability of nanoparticles as drug delivery systems. The group encapsulated ciprofloxacin and fluconazole in fibrin nanoparticles and showed that, in addition to the ability for sustained drug delivery, there was good antibacterial and antifungal activity. The *in vitro* toxicity of the nanoparticles was adequately viable, further supporting the future application of nanoparticles for such drug delivery purposes.

One recent discovery of interest is the use of curcumin with nanoparticles for wound-healing purposes. Curcumin (diferuloylmethane) is the active ingredient of turmeric, an Asian household spice that has been used in traditional remedies [23]. Besides antimicrobial activity [24], curcumin has been shown to demonstrate antineoplastic, antiinflammatory, and antioxidant activity as well as the ability to promote wound healing [25–27]. That being said, the use of curcumin is restricted by its limited oral bioavailability, low aqueous solubility, and rapid breakdown *in vivo* [28]. Recently, Krausz et al. published a paper on the use of curcumin encapsulated in nanoparticles as an antimicrobial and wound-healing agent [29]. The group incorporated curcumin into silane composite nanoparticles and subjected them to a variety of tests, including *in vitro* release, microbial activity, and cytotoxicity studies as well as *in vivo* murine burn model studies. The results showed that the curcumin nanoparticles exhibited significant antimicrobial effects, especially toward MRSA (by disrupting the cellular architecture of MRSA). The nanoparticles managed to reduce the bacterial burden in MRSA-infected burn wounds. In addition, the curcumin nanoparticles also showed enhanced wound-healing activity (Fig. 23.4) [29], with improved granulation tissue synthesis, collagen deposition, and angiogenesis.

Inherent Antimicrobial Properties of Metal Nanoparticles

Antimicrobial activity has been discovered in many metals, such as silver, titanium, copper, zinc, and manganese, when in nanoparticle form. Silver, in particular, has been widely researched for its use for antimicrobial purposes. Silver nanoparticles are some of the most popular and extensively studied areas in nanotechnology.

Metallic silver is inert and does not kill microorganisms until it has been ionized, which it readily does in aqueous media. First, reactive oxygen species (ROS) were thought to mediate the antibacterial activity of silver [30]. In 2005, Yamanaka et al. reported that silver ions are capable of interacting with ribosomes and subsequently interfering with the expression of enzymes and proteins that are essential to energy production [31]. It is also thought that silver ions are capable of binding to microbial deoxyribonucleic acid (DNA), disrupting the integrity of the DNA structure.

In addition, silver ions can also bind to cell walls and block microbial respiratory enzyme pathways [32]. More recently, it has been demonstrated that silver can bind to and inhibit the bacterial enzyme tryptophanase, and this leads to reduced biofilm growth [33,34]. It has also been shown that the antibacterial action of silver nanoparticles can be synergistic with streptomycin, kanamycin, and polymyxin B therapy [35]. Besides antimicrobial activity, *in vivo* studies have shown that silver nanoparticles can reduce inflammation by modulating inflammatory cytokines, leading to accelerated wound healing and less scarring [36]. Silver ions are also able to promote the proliferation of keratinocytes as well as improve wound contraction via stimulating the differentiation of fibroblasts into myofibroblasts [37].

While silver formulations such as silver sulfadiazine or silver nitrate have been utilized to treat wounds for quite some time, a variety of silver nanoparticle-containing wound dressings are being introduced to treat burns, skin ulcers, and other cutaneous wounds. For instance, the Acticoat range by Smith and Nephew consists of silver-based antimicrobial wound dressings. These are usually based on a scaffold that releases nanocrystalline silver over time. Other commercially available silver dressings include Silverlon, PolyMem Silver, and Aquacel Ag.

A meta-analysis of randomized controlled trials to compare the use of nanocrystalline silver with silver sulfadiazine or silver nitrate was performed by Gravante et al. [38]. With the primary outcome being the prevention of infection and the secondary outcomes being reduction of pain, hospitalization length, and costs, the authors showed that treatment with nanocrystalline silver was better than that with the older formulations. Not only was there a lower incidence of infection, but there was less pain as well (probably because its longer lasting action required fewer dressing changes). The costs were subsequently lower due to fewer dressing changes and shorter hospitalization.

Besides silver, other metals also show antimicrobial properties. For instance, titanium dioxide (TiO₂) nanoparticles were used to create a nano-titanium dioxide collagen artificial skin (NTCAS) by Peng et al. in 2008. After testing the NTCAS on wounded animals, they demonstrated that the NTCAS showed favorable antibacterial properties (attributed to the photocatalytic activity of TiO₂ nanoparticles) as well as accelerated healing [39]. Another study looked at green-synthesized TiO₂ nanoparticles and their wound-healing properties [40]. The group showed accelerated wound healing in Wistar Albino rats, including improved wound closure, collagen deposition, and wound contraction.

Copper is a metal known for its antimicrobial and antiinflammatory properties, despite there being less research into the use of copper nanoparticles compared

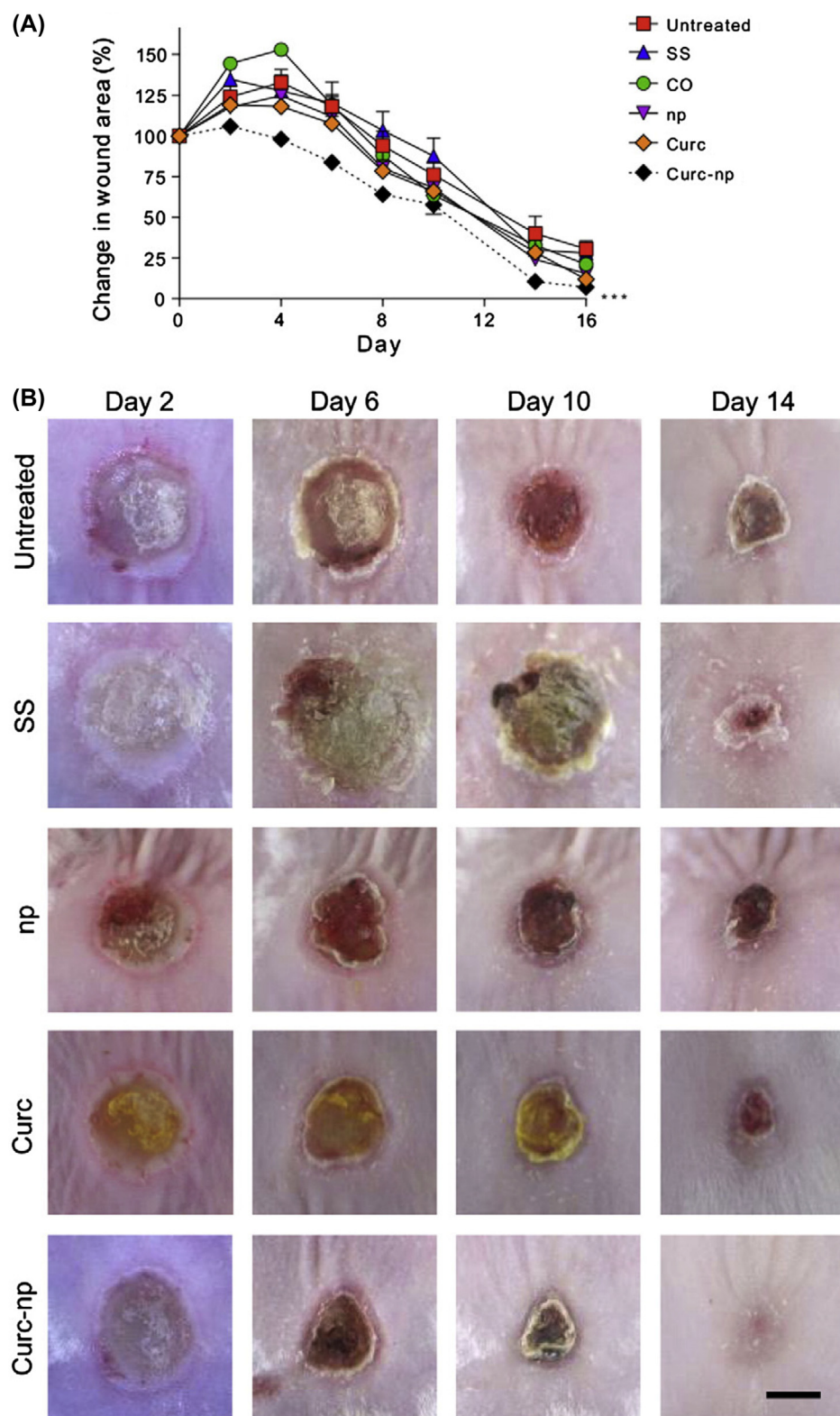


FIGURE 23.4 (A) Changes in a wound area over time. (B) Wound site of the murine burn wound model over 14 days. SS, silver sulfadiazine; CO, coconut oil control; Curc, curcumin; Curc-np, curcumin nanoparticles; np, nanoparticle controls. Reproduced with permission from Tiwari M, Narayanan K, Thakar MB, Jagani HV, Venkata Rao J. Biosynthesis and wound healing activity of copper nanoparticles. *IET Nanobiotechnol* 2014;8(4):230–7.

to silver. Tiwari et al. managed to biosynthesize copper nanoparticles using *Pseudomonas aeruginosa* [41]. The biosynthesized copper nanoparticles were found to be more effective against Gram-positive bacteria compared to Gram-negative bacteria. Antimicrobial activity was thought to be due to cytoplasmic leakage induced by rupturing cell walls. Wound excision models showed accelerated healing for copper nanoparticle-treated subjects compared to controls as well.

Another example of a metal with antibacterial properties is magnesium. It has been demonstrated that magnesium oxide nanoparticles have antibacterial properties [42]. Compared to other materials, magnesium is thought to be more stable and less toxic. At the same time, magnesium oxide nanoparticles can be synthesized from readily available precursors at a low cost.

STEMMING INFLAMMATION

Limiting excessive inflammation is important in wound healing. While there exist corticosteroids and nonsteroidal antiinflammatory drugs for this purpose, these drugs can have systemic side effects, as well as possibly counterproductive actions in terms of their inhibitory actions on fibroblasts and keratinocytes. Nanoparticles thus open up new possibilities of modulating the inflammation stage to accelerate wound healing with minimal side effects.

Norling et al. synthesized humanized nanoparticles using human neutrophil-derived microparticles [43]. Two different lipid mediators (thought to actively promote inflammation resolution), aspirin-triggered resolving D₁ and a lipoxin A₄ analog, were incorporated into the nanoparticles. In murine models, the nanoparticles showed antiinflammatory activity by inhibiting polymorphonuclear cell recruitment. Besides that, Kang et al. used liposomes to deliver celastrol, an antiinflammatory drug, to wound sites [44]. The liposomes were coated with Id-HA, a specific domain of lymphocyte function-associated antigen-1, which binds to intracellular adhesion molecule-1 (ICAM1). As such, the liposomes were capable of targeted delivery to ICAM1-expressing cells, namely the components of inflammation.

A novel approach to stemming inflammation in wound healing involved the use of small interfering ribonucleic acids (siRNAs). These short, double-stranded RNA molecules activate RNA-induced silencing complexes (RISCs) intrinsic to mammalian cells that then identify and subsequently cleave messenger RNA (mRNA). This provides gene-specific silencing that can then be used to mediate the expression of pro-inflammatory molecules during inflammation. Nelson et al. report using pH-responsive micelles,

known as smart polymer nanoparticles (SPNs), and a polyurethane-based synthetic scaffold to deliver siRNAs to skin wounds [45]. The results so far are promising, and there is potential for the group's approach to be translated into clinical applications in the future.

STIMULATING PROLIFERATION

In this section, we will look at how nanoparticles can be used to stimulate the proliferation phase. Numerous biological factors, mainly proteins, are involved in the healing process. This has spurred on efforts to improve wound healing by simulating the action of endogenous factors such as growth factors. The challenges faced in such an approach include difficulty in modifying the therapeutic agent such that it behaves like the endogenous substance in vivo. In addition, another major limitation of biomimicry is that the half-lives of most proteins involved in wound-healing cascades tend to be very short. This is because in the body, the cascades are kept under control by tightly regulating the synthesis and breakdown of their constituent components [1]. By using nanoparticles as a delivery system, effective release of such regenerative factors can be sustained at the wound site.

DELIVERY AND ELUTION OF BIOLOGICAL FACTORS

Polymeric nanoparticles are usually used as the delivery system of choice. The active biological factor can be encapsulated within the nanoparticle or adsorbed at the surface of the nanoparticle. Substance release is governed by diffusion and the degradation of the polymer matrix. Poly(lactic acid) (PLA) and poly(lactic-co-glycolic) acid (PLGA) are two examples of polymers that are biocompatible and biodegradable, thus making them suitable for this purpose.

Recombinant human epidermal growth factor (rhEGF) is a 53-amino-acid-long, single-chain polypeptide created to mimic the action of endogenous epidermal growth factor (EGF). It can stimulate the proliferation and differentiation of epithelial tissues, particularly the intestinal mucosa, corneal epithelial tissue, lung, and tracheal epithelia. However, due to its quick breakdown by enzymes and poor transport across the gastrointestinal membrane, a delivery system capable of sustained rhEGF release is necessary. Han et al. managed to encapsulate rhEGF in biodegradable PLA microspheres using a solvent-evaporation method [46]. In rat models, it was shown that the microspheres were capable of sustaining rhEGF release such that the

plasma concentration of rhEGF was maintained at a relatively high level over 11 days. In gastric ulcer-healing tests, it was also shown that the rhEGF-containing microspheres were effective for accelerating ulcer healing when the concentration was sufficient. In another study, Chu et al. prepared rhEGF nanoparticles using PLGA [47]. The group then tested their nanoparticles on diabetic rats with full-thickness wounds. The study showed that subjects treated with rhEGF nanoparticles exhibited the most fibroblast proliferation, along with the fastest healing rate. This was done compared to three other groups treated with rhEGF stock solution, empty nanoparticles, and phosphate-buffered saline, respectively. Seven days after administration of treatment, subjects treated with rhEGF nanoparticles showed around 68% wound healing compared to 60%, 67%, and 54% in subjects treated with saline, rhEGF stock solution, and empty nanoparticles, respectively. Hence, it seems reasonable to say that polymeric nanoparticle delivery greatly enhances the effects of rhEGF on wound healing.

A slightly different approach to delivering rhEGF is the use of lipid nanoparticles. Lipid nanoparticles can be solid lipid nanoparticles (SLNs) or nanostructured lipid carriers (NLCs). The main difference between SLNs and NLCs is that NLCs are prepared using liquid lipid, and this enhances the loading capacity of the nanoparticles as well as reduces content leakage [48,49]. After loading rhEGF into SLNs and NLCs, Gainza et al. subjected them to *in vivo* tests in addition to *in vivo* tests on full-thickness excisional wounds in diabetic mice [50]. The *in vitro* tests revealed that there was higher bioactivity in all cell lines studied for the nanoparticles compared to free rhEGF. The nanoparticles also enhanced wound healing in the murine wound models. The same group then went on to investigate the properties of rhEGF-loaded NLCs on porcine full-thickness excisional wound models [51]. The results confirmed that the rhEGF-NLCs contributed to skin regeneration, with enhanced microvasculature, fibroblast migration and proliferation, and collagen deposition as well as better inflammatory modulation.

FGF has been known to recruit and stimulate the growth of fibroblasts and endothelial cells. It can also enhance collagenase synthesis and stimulate angiogenesis [52,53]. However, again, due to its short half-life, methods of sustained delivery have to be developed. Kawai et al. managed to incorporate basic FGF into gelatin microspheres [54]. The gelatin was sourced from bovine bone. The microspheres were then tested on pressure-induced decubitus ulcer model diabetic mice. This was done by implanting an artificial dermis impregnated with the microspheres into the wound site. The results showed that the microspheres resulted in sustained release of FGF, leading to accelerated

healing with infection being cleared. Angiogenesis was also enhanced.

PDGF was the first growth factor to be approved by the US Food and Drug Administration for use in diabetic foot ulcers. It has been shown to enhance wound healing via stimulating granulation tissue formation. That being said, its rapid clearance by the circulation meant that high and repeated doses of PDGF were required. This again incited considerable interest in utilizing nanoparticles for the delivery of PDGF. Wei et al. had previously developed a biodegradable nanofibrous scaffold in which they then incorporated recombinant human PDGF-BB-containing microspheres [55]. *In vitro*, they managed to show controlled and sustained PDGF-BB release profiles. The molecular weight and composition of the PLGA microspheres can be modified to provide control over the release kinetics of their contents. The same did another study in 2008 [56], and it was shown that when implanted into midsagittal incisions of rats, PDGF-containing PLGA microspheres showed better angiogenesis and tissue infiltration compared to scaffolds simply coated with PDGF. Another recent interesting development came from Zavan et al. in 2009 [57]. The group incorporated PDGF in hyaluronan-based porous nanoparticles. Hyaluronic acid is a major component of the ECM and is known to be involved in the tissue repair process from the inflammatory stage right to granulation tissue formation and re-epithelialization. Thus, Zavan et al. managed to create nanoparticles in which both the growth factor and the nanocarrier have important roles in wound healing. As the release of PDGF in this case depended on the degradation rate of the polymeric matrix, and PDGF has a high affinity for the polymer, promoters were necessary to degrade the polymeric matrix for growth factor release. This provides another level of control over the release kinetics. *In vivo* tests showed that the nanoparticles simulated the re-epithelialization process, with improved ECM deposition and increased wound breaking strength.

A relatively new entry into this field is LL37, a host defense peptide of the innate immune system. Its inactive precursor has been detected in many different types of cells such as mast cells, neutrophils, macrophages, and natural killer cells, to name a few [58]. LL37 has multiple roles in immunomodulation, including antimicrobial activity, chemotaxis, modulation of the pro-inflammatory response, and cell differentiation and proliferation [59]. Like most of the molecules discussed earlier in this chapter, its half-life within the circulation is too short for effective direct administration. Chereddy et al. created LL37-containing PLGA nanoparticles and investigated their properties and wound-healing ability [60]. The results showed that wounded mice treated with PLGA-LL37 nanoparticles

TABLE 23.4 Developments in Recent Years of Biological Factor Delivery Systems

Biological Factor	Delivery System	Year
rhEGF [46]	PLA microspheres	2001
rhEGF [47]	PLGA nanoparticles	2010
rhEGF [50]	Lipid nanoparticles	2014
rhEGF [51]	Lipid nanoparticles	2015
FGF [54]	Gelatin microspheres	2005
PDGF [55]	PLGA nanospheres	2006
PDGF [57]	Hyaluronan-based porous nanoparticles	2009
LL37 [60]	PLGA nanoparticles	2014

rhEGF, recombinant human epidermal growth factor; FGF, fibroblast growth factor; PDGF, platelet-derived growth factor; PLA, poly(lactic acid); PLGA, poly(lactic-co-glycolic) acid.

exhibited enhanced dermal wound closure compared to the controls, with better re-epithelialization and formation of granulation tissue. PLGA-LL37 nanoparticles also enhanced angiogenesis and decreased myeloperoxidase activity, which can be used as an indicator of less inflammatory infiltration. This introduces the possibility of LL37 nanoparticles being used as a wound-healing agent, as long as sustained delivery is achieved.

Table 23.4 summarizes a few examples of delivery systems used to deliver biological factors that have been studied in recent years.

GENE THERAPY

For wound healing and skin regeneration, VEGF high-expressing stem cells have been developed to promote angiogenesis. That being said, there are limitations such as insufficient expression of angiogenic factors and low cell viability post transplantation. A group attempted to solve these problems by using nonviral, biodegradable polymeric nanoparticles to incorporate the human VEGF (hVEGF) gene into human mesenchymal stem cells (hMSCs) and human embryonic stem cell–derived cells (hESdCs) [61]. After treatment, the stem cells showed significantly improved hVEGF expression, cell viability, and target tissue engraftment. When transplanted into murine ischemic hind limbs, the treated stem cells exhibited enhanced angiogenesis and limb salvage, with reduced muscle degeneration and tissue fibrosis. More recently, polymeric nanoparticles have been used to modify adipose-derived stem cells such that they overexpress VEGF [62]. The treated stem cells subsequently improved angiogenesis in a murine hind limb ischemia model.

The concept of using nanoparticles to deliver genes into stem cells was also utilized in a recent study by Peng et al. [63]. The group used β -cyclodextrin-linked polyethylenimines to create nonviral gene delivery vectors. Together with a β -tricalcium phosphate (β -TCP)-incorporated gelatin scaffold, the VEGF165 gene was delivered into epidermal stem cells (ESCs). Topical application of the treated ESCs enhanced skin re-epithelialization, dermal collagen synthesis, hair follicle regeneration, and angiogenesis.

The expression of the sonic hedgehog (SHH) gene promotes tissue regeneration by stimulating angiogenic pathways. Park et al. utilized biodegradable cationic poly(β -amino esters) (PBAE) nanoparticles for intradermal delivery of the SHH gene in murine full-thickness wound models [64]. They used amine end-modified PBAEs, which have been shown to be more effective for intracellular DNA uptake [65]. Treated mice showed elevated expression of angiogenic growth factor, VEGF, and stromal cell–derived factor-1 α . Wound closure was subsequently enhanced, with improved angiogenesis and epidermal regeneration.

Another interesting development in this area is the use of microRNAs (miRNAs), which are involved in wound-healing processes such as inflammation, angiogenesis, cell differentiation, and migration. Li et al. showed that miR-Pirate378a (anti-miR-378a) transgenic mice had enhanced wound healing due to upregulation of vimentin and β 3 integrin [66]. There was improved fibroblast differentiation and migration as well as improved angiogenesis. Following on from that, they treated mice with gold nanoparticles conjugated with miR-Pirate378a. This was done via intradermal injections. Enhanced healing was seen, and thus the potential use of miRNAs to modulate wound healing can be pursued in the future.

MATURATION

Compared to inflammation and proliferation, less effort has focused on enhancing the maturation/remodeling stage. One of the causes of delayed healing can be excessive proteolytic activity. Thus, it seems reasonable for research efforts to focus on protease inhibitors. Norling et al., who were mentioned earlier in this chapter (see Stemming Inflammation), developed human-derived nanoparticles incorporated with protease inhibitors. In murine models, as polymorphonuclear cell influx decreases, the overall effect was pro-resolution as well.

Potential targets to be investigated during this stage include MMPs and specific tissue inhibitors of metalloproteinases (TIMPs). Remodeling involves a fine balance being struck between collagen breakdown and

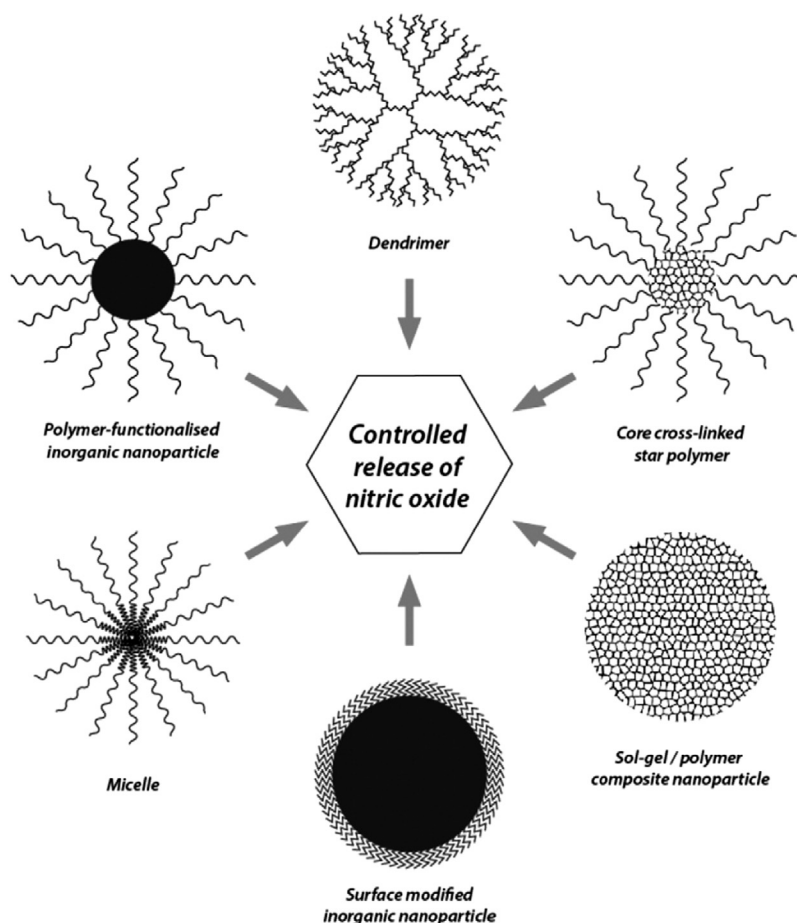


FIGURE 23.5 Different nanomaterial-based delivery platforms for NO.

production, and involves MMP action. MMP activity, in turn, is modulated by TIMPs. In the past, Chellat et al. utilized chitosan–DNA nanoparticles to modify the behavior of THP1 human macrophages. The results showed that the macrophages secreted less pro-inflammatory cytokines but more MMP9 after 24–48 h of incubation. Since MMP9 secretion is enhanced without eliciting an inflammatory response, the group proposed that chitosan–DNA nanoparticles can be a feasible way to modulate the remodeling stage.

NITRIC OXIDE

Nitric oxide (NO) is a gasotransmitter with important roles in intra- and extracellular signaling. Considering that NO is implicated in many body processes, it is thus unsurprising that it has been widely studied for its potential therapeutic applications. With regard to NO delivery, like many other therapeutic substances, important criteria to be considered include making the material easily applicable as well as making the period of delivery therapeutically relevant [67]. Nanomaterials

can potentially fulfill these criteria, and hence different methods of NO delivery involving nanomaterials have been studied (Fig. 23.5) [68].

In wound healing, NO is involved in all stages of the repair process, with roles in vasodilation, inhibiting platelet aggregation, angiogenesis, collagen formation, cell proliferation, and wound contraction. In addition, the antimicrobial properties of NO are also well-known. Different groups have thus investigated the possibility of using nanoparticles for controlled release of NO at wound sites.

Blecher et al. tested the wound-healing abilities of sol-gel-derived NO-releasing nanoparticles on murine models with 5 mm excision wounds [69]. The mice used were nonobese, diabetic, severe combined immunodeficiency mice. The NO nanoparticles were released in a sustained manner. Besides controls, the NO nanoparticle treatment was being compared to a topical NO-releasing platform, diethylenetriamine. The results of the study showed that out of all groups, the subjects treated with NO nanoparticles showed the fastest wound healing. Histologically, there was also less inflammation, more collagen deposition, and more angiogenesis. This

supported the use of NO nanoparticles for treating wounds, including in immunocompromised patients.

In another study, Han et al. utilized sol-gel particles created by Friedman et al. to study the efficacy of NO nanoparticles on wound healing [70]. In vitro, NO nanoparticles increased migration of human dermal fibroblasts. In addition, there was increased expression of type I and type III collagen. NO nanoparticles also managed to increase angiogenesis and decrease neutrophil migration at the wound site.

The antimicrobial properties of NO have been well documented. NO is thought to have three main pathways of antimicrobial activity [1,68]: direct DNA damage through the deamination of cytosine, guanine, and adenine by forming nitrosating intermediates and by radical-induced scission or modification of DNA strands [2]; inhibition of DNA repair enzymes by S-nitrosation of the -SH moiety of cytosine residues [3]; and facilitating lipid peroxidation via the formation of secondary species like peroxynitrite and nitrogen dioxide. Table 23.5 summarizes some of the developments in NO delivery using nanoparticles for antimicrobial purposes in recent years.

Hetrick et al. prepared NO-releasing silica nanoparticles by co-condensation of tetraalkoxysilane with aminoalkoxysilane modified with diazeniumdiolate NO donors [71]. The group then compared the antibacterial properties of the nanoparticles against *S. aureus* and *P. aeruginosa* with a small molecule NO donor. The NO-releasing silica nanoparticles were shown to be more effective at killing bacteria than the NO donor. At concentrations required for bactericidal activity, there was minimal cell toxicity when the nanoparticles were tested on L929 mouse fibroblasts.

Obviously, the nanoparticles can have different effectiveness against different kinds of bacteria as well. In a later study, Carpenter et al. synthesized quaternary ammonium (QA)-functionalized silica nanoparticles with and without NO-releasing capabilities and compared their bactericidal properties against *S. aureus* and *P. aeruginosa* [72]. The results showed that NO-releasing nanoparticles were more effective against the Gram-negative *P. aeruginosa*, while QA-functionalized nanoparticles had a greater effect against the Gram-positive *S. aureus*. Nanoparticles that are both NO-releasing and QA-functionalized showed increased efficacy against *S. aureus* but had the same level of effect against *P. aeruginosa* as only NO-release nanoparticles. It thus seems reasonable to suggest that, depending on the type of microorganism targeted, modifications to nanoparticles can have vastly different effects.

In addition, in nanoparticle geometry, dimensions have an effect on their bactericidal abilities as well. In one study, silica nanorods of different aspect ratios have been investigated for their antimicrobial properties

against *S. aureus* and *P. aeruginosa* [73]. It was shown then that higher aspect ratio nanorods were more effective at killing the bacteria.

Worley et al. recently investigated the use of quaternary ammonium-functionalized dendrimers with and without NO-releasing ability against *S. aureus* and *P. aeruginosa* [74]. Polyamidoamine dendrimers were modified with quaternary ammonium epoxides to produce dendrimers with both quaternary ammonium groups and secondary amine groups at the periphery. The different quaternary ammonium epoxides used resulted in ammonium moieties with either three methyl or two methyl and a butyl, octyl, or dodecyl substituent. The study showed that dendrimers with longer chained quaternary ammonium groups (octyl and dodecyl moieties) were more effective at killing the bacteria. That being said, NO-releasing capability made little difference to the antimicrobial activity of the longer chained functional dendrimers. In contrast, NO-releasing capability significantly increased the antibacterial properties of shorter chained functional dendrimers (methyl, and butyl moieties).

Biofilm formation is an emerging challenge for antimicrobial therapy as biofilms tend to show increased resistance to antibacterial agents [75]. The formation of a resistant ECM around the biofilm further reduces the effectiveness of antimicrobials. NO has been shown to induce biofilm dispersal in a wide range of microbes via a cyclic diguanosine monophosphate (cGMP) pathway. Multiple studies have demonstrated that NO-delivering nanoparticles are effective in inhibiting biofilm formation and/or eradicating biofilm. The nanoparticles investigated include star polymers [76], silica nanospheres and nanorods [77], as well as polyamidoamine dendrimers [78]. The study by Slomberg et al. demonstrated that nanoparticle shape and size had an effect on biofilm inhibition [77]. The group prepared different sized NO-releasing silica nanospheres as well as silica nanorods with different aspect ratios. With regard to particle size, the group showed that smaller particles (14 and 50 nm) were generally more effective against both *S. aureus* and *P. aeruginosa* biofilms. When it comes to shape, nanorods were generally more effective than spheres at delivering NO and eradicating biofilm, with higher aspect ratios resulting in better antibacterial activity.

The group that tested the properties of NO-releasing amphiphilic poly(amidoamine) dendrimers found that external functionalities had quite a significant impact on the efficacy and biocompatibility of the nanoparticles [78]. They found that while hydrophilic and amphiphilic externalities showed the most effective eradication of *P. aeruginosa* biofilm, the ratio of hydrophobic to hydrophilic externalities was best at 7:3 or 5:5 as they balanced efficacy with minimal toxicity.

TABLE 23.5 Recent Developments in Nanoparticle NO Delivery for Antimicrobial Purposes

Nanoparticles	Microbe(s) studied	Study context	Results	Year
NO-releasing silica nanoparticles [71]	<i>S. aureus</i> and <i>P. aeruginosa</i>	In vitro	Nanoparticles were better at killing bacteria than NO donors, with minimal cell toxicity.	2008
Silica nanorods functionalized with aminoalkoxysilanes and N-diazeniumdiolate NO donors [73]. NO release kinetics are controlled by modifying the particle surface	<i>S. aureus</i> and <i>P. aeruginosa</i>	In vitro	Bactericidal efficacy increases with increasing aspect ratio and initial NO flux.	2013
Quaternary ammonium (QA)-functionalized silica nanoparticles [72]	<i>S. aureus</i> and <i>P. aeruginosa</i>	In vitro	NO-releasing nanoparticles were more effective against <i>P. aeruginosa</i> , while QA-functionalized nanoparticles were better against <i>S. aureus</i> . NO-releasing QA-functionalized nanoparticles showed improved efficacy against <i>S. aureus</i> .	2012
QA-functionalized, NO-releasing dendrimers [74]	<i>S. aureus</i> and <i>P. aeruginosa</i>	In vitro	Longer chained functional dendrimers had better antimicrobial properties but with little difference made by NO-releasing capability. For shorter chain QA groups, increased NO-releasing capability significantly increased bactericidal properties.	2014
Core cross-linked star polymers [76]	<i>P. aeruginosa</i>	In vitro	Sustained delivery of NO and effective prevention of cell attachment and biofilm formation.	2014
NO-releasing silica nanospheres and nanorods [77]. Nanospheres have different sizes, while nanorods have different aspect ratios	<i>S. aureus</i> and <i>P. aeruginosa</i>	In vitro	Nanorods were better than nanospheres at NO delivery and biofilm inhibition. Smaller size and higher aspect ratio led to greater efficacy.	2013
NO-releasing amphiphilic poly(amidoamine) (PAMAM) dendrimers [78]	<i>P. aeruginosa</i>	In vitro	While there was bactericidal activity against <i>P. aeruginosa</i> biofilms, dendrimer size and external functionalities proved important in balancing efficacy with biocompatibility. A roughly equal ratio of hydrophilic and hydrophobic functionalities proved to be most effective at destroying biofilms without compromising murine fibroblast viability.	2013
Sol-gel derived NO-releasing nanoparticles in conjunction with glutathione [79]	<i>P. aeruginosa</i>	In vitro and in vivo	In vitro, NO nanoparticles inhibited <i>P. aeruginosa</i> growth for 8 h, while NO nanoparticles and glutathione inhibited growth for 24 h. In vivo, NO nanoparticles co-administered with glutathione accelerated wound closure in lymphocyte-deficient, nonobese, diabetic/severe combined immunodeficient mice.	2012
Sol-gel-based NO-releasing nanoparticles [80]	Methicillin-resistant <i>S. aureus</i> (MRSA)	In vivo	Elimination of both methicillin-resistant and methicillin-sensitive <i>S. aureus</i> . Improved wound healing with decreased inflammation, less collagen degradation, and more preservation of architecture.	2009

TABLE 23.5 Recent Developments in Nanoparticle NO Delivery for Antimicrobial Purposes—cont'd

Nanoparticles	Microbe(s) studied	Study context	Results	Year
Sol-gel-based NO-releasing nanoparticles [81]	MRSA	In vitro and in vivo	NO nanoparticles have antibacterial activity both in vitro and in vivo. Topical or intradermal administration of NO nanoparticles into abscesses enhanced resolution, reduced bacterial load, and improved skin architecture. There was reduced angiogenesis as well, preventing bacterial spread from the abscesses.	2009
Sol-gel-based NO-releasing nanoparticles [83]	<i>Candida albicans</i>	In vivo	Antifungal activity demonstrated in a murine burn model infected with <i>C. albicans</i> . An accelerated healing rate was observed. There was also modified leukocyte infiltration, reduced fungal burden, and reduced collagen degradation.	2012

When it comes to in vivo studies, Chouake et al. studied the action of NO-releasing nanoparticles on *P. aeruginosa* infection [79]. The group administered sol-gel-derived particles in conjunction with glutathione (for in situ S-nitrosoglutathione generation) into murine excisional wound models infected with *P. aeruginosa*. They found that wound closure was significantly accelerated with lower bacterial burden, then NO nanoparticles were coadministered with glutathione. Another group tested sol-gel-based NO-releasing nanoparticles on wounds infected with methicillin-resistant *S. aureus* (MRSA) [80]. Besides eliminating both MRSA and methicillin-sensitive *S. aureus*, nanoparticle application also accelerated wound healing in Balb/c mice, with less tissue damage, more dermal architecture preservation, as well as high collagen content. Han et al. also showed similar results when investigating the topical and intradermal application of sol-gel-based NO-releasing nanoparticles on MRSA-infected wounds [81]. Topical administration of the nanoparticles resulted in less inflammation, more fibrin deposition, and decreased bacterial load. Topical and intradermal administration of nanoparticles to MRSA-infected abscesses also helped to resolve them. These results showed that NO-releasing nanoparticles can potentially be a new generation of antimicrobial therapy against resistant microbes.

That being said, there is always the possibility that microbes can develop resistance to exogenous NO therapy as well. Privett et al. carried out spontaneous and serial passage mutagenesis assays with *S. aureus*, MRSA, *S. epidermis*, *E. coli*, and *P. aeruginosa* to investigate the development of resistance to nitrosated sol-gel particles [82]. No evidence of resistance development was seen, and the authors attributed this to NO exerting antimicrobial action via multiple pathways, thus

making resistance development too complex to be evident in a short study. However, the adaptability of bacteria should not be taken lightly, and there is always the possibility of resistant strains emerging.

Besides bacteria, NO-releasing nanoparticles can potentially be used as antifungals as well. Macherla et al. investigated sol-gel-based NO-releasing nanoparticles on murine burn injury models infected with *Candida albicans* [83]. In addition to inhibiting fungal proliferation, NO-releasing nanoparticles also accelerated the burn-healing process and prevented the further spread of the fungus. That being said, controls with non-NO-releasing nanoparticles showed some fungal inhibition as well, although not to the extent of that with NO-releasing nanoparticles.

All in all, there is substantial evidence to show that nanoparticle delivery can significantly improve the therapeutic potential and efficacy of NO, and this has tremendous implications for wound treatment in the future.

TOXICITY OF NANOPARTICLES

Like any other therapy under development, the toxic effects of nanoparticles, if any exist, have to be assessed. The maximum tolerated dose will have to be weighed against dose efficacy before any nanoparticle-based treatment can be deemed viable. Studies have been performed on the inherent toxicity of nanoparticles, especially metal nanoparticles, and it has been shown that there can be potentially harmful side effects if their use is not regulated appropriately.

As so much focus has been put on the development of silver nanoparticles, their toxicity has also been perhaps

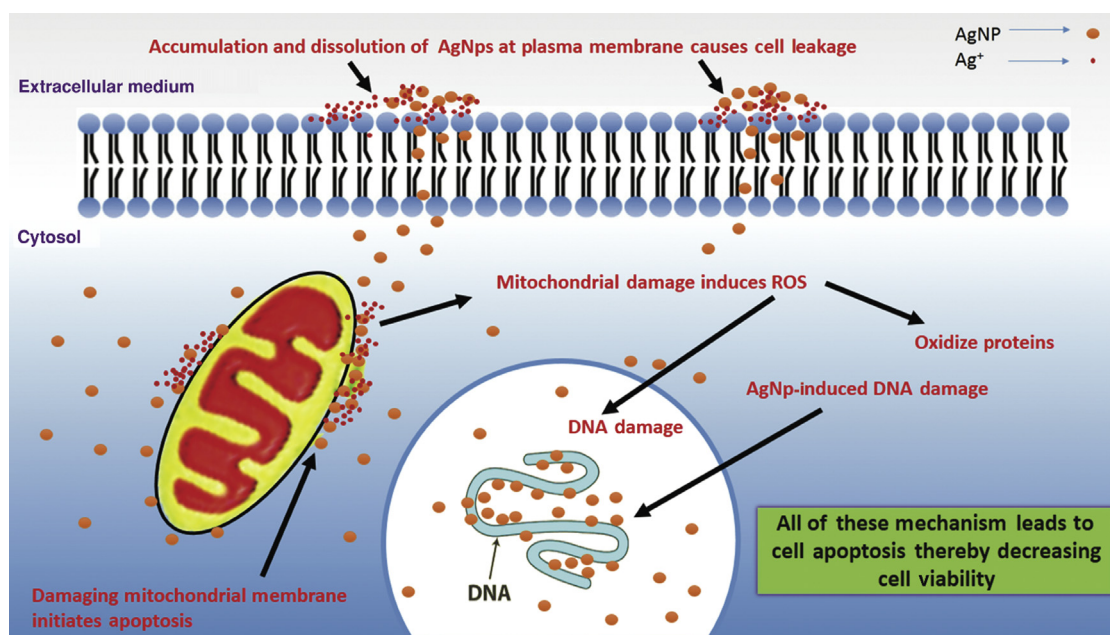


FIGURE 23.6 Toxicity of silver nanoparticles. AgNP, silver nanoparticles; DNA: deoxyribonucleic acid; ROS, reactive oxygen species. Reproduced with permission from Dos Santos CA, Seckler MM, Ingle AP, et al. *Silver nanoparticles: therapeutic uses, toxicity, and safety issues.* *J Pharm Sci* 2014; 103(7):1520–6017.

the most widely studied. A 28-day systemic toxicity study conducted by De Jong et al. showed that when administered intravenously into rats, 20–100-nm-sized silver nanoparticles accumulate in the spleen, liver, lymph nodes, and other organs [84]. Liver damage was suggested by increased levels of phosphatase, alanine transaminase, and aspartate transaminase. In another study by Bidgoli et al., the toxicity of nanosilver wound dressings was tested on murine models [85]. It was shown that there was minor hepatotoxicity at the end of the study. With the liver being arguably the most important metabolic organ in the body, it is unsurprising that, like most drugs, the most common finding in silver nanoparticle toxicology studies is liver damage when there is excessive accumulation [86]. Argyria, the discoloration of the skin or organs, may also be a potential cosmetic side effect of silver nanoparticles.

Dos Santos et al. have summarized the various mechanisms in which silver nanoparticles can compromise cell viability, and this is schematically shown in Fig. 23.6 [86]. Basically, the various mechanisms include triggering apoptosis, DNA damage, increasing mitochondrial membrane permeability, and the accumulation of ROS. It is thought that these mechanisms can occur independently or simultaneously [87]. Another theory regarding silver nanoparticle toxicity is related to the release of silver ions from the nanoparticles. The silver ions disrupt cell membrane integrity and can also affect respiratory chain enzymes, compromising mitochondrial function [88,89].

That being said, another review showed that when it comes to silver exposure from the use of silver-containing wound-healing products, systemic toxicity is rare and unlikely except in cases where there is prolonged and extensive use of said products, for instance in severe burn wounds covering large areas [90]. This is because the body has multiple mechanisms to dispose of silver even if it is systemically absorbed (Fig. 23.7) [90]. The authors concluded that when it comes to silver-containing wound dressings, the potential for toxicity is still relatively low.

Besides silver, the toxicity of other nanoparticles such as those made of titanium or copper has been studied, albeit to a lesser extent. A group has recently shown that TiO₂ nanoparticles may contribute to brain damage in mice [91]. The accumulation of TiO₂ nanoparticles in the brain can lead to oxidative stress, excessive proliferation of glial cells, tissue necrosis, and apoptosis of hippocampal cells. Gene expression is thought to be affected. With regard to copper, the uptake of copper oxide (CuO) nanoparticles by cultured astrocytes can lead to compromised cell viability as well [92].

It is known that the use of nanoparticles for targeted drug delivery means that the systemic toxicity of drugs can be reduced. That being said, we must also account for the inherent toxicity of the nanoparticles themselves when developing nanoparticle-based therapies. A balance must be struck when deciding appropriate nanoparticle dosage to allow for maximum effect with the least chance of side effects.

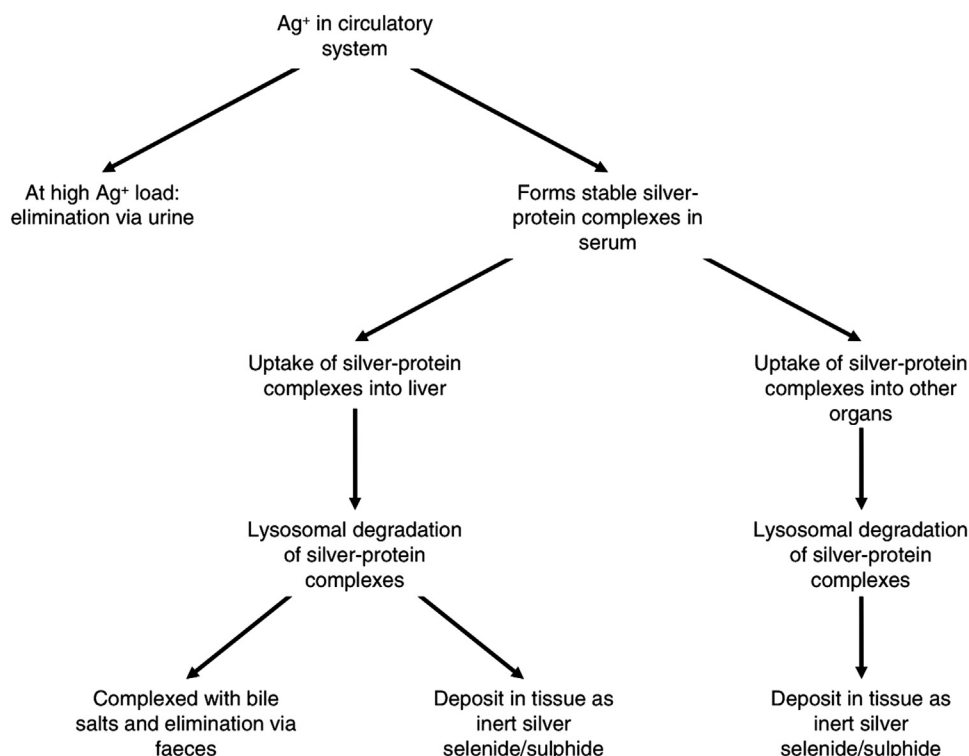


FIGURE 23.7 Possible pathways for the metabolism, detoxification, and elimination of silver ions after systemic absorption. *Reproduced with permission from Walker M, Parsons D. The biological fate of silver ions following the use of silver-containing wound care products e a review. Int Wound J 2014;11(5):496–504.*

WHAT NEXT?

To encapsulate things, the use of nanoparticle-based therapies is an exciting new field in wound treatment, with endless prospects and possibilities. Whether these therapies involve the delivery of substances or promote wound healing due to the inherent properties of the nanoparticles, there are promises of achieving greater efficacy and specificity, with fewer systemic side effects. In addition, compared to conventional antibiotics, nanoparticle-based antibacterial therapies may also be less likely to result in bacteria developing resistance. Current treatments that involve nanoparticles have also demonstrated successful track records. However, much is yet to be discovered regarding the effects of nanoparticles on the human body, and for this reason, the development of nanoparticle-based therapies should be undertaken with a reasonable amount of caution. Working to improving the efficacy of nanoparticle wound treatments should go hand-in-hand with investigating the long- and short-term effects of said treatments, as well as the mechanisms underlying them.

That being said, we are currently approaching what can be considered the golden age of nanotechnology, with research occurring at an exponential rate. With new ways of manipulating nanomaterials into

nanoparticles emerging rapidly, it seems reasonable to be optimistic about developing methods of synthesizing nanoparticles, whether in vitro or in situ, that can maximize efficacy without compromising the safety of the patient, the people administering the treatment, or the environment in general. Further development in this emerging field will definitely have a positive impact on the treatment of wounds, especially chronic wounds, which pose a significant burden on quality of life and the healthcare industry.

List of Acronyms and Abbreviations

CNT	Carbon nanotube
CuO	Copper oxide
DNA	Deoxyribonucleic acid
ECM	Extracellular matrix
ESC	Epidermal stem cell
FGF	Fibroblast growth factor
GMP	Guanosine monophosphate
hESdC	Human embryonic stem cell–derived cell
hMSC	Human mesenchymal stem cell
hVEGF	Human vascular endothelial growth factor
ICAM1	Intracellular adhesion molecule-1
LPN	Lipid–polymer hybrid nanoparticle
miRNA	Micro–ribonucleic acid
MMP	Matrix metalloproteinase
mRNA	Messenger ribonucleic acid

MRSA Methicillin-resistant *Staphylococcus aureus*
NLC Nanostructured lipid carrier
NO Nitric oxide
NTCAS Nano–titanium dioxide collagen artificial skin
PBAE Poly(β -amino esters)
PCL Polycaprolactone
PLA Poly(lactic acid)
PLGA Poly(lactic-co-glycolic)acid
PLN Platelet-like nanoparticle
QA Quaternary ammonium
rhEGF Recombinant human epidermal growth factor
RISC RNA-induced silencing complex
ROS Reactive oxygen species
SHH Sonic hedgehog
siRNA Small interfering ribonucleic acid
SLN Solid lipid nanoparticle
SPN Smart polymer nanoparticle
TGF- α Transforming growth factor- α
TGF- β Transforming growth factor β
TIMP Tissue inhibitor of metalloproteinase
TiO₂ Titanium dioxide
UV Ultraviolet
VEGF Vascular endothelial growth factor
vWF von Willebrand factor
 β -TCP β -Tricalcium phosphate
 γ -Fe₂O₃ Maghemite

References

- [1] Singer AJ, Clark RAF. Cutaneous wound healing. *New Engl J Med* 1999;341(10):738–46.
- [2] Boateng JS, Matthews KH, Stevens HN, Eccleston GM. Wound healing dressings and drug delivery systems: a review. *J Pharm Sci* 2008;97(8):2892–923.
- [3] Mayet N, Choonara YE, Kumar P, et al. A comprehensive review of advanced biopolymeric wound healing systems. *J Pharm Sci* 2014;103(8):2211–30.
- [4] Leong M, Phillips LG. Wound healing. In: Sabiston DC, Townsend CM, editors. *Sabiston textbook of surgery: the biological basis of modern surgical practice*. 19th ed. Philadelphia (PA): Elsevier Saunders; 2012. p. 151–77.
- [5] Stadelmann WK, Digenis AG, Tobin GR. Physiology and healing dynamics of chronic cutaneous wounds. *Am J Surg* 1998;176(2, Suppl. 1):26S–38S.
- [6] Hadinoto K, Sundaresan A, Cheow WS. Lipid-polymer hybrid nanoparticles as a new generation therapeutic delivery platform: a review. *Eur J Pharm Biopharm* 2013;85(3 Pt A):427–43.
- [7] Anselmo AC, Modery-Pawlowski CL, Menegatti S, et al. Platelet-like nanoparticles: mimicking shape, flexibility, and surface biology of platelets to target vascular injuries. *ACS nano* 2014; 8(11):11243–53.
- [8] Yoo JW, Irvine DJ, Discher DE, Mitragotri S. Bio-inspired, bio-engineered and biomimetic drug delivery carriers. *Nat Rev Drug Discov* 2011;10(7):521–35.
- [9] Coughlin SR. Thrombin signalling and protease-activated receptors. *Nature* 2000;407(6801):258–64.
- [10] Lundblad RL, Bradshaw RA, Gabriel D, Ortel TL, Lawson J, Mann KG. A review of the therapeutic uses of thrombin. *Thromb Haemost* 2004;91(5):851–60.
- [11] Jesty J. The kinetics of inhibition of alpha-thrombin in human plasma. *J Biol Chem* 1986;261(22):10313–8.
- [12] Ziv O, Lublin-Tennenbaum T, Margel S. Synthesis and characterization of thrombin conjugated γ -Fe₂O₃ magnetic nanoparticles for hemostasis. *Adv Eng Mater* 2009;11(12):B251–60.
- [13] Ziv-Polat O, Topaz M, Brosh T, Margel S. Enhancement of incisional wound healing by thrombin conjugated iron oxide nanoparticles. *Biomaterials* 2010;31(4):741–7.
- [14] Meddahi-Pellé A, Legrand A, Marcellan A, Louedec L, Letourneur D, Leibler L. Organ repair, hemostasis, and in vivo bonding of medical devices by aqueous solutions of nanoparticles. *Angew Chem Int Ed* 2014;53(25):6369–73.
- [15] Qadan M, Cheadle WG. Common microbial pathogens in surgical practice. *Surg Clin North Am* 2009;89(2):295–310. vii.
- [16] Maham A, Tang Z, Wu H, Wang J, Lin Y. Protein-based nanomedicine platforms for drug delivery. *Small (Weinheim an der Bergstrasse, Germany)* 2009;5(15):1706–21.
- [17] Christian P, Von der Kammer F, Baalousha M, Hofmann T. Nanoparticles: structure, properties, preparation and behaviour in environmental media. *Ecotoxicology (London, England)* 2008; 17(5):326–43.
- [18] Chakraborty SP, Sahu SK, Mahapatra SK, et al. Nanoconjugated vancomycin: new opportunities for the development of anti-VRSA agents. *Nanotechnology* 2010;21(10):105103.
- [19] Turos E, Shim J-Y, Wang Y, et al. Antibiotic-conjugated polyacrylate nanoparticles: new opportunities for development of anti-MRSA agents. *Bioorg Med Chem Lett* 2007;17(1):53–6.
- [20] Jung SM, Yoon GH, Lee HC, Shin HS. Chitosan nanoparticle/PCL nanofiber composite for wound dressing and drug delivery. *J Biomater Sci Polym Ed* 2015;26(4):252–63.
- [21] Ghadiri M, Chrzanowski W, Rohanizadeh R. Antibiotic eluting clay mineral (Laponite(R)) for wound healing application: an in vitro study. *J Mater Sci Mater Med* 2014;25(11):2513–26.
- [22] Alphonsa BM, Sudheesh Kumar PT, Praveen G, Biswas R, Chennazhi KP, Jayakumar R. Antimicrobial drugs encapsulated in fibrin nanoparticles for treating microbial infested wounds. *Pharm Res* 2014;31(5):1338–51.
- [23] Nguyen TA, Friedman AJ. Curcumin: a novel treatment for skin-related disorders. *J Drugs Dermatol* 2013;12(10):1131–7.
- [24] Gunes H, Gulen D, Mutlu R, Gumus A, Tas T, Topkaya AE. Antibacterial effects of curcumin: an in vitro minimum inhibitory concentration study. *Toxicol Ind Health* 2013;32(2).
- [25] Anand P, Sundaram C, Jhurani S, Kunnumakkara AB, Aggarwal BB. Curcumin and cancer: an “old-age” disease with an “age-old” solution. *Cancer Lett* 2008;267(1):133–64.
- [26] Sandur SK, Ichikawa H, Pandey MK, et al. Role of pro-oxidants and antioxidants in the anti-inflammatory and apoptotic effects of curcumin (diferuloylmethane). *Free Radic Biol Med* 2007; 43(4):568–80.
- [27] Kulac M, Aktas C, Tulubas F, et al. The effects of topical treatment with curcumin on burn wound healing in rats. *J Mol Histol* 2013; 44(1):83–90.
- [28] Flora G, Gupta D, Tiwari A. Nanocurcumin: a promising therapeutic advancement over native curcumin. *Crit Rev Ther Drug Carrier Syst* 2013;30(4):331–68.
- [29] Krausz AE, Adler BL, Cabral V, et al. Curcumin-encapsulated nanoparticles as innovative antimicrobial and wound healing agent. *Nanomedicine* 2015;11(1):195–206.
- [30] Le Pape H, Solano-Serena F, Contini P, Devillers C, Maftah A, Leprat P. Involvement of reactive oxygen species in the bactericidal activity of activated carbon fibre supporting silver; Bactericidal activity of ACF(Ag) mediated by ROS. *J Inorg Biochem* 2004;98(6):1054–60.
- [31] Yamanaka M, Hara K, Kudo J. Bactericidal actions of a silver ion solution on *Escherichia coli*, studied by energy-filtering transmission electron microscopy and proteomic analysis. *Appl Environ Microbiol* 2005;71(11):7589–93.
- [32] Castellano JJ, Shafii SM, Ko F, et al. Comparative evaluation of silver-containing antimicrobial dressings and drugs. *Int Wound J* 2007;4(2):114–22.

- [33] Scherzer R, Gdalevsky GY, Goldgur Y, Cohen-Luria R, Bittner S, Parola AH. New tryptophanase inhibitors: towards prevention of bacterial biofilm formation. *J Enzyme Inhib Med Chem* 2009; 24(2):350–5.
- [34] Wigginton NS, de Titta A, Piccapietra F, et al. Binding of silver nanoparticles to bacterial proteins depends on surface modifications and inhibits enzymatic activity. *Environ Sci Technol* 2010; 44(6):2163–8.
- [35] Jain J, Arora S, Rajwade JM, Omray P, Khandelwal S, Paknikar KM. Silver nanoparticles in therapeutics: development of an antimicrobial gel formulation for topical use. *Mol Pharma* 2009;6(5):1388–401.
- [36] Widgerow AD. Nanocrystalline silver, gelatinases and the clinical implications. *Burns* 2010;36(7):965–74.
- [37] Liu X, Lee P-y, Ho C-m, et al. Silver nanoparticles mediate differential responses in keratinocytes and fibroblasts during skin wound healing. *ChemMedChem* 2010;5(3):468–75.
- [38] Gravante G, Caruso R, Sorge R, Nicoli F, Gentile P, Cervelli V. Nanocrystalline silver: a systematic review of randomized trials conducted on burned patients and an evidence-based assessment of potential advantages over older silver formulations. *Ann Plast Surg* 2009;63(2):201–5.
- [39] Peng CC, Yang MH, Chiu WT, et al. Composite nano-titanium oxide-chitosan artificial skin exhibits strong wound-healing effect—an approach with anti-inflammatory and bactericidal kinetics. *Macromol Biosci* 2008;8(4):316–27.
- [40] Sankar R, Dhivya R, Shivashangari KS, Ravikumar V. Wound healing activity of *Origanum vulgare* engineered titanium dioxide nanoparticles in wistar albino rats. *J Mater Sci Mater Med* 2014; 25(7):1701–8.
- [41] Tiwari M, Narayanan K, Thakar MB, Jagani HV, Venkata Rao J. Biosynthesis and wound healing activity of copper nanoparticles. *IET Nanobiotechnol* 2014;8(4):230–7.
- [42] Tang Z-X, Lv B-F. MgO nanoparticles as antibacterial agent: preparation and activity. *Braz J Chem Eng* 2014;31:591–601.
- [43] Norling LV, Spite M, Yang R, Flower RJ, Perretti M, Serhan CN. Cutting edge: humanized nano-proresolving medicines mimic inflammation-resolution and enhance wound healing. *J Immunol* (Baltimore, Md: 1950) 2011;186(10):5543–7.
- [44] Kang S, Park T, Chen X, et al. Tunable physiologic interactions of adhesion molecules for inflamed cell-selective drug delivery. *Biomaterials* 2011;32(13):3487–98.
- [45] Nelson CE, Gupta MK, Adolph EJ, Guelcher SA, Duvall CL. siRNA delivery from an injectable scaffold for wound therapy. *Adv Wound Care* 2013;2(3):93–9.
- [46] Han K, Lee K-D, Gao Z-G, Park J-S. Preparation and evaluation of poly(l-lactic acid) microspheres containing rhEGF for chronic gastric ulcer healing. *J Control Release* 2001;75(3):259–69.
- [47] Chu Y, Yu D, Wang P, Xu J, Li D, Ding M. Nanotechnology promotes the full-thickness diabetic wound healing effect of recombinant human epidermal growth factor in diabetic rats. *Wound Repair Regen* 2010;18(5):499–505.
- [48] Muller RH, Radtke M, Wissing SA. Solid lipid nanoparticles (SLN) and nanostructured lipid carriers (NLC) in cosmetic and dermatological preparations. *Adv Drug Deliv Rev* 2002;54(Suppl. 1):S131–55.
- [49] Souto EB, Wissing SA, Barbosa CM, Muller RH. Development of a controlled release formulation based on SLN and NLC for topical clotrimazole delivery. *Int J Pharm* 2004;278(1):71–7.
- [50] Gainza G, Pastor M, Aguirre JJ, et al. A novel strategy for the treatment of chronic wounds based on the topical administration of rhEGF-loaded lipid nanoparticles: in vitro bioactivity and in vivo effectiveness in healing-impaired db/db mice. *J Control Release* 2014;185:51–61.
- [51] Gainza G, Bonafonte DC, Moreno B, et al. The topical administration of rhEGF-loaded nanostructured lipid carriers (rhEGF-NLC) improves healing in a porcine full-thickness excisional wound model. *J Control Release* 2015;197:41–7.
- [52] Gospodarowicz D, Neufeld G, Schweigerer L. Molecular and biological characterization of fibroblast growth factor, an angiogenic factor which also controls the proliferation and differentiation of mesoderm and neuroectoderm derived cells. *Cell Differ* 1986; 19(1):1–17.
- [53] Bikfalvi A, Savona C, Perollet C, Javerzat S. New insights in the biology of fibroblast growth factor-2. *Angiogenesis* 1998;1(2): 155–73.
- [54] Kawai K, Suzuki S, Tabata Y, Nishimura Y. Accelerated wound healing through the incorporation of basic fibroblast growth factor-impregnated gelatin microspheres into artificial dermis using a pressure-induced decubitus ulcer model in genetically diabetic mice. *Br J Plast Surg* 2005;58(8):1115–23.
- [55] Wei G, Jin Q, Giannobile WV, Ma PX. Nano-fibrous scaffold for controlled delivery of recombinant human PDGF-BB. *J Control Release* 2006;112(1):103–10.
- [56] Jin Q, Wei G, Lin Z, et al. Nanofibrous scaffolds incorporating PDGF-BB microspheres induce chemokine expression and tissue neogenesis in vivo. *PLoS One* 2008;3(3):e1729.
- [57] Zavan B, Vindigni V, Vezzù K, et al. Hyaluronan based porous nano-particles enriched with growth factors for the treatment of ulcers: a placebo-controlled study. *J Mater Sci Mater Med* 2009; 20(1):235–47.
- [58] Vandamme D, Landuyt B, Luyten W, Schoofs L. A comprehensive summary of LL-37, the lactotum human cathelicidin peptide. *Cell Immunol* 2012;280(1):22–35.
- [59] Steinstraesser L, Koehler T, Jacobsen F, et al. Host defense peptides in wound healing. *Mol Med (Cambridge, Mass)* 2008; 14(7–8):528–37.
- [60] Cherreddy KK, Her CH, Comune M, et al. PLGA nanoparticles loaded with host defense peptide LL37 promote wound healing. *J Control Release* 2014;194:138–47.
- [61] Yang F, Cho S-W, Son SM, et al. Genetic engineering of human stem cells for enhanced angiogenesis using biodegradable polymeric nanoparticles. *Proc Natl Acad Sci* 2010;107(8):3317–22.
- [62] Keeney M, Deveza L, Yang F. Programming stem cells for therapeutic angiogenesis using biodegradable polymeric nanoparticles. *J Vis Exp* 2013;79:e50736.
- [63] Peng LH, Wei W, Qi XT, et al. Epidermal stem cells manipulated by pDNA-VEGF165/CYD-PEI nanoparticles loaded gelatin/beta-TCP matrix as a therapeutic agent and gene delivery vehicle for wound healing. *Mol Pharm* 2013;10(8):3090–102.
- [64] Park HJ, Lee J, Kim MJ, et al. Sonic hedgehog intradermal gene therapy using a biodegradable poly(beta-amino esters) nanoparticle to enhance wound healing. *Biomaterials* 2012;33(35):9148–56.
- [65] Sunshine J, Green JJ, Mahon KP, et al. Small molecule end group of linear polymer determines cell-type gene delivery efficacy. *Adv Mater (Deerfield Beach, Fla)* 2009;21(48):4947–51.
- [66] Li H, Chang L, Du WW, et al. Anti-microRNA-378a enhances wound healing process by upregulating integrin beta-3 and vimentin. *Mol Ther* 2014;22(10):1839–50.
- [67] Friedman AJ, Han G, Navati MS, et al. Sustained release nitric oxide releasing nanoparticles: characterization of a novel delivery platform based on nitrite containing hydrogel/glass composites. *Nitric Oxide* 2008;19(1):12–20.
- [68] Quinn JE, Whittaker MR, Davis TP. Delivering nitric oxide with nanoparticles. *J Control Release* 2015;(0).
- [69] Blecher K, Martinez LR, Tuckman-Vernon C, et al. Nitric oxide-releasing nanoparticles accelerate wound healing in NOD-SCID mice. *Nanomedicine* 2012;8(8):1364–71.
- [70] Han G, Nguyen LN, Macherla C, et al. Nitric oxide-releasing nanoparticles accelerate wound healing by promoting fibroblast migration and collagen deposition. *Am J Pathol* 2012;180(4): 1465–73.

- [71] Hetrick EM, Shin JH, Stasko NA, et al. Bactericidal efficacy of nitric oxide-releasing silica nanoparticles. *ACS Nano* 2008;2(2): 235–46.
- [72] Carpenter AW, Worley BV, Slomberg DL, Schoenfisch MH. Dual action antimicrobials: nitric oxide release from quaternary ammonium-functionalized silica nanoparticles. *Biomacromolecules* 2012;13(10):3334–42.
- [73] Lu Y, Slomberg DL, Sun B, Schoenfisch MH. Shape- and nitric oxide flux-dependent bactericidal activity of nitric oxide-releasing silica nanorods. *Small* (Weinheim an der Bergstrasse, Germany) 2013;9(12):2189–98.
- [74] Worley BV, Slomberg DL, Schoenfisch MH. Nitric oxide-releasing quaternary ammonium-modified poly(amidoamine) dendrimers as dual action antibacterial agents. *Bioconjug Chem* 2014;25(5): 918–27.
- [75] Costerton JW, Stewart PS, Greenberg EP. Bacterial biofilms: a common cause of persistent infections. *Science* (New York, NY) 1999; 284(5418):1318–22.
- [76] Duong HT, Jung K, Kutty SK, et al. Nanoparticle (star polymer) delivery of nitric oxide effectively negates *Pseudomonas aeruginosa* biofilm formation. *Biomacromolecules* 2014;15(7):2583–9.
- [77] Slomberg DL, Lu Y, Broadnax AD, Hunter RA, Carpenter AW, Schoenfisch MH. Role of size and shape on biofilm eradication for nitric oxide-releasing silica nanoparticles. *ACS Appl Mater Inter* 2013;5(19):9322–9.
- [78] Lu Y, Slomberg DL, Shah A, Schoenfisch MH. Nitric oxide-releasing amphiphilic poly(amidoamine) (PAMAM) dendrimers as antibacterial agents. *Biomacromolecules* 2013;14(10):3589–98.
- [79] Chouake J, Schairer D, Kutner A, et al. Nitrosoglutathione generating nitric oxide nanoparticles as an improved strategy for combating *Pseudomonas aeruginosa*-infected wounds. *J Drugs Dermatol* 2012;11(12):1471–7.
- [80] Martinez LR, Han G, Chacko M, et al. Antimicrobial and healing efficacy of sustained release nitric oxide nanoparticles against *Staphylococcus aureus* skin infection. *J Invest Dermatol* 2009; 129(10):2463–9.
- [81] Han G, Martinez LR, Mihi MR, Friedman AJ, Friedman JM, Nosanchuk JD. Nitric oxide releasing nanoparticles are therapeutic for *Staphylococcus aureus* abscesses in a murine model of infection. *PLoS One* 2009;4(11):e7804.
- [82] Privett BJ, Broadnax AD, Bauman SJ, Riccio DA, Schoenfisch MH. Examination of bacterial resistance to exogenous nitric oxide. *Nitric oxide* 2012;26(3):169–73.
- [83] Macherla C, Sanchez DA, Ahmadi MS, et al. Nitric oxide releasing nanoparticles for treatment of *Candida albicans* burn infections. *Front Microbiol* 2012;3:193.
- [84] De Jong WH, Van Der Ven LTM, Sleijffers A, et al. Systemic and immunotoxicity of silver nanoparticles in an intravenous 28 days repeated dose toxicity study in rats. *Biomaterials* 2013; 34(33):8333–43.
- [85] Bidgoli SA, Mahdavi M, Rezayat SM, Korani M, Amani A, Ziarati P. Toxicity assessment of nanosilver wound dressing in Wistar rat. *Acta Med Iranica* 2013;51(4):203–8.
- [86] Dos Santos CA, Seckler MM, Ingle AP, et al. Silver nanoparticles: therapeutical uses, toxicity, and safety issues. *J Pharm Sci* 2014; 103(7):1931–44.
- [87] Gupta I, Duran N, Rai M. Nano-silver toxicity: emerging concerns and consequences in human health. In: Cioffi N, Rai M, editors. *Nano-antimicrobials*. Springer Berlin Heidelberg; 2012. p. 525–48.
- [88] Morones JR, Elechiguerra JL, Camacho A, et al. The bactericidal effect of silver nanoparticles. *Nanotechnology* 2005;16(10): 2346–53.
- [89] Park S, Lee YK, Jung M, et al. Cellular toxicity of various inhalable metal nanoparticles on human alveolar epithelial cells. *Inhal Toxicol* 2007;19(Suppl. 1):59–65.
- [90] Walker M, Parsons D. The biological fate of silver ions following the use of silver-containing wound care products – a review. *Int Wound J* 2014;11(5):496–504.
- [91] Ze Y, Hu R, Wang X, et al. Neurotoxicity and gene-expressed profile in brain-injured mice caused by exposure to titanium dioxide nanoparticles. *J Biomed Mater Res Part A* 2014;102(2): 470–8.
- [92] Bulcke F, Thiel K, Dringen R. Uptake and toxicity of copper oxide nanoparticles in cultured primary brain astrocytes. *Nanotoxicology* 2014;8(7):775–85.

Quantum Dot Migration Through Natural Barriers and Distribution in the Skin

R. Rotomskis

Vilnius University, Vilnius, Lithuania

OUTLINE

Introduction	307	<i>Intracellular Localization in the Dermis</i>	315
Skin as a Barrier	308	<i>QD Migration Pathways in the Tissues and Localization in Other Tissue Structures</i>	315
Quantum Dots	309	Conclusion	318
<i>Distribution in the Skin of Topically Applied QDs</i>	310	References	319
<i>QD Distribution and Accumulation at the Epidermal–Dermal Junction</i>	312		
<i>Importance of the Transappendageal Pathway in QD Delivery</i>	313		

INTRODUCTION

One of the fastest growing scientific fields is that of discovery and application of various materials at the nanoscale. This growth in nanotechnology has translated into an explosion in the amount and variety of nanoparticles (NPs) that are used every day in a wide variety of scientific disciplines and consumer products. Expectations of the benefits of nanotechnology are positive and have spread through all academic sectors of medicine, the wider scientific community, and industry in a general way [1]. The public could come in contact with nanomaterials intentionally after applying topical cosmetic preparations containing NPs, or unintentionally through the handling of products used in daily life containing NPs [2,3]. NPs are used in applications ranging from targeted fluorescent labels in the life sciences [4], ultraviolet radiation (UVR)-protective cosmetics [5], and bacterial inhibitors [6,7] in food storage containers to wound care products and baby pacifiers. Concurrent with this growth, however, there are increasing environmental and human health concerns [8–11].

The application of nanoparticles in dermatology and cosmetology represents an emerging field and is closely connected with the question of risk assessment, as the potential for, and consequences of, the penetration of such particles into living human tissue has not been determined conclusively. In the medical sector, extensive research activities are in progress to develop nanoparticles, which can be used as efficient carriers for drug delivery through the skin barrier. In contrast, in cosmetic products, particles are mostly required to remain on the skin surface to fulfill their beneficial effect [1,12]. In recent years, the number of products containing nanosized material has increased, because NPs exhibit unique size-dependent physical and chemical properties that can be advantageous in delivery of drugs to the skin [11]. NPs can be composed of lipids, sugars, degradable or nondegradable polymers, metals, and organic or inorganic compounds.

Nanocarriers can translocate intact into the skin without being degraded, or else they can be degraded at or near the skin surface, and the incorporated therapeutic molecule that is released can penetrate the skin layers. The

interaction of NPs with the skin depends on the physico-chemical properties of the NPs, such as size, surface charge, properties of nanomaterial used, drug-loading efficiency, lamellarity, and mode of application.

NPs have several advantages over chemical penetration enhancers, such as a sustained drug release for a prolonged period of time and better protection of encapsulated materials from chemical degradation. For optimum topical delivery of drugs into the skin, it is essential that the carrier releases the encapsulated drug, which can be further absorbed through the skin layers and through subcutaneous structures that are involved in the disease [11,13].

The question of whether or not NPs can penetrate the healthy skin barrier in vivo remains largely unanswered. Some studies suggest that TiO₂ NPs suspended in a cosmetic-type emulsion do not penetrate the stratum corneum (SC) of the skin when applied ex vivo to porcine skin [14] and in vivo to human skin [15–17]. However, other researchers have examined the question of skin penetration by employing different types of NPs (oxides, metals, and polymers) and using ex vivo skin models, and again contrasting results suggesting both high and low levels of NP penetration have been reported [18–21]. These inconsistencies may relate to differences in the core size or shape of the NPs [22] and in addition highlight the need for standardization of experimental techniques if ex vivo skin models are used.

Of particular concern are UVR-protective cosmetics and sunscreens. Therefore, there is a big need to examine changes in skin permeability to NP penetration following exposure to activating UVR or when the SC is compromised by physical or chemical assaults.

Among inorganic NPs, the extent of skin penetration of TiO₂ and ZnO NPs has been investigated intensively by several research groups [24] because of their high value to the pharmaceutical industry; these NPs are frequently employed as inorganic physical sun blockers [2]. Consumer products often contain significant amounts of ZnO and TiO₂ NPs, and they are marketed for use on a daily basis. Sunscreen products with a high SPF (sun protection factor) are often applied on a repeated basis to skin that has suffered sun exposure sufficient enough to have initiated the biological UVR-induced skin repair processes. These processes are known to weaken the inside-out skin barrier function as measured by transepidermal water loss, which is believed to result from a disorganization of the intercellular lipid lamellae [25].

Given the growing commercial and scientific interest in these NPs, their safety and effectiveness as well as their regulatory status have been repeatedly reviewed in literature [2,26,27]. Naturally, we are exposed to sunlight and, in combination with the explosion in the amount of NPs that are used every day in a wide variety

of scientific disciplines and consumer products, it is possible the combination could be dangerous for our lives. Therefore, it is important to ascertain the potential effect of UVR exposure on the skin barrier function with respect to NP penetration, and examine changes in skin permeability to NP penetration following exposure to activating UVR or when the SC is compromised by physical or chemical assault.

SKIN AS A BARRIER

The skin is a protective barrier against external mechanical, chemical, microbial, and physical assaults. Because of skin's large surface area and easy accessibility, skin delivery also has potential application in drug delivery. Skin delivery is mainly focused on topical delivery to treat local skin conditions or transdermal drug delivery, which involves the delivery of drugs through skin layers into the systemic circulation. The global term *percutaneous/dermal absorption* describes the passage of compounds across the skin. The process is divided into three steps: *penetration*, the entry of substance into a particular skin layer; *permeation*, the penetration through one layer into another; and, finally, *resorption*, the uptake into the vascular system [28]. Following topical application of NP-containing formulations, absorption of active compounds can follow *transcellular* (intracellular), *intercellular*, or *transappendageal* (follicular) pathways [28]. Topical or transdermal delivery offers several advantages over the conventional oral and intravenous dosage forms, such as prevention of first-pass metabolism, minimization of pain, and possible controlled release of drugs [29].

Skin is a unique barrier composed of several highly organized and heterogeneous layers, and it includes a number of appendages such as hair follicles, and sweat and sebaceous glands. Physiologically, skin is composed of three layers [28]:

Epidermis: Composed of SC is a 10–20 µm thick membrane consisting of dead cells (corneocytes) embedded in a lipid matrix as a hydrophobic layer and the viable epidermis, being a living hydrophilic layer.

Dermis: A hydrophilic layer irrigated by the blood circulation and composed of a gel in which a densely network of fibers (collagen and elastin) provides mechanical strength to skin. Any substrate reaching dermis can pass into the systemic circulation.

Hypodermis: The hypodermis (subcutaneous connective tissue) is made of fatty tissues (adipocytes).

Epidermis is an epithelium divided into two distinct parts: the SC, a hydrophobic layer (13% water) made

from dead cells resulting in horny texture, and the viable epidermis (70% water). Dead cells (corneocytes) embedded in a lipid matrix are bound together by corneodesmosomes. The layered structure of skin is continuously renewed and provides efficient protection against the penetration of foreign substances—especially SC. The SC is the outermost layer of the skin and is composed of a 10–15 μm thick matrix of dehydrated and dead keratinocytes that are embedded in highly ordered lipid layers, which serve as a cover [30]. The SC is the foremost barrier that protects our body from the entry of external materials into the skin. The viable epidermis is approximately 100–150 μm thick and composed of multiple layers of keratinocytes and several other types of cells. The structure of SC may be presented as a bricks-and-mortar wall. The “bricks” are made of cornified dead cells filled with keratin and are embedded in the mortar composed of multiple stacks of lipid lamellae. A hydrophilic substance cannot penetrate the skin easily because it cannot enter the hydrophobic SC layer. A hydrophobic substance easily enters the SC, but it remains localized inside it since the next layer is hydrophilic [28].

The dermis contains a network of blood capillaries, lymphatic vessels, and nerve endings. The subcutaneous tissue or hypodermis resides below the dermis and is composed of loose-textured, white, fibrous connective tissue in which fat and elastic fibers are intermingled [31]. In addition to three main layers, several pilosebaceous units and sweat glands are dispersed throughout the skin. However, from a penetration perspective, only epidermis and dermis are important, along with the outermost layer of epidermis (SC), to which the main barrier function of the skin is attributed [32,33].

The NPs can enter the skin through three distinct pathways: (1) the intercellular pathway, which is through the lipid matrix occupying the intercellular spaces of the keratinocytes; (2) the transcellular pathway, which is through the keratinocytes; and (3) the transappendageal pathway, which is across hair follicles, sebaceous glands, and sweat glands [34,35]. The intercellular pathway through the intercellular lipids predominates over the intracellular one [28,36]. Hydrophobic drugs or NPs obviously penetrate skin by the intercellular route. Hydrophilic molecules prefer to pass the SC by the intracellular pathway through the corneocytes. However, it is necessary for penetrating molecules to cross the intercellular lipids in order to jump from one corneocyte to another. Penetration must therefore be a partially intercellular pathway, and this route may be rate determining. The diffusion of NPs through the skin may also occur through defects in the skin structure. The hair shaft and sweat glands, which constitute breaks in the continuity of the SC,

can create an additional path, thus providing a follicular pathway.

Earlier reported studies demonstrated that skin appendages are not a major penetration pathway, as these cover only 0.1% of the skin surface area, and therefore permeation in the skin has been mainly assumed to be through the lipid matrix of the SC [38]. In contrast, recent investigations have demonstrated that the transappendageal route is in fact an efficient penetration pathway and acts as a reservoir for topically applied substances [34,38]. Therefore, besides diffusional pathways, the transappendageal route appears to be one of the important pathways in skin permeation.

The excellent biological barrier, the skin, has been addressed in several recent studies regarding NP penetration [1,11,24,39,40].

QUANTUM DOTS

Semiconductor nanocrystals, or quantum dots (QDs), have great potential for use as diagnostic and imaging agents in biomedicine and as semiconductors in industrial applications. Due to their quantum confinement effects, QD NPs have unique optical and electronic properties; specifically, they emit strong and photostable fluorescence and are suitable for biomedical imaging. QDs are excellent fluorophores with a narrow-sized tunable emission spectral band quantum yield, are photostable, and exist in a nonaggregated state in commercially available aqueous suspensions. Unlike other engineered nanostructures, QDs are easily detected because of their unusually intense and photostable fluorescence.

QDs are commercially available as heterogeneous NPs in various sizes and shapes that consist of a colloidal core surrounded by one or more surface coatings. Surface coatings are frequently applied to customize QDs for specific applications, such as the use of hydrophilic coatings to increase solubility in a biologically compatible medium; coatings (or “shells”) that reduce leaching of metals from the core [41]; and reactive surface groups that facilitate conjugation to therapeutic and diagnostic macromolecules, such as receptor ligands, or antibodies [42]. The surface modifications [e.g., a CdSe core with a ZnS shell and a polyethylene glycol (PEG) coating that has been surface modified with carboxyl groups (COOH) or amine groups (NH₂)], however, may contribute to toxicological effects. These organic coatings overcame the problem of hydrophobic QD aggregation in water and partly in physiological solutions, by way of electrostatic repulsion due to the surface charge in the cases of QD-NH₂ and QD-COOH, and in the case of QD-PEG by rendering the NPs more hydrophilic, in combination with steric

hindrance. Thus, QDs are readily accessible tools by which the nanotoxicologist can determine the permeability of skin to engineered nanostructures with differing physicochemical properties, the results of which are of both practical and heuristic importance.

QDs' interaction with skin [22,23,39,43,45–49] is also of primary interest, as the occurrence of QDs in the life sciences and other technical applications is rising [9] and has consequently increased the risk of skin exposure to QDs that may affect manufacturers, researchers, and consumers. Their initial study investigated commercially available QDs with two core–shell sizes and shapes with three different surface coatings (QD-NH₂, QD-COOH, and QD-PEG), to determine if QDs could penetrate intact skin in a size- and coating-dependent manner [22]. To study these effects of size and coating of QDs on skin penetration, Ryman-Rasmussen and co-workers [22] used two core–shell sizes and shapes (spherical and ellipsoid) of QDs with three types of surface coatings: neutral (QD-PEG), anionic (QD-NH₂), and cationic (QD-COOH). Spherical shaped 4.6 nm core–shell diameter QDs with neutral and anionic coatings penetrated only up to the epidermal layers, while cationic charged spherical QDs were localized in the dermis within 8 h. In contrast, neutral and cationic charged ellipsoid-shaped 12 nm (major axis) by 6 nm core–shell diameter QDs penetrated the skin within 8 h, but the anionic charged ellipsoid QDs needed 24 h to show penetration. This study demonstrates that exposure of intact skin to QDs results in penetration throughout the epidermis and deep into the dermis in some cases. Chu and coauthors demonstrated that CdTe QDs were able to penetrate through mouse skin, and may further migrate into the heart, liver, spleen, lung, kidney, and brain under normal animal temperature conditions [43].

In a more recent follow-up study, contrasting results were reported: minimal penetration of CdSe/CdS–PEG coated water-soluble QDs (hydrodynamic radius 39–40 nm) through ex vivo porcine skin was found, with the bulk of the QDs remaining in the SC [23]. Zhang and coworkers [23] showed that nail-shaped, PEG-coated QDs with a diameter less than 40 nm can penetrate the uppermost layers of SC lipids (intercellular space) and outer root sheath of hair follicles. In addition, substantial QD penetration, after rat skin was abraded and treated with QDs, was shown [44]. However, penetration into the viable epidermis was minimal in skin that had been tape-stripped. QDs skin penetration and toxicity depend on physicochemical properties like size, shape, chemical structure of the core–shell and surface coating, charge, and pH of the applied vehicle.

The data presented by Prow et al. [45] reinforced observations by Monteiro-Riviere et al. [50] showing that QDs generally do not penetrate through intact human SC into the viable epidermis; however, PEG-coated QDs can penetrate the viable epidermis when

applied in the manufacturer's solution at pH 8.3. For intact human skin mounted in static penetration cells, negligible QD-COOH or QD-PEG-NH₂ fluorescence was detectable deep in the SC [45]. Perturbations of the SC, such as tape stripping, can lead to QDs' penetration into the viable epidermis [45]. Importantly, negligible penetration of QDs was seen in mature pig skin that is consistent with the lack of penetration of larger NPs reported by others in mature pig skin [51,52]. There is some evidence that NPs smaller than 10 nm do penetrate human skin [19,53].

QD penetration depends on specific conditions [22,44,46,50,54,55]. Viewed together, these observations suggest that larger NPs such as QDs and ZnO have minimal penetration into human skin, but penetration can occur into tape-stripped human skin. Importantly, the major problem with this body of work is the emphasis on using multiple different animal models with a varied range of experimental conditions, including the manufacturer-supplied QD buffer solutions used by Ref. [22].

At the present time, it is important to determine if QDs can penetrate healthy and/or barrier-compromised skin as potential toxicological consequences may result if QDs are taken up by epidermal skin cells and/or translocated to secondary sites. When the SC is severely compromised, QD penetration occurs into the viable epidermis and dermis. Occupational exposure to workers who suffer from skin defects or a compromised skin barrier due to wounds, scrapes, or diseased skin is likely to lead to increased NP penetration into the injured skin area.

Collectively, current literature points to the understanding that QD penetration through healthy intact skin is very low. However, such penetration will increase when the physical barrier of the skin is compromised. Nonetheless, there remains a significant knowledge gap, and confusion remains concerning the topic. Areas for future research still include the relationship between QDs' properties and property for skin penetration; the potential influence of gender, skin age, and body site on QD penetration; the recognition and correlations between the physical, biological, and immunological skin barriers; the penetration pathways and distribution of QDs within the skin and in the body; and clearance of the QDs from the lower layers of the skin by diffusion and/or via the blood and lymphatic system of the organism.

Distribution in the Skin of Topically Applied QDs

Topically applied QDs have been widely investigated by several groups [22,44,46,48,52,54,55] and were found to have accumulated in the SC; no penetration to deeper layers of epidermis was detected. QD permeability through the skin was investigated by topical application

of aqueous QD solution onto shaved mouse skin. One hour after incubation, mouse skin was prepared for microscopy analysis. QDs preferentially were collected in the upper layers of the SC (Fig. 24.1). The results showed that QDs accumulate in SC and are prevented from passing to the deeper layers of the epidermis (Fig. 24.1). QD penetration deep to the hair follicles was partially limited, and the QDs' red fluorescence in the hair follicles showed no transfollicular migration of QDs into deeper structures of the skin.

These data support earlier findings that QDs are prevented from passage to the viable epidermis due to the barrier properties of SC. The QDs' retention in the superficial layer of epidermis is primarily caused by the dense cellular network, which is tightly interconnected with lipids and proteins, which all together create a highly impermeable barrier for various exogenous compounds [37]. As mentioned earlier in this chapter, epidermis is an epithelium divided into two distinct parts: a hydrophobic layer (13% water) made from dead cells resulting in horny texture, the SC; and the hydrophilic layer (70% water), which is viable epidermis. Water-soluble hydrophilic QDs cannot

penetrate the outer skin layer easily because they cannot enter the hydrophobic SC layer.

Therefore, the CdSe/ZnS QDs that are coated with methoxy-polyethylene glycol (mPEG), abbreviated CdSe/ZnS-mPEG (Qtracker-655, $\lambda_{PL} = 655 \pm 5$ nm, nonfunctionalized; Invitrogen), and the CdTe QDs that are coated with mercaptopropionic acid, abbreviated CdTe-MPA ($\lambda_{PL} = 630 \pm 5$ nm, PlasmaChem GmbH), are stopped inside of the SC (Fig. 24.1).

QDs can penetrate the skin by getting through the SC intracellular lipid lamellae along the edges of differentiated corneocytes [54] or via the intracellular penetration pathway [56,57]; however, it is possible to conclude that alternations in hydrophobicity and hydrophilicity inside the SC create the properties of the first barrier (Fig. 24.1) for QD penetration through the skin. Amphiphilic coating of the QDs could help them easier penetrate the first barrier in the SC layer of the skin.

The results of the topically applied QD penetration through the skin has been widely discussed in recent papers [39,40,44,47,50,54]. Mortensen and Gratiery with coworkers showed that SC of the healthy skin protects deeper skin structures from QD exposure [39,54].

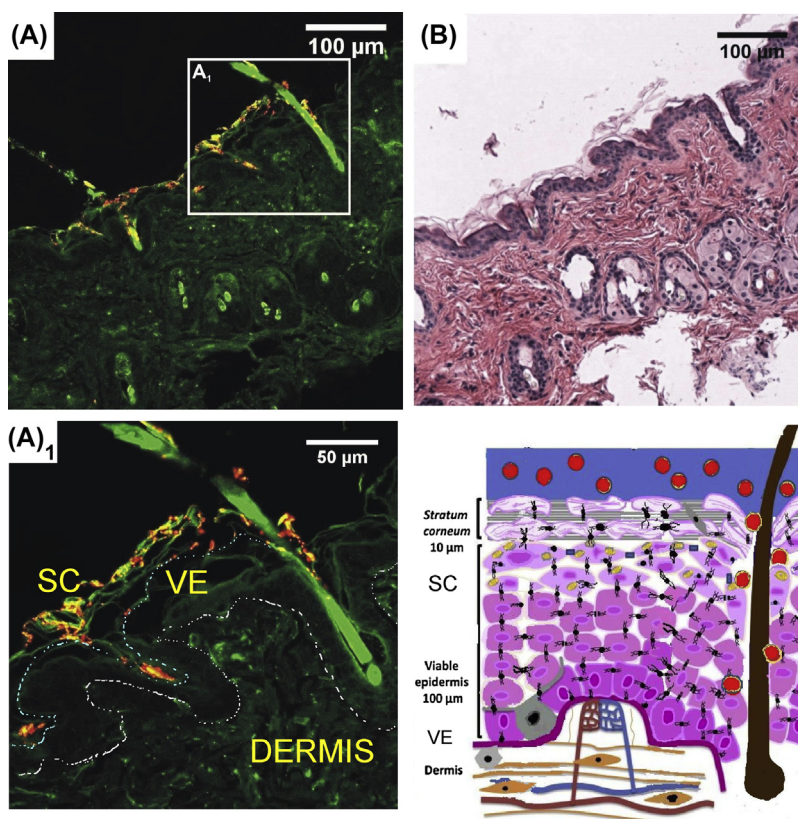


FIGURE 24.1 Confocal fluorescence microscopy (A,A₁: unstained) and bright-field microscopy (B: HE stain) images of mice skin slices 2 h after topical application of CdSe–ZnS-mPEG QD 0.4 µM solution in vivo on shaved mice skin. Red and yellow colors represent the QDs' (A,A₁) distribution in the superficial layers of the stratum corneum, but not in the deeper layers of viable epidermis or dermis. Green color reflects the autofluorescence of the tissue structure. Dotted lines indicate the borders of viable epidermis with stratum corneum and with dermis.

On the other hand, Chu and coworkers detected the penetration of mercaptopropionic acid-coated QDs through mouse skin *in vivo* and *in vitro*, and it displayed QD emission in the underlying muscle [43]. However, the detailed localization of the QDs was not presented. QDs coated with PEG (which is known to increase the hydrodynamic diameter of the QDs and is an important factor in QD penetration through biobarriers [22,58]) were used in our experiments; therefore, the PEG coating could determine different QD permeability from that reported by Chu et al. [43].

It was also shown that NPs of different types, particularly gold NPs, are able to cross the skin barrier, and that the transfer efficacy depended on size as well as the polarity and hydrophilicity of the NPs surface [59,60].

In summary, it can be concluded that skin permeability for NPs depends on the type and physicochemical properties of NPs (size, shape, surface coating, etc.) as well as on the experimental model used; therefore, each type of NP should be investigated

independently in order to assess the potential beneficial or harmful effects of their applications. Taking this data into account, in general, the potential applications of QDs to act as carriers delivering drugs into intact skin might be limited, and are probably only of interest for partially damaged skin [39].

QD Distribution and Accumulation at the Epidermal–Dermal Junction

Fig. 24.2 depicts the patterns of QD distribution in mouse skin after subcutaneous injection. The epidermis and hair follicles exhibited no fluorescence in the range of 600–690 nm, which was used for the QD detection when excited at $\lambda_{\text{ex}} = 488$ nm. The nonhomogeneously distributed red fluorescence was detected in the dermis, in the hypodermis, and between the underlying muscle fibers 1 h after the subcutaneous injection of the QDs (Fig. 24.2A). The QDs' accumulation pattern after 24 h did not significantly differ from the samples taken after

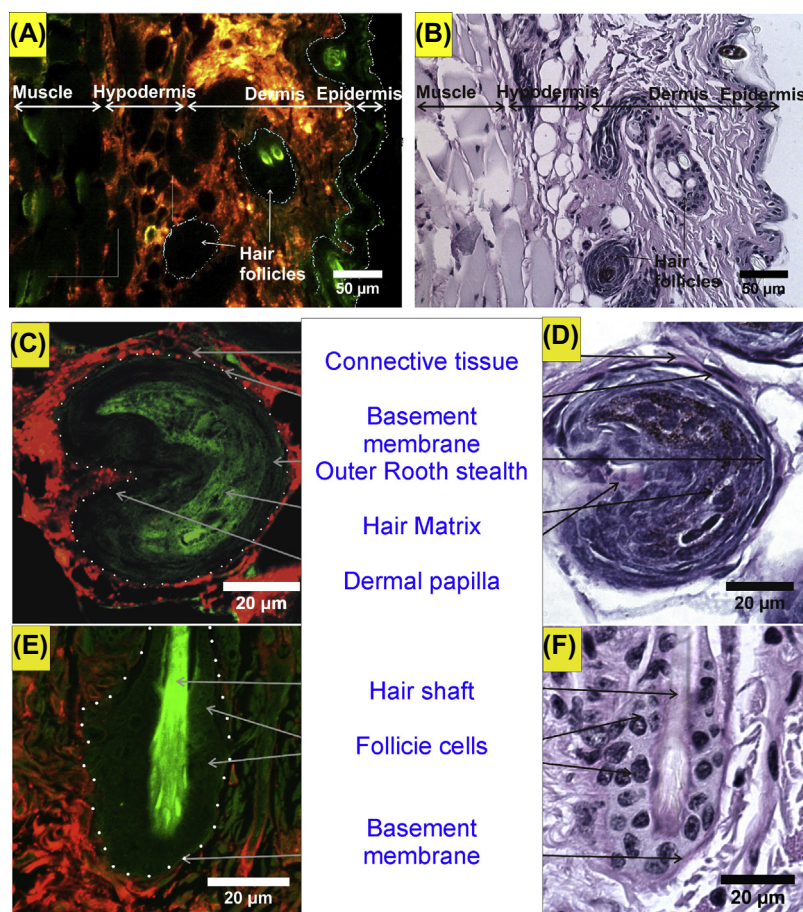


FIGURE 24.2 Confocal fluorescence microscopy (A,C,E: unstained) and bright-field microscopy (B,D,F: PAS stain) images of mice skin (A,B), a longitudinal section of the hair bulb (C,D), and hair follicle (E,F) 24 h after subcutaneous injection of 0.2 mL 0.4 μM CdSe–ZnS–mPEG QD solution. The QD (red/yellow) are distributed in the connective tissue, but high QD fluorescence contrast at the dermal–epidermal junction indicates that QDs are sequestered by the BM from passing to the hair follicle. Dotted lines indicate the border between the epidermis and dermis.

1 h. Subcutaneously injected QDs were distributed widely in the dermis and hypodermis, and penetrated between the underlying muscle fibers. QDs migrate freely within the loose connective tissue of the dermis. Demonstration of high QD accumulation along the epidermal–dermal junction basement membrane (BM) without passing to the epidermis and no permeability to the dermal–epidermal junction after subcutaneous injection was presented [48]. Meanwhile, after topical application of QDs, red fluorescence of the accumulated QDs was detected on the upper layer of the SC without any deep penetration to the viable epidermal or dermal layers (Fig. 24.1). It is an interesting observation because in most studies the barrier properties of the skin are attributed to the SC [19,61].

The role of the BM in the overall skin permeability to NPs has not been widely discussed in the literature. Baroli and coworkers [19] investigated metallic NP penetration through human skin *ex vivo* and showed that NPs mainly accumulated in the SC with little penetration to the viable epidermal layers, particularly to the stratum granulosum. However, the authors did not observe NP permeation to the dermis [19]. Kuhler and coworkers investigated the penetration of fluorescently labeled solid lipid NPs and dendrimeric core–multishell NPs, and they observed the concentration decrease from the SC toward the deeper skin layers for both NP types [10]. Fullerenes were applied to human skin biopsies, and they permeated the epidermis but could not penetrate the BM [8].

The main proposed mechanisms of drug delivery through the skin are the intracellular diffusion of hydrophobic particles through cellular membranes and the transcellular penetration of hydrophilic NPs [19,47]. The presented experimental data show that QDs are impermeable to the dermal–epidermal junction after subcutaneous injection. Unlike cellular epidermis, the BM barrier arises from densely packed protein layers [7], and there are no specific carriers, lipid membranes, or transcellular spaces that are characteristic to the epidermis. In this way, the BM acts as a passive filter to exclude NPs, and it determines the high BM resistance for NP transport in both directions: epidermal–dermal [8,19,47] and dermal–epidermal, as indicated in the study [48]. The NP transport across the BM should depend on the physicochemical properties of the NPs, as the penetration through other biological barriers was shown to be sensitive to the size, surface charge, hydrophilicity, and biofunctionalization of NPs [6,20].

NP retention by the BM might be used for evaluating the integrity of the epidermal–dermal junction. Bennett and coworkers applied ferritin NPs for magnetic resonance imaging of the BM in the kidney [62]. The cationic NPs were observed accumulated in the BM of the glomerules and in the filtration slits between the podocytes.

The NPs penetrated only through the fenestrations that are characteristic of glomerular capillaries. The BM of the epidermis lacks these fenestrations, and it is integral, but some mechanical or radiation damage might disintegrate the BM structure and alter its barrier capacity for the NPs. Therefore, NPs could be used to assess the integrity and physiological state of the BM.

After subcutaneous injection, QDs are homogeneously distributed in the dermis, indicating that the loose network of dermal fibers allows QD diffusion within this tissue (Fig. 24.2). It can be seen that the QD pattern resembles the arrangement of collagen fibers, indicating that the fibers are continuously covered with QDs. It shows that QDs interact with the biomolecules of the extracellular matrix. The detailed analysis of the samples using confocal microscopy revealed that QDs were abundantly accumulated along the epidermal–dermal junction, without crossing this border. The QDs were prevented from gaining access to the epidermis (Fig. 24.2A). In this way, the epidermal–dermal junction creates a protective layer to prevent QD penetration to the epidermis.

Importance of the Transappendageal Pathway in QD Delivery

As many compounds are impermeable to the SC, much attention has been paid to the use of the pilosebaceous unit as an alternative drug delivery pathway [40,63,64]. The hair follicles extend deep into the skin, and the thickness of the SC layer is progressively reduced going deeper into the follicle. The lower part of the hair infundibulum has only a weak barrier as the corneocytes are smaller and crumbly, which increases the permeability for drugs [35]. Moreover, there is also a rich capillary blood supply available in the follicle to distribute absorbed substances systemically.

One of the main features of QDs in dermatological application is their tendency to penetrate and accumulate deep in the SC close to hair follicles (Fig. 24.1). However, the role of hair follicles in the penetration process is often neglected based on the fact that the total area of the orifices of hair follicles occupies only approximately 0.1% of the total skin surface area [38]. In contrast, NPs can increase the penetration of encapsulated drug through hair follicles [38]. Furthermore, it was calculated that the storage time of particle-based drug delivery systems in the hair follicles was 10 days compared to only a short-term storage time in the SC. The rigid hair shaft acts as a geared pump because of the zigzag structure of the cuticular layers along the hair shaft, and it moves particles deeper into hair follicles. The hair follicle acts as a long-term reservoir for QDs because of relatively slow depletion of stored QDs by penetration into

deeper tissue layers, or by slow secretion with sebum production [35,63].

The optimization of drug delivery to and via the hair follicles is gaining more and more importance as it has been recognized that the hair follicles are an interesting target site for topical applications. Follicles are closely surrounded by capillaries and antigen-presenting cells, are associated with sebaceous glands, and contain the niche of stem cells in the bulge region of the hair follicle. It has been demonstrated that the penetration depth of the particles can be influenced by their size, resulting in the possibility of a differential targeting of specific follicular structures. The follicular penetration mechanisms and storage properties of particles are discussed in reviews [34,39].

Topically applied substances can permeate faster with higher concentrations in skin containing hair follicles as compared to skin with hair follicle blockage [65]. The interfollicular epidermis and epithelium of acroinfundibulum form a tight barrier, but the corneocytes in the lower follicular tract are incomplete as the corneocytes in this area are small and not completely differentiated [66]. Therefore, particles carrying the drug can provide an increased drug penetration into the viable epidermis. The particles penetrate down to different depths depending on their size. Only 40 nm NPs, but not 750 or 1500 nm NPs, can deliver vaccine compounds transcutaneously into the skin to reach human antigen-presenting cells [67]. Fluorescence microscopy and laser scanning microscopy showed that transcutaneously applied 40 nm NPs can penetrate through follicular pathway into the perifollicular dermis, and can therefore cross through the meshwork of follicular openings. Targeting several sites in the hair follicle such as the opening of the sebaceous gland or the bulge region can be achieved by taking advantage of size-dependent mechanisms of NP transport [20]. Not all hair follicles contain NPs when they are topically applied as some hair follicles remain closed while others remain open [38].

Fig. 24.2C–F represents the longitudinal section of a hair follicle. QDs are found in the dermis around the hair follicle, but they are prevented from penetrating the outer root sheath cells or deeper hair follicle layers (Fig. 24.2C and E). There was also no QD accumulation in the sebaceous glands [48]. High QD fluorescence contrast was observed in the dermal papilla compared to the hair bulb cells (Fig. 24.2C–F). This means that QD transport to the hair matrix from the dermal papilla is limited or even completely prevented. PAS staining, which is used for the imaging of the BM [7], showed that QDs do not cross the BM barrier in the hair bulb, indicating that this structure is highly impermeable to PEG-coated QDs (Fig. 24.2C and E).

QD diffusion in the tissues is limited by certain extracellular structures that prevent QDs from passing to the

epidermis, hair follicles, nerves, blood vessel walls, and sebaceous and sweat glands [48]. The hair follicles extend deep into the skin, and, as mentioned, the thickness of the SC layer is progressively reduced when going deeper into the follicle. Figs. 24.1 and 24.2 shows that QDs accumulate abundantly along the dermal–follicle junction, but they do not penetrate across this barrier. QDs are prevented from passing to the hair bulb even in the anagen phase of the hair cycle (characterized by the presence of dermal papilla) (Fig. 24.2C), when the cells grow most rapidly and internalize extracellular substances most efficiently. The fact that even highly proliferating cells of the hair bulb do not internalize QDs indicates that QD transport from the dermis to the hair matrix is strongly limited or even completely prevented. It confirms the significance of the BM as the preventive structure for NP migration and may explain the low efficiency of transfollicular transport of NPs reported by others. Lademan and coworkers investigated the follicular penetration of polymeric NPs (size 320 nm) and showed that NPs penetrate deeply into the hair follicles, providing long-term deposition in the epidermis [63]. NPs accumulated along the epidermal–dermal junction. However, the NP penetration from the follicle to the dermis was not discussed. Similar results were presented in a recent study, where drug-loaded polymeric NPs (size 30–96 nm) penetrated deeply into the hair follicle, but they were sequestered from passing to the dermis [68]. Vogt and colleagues have shown that transcutaneously applied 40 nm NPs penetrated the skin predominantly via the follicular route and possibly into the perifollicular dermis, by entering the meshwork of Langerhans cells, which are particularly concentrated in the upper parts of human hair follicles [67]. However, intercellular migration to the dermis was not observed. These reports show that NPs are impermeable to the follicular–dermal junction after topical application. Our results complement these studies as we showed QD retention by the dermal–follicular junction from the dermal compartment (Fig. 24.2). The limited transfollicular transfer of QDs may be explained by attributing the QD barrier properties to the BM.

Limited transfollicular QD penetration can be advantageous for drug delivery as QDs provide rapidly penetrating carriers that can effectively penetrate the hair canal and create a drug depot without passing to other tissues of the body. Whereas the intercellular penetration of particles seems to be unlikely, the hair follicle has been shown to be a relevant penetration pathway for particles as well as an important long-term reservoir.

Through careful analysis of the discussed literature and presented data, it could be concluded that nondamaged healthy skin in normal conditions is impermeable to QDs.

Intracellular Localization in the Dermis

Intracellular uptake of QDs by dermal cells was detected. QDs in the dermis were mainly found adherent to the extracellular dermal fibers; however, confocal microscopy analysis revealed that there were some cells that contain internalized QDs (Fig. 24.3).

These cells mainly accumulate QDs in their cytoplasm, but they are located in vesicular structures instead of being homogeneously distributed [56,57]. QDs are abundantly accumulated in the perinuclear area, but they are not found inside the nuclei (Fig. 24.3). These cells do not show any morphological signs of toxicity or abnormality, indicating that QDs would have been actively internalized by a regulated mechanism (endocytosis) instead of passively leaking through the intact cell membrane. The observed QDs' fluorescence pattern resembles QDs localizing in endosomes and/or endoplasmic reticulum [56,57]. Spectroscopic examination revealed that the fluorescence spectra of the intracellularly located QDs match the spectra obtained in saline solution (Fig. 24.3). This means that spectroscopic properties of QDs are retained in vivo and QDs are prevented from degradation in cellular compartments.

Analysis of the bright-field images of slides of stained tissue allows cells containing QDs to be differentiated. QDs accumulate inside the cells, which exhibit granulated cytoplasm (Fig. 24.3, square contour). According to skin physiology, such granules might be attributed to mast cells. However, QDs were not observed inside the muscle fibers and the adipocytes despite an abundant accumulation around these cells (Fig. 24.3).

According to morphological analysis, QDs were internalized by different cell types, indicating that the QDs' uptake depends on the cell type. One cell type was identified as mast cells. Kuchler with coworkers showed intracellular uptake of NPs to the keratinocytes in vitro [69]. They were distributed in the cytoplasm, mostly in the perinuclear region with no accumulation in the nuclei [70]. There are several types of dermal cells whose endocytic activity for NPs was shown earlier in vitro (cell cultures). Fullerenes were found accumulated in the lysosomes, mitochondria, and endoplasmic reticulum of human mast cells [71]. Fibroblasts were reported to accumulate gold NPs [72] and QDs [73] in the vacuoles and lysosomes. QDs were also found to be rapidly endocytosed by dendritic cells [74] and macrophages [75] and to localize in the lysosomes. However, NPs' intracellular uptake in vivo has not been extensively described.

Cellular uptake of drug-loaded NPs can become clinically relevant when they are applied to damaged skin. In the case of dendritic cells, QDs that were taken up could be later transported to the regional lymph nodes. On the other hand, intracellular uptake and localization

increase the risk of toxic effects as well. A current in vitro study showed that QDs could modulate the expression of genes known to be associated with inflammatory (IL1 β , CCL2, and IRAK2), immune (IL1, IL6, PGLYRP1, SERPINA1, and IL10), and apoptotic (CASP1 and ADORA2A) responses in human keratinocytes and dermal fibroblasts [76]. QDs also caused significant cytotoxicity. Pernodet and coworkers reported that gold NPs induced abnormalities in the construction of actin filaments and extracellular matrix, and inhibited fibroblast proliferation, adhesion, and motility [72]. The degradation of QDs and the release of toxic compounds in vivo after oral [77] and intravenous administration [78] were reported. Active cellular uptake and accumulation of QDs in dermal cells in vivo were detected (Fig. 24.3), and this could induce inflammatory and immune responses in vivo as well. The prolonged accumulation of NPs increases the time for adverse processes to occur, as the NPs are not totally cleared from the tissues.

QD Migration Pathways in the Tissues and Localization in Other Tissue Structures

As the abundant QD retention in the dermis was observed up to 24 h, we hypothesized that QDs could be excreted via sweat glands to the skin surface. To elucidate this presumption, QDs were injected into the mouse foot-pad since the highest density of the sweat glands is in the foot-pad [79]. The results of the microscopic tissue analysis showed that QDs were found accumulated in the dermis surrounding the sweat glands, but there was no QD permeation into the epithelial cells of the sweat glands (Fig. 24.4A and B).

QDs were observed in the epineurium of the peripheral nerves (Fig. 24.4C and D). However, QD fluorescence outlined the borders of the nerve without deeper penetration into the densely packed tissue of the perineurium. Similarly, QDs accumulated in the tunica adventitia of the large blood vessels, but they were prevented from passing to the tunica media (Fig. 24.4E and F). These observations show that QDs diffuse in the loose connective tissue but are unable to permeate the barriers of tightly organized collagen fibrils.

Fluorescence microscopy analysis showed that the QDs' fluorescence pattern mainly resembled the collagen network, indicating possible QD adherence to the extracellular proteins. The QDs' interaction with proteins was shown earlier [80]. QD adherence to the tissue proteins influences QD retention in the injection site and results in prolonged clearance. It might be used as a beneficial route for intradermal drug delivery and prolonged drug release for therapeutic purposes. The possible effects of long-term QD accumulation in the dermis are poorly understood. Kwan and coauthors

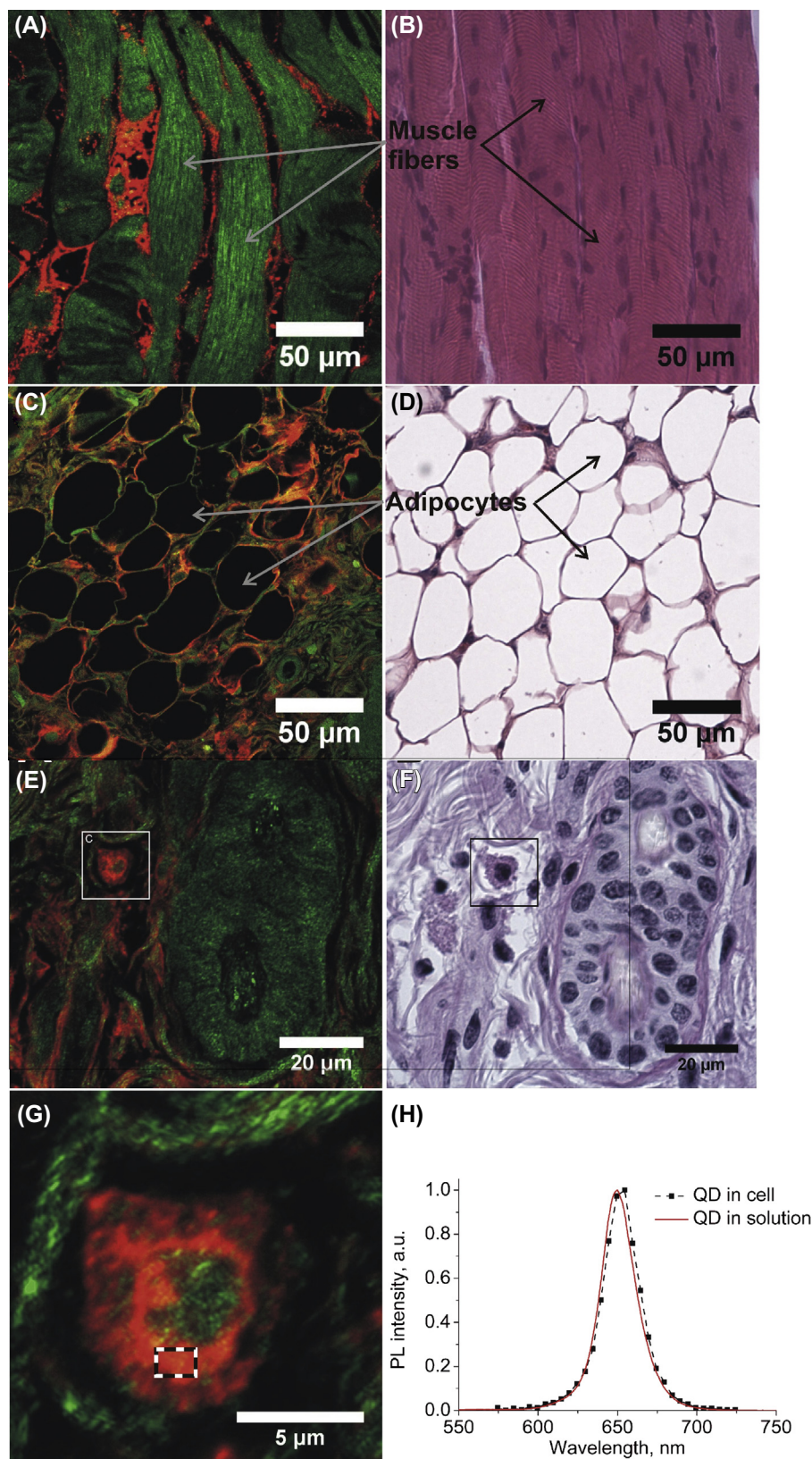


FIGURE 24.3 Fluorescence (A,C,E,G: unstained) and bright-field microscopy (B,D,F: PAS stained) images of mice skin showing intracellular QD (red/yellow) uptake in vivo 1 h after CdSe-ZnS-mPEG QD injection. QD (red/yellow) distribution between the muscle fibers (A,B) and adipocytes (C,D) was detected. No intracellular QD uptake by these cells was observed. The cells marked with white contour show the presence of QDs in the cytoplasm. Enlarged image (G) of a single cell reveals a heterogeneous QD pattern and high accumulation in the perinuclear region. QD emission spectrum (H) in the cell (from rectangle in G) matches the QD spectrum in the saline solution, indicating no spectroscopic changes in vivo.

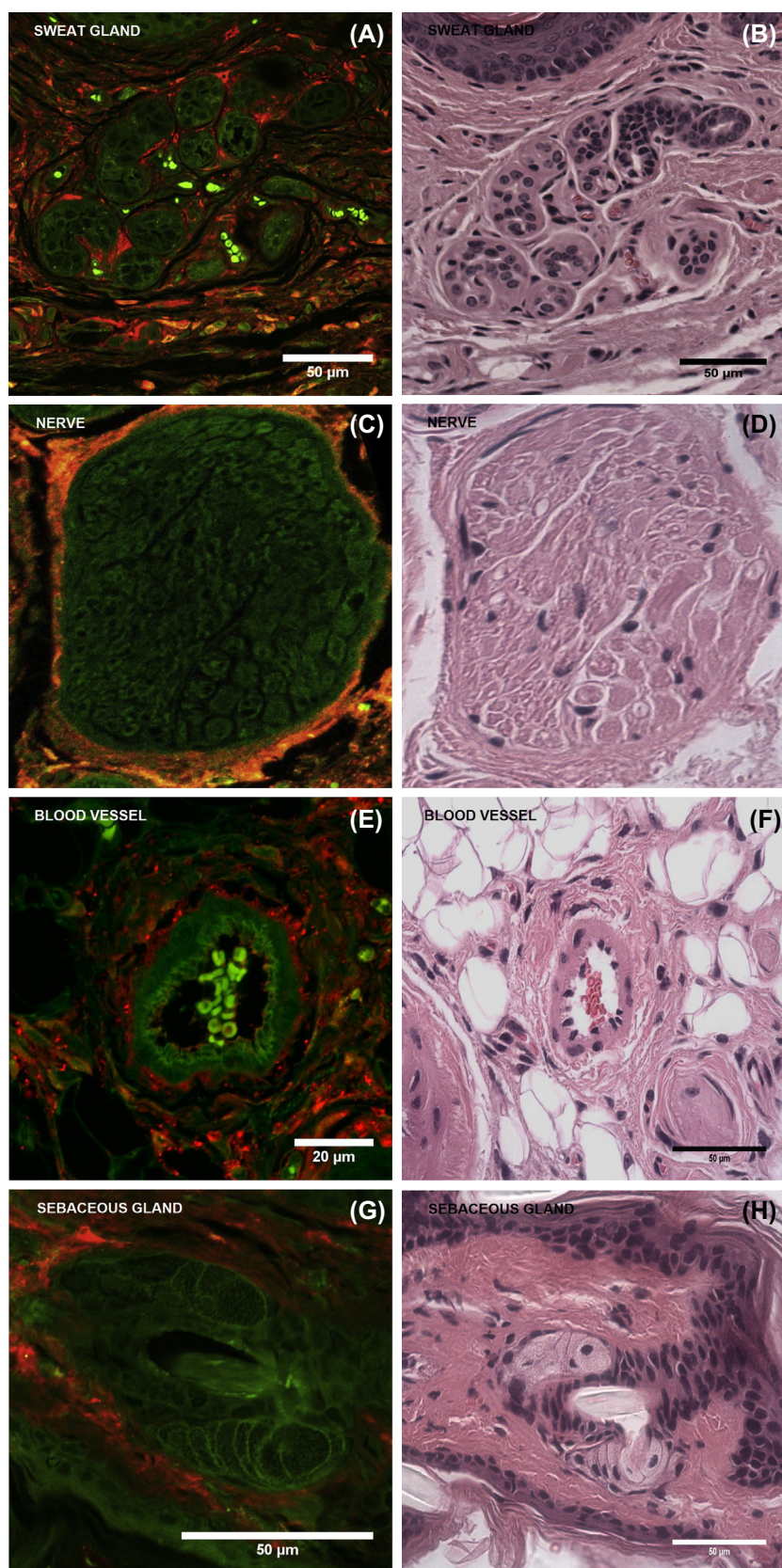


FIGURE 24.4 Fluorescence (A,C,E,G: unstained) and bright-field microscopy (B,D,F,H: HE stained) images of mice dermis showing QD (red/yellow) accumulation in the connective tissue around the sweat gland ducts (A), peripheral nerve (C), outlining artery (E), and sebaceous gland (G) borders *in vivo* 1 h after subcutaneous injection of 0.2 mL 0.4 μM CdSe-ZnS-mPEG QDs. There is no QD accumulation in the sweat and sebaceous glands, in the tunica media of the artery, or inside the nerve. There is no QD accumulation in the ducts or lumen of sweat glands, or in the tunica media of the artery and capillaries, despite abundant QD accumulation in the surrounding connective tissue of dermis, indicating that QDs are unable to permeate the barriers of tightly organized collagen fibrils.

investigated the effect of silver NP (AgNP) treatment for wound healing [81]. The authors found that AgNP-treated skin had better mechanical properties and higher contents of collagen type I and type III than the untreated group. NP treatment also improved the organization of collagen fibrils within the tissue. Platinum NPs showed efficient protection from ultraviolet light-induced inflammatory processes in mice skin [82]. These reports indicate that NPs may induce physiological alterations in the dermis and emphasize the need for comprehensive knowledge of NP interactions with biological tissue.

The long-term retention of QDs in the dermis suggests that they might be excreted to the skin surface, as has been shown for organic molecules including drugs [83]. However, after subcutaneous injection, QDs do not penetrate epithelial cells of the sweat glands (primarily because of the BM barrier). This minimizes the possibility that QDs could be excreted from the organism with the sweat as this would first of all require QD uptake to the sweat glands.

QDs were unable to penetrate the nerves and accumulated along the perineurium (Fig. 24.4), but they were dispersed in the surrounding connective tissue, or epineurium. The epifascicular epineurium consists of areolar connective tissue with loose bundles of collagen fibrils. However, the perineurium has a more organized structure and is usually represented as a sheet of collagen fibrils forming an undulating lacework structure. Therefore, it was assumed that the differences in extracellular collagen organization determined the limited QD diffusion into the perineurium and resulted in the observed QD distribution pattern in the tissue.

Similarly, QDs were also not detected in the muscle fibers, but distributed in the connective tissue between the muscle fascicles (Fig. 24.3). QDs were also detected in the tunica adventitia of the blood vessels, but they were prevented from permeation into the tunica media (Fig. 24.4). These observations indicate that QD diffusion through the tissues is limited and depends on the structure and physical organization of the connective tissue. QDs can migrate in the loosely organized tissue (epineurium, epimysium, and tunica adventitia), but they are not able to penetrate between the densely organized connective tissue fibers of the perineurium or endomysium and the densely packed smooth muscle fibers of the tunica media.

In general, QDs may leave the injected tissue by (1) passive diffusion through tissue, (2) blood circulation, or (3) lymphatic drainage. The limited QD diffusion through the tissue contributes greatly to the slow clearance of QDs away from the injection site. As QDs are highly impermeable to the BM, it might greatly contribute to the inefficient uptake to the blood vessels as the capillary uptake mainly depends on the QDs' penetration through the vessel wall. Slow capillary uptake should be primarily determined by the limited

QD diffusion through the basement membrane that lines the endothelium.

CONCLUSION

First of all, one can state that the penetration of particulate materials into skin is a very complex issue. *Ab initio* predictions are therefore not (yet) a practical approach to describe the penetration processes [24,39,84]. For this reason, to date only experimental data for particle penetration are available, and they also will be indispensable in the future. Looking at Table 2 in Ref. [84], problematic data might be the results of the penetration and permeation of QDs. The findings in two papers [22,43] are really surprising and unexpected, and, with respect to other data on QD penetration, their reliability might be questioned [84]. Our findings show that the application of QDs onto healthy skin is greatly hindered by the strong mechanical barrier properties of the SC. Although some preferable accumulation is observed in the skin furrows and around hair follicles, no deeper penetration was found, and the QDs were never detected in the epidermis or dermis layers (Fig. 24.1). This might exclude the possibility of any systemic toxicity from the topical application of QDs on healthy skin.

However, permeation through compromised skin or skin with any change in composition or structure that may alter its barrier properties is expected to be different from permeation of intact skin. An example is the penetration of QDs into deep epidermal and dermal layers of abraded skin [44] as well as 30 times stripped [45]. The QDs could not penetrate beyond the SC in all of the tested skin types except the abraded type, in which QDs could be found in the dermis, suggesting a higher risk for patients with compromised skin barriers [44,45].

Carbon dioxide laser can remove the SC, thus enhancing QD delivery via skin. Lee and coauthors investigated the skin permeation of carboxylated QDs assisted by carbon dioxide laser resurfacing [85]. The predominant routes for laser-mediated delivery were intercellular and follicular transport. With respect to the skin images by fluorescence microscopy, the QDs were detected in the dermis due to the deposition in the hair follicles.

Mortensen et al. have demonstrated that UVR exposure increases the risk of QD penetration into the mouse skin, but still at low levels [54,86]. UVR exposure [25,87] increases the ability of QDs to move through the SC and into the lower layers of the skin more than the hyperproliferative thickening response [88] works against penetration. The presented results match well with the minimal levels of QD penetration through intact skin as seen elsewhere [23], with increased penetration observable in damaged

skin [44,54]. QD collection in folds, follicles, and defects was seen in both the control and UVR-exposed samples [86].

In recent decades, many investigations have been reported that the appendageal pathway should be taken into consideration as an efficient route for drug permeation [34,89]. However, although some preferable QD accumulation is observed in the skin furrows and around hair follicles, no deeper penetration was found in the healthy skin.

The presented results show that subcutaneously injected QDs distribute in the dermis, hypodermis, and muscle tissue (Fig. 24.2). QDs migrate in the connective tissue, and they penetrate between the muscle fibers and adipocytes (Fig. 24.3). However, QD diffusion in the tissue is limited by specific dermal structures, and, therefore, QD fluorescence is absent in the epidermis, hair follicles, and sebaceous and sweat glands (Figs. 24.2 and 24.3). All these structures are lined by the basement membrane that organizes the epithelial cells and plays a major role as the limiting factor for QD migration in the skin. QDs are prevented from passing through the densely organized fibrils of the connective tissue coating in the peripheral nerves, blood vessel walls, and muscle fascicles (Fig. 24.4).

References

- [1] Antonio JR, Antonio CR, Cardeal ILS, Ballavenuto JMA, Oliveira JR. Nanotechnology in dermatology. *An Bras Dermatol* 2014;89(1):126–36.
- [2] Newman MD, Stotland M, Ellis JI. The safety of nanosized particles in titanium dioxide- and zinc oxide-based sunscreens. *J Am Acad Dermatol* 2009;61:685–92.
- [3] Nohynek GJ, Dufour EK. Nano-sized cosmetic formulations or solid nanoparticles in sunscreens: a risk to human health? *Arch Toxicol* 2012;86:1063–75.
- [4] Akermann ME, Chan WCW, Laakkonen P, Bhatia SN, Ruoslahti E. Nanocrystal targeting in vivo. *PNAS* 2002;99:12617–21.
- [5] Emeline AV, Kuznetsov VN, Ryabchuk VK, Serpone N. On the way to the creation of next generation photoactive materials. *Environ Sci Pollut Res* 2012;19:3666–75.
- [6] Chen X, Schluesener HJ. Nanosilver: a nanoparticle in medical application. *Toxicol Lett* 2008;176(1):1–12.
- [7] Rai M, Yadav A, Gade A. Silver nanoparticles as a new generation of antimicrobials. *Biotechnol Adv* 2009;27:76–83.
- [8] Oberdorster G, Oberdorster E, Oberdorster J. Nanotoxicology: an emerging discipline evolving from studies of ultrafine particles. *J Environ Health Perspect* 2005;113(7):823–39.
- [9] Hardman RA. Toxicologic review of quantum dots: toxicity depends on physicochemical and environmental factors. *Environ Health Perspect* 2006;114(2):165–72.
- [10] Zhao Y, Ng KW. Nanotoxicology in the skin: how deep is the issue? *Nano LIFE* 2014;4(1). 1440004–1/1440004–8.
- [11] Dianzani C. Drug delivery nanoparticles in skin cancers. *Biomed Res Int* 2014;895986. <http://dx.doi.org/10.1155/2014/895986>. Published online 2014 July 2.
- [12] Lademann J, Richter H, Schanzer S, Knorr F, Meinke M, Sterry W, et al. Penetration and storage of particles in human skin: perspectives and safety aspects. *Eur J Pharm Biopharm* 2011;77(3):465–8.
- [13] de Leeuw J, de Vrijlder HC, Bjerring P, Neumann HA. Liposomes in dermatology today. *J Eur Acad Dermatol Venereol* 2009;23: 505–16.
- [14] Gamer AO, Leibold E, van Ravenzwaay B. The in vitro absorption of microfine zinc oxide and titanium dioxide through porcine skin. *Toxicol In Vitro* 2006;20:301–7.
- [15] Lademann J, Weigmann H, Rickmeyer C, Barthelmes H, Schaefer H, Mueller G, et al. Penetration of titanium dioxide microparticles in a sunscreen formulation into the horny layer and the follicular orifice. *Skin Pharmacol Appl Skin Physiol* 1999;12: 247–56.
- [16] Pflücker F, Wendel V, Hohenberg H, Gärtner E, Will T, Pfeiffer S, et al. The human stratum corneum layer: an effective barrier against dermal uptake of different forms of topically applied micronised titanium dioxide. *Skin Pharm Appl Skin Physiol* 2001;14(Suppl. 1):92–7.
- [17] Schulz J, Hohenberg H, Pflücker F, Gärtner E, Will T, Pfeiffer S, et al. Distribution of sunscreens on skin. *Adv Drug Deliv Rev* 2002;54–63(Suppl. 1):S157.
- [18] Rouse JG, Yang J, Barron AR, Monteiro-Riviere NA. Fullerene-based amino acid nanoparticle interactions with human epidermal keratinocytes. *Toxicol In Vitro* 2006;20(8):1313–20.
- [19] Baroli B, Ennas MG, Loffredo F, Isola M, Pinna R, López-Quintela MA. Penetration of metallic nanoparticles in human full-thickness skin. *J Invest Dermatol* 2007;127:1701–12.
- [20] Toll R, Jacobi U, Richter H, Lademann J, Schaefer H, Blume-Peytavi U. Penetration profile of microspheres in follicular targeting of terminal hair follicles. *J Invest Dermatol* 2004;123:168–76.
- [21] Tinkle SS, Antonini JM, Rich BA, Roberts JR, Salmen R, DePree K, et al. Skin as a route of exposure and sensitization in chronic beryllium disease. *Environ Health Perspect* 2003;111:1202–8.
- [22] Ryman-Rasmussen JP, Riviere JE, Monteiro-Riviere NA. Penetration of intact skin by quantum dots with diverse physicochemical properties. *Toxicol Sci* 2006;91:159–65.
- [23] Zhang LW, Yu WW, Colvin VL, Monteiro-Riviere NA. Biological interactions of quantum dot nanoparticles in skin and in human epidermal keratinocytes. *Toxicol Appl Pharmacol* 2008;228: 200–11.
- [24] Lahouta HI, Schneider N. Interaction of inorganic nanoparticles with the skin barrier: current status and critical review. *Nanomedicine* 2013;9:39–54.
- [25] Jiang SJ, Chen JY, Lu ZF, Yao J, Che DF, Zhou XJ. Biophysical and morphological changes in the stratum corneum lipids induced by UVB irradiation. *J Dermatol Sci* 2006;44:29–36.
- [26] Schilling K, Bradford B, Castelli D, Dufour E, Nash JF, Pape W, et al. Human safety review of “nano” titanium dioxide and zinc oxide. *Photochem Photobiol Sci* 2010;9:495–509.
- [27] Smijs TG, Pavel S. Titanium dioxide and zinc oxide nanoparticles in sunscreen: focus on their safety and effectiveness. *Nanotechnol Sci Appl* 2011;4:95–112.
- [28] Bolzinger MA, Briançon S, Pelletier J, Chevalier Y. Penetration of drugs through the skin, a complex rate-controlling membrane. *Curr Opin Colloid Interface Sci* 2012;17:156–65.
- [29] Teo LA, Shearwood C, Chye Ng K, Lu J, Moomchala S. Transdermal microneedles for drug delivery applications. *Mater Sci Eng B* 2006;132:151–4.
- [30] Bouwstra JA, Honeywell-Nguyen PL, Gooris GS, Ponc M. Structure of the skin barrier and its modulation by vesicular formulations. *Prog Lipid Res* 2003;42:1–36.
- [31] Kanikkannan N, Kandimalla K, Lamba SS, Singh M. Structure-activity relationship of chemical penetration enhancers in transdermal drug delivery. *Curr Med Chem* 2000;7:593–608.
- [32] Menon GK. New insights into skin structure: scratching the surface. *Adv Drug Deliv Rev* 2002;54(Suppl. 1):S3–17.
- [33] Lee SH, Jeong SK, Ahn SK. An update of the defensive barrier function of skin. *Yonsei Med J* 2006;47:293–306.
- [34] Patzelt A, Lademann J. Drug delivery to hair follicles. *Expert Opin Drug Deliv* 2013;10(6):787–97.
- [35] Desai P, Patlolla RR, Singh M. Interaction of nanoparticles and cell-penetrating peptides with skin for transdermal drug delivery. *Mol Membr Biol* 2010;27(7):247–59.

- [36] Elias PM. Epidermal lipids, barrier function, and desquamation. *J Invest Dermatol* 1983;80:44s–9s.
- [37] Hadgraft J. Modulation of the barrier function of the skin. *Skin Pharmacol Appl Skin Physiol* 2001;14:72–81.
- [38] Lademann J, Knorr F, Richter H, Blume-Peytavi U, Vogt A, Antoniou C, et al. Hair follicles – an efficient storage and penetration pathway for topically applied substances. *Skin Pharmacol Physiol* 2008;21:150–5.
- [39] Gratieri T, Schaefer UF, Jing L, Gao M, Kostka KH, Lopez RF, et al. Penetration of quantum dot particles through human skin. *J Biomed Nanotechnol* 2010;6:586–95.
- [40] Lademann J, Knorr F, Richter H, Jung S, Meinke MC, Ruhl E, et al. Hair follicles as a target structure for nanoparticles. *J Innovative Opt Health Sci* 2015;8(4):1530004 (1-8).
- [41] Derfus AM, Chan WCW, Bhatia SN. Probing the cytotoxicity of semiconductor quantum dots. *Nano Lett* 2004;4:11–8.
- [42] Michalet X, Pinaud FF, Bentolila LA, Tsay JM, Doose S, Li JJ, et al. Quantum dots for live cells, in vivo imaging, and diagnostics. *Science* 2005;307(5709):538–44.
- [43] Chu M, Wu Q, Wang J, Hou S, Miao Y, Peng J, et al. In vitro and in vivo transdermal delivery capacity of quantum dots through mouse skin. *Nanotechnology* 2007;18:455103 (6 pp.).
- [44] Zhang LW, Monteiro-Riviere NA. Assessment of quantum dot penetration into intact, tape-stripped, abraded and flexed rat skin. *Skin Pharmacol Physiol* 2008;21:166–80.
- [45] Prow TW, Monteiro-Riviere NA, Inman AO, Grice JE, Chen X, Zhao X, et al. Quantum dot penetration into viable human skin. *Nanotoxicology* 2012;6(2):173–85.
- [46] Jeong SH, Kim JH, Yi SM, Lee JP, Kim JH, Sohn KH, et al. Assessment of penetration of quantum dots through in vitro and in vivo human skin using the human skin equivalent model and the tape stripping method. *Biochem Biophys Res Commun* 2010;394:612–5.
- [47] Prow TW, Grice JE, Lin LL, Faye R, Butler M, Becker W, et al. Nanoparticles and microparticles for skin drug delivery. *Adv Drug Deliv Rev* 2011;63:470–91.
- [48] Kulvietis V, Zurauskas E, Rotomskis R. Distribution of polyethylene glycol quantum dots in mice skin. *Exp Dermatol* 2013;22:157–9.
- [49] Lei T, Zhang CL, Song GM, Jin X, Xu ZW. In vivo skin penetration and metabolic path of quantum dots. *Sci China Life Sci* 2013;56:181–8.
- [50] Monteiro-Riviere NA, Zhang LW. Assessment of quantum dot penetration into skin in different species under different mechanical actions. In: Linkov I, Steevens J, editors. *Nanomaterials: risks and benefits*. Dordrecht (Netherlands): Springer; 2008. p. 41–52.
- [51] Wu X, Landfester K, Musyanovych A, Guy RH. Disposition of charged nanoparticles after their topical application to the skin. *Skin Pharmacol Physiol* 2010;23:117–23.
- [52] Wu X, Price GJ, Guy RH. Disposition of nanoparticles and an associated lipophilic permeant following topical application to the skin. *Mol Pharm* 2009;6:1441–8.
- [53] Monteiro-Riviere NA, Baroli B. Nanomaterial penetration. In: Monteiro-Riviere NA, editor. *Toxicology of the skin – target organ series*, vol. 29. New York: Informa Healthcare; 2010. p. 333–46 [chapter 22].
- [54] Mortensen LJ, Oberdörster G, Pentland AP, Delouise LA. In vivo skin penetration of quantum dot nanoparticles in the murine model: the effect of UVR. *Nano Lett* 2008;8:2779–87.
- [55] Gopee NV, Roberts DW, Webb P, Cozart CR, Siitonen PH, Latendresse JR, et al. Quantitative determination of skin penetration of PEG-coated CdSe quantum dots in dermabrased but not intact SKH-1 hairless mouse skin. *Toxicol Sci* 2009;111(1):37–48.
- [56] Damalakiene L, Karabanovas V, Bagdonas S, Valius M, Rotomskis R. Intracellular distribution of nontargeted quantum dots after natural uptake and microinjection. *Int J Nanomed* 2013;8:555–68.
- [57] Karabanovas V, Zitkus Z, Kuciauskas D, Rotomskis R, Valius M. Surface properties of quantum dots define their cellular endocytotic routes, mitogenic stimulation and suppression of cell migration. *Int J Biomed Nanotech* 2014;10(5):775–86.
- [58] Choi HS, Liu W, Misra P, Tanaka E, Zimmer JP, Itty Ipe B, et al. Renal clearance of quantum dots. *Nat Biotechnol* 2007;25(10):1165–70.
- [59] Sonavane G, Tomoda K, Makino K. Biodistribution of colloidal gold nanoparticles after intravenous administration: effect of particle size. *Colloids Surf B Biointerfaces* 2008;66:274–80.
- [60] Labouta HI, el-Khordagui LK, Kraus T, Schneider M. Mechanism and determinants of nanoparticle penetration through human skin. *Nanoscale* 2011;3(12):4989–99.
- [61] Monteiro-Riviere NA, Wiench K, Landsiedel R, Schulte S, Inman AO, Riviere JE. Safety evaluation of sunscreen formulations containing titanium dioxide and zinc oxide nanoparticles in UVB sunburned skin: an in vitro in vivo study. *Toxicol Sci* 2011;123:264–80.
- [62] Bennett KM, Zhou H, Sumner JP, Dodd SJ, Bouraoud N, Doi K, et al. MRI of the basement membrane using charged nanoparticles as contrast agents. *Magn Reson Med* 2008;60:564–74.
- [63] Lademann J, Richter H, Teichmann A, Otberg N, Blume-Peytavi U, Luengo J, et al. Nanoparticles – an efficient carrier for drug delivery into the hair follicles. *Eur J Pharm Biopharm* 2007;66:159–64.
- [64] Lademann J, Richter H, Schaefer UF, Blume-Peytavi U, Teichmann A, Otberg N, et al. Hair follicles – a long-term reservoir for drug delivery. *Skin Pharmacol Physiol* 2006;19:232–6.
- [65] Otberg N, Patzelt A, Rasulev U, Hagemester T, Linscheid M, Sinkgraven R, et al. The role of hair follicles in the percutaneous absorption of caffeine. *Br J Clin Pharmacol* 2008;65:488–92.
- [66] Rancan F, Papakostas D, Hadam S, Hackbarth S, Delair T, Primard C, et al. Investigation of polylactic acid (PLA) nanoparticles as drug delivery systems for local dermatotherapy. *Pharm Res* 2009;26:2027–36.
- [67] Vogt A, Combadiere B, Hadam S, Stieler KM, Lademann J, Schaefer H, et al. 40 nm, but not 750 or 1500 nm, nanoparticles enter epidermal CD1a+ cells after transcutaneous application on human skin. *J Invest Dermatol* 2006;126:1316–22.
- [68] Morgen M, Lu GW, Du D, Stehle R, Lembke F, Cervantes J, et al. Targeted delivery of a poorly water-soluble compound to hair follicles using polymeric nanoparticle suspensions. *Int J Pharm* 2011;416:314–22.
- [69] Kuchler S, Radowski MR, Blaschke T, Dathe M, Plendl J, Haag R, et al. Nanoparticles for skin penetration enhancement – a comparison of dendritic core-multishell nanotransporters and solid lipid nanoparticles. *Naunyn-Schmiedeberg's Arch Pharmacol* 2009;379:8.
- [70] Kuchler S, Wolf NB, Heilmann S, Weindl G, Helfmann J, Yahya MM, et al. 3D – wound healing model: influence of morphine and solid lipid nanoparticles. *J Biotechnol* 2010;148(1):24–30.
- [71] Dellinger A, Zhou Z, Norton SK, Lenk R, Conrad D, Kepley CL. Uptake and distribution of fullerenes in human mast cells. *Nanomedicine* 2010;6:575–82.
- [72] Pernodet N, Fang X, Sun Y, Bakhtina A, Ramakrishnan A, Sokolov J, et al. Adverse effects of citrate/gold nanoparticles on human dermal fibroblasts. *Small* 2006;2:766–73.
- [73] Damalakiene L, Bagdonas S, Rotomskis R, Karabanovas V, Ger M, Valius M. Influence of growth factor on internalization pathway of quantum dots into cells: PDGF effects internalization of QDs. *Nanotechnology* 2009:465–8. IEEE-NANO 2009.
- [74] Sen D. Quantum dots for tracking dendritic cells and priming an immune response in vitro and in vivo. *PLoS One* 2008;3(9):e3290 (1-13).
- [75] Clift MJD, Brandenberger C, Rothen-Rutishauser B, Brown DM, Stone V. The uptake and intracellular fate of a series of different surface coated quantum dots in vitro. *Toxicology* 2011;286:58–68.

- [76] Romoser AA, Chen PL, Berg JM, Seabury C, Ivanov I, Criscitiello MF, et al. Quantum dots trigger immunomodulation of the NF κ B pathway in human skin cells. *Mol Immunol* 2011; 48(12–13):1349–59.
- [77] Karabanovas V, Zakarevicius E, Sukackaite A, Streckyte G, Rotomskis R. Examination of the stability of hydrophobic (CdSe)ZnS quantum dots in the digestive tracts of rats. *Photochem Photobiol Sci* 2008;7:725–9.
- [78] Lin CH, Chang LW, Chang H, Yang MH, Yang CS, Lai WH, et al. The chemical fate of the Cd/Se/Te-based quantum dot 705 in the biological system: toxicity implications. *Nanotechnology* 2009;20: 215101 (9 pp.).
- [79] Kennedy WR, Sakuta M, Quick DC. Rodent eccrine sweat glands: a case of multiple efferent innervation. *Neuroscience* 1984;11(3): 741–9.
- [80] Poderys V, Matulionyte M, Selskis A, Rotomskis R. Interaction of water-soluble CdTe quantum dots with bovine serum albumin. *Nanoscale Res Lett* 2011;6(9). <http://dx.doi.org/10.1007/s11671-010-9740-9>.
- [81] Kwan KH, Liu X, To MK, Yeung KW, Ho CM, Wong KK. Modulation of collagen alignment by silver nanoparticles results in better mechanical properties in wound healing. *Nanomedicine* 2011; 7(4):497–504. <http://dx.doi.org/10.1016/j.nano.2011.01.003>. Epub 2011 January 25.
- [82] Yoshihisa Y, Honda A, Zhao QL, Makino T, Abe R, Matsui K, et al. Protective effects of platinum nanoparticles against UV-light-induced epidermal inflammation. *Exp Dermatol* 2010; 19(11):1000–6. <http://dx.doi.org/10.1111/j.1600-0625.2010.01128.x>. Epub 2010 August 31.
- [83] Barnes AJ, Brunet BR, Choo RE, Mura P, Johnson RE, Jones HE, et al. Excretion of methadone in sweat of pregnant women throughout gestation after controlled methadone administration. *Ther Drug Monit* 2010;32(4):497–503.
- [84] Schneider M, Stracke F, Hansen S, Schaefer UF. Nanoparticles and their interaction with dermal barrier. *Dermatoendocrinology* 2009;1(4):197–206.
- [85] Lee WA, Chen SC, Al-Suwayeh SA, Yang HH, Li YC, Fang JY. Skin permeation of small-molecule drugs, macromolecules and nanoparticles mediated by a fractional carbon dioxide laser: the role of hair follicles. *Pharm Res* 2013;30:792–802.
- [86] Mortensen LO, Zheng H, Faulknor R, De Benedetto A, Beck L, DeLouise LA. Increased in vivo skin penetration of quantum dot with UVR and in vivo quantum dot cytotoxicity. *Proc SPIE* 2009;7189:718919. 1–12.
- [87] Jiang SJ, Chu AW, Lu ZF, Pan MH, Dhe DF, Zhou XJ. Ultraviolet B-induced alterations of the skin barrier and epidermal calcium gradient. *Exp Dermatol* 2007;16(12):985–92.
- [88] Brouxhon S, Konger RL, VanBuskirk J, Sheu TJ, Ryan J, Erdle B, et al. Deletion of prostaglandin E₂ EP₂ receptor protects against ultraviolet-induced carcinogenesis, but increases tumour aggressiveness. *J Invest Dermatol* 2007;127(2):439–46.
- [89] Fang CL, Aljuffali IA, Li YC, Fang JY. Delivery and targeting of nanoparticles into hair follicles. *Ther Deliv* 2014; 5(9):991–1006.

Nanomedicines for the Eye: Current Status and Future Development

A.A. Attama¹, J.N. Reginald-Opara¹, E.M. Uronnachi², E.B. Onuigbo¹

¹University of Nigeria, Nsukka, Enugu State, Nigeria; ²Nnamdi Azikiwe University, Awka, Anambra State, Nigeria

OUTLINE

Introduction	323	<i>Emulsion Solvent Evaporation Method</i>	331
Barriers to Effective Drug Delivery to the Eye	324	<i>Double-Emulsion Solvent Evaporation Method</i>	332
Challenges to Drug Delivery to the Anterior Segment of the Eye	324	<i>Salting-Out Method</i>	332
Challenges to Drug Delivery to the Posterior Segment of the Eye	324	<i>Ionic Gelation Method</i>	332
Drug Transporters in Eye	326	<i>Emulsification Solvent Diffusion Method</i>	332
Nanomedicine Paradigms in Ocular Diseases	326	<i>Supercritical Fluid Method</i>	332
Nanomedicines for Ocular Application	326	<i>Rapid Expansion Supercritical Solution (RESS)</i>	333
Advantages of Ocular Nanomedicines	327	<i>Homogenization Method</i>	333
Disadvantages of Ocular Nanomedicines	327	Characterization of Nanomedicines	333
Novel Nanomedicines for Ocular Delivery	327	Morphology and Particle Size Determination	333
Requirements for Ocular Nanosystems	328	Loading Capacity	334
Nanoparticles	328	Surface Charge or Zeta Potential	334
Polymer-Based Nanomedicines for the Eye	328	Crystallinity	334
Nanosuspensions	329	Drug Release	334
Nanocrystals	329	In Vitro Determination	334
Dendrimers	330	Ex Vivo Evaluation and Use of Bioengineered Cornea	334
Liposomes	330	In Vivo Evaluation	334
Microemulsions and Nanoemulsions	331	Conclusion and Future Prospects	334
Production of Nanomedicines	331	References	335
Nanoprecipitation Method	331		

INTRODUCTION

The eye is divided into anterior and posterior segments [1], and this anatomical division affects the design of drug

delivery system depending on the site of infection. Drug delivery to the eye can be broadly classified into delivery to the anterior and delivery to the posterior segments. Conventional formulations like solutions, suspensions,

and ointments have been shown to be suboptimal in the treatment of ocular diseases. More than 90% of the marketed ophthalmic formulations are in the form of solutions, which mainly target the diseases in the anterior segment of the eye [2].

The bioavailability of an ophthalmic drug is limited by some physiological constraints, for example the relatively impermeable corneal barrier. The cornea (Fig. 25.1) consists of three membranes—the epithelium, the endothelium, and inner stroma—which are the main absorptive barriers [3,4]. The epithelium facing the tears with lipophilic cellular layers acts as a barrier to ion transport. The tight junctions of the corneal epithelium serve as a selective barrier for small molecules and prevent the diffusion of macromolecules through the paracellular route. The stroma beneath the epithelium is a highly hydrophilic layer making up 90% of the cornea. The corneal endothelium is responsible for maintaining normal corneal hydration. Therefore, the more lipophilic the drugs are, the more resistance they will find crossing the stroma. The more hydrophilic the drug is, the more resistant the epithelium is to its passage, though the stroma and endothelium are limited in their resistance [5].

Some physicochemical properties of drugs, such as lipophilicity, solubility, molecular size and shape, charge, and degree of ionization, affect the route and rate of permeation through the corneal membrane in the cul-de-sac.

The anatomy, physiology, and barrier function of the cornea compromise the rapid absorption of drugs. Frequent instillations of eye drops are necessary to

maintain a therapeutic drug level in the tear film or at the site of action. However, the use of highly concentrated solutions may induce toxic side effects and cellular damage at the ocular surface.

BARRIERS TO EFFECTIVE DRUG DELIVERY TO THE EYE

The specific challenge of designing a therapeutic system is to achieve an optimal concentration of a drug at the site of action for the appropriate duration to provide ocular delivery systems with high therapeutic efficacy. The observed poor bioavailability of drugs from ocular dosage forms is mainly due to the precorneal loss factors or barriers preventing ocular topically or systemically administered drugs from reaching posterior segments.

Challenges to Drug Delivery to the Anterior Segment of the Eye

For diseases of the eye, topical administration is usually preferred over systemic administration. Any drug molecule administered by the ocular route has to cross the precorneal barriers. These are the first barriers that limit the penetration of an active ingredient into the eye, resulting in poor bioavailability from ocular dosage forms [6]. The precorneal loss factors are shown in Box 25.1.

Those factors in Box 25.1 are the major challenges to anterior segment drug delivery following topical administration. Due to these physiological and anatomical constraints, only a small fraction of the drug, effectively 1% or even less of the instilled dose, is ocularly absorbed. To be clinically effective, topical formulation has to possess a balance between lipophilicity and hydrophilicity with higher contact time [7].

Challenges to Drug Delivery to the Posterior Segment of the Eye

Topical ocular medications do not reach the posterior segment drug targets because of the high efficiency of the blood–ocular barrier (BOB), typified by the blood–retinal barrier (BRB) (Fig. 25.2) [8] and the blood–aqueous barrier (BAB). The BAB refers to the barriers, which restrict movement of substances from the plasma to the aqueous humour of the eye. BAB usually located in the ciliary body includes vascular endothelium, stroma, basement membrane, pigmented and non-pigmented epithelium. This barrier “pumps” out applied liquid eye medication through production of more aqueous humour and subsequent drainage through the trabecular meshwork/canal of Schlemm

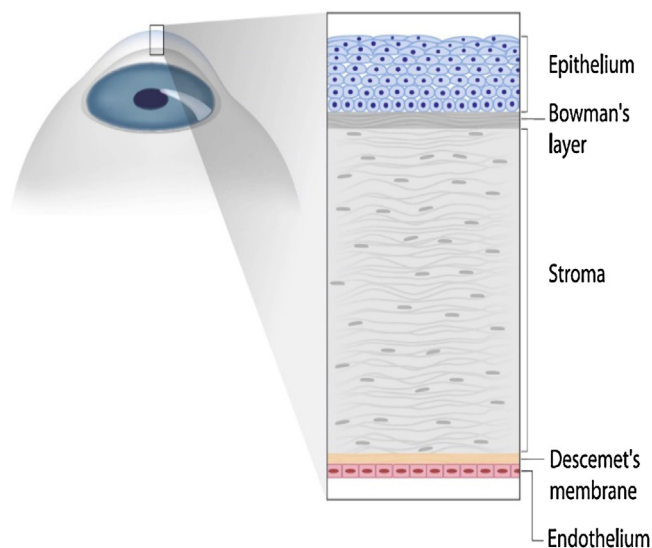


FIGURE 25.1 Cornea structure. Source: Sharif MS, Qahwaji R, Shahamatnia E, Alzubaidi R, Ipson S, Brahma A. An efficient intelligent analysis system for confocal corneal endothelium images. *Comput Methods Programs Biomed* 2015;122(3):421-36.

BOX 25.1

PRECORNEAL LOSS FACTORS

- Solution drainage
- Loss due to evaporation.
- Presystemic metabolism
- Lacrimation
- Tear dynamics: tear dilution, tear turnover
- Conjunctival absorption
- Nonproductive absorption (conduit drainage)
- Protein binding
- Transient residence time in the cul-de-sac
- The relative impermeability of the corneal epithelial membrane.

(trabecular pathway) of uveoscleral pathway (Fig. 25.3) [9], draining into the systemic circulation. This process drastically reduces the concentration of the applied medication which enters the aqueous humour. The BOB physically separates blood vessels from internal segment of eye, controlling passage of any particle or chemical into ocular tissues. Ocular medications administered via local or systemic routes must overcome this barrier to achieve adequate concentration and maintenance in retina and vitreous. BRB, which is selectively permeable to more lipophilic molecules, mainly governs the entry of drug molecules into posterior segment of the eye [10]. This BOB physically separates blood vessels

from the internal segment of the eye, controlling passage of any particle or chemical into ocular tissues. Ocular medications administered via local or systemic routes must overcome this barrier to achieve adequate concentration and maintenance in retina and vitreous. BRB, which is selectively permeable to more lipophilic molecules, mainly governs the entry of drug molecules into the posterior segment of the eye [10].

The tight junctions of BRB restrict the entry of systemically administered drugs into the retina. High vitreal drug concentrations achievable almost only by intravitreal injection are required in the treatment of posterior segment diseases. A very big challenge for the posterior

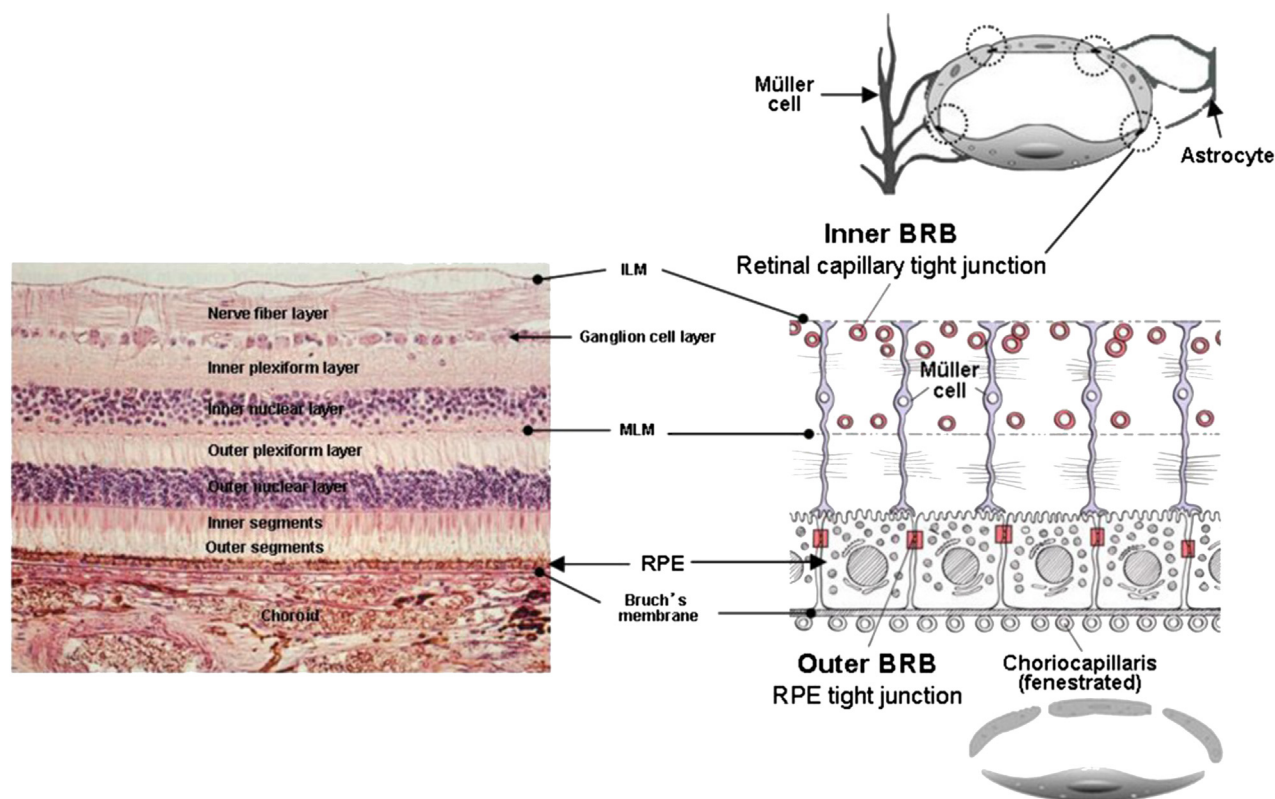


FIGURE 25.2 The blood–retinal barrier (BRB). Source: Kuno N, Fujii S. Recent advances in ocular drug delivery systems. *Polymers* 2011;3(1):193–221. Available from: <http://www.mdpi.com/2073-4360/3/1/193/html>.

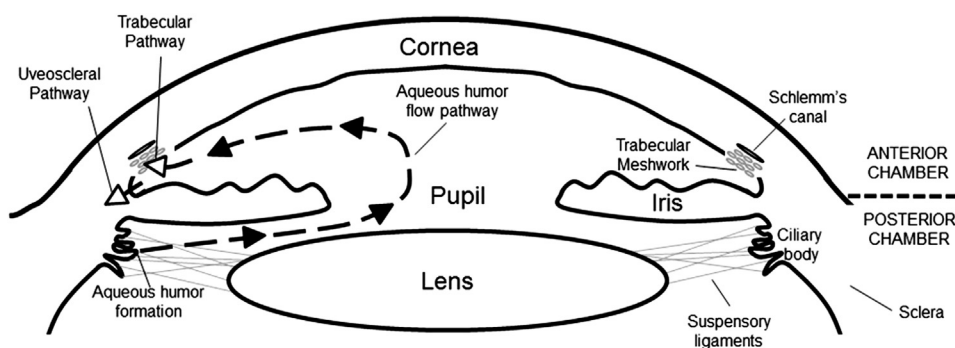


FIGURE 25.3 Aqueous humour flow pathway. Source: Ito YA, Walter MA, 2013. *Genetics and Environmental Stress Factor Contributions to Anterior Segment Malformations and Glaucoma*. In: *Glaucoma - Basic and Clinical Aspects*, Rumelt S. (Ed.). Available from: <http://www.intechopen.com/books/glaucoma-basic-and-clinical-aspects/ngenetics-and-environmental-stress-factor-contributions-to-anterior-segment-malformations-and-glauco>.

segment is to maintain the therapeutic drug concentration over prolonged periods and minimize the number of injections. This presents a lot of problems necessitating the development of novel ocular drug delivery systems.

Drug Transporters in Eye

The traditional approach to improve ocular bioavailability is to modify the drug chemically to achieve the desired solubility and lipophilicity. However, a more rational approach would be a transporter-targeted modification of the drug. Transporters are membrane-bound proteins that play an important role in active transport of nutrients across biological membranes. The presence of transporters has been reported on various ocular tissues, but the focus here is on the epithelia of the cornea, conjunctiva, and retina. Two types of transporter systems are of interest in ocular drug delivery: efflux transporters and influx transporters. The efflux transporters belong to the adenosine triphosphate (ATP) binding cassette superfamily, whereas influx transporters belong to the solute carrier (SLC) superfamily. Efflux transporters lower bioavailability by effluxing the molecules out of the cell membrane and cytoplasm. Prominent efflux transporters identified on ocular tissues include P-gp, multidrug resistance protein (MRP), and breast cancer resistant proteins (BCRPs). Various authors reviewed the emerging role of transporters in ocular drug delivery [11–14].

nanomedicines can be designed to successfully circumvent the blood–ocular barriers. Since encapsulation of drugs can grant further protection as well as prolonged and controlled release, they offer better promise for some chronic ocular diseases like chronic cytomegalovirus (CMV) retinitis, in which the intravitreal delivery of ganciclovir seems to be the preferred strategy [15].

Piloplex, consisting of pilocarpine ionically bound to poly(methyl)methacrylate–co-acrylic acid, is a nanoscaled colloidal carrier system effectively used in glaucoma patients as twice-daily instillations. Multidimensional mechanisms appear to be involved for the pharmacologic action of ocular nanosystems, including extending the time of drug residency in the cornea or conjunctiva, sustaining drug release from its carrier, reducing the precorneal drug loss, and targeting the desired ocular tissues [15–17]. Thus, it is highly desirable to exploit bioadhesive materials for the formulation of nanosystems to be retained in the cul-de-sac after topical administration.

Erodible nanosystems are superior because the self-eroding process of the hydrolyzable polymer exerts less harm on tissue [18,19]. For treatment of chronic ocular diseases (eg, CMV retinitis), localized prolonged nanomedicines can be effectively used as a safer alternative to frequent injections that may cause cataract development, retinal detachment, endophthalmitis, and vitreous hemorrhage [15].

NANOMEDICINE PARADIGMS IN OCULAR DISEASES

Based upon the biological architecture of the eye together with the physicochemical characteristics of the nanostructured medicines (ie, particle charge, surface properties, and relative hydrophobicity),

NANOMEDICINES FOR OCULAR APPLICATION

Nanomedicine is the medical application of nanotechnology, nanodevices, and nanomaterials for tissue repair and drug delivery for the treatment of human diseases. Topical eye drops are the most commonly used method of medication for the prevention and

intervention of corneal defects. Nevertheless, these drugs are often ineffective due to poor patient compliance, low penetration through the epithelial barrier, and unwanted side effects. In the field of cornea, nanomedicine research has particularly focused on imaging, prevention, and/or reduction of corneal opacities and neovascularization [20–24].

Advantages of Ocular Nanomedicines

The advantages offered by nanotechnology-based ocular drug delivery over the conventional dosage forms cannot be overemphasized. These include [25]:

- Achievement of a sustained and controlled drug delivery.
- Increased accurate dosing overcoming the pulsed dosing produced by conventional dosage forms.
- Well-tolerated dosage form with adhesive properties that could prolong the residence time of drug in the cul-de-sac, prevent tear washout, and increase ocular bioavailability.
- No impairment of sight due to the small dimensions of the delivery system.
- Reduced need for repeated instillation as a result of prolonged drug release, leading to better patient compliance and improved therapeutic performance.
- Circumvention of protective barriers like drainage, lacrimation, and conjunctival absorption.
- Provision of drug protection against metabolic enzymes (eg, peptidases and nucleases) and degradation.
- Targeted drug delivery toward affected tissues, reducing possible side effects and required dose.

Disadvantages of Ocular Nanomedicines

One of the disadvantages of nanotechnological-based drug delivery systems formulated for administration to the eye is the possibility of toxicity. The toxicity of nanoparticles in ocular tissues can be affected by many factors, including chemistry, size, dose, the time of assessment, and the biodistribution pattern of the particles in the eye. Even though many of the studies have focused on the efficacy of the formulations, recent studies assessed the toxicity based on histological evaluation, immunohistochemistry, inflammation, and neuronal toxicity [26]. Luty et al. [27] compared the safety of chitosan, poly(((cholesteryl oxocarbonylamido ethyl) methyl bis(ethylene) ammonium iodide) ethyl phosphate) (PCEP), and magnetic nanoparticles that have been investigated as ocular gene delivery vehicles. Recently, Goldberg et al. reported the effect of magnetic nanoparticle size on ocular toxicity in Sprague–Dawley rats [28].

In addition, some of the materials utilized for nanomedicines are not biodegradable; as a result, accumulation in the body (particularly in the eye tissues) over a long period of time would pose a threat to the eye. The stability of the drug in some of the nanobased formulations is not guaranteed after a prolonged period of time.

Some bioadhesive polymers are associated with problems like blurred vision and formation of a veil in the corneal area, leading to loss of eyesight.

The problem of particle growth after a prolonged period of time is also a challenge for nanomedicines, especially with nanosuspensions.

NOVEL NANOMEDICINES FOR OCULAR DELIVERY

Different drug delivery strategies have been studied for ocular delivery systems (Fig. 25.4). The various approaches fall into two main categories: bioavailability improvement and controlled-release drug delivery. Improvement in bioavailability and the duration of action of ocular active drugs are based on maximizing corneal drug absorption and minimizing precorneal drug loss [29]. Tactical design of novel delivery systems would lead to sustained drug delivery, which may provide controlled and continuous delivery of ocular active drugs. Microparticulates (micromedicines) and nanoparticulates (nanomedicines) have been shown to improve the ophthalmic bioavailability of the drugs and to control the release of the ophthalmic drugs to the anterior segment of the eye. The nanomedicines investigated for ocular drug delivery include, among

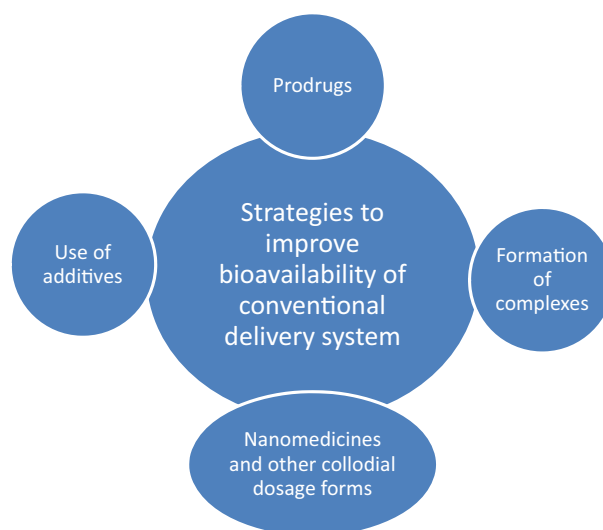


FIGURE 25.4 Strategies to improve low ocular bioavailability of conventional delivery systems.

others, liposomes, niosomes, solid lipid nanoparticles, nanostructured lipid carriers, polymer-based nanoparticles, nanosuspensions, nanoemulsions, nanospheres, nanocapsules, dendrimers, and others. These delivery systems have been shown to provide different degrees of bioavailability enhancement or controlled release of ocular active drugs. Particulates such as nanoparticles, nanocapsules, submicron emulsions, and nanosuspensions improved the bioavailability of ocularly applied drugs [30,31].

Colloidal systems, both in liquid form (eg, micro- and nanoemulsions) and in solid form (eg, nanoparticles), have excellent potential for interaction with the eye. Due to their size and the characteristics of their surface, they are taken up strongly by the cornea, forming a drug reservoir and thus improving the permanence of drugs at the aqueous and vitreous humor levels and enhancing efficacy in treating diseases of the anterior eye through targeting.

Nanoparticles are nanometer-sized structures designed as drug carriers in which the active ingredient is dissolved, entrapped/encapsulated, or adsorbed. Different nanoparticles afford different drug release kinetics, capacities, and stability, and they represent promising drug carriers for ophthalmic applications. Nanoforms of ocular drugs can achieve sustained intravitreal therapeutic drug concentrations and thus significantly enhance the ocular bioavailability of many ocular drugs in comparison with normal aqueous eye solutions [32]. These particulate delivery systems can improve patient compliance and may reduce systemic side effects. Nanoparticles have been engineered from various synthetic and natural biocompatible polymers, but those derived from natural polymers that are biocompatible, biodegradable, nontoxic, and nonantigenic are favored.

Requirements for Ocular Nanosystems

- Adequate control of particle size below irritancy threshold
- A balance of lipophilic and hydrophilic character
- Drugs with high activity at low dose
- Nonirritancy, to not provoke lachrymal secretion and reflex blinking
- Low tendency to form thick films
- Favorable rheological properties.

Nanoparticles

Nanoparticles are roughly defined as particles with a diameter smaller than 1 μm , consisting of various biodegradable materials, such as natural or synthetic polymers, lipids, phospholipids, and even metals. Drugs can be either integrated in the matrix or attached

to the surface. Nanoparticles made up of various biodegradable polymers like polylactide (PLA), polycyanoacrylate, poly(D,L-lactides), and natural polymers like chitosan, gelatin, sodium alginate, and albumin can be used effectively for efficient drug delivery to the ocular tissues [33]. Nanoparticulates have submicron properties, such as high surface area and energy and movement of the particles in liquid media (Brownian motion). The surface charge of nanoparticles determines the performance of the nanoparticle system in the body [34]. The particle size of externally applied colloidal carriers influences absorption or permeation through the ocular barriers. Delivery of drugs to the posterior site of the eye by application of drug solution is very difficult. The possibility of drug-loaded nanoparticles to reach the posterior site of ocular tissues and deliver drugs at targeted sites at effective therapeutic concentration is very high for various disorders like age-related macular degeneration, retinitis, diabetic retinopathy, and corneal/conjunctival squamous cell carcinoma [35].

Polymer-Based Nanomedicines for the Eye

Polymeric nanoparticles are colloidal carriers with diameters ranging from 10 to 1000 nm. They have been widely studied as topical ocular drug delivery systems because of their enhanced adherence to the ocular surface and their controlled release of drugs [36,37]. These systems allow a greater amount of design flexibility in terms of the size, surface charge, and composition to improve drug penetration, retention time, and sustain drug delivery. In addition, they can be formulated and administered as eye drops, which makes them ideal candidates for the treatment of corneal diseases. Some of the polymers that have been used are PLA, PLGA, poly 3-caprolactone (PCL), and polyethyleneimine (PEI)-conjugated nanoparticles [38–40].

A literature survey revealed the most commonly used polymers in ophthalmic drug formulations as: poly(alkyl cyanoacrylates), PCL, and poly(lactic acid)/poly(lactic-co-glycolic acid) (PLA, PGA, and PLGA). Moreover, some others such as chitosan, Eudragit RL, Eudragit RS, PS, poly(acrylic acid), and bovine serum albumin (BSA) have also been exploited for ocular delivery as drug-loaded nanoformulations.

Given that the surface of the ocular tissues (eg, cornea conjunctiva) is negatively charged, cationic colloidal nanoparticles are expected to confer better penetration potential through the ocular membranes and barriers. Of the polymers used for ocular delivery, few polymers (eg, chitosan, Eudragit RL, and Eudragit RS) yield positively charged nanoparticles [16]. Among the biodegradable polymers, the poly(lactic-co-glycolic acid) copolymers (PLA, PGA, and PLGA) have been widely

utilized as the most promising biodegradable materials, and they have also been reported to be the safest polymers successfully used *in vivo* with no significant toxicity [41–44].

Agnihotri and Vavia [41] successfully loaded diclofenac sodium in PLGA nanosuspensions, which were applied to rabbit eye and examined with a modified Draize test. These polymeric nanoparticles seemed to be devoid of any irritant effect on cornea, iris, and conjunctiva. PLGA nanoparticles incorporating flurbiprofen decreased inflammation in the rabbit eye after topical instillation [45]. Furthermore, the intravitreal injections of a suspension of polylactic acid micro- and nanospheres containing 1% adriamycin/doxorubicin were reported to provide sustained, first-order release for approximately 2 weeks.

Chitosan, a deacetylated chitin, is a biodegradable, biocompatible, and nontoxic polymer whose nanoparticles have been demonstrated to penetrate effectively conjunctival and corneal epithelial cells. It is a promising ophthalmic vehicle because of its probable superior mucoadhesiveness caused by electrostatic interactions with the negative charges of the mucosal layers.

Cyclosporine A–loaded chitosan nanoparticles resulted in significantly higher corneal and conjunctival drug levels than those treated with a suspension of cyclosporin A in a chitosan aqueous solution or in water [46]. It has also been demonstrated that the amounts of fluorescent nanoparticles in cornea and conjunctiva were significantly higher than those of a control solution. These amounts were fairly constant for up to 24 h. Also, a higher retention of chitosan nanoparticles in the conjunctiva compared with in the cornea was observed [47].

Nanosuspensions

Nanosuspensions consist of pure, poorly water-soluble drugs suspended in an appropriate dispersion medium. Nanosuspension technology can be better utilized for drug compounds that form crystals with high energy content, which renders them insoluble in either organic (lipophilic) or hydrophilic media. Suspensions of polymeric nanoparticles, which are prepared from inert polymeric resins, can be utilized as important drug delivery vehicles, capable of prolonging drug release and enhancing bioavailability. Since these carriers do not irritate cornea, iris, or conjunctiva, they act as an inert carrier for ophthalmic drugs [48]. Flurbiprofen (FLU), loaded in polymeric nanoparticle suspensions prepared from Eudragit RS 100 and Eudragit RL 100 polymer resins, is reported to prevent myosis induced during extracapsular cataract surgery. FLU is a nonsteroidal antiinflammatory drug (NSAID) that inhibits cyclooxygenase and, thus, antagonizes papillary

constriction during intraocular surgery. It also reduces the infiltration of polymorphonuclear leukocytes (PMNs) in the aqueous humor and, thus, significantly decreases postsurgical edema following intraocular surgery. The positive charge on the nanoparticle surface facilitates their adhesion to the corneal surface [49]. Thus, it can be accepted that the use of nanosuspensions in ophthalmic pharmaceutical formulations is an attractive research area, offering a great possibility to overcome the inherent difficulties associated with ocular drug delivery [50]. Nanosuspensions have a mean size around 100 nm and a positive charge; this makes them suitable for ophthalmic applications.

Eudragit RS100 possesses appropriate stability and size distribution characteristics together with positive surface charge, and it is considered a suitable ocular drug carrier [49]. The positively charged Eudragit RS100 nanoformulations may interact with anionic mucins presented in the tear film, and cause consequential prolongation of drug residency time on the corneal surface [51]. The ERL nanoparticles containing cloricromene (a coumarine derivative with antithrombotic and antiischemic activities) with positive zeta potential values (+27.3 mV) and a particle size of 80 nm were topically applied to rabbit eyes and showed no sign of toxicity or irritation to ocular tissues. A sustained release was observed *in vitro* as well as *in vivo*, resulting in a doubled area under the curve compared with an aqueous solution [52].

Nanosuspensions of methylprednisolone acetate were formulated using Eudragit RS and assessed for inhibition of inflammatory symptoms in rabbits with endotoxin-induced uveitis. It was found that the utilization of MPA-ERS nanosuspensions confers a controlled ocular delivery of MPA [53]. Application of nanosuspensions as a noninvasive approach seems to be a safer controlled ocular delivery of antiinflammation agents for inhibition of uveitis symptoms. Similar results have been reported for ibuprofen and flurbiprofen [49,54].

Nanocrystals

Nanocrystals are nanoparticles composed of 100% drug without any matrix material, typically with a size range between 200 and 500 nm [33]. The physicochemical properties of nanocrystals depend on the type of stabilizer—that is, nonionic surfactants (eg, polysorbates, poloxamines, and poloxamer) and ionic surfactants (eg, bile salts and alkyl-sulfonates). Drug nanocrystals can be considered as a universal formulation approach for delivery of poorly soluble drugs. The salient advantage of nanocrystals is the fact that they can be delivered through various administration routes,

including ophthalmic means, to create systems with prolonged retention times. They are also a simple drug delivery system that is easy to produce and use. Currently, there are few studies investigating NSAIDs in the form of nanocrystals for ophthalmic application, because the major prerequisite for nanocrystal formulation is the hardness of the drug crystals [55].

Dendrimers

Dendrimers are macromolecular compounds made up of a series of branches around an inner core. They are attractive systems for drug delivery because of their nanometer size range, ease of preparation and functionalization, and ability to display multiple copies of surface groups for biological recognition processes. As a result, they can be used as an effective vehicle for ophthalmic drug delivery [56]. Robinson et al. [56] suggested the use of bioadhesive polymers, such as PAAs, to improve drug delivery and release by optimizing contact with the absorbing area in order to prolong residence time and decrease dosage frequency. These bioadhesive polymers, however, are associated with problems like blurred vision and formation of a veil in the corneal area, leading to loss of eyesight. However, these problems are circumvented when dendrimers like poly(amidoamine) (PAMAM) are used, which are liquid or semisolid polymers and have several amine, carboxylic, and hydroxyl surface groups, which increase with the generation number (G0, G1, G2, etc.). This exceptional architecture of PAMAM dendrimers allows excellent solubilization of poorly water-soluble drugs into their inner zones containing cascading tiers of branch cells with radial connectivity to the initiator core and an exterior or surface region of terminal moieties. So, greater possibilities can be explored by using dendrimers as ophthalmic drug delivery vehicles [57].

Dendrimers are composed of concentric, geometrically progressive layers created through radial amplification from a single, central initiator core molecule containing either three or four reactive sites such as ammonia or ethylene diamine. These nanoscale macromolecules are three-dimensional and highly branched monodispersed nanostructures that are obtained by an iterative sequence of reaction steps producing a precise, unique branching structure [58].

These nanostructures provide globular nanosystems of 1–100 nm depending on the molecular weight and number of generations. A nanostructure's surface ultimately determines its interactions with its environment, as a result of which drugs and genes can be incorporated with and released in a controlled manner [59]. Interestingly, the influence of a controlled incremental increase in size, molecular weight, and number of amine, carboxylate, and hydroxyl surface groups in

several series of PAMAM dendrimers for controlled ocular drug delivery was investigated. The residence time for various generations of the dendrimers (1.5, 2–3.5, and 4) in the New Zealand albino rabbit resulted in longer residence time for the solutions containing dendrimers with carboxylic and hydroxyl surface groups, which largely depended on size and molecular weight [60].

The dendrimer surface could be further modified for enhanced performance in the formulation of ocular nanomedicines and to deliver an anti-vascular endothelial growth factor (VEGF) oligonucleotide (ODN) into the eyes of rats [61].

Liposomes

Liposomal nanomedicines (LNMs) were first developed to encapsulate small conventional therapeutic drugs; the earliest attempts involved passive entrapment of drugs, resulting in rapid production of stable, homogeneous populations of large unilamellar vesicles (100 nm). Owing to the composition of LNMs, they are biodegradable and relatively nontoxic, which make them interesting as drug delivery systems. Due to the unique architecture of the nanoliposomes, they facilitate drug absorption through the corneal and conjunctival epithelial cells [62].

Liposomes are closed vesicles (small lipid vesicles) composed of a phospholipid bilayer, and water-soluble drugs can be incorporated into their aqueous phase, whereas lipid-soluble drugs can be incorporated into their lipid phase [63]. Liposomes have various advantages as drug carriers:

1. Because they are noncovalent aggregates, their lipid composition, size, and electric charge can be easily controlled [64,65].
2. Their modification, with surface polymers, carbohydrates, and antibodies, can be easily achieved to facilitate targeting [66].
3. Liposomes have almost no toxicity and low antigenicity [67].
4. Liposomes can be biodegradable and metabolized in vivo [67].
5. Properties such as membrane permeability can be controlled to some extent [68].
6. Liposomes can hold various types of solutes with different properties and molecular weights, such as fat-soluble molecules [68] water-soluble molecules [69], and amphiphilic molecules [70].

Because of these characteristics, studies have been conducted on the intravitreal injection of drug-bearing liposomes and have demonstrated that the release of the drug can be controlled, the half-life of the drug inside the vitreous body can be prolonged, and the toxicity of the drug can be reduced [71–76].

The stability of the drug inside the vitreous humor can be improved even further by adding polyethylene glycol (PEG) to the surface of the liposomes, since PEG modification of liposomes sterically stabilizes them by covering the liposomal surface with a fixed aqueous layer [76]. Other reports have also demonstrated the usefulness of liposomal formulations after intravitreal injection using the following drugs: amikacin, amphotericin B, a model antisense oligonucleotide, bevacizumab, cyclosporine, 5-fluorouridine 5'-monophosphate, fluconazole, GCV, gentamicin, tacrolimus, tobramycin, vasoactive intestinal peptide, an angiogenesis inhibitor, tilisolol, and ofloxacin [77].

Liposomes and other artificial vesicles such as niosomes and disomes have been successfully utilized as vehicles for ophthalmic drugs (eg, oligonucleotides, acetazolamide, pilocarpine HCl, cyclopentolate, and timolol maleate), resulting in improved ocular bioavailability. Of these, positively charged nanostructures seem to be preferentially captured at the negatively charged corneal surface and slow down drug elimination by lacrimal flow [15,78].

Microemulsions and Nanoemulsions

Microemulsions have good tissue permeability because of the small size of the micelles and the presence of a surfactant among the components, and they have proven to be effective for ophthalmic drugs [79]. The instillation of microemulsions containing dexamethasone in the eyes of rabbits enhanced intraocular permeability [80].

Nanoemulsions are nanometer droplets made by the heterogeneous dispersions of two immiscible liquids (oil-in-water or water-in-oil) to provide a transparent ocular drug delivery system. They are unique as they can solubilize both hydrophobic and hydrophilic drugs to improve the stability, half-life, and therapeutic efficacy of the drug delivery. Moreover, they provide a large interfacial area compared to the small droplet size. For example, lecithins have been used as the major emulsifiers in the preparation of ocular nanoemulsions [20,81].

PRODUCTION OF NANOMEDICINES

There are many methods for producing nanomedicines, which depend, among other things, on the raw materials and the physicochemical properties of the drug. Preparation methods of nanoparticles include the following: nanoprecipitation, emulsion/solvent evaporation, the double-emulsion solvent evaporation method, the salting-out method, ionic gelation, emulsification solvent diffusion, the dialysis method, the

supercritical fluid method, and the high-pressure homogenization method.

Nanoprecipitation Method

This can also be referred to as the solvent displacement method. Here, an organic solvent miscible with water is used to dissolve the polymer. The drug is then incorporated into this mixture. The polymer-drug-solvent mixture is then injected into an aqueous phase containing a surfactant or stabilizer. When the organic phase comes in contact with the aqueous phase, diffusion of the organic solvent into the aqueous phase leaves "less solvent" available for polymer dissolution, thereby causing the polymer and drug to precipitate out of the solution. This can be attributed to a difference in the selective affinities of the solvent for the polymer and water, leading to a displacement reaction that causes the polymer existing in the molecular state in the organic solvent to be precipitated as nanoparticles. Also, at the liquid interface exists a surface tension that, alongside solvent flow and diffusion, causes turbulence that gives rise to polymer-containing solvent droplets. Upon evaporation of the solvent, polymer precipitates containing the drug are formed in the nanosize range [82,83]. This method is suitable for hydrophobic drugs and has been used by several authors to successfully produce nanoparticles [84–86].

Emulsion Solvent Evaporation Method

As the name implies, this involves two steps: emulsion formation, and solvent removal via evaporation. It is suitable for forming polymeric nanoparticles. Here, a suitable polymer and organic solvent are selected. The organic solvent must be capable of dissolving both the polymer and the drug. Frequently used organic solvents include ethylacetate, chloroform, and dichloromethane. However, toxicity has limited the use of chloroform and dichloromethane in recent times.

The polymer and drug are first dissolved in a suitable quantity of the solvent to form the organic phase. The surfactant and water are mixed together to form the aqueous phase. Subsequently, both phases are mixed together and homogenized using an emulsifier or homogenizer (eg, Ultra Turrax homogenizer). This yields an oil-in-water (o/w) emulsion. Continuous stirring of the emulsion formed leads to an evaporation of the organic solvent. Removal of the organic solvent causes a precipitation of the drug-containing polymer, yielding nanoparticles, the size of which depends on factors such as surfactant concentration, homogenization speed, and time. Ultracentrifugation of the mixture leads to a separation of the two phases. The nanoparticles can then be collected; washed with distilled water to remove any

residual organic solvent on their surface; and then dried, lyophilized, or removed by decreased pressure under a vacuum environment. This method is suitable for lipophilic drugs, but it is limited by the use of organic solvents that may be hazardous to humans and animals [87,88].

Double-Emulsion Solvent Evaporation Method

This is a modification of the emulsion solvent evaporation method. Here, a multiple emulsion (w/o/w) is formed as a result of a double emulsification process. Usually, a hydrophilic drug is mixed with water and incorporated into the polymer-containing organic solvent. This mixture is then emulsified to form a water-in-oil (w/o) emulsion. The emulsion thus formed is then added to a second aqueous phase (containing a surfactant) and stirred continuously to form a w/o/w emulsion. This method is suitable for preparing hydrophilic drugs and has been successfully used by several researchers to prepare such drugs [89–92].

Salting-Out Method

In this method, electrolytes with suitable solubility in water are used. When added to the organic solvent–water mixture, they precipitate the organic solvent from the water mixture, hence the term *salting out*. Usually, the polymer and drug are mixed with a suitable organic solvent. This is then mixed with an aqueous solution containing a stabilizer and the salting-out agent (eg, magnesium chloride, calcium chloride, or sucrose) [93,94].

Ionic Gelation Method

Here, biodegradable polymers like chitosan, sodium alginate, and gelatin are used [94]. It involves a complexation process in which a charged hydrophilic polymer is complexed with a multivalent cation (eg, CaCl_2) or polyanion (eg, sodium tripolyphosphate) to form nanometer-sized highly viscous gel particles. The gelation arises from electrostatic interaction between the positively charged polymer and the negatively charged polyanion, leading to a phase transition from liquid to gel at room temperature. This method was first reported by Calvo et al. [95] for the preparation of chitosan-based nanoparticles.

Emulsification Solvent Diffusion Method

This is a modified version of the solvent evaporation method. In this technique, an organic solvent mixture can be used (eg, acetone and dichloromethane). The

polymer is first dissolved in this organic solvent mix and subsequently added to a surfactant-containing aqueous phase with moderate stirring. This leads to an emulsification process. After emulsification, the emulsion droplets formed are a mixture of drug, polymer, and organic solvent. The water-miscible organic solvent then diffuses into the aqueous external phase due to its selective affinity for water as well as lower concentration in the aqueous phase. This causes a “shrinking” of the emulsion droplets leading to “nanosized” particles. This process is facilitated by the gentle mechanical stirring that takes place continuously after the emulsion is formed. Consequently, the polymer–drug combination is then precipitated out of the bulk solution as nanoparticles [96,97]. Nanoparticle recovery can then be facilitated by ultracentrifugation and filtration. The collected nanoparticles are then washed with water and freeze-dried to remove any residual solvents present. Polymer–solvent ratio, homogenization speed and time, surfactant type, and concentration are some of the factors that affect the ultimate size of the nanoparticles. The evaporation of the solvent dichloromethane will lead to particle agglomeration that is further increased if the polymer solution volume is high. This process, however, has scale-up limitations since the ultracentrifugation process required to recover the nanoparticles cannot be optionally utilized industrially. The toxicity of the solvent, dichloromethane, also poses a health concern.

Consequently, other less toxic solvents have been explored. Murakami et al. [96] explored the possibility of using a modified approach in which a less toxic solvent (eg, methanol or ethanol) was employed and an exclusively low hydrolyzation and polymerization grade of polyvinyl alcohol (PVA) was used. This thus gave rise to an ethanol–acetone or methanol–acetone mixture. Their study showed that the replacement of dichloromethane with ethanol or methanol had the twin effect of preventing agglomeration of particles even at high polymer solution volumes as well as simplification of the nanoparticle recovery process. A simple ultrafiltration process is employed in sample recovery since both solvents are water miscible and thus could easily diffuse out of the polymer–drug–solvent mixture. A limitation of this method is the large volumes of solvents required. Also, only hydrophobic drugs can be produced via this method.

Supercritical Fluid Method

The commonly used methods here are the supercritical antisolvent (SAS) process and the rapid expansion supercritical solution (RESS). The SAS approach involves the use of two miscible liquids,

one of which is a supercritical fluid. Examples of supercritical fluids include supercritical CO₂, supercritical ethylene, supercritical ammonia, and supercritical ethane. However, among these, supercritical CO₂ is mostly favored for use in pharmaceutical formulations due to its nontoxicity, nonflammability, as well as low cost [98,99].

In this technique, the solute (drug) is usually soluble in the nonsupercritical fluid. The drug and polymer are first dissolved in the organic solvent and then emulsified in a surfactant-containing aqueous medium. After emulsification, o/w emulsion is formed containing an internal phase made of organic solvent, polymer, and drug. A supercritical fluid is then passed through this emulsion at the temperature and pressure needed to maintain it in the supercritical state. This fluid extracts the organic solvent, thus causing a precipitation of the polymer/lipid-containing nanoparticles as a result of a selective affinity and extraction of the solvent by the supercritical fluid in the aqueous solution. The nanoparticles are then collected via ultracentrifugation or ultrafiltration [82,100].

Rapid Expansion Supercritical Solution (RESS)

This is suitable for forming particles in the nanometer size range. Particles thus formed exhibit improved dissolution behavior, making them suitable for poorly soluble drugs. In this method, the solute is dissolved in a supercritical fluid. This solution is then passed through a tiny nozzle into a region of lower pressure. The lowering of the pressure causes the supercritical fluid to expand rapidly, thus losing its "solvent power." This leads to a precipitation of the solute particles. A major drawback of this method is the production of micrometer-sized particles alongside those in the nanometer range. In order to overcome this, the technique of rapid expansion of supercritical fluid into liquid solvent was developed. In this technique, a liquid solvent is introduced into which the supercritical fluid expands. The presence of this solvent reduces particle agglomeration that usually occurs in the former method, thus enabling the production of particles predominantly in the nanometer range [101].

Homogenization Method

This comprises two techniques: the hot-melt homogenization technique for heat-stable drugs, and the cold-melt homogenization technique for heat-labile drugs. Particle size of drugs is decreased by impact, shear, cavitation, and turbulence [102]. In the hot homogenization method, the lipid is melted at a temperature that is about 10 °C above its melting temperature. The

surfactant solution is also heated to the same temperature to prevent congealing of the lipid matrix during homogenization. The mixture is subjected to high-pressure homogenization using an Ultra-Turrax homogenizer at the same temperature for a specific time duration. Usually, repeat cycles are carried out to produce desired particle sizes as well as ensure homogeneity of particles. In some instances, supercooled melts are formed, arising from an inability of the lipid droplets to crystallize in solution at the reduced temperature. Typical problems with this method include thermal degradation of heat-labile drugs, leaking of drugs out of the lipid upon cooling, and the formation of supercooled melts [103]. The cold homogenization technique was developed to overcome the challenges of the hot homogenization method. Here, the lipid is first melted, and drug is dissolved/dispersed in it. This mixture is then cooled under dry ice or liquid nitrogen to ensure crystallization, and then ground with a suitable mill (eg, ball mill, jet mill, or mortar mill) to form microparticles [104,105]. After milling, the microparticles formed are dispersed in a cold surfactant solution and homogenized at or below room temperature to yield nanoparticles. Lyophilization could be carried out to increase the stability of the formed nanoparticles. For an effective lyophilization process, cryoprotectants (eg, mannitol, sucrose, and sorbitol) are added to protect the integrity of the nanoparticles during the freeze-drying process.

CHARACTERIZATION OF NANOMEDICINES

Nanoparticles are assessed using the following parameters: morphology and particle size, surface charge, stability, crystallinity, drug loading, deformability, and so on.

Morphology and Particle Size Determination

Here, microscopy is most frequently used to determine this. Frequently used equipment includes a scanning electron microscope (SEM), transmission electron microscope (TEM), atomic force microscope (AFM), and freeze fracture cryo-TEM. These microscopic techniques all give three-dimensional images of the nanoparticles. However, the SEM has a limitation of giving a three-dimensional image of the particles without determining their particle size. An AFM can be used to visualize, image, and measure the particle size of nanoparticles. Dynamic light scattering can also be used to determine particle size and size distribution (polydispersity index) of nanoparticles. The results are often

presented as mean particle size and polydispersity index (PDI). PDI values between 0.1 and 0.25 are most acceptable as they indicate a narrow size distribution, while PDI values greater than 0.5 suggest a wide size distribution of nanoparticles [106,107].

Loading Capacity

This is usually determined when preparing solid lipid nanoparticles. It is a measure of the drug-carrying capacity of the lipid phase. It is usually expressed as a percentage of the entrapped drug relative to the lipid phase (lipid and drug) [108]. Solubility of the drug in the lipid melt as well as polymorphic form of the lipid or chemical and physical structure of the solid lipid matrix are some of the factors affecting the loading capacity of a lipid matrix [109].

Surface Charge or Zeta Potential

The ability of nanoparticles to exist singly or in aggregates is a function of their surface charge or zeta potential. Usually, a zetasizer is used to measure this. Some zetasizers can measure both the surface charge and size of particles, thus performing a dual purpose [110].

Crystallinity

Crystallinity determinations are usually performed with differential scanning calorimetry (DSC) or X-ray powder diffraction (XRPD) using a wide-angle X-ray powder diffraction (WAXD). DSC measurements give the melting enthalpies of the drug substances, excipients, and drug–excipient combinations. These could be useful in determining the compatibility of excipients with drug and other substances as well as determining the presence of polymorphs. Information on the ability of the formulated nanomedicines to retain the incorporated drug could be obtained from these measurements.

DRUG RELEASE

Drug release studies are usually carried out in vitro, ex vivo, or in vivo.

In Vitro Determination

This involves determining drug release in simulated body fluids and using artificial membranes of different molecular weight cutoffs to mimic the barrier provided by the cornea. Usually, drug release from nanoparticles can occur via any of these three mechanisms:

1. Erosion of the matrix to release drugs from the core.

2. Swelling and subsequent diffusion of drug molecules out of the nanoparticle matrix.
3. Desorption of the drug molecules bound to the surface of these nanoparticles. This mechanism or phenomenon is usually responsible for the “burst effect” experienced with some formulations. Thorough washing of the nanoparticles after preparation could prevent this in cases where there are surface-bound drug molecules.

Ex Vivo Evaluation and Use of Bioengineered Cornea

In ex vivo studies, viable excised cornea from rabbit, pig, goat, or other mammals is used as the permeability barrier. Alternatively, a construct of the cornea is bioengineered in the laboratory and used as the permeability barrier to assess ocular formulations [6,111]. Bioengineering of cornea is done using stroma and epithelial cells obtained from donor cornea.

In Vivo Evaluation

The modified release properties of nanoparticles as well as their small particle size make them useful for delivering a vast array of drugs, both oral and parenteral. The intended use of the drug and administration route will determine the animal species and model to be used for in vivo evaluation. Typical assays carried out include pharmacokinetic and pharmacodynamic evaluations of administered drugs, as well as toxicity profiling of the administered nanoparticles usually because of the size of these particles. Nanoparticles can be taken up by cells or pass across biological membranes via different mechanisms (eg, passive diffusion, movement across tight junctions, or endocytosis). Nanoparticle characteristics such as lipophilicity and surface charge influence passive diffusion across biological membranes [112–114].

CONCLUSION AND FUTURE PROSPECTS

The loss of sight is always devastating to any person, and a patient would do anything to avoid blindness. This raises the expectations of the pharmaceutical industries in drug development for ophthalmology. Therefore, any nanomedicine developed for the eye would have a large market. Ocular nanomedicines could achieve noninvasive sustained drug release for eye disorders in both anterior and posterior segments of the eye. While designing nanomedicines for the eye, a clear understanding of the complexities of the pathological conditions and physiological barriers in normal and diseased eyes

would greatly facilitate further development of the process. An ideal nanomedicine should achieve an effective drug concentration at the target tissue for an extended period of time while minimizing systemic exposure, and it should be both comfortable and easy to use. One of the methods to overcome the drawbacks of present nanoparticle delivery systems is to combine technologies as obtained in lipogelosomes, bioadhesives, and hybrid nanoparticles. This would increase significantly ocular bioavailability of topically administered drugs. Many novel products are expected to appear in the field of ophthalmology in the near future.

References

- [1] Barar J, Asadi M, Mortazavi-Tabatabaei SA, Omid Y. *J Ophthalmic Vis Res* 2009;4(4):238–52.
- [2] Lang JC. *Adv Drug Deliv Rev* 1995;16:39–43.
- [3] https://www.google.com.ng/search?q=cornea+anatomy&rlz=1C2REZB_enNG632NG632&biw=1024&bih=461&tbm=isch&tbo=u&source=univ&sa=X&sqi=2&ved=0CCcQ7AlqFQoTCOu6mrPNpqcCFQIMFAodDh8HQA#imgsrc=2qdyP-UEgNUTM%3A.
- [4] https://www.google.com.ng/search?q=cornea+anatomy&rlz=1C2REZB_enNG632NG632&biw=1024&bih=461&tbm=isch&tbo=u&source=univ&sa=X&sqi=2&ved=0CCcQ7AlqFQoTCOu6mrPNpqcCFQIMFAodDh8HQA#imgsrc=CNmsQEFKNJ3QTM%3A.
- [5] Patel PB, Shastri DH, Shelat PK, Shukla AK. *Sys Rev Pharm* 2010; 1:113–20.
- [6] Attama AA, Reichl S, Müller-Goymann CC. *Curr Eye Res* 2009; 34(8):698–705.
- [7] Anand BS, Dey S, Mitra AK. *Expert Opin Biol Ther* 2002;2: 607–20.
- [8] Kuno N, Fujii S. *Polymers* 2011;3(1):193–221. <http://dx.doi.org/10.3390/polym3010193>. <http://www.mdpi.com/2073-4360/3/1/193/htm>.
- [9] Ito YA, Walter MA. In: Shimon Rumelt, editor. *InTech*, <http://dx.doi.org/10.5772/54653>. Available from: <http://www.intechopen.com/books/glaucoma-basic-and-clinical-aspects/ngenetics-and-environmental-stress-factor-contributions-to-anterior-segment-malformations-and-glauco>.
- [10] Duvvuri S, Majumdar S, Mitra AK. *Expert Opin Biol Ther* 2003;3: 45–56.
- [11] Gaudana R, Ananthula HK, Parenky A, Mitra AK. *AAPS J* 2010; 12(3):348–60.
- [12] Gaudana R, Jwala J, Boddu SH, Mitra AK. *Pharm Res* 2009;26(5): 1197–216.
- [13] Mannerman E, Vellonen KS, Urtti A. *Adv Drug Deliv Rev* 2006; 58(11):1136–63.
- [14] Dey S, Anand BS, Patel J, Mitra AK. *Expert Opin Biol Ther* 2003; 3(1):23–44.
- [15] Sahoo SK, Dilnawaz F, Krishnakumar S. *Drug Discov Today* 2008;13(3–4):144–51.
- [16] Bu HZ, Gukasyan HJ, Goulet L, Lou XJ, Xiang C, Koudriakova T. *Curr Drug Metab* 2007;8(2):91–107.
- [17] Vandervoort J, Ludwig A. *Nanomedicine* 2007;2(1):11–21.
- [18] Herrero-Vanrell R, Refojo MF. *Adv Drug Deliv Rev* 2001;52(1): 5–16.
- [19] Jose-Alonso M. *Biomed Pharmacother* 2004;58(3):168–72.
- [20] Chaurasia SS, Lim RR. *J Funct Biomater* 2015;6:277–98.
- [21] Sharma A, Tandon A, Tovey JC, Gupta R, Robertson JD, Fortune JD, Klibanov AM, Cowden JW, Rieger FG, Mohan RR. *Nanomedicine* 2011;7:505–13.
- [22] Sharma A, Rodier JT, Tandon A, Klibanov AM, Mohan RR. *Mol Vis* 2012;18:2598–607.
- [23] Chowdhury S, Guha R, Trivedi R, Kompella UB, Konar A, Hazra S. *PLoS One* 2013;8:e70528.
- [24] Tandon A, Sharma A, Rodier JT, Klibanov AM, Rieger FG, Mohan RR. *PLoS One* 2013;8:e66434.
- [25] Rajasekaran A, Arul Kumaran KSG, Preetha JP, Karthika K. *Int J PharmTech Res* 2010;2:668–74.
- [26] Qingguo X, Kambhampai SP, Kannan RM. *Middle East Afr J Ophthalmol* 2013;20:26–37.
- [27] Prow TW, Bhutto I, Kim SY, Grebe R, Merges C, McLeod DS. *Nanomedicine* 2008;4:340–9.
- [28] Raju HB, Hu Y, Vedula A, Dubovy SR, Goldberg JL. *PLoS One* 2011;6:e17452.
- [29] Lambert G, Guilatt RL. *Drug development report industry: overview details*, vol. 33; 2005. p. 1–2.
- [30] Wattman SR, Patrowicz TC. *Invest Ophthalmol* 1970;9:966–70.
- [31] Schoenwald RD, Smolen VF. *J Pharm Sci* 1971;60:1039–45.
- [32] <http://www.medscape.com/viewarticle/708608>.
- [33] Bourgies J, Alanso M. *Invest Ophthalmol Vis Sci* 2003;440: 3562–9.
- [34] He C, Hu Y, Yin L, Tang C, Yin C. *Biomaterials* 2010;31(13): 3657–66.
- [35] Pignatello R, Ricupero P, Bucolo C, Maugeri F, Maltese F, Puglisi G. *AAPS PharmSciTech* 2006;7:192–8.
- [36] Kompella UB, Sundaram S, Raghava S, Escobar ER. *Mol Vis* 2006; 12:1185–98.
- [37] Jwala J, Boddu SH, Shah S, Sirimulla S, Pal D, Mitra AK. *J Ocul Pharmacol Ther* 2011;27:163–72.
- [38] Giannavola C, Bucolo C, Maltese A, Paolino D, Vandelli MA, Puglisi G, Lee VHL, Frest M. *Pharm Res* 2003;20:584–90.
- [39] Qaddoumi MG, Ueda H, Yang J, Davda J, Labhasetwar V, Lee VHL. *Pharm Res* 2004;21:641–8.
- [40] Marchal-Heussler L, Sirbat D, Hoffman M, Maincent P. *Pharm Res* 1993;10:386–90.
- [41] Agnihotri SM, Vavia PR. *Nanomedicine* 2009;5(1):90–5.
- [42] Athanasiou KA, Niederauer GG, Agrawal CM. *Biomaterials* 1996;17(2):93–102.
- [43] Dong X, Shi W, Yuan G, Xie L, Wang S, Lin P. *Graefes Arch Clin Exp Ophthalmol* 2006;244(4):492–7.
- [44] Kobayashi H, Shiraki K, Ikada Y. *J Biomed Mater Res* 1992;26(11): 1463–76.
- [45] Vega E, Egea MA, Valls O, Espina M, Garcia ML. *J Pharm Sci* 2006;95:2393–405.
- [46] De Campos AM, Diebold Y, Carvalho EL, Sanchez A, Alonso MJ. *Pharm Res* 2004;21(5):803–10.
- [47] De Campos AM, Sanchez A, Alonso MJ. *Int J Pharm* 2001; 224(1–2):159–68.
- [48] Van Erdenbrugh B, Froyen L, Vanden Hotter G. *Eur J Pharm Sci* 2008;35:127–35.
- [49] Pignatello R, Bucolo C, Ferrara P, Maltese A, Puleo A, Puglisi G. *Eudragit RS 100*. *Eur J Pharm Sci* 2002;16(1–2):53–61.
- [50] Sting GL, Ing GB, Van Deltlen RG, Younge BR, Leavitt JA. *Eur J Pharm Sci* 1996;103:890–8.
- [51] Dillen K, Vandervoort J, Van den Mooter G, Ludwig A. *Int J Pharm* 2006;314(1):72–82.
- [52] Bucolo C, Maltese A, Maugeri F, Busa B, Puglisi G, Pignatello R. *J Pharm Pharmacol* 2004;56(7):841–6.
- [53] Adibkia K, Omid Y, Siahi MR, Javadzadeh AR, Barzegar-Jalali M, Barar J, et al. *J Ocul Pharmacol Ther* 2007;23(5):421–32.
- [54] Pignatello R, Bucolo C, Spedalieri G, Maltese A, Puglisi G. *Biomaterials* 2002;23(15):3247–55.
- [55] Patton TF, Robinson JR. *J Pharm Sci* 1975;64:1312–6.
- [56] Milhe OM, Myles C, M Kawase JY. *Int J Pharm* 2000;197:239–41.
- [57] Loftsson T, Már Másson T, Jarvein T. *Expert Opin Drug Deliv* 2005;2:335–51.

- [58] Loutsch JM, Ong D, Hill JM. In: Mitra MK, editor. Ophthalmic drug delivery systems. New York (USA): Marcel Dekker, Inc.; 2003. p. 467–92.
- [59] Vandervoort J, Ludwig A. *Eur J Pharm Biopharm* 2004;57(2): 251–61.
- [60] Vandamme TF, Brobeck L. *J Control Release* 2005;102(1):23–38.
- [61] Marano RJ, Toth I, Wimmer N, Brankov M, Rakoczy PE. *Gene Ther* 2005;12(21):1544–50.
- [62] Fenwick BW, Cullis PR. *Expert Opin Drug Deliv* 2008;5(1):25–44.
- [63] Allen TM, Cullis PR. *Science* 2004;303:1818–22.
- [64] Bangham AD, Horne RW. *J Mol Biol* 1964;8:660–8.
- [65] Oku N. *Adv Drug Deliv Rev* 1999;40(1–2):63–73.
- [66] Sapra P, Tyagi P, Allen TM. *Curr Drug Deliv* 2005;2(4):369–81.
- [67] van Rooijen N, van Nieuwmege R. *Immunol Commun* 1980; 9(3):243–56.
- [68] Lopez-Berestein G, Mehta R, Hopfer R, Mehta K, Hersh EM, Juliano R. *Cancer Drug Deliv* 1983;1(1):37–42.
- [69] Oku N, Nojima S, Inoue K. *Biochim Biophys Acta* 1980;595(2): 277–90.
- [70] Klibanov AL, Maruyama K, Torchilin VP, Huang L. *FEBS Lett* 1990;268(1):235–7.
- [71] Tremblay C, Barza M, Szoka F, Lahav M, Baum J. *Invest Ophthalmol Vis Sci* 1985;26(5):711–8.
- [72] Barza M, Baum J, Tremblay C, Szoka F, D'Amico DJ. *Am J Ophthalmol* 1985;100(2):259–63.
- [73] Fishman PH, Peyman GA, Lesar T. *Invest Ophthalmol Vis Sci* 1986;27(7):1103–6.
- [74] Peyman GA, Khoobehi B, Tawakol M, et al. *Retina* 1987;7(4):227–9.
- [75] Peyman GA, Schulman JA, Khoobehi B, Alkan HM, Tawakol ME, Mani H. *Retina* 1989;9(3):232–6.
- [76] Bochot A, Fattal E, Boutet V, et al. *Invest Ophthalmol Vis Sci* 2002; 43(1):253–9.
- [77] Honda M, Asai T, Oku N, Araki Y, Tanaka M, Ebihara N. *Int J Nanomed* 2013;8:495–504.
- [78] Kaur IP, Garg A, Singla AK, Aggarwal D. *Int J Pharm* 2004;269(1): 1–14.
- [79] Vandamme TF. *Prog Retin Eye Res* 2002;21(1):15–34.
- [80] Fialho SL, da Silva-Cunha A. *Clin Experiment Ophthalmol* 2004; 32(6):626–32.
- [81] Calvo P, Vila-Jato JL, Alonso MJ. *J Pharm Sci* 1996;85:530–6.
- [82] Mudgit M, Gupta W, Nagpal M, Pawar P. *Int J Pharm Pharm Sci* 2012;4(2).
- [83] Mandal B, Alexander KS, Riga AT. *J Pharm Pharm Sci* 2010;13(4): 510–23.
- [84] Ahuja M, Dhake SA, Sharma SK, Majumdar KD. *J Microencapsul* 2011;28(1):37–45.
- [85] Aksungur P, Demirbilek M, Denkbaz EB, Vandervoort J, Ludwig A, Unlu N. *J Control Release* 2011;151(3):286–94.
- [86] Yoncheva K, Vandervoort J, Ludwig A. *Pharm Dev Technol* 2011; 6(1):29–35.
- [87] Song CX, Labhasetwar V, Murphy H, Qu X, Humphrey WR, Shebuski RJ, Levy RJ. *J Control Release* 1997;43:197–212.
- [88] Pal SL, Jana U, Manna PK, Mohanta GP, Manavalan R. *J Appl Pharm Sci* 2011;01(06):228–34.
- [89] Pinon-Segundo E, Nava-Arzaluz MA, Lechuga-Ballesteros D. *Recent Pat Drug Deliv Formul* 2012;6(3):224–35.
- [90] Alshamson AWS. *Saudi Pharm J* 2014;22(3).
- [91] Liu J, Qiu Z, Wang S, Zhou L, Zhang S. *Biomed Mater* 2010; 5(6).
- [92] Hussein AS, Abdullah N, Fakrul-razi A. *Adv Polym Tech* 2013; 32(1):E486–504.
- [93] Reis CP, Neufeld JR, Ribeiro AJ, Veiga F. *Nanotech Biol Med* 2006; 2:8–21.
- [94] Nagavarma BVN, Yadav KSH, Ayaz A, Vasudha LS, Shivakumar HG. *Asian J Pharm Clin Res* 2012;5(3).
- [95] Calvo P, Remunan-Lopez C, Vila-Jato JL, Alonso MJ. *J Appl Polym Sci* 1997;63:125–32.
- [96] Murakami H, Kobayashi M, Takeuchi H, Kawashima Y. *Int J Pharm* 1999;187:143–52.
- [97] Niwa T, Takeuchi H, Hino T, Kunou N, Kawashima Y. *J Control Release* 1993;25:89–98.
- [98] Sauceau M, Letourneau JJ, Freiss B, Richon D, Fages J. *J Supercrit Fluids* 2004;31(2):133–40.
- [99] Ting SST, Macnaughton SJ, Tomasko DL, Foster NR. *Ind Eng Chem Res* 1993;32(7):1471–81.
- [100] Chattopadhyaya P, Shekunova BY, Yimb D, et al. *Adv Drug Deliv Rev* 2007;59:444–5.
- [101] Meziani MJ, Pathak P, Hurezeanu R, Thies MC, Enick RM, Sun YP. *Angew Chem Int Ed* 2004;43:7047.
- [102] Pathak P, Mohammed J, Meziani J, Sun Y-P. *Expert Opin Drug Deliv* 2005;2(4):747–61.
- [103] Shukla D, Chakraborty S, Singh S, Mishra B. *Expert Opin Drug Deliv* 2011;8(2):207–24.
- [104] Wan F, You J, Sun Y, et al. *Int J Pharm* 2008;359:104–10.
- [105] Kamiya S, Yamada M, Kurita T, et al. *Int J Pharm* 2008;354: 242–7.
- [106] Lu XY, Wu DC, Li ZY, et al. *Prog Mol Biol Transl Sci* 2011;104: 299–323.
- [107] Cho EJ, Holback H, Lu KC, et al. *Mol Pharm* 2013;10(6): 2093–110.
- [108] Bilati U, Allemann E, Doelker E. *J Microencapsul* 2005;22: 205–14.
- [109] Attama AA, Momoh MA, Builders PF. Lipid nanoparticulate drug delivery systems: A revolution in dosage form design and development. In: Sezer AD, editor. *Recent Advances in Novel Drug Carrier Systems*. Croatia: InTech; 2012. p. 107–40.
- [110] Cooper DL, Harirforoosh S. *PLoS One* 2014;9(1):e87326.
- [111] Attama AA, Reichl S, Müller-Goymann CC. *Int J Pharm* 2008;355: 307–13.
- [112] Cooper DL, Londer CM, Harirforoosh S. *Expert Opin Drug Deliv* 2014;11(10):1661–80.
- [113] Sonaje K, Chuang EY, Lin KJ, et al. *Mol Pharm* 2012;9(5): 1271–9.
- [114] Fenart L, Casanova A, Dehouck B, et al. *J Pharmacol Exp Ther* 1999;291(3):1017–22.

Bioinspired Nanotechnologies for Skin Regeneration

S. Tavakol^{1,2,a}, S. Jalili-Firoozinezhad^{3,a},
O. Mashinchian^{4,5,a}, M. Mahmoudi^{2,6}

¹Iran University of Medical Sciences, Tehran, Iran; ²Tehran University of Medical Sciences, Tehran, Iran; ³University of Lisbon, Lisbon, Portugal; ⁴Nestlé Institute of Health Sciences, Lausanne, Switzerland; ⁵École Polytechnique Fédérale de Lausanne (EPFL), Lausanne, Switzerland; ⁶Stanford University School of Medicine, Stanford, CA, United States

OUTLINE

Introduction to Skin Anatomy	337	Skin Aging	342
<i>Epidermis Layer</i>	338	Advanced Fabrication Strategies in Design of Skin	
<i>Basement Membrane</i>	338	Regeneration Scaffolds	343
<i>Dermis and Hypodermis</i>	338	<i>Electrospinning</i>	343
Frontiers in Skin Regeneration	338	<i>Self-assembly</i>	344
Skin Wound Regeneration	338	<i>Cell-Imprinted Substrates</i>	345
<i>Nanoparticles in Wound Healing</i>	339	<i>Skin 3D Bioprinting</i>	345
Nanoporous Anodic Aluminum Oxide (AAO)	339	Conclusion	347
Metallic Nanoparticles	339	References	348
Nonmetallic NPs	340		
<i>Nanofibers in Wound Healing</i>	341		
Natural Polymer Nanofibers	341		
Synthetic Polymer Nanofibers	342		

INTRODUCTION TO SKIN ANATOMY

For a better designing of bioinspired skin substitute, one should have a basic knowledge of the skin structure. Skin (integument) is the largest organ by both weight (10–20%) and surface area (approximately 1.8 m²) in an adult human body [1]. The skin has multistructural layers. The outermost layer is an epidermis layer

containing keratinocytes, melanocytes, Langerhans, and Merkel cells. The outermost layer is connected to the dermis layer (connective tissue) through the basement membrane. However, a dermis layer (sweat glands, hair follicles, nervous cells, lymph, and blood vessels) has been attached to the loose connective tissue and is rich in fat. This deeper layer is called the subcutis (hypodermis) [2].

^a These authors contributed equally to this work.

Epidermis Layer

Epidermis layer varies in thickness ranging from 0.05 to 1.5 mm [2], and its turnover is 35–45 days [3]. It is a stratified squamous epithelium; its major cells are keratinocytes, which are involved in keratin synthesis; and it comprises five layers: stratum corneum, lucidum, granulosum, spinosum, and basale. However, stratum lucidum usually is not easily detectable in the thin epidermis layer. Each of these layers, according to their specific cell distribution, has its own task. Merkel cells and melanocytes involved in light touch sensation and ultraviolet (UV) protection are mainly found in stratum basale, while immunologic cells predominantly locate in the middle of stratum spinosum.

In fact, mature keratinocytes in the form of hexagonal and nonviable cornfield cells (corneocytes) are found in stratum corneum. Nevertheless, each one is surrounded by a protein envelope and lipid bilayer. Keratin inside the corneocytes (10–30 layers) results in the corneocyte absorbing three times its weight in water [2,4].

Basement Membrane

This layer has a complex structure with a capillary projection from the dermis layer that is involved in epidermis nourishment. It is notable that this layer gets flattened during the aging process [2].

Dermis and Hypodermis

The dermis layer varies in thickness ranging from 0.6 to 3 mm, and it is composed of a thin papillary and a thicker reticular layer. Up to 70% of dermis is composed of collagen fibers (having the major share), elastin, and proteoglycan. These biomaterials are responsible to provide strength, elasticity, viscosity, and hydration of skin. Besides sweat glands, lymphatic glands, papillary, nerve cells and fibers, striated muscles, and hair follicles are present in this layer [2]. In fact, the dermis and hypodermis layers are largely composed of connective and fat tissue, respectively. The main role of hypodermis is related to insulator and mechanical shock absorbing [4].

FRONTIERS IN SKIN REGENERATION

Due to the fact that major damage to the skin, as a critical bodily barrier, can endanger human life, exploration and development of new strategies to regenerate skin substitutes are of urgent need in the medical community. To the best of our knowledge, for the first time, Billingham and Reynolds grew sheets of pure epidermis in cell culture for the application in wound healing in 1952 [5]. Then, Karasek and Charlton used collagen gel

to grow postembryonic skin epithelial cells in 1971 [6], while Bell et al. used grown human fibroblasts on rat tail tendon collagen [7]. Later, investigations of Bell and coworkers on co-culture of neonatal epidermal keratinocytes, dermal fibroblasts, and melanocytes disclosed that in the presence of UV light, pigment transferred from the melanocytes to keratinocytes [8–12]. Green's group isolated and propagated human keratinocytes and applied the cells in clinical application about 30 years ago. He discovered that both epithelial cells and connective tissue are necessary for skin regeneration. However, epithelial cells are also needed for the growth of connective tissue and the other way around, as they have capability to stimulate each other's growth [13,14].

During recent years, nanoscience approaches have been recognized as promising methods to develop skin substitutes to overcome obstacles in wound healing, skin regeneration, and aging problems. In the “Skin Wound Regeneration” section, the wound-healing process is discussed in more detail.

SKIN WOUND REGENERATION

According to a previous report, approximately 1.3–3 million people in the United States suffer from pressure ulcers, and more than 10–15% of diabetic patients are at risk of developing ulcer due to disturbances in cellular and biochemical events involved in the skin's integrity and regeneration [15].

Four events are involved in wound healing: hemostatic, inflammation, proliferation, and remodeling [16]. The first step following injury is hemostatic events. Afterward, the coagulation and complement cascade trigger, and degranulation of platelets happen, and platelet-derived growth factor (PDGF), transforming growth factor- β (TGF- β), endothelial growth factor (EGF), fibroblast growth factor (FGF), platelet-derived angiogenesis factor, serotonin, bradykinin, thromboxane A₂, platelet-activating factor, platelet factor IV, histamine, and prostaglandins are released from the platelets [16,17]. After release of cytokines and growth factors derived from platelets, inflammatory responses along with infiltration of immune cells (eg, neutrophils and macrophages) are started; these result in cellular debris removal and bacteria killing by macrophages and secretion of chemical components by neutrophils. This phase will take about 6 days [17].

The third stage starts 2–3 days post injury; it is involved in angiogenesis and extracellular matrix (ECM) formation by fibroblasts and endothelial cells' activation and proliferation in response to chemokines derived from the previous stage [18,19]. The final outcome of this stage is migration of keratinocytes to

the injury sites, and tissue granulation [16]. Usually 3 weeks post injury, the last stage of wound healing starts off with wound remodeling and contraction, which take up to 2 years [19]. In this stage, type III collagen fibers are exchanged with type I collagen to enable cross-linking of collagen fibers [20,21]. However, remodeling of collagen fiber into an organized structure never induces strength more than 80% of that of the intact skin [22].

The largest obstacle in a chronic wound is related to an imbalance between production and degradation of some molecules, such as collagen. In fact, a higher quantity of protease [like matrix metalloproteinase (MMP)] [23] and lower cytokines and growth factors [24] exist in a chronic wound as compared to an acute wound. Besides, the main problem in burn injuries is related to severe damage of the skin's capillaries. In diabetic foot ulcers, however, the healing process cannot progress to the remodeling phase, and other mechanisms are involved in delaying wound healing [25]. With regard to the problems raised, it is critical to find methodologies to effect expedited wound closure with inherent skin appendages. As re-epithelialization is necessary for entire cell–cell contact between keratinocytes, the bio-inspired substitutes and skin grafts that keep moisture in the wound bed will safeguard favorable re-epithelialization. To that end, nanotopography mechanotransduction signals derived from the mechanical strength and porosity of the scaffold create an ideal engineered ECM for the cells involved in the skin regeneration cascade and improve wound repairing. The following sections of this chapter will look at the application of bioinspired nanosubstrates for wound healing in more detail.

Nanoparticles in Wound Healing

Nanoporous Anodic Aluminum Oxide (AAO)

In 2004, Poinern et al. developed a nanoporous AAO. Their investigation revealed that keratinocytes could properly attach to the AAO nanosubstrate [26]. Later on, researchers found that variation of pore sizes in the AAO nanostructures can trigger the rate of cell (eg, keratinocytes and fibroblast epidermal cells) proliferation and migration [27].

To that end, Cellumina Pty Ltd brought out a nanoporous AAO with channels of 50–200 μm thicknesses for burn-healing applications. They supposed that skin cells could attach to this substrate and properly proliferate. Then, proliferated autologous cells could detach or remain with the nanostructured substrate and be applied on the burn-wound bed. The nanoporous structures are capable of exchanging oxygen–CO₂ (gases) and fluids to the cells and make the substrate breathable.

In addition, the substrates can also inhibit bacterial infection, which is one of the main issues for in vivo use of biomaterials [28–31]. It is also notable that the nanotopographical structure of the AAO could have positive influences on keratinocyte behavior. Others advantages of nanosubstrate AAO are their easy sterilization, nondegradation, and lack of cytotoxic effect on cells [26,27].

Metallic Nanoparticles

Reports demonstrated that inflammation induces scar formation at the site of injury. A decreased level of interleukin-6 (IL6, a stimulator of fibroblast formation and macrophage chemotaxis and activation) [32] and tumor necrosis factor- α (TNF α) [33,34] resulted in scarless wounds as seen in fetal wounds. However, interferon- γ (IFN γ , a potent antagonist of fibrogenesis and a vital factor in skin remodeling) and IL10 (which decreases neutrophil and macrophage infiltration) [35,36] play critical roles in scarless wound healing [37–40].

To manipulate pro-inflammatory responses in the wound site, Tian et al. compared the antibacterial and wound-healing potential of sulfadiazine and silver nanoparticles (AgNPs) in a rat model of deep, partial-thickness, and burn wounds. Their study revealed that AgNPs have higher healing and antibacterial potential with normal hair growth and less hypertrophic scarring compared to the sulfadiazine group. Nevertheless, antibiotics such as amoxicillin and metronidazole delayed wound healing. It is notable that AgNPs decrease messenger RNA (mRNA) expression of TGF β 1 and IL6 genes and induce overexpression of VEGF, IL10, and IFN γ . The burn wound model also showed less neutrophil and serum expression of hemopexin (Hpx), haptoglobin (Hpg), and serum amyloid protein component P (SAP) on the 10th day post burn as compared to sulfadiazine. Also, this strategy could heal wounds in diabetic mice [41]. It is assumed that the toxic mechanism of AgNPs is related to its influence on bacterial cell walls and cell membranes [42], whereas the toxic effect of silver ions is associated with bacterial enzyme inhibition and DNA binding [43]. It is notable that Widgerow's investigation confirmed wound-healing improvement through reduction of inflammatory and pro-inflammatory cytokines, induced apoptosis of neutrophils, and decreased MMP activity and TGF β expression [44].

Heydarnejad and coworkers assessed the wound-healing efficacy of AgNPs (40 nm) in innate immunosuppressed mice. They evaluated the levels of TGF β , complement component C3, C-reactive protein (CRP), and rheumatoid factor (RF) in serum of mice 14 days post treatment. The results disclosed that although there is a significant difference between the levels of TGF β , C3, CRP, and RF at day 2 and the treatment group showed

significantly lower levels of C3, CRP, and RF, the concentration of TGF- β was decreased significantly in both treatment and control groups on the 7th and 14th days. However, the C3 level of the treated group was considerably higher than that of the control group on the 14th day, and the levels of C3, CRP, and RF in the AgNP group were not meaningfully decreased compared to the second day [45].

It is believed that AgNPs influence wound healing through wound contraction. These NPs increase the proliferation and migration rates of keratinocytes and myofibroblast-derived fibroblast differentiation. In fact, AgNPs have different effects depending on the cell types. They induce proliferation efficacy in keratinocytes while inhibiting proliferation of fibroblasts (decrease of collagen I) and differentiating them into myofibroblasts (overexpression of α -SMA) [46]. Inhibition of fibroblast proliferation might be considered a well-suited option in antifibrosis therapy.

In another study, To et al. investigated improving the mechanical property effect of regenerated skin with AgNPs [47]. The results disclosed that AgNPs, through modulating collagen formation and deposition, increase the tensile modulus to 4.9 MPa. However, the tensile modulus of normal skin is 4.7 MPa, while the untreated group assigned 1.2 MPa. In fact, it seems that the AgNP treatment group, through increment of collagen density and protein-to-collagen ratio as compared to untreated group, increased the fiber diameter with a well-oriented structure, strengthened the mechanical properties of skin, and resulted in accelerated scarless healing in mice. However, inhibition of uncontrolled collagen formation by AgNPs would be another mechanism of scarless healing [48]. In 2011, Adhya conducted a clinical assessment in India on patients with 2 degrees burn injury and compared the healing efficacy of silver sulfadiazine as compared to AgNPs weekly for 4 weeks. The data showed 80.6% burn healing of patients with AgNPs as compared to 48.1% by silver sulfadiazine [49].

In the predetermined examples, the AgNPs were applied in the colloidal suspension; however, it is also possible to entrap the particles in scaffolds. Wu and coworkers impregnated AgNPs on cellulose nanofiber and improved its wound-healing efficacy and biocompatibility [50]. Kaler et al. prepared AgNP gel via Carbopol Ultrez 10 NF and investigated its burn-healing capability in a male SD rat burn model. Data revealed that AgNP gel induced accelerated scarless wound healing and a higher degree of cell integrity as analyzed by the TEWEL test, as compared to heal and Carbopol Ultrez 10 NF [51].

In summary, one could claim that the wound-healing potential of AgNPs is related to AgNPs' antiinflammatory and antibacterial efficacies along with wound contraction, which affects collagen deposition. However,

the shortcoming of the particles is their possible cytotoxic effects on normal and healthy cells, which might induce detrimental tissue responses in open wounds [52,53].

It is well understood that skin humidity improves wound healing [54]; in this case, the body temperature can provide the proper environment for bacterial growth [55]. In order to overcome this issue, Peng and coworkers prepared a collagen composite containing nano-TiO₂ and chitosan and evaluated its healing efficacy together with their killing effects on bacteria. They demonstrated that this composite has simultaneous bactericidal (due to the presence of TiO₂) and wound-healing (mainly because of the chitosan component) properties. While the level of expression of TNF α remained constant, IL6 was increased (but still was significantly lower than that of the control group) [56].

At least 200 enzymes in the human body (eg, DNA, RNA polymerases, and MMPs) that are involved in tissue repair need zinc ions for proper activity. Earlier studies revealed its antibacterial potential [57] and influence on keratinocytes [58]. Investigations revealed that zinc oxide accelerated wound healing through enhancement of re-epithelization as compared to zinc sulfate [59]. To that end, Kumar et al. prepared wound dressings containing β -chitin and zinc oxide nanoparticles. The results indicated that this bandage at the low concentration of zinc oxide showed higher cell viability (80–90%) compared to the high concentration (60–70%). Besides, wound healing with higher collagen deposition efficacy accelerated blood clot formation, platelet activation, and collagen deposition and a higher migration rate of fibroblasts and keratinocytes, as observed in a rat model. However, it seems that nano-zinc oxide in this study has improved wound healing [60,61].

The iron oxide NPs could be conjugated with thrombin and increase its bioavailability as a critical factor in triggering early pathways in wound healing. The data showed that thrombin-bounded NPs have a higher half-life in the body and induce stronger tensile strength compared to thrombin alone [62].

Nonmetallic NPs

Reduction of conspicuous facial pores is a beneficial attribute in cosmetics products, and several methods have been investigated to cure this. In 2013, researchers conducted a clinical assessment on healthy women with conspicuous facial pores. Fullerene lotion applied twice a day on the face of women for 8 weeks comprised the treatment group. They also applied water-soluble polyvinylpyrrolidone (PVP)-wrapped fullerene in reconstructed human epidermis and evaluated UVB-induced prostaglandin E2 (PGE2) production. Results indicated that fullerene lotion significantly (17.6%)

decreased the number of conspicuous pores; besides, it decreased production of PGE₂ (18.3%) in reconstructed human epidermis. It might be concluded that fullerene influences melanogenesis, mainly through the suppression of PGE₂ and partially by UV absorption. It seems that keratinocytes and melanocytes are target cells of fullerene [63,64].

Encapsulation of growth factors in carriers has already investigated by several researchers. Growth factors are involved in cell proliferation and differentiation pathways by modulating signal transduction [65–67]. Their encapsulation into nanocarriers results in their protection against degradation and increases their bioactivity. Besides, increased systemic circulation lifetime, sustained and controlled release [68,69], and ineffective release in untargeted sites are other advantages of growth factors encapsulated into nanocarriers as compared to traditional carriers [67]. The most important growth factors for skin regeneration are TGF β , the FGF family, vascular endothelial growth factor (VEGF), epidermal growth factor (EGF), and keratinocyte growth factor (KGF). To the best of our knowledge, only recombinant human PDGF beta polypeptide (PDGF-BB) has been approved by the US Food and Drug Administration (FDA) for application in diabetic foot ulcers [70].

Nitric oxide (NO) derived from amino acid L-arginine is a radical involved in cell proliferation, collagen formation, and wound contraction. NO is synthesized by inflammatory cells in the early stages of wound healing [71]. Taking advantage of NO's role in wound healing, researchers developed a silane nanoporous gel containing NO in a sustained-release manner. This nanosystem releases NO when faced with moisture, and it was useful in wound-healing applications [72]. In another study, Norling et al. fabricated a humanized NP containing aspirin-triggered resolvin D1 (AT-RvD1) or a lipoxin A₄ (LXA₄) analog, and evaluated their wound-healing and inflammatory responses in mice. Employing MMP inhibitors has the potential to delay growth factor degradation. To this end, the obtained data indicated that wound healing occurs with a decrease of inflammatory response [73].

Trentin and coworkers designed fibrin matrix entrapped peptide–DNA NPs loading HIF1- α lacking the oxygen-sensitive degradation domain (HIF1 α ODD) and investigated the angiogenesis efficacy for wound-healing application. Assessments revealed that this NP can induce a higher degree of angiogenesis compared to VEGFA165 protein alone [74,75].

As opioids promote keratinocyte migration, their encapsulation into nanocarriers could be of interest. Kuchler disclosed that morphine-loaded solid lipid nanoparticles encourage re-epithelialization and accelerate wound closure along with prolonged opioid release [76].

Curcumin, as an active ingredient of turmeric, has antiinflammatory [77] and wound-healing efficacy [78]. However, its low water solubility and oral availability and rapid profile of degradation limit clinical usage; in this case, its loading into a nanocarrier is an alternative way to overcome the drawbacks and, thus, pass the compound through the intercellular skin barrier [79]. Its nanoformulation is under preclinical and clinical studies of wound healing and inflammation [79–81]. Keausz and coworkers developed a silane composite NP containing curcumin via the sol-gel method and investigated its wound-healing efficacy in a burn model of mice. They indicated that nanocurcumin could increase bacterial morbidity in burn sites and collagen deposition [82], keratinocyte migration, granulation tissue formation, and new vessel formation compared with the untreated group, and at the end it accelerates burn healing [82]. Other mechanisms of curcumin in wound healing are improving re-epithelialization, fibronectin production, and myofibroblast contraction [83], which act through the TGF β pathway, NO synthase [84], and antiinflammatory mechanisms [85].

A calcium-mediated process is involved in wound healing [86] and modulates infiltration of inflammatory cells, proliferation of fibroblasts, and migration of keratinocytes. In this case, using calcium during the wound-healing process could affect the therapeutic efficacy of conventional approaches [87,88]. Clinically, calcium alginate dressing is used for healing chronic wounds [89], and its effective mechanism might be the release of calcium at the wound site. However, this component is not favorably effective in acute wound healing [86,90]. Kawai and coworkers designed a calcium-based NP for calcium delivery to acute wound beds. At the wound site, where the pH is about 5–6 (acidic), the calcium–phosphate minerals degrade and release the calcium. In contrast, there is no trace of degradation in the healthy parts (with normal pH).

Nanofibers in Wound Healing

Natural Polymer Nanofibers

Collagen type I nanofiber is one the most famous natural polymers applied in skin scaffolds. Due to its similarity to skin collagen structure, it can induce keratinocyte adhesion, proliferation, and differentiation and suppress wound contraction, leading to effective wound healing. Fish scale collagen in combination with chito-oligosaccharides exhibited fibroblast adhesion and proliferation along with antibacterial efficacy [91]. Zhou et al. developed tilapia collagen nanofibers for wound dressing. This nanofiber does not alter CD4⁺/CD8⁺ lymphocytes and the level of immunoglobulin G and M in rats, but it increases cell viability

of human fibroblasts and keratinocytes. However, the fiber could induce overexpression of genes involved in epidermal differentiation, including involucrin, filaggrin, and type I transglutaminase of HaCaTs. Besides, upregulated TGF β 1 induces collagen formation and accelerates wound healing at the final stage. These significant healing effects might be related to the similarity of artificial fiber structures to ECM topography, hydrophilicity, and collagen amino acids involve in healing [92].

Gelatin, an acidic and basic degraded form of collagen, induces high cell infiltration. When gelatin is applied with nanosilver, it can possess antibacterial properties [93]. Protein fibers in dermis (eg, collagen, laminin, keratin, and fibronectin) have diameters of 30–130 nm, and this topography is responsible for cell migration and proliferation [94]. Due to their large surface area and proper porosities (causing good oxygen and water permeability), the construction of skin scaffolds by electrospun nanofibers is a subject of intense interest. The fiber composition could be chosen from synthetic polymers, including degradable (chitosan and gelatin) and nondegradable polymers [poly lactic acid (PLA) and polyvinyl alcohol (PVA)], for proper construction of a skin scaffold [95].

Chitosan nanofiber is another natural polymer that is ideal for skin scaffold preparation, although its poor solubility limits its application. In order to enhance its solubility, chitosan nanofibers can be blended with other materials like PVA [96,97] and gelatin [98]; the obtained composites have demonstrated considerable acceleration in the wound-healing process.

Hyaluronic acid (HA) is another important nanofiber for skin regeneration. It induces angiogenesis and is effective in all stages of skin regeneration [99,100].

Hypoxia (lack of oxygen transfer in the tissue) is one of the major problems in the regeneration of damaged tissues like skin. In order to change hypoxia into a normal condition, researchers entrapped myoglobin and hemoglobin in the nanofibers; the results demonstrated successful wound healing, gas exchange, hydration protection, and wound hypoxia inhibition (mainly via oxygen release from hydrophilic nanofibers) [97,101].

Synthetic Polymer Nanofibers

Synthetic polymers such as poly(3-hydroxybutyrate-co-3-hydroxyvalerate) (PHBV), poly caprolactone (PCL), polyurethane (PU), poly(lactide-co-glycolide) (PLGA), and poly(L-lactide) (PLLA) have been considered as nanofibers for wound-healing applications [102]. Each polymer has its own pros and cons; for example, it is demonstrated that although PLGA has good antiadhesive potential and FDA approval, its acidic degradation products could damage the surrounding tissue [103]. PCL has FDA approval and showed promising

effects on promoting diabetic wound healing; however, it has major shortcomings like a high elasticity amount and slow degradation rate [104,105]. It is indicated that PHBV nanofibers induce adhesion and proliferation of human fibroblasts and keratinocytes, but their hydrophobic nature makes some difficulties regarding its integration to the host tissue [106]. PU nanofibers have good mechanical strength and exhibited a moist environment for burns, but they have the same high-hydrophobicity problem as PHBV [107,108].

Wei and coworkers designed a PLLA nanofibrous scaffold containing PLGA microspheres loaded with recombinant human PDGF-BB. This nanocomposite could inhibit the initial burst effects that showed constant bioactivity of the drug for the first day [109]. Plasma-treated gelatin-based electrospun nanofibers consisting of PLLA and ϵ -caprolactone, by improving cell adhesion and proliferation, accelerated wound healing [110]. Jin and coworkers developed a gelatin and poly(L-lactic acid)-co-poly(ϵ -caprolactone) nanofiber containing EGF, insulin, hydrocortisone, and retinoic acid with two different methods: the precise core-shell structure and blended format. Using these two structures, they then probed the epithelial differentiation efficacy of adipose-derived stem cells. The results revealed that the core-shell structure has stronger effects on the differentiation process toward epithelial cells, mainly due to the controlled release of predetermined biomolecules [111].

SKIN AGING

Skin aging is related to decrease of collagen components in an age-dependent manner that results in skin thinning in older people [112,113]. It is noteworthy that intrinsic and extrinsic factors can control the kinetics of skin aging. The aging process is started by reactive oxygen species (ROS) production. Intrinsic oxidative stress that influences skin aging mainly occurs due to hormonal changes and genetic factors [114,115], while extrinsic oxidative stress depends on UV irradiation, stress, illnesses, an unbalanced diet, smoking, lack of exercise, and other pollutants [116,117]. However, both intrinsic and extrinsic factors can have synergetic effects. In the presence of ROS, nitrogen-activated protein kinases activate, leading to the production of activator protein-1 (AP1), which triggers the release of MMPs. Finally, collagenase, gelatinase, and other biomolecules are formed that can enzymatically degrade collagen [118].

Ngan and coworkers prepared a fullerene nanoemulsion; the compound was applied to the face of women and men twice a day. After treatment for 28 days, skin hydration and transepidermal water loss were evaluated [119]. It was found that fullerene significantly

increases skin hydration and water content of the stratum corneum. In addition, it acted as a scavenger of ROS and converts it to lipid autoxidation [120].

Sashwati et al. designed 60–100 nm nanoparticles containing boswellia (ie, a painkiller extracted from a shrubby tree) and evaluated their antiaging efficacy along with impulse light laser. They found that these nanoparticles exhibited decrement of wrinkle depth, firming of the skin, and treatment of inflammatory skin disease [121].

Since another cause of accumulated ROS in cells is the loss of superoxide dismutase (Sod1), one can expect that the use of noble metal NPs could be of help. During the past 60 years in Japan, people have used a combination of palladium and platinum for chronic disease treatment [122]. Shibuya and coworkers fabricated a palladium and platinum NP for antiaging applications, and their finding showed that this NP exhibits SOD and catalase activity and inverts skin thinning related to lipid peroxidation in null SOD mice. Besides, it overexpressed *Colla1*, *Mmp2*, *Has2*, *TNF α* , *IL6*, and *p53* genes in null SOD mice. It seems that palladium and platinum NPs might be effective in antiaging applications [122,123].

ADVANCED FABRICATION STRATEGIES IN DESIGN OF SKIN REGENERATION SCAFFOLDS

Advanced approaches have emerged to recreate the skin ECM, overcoming limitations of autografts and allografts. In this section, we review different methods that are in use to fabricate micro- and nanoscaled scaffolds, including electrospinning, self-assembly, organ-on-chips, and cell-imprinting strategies, for skin tissue regeneration. We also touch upon the most recent advances in the bottom-up approaches for generating scaffolds resembling the structure and function of healthy skin.

Electrospinning

The ECM of dermis and basal lamina is composed of an intricate network of nanofibers, including proteoglycans, structural proteins (eg, collagen and elastin), and specialized proteins (eg, fibronectin), which not only provide structural integrity to skin but also regulate the functioning of residing cells [124–126]. Thus, nanofibrous scaffolds can be a great fit for recapitulating the architecture of native ECM and, hence, generating a functional replacement for the injured or missing skin [127,128]. Among different nanofiber fabrication strategies, electrospinning has emerged as a simple, inexpensive, and scalable method capable of reproducing nanoscale structures from a wide variety of polymers [102,129]. By applying a high-power voltage to a polymer solution, an electrostatically driven jet of polymer is ejected from a syringe, flown across an air gap, and layered on a collector in the form of nanometer- to micron-diameter fibers with interconnected pores (Fig. 26.1). Different process parameters (eg, polymer molecular weight, solvent quality, electrical voltage, polymer flow rate, and collector-to-syringe distance) and environmental factors (like temperature and humidity) affect the morphology and mechanics of fiber mats [130,131]. Moreover, while static targets collect the fibers in random orientation, rotating mandrels yield aligned fibers; thus, depending on the solution features, ambient conditions, process variables, and type(s) of collector, a variety of fiber patterns and architectures can be obtained to address tissue-engineering requirements in different contexts [132].

In the context of skin regeneration, to date, a variety of natural and synthetic materials have been utilized to produce electrospun nanofibers [133]. The high surface area, microporous structure, and high aspect ratio of electrospun nanofibers enhance their oxygen permeability, nutrient and metabolite exchange, medium uptake, and adsorption of bioactive

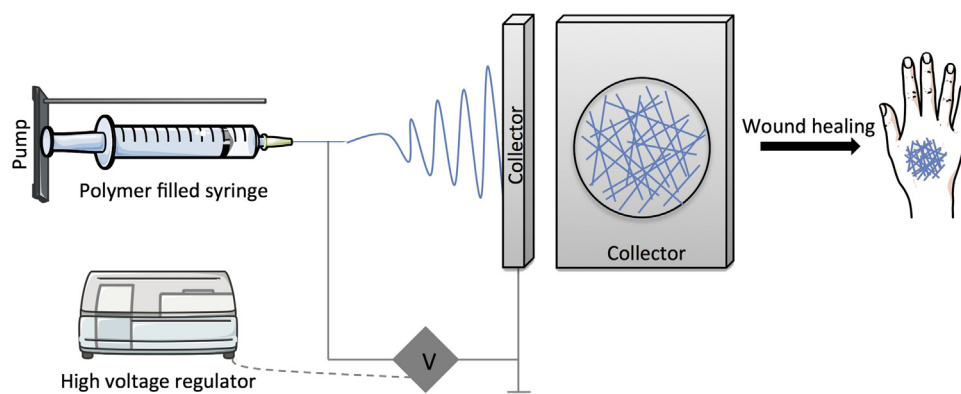


FIGURE 26.1 Schematic representation of electrospinning process for skin regeneration.

proteins, making them ideal wound dressings [134]. These substrates play an important role in protecting the wound area from potential dehydration and external mechanical forces; however, to provide proper molecular signaling, improve cellular function, and achieve successful skin regeneration, bioactive agents could be added to these nanostructured scaffolds [135,136]. Biofunctionalization of scaffolds is performed via blend, coaxial, and emulsion electrospinning, and postspinning, treatments [137–139]. Mixing either natural polymers or biomolecules with synthetic polymers before a spinning process results in entrapping bioactive agents and improving cellular behaviors (ie, adhesion and proliferation); however, as the agents are charged, they scape toward the surface of nanofibers, which reduce their lifetime and increase burst release propensity [140,141]. In core–shell nanofibers that are produced via coaxial electrospinning, the shell contains a polymer that protects the bioactive molecules encapsulated in the core and enables a sustained release of them [142]. Different process parameters, such as flow rate and rheology of polymer solution, influence the growth factor encapsulation efficiency. Core–shell nanofibers have been confirmed to be effective on full-thickness wounds in various studies [143–145]. As a recent approach, emulsion electrospinning is utilized to fabricate core–sheath fibers from an emulsion of bioactive factors and polymer. This technique provides high encapsulation efficiency, enhances targeted delivery, and improves biological activity; however, challenges still remain in even distribution of growth factors throughout the fiber structure [146,147]. Core–sheath nanofibers have been shown to greatly improve wound healing with complete re-epithelialization while containing biochemicals [eg, basic fibroblast growth factor (bFGF)] [148]. Postelectrospinning processing includes biofunctionalization through physical surface absorption and chemical conjugation approaches [149,150]. Poly(methylmethacrylate) mesh coated with collagen I showed enhanced levels of cell attachment and growth [151], and EGF immobilization onto a PCL–collagen scaffold increased the differentiation ability of cultured human dermal keratinocytes [152].

To address poor migration of cells into electrospun scaffolds, different systems might be followed to increase the porosity of scaffolds or the potential of cells to infiltrate deeply in the construct. In one approach, scaffolds were fabricated through layer-by-layer assembly and by stacking multiple layers of nano- and microfibers to create large pores within small fibers [153,154]. In yet another approach, multilayered cell-scaffold structures were generated by continuously sandwiching fibroblasts and keratinocytes within the construct while electrospinning an alternating

PCL–collagen nanofibrous mat. In doing so, infiltration of cells into the scaffold is enhanced, and hence, a bilayer skin substitute with desired thickness could be produced [155,156]. The use of sacrificial material through a co-electrospinning procedure can also be exploited to increase the porosity of the scaffolds. For instance, co-electrospinning of polyethylene oxide, with high degradability, and polycaprolactone improved the penetration of cultivated cells compared to polycaprolactone mats with no polyethylene oxide [157].

The electrospinning technique, owing to its simplicity, monetary value, and high-adaptability nature, is considered an ideal strategy for fabricating natural and synthetic nanofibrous dressings and scaffolds suitable for wound healing and skin regeneration. Although electrospun scaffolds provide a great template to recapitulate native ECM architecture, the incorporation of bioactive agents, such as ECM proteins, growth factors, and genes, further improves cellular adhesion, infiltration, proliferation, and differentiation. Nanofibrous scaffolds, especially biofunctionalized fiber mats, can be considered promising materials for skin tissue-engineering applications.

Self-assembly

A highly promising group of materials for regenerative medicine applications is composed of nanostructures capable of not only interacting with cell proteins and receptors and thus regulating different cellular processes, but also self-assembling into well-defined supramolecular morphologies [158]. Biocompatible, biodegradable, and bioactive hydrogels can be developed using the self-assembling approaches and delivered through noninvasive procedures in various tissue-engineering prospects [159]. RAD-based peptides, for instance, self-assemble into ribbons and nanofibers, and provide 3D hydrogels that approximate native ECM for various cells. RAD16-I, as a member of the RADs family, forms 3D nanofibrous constructs with pore sizes of about 50–200 nm that are used as wound dressing. While tested in a second-degree burn model, RAD16-I not only accelerated wound contraction compared to collagen type I, chitosan, and polylactic acid scaffolds, but also enhanced expression of FGF and EGF [160]. To produce a synthetic skin, in another study, RAD16-I gel was cultivated with fibroblasts for 3 weeks to create dermis and then layered with keratinocytes for 1 week to form epidermis. Given the nanofibrillar nature of the peptide hydrogel, fibroblasts aggregated at fiber junctions while they evenly distributed within collagen or Matrigel samples. As expected, fibroblasts remained functional by expressing collagen I, keratinocytes

differentiated in the epidermis, and basement membrane was developed between the dermal and epidermal layers [161]. So, in the context of skin regeneration, self-assembling peptides could offer a promising cure for wounds.

Peptide amphiphiles (PAs), a class of self-assembled nanofibers composed of a hydrophilic peptide head and a hydrophobic alkyl tail, have been broadly studied for soft-tissue engineering [162]. Self-assembly into nanofibers occurs once electrostatic repulsion between molecules is reduced, for instance by tuning the pH or by adding ion-containing solutions, such as cell culture medium. The resulting nanofibers have diameters smaller than those of electrospun fibers (ie, 10 nm), but in the range of native ECM [163–165]. Although bioactivity of PAs is enhanced by adding chemical signals (eg, the RGD motif), the high complexity and poor mechanical strength of these supramolecular materials challenge their application in large-scale scaffold fabrication [165]. However, by incorporating other biopolymers and designing planar sheets or membranes while developing PA systems, these limitations could be overcome. By combining PA solution with an aqueous solution of high-molecular-weight HA, hierarchically structured sacs and membranes with tunable size and shape are formed by self-assembly and could find utilization in large, thick-tissue regeneration [166]. Using PA with binding affinity for heparin, and incorporating FGF2 and VEGF, PA–HA membranes considerably and rapidly enhanced angiogenesis *in vitro* [167]. These findings suggest that PA-based materials are well suited toward wound healing and skin regeneration.

Cell-Imprinted Substrates

The skin, as a tissue that continuously regenerates during normal homeostasis and after wounding, is supported by stem cells. However, a lack of proper microenvironmental cues affects the behavior of stem cells in both *in vitro* and *in vivo* environments. Matrix-mediated traits, such as surface micro- and nanotopography, and structural ECM cues can greatly regulate a stem cell's fate [168–171]. In this regard, cell imprinting has been introduced as a novel approach to define an optimized niche microenvironment by casting the cell morphologies [171]. In the context of skin regeneration, cell-imprinting technology has been recently recruited to provide bioinspired topography at the micro- and nanolevels using 3D surface casting of the morphology of keratinocytes. Cell-imprinted biomimetic platforms that served for differentiation of adipose-derived stem cells directed their shape and characteristics toward keratinocytes (Fig. 26.2) [172]. Given the efficient and cost-effective

differentiation of stem cells toward skin cells, this technology could find utilization for wound-healing applications.

Skin 3D Bioprinting

3D bioprinting is a process for patterning and assembling complex functional living architectures through controlled layer-by-layer positioning of biological hydrogels, viable cells, and ECM components in a gradient fashion [173]. Having a 3D image of a desired living tissue and benefiting from computer-aided design and computer-aided manufacturing (CAD and CAM, respectively) systems, 3D bioprinting serves as a novel tool for not only generating and transplanting several tissues and organs, but also creating high-throughput models for drug discovery and development [174,175]. Although small (ie, a few 100 micrometer-sized) or less sophisticated structures, such as cartilage as an avascular and aneural tissue, are facile to print, challenges still remain in reproducing larger and multicomponent tissues like skin, and spatially arrange complex ECM traits in a proper resolution [176]. One of the main challenges is to transfer all nanotopographies existing in the ECM into the printed organs.

To recapitulate organ- and tissue-level functionality, as yet, various technologies, namely inkjet, microextrusion, and laser-assisted printing, have been developed [177–179]. The principle is to print cells within a biological material, or layer cell-free hydrogels in a controlled manner; however, based on the intended resolution, type of material, and viability of cells, each of these technologies could be used. Laser-assisted bioprinting (LAB), for example, has been utilized to generate a fully cellularized skin equivalent by precise placement of fibroblasts and keratinocytes in a 3D spatial pattern on a Matrigel matrix. This graft was fully connected to the edges of a full-thickness skin wound *in vivo*, where keratinocytes created a multilayered epidermis and fibroblasts produced collagen. Thanks to printing different cell types in an intricate pattern, new blood vessels were also formed in a relatively short timeframe after *in vivo* transplantation [180]. Thus, LAB could be used to print cellular constructs that subsequently form a tissue resembling the native skin. However, further challenges should be addressed to scale up this system for larger tissue sizes.

In vivo bioprinting, as an alternative approach, could be used to directly print cells and materials into wound or burn defects [181] (Fig. 26.3). In this context, an inkjet approach has been employed to recreate functional skin *in situ* by uniform depositing of a stem cell–hydrogel complex throughout the full-thickness wound area. Amniotic fluid–derived stem cells (AFSCs) with minimal immunogenicity properties were mixed with

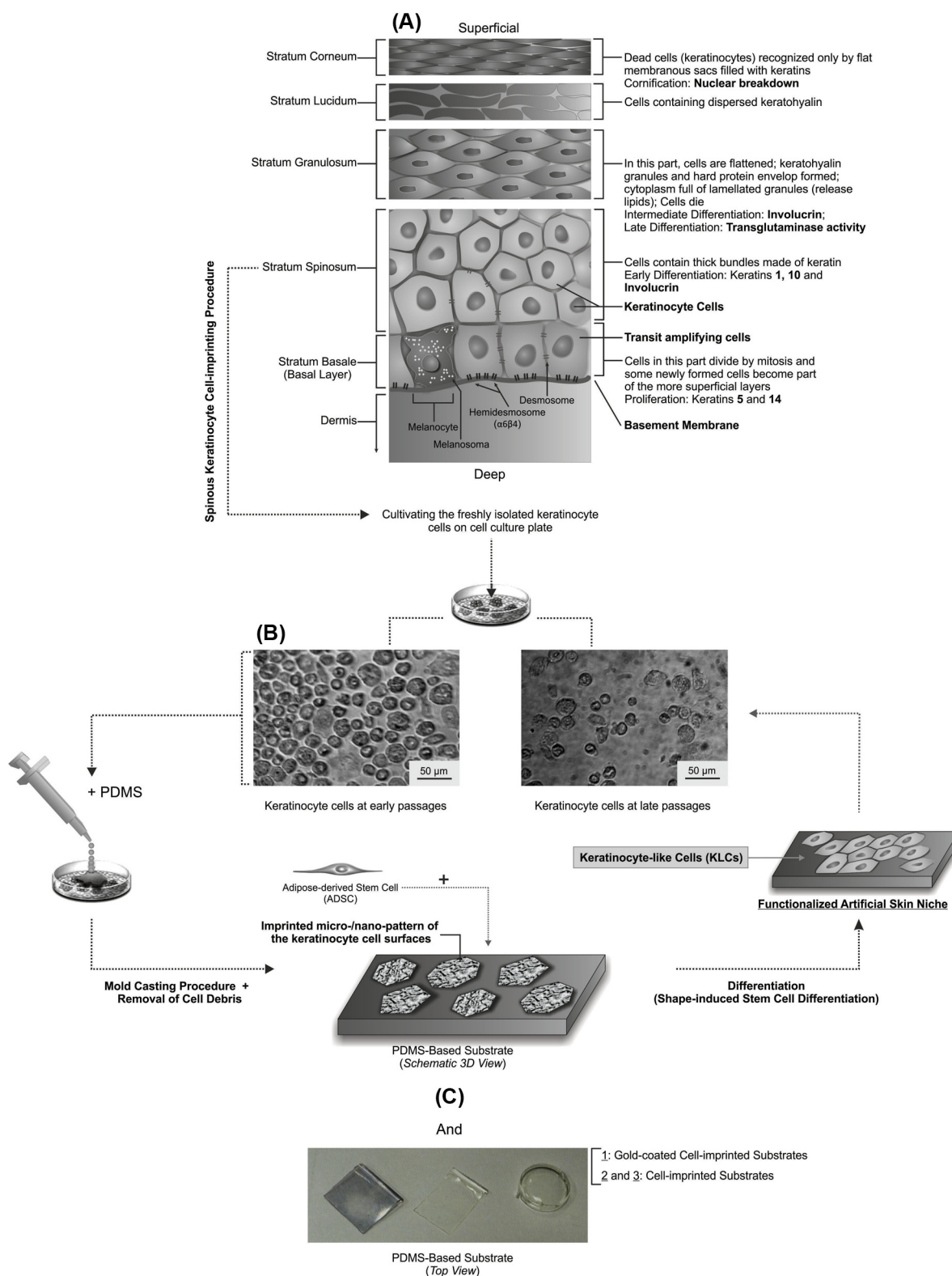


FIGURE 26.2 (Upper middle) Detailed illustration of the architecture of the basal-to-spinous layer transition. (Lower middle) Schematic of the experimental setup and artificial skin niche study steps. (A) The epidermal differentiation procedure is illustrated (ie, a basement membrane at the base, the proliferative basal layer, and the four differentiation stages: the stratum spinosum layer, stratum granulosum layer, stratum lucidum layer, and outermost stratum corneum). (B) The cultured keratinocyte cells on different well plates at different passage levels are shown in this schematic. (C) The keratinocytes were grown on a cell culture plate, and their complete morphologies at different stages were transferred to a silicone replica by a mold-casting procedure in order to fabricate the PDMS-based substrate. This unique structure could be used as a novel platform to manipulate the stem cells to achieve production of the keratinocyte-like cells. *Reprinted with permission from Mashinchian O, Bonakdar S, Taghinejad H, Satarifard V, Heidari M, Majidi M, et al. Cell-imprinted substrates act as an artificial niche for skin regeneration. ACS Appl Mater Interfaces 2014;6(15):13280–92.*

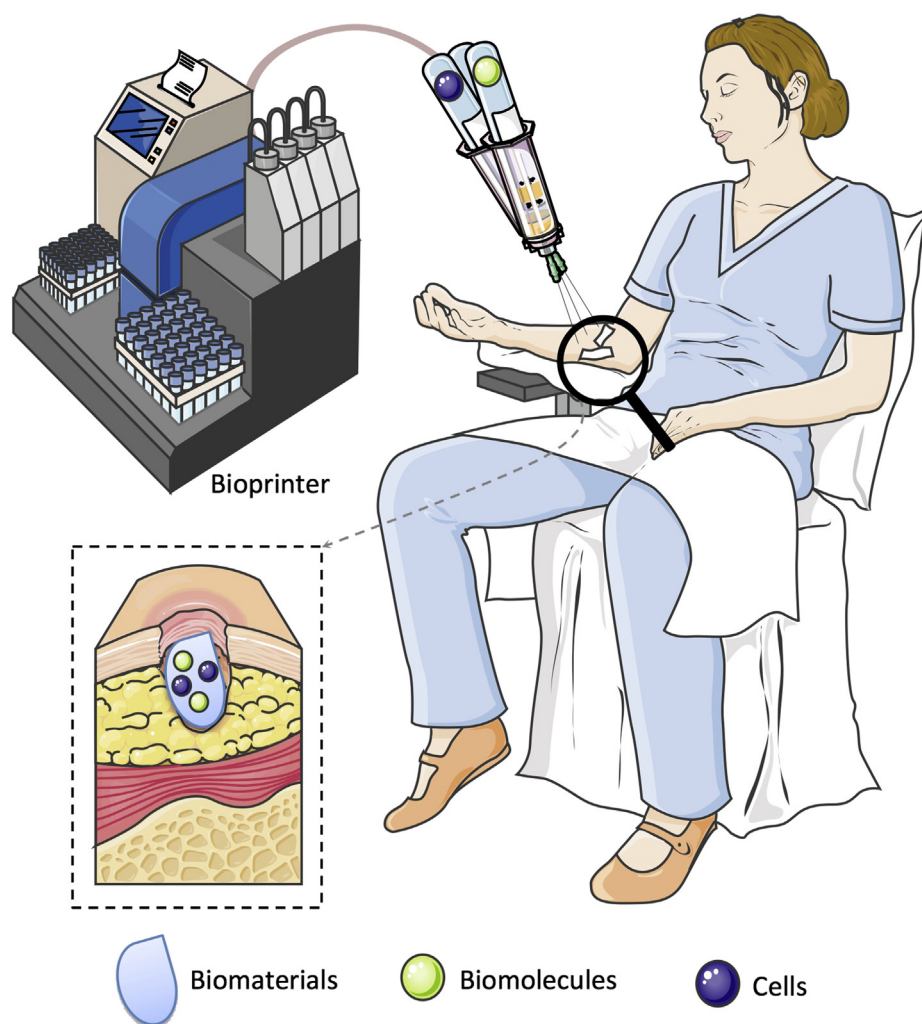


FIGURE 26.3 Schematic illustration of a multineedle bioprinting system for in situ fabrication of skin substitutes.

fibrin–collagen gel and directly layered over the defect site. Wound coverage and angiogenesis into AFSC–gel treated wounds were enhanced as compared to gel-only control, likely due to secretion of a number of trophic factors essential for wound healing [182]. Therefore, bioprinter-based delivery of cell matrix components has the potential to regenerate functional skin tissue; nonetheless, further progress in the speed and resolution of printers might open new doors toward effective wound healing immediately after injuries.

Given the potential of precise patterning of a mixed solution of keratinocytes, fibroblasts, melanocytes, and stem cells within the hydrogels that possesses suitable gelation time, mechanical properties, degradability, and immunological response [181,183], 3D bioprinting could not only overcome limitations of conventional skin-engineering approaches but also serve as a great means of drug testing and treating cosmetic skin defects.

CONCLUSION

Current advances in regenerative medicine and tissue engineering represent a great opportunity to advance novel therapies or enhance the effectiveness of available treatments. To this end, using nanotechnology-based knowledge allows better control over physical and biological properties of diverse biomaterials. Numerous studies are being conducted on the use of biomaterials by incorporation of stem cells in order to generate artificial skin. Nevertheless, the success of these approaches has been limited by the availability of different types of stem cells and their efficiency in regeneration procedures. Correspondingly, an ideal artificial structure for regenerative medicine should have the same characteristics or properties as the native tissue. Thus, biomimetic substrates and scaffolds that can modulate the stem cell differentiation and proliferation were proposed to further mimic the permutations of skin tissue.

References

- [1] Degim IT. Understanding skin penetration: computer aided modeling and data interpretation. *Curr Comput-Aided Drug Des* 2005;1(1):11–9.
- [2] Zaidi Z, Lanigan SW. *Skin: structure and function. Dermatology in clinical practice*. Springer; 2010. p. 1–15.
- [3] Saladin K. *Anatomy and physiology: the unity of form and function*. New York: McGraw Hill; 2007.
- [4] Proksch E, Brandner JM, Jensen JM. The skin: an indispensable barrier. *Exp Dermatol* 2008;17(12):1063–72.
- [5] Billingham R, Reynolds J. Transplantation studies on sheets of pure epidermal epithelium and on epidermal cell suspensions. *Br J Plast Surg* 1952;5(1):25–36.
- [6] Karasek MA, Charlton ME. Growth of postembryonic skin epithelial cells on collagen gels. *J Invest Dermatol* 1971;56(3):205–10.
- [7] Bell E, Ivarsson B, Merrill C. Production of a tissue-like structure by contraction of collagen lattices by human fibroblasts of different proliferative potential in vitro. *Proc Natl Acad Sci* 1979;76(3):1274–8.
- [8] Sarber R, Hull B, Merrill C, Sorzano T, Bell E. Regulation of proliferation of fibroblasts of low and high population doubling levels grown in collagen lattices. *Mech Ageing Dev* 1981;17(2):107–17.
- [9] Mauch C, Hatamochi A, Scharffetter K, Krieg T. Regulation of collagen synthesis in fibroblasts within a three-dimensional collagen gel. *Exp Cell Res* 1988;178(2):493–503.
- [10] Bell E, Parenteau N, Gay R, Nolte C, Kemp P, Bilbo P, et al. The living skin equivalent: its manufacture, its organotypic properties and its responses to irritants. *Toxicol In Vitro* 1991;5(5):591–6.
- [11] Todd C, Hewitt S, Kempenaar J, Noz K, Thody A, Ponc M. Co-culture of human melanocytes and keratinocytes in a skin equivalent model: effect of ultraviolet radiation. *Arch Dermatol Res* 1993;285(8):455–9.
- [12] Bessou S, Surlève-Bazeille JE, Sorbier E, Taieb A. Ex vivo reconstruction of the epidermis with melanocytes and the influence of UVB. *Pigment Cell Res* 1995;8(5):241–9.
- [13] Green H. The birth of therapy with cultured cells. *Bioessays* 2008;30(9):897–903.
- [14] De Luca M, Pellegrini G, Green H. Regeneration of squamous epithelia from stem cells of cultured grafts. *Regen Med* 2006;1.
- [15] Kuehn BM. Chronic wound care guidelines issued. *JAMA* 2007;297(9):938–9.
- [16] Stadelmann WK, Digenis AG, Tobin GR. Physiology and healing dynamics of chronic cutaneous wounds. *Am J Surg* 1998;176(2):265–385.
- [17] Werner S, Grose R. Regulation of wound healing by growth factors and cytokines. *Physiol Rev* 2003;83(3):835–70.
- [18] Tuzlakoglu K, Bolgen N, Salgado A, Gomes ME, Piskin E, Reis R. Nano- and micro-fiber combined scaffolds: a new architecture for bone tissue engineering. *J Mater Sci Mater Med* 2005;16(12):1099–104.
- [19] Witte MB, Barbul A. General principles of wound healing. *Surg Clin North Am* 1997;77(3):509–28.
- [20] Guo S, DiPietro LA. Factors affecting wound healing. *J Dent Res* 2010;89(3):219–29.
- [21] Gosain A, DiPietro LA. Aging and wound healing. *World J Surg* 2004;28(3):321–6.
- [22] Madden JW, Peacock Jr EE. Studies on the biology of collagen during wound healing. I. Rate of collagen synthesis and deposition in cutaneous wounds of the rat. *Surgery* 1968;64(1):288.
- [23] Bennett NT, Schultz GS. Growth factors and wound healing: Part II. Role in normal and chronic wound healing. *Am J Surg* 1993;166(1):74–81.
- [24] Chen C, Schultz GS, Bloch M, Edwards PD, Tebes S, Mast BA. Molecular and mechanistic validation of delayed healing rat wounds as a model for human chronic wounds. *Wound Repair Regen* 1999;7(6):486–94.
- [25] Jeffcoate WJ, Harding KG. Diabetic foot ulcers. *Lancet* 2003;361(9368):1545–51.
- [26] Poinern G, Fawcett D, Ng Y, Ali N, Brundavanam R, Jiang Z-T. Nanoengineering a biocompatible inorganic scaffold for skin wound healing. *J Biomed Nanotechnol* 2010;6(5):497–510.
- [27] Parkinson LG, Giles NL, Adcroft KF, Fear MW, Wood FM, Poinern GE. The potential of nanoporous anodic aluminium oxide membranes to influence skin wound repair. *Tissue Eng Part A* 2009;15(12):3753–63.
- [28] Subbiahdoss G, Sharifi S, Grijpma DW, Laurent S, van der Mei HC, Mahmoudi M, et al. Magnetic targeting of surface-modified superparamagnetic iron oxide nanoparticles yields antibacterial efficacy against biofilms of gentamicin-resistant staphylococci. *Acta Biomater* 2012;8(6):2047–55.
- [29] Mahmoudi M, Serpooshan V. Silver-coated engineered magnetic nanoparticles are promising for the success in the fight against antibacterial resistance threat. *ACS Nano* 2012;6(3):2656–64.
- [30] Hajipour MJ, Fromm KM, Ashkarran AA, de Aberasturi DJ, de Larramendi IR, Rojo T, et al. Antibacterial properties of nanoparticles. *Trends Biotechnol* 2012;30(10):499–511.
- [31] Tavakol S, Nikpour MR, Hoveizi E, Tavakol B, Rezayat SM, Adabi M, et al. Investigating the effects of particle size and chemical structure on cytotoxicity and bacteriostatic potential of nano hydroxyapatite/chitosan/silica and nano hydroxyapatite/chitosan/silver; as antibacterial bone substitutes. *J Nanopart Res* 2014;16(10):1–13.
- [32] Liechty KW, Adzick NS, Crombleholme TM. Diminished interleukin 6 (IL-6) production during scarless human fetal wound repair. *Cytokine* 2000;12(6):671–6.
- [33] Ghahary A, Shen Y, Scott PG, Gong Y, Tredget EE. Enhanced expression of mRNA for transforming growth factor-, type I and type III procollagen in human post-burn hypertrophic scar tissues. *J Lab Clin Med* 1993;122:465.
- [34] Whitby DJ, Ferguson MW. Immunohistochemical localization of growth factors in fetal wound healing. *Dev Biol* 1991;147(1):207–15.
- [35] Sato Y, Ohshima T, Kondo T. Regulatory role of endogenous interleukin-10 in cutaneous inflammatory response of murine wound healing. *Biochem Biophys Res Commun* 1999;265(1):194–9.
- [36] Szpadarska A, Zuckerman J, DiPietro L. Differential injury responses in oral mucosal and cutaneous wounds. *J Dent Res* 2003;82(8):621–6.
- [37] Dans MJ, Isseroff R. Inhibition of collagen lattice contraction by pentoxifylline and interferon-alpha, -beta and -gamma. *J Invest Dermatol* 1994;102(1):118–21.
- [38] Tamai K, Ishikawa H, Mauviel A, Uitto J. Interferon-gamma coordinately upregulates matrix metalloproteinase (MMP)-1 and MMP-3, but not tissue inhibitor of metalloproteinases (TIMP), expression in cultured keratinocytes. *J Invest Dermatol* 1995;104(3):384–90.
- [39] Tredget EE, Wang R, Shen Q, Scott PG, Ghahary A. Transforming growth factor-beta mRNA and protein in hypertrophic scar tissues and fibroblasts: antagonism by IFN-alpha and IFN-gamma in vitro and in vivo. *J Interferon Cytokine Res* 2000;20(2):143–52.
- [40] Broker BJ, Rosen D, Amsberry J, Schmidt R, Sailor L, Pribitkin EA, et al. Keloid excision and recurrence prophylaxis via intradermal interferon-gamma injections: a pilot study. *Laryngoscope* 1996;106(12):1497–501.
- [41] Tian J, Wong KK, Ho CM, Lok CN, Yu WY, Che CM, et al. Topical delivery of silver nanoparticles promotes wound healing. *Chem-MedChem* 2007;2(1):129–36.

- [42] Chamakura K, Perez-Ballesterio R, Luo Z, Bashir S, Liu J. Comparison of bactericidal activities of silver nanoparticles with common chemical disinfectants. *Colloids Surf B Biointerfaces* 2011; 84(1):88–96.
- [43] Jung WK, Koo HC, Kim KW, Shin S, Kim SH, Park YH. Antibacterial activity and mechanism of action of the silver ion in *Staphylococcus aureus* and *Escherichia coli*. *Appl Environ Microbiol* 2008;74(7):2171–8.
- [44] Widgerow AD. Nanocrystalline silver, gelatinases and the clinical implications. *Burns* 2010;36(7):965–74.
- [45] Heydarnejad MS, Rahnama S, Mobini-Dehkordi M, Yarmohammadi P, Aslnai H. Silver nanoparticles accelerate skin wound healing in mice (*Mus musculus*) through suppression of innate immune system. *Nanomomed J* 2013;1(2):79–87.
- [46] Liu X, Lee PY, Ho CM. Silver nanoparticles mediate differential responses in keratinocytes and fibroblasts during skin wound healing. *ChemMedChem* 2010;5(3):468–75.
- [47] To M, Kwan K, Liu X, Yeung K, Wong K, editors. The modulating action of silver nanoparticles on collagen deposition in producing scarless wound healing. TERMIS-NA 2010 Annual Conference; 2010.
- [48] MKT T, Kwan K, Liu X, Yeung K, Wong K. The modulating action of silver nanoparticles on collagen deposition in producing scarless wound healing. ORS; 2011. Annual Meeting 2011.
- [49] Adhya A, Bain J, Ray O, Hazra A, Adhikari S, Dutta G, et al. Healing of burn wounds by topical treatment: a randomized controlled comparison between silver sulfadiazine and nanocrystalline silver. *J Basic Clin Pharm* 2015;6(1):29–34.
- [50] Wu J, Zheng Y, Song W, Luan J, Wen X, Wu Z, et al. In situ synthesis of silver-nanoparticles/bacterial cellulose composites for slow-released antimicrobial wound dressing. *Carbohydr Polym* 2014;102:762–71.
- [51] Kaler A, Mittal AK, Katariya M, Harde H, Agrawal AK, Jain S, et al. An investigation of in vivo wound healing activity of biologically synthesized silver nanoparticles. *J Nanopart Res* 2014; 16(9):1–10.
- [52] Samberg ME, Oldenburg SJ, Monteiro-Riviere NA. Evaluation of silver nanoparticle toxicity in skin in vivo and keratinocytes in vitro. *Environ Health Perspect* 2010;118(3):407.
- [53] DeLouise LA. Applications of nanotechnology in dermatology. *J Invest Dermatol* 2012;132:964–75.
- [54] Hess CT. Checklist for factors affecting wound healing. *Adv Skin Wound Care* 2011;24(4):192.
- [55] Mao JS, Zhao LG, Yin YJ, De Yao K. Structure and properties of bilayer chitosan–gelatin scaffolds. *Biomaterials* 2003;24(6): 1067–74.
- [56] Peng CC, Yang MH, Chiu WT, Chiu CH, Yang CS, Chen YW, et al. Composite nano-titanium oxide–chitosan artificial skin exhibits strong wound-healing effect—an approach with anti-inflammatory and bactericidal kinetics. *Macromol Biosci* 2008; 8(4):316–27.
- [57] Nair S, Sasidharan A, Rani VD, Menon D, Nair S, Manzoor K, et al. Role of size scale of ZnO nanoparticles and microparticles on toxicity toward bacteria and osteoblast cancer cells. *J Mater Sci Mater Med* 2009;20(1):235–41.
- [58] Kocbek P, Teskač K, Kreft ME, Kristl J. Toxicological aspects of long-term treatment of keratinocytes with ZnO and TiO₂ nanoparticles. *Small* 2010;6(17):1908–17.
- [59] Ågren MS, Chvapil M, Franzén L. Enhancement of re-epithelialization with topical zinc oxide in porcine partial-thickness wounds. *J Surg Res* 1991;50(2):101–5.
- [60] Kumar S, Lakshmanan V-K, Raj M, Biswas R, Hiroshi T, Nair SV, et al. Evaluation of wound healing potential of β -chitin hydrogel/nano zinc oxide composite bandage. *Pharm Res* 2013;30(2): 523–37.
- [61] Sudheesh Kumar P, Lakshmanan V-K, Anilkumar T, Ramya C, Reshmi P, Unnikrishnan A, et al. Flexible and microporous chitosan hydrogel/nano ZnO composite bandages for wound dressing: in vitro and in vivo evaluation. *ACS Appl Mater Interfaces* 2012;4(5):2618–29.
- [62] Ziv-Polat O, Topaz M, Brosh T, Margel S. Enhancement of incisional wound healing by thrombin conjugated iron oxide nanoparticles. *Biomaterials* 2010;31(4):741–7.
- [63] Xiao L, Matsubayashi K, Miwa N. Inhibitory effect of the water-soluble polymer-wrapped derivative of fullerene on UVA-induced melanogenesis via downregulation of tyrosinase expression in human melanocytes and skin tissues. *Arch Dermatol Res* 2007;299(5–6):245–57.
- [64] Inui S, Mori A, Ito M, Hyodo S, Itami S. Reduction of conspicuous facial pores by topical fullerene: possible role in the suppression of PGE₂ production in the skin. *J Nanobiotechnol* 2014;12(1):6.
- [65] Yao C, Markowicz M, Pallua N, Noah EM, Steffens G. The effect of cross-linking of collagen matrices on their angiogenic capability. *Biomaterials* 2008;29(1):66–74.
- [66] Karakeçili AG, Satriano C, Gümüşdereioğlu M, Marletta G. Enhancement of fibroblastic proliferation on chitosan surfaces by immobilized epidermal growth factor. *Acta Biomater* 2008; 4(4):989–96.
- [67] Chen F-M, Zhang M, Wu Z-F. Toward delivery of multiple growth factors in tissue engineering. *Biomaterials* 2010;31(24): 6279–308.
- [68] Rajam M, Pulavendran S, Rose C, Mandal A. Chitosan nanoparticles as a dual growth factor delivery system for tissue engineering applications. *Int J Pharm* 2011;410(1):145–52.
- [69] Gao P, Nie X, Zou M, Shi Y, Cheng G. Recent advances in materials for extended-release antibiotic delivery system. *J Antibiot* 2011;64(9):625–34.
- [70] Senet P, Vicaut E, Beneton N, Debure C, Lok C, Chosidow O. Topical treatment of hypertensive leg ulcers with platelet-derived growth factor-BB: a randomized controlled trial. *Arch Dermatol* 2011;147(8):926–30.
- [71] Schäffer M, Efron PA, Thornton FJ, Klingel K, Gross SS, Barbul A. Nitric oxide, an autocrine regulator of wound fibroblast synthetic function. *J Immunol* 1997;158(5):2375–81.
- [72] Friedman AJ, Han G, Navati MS, Chacko M, Gunther L, Alfieri A, et al. Sustained release nitric oxide releasing nanoparticles: characterization of a novel delivery platform based on nitrite containing hydrogel/glass composites. *Nitric Oxide* 2008; 19(1):12–20.
- [73] Norling LV, Spite M, Yang R, Flower RJ, Perretti M, Serhan CN. Cutting edge: humanized nano-proresolving medicines mimic inflammation-resolution and enhance wound healing. *J Immunol* 2011;186(10):5543–7.
- [74] Metcalfe AD, Ferguson MW. Tissue engineering of replacement skin: the crossroads of biomaterials, wound healing, embryonic development, stem cells and regeneration. *J R Soc Interface* 2007;4(14):413–37.
- [75] Trentin D, Hall H, Wechsler S, Hubbell JA. Peptide-matrix-mediated gene transfer of an oxygen-insensitive hypoxia-inducible factor-1 α variant for local induction of angiogenesis. *Proc Natl Acad Sci USA* 2006;103(8):2506–11.
- [76] Küchler S, Wolf NB, Heilmann S, Weindl G, Helfmann J, Yahya MM, et al. 3D-wound healing model: influence of morphine and solid lipid nanoparticles. *J Biotechnol* 2010; 148(1):24–30.
- [77] Sandur SK, Ichikawa H, Pandey MK, Kunnumakkara AB, Sung B, Sethi G, et al. Role of pro-oxidants and antioxidants in the anti-inflammatory and apoptotic effects of curcumin (diferuloylmethane). *Free Radic Biol Med* 2007;43(4):568–80.

- [78] Kulac M, Aktas C, Tulubas F, Uygur R, Kanter M, Erboğa M, et al. The effects of topical treatment with curcumin on burn wound healing in rats. *J Mol Histol* 2013;44(1):83–90.
- [79] Flora G, Gupta D, Tiwari A. Nanocurcumin: a promising therapeutic advancement over native curcumin. *Crit Rev Ther Drug Carrier Syst* 2013;30(4).
- [80] Chereddy KK, Coco R, Memvanga PB, Ucarar B, des Rieux A, Vandermeulen G, et al. Combined effect of PLGA and curcumin on wound healing activity. *J Control Release* 2013;171(2):208–15.
- [81] Aggarwal BB, Harikumar KB. Potential therapeutic effects of curcumin, the anti-inflammatory agent, against neurodegenerative, cardiovascular, pulmonary, metabolic, autoimmune and neoplastic diseases. *Int J Biochem Cell Biol* 2009;41(1):40–59.
- [82] Krausz AE, Adler BL, Cabral V, Navati M, Doerner J, Charafeddine RA, et al. Curcumin-encapsulated nanoparticles as innovative antimicrobial and wound healing agent. *Nanomedicine* 2015;11(1):195–206.
- [83] Sidhu GS, Singh AK, Thaloor D, Banaudha KK, Patnaik GK, Srimal RC, et al. Enhancement of wound healing by curcumin in animals. *Wound Repair Regen* 1998;6(2):167–77.
- [84] Mani H, Sidhu GS, Kumari R, Gaddipati JP, Seth P, Maheshwari RK. Curcumin differentially regulates TGF- β 1, its receptors and nitric oxide synthase during impaired wound healing. *Biofactors* 2002;16(1–2):29–43.
- [85] Cheppudira B, Fowler M, McGhee L, Greer A, Mares A, Petz L, et al. Curcumin: a novel therapeutic for burn pain and wound healing. *Expert Opin Invest Drugs* 2013;22(10):1295–303.
- [86] Lansdown AB. Calcium: a potential central regulator in wound healing in the skin. *Wound Repair Regen* 2002;10(5):271–85.
- [87] Jadali A, Ghazizadeh S. Protein kinase D is implicated in the reversible commitment to differentiation in primary cultures of mouse keratinocytes. *J Biol Chem* 2010;285(30):23387–97.
- [88] Bikle DD, Ng D, Tu C-L, Oda Y, Xie Z. Calcium-and vitamin D-regulated keratinocyte differentiation. *Mol Cell Endocrinol* 2001;177(1):161–71.
- [89] Motta G. Calcium alginate topical wound dressings: a new dimension in the cost-effective treatment for exudating dermal wounds and pressure sores. *Ostomy Wound Manage* 1988;25: 52–6.
- [90] Huang JS, Mukherjee JJ, Chung T, Crilly KS, Kiss Z. Extracellular calcium stimulates DNA synthesis in synergism with zinc, insulin and insulin-like growth factor I in fibroblasts. *Eur J Biochem* 1999;266(3):943–51.
- [91] Wang Y, Zhang C-L, Zhang Q, Li P. Composite electrospun nanomembranes of fish scale collagen peptides/chitosan-oligosaccharides: antibacterial properties and potential for wound dressing. *Int J Nanomed* 2011;6:667–76.
- [92] Zhou T, Wang N, Xue Y, Ding T, Liu X, Mo X, et al. Development of biomimetic tilapia collagen nanofibers for skin regeneration through inducing keratinocytes differentiation and collagen synthesis of dermal fibroblasts. *ACS Appl Mater Interfaces* 2015;7(5): 3253–62.
- [93] Rujitanaroj P-o, Pimpha N, Supaphol P. Wound-dressing materials with antibacterial activity from electrospun gelatin fiber mats containing silver nanoparticles. *Polymer* 2008;49(21): 4723–32.
- [94] Vracko R. Basal lamina scaffold-anatomy and significance for maintenance of orderly tissue structure: a review. *Am J Pathol* 1974;77(2):313.
- [95] Tocco I, Zavan B, Bassetto F, Vindigni V. Nanotechnology-based therapies for skin wound regeneration. *J Nanomater* 2012;2012:4.
- [96] Sundaramurthi D, Vasanthan KS, Kuppan P, Krishnan UM, Sethuraman S. Electrospun nanostructured chitosan–poly (vinyl alcohol) scaffolds: a biomimetic extracellular matrix as dermal substitute. *Biomed Mater* 2012;7(4):045005.
- [97] Zhou Y, Yang D, Chen X, Xu Q, Lu F, Nie J. Electrospun water-soluble carboxyethyl chitosan/poly (vinyl alcohol) nanofibrous membrane as potential wound dressing for skin regeneration. *Biomacromolecules* 2007;9(1):349–54.
- [98] Dhandayuthapani B, Krishnan UM, Sethuraman S. Fabrication and characterization of chitosan-gelatin blend nanofibers for skin tissue engineering. *J Biomed Mater Res B Appl Biomater* 2010;94(1):264–72.
- [99] Leach JB, Bivens KA, Patrick CW, Schmidt CE. Photocrosslinked hyaluronic acid hydrogels: natural, biodegradable tissue engineering scaffolds. *Biotechnol Bioeng* 2003;82(5):578–89.
- [100] Uppal R, Ramaswamy GN, Arnold C, Goodband R, Wang Y. Hyaluronic acid nanofiber wound dressing—production, characterization, and in vivo behavior. *J Biomed Mater Res B Appl Biomater* 2011;97(1):20–9.
- [101] Barnes CP, Sell SA, Boland ED, Simpson DG, Bowlin GL. Nanofiber technology: designing the next generation of tissue engineering scaffolds. *Adv Drug Deliv Rev* 2007;59(14): 1413–33.
- [102] Sundaramurthi D, Krishnan UM, Sethuraman S. Electrospun nanofibers as scaffolds for skin tissue engineering. *Polym Rev* 2014;54(2):348–76.
- [103] Kumbar SG, Nukavarapu SP, James R, Nair LS, Laurencin CT. Electrospun poly (lactic acid-co-glycolic acid) scaffolds for skin tissue engineering. *Biomaterials* 2008;29(30):4100–7.
- [104] Chong E, Phan T, Lim I, Zhang Y, Bay B, Ramakrishna S, et al. Evaluation of electrospun PCL/gelatin nanofibrous scaffold for wound healing and layered dermal reconstitution. *Acta Biomater* 2007;3(3):321–30.
- [105] Venugopal J, Ramakrishna S. Biocompatible nanofiber matrices for the engineering of a dermal substitute for skin regeneration. *Tissue Eng* 2005;11(5–6):847–54.
- [106] Kuppan P, Vasanthan KS, Sundaramurthi D, Krishnan UM, Sethuraman S. Development of poly (3-hydroxybutyrate-co-3-hydroxyvalerate) fibers for skin tissue engineering: effects of topography, mechanical, and chemical stimuli. *Biomacromolecules* 2011;12(9):3156–65.
- [107] Heo DN, Yang DH, Lee JB, Bae MS, Kim JH, Moon SH, et al. Burn-wound healing effect of gelatin/polyurethane nanofiber scaffold containing silver-sulfadiazine. *J Biomed Nanotechnol* 2013;9(3):511–5.
- [108] Kim SE, Heo DN, Lee JB, Kim JR, Park SH, Jeon SH, et al. Electrospun gelatin/polyurethane blended nanofibers for wound healing. *Biomed Mater* 2009;4(4):044106.
- [109] Wei G, Jin Q, Giannobile WV, Ma PX. Nano-fibrous scaffold for controlled delivery of recombinant human PDGF-BB. *J Control Release* 2006;112(1):103–10.
- [110] Chandrasekaran AR, Venugopal J, Sundararajan S, Ramakrishna S. Fabrication of a nanofibrous scaffold with improved bioactivity for culture of human dermal fibroblasts for skin regeneration. *Biomed Mater* 2011;6(1):015001.
- [111] Jin G, Prabhakaran MP, Kai D, Ramakrishna S. Controlled release of multiple epidermal induction factors through core–shell nanofibers for skin regeneration. *Eur J Pharm Biopharm* 2013; 85(3):689–98.
- [112] Shuster S, Black MM, Mcvitie E. The influence of age and sex on skin thickness, skin collagen and density. *Br J Dermatol* 1975; 93(6):639–43.
- [113] Naylor EC, Watson RE, Sherratt MJ. Molecular aspects of skin ageing. *Maturitas* 2011;69(3):249–56.
- [114] Floyd RA, Townner RA, He T, Hensley K, Maples KR. Translational research involving oxidative stress and diseases of aging. *Free Radic Biol Med* 2011;51(5):931–41.
- [115] Masaki H. Role of antioxidants in the skin: anti-aging effects. *J Dermatol Sci* 2010;58(2):85–90.

- [116] Farage M, Miller K, Elsner P, Maibach H. Intrinsic and extrinsic factors in skin ageing: a review. *Int J Cosmet Sci* 2008;30(2): 87–95.
- [117] Pinnell SR. Cutaneous photodamage, oxidative stress, and topical antioxidant protection. *J Am Acad Dermatol* 2003;48(1):1–22.
- [118] Rittié L, Fisher GJ. UV-light-induced signal cascades and skin aging. *Ageing Res Rev* 2002;1(4):705–20.
- [119] Ngan CL, Basri M, Tripathy M, Karjiban RA, Abdul-Malek E. Skin intervention of fullerene-integrated nanoemulsion in structural and collagen regeneration against skin aging. *Eur J Pharm Sci* 2015;70:22–8.
- [120] Cataldo F. Interaction of C 60 fullerene with lipids. *Chem Phys Lipids* 2010;163(6):524–9.
- [121] Enhanced skin structure through innovative anti-aging treatment with intense pulsed light (IPL) and boswellia nanoparticles. *Ästhetische Dermatol* 2009;4:28–33.
- [122] Shibuya S, Ozawa Y, Watanabe K, Izuo N, Toda T, Yokote K, et al. Palladium and platinum nanoparticles attenuate aging-like skin atrophy via antioxidant activity in mice. *PLoS One* 2014;9.
- [123] Shibuya S, Ozawa Y, Yokote K, Shimizu T. Palladium and platinum nanoparticles attenuate aging-like skin atrophy via antioxidant activity. *Free Radic Biol Med* 2014;(76):S90.
- [124] Clark RA, Ghosh K, Tonnesen MG. Tissue engineering for cutaneous wounds. *J Invest Dermatol* 2007;127(5):1018–29.
- [125] Gurtner GC, Werner S, Barrandon Y, Longaker MT. Wound repair and regeneration. *Nature* 2008;453(7193):314–21.
- [126] Mitsiadis TA, Barrandon O, Rochat A, Barrandon Y, De Bari C. Stem cell niches in mammals. *Exp Cell Res* 2007;313(16): 3377–85.
- [127] Bowlin GL. A new spin on scaffold. *Mater Today* 2004;7(5):64.
- [128] Ayres CE, Jha BS, Sell SA, Bowlin GL, Simpson DG. Nanotechnology in the design of soft tissue scaffolds: innovations in structure and function. *Wiley Interdiscip Rev Nanomed Nanobiotechnol* 2010;2(1):20–34.
- [129] Lim SH, Mao H-Q. Electrospun scaffolds for stem cell engineering. *Adv Drug Deliv Rev* 2009;61(12):1084–96.
- [130] Agarwal S, Wendorff JH, Greiner A. Use of electrospinning technique for biomedical applications. *Polymer* 2008;49(26):5603–21.
- [131] Braghirolli DI, Steffens D, Pranke P. Electrospinning for regenerative medicine: a review of the main topics. *Drug Discov Today* 2014;19(6):743–53.
- [132] Ingavle GC, Leach JK. Advancements in electrospinning of polymeric nanofibrous scaffolds for tissue engineering. *Tissue Eng Part B Rev* 2013;20(4):277–93.
- [133] Norouzi M, Boroujeni SM, Omidvarkordshouli N, Soleimani M. Advances in skin regeneration: application of electrospun scaffolds. *Adv Healthcare Mater* 2015;4.
- [134] Beachley V, Wen X. Polymer nanofibrous structures: fabrication, biofunctionalization, and cell interactions. *Prog Polym Sci* 2010; 35(7):868–92.
- [135] Jayarama Reddy V, Radhakrishnan S, Ravichandran R, Mukherjee S, Balamurugan R, Sundarrajan S, et al. Nanofibrous structured biomimetic strategies for skin tissue regeneration. *Wound Repair Regen* 2013;21(1):1–16.
- [136] Gainza G, Villullas S, Pedraz JL, Hernandez RM, Igartua M. Advances in drug delivery systems (DDSs) to release growth factors for wound healing and skin regeneration. *Nanomedicine* 2015;11.
- [137] Peh P, Lim NSJ, Blocki A, Chee SML, Park HC, Liao S, et al. Simultaneous delivery of highly diverse bioactive compounds from blend electrospun fibers for skin wound healing. *Bioconjug Chem* 2015;26.
- [138] Mirdailami O, Soleimani M, Dinarvand R, Khoshayand MR, Norouzi M, Hajarizadeh A, et al. Controlled release of rhEGF and rhbFGF from electrospun scaffolds for skin regeneration. *J Biomed Mater Res Part A* 2015;103.
- [139] Choi JS, Kim HS, Yoo HS. Electrospinning strategies of drug-incorporated nanofibrous mats for wound recovery. *Drug Deliv Transl Res* 2015;5(2):137–45.
- [140] Dai X-Y, Nie W, Wang Y-C, Shen Y, Li Y, Gan S-J. Electrospun emodin polyvinylpyrrolidone blended nanofibrous membrane: a novel medicated biomaterial for drug delivery and accelerated wound healing. *J Mater Sci Mater Med* 2012;23(11):2709–16.
- [141] Schneider A, Wang X, Kaplan D, Garlick J, Egles C. Bio-functionalized electrospun silk mats as a topical bioactive dressing for accelerated wound healing. *Acta Biomater* 2009;5(7): 2570–8.
- [142] Szentivanyi A, Chakradeo T, Zernetsch H, Glasmacher B. Electrospun cellular microenvironments: understanding controlled release and scaffold structure. *Adv Drug Deliv Rev* 2011;63(4): 209–20.
- [143] Norouzi M, Shabani I, Ahvaz HH, Soleimani M. PLGA/gelatin hybrid nanofibrous scaffolds encapsulating EGF for skin regeneration. *J Biomed Mater Res Part A* 2014;103.
- [144] Blackstone BN, Drexler JW, Powell HM. Tunable engineered skin mechanics via coaxial electrospun fiber core diameter. *Tissue Eng Part A* 2014;20(19–20):2746–55.
- [145] Wu L, Li H, Li S, Li X, Yuan X, Li X, et al. Composite fibrous membranes of PLGA and chitosan prepared by coelectrospinning and coaxial electrospinning. *J Biomed Mater Res Part A* 2010;92(2):563–74.
- [146] Wade RJ, Burdick JA. Advances in nanofibrous scaffolds for biomedical applications: from electrospinning to self-assembly. *Nano Today* 2014;9(6):722–42.
- [147] Hu C, Cui W. Hierarchical structure of electrospun composite fibers for long-term controlled drug release carriers. *Adv Healthcare Mater* 2012;1(6):809–14.
- [148] Yang Y, Xia T, Zhi W, Wei L, Weng J, Zhang C, et al. Promotion of skin regeneration in diabetic rats by electrospun core-sheath fibers loaded with basic fibroblast growth factor. *Biomaterials* 2011;32(18):4243–54.
- [149] Pettikiriarachchi JT, Parish CL, Nisbet DR, Forsythe JS. Architectural and surface modification of nanofibrous scaffolds for tissue engineering. *Nanotechnol Life Sci* 2012. <http://dx.doi.org/10.1002/9783527610419.ntls0258>.
- [150] Xin S, Li X, Wang Q, Huang R, Xu X, Lei Z, et al. Novel layer-by-layer structured nanofibrous mats coated by protein films for dermal regeneration. *J Biomed Nanotechnol* 2014;10(5):803–10.
- [151] Polini A, Pagliara S, Stabile R, Netti GS, Roca L, Praticchizzo C, et al. Collagen-functionalised electrospun polymer fibers for bioengineering applications. *Soft Matter* 2010;6(8):1668–74.
- [152] Gümüşderelioğlu M, Dalkıranoğlu S, Aydın R, Çakmak S. A novel dermal substitute based on biofunctionalized electrospun PCL nanofibrous matrix. *J Biomed Mater Res Part A* 2011;98(3):461–72.
- [153] Pham QP, Sharma U, Mikos AG. Electrospun poly (ϵ -caprolactone) microfiber and multilayer nanofiber/microfiber scaffolds: characterization of scaffolds and measurement of cellular infiltration. *Biomacromolecules* 2006;7(10):2796–805.
- [154] Pu J, Yuan F, Li S, Komvopoulos K. Electrospun bilayer fibrous scaffolds for enhanced cell infiltration and vascularization in vivo. *Acta Biomater* 2015;13:131–41.
- [155] Yang X, Shah JD, Wang H. Nanofiber enabled layer-by-layer approach toward three-dimensional tissue formation. *Tissue Eng Part A* 2008;15(4):945–56.
- [156] Ma B, Xie J, Jiang J, Wu J. Sandwich-type fiber scaffolds with square arrayed microwells and nanostructured cues as micro-skin grafts for skin regeneration. *Biomaterials* 2014;35(2):630–41.
- [157] Baker BM, Gee AO, Metter RB, Nathan AS, Marklein RA, Burdick JA, et al. The potential to improve cell infiltration in composite fiber-aligned electrospun scaffolds by the selective removal of sacrificial fibers. *Biomaterials* 2008;29(15):2348–58.

- [158] Hirst AR, Escuder B, Miravet JF, Smith DK. High-tech applications of self-assembling supramolecular nanostructured gel-phase materials: from regenerative medicine to electronic devices. *Angew Chem Int Ed* 2008;47(42):8002–18.
- [159] Maude S, Ingham E, Aggeli A. Biomimetic self-assembling peptides as scaffolds for soft tissue engineering. *Nanomedicine* 2013; 8(5):823–47.
- [160] Meng H, Chen L, Ye Z, Wang S, Zhao X. The effect of a self-assembling peptide nanofiber scaffold (peptide) when used as a wound dressing for the treatment of deep second degree burns in rats. *J Biomed Mater Res B Appl Biomater* 2009;89(2):379–91.
- [161] Kao B, Kadomatsu K, Hosaka Y. Construction of synthetic dermis and skin based on a self-assembled peptide hydrogel scaffold. *Tissue Eng Part A* 2009;15(9):2385–96.
- [162] Webber MJ, Tongers J, Renault M-A, Roncalli JG, Losordo DW, Stupp SI. Development of bioactive peptide amphiphiles for therapeutic cell delivery. *Acta Biomater* 2010;6(1):3–11.
- [163] Matson JB, Stupp SI. Self-assembling peptide scaffolds for regenerative medicine. *Chem Commun* 2012;48(1):26–33.
- [164] Cui H, Webber MJ, Stupp SI. Self-assembly of peptide amphiphiles: from molecules to nanostructures to biomaterials. *Pept Sci* 2010;94(1):1–18.
- [165] Matson JB, Zha RH, Stupp SI. Peptide self-assembly for crafting functional biological materials. *Curr Opin Solid State Mater Sci* 2011;15(6):225–35.
- [166] Capito RM, Azevedo HS, Velichko YS, Mata A, Stupp SI. Self-assembly of large and small molecules into hierarchically ordered sacs and membranes. *Science* 2008;319(5871):1812–6.
- [167] Chow LW, Bitton R, Webber MJ, Carvajal D, Shull KR, Sharma AK, et al. A bioactive self-assembled membrane to promote angiogenesis. *Biomaterials* 2011;32(6):1574–82.
- [168] Tay CY, Irvine SA, Boey FY, Tan LP, Venkatraman S. Micro-/nano-engineered cellular responses for soft tissue engineering and biomedical applications. *Small* 2011;7(10):1361–78.
- [169] Groeber F, Holeiter M, Hampel M, Hinderer S, Schenke-Layland K. Skin tissue engineering—in vivo and in vitro applications. *Adv Drug Deliv Rev* 2011;63(4):352–66.
- [170] Mashinchian O, Turner L-A, Dalby MJ, Laurent S, Shokrgozar MA, Bonakdar S, et al. Regulation of stem cell fate by nanomaterial substrates. *Nanomedicine* 2015;10(5):829–47.
- [171] Mahmoudi M, Bonakdar S, Shokrgozar MA, Aghaverdi H, Hartmann R, Pick A, et al. Cell-imprinted substrates direct the fate of stem cells. *ACS Nano* 2013;7(10):8379–84.
- [172] Mashinchian O, Bonakdar S, Taghinejad H, Satarifard V, Heidari M, Majidi M, et al. Cell-imprinted substrates act as an artificial niche for skin regeneration. *ACS Appl Mater Interfaces* 2014;6(15):13280–92.
- [173] Murphy SV, Atala A. 3D bioprinting of tissues and organs. *Nat Biotechnol* 2014;32(8):773–85.
- [174] Seol Y-J, Kang H-W, Lee SJ, Atala A, Yoo JJ. Bioprinting technology and its applications. *Eur J Cardiothorac Surg* 2014;ezu148.
- [175] Sinha G. Cell presses. *Nature Biotechnol* 2014;32.
- [176] Jakab K, Norotte C, Marga F, Murphy K, Vunjak-Novakovic G, Forgacs G. Tissue engineering by self-assembly and bioprinting of living cells. *Biofabrication* 2010;2(2):022001.
- [177] Lee V, Singh G, Trasatti JP, Bjornsson C, Xu X, Tran TN, et al. Design and fabrication of human skin by three-dimensional bioprinting. *Tissue Eng Part C Methods* 2013;20(6):473–84.
- [178] Lee W, Debasitis JC, Lee VK, Lee J-H, Fischer K, Edminster K, et al. Multi-layered culture of human skin fibroblasts and keratinocytes through three-dimensional freeform fabrication. *Biomaterials* 2009;30(8):1587–95.
- [179] Koch L, Deiwick A, Schlie S, Michael S, Gruene M, Coger V, et al. Skin tissue generation by laser cell printing. *Biotechnol Bioeng* 2012;109(7):1855–63.
- [180] Michael S, Sorg H, Peck C-T, Koch L, Deiwick A, Chichkov B, et al. Tissue engineered skin substitutes created by laser-assisted bioprinting form skin-like structures in the dorsal skin fold chamber in mice. *PLoS One* 2013;8(3):e57741.
- [181] Sofokleous P, Stride E, Bonfield W, Edirisinghe M. Design, construction and performance of a portable handheld electrohydrodynamic multi-needle spray gun for biomedical applications. *Mater Sci Eng C* 2013;33(1):213–23.
- [182] Skardal A, Mack D, Kapetanovic E, Atala A, Jackson JD, Yoo J, et al. Bioprinted amniotic fluid-derived stem cells accelerate healing of large skin wounds. *Stem Cells Transl Med* 2012; 1(11):792.
- [183] Algizlan H, Varada S. Three-dimensional printing of the skin. *JAMA Dermatol* 2015;151(2):207.

Imaging Nanoparticle Skin Penetration in Humans

L.L. Lin, M. Yamada, T.W. Prow

The University of Queensland, Brisbane, QLD, Australia

OUTLINE

Introduction	353	<i>Single-Photon Microscopy</i>	359
Skin Structure and Barrier Functions on Nanoparticle Penetration	354	<i>Optical Coherence Tomography</i>	361
<i>Skin Structure</i>	354	Conclusions and Perspectives	363
<i>Mechanism of Nanoparticle Penetration into Skin</i>	355	List of Acronyms and Abbreviations	364
<i>Factors Affecting Nanoparticle Penetration</i>	356	References	364
Noninvasive Microscopy Techniques	357		
<i>Multiphoton Microscopy (MPM) and Time-Related Single-Photon Counting</i>	358		

INTRODUCTION

Our skin is being increasingly exposed to nanoparticles from both environmental and manmade sources. Nanoparticles originate from natural sources like particulates formed during volcano eruptions, cosmic sources such as meteorite collisions with earth, or even desert dust storms that drive particulates into the upper atmosphere [1]. Manmade nanoparticle material is being mass produced, for example, zinc oxide (ZnO) and titanium dioxide (TiO₂). Both of these materials are milled to the micro- and nanoscale for personal care and pharmaceutical applications. The global ZnO market is currently 1200 kilotons [2] with TiO₂, a pigment and sunscreen active, being produced at 5000 tons per year in 2010. Of which, an estimated 1300 tons were used for personal care products in 2005 [3]. Thus, there is a real need to understand how these nanoparticles interact with our skin.

Nanoparticle skin interactions are the focus of significant research efforts, but there are relatively few approaches that can be adapted to the clinical setting where the need for new information is greatest. The long list of personal care products that contain nanoparticles are considered to be relatively safe, but we do not know how these nanoparticles interact with the complex biology that exists in skin. One of the relevant questions that drive the field is that of nanoparticle penetration into the viable skin. The skin is an outstanding barrier to topical nanoparticles. The epidermal layer, or outermost skin strata, is constantly turning over and shedding outer layers. This creates a situation where penetrating nanoparticles can be shed quickly from the outer layers, especially with normal skin care practices like washing with soap and water [4].

The ideal analytical method for studying nanoparticle penetration and residence time in skin would be a

quantitative, sensitive, and noninvasive approach that could distinguish nanoparticles from microparticles and skin. Clinical studies have significant barriers to invasive sampling approaches because tissue has to be biopsied from the volunteer, which is expensive and can put the patient at risk. This limits conventional nanoparticle research approaches like electron microscopy and elemental analysis. Imaging is particularly suited to studying some nanoparticles but is also limited by several factors, including resolution and specificity. Imaging is noninvasive and can be semiquantitative or quantitative depending on the approach. Nonlinear optical imaging approaches have some exceptional benefits that include high specificity when combined with advanced acquisition instrumentation, high optical resolution, no requirement for dyes, and biocompatibility. There are a number of imaging devices available for clinical use that involve light, confocal, and nonlinear optical imaging options.

Clinical skin-imaging technology has improved over the last decade. We now have an array of clinical imaging options that can help to investigate nanoparticle–skin interactions. Our 2011 publication on the penetration of gold nanoparticles (Au-NPs) in human skin is an example where clinical imaging technologies were applied (Fig. 27.1) [5]. The imaging data from conventional dermoscopy showed aggregation in the skin furrows, a common phenomenon in nanoparticle-treated skin that we have observed time and time again. The color changes we observed with dermoscopy hinted at the aggregation status of the Au-NPs. Reflectance confocal microscopy was useful for imaging aggregates in the skin furrows, but there is a lack of specificity with this approach. It was relatively difficult to differentiate between reflectance from stratum corneum (SC) and Au-NPs. This issue was resolved with the use of multiphoton imaging coupled with time-correlated single-photon counting. We were able to use fluorescence lifetime measurements to differentiate signal from skin and that from Au-NPs. This approach was central to our focus on evaluating nanoparticle penetration into skin. No other analytical method enables this type of experimental design. We see imaging as a necessary method to investigate nanoparticle–skin interactions in humans.

SKIN STRUCTURE AND BARRIER FUNCTIONS ON NANOPARTICLE PENETRATION

Skin Structure

The skin makes up 16% of body weight, with a surface area of 1.8 m [2], which makes it the largest organ

of the body. The most important function of skin is to allow and limit the inward and outward passage of water, electrolytes, and various substances. The skin provides protection against microorganisms, ultraviolet radiation, toxic agents, and mechanical insults. The skin consists of three main layers: epidermis, dermis, and hypodermis. The epidermis and dermis play important roles from the perspective of nanoparticle penetration.

The epidermis is the outermost skin layer and serves as the physical and chemical barrier between the interior body and the environment. The main cells of the epidermis are the keratinocytes, which synthesize the structural protein keratin. There are four sublayers within the epidermis (top to bottom): SC, being the outer most nonliving keratinocytes; stratum granulosum; stratum spinosum; and stratum basale, which contains important cells with specific functions (eg, Langerhans cells, melanocytes, and Merkel cells). The keratinocytes in the basal layer undergo differentiation as they mature and migrate from the lower layers toward the surface of the skin. This process keeps the epidermis healthy and intact by a continuous regeneration and renewal of its components [6]. The major defense layer of the epidermis is the SC. The SC prevents the entrance of chemical and biological agents and is made up of layers of hexagonal-shaped, nonviable cornified cells known as corneocytes. Corneocytes are filled with keratin and keratin cross-linked with filaggrin. It is the shape and orientation of keratin proteins that provide additional mechanical strength to the SC. Together with the interactions between the macro- and microstructures of the SC, and organization of the complex SC lipid matrix, the outcome is the barrier action of the SC to keep out the majority of foreign compounds that people are exposed to.

The dermis is below the epidermis and is composed of a tough, supportive protein matrix. It is made of two layers, a thin papillary layer and a thick reticular layer. The dermis is made up of fibroblasts, which produce collagen, elastin, and structural proteoglycans that make up the supportive matrix. Collagen fibers make up 70% of the dermis, providing the skin with strength and toughness while maintaining elasticity and flexibility. Because of the organization of the matrix, the dermis provides minimal barrier properties to small drugs. The capillary anastomoses within the dermis transport nutrients and oxygen to the epidermis, while clearing the dermis from penetrated foreign agents and cell metabolic products. A review by Baroli discusses in detail how the different cellular components and structures within the skin provide defensive functions toward nanoparticle penetration [7].

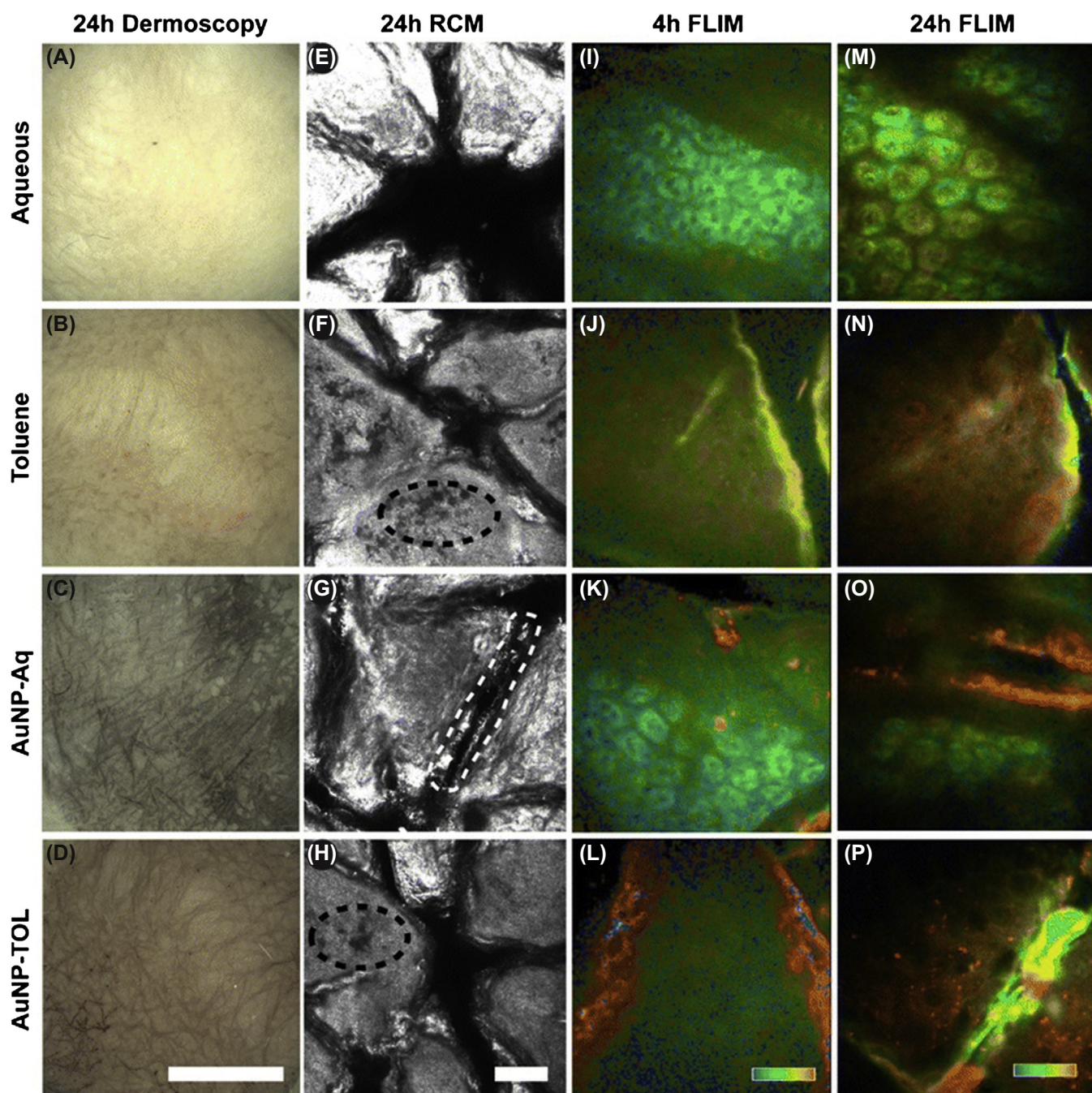


FIGURE 27.1 Noninvasive imaging of nanoparticle-treated excised human skin. The surfaces of skin samples treated with aqueous solution, toluene, AuNP-Aq, and AuNP-TOL were imaged using dermoscopy (A–D) and RCM (E–H) at 24 h. Abnormal structures were observed in toluene-treated skin (F, H; *black dashed line*). The white dashed line highlights highly reflective particles on the surface of the skin (G). FLIM images of the skin were taken at 4 h (I–L) and 24 h (M–P) post treatment. The pseudocolored MPT–FLIM images are $\alpha 1\%$ 50–100 from blue to red. Blue-green coloration indicates cellular autofluorescence (ie, NADPH), and AuNP luminescence is orange to red (K, L, O, P). Scale bars: 4 mm (D); 50 μm (H, L, P) [35].

Mechanism of Nanoparticle Penetration into Skin

Topical formulations when applied onto skin can deliver active compounds into the deeper region of the

skin (epidermis and/or dermis) through a number of ways. Fig. 27.2 shows the three potential pathways of particle transport across the SC. It was first believed that transporting compounds across the SC through the transepidermal pathway was the main mechanism

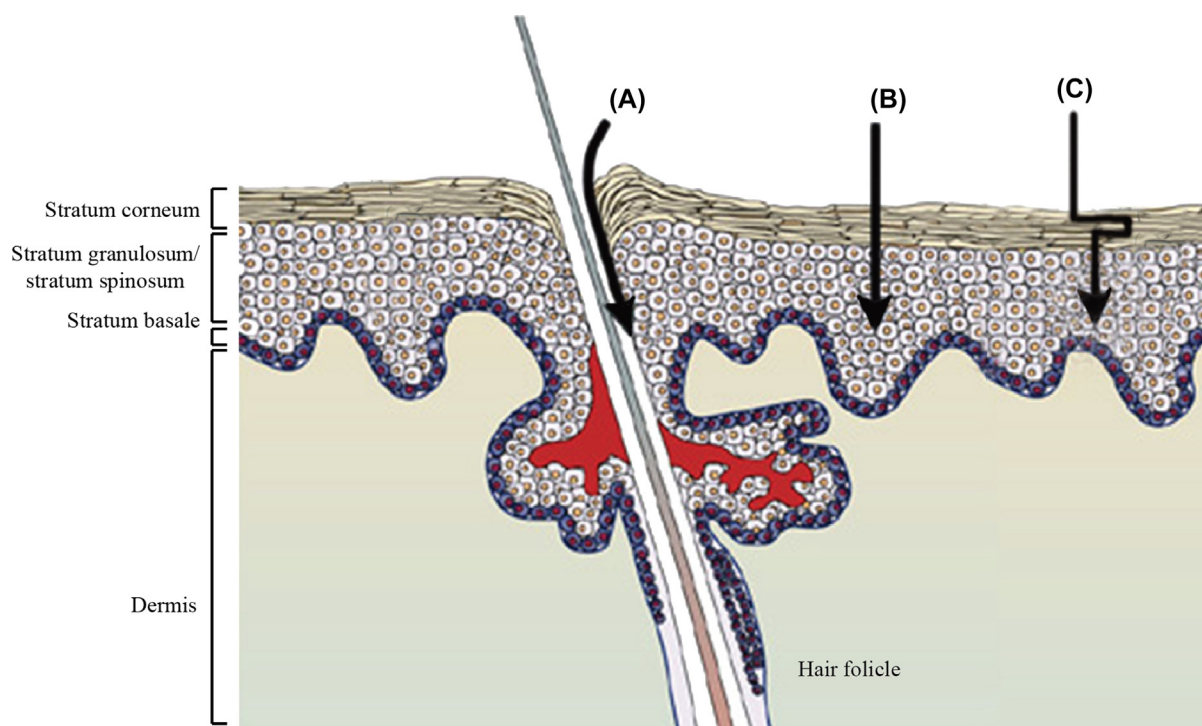


FIGURE 27.2 Potential transport pathways of particles across skin barrier. The primary skin barrier is made up of a nonliving layer of keratinocytes that is approximately 10–20 μm thick. Particles can pass through the barrier into the deeper regions of the skin by the transappendageal route through hair follicles or sweat glands (A); the transepidermal route via keratinocytes (B); or intercellular lipids (C). Adapted from Prausnitz MR, Mitragotri S, Langer R. Current status and future potential of transdermal drug delivery. *Nat Rev Drug Discov* 2004;3(2):115–24.

of skin penetration. Yet this is not likely in most cases, given that it requires repeated partitioning of the particle between lipophilic and hydrophilic compartments to get past layers of the intracellular matrix of keratin and keratohyalin, which is mostly impenetrable [8]. Evidence shows that the intercellular pathway is common for most penetrants [7,9]. Large molecules or particles could not move freely into the deeper layer of skin as they may be physically restricted within the lipid channels. Smaller molecules may diffuse into intercellular spaces, and the rate of diffusion is driven by their lipophilicity and other physicochemical properties, including molecular weight, solubility, and hydrogen bonding ability [10]. Wang, Kasting, and Nitsche have shown evidence to support the significance of the transcellular pathway [11], even for lipophilic molecules, but this issue remains controversial.

We and others have found that skin appendages such as hair follicles, sweat glands, and sebaceous glands may be an alternative route of delivery, even though these features are relatively sparse across the skin surface [5,12,13]. These appendages provide open channels on the skin surface that may facilitate penetration of nanoparticles through a *trans*-follicular pathway. The physical structure of the hair follicles could also promote accumulation and storage of particles, as supported by

studies looking at penetration of topical caffeine and minoxidil across intact skin barrier through uptake into appendages [14,15]. The mechanism for small molecules and nanoparticles may be governed differently, and it is still largely undefined for the latter.

Factors Affecting Nanoparticle Penetration

Nanoparticle penetration into skin due to unintended nanoparticle exposure remains a significant issue in terms of environmental, health, and safety perspectives. In general, the risk for nanoparticles and microparticles to penetrate skin is thought to be negligible in intact skin. However, in the case when skin barrier is compromised, the possibility of particle penetration is enhanced. We have investigated the penetration of 35 nm ZnO nanoparticles (ZnO-NPs) in psoriatic patients by quantifying surface-enhanced multiphoton photoemission signals generated from the particles. Concentrated ZnO-NP signals were observed in the lesion furrows but remained on the surface of the skin in both lesion and nonlesional regions. We observed comparable signals from treated and untreated, lesion and nonlesional sites, and our results supported findings reported in a TGA review [16]. The review concluded, based on existing evidence, that the lack of

nanoparticle penetration in volunteers with psoriasis was the reason for the absence of increase in systemic zinc levels.

Other than the condition of skin, the physiochemical properties of the nanoparticle were found to be significant contributors to skin penetration. The most important nanoparticle property that influences skin penetration is the size of the nanoparticle. Different nanoparticles of various sizes have been studied in human and animal models. Sonavane et al. described a size-dependent permeation of Au-NPs into rat skin [17]. They found enhanced permeation with 15 nm Au-NPs compared to 102 and 198 nm Au-NPs, and the permeability coefficient decreases as the particle size increases. This finding was corroborated by a study that reported greater penetration in excised human skin with 6 nm Au-NPs than 15 nm particles [18]. ZnO-NPs of varying sizes from 20 to 200 nm, in contrast, were only restricted to the SC and within the skin furrows [19–22]. The study evaluating the influence of nanoparticle size on penetration through the follicular pathway revealed different outcomes [23]. Patzelt et al. reported that there was a trend of deeper penetration in the hair follicle with increased particle sizes of poly(lactic-co-glycolic acid) particles for up to 643 nm, and depth of penetration decreased with 860 nm particles. The depth of penetration was significantly increased with larger particles with exceptions to 300, 470, and 860 nm particles ($p < .05$). The size-dependent penetration profile was the same for silica particles in the same study, where deepest penetration was observed with 646 nm particles. They correlated the penetration profiles of the poly(lactic-co-glycolic acid) and silica particles in their study to the morphometry of follicle length, infundibulum, and the bulge region of the hair follicle reported by Vogt et al. [24]. They advocated that the delivery of particles can be selectively targeted to different parts of the hair follicle by the particle diameter. This phenomenon was also discussed by Lademann et al. [25]. The group has shown that optimal penetration and accumulation of particles occur if the applied particles have similar thickness as the cuticula.

Nanoparticles come in various forms and shapes. The ability to penetrate and the choice of route may depend on whether the nanoparticle is rigid or deformable. Deformable nanoparticles are typically made of polymer, or they could be nanosomes (small lipid vesicles) or composites comprising a deformable surfactant layer and a nondeformable inorganic core. A study using larger flexible nanosomes, known as flexosomes, have shown that deformable particles overcome the SC by opening intercellular hydrophilic pathways through transdermal water concentration gradients [26]. The lamellar structure of flexosomes

has the ability to deform and fit into the passages between the cells. The force produced by the gradient then drives them through the SC and into the epidermal layer. For example, Geusens et al. have shown that secosomes, a form of ultra-flexible liposomes, have enhanced skin penetration compared to rigid or partially rigid liposomes [27]. The surface charge and polarity of the nanoparticle may also influence its ability to penetrate the skin barrier. In theory, positively charged nanoparticles are favored as the surface of skin and hair is negatively charged under physiological conditions. There are a number of studies examining the effects of surface properties on skin penetration, but the outcomes are not consistent [28–32].

In addition to those factors discussed in the earlier sections, the penetration of nanoparticles can be enhanced by formulations, exposure of time, and physical or mechanical approaches. Labouta and Schneider have discussed current evidence on how these factors could affect skin penetration [33].

Almost all of the studies have employed one or more imaging techniques to assess the penetration outcome of particles or nanoparticles. However, not many have studied the penetration of nanoparticles in humans. This may be limited by the accessibility of noninvasive imaging tools and the ethics regulation issues in human volunteer studies.

NONINVASIVE MICROSCOPY TECHNIQUES

Studying nanomaterial penetration into human skin has proven to be a challenging field. Most studies rely on the use of invasive sampling methods such as biopsied skin or excised human skin [7,34–36] or animal models [37–39]. The extensive use of these ex vivo methods in industry and academic research is tied to benefits like having fewer regulatory issues to overcome and less time-consuming experiments. The accuracy of these in vitro experiments, on the other hand, relies strongly on study approach in terms of skin model, experimental setup, and analytical method [33]. In vivo assessment on human volunteers for defining nanoparticle penetration remains the most relevant model but is challenging due to health, safety, and ethical reasons. Noninvasive imaging techniques provide real-time risk assessment on nanoparticle exposure and penetration in humans without requiring invasive sampling. Here, we discuss some of the imaging technologies that are commonly used to localize nanoparticles in human volunteer skin.

Multiphoton Microscopy (MPM) and Time-Correlated Single-Photon Counting

MPM or multiphoton tomography offers high-contrast imaging with submicron spatial resolution and picosecond temporal resolution in biological tissues [40]. MPM can be coupled with multimodal imaging technologies (eg, Raman spectroscopy, reflectance, fluorescence lifetime imaging (FLIM), optical coherence tomography (OCT), and photoacoustic) to facilitate noninvasive, real-time imaging in human volunteers. This technology has the highest resolution in noninvasive clinical imaging [41] compared to ultrasound, OCT, reflectance confocal microscopy (RCM), and Raman microscopy [42,43]. This has attracted researchers to apply it to a wide range of biological applications, including assessment of skin conditions [44,45], in vivo cell-trafficking tracking [46], metabolic imaging [47], drug delivery [22], and stem cell optoinjection [48]. Yet the application of this technology has been limited by the substantial acquisition ($\sim 300,000\text{€}$) and maintenance cost of the instrument due to the need for a femtosecond excitation laser source.

The majority of the MPM systems are built using Mai-Tai (Newport/Spectra Physics) or Chameleon (Coherent Inc.) 80 MHz/fs, near-infrared, titanium–sapphire tunable laser (Fig. 27.3). MPM has the ability to separate nanoparticle signals from endogenous fluorophores, such as nicotinamide adenine dinucleotide phosphate (NADPH), keratin, porphyrins, elastin, and so on. MPM–FLIM systems paired with time-correlated single-photon counting (TCSPC) detectors [49] allow

the simultaneous assessment of endogenous fluorophores and nanomaterials without the need for fluorescent dyes, which are not possible with other techniques [50]. The use of high numerical aperture objectives (>1 NA) and low laser powers (<40 mW) in MPM systems enables a tiny subfemtoliter focal volume. This results in superior lateral ($<1\text{ }\mu\text{m}$) and axial resolutions ($1\text{--}2\text{ }\mu\text{m}$) in tissue imaging, facilitating experiments to characterize or localize nanoparticles' exposure to biologically relevant structures at a resolution that is not possible with other imaging technologies [51].

The fact that nanotechnologies are a fast-growing market and are already in use in a variety of consumer products means that people are increasingly exposed to newly developed nanomaterials. A number of studies have shown that nanoparticles can be toxic to living cells [52,53], and the question of whether existing approaches can accurately assess risks of these nanoparticles to human health remains debatable. One of the fundamental strategies to assess this risk is by determining whether the nanoparticles breach the skin barrier and reach viable tissue. MPM has been exceptionally useful in nanotoxicology investigations to track the fate of nanoparticles in biological systems [54–57] and to study their interaction with human skin [20,35,58]. The gold standard for studying localization of individual nanoparticles, and their size and distribution within cells and tissues, is transmission electron microscopy (TEM). This technique also has the ability to characterize the elemental component of the nanoparticles. However, the downsides of TEM compared to MPM are the need for sample acquisition and processing, and the lack of

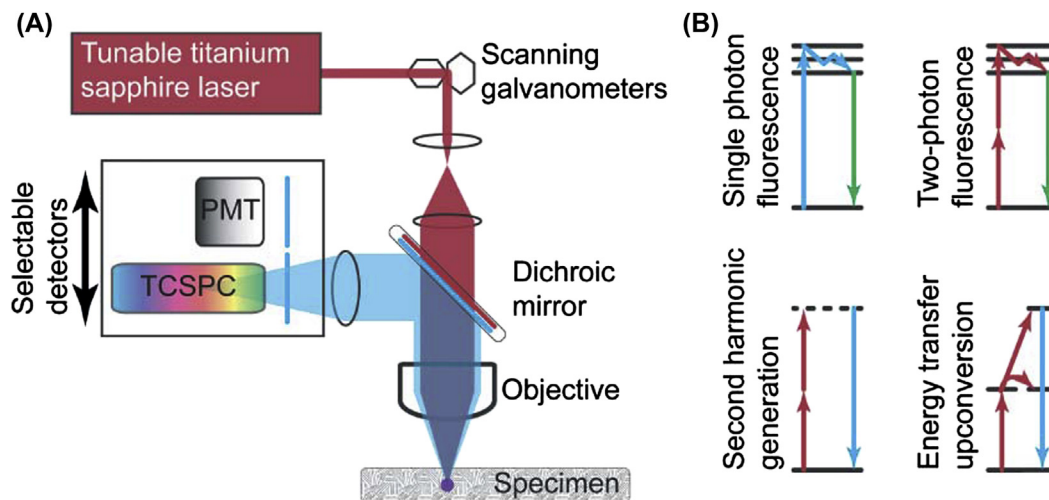


FIGURE 27.3 Schematic of MPM and energy transfer diagrams. (A) The components of MPM include a tunable titanium–sapphire laser source and scanning galvanometers to raster scan the excitation beam over the imaging area. The excitation beam (red) passes through a dichroic mirror and optical lenses before reaching the sample. The emitted light (blue) then passes back to the lenses and is reflected to one or more detectors by the dichroic mirror. Photomultiplier tube and TCSPC detectors can be stationary or be selected depending on the application. (B) Energy transfer diagrams for single-photon fluorescence, two-photon fluorescence, second harmonic generation, and energy transfer upconversion [80].

quantitative results with TEM. TEM also requires significant training for users, as highly technical and demanding protocols are involved.

MPM–FLIM, in contrast, is more favorable given the ability to isolate and quantify metal nanoparticles and quantum dots resulting from multiphoton-enhanced photoluminescence (MEP) [20,59,60], without the ethical or compliance implications from multiple biopsies in healthy skin. FLIM quantifies the time that photons interacted with a sample using TCSPC detectors and provides the fluorescence decay curves for each pixel. The numerical lifetimes (τ_1 and τ_2) and amplitudes ($\alpha_1\%$ and $\alpha_2\%$) of fast and slow decay components can be extracted from the FLIM images when fitted to a decay profile. In the case of examining a complex medium, for instance nanoparticles within skin, a double-exponential decay profile can be applied during data processing. These numerical outputs can be analyzed to differentiate nanoparticle signals from endogenous signals. However, as described in our previous study [20] with ZnO-NPs, the separation of nanoparticle signals from skin autofluorescence is not straightforward. The emission signals for NADPH and ZnO-NPs were spectrally overlapped, but the signals could be separated using FLIM [20]. ZnO-NPs undergo ultrafast MEP, and the proportion of photons that return to the detector will be nearly 100%. Photons resulting from MEP have short lifetime components, while NADPH has both long and short lifetime components. The separation of ZnO-NP signals can be confounded by the shift in a fluorescence lifetime histogram of NADPH of a given pixel resulting from alterations in the microenvironment (eg, binding of protein). The amplitudes of the decay components, however, remain unchanged with microenvironment alterations and were the key to separating the nanoparticle signals from autofluorescence [20] (Fig. 27.4). The MEP signal from ZnO-NPs was detected within 95–100 amplitudes of the fast decay component ($\alpha_1\%$), while the fluorescence lifetime signal of skin autofluorescence ranges from 55 to 95 [20].

A related but less stringent (and less costly) strategy for differentiating ZnO-NP signals from skin autofluorescence is through the isolation of second harmonic generation (SHG) and hyper-Rayleigh scattering (HRS) from spectrally resolved broadband detection [61]. A metal oxide nanoparticle such as a ZnO-NP has the ability to generate both coherent and incoherent radiation at half the excitation wavelength; these are also known as SHG and HRS, respectively. SHG–HRS signals are highly specific to ZnO-NPs in the viable epidermis and are not affected by the presence of dissolved zinc and autofluorescence within the tissue. Spectrally resolved broadband detection was achieved with the addition of two charge-coupled device cameras and two photo multipliers to the MPM systems. A 300–700 nm

broadband filter with a spectral width of 14 nm and an interference filter of full width at half maximum, transmitting at 380 nm, were added in front of the photo multipliers to separate the spectrally broad autofluorescence signal and spectrally narrow SHG–HRS signals. Consistent with our findings [20], Davin et al. also reported that ZnO-NPs are located within the furrows and wrinkles and did not penetrate the viable epidermis [61]. Others, including Zvyagin et al. and Gratieri et al., also did not observe any evidence of nanoparticles penetration into skin [57,62] with the use of MPM systems.

Single-Photon Microscopy

Single-photon confocal microscopy, which is also commonly known as laser scanning confocal microscopy (LSCM), is more frequently used to track fluorescent nanoparticles in cells [63,64], within tissues [31,35,65], and even in vivo [5,66,67]. The benefits of LSCM are the ease of use and the availability of relatively inexpensive equipment. One of the key benefits of using LSCM for in vivo nanoparticle imaging is that the optical sections acquired are free from artifacts commonly seen in sections that are generated during tissue processing. However, the nanoparticles need to be intrinsically fluorescent or have fluorescent tags to be detected by this form of microscopy. Consequently, the range of lasers (eg, argon, krypton–argon, helium–neon, and helium–cadmium) for which efficient fluorophore excitation can be achieved could be a limiting factor of LSCM [68]. Another problem with this technique is the risk of damage to both viable tissue and the fluorophore resulting in photobleaching [69].

Single-photon microscopy may not have as superior penetration depth and contrast compared to MPM systems. However, many of these imaging technologies are seen as complementary and often are paired to improve assessment [70]. Clinical imaging technologies such as dermoscopy and reflectance confocal microscopy (RCM), the latter of which is a form of single-photon microscopy, were used to complement MPM imaging as seen in Fig. 27.1. RCM can provide high-resolution ($<1.25\ \mu\text{m}$ in the horizontal plane and $<5.0\ \mu\text{m}$ in the vertical plane) in vivo imaging for up to 200 μm in skin, and it enables collection of large mosaics (maximum of $8\times 8\ \text{mm}^2$) that provides valuable information on nanoparticles aggregation and changes in tissue morphology and architecture.

The typical configuration of a single-photon confocal microscope includes a laser light source to illuminate a fluorescent derivative, a condenser, objective lenses, and a point detector. Unlike MPM systems, the focal point from the excitation beam is focused through a pinhole that is placed in front of the detector, blocking

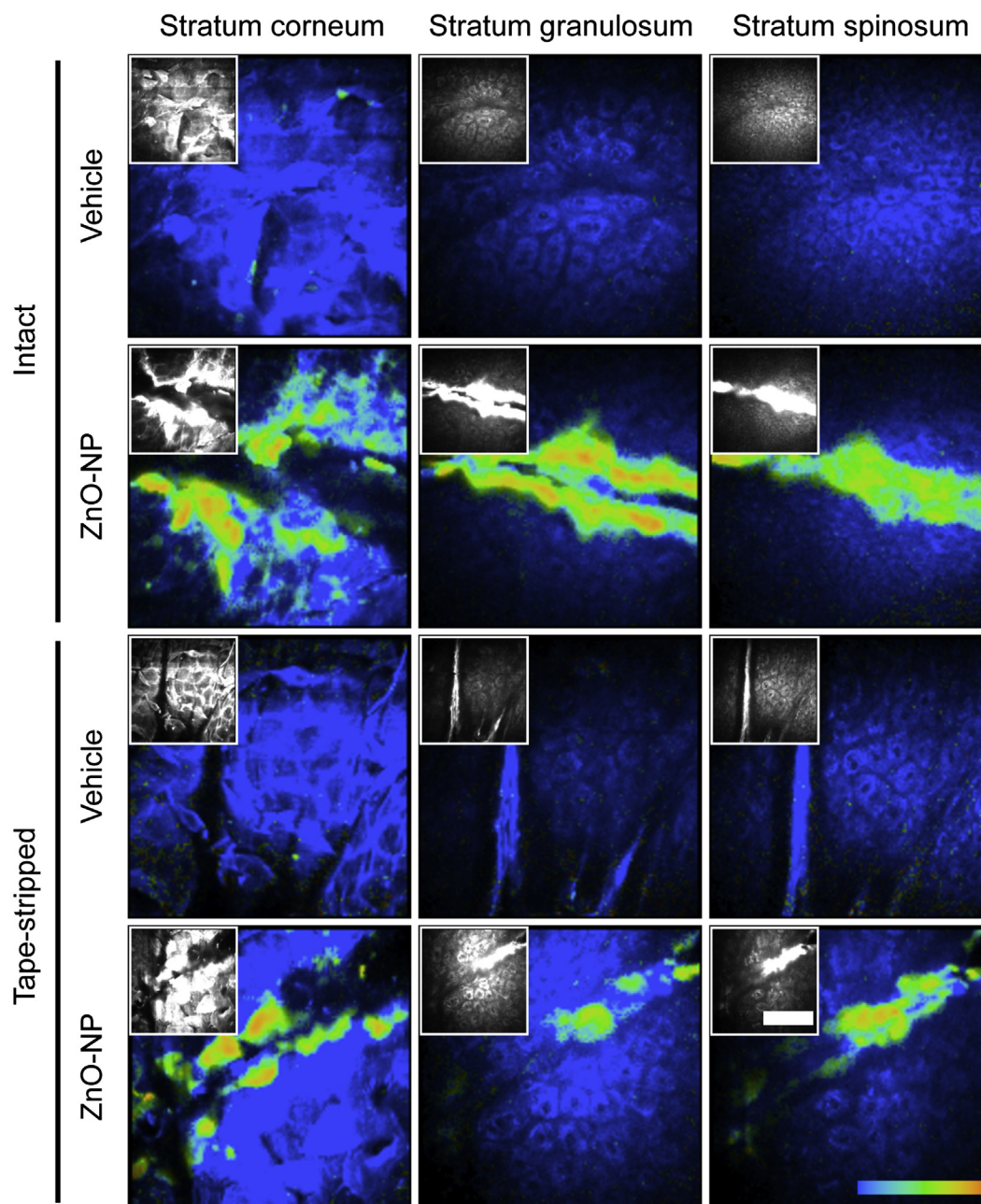


FIGURE 27.4 In vivo MPM-FLIM images of intact and tape-stripped skin taken at different depths post 24 h treatment with either ZinClear-S 60 CCT (ZnO nanoparticles dispersed in caprylic/capric triglycerides) or CCT (vehicle). Each image is $214 \times 214 \times 1 \mu\text{m}^3$. Autofluorescence is blue ($\alpha 1\%$ 0–85) and ZnO-NPs are green-red ($\alpha 1\%$ 90–100) in the color images. The grayscale insets are intensity-only images. The color scale bar represents $\alpha 1\%$ 85–100, blue-red [20].

out scattered light that is out of focus. The high-contrast image from RCM is based on backscattering of light, and it is governed by the refractive index of the structures compared to the surrounding medium [71]. Structures in the grayscale reflectance images that appear bright have components with a high reflective index compared to the surrounding tissue. In skin, components like melanin, keratin, and collagen are highly reflective. The commercially available RCM systems from Lucid

Inc. uses relatively low laser power between 1 and 25 mW, and they have either a single wavelength (830 nm) or multiple wavelengths (488, 658, and 758 nm) with fluorescence imaging capacity.

Most studies that use LSCM to investigate nanoparticle penetration into skin were carried out in either excised human [7,34,35,62] or animal skin [12,37,38,72]. We are the first group to report the use of RCM systems for the assessment of a topical nanoparticle penetration

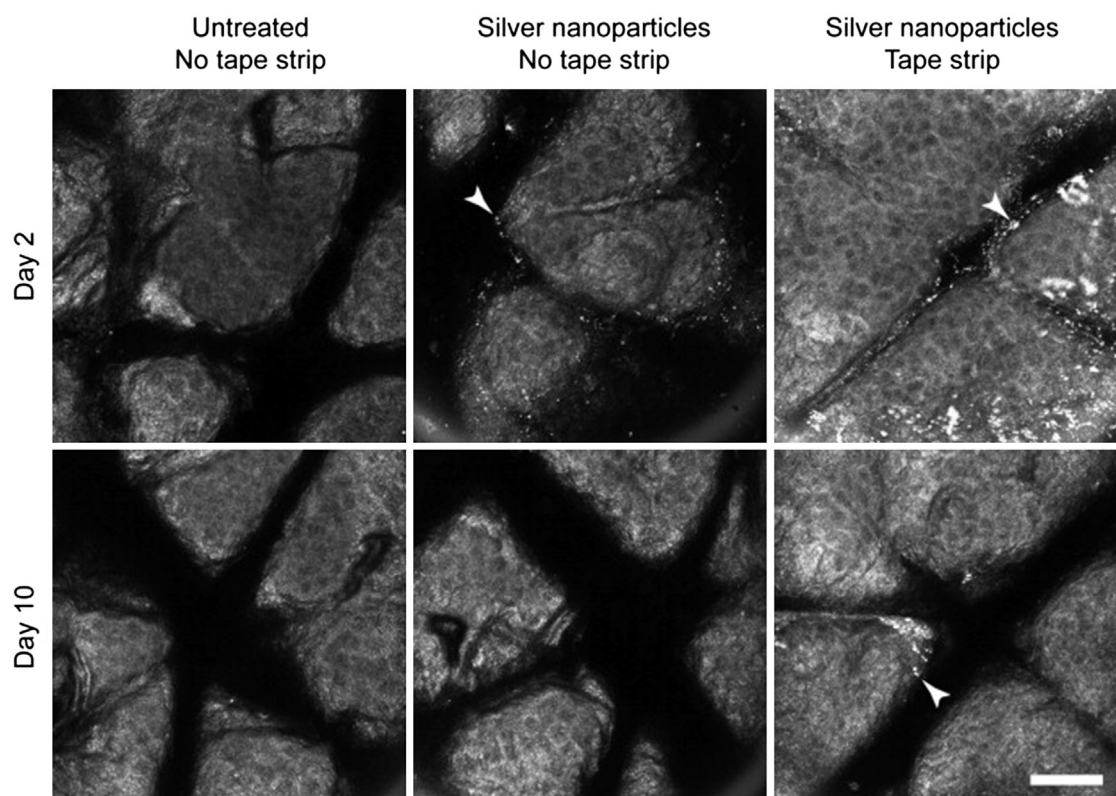


FIGURE 27.5 In vivo RCM images of untreated, and intact and tape-stripped, skin that was treated with Ag-NPs. Silver nanoparticle aggregates (white arrowheads) were observed within the skin furrows at 2 and 6 days (data not shown) after application in intact and tape-stripped skin. No aggregates were seen after 10 days in intact skin, but discrete aggregates were observed in tape-stripped skin. Each image is $0.5 \times 0.5 \text{ mm}^2$ [5].

profile in human volunteers [5]. A commercial spray containing silver NPs (Ag-NPs) of $<50 \text{ nm}$ was applied to intact and tape-stripped skin. Relatively large Ag-NP aggregates (Fig. 27.5, white arrowheads) were observed on the skin surface after 48 h, particularly in the furrows, and were tracked for up to 10 days using RCM (Fig. 27.5). We detected no aggregates in intact skin 10 days post treatment, while the aggregates in tape-stripped skin appeared to persist on the surface of skin, within furrows, and in hair follicles. Morphological assessment from RCM images suggested no abnormalities associated with Ag-NP treatment. The ratio of $\alpha 1\%:\alpha 2\%$ from the MPM-FLIM data was also analyzed in the same study to determine whether Ag-NPs have any metabolic effects on skin. The study concluded with no statistically significant differences in NADPH intensity and lifetime in untreated and treated skin, including tape-stripped skin. Additionally, the data showed that there were depth-dependent differences in NADPH intensity and lifetime that supported the idea that metabolic activity changes with depth. RCM is a highly relevant clinical imaging tool to nanotoxicology research, given its capacity to identify metal nanoparticle aggregates and to rapidly assess skin morphology and architecture changes in human studies.

Optical Coherence Tomography

OCT generates two-dimensional or three-dimensional, cross-sectional, depth-resolved images using low-coherent interferometry in the near-infrared wavelengths. Detailed principles of OCT can be found in the article by Fercher [73]. In brief, the technology uses an interferometry technique to collect structural data from complex media such as skin. Two light paths are used in OCT: one (the reference beam) goes to a reference mirror, and the other (the probing beam) passes through the galvanometer scanning mirrors and optics to the sample (Fig. 27.6A). A reference profile is generated from the reflectivity from the mirror path and is compared to the sample path. High light-scattering components within the tissue will produce increased interference and appear as bright areas in the OCT image (Fig. 27.6B).

OCT is analogous to ultrasound and RCM imaging but with critical differences. OCT uses light, while ultrasound images are acquired through sound. OCT quantifies differences in wave propagation information through interferometry, whereas RCM detects the level of backscattered light from samples. There are several favorable features of OCT that make it a useful tool for nanoparticle imaging in volunteers. The relatively long

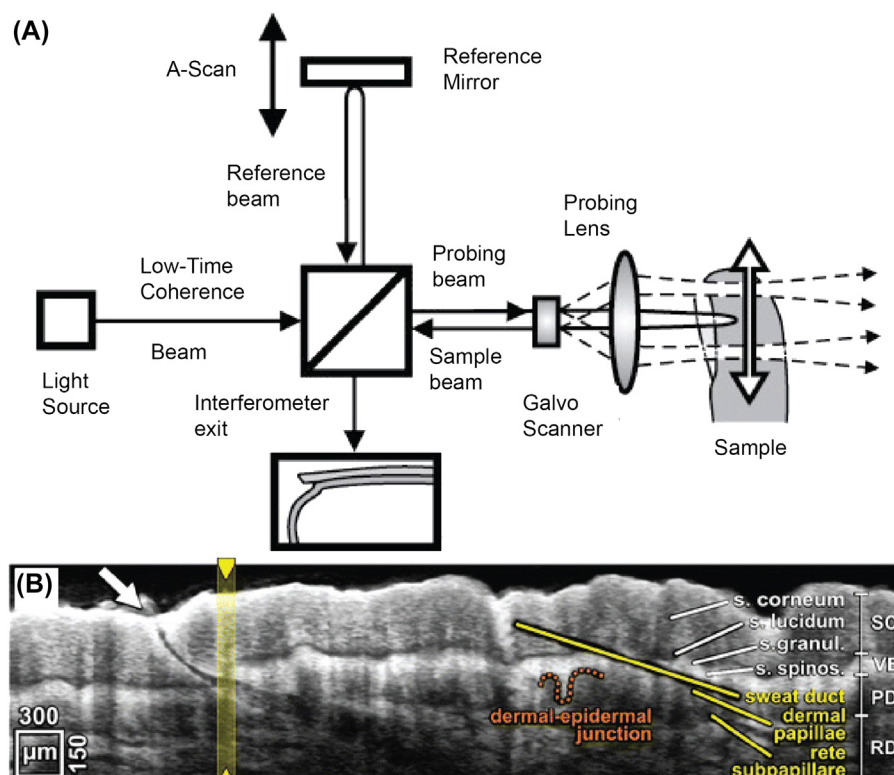


FIGURE 27.6 Schematic of OCT imaging and images of healthy human skin. The acquisition of depth and lateral data is decoupled. Lateral scanning (*open double arrow*) is performed by the moving focus of the probing beam and directed to the sample after focusing through the galvanometer scanning mirrors and optics. Depth data (A-scan) are obtained by depth shifting the coherence window with the reference mirror (A). (B) An example of healthy skin applied with microneedle where different strata of the skin and the site of microneedle application (*white arrow*) can be observed [73,81]. SC, Stratum corneum; VE, viable epidermis; PD, papillary dermis; RD, reticular dermis.

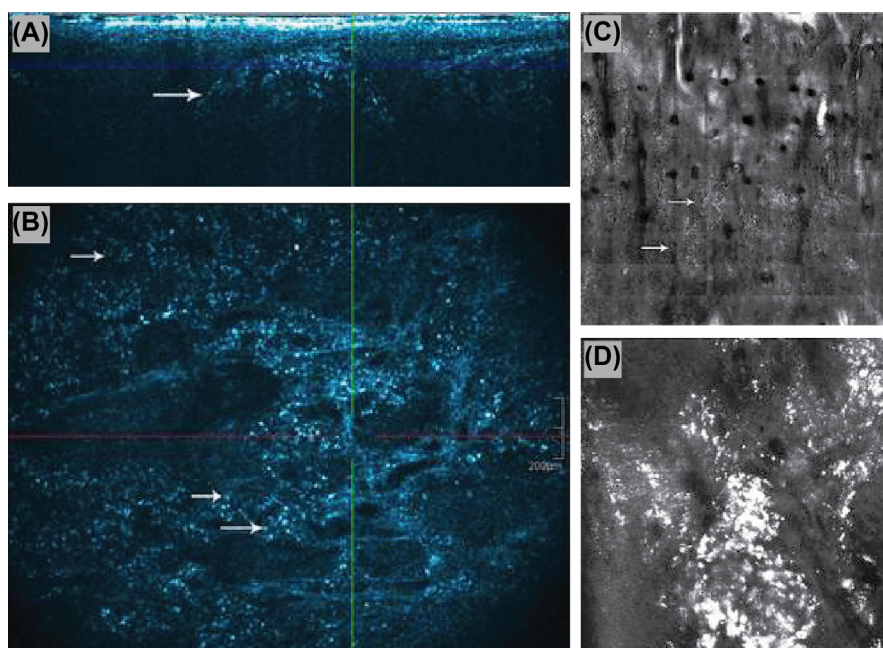


FIGURE 27.7 Clustered pigmentation can be observed below the epidermis from a cross-sectional high-definition optical coherence tomography image, and the formation of round granuloma-like structures is indicated by the *white arrow* (A). Scattered pigment can be located at the subepidermal level based on the en-face image. The *white arrows* in (B) indicate bright structures with a dark center that may correspond to pigment-loaded macrophages. A $5 \times 5 \text{ mm}^2$ RCM mosaic image reveals the distribution of pigment structures (*white arrows*) (C), while highly reflective structures corresponding to the pigment can be observed from a single field of view ($0.5 \times 0.5 \text{ mm}^2$) (D) [76].

wavelength light in OCT imaging enables deep penetration, and up to 2 to 3 mm penetration depth can be achieved in most tissues. OCT has an axial resolution of 1–15 μm that would enable architectural morphology and certain cellular features to be resolved without the need for fluorescent dyes or contrast agents. Similar to most noninvasive imaging technologies, imaging can be done without the need for excision or tissue processing.

OCT is an emerging technology that will be highly relevant for analysis of nanoparticle exposure and penetration in vivo [74–77]. Given that OCT has low contrast levels in biological tissue, inorganic nanoparticles were used as contrast agents to overcome this limitation. The use of nanoparticles to improve OCT contrast in biological tissues was, however, limited due to potential toxicity. Previous studies have supported the use of OCT for in vivo imaging of nanoparticle penetration, not just for diagnostic purposes but also as a relevant tool for studying skin penetration upon exposure.

An example by Maier et al. showed that OCT has the ability to localize carbon nanoparticles and assess morphological changes in a 40-year-old female's lip after undergoing a permanent lip-lining procedure [76]. The carbon nanoparticle-containing pigment was identified as bright clusters of particles dispersed in the epidermis and superficial dermis using high-definition OCT and RCM (Fig. 27.7). They also detected macrophages loaded with pigment within a noninfectious granuloma consisting of highly reflective structures in both high-definition OCT and RCM images. The presence of the nodular granuloma containing lymphohistiocytic infiltrates was further confirmed by histopathological findings from a skin biopsy.

CONCLUSIONS AND PERSPECTIVES

The advances in nanotechnology have called for the need to assess potential health risks of new nanoparticles in humans. One of the first questions to determine whether a particular nanoparticle causes toxicity is to find out if the particle can overcome the skin barrier and penetrate living tissues of the skin. Current methodologies to investigate skin penetration mostly consist of invasive techniques that make human studies difficult and can involve substantial amounts of tissue processing. Noninvasive imaging provides an alternative and complementary method for more accurate assessments of nanotoxicity in the whole, as the study can be carried out in human volunteers with minimal issues. This form of analysis also allows for longitudinal studies of nanotoxicity, which are impossible with destructive analytical approaches. That said, there are several

limitations to consider before imaging nanoparticles in skin.

One limitation of imaging nanoparticles in skin is the vast difference in the size of skin features and the diameter of nanoparticles; for example, skin features are measured in micrometers, whereas nanoparticle features are measured in nanometers. The size of a single nanoparticle is at least 30,000 times smaller than a single keratinocyte [78]; one practical limitation is that when we image different skin strata, with hematoxylin and eosin (H&E)-stained sections for instance, we will not be able to visualize the nanoparticles with the same light microscope due to insufficient magnification and resolution. We can approach this in two ways. One is to use electron microscopy to study individual nanoparticles at subcellular resolution, with the limitations of analyzing only a small area and the risk of overinterpreting artifacts. Another is the use of noninvasive imaging techniques to assess the skin organization, disregarding probable errors in the number of nanoparticles and their location. The ideal approach for studying toxicity of a nanoparticle would be to combine high-resolution imaging in excised human skin and noninvasive imaging technologies in human volunteers.

The ability to differentiate what is and is not a nanoparticle is one of the most challenging aspects of studying nanoparticles in skin. For example, the actual concentration exposed to skin in reality may be below the detectable limit of the imaging tool available, but that does not conclude that there are no nanoparticles that had penetrated the skin. It is also possible that a researcher might not visualize the nanoparticles the same way others reported in their studies. We routinely image high concentrations of nanoparticles blotted onto paper as a positive control when setting up a new experiment. This approach helps us to more accurately interpret the imaging data and avoid artifacts.

The use of these imaging instruments becomes increasingly intricate as the complexity of these machines increases. Each imaging modality has pros and cons in terms of imaging nanoparticles in skin and potential artifacts. Individual nanoparticles can be resolved with TEM, but only a small sample can be analyzed, in addition to the invasive sample preparation process. Functional readouts such as NADPH and quantity of nanoparticles can be extracted from MPM, but this requires an experienced user, and significant misinterpretation of data can occur otherwise. LSCM offers high xy resolution but has poor depth resolution when it comes to nanoparticles. RCM is easy to use in clinical settings but could only visualize highly reflective materials on the surface of the skin in this context. OCT can provide outstanding depth data but has low contrast in biological tissues. Multimodality imaging combines the strengths of individual modalities while

overcoming their limitations. We believe that integrating multiple imaging modalities can improve skin penetration data and provide more accurate and comprehensive information for diagnosis of diseases.

List of Acronyms and Abbreviations

Ag-NP Silver nanoparticle
Au-NP Gold nanoparticle
CCT Caprylic/capric triglyceride
FLIM Fluorescence lifetime imaging microscopy
HRS Hyper-Rayleigh scattering
LSCM Laser scanning confocal microscopy
MPM Multiphoton microscopy
NADPH Nicotinamide adenine dinucleotide phosphate
OCT Optical coherent tomography
RCM Reflectance confocal microscopy
SHG Second harmonic generation
TCSPC Time-correlated single photon counting
TEM Transmission electron microscopy
TiO₂-NP Titanium dioxide nanoparticle
ZnO-NP Zinc oxide nanoparticle

References

- [1] Lungu M, Neculae A, Bunoiu M, Biris CG. Nanoparticles' promises and risks: characterization, manipulation, and potential hazards to humanity and the environment. Cham: Springer; 2014.
- [2] ZOFA.ORG. Zinc Oxide Producers Association 2015 Available from: <http://www.zopa.org/>.
- [3] Weir A, Westerhoff P, Fabricius L, Hristovski K, von Goetz N. Titanium dioxide nanoparticles in food and personal care products. *Environ Sci Technol* 2012;46(4):2242–50.
- [4] Raphael AP, Sundh D, Grice JE, Roberts MS, Soyer HP, Prow TW. Zinc oxide nanoparticle removal from wounded human skin. *Nanomedicine (Lond)* 2013;8(11):1751–61.
- [5] Prow TW, Grice JE, Lin LL, Faye R, Butler M, Becker W, et al. Nanoparticles and microparticles for skin drug delivery. *Adv Drug Deliv Rev* 2011;63(6):470–91.
- [6] Menon GK. New insights into skin structure: scratching the surface. *Adv Drug Deliv Rev* 2002;54(Suppl. 1):S3–17.
- [7] Baroli B, Ennas MG, Loffredo F, Isola M, Pinna R, López-Quintela MA. Penetration of metallic nanoparticles in human full-thickness skin. *J Invest Dermatol* 2007;127(7):1701–12.
- [8] Scheuplein RJ, Blank IH. Permeability of the skin. *Physiol Rev* 1971;51(4):702–47.
- [9] Elias PM, Friend DS. The permeability barrier in mammalian epidermis. *J Cell Biol*. 1975;65(1):180–91.
- [10] Potts RO, Guy RH. A predictive algorithm for skin permeability: the effects of molecular size and hydrogen bond activity. *Pharm Res* 1995;12(11):1628–33.
- [11] Wang TF, Kasting GB, Nitsche JM. A multiphase microscopic diffusion model for stratum corneum permeability. II. Estimation of physicochemical parameters, and application to a large permeability database. *J Pharm Sci* 2007;96(11):3024–51.
- [12] Alvarez-Román R, Naik A, Kalia YN, Guy RH, Fessi H. Skin penetration and distribution of polymeric nanoparticles. *J Controlled Release* 2004;99(1):53–62.
- [13] Roberts MS, Walters KA. Human skin morphology and dermal absorption. In: *Dermal absorption and toxicity assessment*. 2nd ed. 2007. p. 1–15.
- [14] Grice JE, Ciotti S, Weiner N, Lockwood P, Cross SE, Roberts MS. Relative uptake of minoxidil into appendages and stratum corneum and permeation through human skin in vitro. *J Pharm Sci* 2010;99(2):712–8.
- [15] Liu X, Grice JE, Lademann J, Otberg N, Trauer S, Patzelt A, et al. Hair follicles contribute significantly to penetration through human skin only at times soon after application as a solvent deposited solid in man. *Br J Clin Pharmacol* 2011;72(5):768–74.
- [16] TGA. A review of the scientific literature on the safety of nanoparticulate titanium dioxide or zinc oxide in sunscreens. 2009.
- [17] Sonavane G, Tomoda K, Sano A, Ohshima H, Terada H, Makino K. In vitro permeation of gold nanoparticles through rat skin and rat intestine: effect of particle size. *Colloids Surf B Biointerfaces* 2008;65(1):1–10.
- [18] Labouta HI, el-Khordagui LK, Kraus T, Schneider M. Mechanism and determinants of nanoparticle penetration through human skin. *Nanoscale* 2011;3(12):4989–99.
- [19] Gontier E, Ynsa M-D, Biró T, Hunyadi J, Kiss B, Gáspár K, et al. Is there penetration of titania nanoparticles in sunscreens through skin? A comparative electron and ion microscopy study. *Nanotoxicology* 2008;2(4):218–31.
- [20] Lin LL, Grice JE, Butler MK, Zvyagin AV, Becker W, Robertson TA, et al. Time-correlated single photon counting for simultaneous monitoring of zinc oxide nanoparticles and NAD(P)H in intact and barrier-disrupted volunteer skin. *Pharm Res* 2011;28(11):2920–30.
- [21] Pflucker F, Wendel V, Hohenberg H, Gartner E, Will T, Pfeiffer S, et al. The human stratum corneum layer: an effective barrier against dermal uptake of different forms of topically applied micronised titanium dioxide. *Skin Pharmacol Appl Skin Physiol* 2001;14(Suppl. 1):92–7.
- [22] Roberts MS, Roberts MJ, Robertson TA, Sanchez W, Thorling C, Zou Y, et al. In vitro and in vivo imaging of xenobiotic transport in human skin and in the rat liver. *J Biophotonics* 2008;1(6):478–93.
- [23] Patzelt A, Richter H, Knorr F, Schäfer U, Lehr C-M, Dähne L, et al. Selective follicular targeting by modification of the particle sizes. *J Controlled Release* 2011;150(1):45–8.
- [24] Vogt A, Hadam S, Heiderhoff M, Audring H, Lademann J, Sterry W, et al. Morphometry of human terminal and vellus hair follicles. *Exp Dermatol* 2007;16(11):946–50.
- [25] Lademann J, Patzelt A, Richter H, Antoniou C, Sterry W, Knorr F. Determination of the cuticle thickness of human and porcine hairs and their potential influence on the penetration of nanoparticles into the hair follicles. *J Biomed Opt* 2009;14(2):021014.
- [26] Cevc G, Blume G. Lipid vesicles penetrate into intact skin owing to the transdermal osmotic gradients and hydration force. *Biochim Biophys Acta* 1992;1104(1):226–32.
- [27] Geusens B, Van Gele M, Braat S, De Smedt SC, Stuart MCA, Prow TW, et al. Flexible nanosomes (SECosomes) enable efficient siRNA delivery in cultured primary skin cells and in the viable epidermis of ex vivo human skin. *Adv Funct Mater* 2010;20(23):4077–90.
- [28] Jung S, Patzelt A, Otberg N, Thiede G, Sterry W, Lademann J. Strategy of topical vaccination with nanoparticles. *J Biomed Opt* 2009;14(2):021001.
- [29] Kohli AK, Alpar HO. Potential use of nanoparticles for transcutaneous vaccine delivery: effect of particle size and charge. *Int J Pharm* 2004;275(1–2):13–7.
- [30] Lopez RF, Seto JE, Blankschtein D, Langer R. Enhancing the transdermal delivery of rigid nanoparticles using the simultaneous application of ultrasound and sodium lauryl sulfate. *Biomaterials* 2011;32(3):933–41.
- [31] Prow TW, Monteiro-Riviere NA, Inman AO, Grice JE, Chen X, Zhao X, et al. Quantum dot penetration into viable human skin. *Nanotoxicology* 2012;6(2):173–85.

- [32] Ryman-Rasmussen JP, Riviere JE, Monteiro-Riviere NA. Penetration of intact skin by quantum dots with diverse physicochemical properties. *Toxicol Sci* 2006;91(1):159–65.
- [33] Labouta HI, Schneider M. Interaction of inorganic nanoparticles with the skin barrier: current status and critical review. *Nanomed: Nanotechnol, Biol Med* 2013;9(1):39–54.
- [34] Cross SE, Innes B, Roberts MS, Tsuzuki T, Robertson TA, McCormick P. Human skin penetration of sunscreen nanoparticles: in-vitro assessment of a novel micronized zinc oxide formulation. *Skin Pharmacol Physiol* 2007;20(3):148–54.
- [35] Labouta HI, Liu DC, Lin LL, Butler MK, Grice JE, Raphael AP, et al. Gold nanoparticle penetration and reduced metabolism in human skin by toluene. *Pharm Res* 2011;28(11):2931–44.
- [36] Wissing S, Müller R. Solid lipid nanoparticles as carrier for sunscreens: in vitro release and in vivo skin penetration. *J Controlled Release* 2002;81(3):225–33.
- [37] Mortensen LJ, Oberdörster G, Pentland AP, DeLouise LA. In vivo skin penetration of quantum dot nanoparticles in the murine model: the effect of UVR. *Nano Lett* 2008;8(9):2779–87.
- [38] Ostrowski A, Nordmeyer D, Boreham A, Brodwolf R, Mundhenk L, Fluhr JW, et al. Skin barrier disruptions in tape stripped and allergic dermatitis models have no effect on dermal penetration and systemic distribution of AHAPS-functionalized silica nanoparticles. *Nanomedicine* 2014;10(7):1571–81.
- [39] Wu J, Liu W, Xue C, Zhou S, Lan F, Bi L, et al. Toxicity and penetration of TiO₂ nanoparticles in hairless mice and porcine skin after subchronic dermal exposure. *Toxicol Lett* 2009;191(1):1–8.
- [40] König K, Riemann I. High-resolution multiphoton tomography of human skin with subcellular spatial resolution and picosecond time resolution. *J Biomed Opt* 2003;8(3):432–9.
- [41] Gibson EA, Masihzadeh O, Lei TC, Ammar DA, Kahook MY. Multiphoton microscopy for ophthalmic imaging. *J Ophthalmol* 2011;2011, 870879.
- [42] König K, Speicher M, Buckle R, Reckfort J, McKenzie G, Welzel J, et al. Clinical optical coherence tomography combined with multiphoton tomography of patients with skin diseases. *J Biophotonics* 2009;2(6–7):389–97.
- [43] König K, Speicher M, Kohler MJ, Scharenberg R, Kaatz M. Clinical application of multiphoton tomography in combination with high-frequency ultrasound for evaluation of skin diseases. *J Biophotonics* 2010;3(12):759–73.
- [44] Koehler MJ, König K, Elsner P, Bückle R, Kaatz M. In vivo assessment of human skin aging by multiphoton laser scanning tomography. *Opt Lett* 2006;31(19):2879–81.
- [45] Paoli J, Smedh M, Wennberg A-M, Ericson MB. Multiphoton laser scanning microscopy on non-melanoma skin cancer: morphologic features for future non-invasive diagnostics. *J Invest Dermatol* 2008;128(5):1248–55.
- [46] Fujisaki J, Wu J, Carlson AL, Silberstein L, Putheti P, Larocca R, et al. In vivo imaging of Treg cells providing immune privilege to the haematopoietic stem-cell niche. *Nature* 2011;474(7350):216–9.
- [47] Skala MC, Ricking KM, Bird DK, Gendron-Fitzpatrick A, Eickhoff J, Eliceiri KW, et al. In vivo multiphoton fluorescence lifetime imaging of protein-bound and free nicotinamide adenine dinucleotide in normal and precancerous epithelia. *J Biomed Opt* 2007;12(2):024014.
- [48] Foldes-Papp Z, König K, Studier H, Buckle R, Breunig HG, Uchugonova A, et al. Trafficking of mature miRNA-122 into the nucleus of live liver cells. *Curr Pharm Biotechnol* 2009;10(6):569–78.
- [49] Becker W, Bergmann A, Haustein E, Petrusek Z, Schwille P, Biskup C, et al. Fluorescence lifetime images and correlation spectra obtained by multidimensional time-correlated single photon counting. *Microsc Res Tech* 2006;69(3):186–95.
- [50] Helmchen F, Denk W. Deep tissue two-photon microscopy. *Nat Methods* 2005;2(12):932–40.
- [51] Zipfel WR, Williams RM, Christie R, Nikitin AY, Hyman BT, Webb WW. Live tissue intrinsic emission microscopy using multiphoton-excited native fluorescence and second harmonic generation. *Proc Natl Acad Sci USA* 2003;100(12):7075–80.
- [52] Lewinski N, Colvin V, Drezek R. Cytotoxicity of nanoparticles. *Small* 2008;4(1):26–49.
- [53] Samberg ME, Oldenburg SJ, Monteiro-Riviere NA. Evaluation of silver nanoparticle toxicity in skin in vivo and keratinocytes in vitro. *Environ Health Perspect* 2010;118(3):407–13.
- [54] Kolonics A, Csiszovszki Z, Toke ER, Lorincz O, Haluszka D, Szipocs R. In vivo study of targeted nanomedicine delivery into Langerhans cells by multiphoton laser scanning microscopy. *Exp Dermatol* 2014;23(8):596–605.
- [55] Roberts MS, Dancik Y, Prow TW, Thorling CA, Lin LL, Grice JE, et al. Non-invasive imaging of skin physiology and percutaneous penetration using fluorescence spectral and lifetime imaging with multiphoton and confocal microscopy. *Eur J Pharm Biopharm* 2011;77(3):469–88.
- [56] Teubl BJ, Leitinger G, Schneider M, Lehr CM, Fröhlich E, Zimmer A, et al. The buccal mucosa as a route for TiO₂ nanoparticle uptake. *Nanotoxicology* 2015;9(2):253–61.
- [57] Zvyagin AV, Zhao X, Gierden A, Sanchez W, Ross JA, Roberts MS. Imaging of zinc oxide nanoparticle penetration in human skin in vitro and in vivo. *J Biomed Opt* 2008;13(6):064031.
- [58] Graf BW, Chaney EJ, Marjanovic M, De Lizio M, Valero MC, Boppart MD, et al. In vivo imaging of immune cell dynamics in skin in response to zinc-oxide nanoparticle exposure. *Biomed Opt Express* 2013;4(10):1817–28.
- [59] Liang X, Grice JE, Zhu Y, Liu D, Sanchez WY, Li Z, et al. Intravital multiphoton imaging of the selective uptake of water-dispersible quantum dots into sinusoidal liver cells. *Small* 2015;11(14):1711–20.
- [60] Zhu Y, Choe CS, Ahlberg S, Meinke MC, Alexiev U, Lademann J, et al. Penetration of silver nanoparticles into porcine skin ex vivo using fluorescence lifetime imaging microscopy, Raman microscopy, and surface-enhanced Raman scattering microscopy. *J Biomed Opt* 2015;20(5):051006.
- [61] Darvin ME, König K, Kellner-Hoefer M, Breunig HG, Werncke W, Meinke MC, et al. Safety assessment by multiphoton fluorescence/second harmonic generation/hyper-Rayleigh scattering tomography of ZnO nanoparticles used in cosmetic products. *Skin Pharmacol Physiol* 2012;25(4):219–26.
- [62] Gratieri T, Schaefer UF, Jing L, Gao M, Kostka KH, Lopez RF, et al. Penetration of quantum dot particles through human skin. *J Biomed Nanotechnol* 2010;6(5):586–95.
- [63] Lewin M, Carlesso N, Tung C-H, Tang X-W, Cory D, Scadden DT, et al. Tat peptide-derivatized magnetic nanoparticles allow in vivo tracking and recovery of progenitor cells. *Nat Biotechnol* 2000;18(4):410–4.
- [64] Selvi BR, Jagadeesan D, Suma BS, Nagashankar G, Arif M, Balasubramanyam K, et al. Intrinsically fluorescent carbon nanospheres as a nuclear targeting vector: delivery of membrane-impermeable molecule to modulate gene expression in vivo. *Nano Lett* 2008;8(10):3182–8.
- [65] Prow T, Grebe R, Merges C, Smith JN, McLeod DS, Leary JF, et al. Nanoparticle tethered antioxidant response element as a biosensor for oxygen induced toxicity in retinal endothelial cells. *Mol Vis* 2006;12:616–25.
- [66] de Campos A, Diebold Y, Carvalho ES, Sánchez A, José Alonso M. Chitosan nanoparticles as new ocular drug delivery systems: in vitro stability, in vivo fate, and cellular toxicity. *Pharm Res* 2004;21(5):803–10.
- [67] Prow TW, Bhutto I, Kim SY, Grebe R, Merges C, McLeod DS, et al. Ocular nanoparticle toxicity and transfection of the retina and retinal pigment epithelium. *Nanomedicine* 2008;4(4):340–9.

- [68] Brelje TC, Wessendorf MW, Sorenson RL. Multicolor laser scanning confocal immunofluorescence microscopy: practical application and limitations. *Methods Cell Biol.* 2002;70:165–244.
- [69] Pedley KC. Applications of confocal and fluorescence microscopy. *Digestion* 1997;58(Suppl. 2):62–8.
- [70] Hwang JY, Park J, Kang BJ, Lubow DJ, Chu D, Farkas DL, et al. Multimodality imaging in vivo for preclinical assessment of tumor-targeted doxorubicin nanoparticles. *PLoS One* 2012;7(4): e34463.
- [71] Gareau DS, Patel YG, Rajadhyaksha M. Basic principles of reflectance confocal microscopy. In: *Reflectance confocal microscopy of cutaneous tumors*; 2008. p. 1–6.
- [72] Rouse JG, Yang J, Ryman-Rasmussen JP, Barron AR, Monteiro-Riviere NA. Effects of mechanical flexion on the penetration of fullerene amino acid-derivatized peptide nanoparticles through skin. *Nano Lett* 2007;7(1):155–60.
- [73] Fercher AF. Optical coherence tomography – development, principles, applications. *Z für Medizinische Physik* 2010;20(4):251–76.
- [74] Kim CS, Wilder-Smith P, Ahn Y-C, Liaw L-HL, Chen Z, Kwon YJ. Enhanced detection of early-stage oral cancer in vivo by optical coherence tomography using multimodal delivery of gold nanoparticles. *J Biomed Opt* 2009;14(3):034008.
- [75] Kirillin M, Shirmanova M, Sirotkina M, Bugrova M, Khlebtsov B, Zagaynova E. Contrasting properties of gold nanoshells and titanium dioxide nanoparticles for optical coherence tomography imaging of skin: Monte Carlo simulations and in vivo study. *J Biomed Opt* 2009;14(2):021017.
- [76] Maier T, Flaig MJ, Ruzicka T, Berking C, Pavicic T. High-definition optical coherence tomography and reflectance confocal microscopy in the in vivo visualization of a reaction to permanent make-up. *J Eur Acad Dermatol Venereol* 2015;29(3):602–6.
- [77] Zagaynova EV, Shirmanova MV, Kirillin MY, Khlebtsov BN, Orlova AG, Balalaeva IV, et al. Contrasting properties of gold nanoparticles for optical coherence tomography: phantom, in vivo studies and Monte Carlo simulation. *Phys Med Biol* 2008;53(18):4995–5009.
- [78] Utah TUo. Genetic Science Learning Center [Interactive]. 2015 Available from: <http://learn.genetics.utah.edu/content/cells/scale/>.
- [79] Prausnitz MR, Mitragotri S, Langer R. Current status and future potential of transdermal drug delivery. *Nat Rev Drug Discov* 2004;3(2):115–24.
- [80] Prow TW. Multiphoton microscopy applications in nanodermatology. *Wiley Interdiscip Rev Nanomed Nanobiotechnol* 2012;4(6):680–90.
- [81] Coulman S, Birchall J, Alex A, Pearton M, Hofer B, O'Mahony C, et al. In vivo, in situ imaging of microneedle insertion into the skin of human volunteers using optical coherence tomography. *Pharm Res* 2011;28(1):66–81.

EGF-Loaded Nanofibers for Skin Tissue Engineering

M. Norouzi¹, M. Soleimani²

¹Stem Cell Technology Research Center, Tehran, Iran; ²Tarbiat Modares University, Tehran, Iran

OUTLINE

Introduction	367	Conclusion	372
Epidermal Growth Factor Mechanisms of Action	367	Glossary	372
Topical Delivery of Epidermal Growth Factor	368	References	372
Epidermal Growth Factor-Loaded Nanofibers	368		

INTRODUCTION

Epidermal growth factor (EGF) was first isolated from mouse salivary glands by Stanley Cohen in 1962 as part of the Nobel Prize-winning project of discovery of the growth factors (GFs). Thereupon, GF therapy has progressed for treatment of wounds into clinical practice [1–4].

EGF is a polypeptide of 53 amino acids that is secreted by platelets, macrophages, and fibroblasts. After an acute injury, EGF is upregulated, enhancing re-epithelialization and tensile strength in wounds [2,5–7]. The EGF family comprises various members such as EGF, transforming growth factor- α (TGF- α), heparin-binding EGF (HB-EGF), and amphiregulin, which act in autocrine and paracrine manners on their specific cell membrane receptors [6,8,9].

Clinical trials revealed that topical application of EGF can accelerate the rate of epidermal regeneration at the donor sites of split-thickness skin grafts and second-degree burn sites, and also enhance the healing process of chronic wounds [5,10,11]. For instance, in a clinical experiment, better wound recovery of diabetic foot

ulcers has been reported for the wounds treated with a 0.04% EGF-cream compared to those treated with a 0.02% EGF-cream or the cream without EGF at the end of 12 weeks [10].

EPIDERMAL GROWTH FACTOR MECHANISMS OF ACTION

Generally, EGF is involved in the stimulation, proliferation, and migration of keratinocytes, endothelial cells, and fibroblasts; secretion of natural extracellular matrix (ECM) protein; as well as formation of granulation tissue [9,12,13].

EGF interacts with epidermal growth factor receptor (EGFR), a protein tyrosine kinase receptor that is localized throughout the entire epidermis and particularly in the basal layer, and it activates several pathways, which leads to dimerization of the receptor, autophosphorylation, and tyrosine phosphorylation of downstream proteins. In fact, activation of EGFR is responsible for several biological events, including cell migration, proliferation, differentiation, cytoprotection,

and apoptosis. Also, EGFR plays an important role in re-epithelialization of wounds through increasing cell migration and proliferation in acute wounds [2,6,9].

Nevertheless, the bioavailability and the effect of EGF in chronic diabetic ulcers are less pronounced than in the acute wounds owing to the irregular response of skin cells to stimulation with EGF. In fact, based on the *ex vivo* studies, EGF is upregulated after acute injury, leading to an increased expression of keratins K6 and K16 and enhanced re-epithelialization. In contrast, downregulation of EGF and EGFR, mislocalization of EGFR in the cytoplasm of keratinocytes instead of the membrane, and the proteolytic environment cause inhibition of epithelialization in the chronic wounds [2,14,15]. However, it has been reported that the addition of metalloproteinase inhibitors can prevent degradation of exogenous EGF and EGFR in the proteolytic environment of the chronic ulcers [2].

However, findings have shown that EGFR is overexpressed in solid tumors, which is associated with tumor growth and metastasis. Therefore, active targeting of EGF to the cancer cells can be achieved through the conjugation approach [9,16,17]. Additionally, EGFR inhibitors (EGFRIs) have become a therapeutic candidate for cancer therapy. Therefore, EGF and EGFR therapies can play a role in the treatment of both wounds and cancer. However, alternative treatments such as downstreaming of phosphoinositol-3 kinase (PI3K) and Janus kinase 1 (JAK1) molecules utilizing different inhibitors can be applied to cancer without inhibiting EGFR signaling that is essential for normal wound healing [9].

Notwithstanding, topical administration or subcutaneous injection of EGF may induce hyperplasia and hypertrophy of skin keratinocytes and fibroblasts as well as thickening of the corneous layer, depending on the dose and length of the exposure time [2,18,19]. In addition, some studies on the long-term systemic administration of EGF revealed that although EGF may play a role in cancer development, it is not an initiating agent [20].

TOPICAL DELIVERY OF EPIDERMAL GROWTH FACTOR

Many clinical experiments have reported the topical application of EGF for wound healing and its intravenous, oral, and rectal applications for gastrointestinal damages [18,21]. However, insignificant results of the topical administration of EGF were attributed to its short half-life; a hostile microenvironment rich in protease activity, which degrades EGF quickly; and inefficacious delivery of EGF failing to reach effective dosages in an appropriately sustained manner. Furthermore, considering the fact that the wound-healing process depends

on several other growth factors, such as basic fibroblast growth factor (bFGF), keratinocyte growth factor (KGF), vascular endothelial growth factor (VEGF), and platelet-derived growth factor (PDGF), drug delivery systems capable of programmed release of multiple GFs may be found more effective than a single bolus application [11,22–24].

Consequently, some efforts have been made to develop new systems capable of delivering multiple growth factors in a controlled pattern and protect them against *in vivo* degradation. To this end, polymer-based systems such as micro- and nanoparticles [25,26], hydrogels [27], and nanofibrous scaffolds [28,29] have been utilized extensively.

Generally, the high specific surface area of nanofibers leads to enhanced dermal drug delivery. Moreover, electrospun nanofibrous scaffolds are capable of mimicking the ECM architecture, which ameliorates cell attachment, proliferation, and migration [30,31].

Electrospinning is considered as a straightforward and multifunctional technique to fabricate ultrafine fibers with the diameter in the range of nanometers to micrometers. The electrospinning apparatus consists of a high-voltage power supply, a syringe containing the polymer solution, a digital syringe pump, and a conductive collection device. The fundamental of the electrospinning is based on applying high voltage to the polymer solution in order to overcome its liquid surface tension and enable the formation of the polymer jet. Afterward, the polymer jet is elongated by the electrostatic repulsion and moved toward the collection device while the solvent is being evaporated, and finally the nanofibers are deposited on the target [30,32,33].

Several studies reported superior wound-healing ability of GF-loaded nanofibers *in vivo* compared to the GF-free nanofibers. In addition, the superiority of a sustained release of GFs from nanofibers over a solution of GFs on the continuous cell mitosis has been reported [34,35].

EPIDERMAL GROWTH FACTOR-LOADED NANOFIBERS

Several reports discuss the incorporation of EGF into electrospun nanofibers for the purposes of wound healing and skin regeneration (Table 28.1). Generally, blend electrospinning, emulsion electrospinning, coaxial electrospinning, as well as immobilization are the most common techniques to fabricate GF-loaded nanofibers [30]. These techniques have been reviewed by Yoo et al. [36] and Rieger et al. [37].

Briefly, in blend electrospinning, biomolecules are added to the polymer solution prior to the spinning

TABLE 28.1 Electrospun Scaffolds Containing EGF for the Purpose of Skin Regeneration

Growth factor	Polymer	Solvent	Cell	Method	References
EGF	PCL and PCL–PEG/ PCL	Methanol, chloroform	Keratinocyte	Immobilization	[29]
EGF	PLGA/gelatin	Chloroform, acetone/ acetic acid	HDF	Emulsion	[28]
EGF	Silk fibroin	LiBr	HDF	Blend	[46]
EGF	PCL and PCL/collagen	PCL: DMF, DCM PCL/collagen: HFIP	HDK	Immobilization	[47]
EGF	Gelatin, PLLACL/ P3GF	P3HT: chloroform/ methanol Gelatin, PLLACL: HFIP	Fibroblasts and ADSCs	Coaxial	[48]
EGF (and insulin, hydrocortisone, and retinoic acid)	Gelatin/PLLACL	HFIP	ADSC	Blend/coaxial	[45]
EGF (and silver sulfadiazine)	Silk/PEO	—	—	Blend/coating	[42]
bFGF/EGF	PCL-PEG	Methanol, chloroform	Keratinocyte and fibroblast	Coaxial/ immobilization	[34]
bFGF/EGF	PLGA/PEO	Chloroform, DMF/ water	HSF	Encapsulation of GFs in microspheres then blend electrospinning	[41]
bFGF, EGF, VEGF, PDGF	Collagen-hyaluronic acid/gelatin nanoparticle	Hyaluronic acid: NaOH/DMF Collagen: acetic acid	HUVEC	Blend: bEGF/EGF In nanoparticle: VEGF/ PDGF	[26]

ADSC, Adipose-derived stem cell; bFGF, basic fibroblast growth factor; DCM, dichloromethane; DMF, dimethylformamide; HDF, human dermal fibroblast; HDK, human dermal keratinocyte; HFIP, hexafluoroisopropanol; HUVEC, human umbilical vein endothelial cell; PCL, poly(ϵ -caprolactone); PDGF-BB, platelet-derived growth factor-BB; PEG, poly(ethylene glycol); PLGA, poly(lactate-co-glycolic acid); PLLACL, poly(L-lactic acid)-co-poly(ϵ -caprolactone); P3GF, P3HT + EGF; P3HT, poly (3-hexylthiophene); VEGF, vascular endothelial growth factor.

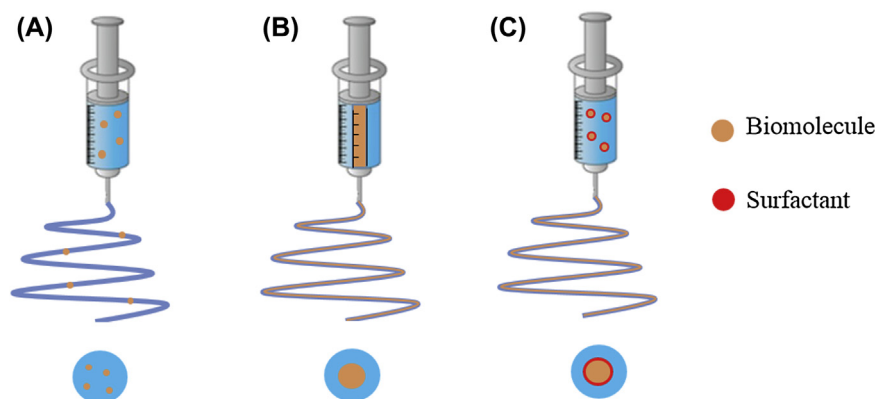


FIGURE 28.1 Scheme of the spinnerets loaded with biomolecules for (A) blend, (B) coaxial, and (C) emulsion electrospinning.

process. Inasmuch as most of the biomolecules are charged molecules, they migrate toward the surface of the forming fibers because of the charge repulsion during the electrospinning. In coaxial electrospinning, two concentrically arranged nozzles are employed for the polymer and the biomolecule-incorporated solution to form a core-shell structure in which the shell is made of the polymer and the core is made of the biomolecule. In emulsion electrospinning, an emulsion of biomolecule and polymer stabilized by a surfactant is utilized to embed the drug in the fibers [30,32,36,38]. Fig. 28.1 shows these three techniques schematically.

In one study, Choi et al. [34] prepared an amine-functionalized block copolymer of a poly(ϵ -caprolactone)-poly(ethylene glycol) (PCL-PEG) electrospun nanofibrous scaffold containing bFGF and EGF. To this end, bFGF solution was encapsulated as a core layer in a shell layer of PCL-PEG by coaxial electrospinning. Then, EGF was immobilized on the surface of the nanofibers via conjugating surface-exposed amine groups of the nanofibers to the carboxylate groups of EGF. Accordingly, EGF was exposed to cells on the surface of nanofibers, and it exhibited a release rate of c. 2% in one week, which was ascribed to the polymer degradation. On the other hand, bFGF showed a burst release

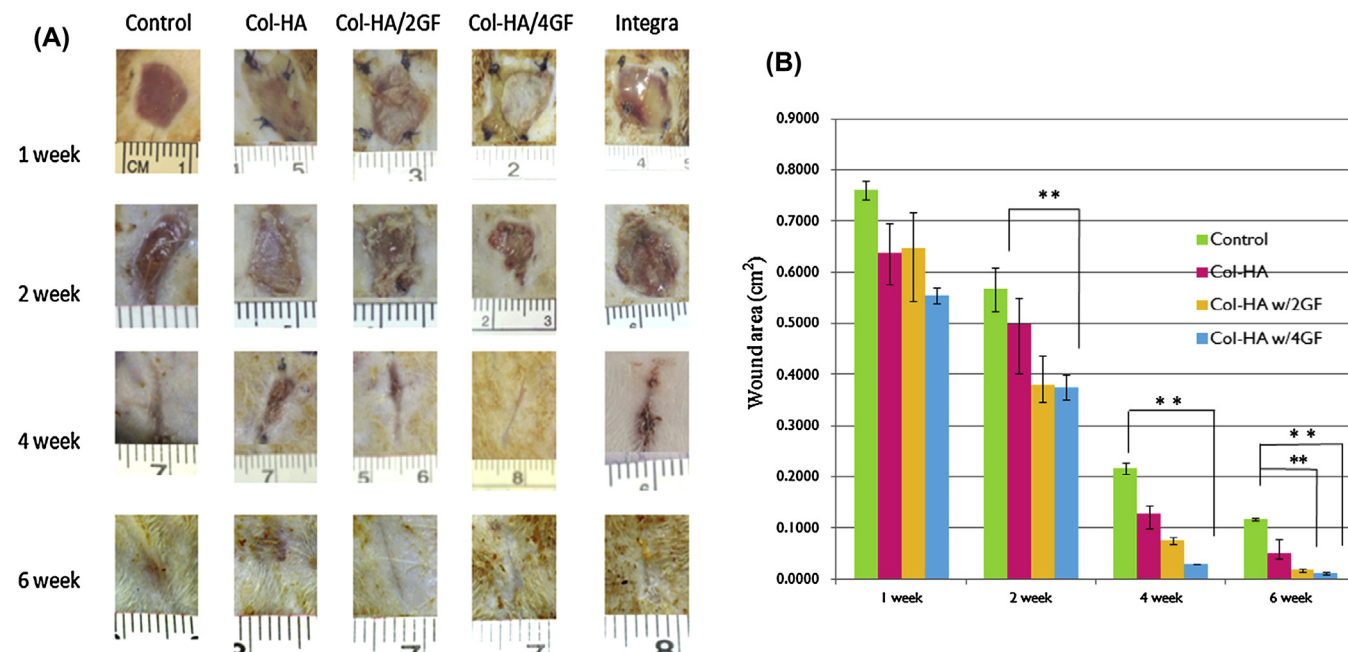


FIGURE 28.2 Evaluation of wound closure of diabetic rats at different time points. (A) Appearance of wounds, (B) statistical data of wound area (** $p < 0.01$, * $p < 0.05$). 2GF: EGF and bFGF; 4GF: EGF, bFGF, PDGF-BB, and VEGF. Adapted from Lai H-J, Kuan C-H, Wu H-C, Tsai J-C, Chen T-M, Hsieh D-J, et al. Tailored design of electrospun composite nanofibers with staged release of multiple angiogenic growth factors for chronic wound healing. *Acta Biomater* 2014;10:4156–66.

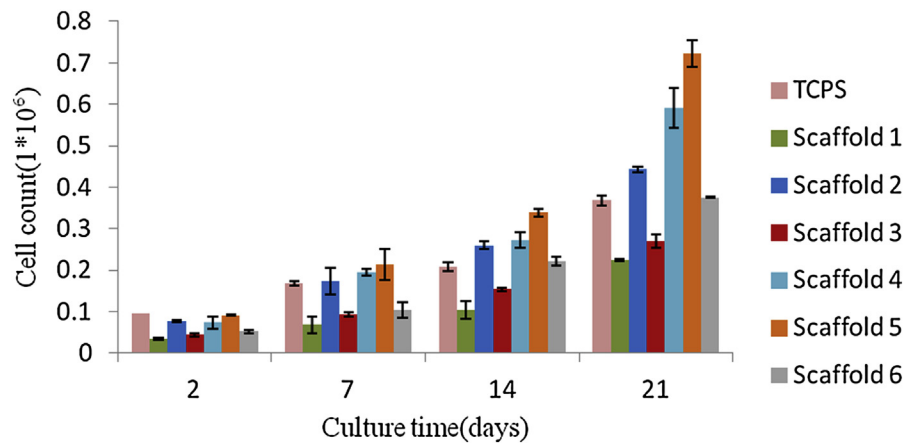


FIGURE 28.3 Proliferation of HSF seeded on PLGA–PEO scaffolds with different release patterns of EGF and bFGF. Scaffold 1: no GFs; scaffold 2: EGF; scaffold 3: bFGF; scaffold 4: dual delivery of EGF and bFGF; scaffold 5: sequential delivery of EGF, then bFGF; scaffold 6: sequential delivery of bFGF, then EGF. Adapted from Mirdailami O, Soleimani M, Dinarvand R, Khoshayand MR, Norouzi M, Hajarizadeh A, et al. Controlled release of rhEGF and rhbFGF from electrospun scaffolds for skin regeneration. *J Biomed Mater Res Part A* 2015;103(10):3374–85.

of about 30% in the first 12 h because of the fast diffusion from the shell layer. This scaffold was reported to be able to increase both human primary keratinocyte and human dermal fibroblast proliferation. Also, an increased rate of wound closure of diabetic ulcers; up-regulated K14, K5, and K1 expressions; and increased cemented matrix of keratin accumulation were observed in vivo.

It is noteworthy to mention that a temporal masking of GFs through conjugation to the biocompatible vehicles can increase biological stability of the GFs [3,8,39]. For instance, Son et al. [40] conjugated EGF to the low-molecular-weight chitosan via a carbodiimide-mediated reaction that enhanced proteolytic and

thermal stability as well as proliferative effect compared to the free EGF.

In another study, a hybrid scaffold made of collagen and hyaluronic acid nanofibers was fabricated with the capability of a fast release of EGF and bFGF and a sustained release of PDGF-BB and VEGF lasting for 1 month. For this purpose, the former were embedded directly into the nanofibers, while the latter were first encapsulated in gelatin nanoparticles. In fact, the initial delivery of bFGF and EGF triggers the wound-healing process, while sustained release of VEGF and PDGF-BB improves the late stages of skin regeneration (Fig. 28.2) [26].

In our laboratory, different types of poly(lactocoglycolic acid)–poly(ethylene oxide) (PLGA–PEO) nanofibrous scaffolds were fabricated in order to obtain single-, dual-, and sequential-release patterns of EGF and bFGF. To this end, various formulations of PLGA microspheres containing EGF or bFGF were prepared and loaded into the electrospinning solution. In fact, adding polyvinyl alcohol (PVA) to the formulation of the microspheres led to a controlled-release rate of the proteins and a reduced burst release. The high levels of proliferation of human skin fibroblast cells were observed when EGF was released either alone or in combination with bFGF (Fig. 28.3, scaffolds 2, 4, and 5), while the highest levels of collagen (types I, III, and IV) and elastin expression were achieved with a single release of EGF [41].

In another study, we prepared a hybrid nanofibrous scaffold of PLGA–gelatin, and EGF was encapsulated in the PLGA nanofibers through emulsion electrospinning (Fig. 28.4). This scaffold showed the features of blood clotting, stimulation of fibroblast proliferation, as well as synthesis of collagen [28]. Gil et al. [42] also observed the most rapid wound-healing responses

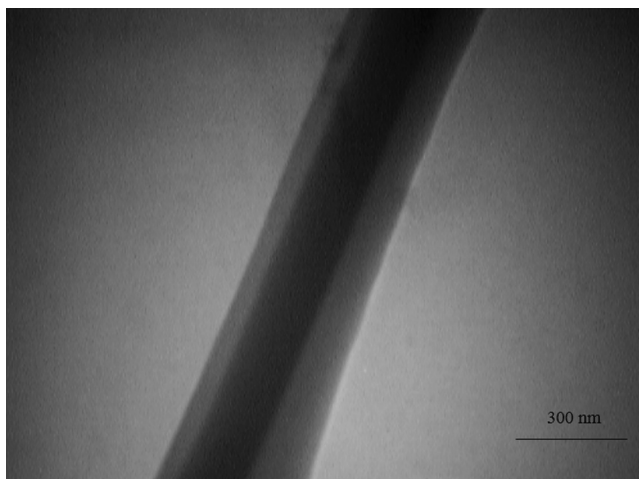


FIGURE 28.4 Transmission electron microscopy image of PLGA nanofiber encapsulating EGF. Adapted from Norouzi M, Shabani I, Ahvaz HH, Soleimani M. PLGA/gelatin hybrid nanofibrous scaffolds encapsulating EGF for skin regeneration. *Journal of biomedical materials research Part A*, 2015;103(7):2225–35.

when the wounds were covered with silk nanofibers coated with EGF–silver sulfadiazine in comparison to Tegaderm 3M and nanofibers alone.

Mesenchymal stem cells (MSCs) derived from either bone marrow or adipose tissue offer appropriate candidates for cell therapy in skin regeneration and wound healing, in view of the fact that they can accelerate wound closure and angiogenesis [43,44]. In order to investigate the epidermal differentiation potential of adipose-derived stem cells (ADSCs), Jin et al. [45] incorporated multiple epidermal induction factors (EIFs), including EGF, insulin, hydrocortisone, and retinoic acid, in gelatin–poly(L-lactic acid)–co-poly(ε-caprolactone) (PLLCL) nanofibers through two electrospinning techniques (ie, blend and core–shell). They reported higher proliferation of ADSCs on the core–shell nanofibers. In addition, differentiation of ADSCs cultured on the core–shell and blend nanofibers to epidermal cells was reported as 62% and 43%, respectively, which was attributed to the sustained release of EGF from the core–shell nanofibers.

CONCLUSION

EGF is a key factor in the normal wound-healing cascade. Due to the obstacles of topical administration of EGF in wound sites such as fast diffusion and degradation, various drug delivery systems have been developed. Amid those, electrospun nanofibers offer both a suitable vehicle with the capability of protection and controlled release of EGF and a substrate for cell attachment. Therefore, a variety of nanofibers loaded with EGF have been fabricated showing superior cellular activities and wound recovery. However, there is still a need to study the effects of the EGF-loaded nanofibers in clinical trials.

Glossary

ADSC Adipose-derived stem cell
bFGF Basic fibroblast growth factor
DCM Dichloromethane
DMF Dimethylformamide
ECM Extracellular matrix
EGF Epidermal growth factor
EGFR Epidermal growth factor inhibitor
EIF Epidermal induction factors
GF Growth factor
HB-EGF Heparin-binding EGF
HDF Human dermal fibroblast
HDK Human dermal keratinocyte
HFIP Hexafluoroisopropanol
HUVEC Human umbilical vein endothelial cell
JaK1 Janus kinase 1
KGF Keratinocyte growth factor
MSC Mesenchymal stem cell

P3GF P3HT + EGF
P3HT Poly(3-hexylthiophene)
PCL Poly(ε-caprolactone)
PDGF-BB Platelet-derived growth factor-BB
PEG Poly(ethylene glycol)
PEO Poly(ethylene oxide)
PI3K Phosphoinositol-3 kinase
PLGA Poly(lacto-co-glycolic acid)
PLLACL Poly(L-lactic acid)–co-poly(ε-caprolactone)
TGF-α Transforming growth factor-alpha
VEGF Vascular endothelial growth factor

References

- [1] Jahovic N, Güzel E, Arbak S, Yeğen BÇ. The healing-promoting effect of saliva on skin burn is mediated by epidermal growth factor (EGF): role of the neutrophils. *Burns* 2004;30:531–8.
- [2] Tiaka EK, Papanas N, Manolakis AC, Georgiadis GS. Epidermal growth factor in the treatment of diabetic foot ulcers: an update. *Perspect Vasc Surg Endovasc Ther* 2012;24(1):37–44. 1531003512442093.
- [3] Hardwicke J, Schmaljohann D, Boyce D, Thomas D. Epidermal growth factor therapy and wound healing—past, present and future perspectives. *Surgeon* 2008;6:172–7.
- [4] Teramatsu Y, Maeda H, Sugii H, Tomokiyo A, Hamano S, Wada N, et al. Expression and effects of epidermal growth factor on human periodontal ligament cells. *Cell Tissue Res* 2014;357:633–43.
- [5] Hong JP, Jung HD, Kim YW. Recombinant human epidermal growth factor (EGF) to enhance healing for diabetic foot ulcers. *Ann Plast Surg* 2006;56:394–8.
- [6] Barrientos S, Stojadinovic O, Golinko MS, Brem H, Tomic-Canic M. Growth factors and cytokines in wound healing. *Wound Repair Regen* 2008;16:585–601.
- [7] Fu X, Fang L, Li H, Li X, Cheng B, Sheng Z. Adipose tissue extract enhances skin wound healing. *Wound Repair Regen* 2007;15: 540–8.
- [8] Hajimiri M, Shahverdi S, Kamalinia G, Dinarvand R. Growth factor conjugation: strategies and applications. *J Biomed Mater Res Part A* 2015;103:819–38.
- [9] Bodnar RJ. Epidermal growth factor and epidermal growth factor receptor: the yin and yang in the treatment of cutaneous wounds and cancer. *Adv Wound Care* 2013;2:24–9.
- [10] Tsang MW, Wong WKR, Hung CS, Lai K-M, Tang W, Cheung EY, et al. Human epidermal growth factor enhances healing of diabetic foot ulcers. *Diabetes Care* 2003;26:1856–61.
- [11] Dinh T, Braunagel S, Rosenblum BI. Growth factors in wound healing: the present and the future? *Clin Podiatric Med Surg* 2015;32:109–19.
- [12] Kim JS, McKinnis VS, Nawrocki A, White SR. Stimulation of migration and wound repair of guinea-pig airway epithelial cells in response to epidermal growth factor. *Am J Respir Cell Mol Biol* 1998;18:66–74.
- [13] Yildirim L, Thanh NT, Seifalian AM. Skin regeneration scaffolds: a multimodal bottom-up approach. *Trends Biotechnol* 2012;30:638–48.
- [14] Papanas N, Maltezos E. Growth factors in the treatment of diabetic foot ulcers: new technologies, any promises? *Int J Low Extrem Wounds* 2007;6:37–53.
- [15] Loots MA, Kenter SB, Au FL, Van Galen W, Middelkoop E, Bos JD, et al. Fibroblasts derived from chronic diabetic ulcers differ in their response to stimulation with EGF, IGF-I, bFGF and PDGF-AB compared to controls. *Eur J Cell Biol* 2002;81:153–60.
- [16] Tseng C-L, Wang T-W, Dong G-C, Wu SY-H, Young T-H, Shieh M-J, et al. Development of gelatin nanoparticles with biotinylated

- EGF conjugation for lung cancer targeting. *Biomaterials* 2007;28:3996–4005.
- [17] Shimada T, Ueda M, Jinno H, Chiba N, Wada M, Watanabe J, et al. Development of targeted therapy with paclitaxel incorporated into EGF-conjugated nanoparticles. *Anticancer Res* 2009;29:1009–14.
 - [18] Acosta JB, Savigne W, Valdez C, Franco N, Alba JS, Rio Ad, et al. Epidermal growth factor intralesional infiltrations can prevent amputation in patients with advanced diabetic foot wounds. *Int Wound J* 2006;3:232–9.
 - [19] Sonnylal S, Xu S, Jones H, Tam A, Sreeram VR, Ponticos M, et al. Connective tissue growth factor causes EMT-like cell fate changes in vivo and in vitro. *J Cell Sci* 2013;126:2164–75.
 - [20] Berlanga-Acosta J, Gavilondo-Cowley J, López-Saura P, González-López T, Castro-Santana MD, López-Mola E, et al. Epidermal growth factor in clinical practice – a review of its biological actions, clinical indications and safety implications. *Int Wound J* 2009;6:331–46.
 - [21] Tuyet HL, Quynh N, Tran T, Vo Hoang Minh H, Bich T, Nguyen D, et al. The efficacy and safety of epidermal growth factor in treatment of diabetic foot ulcers: the preliminary results. *Int Wound J* 2009;6:159–66.
 - [22] Maxson S, Lopez EA, Yoo D, Danilkovitch-Miagkova A, LeRoux MA. Concise review: role of mesenchymal stem cells in wound repair. *Stem Cell Transl Med* 2012;1:142–9.
 - [23] Barrientos S, Brem H, Stojadinovic O, Tomic-Canic M. Clinical application of growth factors and cytokines in wound healing. *Wound Repair Regen* 2014;22:569–78.
 - [24] Mac Cornick S, de Noronha SAAC, Chominski V, de Noronha SMR, Ferreira LM, Gragnani A. Clinical use of growth factors in the improvement of skin wound healing. *Open J Clin Diagn* 2014;4:227.
 - [25] Ulubayram K, Cakar AN, Korkusuz P, Ertan C, Hasirci N. EGF containing gelatin-based wound dressings. *Biomaterials* 2001;22:1345–56.
 - [26] Lai H-J, Kuan C-H, Wu H-C, Tsai J-C, Chen T-M, Hsieh D-J, et al. Tailored design of electrospun composite nanofibers with staged release of multiple angiogenic growth factors for chronic wound healing. *Acta Biomater* 2014;10:4156–66.
 - [27] Hori K, Sotozono C, Hamuro J, Yamasaki K, Kimura Y, Ozeki M, et al. Controlled-release of epidermal growth factor from cationized gelatin hydrogel enhances corneal epithelial wound healing. *J Control Release* 2007;118:169–76.
 - [28] Norouzi M, Shabani I, Ahvaz HH, Soleimani M. PLGA/gelatin hybrid nanofibrous scaffolds encapsulating EGF for skin regeneration. *J Biomed Mater Res Part A* 2015;103(7):2225–35.
 - [29] Choi JS, Leong KW, Yoo HS. In vivo wound healing of diabetic ulcers using electrospun nanofibers immobilized with human epidermal growth factor (EGF). *Biomaterials* 2008;29:587–96.
 - [30] Norouzi M, Boroujeni SM, Omidvarkordshouli N, Soleimani M. Advances in skin regeneration: application of electrospun scaffolds. *Adv Healthc Mater* 2015;4(8):1114–33.
 - [31] Babaeijandaghi F, Shabani I, Seyedjafari E, Naraghi ZS, Vasei M, Haddadi-Asl V, et al. Accelerated epidermal regeneration and improved dermal reconstruction achieved by polyethersulfone nanofibers. *Tissue Eng Part A* 2010;16:3527–36.
 - [32] Norouzi M, Soleimani M, Shabani I, Atyabi F, Ahvaz HH, Rashidi A. Protein encapsulated in electrospun nanofibrous scaffolds for tissue engineering applications. *Polym Int* 2013;62:1250–6.
 - [33] Norouzi M, Zare Y, Kiany P. Nanoparticles as effective flame retardants for natural and synthetic textile polymers: application, mechanism, and optimization. *Polym Rev* 2015;55:531–60.
 - [34] Choi JS, Choi SH, Yoo HS. Coaxial electrospun nanofibers for treatment of diabetic ulcers with binary release of multiple growth factors. *J Mater Chem* 2011;21:5258–67.
 - [35] Yang Y, Xia T, Zhi W, Wei L, Weng J, Zhang C, et al. Promotion of skin regeneration in diabetic rats by electrospun core-sheath fibers loaded with basic fibroblast growth factor. *Biomaterials* 2011;32:4243–54.
 - [36] Yoo HS, Kim TG, Park TG. Surface-functionalized electrospun nanofibers for tissue engineering and drug delivery. *Adv Drug Deliv Rev* 2009;61:1033–42.
 - [37] Rieger KA, Birch NP, Schiffman JD. Designing electrospun nanofiber mats to promote wound healing – a review. *J Mater Chem B* 2013;1:4531–41.
 - [38] Norouzi M, Shabani I, Atyabi F, Soleimani M. EGF-loaded nanofibrous scaffold for skin tissue engineering applications. *Fibers Polym* 2015;16:782–7.
 - [39] Johnson NR, Wang Y. Controlled delivery of heparin-binding EGF-like growth factor yields fast and comprehensive wound healing. *J Control Release* 2013;166:124–9.
 - [40] Son TI, Park SH, Kang HS, Son YS, Kim CH, Jang E-C. Preparation of human epidermal growth factor/low-molecular-weight chitosan conjugates and their effect on the proliferation of human dermal fibroblasts in vitro. *J Ind Eng Chem* 2005;11:34–41.
 - [41] Mirdailami O, Soleimani M, Dinarvand R, Khoshayand MR, Norouzi M, Hajarizadeh A, et al. Controlled release of rhEGF and rhbFGF from electrospun scaffolds for skin regeneration. *J Biomed Mater Res Part A* 2015;103(10):3374–85.
 - [42] Gil ES, Panilaitis B, Bellas E, Kaplan DL. Functionalized silk biomaterials for wound healing. *Adv Healthc Mater* 2013;2:206–17.
 - [43] Dieckmann C, Renner R, Milkova L, Simon JC. Regenerative medicine in dermatology: biomaterials, tissue engineering, stem cells, gene transfer and beyond. *Exp Dermatol* 2010;19:697–706.
 - [44] Chen M, Przyborowski M, Berthiaume F. Stem cells for skin tissue engineering and wound healing. *Crit RevTM Biomed Eng* 2009;37.
 - [45] Jin G, Prabhakaran MP, Kai D, Ramakrishna S. Controlled release of multiple epidermal induction factors through core-shell nanofibers for skin regeneration. *Eur J Pharm Biopharm* 2013;85:689–98.
 - [46] Schneider A, Wang X, Kaplan D, Garlick J, Egles C. Biofunctionalized electrospun silk mats as a topical bioactive dressing for accelerated wound healing. *Acta Biomater* 2009;5:2570–8.
 - [47] Gümüşderelioğlu M, Dalkıranoglu S, Aydın R, Çakmak S. A novel dermal substitute based on biofunctionalized electrospun PCL nanofibrous matrix. *J Biomed Mater Res Part A* 2011;98:461–72.
 - [48] Jin G, Prabhakaran MP, Ramakrishna S. Photosensitive and biomimetic core-shell nanofibrous scaffolds as wound dressing. *Photochem Photobiol* 2014;90:673–81.

Index

‘Note: Page numbers followed by “f” indicate figures, “t” indicate tables and “b” indicates boxes.’

- A**
- ABI-007. *See* Abraxane
- Abraxane, 206, 211
- Absorption, 239
- ABT-737, 195
- N-Acetyl-D-glucosamine, 78
- Acetylated 3-aminopropyltrimethoxysilane (APTMS), 60–61
- Acinetobacter baumannii* (*A. baumannii*), 34, 129–131
- Acitretin, 163
- Acne, nanoemulsions for, 39
- Acne vulgaris, 132–133
- Acoustic streaming, 94
- Acrosyngium, 8–9
- 2-Acrylamido-2-methyl-1-propane sulfonic acid (AMPS), 62
- ACS. *See* American Cancer Society (ACS)
- Actinic keratoses (AKs), 39
- nanoemulsions for, 39
- Activator protein-1 (AP1), 342
- Active targeting, 206
- integrins on surface of endothelial cells, 208
- melanoma, 208–209
- and melanoma-APCs, 207t
- receptors on surface of melanoma cells, 206–208
- Active targeting, 241
- AD. *See* Atopic dermatitis (AD)
- Ad5-mIL-12. *See* Adenovirus vector encoding for IL-12 (Ad5-mIL-12)
- Adenine (A), 203–204
- Adenosine triphosphate (ATP), 16–17
- binding cassette superfamily, 326
- Adenovirus vector encoding for IL-12 (Ad5-mIL-12), 210
- ADI-PEG-20, 211
- Adiponectic mediator, 7–8
- Adipose tissue, 237, 372
- Adipose-derived stem cells (ADSCs), 372
- Adnexa. *See* Epidermal appendages
- ADSCs. *See* Adipose-derived stem cells (ADSCs)
- Advanced fabrication strategies, 343
- basal-to-spinous layer transition, 346f
- cell-imprinted substrates, 345
- electrospinning, 343–344, 343f
- multineedle bioprinting system, 347f
- self-assembly, 344–345
- skin 3D bioprinting, 345–347
- Advanced surfaces, 23
- AFM. *See* Atomic force microscope (AFM)
- AFSCs. *See* Amniotic fluid–derived stem cells (AFSCs)
- Agglomerates, 230–231
- Aggregates, 230–231
- AgNPs. *See* Silver nanoparticles (AgNPs)
- AKs. *See* Actinic keratoses (AKs)
- Akt, 192–193, 203–204
- combination of siRNAs against, 195
- AL. *See* Anionic liposomes (AL)
- 5-ALA. *See* 5-Aminolaevulinic acid (5-ALA)
- Allopurinol, 140
- Allovectin-7, 211
- AmB. *See* Amphotericin B (AmB)
- AmB nanoparticles (AmB-np), 34–35
- AmB-np. *See* AmB nanoparticles (AmB-np)
- American Cancer Society (ACS), 36
- Amine groups (NH₂), 309–310
- Amine-functionalized silica nanoparticles, 26–27
- Amino acids, 91–92, 96
- 5-Aminolaevulinic acid (5-ALA), 39, 142–143, 161, 181–182, 276–277
- PDT, 142–143
- 3-Aminopropyltriethoxysilane (APTES), 26–27
- Amniotic fluid–derived stem cells (AFSCs), 345–347
- Amorphous silica oxide, 80
- Amphiphilic coating, 311
- Amphotericin B (AmB), 34–35, 140
- AMPS. *See* 2-Acrylamido-2-methyl-1-propane sulfonic acid (AMPS)
- Anagen phase, 9–10
- Anhidrotic ectodermal dysplasia, 8
- Anionic liposomes (AL), 210
- Anti-CTLA-4. *See* Anticytotoxic T lymphocyte-associated antigen-4 (Anti-CTLA-4)
- Anti-EGFR. *See* Anti–epidermal growth factor receptor (Anti-EGFR)
- Antiaging
- cosmetics, 240
- skincare cosmetics, 240
- Antibacterial agent, 101
- nitric oxide releasing NPs as, 129–131
- Antibiotic resistance, 33
- Anticancer agents nanodelivery in melanoma
- nanodelivery in melanoma therapy, 190–191
- nanoparticle containing both 5-FU and siRNA, 191f
- nanoparticle drug delivery systems relevant to melanoma, 191–192
- nanotechnology
- in chemotherapy of melanoma, 192
- in combination therapy of melanoma, 197–198
- in melanoma immunotherapy, 195–197
- in targeted therapy against melanoma, 192–195
- in targeting mitochondrial apoptotic pathway, 195
- Anticytotoxic T lymphocyte-associated antigen-4 (Anti-CTLA-4), 182, 205
- Anti–epidermal growth factor receptor (Anti-EGFR), 37, 101
- Antifungal agent, 35
- nitric oxide releasing NPs as, 131–132
- Antigen-presenting cells (APCs), 208
- Antimicrobial agents delivery, 292–293, 294f
- Antimicrobial applications, 292
- antimicrobial agents delivery, 292–293, 294f
- inherent antimicrobial properties of metal nanoparticles, 293–295
- Antimicrobial nanoemulsion, 39
- Antimicrobial therapy, 127
- nitric oxide releasing NPs
- as antibacterial agent, 129–131
- as antifungal agent, 131–132
- characteristics, 128–129
- future directions, 132–133
- Antimonial derivatives, 136
- Antiovalbumin–immunoglobulin G (IgG), 101–102
- Anti–vascular endothelial growth factor (Anti–VEGF), 330
- Anti–VEGF. *See* Anti–vascular endothelial growth factor (Anti–VEGF)
- AP1. *See* Activator protein-1 (AP1)
- APCs. *See* Antigen-presenting cells (APCs)
- Apocrine glands, 8–9
- Apoptosis, 141, 148
- of keratinocytes, 141–142, 148
- APTES. *See* 3-Aminopropyltriethoxysilane (APTES)
- APTMS. *See* Acetylated 3-aminopropyltrimethoxysilane (APTMS)

- ARG1. *See* Arginase-1 (ARG1)
 Arginase-1 (ARG1), 204
 Arginine, glycine, and asparagine (RGD peptides), 17
 Argyria, 22
 Aspirin-triggered resolvin D1 (AT-RvD1), 341
 Atomic force microscope (AFM), 333–334
 Atopic dermatitis (AD), 63, 68, 167. *See also* Cutaneous leishmaniasis (CL)
 clinical features, 168
 epidemiology, 168–169
 pathophysiology, 167–168
 treatment, 169
 nanoparticles use, 170–173
 nanotechnology risks, 173
 “Atopic march”, 167
 ATP. *See* Adenosine triphosphate (ATP)
 Au-NRs. *See* Gold nanorods (Au-NRs)
 AuNPs. *See* Gold nanoparticles (AuNPs)
 Australia’s Therapeutic Goods Administration (TGA), 252
 Autonomic nervous system, 7
 Autonomous nervous system, 7
 Avobenzone, 229, 231
 Azobenzene, 91–92
- B**
 BAB. *See* Blood–aqueous barrier (BAB)
 Basal cell carcinoma (BCC), 181
 Basal lamina, ECM of, 343
 Basal layer, 3–4
 Basal-to-spinous layer transition, 345, 346f
 Basement membrane (BM), 312–313
 Basement membrane, 338
 basic fibroblast growth factor (bFGF), 343–344, 368
 Bathing, 169
 BCC. *See* Basal cell carcinoma (BCC)
 Bedsore, 257
 Betamethasone 17 valerate, 163
 bFGF. *See* basic fibroblast growth factor (bFGF)
 Bioavailability enhancement, 327–328
 Biocompatible, 74
 inorganic nanocarriers, 80
 organic nanocarriers, 79–80
 Bioconjugates, 76–77
 Biodegradable, 74
 organic nanocarriers, 77–79
 polypeptides, 77–78
 polysaccharides, 78
 synthetic polymers, 78–79
 Bioengineered cornea, 334
 Biofilm formation, 299
 Bioinspired nanotechnologies for skin regeneration
 advanced fabrication strategies, 343–347
 frontiers in skin regeneration, 338
 skin aging, 342–343
 skin wound regeneration, 338–342
 Biological nanocarriers, 74–76
 Biological polymers, 77
 Blanching, 289
 Blood–retinal barrier (BRB), 324–325, 325f
 Blood–aqueous barrier (BAB), 324–326, 327f
 Blood–ocular barrier (BOB), 324–325
 BM. *See* Basement membrane (BM)
 BOB. *See* Blood–ocular barrier (BOB)
 Boc. *See* tert-Butyl carbamates (Boc)
 Body temperature, regulation of, 11
 Bottom-up synthesis of nanocarriers, 25–27
 Bovine serum albumin (BSA), 291–292, 328
 Brachytherapy. *See* Internal radiation therapy
 BRAF
 combination of siRNAs against, 195
 inhibitors, 205
 mutation, 192–193
 targeted therapy effect, 177
 V600E mutation, 182
 BRB. *See* Blood–retinal barrier (BRB)
 “Bricks”, 308–309
 Brookhaven Instrument, 277
 Brownian motion of nanoemulsions, 240–241
 Brust–Schiffman method, 218
 BSA. *See* Bovine serum albumin (BSA)
 Bulge, 3
 Buparvaquone, 140
- C**
 C-reactive protein (CRP), 339–340
 C16Y, 208
 CA4, 210
 CaCO₃NPs. *See* Calcium carbonate nanoparticles (CaCO₃NPs)
 CAD. *See* Computer-aided manufacturing (CAD)
 Caelyx, 211
 Calcineurin antagonists, 169–170
 Calcium carbonate (CaCO₃), 66
 Calcium carbonate nanoparticles (CaCO₃NPs), 58, 68
 Calcium phosphate (CaPO₄), 66, 80
 nanoparticles, 68
 Calcium-mediated process, 341
 Cancer. *See also* Skin cancer
 immunotherapy, 73–74
 theranostics, NPs in, 178–179
Candida albicans (*C. albicans*), 131–132, 132f
 CaPO₄. *See* Calcium phosphate (CaPO₄)
 Capryl–caproyl macrogol 8–glyceride. *See* Labrasol
 Caprylic acid–capric triglyceride, 120
 Capsaicin, 163–164
 Carbon nanotubes, 17
 Carboxyl groups (COOH), 309–310
 Carrageenan-induced rat paw edema model, 122
 Casein, 76
 Catagen, 9–10
 Cationic lipid, 172
 Cationic lysine–based surfactants, 149
 Cationic polymers, 172
 Cavitation effects, 94
 CCD. *See* Charge-coupled device (CCD)
 CD2. *See* Cluster differentiation 2 (CD2)
 CD47, 196–197
 CDKN2A. *See* Cyclin–dependent kinase inhibitor 2A (CDKN2A)
 Celecoxib, 122–123
 Cell organelles, labeling of, 278
 Cell-imprinted substrates, 345
 Cell-penetrating peptides (CPPs), 74–76, 122–123
 Cellular components, 275–276
 Cerium dioxide, 248
 Ceruminous gland, 8
 cGMP. *See* cyclic diguanosine monophosphate (cGMP)
 Charge-coupled device (CCD), 260
 Chemical enhancement, 93
 Chemical penetration enhancers, 105, 107
 Chemical reactivity, 21
 Chemotherapeutic(s), 36, 128
 agent, 178, 192, 197–198, 209
 drugs, 148, 189–190, 210
 Chemotherapy, 192
 Chitin, 17–18
 Chitin nanofibers (CNFs), 18
 Chitosan (CTS), 35–36, 78, 191, 206, 329
 nanofiber, 342
 NP, 194
 Chlorins derivatives, 143
 Chloroauric acid (HAuCl₄), 25
 Cholesterol, 27
 Chronic inflammation, 137–139
 H&E stained skin sections, 138f
 Chronic wounds, 287
 CL. *See* Cutaneous leishmaniasis (CL)
 Classical cosmetics, 240
 Clinical skin-imaging technology, 354
 Clobetasol, 164
p-Chloromethyl styrene (CMS), 62
 Cluster differentiation 2 (CD2), 157–160
 CMOS. *See* Complementary metal-oxide semiconductor (CMOS)
 CMS. *See* *p*-Chloromethyl styrene (CMS)
 CMV retinitis. *See* Cytomegalovirus retinitis (CMV retinitis)
 CNFs. *See* Chitin nanofibers (CNFs)
 Cochrane database, 142
 Cold homogenization technique, 333
 Collagen, 76
 fibers, 354
 type I nanofiber, 341–342
 Collagenases, 6–7
 Collective surface area, 18–19, 19f
 Colloidal gold, 80
 skin penetration enhancers, 107–108
 Colloidal silica, 63
 Colloidal systems, 115–116, 328
 Combination therapy
 nanotheranostics and, 210–211
 NP in melanoma combination therapy, 210–211
 theranostic NP in melanoma imaging, 210
 Complementary metal-oxide semiconductor (CMOS), 260

- Computer-aided manufacturing (CAD), 345
- Concentrated ZnO-NP signals, 356–357
- Consensus, 248, 252
- Continuous-wave (CW), 107–108
- COOH. *See* Carboxyl groups (COOH)
- Copper, 293–295
- Copper oxide (CuO), 302. *See also* Nitric oxide (NO)
- Copper sulfide nanoparticles (CuSNPs), 58, 65
- Corium, 54
- Cornea, 324, 324f
- Corneocytes, 354
- Cornified envelope, 5
- Cornified layer. *See* Stratum corneum (SC)
- Corticosteroids, 35, 157–160, 164
topical, 169
- Cosmetic dermatology. *See also* Diagnostic dermatology
nanoemulsions for, 40
nanopigments for, 40–41
- Cosmetics, 240
- “Cosmetics Regulation #1223/2009”, 234
- Covalent bonding, 60–61
- CpG oligonucleotides (CpG ODN), 141
endosomal delivery, 149
- CPPs. *See* Cell-penetrating peptides (CPPs)
- CRP. *See* C-reactive protein (CRP)
- CsA. *See* Cyclosporine A (CsA)
- CTLA4. *See* Cytotoxic T lymphocyte-associated antigen-4 (CTLA4)
- CTLs. *See* Cytotoxic T lymphocytes (CTLs)
- CTS. *See* Chitosan (CTS)
- CuO. *See* Copper oxide (CuO)
- curc-np. *See* Curcumin nanoparticles (curc-np)
- Curcumin, 34, 161–164, 293, 341
- Curcumin nanoparticles (curc-np), 34
- CuSNPs. *See* Copper sulfide nanoparticles (CuSNPs)
- Cutaneous leishmaniasis (CL), 135–136.
See also Atopic dermatitis (AD)
disease and therapy, 135–137
NPs in topical therapy, 143
AgNPs failure in *L. major*, 147–148
liposomal conventional drugs, 146–147
liposomes in photodynamic therapy, 148
NO delivery systems, 147
NPs and interaction with pathological skin lesions, 143–146, 145f
perspectives in NPs for CL topical therapy, 148–149
- PM efficacy
immunological considerations, 140–143
pharmacokinetic considerations, 139–140
skin features, 137–139
types, 142f
- Cutaneous neoplasms
nanoliposomes for, 38
nanoparticles for, 36–37
- CW. *See* Continuous-wave (CW)
- cyclic diguanosine monophosphate (cGMP), 299
- Cyclin-dependent kinase inhibitor 2A (CDKN2A), 203–204
- Cyclodextrins, 78
- Cyclosporine A (CsA), 160
- Cytokines, 82, 288
- Cytomegalovirus retinitis (CMV retinitis), 326
- Cytosine (C), 203–204
- Cytotoxic T lymphocyte-associated antigen-4 (CTLA4), 197
- Cytotoxic T lymphocytes (CTLs), 208
- Cytotoxicity, 74–75, 82, 90
- D**
- Dacarbazine, 204–205
- DCL. *See* Diffuse cutaneous leishmaniasis (DCL)
- DCM. *See* Dichloromethane (DCM)
- DCs. *See* Dendritic cells (DCs)
- DC-specific intercellular adhesion molecule-3-grabbing nonintegrin (DC-SIGN), 208
- DDD. *See* Dermal drug delivery (DDD)
- Deacetylated chitin, 329
- Decapitation secretion, 9
- Decoupling in vitro nanotoxicity, 248
- Deep dermis, 239
- Delivers doxorubicin (DOX), 190–192
- Dendrimers, 25, 74, 79–80, 89–90, 179, 191, 242, 330. *See also* Peptide dendrimers
applications in drug delivery, 90
dendrimer-aided solubility
enhancement of drugs, 91
dendrimeric structure, 90
differentiation factors, 90–91
types of, 90
- Dendritic cells (DCs), 157–160, 208, 276
“Dendron”, 242
- Dense cellular network, 311
- Deoxyribonucleic acid (DNA), 75, 293
- Dermabrasion, 108
- Dermal
absorption, 308
biomedical applications, 102
blood, 7
dermal-epidermal junction, 6
penetration, 250, 252
photoaging, 239–240
- Dermal drug delivery (DDD), 179–180
- Dermaportation, 104–105, 108
- Dermatological applications of AuNPs, 100, 100f
applications, 102
skin cancer treatment and imaging, 101
topical and transdermal drug delivery, 101–102
- Dermatological disorders, 242–243
- Dermatology. *See also* Nanodermatology
cosmetic dermatology
nanoemulsions for, 40
nanopigments for, 40–41
diagnostic dermatology
nanoparticles for, 41–42
quantum dots for, 41
nanofibers in, 17–18
- Dermatophagoides pteronyssinus* (Dp), 63
- Dermis, 6, 179, 238, 309, 338, 354
dermal blood, 7
ECM of, 343
layer, 337
lymphatic vessels, 7
mast cells, 7
muscles, 7
nerves, 7
protein fibers in, 342
- Desmosomes, 3–4
- Dexamethasone (DXM), 61–62
- Dextran sulfate (DXS), 61–62
- Diagnostic dermatology. *See also* Cosmetic dermatology
nanoparticles for, 41–42
quantum dots for, 41
- Diagnostic macromolecules, 309–310
- N-Diazoniumdiolate, 128, 129f
- Dichloromethane (DCM), 91
- Diferuloylmethane, 293
- Differential scanning calorimetry (DSC), 121, 334
- Diffuse cutaneous leishmaniasis (DCL), 136–137
- Dimethyl sulfoxide (DMSO), 107
- N,N-Dimethylformamide (DMF), 91
- Dinitrochlorobenzene (DNCB), 68
- Dinitrogen trioxide (N₂O₃), 128
- 1,2-Dioleoyl-3-trimethylammonium-propane (DOTAP), 116–120, 122
- Dioleoylphosphatidylethanolamine (DOPE), 122
- 1,2-Dipalmitoyl-sn-glycero-3-phosphocholine (DPPC), 170–171
- Dipotassium glycyrrhizinate, 116–120
- Disc-shaped nanoparticles, 19
- Dithranol, 160
- DLS. *See* Dynamic light scattering (DLS)
- DLVO theory, 20
- DMF. *See* N, N-Dimethylformamide (DMF)
- DMSO. *See* Dimethyl sulfoxide (DMSO)
- DNA. *See* Deoxyribonucleic acid (DNA)
- DNCB. *See* Dinitrochlorobenzene (DNCB)
- DNDi. *See* Drugs for Neglected Diseases initiative (DNDi)
- Docetaxel (DTX), 206
- “Donnan exclusion effect” of skin, 58–59
- DOPE. *See* Dioleoylphosphatidylethanolamine (DOPE)
- Doppler imaging systems, 258–259
- DOTAP. *See* 1,2-Dioleoyl-3-trimethylammonium-propane (DOTAP)
- Double-emulsion solvent evaporation method, 332
- DOX. *See* Delivers doxorubicin (DOX); Doxorubicin (DOX)
- Doxil, 206
- Doxorubicin (DOX), 77, 206

- Dp. *See* *Dermatophagoides pteronyssinus* (Dp)
 DPPC. *See* 1,2-Dipalmitoyl-sn-glycero-3-phosphocholine (DPPC)
 Drug delivery, 205, 313–314, 323–324
 advantages, 179–180
 application in melanoma cells, 183
 barriers to eye, 324
 aqueous humour flow pathway, 326f
 challenges to anterior segment, 324
 challenges to posterior segment, 324–326
 precorneal loss factors, 325b
 developing AuNP, 181
 SPION application for, 181
 Drug release, 334
 bioengineered cornea, 334
 ex vivo evaluation, 334
 in vitro determination, 334
 in vivo evaluation, 334
 Drugs for Neglected Diseases initiative (DNDi), 136–137
 DSC. *See* Differential scanning calorimetry (DSC)
 DTX. *See* Docetaxel (DTX)
 DXM. *See* Dexamethasone (DXM)
 DXS. *See* Dextran sulfate (DXS)
 Dynamic light scattering (DLS), 277
- E**
 Eccrine sweat glands, 8–9
 ECM. *See* Extracellular matrix (ECM)
 Edge activator, 116–120
 EDS. *See* Energy-dispersive X-ray spectroscopy (EDS)
 EDTA. *See* Ethylenediaminetetraacetic acid (EDTA)
 EGF. *See* Endothelial growth factor (EGF); Epidermal growth factor (EGF)
 EGFR. *See* Epidermal growth factor receptor (EGFR)
 EHMC. *See* Ethylhexyl Methoxycinnamate (EHMC)
 EIFs. *See* Epidermal induction factors (EIFs)
 Elastic liposomes, 161–163
 Electromigration, 95, 108
 Electron beam radiation, 219
 Electron paramagnetic resonance (EPR), 268
 oximetry measurements in skin, 269
 Electrospinning, 343–344, 343f, 368
 Elongated microparticles (EMPs), 223–224, 224f
 Emulsification solvent diffusion method, 332
 Emulsions, 240
 emulsion-based nanocarriers, 164
 solvent evaporation method, 331–332
 Emulsomes, 161
 Endocrine function, 12
 Endocytosis, 22
 Endogenous enzymes, 74–75
 Endothelial growth factor (EGF), 338
 Endothelium, 324
 Endothelial NOS, 128
- Energy-dispersive X-ray spectroscopy (EDS), 106
 Enhanced permeability and retention (EPR), 36, 190, 205–206
 effect, 177
 Enhanced radiosensitization
 GNP production and physicochemical properties, 218
 mechanism of metal radiosensitization, 219
 with metal nanoparticle, 218–221
 other metal-based radiosensitizers, 220–221
 in vivo studies, 219–220
 GNP enhanced radiotherapy in mouse model, 220f
Enterococcus faecium (*E. faecium*), 34–35
 Enzymes, 75
 EPI. *See* Epirubicin (EPI)
 EPI-superparamagnetic Fe₃O₄ nanoparticles (EPI-SPION), 65, 181
 Epidemiology, 168–169
 Epidermal appendages, 8
 apocrine glands, 8–9
 eccrine sweat glands, 8–9
 hair follicle glands, 9–11
 nails, 11
 sebaceous glands, 9–11
 Epidermal basement membrane, 6
 Epidermal growth factor (EGF), 295–296, 367
 EGF-loaded nanofibers, 368–372
 evaluation of wound closure, 370f
 electrospun scaffolds, 369t
 mechanisms of action, 367–368
 topical delivery, 368
 Epidermal growth factor receptor (EGFR), 367–368
 Epidermal induction factors (EIFs), 372
 Epidermal stem cells (ESCs), 297
 Epidermal targeting, 35
 Epidermis, 2, 124, 179, 221–222, 237, 252–253, 308–309, 311, 354
 clustered pigmentation, 362f
 dermal-epidermal junction, 6
 epithelial stem cells, 3–5
 keratinocytes, 3
 layer, 337–338
 nonkeratinocyte cells, 5–6
 structure, 2f, 3
 Epifascicular epineurium, 318
 Epigallocatechin gallate, 102
 Epirubicin (EPI), 65, 181
 Epithelial hair follicle stem cells, 253
 Epithelial stem cells, 3
 basal layer, 3–4
 basement membrane diagram, 5f
 cornified layer, 5
 granular layer, 4–5
 squamous cell layer, 4
 Epithelium, 9, 324
 epidermis, 308–309, 311
 EPR. *See* Electron paramagnetic resonance (EPR); Enhanced permeability and retention (EPR)
- Erodible nanosystems, 326
 ESCs. *See* Epidermal stem cells (ESCs)
 17 β -Estradiol-hemihydrate formulation, 76
 Ethanol, 170–171
 Ethosomes, 160–161, 170–171
 2-(2-Ethoxyethoxy) ethanol. *See* Transcutol
 Ethylenediaminetetraacetic acid (EDTA), 68
 Ethylhexyl Methoxycinnamate (EHMC), 231–232
 Eudragit RS100 nanoformulations, 329
 European Union (EU), 232, 252
 Evaluation methods, 106–107
 Ex vivo studies, 248–249
 ex vivo evaluation, 334
 ex vivo techniques, 248
 Franz diffusion cells, 249f
 Excess surface energy, 19
 Excision, 181–182
 External flagellum, 135
 Extracellular matrix (ECM), 39, 139, 238, 289, 338–339, 367
 of dermis and basal lamina, 343
 Extrinsic factors, 239
 Eye, 323–324
 cornea, 324, 324f
 drug delivery, 323–324
 barriers, 324–326
 drug release, 334
 nanomedicine paradigms in ocular diseases, 326
 nanomedicines
 characterization, 333–334
 for ocular application, 326–327
 for ocular delivery, 327–331
 production, 331–333
- F**
 FA. *See* Folic acid (FA)
 Face-centered cubic material (fcc material), 19
 FasL expression, 141–142, 148
 fcc material. *See* Face-centered cubic material (fcc material)
 FDA. *See* Food and Drug Administration (FDA). *See* US Food and Drug Administration (FDA)
 Ferromagnetic particles (FMP), 209
 FGF. *See* Fibroblast growth factor (FGF)
 FGFR. *See* Fibroblast growth factor receptor (FGFR)
 Fibrin network, 288
 Fibroblast growth factor (FGF), 296, 338
 Fibroblast growth factor receptor (FGFR), 208
 Fibroblasts, 238
 Filaggrin, 4–5, 76–77
 Fine-disperse emulsions. *See* Nanoemulsion
 First-pass effect, 92
 FK506, 163
 Flexible nanoparticles (Flexible NPs), 116–120
 Flexible nanovesicles, 116–120

- Flexible NPs. *See* Flexible nanoparticles (Flexible NPs)
- FLIM. *See* Fluorescence lifetime imaging (FLIM)
- FLU. *See* Flurbiprofen (FLU)
- Fluconazole, 140
- Fluocinolone, 35
- 9-Fluorenylmethyl carbamate (Fmoc), 91
- Fluorescence lifetime imaging (FLIM), 106, 358–359
- Fluorescence microscopy, 38, 314
- Fluorescence resonance energy transfer (FRET), 263–265
- 5-Fluorouracil (5-FU), 96, 181–182, 208
- Flurbiprofen (FLU), 329
- Fmoc. *See* 9-Fluorenylmethyl carbamate (Fmoc)
- FMP. *See* Ferromagnetic particles (FMP)
- Folic acid (FA), 77, 206
- Folic acid receptors (FR), 206–208
- Follicular penetration, 238–239
- “Follicular sink”, 233–234
- Food and Drug Administration (FDA), 189–190
- Formulation adjuvants, 102–104
- Formulation manipulation, 93
- Fourier transform infrared spectroscopy (FT-IR), 121
- FR. *See* Folic acid receptors (FR)
- Fragmentation, 231
- Franz diffusion cell, 105–106
- Free radical production, 231
- FRET. *See* Fluorescence resonance energy transfer (FRET)
- Frontiers in skin regeneration, 338
- FT-IR. *See* Fourier transform infrared spectroscopy (FT-IR)
- 5-FU. *See* 5-Fluorouracil (5-FU)
- Functionalization, 241
- Fungal infections, 39
- G**
- G3 CAOS sensor, 264f
- Gadolinium (Gd), 178–179, 221
- neutron capture therapy, 221
- GAGs. *See* Glycosaminoglycans (GAGs)
- β -Galactosidase, 101–102
- GAPDH. *See* Glyceraldehyde 3-phosphate dehydrogenase (GAPDH)
- Gastrointestinal (GI), 92
- Gastrointestinal distress (GI distress), 35
- Gelatin, 76, 342
- Gelatinases, 6–7
- Gene therapy, 297
- with siRNA, 206
- Generations, 90, 242
- GI. *See* Gastrointestinal (GI)
- GI distress. *See* Gastrointestinal distress (GI distress)
- β -Glucuronic acid, 78
- Glutathione (GSH), 129
- Glyceraldehyde 3-phosphate dehydrogenase (GAPDH), 172
- Glycogen, 16–17
- Glycosaminoglycans (GAGs), 238
- GNPs. *See* Gold nanoparticles (AuNPs)
- Gold, 19
- clusters, 21
- nanoshells, 23–24
- fabrication, 26–27
- Gold nanoparticles (AuNPs), 23–24, 41, 58, 64–65, 99–100, 179, 218, 354
- dermatological applications, 100, 100f
- applications, 102
- skin cancer treatment and imaging, 101
- topical and transdermal drug delivery, 101–102
- enhanced radiotherapy in mouse model, 220f
- interactions with skin barrier, 102–108
- AuNP penetration, 106–107
- factors affecting skin penetration, 102–106
- potential experimental design, 103f
- skin penetration enhancers of colloidal gold, 107–108
- mechanisms of skin penetration, 108–110
- physicochemical properties, 102–104
- production and physicochemical properties, 218
- Gold nanorods (Au-NRs), 41
- Grafted peptide dendrimers, 91
- Granular layer, 4–5
- Granulation tissue, 289
- Graphene oxide, 194–195
- Growth factor–loaded biodegradable scaffolds, 77–78
- GSH. *See* Glutathione (GSH)
- GSNO. *See* s-Nitrosoglutathione (GSNO)
- Guanine (G), 203–204
- H**
- HA. *See* Hyaluronic acid (HA); Hydroxyapatite (HA)
- Hair. *See also* Dermatology; Nanodermatology
- bulb, 9
- color, 9
- formation, 9–10
- Hair follicle(s), 233–234
- cells, 252–253
- glands, 9–11
- stem cells, 3
- Haptoglobin (Hpg), 339
- HB-EGF. *See* Heparin-binding epidermal growth factor (HB-EGF)
- HCuSNPs. *See* Hollow CuS nanoparticles (HCuSNPs)
- HDLs. *See* High-density lipoproteins (HDLs)
- hEGFR. *See* human epidermal growth factor receptor (hEGFR)
- HeLa cells, 276–278, 277f, 281
- Helicobacter pylori* (*H. pylori*), 76
- Hemagglutinin, 75
- Hemopexin (Hpx), 339
- Hemostasis, 290
- Hemostatic events, 338
- Henle’s layer, 9
- Heparin, 81–82
- Heparin-binding epidermal growth factor (HB-EGF), 367
- hESdCs. *See* human embryonic stem cell-derived cells (hESdCs)
- Hexamethyldisiloxane (HMDSO), 268
- nanoemulsions, 268–269
- 3-(1’-Hexyloxyethyl) pyropheophorbide-a (HPPH), 37
- HF. *See* Hydrofluoric acid (HF)
- HIF1-alpha lacking oxygen-sensitive degradation domain (HIF1adODD), 341
- High-density lipoproteins (HDLs), 76
- High-energy gamma/X-ray radiation, 219
- High-Z inorganic nanoparticles, 218
- Histamine, 81–82
- HIV-1. *See* Human immunodeficiency virus-1 (HIV-1)
- HMDSO. *See* Hexamethyldisiloxane (HMDSO)
- hMSCs. *See* human mesenchymal stem cells (hMSCs)
- Hollow CuS nanoparticles (HCuSNPs), 65
- Homeostasis, 252–253
- Homogenization method, 333
- Horseradish peroxidase, 101–102
- Hot-melt homogenization technique, 122, 333
- Hpg. *See* Haptoglobin (Hpg)
- HPPH. *See* 3-(1’-Hexyloxyethyl) pyropheophorbide-a (HPPH)
- HPV. *See* Human papilloma virus (HPV)
- Hpx. *See* Hemopexin (Hpx)
- HRS. *See* Hyper-Rayleigh scattering (HRS)
- human embryonic stem cell-derived cells (hESdCs), 297
- human epidermal growth factor receptor (hEGFR), 37
- Human immunodeficiency virus-1 (HIV-1), 79
- human mesenchymal stem cells (hMSCs), 297
- Human papilloma virus (HPV), 132–133
- rabbit model, 132–133
- Human skin, 237–238
- human vascular endothelial growth factor (hVEGF), 297
- Huxley’s layer, 9
- hVEGF. *See* human vascular endothelial growth factor (hVEGF)
- Hyaluronic acid (HA), 52, 77–78, 121, 296, 342
- Hydrofluoric acid (HF), 91
- Hydrogen tetrachloroaurate ($\text{HAuCl}_4 \cdot 3\text{H}_2\text{O}$), 26–27
- Hydrolyzable bonds, 78f
- Hydrophilic layer, 311
- molecules, 309
- upconversion nanoparticles, 60
- Hydrophilicity, 59, 266
- Hydrophobic layer, 311
- Hydroxyapatite (HA), 61–62

- Hydroxyl radicals (OH radicals), 232
N-Hydroxysuccinimide (NHS), 60–61
 Hyper-Rayleigh scattering (HRS), 359
 Hypericin
 dermatological application, 276
 nanoparticles distribution and in living cells
 incubation of cells, 277–278
 labeling of cell organelles, 278
 PLLA-Hyp nanoparticles
 characterization, 277
 Hypericin with polyvinylpyrrolidone (PVP-Hyp), 276
 Hypericin-loaded PLLA (PLLA-Hyp), 276
 Hypodermis, 7–8, 308, 337–338
 Hypoxia, 257, 342
- I**
 ICAM1. *See* Intracellular adhesion molecule-1 (ICAM1)
 ICPS. *See* Inductively coupled plasma spectroscopy (ICPS)
 ICS. *See* Image correlation spectroscopy (ICS)
 IDO. *See* Indoleamine 2,3-dioxygenase (IDO)
 IFN- α . *See* Interferon- α (IFN- α)
 IFN- α -2 β . *See* Interferon α -2 β (IFN- α -2 β)
 IFN γ . *See* Interferon- γ (IFN γ)
 IgE. *See* Immunoglobulin E (IgE)
 IgG. *See* Antiovalbumin-immunoglobulin G (IgG)
 IM. *See* Imatinib mesylate (IM)
 Image correlation spectroscopy (ICS), 278
 corrections for immobile species, 281
 image collection for variants, 281
 STICCS, 279–280
 STICS, 278–279
 TICS, 279
 Imaging, 353–354
 Imatinib mesylate (IM), 64–65
 Imatinib-loaded sterically stabilized liposomes (SSL-IMA), 210
 Imiquimod (IMQ), 136
 IMMA. *See* Intramuscular meglumine antimoniate (IMMA)
 Immune checkpoint, 196
 Immune response, 51–52
 Immunity priming effects, 168–169
 Immunoglobulin E (IgE), 167
 Immunological abnormalities, 167–168
 Immunological considerations, 140–143
 Immunological function, 11–12
 Immunomodulation, 141
 Immunostimulation, 196
 immunostimulatory effect, 141
 Immunotoxicity, 75
 IMQ. *See* Imiquimod (IMQ)
 In situ polymerization, 62
 In vitro, 252
 cell toxicity, 248
 determination, 334
 In vivo
 EPR oximetry systems, 270f
 evaluation, 334
 studies, 249
 mouse skin, 251f
 impact of particle characteristics, 252
 particle/ion penetration, 249–250
 skin barrier disruption, 250–252
 Indoleamine 2,3-dioxygenase (IDO), 204
 Inducible NOS (iNOS), 128
 Inductively coupled plasma spectroscopy (ICPS), 106
 Infectious disease
 nanoemulsions for, 39
 nanoparticles for, 33–35
 Inflammation, 288, 338
 cutaneous wound, 289f
 inflammatory cytokines, 139
 inflammatory disease, nanoparticles for, 35–36
 Infundibulum, 9
 Ingested silver nanoparticles, 22
 Inner stroma, 324
 Inorganic filters, 229
 formation of aggregates and agglomerates, 230f
 nano TiO₂ and ZnO, 229–231
 TiO₂ primary particles, 230f
 UVattenuation *vs.* wavelength for spherical TiO₂, 231f
 Inorganic nanoparticles, 58
 design criteria, 58
 skin penetration ability, 58–60
 surface engineering strategies, 60–62
 surface modification, 61f
 synthesis
 of boronic acid-functionalized silica nanoparticles, 62f
 of EGFR siRNA-based SNA-NCs, 65f
 for topical application, 66
 calcium carbonate nanoparticles, 68
 calcium phosphate nanoparticles, 68
 QDs, 68–69
 silver nanoparticles, 66–68
 titanium dioxide nanoparticles, 68
 zinc oxide nanoparticles, 68
 for transdermal drug delivery, 63
 CuS nanoparticles, 65
 gold nanoparticles, 64–65
 iron oxide nanoparticles, 65
 silica nanoparticles, 63
 iNOS. *See* Inducible NOS (iNOS)
 Insulin, 48–50
 Integrins, 208
 Integumentary system, 1–2
 Interacellular
 lipid, 238–239
 pathway, 108–109, 309
 route, 180
 Interferon α -2 β (IFN- α -2 β), 204–205
 Interferon- α (IFN- α), 196
 Interferon- γ (IFN γ), 339
 Interleukins, 75
 IL-2, 204–205
 IL10, 75
 IL18, 63
 Intermolecular interactions, 20–21
 Internal radiation therapy, 217–218
- Intracellular
 dynamics
 PLLA-HYP nanoparticles, 281–282
 PVP-HYP, 281–282
 localization, 277f
 pathways, 109
 signaling pathways, 192
 Intracellular adhesion molecule-1 (ICAM1), 295
 Intramolecular bonding, 20, 20t
 Intramuscular meglumine antimoniate (IMMA), 142
 Intravenous (IV), 157–160
 Intrinsic bioactive effects, 241–242
 Intrinsic factors, 239
 Invasomes, 75
 Ionic gelation method, 332
 Ionizing radiation, 210, 217–219
 Iontophoresis, 108
 iontophoresis-mediated permeation, 94–95
 Iridium(II) complexes, 260
 Iron oxide (Fe₃O₄), 65
 Iron oxide nanoparticles (Fe₃O₄NPs), 58, 65, 340
 Isomerization, 231
 Isopropyl alcohol, 122
 Isthmus, 9
 IV. *See* Intravenous (IV)
- J**
 Janus kinase 1 (JaK1), 368
- K**
 Keratinization, 3
 Keratinocyte growth factor (KGF), 341, 368
 Keratinocytes, 3, 81–82, 237, 338, 354
 Ketoprofen (KP), 68, 96
 KGF. *See* Keratinocyte growth factor (KGF)
 KP. *See* Ketoprofen (KP)
- L**
 LAB. *See* Laser-assisted bioprinting (LAB)
 Labrasol, 116–120
 Lamina densa, 6
 Lamina lucida, 6
 Laminin receptor, 208
 Langerhans cells (LCs), 5, 82, 101–102
 Langmuir–Blodgett films, 25
 β -Lapachone, 149
 Laponite, 292–293
 Larger spherical nanomaterials, 17
 Laser scanning confocal microscopy (LSCM), 359–361
 Laser scanning microscopy, 314
 Laser-assisted bioprinting (LAB), 345
 Layer-by-layer (LbL), 64–65
 assembly, 61–62
 methods, 25
 Layer-by-layer polyelectrolyte coated AuNP (LbL-AuNP), 181
 LbL. *See* Layer-by-layer (LbL)
 LbL-AuNP. *See* Layer-by-layer polyelectrolyte coated AuNP (LbL-AuNP)

- LC-silica NPs. *See* Lipid-coated silica nanoparticles (LC-silica NPs)
- LCL. *See* Localized cutaneous leishmaniasis (LCL)
- LCNs. *See* Liquid crystalline nanoparticles (LCNs)
- LCs. *See* Langerhans cells (LCs)
- LDCs. *See* Lipid drug conjugates (LDCs)
- LDLs. *See* Low-density lipoproteins (LDLs)
- LEDs. *See* Light-emitting diodes (LEDs)
- Leishmania*, 135–136
L. aethiopica, 136
L. amazonensis, 136
L. donovani, 141
L. major, 136, 147–148
L. mexicana, 136
L. panamensis, 136
L. tropica, 136
parasites, 139
- Leishmaniasis, 135
- LFA-3. *See* Lymphocyte functional antigen (LFA-3)
- Light responsive drug delivery, 209
- Light-emitting diodes (LEDs), 15
- Light-responsive drug delivery, 209
- Limonene, 116–120
- Lipid, 170
cationic, 172
decreased SC lipids, 167–168
lipid-based
nanocarriers, 25
nanoparticles, 33, 191
nanoparticle preparations, 170
- Lipid based vesicular nanocarriers, 160–163
antipsoriatic drug delivery
nano-bullets, 161f
nanocarriers, 162t
- Lipid drug conjugates (LDCs), 33
- Lipid nanoparticles (LNs), 63, 192
- Lipid-coated silica nanoparticles (LC-silica NPs), 59
- Lipid-polymer hybrid nanoparticles (LPNs), 290
- α -Lipolic acid, 102
- Liposomal conventional drugs, 146–147
preclinical or clinical studies, 146t
- Liposomal nanomedicines (LNMs), 330
- Liposome, 75–76, 82, 160
in photodynamic therapy, 148
- Liposome-protamine-hyaluronic acid (LPH), 197
- Liposomes, 27, 38, 101, 160, 178, 242, 295, 330–331
elastic, 161–163
- Liposomes, rigid, 144
- Lipoxin A₄ (LXA₄), 341
- Liquid crystalline nanoparticles (LCNs), 35
- Living cells, nanoparticles distribution and hypericin in
incubation of cells, 277–278
labeling of cell organelles, 278
PLLA-Hyp nanoparticles
characterization, 277
- LNMs. *See* Liposomal nanomedicines (LNMs)
- LNs. *See* Lipid nanoparticles (LNs); Lymph nodes (LNs)
- Localized cutaneous leishmaniasis (LCL), 136
- Lohmann Therapie-Systeme AG (LTS), 54
- Lotus leaf surface, 23
- Low-density lipoproteins (LDLs), 76
- LPH. *See* Liposome-protamine-hyaluronic acid (LPH)
- LPNs. *See* Lipid-polymer hybrid nanoparticles (LPNs)
- LSCM. *See* Laser scanning confocal microscopy (LSCM)
- LTS. *See* Lohmann Therapie-Systeme AG (LTS)
- LXA₄. *See* Lipoxin A₄ (LXA₄)
- Lymph nodes (LNs), 208
- Lymphatic vessels, 7
- Lymphocyte functional antigen (LFA-3), 157–160
- Lyophilization, 333
- Lysine, 91–92
- Lysosomes, 16–17
- M**
- “M2-like” macrophage phenotype, 139
- mAb. *See* Monoclonal antibody (mAb)
- Macrophages, 288
- Magnetic NPs (MNPs), 181–182, 210
- Magnetic particle focusing, 23
- Magnetic resonance image-guided focused ultrasound (MRI-GFU), 222–223
- Magnetic resonance imaging (MRI), 210
oxygen sensing on, 267–268
- Magnetophoresis, 222–223
- Major histocompatibility complex (MHC), 157–160
- MAL. *See* Methyl aminolevulinate (MAL); Methyl-5-aminolaevulinate (MAL)
- Man-PEG bubble lipoplexes, 210
- Manganese (Mn), 178–179
- Manmade nanoparticle material, 353
- MAPK pathway. *See* Mitogen-activated protein kinase (MAPK pathway)
- Marqibo, 211
- MART-1. *See* Melanoma antigen recognized by T-cells 1 (MART-1)
- Mast cells, 7
- Matrix metalloproteinases (MMPs), 6–7, 139, 239–240, 289–290, 297–298, 339
- Maturation, 289–290, 297–298
- MB. *See* Methylene blue (MB)
- MBs. *See* Molecular beacons (MBs)
- MC calculations. *See* Monte Carlo calculations (MC calculations)
- MC-ICP-MS. *See* Multicollector inductively coupled plasma mass spectrometry (MC-ICP-MS)
- MC1R. *See* Melanocortin 1 receptor (MC1R)
- MCL. *See* Mucocutaneous leishmaniasis (MCL)
- MCM-41. *See* Mesoporous silicate (MCM-41)
- MD simulations. *See* Molecular dynamic simulations (MD simulations)
- MDR. *See* Multiple drug resistance (MDR)
- MDSCs. *See* Myeloid-derived suppressor cells (MDSCs)
- Mechanical penetration enhancers, 105
- Melanin, 5
- Melanocortin 1 receptor (MC1R), 203–204
- Melanocyte-stimulating hormone (MSH), 41, 209
- Melanocytes, 5
- Melanoma, 182, 189–190, 203–204
genetic mutations and immunobiological changes, 204f
limitations of conventional treatments for, 204–205
nanomedicine in melanoma clinical trials, 211–212
nanoparticle containing both 5-FU and siRNA, 191f
nanoparticle drug delivery systems relevant to, 191–192
nanotechnology
in chemotherapy, 192
in combination therapy, 197–198
in melanoma immunotherapy, 195–197
in targeted therapy against, 192–195
nanotechnology-based targeted drug delivery, 205
signaling pathways, 193f
targeted NP drug delivery for, 205–211
active targeting, 206–209
nanotheranostics and combination therapy, 210–211
stimuli-responsive drug delivery and triggered release, 209–210
- Melanoma, targeting, 208–209
- Melanoma antigen recognized by T-cells 1 (MART-1), 208
- Melanoma cells
targeting receptors on surface, 206–208
- MEP. *See* Multiphoton-enhanced photoluminescence (MEP)
- Merkel cells, 6
- MEs. *See* Microemulsions (MEs)
- Mesenchymal stem cells (MSCs), 372
- Mesoporous silica nanoparticles (MSNs), 265f
- Mesoporous silica oxide, 80
- Mesoporous silicate (MCM-41), 232
- messenger RNA (mRNA), 64–65, 295, 339
- Metal nanoparticles, 33, 219, 221. *See also* Nanoparticles
antimicrobial properties, 293–295
application in brachyirradiation for nonmelanoma skin cancers, 223–225
EMP enhanced radiotherapy in human skin, 225f
vziable human skin, 224f

- Metal nanoparticles (Continued)
 enhanced radiosensitization, 218–221
 AgNPs production and physicochemical properties, 218
 GNP enhanced radiotherapy in mouse model, 220f
 mechanism of metal radiosensitization, 219
 metal-based radiosensitizers, 220–221
 in vivo studies, 219–220
 enhanced radiotherapy in dermatology, 217
 high-Z inorganic nanoparticles, 218
 radiation therapy, 217–218
 targeted delivery to tumor tissues, 221–223
 multiphoton tomography, 223f
 sites in skin for nanoparticle delivery, 222f
- Metal oxide nanoparticles, 120–121, 248
 decoupling in vitro nanotoxicity from risk to human health, 248
 ex vivo studies, 248–249
 Franz diffusion cells, 249f
 remaining knowledge gaps, 252–253
 in vivo studies, 249–252
 mouse skin, 251f
 impact of particle characteristics, 252
 particle/ion penetration, 249–250
 skin barrier disruption, 250–252
- Metal radiosensitization mechanism, 219
- Metallic nanoparticles, 339–340
- Metallic NPs (MNPs), 181–182
- Metalloproteinases, 141–142, 148
- Methicillin-resistant *S. aureus* (MRSA), 34, 129–130, 130f, 292–293, 301
- Methotrexate (MTX), 35, 160–161
- Methoxy polyethylene glycol (mPEG), 17, 64–65
- 8-Methoxypsoralen with UVA radiation (PUVA), 157–160
- Methyl aminolevulinate (MAL), 181–182
- Methyl-5-aminolaevulinate (MAL), 39
- Methylene blue (MB), 142
- N-Methylthiolated β -lactams, 292
- MHC. *See* Major histocompatibility complex (MHC)
- MIC. *See* Minimum inhibitory concentration (MIC)
- Microbial response, 51–52
- Microemulsions (MEs), 63, 164, 331
- Microencapsulated retinol, 39
- Microfibrils, 16–17
- Microneedle (MN), 47–48, 48f, 222–223
 assuring patient confidence in, 50–51
 combining hydrogel-forming microneedles, 49f
 devices, 54f
 ensuring patient safety, 51–52
 future applications, 50
 materials, 48–50
 MN-based transdermal delivery systems, 47–48
 patients and healthcare professionals, 51
 regulatory issues, 52–53
 as viable commercial technology, 53–54
 microRNAs (miRNAs), 297
- Microspheres, 164
- Microstructured transdermal systems (MTS), 53
- Miltefosine (MIL), 140
- Mini-emulsion technique, 277
- Mini-emulsions. *See* Nanoemulsion
- Minimum inhibitory concentration (MIC), 34–35
- miRNAs. *See* microRNAs (miRNAs)
- Mitochondrial apoptotic pathway, nanotechnology in, 195
- Mitochondrion, 195
- Mitogen-activated protein kinase (MAPK pathway), 189–190, 193–194, 203–204
- MMPs. *See* Matrix metalloproteinases (MMPs)
- MN. *See* Microneedle (MN)
- MNPs. *See* Magnetic NPs (MNPs); Metallic NPs (MNPs)
- Molecular beacons (MBs), 182–183, 183f
- Molecular dynamic simulations (MD simulations), 21–22
- Molecular oxygen, 257
- Molecular weight (MW), 139–140
- Moll's gland, 8
- Monoclonal antibody (mAb), 205
- Mononuclear phagocytic system (MPS), 205
- Monte Carlo calculations (MC calculations), 220
- Mouse mammary carcinoma model, 219
 GNP enhanced radiotherapy in, 220f
- mPEG. *See* Methoxy polyethylene glycol (mPEG)
- MPM. *See* Multiphoton microscopy (MPM)
- MPM–FLIM. *See* Multiphoton tomography–fluorescence lifetime imaging (MPM–FLIM)
- MPS. *See* Mononuclear phagocytic system (MPS)
- MRI. *See* Magnetic resonance imaging (MRI)
- MRI-GFU. *See* Magnetic resonance image–guided focused ultrasound (MRI-GFU)
- mRNA. *See* messenger RNA (mRNA)
- MRSA. *See* Methicillin-resistant *S. aureus* (MRSA)
- MSCs. *See* Mesenchymal stem cells (MSCs)
- MSH. *See* Melanocyte-stimulating hormone (MSH)
- MSNs. *See* Mesoporous silica nanoparticles (MSNs)
- mTHPC. *See* M-Tetrahydroxyphenylchlorin (mTHPC)
- MTS. *See* Microstructured transdermal systems (MTS)
- MTX. *See* Methotrexate (MTX)
- Mucocutaneous leishmaniasis (MCL), 136–137
- Multicollector inductively coupled plasma mass spectrometry (MC-ICP-MS), 250
- Multineedle bioprinting system, 345–347, 347f
- Multiphoton microscopy (MPM), 103–104, 106, 358–359
- Multiphoton tomography with fluorescence lifetime imaging microscopy (MPT–FLIM)
- Multiphoton tomography–fluorescence lifetime imaging (MPM–FLIM), 120, 359
 images of intact and tape-stripped skin, 359
- Multiphoton-enhanced photoluminescence (MEP), 359
- Multiple drug resistance (MDR), 36, 205
 MDR1, 36
- Muscles, 7
- MW. *See* Molecular weight (MW)
- Myc, 194
- Myeloid-derived suppressor cells (MDSCs), 204
- ## N
- n-3 polyunsaturated fatty acids (n-3 PUFAs), 168
- N₂O₃. *See* Dinitrogen trioxide (N₂O₃)
- Nab-paclitaxel, 192
- Nails, 11
- Naked probe molecules, 260
- NALP-3 inflammasome, 145
- Nano TiO₂ and ZnO
 safety concerns for, 232–234
 combination TiO₂ and ZnO skin penetration studies, 234t
 TiO₂ skin penetration studies, 233t
 ZnO skin penetration studies, 233t
- Nanobridging, 292
- Nanocarriers, 26f, 73–74, 75f, 181, 307–308
 biocompatible inorganic, 80
 biocompatible organic, 79–80
 bioconjugates, 76–77
 biodegradability and biocompatibility in skin, 80–83, 81f
 biodegradable organic, 77–79
 biological, 74–76
 bottom-up synthesis, 25–27
- Nanocrystals, 329–330
- Nanodelivery benefits in melanoma therapy, 190–191
- Nanodermatology, 20, 32. *See also* Dermatology
- nanomaterials, 32
 cosmetic roles, 40–41
 diagnostic roles, 41–42
 nanoemulsions, 38–39
 nanoliposomes, 38
 nanoparticles, 33–38
 nanoscaffold wound dressings, 39–40
 selective accumulation, 33f
 stratum corneum, 32f
- Nanoemulsions, 38–39, 115–116, 170, 240–242, 331
 antiaging cosmetics, 240
 for cosmetic dermatology, 40
 ECM, 238

- epidermis, 237
- mechanisms of action, 241f
- nanocarriers, 240f, 242
- for prevention and treatment of
 - photoaging, 242–243
- skin aging, 239–240
- skin permeability, 238–239
 - skin barrier, 238f
- types, 241f
- Nanoencapsulation, 231–232
- Nanofibers, 17
 - chitin, 17–18, 33
 - core–shell, 343–344
 - EGF-loaded, 368–372
 - electrospun, 343–344
 - in wound healing
 - natural polymer nanofibers, 341–342
 - synthetic polymer nanofibers, 342
- Nanoformulations for skin, 115–116
 - nanoparticle application to skin, 117t–119t
 - penetration, 116f
- Nanogels, 77, 79–80
- Nanoliposomes, 38
- Nanomaterials, 17, 31–32
 - cosmetic roles, 40
 - nanoemulsions for cosmetic dermatology, 40
 - nanopigments for cosmetic dermatology, 40–41
 - diagnostic roles, 41
 - nanoparticles for diagnostic dermatology, 41–42
 - quantum dots for diagnostic dermatology, 41
 - larger spherical nanomaterials, 17
 - log scale, 16f
 - 1D nanomaterials, 17–18
 - oxygen sensors, 263–265
 - approaches to immobilize oxygen probes, 265f
 - G3 CAOS sensor, 264f
 - photodynamic model of MSNs, 265f
 - targeted ratiometric Oxyphor
 - G2-loaded oxygen nanosensor, 266f
 - and sizes of things, 16–17
 - synthesis, 24–25
 - bottom-up synthesis of nanocarriers, 25–27
 - self-assembly, 25
 - self-organization, 25
 - 2D nanomaterials, 18
 - 0D nanomaterials, 17
- Nanomedicines, 157, 190
 - for antipsoriatic drug therapy, 160
 - emulsion-based nanocarriers, 164
 - lipid based vesicular nanocarriers, 160–163
 - nanoparticulate carriers, 163–164
 - polymeric nanocarriers, 164–165
 - characterization, 333–334
 - in melanoma clinical trials, 211–212
 - for ocular application, 326–327
 - Advantages of Ocular Nanomedicines, 327
 - Disadvantages of Ocular Nanomedicines, 327
 - for ocular delivery, 327–328
 - dendrimers, 330
 - liposomes, 330–331
 - microemulsions, 331
 - nanocrystals, 329–330
 - nanoemulsions, 331
 - nanoparticles, 328
 - nanosuspensions, 329
 - polymer-based nanomedicines for eye, 328–329
 - requirements for ocular nanosystems, 328
 - strategies to improving low ocular bioavailability, 327
 - paradigms in ocular diseases, 326
 - production, 331
 - double-emulsion solvent evaporation method, 332
 - emulsification solvent diffusion method, 332
 - emulsion solvent evaporation method, 331–332
 - homogenization method, 333
 - ionic gelation method, 332
 - nanoprecipitation method, 331
 - RESS, 333
 - salting-out method, 332
 - supercritical fluid method, 332–333
- Nanoparticle skin penetration
 - affecting factors, 356–357
 - analytical method for studying, 353–354
 - barrier functions, 354–357
 - imaging, 353–354
 - mechanism into skin, 355–356
 - noninvasive imaging, 355f
 - noninvasive microscopy techniques, 357
 - MPM, 358–359, 358f
 - OCT, 361–363, 362f
 - single-photon microscopy, 359–361
 - time-correlated single-photon counting, 358–359
 - skin structure, 354–357
 - transport pathways of particles across skin barrier, 356f
- Nanoparticle-based antitumor vaccination, 73–76, 82–83
- Nanoparticle-based theranostics
 - NPs for transdermal drug delivery, 179–181
 - NPs in cancer theranostics, 178–179
 - in skin cancer, 181–183
 - MBs, 183f
 - nanovehicles in therapy and diagnosis, 183t–184t
- Nanoparticles (NPs), 33–38, 115, 177, 190, 192, 196, 205, 221, 230–231, 248, 259, 262–263, 290, 290t, 307–309, 313, 328, 353, 357
 - active targeting and internalization of therapeutic, 206
 - applications in wound healing, 290
 - hemostasis, 290
 - nanobridging, 292
 - platelets, 290–291
 - thrombin, 291–292, 291f
- combination
 - with penetration enhancers, 124
 - of siRNAs against BRAF and Akt in, 195
- for cutaneous neoplasms, 36–37
- for diagnostic dermatology, 41–42
- drug delivery systems relevant to melanoma, 191–192
- encapsulation, 34–35
- flexible, 116–120
- formulations, 267
- for infectious disease, 33–35
- for inflammatory disease, 35–36
- metal oxide, 120–121
- oxygen probes, 265
- paramagnetic materials, 269
- penetration of variably sized, 123f
- in photoacoustic tomography for cancer detection, 41f
- for photoprotection, 37–38
- Polymer-based, 123–124
- PtTFPP within, 263–265
- recovery, 332
- releasing encapsulated drugs, 34f
- and skin, 115, 117t–119t
 - interactions, 353
 - structure and penetration routes, 59f
- sources of materials for polymeric, 290t
- for targeted delivery to hair follicles and sebaceous glands, 124
- in topical therapy of CL, 143
 - AgNPs failure in *L. major*, 147–148
- liposomal conventional drugs, 146–147
- liposomes in photodynamic therapy, 148
- NO delivery systems, 147
- NPs and interaction with pathological skin lesions, 143–146, 145f
- toxicity, 301–302
 - pathways for metabolism, 303f
 - silver nanoparticles, 302f
- types, 263–265
- use for AD treatment, 170–173
- in wound healing
 - metallic nanoparticles, 339–340
 - nanoporous AAO, 339
 - nonmetallic NPs, 340–341
- Nanoparticles safety, 248
- Nanoparticulate(s), 328
 - carriers, 163–164
 - platforms, 129
 - systems, 180
- Nanopass Technologies, 53
- Nanopigments for cosmetic dermatology, 40–41
- Nanoporous anodic aluminum oxide (Nanoporous AAO), 339
- Nanoprecipitation method, 331

- Nanoscience, 15–16
 nanomaterials
 and sizes of things, 16–17
 synthesis, 24–27
 types, 17–18
 physical and chemical properties, 18
 advanced surfaces, 23
 chemical reactivity, 21
 collective surface area, 18–19, 19f
 intermolecular interactions, 20–21
 optical and magnetic properties, 23–24
 particle shape, 19
 particle stability, 19–20
 penetration, permeability, solution, transport properties, 21–23
 S/V ratio, 19
 specific surface area, 18–19
 surface energy, 19–20
 tumor ablation, 24f
- Nanoshells, 17, 23–24
- Nanosized particles of TiO₂, 248
- Nanosized particles of ZnO, 248
- Nanostructured lipid carriers (NLCs), 33, 76, 115–116, 122–123, 143–144, 163, 170, 296
- Nanosuspensions, 329
- Nanotechnology, 15–16, 73–74, 99–100, 115, 127, 229, 240, 247, 293
 in chemotherapy of melanoma, 192
 in combination therapy of melanoma, 197–198
 in melanoma immunotherapy, 195–197
 CD47, 196–197
 CTLA4, 197
 immune checkpoint, 196
 immunostimulation, 196
 PD-L1, 197
 Nanotechnology Task Force, 235
 in photoprotection, 229
 inorganic filters, 229–231
 organic filters and, 231–232
 regulatory state of nanoparticles in sunscreens, 234–235
 safety concerns for nano TiO₂ and ZnO, 232–234
 risks, 173
 in T-cell and macrophage activation, 196f
 in targeted therapy against melanoma, 192–195
 combination of siRNAs against BRAF and Akt in nanoparticle, 195
 MAPK pathway, 193–194
 nanotechnology in signaling pathways in melanoma, 194–195
 PI3K/Akt pathway, 194
 signaling pathways in melanoma, 193f
 in targeting mitochondrial apoptotic pathway, 195
- Nanotechnology-based nano-bullets in antipsoriatic drug delivery
 nanomedicines for antipsoriatic drug therapy, 160
 emulsion-based nanocarriers, 164
 lipid based vesicular nanocarriers, 160–163
 nanoparticulate carriers, 163–164
 polymeric nanocarriers, 164–165
 pathophysiology and pharmacotherapy for psoriasis, 157–160
 eminent pathways in pathogenesis of psoriasis, 158f
 psoriasis pharmacotherapy, 159t
- Nanotechnology–based targeted drug delivery, 205
- Nanotheranostics
 and combination therapy, 210–211
 NP in melanoma combination therapy, 210–211
 theranostic NP in melanoma imaging and therapy, 210
- Nano–titanium dioxide collagen artificial skin (NTCAS), 293
- Nanotoxicology, 28
- Natural polymer nanofibers, 341–342
- NB-002 nanoemulsion, 39
- Near-infrared (NIR), 64–65, 259
 light, 209
 oxygen sensing, 259
 radiation, 17, 23–24, 99–100
- Near-infrared spectroscopy (NIRS), 259
- Necrosis, 141
- Nerves, 7
- Neuraminidase, 75
- Neuronal NOS, 128
- Neutrophils, 149
 apoptosis, 141
- New world cutaneous leishmaniasis (NWCL), 136, 141
- NF- κ B. *See* Nuclear factor kappa-light-chain-enhancer of activated B cells (NF- κ B)
- NH₂. *See* Amine groups (NH₂)
- NHS. *See* N-Hydroxysuccinimide (NHS)
- Niche microenvironment, 345
- Niosomes, 161–163, 170–171
- NIR. *See* Near-infrared (NIR)
- NIRS. *See* Near-infrared spectroscopy (NIRS)
- Nisosomes, 242
- Nitric oxide (NO), 33–34, 127, 139, 298–301, 341
 delivery systems, 147
 nanomaterial-based delivery platforms for, 298f
 nanoparticle NO delivery, 300t–301t
 photodonor, 181–182
 physical characteristics and physiological role, 128
- Nitric oxide–releasing nanoparticles (NO-np), 33–34, 128, 130–131
 as antibacterial agent, 129–131
 as antifungal agent, 131–132
 characteristics, 128–129
 minimal toxicity to fibroblasts, 130f
 nitric oxide releasing sol–gel nanoplateforms, 129f
 future directions, 132–133
- platforms, 127–133, 130f
 S. aureus, 131f
 subcutaneous abscess area decreased after treatment, 130f
- Nitrogen dioxide (NO₂), 128
- s-Nitrosocaptopril nanoparticles (SNO-CAP-np), 129–130
- s-Nitrosoglutathione (GSNO), 129–130
- S-Nitrosothiols, 128
- Nitroxides, 269
- Nivolumab, 197–198, 205
- NLCs. *See* Nanostructured lipid carriers (NLCs)
- NMR. *See* Nuclear magnetic resonance (NMR)
- NO. *See* Nitric oxide (NO)
- NO synthase (NOS), 128
- NO-np. *See* Nitric oxide–releasing nanoparticles (NO-np)
- NO₂. *See* Nitrogen dioxide (NO₂)
- Nonimmunogenic delivery system, 75–76
- Nonkeratinocyte cells
 LCs, 5
 melanocytes, 5
 merkel cells, 6
- Nonmelanoma skin cancers, 217
 EMP enhanced radiotherapy in human skin, 225f
 metal nanoparticle application in brachyradiation for, 223–225
 vziabie human skin, 224f
- Nonmetallic NPs, 340–341
- Nonpharmacologic treatments, 169
- Nonsteroidal antiinflammatory drug (NSAID), 329
- Nonvirulent, 75
- NOS. *See* NO synthase (NOS)
- NPs. *See* Nanoparticles (NPs)
- NSAID. *See* Nonsteroidal antiinflammatory drug (NSAID)
- NTCAS. *See* Nano–titanium dioxide collagen artificial skin (NTCAS)
- Nuclear factor kappa-light-chain-enhancer of activated B cells (NF- κ B), 194
- Nuclear magnetic resonance (NMR), 268
- Numerous downstream effects, 128
- NWCL. *See* New world cutaneous leishmaniasis (NWCL)
- O**
- O/O emulsions. *See* Oil-in-oil emulsions (O/O emulsions)
- O/W emulsions. *See* Oil-in-water emulsions (O/W emulsions)
- OAM. *See* Oleylamine (OAM)
- OCT. *See* Optical coherence tomography (OCT)
- Octadecylsiloxane (ODS), 18
- Octyl methoxycinnamate (OMC), 231–232
- Ocular delivery, nanomedicines for, 327–328
 dendrimers, 330
 liposomes, 330–331
 microemulsions, 331

- nanocrystals, 329–330
 nanoemulsions, 331
 nanoparticles, 328
 nanosuspensions, 329
 polymer-based nanomedicines for eye, 328–329
 requirements for ocular nanosystems, 328
 strategies to improving low ocular bioavailability, 327
- Ocular nanomedicines
 advantages, 327
 disadvantages, 327
- Ocular nanosystems, requirements for, 328
- ODN. *See* Oligonucleotide (ODN)
- ODS. *See* Octadecylsiloxane (ODS)
- OH radicals. *See* Hydroxyl radicals (OH radicals)
- Oil-in-oil emulsions (O/O emulsions), 240
- Oil-in-water emulsions (O/W emulsions), 240, 331–332
- Olanzapine, 124
- Old world cutaneous leishmaniasis (OWCL), 136, 141
- Oleic acid, 116–120
- Oleylamine (OAM), 172
- Oligonucleotide (ODN), 330
- OMC. *See* Octyl methoxycinnamate (OMC)
- Omega-3 fatty acids, 164
- One-dimensional nanomaterials (1D nanomaterials), 17–18
- Onychomycosis, 132–133
- Optical and magnetic properties, nanomaterials, 23–24
- Optical coherence tomography (OCT), 50, 358, 361–363, 362f
- Organic filters, 231–232
- Organic nanoparticles, 57–58. *See also* Inorganic nanoparticles
- Organic UV filters, 229, 231, 243
- OS. *See* Overall survival (OS)
- Osmium complexes, 260
- Ovalbumin (OVA), 64–65
- Overall survival (OS), 204
- OWCL. *See* Old world cutaneous leishmaniasis (OWCL)
- Oxidative biomarkers, 232
- Oxybenzone, 229, 231
- Oxygen (O₂), 257
 probe molecules, 263
 sensing in skin, 257–258
- Oxygen saturation (StO₂), 259
- Oxygen sensing
 on magnetic resonance techniques, 267–268
 oxygen calibration curve, 268f
 particle oxygen sensors, 268–269
 skin oxygen sensing, 269
 nanomaterials in, 259
 on phosphorescence quenching, 259–260
 nanomaterial oxygen sensors, 263–265
 phosphorescent probes, 260–262
 sensor matrix, 262–263
 skin oxygen sensing, 265–267
- in skin, 257–258
 techniques for, 258–259
- P**
- P/S. *See* Penicillin–streptomycin (P/S)
- PAA. *See* Poly(acrylic acid) (PAA)
- Paclitaxel (PTX), 18, 192, 206, 210
 paclitaxel–siRNA nanoparticles, 36
- PAMAM dendrimers. *See* Polyamidoamine dendrimers (PAMAM dendrimers)
- PAMAMOS. *See* Poly(amidoamine-organosilicon) (PAMAMOS)
- PAN. *See* Polyacrylonitrile (PAN)
- Papillary dermis, 238
- Paromomycin (PM), 136
 immunological considerations, 140–143
 pharmacokinetic considerations, 139–140
- Paromomycin-methylbenzethonium chloride (PM-MBCL), 136
- Particle
 characteristics, 252
 oxygen sensors, 268–269
 penetration, 248–249
 shape, 19, 60
 size, 60
 stability, 19–20
- PAs. *See* Peptide amphiphiles (PAs)
- Passive targeting, 241
 to extending blood circulation time, 205–206
- PAT. *See* Photoacoustic tomography (PAT)
- Pathophysiology, 167–168
- Patient safety, 51–52
- PBAE. *See* Poly(β -amino esters) (PBAE)
- PCEP. *See* Poly(((cholesteryl oxocarbonylamido ethyl) methyl bis(ethylene) ammonium iodide) ethyl phosphate) (PCEP)
- PCL. *See* Poly(ϵ -caprolactone) (PCL)
- PCL–PEG. *See* Poly(ϵ -caprolactone)–poly(ethylene glycol) (PCL–PEG)
- PCV-2. *See* Porcine circovirus type 2 (PCV-2)
- PD-1, 197, 205
- PD-L1. *See* Programmed death ligand-1 (PD-L1)
- PDAC–PSS. *See* Poly-(diallyldimethylammonium chloride)–poly(styrene sulfonate) (PDAC–PSS)
- PDGF. *See* Platelet-derived growth factor (PDGF)
- PDGF beta polypeptide (PDGF-BB), 341
- PDGF-BB. *See* PDGF beta polypeptide (PDGF-BB)
- PDI. *See* Polydispersity index (PDI)
- PDMS. *See* Polydimethylsiloxane (PDMS)
- PDT. *See* Photodynamic therapy (PDT)
- PEBBLE. *See* Probe-encapsulated by biologically localized embedding (PEBBLE)
- PEG. *See* Polyethylene glycol (PEG)
- PEG-octaoxyethylene laurate ester (PEG-8-L), 116–120
- PEI. *See* Polyethylenimine (PEI)
- PEMF. *See* Pulsed electromagnetic fields (PEMF)
- Penetration enhancer vesicles (PEVs), 116–120
- Penetration process, 21–23, 308, 313–314
- Penicillin–streptomycin (P/S), 277–278
- Pentamidine, 140
- Peptide amphiphiles (PAs), 345
- Peptide dendrimers. *See also* Dendrimers
 advantages, 92
 alternative class of dendrimers, 91
 synthesis, 91–92
 transdermal drug delivery, 93–96
 as drug carriers, 94–95
 drug peptide dendrimeric conjugates effect, 96
 iontophoresis-mediated permeation, 94–95
 RP-HPLC method development, 93–94
 sonophoresis-mediated permeation, 94
- Peptides, 208
- Percutaneous absorption, 308
- Perfluorocarbons (PFCs), 268
- Permeability, 21–23
- Permeation, 308
- Peroxynitrite (OONO⁻), 128
- PEVs. *See* Penetration enhancer vesicles (PEVs)
- PFCs. *See* Perfluorocarbons (PFCs)
- PFS. *See* Progression-free survival (PFS)
- PGA. *See* Poly(glycolic acid) (PGA)
- PGE2. *See* Prostaglandin E2 (PGE2)
- pH responsive drug delivery, 209
- Pharmacokinetic(s), 73–74
 behavior, 90
 considerations, 139–140
- PHBV. *See* Poly(3- ϵ -hydroxybutyrate–co-3- ϵ -hydroxyvalerate) (PHBV)
- Phenotypes, 136
- Phosphatidylcholine, 116–120, 242
- Phosphatidylinositol 3-kinase. *See* Phosphoinositol-3 kinase (PI3K)
- Phosphoinositol-3 kinase (PI3K), 203–204, 368
 PI3K/Akt pathway, 193–194
- Phospholipase A2 (PLA2), 141
- Phospholipid, 27, 170–171
- Phosphorescence, 259
 oxygen sensing on quenching, 259–260
- Phosphorescent probes, 260–262
 oxygen-sensing phosphors, 261f
- Photoacoustic tomography (PAT), 41
- Photoaging, 239
 nanoemulsions for prevention and treatment, 242–243
- Photodynamic therapy (PDT), 36–37, 136, 142, 181–182, 209, 275–276. *See also* Image correlation spectroscopy (ICS)
- liposomes in, 148

- Photodynamic therapy, 75
 Photoprotection, 231
 nanoparticles for, 37–38
 Photosensitizers (PS), 142, 181–182
 Photostability, 231
 Photothermal therapy, 99–100
 PHPMA. *See* Poly(N-(2-hydroxypropyl) methacrylamide) (PHPMA)
 Phthalocyanine derivatives, 143
 Physical adsorption approaches, 60
 Physical penetration, 93
 Phytosphingosine (PS), 170
 PI3K. *See* Phosphoinositol-3 kinase (PI3K)
 Piloplex, 326
 PKC. *See* Protein kinase C (PKC)
 PKDL. *See* Post-kala-azar dermal leishmaniasis (PKDL)
 PLA. *See* Poly(lactic acid) (PLA). *See* Polylactide (PLA)
 PLA2. *See* Phospholipase A2 (PLA2)
 Planck's constant, 24
 Plasma, 92
 Platelet-derived growth factor (PDGF), 296, 338, 368
 Platelet-inspired nanoparticles, 290–291
 Platelet-like nanoparticles (PLNs), 291
 Platelets, 290–291
 Platinum, 221
 Platinum octaethylporphyrin (PtOEP), 263–265
 Platinum tetrakis(pentafluorophenyl) porphyrin (PtTFPP), 263–265
 PLGA. *See* Poly(lactic-co-glycolic acid) (PLGA)
 PLGA–PEO. *See* Poly(lacto-co-glycolic acid)–poly(ethylene oxide) (PLGA–PEO)
 PLLA. *See* Poly L-lactic acid (PLLA)
 PLLA-Hyp. *See* Hypericin-loaded PLLA (PLLA-Hyp)
 PLLCL. *See* Poly(L-lactic acid)-co-poly-(ϵ -caprolactone) (PLLCL)
 PLNs. *See* Platelet-like nanoparticles (PLNs)
 PM. *See* Paromomycin (PM)
 PM-MBCL. *See* Paromomycin-methylbenzethonium chloride (PM-MBCL)
 PMMA. *See* Polymethylmethacrylate (PMMA)
 PNIPA. *See* Poly(N-isopropylacrylamide) (PNIPA)
 PNP. *See* Polymeric nanoparticles (PNP)
 Point spread function (PSF), 106
 Poly L-lactic acid (PLLA), 275–276, 342.
 See also Image correlation spectroscopy (ICS)
 PLLA-based NPs, 276
 dermatological application, 276–277
 PLLA-HYP nanoparticles
 characterization, 277
 flow velocities of organelles, 282t
 incubation of cells with, 277–278
 intracellular dynamics, 281–282
 Poly-(diallyldimethylammonium chloride)–poly(styrene sulfonate) (PDAC–PSS), 61–62
 Poly-alkyl-cyanoacrylates, 275–276
 Poly-depsipeptides, 77–78
 Poly-L-lysine dendrimers, 191
 Poly(((cholesteryl oxocarbonylamido ethyl) methyl bis(ethylene) ammonium iodide) ethyl phosphate) (PCEP), 327
 Poly(3- ϵ -hydroxybutyrate–co–3- ϵ -hydroxyvalerate) (PHBV), 342
 Poly(acrylic acid) (PAA), 79–80
 Poly(amidoamine-organosilicon) (PAMAMOS), 90
 Poly(aminoamine), 191
 Poly(carboxybetaine acrylamide) (polyCBAA), 21
 Poly(ϵ -caprolactone)–poly(ethylene glycol) (PCL–PEG), 370–371
 Poly(glycolic acid) (PGA), 78–79
 Poly(L-arginine), 61–62
 Poly(L-lactic acid)-co-poly-(ϵ -caprolactone) (PLLCL), 372
 Poly(lactic acid) (PLA), 21, 77–79, 295, 328, 342
 Poly(lactic-co-glycolic acid) (PLGA), 25, 123–124, 143–144, 181–182, 206, 295, 328, 342
 PLGA-LL37 nanoparticles, 296–297
 Poly(lactide–co–glycolide). *See* Poly(lactic-co-glycolic acid) (PLGA)
 Poly(lacto-co-glycolic acid)–poly(ethylene oxide) (PLGA–PEO), 371
 Poly(L–lactide). *See* Poly L-lactic acid (PLLA)
 Poly(N-(2-hydroxypropyl) methacrylamide) (PHPMA), 79–80
 Poly(N-isopropylacrylamide) (PNIPA), 79–80, 263–265
 Poly(N-vinylpyrrolidone) (PVP), 79–80
 Poly(propyleneimine), 191
 Poly(propyleneimine) (PPI), 80
 Poly(styrene-block-vinylpyridine), 263–265
 Poly(β -amino esters) (PBAE), 297
 Poly(γ -glutamic acid), 77
 Poly(ϵ -caprolactone) (PCL), 78–79, 172, 196, 292–293, 328, 342
 Polyacrylonitrile (PAN), 262–263
 Polyamidoamine dendrimers (PAMAM dendrimers), 80, 90, 92, 299, 330
 Polycaprolactone. *See* Poly(ϵ -caprolactone) (PCL)
 polyCBAA. *See* Poly(carboxybetaine acrylamide) (polyCBAA)
 Polydimethylsiloxane (PDMS), 262–263
 Polydispersity index (PDI), 333–334
 Polyethylene glycol (PEG), 22, 33, 58–59, 79–80, 128, 205–206, 241, 309–310, 331
 PEG-Intron, 211
 PEG–functionalized, 104
 Polyethylenimine (PEI), 64–65, 80, 172, 196, 328
 Polylactide (PLA), 328
 Polymeric nanoparticles (PNP), 33, 171–172, 290
 Polymeric/polymer(s), 191
 cationic, 172
 micelles, 178–179
 nanocarriers, 164–165
 NP PLGA, 194
 polymer-based nanomedicines for eye, 328–329
 polymer-based nanoparticles, 123–124
 Polymethylmethacrylate (PMMA), 62
 Polypeptides, 77–78
 Polypropylene imine dendrimers (PPI dendrimers), 90
 Polysaccharides, 78
 Polystyrene (PS), 262–263, 266
 Polystyrene sulfonate (PSS), 64–65
 Polyurethane (PU), 342
 Polyvinyl alcohol (PVA), 332, 342
 Polyvinylpyrrolidone (PVP), 340–341.
 See also Image correlation spectroscopy (ICS)
 PVP-HYP nanoparticles
 flow velocities of organelles, 282t
 intracellular dynamics, 281–282
 PVP-Hyp photosensitizer
 incubation of cells with, 277–278
 Porcine circovirus type 2 (PCV-2), 27
 Porous materials, 232
 Post-kala-azar dermal leishmaniasis (PKDL), 136
 Potential carcinogenicity, 82
 PPI. *See* Poly(propyleneimine) (PPI)
 PPI dendrimers. *See* Polypropylene imine dendrimers (PPI dendrimers)
 PpIX. *See* Protoporphyrin IX (PpIX)
 Preclinical studies, 64–65
 Precorneal loss factors, 325b
 Prickle cell layer. *See* Squamous cell layer
 Probe-encapsulated by biologically localized embedding (PEBBLE), 263–265
 Professional antigen-presenting cells, 11–12
 Programmed death ligand-1 (PD-L1), 197, 204
 Progression–free survival (PFS), 205
 Proliferation, 289, 338
 Prostaglandin E2 (PGE2), 340–341
 Prostate specific membrane antigen (PSMA), 190, 206
 Protein kinase C (PKC), 141
 Protein(s), 21
 corona, 21
 fibers in dermis, 342
 sponge effect, 209
 Protoporphyrin IX (PpIX), 276–277
 PS. *See* Photosensitizers (PS); Phytosphingosine (PS); Polystyrene (PS)
Pseudomonas aeruginosa (*P. aeruginosa*), 80, 293–295, 299
 PSF. *See* Point spread function (PSF)

- PSMA. *See* Prostate specific membrane antigen (PSMA)
- Psoriasis, 157
- pathophysiology and pharmacotherapy for, 157–160
- pharmacotherapy, 159t
- PSS. *See* Polystyrene sulfonate (PSS)
- PtOEP. *See* Platinum octaethylporphyrin (PtOEP)
- PtTFPP. *See* Platinum
- tetrakis(pentafluorophenyl) porphyrin (PtTFPP)
- PTX. *See* Paclitaxel (PTX)
- PU. *See* Polyurethane (PU)
- Pulse oximeter, 259
- Pulsed electromagnetic fields (PEMF), 223
- PUVA. *See* 8-Methoxypsoralen with UVA radiation (PUVA)
- PVA. *See* Polyvinyl alcohol (PVA)
- PVP. *See* Poly(N-vinylpyrrolidone) (PVP); Polyvinylpyrrolidone (PVP)
- PVP-Hyp. *See* Hypericin with polyvinylpyrrolidone (PVP-Hyp)
- Q**
- Q10-NLC formulation, 122
- QA. *See* Quaternary ammonium (QA)
- Quantum dots (QDs), 17, 58–59, 68–69, 143–144, 210, 307, 309–311, 313–315, 318
- for diagnostic dermatology, 41
- distribution and accumulation at epidermal–dermal junction, 312–313
- confocal fluorescence microscopy, 312f
- distribution in skin, 310–312
- confocal fluorescence microscopy, 311f
- intracellular localization in dermis, 315
- migration pathways, 313–314
- nanocarriers, 307–308
- SC, 308
- skin as barrier, 308–309
- skin repair processes, 308
- transappendageal pathway in delivery, 313–314
- Quantum wires, 17
- Quantum yield (QY), 260
- Quaternary ammonium (QA), 299
- QY. *See* Quantum yield (QY)
- R**
- RAD16-I gel, 344–345
- Radiation therapy, 217–218
- Raman microscopy, 358
- Rapid expansion supercritical solution (RESS), 332–333
- Raynaud's phenomenon, 258
- RCM. *See* Reflectance confocal microscopy (RCM)
- Re-epithelialization, 339
- Reactive nitrogen oxide species (RNOS), 33–34, 128
- Reactive oxygen species (ROS), 21, 37, 66–67, 141, 160, 181–182, 204, 219, 232, 239, 293, 342
- Recombinant human epidermal growth factor (rhEGF), 295–296
- Reflectance confocal microscopy (RCM), 103–104, 358–359
- images of untreated, and intact and tape-stripped, skin, 361f
- Regulatory issues, 52–53
- Regulatory T cells (Treg cells), 204
- Remodeling, 338
- RES. *See* Reticuloendothelial system (RES)
- Resorption, 308
- RESS. *See* Rapid expansion supercritical solution (RESS)
- Resveratrol, 160
- Reticuloendothelial system (RES), 20–21, 178
- Retinoid X receptor (RXR), 163
- Retinoids, 242–243
- Retinol, 121
- Retinyl palmitate oil, 242–243
- Reverse-phase high-performance liquid chromatography (RP-HPLC), 92
- RF. *See* Rheumatoid factor (RF)
- RGD peptides. *See* Arginine, glycine, and asparagine (RGD peptides)
- rhEGF. *See* Recombinant human epidermal growth factor (rhEGF)
- Rheumatoid factor (RF), 339–340
- Rhodamine, 195
- RISCs. *See* RNA-induced silencing complexes (RISCs)
- RNA-induced silencing complexes (RISCs), 295
- RNOS. *See* Reactive nitrogen oxide species (RNOS)
- Rod
- rod-shaped nanoparticles, 19
- rod-shaped particles, 22
- Rod/OVA/SO, 64–65
- ROS. *See* Reactive oxygen species (ROS)
- RP-HPLC. *See* Reverse-phase high-performance liquid chromatography (RP-HPLC)
- RXR. *See* Retinoid X receptor (RXR)
- S**
- S/V ratio. *See* Surface-to-volume ratio (S/V ratio)
- Salidroside, 27
- liposomes, 27
- Salting-out method, 332
- SAMs. *See* Self-assembled monolayers (SAMs)
- Sandfly, 137–138
- SAP. *See* Serum amyloid protein P (SAP)
- SAS process. *See* Supercritical antisolvent process (SAS process)
- SC. *See* Stratified corneum (SC)
- Scanning electron microscopy (SEM), 106, 333–334
- Scavenger-receptor-mediated pathway, 82
- SCC. *See* Squamous cell carcinoma (SCC)
- Sebaceous follicles, 10–11
- Sebaceous glands, 9–11
- Sebum flow, 253
- Second harmonic generation (SHG), 359
- Secosomes, 116–120
- Secreted protein, acidic, and rich in cysteine (SPARC), 61–62
- Self-assembled monolayers (SAMs), 25
- Self-assembly, 25, 344–345
- Self-organization, 25
- SEM. *See* Scanning electron microscopy (SEM)
- Semiconductor quantum dots, 24
- Sensor foil scheme, 267f
- Sensor matrix, 262–263
- Sensory organ, 12
- Serum amyloid protein P (SAP), 339
- sGC. *See* Soluble guanylyl cyclase (sGC)
- Shaft cuticle, 9
- SHG. *See* Second harmonic generation (SHG)
- SHH. *See* Sonic hedgehog (SHH)
- Shunt route, 180
- SI-ATRP process. *See* Surface-initiated atom transfer radical polymerization process (SI-ATRP process)
- Si(OC₂H₅)₄. *See* Tetraethylorthosilicate (TEOS)
- Signal regulatory protein- α (SRP α), 196–197
- Silica nanoparticles, 25–26, 63
- Silicone, 266
- Silver (Ag), 21, 143–145
- Silver nanoparticles (AgNPs), 39, 58, 66–68, 147–148, 220, 339–340
- Simvastatin, 124
- Single-photon confocal microscopy, 359
- Single-photon microscopy, 359–361
- Singlet oxygen ((1)O₂), 181–182
- siRNAs. *See* Small interfering ribonucleic acids (siRNAs)
- Sitamaquine, 140
- Skin, 1, 287, 308, 353
- aging, 239–240, 342–343
- anatomy, 337–338
- appearance, 240
- appendages, 238–239, 356
- barrier, 238f
- biodegradability and biocompatibility in, 75f, 80–83, 81f
- delivery, 308
- dermis, 6–7
- epidermal appendages, 8–11
- epidermis, 2
- dermal-epidermal junction, 6
- epithelial stem cells, 3–5
- keratinocytes, 3
- nonkeratinocyte cells, 5–6
- structure, 2f, 3
- functions, 11, 11t
- endocrine function, 12
- immunological function, 11–12
- preventing loss of essential body fluids, 11

Skin (Continued)

- protecting against toxic substances
 - penetration, 11
 - regulation of body temperature, 11
 - sensory organ, 12
- hypodermis, 7–8
- immune system cells, 74
- penetration studies, 106
- permeability, 238–239
- permeation studies, 106
- regeneration, 368
 - electrospun scaffolds containing EGF, 369t
 - frontiers in, 338
 - MSCs, 372
- repair processes, 308
- skin-based biomedical applications, 99–100
- structure, 237
 - in nanoparticle penetration, 354–357
- 3D bioprinting, 345–347
- wound healing
 - nanofibers in, 341–342
 - nanoparticles in, 339–341
- wound regeneration, 338–342
- Skin barrier, 221, 308–309
 - AuNPs interactions with, 251
 - evaluation methods, 107–108
 - factors affecting skin penetration of AuNPs, 252
 - skin penetration enhancers of colloidal gold, 107–108
 - disruption, 250–252
- Skin cancer, 178, 181–183, 217
 - MBs, 183f
 - nanoparticle-based theranostics in
 - NPs for transdermal drug delivery, 179–181
 - NPs in cancer theranostics, 178–179
 - nanovehicles in therapy and diagnosis, 183t–184t
 - treatment, 36
 - treatment and imaging, 101
- Skin oxygen sensing
 - on magnetic resonance techniques, 269
 - tumor pO₂, 270f
 - in vivo EPR oximetry systems, 270f
 - on phosphorescence quenching, 265–267
 - sensor foil scheme, 267f
- Skin penetration
 - ability of inorganic nanoparticles, 58
 - hydrophilicity, 59
 - particle shape, 60
 - particle size, 60
 - surface charge, 58–59
 - in vivo silica permeation amounts, 60t
 - enhancers of colloidal gold, 107–108
 - chemical penetration enhancers, 107
 - dermaporation, 108
 - iontophoresis, 108
 - thermal ablation, 107–108
 - ultrasound, 107
 - factors affecting AuNPs, 102–106
 - experimental variables and experimental configuration, 105–106
 - formulation adjuvants, 102–104
 - physicochemical properties of AuNPs, 102–104
 - skin origin and condition, 104–105
 - potential mechanisms, 108–110
 - penetration pathways of AuNPs, 109f
 - SLNPs. *See* Solid lipid nanoparticles (SLNs)
 - SLNs. *See* Solid lipid nanoparticles (SLNs)
 - SLS. *See* Sodium lauryl sulfate (SLS)
 - Small interfering ribonucleic acids (siRNAs), 36, 60–61, 76, 99–100, 116–120, 172, 205, 295
 - Smart delivery, 209
 - Smart polymer nanoparticles (SPNs), 295
 - SNO-CAP-np. *See* s-Nitrosocaptopril nanoparticles (SNO-CAP-np)
 - SO dispersion system. *See* Solid-in-oil dispersion system (SO dispersion system)
 - Sod1. *See* Superoxide dismutase (Sod1)
 - Sodium borohydride (NaBH₄), 25, 218
 - Sodium lauryl sulfate (SLS), 105, 223
 - Solar filters, 243
 - Sol–gel
 - process, 25–26
 - sol–gel-based platform, 128, 129f
 - Solid lipid nanoparticles (SLNs), 33, 35, 57–58, 76, 115–116, 121–122, 143–144, 163, 170, 178, 296
 - Solid-in-oil dispersion system (SO dispersion system), 64–65
 - Solid-phase combinatorial methods, 91
 - Solid-phase peptide synthesis (SPPS), 91
 - Soluble guanylyl cyclase (sGC), 128
 - Solvent displacement method, 331
 - Solvo-thermal approach, 60
 - Somatostatin receptor (SSTR), 190, 208
 - Sonic hedgehog (SHH), 297
 - Sonophoresis, 222–223
 - sonophoresis-mediated permeation, 94
 - acoustic streaming, 94
 - cavitation effects, 94
 - thermal effects, 94
 - SPARC. *See* Secreted protein, acidic, and rich in cysteine (SPARC)
 - Spatiotemporal image correlation spectroscopy (STICS), 278–279
 - Spatiotemporal image cross-correlation spectroscopy (STICCS), 276, 278–280
 - Specific surface area, 18–19
 - SPFs. *See* Sun protection factors (SPFs)
 - Spherical particles, 25
 - SPION. *See* Superparamagnetic iron oxide NPs (SPION)
 - SPNs. *See* Smart polymer nanoparticles (SPNs)
 - Spongiosis, 168
 - SPPS. *See* Solid-phase peptide synthesis (SPPS)
 - Squamous cell carcinoma (SCC), 101, 181
 - Squamous cell layer, 4
 - SRP α . *See* Signal regulatory protein-alpha (SRP α)
 - SSA. *See* Sulfonic acid sodium salt (SSA)
 - SSL-IMA. *See* Imatinib–loaded sterically stabilized liposomes (SSL-IMA)
 - SSTR. *See* Somatostatin receptor (SSTR)
 - Staphylococcus aureus* (*S. aureus*), 79, 129–130, 131f, 292, 299
 - STAT1, 196
 - STAT3, 194–195
 - Stemming inflammation, 295
 - Stern–Volmer equation, 259–260
 - STICCS. *See* Spatiotemporal image cross-correlation spectroscopy (STICCS)
 - STICS. *See* Spatiotemporal image correlation spectroscopy (STICS)
 - Stimulating proliferation, 295
 - Stimuli-responsive, 209
 - drug delivery, 209
 - light responsive, 209
 - pH responsive, 209
 - temperature responsive, 209
 - and triggered release, 209
 - ultrasound responsive, 210
 - StO₂. *See* Oxygen saturation (StO₂)
 - Stokes–Einstein equation, 21–22
 - Stratum corneum (SC), 5, 32, 32f, 57–58, 76, 81–82, 93–95, 95f, 99–100, 138, 140, 167–168, 179–180, 220–221, 231–232, 237–238, 308–309, 354–356
 - lipid lamellar regions, 116–120
 - lipids, 40
 - Stratum germinativum. *See* Basal layer
 - Stratum granulosum. *See* Granular layer
 - Stratum spinosum. *See* Squamous cell layer
 - Streptomyces tsukubaensis* (*S. tsukubaensis*), 163
 - Stromelysins, 6–7
 - Subcutis. *See* Hypodermis
 - Sublamina densa, 6
 - Submicron emulsions. *See* Nanoemulsion
 - Substrates, 339, 343–344
 - cell-imprinted, 345
 - Sulfonic acid sodium salt (SSA), 62
 - Sun protection factors (SPFs), 122, 231, 243
 - Sunscreen, 229, 250–251
 - nanoemulsions, 243
 - regulatory state of nanoparticles in, 234–235
 - Supercritical antisolvent process (SAS process), 332–333
 - Supercritical fluid method, 332–333
 - Superoxide dismutase (Sod1), 343
 - Superparamagnetic hematite (Fe₂O₃), 17
 - Superparamagnetic iron oxide NPs (SPION), 179
 - Suprabasal cells, 4
 - Supramolecular chemistry, 25
 - Supramolecules, 25
 - Surface
 - charge, 58–59
 - coatings, 310

- energy, 19–20
mitigation, 20
engineering strategies, 60–62
plasmon, 23
tension, 19
- Surface-initiated atom transfer radical polymerization process (SI-ATRP process), 62
- Surface-to-volume ratio (S/V ratio), 19
- Symptomatic treatment, 169
- Synergistic ratio, 211
- Synthetic nanocarriers, 74
- Synthetic polymer nanofibers, 342
- Synthetic polymers, 77–79
- T**
- T cells, 138–139
- T lymphocyte activation, 157–160
- T-regulatory cells, 138–139
- T.R.U.E. patch test. *See* Thin Layer Rapid Use Epicutaneous test (T.R.U.E. patch test)
- Tacrolimus, 35, 163
- TAMC. *See* Total Aerobic Microbial Count (TAMC)
- Tamoxifen, 160
- Tape stripping, 310
- Targeted delivery to tumor tissues, 221–223
multiphoton tomography, 223f
sites in skin for nanoparticle delivery, 222f
- Targeted NP drug delivery for melanoma therapy
active targeting, 206
melanoma and melanoma-APCs, 207f
targeting integrins on surface of endothelial cells, 208
targeting melanoma, 208–209
targeting receptors on surface of melanoma cells, 206–208
nanotheranostics and combination therapy, 210–211
NP in melanoma combination therapy, 210–211
theranostic NP in melanoma imaging and therapy, 210
passive targeting, 205–206
stimuli-responsive drug delivery and triggered release, 209–210
light responsive, 209
pH responsive, 209
temperature responsive, 209
ultrasound responsive, 210
- TAT-NLCs. *See* Transactivating transcriptional activator (TAT-NLCs)
- Taxoprexin, 211
- β -TCP. *See* β -Tricalcium phosphate (β -TCP)
- TDD. *See* Transdermal drug delivery (TDD)
- TDDS. *See* Transdermal drug delivery systems (TDDS)
- Teflon nanoparticles, 15
- Tegumentary leishmaniasis, 135–136
- TEM. *See* Transmission electron microscopy (TEM)
- Temoporfin. *See* M-tetrahydroxyphenylchlorin (mTHPC)
- Temperature responsive, 209
- Temporal ICS (TICS), 278
- TEOS. *See* Tetraethylorthosilicate (TEOS)
- Terpene penetration enhancers, 124
- tert-Butyl carbamates (Boc), 91
- M-Tetrahydroxyphenylchlorin (mTHPC), 160–161
- Tetraethylorthosilicate (TEOS), 25–26
- 5,10,15,20-Tetrakis(4-hydroxyphenyl)-21H,23H-porphine (tHPP), 37
- Tetramethylammonium hydroxide (TMAOH), 58–59
- TEWL. *See* Transepidermal water loss (TEWL)
- TF. *See* Transferrin (TF)
- TFA. *See* Trifluoroacetic acid (TFA)
- TFG- β . *See* Transforming growth factor- β (TFG- β)
- TfR. *See* Transferrin receptors (TfR)
- TGA. *See* Australia's Therapeutic Goods Administration (TGA)
- TGF α . *See* Transforming growth factor- α (TGF α)
- Theranostics, 25, 177, 210
- Thermal ablation, 107–108
- Thermal effects, 94
- Thin Layer Rapid Use Epicutaneous test (T. R. U. E. patch test), 22–23
- tHPP. *See* 5,10,15,20-Tetrakis(4-hydroxyphenyl)-21H,23H-porphine (tHPP)
- Thrombin, 291–292, 291f
- Thymic stromal lymphopoietin (TSLP), 63, 173
- Thymine (T), 203–204
- TICS. *See* Temporal ICS (TICS)
- TILs. *See* Tumor infiltrating lymphocytes (TILs)
- Time-correlated single-photon counting, 358–359
- TIMPs. *See* Tissue inhibitors of matrix metalloproteinases (TIMPs)
- Tinosorb A2B, 232
- Tissue inhibitors of matrix metalloproteinases (TIMPs), 6–7, 139, 239–240, 297–298
- Tissue oxygen sensing, 258–259
- Titanium dioxide (TiO₂), 21, 37–38, 66, 102, 115–116, 229–230, 248–250, 293, 353
NPs, 58, 68, 120
- TLR. *See* Toll-like receptor (TLR)
- TMAOH. *See* Tetramethylammonium hydroxide (TMAOH)
- TNF α . *See* Tumor necrosis factor- α (TNF α)
- α -Tocopherol, 78
- Toll-like receptor (TLR), 141
- Topical corticosteroids, 169
- Topical drug delivery, 101–102, 179–180
- Topical eye drops, 326–327
- Topical nanoparticle penetration
combination of NPs with penetration enhancers, 124
flexible nanovesicles, 116–120
flexible NPs, 116–120
metal oxide NPs, 120–121
nanoformulations for skin, 115–116
nanoparticles and skin, NLCs, 122–123
NPs for targeted delivery to hair follicles and sebaceous glands
polymer-based NPs, 123–124
SLNs, 121–122
- Total Aerobic Microbial Count (TAMC), 53
- Total Combined Yeasts and Molds Count (TYMC), 53
- TP. *See* Triptolide (TP)
- TRAIL-expressing inflammatory cells, 139
- Trans-epithelial transport, 90
- Transactivating transcriptional activator (TAT-NLCs), 122–123
- Transappendageal pathway, 309
in QDs delivery, 313–314
- Transcellular routes, 238–239
- Transcutaneous oxygen tension (TcPO₂), 258
- Transcutaneous vaccination, 101–102
- Transcutol, 116–120
- Transdermal biomedical applications, 102
- Transdermal delivery, 47–50, 92. *See also* Microneedle (MN)
therapeutics, 101–102
- Transdermal drug, 68
- Transdermal drug delivery (TDD), 92, 101–102, 179–180
NPs for, 179–181
transdermal penetration mechanisms, 180f
- Transdermal drug delivery systems (TDDS), 57, 92
approaches, 93
ideal candidates, 92–93
peptide dendrimers in, 93–96
as drug carriers, 94–95
drug–peptide dendrimeric conjugates effect, 96
iontophoresis-mediated permeation, 94–95
RP-HPLC method development, 93–94
sonophoresis-mediated permeation, 94
SC, 93
- Transdermal penetration mechanisms, 180f
- Transepidermal water loss (TEWL), 50, 115–116, 168, 241–242, 308
measurement, 105
- Transferosomes, 170–171
- Transferrin (TF), 77, 206–208
- Transferrin receptors (TfR), 206–208
- Transferosomes, 116–120
- Transfollicular
pathways, 109
penetration, 124

- Transforming growth factor- α (TGF α), 288, 367
 Transforming growth factor- β (TGF- β), 6–7, 338
 Transmission electron microscopy (TEM), 32, 103, 230–231, 251, 277, 288, 333–334, 358–359
 Treg cells. *See* Regulatory T cells (Treg cells)
 Tretinoin (TTN), 163–164
 β -Tricalcium phosphate (β -TCP), 297
Trichophyton mentagrophytes (*T. mentagrophytes*), 132
 Trifluoroacetic acid (TFA), 91
 Triphenyl phosphine (PPhe₃), 25
Tripterygium wilfordii (*T. wilfordii*), 163
 Triptolide (TP), 163
 TSLP. *See* Thymic stromal lymphopoietin (TSLP)
 TTN. *See* Tretinoin (TTN)
 Tumor ablation, 24f
 Tumor cells, 36
 Tumor infiltrating lymphocytes (TILs), 204
 Tumor necrosis factor- α (TNF α), 339
 Turkevich method, 218
 Two-dimensional diffusion, 279
 Two-dimensional Gaussian function, 278–279
 Two-dimensional nanomaterials (2D nanomaterials), 17–18
 TYMC. *See* Total Combined Yeasts and Molds Count (TYMC)
 TYR. *See* Tyrosinase (TYR)
 Tyrosinase (TYR), 203–204
 TyroSpheres, 164–165
- U**
 UDL. *See* Ultradeformable liposomes (UDL)
 Ultra-Turrax homogenizer, 333
 Ultradeformable liposomes (UDL), 148, 170–171
 Ultrafine chitin nanofibers, 18
 Ultrasound (US), 107, 183, 210
 Ultraviolet (UV), 21, 157, 168, 209, 217, 229
 attenuation, 231
 filters, 243
 protection, 338
 UV-induced ROS, 239–240
 Ultraviolet A (UVA), 276
 filters, 120
 Ultraviolet B (UVB), 12
 filters, 120, 251
 Ultraviolet radiation (UVR), 37, 203–204, 239–240, 248, 307
- Unstable microemulsions. *See* Nanoemulsion
 Upconversion nanoparticles, 60
 US. *See* Ultrasound (US)
 US Food and Drug Administration (FDA), 57, 204–205, 229–230, 275–276, 296, 341
 UV. *See* Ultraviolet (UV)
 UVA. *See* Ultraviolet A (UVA)
 UVB. *See* Ultraviolet B (UVB)
 UVR. *See* Ultraviolet radiation (UVR)
- V**
 van der Waals forces, 20, 27
 Vancomycin, 130–131, 292
 Vascular endothelial growth factor (VEGF), 194, 288, 341, 368
 VEGF-siRNA, 206
 Vater–Pacinian corpuscles, 7
 VEGF. *See* Vascular endothelial growth factor (VEGF)
 Vesicles, 115–116
 Virosomes, 75
 Virus-like particles (VLPs), 74–75
 Visceral leishmaniasis (VL), 135–136
 VL. *See* Visceral leishmaniasis (VL)
 VLPs. *See* Virus-like particles (VLPs)
 von Willebrand Factor (vWF), 290–291
- W**
 W/O emulsions. *See* Water-in-oil emulsions (W/O emulsions)
 W/W emulsions. *See* Water-in-water emulsions (W/W emulsions)
 Water contact angle (WCA), 23
 Water-in-oil emulsions (W/O emulsions), 240, 332
 Water-in-water emulsions (W/W emulsions), 240
 WAXD. *See* Wide-angle X-ray powder diffraction (WAXD)
 WCA. *See* Water contact angle (WCA)
 Weanling piglets, 120–121
 “Whitening effect”, 229–230
 WHO. *See* World Health Organization (WHO)
 Wide-angle X-ray powder diffraction (WAXD), 334
 World Health Organization (WHO), 136–137
 Wound, 287
 repair, 287–288
 stages, 288t
 types, 288f
- Wound healing, 39, 287, 290, 368, 371–372
 antimicrobial applications, 292
 antimicrobial agents delivery, 292–293, 294f
 inherent antimicrobial properties of metal nanoparticles, 293–295
 biological factors, delivery and elution, 295–297, 297t
 EGF for, 368
 gene therapy, 297
 inflammation, 288
 cutaneous wound, 289f
 maturation, 289–290, 297–298
 nanofibers
 natural polymer nanofibers, 341–342
 synthetic polymer nanofibers, 342
 nanoparticles, 290, 290t
 applications in, 290
 hemostasis, 290
 metallic nanoparticles, 339–340
 nanobridging, 292
 nanoporous AAO, 339
 nonmetallic NPs, 340–341
 NO delivery, 300t–301t
 pathways for metabolism, 303f
 platelets, 290–291
 silver nanoparticles, 302f
 sources of materials for polymeric, 290t
 thrombin, 291–292, 291f
 toxicity, 301–302
 NO, 298–301
 proliferation, 289
 stemming inflammation, 295
 stimulating proliferation, 295
 Wrinkly skin, 240
- X**
 X-ray powder diffraction (XRPD), 334
- Z**
 Zero-dimensional nanomaterials (0D nanomaterials), 17
 Zinc oxide (ZnO), 37–38, 66, 102, 115–116, 229–230, 248–249, 252, 353
 Zinc oxide nanoparticles (ZnONPs), 22–23, 58, 68, 120, 356–357, 359
 Zinc phthalocyanine (ZnPC), 148
 Zn²⁺ cation, 22–23
 ZnO. *See* Zinc oxide (ZnO)
 ZnONPs. *See* Zinc oxide nanoparticles (ZnONPs)
 ZnPC. *See* Zinc phthalocyanine (ZnPC)